VOLUME 28 / NUMBER 3
FEBRUARY 8, 1990
ACC. NOS. N90-11692 TO N90-12494

STAR

AN ABSTRACT JOURNAL

Scientific and Technical Aerospace Reports

PRODUCED BY THE
SCIENTIFIC AND TECHNICAL
INFORMATION
DIVISION

NASA

NATIONAL AERONAUTICS AND SPACE ADMINISTRATION

WHAT YOU CAN DO FOR *STAR*

All users of this abstract service are urged to forward reports to be considered for announcement in *STAR*. This will aid NASA in its efforts to provide the fullest possible coverage of all scientific and technical publications that might support aeronautics and space research and development. If you have prepared relevant reports (other than those that you will transmit to NASA, DOD, or DOE through the usual contract- or grant-reporting channels), please send them for consideration to the NASA Scientific and Technical Information Facility, P.O. Box 8757, BWI Airport, MD 21240.

Reprints of journal articles, book chapters, and conference papers are also welcome. These will be considered for announcement in *STAR's* companion journal, *International Aerospace Abstracts*.

You may specify a particular source to be included in a report announcement if you wish; otherwise the report will be placed on public sale at the National Technical Information Service. Copyrighted publications will be announced but not distributed or sold.

PURCHASE OF *STAR*

The semimonthly issues are available to registered users on annual subscription from the NASA Scientific and Technical Information Facility, ATTN: Registration Services, P.O. Box 8757, BWI Airport, MD 21240. *STAR* is publicly available on annual subscription from the Superintendent of Documents, U.S. Government Printing Office, Washington, DC 20402.

PUBLISHED BY:

UNITED STATES GOVERNMENT
NATIONAL AERONAUTICS AND SPACE ADMINISTRATION
SCIENTIFIC AND TECHNICAL INFORMATION DIVISION
Scientific and Technical Aerospace Reports, Volume 28, is prepared by the NASA Scientific and Technical Information Facility operated for the National Aeronautics and Space Administration by RMS Associates.

The Administrator of the National Aeronautics and Space Administration has determined that the publication of this periodical is necessary in the transaction of the public business required by law of this agency. Use of funds for printing this periodical has been approved by the Director of the Office of Management and Budget through March 22, 1991.

US ISSN 0036-8741

Scientific and Technical Aerospace Reports (STAR) is issued twice a month and contains abstracts and indexes of meeting papers, conference proceedings, and unlimited distribution reports that have been added to the NASA Scientific and Technical Information Database during the preceding period. These citations may also be accessed online via NASA/RECON or via AIAA's Aerospace Database (File 108) through Dialog Information Services, Inc.

STAR subject coverage includes all aerospace-related areas that will help NASA achieve its mission. Material is gathered from all over the world and includes significant input from many countries under exchange and access agreements.

Consult the indexes at the back of this volume to help zero in on what you are looking for. These include:

Subject Index
Personal Author Index
Corporate Source Index
Contract Number Index
Report/Accession Number Index

STAR's companion abstract journal *International Aerospace Abstracts* should be used if you are looking for references to periodicals, books, and published meeting papers or conference proceedings.

Questions and comments should be addressed to:

NASA Scientific and Technical Information Facility
User Services
P.O. Box 8757
BWI Airport, MD 21240
301-621-0150

VOLUME 28 NUMBER 3 / FEBRUARY 8, 1990

TABLE OF CONTENTS

AERONAUTICS

Includes aeronautics (general); aerodynamics; air transportation and safety; aircraft communications and navigation; aircraft design, testing and performance; aircraft instrumentation; aircraft propulsion and power; aircraft stability and control; and research and support facilities (air).

For related information see also *Astronautics.*

01 AERONAUTICS (GENERAL) 299

02 AERODYNAMICS 299

Includes aerodynamics of bodies, combinations, wings, rotors, and control surfaces; and internal flow in ducts and turbomachinery.

For related information see also *34 Fluid Mechanics and Heat Transfer.*

03 AIR TRANSPORTATION AND SAFETY 302

Includes passenger and cargo air transport operations; and aircraft accidents.

For related information see also *16 Space Transportation* and *85 Urban Technology and Transportation.*

04 AIRCRAFT COMMUNICATIONS AND NAVIGATION 303

Includes digital and voice communication with aircraft; air navigation systems (satellite and ground based); and air traffic control.

For related information see also *17 Space Communications, Spacecraft Communications, Command and Tracking* and *32 Communications and Radar.*

05 AIRCRAFT DESIGN, TESTING AND PERFORMANCE 305

Includes aircraft simulation technology.

For related information see also *18 Spacecraft Design, Testing and Performance* and *39 Structural Mechanics.* For land transportation vehicles see *85 Urban Technology and Transportation.*

06 AIRCRAFT INSTRUMENTATION 306

Includes cockpit and cabin display devices; and flight instruments.

For related information see also *19 Spacecraft Instrumentation* and *35 Instrumentation and Photography.*

07 AIRCRAFT PROPULSION AND POWER 306

Includes prime propulsion systems and systems components, e.g., gas turbine engines and compressors; and onboard auxiliary power plants for aircraft.

For related information see also *20 Spacecraft Propulsion and Power, 28 Propellants and Fuels,* and *44 Energy Production and Conversion.*

08 AIRCRAFT STABILITY AND CONTROL 308

Includes aircraft handling qualities; piloting; flight controls; and autopilots.

For related information see also *05 Aircraft Design, Testing and Performance.*

09 RESEARCH AND SUPPORT FACILITIES (AIR) 310

Includes airports, hangars and runways; aircraft repair and overhaul facilities; wind tunnels; shock tubes; and aircraft engine test stands.

For related information see also *14 Ground Support Systems and Facilities (Space).*

ASTRONAUTICS

Includes astronautics (general); astrodynamics; ground support systems and facilities (space); launch vehicles and space vehicles; space transportation; space communications, spacecraft communications, command and tracking; spacecraft design, testing and performance; spacecraft instrumentation; and spacecraft propulsion and power.

For related information see also *Aeronautics.*

12 ASTRONAUTICS (GENERAL) 311

For extraterrestrial exploration see *91 Lunar and Planetary Exploration.*

13 ASTRODYNAMICS N.A.

Includes powered and free-flight trajectories; and orbital and launching dynamics.

14 GROUND SUPPORT SYSTEMS AND FACILITIES (SPACE) 312

Includes launch complexes, research and production facilities; ground support equipment, e.g., mobile transporters; and simulators.

For related information see also *09 Research and Support Facilities (Air).*

15 LAUNCH VEHICLES AND SPACE VEHICLES N.A.

Includes boosters; operating problems of launch/space vehicle systems; and reusable vehicles.

For related information see also *20 Spacecraft Propulsion and Power.*

16 SPACE TRANSPORTATION 312

Includes passenger and cargo space transportation, e.g., shuttle operations; and space rescue techniques.

For related information see also *03 Air Transportation and Safety* and *18 Spacecraft Design, Testing and Performance.* For space suits see *54 Man/System Technology and Life Support.*

17 SPACE COMMUNICATIONS, SPACECRAFT COMMUNICATIONS, COMMAND AND TRACKING N.A.

Includes telemetry; space communications networks; astronavigation and guidance; and radio blackout.

For related information see also *04 Aircraft Communications and Navigation* and *32 Communications and Radar.*

18 SPACECRAFT DESIGN, TESTING AND PERFORMANCE 317

Includes satellites; space platforms; space stations; spacecraft systems and components such as thermal and environmental controls; and attitude controls.

For life support systems see *54 Man/System Technology and Life Support*. For related information see also *05 Aircraft Design, Testing and Performance, 39 Structural Mechanics,* and *16 Space Transportation.*

19 SPACECRAFT INSTRUMENTATION N.A.

For related information see also *06 Aircraft Instrumentation* and *35 Instrumentation and Photography.*

20 SPACECRAFT PROPULSION AND POWER 318

Includes main propulsion systems and components, e.g. rocket engines; and spacecraft auxiliary power sources.

For related information see also *07 Aircraft Propulsion and Power, 28 Propellants and Fuels, 44 Energy Production and Conversion,* and *15 Launch Vehicles and Space Vehicles.*

CHEMISTRY AND MATERIALS

Includes chemistry and materials (general); composite materials; inorganic and physical chemistry; metallic materials; nonmetallic materials; propellants and fuels; and materials processing.

23 CHEMISTRY AND MATERIALS (GENERAL) N.A.

24 COMPOSITE MATERIALS 318

Includes physical, chemical, and mechanical properties of laminates and other composite materials.

For ceramic materials see *27 Nonmetallic Materials.*

25 INORGANIC AND PHYSICAL CHEMISTRY 321

Includes chemical analysis, e.g., chromatography; combustion theory; electrochemistry; and photochemistry.

For related information see also *77 Thermodynamics and Statistical Physics.*

26 METALLIC MATERIALS 325

Includes physical, chemical, and mechanical properties of metals, e.g., corrosion; and metallurgy.

27 NONMETALLIC MATERIALS 330

Includes physical, chemical, and mechanical properties of plastics, elastomers, lubricants, polymers, textiles, adhesives, and ceramic materials.

For composite materials see *24 Composite Materials.*

28 PROPELLANTS AND FUELS 333

Includes rocket propellants, igniters and oxidizers; their storage and handling procedures; and aircraft fuels.

For related information see also *07 Aircraft Propulsion and Power, 20 Spacecraft Propulsion and Power,* and *44 Energy Production and Conversion.*

29 MATERIALS PROCESSING 334

Includes space-based development of products and processes for commercial application.

For biological materials see *55 Space Biology.*

ENGINEERING

Includes engineering (general); communications and radar; electronics and electrical engineering; fluid mechanics and heat transfer; instrumentation and photography; lasers and masers; mechanical engineering; quality assurance and reliability; and structural mechanics.

For related information see also *Physics.*

31 ENGINEERING (GENERAL) 334

Includes vacuum technology; control engineering; display engineering; cryogenics; and fire prevention.

32 COMMUNICATIONS AND RADAR 336

Includes radar; land and global communications; communications theory; and optical communications.

For related information see also *04 Aircraft Communications and Navigation* and *17 Space Communications, Spacecraft Communications, Command and Tracking.* For search and rescue see *03 Air Transportation and Safety,* and *16 Space Transportation.*

33 ELECTRONICS AND ELECTRICAL ENGINEERING 341

Includes test equipment and maintainability; components, e.g., tunnel diodes and transistors; microminiaturization; and integrated circuitry.

For related information see also *60 Computer Operations and Hardware* and *76 Solid-State Physics.*

34 FLUID MECHANICS AND HEAT TRANSFER 345

Includes boundary layers; hydrodynamics; fluidics; mass transfer and ablation cooling.

For related information see also *02 Aerodynamics* and *77 Thermodynamics and Statistical Physics.*

35 INSTRUMENTATION AND PHOTOGRAPHY 349

Includes remote sensors; measuring instruments and gauges; detectors; cameras and photographic supplies; and holography.

For aerial photography see *43 Earth Resources and Remote Sensing.* For related information see also *06 Aircraft Instrumentation* and *19 Spacecraft Instrumentation.*

36 LASERS AND MASERS 352

Includes parametric amplifiers.

For related information see also *76 Solid-State Physics.*

37 MECHANICAL ENGINEERING 354

Includes auxiliary systems (nonpower); machine elements and processes; and mechanical equipment.

38 QUALITY ASSURANCE AND RELIABILITY 356

Includes product sampling procedures and techniques; and quality control.

39 STRUCTURAL MECHANICS 356

Includes structural element design and weight analysis; fatigue; and thermal stress.

For applications see *05 Aircraft Design, Testing and Performance* and *18 Spacecraft Design, Testing and Performance.*

GEOSCIENCES

Includes geosciences (general); earth resources and remote sensing; energy production and conversion; environment pollution; geophysics; meteorology and climatology; and oceanography.

For related information see also *Space Sciences.*

42 GEOSCIENCES (GENERAL) 360

43 EARTH RESOURCES AND REMOTE SENSING 365

Includes remote sensing of earth resources by aircraft and spacecraft; photogrammetry; and aerial photography.

For instrumentation see *35 Instrumentation and Photography.*

44 ENERGY PRODUCTION AND CONVERSION 366

Includes specific energy conversion systems, e.g., fuel cells; global sources of energy; geophysical conversion; and windpower.

For related information see also *07 Aircraft Propulsion and Power, 20 Spacecraft Propulsion and Power,* and *28 Propellants and Fuels.*

45 ENVIRONMENT POLLUTION 367

Includes atmospheric, noise, thermal, and water pollution.

46 GEOPHYSICS 369

Includes aeronomy; upper and lower atmosphere studies; ionospheric and magnetospheric physics; and geomagnetism.

For space radiation see *93 Space Radiation.*

47 METEOROLOGY AND CLIMATOLOGY 373

Includes weather forecasting and modification.

48 OCEANOGRAPHY 376

Includes biological, dynamic, and physical oceanography; and marine resources.

For related information see also *43 Earth Resources and Remote Sensing.*

LIFE SCIENCES

Includes life sciences (general); aerospace medicine; behavioral sciences; man/system technology and life support; and space biology.

51 LIFE SCIENCES (GENERAL) 377

52 AEROSPACE MEDICINE 379

Includes physiological factors; biological effects of radiation; and effects of weightlessness on man and animals.

53 BEHAVIORAL SCIENCES 382

Includes psychological factors; individual and group behavior; crew training and evaluation; and psychiatric research.

54 MAN/SYSTEM TECHNOLOGY AND LIFE SUPPORT 383

Includes human engineering; biotechnology; and space suits and protective clothing.

For related information see also *16 Space Transportation.*

55 SPACE BIOLOGY N.A.

Includes exobiology; planetary biology; and extraterrestrial life.

MATHEMATICAL AND COMPUTER SCIENCES

Includes mathematical and computer sciences (general); computer operations and hardware; computer programming and software; computer systems; cybernetics; numerical analysis; statistics and probability; systems analysis; and theoretical mathematics.

59 MATHEMATICAL AND COMPUTER SCIENCES (GENERAL) 384

60 COMPUTER OPERATIONS AND HARDWARE 384

Includes hardware for computer graphics, firmware, and data processing.

For components see *33 Electronics and Electrical Engineering.*

61 COMPUTER PROGRAMMING AND SOFTWARE 385

Includes computer programs, routines, algorithms, and specific applications, e.g., CAD/CAM.

62 COMPUTER SYSTEMS 388

Includes computer networks and special application computer systems.

63 CYBERNETICS 390

Includes feedback and control theory, artificial intelligence, robotics and expert systems.

For related information see also *54 Man/System Technology and Life Support.*

64 NUMERICAL ANALYSIS 391

Includes iteration, difference equations, and numerical approximation.

65 STATISTICS AND PROBABILITY 396

Includes data sampling and smoothing; Monte Carlo method; and stochastic processes.

66 SYSTEMS ANALYSIS N.A.

Includes mathematical modeling; network analysis; and operations research.

67 THEORETICAL MATHEMATICS 398

Includes topology and number theory.

PHYSICS

Includes physics (general); acoustics; atomic and molecular physics; nuclear and high-energy physics; optics; plasma physics; solid-state physics; and thermodynamics and statistical physics.

For related information see also *Engineering.*

70 PHYSICS (GENERAL) 398

For precision time and time interval (PTTI) see *35 Instrumentation and Photography;* for geophysics, astrophysics or solar physics see *46 Geophysics, 90 Astrophysics,* or *92 Solar Physics.*

71 ACOUSTICS 400

Includes sound generation, transmission, and attenuation.

For noise pollution see *45 Environment Pollution.*

72 ATOMIC AND MOLECULAR PHYSICS 401

Includes atomic structure, electron properties, and molecular spectra.

73 NUCLEAR AND HIGH-ENERGY PHYSICS 403

Includes elementary and nuclear particles; and reactor theory.

For space radiation see *93 Space Radiation.*

74 OPTICS 404

Includes light phenomena and optical devices.

For lasers see *36 Lasers and Masers.*

75 PLASMA PHYSICS 406

Includes magnetohydrodynamics and plasma fusion.

For ionospheric plasmas see *46 Geophysics.* For space plasmas see *90 Astrophysics.*

76 SOLID-STATE PHYSICS 409

Includes superconductivity.

For related information see also *33 Electronics and Electrical Engineering* and *36 Lasers and Masers.*

77 THERMODYNAMICS AND STATISTICAL PHYSICS 414

Includes quantum mechanics; theoretical physics; and Bose and Fermi statistics.

For related information see also *25 Inorganic and Physical Chemistry* and *34 Fluid Mechanics and Heat Transfer.*

SOCIAL SCIENCES

Includes social sciences (general); administration and management; documentation and information science; economics and cost analysis; law, political science, and space policy; and urban technology and transportation.

80 SOCIAL SCIENCES (GENERAL) 415

Includes educational matters.

81 ADMINISTRATION AND MANAGEMENT 415

Includes management planning and research.

82 DOCUMENTATION AND INFORMATION SCIENCE 416

Includes information management; information storage and retrieval technology; technical writing; graphic arts; and micrography.

For computer documentation see *61 Computer Programming and Software.*

83 ECONOMICS AND COST ANALYSIS 419

Includes cost effectiveness studies.

84 LAW, POLITICAL SCIENCE AND SPACE POLICY 419

Includes NASA appropriation hearings; aviation law; space law and policy; international law; international cooperation; and patent policy.

85 URBAN TECHNOLOGY AND TRANSPORTATION 419

Includes applications of space technology to urban problems; technology transfer; technology assessment; and surface and mass transportation.

For related information see *03 Air Transportation and Safety, 16 Space Transportation,* and *44 Energy Production and Conversion.*

SPACE SCIENCES

Includes space sciences (general); astronomy; astrophysics; lunar and planetary exploration; solar physics; and space radiation.

For related information see also *Geosciences.*

88 SPACE SCIENCES (GENERAL) N.A.

89 ASTRONOMY 420

Includes radio, gamma-ray, and infrared astronomy; and astrometry.

90 ASTROPHYSICS 420

Includes cosmology; celestial mechanics; space plasmas; and interstellar and interplanetary gases and dust.

For related information see also *75 Plasma Physics.*

91 LUNAR AND PLANETARY EXPLORATION 422

Includes planetology; and manned and unmanned flights.

For spacecraft design or space stations see *18 Spacecraft Design, Testing and Performance.*

92 SOLAR PHYSICS 429

Includes solar activity, solar flares, solar radiation and sunspots.

For related information see *93 Space Radiation.*

93 SPACE RADIATION 435

Includes cosmic radiation; and inner and outer earth's radiation belts.

For biological effects of radiation see *52 Aerospace Medicine.* For theory see *73 Nuclear and High-Energy Physics.*

GENERAL

Includes aeronautical, astronautical, and space science related histories, biographies, and pertinent reports too broad for categorization; histories or broad overviews of NASA programs.

99 GENERAL 436

Note: N.A. means that no abstracts were assigned to this category for this issue.

SUBJECT INDEX I-1
PERSONAL AUTHOR INDEX I-53
CORPORATE SOURCE INDEX I-61
CONTRACT NUMBER INDEX I-71
REPORT/ACCESSION NUMBER INDEX I-75
APPENDIX—ABOUT STAR A-1

TYPICAL CITATION AND ABSTRACT

NASA SPONSORED

ON MICROFICHE

ACCESSION NUMBER	**N90-10004*#** Sverdrup Technology, Inc., Cleveland, OH.	**CORPORATE SOURCE**
TITLE	**A SUPERSONIC THROUGH-FLOW FAN ENGINE AIRFRAME INTEGRATION STUDY Final Report**	
AUTHOR	Paul J. Barnhart Sep. 1989 11 p Presented at the Aircraft Design, Systems and Operations Conference, Seattle, WA, 31 Jul. - 2 Aug. 1989; cosponsored by AIAA, AHS, and ASEE	**PUBLICATION DATE**
CONTRACT OR GRANT	(Contract NAS3-25266)	
REPORT NUMBERS	(NASA-CR-185140; E-5068; NAS 1.26:185140; AIAA-89-2140)	
AVAILABILITY SOURCE	Avail: NTIS HC A03/MF A01 CSCL 01A	**COSATI CODE**
PRICE CODE	A03/MF A01	

Engine airframe integration effects are investigated for superonsic through-flow fan engines installed on a Mach 3.20 supersonic cruise vehicle. Six different supersonic through-flow fan engine installations covering the effects of engine size, nacelle contour, nacelle placement, and approximate bypass plume effects are presented. The different supersonic through-flow fan installations are compared with a conventional turbine bypass engine configuration on the same basic airframe. The supersonic through-flow fan engine integrations are shown to be comparable to the turbine bypass engine configuration on the basis of installed nacelle wave drag. The supersonic through-flow fan engine airframe integrated vehicles have superior aerodynamic performance on the basis of maximum lift-to-drag ratio than the turbine bypass engine installation over the entire operating Mach number range from 1.10 to 3.20. When approximate bypass plume modeling is included, the supersonic through-flow fan engine configuration shows even larger improvements over the turbine bypass engine configuration. Author

VOLUME 28 NUMBER 3 / FEBRUARY 8, 1990

Scientific and Technical Aerospace Reports

A Semimonthly Publication of the National Aeronautics and Space Administration

01 AERONAUTICS (GENERAL)

N90-11692*# National Aeronautics and Space Administration. Ames Research Center, Moffett Field, CA.
REVIEW AND ANALYSIS OF THE DNW/MODEL 360 ROTOR ACOUSTIC DATA BASE
R. A. Zinner, D. A. Boxwell, and R. H. Spencer (Boeing Helicopter Co., Philadelphia, PA.) Nov. 1989 26 p Presented at the 15th European Rotorcraft Forum, Amsterdam, Netherlands, 12-15 Sep. 1989
(NASA-TM-102253; A-89213; NAS 1.15:102253; USAAVSCOM-TM-89-A-002) Avail: NTIS HC A03/MF A01 CSCL 01B

A comprehensive model rotor aeroacoustic data base was collected in a large anechoic wind tunnel in 1986. Twenty-six microphones were positioned around the azimuth to collect acoustic data for approximately 150 different test conditions. A dynamically scaled, blade-pressure-instrumented model of the forward rotor of the BH360 helicopter simultaneously provided blade pressures for correlation with the acoustic data. High-speed impulsive noise, blade-vortex interaction noise, low-frequency noise, and broadband noise were all captured in this extensive data base. Trends are presentes for each noise source, with important parametric variations. The purpose of this paper is to introduce this data base and illustrate its potential for predictive code validation.
Author

N90-11693* National Aeronautics and Space Administration, Washington, DC.
AERONAUTICAL ENGINEERING: A CONTINUING BIBLIOGRAPHY WITH INDEXES (SUPPLEMENT 243)
Sep. 1989 122 p
(NASA-SP-7037(243); NAS 1.21:7037(243)) Avail: NTIS HC A06; NTIS standing order as PB89-914100, $10.50 domestic, $21.00 foreign CSCL 01B

This bibliography lists 423 reports, articles, and other documents introduced into the NASA scientific and technical information system in August 1989. Subject coverage includes: design, construction and testing of aircraft and aircraft engines; aircraft components, equipment and systems; ground support systems; and theoretical and applied aspects of aerodynamics and general fluid dynamics.
Author

N90-11694* National Aeronautics and Space Administration, Washington, DC.
AERONAUTICAL ENGINEERING: A CONTINUING BIBLIOGRAPHY WITH INDEXES (SUPPLEMENT 244)
Oct. 1989 136 p
(NASA-SP-7037(244); NAS 1.21:7037(244)) Avail: NTIS HC A07; NTIS standing order as PB89-914100, $10.50 domestic, $21.00 foreign CSCL 01B

This bibliography lists 465 reports, articles, and other documents introduced into the NASA scientific and technical information system in September 1989. Subject coverage includes: design, construction and testing of aircraft and aircraft engines; aircraft components, equipment and systems; ground support systems; and theoretical and applied aspects of aerodynamics and general fluid dynamics.
Author

02 AERODYNAMICS

Includes aerodynamics of bodies, combinations, wings, rotors, and control surfaces; and internal flow in ducts and turbomachinery.

For related information see also *34 Fluid Mechanics and Heat Transfer.*

N90-11695*# Notre Dame Univ., IN.
THE STRUCTURE OF SEPARATED FLOW REGIONS OCCURRING NEAR THE LEADING EDGE OF AIRFOILS - INCLUDING TRANSITION Semiannual Status Report, period ending 30 May 1989
May 1989 33 p
(Grant NsG-1419)
(NASA-CR-185853; NAS 1.26:185853) Avail: NTIS HC A03/MF A01 CSCL 01A

Laser Doppler Velocimeter data, static pressure data, and smoke flow visualization data was obtained and analyzed to correlate with separation bubble data. The Eppler 387 airfoil was focused on at a chord Reynolds number of 100,000 and an angle of attack of 2 deg. Additional data was also obtained from the NACA 663-018 airfoil at a chord Reynolds number of 160,000 and an angle of attack of 12 deg. The structure and behavior of the transition separation bubble was documented along with the redeveloping boundary layer after reattachment over an airfoil at low Reynolds numbers. The understanding of the complex flow phenomena was examined so that analytic methods for predicting their formation and development can be improved. These analytic techniques have applications in the design and performance prediction of airfoils operating in the low Reynolds number flight regime.
Author

N90-11696# National Aerospace Lab., Tokyo (Japan). V/STOL Aircraft Research Group.
WIND TUNNEL TEST OF CAD USB-STOL SEMI-BORNE PROTOTYPE
Masahiro Okuyama, Hitoshi Takahashi, Kakutoshi Fujieda, Toshimi Fujita, and Akihito Iwasaki Mar. 1987 34 p In JAPANESE
(NAL-TM-566; ISSN-0452-2982; JTN-88-80061) Avail: NTIS HC A03/MF A01

The National Aerospace Laboratories (NAL) is researching and developing an experimental fan-jet Short Take-Off and Landing (STOL) plane. Aerodynamic research on the shape of the STOL plane was started in 1983. Research on aerodynamic elements was completed and the obtained results were fed to the existing Computer Aided Design (CAD). Based on its program, the shape of the main wing of the plane was designed. A prototype having the main wing shape obtained with CAD was fabricated during 1984 and 1985. Described here are the results of wind tunnel tests that were conducted to determine the basic aerodynamic characteristics of the prototype under the new design. Tests of each flap mode with no wind load, effects of Vortex Generator (VG) with no wind load, effects of a deflector nozzle, effects of the Upper Surface Blowing (USB) flap angle with ventilation, effects of front and rear flap angles, and VG effects with ventilation were analyzed. Data to determine the characteristics of the three longitudinal components of force during crusing, taking off and landing modes was also obtained. A comparison of the data with

the experimental data of the STOL plane ASUKA was made.
NASDA

N90-11697# National Aerospace Lab., Tokyo (Japan). Second Airframe Div.
ACOUSTIC-THERMAL ENVIRONMENT FOR USB FLAP STRUCTURE. REPORT 1: GROUND SIMULATION TEST RESULTS
Masaaki Sano, Kouichi Egawa, and Syunji Endoh Jan. 1987 16 p In JAPANESE
(NAL-TM-567; ISSN-0452-2982; JTN-88-80062) Avail: NTIS HC A03/MF A01

Upper Surface Blowing (USB) flap structure, which is one of the high-lift generating units in the low-noise Short Take-off and Landing (STOL) aircraft ASUKA, characteristically receives great thermal and acoustic loads. In terms of the design, an acoustic load test was made in the laboratory, with partial structure models to get various basic data. At the same time, it was confirmed that there was not any damage due to acoustic fatigue or harmful deformation. The design conditions of USB flap structure, however, were set under various hypothetical factors. Furthermore, the test conditions with the partial structure model were limited by a load device. For these reasons, it was necessary to obtain more accurate design data for acoustic fatigue-proof design. The USB flap acoustic and thermal environment and its structure response characteristics were measured, as part of the ground simulation test made in National Aerospace Laboratory (NAL) Kakuda Laboratory in November 1981 and September 1982 with a view to grasping the total characteristics of USB high-lift unit. In addition to the measurement results, the initial design conditions and partial structure model test results are evaluated. NASDA

N90-11698*# Institute for Computer Applications in Science and Engineering, Hampton, VA.
NEAR-PLANAR TS WAVES AND LONGITUDINAL VORTICES IN CHANNEL FLOW: NONLINEAR INTERACTION AND FOCUSING Final Report
P. Hall and F. T. Smith (University Coll., London, England) Sep. 1989 37 p Submitted for publication
(Contract NAS1-18605)
(NASA-CR-181928; NAS 1.26:181928; ICASE-89-47) Avail: NTIS HC A03/MF A01 CSCL 01A

The nonlinear interaction between planar or near-planar Tollmien-Schlichting waves and longitudinal vortices, induced or input, is considered theoretically for channel flows at high Reynolds numbers. Several kinds of nonlinear interaction, dependent on the input amplitudes and wavenumbers or on previously occurring interactions, are found and inter-related. The first, Type 1, is studied the most here and it usually produces spanwise focusing of both the wave and the vortex motion, within a finite scaled time, along with enhancement of both their amplitudes. This then points to the nonlinear interaction Type 2 where new interactive effects come into force to drive the wave and the vortex nonlinearly. Types 3, 4 correspond to still higher amplitudes, with 3 being related to 2, while 4 is connected with a larger-scale interaction 5 studied in an allied paper. Both 3, 4 are subsets of the full three-dimensional triple-deck-lie interaction, 6. The strongest nonlinear interactions are those of 4, 5, 6 since they alter the mean-flow profile substantially, i.e., by an 0(1) relative amount. All the types of nonlinear interaction however can result in the formation of focussed responses in the sense of spanwise concentrations and/or amplifications of vorticity and wave amplitude. Author

N90-11699*# National Aeronautics and Space Administration. Ames Research Center, Moffett Field, CA.
COMPUTER SIMULATION OF AIRCRAFT AERODYNAMICS
Mamoru Inouye Oct. 1989 11 p Presented at the 27th Aircraft Symposium, Fukuoka, Japan, 18-20 Oct. 1989; sponsored by Japan Society for Aeronautical and Space Sciences
(NASA-TM-102221; A-89227; NAS 1.15:102221) Avail: NTIS HC A03/MF A01 CSCL 01A

The role of Ames Research Center in conducting basic aerodynamics research through computer simulations is described. The computer facilities, including supercomputers and peripheral equipment that represent the state of the art, are described. The methodology of computational fluid dynamics is explained briefly. Fundamental studies of turbulence and transition are being pursued to understand these phenomena and to develop models that can be used in the solution of the Reynolds-averaged Navier-Stokes equations. Four applications of computer simulations for aerodynamics problems are described: subsonic flow around a fuselage at high angle of attack, subsonic flow through a turbine stator-rotor stage, transonic flow around a flexible swept wing, and transonic flow around a wing-body configuration that includes an inlet and a tail. Author

N90-11700*# National Aeronautics and Space Administration. Ames Research Center, Moffett Field, CA.
APPLICATION OF THE WIDE-FIELD SHADOWGRAPH TECHNIQUE TO ROTOR WAKE VISUALIZATION
Thomas R. Norman and Jeffrey S. Light Oct. 1989 20 p Presented at the 15th European Rotorcraft Forum, Amsterdam, Netherlands, 12-15 Sep. 1989
(NASA-TM-102222; A-89229; NAS 1.15:102222) Avail: NTIS HC A03/MF A01 CSCL 01A

The wide field shadowgraph technique is reviewed along with its application to the visualization of rotor wakes. In particular, current experimental methods and data reduction requirements are discussed. Sample shadowgraphs are presented. These include shadowgraphs of model-scale helicopter main rotors and tilt rotors, and full scale tail rotors, both in hover and in forward flight.
Author

N90-11701*# National Aeronautics and Space Administration. Ames Research Center, Moffett Field, CA.
AN EXPERIMENTAL INVESTIGATION OF HELICOPTER ROTOR HUB FAIRING DRAG CHARACTERISTICS
D. Y. Sung, M. B. Lance (Planning Research Corp., Hampton, VA.), L. A. Young, and R. H. Stroub Sep. 1989 60 p
(NASA-TM-102182; A-89096; NAS 1.15:102182) Avail: NTIS HC A04/MF A01 CSCL 01A

A study was done in the NASA 14- by 22-Foot Wind Tunnel at Langley Research Center on the parasite drag of different helicopter rotor hub fairings and pylons. Parametric studies of hub-fairing camber and diameter were conducted. The effect of hub fairing/pylon clearance on hub fairing/pylon mutual interference drag was examined in detail. Force and moment data are presented in tabular and graphical forms. The results indicate that hub fairings with a circular-arc upper surface and a flat lower surface yield maximum hub drag reduction; and clearance between the hub fairing and pylon induces high mutual-interference drag and diminishes the drag-reduction benefit obtained using a hub fairing with a flat lower surface. Test data show that symmetrical hub fairings with circular-arc surfaces generate 74 percent more interference drag than do cambered hub fairings with flat lower surfaces, at moderate negative angle of attack. Author

N90-11702*# West Virginia Univ., Morgantown. Dept. of Mechanical and Aerospace Engineering.
THREE COMPONENT LASER DOPPLER MEASUREMENTS IN AN AXISYMMETRIC JET Final Report, May 1987 - May 1989
John M. Kuhlmann and Robert W. Gross Oct. 1989 41 p
(Grant NAG1-748)
(NASA-CR-181908; NAS 1.26:181908) Avail: NTIS HC A03/MF A01 CSCL 01A

A three-component laser Doppler anemometer (LDA) was used to acquire a detailed set of three-dimensional mean and fluctuating velocity measurements in a low-speed air jet entering a stagnant ambient, over the first 20 jet exit diameters along the jet trajectory. These data are physically consistent with previous measurements in axisymmetric jets. The relative difficulty of obtaining three-dimensional and two-dimensional LDA data is briefly discussed. Author

N90-11703*# National Aeronautics and Space Administration. Langley Research Center, Hampton, VA.
THE UPWIND CONTROL VOLUME SCHEME FOR UNSTRUCTURED TRIANGULAR GRIDS
Michael Giles, W. Kyle Anderson, and Thomas W. Roberts (Vigyan Research Associates, Inc., Hampton, VA.) Sep. 1989 23 p
(NASA-TM-101664; NAS 1.15:101664) Avail: NTIS HC A03/MF A01 CSCL 01A

A new algorithm for the numerical solution of the Euler equations is presented. This algorithm is particularly suited to the use of unstructured triangular meshes, allowing geometric flexibility. Solutions are second-order accurate in the steady state. Implementation of the algorithm requires minimal grid connectivity information, resulting in modest storage requirements, and should enhance the implementation of the scheme on massively parallel computers. A novel form of upwind differencing is developed, and is shown to yield sharp resolution of shocks. Two new artificial viscosity models are introduced that enhance the performance of the new scheme. Numerical results for transonic airfoil flows are presented, which demonstrate the performance of the algorithm. Author

N90-11704*# Bolt, Beranek, and Newman, Inc., Cambridge, MA.
SOME IMPLICATIONS OF THE ISOTROPIC MOMENTARILY FROZEN ASSUMPTIONS FOR THE SPAN-MAT PROGRAM Final Report
W. D. Mark Jun. 1986 29 p
(Contract NAS1-16521)
(NASA-CR-181937; NAS 1.26:181937; BBN-TM-938) Avail: NTIS HC A03/MF A01 CSCL 01A

Potential tests using turbulence velocity histories measured in the SPAN-MAT Program are outlined to determine validity of the homogeneous, momentarily frozen assumptions for the vertical turbulence velocity component and the homogeneous, isotropic, momentarily frozen assumptions for the horizontal turbulence velocity components. In addition, methods are reviewed for prediction of the crosscorrelation function between any two spatially separated turbulence velocity components using the homogeneous, isotropic, momentarily frozen assumptions and measurements of the transverse and longitudinal turbulence velocity components. Author

N90-11705# United Technologies Research Center, East Hartford, CT.
INVESTIGATION OF ADVANCED MIXER-EJECTOR EXHAUST SYSTEM Progress Report No. 3, 15 Apr. - 15 Jul. 1989
2 Aug. 1989 6 p
(Contract N00014-88-C-0654)
(AD-A211943; UTRC/R89-957928-3) Avail: NTIS HC A02/MF A01 CSCL 21/2

A combined experimental and analytical investigation is being conducted to study advanced mixer-ejector exhaust systems. The program is designed to provide benchmark experimental data relative to several advanced mixer-ejector exhaust system configurations; in addition, analytical flowfield development and plume assessment calculations was performed. Exhaust mixing, ejector pumping, and the mixer-ejector exit plane 3-D velocity field was investigated. A slot nozzle ejector configuration was investigated under a gas dynamic research program, in order to provide a baseline with which to compare mixer-ejector results. The JETPATH code was used to calculate flowfield development downstream of the mixer-ejector for the purpose of generating aerodynamic input for plume assessment calculations. Plume assessment calculations was performed using the IPAT code. In addition, an experimental compressibility assessment of convoluted exhaust nozzle mixing effectiveness was performed. This involves low speed testing of an advanced mixer nozzle which was tested previously at a supersonic operating condition. The compressibility assessment assisted a parallel contract to develop improved prediction procedures for vortical flowfield development downstream of convoluted trailing edge configurations. GRA

N90-11706# Stanford Univ., CA. Dept. of Aeronautics and Astronautics.
UNSTEADY AERODYNAMICS WITH APPLICATIONS TO FLIGHT MECHANICS Final Report, 1 Apr. 1984 - 31 Mar. 1989
Holt Ashley Jun. 1989 20 p
(Grant AF-AFOSR-0099-84; AF Proj. 2307)
(AD-A211944; AFOSR-89-1136TR) Avail: NTIS HC A03/MF A01 CSCL 01/1

Unsteady airload measurements have been made on a series of low aspects ratio delta wings subjected to transient pitch motions. These data have been qualified and discussed in several publication which are listed. In addition a discussion on the relevance of unsteady transient airloads to flight mechanics is included. GRA

N90-11707# Stanford Univ., CA. Dept. of Mechanical Engineering.
ACTIVE CONTROL OF UNSTEADY AND SEPARATED FLOW STRUCTURES Final Technical Report, 15 Apr. 1986 - 14 Apr. 1989
John K. Eaton and Dennis J. Koga May 1989 61 p
(Grant AF-AFOSR-0159-86; AF Proj. 2307)
(AD-A212109; AFOSR-89-1210TR) Avail: NTIS HC A04/MF A01 CSCL 01/1

The objective of the research program was to formulate an active flow control method to change the vorticity and convection characteristics of a modelled dynamic stall vortex. Flow visualization, surface pressure and laser Doppler anemometer measurements were obtained. A potential flow model was developed as a state estimator and several flow control strategies were examined. GRA

N90-11708# California Inst. of Tech., Pasadena. Graduate Aeronautical Labs.
CONTROL OF TURBULENT MIXING LAYERS Final Report, 1 Jun. 1984 - 31 Dec. 1988
Paul E. Dimotakis and Manoocher M. Koochesfahani (Michigan State Univ., East Lansing.) 30 Apr. 1989 36 p
(Contract F49620-86-C-0134; AF-AFOSR-0120-84; AF Proj. 2308)
(AD-A211413; AFOSR-89-1036TR) Avail: NTIS HC A03/MF A01 CSCL 01/1

Study of the open-loop forcing of the shear layer by a pitching airfoil led to the following results: it is possible to induce very large changes in the shear layer growth rate downstream of the disturbance location, while leaving the portion of the layer between the splitter plate and the disturbance location essentially unaffected; upstream forcing can be used to modify the shear layer in the region upstream of the disturbance; two different mechanisms are responsible for coupling such disturbances to the flow in the cases of upstream and downstream forcing. An investigation into the structure of the wake of a pitching airfoil in a uniform stream revealed that the proper choice of the pitch oscillation parameters can result in significant alterations of the wake. In particular, flow regimes corresponding to wake, jet, double-wake and mixed jet-wake structures can be generated. Further study of the axial flow along the wake vortices indicated that the magnitude of the flow increases approximately linearly with both the amplitude and frequency of oscillation. The closed-loop feedback phase of the project was initiated by the demonstration of a cancellation experiment in a forced turbulent shear layer. GRA

N90-11709# ESDU International Ltd., London (England).
NORMAL-FORCE-CURVE AND PITCHING-MOMENT-CURVE SLOPES OF FOREBODY-CYLINDER COMBINATIONS AT ZERO ANGLE OF ATTACK FOR MACH NUMBERS UP TO 5
Apr. 1989 22 p Supersedes ESDU-86029 and ESDU-88026
(ESDU-89008; ESDU-86029; ESDU-88026; ISBN-0-85679-679-4; ISSN-0141-397X) Avail: ESDU

This Data Item 89008, an addition to the Aerodynamics Subseries, uses data drawn from the literature to produce semi-empirical correlations for the aerodynamic characteristics of cone and ogive forebodies, either sharp or with varying degrees of spherical blunting, on cylindrical afterbodies. The correlations provide the two slopes as the sum of three contributions: the inviscid loading distribution at angle of attack, the changes caused by the boundary layer displacement thickness, and the skin friction contribution. A fully turbulent boundary layer is assumed and the correlations are expected to apply to all axisymmetric forebody shapes whether or not there is a smooth-surface transition from the forebody to the cylinder. The correlations are presented graphically and the ranges of geometries and flow conditions studied are tabulated. Two worked examples illustrate their application in practice. ESDU

N90-11710# Centre Aeroporte de Toulouse (France).
PERFORMANCE AND QUALITY OF A WING TYPE PARACHUTE: PARAMETRIC ANALYSIS Final Report [ETUDE PARAMETRIQUE DES PERFORMANCES ET DES QUALITES DE VOL D'UN PARACHUTE DE TYPE AILE]
Patrick Chavanon Nov. 1988 159 p In FRENCH Sponsored by the Ministere de la Defense, Paris, France
(Rept-88-19; ETN-89-95024) Avail: NTIS HC A08/MF A01

The parametric study of the quality and performance of a (wing) type parachute, is reported. The aim of the analysis is the improvement of the parachute equilibrium and control in operating conditions. In the scope of the work, the aerodynamic coefficients and efforts and the simulation program are discussed. The suspending rope lengths, the parachute surface, and the parachute setting are taken into account. The landing and pulling back dynamics are investigated. ESA

N90-11711# Deutsche Forschungs- und Versuchsanstalt fuer Luft- und Raumfahrt, Goettingen (Germany, F.R.). Abteillung Instationaere Aerodynamik.
STEADY AND UNSTEADY POTENTIAL FLOW AROUND THIN ANNULAR WINGS AND ENGINES WITH SIMULATION OF JET ENGINE FLOW
Edgar Katzer Feb. 1989 84 p In GERMAN; ENGLISH summary
(DFVLR-FB-89-18; ISSN-0171-1342; ETN-89-95313) Avail: NTIS HC A05/MF A01; DFVLR, VB-PL-DO, Postfach 90 60 58, 5000 Cologne, Federal Republic of Germany, 32 deutsche marks

The unsteady incompressible flow around oscillating jet engines and ring airfoils is analyzed numerically. A thin axisymmetric surface approximates the geometry, and the jet is simulated by a vortex cylinder. A new and efficient Fourier-panel method is derived by a Fourier decomposition of the flow which allows reduction of the problem by one dimension. A higher order vorticity distribution on the body represents the flow and extremely accurate results are obtained for a few panels. The unsteady flow is calculated with a time marching procedure. The influences of frequency diameter and jet on the unsteady forces and moments is investigated for jet engines and ring airfoils displaying harmonic heave and pitch oscillations. Empirical approximations valid for small diameters are derived. It is found that there are vanishing influences of the jet on the aerodynamic forces and only minor influences on the moments for engines with small diameters. Highly nonlinear influences of the jet and oscillation frequency appear with increasing diameter. The importance of these results in designing the extreme high-bypass engines of future aircraft is stressed. ESA

N90-11712# Cranfield Inst. of Tech., Bedford (England). College of Aeronautics.
THE DETERMINATION OF THE AERODYNAMIC CHARACTERISTICS OF AN OGIVE-CYLINDER BODY IN SUBSONIC, CURVED, INCOMPRESSIBLE FLOW, AND AN ASSESSMENT OF THE EFFECT OF FLOW CURVATURE
D. I. T. P. Llewelyn-Davies Dec. 1987 117 p
(Contract RAE-2028/131-XRAW)
(Rept-87-13; ISBN-0-947767-90-8; ETN-89-95575) Avail: NTIS HC A06/MF A01; Cranfield Inst. of Technology, College of Aeronautics, Cranfield, Bedford MK43 0AL, England 7.50 Sterling pounds

Tests on a fineness ratio ogive-cylinder body made in a curved flow are described. Theoretical estimates are made of the aerodynamic characteristics of the model using the SPARV panel method, and slender-body and linear theory. The pressure distributions over the model are measured over a pitch range of -6.4 to 11.6 degrees measured relative to the nominal flow direction at the center of the model. The local loadings and overall loads are obtained by successive integration of the pressures. The experimental results show that unexpectedly high loadings are present over the whole of the afterbody and these dominate the aerodynamic characteristics giving high normal-force and a rearward centre of pressure position as compared with the results obtained from tests made in the straight flow provided by a windtunnel. ESA

N90-11713# Cranfield Inst. of Tech., Bedford (England). College of Aeronautics.
INCOMPRESSIBLE FLOW ABOUT ELLIPSOIDS OF REVOLUTION
P. A. T. Christopher Feb. 1988 21 p
(Rept-88-02; ISBN-0-947767-86-X; ETN-89-95576) Avail: NTIS HC A03/MF A01; Cranfield Inst. of Technology, College of Aeronautics, Cranfield, Bedford MK43 0AL, England 7.50 sterling pounds

A derivation of the exact equivalent source and doublet distributions, associated with the flow around a prolate ellipsoid of revolution, is presented. The derivation provides a valuable alternative approach to the classical one, does not require a knowledge of the theory of spherical harmonics, and lends itself to a ready comparison with slender-body theory. ESA

03 AIR TRANSPORTATION AND SAFETY

Includes passenger and cargo air transport operations; and aircraft accidents.

For related information see also *16 Space Transportation* and *85 Urban Technology and Transportation.*

N90-11714# Federal Aviation Administration, Atlantic City, NJ. Technical Center.
FLAMMABILITY, SMOKE, AND DRY ARC TRACKING TESTS OF AIRCRAFT ELECTRICAL WIRE INSULATIONS Final Report
Patricia L. Cahill Jul. 1989 23 p
(DOT/FAA/CT-89/21) Avail: NTIS HC A03/MF A01

Although three different laboratory-scale tests were evaluated in this wire program, only the sixty-degree test is currently required by the Federal Aviation Administration (FAA). All test specimens with the exception of MIL-W-5086/1-PVC nylon passed this test with average burn lengths within the 3-inch maximum and no flame time. The MIL-W-5086/1 samples marginally passed the 30-second flame time, and the average burn length was greater than the 3-inch maximum specified in the FAR. The smoke test method used in this program called for a straight pilot burner when testing insulated conductor specimens. However, data for a multidirectional pilot burner are also included. Large variations in D(sub s) occurred between the two burners for ETFE constructions at both the 5- and 20-minute test points. The MIL-W-81381/12 aromatic polyimide and the composite construction (Teflon/polyimide/Teflon or TPT) showed no appreciable difference in D(sub s) between the two burner types. Moreover, test duration did not affect smoke generation for these two samples. A direct correlation can be seen between dry arc tracking tests and wet arc tracking tests (DOT/FAA/CT-88/4). The halogenated polymers formed no conductive chars upon thermal decomposition and, therefore, no dry arc tracking. Author

N90-11715# Naval Postgraduate School, Monterey, CA. Dept. of Computer Science.
POST CRASH FLIGHT ANALYSIS: VISUALIZING FLIGHT RECORDER DATA M.S. Thesis
Mark Jay Christian Jun. 1989 97 p
(AD-A212063) Avail: NTIS HC A05/MF A01 CSCL 01/2

Previous research has produced a real-time, three dimensional, interactive moving platform simulator (MPS). The simulator utilizes

Defense Mapping Agency digital terrain elevation data to generate the three dimensional terrain and runs on Silicon Graphics, Inc. IRIS 4D/70GT graphics workstations. The MPS system was used as a basis for a variety of military applications. The modifications of the MPS system for use as a crash investigation tool for the U.S. Army aircraft mishaps are presented. Flight recorder data from the mishap aircraft is used to graphically reconstruct the flight of the aircraft. Flight attitudes, gauge readings, switch positions, warning and advisory light indicators, and flight control inputs are displayed. The visualization of the flight recorder data greatly aids in the analysis of the causes of an aircraft mishap.
GRA

N90-11716# Limoges Univ. (France). Inst. de Recherches en Communications Optiques et Microondes.
NUMERICAL SIMULATION OF AEROPLANE RESPONSE TO A LIGHTNING INJECTION Final Report [SIMULATION NUMERIQUE DE LA REPONSE D'UN AVION A UNE INJECTION DE LA FOUDRE]
B. Jecko and A. Roussaud 1989 146 p In FRENCH
(Contract DRET-87/1497/DS/SR2)
(ETN-89-95271) Avail: NTIS HC A07/MF A01

Aeroplane response to the electromagnetic impulsions of lightning is investigated. The process is analyzed as a diffraction of the electromagnetic waves by wirelike structures. This model is applied to the lightning channel formation. The resonance in the cylinder (representative of the airplane and the lightning injection model coupling) is demonstrated. The development of positive and negative beam leads during lightning are modeled. It is shown that the current impulsions generated in the airborne electronic equipment during lightning, must be taken into account in signal transmissions. ESA

N90-11717 Civil Aviation Authority, London (England).
UK AIRMISSES INVOLVING COMMERCIAL AIR TRANSPORT, MAY-AUGUST 1988
May 1989 87 p
(ISSN-0951-6301; ETN-89-95249) Copyright Avail: Civil Aviation Authority, Greville House, 37 Gratton Road, Cheltenham, United Kingdom, 5 sterling pounds

Statistics regarding the number of airmisses in Great Britain over the period from 1978 to 1988 are provided. Detailed accounts of airmisses that occurred between May and August 1988 are given. A summary of the working groups discussion concerning each airmiss reported during this period is provided. The procedure by which airmisses are processed is outlined. ESA

N90-11718 Civil Aviation Authority, London (England).
UK AIRMISSES INVOLVING COMMERCIAL AIR TRANSPORT
Aug. 1988 53 p
(CAA-2/88; ISSN-0951-6301; ETN-89-95533) Copyright Avail: Civil Aviation Authority, Greville House, 37 Gratton Road, Cheltenham, United Kingdom, 5 sterling pounds

The commercial airmiss reports for the period from Sep. - Dec. 1987 are listed. The procedures involved in reporting, investigating and categorizing air misses are summarized. Full transcripts of the airmiss report data for the study period are provided. These include a summary of the working group's discussions and an assessment of risk and cause for each airmiss cited. ESA

N90-11719 Civil Aviation Authority, London (England).
AIRCRAFT CABIN FIRE SUPPRESSION BY MEANS OF AN INTERIOR WATER SPRAY SYSTEM
R. T. Whitfield, Q. dAWhitfield, and J. Steel Jul. 1988 69 p
Original contains color illustrations
(CAA-Paper-88014; ETN-89-95535) Copyright Avail: Civil Aviation Authority, Greville House, 37 Gratton Road, Cheltenham, United Kingdom, 10 sterling pounds

Tests carried out using a fully furnished Trident aircraft to determine the effectiveness of an interior water spray system in preserving a survivable cabin environment in the face of an external fuel fire are described. The water spray system should delay penetration of an external fire, minimize the combustion of cabin furnishings, prevent the buildup of unsurvivable temperatures within the cabin, and delay the transfer of combustion products, including toxic gases into the occupied areas of the cabin. In three tests, during which the aircraft structure suffered increasing external damage, the water spray prevented fire damage in the cabin and delayed the migration of toxic fumes. ESA

04 AIRCRAFT COMMUNICATIONS AND NAVIGATION

Includes digital and voice communication with aircraft; air navigation systems (satellite and ground based); and air traffic control.

For related information see also *17 Space Communications, Spacecraft Communications, Command and Tracking* and *Communications and Radar.*

N90-11720# Army Engineer Topographic Labs., Fort Belvoir, VA.
SENTINEL SATELLITE POSITIONAL PRECISION DERIVED FROM THE NAVSTAR GLOBAL POSITIONING SYSTEM Technical Report, Jun. - Dec. 1988
Michael A. Crombie 16 Aug. 1989 23 p
(DA Proj. 4A7-62707-A8-55)
(AD-A211876; ETL-0544) Avail: NTIS HC A03/MF A01
CSCL 17/7

Error estimates of position are presented for a variety of symmetric circular satellite constellations when four or five observations are made on NAVSTAR GPS satellites. Results are calculated in terms of minimum PDOP and expected outages.
GRA

N90-11721# Rockwell International Science Center, Thousand Oaks, CA.
MULTICOLOR ELECTROCHROMIC DISPLAYS EXPLORATORY DEVELOPMENT Final Report, 1 Aug. 1985 - 31 Mar. 1988
M. M. Nicholson, S. Lewkowitz, and F. A. Pizzarello Jul. 1989 89 p
(Contract N00014-85-C-0415)
(AD-A212004; SC5433.FR) Avail: NTIS HC A05/MF A01
CSCL 09/5

Multicolor electrochromic cells using a rare-earth diphthalocyanine as the switchable material offer advantages over other flat-panel technologies for several types of information displays. This exploratory development effort addressed the issues of cycle life, red-color improvement, and counter-electrode performance. Major increases in the orange/green or orange/blue-green cycle life of lutetium diphthalocyanine electrodes in aqueous chloride electrolytes were achieved, respectively, by the use of Nafion binder on the dye film and by incorporation of 2-acrylamido-2-methylpropanesulfonic acid (AMPS) in the liquid electrolyte. Three failure modes were identified from changes in the switching charge and absorption spectra that occurred during long-term voltage-pulse cycling. GRA

N90-11722# Royal Signals and Radar Establishment, Malvern (England).
A SIMULATION STUDY OF LANDING TIME ALLOCATION PROCEDURES FOR USE IN COMPUTER-ASSISTED AIR TRAFFIC MANAGEMENT SYSTEMS
A. J. Budd 28 Apr. 1989 13 p
(AD-A212159; RSRE-Memo-4132; DRIC-BR-110739) Avail: NTIS HC A03/MF A01 CSCL 01/5

During busy periods at major airports, inbound aircraft have to queue for use of the landing runway. In future air traffic systems it is likely that controllers will be able to make use of computer-proposed landing sequences and speed control advice. One proposed method for allocating aircraft landing times in such systems is the Time Horizon method. According to this method, a preferred landing time is calculated for each aircraft some way out from the airport, and a planned landing time is allocated at a fixed time before the aircraft's preferred landing time. This memorandum reports on a computer simulation study to demonstrate and quantify the effect of the time horizon method. GRA

N90-11723# Anacapa Sciences, Inc., Fort Rucker, AL.
EFFECTS OF THE ADVANCED MAP INTERPRETATION AND TERRAIN ANALYSIS COURSE ON CONTOUR-LEVEL NAVIGATION PERFORMANCE Research Report, Sep. 1987 - Sep. 1988
Dudley J. Terrell Jun. 1989 30 p
(Contract MDA903-87-C-0523; DA Proj. 2Q2-63007-A-795)
(AD-A212163; ASI690-314-88; ARI-RR-1528) Avail: NTIS HC A03/MF A01 CSCL 05/6

The effectiveness of the Advanced Map Interpretation and Terrain Analysis Course (MITAC) was evaluated and two strategies of error remediation in computer-based training were compared. Forty-one OH-58 student pilots were given an inflight contour-level navigation pretest at the beginning of the Basic Combat Skills (BCS) course. Two experimental groups, with 14 subjects per group, received navigation training with the Advanced MITAC in addition to the standard BCS training. The two groups differed only in the manner in which Advanced MITAC errors were remediated. For one group, errors were followed by a computer presentation of the correct answer and a brief explanation of the navigation strategy that would have produced the correct answer (i.e., computer-remediated). For the other group, errors were followed by a requirement to work the navigation problem again (i.e., self-remediated). A control group of 13 subjects received only the standard BCS training. At the end of the BCS course, a significantly larger proportion of experimental subjects than control subjects performed perfectly on an inflight navigation posttest. Of the experimental subjects who did not perform perfectly, those in the self-remediated group tended to stray slightly farther and to spend more time off course than those in the computer-remediated group. GRA

N90-11724# Massachusetts Inst. of Tech., Cambridge. Lab. for Information and Decision Systems.
ON THE GENERATION OF A VARIABLE STRUCTURE AIRPORT SURFACE TRAFFIC CONTROL SYSTEM
Jacques J. Demael and Alexander H. Levis Aug. 1989 25 p
(Contract N00014-84-K-0519)
(AD-A211306; LIDS-P-1899) Avail: NTIS HC A02/MF A01 CSCL 17/7

A quantitative approach for modeling variable structure decision making organizations is presented. In these organizations, the interactions between the decisionmakers can change, depending on the task being processed. Using Colored Petri Nets as the appropriate mathematical formalism, an algorithm is presented for generating such variable structures. The approach is illustrated through the modeling and design of a hypothetical Airport Surface Traffic Control System. GRA

N90-11725# Maryland Univ., College Park. Center for Automation Research.
VISION-BASED NAVIGATION FOR AUTONOMOUS GROUND VEHICLES Summary Report
Larry S. Davis Aug. 1989 23 p
(Contract DACA76-84-C-0004)
(AD-A211584; ETL-0543) Avail: NTIS HC A02/MF A01 CSCL 12/9

This is a summary report for contract DACA76-84-C-0004, Vision Based Navigation for Autonomous Ground Vehicles. The research resulted in seventeen technical reports (list appended to this report, with abstracts), many of which were subsequently published in journals, conferences and workshops. Additionally, the project involved close collaboration with the Martin Marietta Corporation, Denver, Colorado, in the development and testing the vision algorithms for navigation of roads and road networks. Several experiments were run on the Martin Autonomous Land Vehicle using programs developed at the University of Maryland, and some critical components of Martin Marietta's visual navigation system were based on fundamental research conducted at the University of Maryland and under support of this contract specifically, the overall framework of a focus-of-attention vision system, in which detailed analyses are performed on selected windows of images of roads, and the shape-from-contour algorithms (e.g., the zero bank algorithm) that allowed the vehicle software to recover an accurate three-dimensional road model from monocular imagery, thus saving the autonomous land vehicle (ALV) from having to perform costly, and less reliable, analyses based on either stereo or motion. GRA

N90-11726# Federal Aviation Administration, Atlantic City, NJ. Technical Center.
SIMULATIONS FOR COMPUTER CENTERLINE APPROACH Report, Jul. 1989
Barry R. Billmann and Christopher J. Wolf Aug. 1989 18 p
(DOT/FAA/CT-TN89/41) Avail: NTIS HC A03/MF A01

Position computation for any Microwave Landing System (MLS) Area Navigation (RNAV) approach has an associated accuracy. This acuracy is affected by several error sources: MLS signal source errors, data word granularity in describing MLS ground station siting, and the MLS RNAV coordinate transformation algorithm. The International Civil Aviation Organization (ICAO) signal source errors and allowable degradation, specified in ICAO Annex 10, were used in their simulations. Since the coordinate transformation algorithms are nonlinear, it is necessary to use Monte Carlo simulation techniques to determine the magnitude of position determination accurcy in the presence of MLS signal source errors. The result of simulations undertaken by the Federal Aviation Administration (FAA) Technical Center to determine the accuracy of the RNAV at the Categories 1 and 2 minima, and at 50 feet above ground level for Category 3 in the presence of the MLS signal source errors and associated allowable error degradation are presented. Author

N90-11727# Deutsche Forschungs- und Versuchsanstalt fuer Luft- und Raumfahrt, Oberpfaffenhofen (West Germany). Abteilung HF-Verfahren.
NAVIGATION EXPERIMENT NAVEX: DATA STORAGE AND PROCESSING
Jens Hammesfahr Oct. 1988 46 p In GERMAN; ENGLISH summary Report will also be announced as translation (ESA-TT-1175)
(DFVLR-Mitt-89-09; ISSN-0176-7739; ETN-89-95300) Avail: NTIS HC A03/MF A01; DFVLR, VB-PL-DO, Postfach 90 60 58, 5000 Cologne, Fed. Republic of Germany, 19 DM

The format of the data stored during the NAVEX (navigation experiment) experiment is outlined. The names of all NAVEX data files in the DFVLR (Deutsche Forschungs und Versuchsanstalt fur Luft und Raumfahrt) central computer are listed. Apparent data outliers are described as far as they are known by the data evaluation. Complete lists of overfly dates and signals are provided. The operating parameters of the tracking stations are described. ESA

N90-11728# Deutsche Forschungs- und Versuchsanstalt fuer Luft- und Raumfahrt, Oberpfaffenhofen (West Germany). Abteilung Hochfrequenzverfahren.
NAVIGATION EXPERIMENT NAVEX: THE EQUIPMENT DELAY TIMES IN THE SPACELAB MISSION D1
Jens Hammesfahr and Anita Zimmermann Nov. 1988 44 p In GERMAN; ENGLISH summary Report will also be announced as translation (ESA-TT-1176)
(DFVLR-Mitt-89-10; ISSN-0176-7739; ETN-89-95301) Avail: NTIS HC A03/MF A01; DFVLR, VB-PL-DO, Postfach 90 60 58, 5000 Cologne, Fed. Republic of Germany, 18 DM

The self test delay times of the NAVEX (navigation experiment) stations and their correlations with temperature are shown. These delay times are related to the delay times when the timing signals are passing the equipment. Diagrams of the circuits and the self test delay times are provided for all the tests. ESA

N90-11729 Civil Aviation Authority, London (England). Air Traffic Control Evaluation Unit.
THE 1987 SURVEY OF TRACK KEEPING AND ALTITUDES ON HEATHROW AND GATWICK STANDARD INSTRUMENT DEPARTURE ROUTES (DAY)
C. K. Townend and L. J. Wells Aug. 1988 84 p
(CAA-Paper-88010; EU619; Rept-542; ETN-89-95534) Copyright Avail: Civil Aviation Authority, Greville House, 37 Gratton Road, Cheltenham, United Kingdom

A summary of the track keeping of aircraft departing from Heathrow and Gatwick, (England), airports between the hours of 0700 to 2300 local time in relation to the published standard instrument departure routes is presented. The results of that survey, showing the variation in aircraft lateral displacement and altitude at specific distances along each route, are presented. ESA

N90-11730*# Ohio Univ., Athens. Avionics Engineering Center.
DISCRETE FILTERING TECHNIQUES APPLIED TO SEQUENTIAL GPS RANGE MEASUREMENTS
Frank vanGraas Dec. 1987 43 p
(Contract NAS2-11969)
(NASA-CR-177472; NAS 1.26:177472) Avail: NTIS HC A03/MF A01 CSCL 17G

The basic navigation solution is described for position and velocity based on range and delta range (Doppler) measurements from NAVSTAR Global Positioning System satellites. The application of discrete filtering techniques is examined to reduce the white noise distortions on the sequential range measurements. A second order (position and velocity states) Kalman filter is implemented to obtain smoothed estimates of range by filtering the dynamics of the signal from each satellite separately. Test results using a simulated GPS receiver show a steady-state noise reduction, the input noise variance divided by the output noise variance, of a factor of four. Recommendations for further noise reduction based on higher order Kalman filters or additional delta range measurements are included. Author

05 AIRCRAFT DESIGN, TESTING AND PERFORMANCE

Includes aircraft simulation technology.
For related information see also *18 Spacecraft Design, Testing and Performance* and *39 Structural Mechanics.*For land transportation vehicles see *85 Urban Technology and Transportation.*

N90-11731# National Center for Atmospheric Research, Boulder, CO. Atmospheric Technology Div.
SCIENTIFIC JUSTIFICATION AND DEVELOPMENT PLAN FOR A MID-SIZED JET RESEARCH AIRCRAFT
William A. Cooper, Warren B. Johnson, James E. Ragni, Gilbert L. Summers, and M. Norman Zrubek Jun. 1989 71 p
(Grant NSF ATM-87-09659)
(PB89-208995; NCAR/TN-337-EDD) Avail: NTIS HC A04/MF A01 CSCL 01C

Extensive inputs from the atmospheric sciences community, especially those at the Second NCAR Research Aircraft Fleet Workshop in April 1987, have identified a number of critical observational needs of research studies in global climate, atmospheric chemistry, mesoscale storm structure and dynamics, cloud physics, and stratospheric-tropospheric exchange that cannot be met with NCAR's current aircraft. The 1987 Fleet Workshop, as well as a similar workshop held earlier in 1982, resulted in strong recommendations that NCAR replace its aging Sabreliner with an advanced mid-sized jet to provide these needed capabilities. These inputs are followd up, and a plan for implementation of these recommendations is offered. Author

N90-11732*# National Aeronautics and Space Administration. Hugh L. Dryden Flight Research Facility, Edwards, CA.
FLUTTER CLEARANCE OF THE F-18 HIGH-ANGLE-OF-ATTACK RESEARCH VEHICLE WITH EXPERIMENTAL WINGTIP INSTRUMENTATION PODS
Lawrence C. Freudinger Oct. 1989 21 p
(NASA-TM-4148; H-1528; NAS 1.15:4148) Avail: NTIS HC A03/MF A01 CSCL 01C

An F-18 aircraft was modified with wingtip instrumentation pods for use in NASA's high-angle-of-attack research program. Ground vibration and flight flutter testing were performed to clear an acceptable flight envelope for the aircraft. Flight test utilized atmospheric turbulence for structural excitation; the aircraft displayed no adverse aeroelastic trends within the envelope tested. The data presented in this report include mode shapes from the ground vibration and estimates of frequency and damping as a function of Mach number. Author

N90-11733*# Texas A&M Univ., College Station. Dept. of Aerospace Engineering.
DEVELOPMENT OF DIRECT-INVERSE 3-D METHODS FOR APPLIED TRANSONIC AERODYNAMIC WING DESIGN AND ANALYSIS Final Report, Oct. 1985 - Aug. 1989
Leland A. Carlson Oct. 1989 394 p
(Grant NAG1-619; TAMRF Proj. RF-5373)
(NASA-CR-186036; NAS 1.26:186036; TAMRF-5373-8903)
Avail: NTIS HC A17/MF A03 CSCL 01C

An inverse wing design method was developed around an existing transonic wing analysis code. The original analysis code, TAWFIVE, has as its core the numerical potential flow solver, FLO30, developed by Jameson and Caughey. Features of the analysis code include a finite-volume formulation; wing and fuselage fitted, curvilinear grid mesh; and a viscous boundary layer correction that also accounts for viscous wake thickness and curvature. The development of the inverse methods as an extension of previous methods existing for design in Cartesian coordinates is presented. Results are shown for inviscid wing design cases in super-critical flow regimes. The test cases selected also demonstrate the versatility of the design method in designing an entire wing or discontinuous sections of a wing. Author

N90-11734# Air Force Systems Command, Wright-Patterson AFB, OH. Foreign Technology Div.
PILOTLESS AIRPLANES
5 Jul. 1989 83 p Transl. into ENGLISH of Guo Fang Gong Ye Chu Ban She (Peoples Republic of China), May 1981 p 1-72
(AD-A211719; FTD-ID(RS)T-0392-89) Avail: NTIS HC A05/MF A01 CSCL 01/3

This book provides a concise introduction to pilotless airplanes, using every-day, easy-to-understand language and clearly drawn illustrations. The structural characteristics of pilotless airplanes are discussed, and a history of their development is provided. Special emphasis is given to the problem of how control systems guide pilotless airplanes in carrying out a variety of tasks. Examples of the uses of pilotless airplanes are given, and projections are made concerning their future prospects. Topics discussed include: Take-off and recovery; Essentials of their control systems; Automatic pilot; Navigation equipment; and Telemetry and remote control; Uses and developmental trends -- As target drones; Pilotless reconnaissance planes as electronic opposition devices, warplanes, specimen collectors and observation planes, planes for scientific studies, and geological prospecting planes. GRA

N90-11735# Aeritalia S.p.A., Turin (Italy). Gruppo Velivoli di Combattimento.
PROBLEMS RELATED TO THE ACQUISITION, PROCESSING AND UTILIZATION OF THE MODAL PARAMETERS MEASURED IN FLIGHT TESTS IN ORDER TO OBTAIN THE FULL ENVELOPE FOR FLUTTER [PROBLEMATICHE LEGATE ALL'ESTRAZIONE, ALL'ELABORAZIONE ED AL SUCCESSIVO UTILIZZO DEI PARAMETRI MODALI MISURATI IN VOLO ALLO SCOPO DI RAGGIUNGERE IL PIENO INVILUPPO DAL PUNTO DI VISITA DEL FLUTTER]

M. Guadagno, G. Guiffre, and M. Marchitti (Aeritalia S.p.A., Caselle Torinese, Italy) 1987 23 p In ITALIAN Presented at the 9th Congresso Nazionale della Associazione Italiana di Aeronautica ed Astronautica, Palermo, Italy, 26-28 Oct. 1987
(ETN-89-95210) Avail: NTIS HC A03/MF A01

Problems related to the aeroelastic flight qualification of the AMX combat aircraft are discussed. The prediction studies allowed the identification of a certain number of couplings, which were monitored during the test flights. The transducer installed measured the evolution of the design critical frequencies and of those which could generate criticality for given variations in mass or rigidity. The approach is demonstrated functionally and relatively fast to verify the matching of mathematical models and for optimizing signal analysis techniques. ESA

06 AIRCRAFT INSTRUMENTATION

Includes cockpit and cabin display devices; and flight instruments.

For related information see also *19 Spacecraft Instrumentation* and *35 Instrumentation and Photography.*

N90-11736*# National Aeronautics and Space Administration. Langley Research Center, Hampton, VA.
TRANSPORT SYSTEMS RESEARCH VEHICLE COLOR DISPLAY SYSTEM OPERATIONS MANUAL
Wesley C. Easley and Larry E. Johnson Oct. 1989 31 p
(NASA-TM-101577; NAS 1.15:101577) Avail: NTIS HC A03/MF A01 CSCL 01D

A recent upgrade of the Transport Systems Research Vehicle operated by the Advanced Transport Operating Systems Program Office at the NASA Langley Research Center has resulted in an all-glass panel in the research flight deck. Eight ARINC-D size CRT color displays make up the panel. A major goal of the display upgrade effort was ease of operation and maintenance of the hardware while maintaining versatility needed for flight research. Software is the key to this required versatility and will be the area demanding the most detailed technical design expertise. This document is is intended to serve as a single scurce of quick reference information needed for routine operation and system level maintenance. Detailed maintenance and modification of the display system will require specific design documentation and must be accomplished by individuals with specialized knowledge and experience. Author

07 AIRCRAFT PROPULSION AND POWER

Includes prime propulsion systems and systems components, e.g., gas turbine engines and compressors; and onboard auxilliary power plants for aircraft.

For related information see also *20 Spacecraft Propulsion and Power, 28 Propellants and Fuels,* and *44 Energy Production and Conversion.*

N90-11737# National Aerospace Lab., Tokyo (Japan). Aeroengine Div.
EFFECTS OF A HEAT CYCLE ON MATERIAL STRENGTH
Tameharu Ikeda Jan. 1987 14 p In JAPANESE
(NAL-TM-562; ISSN-0452-2982; JTN-88-80057) Avail: NTIS HC A03/MF A01

Pyrogenic components of thermal engines that are frequently started and stopped, such as in aircraft jet engines, are repetitively subjected to heating and cooling due to engine starts and stops. Therefore, the non-steady thermal stresses that result must be taken into consideration. These thermal stress are caused by many compounded conditions such as changes in heating and cooling speeds, heat transfer, thermal conduction, thermal expansion, specific heat and the shapes of parts and members. Heating and cooling tests of T3 treated sheets of high-tension aluminum alloy 2024S and cast iron are discussed. The cast iron test was conducted by repeated heating and cooling to study cracking and propagation of high-temperature parts and materials. The tests were conducted in a wind tunnel for thermal shock tests. NASDA

N90-11738*# Lockheed Aeronautical Systems Co., Marietta, GA.
PROPFAN TEST ASSESSMENT (PTA): FLIGHT TEST REPORT
B. H. Little, H. W. Bartel, N. N. Reddy, G. Swift, C. C. Withers, and P. C. Brown (United Technologies Corp., Windsor Locks, CT.) Apr. 1989 276 p
(Contract NAS3-24339)
(NASA-CR-182278; NAS 1.26:182278; LG89ER0026) Avail: NTIS HC A13/MF A02 CSCL 21E

The Propfan Test Assessment (PTA) aircraft was flown to obtain glade stress and noise data for a 2.74m (9 ft.) diameter single rotation propfan. Tests were performed at Mach numbers to 0.85 and altitudes to 12,192m (40,000 ft.). The propfan was well-behaved structurally over the entire flight envelope, demonstrating that the blade design technology was completely adequate. Noise data were characterized by strong signals at blade passage frequency and up to 10 harmonics. Cabin noise was not so high as to preclude attainment of comfortable levels with suitable wall treatment. Community noise was not excessive. Author

N90-11739*# Lockheed Aeronautical Systems Co., Marietta, GA.
PROPFAN TEST ASSESSMENT (PTA) Final Report
B. H. Little, D. T. Poland, H. W. Bartel, C. C. Withers, and P. C. Brown (United Technologies Corp., Windsor Locks, CT.) Jul. 1989 676 p
(Contract NAS3-24339)
(NASA-CR-185138; NAS 1.26:185138; LG89ER0064) Avail: NTIS HC A99/MF A04 CSCL 21E

The objectives of the Propfan Test Assessment (PTA) Program were to validate in flight the structural integrity of large-scale propfan blades and to measure noise characteristics of the propfan in both near and far fields. All program objectives were met or exceeded, on schedule and under budget. A Gulfstream Aerospace Corporation GII aircraft was modified to provide a testbed for the 2.74m (9 ft) diameter Hamilton Standard SR-7 propfan which was driven by a 4475 kw (600 shp) turboshaft engine mounted on the left-hand wing of the aircraft. Flight research tests were performed for 20 combinations of speed and altitude within a flight envelope that extended to Mach numbers of 0.85 and altitudes of 12,192m (40,000 ft). Propfan blade stress, near-field noise on aircraft surfaces, and cabin noise were recorded. Primary variables were propfan power and tip speed, and the nacelle tilt angle. Extensive low altitude far-field noise tests were made to measure flyover and sideline noise and the lateral attenuation of noise. In coopertion with the FAA, tests were also made of flyover noise for the aircraft at 6100m (20,000 ft) and 10,668m (35,000 ft). A final series of tests were flown to evaluate an advanced cabin wall noise treatment that was produced under a separate program by NASA-Langley Research Center. Author

N90-11740*# National Aeronautics and Space Administration. Lewis Research Center, Cleveland, OH.
STOVL PROPULSION SYSTEM VOLUME DYNAMICS APPROXIMATIONS
Colin K. Drummond 1989 11 p Presented at the 1989 Winter Annual Meeting, San Francisco, CA, 10-15 Dec. 1989, sponsored by ASME
(NASA-TM-102397; E-5147; NAS 1.15:102397) Avail: NTIS HC A03/MF A01 CSCL 21E

Two approaches to modeling turbofan engine component volume dynamics are explored and compared with a view toward application to real-time simulation of short take-off vertical landing (STOVL) aircraft propulsion systems. The first (and most popular) approach considers only heat and mass balances; the second approach includes a momentum balance and substitutes the heat equation with a complete energy balance. Results for a practical test case are presented and discussed. Author

N90-11741*# National Aeronautics and Space Administration. Hugh L. Dryden Flight Research Facility, Edwards, CA.

MEASUREMENT EFFECTS ON THE CALCULATION OF IN-FLIGHT THRUST FOR AN F404 TURBOFAN ENGINE

Timothy R. Conners Sep. 1989 24 p Presented at the AIAA Joint Propulsion Conference, Monterey, CA, 10-14 Jul. 1989 Previously announced in IAA as A89-46777

(NASA-TM-4140; H-1556; NAS 1.15:4140; AIAA-89-2364) Avail: NTIS HC A03/MF A01 CSCL 21E

A study was performed that investigates parameter measurement effects on calculated in-flight thrust for the General Electric F404-GE-400 afterburning turbofan engine which powered the X-29A forward-swept wing research aircraft. Net-thrust uncertainty and influence coefficients were calculated and are presented. Six flight conditions were analyzed at five engine power settings each. Results were obtained using the mass flow-temperature and area-pressure thrust calculation methods, both based on the commonly used gas generator technique. Thrust uncertainty was determined using a common procedure based on the use of measurement uncertainty and influence coefficients. The effects of data nonlinearity on the uncertainty calculation procedure were studied and results are presented. The advantages and disadvantages of using this particular uncertainty procedure are discussed. A brief description of the thrust-calculation technique along with the uncertainty calculation procedure is included. Author

N90-11742*# National Aeronautics and Space Administration. Ames Research Center, Moffett Field, CA.

WAVE COMBUSTORS FOR TRANS-ATMOSPHERIC VEHICLES

Gene P. Menees, Henry G. Adelman, Jean-Luc Cambier (Eloret Corp., Palo Alto, CA.), and Jeffrey V. Bowles Oct. 1989 10 p Presented at the 9th International Symposium on Airbreathing Engines, Athens, Greece, 4-8 Sep. 1989

(NASA-TM-102238; A-89251; NAS 1.15:102238) Avail: NTIS HC A02/MF A01 CSCL 21E

The Wave Combustor is an airbreathing hypersonic propulsion system which utilizes shock and detonation waves to enhance fuel-air mixing and combustion in supersonic flow. In this concept, an oblique shock wave in the combustor can act as a flameholder by increasing the pressure and temperature of the air-fuel mixture and thereby decreasing the ignition delay. If the oblique shock is sufficiently strong, then the combustion front and the shock wave can couple into a detonation wave. In this case, combustion occurs almost instantaneously in a thin zone behind the wave front. The result is a shorter, lighter engine compared to the scramjet. This engine, which is called the Oblique Detonation Wave Engine (ODWE), can then be utilized to provide a smaller, lighter vehicle or to provide a higher payload capability for a given vehicle weight. An analysis of the performance of a conceptual trans-atmospheric vehicle powered by an ODWE is given here. Author

N90-11743# Dayton Univ., OH.

COMPUTATION OF RAMJET INTERNAL FLOWFIELDS Final Report, Jan. 1986 - Dec. 1988

James N. Scott, Wilbur L. Hankey, and Thomas P. Gielda May 1989 91 p

(Contract F33615-86-C-2615)

(AD-A212001; WRDC-TR-89-2025) Avail: NTIS HC A05/MF A01 CSCL 21/1

This document reports on the computation of Ramjet Internal Flowfields. It is divided into two sections, i.e., subsonic and supersonic combustion. To numerically simulate subsonic combustion, the time-dependent Navier-Stokes equations are used with additional species equations incorporated to model hydrocarbon-air combustion. To compute supersonic combustion, the parabolized Navier-Stokes equations are utilized (PNS) with species equations to simulate hydrogen-air combustions. Model cases are computed and compared with limited experimental data. GRA

N90-11744# Princeton Univ., NJ. Dept. of Mechanical and Aerospace Engineering.

AFRAPT (AIR FORCE RESEARCH IN AERO PROPULSION TECHNOLOGY) TRAINEE PROGRAM

Irvin Glassman 13 Jun. 1989 3 p

(Grant AF-AFOSR-0292-85; AF Proj. 2308)

(AD-A211540; AFOSR-89-1182TR) Avail: NTIS HC A01/MF A01 CSCL 05/9

Four AFRAPT students were in residence in Princeton University's Department of Mechanical and Aerospace Engineering during the subject period. Two have been awarded M.S.E. degrees and accepted positions in the aircraft propulsion fields. Another will receive the M.S.E. degree in 1989 and has also accepted a position in the jet engine field. The fourth has continued his studies to pursue the Ph.D. degree. These students performed their industrial traineeships with General Electric-Cincinnati, Pratt and Whitney East Hartford and West Palm Beach, and United Technologies Research Center. GRA

N90-11745# Aeronautical Research Labs., Melbourne (Australia).

AN OPEN-LOOP TRANSIENT THERMODYNAMIC MODEL OF THE COUGUAR TURBOJET

P. C. Frith Apr. 1989 69 p

(AD-A211774; ARL-PROP-TM-457; DODA-AR-005-582) Avail: NTIS HC A04/MF A01 CSCL 21/5

An open-loop, transient, thermodynamic model of the single-spool Couguar turbojet was developed for use in both fault diagnosis and engine control research work. The model is based on TURBOTRANS, a generic engine modeling computer program, and it was calibrated against test cell measurements of the steady-state running line. The model provided good predictions of a series of accelerations and decelerations over the operating range of the turbojet. Estimates of the steady-states gains and time constants, across the speed range of the engine, are also presented. GRA

N90-11746# Rolls-Royce Ltd., Derby (England). Product Support Dept.

THE RB199: AN IN-SERVICE SUCCESS

K. Flanders 13 Apr. 1987 7 p Presented at the SBAC Symposium (Multi Purpose Combat Aircraft), Belgrade, Yugoslavia, 13-14 Apr. 1987

(PNR90544; ETN-89-95542) Copyright Avail: NTIS HC A02/MF A01

The performance of the RB199 engine is assessed. The modular design, on-condition maintenance and flexibility of the engine are described. There is no fixed time between overhauls on these engines. Repairs are carried out only to remedy a diagnosed fault. The reliability rates nonetheless compare favorably with any other military engine. The maintenance record for these engines, which have completed over 500,000 flying hours in Tornado aircraft, is fully documented. ESA

N90-11747# Rolls-Royce Ltd., Derby (England).

ADVANCED TECHNOLOGY IN MILITARY GAS TURBINE DESIGN AND MANUFACTURE

B. J. Quinn 13 Apr. 1987 9 p Presented at the SBAC Symposium (Multi Purpose Combat Aircraft), Belgrade, Yugoslavia, 13-14 Apr. 1987

(PNR90545; ETN-89-95543) Copyright Avail: NTIS HC A02/MF A01

The interaction of design and manufacturing technology in achieving high engine and component efficiency is described. The use of high precision three dimensional aerodynamic design and manufacturing methods is described. The goal of the research, to obtain a high thrust/weight ratio in combat, but a low fuel consumption while patrolling to minimize aircraft size, is outlined. This goal is achieved by using high flame temperatures, medium bypass ratios, high overall pressure ratios and good component efficiencies. ESA

N90-11748# Rolls-Royce Ltd., Derby (England). Controls and Electronics Group.
ENGINE CONTROLS FOR THE 1990'S
V. A. Fisher 13 Apr. 1987 6 p Presented at the SBAC (Multi Purpose Combat Aircraft), Belgrade, Yugoslavia, 13-14, Apr. 1987
(PNR90546; ETN-89-95544) Copyright Avail: NTIS HC A02/MF A01

The development of controls with increased emphasis on minimum hydromechanics and use of digital techniques is discussed. Changes in the way that designs are specified, and subsequent changes in maintenance attitudes are necessary, to fully exploit these more sophisticated systems. The concept of the engine control systems for the 1990s is described. Arguments of how integrity, reliability and control system performance will be obtained are presented. ESA

N90-11749# Rolls-Royce Ltd., Derby (England).
FUTURE MILITARY POWERPLANTS
W. J. Lewis 21 May 1988 20 p Presented at the I. Mech. E. Seminar for 21st Century Aero-Engine Design, 21 May 1988
(PNR90554; ETN-89-95547) Copyright Avail: NTIS HC A03/MF A01

The importance of fighter aircraft engine development as the leading edge of technological development is outlined. It is expected that fighter engines of the next century will continue to follow the trends already established. Thrust over weight ratios will increase and fuel consumption and costs will be reduced. The use of composites will become more widespread. It is likely that development of new materials, manufacturing processes, and aerodynamic and thermodynamic techniques will be the major areas of technological development. ESA

N90-11750# National Aerospace Lab., Amsterdam (Netherlands). Structures and Materials Dept.
COATINGS FOR GAS TURBINE COMPRESSORS
H. J. Kolkman 8 Jul. 1988 10 p Presented at the Materials Developments in Turbomachinery Design Conference, Cambridge, United Kingdom, 12-14 Sep. 1988 Sponsored in part by the Royal Netherlands Air Force
(NLR-MP-88045-U; ETN-89-95057) Avail: NTIS HC A02/MF A01

A number of compressor coatings with supposedly high erosion resistance are investigated. Both the erosion and corrosion resistances of these coatings are investigated under simulated service conditions in the NLR (National Aerospace Laboratory) compressor test rig. Uncoated helicopter jet engine compressors have experienced severe pitting problems in the Western European environment. Moisture absorbed by hydroscopic salts, acidified by air pollutants such as sulfur dioxide and nitrogen dioxide, caused pitting corrosion (manifested by the presence of metal ions). Magnesium chloride, a natural marine salt, supplies the chloride ions which attack the protective oxide layer of stainless steels. It is concluded that the ideal compressor coating is not yet available. ESA

08 AIRCRAFT STABILITY AND CONTROL

Includes aircraft handling qualities; piloting; flight controls; and autopilots.

For related information see also *05 Aircraft Design, Testing and Performance.*

N90-11751*# National Aeronautics and Space Administration. Langley Research Center, Hampton, VA.
LOW-SPEED WIND-TUNNEL STUDY OF REACTION CONTROL-JET EFFECTIVENESS FOR HOVER AND TRANSITION OF A STOVL FIGHTER CONCEPT
Donald R. Riley, Gautam H. Shah, and Richard E. Kuhn (Kuhn, Richard E., San Diego, CA) Washington Dec. 1989 39 p
(NASA-TM-4147; L-16616; NAS 1.15:4147) Avail: NTIS HC A03/MF A01 CSCL 01C

A brief wind-tunnel study was conducted in the Langley 12-Foot Low-Speed Tunnel to determine reaction control-jet effectiveness and some associated aerodynamic characteristics of a 15 percent scale model of the General Dynamics E-7A STOVL fighter/attack aircraft concept applicable to hover and transition flight. Tests were made with the model at various attitude angles in the tunnel test section and at various tunnel airspeeds for a range of control-jet nozzle pressure ratios. Eight reaction control-jets were tested individually. Four jets were at the design baseline locations providing roll, pitch, and yaw control. Comparisons of measured data with values calculated using empirical methods were made where possible. Author

N90-11752*# National Aeronautics and Space Administration. Ames Research Center, Moffett Field, CA.
APPLICATIONS OF FLIGHT CONTROL SYSTEM METHODS TO AN ADVANCED COMBAT ROTORCRAFT
Mark B. Tischler, Jay W. Fletcher, Patrick M. Morris (Army Aviation Research and Development Command, Moffett Field, CA.), and George T. Tucker Jul. 1989 62 p Presented at the Royal Aeronautical Society International Conference on Helicopter Handling Qualities and Control, London, England, 15-17 Nov. 1988
(NASA-TM-101054; A-89006; USAAVSCOM-CP-89-A-002; NAS 1.15:101054; AD-A211906) Avail: NTIS HC A04/MF A01 CSCL 01/3

Advanced flight control system design, analysis, and testing methodologies developed at the Ames Research Center are applied in an analytical and flight test evaluation of the Advanced Digital Optical Control System (ADOCS) demonstrator. The primary objectives are to describe the knowledge gained about the implications of digital flight control system design for rotorcraft, and to illustrate the analysis of the resulting handling-qualities in the context of the proposed new handling-qualities specification for rotorcraft. Topics covered in-depth are digital flight control design and analysis methods, flight testing techniques, ADOCS handling-qualities evaluation results, and correlation of flight test results with analytical models and the proposed handling-qualities specification. The evaluation of the ADOCS demonstrator indicates desirable response characteristics based on equivalent damping and frequency, but undersirably large effective time-delays (exceeding 240 m sec in all axes). Piloted handling-qualities are found to be desirable or adequate for all low, medium, and high pilot gain tasks; but handling-qualities are inadequate for ultra-high gain tasks such as slope and running landings. Author

N90-11753*# National Aeronautics and Space Administration. Hugh L. Dryden Flight Research Facility, Edwards, CA.
A DESIGN PROCEDURE FOR THE HANDLING QUALITIES OPTIMIZATION OF THE X-29A AIRCRAFT
John T. Bosworth and Timothy H. Cox Sep. 1989 21 p Presented at the Guidance, Navigation, and Control Conference, Boston, MA, 14-16 Aug. 1989 Previously announced in IAA as A89-52529
(NASA-TM-4142; H-1548; NAS 1.15:4142; AIAA-89-3428) Avail: NTIS HC A03/MF A01 CSCL 01C

A design technique for handling qualities improvement was developed for the X-29A aircraft. As with any new aircraft, the X-29A control law designers were presented with a relatively high degree of uncertainty in their mathematical models. The presence of uncertainties, and the high level of static instability of the X-29A caused the control law designers to stress stability and robustness over handling qualities. During flight test, the mathematical models of the vehicle were validated or corrected to match the vehicle dynamic behavior. The updated models were then used to fine tune the control system to provide fighter-like handling characteristics. A design methodology was developed which works within the existing control system architecture to provide improved handling qualities and acceptable stability with a minimum of cost in both implementation as well as software verification and validation. IAA

N90-11754# Technische Hogeschool, Delft (Netherlands). Dept. of Aerospace Engineering.

STABILITY AND CONTROL DERIVATIVES OF THE DE HAVILLAND DHC-2 BEAVER AIRCRAFT

R. T. H. Tjee and J. A. Mulder Aug. 1988 151 p
(PB89-217525; LR-556) Avail: NTIS HC A08/MF A01 CSCL 01C

The report presents a database of stability derivatives of the De Havilland DHC-2 BEAVER experimental aircraft of the Delft University of Technology at various stationary nominal flight conditions. To compute these stability derivatives a nonlinear aerodynamic model is used. The flight test data of this model is based on data derived from the DHC-2 BEAVER test flights of the 1977 and 1978 period. The stability derivatives are presented at several nominal flight conditions throughout the normally used flight envelope of the aircraft. GRA

N90-11755*# Air Force Geophysics Lab., Hanscom AFB, MA. Space Physics Div.

A BEAM INDUCED UPSET DURING THE FLIGHT OF THE ECHO-7 ROCKET

Perry R. Malcolm, William J. Burke, and George P. Murphy 13 Jan. 1989 24 p
(Grant NsG-5088; AF Proj. 7601)
(NASA-CR-186089; NAS 1.26:186089; AD-A211830; AFGL-TR-89-0021; AFGL-ERP-1018) Avail: NTIS HC A03/MF A01 CSCL 22/1

During the flight of the ECHO-7 rocket, electron beams with energies and currents up to 40 keV and 250 mA were emitted at pitch angles controlled by a deflection magnet and successfully detected upon reflection in the southern ionosphere. Three anomalies occurred onboard the beam emitting main payload, one of which is presented in detail. While emitting at 36 keV and 180 mA and with the deflection magnet turned off, the vehicle potential was measured to be greater than 5 kV. During a 30 ms pulse of gas from the attitude control system the vehicle rapidly discharged, a power converter for several diagnostic sensors failed, and a safety circuit was activated to shut the electron beam off. Two qualitative models of the consequences of ionization of the neutral cloud by beam and return current electrons are examined. An understanding of the interactions of neutral gas clouds with charged vehicles is of capital importance for the design of reliable high-power space platforms. GRA

N90-11756# Techno-Sciences, Inc., Greenbelt, MD.

ROBUST CONTROL DESIGN FOR FLIGHT CONTROL Final Report, Jul. 1988 - Mar. 1989

William H. Bennett, Harold G. Kwatny, and Keith Glover Jul. 1989 92 p
(Contract F33615-88-C-3606)
(AD-A211957; TSI-89-04-06-WB; WRDC-TR-89-3063) Avail: NTIS HC A05/MF A01 CSCL 01/4

The application of new and advanced methods of control law synthesis for robust stabilization were studied with respect to a combination of both unstructured model uncertainty (arising from neglected parasitic dynamics) and structured model uncertainty (arising from parametric variations which occur as flight conditions change). Efforts focused on the characterization of a class of nonlinear models for longitudinal dynamics of aircraft in level flight subject to changes in static stability. Such relaxed stability aircraft configurations are currently at issue in a wide variety of advanced designs including commercial transport and high performance aircraft. The control design approach employs H-infinity synthesis methods for optimal robust stabilization for the unstructured model uncertainty, and the requirement of worst case (i.e., robust) design for parametric uncertainty is included using a minimax optimization criteria. A class of flight control models with physically based parametric uncertainty were examined. For these models, the solution of the minimax or worst case design is achieved by a straightforward procedure which can be readily combined with the requirements for robustness to parasitic dynamics using the closed form solution of the optical robust stabilization method. GRA

N90-11757*# National Aeronautics and Space Administration. Langley Research Center, Hampton, VA.

COMPARISON OF FLYING QUALITIES DERIVED FROM IN-FLIGHT AND GROUND-BASED SIMULATORS FOR A JET-TRANSPORT AIRPLANE FOR THE APPROACH AND LANDING PILOT TASKS

William D. Grantham Washington Dec. 1989 32 p
(NASA-TP-2962; L-16609; NAS 1.60:2962) Avail: NTIS HC A03/MF A01 CSCL 01C

The primary objective was to provide information to the flight controls/flying qualities engineer that will assist him in determining the incremental flying qualities and/or pilot-performance differences that may be expected between results obtained via ground-based simulation (and, in particular, the six-degree-of-freedom Langley Visual/Motion Simulator (VMS)) and flight tests. Pilot opinion and performance parameters derived from a ground-based simulator and an in-flight simulator are compared for a jet-transport airplane having 32 different longitudinal dynamic response characteristics. The primary pilot tasks were the approach and landing tasks with emphasis on the landing-flare task. The results indicate that, in general, flying qualities results obtained from the ground-based simulator may be considered conservative-especially when the pilot task requires tight pilot control as during the landing flare. The one exception to this, according to the present study, was that the pilots were more tolerant of large time delays in the airplane response on the ground-based simulator. The results also indicated that the ground-based simulator (particularly the Langley VMS) is not adequate for assessing pilot/vehicle performance capabilities (i.e., the sink rate performance for the landing-flare task when the pilot has little depth/height perception from the outside scene presentation). Author

N90-11758# Dynetics, Inc., Huntsville, AL.

ADAPTIVE CONTROL LAW DESIGN FOR MODEL UNCERTAINTY COMPENSATION Final Report, Aug. 1988 - Jan. 1989

J. E. Sorrells 14 Jun. 1989 96 p
(Contract F33615-88-C-3609; AF Proj. 3005)
(AD-A211712; TR-89-WPAFB-3609-033; WRDC-TR-89-3061)
Avail: NTIS HC A05/MF A01 CSCL 01/4

Disturbance Accommodating Control (DAC) principles were applied to the design of a baseline aerospace flight control system. The resulting DAC controller designs were evaluated in terms of their ability to maintain an ideal model response when the closed loop system was subjected to significant uncertainties. These uncertainties included parameter perturbations, external disturbances, and unmodelled dynamics. The DAC designs were compared to other adaptive techniques, including Self-Tuning Regulator (STR) and Model Reference Adaptive Control (MRAC) concepts. These designs were also compared to a classical Proportional-Integral-Derivative (PID) controller. All of the adaptive controller designs were judged relative to each other and relative to the PID design, in terms of performance, design, complexity, and confidence of operation (reliability). In every case the controllers designed using Dynetics innovative approach were able to equal or surpass the STR and MRAC controllers in terms of performance robustness while preserving a linear time-invariant implementation structure. GRA

N90-11759# Aeritalia S.p.A., Turin (Italy). Gruppo Velivoli da Combattimento.

EVOLUTION OF FLIGHT COMMANDS IN AERITALIA DESIGN [EVOLUZIONE DEI COMANDI DI VOLO NELLA PROGETTAZIONE AERITALIA]

Gian Mario Avagnina and Pier Luigi Ferraris 1989 13 p In ITALIAN; ENGLISH summary
(ETN-89-95211) Avail: NTIS HC A03/MF A01

An overview of the aircrafts designed either independently or in collaboration is made with reference to handling qualities and flight control system design problems. The analysis shows that the technological evolution transformed both the aerodynamic configuration and the basic design of the control system. ESA

N90-11760# Deutsche Forschungs- und Versuchsanstalt fuer Luft- und Raumfahrt, Oberpfaffenhofen (West Germany). Abteilung Regelung.
CONTROLLER DESIGN FOR ACTIVE VIBRATION SUPPRESSION OF A HELICOPTER
Norbert Gaus and Reinhold Steinhauser Jan. 1989 141 p In GERMAN; ENGLISH summary
(DFVLR-FB-89-20; ISSN-0171-1342; ETN-89-95315) Avail: NTIS HC A07/MF A01; DFVLR, VB-PL-DO, Postfach 90 60 58, 5000 Cologne, Federal Republic of Germany, 49.50 deutsche marks

A controller is designed to suppress vibrations, which are transmitted from the helicopter rotor to its fuselage. To solve the corresponding regulator problem by output-feedback, notch-filters are introduced in the controller structure. A comprehensive linear system analysis, where invariant system zeros give major hints, leads to a suitable extension of the controller structure and an initial controller design. The final controller coefficients are determined by optimizing a vector performance index. The result is compared to linear quadratic optimal controllers and then checked for robustness taking both model extensions and sensor or actuator failing into consideration. ESA

09 RESEARCH AND SUPPORT FACILITIES (AIR)

Includes airports, hangars and runways; aircraft repair and overhaul facilities; wind tunnels; shock tubes; and aircraft engine test stands.

For related information see also *14 Ground Support Systems and Facilities (Space).*

N90-11761 Federal Aviation Administration, Atlantic City, NJ.
ANALYSIS OF HELIPORT ENVIRONMENTAL DATA: INDIANAPOLIS DOWNTOWN HELIPORT, WALL STREET HELIPORT. VOLUME 2: WALL STREET HELIPORT DATA PLOTS
Rosanne M. Weiss, John G. Morrow, Donald Gallagher, Mark DiMeo, and Scott Erlichman May 1989 1128 p
(DOT/FAA/CT-TN87/54-Vol-2) Avail: Issuing Activity

During the summer of 1987 heliport environmental data were collected at Indianapolis Downtown Heliport and at New York's Wall Street Heliport. The purpose of this data collection activity was to obtain measures of rotorwash in the heliport environment due to maneuvering helicopters, and to obtain pilot perceptions and observations concerning maneuvering and parking separation criteria. Ten wind vector transmitters were situated at various locations around the heliport in order to gather information to describe the rotorwash induced wind speed and direction changes. Pilot interviews were also conducted at these heliports. Volume 1 of this report provides a summary of the results of this activity. Volume 3 provides the plots generated from the wind sensor data collected at the Indianapolis Downtown Heliport. This volume (Volume 2) provides the plots generated from the wind sensor data collected at New York's Wall Street Heliport. The results of this study will be considered in future modifications of the Federal Aviation Administration (FAA) Heliport Design Advisory Circular, AC 150/5390-2. Author

N90-11762# Federal Aviation Administration, Atlantic City, NJ. Technical Center.
ILS MATHEMATICAL MODELING STUDY OF THE EFFECTS OF PROPOSED HANGAR CONSTRUCTION AT THE ORLANDO INTERNATIONAL AIRPORT, RUNWAY 17R, ORLANDO, FLORIDA Technical Report, Aug. 1989
James D. Rambone and John E. Walls Sep. 1989 21 p
(DOT/FAA/CT-TN89/52) Avail: NTIS HC A03/MF A01

Described here is the instrument landing system (ILS) math modeling performed by the Federal Aviation Administration (FAA) Technical Center at the request of the Southern Region. Computed localizer data are presented showing the effects of two hangar buildings (Braniff and Comair) on the performance of an ILS localizer proposed for runway 17R at the Orlando International Airport. The Southern Region is concerned that radio frequency (RF) signal reflections from the two hangars may degrade the localizer course beyond Category II/III tolerances. Modeled course structure results indicate that Category II/III localizer performance should be obtained with the Wilcox Mark II, 14-element, dual-frequency log periodic antenna with both hangar buildings constructed at the currently proposed locations. Computed clearance orbit results indicate satisfactory linearity, course crossover, and signal clearance levels. Data are also presented showing the computed performance for a glide slope proposed for runway 17R at the Orlando International Airport. The null reference glide slope will be located 1050 feet back from runway threshold and 400 feet left offset of centerline. Glide slope modeling computed only the effect of terrain in front of the antenna system and was conducted with the GTD-2D model because of limited terrain data availability. Modeled path structure and level run plots are provided for the proposed null reference system. Author

N90-11763# Analytics, Inc., Willow Grove, PA.
HUMAN OPERATOR SIMULATOR (HOS) 4 USER'S GUIDE Final Report, 1987 - 1988
Jun. 1989 267 p
(AD-A212007) Avail: NTIS HC A12/MF A02 CSCL 05/9

This is the user's guide for the Human Operator Simulator (HOS) 4. HOS 4 was developed to aid in the design and evaluation of interfaces between operators or maintainers and weapon system hardware and software. HOS 4 can be used to simulate manned systems on IBM-AT or compatible computers by producing both system and human performance estimates based, in part, on micromodels of basic human processes. A set of micromodels is included in HOS. The user's guide provides the information required to install HOS, create new simulations, create new micromodels, edit existing simulations and micromodels, and run HOS simulations. GRA

N90-11764# Army Research Inst. of Environmental Medicine, Natick, MA.
AIR VELOCITY MAPPING OF ENVIRONMENTAL TEST CHAMBERS
Stephen KW. Chang and Richard R. Gonzalez Jul. 1989 25 p
(DA Proj. 3E1-62787-A8-78)
(AD-A212082; USARIEM-M65-89) Avail: NTIS HC A03/MF A01 CSCL 14/2

The air velocity profile of the U.S. Army Research Institute of Environmental Medicine articulated manikin chamber was mapped using an anemometer tree system. It was found that the air velocity within the chamber was a disparate property. Air velocities were significantly different at different chamber fan speed settings, and at different heights in the chamber. Airflow patterns in such an environmental chamber are an inherent function of conventional chamber construction, but influenced by external factors such as equipment situated within the chamber. The practice of employing a single thermal or cup anemometer to monitor chamber air velocity is, in general, totally inadequate. GRA

N90-11765# Wichita State Univ., KS. Inst. for Aviation Research.
STALL/SPIN/FLIGHT SIMULATION Final Report
M. G. Nagati Sep. 1989 68 p
(Contract DTFA03-86-C-00041)
(DOT/FAA/CT-88/28) Avail: NTIS HC A04/MF A01

The work performed for stall-spin resistant design aids for aircraft is summarized. Two major areas were investigated. First, the solution of the non-linear equations of motion with on-line computation of the aerodynamic moments and visual display of the pilot's view and views of the aircraft. This enables evaluation of the simulator and the quality of the solution by pilots and engineers. Second, a method for predicting the aerodynamics of wings near and beyond stall was developed. It serves the purpose of selecting planforms for spin resistant aircraft. This work demonstrates the viability and promise of these approaches against spin. Author

N90-11766# Aeritalia S.p.A., Turin (Italy). Gruppo Velivoli da Combattimento.

THE AERODYNAMIC EXPERIMENTAL CENTER OF AERITALIA: COMBAT AIRCRAFT GROUP [IL CENTRO DI SPERIMENTAZIONE AERODINAMICA DELL'AERITALIA - GRUPPO VELIVOLI DA COMBATTIMENTO]

E. Barbantini and G. Bucciantini 1989 19 p In ITALIAN
(ETN-89-95213) Avail: NTIS HC A03/MF A01

The two subsonic wind tunnels developed to test transport (G222) and combat (G91y, tornado, AMX) aircraft design are described. The design principles and the integration of experimental tests with theoretical aerodynamics mathematical models are discussed. The second wind tunnel is smaller and adapted to flow visualization and preliminary test studies. ESA

N90-11767# Deutsche Forschungs- und Versuchsanstalt fuer Luft- und Raumfahrt, Cologne (Germany, F.R.).

CRYOGENIC FREE JETS

Knud Kindler (Deutsche Forschungs- und Versuchsanstalt fuer Luft- und Raumfahrt, Cologne, Germany, F.R.) Jul. 1989 73 p Transl. into ENGLISH of Tieftemperaturfreistrahlen (Cologne, Fed. Republic of Germany, DFVLR), Jun. 1988 62 p Original language document was announced as N88-27210
(ESA-TT-1128; DFVLR-FB-88-16; ETN-89-95517) Avail: NTIS HC A04/MF A01; originial German version available from DFVLR, VB-PL-DO, Postfach 90 60 58, 5000 Cologne, Fed. Republic of Germany, 25.50 Deutsche marks

The differences in the development of cryogenic jets and of uncooled free jets, in the region near the origin of the jet, are investigated. The results show no differences in the velocity distribution between the two types of jets. However, marked differences in the development of the temperature field are observed. The decrease in the entrainment mass flow is shown to be due to the density difference between the jet and its environment. It is partly compensated, in the case of the cryogenic jet, by the sink effect of the low energy level of the cryogenic jet. ESA

N90-11768# Royal Aerospace Establishment, Farnborough (England).

COMPARISON OF THE RESULTS OF TESTS ON A300 AIRCRAFT IN THE RAE 5 METRE AND ONERA F1 WIND TUNNELS

C. Quemard and P. B. Earnshaw 26 May 1988 28 p Previously announced as N89-16849
(RAE-TM-Aero-2130; BR108113; ETN-89-94334) Copyright Avail: Defence Research Information Centre, Kentigern House, 65 Brown Street, Glasgow, G2 8EX, Scotland

Studies of the A300 Airbus aircraft were carried out in two pressurized low speed wind tunnels. Initially comparison of the results obtained in the two facilities, with the same model mounted on an identical three strut support, showed discrepancies which in the case of lift coefficient amounted to 2.5 percent. Comparison of all of the procedures used in processing the measurements led to a series of modifications in data reduction techniques in the two facilities. When these modifications are all taken into account, the results on lift and drag on the A300 provided by the two tunnels show good agreement, confirming the accuracy of the measurement techniques and the broad framework of the corrections. ESA

12 ASTRONAUTICS (GENERAL)

For extraterrestrial exploration see *91 Lunar and Planetary Exploration.*

N90-11769# Air Force Systems Command, Wright-Patterson AFB, OH. Foreign Technology Div.

SPACE FLIGHT (SELECTED ARTICLES)

7 Jul. 1989 7 p Transl. into ENGLISH from Hangtian (China), no. 5, 26 Sep. 1988 p 6
(AD-A212068; FTD-ID(RS)T-0594-89) Avail: NTIS HC A02/MF A01 CSCL 05/2

This Chinese translations provides brief biographical sketches of: (1) Chinese rocket specialist LI Naiji; and (2) solid propellant specialist CUI Gouliang. GRA

N90-11770*# Arizona Univ., Tucson. Dept. of Aerospace and Mechanical Engineering.

AUTONOMOUS SPACE PROCESSOR FOR ORBITAL DEBRIS Final Report, 1988 - 1989

Kumar Ramohalli, David Campbell, Jeff P. Brockman, Bruce Carter, Leslie Donelson, Lawrence E. John, Micky C. Marine, and Dan D. Rodina 1989 81 p Presented at the Universities Space Research Association Summer Conference, Huntsville, AL, 12-16 Jun. 1989 Prepared for Universities Space Research Association, Houston, TX
(Contract NASw-4435)
(NASA-CR-186043; NAS 1.26:186043) Avail: NTIS HC A05/MF A01 CSCL 22A

This work continues to develop advanced designs toward the ultimate goal of a GETAWAY SPECIAL to demonstrate economical removal of orbital debris utilizing local resources in orbit. The fundamental technical feasibility was demonstrated last year through theoretical calculations, quantitative computer animation, a solar focal point cutter, a robotic arm design and a subscale model. During this reporting period, several improvements are made in the solar cutter, such as auto track capabilities, better quality reflectors and a more versatile framework. The major advance has been in the design, fabrication and working demonstration of a ROBOTIC ARM that has several degrees of freedom. The functions were specifically tailored for the orbital debris handling. These advances are discussed here. Also a small fraction of the resources were allocated towards research in flame augmentation in SCRAMJETS for the NASP. Here, the fundamental advance was the attainment of Mach numbers up to 0.6 in the flame zone and a vastly improved injection system; the current work is expected to achieve supersonic combustion in the laboratory and an advanced monitoring system. Author

N90-11771*# Auburn Univ., AL.

DESIGN OF A SOLAR SAIL MISSION TO MARS Final Report

Richard Eastridge, Kerry Funston, Aminat Okia, Joan Waldrop, and Christopher Zimmerman 5 May 1989 61 p
(Contract NASw-4435)
(NASA-CR-186045; NAS 1.26:186045) Avail: NTIS HC A04/MF A01 CSCL 22A

An evaluation of the design of the solar sail includes key areas such as structures, sail deployment, space environmental effects, materials, power systems, telemetry, communications, attitude control, thermal control, and trajectory analysis. Deployment and material constraints determine the basic structure of the sail, while the trajectory of the sail influences the choice of telemetry, communications, and attitude control systems. The thermal control system of the sail for the structures and electronics takes into account the effects of the space environment. Included also are a cost and weight estimate for the sail. Author

N90-11772# Technische Univ., Brunswick (Germany, F.R.). Inst. fuer Raumflug- und Reaktortechnik.

THE TIME EVALUATION OF THE NUMBER OF SPACE PROBES AND DEBRIS AT DIFFERENT ORBIT HEIGHTS WITH A VIEW TO A FUTURE COLLISION RISK IN SPACE Final Report [DIE ZEITLICHE ENTWICKLUNG DER ANZAHL VON RAUMFLUGOBJEKTEN UND TRUEMMERN IN VERSCHIEDENEN BAHNHOEHEN IM HINBLICK AUF EIN ZUKUENFTIGES KOLLISIONSISIKO IM WELTRAUM]

P. Eichler and D. Rex 1987 86 p In GERMAN
(Contract BMFT-01-OV-86-810)
(R-8718; ETN-89-94626) Avail: NTIS HC A05/MF A01

A data base for the calculation of the collision in space probability for different possible scenarios is established. An extensive literature study is performed. A simplied assumption for the determination of the collision probability is presented. The occupation density of the cataloged artificial objects is given, and that of noncataloged small artificial objects is estimated. The future evolution of the occupation density and collision probability is discussed. The orbit parameter data set of all objects with diameter larger than one cm in the earth orbit is presented. A computer program for the simulation of the time evolution of the number and the orbit parameter distribution of orbits in the earth orbit is developed. ESA

13 ASTRODYNAMICS

Includes powered and free-flight trajectories; and orbital and launching dynamics.

No abstracts in this category.

14 GROUND SUPPORT SYSTEMS AND FACILITIES (SPACE)

Includes launch complexes, research and production facilities; ground support equipment, e.g., mobile transporters; and simulators.

For related information see also *09 Research and Support Facilities (Air).*

N90-11773# Hughes Research Labs., Malibu, CA.
PLASMA-ANODE ELECTRON GUN RESEARCH Final Report, Jul. 1986 - 15 Feb. 1989
Robert W. Schumacher and Joseph Santoru 30 May 1989 61 p
(Contract F49620-86-C-0105)
(AD-A211547; AFOSR-89-1190TR) Avail: NTIS HC A04/MF A01 CSCL 09/1

The plasma-anode electron gun (PAG) is a new cold-cathode electron source which exhibits many novel features. These include instant starting, no cathode heater power, minimal vacuum requirements, a nonpoisoning cathode, long-pulse operation without gap closure, and beam modulation at ground potential with constant beam energy. The basic concept involves a collective interaction between counterpropagating streams of electrons and ions in a high-voltage diode gap. A Pierce electron-gun configuration is employed, but the thermionic cathode is replaced with a cold, secondary-electron-emitting electrode. Electron emission is stimulated by bombarding the cathode with high-energy ions. The ions are injected into the high-voltage gap through a gridded structure from a plasma source, which is embedded inside the anode electrode. The gridded structure serves as both a cathode for the plasma discharge and as an anode for the PAG. As high-voltage ions impact the cathode surface, secondary electrons are emitted, accelerated back through the diode gap, and focused through an on-axis aperture in the anode. Under this program, a modified Herrmannsfeldt computer code was constructed that calculates electron and ion trajectories and limiting particle currents in realistic geometries in the self-consistent space-charge fields of both particle species. GRA

15 LAUNCH VEHICLES AND SPACE VEHICLES

Includes boosters; operating problems of launch/space vehicle systems; and reusable vehicles.

For related information see also *20 Spacecraft Propulsion and Power.*

No abstracts in this category.

16 SPACE TRANSPORTATION

Includes passenger and cargo space transportation, e.g., shuttle operations; and space rescue techniques.

For related information see also *03 Air Transportation and Safety* and *18 Spacecraft Design, Testing and Performance.* For space suits see *54 Man/System Technology and Life Support.*

N90-11774*# McDonnell-Douglas Astronautics Co., Houston, TX.
INDEPENDENT ORBITER ASSESSMENT (IOA): ANALYSIS OF THE DISPLAYS AND CONTROLS SUBSYSTEM
W. H. Trahan and E. E. Prust 1 Dec. 1987 182 p
(Contract NAS9-17650)
(NASA-CR-185563; NAS 1.26:185563; Rept-1.0-WP-VA87001-06)
Avail: NTIS HC A09/MF A01 CSCL 22B

The results of the Independent Orbiter Assessment (IOA) of the Failure Modes and Effects Analysis (FMEA) and Critical Items List (CIL) are presented. The IOA approach features a top-down analysis of the hardware to determine failure modes, criticality, and potential critical items. To preserve independence, this analysis was accomplished without reliance upon the results contained within the NASA FMEA/CIL documentation. This report documents the independent analysis results corresponding to the Orbiter Displays and Controls (D and C) subsystem hardware. The function of the D and C hardware is to provide the crew with the monitor, command, and control capabilities required for management of all normal and contingency mission and flight operations. The D and C hardware for which failure modes analysis was performed consists of the following: Acceleration Indicator (G-METER); Head Up Display (HUD); Display Driver Unit (DDU); Alpha/Mach Indicator (AMI); Horizontal Situation Indicator (HSI); Attitude Director Indicator (ADI); Propellant Quantity Indicator (PQI); Surface Position Indicator (SPI); Altitude/Vertical Velocity Indicator (AVVI); Caution and Warning Assembly (CWA); Annunciator Control Assembly (ACA); Event Timer (ET); Mission Timer (MT); Interior Lighting; and Exterior Lighting. Each hardware item was evaluated and analyzed for possible failure modes and effects. Criticality was assigned based upon the severity of the effect for each failure mode. Author

N90-11775*# McDonnell-Douglas Astronautics Co., Houston, TX.
INDEPENDENT ORBITER ASSESSMENT (IOA): ASSESSMENT OF THE ORBITER MAIN PROPULSION SYSTEM FMEA/CIL, VOLUME 1
B. C. Slaughter 26 Feb. 1988 623 p
(Contract NAS9-17650)
(NASA-CR-185559-Vol-1; NAS 1.26:185559-Vol-1; Rept-1.0-WP-VA88003-33-Vol-1) Avail: NTIS HC A99/MF A04 CSCL 22B

The results of the Independent Orbiter Assessment (IOA) of the Failure Modes and Effects Analysis (FMEA) and Critical Items List (CIL) are presented. The IOA effort first completed an analysis of the Main Propulsion System (MPS) hardware, generating draft failure modes and potential critical items. To preserve independence, this analysis was accomplished without reliance upon the results contained within the NASA FMEA/CIL documentation. The IOA results were then compared to available data from the Rockwell Downey/NASA JSC FMEA/CIL review.

The Orbiter MPS is composed of the Propellant Management Subsystem (PMS) consisting of the liquid oxygen (LO2) and liquid hydrogen (LH2) subsystems and the helium subsystem. The PMS is a system of manifolds, distribution lines, and valves by which the liquid propellants pass from the External Tank to the Space Shuttle Main Engine (SSME). The helium subsystem consists of a series of helium supply tanks and their associated regulators, control valves, and distribution lines. Volume 1 contains the MPS description, assessment results, ground rules and assumptions, and some of the IOA worksheets. Author

N90-11776*# McDonnell-Douglas Astronautics Co., Houston, TX.
INDEPENDENT ORBITER ASSESSMENT (IOA): ASSESSMENT OF THE MAIN PROPULSION SUBSYSTEM FMEA/CIL, VOLUME 2
K. A. Holden 26 Feb. 1988 572 p
(Contract NAS9-17650)
(NASA-CR-185559-Vol-2; NAS 1.26:185559-Vol-2; Rept-1.0-WP-VA88003-33-Vol-2) Avail: NTIS HC A24/MF A03
CSCL 22B

The results of the Independent Orbiter Assessment (IOA) of the Failure Modes and Effects Analysis (FMEA) and Critical Items List (CIL) are presented. The IOA effort first completed an analysis of the Main Propulsion System (MPS) hardware, generating draft failure modes and potential critical items. To preserve independence, this analysis was accomplished without reliance upon the results contained within the NASA FMEA/CIL documentation. The IOA results were than compared to available data from the Rockwell Downey/NASA JSC FMEA/CIL review. Volume 2 continues the presentation of IOA worksheets for MPS hardware items. Author

N90-11777*# McDonnell-Douglas Astronautics Co., Houston, TX.
INDEPENDENT ORBITER ASSESSMENT (IOA): ASSESSMENT OF THE MAIN PROPULSION SUBSYSTEM FMEA/CIL, VOLUME 3
K. A. Holden 26 Feb. 1988 566 p
(Contract NAS9-17650)
(NASA-CR-18559-Vol-3; NAS 1.26:18559-Vol-3; Rept-1.0-WP-VA88003-33-Vol-3) Avail: NTIS HC A24/MF A03
CSCL 22B

The results of the Independent Orbiter Assessment (IOA) of the Failure Modes and Effects Analysis (FMEA) and Critical Items List (CIL) are presented. The IOA effort first completed an analysis of the Main Propulsion System (MPS) hardware, generating draft failure modes and potential critical items. To preserve independence, this analysis was accomplished without reliance upon the results contained within the NASA FMEA/CIL documentation. The IOA results were then compared to available data from the Rockwell Downey/NASA JSC FMEA/CIL review. Volume 3 continues the presentation of IOA worksheets and includes the potential critical items list. Author

N90-11778*# McDonnell-Douglas Astronautics Co., Houston, TX.
INDEPENDENT ORBITER ASSESSMENT (IOA): ASSESSMENT OF THE MAIN PROPULSION SUBSYSTEM FMEA/CIL, VOLUME 4
B. C. Slaughter 26 Feb. 1988 511 p
(Contract NAS9-17650)
(NASA-CR-185559-Vol-4; NAS 1.26:185559-Vol-4; Rept-1.0-WP-VA88003-33-Vol-4) Avail: NTIS HC A22/MF A03
CSCL 22B

The results of the Independent Orbiter Assessment (IOA) of the Failure Modes and Effects Analysis (FMEA) and Critical Items List (CIL) are presented. The IOA effort first completed an analysis of the Main Propulsion System (MPS) hardware, generating draft failure modes and potential critical items. To preserve independence, this analysis was accomplished without reliance upon the results contained within the NASA FMEA/CIL documentation. The IOA results were than compared to available data from the Rockwell Downey/NASA JSC FMEA/CIL review. Volume 4 contains the IOA analysis worksheets and the NASA FMEA to IOA worksheet cross reference and recommendations. Author

N90-11779*# McDonnell-Douglas Astronautics Co., Houston, TX.
INDEPENDENT ORBITER ASSESSMENT (IOA): ASSESSMENT OF THE ELECTRICAL POWER DISTRIBUTION AND CONTROL SUBSYSTEM, VOLUME 1
K. R. Schmeckpeper 26 Feb. 1988 682 p
(Contract NAS9-17650)
(NASA-CR-185557-Vol-1; NAS 1.26:185557-Vol-1; Rept-1.0-WP-VA88003-23-Vol-1) Avail: NTIS HC A99/MF A04
CSCL 22B

The results of the Independent Orbiter Assessment (IOA) of the Failure Modes and Effects Analysis (FMEA) and Critical Items List (CIL) are presented. The IOA first completed an analysis of the Electrical Power Distribution and Control (EPD and C) hardware, generating draft failure modes and potential critical items. To preserve independence, this analysis was accomplished without reliance upon the results contained within the NASA FMEA/CIL documentation. The IOA results were then compared to the NASA FMEA/CIL baseline with proposed Post 51-L updates included. A resolution of each discrepancy from the comparison is provided through additional analysis as required. This report documents the results of that comparison for the Orbiter EPD and C hardware. The IOA product for the EPD and C analysis consisted of 1671 failure mode analysis worksheets that resulted in 468 potential critical items being identified. Comparison was made to the proposed NASA Post 51-L baseline which consisted of FMEAs and 158 CIL items. Volume 1 contains the EPD and C subsystem description, analysis results, ground rules and assumptions, and some of the IOA worksheets. Author

N90-11780*# McDonnell-Douglas Astronautics Co., Houston, TX.
INDEPENDENT ORBITER ASSESSMENT (IOA): ASSESSMENT OF THE ELECTRICAL POWER DISTRIBUTION AND CONTROL SUBSYSTEM, VOLUME 2
K. R. Schmeckpeper 26 Feb. 1988 652 p
(Contract NAS9-17650)
(NASA-CR-185557-Vol-2; NAS 1.26:185557-Vol-2; Rept-1.0-WP-VA88003-23-Vol-2) Avail: NTIS HC A99/MF A04
CSCL 22B

The results of the Independent Orbiter Assessment (IOA) of the Failure Modes and Effects Analysis (FMEA) and Critical Items List (CIL) are presented. The IOA first completed an analysis of the Electrical Power Distribution and Control (EPD and C) hardware, generating draft failure modes and potential critical items. To preserve independence, this analysis was accomplished without reliance upon the results contained within the NASA FMEA/CIL documentation. The IOA results were then compared to the NASA FMEA/CIL baseline with proposed Post 51-L updates included. A resolution of each discrepancy from the comparison is provided through additional analysis as required. This report documents the results of that comparison for the Orbiter EPD and C hardware. Volume 2 continues the presentation of IOA worksheets. Author

N90-11781*# McDonnell-Douglas Astronautics Co., Houston, TX.
INDEPENDENT ORBITER ASSESSMENT (IOA): ASSESSMENT OF THE ELECTRICAL POWER DISTRIBUTION AND CONTROL SUBSYSTEM, VOLUME 3
K. R. Schmeckpeper 26 Feb. 1988 651 p
(Contract NAS9-17650)
(NASA-CR-185557-Vol-3; NAS 1.26:185557-Vol-3; Rept-1.0-WP-VA88003-23-Vol-3) Avail: NTIS HC A99/MF A04
CSCL 22B

The results of the Independent Orbiter Assessment (IOA) of the Failure Modes and Effects Analysis (FMEA) and Critical Items List (CIL) are presented. The IOA first completed an analysis of the Electrical Power Distribution and Control (EPD and C) hardware, generating draft failure modes and potential critical items. To preserve independence, this analysis was accomplished without reliance upon the results contained within the NASA FMEA/CIL documentation. The IOA results were then compared to the NASA FMEA/CIL baseline with proposed Post 51-L updates included. A resolution of each discrepancy from the comparison is provided through additional analysis as required. This report documents the results of that comparison for the Orbiter EPD and C hardware. Volume 3 continues the presentation of IOA worksheets and contains the potential critical items list and the NASA FMEA to IOA worksheet cross reference and recommendations. Author

N90-11782*# McDonnell-Douglas Astronautics Co., Houston, TX.
INDEPENDENT ORBITER ASSESSMENT (IOA): ANALYSIS OF THE ACTIVE THERMAL CONTROL SUBSYSTEM
S. K. Sinclair and W. E. Parkman 1 Dec. 1987 375 p
(Contract NAS9-17650)
(NASA-CR-185553; NAS 1.26:185553; Rept-1.0-WP-VA87001-05)
Avail: NTIS HC A16/MF A02 CSCL 22B

The results of the Independent Orbiter Assessment (IOA) of the Failure Modes and Effects Analysis (FMEA) and Critical Items List (CIL) are presented. The IOA approach features a top-down analysis of the hardware to determine failure modes, criticality, and potential critical (PCIs) items. To preserve independence, this analysis was accomplished without reliance upon the results contained within the NASA FMEA/CIL documentation. The independent analysis results corresponding to the Orbiter Active Thermal Control Subsystem (ATCS) are documented. The major purpose of the ATCS is to remove the heat, generated during normal Shuttle operations from the Orbiter systems and subsystems. The four major components of the ATCS contributing to the heat removal are: Freon Coolant Loops; Radiator and Flow Control Assembly; Flash Evaporator System; and Ammonia Boiler System. In order to perform the analysis, the IOA process utilized available ATCS hardware drawings and schematics for defining hardware assemblies, components, and hardware items. Each level of hardware was evaluated and analyzed for possible failure modes and effects. Criticality was assigned based upon the severity of the effect for each failure mode. Of the 310 failure modes analyzed, 101 were determined to be PCIs. Author

N90-11783*# McDonnell-Douglas Astronautics Co., Houston, TX.
INDEPENDENT ORBITER ASSESSMENT (IOA): FMEA/CIL ASSESSMENT Interim Report
Mo J. Saiidi, L. J. Swain, and J. M. Compton 9 Mar. 1988 100 p
(Contract NAS9-17650)
(NASA-CR-185550; NAS 1.26:185550; Rept-1.0-WP-VA88003-40)
Avail: NTIS HC A05/MF A01 CSCL 22B

The results of the Independent Orbiter Assessment (IOA) of the Failure Modes and Effects Analysis (FMEA) and Critical Items List (CIL) are presented. Direction was given by the Orbiter and GFE Projects Office to perform the hardware analysis and assessment using the instructions and ground rules defined in NSTS 22206. The IOA analysis features a top-down approach to determine hardware failure modes, criticality, and potential critical items. To preserve independence, the anlaysis was accomplished without reliance upon the results contained within the NASA and prime contractor FMEA/CIL documentation. The assessment process compares the independently derived failure modes and criticality assignments to the proposed NASA Post 51-L FMEA/CIL documentation. When possible, assessment issues are discussed and resolved with the NASA subsystem managers. The assessment results for each subsystem are summarized. The most important Orbiter assessment finding was the previously unknown stuck autopilot push-button criticality 1/1 failure mode, having a worst case effect of loss of crew/vehicle when a microwave landing system is not active. Author

N90-11784*# McDonnell-Douglas Astronautics Co., Houston, TX.
INDEPENDENT ORBITER ASSESSMENT (IOA): ASSESSMENT OF THE GUIDANCE, NAVIGATION, AND CONTROL SUBSYSTEM FMEA/CIL
W. H. Trahan, R. A. ODonnell, K. C. Pietz, and L. J. Drapela 23 Jan. 1988 273 p
(Contract NAS9-17650)
(NASA-CR-185552; NAS 1.26:185552; Rept-1.0-WP-VA88003-06)
Avail: NTIS HC A12/MF A02 CSCL 22B

The results of the Independent Orbiter Assessment (IOA) of the Failure Modes and Effects Analysis (FMEA) and Critical Items List (CIL) are presented. The IOA effort first completed an analysis of the Guidance, Navigation, and Control System (GNC) hardware, generating draft failure modes and potential critical items. To preserve independence, this analysis was accomplished without reliance upon the results contained within the NASA FMEA/CIL documentation. The IOA results were then compared to the NASA FMEA/CIL baseline with proposed Post 51-L updates included. A resolution of each discrepancy from the comparison is provided through additional analysis as required. The results of that comparison for the Orbiter GNC hardware is documented. The IOA product for the GNC analysis consisted of 141 failure mode worksheets that resulted in 24 potential critical items being identified. Comparison was made to the NASA baseline which consisted of 148 FMEAs and 36 CIL items. This comparison produced agreement on all but 56 FMEAs which caused differences in zero CIL items. Author

N90-11785*# McDonnell-Douglas Astronautics Co., Houston, TX.
INDEPENDENT ORBITER ASSESSMENT (IOA): ASSESSMENT OF THE ELECTRICAL POWER DISTRIBUTION AND CONTROL/ELECTRICAL POWER GENERATION (EPD AND C/EPG) FMEA/CIL
C. N. McCants and M. Bearrow 26 Feb. 1988 444 p
(Contract NAS9-17650)
(NASA-CR-185542; NAS 1.26:185542; Rept-1.0-WP-VA88003-33)
Avail: NTIS HC A19/MF A03 CSCL 22B

The results of the Independent Orbiter Assessment (IOA) of the Failure Modes and Effects Analysis (FMEA) and Critical Items List (CIL) are presented. The IOA effort first completed an analysis of the Electrical Power Distribution and Control/Electrical Power Generation (EPD and C/EPG) hardware, generating draft failure modes and potential critical items. To preserve independence, this analysis was accomplished without reliance upon the results contained within the NASA FMEA/CIL documentation. The IOA results were then compared to the NASA FMEA/CIL baseline with proposed Post 51-L updates included. A resolution of each discrepancy from the comparison was provided through additional analysis as required. The results of that comparison is documented for the Orbiter EPD and C/EPG hardware. The IOA product for the EPD and C/EPG analysis consisted of 263 failure mode worksheets that resulted in 42 potential critical items being identified. Comparison was made to the NASA baseline which consisted of 211 FMEA and 47 CIL items. Author

N90-11786*# McDonnell-Douglas Astronautics Co., Houston, TX. Engineering Services.
INDEPENDENT ORBITER ASSESSMENT (IOA): ANALYSIS OF THE LIFE SUPPORT AND AIRLOCK SUPPORT SUBSYSTEMS
Jim Arbet, R. Duffy, K. Barickman, and Mo J. Saiidi 2 Nov. 1987 594 p
(Contract NAS9-17650)
(NASA-CR-185539; NAS 1.26:185539; Rept-1.0-WP-VA87001-02)
Avail: NTIS HC A25/MF A04 CSCL 22B

The results of the Independent Orbiter Assessment (IOA) of the Failure Modes and Effects Analysis (FMEA) and Critical Items List (CIL) are presented. The IOA approach features a top-down analysis of the hardware to determine failure modes, criticality, and potential critical items. To preserve independence, this analysis was accomplished without reliance upon the results contained within the NASA FMEA/CIL documentation. This report documents the independent analysis results corresponding to the Orbiter Life Support System (LSS) and Airlock Support System (ALSS). Each level of hardware was evaluated and analyzed for possible failure modes and effects. Criticality was assigned based upon the severity of the effect for each failure mode. The LSS provides for the management of the supply water, collection of metabolic waste, management of waste water, smoke detection, and fire suppression. The ALSS provides water, oxygen, and electricity to support an extravehicular activity in the airlock. Author

N90-11787*# McDonnell-Douglas Astronautics Co., Houston, TX.
INDEPENDENT ORBITER ASSESSMENT (IOA): ASSESSMENT OF THE ORBITAL MANEUVERING SYSTEM FMEA/CIL, VOLUME 1
Chet D. Prust, W. A. Haufler, and A. J. Marino 26 Feb. 1988 618 p
(Contract NAS9-17650)
(NASA-CR-185544-Vol-1; NAS 1.26:185544-Vol-1; Rept-1.0-WP-VA88003-30-Vol-1) Avail: NTIS HC A99/MF A04
CSCL 22B

The results of the Independent Orbiter Assessment (IOA) of the Failure Modes and Effects Analysis (FMEA) and Critical Items List (CIL) are presented. The IOA effort first completed an analysis of the Orbital Maneuvering System (OMS) hardware and Electrical Power Distribution and Control (EPD and C), generating draft failure modes and potential critical items. To preserve independence, this analysis was accomplished without reliance upon the results contained within the NASA FMEA/CIL documentation. The IOA results were then compared to the proposed Post 51-L NASA FMEA/CIL baseline. This report documents the results of that comparison for the Orbiter OMS hardware. The IOA analysis defined the OMS as being comprised of the following subsystems: helium pressurization, propellant storage and distribution, Orbital Maneuvering Engine, and EPD and C. The IOA product for the OMS analysis consisted of 284 hardware and 667 EPD and C failure mode worksheets that resulted in 160 hardware and 216 EPD and C potential critical items (PCIs) being identified. A comparison was made of the IOA product to the NASA FMEA/CIL baseline which consisted of 101 hardware and 142 EPD and C CIL items. Author

N90-11788*# McDonnell-Douglas Astronautics Co., Houston, TX.
INDEPENDENT ORBITER ASSESSMENT (IOA): ASSESSMENT OF THE ORBITAL MANEUVERING SUBSYSTEM, VOLUME 2
W. A. Haufler 26 Feb. 1988 601 p
(Contract NAS9-17650)
(NASA-CR-185544-Vol-2; NAS 1.26:185544-Vol-2; Rept-1.0-WP-VA88003-30-Vol-2) Avail: NTIS HC A99/MF A04
CSCL 22B

The results of the Independent Orbiter Assessment (IOA) of the Failure Modes and Effects Analysis (FMEA) and Critical Items List (CIL) are presented. The IOA effort first completed an analysis of the Orbital Maneuvering System (OMS) hardware and electrical power distribution and control (EPD and C), generating draft failure modes and potential critical items. To preserve independence, this analysis was accomplished without reliance upon the results contained within the NASA FMEA/CIL documentation. The IOA results were then compared to the proposed Post 51-L NASA FMEA/CIL baseline. This report documents the results of that comparison for the Orbiter OMS hardware and EPD and C systems. Volume 2 continues the presentation of IOA worksheets and contains the critical items list and the NASA FMEA to IOA worksheet cross reference and recommendations. Author

N90-11789*# McDonnell-Douglas Astronautics Co., Houston, TX.
INDEPENDENT ORBITER ASSESSMENT (IOA): ASSESSMENT OF THE COMMUNICATION AND TRACKING SUBSYSTEM, VOLUME 1
W. C. Long 18 Mar. 1988 652 p
(Contract NAS9-17650)
(NASA-CR-185528-Vol-1; NAS 1.26:185528-Vol-1; Rept-1.0-WP-VA88005-10-Vol-1) Avail: NTIS HC A99/MF A04
CSCL 22B

The results of the Independent Orbiter Assessment (IOA) of the Failure Modes and Effects Analysis (FMEA) and Critical Items List (CIL) are presented. The IOA effort first completed and analysis of the Communication and Tracking hardware, generating draft failure modes and potential critical items. To preserve independence, this analysis was accomplished without reliance upon the results contained within the NASA FMEA/CIL documentation. The IOA results were then compared to the NASA FMEA/CIL baseline. A resolution of each discrepancy from the comparison is provided through additional analysis as required. This report documents the results of that comparison for the Orbiter Communication and Tracking hardware. The IOA product for the Communication and Tracking consisted of 1,108 failure mode worksheets that resulted in 298 critical items being identified. Comparison was made to the NASA baseline which consists of 697 FMEAs and 239 CIL items. The comparison determined if there were any results which had been found by IOA but were not in the NASA baseline. This comparison produced agreement on all but 407 FMEAs which caused differences in 294 CIL items. Volume 1 contains the subsystem description, assessment results, ground rules and assumptions, and some of the IOA worksheets. Author

N90-11790*# McDonnell-Douglas Astronautics Co., Houston, TX.
INDEPENDENT ORBITER ASSESSMENT (IOA): ASSESSMENT OF THE COMMUNICATION AND TRACKING SUBSYSTEM, VOLUME 2
W. C. Long 18 Mar. 1988 602 p
(Contract NAS9-17650)
(NASA-CR-185528-Vol-2; NAS 1.26:185528-Vol-2; Rept-1.0-WP-VA88005-10-Vol-2) Avail: NTIS HC A99/MF A04
CSCL 22B

The results of the Independent Orbiter Assessment (IOA) of the Failure Modes and Effects Analysis (FMEA) and Critical Items List (CIL) are presented. The IOA effort first completed and analysis of the Communication and Tracking hardware, generating draft failure modes and potential critical items. The IOA results were then compared to the NASA FMEA/CIL baseline. A resolution of each discrepancy from the comparison is provided through additional analysis as required. This report documents the results of that comparison for the Orbiter Communication and Tracking hardware. Volume 2 continues the presentation of IOA worksheets. Author

N90-11791*# McDonnell-Douglas Astronautics Co., Houston, TX.
INDEPENDENT ORBITER ASSESSMENT (IOA): ASSESSMENT OF THE COMMUNICATION AND TRACKING SUBSYSTEM, VOLUME 3
W. C. Long 18 Mar. 1988 545 p
(Contract NAS9-17650)
(NASA-CR-185528-Vol-3; NAS 1.26:185528-Vol-3; Rept-1.0-WP-VA88005-10-Vol-3) Avail: NTIS HC A23/MF A03
CSCL 22B

The results of the Independent Orbiter Assessment (IOA) of the Failure Modes and Effects Analysis (FMEA) and Critical Items List (CIL) are presented. The IOA effort first completed and analysis of the Communication and Tracking hardware, generating draft failure modes and potential critical items. The IOA results were then compared to the NASA FMEA/CIL baseline. A resolution of each discrepancy from the comparison is provided through additional analysis as required. This report documents the results of that comparison for the Orbiter Communication and Tracking hardware. Volume 3 continues the presentation of IOA worksheets and contains the potential critical items list, detailed analysis, and the NASA FMEA to IOA worksheet cross reference and recommendations. Author

N90-11792*# McDonnell-Douglas Astronautics Co., Houston, TX.

INDEPENDENT ORBITER ASSESSMENT (IOA): ASSESSMENT OF THE HYDRAULICS/WATER SPRAY BOILER SUBSYSTEM

M. C. Bynum, J. D. Duval, W. E. Parkman, and W. R. Davidson
2 Mar. 1988 619 p
(Contract NAS9-17650)
(NASA-CR-185537; NAS 1.26:185537) Avail: NTIS HC A99/MF A04 CSCL 22B

The results of the Independent Orbiter Assessment (IOA) of the Failure Modes and Effects Analysis (FMEA) and Critical Items List (CIL) are presented. The IOA effort first completed an analysis of the Hydraulics/Water Spray Boiler (HYD/WSB) hardware, generating draft failure modes and potential critical items. To preserve independence, this analysis was accomplished without reliance upon the results contained within the NASA FMEA/CIL documentation. The IOA results were then compared to the NASA FMEA/CIL baseline with proposed Post 51-L updates included. A resolution of each discrepancy from the comparison is provided through additional analysis as required. This report documents the results of that comparison for the Orbiter HYD/WSB hardware. The IOA product for the HYD/WSB analysis consisted of 447 failure mode worksheets that resulted in 183 potential critical items being identified. Comparison was made to the NASA baseline which consisted of 364 FMEAs and 111 CIL items. This comparison produced agreement on all but 68 FMEAs which caused differences in 23 CIL items. Author

N90-11793*# McDonnell-Douglas Astronautics Co., Houston, TX.

INDEPENDENT ORBITER ASSESSMENT (IOA): ASSESSMENT OF THE REACTION CONTROL SYSTEM, VOLUME 1

Chet D. Prust and Dan W. Hartman 26 Feb. 1988 882 p
(Contract NAS9-17650)
(NASA-CR-185543-Vol-1; NAS 1.26:185543-Vol-1; Rept-1.0-WP-VA88003-12-Vol-1) Avail: NTIS HC A99/MF E06 CSCL 22B

The results of the Independent Orbiter Assessment (IOA) of the Failure Modes and Effects Analysis (FMEA) and Critical Items List (CIL) are presented. The IOA effort first completed an analysis of the aft and forward Reaction Control System (RCS) hardware, and Electrical Power Distribution and Control (EPD and C), generating draft failure modes and potential critical items. To preserve independence, this analysis was accomplished without reliance upon the results contained within the NASA FMEA/CIL documentation. The IOA results were then compared to the proposed Post 51-L NASA FMEA/CIL baseline. This report documents the results of that comparison for the Orbiter RCS hardware and EPD and C systems. The IOA product for the RCS analysis consisted of 208 hardware and 2064 EPD and C failure mode worksheets that resulted in 141 hardware and 449 EPD and C potential critical items (PCIs) being identified. A comparison was made of the IOA product to the NASA FMEA/CIL baseline. After comparison and discussions with the NASA subsystem manager, 96 hardware issues, 83 of which concern CIL items or PCIs, and 280 EPD and C issues, 158 of which concern CIL items or PCIs, and 280 EPD and C issues, 158 of which concern CIL items or PCIs, remain unresolved. Volume 1 contains the subsystem description, assessment results, and some of the IOA worksheets. Author

N90-11794*# McDonnell-Douglas Astronautics Co., Houston, TX.

INDEPENDENT ORBITER ASSESSMENT (IOA): ASSESSMENT OF THE REACTION CONTROL SYSTEM, VOLUME 2

Chet D. Prust and Dan W. Hartman 26 Feb. 1988 702 p
(Contract NAS9-17650)
(NASA-CR-185543-Vol-2; NAS 1.26:185543-Vol-2; Rept-1.0-WP-VA88003-12-Vol-2) Avail: NTIS HC A99/MF A04 CSCL 22B

The results of the Independent Orbiter Assessment (IOA) of the Failure Modes and Effects Analysis (FMEA) and Critical Items List (CIL) are presented. The IOA effort first completed an analysis of the aft and forward Reaction Control System (RCS) hardware and Electrical Power Distribution and Control (EPD and C), generating draft failure modes and potential critical items. The IOA results were then compared to the proposed Post 51-L NASA FMEA/CIL baseline. This report documents the results of that comparison for the Orbiter RCS hardware and EPD and C systems. Volume 2 continues the presentation of IOA worksheets. Author

N90-11795*# McDonnell-Douglas Astronautics Co., Houston, TX.

INDEPENDENT ORBITER ASSESSMENT (IOA): ASSESSMENT OF THE REACTION CONTROL SYSTEM, VOLUME 3

Chet D. Prust and Dan W. Hartman 26 Feb. 1988 803 p
(Contract NAS9-17650)
(NASA-CR-185543-Vol-3; NAS 1.26:185543-Vol-3; Rept-1.0-WP-VA88003-12-Vol-3) Avail: NTIS HC A99/MF E06 CSCL 22B

The results of the Independent Orbiter Assessment (IOA) of the Failure Modes and Effects Analysis (FMEA) and Critical Items List (CIL) are presented. The IOA effort first completed an analysis of the aft and forward Reaction Control System (RCS) hardware and Electrical Power Distribution and Control (EPD and C), generating draft failure modes and potential critical items. The IOA results were then compared to the proposed Post 51-L NASA FMEA/CIL baseline. This report documents the results of that comparison for the Orbiter RCS hardware and EPD and C systems. Volume 3 continues the presentation of IOA worksheets. Author

N90-11796*# McDonnell-Douglas Astronautics Co., Houston, TX.

INDEPENDENT ORBITER ASSESSMENT (IOA): ASSESSMENT OF THE REACTION CONTROL SYSTEM, VOLUME 4

Chet D. Prust and Dan W. Hartman 26 Feb. 1988 732 p
(Contract NAS9-17650)
(NASA-CR-185543-Vol-4; NAS 1.26:185543-Vol-4; Rept-1.0-WP-VA88003-12-Vol-4) Avail: NTIS HC A99/MF A04 CSCL 22B

The results of the Independent Orbiter Assessment (IOA) of the Failure Modes and Effects Analysis (FMEA) and Critical Items List (CIL) are presented. The IOA effort first completed an analysis of the aft and forward Reaction Control System (RCS) hardware and Electrical Power Distribution and Control (EPD and C), generating draft failure modes and potential critical items. The IOA results were then compared to the proposed Post 51-L NASA FMEA/CIL baseline. This report documents the results of that comparison for the Orbiter RCS hardware and EPD and C systems. Volume 4 continues the presentation of IOA worksheets and contains the potential critical items list. Author

N90-11797*# McDonnell-Douglas Astronautics Co., Houston, TX.

INDEPENDENT ORBITER ASSESSMENT (IOA): ASSESSMENT OF THE REACTION CONTROL SYSTEM, VOLUME 5

Chet D. Prust and Dan W. Hartman 26 Feb. 1988 693 p
(Contract NAS9-17650)
(NASA-CR-185543-Vol-5; NAS 1.26:185543-Vol-5; Rept-1.0-WP-VA88003-12-Vol-5) Avail: NTIS HC A99/MF A04 CSCL 22B

The results of the Independent Orbiter Assessment (IOA) of the Failure Modes and Effects Analysis (FMEA) and Critical Items List (CIL) are presented. The IOA effort first completed an analysis of the aft and forward Reaction Control System (RCS) hardware and Electrical Power Distribution and Control (EPD and C), generating draft failure modes and potential critical items. The IOA results were then compared to the proposed Post 51-L NASA FMEA/CIL baseline. This report documents the results of that comparison for the Orbiter RCS hardware and EPD and C systems. Volume 5 contains detailed analysis and superseded analysis worksheets and the NASA FMEA to IOA worksheet cross reference and recommendations. Author

17 SPACE COMM., SPACECRAFT COMM., COMMAND & TRACKING

Includes telemetry; space communications networks; astronavigation and guidance; and radio blackout.

For related information see also *04 Aircraft Communications and Navigation* and *32 Communications and Radar.*

No abstracts in this category.

18 SPACECRAFT DESIGN, TESTING AND PERFORMANCE

Includes satellites; space platforms; space stations; spacecraft systems and components such as thermal and environmental controls; and attitude controls.

For life support systems see *54 Man/System Technology and Life Support.* For related information see also *05 Aircraft Design, Testing and Performance, 39 Structural Mechanics,* and *16 Space Transportation.*

N90-11798*# National Aeronautics and Space Administration. Lyndon B. Johnson Space Center, Houston, TX.
DOCKING SYSTEM FOR SPACECRAFT Patent Application
Jon B. Kahn, inventor (to NASA) 30 Dec. 1988 21 p
(NASA-Case-MSC-21327-1; NAS 1.71:MSC-21327-1; US-Patent-Appl-SN-292121) Avail: NTIS HC A03/MF A01 CSCL 22B

A mechanism is disclosed for the docking of a spacecraft to a space station where a connection for transfer of personnel and equipment is desired. The invention comprises an active docking structure on a spacecraft and a passive docking structure on the station. The passive structure includes a docking ring mounted on a tunnel structure fixed to the space station. The active structure includes a docking ring carried by an actuator-attenuator devices, each attached at one end to the ring and at its other end in the spacecraft payload bay. The devices respond to command signals for moving the docking ring between a stowed position in the spacecraft to a deployed position suitable for engagement with the docking ring. The devices comprise means responsive to signals of sensed loadings to absorb impact energy and retraction means for drawing the coupled spacecraft and station into final docked configuration and moving the tunnel structure to a berthed position in the spacecraft. Latches couple the spacecraft and space station upon contact of the docking rings and latches establish a structural tie between the spacecraft when retracted. NASA

N90-11799# Technische Hogeschool, Delft (Netherlands). Faculty of Aerospace Engineering.
PROJECT AENEAS: A FEASIBILITY STUDY FOR CREW EMERGENCY RETURN VEHICLE
H. Buning Jul. 1988 252 p
(PB89-217020; LR-558) Avail: NTIS HC A12/MF A02 CSCL 22B

The goal of Project AENEAS was to design a Crew Emergency Return Vehicle for the International Space Station. This vehicle has to be able to perform the following Mission Definitions: a non-time critical retreat from Space Station, in case the Space Shuttle is not available for a long time; a time critical retreat to Earth in case of a Space Station contingency; and an ambulance return under medical tolerant conditions. In order to cover the different aspects of the design, the 29 participating engineering students were divided into eight groups, which in their turn were assembled into three major divisions: a spacecraft engineering division. Topics covered in the report include the following: Systems requirements; space station interface; human factors; power and communication; propulsion; spacecraft integration; orbital operations; reentry; landing and recovery; limits of design and cost aspects. GRA

N90-11800*# Naval Postgraduate School, Monterey, CA. Space Systems Academic Group.
PETITE AMATEUR NAVY SATELLITE (PANSAT) Final Report
1989 21 p
(Contract NASw-4435)
(NASA-CR-186049; NAS 1.26:186049) Avail: NTIS HC A03/MF A01 CSCL 22B

The subsystem and structural design of the Naval Post Graduate School's Petite Amateur Navy Satellite (PANSAT) is described. The objectives of PANSAT are: (1) to provide an ideal educational tool for officer students; (2) to provide digital store-and-forward communications, or packet radio, for the amateur radio community; and (3) to provide a low-cost space-based platform for small experiments. PANSAT will be launched from the Shuttle at a nominal altitude of 200 nmi. and an inclination of at least 37 deg. Since there is no attitude control, eight dipole whip antennas will be used to provide isotropic ground coverage for communications. FM digital communications will be used with up-link and down-link on a single frequency in the amateur band of 144 to 146 MHz or 437 to 438 MHz. The satellite's communications subsystem, data processor and sequencer, power subsystem, structure subsystem, and experiment payload are described. The major experiment being considered will test the on-orbit annealing of radiation damaged solar cells. M.G.

N90-11801# Aerospace Corp., El Segundo, CA. Chemistry and Physics Lab.
PHOTOLYSIS OF SPACECRAFT CONTAMINANTS
Thomas B. Stewart, Graham S. Arnold, David F. Hall, and H. D. Marten 1 Jul. 1989 68 p
(Contract F04701-85-C-0086)
(AD-A211715; TR-0086(6403-01)-1; SD-TR-89-45) Avail: NTIS HC A04/MF A01 CSCL 22/2

Self-contamination of sensitive spacecraft surfaces has long been recognized as potentially limiting the performance, and even the useful life, of a spacecraft. It has become clear that photochemical reactions, induced by solar vacuum ultraviolet (VUV) illumination, play a substantial role in contaminant deposition. A series of laboratory measurements of the absolute rates of adsorption, desorption, and VUV-induced deposition of contaminants under simulated spacecraft conditions are described in this report. The rates measured are sufficient to explain anomalous radiator degradation on the Satellite Data Systems spacecraft radiator. The dependence of the deposition rate on substrate identity and temperature and on contaminant identity and flux is discussed, and a simple kinetic model that describes most experimental observations is presented. GRA

N90-11802*# Mississippi State Univ., Mississippi State. Dept. of Electrical Engineering.
SPACELAB SYSTEM ANALYSIS MARSHALL AVIONICS SYSTEM TESTBED (MAST) Final Report
Frank Ingels, John Owens, and Steven Daniel 31 Oct. 1989 41 p
(Contract NAS8-36717)
(NASA-CR-183804; NAS 1.26:183804; MSU-EE-FIN-20B-89)
Avail: NTIS HC A03/MF A01 CSCL 22B

A synopsis of the visits to avionics test facilities is presented. A list of recommendaions for the MAST facility is also included. Author

19 SPACECRAFT INSTRUMENTATION

For related information see also *06 Aircraft Instrumentation* and *35 Instrumentation and Photography.*

No abstracts in this category.

20 SPACECRAFT PROPULSION AND POWER

Includes main propulsion systems and components, e.g., rocket engines; and spacecraft auxilliary power sources.

For related information see also *07 Aircraft Propulsion and Power, 28 Propellants and Fuels, 44 Energy Production and Conversion,* and *15 Launch Vehicles and Space Vehicles.*

N90-11803# National Aerospace Lab., Kakuda (Japan).
PROGRAM FOR HIGH SPEED COMPUTATION OF PHYSICAL PROPERTIES OF PROPELLANTS AND COMBUSTION GAS OF AN LH2/LOX ROCKET ENGINE
Yoshio Wakamatsu, Takeshi Karita, and Akio Kanmuri Mar. 1987 41 p In JAPANESE
(NAL-TM-564; ISSN-0452-2982; JTN-88-80059) Avail: NTIS HC A03/MF A01

The equation of state of hydrogen and oxygen as a propellant, well as the gas produced through their combustion, and the values of thermodynamic, transport and the physical properties are necessary at all development stages and for the study of hydrogen/oxygen rocket engines. Calculation of physical properties is repeated at frequent intervals, particularly in the simulation of the dynamic characteristics in the starting and stopping of rocket engines. Therefore, it is necessary to take a serious view of the calculation speed in the subprograms for the physical-property calculations used in simulation. The physical property calculation codes published so far are universal and accurate for several kinds of materials. Nevertheless, their balance with calculation speed is not always satisfactory. The specifications and the application results of TROY (Time-saving Routine for H2 and O2 Properties) and the codes for calculating the physical properties of the hydrogen, oxygen and combustible gas of hydrogen/oxygen rockets are discussed. NASDA

N90-11804*# National Aeronautics and Space Administration. Lewis Research Center, Cleveland, OH.
THE FUEL CELL IN SPACE: YESTERDAY, TODAY AND TOMORROW
Marvin Warshay and Paul R. Prokopius Sep. 1989 11 p
Presented at the Grove Anniversary (1839-1989) Fuel Cell Symposium, London, England, 18-21 Sep. 1989; sponsored in part by the Royal Institution
(NASA-TM-102366; E-5084; NAS 1.15:102366) Avail: NTIS HC A03/MF A01 CSCL 10B

The past, present, and future of space fuel cell power systems is reviewed, starting with the first practical fuel cell by F.T. Bacon which led to the 1.5 kW Apollo alkaline fuel cell. However, the first fuel cell to be used for space power was the Gemini 1.0 kW Acid IEM fuel cell. The successor to the Apollo fuel cell is today's 12 kW Orbiter alkaline fuel cell whose technology is considerably different and considerably better than that of its ancestor, the Bacon cell. And in terms of specific weight there has been a steady improvement from the past to the present, from the close to 200 lb/kW of Apollo to the 20 lb/kW of the orbiter. For NASA future Lunar and Martian surface power requirements the regenerative fuel cell (RFC) energy storage system is enabling technology, with the alkaline and the PEM the leading RFC candidate systems. The U.S. Air Force continues to support fuel cell high power density technology development for its future short duration applications. Author

N90-11805*# Grumman Aerospace Corp., Bethpage, NY. Space Systems.
CONCEPTUAL DESIGN OF LIQUID DROPLET RADIATOR SHUTTLE-ATTACHED EXPERIMENT Final Report
Shlomo L. Pfeiffer Oct. 1989 60 p
(Contract NAS3-25357)
(NASA-CR-185164; NAS 1.26:185164) Avail: NTIS HC A04/MF A01 CSCL 10B

The conceptual design of a shuttle-attached liquid droplet radiator (LDR) experiment is discussed. The LDR is an advanced, lightweight heat rejection concept that can be used to reject heat from future high-powered space platforms. In the LDR concept, submillimeter-sized droplets are generated, pass through space, radiate heat before they are collected, and recirculated back to the heat source. The LDR experiment is designed to be attached to the shuttle longeron and integrated into the shuttle bay using standard shuttle/experiment interfaces. Overall power, weight, and data requirements of the experiment are detailed. The conceptual designs of the droplet radiator, droplet collector, and the optical diagnostic system are discussed in detail. Shuttle integration and safety design issues are also discussed. Author

N90-11806*# Grumman Aerospace Corp., Bethpage, NY.
CONCEPTUAL DESIGN OF LIQUID DROPLET RADIATOR SHUTTLE-ATTACHED EXPERIMENT TECHNICAL REQUIREMENTS DOCUMENT
Shlomo L. Pfeiffer Oct. 1989 31 p
(Contract NAS3-25357)
(NASA-CR-185165; NAS 1.26:185165) Avail: NTIS HC A03/MF A01 CSCL 10B

The technical requirements of a shuttle-attached Liquid Droplet Radiator (LDR) experiment are discussed. The Liquid Droplet Radiator is an advanced lightweight heat rejection concept that can be used to reject heat from future high powered space platforms. In the LDR concept, submillimeter sized droplets are generated, pass through space, and radiate heat before they are collected and recirculated back to the heat source. The LDR experiment is designed to be attached to the shuttle longeron and integrated into the shuttle bay using standard shuttle/experiment interfaces. Overall power, weight, and data requirements of the experiment are detailed. Shuttle integration and safety design issues are discussed. An overview of the conceptual design of the experiment is presented. Details of the conceptual design are not discussed here, but rather in a separate Final Report. Author

23 CHEMISTRY AND MATERIALS (GENERAL)

No abstracts in this category.

24 COMPOSITE MATERIALS

Includes physical, chemical, and mechanical properties of laminates and other composite materials.

For ceramic materials see *27 Nonmetallic Materials.*

N90-11807*# Wyoming Univ., Laramie. Composite Materials Group.
STATIC TENSILE AND TENSILE CREEP TESTING OF FOUR BORON NITRIDE COATED CERAMIC FIBERS AT ELEVATED TEMPERATURES Final Report
Scott L. Coguill, Donald F. Adams, and Richard S. Zimmerman Aug. 1989 135 p
(Grant NAG2-470)
(NASA-CR-184999; NAS 1.26:184999; UW-CMRG-R-89-123) Avail: NTIS HC A07/MF A01 CSCL 11D

Six types of uncoated ceramic fibers were static tensile and tensile creep tested at various elevated temperatures. Three types of boron nitride coated fibers were also tested. Room temperature static tensile tests were initially performed on all fibers, at gage lengths of 1, 2, and 4 inches, to determine the magnitude of end effects from the gripping system used. Tests at one elevated temperature, at gage lengths of 8 and 10 inches, were also conducted, to determine end effects at elevated temperatures.

Fiber cross sectional shapes and areas were determined using scanning electron microscopy. Creep testing was typically performed for 4 hours, in an air atmosphere. Author

N90-11808*# National Aeronautics and Space Administration. Lewis Research Center, Cleveland, OH.

AN INTEGRATED METHODOLOGY FOR OPTIMIZING STRUCTURAL COMPOSITE DAMPING

D. A. Saravanos and C. C. Chamis 1989 25 p Presented at the 1989 Winter Annual Meeting of the ASME, San Francisco, CA, 10-15 Dec. 1989

(NASA-TM-102343; E-5051; NAS 1.15:102343) Avail: NTIS HC A03/MF A01 CSCL 11D

A method is presented for tailoring plate and shell composite structures for optimal forced damped dynamic response. The damping of specific vibration modes is optimized with respect to dynamic performance criteria including placement of natural frequencies and minimization of resonance amplitudes. The structural composite damping is synthesized from the properties of the constituent materials, laminate parameters, and structural geometry based on a specialty finite element. Application studies include the optimization of laminated composite beams and composite shells with fiber volume ratios and ply angles as design variables. The results illustrate the significance of damping tailoring to the dynamic performance of composite structures, and the effectiveness of the method in optimizing the structural dynamic response. Author

N90-11809# Karlsruhe Univ. (Germany, F.R.). Fakultaet fuer Maschinenbau.

INTERLAMINAR STRESS CONCENTRATION IN FIBER COMPOSITES Ph.D. Thesis [INTERLAMINARE SPANNUNGSKONZENTRATIONEN IN FASERVERBUNDWERKSTOFFEN]

Martin Woertler 2 Feb. 1988 152 p In GERMAN

(ETN-89-94670) Avail: NTIS HC A08/MF A01

A measuring system is further developed and calibrated in order to allow the experimental analysis of stress concentration problems in free edges and notches of fiber composite laminates, and correlation with theoretical results. The numerical treatment of the edge effect problem using a finite element model is outlined. The roentgenographic measurement of distortions and stresses is explained. The measuring setup (diffractometer, interference line shift) and the systematic and statistic errors are discussed. Tests are performed on metal-epoxy samples, and carbon fiber reinforced laminates and strips. The results are confirmed by finite element simulations. The scattering of results from different identical samples and the measuring speed need improvement. The method allows direct stress measurements in the highly loaded, interlaminar range of multilayer composites, including notches and delamination points. ESA

N90-11810# Drexel Univ., Philadelphia, PA.

INORGANIC COMPOSITE MATERIALS IN JAPAN: STATUS AND TRENDS

M. J. Koczak, K. Prewo, A. Mortensen, S. Fishman, M. Barsoum, and R. Gottschall Sep. 1988 73 p

(PB89-230015) Avail: NTIS HC A04/MF A01 CSCL 11D

Japan's high performance composite research activities and applications are reviewed by six authors who teamed as a study group in September 1988, in order to assess selected research areas of composite activities. The summary of the study group visits are detailed in the subsequent sections: advance composite material programs; ceramic fibers and whiskers; metal matrix composites; ceramic matrix composites; and composite applications and future directions. Several developments in high temperature metals and polymer and metal matrix composites were achieved over an eight-year program. In the composites area, the areas of fiber and whisker developments, ceramic powder processing and applications of metal matrix composites are particularly notable and are reviewed. Toyota's application of wear resistant metal matrix composites for automotive diesel piston fabrication continues to be significant with other structural and wear applications currently being considered and sought. The efforts in ceramic matrix composites are more on a laboratory and developmental stage and have not matured to a manufacturing production stage with the notable exception of the Nissan turbocharger. GRA

N90-11811# Fermi National Accelerator Lab., Batavia, IL.

THERMAL CONDUCTION OF SSC (SUPERCONDUCTING SUPER COLLIDER) WIRE

M. Kuchnir and J. L. Tague Aug. 1989 4 p Presented at the International Cryogenic Materials Conference, Los Angeles, CA, 24-28 Jul. 1989

(Contract DE-AC02-76CH-03000)

(DE89-016710; FNAL-TM-1613; CONF-890701-3) Avail: NTIS HC A01/MF A01

A method suitable for measuring the thermal conductivity of good thermal conductors at low temperatures was implemented. It successfully served its purpose: to detect the effect of doping with manganese, the interfilament part of the copper matrix of the superconducting wire used in the magnets of the Superconducting Super Collider. It uses two heaters and one thermometer per sample, reducing the accuracy requirement on the thermometers, automatically compensating for zero offsets and reducing the number of critical thermal contacts. Commercially available strain gauges are used as heaters. DOE

N90-11812# Lawrence Livermore National Lab., CA. Chemistry and Materials Science.

SHORT PERIOD MULTILAYERS: INTERFACE DOMINATED STRUCTURES

A. F. Jankowski Jul. 1989 25 p Presented at the American Crystallographic Association Annual Meeting, Seattle, WA, 23-29 Jul. 1989

(Contract W-7405-eng-48)

(DE89-017536; UCRL-100869; CONF-890771-4) Avail: NTIS HC A03/MF A01

The dimensional scale of materials synthesis techniques have extended to an atomic level. As such, the structure and properties of composite materials are unlike those of the bulk constituents. This is especially true for the case of artificially composition modulated materials, i.e., multilayers. The statistical presence of interfaces is high in short period multilayers, which in turn affects the stable configuration of atoms in the lattice. The metastable arrangement which results from the one-dimensional ordering in metallic multilayers will be examined using diffraction techniques. The careful selection of compatible materials has enabled the fabrication of amorphous superlattices with near monolayer composition modulation. An examination of these structures and their use in X-ray optical systems will be presented. DOE

N90-11813# Pacific Northwest Lab., Richland, WA.

STOCHASTIC PROPAGATION OF AN ARRAY OF PARALLEL CRACKS: EXPLORATORY WORK ON MATRIX FATIGUE DAMAGE IN COMPOSITE LAMINATES

R. E. Williford Sep. 1989 37 p

(Contract DE-AC06-76RL-01830)

(DE89-017837; PNL-6903) Avail: NTIS HC A03/MF A01

Transverse cracking of polymeric matrix materials is an important fatigue damage mechanism in continuous-fiber composite laminates. The propagation of an array of these cracks is a stochastic problem usually treated by Monte Carlo methods. However, this exploratory work proposes an alternative approach wherein the Monte Carlo method is replaced by a more closed-form recursion relation based on fractional Brownian motion. A fractal scaling equation is also proposed as a substitute for the more empirical Paris equation describing individual crack growth in this approach. Preliminary calculations indicate that the new recursion relation is capable of reproducing the primary features of transverse matrix fatigue cracking behavior. Although not yet fully tested or verified, this cursion relation may eventually be useful for real-time applications such as monitoring damage in aircraft structures. DOE

N90-11814# Illinois Univ., Urbana-Champaign.
PROCESSING AND CHARACTERIZATION OF ALUMINA PLATELET-REINFORCED MULLITE COMPOSITES M.S. Thesis
Scott D. Crudele Aug. 1989 112 p
(Contract DE-AC02-76ER-01198)
(DE90-000057; DOE/ER-01198/T37) Avail: NTIS HC A06/MF A01

The alumina-mullite system may be a candidate for high temperature composites because alumina and mullite are chemically stable in air up to 1630 C. Twenty volume percent of approximately 5 or 40 (mu)m alumina platelets were hot pressed in a 3:2 mullite matrix. The microstructure revealed strong bonding at the alumina-mullite interface and stress cracks in the mullite. Consequently, tin oxide and nickel aluminate coatings were applied to the platelets and the hot pressed and sintered composite microstructure was analyzed. Results indicate that tin oxide volatizes during hot pressing leaving no trace of tin at the interface. Also, nickel aluminate may act as a debonding phase between alumina and mullite; however, the nickel aluminate does not form a continuous layer at the interface via sintering or hot pressing. DOE

N90-11815# Colorado School of Mines, Golden. Center for Welding and Joining Research.
INVESTIGATIONS INTO THE INFILTRATION KINETICS, WETTABILITY, AND INTERFACIAL BOND STRENGTH OF Al/SIC COMPOSITES Annual Report
Glen R. Edwards and David L. Olson Jul. 1989 63 p
(Contract N00014-88-K-0500)
(AD-A211924; CSM-MT-CWR-089-038) Avail: NTIS HC A04/MF A01 CSCL 11/4

The theoretical model and the experimental setup used for porous compact studies are described in previous reports. In this phase of the study, unsintered compacts of Silicon carbide particles were infiltrated with pure aluminum. The infiltration distance, the distance to which the liquid metal penetrates the porous compact, was measured as a function of time different temperatures and pressures. The results are plotted as infiltration distance versus time in accordance with a theoretical analysis previously reported. (A least square analysis was carried out to fit a straight line through the data points). GRA

N90-11816# Army Lab. Command, Watertown, MA. Material Technology Lab.
DEFORMATION BEHAVIOR OF SiC/2014 Al METAL-MATRIX COMPOSITE Final Report
Shun-Chin Chou, Dattatraya P. Dandekar, Julius Frankel, Jibmitra Ganguly, John L. Green, Anthony G. Martin, Ronald A. Swanson, and Craig Lopatin (Dayton Univ., OH.) May 1989 53 p
(AD-A212095; MTL-TR-89-42) Avail: NTIS HC A04/MF A01 CSCL 11/4

The deformation behavior of a composite composed of 25-volume-percent silicon carbide (SiC) whiskers in 2014 aluminum matrix was studied. Specimens were taken from a hot isostatically pressed cylindrical billet, then tested at various loading conditions and strain rates. Mechanical deformation of the composite was performed using tension, compression, torsion, Bauschinger effect, and fracture toughness testing. Deformation of the composite under shock loading/unloading and spallation threshold were determined. Elastic wave velocities at high pressures to 1.5 GPa and volume compression to 4.5 GPa were measured to determine the pressure dependence of elastic constants and isothermal and adiabatic equations of state. GRA

N90-11817# Tufts Univ., Medford, MA. Lab. for Materials and Interfaces.
IN-SITU CURE MONITORING OF COMPOSITES BY FIBER-OPTIC MOLECULAR SENSORS Technical Report No. 15, 1988 - 1989
Nakho Sung, Wenbin Dang, and Chong Sook Paik Sung (Connecticut Univ., Storrs.) 10 Aug. 1989 3 p Presented at the 2nd Topical Conference on Emerging Technologies on Materials, San Francisco, CA, 6-8 Nov. 1989; sponosred by AIChE Sponsored by ONR, Arlington, VA
(AD-A211495) Avail: NTIS HC A02/MF A01 CSCL 07/6

In-Situ Cure Monitoring of Composites by Fiber-Optic Molecular Sensors is examined. Recently, a new technique was developed for monitoring cure reactions in network forming polymers by using reactive molecular sensors. Diaminoazobenzene (DAA), for example, generates sensitive signals in UV-Visible and fluorescence spectra as a function of cure reaction in epoxy, such as DGEBA/DDS system. This describes the current efforts on the application of molecular sensors to composite cure monitoring via remote sensing fiber-optics probes. A custom-built fiber-optic fluorimeter allows on-line sensing of fluorescence signals directly from the cure environment. Different optrode configurations are developed to probe the structure at the local sites of surface, bulk, and interface. GRA

N90-11818# United Technologies Research Center, East Hartford, CT.
CARBON FIBER REINFORCED GLASS MATRIX COMPOSITES FOR STRUCTURAL SPACE BASED APPLICATIONS Final Report, 1 Jul. 1987 - 31 May 1989
W. K. Tredway and K. M. Prewo 31 Jul. 1989 108 p
(Contract N00014-85-C-0332)
(AD-A211682; UTRC/R89-917704-1) Avail: NTIS HC A06/MF A01 CSCL 11/4

A variety of ultrahigh elastic modulus pitch based carbon fibers were combined with several different glass and glass-ceramic matrix compositions to produce unidirectionally reinforced composites. Composite performance was evaluated in several different areas, including tensile stress-strain behavior, flexural properties at both room and elevated temperature, thermal expansion, and fracture behavior. Pitch fiber reinforced glass matrix composites demonstrated high tensile strength (540 to 790 MPa), high elastic modulus (300 to 350 GPa), and high specific stiffness (135 to 165x 107 cm). Residual matrix tensile stress resulting from differential thermal contraction between fiber and matrix was shown to have a strong influence on composite behavior. Pitch/Glass composites were found to exhibit fairly linear coefficient of thermal expansion behavior in the longitudinal direction over the temperature range of -150 to 100 C. High temperature matrix compositions were developed which maintained the excellent tensile properties of pitch fiber reinforced composites while giving them the capability to preserve structural integrity up to temperatures of at least 800 C. GRA

N90-11819# Aeritalia S.p.A., Turin (Italy). Lab. Strutture e Ricerche sui Materiali.
CHOICE AND CHARACTERIZATION OF NEW MATERIALS FOR AEROSPACE APPLICATIONS [CARATTERIZZAZIONE E SCELTA DI MATERIALI INNOVATIVI PER IMPIEGHI AEROSPAZIALI]
F. Cipri 1989 18 p In ITALIAN
(ETN-89-95219) Avail: NTIS HC A03/MF A01

Some results covering mechanical properties of product families used for aircraft structures are reported, and the development of new materials and technology which will be used in aerospace projects are discussed. The criteria followed in the choice of composite materials for the primary structures design of advanced aircraft are detailed. ESA

N90-11820# Aeritalia S.p.A., Turin (Italy). Gruppo Velivoli da Combattimento.
A NEW TEST PROCEDURE FOR A WING MADE WITH CARBON FIBER COMPOSITES [UNA NUOVA TECNICA DI PROVA PER UN'ALA IN COMPOSITO DI FIBRA DI CARBONIO]
Eraldo Padovano and Vincenzo Vallone 1989 7 p In ITALIAN
(ETN-89-95220) Avail: NTIS HC A02/MF A01

The testing method applied to full size delta shape half wings of a fighter aircraft is presented. It consists of discrete loading applied by means of hydraulic devices which reproduce the distribution of shear and torque to which the wing is subjected under aerodynamic and inertia loadings. The experimental setup is described. Block diagrams detailing load control and data acquisition are presented. ESA

N90-11821*# Lockheed-California Co., Burbank.
TRANSPORT COMPOSITE FUSELAGE TECHNOLOGY: IMPACT DYNAMICS AND ACOUSTIC TRANSMISSION Final Report
A. C. Jackson, F. J. Balena, W. L. LaBarge, G. Pei, W. A. Pitman, and G. Wittlin Washington Dec. 1986 163 p
(Contract NAS1-17698)
(NASA-CR-4035; NAS 1.26:4035; LR-31038) Avail: NTIS HC A08/MF A01 CSCL 11D

A program was performed to develop and demonstrate the impact dynamics and acoustic transmission technology for a composite fuselage which meets the design requirements of a 1990 large transport aircraft without substantial weight and cost penalties. The program developed the analytical methodology for the prediction of acoustic transmission behavior of advanced composite stiffened shell structures. The methodology predicted that the interior noise level in a composite fuselage due to turbulent boundary layer will be less than in a comparable aluminum fuselage. The verification of these analyses will be performed by NASA Langley Research Center using a composite fuselage shell fabricated by filament winding. The program also developed analytical methodology for the prediction of the impact dynamics behavior of lower fuselage structure constructed with composite materials. Development tests were performed to demonstrate that the composite structure designed to the same operating load requirement can have at least the same energy absorption capability as aluminum structure. Author

N90-11822*# Douglas Aircraft Co., Inc., Long Beach, CA.
MANUAL FOR PROGRAM PSTRESS: PEEL STRESS COMPUTATION
Derek A. Barkey and Ram C. Madan Dec. 1987 41 p
(Contract NAS1-17970)
(NASA-CR-178408; NAS 1.26:178408) Avail: NTIS HC A03/MF A01 CSCL 11D

Described is the use of the interactive FORTRAN computer program PSTRESS, which computes a closed form solution for two bonded plates subjected to applied moments, vertical shears, and in-plane forces. The program calculates in-plane stresses in the plates, deflections of the plates, and peel and shear stresses in the adhesive. The document briefly outlines the analytical method used by PSTRESS, describes the input and output of the program, and presents a sample analysis. The results of the latter are shown to be within a few percent of results obtained using a NASTRAN finite element analysis. An appendix containing a listing of PSTRESS is included. Author

25 INORGANIC AND PHYSICAL CHEMISTRY

Includes chemical analysis, e.g., chromatography; combustion theory; electrochemistry; and photochemistry.

For related information see also *77 Thermodynamics and Statistical Physics.*.

N90-11823*# National Aeronautics and Space Administration. Langley Research Center, Hampton, VA.
CATALYST FOR CARBON MONOXIDE OXIDATION Patent Application
Billy T. Upchurch, inventor (to NASA), Irvin M. Miller, inventor (to NASA), David R. Brown, inventor (to NASA), Patricia P. Davis, inventor (to NASA), David R. Schryer, inventor (to NASA), Kenneth G. Brown, inventor (to NASA), and John D. VanNorman, inventor (to NASA) (Old Dominion Univ., Norfolk, VA.) 18 Jan. 1989 11 p
(NASA-Case-LAR-14155-1-SB; NAS 1.71:LAR-14155-1-SB; US-Patent-Appl-SN-298150) Avail: NTIS HC A03/MF A01 CSCL 07D

A catalyst is disclosed for the combination of CO and O2 to form CO2, which includes a platinum group metal (e.g., platinum); a reducable metal oxide having multiple valence states (e.g., SNO2); and a compound which can bind water to its structure (e.g., silica gel). This catalyst is ideally suited for application to high-powered pulsed, CO2 lasers operating in a sealed for closed-cycle condition NASA

N90-11824*# National Aeronautics and Space Administration. Lewis Research Center, Cleveland, OH.
STEAM COOLED RICH-BURN COMBUSTOR LINER Patent
Donald F. Schultz, inventor (to NASA) 11 Apr. 1989 7 p
Filed 23 Dec. 1982 Supersedes N83-17628 (21 - 8, p 1149)
(NASA-Case-LEW-13609-1; US-Patent-4,819,438; US-Patent-Appl-SN-452465; US-Patent-Class-60-730; US-Patent-Class-60-732; US-Patent-Class-165-83; US-Patent-Class-165-81; US-Patent-Class-165-156; US-Patent-Class-431-352) Avail: U.S. Patent and Trademark Office CSCL 21B

Stress on the wall of the primary combustor is minimized. Thus, the steam pressure in the inlet manifold is approximately the same as the combustor discharge pressure at the throat, and annular expansion tubes minimize stresses in the jacket. The second combustor accomplishes lean burning of the gases discharged from primary combustor. The combination of the rich burning of heavy fuels followed by lean burning minimizes the NOx in the exhaust gas discharged from combustor. The novelty of the invention appears to lie in cooling a rich burn combustor with spiral streams of saturated steam flowing between the combustor linear and the jacket at a predetermined pressure; the jacket including stress relief means. NASA

N90-11825*# Missouri Univ., Rolla. Dept. of Mechanical and Aerospace Engineering.
ANALYSIS OF OPPOSED JET HYDROGEN-AIR COUNTER FLOW DIFFUSION FLAME
Y. H. Ho and K. M. Isaac Oct. 1989 84 p
(Grant NAG1-861)
(NASA-CR-182366; NAS 1.26:182366; MAE-TM-25) Avail: NTIS HC A05/MF A01 CSCL 21B

A computational simulation of the opposed-jet diffusion flame is performed to study its structure and extinction limits. The present analysis concentrates on the nitrogen-diluted hydrogen-air diffusion flame, which provides the basic information for many vehicle designs such as the aerospace plane for which hydrogen is a candidate as the fuel. The computer program uses the time-marching technique to solve the energy and species equations coupled with the momentum equation solved by the collocation method. The procedure is implemented in two stages. In the first stage, a one-step forward overal chemical reaction is chosen with the gas phase chemical reaction rate determined by comparison with experimental data. In the second stage, a complete chemical reaction mechanism is introduced with detailed thermodynamic and transport property calculations. Comparison between experimental extinction data and theoretical predictions is discussed. The effects of thermal diffusion as well as Lewis number and Prandtl number variations on the diffusion flame are also presented. Author

N90-11826# Case Western Reserve Univ., Cleveland, OH. Dept. of Chemistry.
IN-SITU SPECTROSCOPIC STUDIES OF TRANSITION METAL MACROCYCLES AS CATALYSTS FOR THE ELECTROCHEMICAL REDUCTION OF OXYGEN Annual Report, Dec. 1987 - Nov. 1988
Daniel A. Scherson and Ernest Yeager May 1989 47 p
(Contract GRI-5086-260-1403)
(PB89-219273; GRI-89/0123) Avail: NTIS HC A03/MF A01 CSCL 07D

The vibrational, electronic, and structural properties of transition metal macrocycles adsorbed on electrode surfaces are being investigated with an array of in situ spectroscopic techniques. The techniques include potential difference Fourier transform infrared spectroscopy, electrochemically modulated infrared spectroscopy, electromodulated reflection absorption spectroscopy in the UV-vis spectral region, Mossbauer spectroscopy in the transmission, and conversion electron modes and x ray absorption fine structure. The information arising from the use of the techniques is being complemented by conventional electrochemical measurements, and scanning tunneling microscopy as a means of imaaging transition metal macrocycles adsorbed on metal surfaces. The studies are aimed at gaining a basic understanding of the factors that control the electrocatalytic activity of transition metal macrocycles adsorbed on electrode surfaces for the electrochemical reduction of dioxygen. GRA

N90-11827# Helsinki Univ. of Technology, Espoo (Finland). Lab. of Physics.
COMPUTER SIMULATIONS OF RADIATION DAMAGE IN AMORPHOUS SOLIDS
J. Laakkonen and R. M. Nieminen 1989 67 p
(PB89-212682; Rept-186(1989)) Avail: NTIS HC A04/MF A01
CSCL 07D

Microscopic radiation damage in a Lennard-Jones amorphous solid is investigated by computer simulations of collision cascades. Molecular dynamnics simulations with various primary knock-on atom (PKA) energies and directions are carried out. Energy outflow from the computational box is accounted for but electronic losses are neglected. The experiments shown the PKA energy to spread rapidly among the nearby atoms, and the atomic trajectories disclose such features as replacement collision sequences and focused chains. Vacancies are created in the central region of the cascade and are surrounded by a cloud of interstitials. The defects mainly disappear independently of each other, the vacancies faster than the interstitials. Recombination plays a minor role. At the end of a simulation all the defects created have vanished and little change in the sample volume or structure is observed. The threshold energy for a permanent displacement is found for various PKA directions. The validity of the modified Kinchin-Pease model for an amorphous solid is discussed. GRA

N90-11828# Morgantown Technology Center, WV. Office of Fossil Energy.
NATURAL GAS TO LIQUIDS Technology Status Report
R. D. Malone, ed. and C. A. Komar, ed. Jan. 1989 23 p
(DE89-000982; DOE/METC-89-0265) Avail: NTIS HC A03/MF A01

In 1984, DOE initiated a program for expanding the knowledge base and for developing concepts, methods, and processes to convert natural gas to liquid fuels. The initial research activities focused on developing a comprehensive understanding of the fundamental mechanisms and kinetics when partially oxidating methane directly to methanol as the basis for designing a process. The goal is to achieve a sufficiently high yield that an operable and economically viable process can be applied to converting remote natural gas to liquids for transportation to U.S. markets. This research project is ongoing and has progressed to include research in catalytic, noncatalytic, and biological conversion processes. These processes are discussed. DOE

N90-11829# Lawrence Livermore National Lab., CA.
SHOCK DISSOCIATION OF MOLECULAR FLUIDS: A POSSIBILITY OF FIRST-ORDER PHASE CHANGE
Francis H. Ree Jul. 1989 2 p Presented at the 30th High Pressure Conference of Japan, Sendai, Japan, 16-18 Oct. 1989 Submitted for publication
(Contract W-7405-eng-48)
(DE89-016647; UCRL-101433; CONF-8910191-1) Avail: NTIS HC A01/MF A01

A relationship is examined between a thermodynamic phase change and molecular dissociation. The recent calculations of dissociation processes; (reversible reactions) H2 yields 2H and N2 yields 2N, have indicated that such a phase change is theoretically possible. The main purpose of this paper is to offer a physical explanation for the predicted phase change. DOE

N90-11830# Los Alamos National Lab., NM.
AIR BREAKDOWN PHOTOGRAPHY IN THE PICOSECOND DOMAIN
George A. Kyrala, Peter H. Y. Lee, Kurt A. Stetler, and Irene I. K. Yu 1989 9 p Presented at the 33rd SPIE Annual International Technical Symposium on Optical and Optoelectronic Applied Science and Engineering, San Diego, CA, 6-11 Aug. 1989
(Contract W-7405-eng-36)
(DE89-016775; LA-UR-89-2671; CONF-890836-12) Avail: NTIS HC A02/MF A01

We have studied the breakdown of air using the Los Alamos Bright Source KrF laser at an irradiance of 1.36 x 10(exp 16) W/sq cm and pulse length of 700 fs. Results of the temporal evolution of various regions of the spark, recorded with an S-20 streak/framing camera, are presented. DOE

N90-11831# Lawrence Livermore National Lab., CA.
CONVERSION OF METHANE TO LIQUID HYDROCARBONS
Michael W. Droege and L. M. Hair Apr. 1989 12 p Presented at the Natural Gas Research and Development, Morgantown, WV, 18-19 Apr. 1989
(Contract W-7405-eng-48)
(DE89-017547; UCRL-100943; CONF-890492-3) Avail: NTIS HC A03/MF A01

The major emphasis of this project is the development of new catalyst materials which facilitate reactions that convert methane to liquid fuels. Reactions of interest include partial oxidation (forming methanol and formaldehyde) or oxidative coupling (forming ethane and ethylene) of methane using oxygen. Our efforts have focused both on describing the gas phase reactions of methane and oxygen that lead to methane oxidation and on development of new catalysts that select and accelerate the partial oxidation or coupling reactions. We have employed a chemical kinetic model (HCT: Hydrodynamics, Chemical kinetics, and Transport) that was developed at this Laboratory to describe homogeneous gas phase reactions. In addition, we have focused on the synthesis and reactions of new catalyst materials that would serve as the basis for methane conversion processes. The catalysts typically consist of an inorganic oxide matrix such as SiO(sub 2) in which early transition metal and lanthanide ions are incorporated into the oxide coordination environment of the matrix. Characterization studies have been used to elucidate both the bulk properties of the catalysts as well as to determine details of the metal ion coordination environment. Reactor studies testing the foregoing catalysts for methane partial oxidation reactions are in progress and the results will be correlated with both the characterization data and with chemical kinetic modelling of the thermal reactions of methane and oxygen. DOE

N90-11832# Lawrence Livermore National Lab., CA.
PHASE BEHAVIOR OF PURE AND MIXED SYSTEMS AT HIGH PRESSURE
Francis H. Ree Jun. 1989 3 p Presented at the AIRAPT and EHPRG International High Pressure Science and Technology Conference, Paderborn, Fed. Republic of Germany, 17-21 Jul. 1989
(Contract W-7405-eng-48)
(DE89-017734; UCRL-100488; CONF-890798-12) Avail: NTIS HC A01/MF A01

The knowledge of intermolecular potentials, equations of state theories, and methods of handling chemical reactions are at a stage where one can perform rigorous calculations on pure and mixture systems at high pressures and temperatures. DOE

N90-11833# Lawrence Livermore National Lab., CA.
CALCULATION OF THE REFRACTIVE INDEX CHANGE IN DISSOCIATING SHOCKED BENZENE
David J. Erskine Aug. 1989 5 p Presented at the American Physical Society Topical Conference on Shock Compression of Condensed Matter, Albuquerque, NM, 14-17 Aug. 1989
(Contract W-7405-eng-48)
(DE89-017737; UCRL-100804; CONF-890812-42) Avail: NTIS HC A01/MF A01

A calculation is made of the refractive index (n) of a shocked solution of hydrocarbon species and spheroidal carbon particles that would be the dissociation products of benzene. The result is evaluated for benzene shocked to 15 GPa or particles of different morphologies. In the case of diamond particles, the refractive index is predicted to decrease through the dissociation from 1.96 to 1.75. For particles of graphite in platelet form (10:1 aspect ratio) the refractive index increases from 1.96 to 2.2. Thus the measurement of n(t) could indicate the morphology of the carbon particulates and the time scale for this reaction, as well as the instantaneous amount of carbon particulate. The latter information is valuable in conjunction with recent Mie scattering experiments for example. DOE

N90-11834# Pennsylvania Univ., Philadelphia.
CATALOGIC HYDROGENATION OF CARBON MONOXIDE Final Progress Report, 15 Sep. 1988 - 14 Sep. 1989
Bradford B. Wayland Sep. 1989 6 p
(Contract DE-FG02-86ER-13615)
(DE89-017813; DOE/ER-13615/3) Avail: NTIS HC A02/MF A01

This project is focused on developing strategies to accomplish the hydrogenation of carbon monoxide to produce organic oxygenates at mild conditions. Our approaches are based on the recognition that rhodium macrocycles have unusually favorable thermodynamic values for producing a series of intermediates implicated in the catalytic hydrogenation of CO. Observations of metalloformyl complexes from reactions of H(sub 2) and CO, and reductive coupling of CO to form metallo (alpha)-diketone species have suggested a multiplicity of routes to organic oxygenates that utilize these species as intermediates. Thermodynamic and kinetic-mechanistic studies are used in constructing energy profiles for a variety of potential pathways, and these schemes are used in guiding the design of new metallospecies to improve the thermodynamic and kinetic factors for individual steps in the overall process. Variation of the electronic and steric effects associated with the ligand arrays along with the influences of the reaction medium provide the chemical tools for tuning these factors. Current studies are directed toward the use of non-macrocyclic ligand complexes that emulate the favorable thermodynamic features associated with rhodium macrocycles, but that also manifest improved reaction kinetics. DOE

N90-11835# California Univ., Berkeley. Lawrence Berkeley Lab. Materials and Chemical Sciences Div.
HIGH TEMPERATURE AND HIGH RESOLUTION UV PHOTOELECTRON SPECTROSCOPY USING SUPERSONIC MOLECULAR BEAMS
Lai-Sheng Wang, J. E. Reutt-Robey, B. Niu, Y. T. Lee, and D. A. Shirley (California Univ., Berkeley.) Jul. 1989 15 p Presented at the 4th International Conference on Electron Spectroscopy, Honolulu, HI, 10-14 Jul. 1989
(Contract DE-AC03-76SF-00098)
(DE90-000176; LBL-27583; CONF-890738-2) Avail: NTIS HC A03/MF A01

A high temperature molecular beam source with electron bombardment heating was built for high resolution photoelectron spectroscopic studies of high temperature species and clusters. This source has the advantages of: producing an intense, continuous, seeded molecular beam, eliminating the interference of the heating mechanism from the photoelectron measurement. Coupling the source with the hemispherical electron energy analyzer, very high resolution HeI(alpha) (584 A) photoelectron spectra of high temperature species can be obtained. Vibrationally-resolved photoelectron spectra of Pb Se, As2, As4, and ZnCl2 are shown to demonstrate the performance of the new source. DOE

N90-11836# Duquesne Univ., Pittsburgh, PA. Dept. of Chemistry.
IRON (III) INITIATED AUTOXIDATION OF 1,2,3,4-TETRAHYDROCARBAZOLE: AN EXAMPLE OF ELECTRON TRANSFER Final Report, 15 Jul. 1988 - 15 Sep. 1989
Bruce Beaver, Garret Veloski, and David Kindelberger 1 Sep. 1989 14 p Sponsored by NRL and ONR
(AD-A211857) Avail: NTIS HC A03/MF A01 CSCL 07/3

The initial stages of the autoxidation of 1,2,3,4-tetrahydrocarbazole in the presence of trace amounts of iron (III) is proposed to involve a non-free radical chain mechanism. This mechanism was designed as electron transfer initiated oxidation (ETIO). The characteristics of this reaction are discussed. GRA

N90-11837# Argonne National Lab., IL.
ANALYTICAL STUDIES OF THREE-DIMENSIONAL COMBUSTION PROCESSES Final Report, Dec. 1982 - Sep. 1988
S. Pratap Vanka May 1989 243 p
(Contract FY1455-88-N0617; AF Proj. 2308)
(AD-A211903; AFWAL-TR-88-2140) Avail: NTIS HC A11/MF A02 CSCL 21/5

This report summarizes the significant contributions from a research program sponsored at Argonne National Laboratory by the Air Force Wright Aeronautical Laboratories, Advanced Propulsion Division. The objectives of this study were to develop advanced computational techniques and physical models for calculating the multidimensional flow and combustion process in subsonic ramjet and ducted rocket configurations. A number of significant accomplishments were made during the course of this study. These include: (1) development of efficient solution techniques for subsonic, elliptic fluid flows; (2) application and assessment of the two-equation turbulence model to swirling and nonswirling flows in a sudden expansion geometry; and (3) analysis of combustion processes in a prototypical ducted rocket configuration. GRA

N90-11838# Harvard Univ., Cambridge, MA.
SELF-ASSEMBLED ORGANIC MONOLAYER FILMS Final Report
15 Aug. 1989 8 p
(AD-A212006) Avail: NTIS HC A02/MF A01 CSCL 07/3

This project comprised three components, all relevant to organic surface chemistry: (1) Polymer Surface Functionalization. This research has developed a comprehensive surface chemistry for surface-oxidized low-density polyethylene film, and used the resulting surface-functionalized materials to define the stability and properties of this class of materials. (2) Self-Assembled Organic Monolayer Films. This work has tested methods for making several classes of self-assembled organic monolayer films, and has examined the structure of these films using a range of spectroscopic techniques (especially x ray photo electron spectroscopy, polarized reflectance infrared spectroscopy, and low-angle x ray reflection). The best ordered monolayers (which are quasi 2-D crystals) are obtained by reaction of alkyltrichlorosilanes on silicon or chemisorption of alkanethiols on gold. (3) Physical-Organic Chemistry of Wetting. Wetting has been extensively explored as a probe of surface structure and composition. It has useful characteristics that complement the spectroscopic methods: it is very sensitive to surface structure, and responds only to the top approx. 5 A of the surface; it is applicable to the solid-liquid interface; it is inexpensive to study. A reasonably sound understanding of static wetting at equilibrium is now in hand; the kinetics of wetting are still being explored. GRA

N90-11839# Helsinki Univ. of Technology, Espoo (Finland). Electromagnetics Lab.
EFFECTIVE PERMEABILITY OF MIXTURES
Ari H. Sihvola and Ismo V. Lindell Feb. 1989 31 p
(PB89-218952; Rept-43; ISBN-951-754-803-6) Avail: NTIS HC A03/MF A01 CSCL 07D

Macroscopic modeling of magnetically heterogeneous materials is reviewed. The emphasis is on mixing formulae that give the effective permeability of a mixture as a function of the component permeabilities, their volume fractions, and the internal structure. Much of the analysis is based on the duality of the electrostatic and magnetostatic problems, which allows the use of dielectric mixing formulae for magnetic mixtures. The low-frequency limitation in applying mixing formulae is that the wavelength of the incident field be smaller than the sizes of the inclusions in the mixture. How to treat losses through mixing rules is also discussed, and different loss mechanisms typical to magnetically non-neutral media are given attention. Author

N90-11840# Iowa Univ., Iowa City. Chemical Research, Development, and Engineering Center.
IMPROVED PATTERN RECOGNITION TECHNIQUES FOR REAL TIME OPERATION Report, Apr. 1986 - Aug. 1988
Gary W. Small May 1989 50 p
(Contract DAAA15-86-C-0034)
(AD-A211395; CRDEC-CR-030) Avail: NTIS HC A03/MF A01 CSCL 15/3

Passive Fourier transform infrared remote sensors have shown tremendous potential for use in the automated detection of atmospheric pollutants. To be maximally effective as an early warning alarm device, however, passive infrared sensors must be able to operate in a variety of infrared backgrounds and under conditions in which the background is rapidly changing. For economic reasons, the sensor should be the simplest device that can meet the aforementioned operational requirements. In the work described here, new signal processing strategies have been developed that allow target chemical species to be detected directly from time-domain infrared data. This methodology eliminates the Fourier transform computation through the development of digital filters keyed to the characteristic infrared frequencies of the target molecules. Through this approach, both the computational and instrumental requirements for the sensor are significantly reduced. The performance of this methodology will be illustrated with a variety of test data. GRA

N90-11841# Pennsylvania State Univ., University Park.
PREMIXED TURBULENT FLAME PROPAGATION Annual Report, 1 Nov. 1987 - 31 Oct. 1988
D. A. Santavicca 10 Apr. 1989 46 p
(Grant AF-AFOSR-0097-87; AF Proj. 2308)
(AD-A211489; AFOSR-89-1183TR) Avail: NTIS HC A03/MF A01 CSCL 21/2

An experimental study has been conducted of turbulence-flame interactions in premixed turbulent flames and their effect on flame-generated turbulence, flame structure and flame propagation. The flame configuration used for this study is that of a freely propagating, one-dimensional (in the mean) turbulent flame which is free of the flame stabilization, free stream shear, and post-flame flow restriction effects of other flame configurations. Flame-generated turbulence has been studied in an atmospheric pressure, propane-air flame at one turbulence condition, where LDV measurements of the mean velocity, turbulence intensity, time scale, energy spectrum, length scale and Reynolds stress have been made as a function of time through the propagating flame front. A three-fold increase in the density weighted turbulent kinetic energy across the flame front is observed. Based on a comparison with similar results from other experiments, this result suggests that the heat release parameter has a greater effect on flame-generated turbulence than the turbulence intensity to laminar flame speed ratio. A heuristic model has been developed which accurately predicts the observed variation in flame structure fractal dimension based on the competition between turbulence which acts to convectively distort the flame surface and burning which acts to smooth the flame surface. GRA

N90-11842# George Washington Univ., Washington, DC. Dept. of Chemistry.
QUANTITATIVE INTERPRETATION OF AUGER LINESHAPES AND ELECTRON/PHOTON STIMULATED DESORPTION Final Report, 1 Jul. 1980 - 31 Mar. 1989
David E. Ramaker 18 Aug. 1989 16 p
(Contract N00014-80-K-0852; RR013)
(AD-A211550) Avail: NTIS HC A02/MF A01 CSCL 07/4

This project has involved a quantitative theoretical interpretation of electron spectroscopic data with a view toward elucidating the chemical environment and electronic structure of atoms in the bulk and adsorbed on solid surfaces. Many-body effects, such as shake satellites, initial core hole screening, and final state hole-hole correlation, etc., have been examined and found to have significant effects on the spectral lineshapes. We have more recently examined electron spectroscopic data for the high temperature superconductors, and for chemisorbed species on metals. Electron/photon stimulated desorption (ESD/PSD) was also of interest. Here, an interpretation of spectroscopic data and comparison with PSD spectral yields was very helpful in obtaining an understanding of the image charge, surface resonances, polarization, and the role of many-body interactions in the desorption mechanism itself. GRA

N90-11843# Minnesota Univ., Minneapolis. Dept. of Chemical Engineering and Materials Science.
EFFECT OF ELECTRICAL DOUBLE LAYER ON TRANSPORT LIMITED CURRENTS AT MICROELECTRODES
John D. Norton, Henry S. White, and Stephen W. Feldberg (Brookhaven National Lab., Upton, NY.) Jul. 1989 35 p
Submitted for publication
(Contract N00014-87-K-0494)
(AD-A211586; TR-6) Avail: NTIS HC A03/MF A01 CSCL 07/4

An analysis of transport of charged and uncharged species associated with a steady-state faradaic process at a spherical microelectrode is reported. Systems comprising various relative concentrations of a redox species are examined and, if charged, its counter ion, and an inert electrolyte. Of particular interest is the behavior of these systems when the thickness of the diffuse double layer (characterized by the Debye length, 1/kappa) and the radius of the electrode (r sub 0) are comparable. Transport of each species is assumed to be governed by the Nernst-Planck equation. A generalized solution obtained using finite-difference simulations demonstrates that significant enhancement or inhibition of the steady-state flux can occur and will depend upon the dimensionless parameter r(sub 0)kappa, upon the relationship between the applied potential, the formal redox potential (Eo'), and the potential of zero charge, and upon the charges and relative concentrations of the species in solution. Analytic solutions for several limiting cases are discussed and serve as simple expositions of the phenomena as well as a verification of the simulations. In infinitely dilute ionic solutions, the limiting flux of ionic species may be computed directly from the Smoluchowski-Debye theory for ionic bimolecular reaction rates. GRA

N90-11844# Dartmouth Coll., Hanover, NH. Dept. of Chemistry.
SYNTHESIS AND CHEMISTRY OF STRAINED AND CONJUGATED FLUOROCARBONS Final Report, 1 Apr. 1986 - 31 Mar. 1989
David M. Lemal 20 Jul. 1989 16 p
(Grant AF-AFOSR-0130-86; AF Proj. 2303)
(AD-A211633; AFOSR-89-1098TR) Avail: NTIS HC A03/MF A01 CSCL 07/3

The chemistry of an array fluorocarbons and fluorocarbon derivatives was studied in order to further the understanding of fluorine as substituent in organic chemistry. Target molecules, all of which incorporated conjugation and/or strain, were chosen on the basis of unusual and/or interesting structural features. The synthesis of many new fluorocarbons and derived molecules was accomplished along with exploration of new synthetic methodology in fluorocarbon chemistry, determination of thermodynamic and kinetic parameters for fluorocarbon valence isomerizations, study of negative hyperconjugation, and examination of mechanisms of fluorocarbon reactions. Much was learned about how to synthesize perfluorinated annulenes and their relatives, and much information was acquired about potential energy surfaces for fluorocarbon valence isomerizations. A study of rotational barriers in alpha-fluoramines revealed that negative hyperconjugation can have powerful energetic consequences even in neutral molecules.

insights into fluorocarbon reaction mechanisms, both thermal and photochemical, have emerged from synthetic explorations as well as from explicitly mechanistic studies. GRA

N90-11845# Ohio State Univ., Columbus. Dept. of Chemistry.

MECHANISM OF ELECTROCHEMICAL ACTIVATION OF CARBON ELECTRODES: ROLE OF GRAPHITE LATTICE DEFECTS

Robert J. Bowling, Richard T. Packard, and Richard L. McCreery 1989 7 p Presented at the 196th Meeting of the American Chemical Society Symposium on Electrocatalysis, Los Angeles, CA, 27-29 Sep. 1988 Submitted for publication
(Grant AF-AFOSR-0071-88; AF Proj. 2303)
(AD-A211644; AFOSR-89-1146TR) Avail: NTIS HC A02/MF A01 CSCL 07/4

By use of Raman spectroscopy as a probe, the relationship between carbon microstructure and increases in the heterogeneous electron-transfer rate for carbon electrodes was examined. A distinctive Raman band at 1360 cm(-1) is proportional to the density of graphitic edge planes and may be used to monitor changes in edge plane density induced by carbon pretreatment procedures. It was shown that electrochemical oxidation of highly ordered pyrolytic graphite (HOPG) caused fracturing of the graphite lattice, thus increasing edge plane density. This result is consistent with other reports from laser activation of HOPG, which correlate increased edge plane density with increased electron-transfer rate. Creation of edge plane is a phenomenon common to both oxidative and nonoxidative activation procedures and is responsible for HOPG activation. Arguments about the involvement of graphitic oxide or oxygen containing functional groups in electron-transfer activation are presented. After the present results are combined with those from the literature, it appears unlikely the oxygen functional groups are involved in electron-transfer activation of several benchmark redox systems on carbon electrodes. GRA

N90-11846# Minnesota Univ., Minneapolis. Dept. of Chemical Engineering and Materials Science.

MOLECULAR DYNAMICS STUDY OF THE PRIMITIVE MODEL OF 1-3 ELECTROLYTE STUDIES

S. H. Suh, L. Mier-y-Teran, Henry S. White, and H. T. Davis Jul. 1989 31 p Submitted for publication
(Contract N00014-87-K-0494)
(AD-A211653; TR-4) Avail: NTIS HC A03/MF A01 CSCL 07/4

Molecular dynamics simulations at constant temperature were carried out for the primitive model of 1-3 electrolyte solutions. Thermodynamics, pair distribution functions, and self-diffusion coefficients were computed to examine the electrostatic effects on the structural and dynamical properties. The simulation results were used to evaluate various theoretical equations, namely, the hypernetted chain approximation. As was observed for symmetrically electrolytes, the latter turns out to be the best approximation. For asymmetrically charged 1-3 electrolytes, it was found that ionic aggregation significantly influenced the dynamical properties of electrolytes. Coherent motion between highly charged negative ions and positive ions surrounding them was deduced from the time dependence of the velocity autocorrelation functions, particularly at concentrations between 0.4 and 4 total molar. GRA

N90-11847# Cincinnati Univ., OH. Nanoelectronics Lab.

REACTIVE ION ETCHING OF SPUTTERED SILICON CARBIDE AND TUNGSTEN THIN FILMS FOR DEVICE APPLICATIONS Final Report

Wen-Sen Pan and Andrew J. Steck 1989 190 p
(Contract N00014-81-K-0605)
(AD-A211711) Avail: NTIS HC A09/MF A01 CSCL 07/2

For high temperature processing and device applications, refractory materials, such as silicon carbide (SiC) and tungsten (W), are actively considered or evaluated as the basic semiconductor and metallization materials for future generations of integrated circuits. In order to pattern fine lines in SiC and W thin films, a selective and anisotropic etching technique needs to be developed for future device applications. Therefore, the etching process including basic mechanisms and process requirement have been chosen as the overall research goals of this project. Reactive ion etching (RIE) of SiC thin films in a variety of fluorinated gas plasmas, such as SF6, CBrF3 and CHF3 mixed with oxygen has been investigated in depth. The best anisotropic profile was observed by using CHF3 gas in the RIE mode. A typical dc bias, -300V, is concluded from etching experiments to determine the dependence of SiC etch rate and physical reaction under RIE mode. Reactive ion etching of tungsten (W) thin film has also been investigated by using the different fluorinated gas plasmas, such as CF4, SF6, CBrF3 and CHF3 mixed with oxygen. The obtaining of anisotropic etching profile in W etching has been suggested and the mechanisms have also been studied. GRA

N90-11848# ESDU International Ltd., London (England).

VAPOUR PRESSURES AND CRITICAL POINTS OF LIQUIDS. HALOGENATED HYDROCARBONS

Apr. 1989 58 p
(ESDU-89006; ISBN-0-85679-677-8; ISSN-0141-4062) Avail: ESDU

This data item 89006, an addition to the Physical Data, Chemical Engineering Subseries, gives vapor pressure for 3-chloropropene and 25 bromo- and chloroalkanes. The data were obtained by a method described in ESDU 84021 involving a critical evaluation of experimental results in the literature, extrapolated by a reliable method into the low pressure region, and fitted by a Wagner equation applying over the full liquid range from the freezing to the critical point. The coefficients for the equation are given for each compound and three tables of vapor pressure values calculated using them are included: in SI units at 5 K and 10 K intervals, in atmospheres at 5 and 10 C intervals; and in lbf/sq in. at 10 F intervals. A table also gives the saturation temperature at various specified pressures, and indicates the possible uncertainty in the calculated values. The sources of the data for each compound are included. ESDU

26 METALLIC MATERIALS

Includes physical, chemical, and mechanical properties of metals, e.g., corrosion; and metallurgy.

N90-11849# Bureau of Mines, Albany, OR.

Fe-Ni-Cr ALLOYS FOR COATINGS AND ELECTROFORMS Report of Investigations, 1989

J. E. Allison, Jr. and G. R. Smith (Bureau of Mines, Washington, DC.) 1988 20 p
(PB89-195846; BUMINES-RI-9213; LC-88-600301) Avail: NTIS HC A03/MF A01 CSCL 11F

An aqueous electrodeposition method for preparing stainless-steel-type coatings was studied. Chromium powder (averaging 3 micrometers diam) was suspended in a ferrous-nickelous sulfate electroplating bath and occluded in the electrodeposited Fe-Ni alloy matrix. Subsequent heat treatment of the resulting composite coating formed the ternary alloy. The occlusion process was affected by the quantity of Cr powder suspended in the electrolyte and by the microstructure and composition of the electrodeposited matrix. Coatings containing up to 21 wt pct Cr were deposited from an electrolyte containing 20 vol pct suspended Cr powder. Heat treatment at 1,100 C for 8 h homogenized the composite coating. Deposition of 44Fe36Ni20Cr alloy coatings (250 micrometers thick) on AISI 1020 carbon steel rods, followed by heat treatment, provided complete protection of the carbon steel during exposure to a boiling 65-pct HNO3 solution. Corrosion rates of 0.6 plus or minus or minus 0.4 mm/yr for the coating in the boiling HNO3 approximate that of 304 stainless steel. Practically shaped electroforms have been prepared by the coating method. Author

N90-11850*# National Inst. of Standards and Technology, Boulder, CO. Chemical Engineering Science Div.
IGNITION CHARACTERISTICS OF THE NICKEL-BASED ALLOY UNS N07718 IN PRESSURIZED OXYGEN
James W. Bransford, Phillip A. Billiard, James A. Hurley, Kathleen M. McDermott, and Isaura Vazquez Apr. 1989 50 p
(NASA-CR-185932; NAS 1.26:185932; PB89-218333; NISTIR-89/3911) Avail: NTIS HC A03/MF A01 CSCL 11F

The development of ignition and combustion in pressurized oxygen atmospheres was studied for the nickel based alloy UNS N07718. Ignition of the alloy was achieved by heating the top. It was found that the alloy would autoheat to destruction from temperatures below the solidus temperature. In addition, endothermic events occurred as the alloy was heated, many at reproducible temperatures. Many endothermic events occurred prior to abrupt increases in surface temperature and appeared to accelerate the rate of increase in specimen temperature. It appeared that the source of some endotherms may increase the oxidation rate of the alloy. Ignition parameters are defined and the temperatures at which these parameters occur are given for the oxygen pressure range of 1.72 to 13.8 MPa (250 to 2000 psia). Author

N90-11851# Lawrence Livermore National Lab., CA.
X RAY DIFFRACTION PATTERNS OF METAL AUROCYANIDES
Walter S. Selig, Gordon S. Smith, Kerstin K. Harding, and Leslie J. Summers Jun. 1989 16 p
(Contract W-7405-eng-48)
(DE89-015188; UCID-21742) Avail: NTIS HC A03/MF A01

Aurocyanides of the following metal cations were prepared: Ag, Hg(II), Ga, Fe(III), Tl(I), Bi, Pb, Mn(II), Ni, Zn, Cu(II), Cd, In, and Co(II). Most of the aurocyanides are of the type M(Au(CN)2)(x) where M is the metal cation and x its valence. However, under some conditions mixed aurocyanides containing K may be formed, such as KCo(Au(CN)2)3. Only Ag and Hg(II) form aurocyanides which are sufficiently insoluble for the potentiometric determination of the aurocyanide anion. The diffraction patterns of the various aurocyanides are reported. DOE

N90-11852# Department of the Navy, Washington, DC.
ELEVATED TEMPERATURE ALUMINUM-TITANIUM ALLOY BY POWDER METALLURGY PROCESS Patent
William E. Frazier, inventor (to Navy) and Michael J. Koczak, inventor (to Navy) 30 May 1989 5 p Filed 29 Jan. 1988
(AD-D014165; US-Patent-4,834,942; US-Patent-Appl-SN-150122)
Avail: U.S. Patent and Trademark Office CSCL 19/6

An aluminum-titanium alloy and a process of making it are disclosed. The alloy consists essentially of aluminum, 4 to 6 wt. percent titanium, 1 to 2 wt. percent carbon, and 0.1 to 0.2 wt. percent oxygen. The alloy is an aluminum matrix supersaturated with titanium, and having throughout a fine, homogeneous dispersion of Al3T1 particles. It is fine grained and has grain boundary dispersion of carbides and oxides, predominantly of aluminum. An aluminum-titanium melt is rapidly solidified and then mechanically alloyed in the presence of a carbon-bearing agent. The resulting powder is degassed and hot consolidated to form articles which exhibit high strength, ductility, and creep resistance at temperatures greater than 200 C. GRA

N90-11853*# Case Western Reserve Univ., Cleveland, OH.
PRECIPITATION STRENGTHENED HIGH STRENGTH, HIGH CONDUCTIVITY Cu-Cr-Nb ALLOYS PRODUCED BY CHILL BLOCK MELT SPINNING Final Report Ph.D. Thesis
David L. Ellis and Gary M. Michal Sep. 1989 231 p
(Grant NGT-50087)
(NASA-CR-185144; NAS 1.26:185144) Avail: NTIS HC A11/MF A02 CSCL 11F

A series of Cu-based alloys containing 2 to 10 a/o Cr and 1 to 5 a/o Nb were produced by chill block melt spinning (CBMS). The melt spun ribbons were consolidated and hot rolled to sheet to produce a supersaturated Cu-Cr-Nb solid solution from which the high melting point intermetallic compound Cr2Nb could be precipitated to strengthen the Cu matrix. The results show that the materials possess electrical conductivities in excess of 90 percent that of pure Cu at 200 C and above. The strengths of the Cu-Cr-Nb alloys were much greater than Cu, Cu-0.6 Cr, NARloy-A, and NARloy-Z in the as-melt spun condition. The strengths of the consolidated materials were less than Cu-Cr and Cu-Cr-Zr below 500 C and 600 C respectively, but were significantly better above these temperatures. The strengths of the consolidated materials were greater than NARloy-Z, at all temperatures. The GLIDCOP possessed similar strength levels up to 750 C when the strength of the Cu-Cr-Nb alloys begins to degrade. The long term stability of the Cu-Cr-Nb alloys was measured by the microhardness of aged samples and the growth of precipitates. The microhardness measurements indicate that the alloys overage rapidly, but do not suffer much loss in strength between 10 and 100 hours which confirms the results of the electrical resistivity measurements taken during the aging of the alloys at 500 C. The loss in strength from peak strength levels is significant, but the strength remains exceptionally good. Transmission electron microscopy (TEM) of the as-melt spun samples revealed that Cr2Nb precipitates formed in the liquid Cu during the chill block melt spinning, indicating a very strong driving force for the formation of the precipitates. The TEM of the aged and consolidated materials indicates that the precipitates coarsen considerably, but remain in the submicron range. Author

N90-11854*# National Aeronautics and Space Administration. Lewis Research Center, Cleveland, OH.
CREEP STRENGTH OF NIOBIUM ALLOYS, Nb-1%Zr AND PWC-11 Final Report
Robert H. Titran 1989 10 p Prepared for presentation at the 7th Symposium on Space Nuclear Power Systems, Albuquerque, NM, 7-11 Jan. 1990; sponsored in part by New Mexico Univ.
(Contract DE-AI03-86SF-16310)
(NASA-TM-102390; E-5102; DOE/NASA/16310-13; NAS 1.15:102390) Avail: NTIS HC A02/MF A01 CSCL 11F

A study is being conducted at NASA Lewis Research Center to determine the feasibility of using a carbide particle strengthened Nb-1 percent Zr base alloy to meet the anticipated temperature and creep resistance requirements of proposed near term space power systems. In order to provide information to aid in the determination of the suitability of the PWC-11 alloy as an alternative to Nb-1 percent Zr in space power systems this study investigated: (1) the long-time high-vacuum creep behavior of the PWC-11 material and the Nb-1 percent Zr alloy, (2) the effect of prior stress-free thermal aging on this creep behavior, (3) the effect of electron beam (EB) welding on this creep behavior, and (4) the stability of creep strengthening carbide particles. Author

N90-11855# Technische Univ., Darmstadt (Germany, F.R.). Fachbereich Maschinenbau.
CREEP AND FRACTURE BEHAVIOR OF HEAT RESISTANT STEELS IN CHARACTERISTIC CASES OF VARIABLE FATIGUE LOADING Ph.D. Thesis [KRIECH- UND BRUCHVERHALTEN WARMFESTER STAEHLE IN KENNZEICHNENDEN FAELLEN VERAENDERLICHER ZEITSTANDBEANSPRUCHUNG]
Ad Kooy 1988 227 p In GERMAN
(ETN-89-94671) Avail: NTIS HC A11/MF A01

The creep behavior of several heat resistant steels is investigated under variable high-cycle loading conditions. The fatigue life under cyclic stress or temperature can be described by a modified lifetime part rule with an accumulation of life time parts. The average relative lifetime for all steels is found to be 0.67 under variable stress and 0.87 under variable temperature (two-valve concept). The measured and calculated lifetimes are shown to agree. The fatigue life under simultaneously variable stress and temperature can be estimated from the tests with only one variable parameter. During all the tests the creep behavior is measured and the creep curves are calculated. The results contribute to the data base for the design and control of high temperature components under variable fatigue loading conditions. ESA

N90-11856# Los Alamos National Lab., NM.
FORMATION AND MODIFICATION OF SURFACE ALLOYS BY EXCIMER LASER MELTING AND RESOLIDIFICATION
Thomas R. Jervis, Michael Nastasi, and Juha-Pekka Hirvonen 1989 15 p Presented at the Microelectronic Integrated Processing Conference, Santa Clara, CA, 8-13 Oct. 1989; sponsored by SPIE
(Contract W-7405-eng-36)
(DE89-016968; LA-UR-89-2930; CONF-8910197-1) Avail: NTIS HC A03/MF A01

The use of pulsed lasers operating in the ultra-violet for the formation and modification of metal alloys opens a range of processing techniques which offer the precision of ion beam techniques but at much higher processing rates. In addition, excimer laser surface processing offers the possibility of new surface modification technologies. Most metals have low reflectivities in the UV, so laser light is coupled strongly to the surface. The short pulse length of these lasers, along with a shallow absorption depth, results in a heated zone which is also quite shallow, of the order of 1 micrometer. Modest fluences, of the order of 1 J/sq cm are sufficient to melt this surface zone. Typical quench rates from the melt are of the order of 10(exp 10) K/sec; high enough to produce amorphous phases in some materials. Mixing by liquid phase diffusion between layers of vacuum evaporated materials and zone refinement can result from multiple melt resolidification events. These techniques make available a large range of alloy compositions on engineering materials. The surface morphology of the processed layers is quite smooth with a surface finish less than 100 nm. Further processing prior to use is therefore not required for most applications. We have studied laser mixing of metals into engineering materials, both metal alloys and ceramics, the formation of ceramic structures on metals, the modification of alloys by surface zone refinement, and the mixing of binary and ternary multilayer structures. DOE

N90-11857# Los Alamos National Lab., NM.
TEMPERATURE DEPENDENT EFFECTS DURING Ag DEPOSITION ON Cu(110)
T. N. Taylor, R. E. Muenchausen, M. A. Hoffbauer, A. W. DeniervanderGon, and J. F. vanderVeen (FOM-Inst. voor Atoomen Molecuulfysica, Amsterdam, Netherlands) 1989 20 p Presented at the 36th American Vacuum Society National Vacuum Symposium, Boston, MA, 23-27 Oct. 1989
(Contract W-7405-eng-36)
(DE89-016987; LA-UR-89-2808; CONF-891093-1) Avail: NTIS HC A03/MF A01

The composition, structure, and morphology of ultrathin films grown by Ag deposition on Cu(110) were monitored as a function of temperature using low energy electron diffraction (LEED), Auger electron spectroscopy (AES), and medium energy ion scattering (MEIS). Aligned backscattering measurements with 150 KeV He ions indicate that the Ag resides on top of the Cu and there is no significant surface compound formation. Measurements with LEED show that the Ag is initially confined to the substrate troughs. Further deposition forces the Ag out of the troughs and results in a split c(2 x 4) LEED pattern, which is characteristic of a distorted Ag(111) monolayer template. As verified by both AES and MEIS measurements, postmonolayer deposition of Ag on Cu(110) at 300K leads to a pronounced 3-D clustering. Ion blocking analysis of the Ag clusters show that the crystallites have a (110)-like growth orientation, implying that the Ag monolayer template undergoes a rearrangement. These data are confirmed by low temperature LEED results in the absence of clusters, which indicate that Ag multilayers grow from a Ag--Cu interface where the Ag is captured in the troughs. Changes observed in the film structure and morphology are consistent with a film growth mechanism that is driven by overlayer strain response to the substrate corrugation. DOE

N90-11858# Oak Ridge National Lab., TN.
INTERNATIONAL SEMINAR ON THE INELASTIC BEHAVIOR OF SOLIDS: MODELS AND UTILIZATION Foreign Trip Report, 28 Aug. - 6 Sep. 1988
M. B. Ruggles 19 Sep. 1988 17 p
(Contract DE-AC05-84OR-21400)
(DE89-017420; ORNL/FTR-3036) Avail: NTIS HC A03/MF A01

The traveler attended the International Seminar on the Inelastic Behavior of Solids: Models and Utilization, and presented an invited paper. Development and validation of constitutive models for complex loading and environmental conditions was the principal subject of the seminar. Session 1. Constitutive Models: Theoretical Development, Analysis and Comparison, and Session 2. Constitutive Models: Experimental Identification and Use, were of particular interest to the ORNL constitutive equations development effort. The traveler also visited the Applied Mechanics Laboratory at the University of Franche-Comte in Besancon and the Laboratory of Mechanics and Technology at the ENSET/Paris University 6 in Cachan. In both laboratories the traveler held discussions regarding inelastic material behavior at room and elevated temperatures, exploratory testing and modeling, and materials testing equipment and techniques. DOE

N90-11859# Colorado School of Mines, Golden.
WELDABILITY OF DUCTILE NICKEL ALUMINIDES
M. C. Maguire, Glen R. Edwards, and S. A. David May 1989 185 p Prepared in cooperation with ORNL, TN
(Contract DE-AC05-84OR-21400)
(DE89-017452; ORNL/Sub-85-27421/03; MT-CWR-089-033) Avail: NTIS HC A09/MF A01

A study was conducted to characterize hot ductility and heat-affected zone (HAZ) cracking behavior as a function of microstructure for a series of Ni(sub 3)Al-based alloys. Slip path length was influenced by grain size and antiphase domain (APD) structures. Grain size was varied by isothermal annealing, and APD structures were produced by oil quenching from temperatures above the ordering transition temperature. The ordering temperature was lowered by adding up to 8 at. pct chromium to a Ni(sub 3)Al+Hf+B alloy. Hot ductility and weldability correlated with grain size and antiphase domain (APD) size. Grain refinement and APD structures reduced slip path lengths and improved hot ductility. In general, hot ductility increased in high chromium alloys, and the highest ductility was observed in alloys with extensive APD structures. A model was developed to describe how a disordered skin at an antiphase domain boundary (APDB) influenced dislocation motion and reduced slip path length. HAZ cracking susceptibility was characterized by performing full penetration autogenous electron beam welds on 0.76 mm sheet. Welds with higher chromium content were less prone to HAZ cracking during welding, and slower welding speeds minimized cracking tendency in all alloys. DOE

N90-11860# Brookhaven National Lab., Upton, NY. Dept. of Physics.
ELECTRONIC STRUCTURE OF TRANSITION METAL ALLOYS AND INTERMETALLICS: CHARGE TRANSFER AND ITS IMPLICATIONS FOR MOESSBAUER EFFECT MEASUREMENTS
R. E. Watson, J. W. Davenport, M. Weinert, and G. W. Fernando 1989 19 p Presented at the International Conference on the Applications of the Mossbauer Effect (ICAME '89), Budapest, Hungary, 4-8 Sep. 1989
(Contract DE-AC02-76CH-00016)
(DE89-017603; BNL-43052; CONF-890933-2) Avail: NTIS HC A03/MF A01

The Moessbauer effect provides several measures of charge transfer and bonding effects in compounds, namely in its measured quadrupole fields and isomer shifts. The isomer shifts offer a unique sampling of such transfer and these shifts will be juxtaposed against other experimental measures. Charge transfer estimates obtained in electronic structure calculations for transition metal alloys are inspected in light of known isomer shift trends and the competing contributions to charge transfer are elucidated. DOE

N90-11861# Lawrence Livermore National Lab., CA.
A RATE-DEPENDENT CONSTITUTIVE MODEL FOR Be
Daniel J. Steinberg Jul. 1989 4 p Presented at the American Physical Society Topical Conference on Shock Compression of

Condensed Matter, Albuquerque, NM, 14-17 Aug. 1989
(Contract W-7405-eng-48)
(DE89-017755; UCRL-101616; CONF-890812-45) Avail: NTIS HC A01/MF A01

The Steinberg-Guinan-Lund rate dependent constitutive model for BCC metals was extended to the HCP metal Be. Computer simulations with this model correctly predict a number of time resolved shock wave experiments. However, the model does not reproduce all the yield strength data at low strain rates. These discrepancies could be due to the different material properties in the different experiments, or simply to limitations of the model. DOE

N90-11862# General Electric Co., Schenectady, NY. Corporate Research and Development Center.
DEFORMATION AND DEFECTS IN LAVES-PHASE INTERMETALLIC COMPOUNDS Final Report, 1 Apr. 1987 - 29 Sep. 1989
James D. Livingston 1989 66 p
(Contract DE-FG02-87ER-45296)
(DE89-017798; DOE/ER-45296/2) Avail: NTIS HC A04/MF A01

Most studies of deformation in intermetallic compounds have been on compounds such as Ni(sub 3)Al, NiAl, and Ti(sub 3)Al whose crystal structures are ordered forms of the basic fcc, bcc, and hcp structures. Most intermetallics have more complex structures, and we have chosen to study the largest class of such compounds, the Laves phases, on which information on deformation and mechanical properties is very limited. The approach was to couple basic mechanical property measurements on representative binary and ternary Laves phase with TEM studies of deformation-induced defects. Effects of temperature and strain rate on flow stress in compression were determined for the prototype cubic (C15) Laves phase MgCu(sub 2). More limited but related data were gathered for hexagonal (C14) MgZn(sub 2), dihexagonal (C36) MgNi(sub 2), and two higher-temperature Laves phase, ZrFe(sub 2) (C15) and TiFe(sub 2)(C14). Effects of stoichiometry were studied in ZrFe(sub 2+x) and TiFe(sub 2+x). Extensive studies by TEM showed the dominant slip systems in C15 and C14 phases, and the deformation-induced dislocation structures, are analogous to those in fcc and hcp metals. Significant solution hardening was demonstrated in C15 Mg(Cu, M)(sub 2), where M = Al,Ni,Si, and Zn. The compositional dependence of solution hardening was characterized in MgCu(sub 2(minus)x)Zn (sub x), and limited data indicated solution hardening in both C15 and C14 (Zr, Ti)Fe(sub 2) compounds. DOE

N90-11863# Brookhaven National Lab., Upton, NY. Dept. of Physics.
NEUTRON SCATTERING STUDIES OF PREMARTENSITIC PHENOMENA
S. M. Shapiro 1989 13 p Presented at the International Conference on Martensitic Phase Transformations, Sydney, Australia, 3-7 Jul. 1989
(Contract DE-AC02-76CH-00016)
(DE90-000025; BNL-43179; CONF-8907114-2) Avail: NTIS HC A03/MF A01

Elastic neutron diffraction and inelastic neutron scattering are ideal techniques for studying premartensitic behavior in metallic alloys. By necessity, real, bulk samples are probed replete with their intrinsic defects. Also, because of the properties of the neutron it is straightforward to probe the behavior of the phonon modes away from the zone center which is probed in the normal ultrasonic techniques. A wide variety of alloys exhibiting martensitic transformations have been studied. It will be shown that most systems undergoing diffusionless transformations exhibit premartensitic behavior in that precursor effects are seen at temperatures well above the matensitic transformation temperature, T(sub M). This behavior manifests itself in an anomalous temperature dependence of the energy of a particular phonon mode as the temperature approaches T(sub M). The wavevector of this mode is frequently away from the zone center (i.e., q (ne) O). This softening is nearly always accompanied by elastic diffuse scattering at the same wavevector. Particular examples to be discussed are the alkali metals, (omega)-phase materials and Ni-based alloys. DOE

N90-11864# Westinghouse Hanford Co., Richland, WA.
FRACTURE TOUGHNESS DATA BASE FOR HT9 AND MODIFIED 9Cr-1Mo IRRADIATED IN SEVERAL REACTORS UP TO APPROXIMATELY 100 dpa
F. H. Huang and M. L. Hamilton (Pacific Northwest Lab., Richland, WA.) Jul. 1989 17 p Submitted for publication
(Contract DE-AC06-87RL-10930)
(DE90-000111; WHC-SA-0667) Avail: NTIS HC A03/MF A01

The purpose was to determine the fracture toughness behavior of HT9 and modified 9Cr-1Mo ferritic steels after neutron exposure to high doses. A summary is presented of the entire fracture toughness database for HT9 and 9Cr-1Mo generated at Hanford. Fracture toughness tests were recently performed on miniature specimens of HT9 and modified 9Cr-1Mo irradiated in FFTF to exposures ranging from 35 to about 100 dpa. At test temperatures ranging from 20 to 430 C values of toughness and tearing modulus at 35 to 100 dpa were no lower than those obtained previously in tests conducted on specimens irradiated in EBR-2, despite differences in orientation between the EBR-2 and FFTF specimens. DOE

N90-11865# California Univ., Berkeley. Lawrence Berkeley Lab. Materials and Chemical Sciences Div.
THE EFFECTS OF TEMPERATURE ON FATIGUE CRACK PROPAGATION IN 310 AUSTENITIC STAINLESS STEEL
Z. Mei, J. W. Chan, and J. W. Morris, Jr. (California Univ., Berkeley.) Jul. 1989 13 p Presented at the International Cryogenic Materials Conference, Los Angeles, CA, 24-28 Jul. 1989
(Contract DE-AC03-76SF-00098)
(DE90-000136; LBL-27375; CONF-890701-7) Avail: NTIS HC A03/MF A01

The fatigue crack propagation rate of 310 austenitic stainless steel was measured at 298 K, 77 K, and 4 K. As temperature decreased the fatigue crack growth rate decreased while the threshold stress intensity increased. At all three temperatures the fatigue crack propagated in a quasi-cleavage mode along a zigzag path. The propagating crack branched to an extent that increased as the temperature decreased. Since no martensite was detected on the crack surfaces and the crack surfaces were smoother at lower temperatures, neither transformation toughening nor roughness-induced crack closure can account for the temperature dependence of the crack growth rate. Various factors that might contribute to the temperature dependence are discussed. DOE

N90-11866# Naval Research Lab., Washington, DC.
LOW TEMPERATURE FORMATION OF TITANIUM ALUMINIDE FILMS USING PHYSICAL VAPOR DEPOSITION Progress Report, May 1987 - Nov. 1988
D. K. Perkins, E. I. Keith, A. Pattnaik, and W. F. Henshaw (Cordec Corp., Lorton, VA.) 21 Aug. 1989 14 p
(AD-A211877; NRL-MR-6393) Avail: NTIS HC A03/MF A01 CSCL 11/6

The crystallization of the two intermetallic phases, alpha 2 and beta, which form in Ti3Al alloyed with Nb was investigated in films deposited using direct current magnetron sputtering. Phase formation was studied in post-deposition annealed films as well as in films deposited on heated substrates. Analysis was carried out using x ray diffraction, scanning electron microscopy, and scanning Auger microprobe analyses. The oxygen content of films formed on heated substrates was 6 at. percent, which is considerably lower than the 26 at. percent oxygen content of post-deposition annealed films. This difference in the oxygen content is postulated to be a result of the microstructural differences in the films. Formation of the intermetallic phases in the films begins at approximately 100 C. GRA

N90-11867# Massachusetts Inst. of Tech., Cambridge. Dept. of Materials Science and Engineering.
KINETIC PROCESSES IN ADVANCED ALLOYS Final Report, 7 Sep. 1986 - 30 Sep. 1987
Kenneth C. Russell 30 Jun. 1989 92 p
(Contract F33601-87-M-3028; AF Proj. 2418)
(AD-A212049; WRDC-TR-89-4051) Avail: NTIS HC A05/MF A01 CSCL 11/6

A study was made of kinetic processes in advanced alloys, in particular prediction of terminal solid solubility extension and grain size in rapidly solidified alloys, and dispersoid formation, stability, and interaction with interfaces. Existing criteria for predicting terminal solid solubility extension were found inadequate. A new criterion based on the Miedema coordinates of electron potential and density was found to have excellent predictive power for Al-based alloys and to show promise for Mg-based and Ti-based alloys. A simple model was developed which for the first time allows easy prediction of grain size in rapid massive solidification of alloys. The model is in agreement with most existing data on massively rapidly solidified (RS) pure metals and alloys. Equations are derived for stability of compound dispersoid particles against coarsening and against dragging by grain boundaries. GRA

N90-11868# Martin Marietta Labs., Baltimore, MD.
A STUDY OF THE HOT WORKABILITY OF Al-8.5 WT PCT Mg ALLOYS FOR ARMOR PLATE APPLICATIONS Final Report, May 1985 - Jan. 1989
Joseph R. Pickens and Frank H. Heubaum Jan. 1989 67 p
(Contract DAAG46-85-C-0034)
(AD-A211680; MML-TR-894(C); MTL-TR-89-3) Avail: NTIS HC A04/MF A01 CSCL 11/6

Hot-torsion tests were conducted to examine the hot workability of standard and enhanced purity Al-8.5 wt percent Mg ingots in both the as-cast and homogenized conditions. The enhanced purity variant showed substantially higher hot ductilities at all homogenization and deformation temperatures investigated with no change in equivalent tensile flow stress. The optimum homogenization practice consists of two stages, namely stage-1 for greater than 5 h at 427 C (800 F) plus greater than 6 h at 482 C (900 F) which provides an equivalent tensile strain-to-failure of approximately 3 as opposed to 1 in the as-cast condition at a strain rate of 0.1/s. The optimal strain rate for hot working this Al-8.5 wt percent Mg alloy is considerably lower than the nominal 1.2/s typically used in commercial practice for many other Al-Mg alloys. In particular, a strain rate between approximately 0.1 and 0.01/s gives the highest measured strain-to-failure for the alloys containing 0 and 2 ppm sodium. High strain rates and/or higher deformation temperatures promote a brittle quasi-cleavage fracture morphology that reflects the alloy's low ductility under these normal commercial hot-working conditions. A rolling trial using laboratory-scale ingots was successfully conducted with minimal edge cracking using the parameters determined from the hot-torsion tests. GRA

N90-11869# Naval Civil Engineering Lab., Port Hueneme, CA.
COATING GALVANIZED STEEL Final Report, Sep. 1982 - Oct. 1985
R. W. Drisko Jun. 1989 29 p
(AD-A211775; NCEL-TN-1794) Avail: NTIS HC A03/MF A01 CSCL 11/3

An experiment was conducted to determine the factors that contribute to deterioration on coatings on galvanizing and how to obtain better coating performance. Variables included six surface treatments, two weathering variations, and five chemical compositions. Coating properties measured were initial bonding to galvanizing and salt fog resistance. Significant conclusions were: (1) wash priming improved both bonding strength of coatings to unweathered galvanizing and salt fog resistance of coatings to both weathered and unweathered galvanizing (no other surface treatment was beneficial), (2) weathering of the galvanizing before coating generally reduced bonding but improved salt fog resistance, (3) the epoxy system performed best of all and did not require wash priming for good performance, and (4) the zinc chromate primer improved salt fog resistance of the alkyd system, but the zinc dust/zinc oxide primer did not. GRA

N90-11870# ESDU International Ltd., London (England).
EFFECT OF FRETTING ON FATIGUE STRENGTH OF ALUMINIUM ALLOYS Abstract Only
Mar. 1989 41 p
(ESDU-89004; ISBN-0-85679-675-1; ISSN-0141-4089) Avail: ESDU

ESDU 89004 presents, in sixteen graphs, plots of stress versus endurance for the results extracted from the literature of over 500 fretting fatigue tests on six alloys. The data allow the effects of clamping pressure and slip amplitude to be seen. Various surface coatings and treatments were used in the tests to try to reduce fretting fatigue, and their effects can be compared. Some tests were made under variable amplitude loading and others in an artificial sea water environment although the majority were in room temperature air. Most of the data related to specimens of identical alloy in mutual slip, but some are for steel, brass or copper sliding against the aluminium alloy, and allow any effect due to the use of different materials to be seen. Each graph is accompanied by a table giving details of the alloy composition and treatment, the testing arrangements and surface treatments applied, and the mechanical properties of the alloy. Author

N90-11871# Technische Hochschule, Darmstadt (Germany, F.R.). Fachbereich Maschinebau.
DETERMINATION AND DESCRIPTION OF THE LONG TERM CREEP BEHAVIOR OF HIGH TEMPERATURE GAS TURBINE MATERIALS Ph.D. Thesis [ERMITTLUNG UND BESCHREIBUNG DES LANGZEITKRIECHVERHALTENS HOCHWARMFESTER GASTURBINENWERKSTOFFEE]
Herbert Bartsch 1985 245 p In GERMAN
(ETN-89-94985) Avail: NTIS HC A11/MF A01

Fatigue tests are performed on typical high temperature gas turbine materials to improve the knowledge of the long term creep behavior. Nickel precision-cast alloys, nickel wrought alloys, and a cobalt alloy, are tested for operational stresses and strains at main utilization temperatures. Additional annealing tests are made to determine the material-specific structural contraction, as well as hot tensile tests to describe the elastoplastic short term behavior. The results improve substantially the knowledge of the long term creep behavior of important gas turbine materials and hence contribute to the improvement of the design and control of high temperature gas turbine components. ESA

N90-11872# Aeritalia S.p.A., Turin (Italy).
THE EVOLUTION OF LIGHT ALLOYS IN THE AEROSPACE INDUSTRY [L'EVOLUZIONE DELLE LEGHE LEGGERE NELL'INDUSTRIA AEROSPAZIALE]
G. Arstento, F. Boschetti, and M. Scolaris 1987 17 p In ITALIAN Presented at the Convegno Associazione Italiana di Metallurgia, Milan, Italy, 3-5 Nov. 1987
(ETN-89-95216) Avail: NTIS HC A03/MF A01

The characteristics of the light alloys used as aircraft construction materials are compared with those available in the past. Studies on the effect of chemical composition and thermal treatments to improve crack propagation and corrosion resistance characteristics are described. The economic factors considered in selection are discussed. ESA

N90-11873# Deutsche Forschungs- und Versuchsanstalt fuer Luft- und Raumfahrt, Cologne (Germany, F.R.). Abteilung Metallurgie.
SIGNIFICANCE OF OXIDE SKINS ON POWDER FOR THE QUALITY OF PM Al MATERIAL Ph.D. Thesis - Technische Hochschule, Aachen
Hugo Schlich Apr. 1989 146 p In GERMAN; ENGLISH summary Report will also be announced as translation (ESA-TT-1178)
(DFVLR-FB-89-11; ISSN-0171-1342; ETN-89-95308) Avail:

NTIS HC A07/MF A01; DFVLR, VB-PL-DO, Postfach 90 60 58, 5000 Cologne, Federal Republic of Germany, 52 deutsche marks

Surface oxide layers (oxides, hydroxides and adsorbates) on atomized aluminum powder are conditioned by degassing. Measurements are made in order to optimize the degassing treatment. The composition and compound states are characterized before and after degassing. In degassed and consolidated powder, less internal defects caused by oxide and hydroxide skins are found. This is due to desorption of adsorbates and dehydration of hydroxides by degassing and to consolidation in vacuum. ESA

N90-11874# Rolls-Royce Ltd., Derby (England).
ALUMINIUM ALLOY DEVELOPMENT FOR AERO ENGINES
David Driver 1 Sep. 1987 6 p
(PNR90548; ETN-89-95545) Copyright Avail: NTIS HC A02/MF A01

The present and potential uses of different aluminium alloys in making aero engines is discussed. The benefits and drawbacks of aluminum-copper alloys, aluminum-zinc-magnesium alloys, cast aluminum-copper alloys, wrought aluminum-copper alloys and miscellaneous aluminum alloys are presented. The experience of Rolls Royce in testing and using such alloys is discussed. An itemized list of miscellaneous aluminum alloys is given. ESA

N90-11875# Royal Aerospace Establishment, Farnborough (England).
DEFORMATION OF Ti-6Al-4V BAR AND EXTRUSION UNDER SUPERPLASTIC FORMING CONDITIONS
D. V. Dunford and P. G. Partridge 29 Jul. 1988 8 p Presented at the International Conference on Superplasticity and Superplastic Forming, Blaine, WA, 1-4 Aug. 1988
(RAE-TM-MAT/STR-1110; BR108283; ETN-89-94203) Copyright Avail: Defence Research Information Centre, Kentigern House, 65 Brown Street, Glasgow, G2 8EX, Scotland

Tests were carried out to compare the superplasticity of Ti-6Al-4V bar and extrusion with that reported for sheet. The flow stresses, m-values, and plastic anisotropy were measured and related to the microstructure. Resulting anisotropy occurs in specimens machined both parallel and perpendicular to the extrusion major axis. Anisotropy also occurs in specimens machined perpendicular, but not parallel to the bar major axis. The anisotropy can be explained in terms of the directionality of the microstructure. It is concluded that for limited strains these conventional product forms, although having nonideal microstructures can be suitable for superplastic forming of components. ESA

N90-11876# Royal Aerospace Establishment, Farnborough (England).
DEFORMATION OF EXTRUDED TITANIUM ALLOYS UNDER SUPERPLASTIC CONDITIONS
D. V. Dunford and P. G. Partridge 29 Jul. 1988 9 p Presented at the 6th World Conference on Titanium, Cannes, France, 6-9 Jun. 1988
(RAE-TM-MAT/STR-1111; BR108112; ETN-89-94333) Copyright Avail: Defence Research Information Centre, Kentigern House, 65 Brown Street, Glasgow, G2 8EX, Scotland

The m-values, microstructure, and deformation behavior of an extruded U-channel section in IMI 550 and IMI 318 were studied under conditions that produce superplasticity in these alloys in thin sheet form. The results are compared with those obtained for bar and sheet. Results for bar and extruded material are similar. The flow stresses in the extruded alloys are greater by a factor 2 than those reported for sheet material and in both product forms the flow stresses are a factor 1.5 to 2 greater in the IMI 550 alloy at 870 C compared with IMI 318 alloy at 925 C. Although the pressure required for IMI 550 was greater, the lower forming temperature may reduce processing costs and subsequent heat treatment may lead to higher strength in the formed product compared with IMI 318 alloy. The m-value data for extruded material suggests more superplastic behavior would be obtained at strain rates lower than the 0.00008/sec used, which is 3 times slower than the superplastic forming rates used for titanium alloy sheet. Processing changes at the billet or extrusion stages can possibly produce a more equiaxed microstructure with a finer grain size. ESA

N90-11877# National Aerospace Lab., Amsterdam (Netherlands). Structures and Materials Div.
FRACTOGRAPHIC AND MICROSTRUCTURAL ANALYSIS OF FATIGUE CRACK GROWTH IN A Ti-6Al-4V FAN DISC FORGING
R. J. H. Wanhill, R. Galatolo (Pisa Univ., Italy), and C. E. W. Looije 30 Jun. 1988 30 p Presented at the AGARD-Coordinated Programme on Engine Disc Materials Sponsored in part by the Royal Netherlands Air Force
(NLR-MP-88028-U; ETN-89-95054) Avail: NTIS HC A03/MF A01

Fractographic and microstructural analyses of a solution treated and aged Ti-6Al-4V fan disc forging are presented. The crack growth process demonstrates many complex interrelated fracture features. A transition in the crack growth curve correlates with a change from structure-sensitive to continuum mode crack growth. A decrease in fracture surface roughness is seen. The significance of such transitions in predicting fatigue crack growth and service failure analysis is discussed. ESA

27 NONMETALLIC MATERIALS

Includes physical, chemical, and mechanical properties of plastics, elastomers, lubricants, polymers, textiles, adhesives, and ceramic materials.

For composite materials see *24 Composite Materials.*

N90-11878# Case Western Reserve Univ., Cleveland, OH. Dept. of Macromolecular Science.
SUPPRESSION OF SIDE CHAIN CRYSTALLIZATION AND TRANSFORMATION OF MONOTROPIC MESOPHASES INTO ENANTIOTROPIC MESOPHASES BY COPOLYMERIZATION OF THE PARENT POLYMERS' MONOMER PAIRS CONTAINING CONSTITUTIONAL ISOMERIC MESOGENIC SIDE GROUPS
V. Percec and D. Tomazos 21 Dec. 1988 23 p Submitted for publication
(Contract N00014-89-J-1828)
(AD-A209066; TR-24) Avail: NTIS HC A03/MF A01 CSCL 07/6

The synthesis and characterization of several copolymers based on the monomer pairs of nyl methacrylate (4-11-MA) and nyl methacrylate (4'-11-MA), nyl acrylate (4-11-AC) and nyl acrylate (4'-11-AC), and 8-(4-methoxy-(4'-oxy)-alpha-methylstilbene(octyl acrylate (4-8-AC) nd 8-(4-methoxy-(4'-oxy)-alpha-methylstilbene(octyl acrylate (4-8-AC) and 8-(4-oxy-(4'methoxy)-alpha-methylstilbene)octyl acrylate (4-8'-AC) are described. In the case of polymers with poly-methacrylate backbones, the copolymerization of the two constitutional isomeric mesogenic monomers cancels the side chain crystallization tendency characteristic of their parent homopolymers. Subsequently, the copolymer presents a broader mesophase temperature range than any of the two parent homopolymers. In the case of polymers with polyacrylate backbones, copolymerization suppresses the tendency towards side chain crystallization and subsequently, transforms one or even two monotropic mesophases into enantiotropic mesophases. GRA

N90-11879# Department of the Army, Washington, DC.
METHOD OF MODIFYING THE DIELECTRIC PROPERTIES OF AN ORGANIC POLYMER FILM Patent Application
Michael Binder, inventor (to Army) and Robert J. Mammone, inventor (to Army) 12 Jun. 1989 10 p
(AD-D014171; US-Patent-Appl-SN-374125) Avail: NTIS HC A02/MF A01 CSCL 07/6

This invention relates in general to a method of modifying the dielectric properties of an organic polymer film by ion implantation and in particular to such a method for modifying the dielectric properties of a film of a Poly-p-Xylylene formed by vapor deposition polymerization. Poly-p-Xylylenes, also known by their trade name of Parylene, are well known conformal coatings that are primarily used as insulators and isolators in electronics. These materials are interesting because of their ability to provide ultrathin films that conform to substrates of varied geometrical shapes and irregularities. GRA

N90-11880*# National Aeronautics and Space Administration. Lewis Research Center, Cleveland, OH.

PLASMA-DEPOSITED AMORPHOUS HYDROGENATED CARBON FILMS AND THEIR TRIBOLOGICAL PROPERTIES

Kazuhisa Miyoshi, John J. Pouch, and Samuel A. Alterovitz Oct. 1989 13 p Submitted for publication
(NASA-TM-102379; E-5118; NAS 1.15:102379) Avail: NTIS HC A03/MF A01 CSCL 11C

Recent work on the properties of diamondlike carbon films and their dependence on preparation conditions are reviewed. The results of the study indicate that plasma deposition enables one to deposit a variety of amorphous hydrogenated carbon (a-C:H) films exhibiting more diamondlike behavior to more graphitic behavior. The plasma-deposited a-C:H can be effectively used as hard, wear-resistant, and protective lubricating films on ceramic materials such as Si(sub 3)N(sub 4) under a variety of environmental conditions such as moist air, dry nitrogrn, and vacuum. Author

N90-11881*# National Aeronautics and Space Administration. Lewis Research Center, Cleveland, OH.

FUNDAMENTAL TRIBOLOGICAL PROPERTIES OF ION-BEAM-DEPOSITED BORON NITRIDE FILMS

Kazuhisa Miyoshi Oct. 1989 25 p Submitted for publication
(NASA-TM-102088; E-4850; NAS 1.15:102088) Avail: NTIS HC A03/MF A01 CSCL 11C

The adhesion, friction, and micromechanical properties of ion-beam-deposited boron nitride (BN) films are reviewed. The BN films are examined in contact with BN metals and other harder materials. For simplicity of discussion, the tribological properties of concern in the processes are separated into two parts. First, the pull-off force (adhesion) and the shear force required to break the interfacial junctions between contacting surfaces are discussed. The effects of surface films, hardness of metals, and temperature on tribological response with respect to adhesion and friction are considered. The second part deals with the abrasion of the BN films. Elastic, plastic, and fracture behavior of the BN films in solid-state contact are discussed. The scratch technique of determining the critical load needed to fracture interfacial adhesive bonds of BN films deposited on substrates is also addressed. Author

N90-11882*# Southwest Research Inst., San Antonio, TX.

SLIDING SEAL MATERIALS FOR LOW HEAT REJECTION ENGINES

Kevin Beaty, James Lankford, and Shannon Vinyard Jul. 1989 134 p Prepared in cooperation with Department of Energy, Washington, DC
(Contracts DEN3-352; DE-AI01-86CE-50162)
(NASA-CR-182262; NAS 1.26:182262; DOE/NASA/0352-3; SwRI-06-7963) Avail: NTIS HC A07/MF A01 CSCL 11A

Sliding friction coefficients and wear rates of promising piston seal materials were measured under temperature, environmental, velocity, and loading conditions that are representative of the low heat rejection (LHR) diesel engine environment. These materials included carbides, oxides, and nitrides. In addition, silicon nitride and partially stablized zirconia disks (cylinder liners) were ion-implanted with TiNi, Ni, Co, and Cr, and subsequently run against carbide pins (piston rings), with the objective of producing reduced friction via solid lubrication at elevated temperature. Friction and wear measurements were obtained using pin-on-disk laboratory experiments and a unique engine friction test rig. Unmodified ceramic sliding couples were characterized at all temperatures by friction coefficients of 0.24 and above during the pin-on-disk tests. The coefficient at 800 C in an oxidizing environment was reduced to below 0.1, for certain material combination, by the ion-implantation of TiNi or Co. This beneficial effect was found to derive from the lubricious Ti, Ni, and Co oxides. Similar results were demonstrated on the engine friction test rig at lower temperatures. The structural integrity and feasibility of engine application with the most promising material combination were demonstrated during a 30-hour single-cylinder, direct-injection diesel engine test. Author

N90-11883# Argonne National Lab., IL. Materials and Components Technology Div.

ION-ASSISTED DEPOSITION OF HIGH-TEMPERATURE LUBRICIOUS SURFACES

G. R. Fenske, A. Erdemir, R. A. Erck, C. C. Cheng, D. E. Busch, R. H. Lee, and F. A. Nichols 1989 32 p Presented at the Joint American Society of Mechanical Engineers/Society of Tribologists and Lubrication Engineers Tribology Conference, Ft. Lauderdale, FL, 16-19 Oct. 1989
(Contract W-31-109-eng-38)
(DE89-012397; CONF-891036-1) Avail: NTIS HC A03/MF A01

High-temperature lubricious surfaces or surface coatings are required in many applications. This paper describes a relatively new surface modification process termed ion assisted deposition, which is capable of forming lubricious layers that are extremely adherent to metallic and ceramic substrates. DOE

N90-11884# Oak Ridge National Lab., TN. Ceramic Science and Technology Div.

CURRENT RESEARCH IN ADVANCED MATERIALS Foreign Trip Report, 29 May - 3 Jun. 1989

D. F. Craig 19 Jun. 1989 15 p
(Contract DE-AC05-84OR-21400)
(DE89-017466; ORNL/FTR-3286) Avail: NTIS HC A03/MF A01

The International Conference on Evolution of Advanced Materials addressed current research in the areas of design, processing, ferrous and nonferrous alloys, ceramics, glasses, composites, and powder metallurgy materials. Technical papers were presented by researchers from 16 countries. The traveler presented an invited lecture on structural ceramics in the advanced materials world. DOE

N90-11885# National Inst. of Standards and Technology, Gaithersburg, MD.

PHOTOLITHOGRAPHY: A NEW TOOL FOR CERAMIC SCIENCE

Juergen Roedel and Andreas M. Glaeser (California Univ., Berkeley. Lawrence Berkeley Lab.) Jun. 1989 19 p Presented at the Spring Meeting of the Materials Research Society, San Diego, CA, 24-28 Apr. 1989
(Contract DE-AC03-76SF-00098)
(DE90-000135; LBL-27303; CONF-890426-29) Avail: NTIS HC A03/MF A01

A recently developed technique combining photolithography, ion beam milling, and hot pressing allows the production of submicron-scale controlled-geometry, controlled-crystallography pore structures in controlled misorientation bicrystals, single crystal-polycrystal ensembles, and polycrystal-polycrystal ensembles. Such microdesigned interfacial structures provide a new tool for studying fundamental aspects of microstructural evolution. Current applications of the technique, opportunities for future research, and future extensions and refinements of the technique are described. DOE

N90-11886# California Univ., Berkeley. Lawrence Berkeley Lab. Materials and Chemical Sciences Div.

DENSIFICATION OF PARTICULATE CERAMIC COMPOSITES: THE ROLE OF HETEROGENEITIES

Lutgard C. DeJonghe and Mohamed N. Rahaman (Missouri Univ., Rolla.) Aug. 1989 11 p Presented at the Spring Meeting of the Materials Research Society, San Diego, CA, 24-28 Apr. 1989
(Contract DE-AC03-76SF-00098)
(DE90-000177; LBL-27643; CONF-890426-30) Avail: NTIS HC A03/MF A01

Inert particulate inclusions in ceramic powder compacts can obstruct densification behavior significantly. The factors that are the causes of this decrease in the sinterability are reviewed. It is concluded that the origin of the sintering difficulty resides in defects that processes such as die compaction introduce during the initial forming of the composite powder compact. Alternative processing methods are suggested that should minimize the negative effects of the dispersed inclusion phase on densification. DOE

N90-11887# Optical Coating Lab., Inc., Dunfermline (Scotland).
VANADIUM DIOXIDE PROTECTIVE DEVICES Final Technical Report
J. S. Orr, H. Gordon, and H. Orr Jun. 1989 33 p
(Contract DAJA45-88-C-0037)
(AD-A212018; R/D-6060-EE-01) Avail: NTIS HC A03/MF A01 CSCL 11/3

This development contract has been carried out in order to answer the increasing requirement for protection of sensitive infrared detectors from pulsed laser radiation in the military environment. The objective of this project was to develop a protective device for use in the 8 to 12 micron wavelength region. The approach has been to exploit the well established optical properties of vanadium dioxide thin films in the infrared. The equipment and methods used to obtain thin films of vanadium dioxide for incorporation in protective devices are presented. A significant development effort has been directed at the inclusion of switching films in antireflection coatings for the 8 to 12 micron band. The subject of this contract was the development of vanadium dioxide optical switches. The aim was to further develop the reactive sputtering process for deposition of vanadium dioxide. Vanadium dioxide can now be deposited on germanium as well as silicon and has been fully characterized. The process stability, repeatability and the quality of the vanadium dioxide has been significantly improved. In particular the optical scatter has been reduced and the dynamic range has been increased. Devices incorporating vanadium dioxide have been manufactured to the required specification and indications are that the devices should fulfill their intended purpose. GRA

N90-11888# Washington Univ., Seattle. Dept. of Materials Science and Engineering.
STRUCTURE/REACTIVITY RELATIONSHIPS OF POLYSILAZANE PRECERAMICS
Kay A. Youngdahl, Jeffrey A. Rahn, Richard M. Laine, Richard A. Kennish, and Gilbert A. Balavoine 1988 8 p Submitted for publication
(Contract N00014-88-K-0305)
(AD-A212028; TR-18) Avail: NTIS HC A02/MF A01 CSCL 07/6

The structure/reactivity relationships of the polysilazanes -(H2SiNMe(x-) and -(MeHSiNH(x-) were examined to develop an understanding of the effects of structure on the composition of the ceramic product produced when these preceramic polysilazanes are pyrolyzed at 5 C/min under nitrogen to 900 C. The evolution of the precursors into amorphous ceramic mixtures was followed by thermogravimetric analysis, diffuse reflectance FTIR, and chemical analysis of intermediates formed during the transformation process. This paper will show how ceramic product selectivity is controlled by molecular structure. GRA

N90-11889# Army Lab. Command, Watertown, MA. Material Technology Lab.
FLEXURE STRENGTH OF ADVANCED CERAMICS: A ROUND ROBIN EXERCISE Final Report
George D. Quinn Jul. 1989 136 p
(AD-A212101; MTL-TR-89-62) Avail: NTIS HC A07/MF A01 CSCL 11/4

A mechanical testing round robin exercise was performed under the auspices of The Technical Cooperation Program (TTCP). TTCP is a collaboration between the defense establishments of Australia, Canada, New Zealand, the United Kingdom, and the United States. TTCP coordinates and shares results from research activities. The work reported was performed by panel P-TP-2, Ceramic Materials, and was concluded in 1987. Flexural strength at room temperature was measured for a sintered alumina and a reaction-bonded silicon nitride. These tests are relevant to advanced structural ceramics. The goal of the exercise was to determine if accurate and consistent results could be obtained by the participants using various test procedures. GRA

N90-11890# Duke Univ., Durham, NC. Dept. of Mechanical Engineering and Materials Science.
POSITRON ANNIHILATION STUDIES OF INTERPENETRATING POLYMER NETWORKS Final Report, 1 Jun. 1986 - 31 May 1989
Annand D. Kasbekar, Phillip L. Jones, and Andrew Crowson 23 Aug. 1989 6 p
(Contract DAAL03-86-C-0015)
(AD-A212162; ARO-23992.2-MA) Avail: NTIS HC A02/MF A01 CSCL 07/6

Positron annihilation lifetime spectroscopy was used to study thermal response and isothermal relaxation in two different molecular weight polystyrene samples over the temperature range of -20 C to 120 C. The lifetime and intensity of the ortho-positronium pickoff component were observed to vary systematically as a function of time, temperature, and molecular weight. A glass transition and secondary transition were detected in the thermal response data for both samples. PALS was also used to study the effects of physical crosslink density on free volume relaxation in polystyrene and polystyrene based interpenetrating polymer networks. The intensity of the o-Ps pickoff component was observed to vary in a consistent and predictable manner as a function of time, temperature, and crosslink density. GRA

N90-11891# Navy Clothing and Textile Research Facility, Natick, MA.
NEW FABRIC DEVELOPMENT PROGRAM Final Report, Dec. 1985 - May 1987
Ruth Tompkins, Roy Dillard, and Norman Audet Feb. 1989 73 p
(AD-A211549; NCTRF-170) Avail: NTIS HC A04/MF A01 CSCL 11/5

This report details an evaluation of potential candidate replacement fabrics for the Navy's 100 percent texturized polyester Certified Navy Twill (CNT) fabric for use in all L-1 and E-1 summer dress white uniforms and in E-1 dinner dress white and summer khaki uniforms. The Navy Clothing and Textile Research Facility (NCTRF) was directed by the Naval Military Personnel Command (NMPC) to conduct this study. GRA

N90-11892# Ceramatec, Inc., Salt Lake City, UT.
NEW MECHANISM FOR TOUGHENING CERAMIC MATERIALS Final Report, 15 Jul. 1987 - 14 Dec. 1988
Raymond A. Cutler and Anil V. Virkar (Utah Univ., Salt Lake City.) 19 May 1989 98 p
(Contract F49620-87-C-0077; DARPA Order 5994)
(AD-A211651; CERMATEC-8961701; AFOSR-89-1097TR) Avail: NTIS HC A05/MF A01 CSCL 11/2

It was determined if ferroelastic switching contributes to toughening in ceramic materials. Domain switching in ZrO_2 single crystals (heat treated to minimize transformation) at 1400 C was used to show that ferroelastic switching is a process which occurs at temperatures in excess of the monoclinic to tetragonal transformation temperature. These data, coupled with fracture toughness measurements of 8 MPa.m 1.2 at 1000 C, show that ferroelastic toughening has the potential for toughening at temperatures in excess of that possible by transformation toughening. Experiments on PZT, $SrZrO_3$ and $Gd_2(MoO_4)_3$ were used to show that ferroelastic switching can contribute to toughening. The time dependence of switching was demonstrated using PZT ceramics. Dopants were added to polycrystalline TZP materials in order to substantially increase their fracture toughness. In the case of SrO additions, strontium aluminate platelets, formed in-situ during sintering, contributed to toughness. GRA

N90-11893# Deutsche Forschungsanstalt fuer Luft- und Raumfahrt, Brunswick (Germany, F.R.). Inst. for Structural Mechanics.

AGING OF CFRP DUE TO LONGTERM STORAGE IN HEATED AIR

Harald Twardy (Deutsche Forschungs- und Versuchsanstalt fuer Luft- und Raumfahrt, Brunswick, Germany, F.R.) Feb. 1989 29 p Transl. into ENGLISH of Alterung von CFK bei Heissluftagerung im Langzeitversuch (Brunswick, Fed. Republic of Germany, DFVLR), Dec. 1987 31 p Original language document was announced as N88-27345
(ESA-TT-1124; DFVLR-FB-88-05; ETN-89-95390) Avail: NTIS HC A03/MF A01; original German version available from DFVLR, VB-PL-DO, Postfach 90 60 58, 5000 Cologne, Fed. Republic of Germany, 15.50 Deutsche marks

The long term aging of carbon fiber reinforced plastic (CFRP), in heated air, is investigated. The influence of environmental conditions such as temperature, humidity, oxygen and UV radiation are taken into account. The thermal aging of seven CFRP materials, in long term storage, and with simultaneous action of air and heat at 100C to 140C, are reported. Isothermal thermogravimetry is applied. The degree of irreversible degradation is determined. Strength measurements indicate the degree of irreversible degradation reached in long term storage. ESA

N90-11894# Defence Research Information Centre, Orpington (England).

DESIGN OF GLUED JOINTS, ELASTOPLASTIC ADHESIVES Progress Report

Maigret, Martin, and Menrath Nov. 1988 58 p Transl. into ENGLISH of Calcul des Assemblages Colles Adhesifs Elastoplastiques (Saint-Medard-en-Jalles, France, Aerospatiale), 1988
(DRIC-T-8168; SNIAS-NT-18926/AG-ET; BR108365; ETN-89-94328) Copyright Avail: Defence Research Information Centre, Kentigem House, 65 Brown Street, Glasgow, G2 8EX, Scotland

Experimental methods for defining the mechanical features of adhesives with elastoplastic properties and methods of calculation for analyzing the behavior of bonded joints are described. Tests of the properties of the adhesive HYSOL EA 9628 NW are described. Calculation methods using the finite element method are developed and the programs are presented. ESA

N90-11895 National Physical Lab., Teddington (England). Div. of Materials Applications.

A MODEL FOR LONG-TERM CREEP AND THE EFFECTS OF PHYSICAL AGEING IN POLY (BUTYLENE TEREPHTHALATE)

G. D. Dean, B. E. Read, and P. E. Tomlins May 1989 33 p
(NPL-DMA(A)-182; ISSN-0143-7313; ETN-89-95540) Copyright Avail: National Physical Lab., Teddington, Middlesex, TW11 0LW, United Kingdom

Creep data for poly butylene terephthalate (PBT) obtained for a range of elapsed times between quenching from 80 C and the start of the creep test is presented. The results enabled further developments to be made to a model which predicts the long term creep compliance in terms of parameters which can be determined from tests of short duration. In the case of PBT, the parameter which represents the distribution of retardation times in the mechanism responsible for creep deformation at long times cannot be determined from short term tests with sufficient accuracy to allow confident predictions of long time behavior. An alternative method is described for determining this parameter based on an analysis of long term tests. The relevance of the model to procedures for accelerated creep testing is discussed. ESA

28 PROPELLANTS AND FUELS

Includes rocket propellants, igniters, and oxidizers; their storage and handling procedures; and aircraft fuels.

For related information see also *07 Aircraft Propulsion and Power, 20 Spacecraft Propulsion and Power,* and *44 Energy Production and Conversion.*

N90-11896# Materials Research Labs., Ascot Vale (Australia).

A CRITICAL ASSESSMENT OF MODELS AVAILABLE FOR THE SHOCK INITIATION OF HETEROGENEOUS EXPLOSIVES

David A. Jones 1989 28 p
(MRL-TR-89-17; AR-005-707) Avail: NTIS HC A03/MF A01

Several recent models for the shock initiation of heterogeneous explosives are presented, concentrating on those models which have proved to be the most successful. Particular attention is given to models of specific interest to the Materials Research Laboratory (MRL), which are capable of simulating the effect of particle size on sensitivity, and can be readily incorporated into single phase hydrodynamic computer codes. Other models are also briefly considered. Recommendations are made regarding the suitability of some of these models for MRL use. Author

N90-11897# Los Alamos National Lab., NM.

SENSITIVITY RELATIONSHIPS IN ENERGETIC MATERIALS

C. B. Storm, J. R. Stine, and J. F. Kramer 1989 36 p Presented at the NATO Advanced Study Institute on Chemistry and Physics of Molecular Processes in Energetic Materials, Sicily, Italy, 2-15 Sep. 1989 Submitted for publication
(Contract W-7405-eng-36)
(DE89-016967; LA-UR-89-2936; CONF-8909182-2) Avail: NTIS HC A03/MF A01

In searching for new explosives one is most concerned with performance (detonation velocity and pressure), thermal properties, and sensitivity. Whether a new candidate explosive is ultimately widely used may well be determined by other factors, such as cost, toxicity, melting point, etc., but the initial research effort is guided by the trinity of performance, thermal stability, and sensitivity. This presents a difficult multifactoral problem in assessing the various molecular properties that contribute to each of these principal selection criteria. For instance, detonation velocity is affected by density, elemental composition, and heat of formation. These factors must be varied together in such a way as to maximize the combined effect on performance. A relationship is shown between impact and shock sensitivity and how a sensitivity index based on oxygen balance can be used to estimate sensitivity in closely related series of molecules is illustrated. It is shown that the critical temperature of an explosive calculated by the Frank-Kamenetskii equation correlated fairly well with the shock sensitivity of the material. This supports the idea that the shock or impact initiation of an explosive is primarily a thermal event and not dominated by pressure driven chemistry. The concept of the trigger linkage in explosives is discussed and it is pointed out that insensitive explosives will require early chemistry that is thermomechanically neutral or endothermic and leads to the build-up of later strongly exothermic chemistry. DOE

N90-11898# Oak Ridge National Lab., TN.

CORRELATING MICROEMULSION FUEL COMPOSITION, STRUCTURE AND COMBUSTION PROPERTIES

W. L. Griffith and A. L. Compere 1989 45 p
(Contract DE-AC05-84OR-21400)
(DE89-017779; ORNL/TM-11248) Avail: NTIS HC A03/MF A01

Microemulsion fuels provide a method for increasing the use of byproduct and biomass materials, including alcohols, in diesel fuels. The ability to replace 50 percent of diesel fuel with byproduct and biomass-derived materials microemulsion fuels could significantly decrease petroleum consumption. However, it is likely that the low particulate and NO sub x emissions characteristic of these fuels will drive the adoption of this technology. The development of a series of short experiments were carried out to determine the fuel composition changes required to support development of microemulsion fuels which have combustion properties acceptable to the public and adequate to support widespread use in current diesel engines. The goal is delineation of microemulsion diesel fuel compositions which have acceptable compression ignition and emissions properties and which permit the replacement of one-third to one-half of current diesel fuel petroleum. A review of the literature on cetane enhancers for conventional and alternative diesel fuels was performed and a small number of enhancers likely to be effective with high-alcohol fuels selected. Based on linear regression analysis of emissions from a passenger diesel engine using alcohol and aqueous microemulsion fuels, correlation between microemulsion solution structure as determined by small-angle neutron scattering and actual NO sub x and particulate emissions was determined. The analysis indicates that solution structure and microemulsion composition play major roles in emissions modification. DOE

N90-11899# Army Belvoir Research and Development Center, Fort Belvoir, VA.
THE PREDICTION OF MIDDLE DISTILLATE FUEL PROPERTIES USING LIQUID CHROMATOGRAPHY-PROTON NUCLEAR MAGNETIC RESONANCE SPECTROSCOPY DATA Final Report, 1987 - 1988
Madeline Swann Jun. 1989 60 p
(AD-A211879; BRDEC-2478) Avail: NTIS HC A04/MF A01 CSCL 21/4

The research was initiated to support the Army's capability to identify the components of fuels which contribute to low temperature performance of fuels. It was discovered that various physical properties of middle distillate fuels can be predicted. The liquid chromatography (LC) H-1 NMR technique was developed to predict physical properties based on chemical structures present in the fuels. The prediction of properties is approached from a group property point of view. In the group property approach, the structure of the molecule is examined for structural features which dictate the physical properties of the compounds. In other words, the physical properties of a molecule or compound are determined by the number of types of chemical groups, i.e., methyl, methylene, methine, etc., present. These LC H-1 NMR predicted property measurements were compared to measurements obtained by the ASTM fuel tests. Most measurements were found to be within experimental error. The research has demonstrated that the LC H-1 NMR approach for measuring various middle distillate fuel properties can be used as an alternative to the ASTM methods of fuel property measurement. GRA

29 MATERIALS PROCESSING

Includes space-based development of products and processes for commercial applications.
For biological materials see *55 Space Biology.*

N90-11900# Naval Postgraduate School, Monterey, CA.
ON-ORBIT ANNEALING OF GALLIUM ARSENIDE SOLAR CELL ARRAYS M.S. Thesis
Robert S. Sommers Jun. 1989 127 p
(AD-A212087) Avail: NTIS HC A07/MF A01 CSCL 10/2

A complete experimental package is developed for the acquisition of current voltage curves and the annealing of Gallium Arsenide solar cells and arrays of cells. This package is designed to be placed aboard a wide variety of satellite buses and to operate with little interface to the satellite system. GRA

31 ENGINEERING (GENERAL)

Includes vacuum technology; control engineering; display engineering; cryogenics; and fire prevention.

N90-11901*# National Aeronautics and Space Administration. Lewis Research Center, Cleveland, OH.
NONINTRUSIVE INERTIAL VIBRATION ISOLATION TECHNOLOGY FOR MICROGRAVITY SPACE EXPERIMENTS
Carlos M. Grodsinsky and Gerald V. Brown 1989 10 p Proposed for presentation at the 28th Aerospace Sciences Meeting, Reno, NV, 8-11 Jan. 1990; sponsored by AIAA
(NASA-TM-102386; E-5127; NAS 1.15:102386; AIAA-90-0741)
Avail: NTIS HC A02/MF A01 CSCL 22A

The dynamic acceleration environment observed on Space Shuttle flights to date and predicted for the Space Station has complicated the analysis of prior microgravity experiments and prompted concern for the viability of proposed space experiments requiring long-term, microgravity environments. Isolation systems capable of providing significant improvements to this environment exist, but at present have not been demonstrated in flight configurations. A summary of the theoretical evaluation for two one degree-of-freedom (DOF) active magnetic isolators and their predicted response to both direct and base excitations is presented. These isolators can be used independently or in concert to isolate acceleration-sensitive microgravity space experiments, dependent on the isolation capability required for specific experimenter needs. Author

N90-11902*# National Aeronautics and Space Administration. Lewis Research Center, Cleveland, OH.
ADVANCES AND DIRECTIONS OF ION NITRIDING/CARBURIZING
Talivaldis Spalvins Sep. 1989 6 p Presented at the 2nd International Ion Nitriding/Carburizing Conference, Cincinnati, OH, 18-20 Sep. 1989; sponsored in part by ASM
(NASA-TM-102398; E-5148; NAS 1.15:102398) Avail: NTIS HC A02/MF A01 CSCL 13B

Ion nitriding and carburizing are plasma activated thermodynamic processes for the production of case hardened surface layers not only for ferrous materials, but also for an increasing number of nonferrous metals. When the treatment variables are properly controlled, the use of nitrogenous or carbonaceous glow discharge medium offers great flexibility in tailoring surface/near-surface properties independently of the bulk properties. The ion nitriding process has reached a high level of maturity and has gained wide industrial acceptance, while the more recently introduced ion carburizing process is rapidly gaining industrial acceptance. The current status of plasma mass transfer mechanisms into the surface regarding the formation of compound and diffusion layers in ion nitriding and carbon build-up ion carburizing is reviewed. In addition, the recent developments in design and construction of advanced equipment for obtaining optimized and controlled case/core properties is summarized. Also, new developments and trends such as duplex plasma treatments and alternatives to dc diode nitriding are highlighted. Author

N90-11903# Allied-Signal Aerospace Co., Kansas City, MO.
COUPLING RULE-BASED AND OBJECT-ORIENTED PROGRAMMING FOR THE CLASSIFICATION OF MACHINED FEATURES
K. E. Hummel Aug. 1989 24 p Presented at the Computers in Engineering Conference, Anaheim, CA, 2 Aug. 1989
(Contract DE-AC04-76DP-00613)
(DE89-017705; KCP-613-4130; CONF-8908153-1) Avail: NTIS HC A03/MF A01

An expert system, XCUT, currently is being developed which will generate process plans for the production of machined parts given descriptions of manufacturing features. Generally speaking, these features form recurring geometric and technological patterns for which an expert process engineer has acquired years of manufacturing experience. Because they capture much of the terminology and methodology of the process engineer, manufacturing features have become a topic of considerable interest in the development of process planning systems. In the XCUT system manufacturing features generally correspond to volumes of material which are to be removed from an initial stock. A language has been developed for XCUT which generates an object-oriented description of a feature as well as methods for extracting relevant information from the feature volume representation. These methods may invoke either procedural code or production rules to deduce the appropriate information. In addition, the language generates a production rule whose conditions use these methods to identify an instance of the appropriate feature body. These rules are then used by the XCUT planning system to automatically classify and define feature instances from the initial solid geometric descriptions. This paper describes the XCUT feature language and illustrates its use for the automatic classification of features. DOE

N90-11904# Allied-Signal Aerospace Co., Kansas City, MO.
MANUFACTURING AND THE MANUFACTURING ENGINEER IN THE YEAR 2000, REVISION
LaRoux K. Gillespie Aug. 1989 20 p Presented at the Curricula 2000 Workshop, Southfield, MI, 16-18 Apr. 1989 Revised
(Contract DE-AC04-76DP-00613)
(DE89-017707; KCP-613-4025-Rev; CONF-8904270-1-Rev)
Avail: NTIS HC A03/MF A01

The recently completed Society of Manufacturing Engineer (SME) Profile 21 study provided a number of insights into the future world of manufacturing and the manufacturing engineer. This presentation provides an overview of the issues and solutions and compellingly sets a much faster pace than we have followed. It presents both shop floor and engineering insights in a manner that commands attention. DOE

N90-11905# Massachusetts Inst. of Tech., Cambridge. Microsystems Research Center.
APPLICATION OF DIMENSIONAL ANALYSIS TO STATISTICAL PROCESS MODELING M.S. Thesis
William P. Wehrle May 1989 54 p
(Contract MDA972-88-K-0008)
(AD-A211881; VLSI-MEMO-89-533) Avail: NTIS HC A04/MF A01 CSCL 07/1

This work explores the use of Dimensional Analysis as a technique for combining the benefits of empirical modeling and analytical modeling for physical processes. Two processes in the semiconductor industry, Low Pressure Chemical Vapor Deposition (LPCVD) of Polysilicon and LPCVD of Low Temperature Oxide, are dimensionally analyzed and experimentally modeled. The group parameters that Dimensional Analysis yields are shown to be physically more significant than the primitive variables, that is variables that are directly and independently controlled, and therefore model processes much better. For each process, the best polynomial regression to experimental data is found for both the dimensionless parameters and the primitive variables. The average ratio of dimensionless parameter model F-tests to primitive variable model F-tests is 5:1 for polysilicon, and 2.25:1 for LTO. Also, an Application theorem, which measures the modeling and design of experiments gain yielded by Dimensional Analysis is presented. This Application theorem parallels the Pi theorem, but to fit the specific needs of manufacturing processes. The experimental aspect of this work involved minimizing the wafer to wafer variance of the Low Temperature Oxide process. This was achieved by designing and performing amd orthogonal array of eighteen experiments that characterized the growth rate of the process. Models of the film deposition for eleven evenly distributed wafers were created and evaluated using the L18 array. GRA

N90-11906# Naval Postgraduate School, Monterey, CA.
DESIGN AND CALIBRATION OF AN ELECTRODYNAMIC DRIVER FOR THE SPACE THERMOACOUSTIC REFRIGERATOR (STAR) M.S. Thesis
David Anthony Harris and Richard Eugene Volkert Jun. 1989 220 p
(AD-A212022) Avail: NTIS HC A10/MF A02 CSCL 13/1

The objective of the STAR project is to test and space qualify a continuous cycle cryogenic refrigeration system for the cooling of sensors and electronics based upon the thermoacoustic heat pumping effect. This thesis describes the design, assembly, and calibration of the electrodynamic driver and its associated performance monitoring and control instrumentation. The electroacoustic efficiency of the driver is measured under different operating conditions utilizing a prototype refrigerator resonator. These results are then compared to modelled efficiencies derived from a computer simulation program that uses the independently-measured individual component parameters to predict the driver performance. Good agreement between measured and predicted efficiencies is observed. Highest electroacoustic efficiencies are shown to occur when the resonance frequencies of the driver and resonator are most closely matched. A maximum electroacoustic efficiency of 50 percent is achieved under these conditions. GRA

N90-11907# Michigan Technological Univ., Houghton.
IMPROVING SNOW ROADS AND AIRSTRIPS IN ANTARCTICA Final Report, Nov. 1986 - Jun. 1988
Sung M. Lee, Wilbur M. Haas, Robert L. Brown, and Albert F. Wuori Jul. 1989 24 p Sponsored by NSF, Washington, DC
(AD-A211588; CRREL-SP-89-22) Avail: NTIS HC A02/MF A01 CSCL 08/12

During the 1986 to 1987 austral summer, snow road and runway test lanes were constructed at McMurdo Station and at South Pole Station. These lanes were monitored during Dec. 1986 to Jan. 1987, and again in Jan. 1988. Test sections were constructed of: (1) tractor-compacted snow topped with a 15 cm layer of rotary blower processed snow, (2) rotary processed and compacted snow in 15-cm layers to a depth of 60 cm, (3) rotary processed and compacted snow in 15-cm layers incorporating wood sawdust additive mixed at 5 percent by volume, and (4) rotary-processed snow with 10 percent sawdust by volume. These test sections were monitored by obtaining temperature and density profiles, Rammsonde hardness profiles, California Bearing Ratio and Clegg surface strength values, and testing for ability to withstand traffic. Wood sawdust added to processed snow in amounts of 5 to 10 percent by volume significantly increases the strength of the resulting snow road or runway. Adequate strengths of the snow/sawdust mixtures were achieved for limited use by wheeled C130 aircraft, but additional processing with heat, water or added compaction appears necessary to produce a 25-cm-thick surface layer adequate for frequent use and to accommodate wheeled C141 aircraft. At McMurdo, it was found that the sawdust was not effective in maintaining the integrity of the surface traffic during the thawing season without additional maintenance, whereas at the South Pole, thawing was not a problem since temperatures remained well below the melting point. GRA

N90-11908# Army Cold Regions Research and Engineering Lab., Hanover, NH.
ICE RUNWAYS NEAR THE SOUTH POLE Special Report
Charles Swithinbank Jun. 1989 47 p
(Contract MIPR-CRREL-89-12)
(AD-A211606; CRREL-SR-89-19) Avail: NTIS HC A03/MF A01 CSCL 01/5

Following an examination of air photographs of the Transantarctic Mountains, 37 blue-ice areas were reconnoitered from the air, using a ski-wheel Twin Otter operating from the South Pole. Two sites were selected as potential airfields for conventional transport aircraft, and ground surveys were made. On the Mill Glacier at 85 deg 06'S, 167 deg 15'E there is an area of smooth and level ice which gives a 7-km run directly into the prevailing wind. Five wheel landings were made there. Alongside Mount Howe there is a large area of level ice at 87 deg 20'S, 149 deg 50'W. It offers a 7-km runway, but there is a strong crosswind component from the prevailing wind and some bumps on the ice surface need to be planed off. Eight wheel landings were made at Mount Howe. GRA

N90-11909# ESDU International Ltd., London (England).
APPLICATION OF PROCESS INTEGRATION TO UTILITIES, COMBINED HEAT AND POWER, AND HEAT PUMPS
Apr. 1989 75 p
(ESDU-89001; ISBN-0-85679-672-7; ISSN-0141-402X) Avail: ESDU

This Data Item 89001, an addition to the Heat Transfer Subseries, shows how the techniques of process integration introduced in ESDU 87030, where they were used to optimize heat exchanger networks, can be extended to design optimally the heat and power systems of a process plant or site. After briefly describing the thermodynamic principles of heating and cooling systems, the various types of heat engines and heat pumps that may be used are introduced, and criteria for their selection to achieve an optimal combined heat and power system are explained. Heat engines include steam and gas turbines and diesel engines, while heat pumps cover mechanical and thermal vapor recompression, refrigeration cycles, and heat transformers. The optimization process covers not only the selection of an appropriate type of utility of the correct size, but also its placement within the process. The application of the techniques is illustrated using the real case study also used in ESDU 87030, and further case studies using current economic and numerical data extend the user's appreciation of the methods. ESDU

N90-11910# Technische Univ., Delft (Netherlands). Faculty of Technical Mathematics and Informatics.
MODELLING AND CONTROL OF A DIFFUSION/LPCVD FURNACE
H. deWaard and W. L. deKoning 1988 25 p
(Rept-88-97; ISSN-0922-5641; ETN-89-95108) Copyright Avail: NTIS HC A03/MF A01

Heat transfer inside a cylindrical resistance diffusion/Low Pressure Chemical Vapor Deposition (LPCVD) furnace is studied with the aim of developing an improved temperature controller. A model of the thermal behavior is derived, which covers the important class of furnaces equipped with semitransparent quartz process tubes. The model takes into account the thermal behavior of the thermocouples. Currently used temperature controllers are shown to be highly inefficient for very large scale integration applications. Based on the model an alternative temperature controller of the LQG (linear quadratic Gaussian) type is proposed which features direct wafer temperature control. Some simulation results are given. ESA

32 COMMUNICATIONS AND RADAR

Includes radar; land and global communications; communications theory; and optical communications.

For related information see also *04 Aircraft Communications and Navigation* and *17 Space Communications, Spacecraft Communications, Command and Tracking.* For search and rescue see *03 Air Transportation and Safety,* and *16 Space Transportation.*

N90-11911# National Oceanic and Atmospheric Administration, Boulder, CO. Wave Propagation Lab.
FURTHER GUIDE FOR THE RETRIEVAL OF DROPSIZE DISTRIBUTIONS IN WATER CLOUDS WITH A GROUND-BASED CLEAR-AIR-SENSING DOPPLER RADAR
Earl E. Gossard (Colorado Univ., Boulder.) and Richard G. Strauch Apr. 1989 55 p
(PB89-196000) Avail: NTIS HC A04/MF A01 CSCL 20N

The report describes a technique for expanding the size range of the dropsize distribution by a factor of 2 by unfolding the Doppler spectrum so that frequencies up to twice the Nyquist frequency are recoverable. Also, a second technique for retrieving the dropsize spectra is introduced and discussed. The technique is the Fourier transform deconvolution of the Doppler frequency spectrum with the turbulent medium in which the drops are embedded. The advantages and limitations are discussed and compared with the iterative method described in detail in the earlier report. The report gives the deconvolution procedure for digital spectra and discusses the random and systematic errors in the process. Author

N90-11912# National Telecommunications and Information Administration, Annapolis, MD.
HANDBOOK OF RADIO WAVE PROPAGATION LOSS (100-20,000 MHz), PART 2
William E. Frazier Apr. 1989 117 p
(PB89-195473; NTIA-89-242-Pt-2) Avail: NTIS HC A06/MF A01 CSCL 20N

The handbook provides estimates of radio wave propagation loss between transmitting and receiving antennas of various heights and transmission frequencies above the assumed smooth earth surface calculated using the NLAMBDA computer model. For many cases involving electromagnetic compatibility analysis, the curves of predicted transmission losses may be used to estimate the transmission losses of the desired and undesired signals. These estimated loss values are given in dB as BASIC MEDIAN TRANSMISSION LOSS for antennas with effective heights up to 5000 meters, operating in the 100 to 20,000 MHz frequency range, over land or sea, at great circle earth surface distances up to 1000 kilometers. The handbook includes curves for the frequencies of 500 MHz, 2000 MHz, 5000 MHz, 7000 MHz, and 20,000 MHz. Author

N90-11913# Institute for Telecommunication Sciences, Boulder, CO.
A NEW APPROACH TO HF (HIGH FREQUENCY) CHANNEL MODELING AND SIMULATION. PART 1: DETERMINISTIC MODEL
L. E. Vogler and J. A. Hoffmeyer Dec. 1988 44 p
(PB89-203962; NTIA-88-240-Pt-1) Avail: NTIS HC A03/MF A01 CSCL 17B

The report describes a new and unique approach for modeling either narrowband or wideband High Frequency (HF) channels. Although narrowband models of the HF channel have existed for many years, they are applicable to only a limited set of actual propagation conditions. The report describes the development of a channel transfer function for the HF channel that accurately models a wide variety of propagation conditions and can be used for the evaluation of wideband HF systems. The first part of the effort developed a model that represents the median channel conditions. Good agreement has been found between the model and wideband propagation measurements taken during relatively stable conditions. The report provides comparisons between ionograms generated by the model and measured wideband ionograms that have been reported in the literature. GRA

N90-11914# Department of the Army, Washington, DC.
A SAW SLANTED ARRAY CORRELATOR (SAC) WITH SEPARATE AMPLITUDE COMPENSATION CHANNEL Patent Application
Elio A. Mariani, inventor (to Army) and William J. Skudera, Jr., inventor (to Army) 26 Jun. 1989 14 p
(AD-D014174; US-Patent-Appl-SN-373537) Avail: NTIS HC A03/MF A01 CSCL 09/4

A Surface Acoustic Wave (SAW) slanted array correlater (SAC) comprises a piezoelectric substrate, an input and an output interdigital transducer deposited on the piezoelectric substrate, a reflective array aligned with the transducers, and an acoustic absorbing film disposed on the substrate between the output transducer and the reflective array. The input and output transducer are slanted at equal and opposite appropriate angles to each other. The reflective array is disposed on the substrate at an angle the same as the angle of emplacement of the output transducer. The transducers comprise a number of interdigital electrodes with varying periodicity, the periodicity being the same for corresponding portions of the two transducers. The reflective array comprises a number of shorted electrodes having a periodicity corresponding to the periodicity of the output transducer. The acoustic absorbing film has a non-uniform width with selected portions having little or no width. GRA

N90-11915*# National Aeronautics and Space Administration. Lewis Research Center, Cleveland, OH.
SATELLITE-MATRIX-SWITCHED, TIME-DIVISION-MULTIPLE-ACCESS NETWORK SIMULATOR
William D. Ivancic, Monty Andro, Lawrence A. Nagy, James M. Budinger, and Mary Jo Shalkhauser Washington Oct. 1989 21 p Proposed for presentation at the 13th AIAA International

Communication Satellite System Conference, 11-15 Mar. 1990
(NASA-TP-2944; E-4813; NAS 1.60:2944) Avail: NTIS HC
A03/MF A01 CSCL 17B

A versatile experimental Ka-band network simulator has been implemented at the NASA Lewis Research Center to demonstrate and evaluate a satellite-matrix-switched, time-division-multiple-access (SMS-TDMA) network and to evaluate future digital ground terminals and radiofrequency (RF) components. The simulator was implemented by using proof-of-concept RF components developed under NASA contracts and digital ground terminal and link simulation hardware developed at Lewis. This simulator provides many unique capabilities such as satellite range delay and variation simulation and rain fade simulation. All network parameters (e.g., signal-to-noise ratio, satellite range variation rate, burst density, and rain fade) are controlled and monitored by a central computer. The simulator is presently configured as a three-ground-terminal SMS-TEDMA network. Author

N90-11916# Helsinki Univ. (Finland). Circuit Theory Lab.
CALIBRATION AND DE-EMBEDDING OF MICROWAVE MEASUREMENTS USING ANY COMBINATION OF ONE- OR TWO-PORT STANDARDS
Kimmo Silvonen Dec. 1987 43 p
(PB89-212674; CT-4; ISBN-951-754-313-1) Avail: NTIS HC
A03/MF A01 CSCL 20N

The determination of the error two-ports in microwave and millimeter-wave measurements is studied using known calibration standards. New explicit equations were derived which allow the use of any combination of standards described with their S-parameters. For singularity reasons different equations are needed, depending on the type of standards. The question of how many standards are really needed is also addressed. According to the results, three are needed, no matter if they are one-or two-ports and reciprocal or not. However, a new method is described that uses only two standards as far as the symmetrical measurement fixture is concerned. It is also shown how to use redundant equations to reduce the errors in over-determined problems. A Calibration And De-Embedding Program CADEP was written for use with the HP 8409C network analyzer and the circuit design program APLAC. GRA

N90-11917# Lawrence Livermore National Lab., CA.
RECENT ADVANCES TO NEC (NUMERICAL ELECTROMAGNETICS CODE): APPLICATIONS AND VALIDATION
G. J. Burke 3 Mar. 1989 26 p Presented at the Conference on Modern Antenna Design Using Computers and Measurement Application To Antenna Problems of Military Interest, Ankara, Turkey, 19-20 Oct. 1989
(Contract W-7405-eng-48)
(DE89-009231; UCRL-100651; CONF-891074-1) Avail: NTIS
HC A03/MF A01

Capabilities of the antenna modeling code NEC are reviewed and results are presented to illustrate typical applications. Recent developments are discussed that will improve accuracy in modeling electrically small antennas, stepped-radius wires and junctions of tightly coupled wires, and also a new capability for modeling insulated wires in air or earth is described. These advances will be included in a future release of NEC, while for now the results serve to illustrate limitations of the present code. NEC results are compared with independent analytical and numerical solutions and measurements to validate the model for wires near ground and for insulated wires. DOE

N90-11918# Sandia National Labs., Albuquerque, NM.
SIMULATION OF THE EMP (ELECTROMAGNETIC PULSE) FROM ESD (ELECTROSTATIC DISCHARGE)
Bill Boverie 1989 11 p Presented at the EOS Electrostatic Discharge Symposium, New Orleans, LA, 26-28 Sep. 1989
(Contract DE-AC04-76DP-00789)
(DE89-014484; SAND-89-0153C; CONF-8909176-1) Avail: NTIS
HC A03/MF A01

Both bounded-wave and TEM-cell structures provide controlled, repeatable testing for ESD-generated EMP. Coaxial transmission line drivers are required for very fast rise times, but Marx generators and peaking capacitors can be used otherwise. The pulse parameters most important to simulate accurately are rise time, peak amplitude, and pulse energy. DOE

N90-11919# Sandia National Labs., Albuquerque, NM. Systems Engineering Div.
VIDEO IMAGING SYSTEMS: A SURVEY
H. Lee Kefauver Jul. 1989 244 p
(Contract DE-AC04-76DP-00789)
(DE89-016920; SAND-89-1784) Avail: NTIS HC A11/MF A02

Recent technological advances in the field of electronics have made video imaging a viable substitute for the traditional Polaroid(trademark) picture used to create photo ID credentials. New families of hardware and software products, when integrated into a system, provide an exciting and powerful toll which can be used simply to make badges or enhance an access control system. The reader is made aware of who is currently in this business and compare their capabilities. DOE

N90-11920# Lawrence Livermore National Lab., CA.
RESISTIVE BLOCK METHODS FOR ELECTROSTATIC FIELD SOLUTIONS WITH INTERNAL ELEMENTS
Dale E. Nielsen, Jr. and John J. Ambrosiano Jul. 1989 5 p
Presented at the 13th Conference on the Numerical Simulation of Plasmas, Santa Fe, NM, 17-20 Sep. 1989
(Contract W-7405-eng-48)
(DE89-017535; UCRL-101396; CONF-890931-6) Avail: NTIS
HC A01/MF A01

The presence of conducting elements (e.g., electrodes) often makes numerical computations of electromagnetic fields within a bounded region awkward. At the interface or boundary between the conducting elements and the vacuum region, appropriate conditions must be prescribed and enforced. Such problems may be more conveniently posed if the elements are simply represented as blocks of material with specific values of resistance, dielectric constant and permitivity. The field solution can then be obtained over the whole region including the conducting elements without the need to specify fields at the interface. We refer to a field solution algorithm that incorporates regions having finite conductivity as a resistive block algorithm. An electromagnetic resistive block algorithm was introduced by Eppley and Drobot which is accurate and robust to timesteps that are large with respect to the resistive decay timescale (tau)(sub R) = (epsilon)/(sigma) ((sigma) is the conductivity and (epsilon) is the dielectric constant). This makes it applicable to problems having regions with metallic conductivities while allowing the solution to be advanced on a timescale appropriate to phenomena of interest, e.g., plasma physics. In this paper we reiterate the electromagnetic algorithm and show how to use the same approach to solve electrostatic problems. DOE

N90-11921# California Univ., Davis. Dept. of Electrical Engineering and Computer Science.
MICROWAVE SIGNAL DETECTION USING MODULATION OF POLYMERIC OPTICAL WAVEGUIDES Final Report, Mar. - Sep. 1988
Stephen T. Kowel, Andre Knoesen, C. A. Eldering, and M. A. Mortazavi Jan. 1989 50 p
(Contract W-7405-eng-48)
(DE89-017545; UCRL-21166; LLNL-B-034291) Avail: NTIS HC
A03/MF A01

The Polymeric Ultrathin Films Program (PUFS) was initiated at UCD during the Fall of 1984. It is a multidisciplinary program of research and graduate education involving faculty from the Department of Electrical and Computer Engineering (Stephen T. Kowel, Andrew Dienes, and Andre Knoesen), the Department of Chemical Engineering (Pieter Stoeve and Brian G. Higgins), the Department of Physics (Lawrence B. Coleman), and the Department of Applied Science (Yin Yeh), and their students. Since the Summer of 1986, a close collaboration has developed with scientists at the Chemistry Division, Naval Weapons Center, China Lake, CA. Thus, the program includes efforts by Dr. Geoffrey Lindsay and Dr. James Hoover, in organic and synthetic chemistry, as well as deposition of ultrathin films, evaluation of film properties, and applications work carried our at UCD. The primary focus of our work is film systems for opto-electronics, especially optical signal conditioning, hybrid computing, and sensing. Some project elements devoted to evaluation of optical fibers and planar waveguides have been performed by professor Richard Selfridge in the Department of Electrical and Computer Engineering at Brigham Young University, Provo, Utah. Support has come from the Air Force Weapons Laboratory, Rome Air Development Center, Lawrence Livermore National Laboratory, and the National Science Foundation. DOE

N90-11922# Brookhaven National Lab., Upton, NY.
MICROWAVE INSTABILITY NEAR TRANSITION ENERGY
J. Wei and S. Y. Lee 1989 6 p Presented at the 14th International Conference on High Energy Accelerators, Tsukuba, Japan, 20-26 Aug. 1989
(Contract DE-AC02-76CH-00016)
(DE90-000107; BNL-43204; CONF-890803-16) Avail: NTIS HC A02/MF A01

Monte Carlo simulation for the microwave instability agrees with analytic calculation solving the Vlasov equation, provided that bunch shape distortion due to coupling is taken into account. DOE

N90-11923# Naval Ocean Systems Center, San Diego, CA. Electronic Material Sciences Div.
SENSITIVITY OF OPTOELECTRONIC RECEIVERS
C. R. Zeisse Mar. 1989 13 p Submitted for publication
(AD-A211823) Avail: NTIS HC A03/MF A01 CSCL 17/5

The formula used to predict wide-band noise of optoelectronic receivers was modified to account for parasitic resistances in the transistor connected to the photodiode. The new formula leaves the total noise unchanged after proper steps were taken to adjust the transistor gate width for minimum noise. The discrepancy between measured and predicted noise of 1.65 micron monolithic InP receivers thus remains largely unexplained. GRA

N90-11924# Defence Research Establishment Pacific, Victoria (British Columbia).
ANALYSIS OF TWO-PASS MODIFIED HOUGH TRANSFORM (MHT) TECHNIQUE FOR THE DETECTION OF WAKE LIKE SIGNALS
M. J. Wilmut and R. F. MacKinnon Mar. 1989 19 p
(AD-A211982; DREP-TM-89-03) Avail: NTIS HC A03/MF A01 CSCL 17/1

In this paper a procedure is developed using the Modified Hough Transform (MHT) for the detection of signals of low signal-to-noise ratio. The signal can be considered as being composed of a sum of narrow lines. The expected number of signal and false lines to be found in an image can be determined as a function of the false alarm probability per decision. The MHT performance is compared to that of the matched filter. The method is applied to noisy images containing a wake-like signal. The MHT is able to detect the signal pattern at signal-to-noise ratios for which the signal is just visible on a good image display system. A two pass system, employing prior knowledge about the signal, gives improved detection performance. GRA

N90-11925# National Inst. of Standards and Technology, Boulder, CO. Electromagnetic Fields Div.
CLUTTER MODELS FOR SUBSURFACE ELECTROMAGNETIC APPLICATIONS
David A. Hill Feb. 1989 46 p Sponsored by Army Belvoir Research Development and Engineering Center, Fort Belvoir, VA
(PB89-229678; NISTIR-89/3909) Avail: NTIS HC A03/MF A01 CSCL 20N

Clutter models for subsurface electromagnetic applications are discussed with emphasis on tunnel detection applications. Random medium models are more versatile and require less detailed information than deterministic models. The Born approximation is used to derive expressions for the incoherent field, and electric and magnetic dipoles are treated in detail. When random inhomogeneities are located in the near field of the dipole source, an electric dipole radiates a larger incoherent field than a magnetic dipole because of its larger reactive electric field. Author

N90-11926# Helsinki Univ. of Technology, Espoo (Finland). Electromagnetics Lab.
EIGENSOLUTIONS FOR THE REFLECTION PROBLEM INVOLVING THE INTERFACE OF TWO CHIRAL HALF SPACES
Ari J. Viitanen, Ismo V. Lindell, Ari H. Sihvola, and Sergei A. Tretyakov Apr. 1989 29 p
(PB89-221592; Rept-46; ISBN-951-754-878-8) Avail: NTIS HC A03/MF A01 CSCL 20N

The Silberstein wave-field decomposition of electromagnetic fields is applied to the problem of wave propagation in chiral medium. The problem involving a planar interface between two chiral media is considered and eigensolutions for the reflection and transmission problems are given. Numerical results are calculated for the eigenpolarizations and reflection coefficients with different incident field polarizations, for the problem involving an interface between isotropic and chiral media. Also, the limit cases of reflection from a half space with only small amount of chirality are studied and it is shown that the chirality gives a second-order effect on the co-polarized reflection coefficient and a first-order effect on cross-polarization. GRA

N90-11927# Helsinki Univ. of Technology, Espoo (Finland). Electromagnetics Lab.
TIME-DOMAIN ANALYTIC AND NUMERIC ANALYSIS OF VERTICAL DIPOLES IN FRONT OF DIELECTRIC PLANAR INTERFACE
Keijo I. Nikoskinen May 1989 22 p
(PB89-221642; Rept-47; ISBN-951-754-899-0) Avail: NTIS HC A03/MF A01 CSCL 20N

Time-domain solutions for fields due to an impulsive vertical magnetic and electric dipole in the presence of a planar dielectric boundary are studied both analytically and numerically. Closed-form expressions for the Hertzian potential are derived in cases when the observation point is on the axis of the dipole or when both the dipole and the observation point are located on the interface. Numerical results are given for more general observation points. GRA

N90-11928# Rome Air Development Center, Griffiss AFB, NY.
PROCEEDINGS OF THE 1988 ANTENNA APPLICATIONS SYMPOSIUM, VOLUME 1 Final Report, 21 Sep. - 23 Sep. 1988
Paul Mayes Jun. 1989 300 p
(AF Proj. 4600)
(AD-A211396; RADC-TR-89-121-Vol-1) Avail: NTIS HC A13/MF A02 CSCL 09/1

The Proceedings of the 1988 Antenna Applications Symposium is a collection of state-of-the-art papers relating to phased array antennas, multibeam antennas, satellite antennas, microstrip antennas, reflector antennas, HF, VHF, UHF and various other antennas. GRA

N90-11929# Naval Research Lab., Washington, DC. Ionospheric Effects Branch.
NRL/VOA MODIFICATIONS TO IONCAP AS OF 12 JULY 1988 Progress Report, Jun. - Dec. 1988
Mark Daehler 2 Aug. 1989 140 p
(AD-A211546; NRL-MR-6514) Avail: NTIS HC A07/MF A01 CSCL 20/14

Modifications made by NRL to IONCAP 85.04, an HF ionospheric propagation prediction computer program are documented. These modifications serve to present the structure of multimode propagation more accurately, to separate the effects on system performance caused by antenna gain and ionospheric structure (thereby making it more suitable for wide area coverage studies), to incorporate a newer noise model, to improve the accuracy of some calculations, to correct a few programming errors, and to make operation more convenient on the computers in use at NRL. GRA

N90-11930# Mitre Corp., Bedford, MA.

PERFORMANCE OF FOUR RAKE MODEMS OVER THE NON-DISTURBED WIDEBAND HF CHANNEL Interim Report, Oct. 1987 - Aug. 1988

Phillip A. Bello Jun. 1989 99 p
(Contract F19628-86-C-0001)
(AD-A211589; MTR-10445; RADC-TR-89-91) Avail: NTIS HC A05/MF A01 CSCL 25/2

The Rake Modem technique was proposed some thirty years ago by R. Price and P. Green as a means for combating multipath when direct sequence spread spectrum signals are transmitted. Performance evaluations are presented for four Rake modems used to communicate over the wide band (e.g., 1-MHz) HF channel. Attention is confined to performance for the non-disturbed HF channel. Consideration is given to the impact of mode Doppler shift and multipath spread due to dispersion. The effects of additive noise, self noise and imperfect channel measurements are included. Results are presented for decision-directed, parallel-probe, serial-probe, and DPSK Rake modems. With a suitable codec, performance to within 1 to 3 dB of the additive white Gaussian noise channel at 0.00001 error rate is predicted, depending upon the modem and the channel dispersion, if Doppler shifts of modes can be tracked to within 0.1 Hz. GRA

N90-11931# Naval Research Lab., Washington, DC.

PACIFIC MARINE RADAR SEA SCATTER EXPERIMENTAL RESULTS

Dennis B. Trizna 22 Aug. 1989 29 p
(AD-A211593; NRL-MR-6506) Avail: NTIS HC A03/MF A01 CSCL 17/9

Results are presented for a low grazing angle marine radar sea scatter experiment conducted in the Pacific Ocean. A wide range of wind speeds and directions resulted in nonequilibrium sea conditions, in contrast to a previous Atlantic experiment in which ocean waves were fully developed. Statistical properties of the radar echoes are parameterized by a dual Weibull model versus wind speed and differ from the North Atlantic data. A modified version of Wetzel's cylindrical plume scattering model satisfactorily describes the sea spike cross section characteristics. For the Weibull distribution representing distributed scatter, a composite scattering model produces neither the correct absolute cross section nor the correct X/S band ratio using Bragg scatter spectral densities derived from high grazing angle radar experiments. Thus, the surface turbulence from a broken crest on the front face of waves may be responsible for the scatter from area-distributed roughness. GRA

N90-11932# Illinois Univ., Urbana. Coordinated Science Lab.

SPECTRAL-DOMAIN ANALYSIS OF FINITE FREQUENCY SELECTIVE SURFACES

Kim Merewether and Raj Mittra Aug. 1989 115 p
(Contract N00014-84-C-0149)
(AD-A211669; UILU-ENG-89-2220) Avail: NTIS HC A06/MF A01 CSCL 20/14

Though frequency selective surfaces have been investigated for over two hundred years, accurate numerical analysis of these surfaces is still in its infancy. In this thesis, the method of moments is applied in the spectral domain to model finite frequency selective surfaces, to study the effects of non-plane-wave sources, and to explore the advantages of gradually adjusting the lattice and shape of the element in a nonuniform frequency selective surface for non-plane-wave excitation. In pursuing these goals, the following topics are discussed in some detail. Because of the limited interest in free-standing surfaces, and because the usual cascade approach is not applicable to finite frequency selective surfaces, a general multilayer Green's function is developed in order to incorporate an arbitrary dielectric support. Because the analysis of finite arrays can be computationally intensive, several strategies are discussed for efficiently filling the matrices generated by the application of the spectral-domain method of moments. A few methods for handling the singularities of the spectral Green's function are briefly mentioned, including a comparison of several adaptive numerical integration routines for integrating functions which are singular or sharply peaked. The effects of finite dimensions are evaluated by comparing the induced currents and reflection coefficients for the finite and periodic arrays. GRA

N90-11933# Alaska Univ., Fairbanks. Geophysical Inst.

HIPAS 1987-88: ULF RESEARCH AND CAMPAIGN SUPPORT Final Report

John V. Olson 18 Aug. 1989 3 p
(Contract N00014-88-K-0240)
(AD-A211720) Avail: NTIS HC A02/MF A01 CSCL 20/14

During the October campaign several intervals were noted in which naturally occurring ULF signals were present during Dr. Ferraro's ELF heating experiments. A one-to-one correlation was found between the ULF and ELF polarization characteristics. ULF pulsations are the result of resonant hydromagnetic waves standing in the earth's magnetic field. They drive currents in the ionosphere, primarily at E region heights above 100 km. The heating experiment, which produced ELF returns, heated electrons below 100 km in the D region. The correlation led us to a series of studies of the casual link between the ULF and ELF signals. A second campaign was held during July 1988. In preparation for this campaign, two data acquisition systems were acquired and placed at two sites in Alaska to supplement the Alaska meridian chain of magnetometers. The first system was placed in Tok, Alaska and the second in Coldfoot, Alaska and both were operated continuously during the period of the campaign. These two sites give us measures of the magnetic fields, and hence the ionospheric currents over a two-dimensional region rather than the one dimensional estimate available using only the Alaska meridian chain. GRA

N90-11934# Massachusetts Inst. of Tech., Lexington. Lincoln Lab.

ASR-9 WEATHER CHANNEL TEST REPORT

Dean C. Puzzo, Seth W. Troxel, Mark A. Meister, Mark E. Weber, and James V. Pieronek 3 May 1989 140 p
(Contracts F19628-85-C-0002; DTFA01-80-Y-10546)
(AD-A211749; ATC-165; DOT/FAA/PS-89-3) Avail: NTIS HC A07/MF A01 CSCL 17/9

The ASR-9, the next generation airport surveillance radar, will be deployed by the FAA at over 100 locations throughout the U.S. The system includes a weather channel designed to provide ATC personnel with timely and accurate weather reflectivity information as a supplement to normal aircraft information. Issues addressed are: whether the ASR-9 weather channel performs according to FAA specifications and whether the ASR-9 weather channel adequately represents weather reflectivity for ATC purposes. Comparisons between data from an ASR-9 in Huntsville, AL, recorded during design qualification and testing, and data from two other reference radars, were used as the basis for the assessment. Several storm cases were analyzed, comprised of stratiform rain, isolated convective storms, squall lines, and cold fronts containing multiple simultaneous convective storms. Results suggest that, with the exception of an apparent 3 dB discrepancy between the weather products of the ASR-9 and the reference radars, the ASR-9 weather channel seems to perform according to FAA specifications. Although the ASR-9 products give a reasonable representation of the extent and severity of potentially hazardous weather in Huntsville, the results suggest that the static storm model used to determine beamfill corrections for the ASR-9 should be optimized for the particular climatic region in which an ASR-9 will be operated. GRA

N90-11935# Physikalisch-Technische Bundesanstalt, Brunswick (Germany, F.R.). Abteilung Elektrizitaet.
CONTRIBUTION OF THE PRECISION DETERMINATION OF NOISE POWERS IN THE MHz AND LOWER GHz FREQUENCY RANGE Ph.D. Thesis - Technischen Univ., Hamburg [EIN BEITRAG ZUR PRAEZISIONSBESTIMMUNG VON RAUSCHLEISTUNGEN IM MHZ- UND UNTEREN GHZ-FREQUENZBEREICH]
Dieter Janik Oct. 1988 194 p In GERMAN
(PTB-E-33; ISBN-3-88314-824-5; ISSN-0341-6720; ETN-89-94612)
Avail: NTIS HC A09/MF A01

Methods are presented for the calibration of noise sources in broadband coaxial noise measuring systems for frequencies between 100 MHz and 8 GHz. The general theoretical fundamentals are outlined. A novel broadband coaxial measuring setup is described. The calibration is performed using a thermal coaxial standard and a precision attenuator at fixed intermediate frequency, providing a relative global measuring accuracy (2 sigma) of about 0.5 percent. For frequencies below 100 MHz coaxial unidirectional transmission lines are not available, and the measuring circuit had to be modified, using synthetic noise sources with pseudorandom pulse generators. A relative global measuring accuracy of 0.1 percent is obtained. ESA

N90-11936# Dortmund Univ. (Germany, F.R.). Lehrstuhl fuer Nachrichtentechnik.
TELEVISION SYSTEMS WITH ENHANCED IMAGE QUALITY FOR NEW BROADBAND CHANNELS Final Report [FERNSEHSYSTEME ERHOEHTER BILDQUALITAET FUER NEUE BREITBANDKANAELE]
W. Boie, E. Guettner, G. Huerkamp, R. Kays, H. Schroeder, M. Silverberg, F. Stoellenwerk, and B. Wendland 1988 117 p In GERMAN
(Contract BMFT-TK-0238-5)
(ETN-89-94622) Avail: NTIS HC A06/MF A01

Methods for improved image transmission via new broadband channels (satellite and cable channels) are developed and demonstrated, with a particular view to future high definition television (HDTV). A digital signal pre- and postprocessing system is designed and realized for a HQ-MAC (high quality-multiplexed analog component) television system, which increases the resolution substantially. The constructed demonstration model shows an impressive quality improvement with respect to standard definition television. Methods for the suppression of jitter are realized. A new high definition progressive production standard is established. A number of improvements in the projector system are realized, with a view to an efficient display for HDTV. ESA

N90-11937 Physics and Electronics Lab. TNO, The Hague (Netherlands).
FEASIBILITY OF GRAPHICS VOICE TELEPHONES FOR THE POST 2000 ERA
A. J. Ruizenaar Sep. 1988 19 p Original contains color illustrations
(Contract A86/KL/045)
(FEL-1988-26; TD88-4381; ETN-89-95074) Copyright Avail: TNO Physics and Electronics Laboratory, P.O. Box 96864, 2509 JG The Hague, Netherlands

The philosophy behind the work and the choice of the implemented technique, concerning developed models of an integrated graphics voice telephone, are discussed. Military user requirements versus technical possibilities, are considered. Based on the feasibility study and the results, the following conclusions are drawn: an integrated graphics voice telephone offers the user extra capabilities besides voice for exchanging messages, sketches or images; voice and data can be handled simultaneously and in the same way over a common radio channel; it is feasible to limit the size of such a multifunctional telephone to a hand-held portable terminal; the use of redundant speech pauses for exchanging data traffic is an attractive method; efficient and state of the art voice and error correcting coding techniques have to be developed in order to increase the technical qualities of the Gravophone; due to the obtained experience and the comments by military planners given during demonstrations, a better overview on user facilities and system requirements is obtained. ESA

N90-11938 Physics and Electronics Lab. TNO, The Hague (Netherlands).
MODELING OF DIFFRACTION REFLECTION AND CLUTTER LOSS IN UHF RADIO WAVE PROPAGATION
J. P. G. M. Linnartz Jun. 1988 120 p
(Contract A84/KL/110)
(FEL-1988-28; TD88-4406; ETN-89-95075) Copyright Avail: TNO Physics and Electronics Laboratory, P.O. Box 96864, 2509 JG The Hague, Netherlands

In the scope of a project for the development of a propagation model, to be used to forecast path losses over operational links and for off-site interfering signals, the propagation of carrier signals is studied. A set of measurements (1270 measurements over 55 paths) is used to analyze several relatively simple models for UHF-propagation over rolling hilly, agricultural and forested terrain in the north German plain. A topological data base and statistical methods are applied to gain insight in the applicability of these models. The accuracy of the models considered ranges from 8 to 12 decibels. Path losses are assumed to be determined in first order by diffraction and groundwave propagation. An accuracy of about 8 decibels can be achieved, if average losses due to scattering of radio waves in the vicinity of the antenna are considered. To avoid large errors, higher resolution is recommended and it is feasible with present technology. ESA

N90-11939 Physics and Electronics Lab. TNO, The Hague (Netherlands).
THEORY AND SIMULATION OF THE OPERATION OF A DOPPLER DIRECTION FINDER IN A MULTIPATH ENVIRONMENT
G. J. M. Janssen Dec. 1988 67 p
(Contract A81/KL/134)
(FEL-1988-56; TD89-0302; ETN-89-95079) Copyright Avail: TNO Physics and Electronics Lab., P.O. Box 96864, 2509 JG The Hague, Netherlands

The theory and simulation programs are presented for direction finders (DF) which use the Doppler principle. Two situations are analyzed: the case that the antenna is a continuously rotating omnidirectional element; and the case that the antenna consists of m elements which are uniformly distributed over the circumference of a circle. The results, for both antenna configurations, show that the system in which samples are taken of the electromagnetic field causes slightly larger bearing errors in a multipath situation, than when the electromagnetic field is continuously sensed. This is caused by the occurrence of the aliasing effect. The simulation programs are powerful tools for more profound research in Doppler DF systems and the use of them. It is shown that multipath signals cause a broadening of the low frequency (LF) spectrum after the frequency modulation detector; and that when the electromagnetic field is sampled, the LF spectrum appears around every multiple of the sample frequency. ESA

N90-11940 Physics and Electronics Lab. TNO, The Hague (Netherlands).
A METHOD TO MODEL FUZE-PERFORMANCE. PART 3: DIFFRACTION OF ELECTROMAGNETIC RADIATION BY AN EDGE
M. H. Vogel Jan. 1989 78 p
(FEL-1989-22-Pt-3; TD89-1167-Pt-3; ETN-89-95083) Copyright Avail: TNO Physics and Electronics Lab., P.O. Box 96864, 2509 JG The Hague, Netherlands

The methods to calculate diffraction of electromagnetic radiation by a wedge, and especially monostatic reflection from the sharp edge of a half-plane. The derived Physical Optics is suited for smooth (perfectly conducting) surfaces. The method of Incremental Length Diffraction Coefficients (ILDC) is chosen because it is suited for edges of finite length and can easily be added to the method of Physical Optics. Experiments show that in many cases the addition of such a method to Physical Optics does not lead to better results than the use of Physical Optics alone. ESA

33 ELECTRONICS AND ELECTRICAL ENGINEERING

Includes test equipment and maintainability; components, e.g., tunnel diodes and transistors; microminiaturization; and integrated circuitry.

For related information see also *60 Computer Operations and Hardware* and *76 Solid-State Physics.*

N90-11941# Department of the Army, Washington, DC.
HIGH POWER, SOLID STATE RF PULSE GENERATORS Patent Application
Lawrence J. Bovino, inventor (to Army), Maurice Weiner, inventor (to Army), and Anderson H. Kim, inventor (to Army) 12 Jun. 1989 30 p
(AD-D014172; US-Patent-Appl-SN-374122) Avail: NTIS HC A03/MF A01 CSCL 10/2

A high power, solid state burst generator for producing RF pulses includes a plurality of transmission lines, such as coaxial cables, having one end connected across a load via a plurality of photoconductive switches, one for each line. The other end of the transmission lines are terminated in open ends and connected to a charging DC voltage. One set of lines is connected to a positive DC voltage +V while the other set is connected to a negative DC voltage -V. A laser is coupled to one end of a plurality of fiber optic lines, each having a different length, for simultaneously launching switch pulses thereon. The other ends of the fiber optic lines are each coupled to a different one of the photoconductive switches for closing and opening the switches in a sequential fashion such that the lines are sequentially discharged through the load to generate a cyclic series of pulses. GRA

N90-11942# Department of the Navy, Washington, DC.
MULTI-STAGE NOISE-REDUCING SYSTEM Patent Application
Harry B. Miller, inventor (to Navy) 20 Mar. 1989 29 p
(AD-D014179; US-Patent-Appl-SN-328651) Avail: NTIS HC A03/MF A01 CSCL 12/9

An electronic noise-reducing system is disclosed which includes a plurality of adaptive filters forming multiple stages of noise reduction and producing greatly increased signal-to-noise ratio. The input for the primary channel of the first adaptive filter, which forms the first noise-reducing stage, is the signal including multitones buried in noise. The reference channel ideally uses signal-free noise as input. The output of the first adaptive filter is used as the input to the primary channel of the second or final adaptive filter, whereas the reference channel thereof is fed with clean noise. The clean noise can be obtained as the output of the intermediate adaptive filter by feeding simultaneously both the primary and reference channels of the intermediate filter with the noise-reduced waveform present at the output of the first noise-reducing filter. GRA

N90-11943*# National Aeronautics and Space Administration. Lewis Research Center, Cleveland, OH.
CHANNELIZED COPLANAR WAVEGUIDE PIN-DIODE SWITCHES
G. E. Ponchak and R. N. Simons (Case Western Reserve Univ., Cleveland, OH.) Nov. 1989 10 p Presented at the European Microwave Conference, London, England, 8 Sep. 1989; sponsored in part by IEEE, IEE, URSI, and EUREL
(NASA-TM-102289; E-4959; NAS 1.15:102289) Avail: NTIS HC A02/MF A01 CSCL 09A

Three different types of p-i-n diode, reflective CPW switches are presented. The first two switches are the series and the shunt mounted diode switches. Each has achieved greater than 15 dB of isolation over a broad bandwidth. The third switch is a narrow band, high isolation switched filter which has achieved 19 dB of isolation. Equivalent circuits and measured performance for each switch is presented. Author

N90-11944# Helsinki Univ. (Finland). Radio Lab.
DESIGN, CONSTRUCTION AND TEST OF A FREQUENCY DOUBLER FOR 183 GHz
Timo J. Tolmunen and Antti V. Raeisaenen Mar. 1989 39 p
(PB89-212591; S-178; ISBN-951-754-826-5) Avail: NTIS HC A03/MF A01 CSCL 09C

The design, construction and test of a frequency doubler for 183 GHz is described. A proper Schottky-varactor is selected and analyzed using harmonic balance techniques to find theoretically available efficiency and output power, and associated impedances. A crossed waveguide mount is then designed using the results of the theoretical analysis and experience from scaled model measurements and from previous multiplier designs at lower frequencies. Differences in the design between higher-order frequency multipliers and a doubler are discussed. The constructed doubler utilizing a VD011 varactor from Farran Technology was tested over the output frequency range of 160-193 GHz. GRA

N90-11945# Sandia National Labs., Albuquerque, NM.
CLEANING OF PRINTED CIRCUIT ASSEMBLIES WITH SURFACE-MOUNTED COMPONENTS
J. S. Arzigian 1989 5 p Presented at the International Telemetry Conference, San Diego, CA, 30 Oct. - 1 Nov. 1989
(Contract DE-AC04-76DP-00789)
(DE89-013609; SAND-89-1382C; CONF-8910106-1) Avail: NTIS HC A01/MF A01

The need for ever-increasing miniaturization of airborne instrumentation through the use of surface mounted components closely placed on printed circuit boards highlights problems with traditional board cleaning methods. The reliability of assemblies which have been cleaned with vapor degreasing and spray cleaning can be seriously compromised by residual contaminants leading to solder joint failure, board corrosion, and even electrical failure of the mounted parts. In addition, recent government actions to eliminate fully halogenated chlorofluorocarbons (CFC) and chlorinated hydrocarbons from the industrial environment require the development of new cleaning materials and techniques. This paper discusses alternative cleaning materials and techniques and results that can be expected with them. Particular emphasis is placed on problems related to surface-mounted parts. These new techniques may lead to improved circuit reliability and, at the same time, be less expensive and less environmentally hazardous than the traditional systems. DOE

N90-11946# Texas Technological Univ., Lubbock. Dept. of Electrical Engineering.
DEVELOPMENT OF HIGH FREQUENCY SPICE MODELS FOR FERRITE CORE INDUCTORS AND TRANSFORMERS
G. Patrick Muyshondt and William M. Portnoy 1989 7 p Presented at the Industry Applications Conference, San Diego, CA, 1-5 Oct. 1989
(Contract DE-AC04-76DP-00789)
(DE89-015121; SAND-89-1626C; CONF-8910156-1) Avail: NTIS HC A02/MF A01

In this work high frequency SPICE models were developed to simulate the hysteresis and saturation effects of toroidal shaped ferrite core inductors and transformers. The models include the nonlinear, multi-valued B-H characteristic of the core material, leakage flux, stray capacitances, and core losses. The saturation effects were modeled using two diode clamping arrangements in conjunction with nonlinear dependent sources. Two possible controlling schemes were developed for the saturation switch. One of the arrangements used the current flowing through a series RC branch to control the switch, while the other used a NAND gate. The NAND gate implementation of the switch proved to be simpler and the parameters associated with it were easier to determine from the measurements and the B-H characteristics of the material. Lumped parameters were used to simulate the parasitic effects. Techniques for measuring these effects are described. The models were verified using manganese-zinc ferrite-type toroidal cores and they have general applicability to all circuit analysis codes equivalent function blocks such as multipliers, adders, and logic components. DOE

N90-11947# Sandia National Labs., Albuquerque, NM.
AN EMPIRICAL FORMULA FOR GAS SWITCH BREAKDOWN DELAY
T. H. Martin 1989 7 p Presented at the 7th IEEE Pulsed Power Conference, Monterey, CA, 12-14 Jun. 1989
(Contract DE-AC04-76DP-00789)
(DE89-017233; SAND-89-1954C; CONF-890665-45) Avail: NTIS HC A02/MF A01

An empirical scaling relationship between the mean electric field and the breakdown time has been found. Many divergent sets of data were used from breakdown experiments on power lines, laser-triggered switches, trigatrons, e-beam triggered gaps, sharp-point electrode to plane gaps, and uniform field gaps. This relationship builds on the Felsenthal and Proud data and extends their breakdown time delay (formative time) data by three orders of magnitude and into the region of interest for triggered gas switching. The data indicates that electrically triggered gaps, laser-triggered gaps, and untriggered gaps are governed by the same time-delay processes. Predictions can be made of trigger gap geometry, trigger delays, and trigger polarity effects. Breakdown delays of sub-centimeter-long to at least 8-meter-long gaps in air with either high or low field-enhanced electrodes are described by this equation. In addition, this relationship appears to be valid for a variety of gases and even accurately predicts the breakdown delay of mixtures of air and SF(sub 6). DOE

N90-11948# Oregon State Univ., Corvallis. Dept. of Electrical and Computer Engineering.
ADJUSTABLE SPEED DRIVE STUDY, PART 1 Summary Report, Jun. 1985 - Sep. 1988
A. Wallace Aug. 1989 69 p
(Contract DE-AI79-85BP-23169)
(DE89-017654; DOE/BP-23169/1) Avail: NTIS HC A04/MF A01

Advances in speed control for motors in recent years, notably those in power electronics, have widened the range of application for several adjustable speed drive (ASD) types to include the smaller horsepower sizes. The dc motor drive, formerly in almost universal use for speed control, is being challenged by the high efficiency induction motor/pulse width modulation (PWM) drive; and for special small horsepower size applications, by the permanent magnet motor/PWM inverter drive or by the switched reluctance motor drive. The main characteristics of the several ASD types suitable for small horsepower size applications are discussed, as well as their unwanted side effects: poor power factor, harmonic distortion of the supply, acoustic noise, and electromagnetic interference. A procedure is recommended for determining which, if any, ASD to use. DOE

N90-11949# Argonne National Lab., IL.
SAFETY CONSIDERATIONS FOR SODIUM-SULFUR BATTERIES FOR ELECTRIC VEHICLES
Frank Stodolsky 1989 11 p Presented at the SAE Conference and Expo on Future Transportation Technology, Vancouver, British Columbia, 6-10 Aug. 1989
(Contract W-31-109-eng-38)
(DE89-017682; CONF-8908144-1) Avail: NTIS HC A03/MF A01

Safety issues and current transport (shipment and in-vehicle use) and environmental regulations applicable to sodium-sulfur batteries for electric vehicles are summarized, and an assessment technique is suggested for evaluating hazards relative to commonly accepted risks. It is found that shipment regulations do not directly apply to sodium-sulfur batteries. Disposal hazards need to be quantified and decommissioning procedures need to be developed to comply with the environmental regulations. The risk assessment could be used to help commercialize sodium-sulfur and other advanced batteries in electric vehicles. DOE

N90-11950# Argonne National Lab., IL. Chemical Technology Div.
FUEL CELLS FOR VEHICLE PROPULSION APPLICATIONS: A THERMODYNAMIC SYSTEMS ANALYSIS
R. Kumar, M. Krumpelt, and B. Misra 1989 7 p Presented at the 24th Intersociety Energy Conversion Engineering Conference, Arlington, VA, 6-11 Aug. 1989
(Contract W-31-109-eng-38)
(DE89-017689; CONF-890815-26) Avail: NTIS HC A02/MF A01

The liquid- and air-cooled phosphoric acid, the proton exchange membrane, and the monolithic solid oxide fuel cell systems were analyzed for use in vehicle propulsion applications. System efficiency and input energy distribution were examined as a function of electrochemical fuel-utilization and other operating parameters. The liquid-cooled phosphoric acid and the monolithic solid oxide fuel cell systems have efficiencies approaching 40 percent; the air-cooled phosphoric acid and the proton exchange membrane fuel cells offer efficiencies near 30 percent. Thus the efficiencies of all of these fuel cell systems are much greater than the efficiencies of internal combustion engines. Our analyses indicate further that these fuel cells should be operated at the highest practical electrochemical fuel utilization rates for best efficiency and dynamic response, as well as minimum component volume and cost. DOE

N90-11951# Lawrence Livermore National Lab., CA.
HIGH GAIN FLUX COMPRESSION GENERATOR FABRICATION ISSUES
J. L. Cutting, D. K. Abe (Maryland Univ., College Park.), J. B. Chase, R. S. Hawke, P. A. Pincosy, H. T. Takemori, and M. L. Fillipucci 21 Jul. 1989 6 p Presented at the 5th International Conference on Megagauss Magnetic Field Generation and Related Topics, Novosibirsk, USSR, 3-7 Jul. 1989
(Contract W-7405-eng-48)
(DE89-017888; UCRL-100642; CONF-890710-18) Avail: NTIS HC A02/MF A01

The fabrication issues involved with a high gain helical flux compression generator are discussed. The generator is 20 cm in diameter, 76 cm long, contains 4500 gm of explosives, and its desired output is 2 million amperes into a 200-nH load. The goal is to attain better than 1000 X current multiplication. To achieve this goal great attention must be made to details such as mechanical fabrication tolerances, repeatability, and assembly techniques. DOE

N90-11952# Brookhaven National Lab., Upton, NY. Dept. of Physics.
SWITCHED POWER WORKSHOP: INTRODUCTION AND SUMMARY
R. B. Palmer (Stanford Univ., CA.) 1988 10 p Presented at the Switched-Power Workshop, Shelter Island, NY, 16-21 Oct. 1988
(Contract DE-AC02-76CH-00016)
(DE90-000036; BNL-42851; CONF-8810135-7) Avail: NTIS HC A02/MF A01

This paper discusses the design of a switched power electron gun. Particular topics discussed are: vacuum photodiode switch; laser switched solid state diodes; gun performance; charging supply; and laser requirements. DOE

N90-11953# California Univ., Berkeley. Lawrence Berkeley Lab.
ADVANCED LIGHT SOURCE MASTER OSCILLATOR
C. C. Lo, B. Taylor, and K. Baptiste Mar. 1989 4 p Presented at the 13th Particle Accelerator Conference, Chicago, IL, 20-23 Mar. 1989
(Contract DE-AC03-76SF-00098)
(DE90-000123; LBL-25974; CONF-890335-254) Avail: NTIS HC A01/MF A01

The Master Oscillator of the Advanced Light Source operates at a frequency of 499.654 MHz which is the 328th harmonic of the storage ring. The oscillator is capable of providing up to a maximum of (plus minus) 500 KHz frequency deviation for various experimental purposes. Provisions for external signal injection as well as using an external signal source were designed into the unit. A power distribution system was also included to provide signals for various parts of the ALS machine and user requirements. The Master Oscillator is made up with modules housed in a Euro chassis. DOE

N90-11954# Thomson-CSF, Orsay (France).
PROCEEDINGS OF THE WORKSHOP ON COMPOUND SEMICONDUCTOR DEVICES AND INTEGRATED CIRCUITS (13TH) HELD IN CABOURG, FRANCE ON 10-12 MAY 1989
12 May 1989 140 p Workshop held in Cabourg, France, 10-12 May 1989
(Contract DAJA45-89-M-0052)
(AD-A211848; R/D-6132-EE-02) Avail: NTIS HC A07/MF A01 CSCL 09/1

This symposium included the following topics: Large area growth of optoelectronic structures in the LP-VPE system; epitaxial growth on InP substrates etched with methane reactive ion etching technique; InP plasma epitaxy; MOVPE grown heterostructures for monolithic integration; parameters estimation tool for GaAs MESFET; two-dimensional simulation of the electron diffusion field-effect transistor; large signal switching model of GaAs MESFETs; very low noise 0.2 micron GaAs MESFET; backgating effect sensitivity to material parameters in HEMT structures; parasitic induced carrier-deconfinement in HFET's as studied by temperature dependent device characterization; and HEMT microwave characteristics at low temperatures. GRA

N90-11955# Massachusetts Inst. of Tech., Cambridge. Lab. for Computer Science.
NEARLY OPTIMAL ALGORITHMS AND BOUNDS FOR MULTILAYER CHANNEL ROUTING
Bonnie Berger, Martin Brady, Donna Brown (Illinois Univ., Urbana.), and Tom Leighton May 1989 49 p Sponsored in part by Xerox Corp., Stamford, CT; International Business Machines Corp., Armonk, NY and AT and T Bell Labs., Murray Hill, NJ
(Contracts N00014-80-C-0622; N00014-87-K-0825; NSF ECS-83-52185; AF-AFOSR-0078-86)
(AD-A211913; VLSI-MEMO-89-545) Avail: NTIS HC A03/MF A01 CSCL 09/1

Channel routing plays an important role in the development of automated layout systems for integrated circuits. Many layout systems first place modules on a chip and then wire together terminals on different modules that should be electrically connected. This wiring problem is often solved by heuristically partitioning the given space into rectangular channels and then assigning to each such channel a set of wires which are to pass through it. This solution reduces a global wiring problem to a set of disjoint (and hopefully easier) local channel routing subproblems. For this reason, the channel routing problem has been intensively studied for over a decade, and numerous heuristics and approximation algorithms have been proposed for its solution. The generic form of the channel routing problem may be described as follows. The channel consists of a rectilinear grid of tracks (or rows) and columns. Along the top and bottom tracks are numbers called terminals, and terminals with the same number form a net. A net with q terminals is called an q-terminal net. The smallest net is a two-terminal net; if q is greater than 2, we have a multiterminal net. The channel routing problem is to connect all the terminals in each net using horizontal and vertical wires which are routed along the underlying rectilinear grid. The goal is to complete the wiring using the minimum number of tracks; i.e., to minimize the width of the channel. GRA

N90-11956# Massachusetts Inst. of Tech., Cambridge. Dept. of Electrical Engineering and Computer Science.
REDUNDANCIES AND DON'T CARES IN SEQUENTIAL LOGIC SYNTHESIS Memorandum Report
Srinivas Devadas, Hi-Keung Tony Ma, and A. Richard Newton (California Univ., Berkeley.) May 1989 12 p Presented at the International Test Conference, Washington, DC, Aug. 1989
(Contract N00014-87-K-0825)
(AD-A211931; VLSI-MEMO-89-538) Avail: NTIS HC A03/MF A01 CSCL 09/1

The relationships between redundant logic and don't care conditions in combinational circuits are well known. Redundancies in a combinational circuit can be explicitly identified using test generation algorithms or implicitly eliminated by specifying don't cares for each gate in the combinational network and minimizing the gates, subject to the don't care conditions. The relationships are explored between redundant logic and don't care conditions in sequential circuits. Stuck-at faults in a sequential circuit may be testable in the combinational sense, but may be redundant because they do not alter the terminal behavior of anon-scan sequential machine. The sequential redundancies result in a faulty State Transition Graph (STG) that is equivalent to the STG of the true machine. A classification is presented of redundant faults in sequential circuits composed of single or interacting finite state machines. GRA

N90-11957# Massachusetts Inst. of Tech., Cambridge. Dept. of Electrical Engineering and Computer Science.
A DIGITAL MODEL FOR LEVEL-CLOCKED CIRCUITRY M.S. Thesis
Alexander Toichi Ishii May 1989 36 p
(Contract N00014-87-K-0825)
(AD-A211937; VLSI-MEMO-89-534) Avail: NTIS HC A03/MF A01 CSCL 09/1

This thesis presents the formal background for a mathematical model for level-clocked circuitry, in which latches are controlled by the levels (high or low) of clock signals rather that transitions (edges) of the clocks. Such level-clocked circuits are frequently used in MOS VSLI design. Our model maps continuous data-domains, such as voltage, into discrete, or digital, data domains, while retaining a continuous notion of time. A level-clocked circuit is represented as a graph G = (V,E) where V consists of digital components--latches and functional elements--and E represents inter-component connections. The majority of this thesis concentrates on developing lemmas and theorems that can serve as a set of axioms when analyzing algorithms based on the model. Key axioms include the fact that circuits in our model generate only well defined digital signals, and the fact that components in our model support and accurately handle the undefined values that electrical signals must take on when they make a transition between valid logic levels. In order to facilitate proofs for circuit properties, the class of computational predicates is defined. A circuit property can be provided by simply casting the property as a computational predicate. GRA

N90-11958# Minnesota Univ., Minneapolis. Dept. of Chemical Engineering and Materials Science.
ASSESSMENT OF THIN FILM BATTERIES BASED ON POLYMER ELECTROLYTES. PART 1: ENERGY DENSITY Technical Report, 15 Jun. 1989
M. Z. Munshi and B. B. Owens 15 Jun. 1989 23 p
(Contract N00014-88-K-0360)
(AD-A212111; TR-15-ONR) Avail: NTIS HC A03/MF A01 CSCL 10/3

The theoretical energy density performance limits for packaged rechargeable lithium polymer electrolyte batteries of both prismatic unipolar and bipolar electrode configurations are discussed. The electrolyte is based on complexes formed between polyethylene oxide and a lithium salt, and the composite cathode is V6O13. The modeling study suggests that specific energies up to 450 Wh/kg are possible for packaged batteries based on both unipolar and bipolar cell designs. This requires the use of low density metallic or metallized plastic current collectors. GRA

N90-11959# Helsinki Univ. of Technology, Espoo (Finland). Radio Lab.
CRYOGENIC SCHOTTKY-MIXER RECEIVER FRONT-END FOR 40-50 GHz
A. Lehto, J. Mallat, M. Mazanek, J. Peltonen, A. Raeisaenen, J.

Syvasalmi, and J. Tuovinen Mar. 1989 22 p
(PB89-221667; S-176; ISBN-951-754-824-9) Avail: NTIS HC A03/MF A01 CSCL 09A

A cryogenic Schottky-mixer front-end was constructed at the Radio Laboratory for radioastronomical observations with the Metsahoivi 13.7 m telescope. The front-end consists of a corrugated feed-horn, ring-filter, Schottky-mixer and FET amplifier at 1.4 GHz, all cooled down to 20 K by a closed cycle helium refrigerator. The beam from the telescope is fed to the feed-horn through a quasi-optical system consisting of an ellipsoid mirror, a flat mirror/chopper and a meniscus lens. The system allows a beam switching of 3 beam-widths and also focusing of the beam of the horn back to a cold reference load within the dewar. The receiver noise temperature (DSB) was measured to the below 200 K from 40 to 52 GHz and the lowest noise temperature to be 122 K at GHz. GRA

N90-11960# Illinois Univ., Urbana-Champaign. Coordinated Science Lab.

A DESIGN METHODOLOGY FOR SELF-TUNING CONTROL OF SYSTEMS WITH INHERENT CONFLICTS Ph.D. Thesis

Stephen Think Hung Jan. 1989 108 p
(Grant NSF ECS-87-15811)
(PB89-219505; UILU-ENG-89-2206; DC-110; NSF/ENG-89009) Avail: NTIS HC A06/MF A01 CSCL 09A

A methodology is outlined for the design of self-tuning controllers for systems with inherent control conflicts. These conflicts arise from either physical phenomena or user specifications. An intrinsic part of this methodology is the extensive collection and computer-aided incorporation of a priori information in the design process to enable realization of controllers of relatively simple structure and of low on-line computational requirements. Such simple solutions to complex problems are often overlooked when a priori information is unnecessarily neglected in some of the more mathematically elegant self-tuning algorithms proposed to date. Another intrinsic element of the methodology is the use of integral manifold and averaging techniques to simplify the analysis and design of self-tuning control of real processes. This serves not to confuse the design engineer, but to demonstrate the practical nature of some of the control theorists tools. GRA

N90-11961# Institute of Electrical and Electronics Engineers, New York, NY.

SOLID-STATE SENSOR AND ACTUATOR Final Report, 16 May 1988 - 15 May 1989

Richard S. Muller IEEE 1988 166 p Workshop held at Hilton Head Island, SC, 6-9 Jun. 1988 Submitted for publication Sponsored by NSF
(Contract DAAL03-88-G-0029)
(AD-A211427; ARO-26222.1-EL-CF; IEEE-88TH0215-4; LC-87-83469) Avail: NTIS HC A08/MF A01 CSCL 09/1

The proceedings of the workshop which were published by IEEE are presented. GRA

N90-11962# Army Missile Command, Redstone Arsenal, AL. Advanced Sensors Directorate.

POWER UP MODIFICATION FOR VIDEO SWITCHER MICROPROCESSOR INTERFACE FOR SENSOR SYSTEM PROCESSING SYSTEM Interim Technical Report, period ending 1988

Jonathan A. Mills Jun. 1989 13 p
(AD-A211543; AD-E951378; AMSMI/TR-RD-AS-88-8) Avail: NTIS HC A03/MF A01 CSCL 09/1

The Power-up Modification of the Video Switch Interface of the SSPS Lab is described. The Video Switcher Microprocessor Interface is used to interface between the SSPS VAX 11/785 and the Video Switcher. The modifications made are: (1) creating a power-up circuit that resets the microprocessor, (2) changing the chip selects from the start-up program, and (3) programming the EPROM to run the start-up program and user interface program. GRA

N90-11963# Rome Air Development Center, Griffiss AFB, NY.

DIELECTRIC COVERED MICROSTRIP PATCH ANTENNAS Final Technical Report, Sep. 1987 - Sep. 1988

Lisa M. Sharpe Nov. 1988 24 p
(AD-A211577; RADC-TR-88-307) Avail: NTIS HC A03/MF A01 CSCL 09/1

Microstrip antennas have many properties that make them suitable for airborne and satellite communications systems. These antennas are low in cost and lightweight. For these reasons, Rome Air Development Center is interested in verifying and augmenting existing design models for these antennas. The theory and results are presented for modeling microstrip antennas that are covered with a sheet of dielectric material. There are several reasons for designing a microstrip antenna covered with a dielectric material. This configuration would allow the modeling of antennas with an integrated radome. A cover layer could possibly be used to support a polarizer; to mount additional antenna elements on top of the cover layer to provide bandwidth enhancements; or to be used as a dual frequency antenna. GRA

N90-11964# Naval Research Lab., Washington, DC. Materials Physics Branch.

SUPERCONDUCTING SWITCH PROGRAM Final Interim Report, Jan. 1987 - Apr. 1988

T. L. Francavilla, S. A. Wolf, and D. U. Gubser 22 Aug. 1989 21 p
(AD-A211580; NRL-MR-6508) Avail: NTIS HC A03/MF A01 CSCL 09/1

The feasibility of a superconducting opening switch is examined. The following is considered: (1) The achievement of critical current densities of over 10(exp 7) A/sq cm in NbN; (2) Determination of the power required to operate a superconducting switch; and (3) Utilization of materials other than NbN in such a switch. GRA

N90-11965# Sheffield Univ. (England). Dept. of Control Engineering.

ADAPTIVE NOISE CANCELLATION FOR A CLASS OF NONLINEAR 2R FILTER

S. A. Billings, M. ElHitmy, and A. R. D. Curtis Feb. 1989 25 p
(RR-351; ETN-89-95138) Avail: NTIS HC A03/MF A01

A Nonlinear AutoRegressive Moving Average model with eXogenous inputs (NARMAX) filter structure is introduced. This filter structure is to be used as a basis for the design of a class of nonlinear filters which can be used for noise cancellation. The design is an extension of the classical 2R filter. It is shown that the filter parameters can be estimated using a suboptimal least squares algorithm originally developed for system identification. Conditions for the convergence of the algorithm are briefly discussed and simulation results are presented which show the effectiveness of the new structure. ESA

N90-11966# Sheffield Univ. (England). Dept. of Control Engineering.

A DISTRIBUTED PIPELINED ARCHITECTURE OF THE RECURSIVE LAGRANGIAN EQUATIONS OF MOTION FOR ROBOT MANIPULATORS WITH VLSI IMPLEMENTATION

A. M. S. Zalzala and A. S. Morris Jan. 1989 50 p
(RR-353; ETN-89-95139) Avail: NTIS HC A03/MF A01

An efficient and fast computation of robot arm joint torques using very large scale integration (VLSI) is discussed. A distributed architecture for the recursive Lagrangian equations of motion is designed to solve the inverse dynamics problem. Lagrangian based equations are found to be more appropriate to implement than the equivalent Newtonian-based or classical Lagrangian-based equations where trajectory planner or controller designs are involved. A symbolic representation for parts of the relevant equations is developed as a contribution to the reduction of complexity. As a result, the utilization of each element in the multiprocessor system is high. The proposed architecture is shown to be adequate for real time applications and computationally efficient. Real time implementation is presented utilizing an Inmos T-800 transputer network, for which programming is performed in the OCCAM programming language, and simulation results are reported for a Puma 560 robot manipulator with six degrees of freedom. The practical system constructed also provides the opportunity to investigate the significance of interprocessor communication. ESA

34 FLUID MECHANICS AND HEAT TRANSFER

Includes boundary layers; hydrodynamics; fluidics; mass transfer; and ablation cooling.

For related information see also *02 Aerodynamics* and *77 Thermodynamics and Statistical Physics.*

N90-11967# National Inst. of Standards and Technology, Gaithersburg, MD. Center for Computing and Applied Mathematics.
ELIMINATION OF SPURIOUS EIGENVALUES IN THE CHEBYSHEV TAU SPECTRAL METHOD
G. B. McFadden, B. T. Murray, and R. F. Boisvert May 1989 19 p Sponsored in part by NASA and National Research Council
(PB89-209282; NISTIR-89/4090) Avail: NTIS HC A03/MF A01 CSCL 20D

Spectral methods have been used to great advantage in hydrodynamic stability calculations; the concepts are described in Orszag's seminal application of the Chebyshev tau method to the Orr-Sommerfeld equation for plane Poiseuille flow in 1971. Orszag discusses both the Chebyshev Galerkin and the Chebyshev tau methods, but presents results for the tau method, which is easier to implement than the Galerkin method. The tau method has the disadvantage that two unstable eigenvalues are produced that are artifacts of the discretization. An extremely simple modification to the Chebyshev tau method is presented which eliminates the spurious eigenvalues. First a simplified model of the Orr-Sommerfeld equaiton discussed by Gottlieb and Orszag was studied. Then the Chebyshev tau method is considered, which has two spurious eigenvalues, and then a modification which eliminates them is described. Finally, results for the Orr-Sommerfeld equation are considered where the modified tau method also eliminates the spurious eigenvalues. The simplicity of the modification makes it a convenient alternative to other approaches to the problem. Author

N90-11968*# Old Dominion Univ., Norfolk, VA.
A STUDY OF THE TEMPORAL STABILITY OF MULTIPLE CELL VORTICES Progress Report, period ending 31 Oct. 1989
Mehdi R. Khorrami Washington Nov. 1989 210 p
(Grant NAG1-530)
(NASA-CR-4261; NAS 1.26:4261) Avail: NTIS HC A10/MF A02 CSCL 20D

The effect of initial mean velocity field on the stability characteristics of longitudinal vortices is documented in detail. The temporal stability of isolated multiple cell vortices is considered. The types of vortices studied include single cell as well as two and three cell vortices. It is shown that cell multiplicity in the vortex core has drastic effects on the stability characteristics. On the basis of numerical calculations, it is concluded that the growth rates of instabilities in multiple cell vortices are substantially larger (two to threefold increases are observed) than those of a single cell vortex. It is also determined that there is a substantial increase in the effective range of axial and azimuthal wavenumbers where instabilities are present. But most importantly, there is the appearance of a variety of viscous modes of instability. In the case of vortices, these latter instabilities which highlight the importance of viscous forces have never been reported before. These effects are discussed in detail for the case of a two cell vortex. Author

N90-11969*# National Aeronautics and Space Administration. Lewis Research Center, Cleveland, OH.
HOPF BIFURCATION IN THE DRIVEN CAVITY
John W. Goodrich, Karl Gustafson, and Kadosa Halasi (Kansas State Univ., Manhattan.) Oct. 1989 52 p Submitted for publication
(NASA Order C-99066-G)
(NASA-TM-102334; E-4957-1; ICOMP-89-21; NAS 1.15:102334)
Avail: NTIS HC A04/MF A01 CSCL 20D

Incompressible two dimensional calculations are reported for the impulsively started lid driven cavity with aspect ratio two. The algorithm is based on the time dependent streamfunction equation, with a Crank-Nicolson differencing scheme for the diffusion terms, and with an Adams-Bashforth scheme for the convection terms. A multigrid method is used to solve the linear implicit equations at each time step. Periodic asymptotic solutions have been found for Re = 10000 and for Re = 5000. The Re = 5000 results are validated by grid refinement calculations. The solutions are shown to be precisely periodic, and care is taken to demonstrate that asymptotic states were reached. A discussion is included about the indicators that are used to show that an asymptotic state was reached, and to show that the asymptotic state is indeed periodic. Author

N90-11970*# National Aeronautics and Space Administration. Ames Research Center, Moffett Field, CA.
SIMULATION OF GLANCING SHOCK WAVE AND BOUNDARY LAYER INTERACTION
Ching-Mao Hung Sep. 1989 13 p Presented at the 8th GAMM Conference, Delft, The Netherlands, 27-29 Sep. 1989
(NASA-TM-102233; A-89241; NAS 1.15:102233) Avail: NTIS HC A03/MF A01 CSCL 20D

Shock waves generated by sharp fins, glancing across a laminar boundary layer growing over a flat plate, are simulated numerically. Several basic issues concerning the resultant three-dimensional flow separation are studied. Using the same number of grid points, different grid spacings are employed to investigate the effects of grid resolution on the origin of the line of separation. Various shock strengths (generated by different fin angles) are used to study the so-called separated and unseparated boundary layer and to establish the existence or absence of the secondary separation. The usual interpretations of the flow field from previous studies and new interpretations arising from the present simulation are discussed. Author

N90-11971# Ohio State Univ., Columbus. Engineering Experiment Station.
DOUBLY-FLUTED TUBES AND ENHANCED TUBES IN CONFINED CROSSFLOW Annual Report, Aug. 1987 - Jul. 1988
Richard N. Christensen and Srinivas Garimella May 1989 104 p
(Contract GRI-5087-260-1538)
(PB89-217921; GRI-89/0019) Avail: NTIS HC A06/MF A01 CSCL 20D

The report describes the results of an ongoing project to investigate the thermal hydraulic characteristics of spirally-enhanced tubes and annuli in heat exchanger applications. Heat transfer enhancement and pressure drop increase data for the turbulent flow regime available in the literature for over sixty spirally enhanced tubes fabricated by different manufacturers was analyzed. A geometric nondimensional parameter known as severity was used to collapse data for Nusselt number increase, friction factor increases and enhancement efficiency for all these tubes. GRA

N90-11972# Los Alamos National Lab., NM.
INDEXES FOR THE PROCEEDINGS OF THE SYMPOSIA (INTERNATIONAL) ON DETONATION, 1951 THROUGH 1985
Sharon L. Crane, William E. Deal, John B. Ramsay, and Bruce E. Takala Aug. 1989 92 p
(Contract W-7405-eng-36)
(DE89-015178; LA-11570-MS) Avail: NTIS HC A05/MF A01

The Proceedings of the eight Detonation Symposia have become the major archival source of information of international research in explosive phenomenology, theory, experimental techniques, numerical modeling, and high-rate reaction chemistry. In many cases, they contain the original reference or the only reference to major progress in the field. For some papers, the information is more complete than the complementary article appearing in a formal journal, yet for others, authors elected to publish only an abstract in the Proceedings. For the large majority of papers, the Symposia Proceedings provide the published reference to a body of work. However, no indexes exist for any of the Proceedings, making it difficult to locate a reference or to perform a preliminary literature search. This report indexes the eight existing Proceedings of the Detonation Symposia by paper titles, topic phrases, authors, and first appearance of acronyms and code names. DOE

N90-11973# Los Alamos National Lab., NM.
SHOCK-INDUCED REACTION IN SEVERAL LIQUIDS
Stephen A. Sheffield and Robert R. Alcon 1989 5 p Presented at the American Physical Society Topical Conference on Shock Compression of Condensed Matter, Albuquerque, NM, 14-17 Aug. 1989
(Contract W-7405-eng-36)
(DE89-016594; LA-UR-89-2718; CONF-890812-23) Avail: NTIS HC A01/MF A01

Single-shock experiments have been completed in several liquids using multiple, embedded, electromagnetic Lagrangian particle velocity and impulse gauges to measure shock waveforms. The liquids include acrylonitrile, bromoform, diiodomethane, phenylacetylene, bromocyclopropane, and carbon disulfide. Some of these are known to exhibit shock-induced reaction and others are considered to be candidates for reaction studies. The universal liquid Hugoniot, which depends only on initial condition sound speed, was used to calculate the unreacted Hugoniot. Sound velocities were measured for those liquids with no data available. The effects of shock-induced reaction are clearly identified in the particle velocity waveforms for some materials, but there are remaining questions about whether reactions occur in others. The most impressive results are that the full reactive, two-wave structure was measured in phenylacetylene. On the reacting materials with two-wave structures, the particle velocity waveforms had a decrease behind the top of the first wave. This is thought to be evidence of an early reaction which occurs at the top of the first (nonreactive) wave. DOE

N90-11974# Los Alamos National Lab., NM. Chemical and Laser Sciences Div.
KIVA REACTIVE HYDRODYNAMICS CODE APPLIED TO DETONATIONS IN HIGH VACUUM
N. Roy Greiner 1989 33 p Presented at the NATO Advanced Study Institute on Chemistry and Physics of Molecular Processes in Energetic Materials, Sicily, Italy, 2-15 Sep. 1989
(Contract W-7405-eng-36)
(DE89-016979; LA-UR-89-2783; CONF-8909182-1) Avail: NTIS HC A03/MF A01

The KIVA reactive hydrodynamics code was adapted for modeling detonation hydrodynamics in a high vacuum. Adiabatic cooling rapidly freezes detonation reactions as a result of free expansion into the vacuum. After further expansion, a molecular beam of the products is admitted without disturbance into a drift tube, where the products are analyzed with a mass spectrometer. How the model is used for interpretation and design of experiments for detonation chemistry is explained. Modeling of experimental hydrodynamic characterization by laser-schlieren imaging and model-aided mapping that will link chemical composition data to particular volume elements in the explosive charge are also discussed. DOE

N90-11975# California Inst. of Tech., Pasadena.
NUMERICAL ANALYSIS, SCIENTIFIC COMPUTING AND FUNDAMENTAL STUDIES OF FLUID MECHANICS Final Report, 1 Apr. 1986 - 31 Mar. 1989
1989 10 p
(Contracts DE-AS03-76ER-72012; DE-AA03-76SF-00767)
(DE89-017554; DOE/ER-72012/T8) Avail: NTIS HC A02/MF A01

This paper briefly discusses the following topics: vortex dynamics, vortical flow and separated flow; free surface flows at low Reynolds number; concurrent linear algebra routines; concurrent continuation and invariant manifolds; concurrent multigrid continuation methods; AUTO-software; Taylor-vortex flows; boundary conditions for infinite domains; numerical and analytical studies of evolutionary systems; numerical methods for stiff differential equations; vortex reconnection; and a study of finite amplitude bifurcations in plane Poiseuille flow. DOE

N90-11976# Lawrence Livermore National Lab., CA.
VISAR WAVE PROFILE MEASUREMENTS IN SUPRA-COMPRESSED HE
David J. Erskine, L. Green, and C. Tarver Aug. 1989 6 p Presented at the American Physical Society Topical Conference on Shock Compression of Condensed Matter, Albuquerque, NM, 14-17 Aug. 1989
(Contract W-7405-eng-48)
(DE89-017736; UCRL-100835; CONF-890812-43) Avail: NTIS HC A02/MF A01

Using a VISAR velocimeter with nanosecond time resolution, wave profiles of the reaction zone were measured in planar TNT and 92.5/7.5 TATB/KEL-F samples impacted by flyer plates from a two stage gas gun, at shock pressures exceeding the detonation pressure. The results indicate that for increasing piston supported pressures the difference between inert and reaction product Hugoniots becomes very small. For TNT, the reaction zone is fairly well defined and does not extend beyond 150 ns. DOE

N90-11977# Lawrence Livermore National Lab., CA.
CHARACTERISTICS OF FLYER IMPACT FOR ONE-DIMENSIONAL SHOCK-WAVE STUDY APPLICATIONS
J. E. Osher, H. H. Chau, G. R. Gathers, and R. C. Weingart 25 Aug. 1989 5 p Presented at the American Physical Society Topical Conference on Shock Compression of Condensed Matter, Albuquerque, NM, 14-17 Aug. 1989
(Contract W-7405-eng-48)
(DE89-017887; UCRL-100901; CONF-890812-47) Avail: NTIS HC A01/MF A01

Lawrence Livermore National Laboratory's (LLNL's) linear, and new coaxial, electric guns was used in a variety of studies involving 1-D shock waves produced by the impact of plastic flyers at velocities up to 18 km/s. Flyer integrity and characteristics of the pressure pulse at impact are compared with code predictions for a variety of flyer thicknesses and velocities. Applications discussed include a study of the net forward impulse gain measured for 0.30-mm-thick flyers at normal incidence on thick targets of 6061-T6 aluminum at atmospheric pressure and under vacuum. DOE

N90-11978*# National Aeronautics and Space Administration. Ames Research Center, Moffett Field, CA.
NEAR-WALL, THREE-DIMENSIONAL TURBULENCE MEASUREMENTS: A CHALLENGE FOR LASER VELOCIMETRY
D. A. Johnson and S. D. Abrahamson (Minnesota Univ., Minneapolis.) Oct. 1989 14 p Presented at the 8th International Congress on Applications of Laser and Electro-Optics, Orlando, FL, 15-20 Oct. 1989
(NASA-TM-102252; A-89261; NAS 1.15:102252) Avail: NTIS HC A03/MF A01 CSCL 20D

A new laser velocimeter approach is presented, which has distinct advantages in near-wall, two- and three-dimensional turbulence measurement applications. The approach does require placing a probe into the flow; but in return, there are some important benefits, such as, the direct measurement of the crossflow velocity, w, at a grazing incidence, and the ability to size optical components for the scale of the flow rather than the size of the facility. Promising resuls were obtained with this approach for a two-dimensional turbulent boundary layer. Author

N90-11979# Army Research Inst. of Environmental Medicine, Natick, MA.
CONVECTIVE HEAT TRANSFER IN HYPOBARIC ENVIRONMENTS
Stephen KW. Chang and Richard R. Gonzalez Jul. 1989 28 p
(DA Proj. 3E1-62787-A8-78)
(AD-A212060; USARIEM-M64-89) Avail: NTIS HC A03/MF A01 CSCL 20/13

The relationship between convective heat transfer and barometric pressure (P sub b), specifically, how hypobaric pressure affects the convective heat transfer coefficient (H sub c) is examined. Five environmental conditions were simulated at elevation of 0 (sea level), 1520 m (5000 ft), 3050 m (10,000 ft), 4570 m (15,000 ft), and 6100 m (20,000 ft). In the chamber, constant temperature (30 C) and wind speed (0.5m/s) were maintained. The convective heat transfer coefficient was determined using the naphthalene sublimation technique. Circular naphthalene disks were affixed to six sites on a stationary copper manikin. The amount of naphthalene weight loss through sublimation was translated to H(sub c) using the Chilton-Colburn j-factor analogy between heat and mass transfer. As elevation increases, P(sub b) decreases; H(sub c) should decrease accordingly, pointing to a diminished convective heat transfer mechanism. Hitherto, the relationship between H(sub c) and P(sub b) was thought to be a nonlinear power function. The results showed that convective transfer indeed decreased at higher elevation, but H(sub c) and (sub b) exhibit a linear relationship. A linear relationship was also obtained from a theoretical derivation. These results suggest that in a hypobaric environment, the convective transfer process becomes even more diminished, and the potential convective heat loss is smaller than the original nonlinear theory would predict. GRA

N90-11980# Mississippi State Univ., Mississippi State. Dept. of Mechanical and Nuclear Engineering.
AN EXPERIMENTAL STUDY OF SURFACE ROUGHNESS EFFECTS ON TURBULENT BOUNDARY LAYER FLOW AND HEAT TRANSFER Annual Report, May 1988 - Mar. 1989
Hugh W. Coleman, Robert P. Taylor, M. H. Hosni, Glenn B. Brown, and Philip H. Love Apr. 1989 153 p
(Grant AF-AFOSR-0178-86; AF Proj. 2307)
(AD-A212099; AFOSR-89-1230TR) Avail: NTIS HC A08/MF A01 CSCL 20/13

The uncertainty analysis, design, and qualification of a Turbulent Heat Transfer Test Facility (THTTF) with a smooth wall test surface are presented, and initial results for a test surface roughened with hemispherical elements spaced four base diameters apart are discussed and compared with calculations from a previously developed discrete element prediction method. A description of the facility and discussions of details of the instrumentation systems, calibration procedures and uncertainties associated with the measurements are documented. GRA

N90-11981# Ben Gurion Univ. of the Negev, Beersheva (Israel).
EXPERIMENTAL INVESTIGATION OF A PLANAR SHOCK WAVE OVER A DOUBLE WEDGE Final Technical Report, 1 Oct. 1987 - 31 Dec. 1988
G. Ben-Dor 31 Dec. 1988 156 p
(Contract DAJA45-87-C-0042)
(AD-A211366; R/D-5838-PH-01) Avail: NTIS HC A08/MF A01 CSCL 20/4

The research project consisted of three different phases: An analytical investigation - During this phase the various reflection processes which can occur when a plane shock wave reflects over a double wedge were predicted. In addition, the transition boundaries between the various reflection processes were established. An experimental investigation was conducted to verify the above mentioned analysis. Some other aspects regarding the reflection of a plane wedge over a double wedge were investigated experimentally. In particular, the wave configuration which is approached asymptotically should be mentioned. A numerical code based on the TVD scheme was developed. The wave configurations as predicted by the numerical code were compared with those obtained experimentally and found to be in excellent agreement. This gave confidence in the numerical code and its predictions regarding the flow field generated during the reflection in general, and the pressure distribution along the wedge surface, in particular. GRA

N90-11982# Pennsylvania State Univ., University Park. Applied Research Lab.
AN INVESTIGATION OF END-WALL VORTEX CAVITATION IN A HIGH REYNOLDS NUMBER AXIAL-FLOW PUMP
Kevin J. Farrell Aug. 1989 182 p Sponsored by Naval Sea Systems Command
(AD-A211426; ARL/PSU/TR-89-004) Avail: NTIS HC A09/MF A01 CSCL 20/4

Relative motion of a turbomachinery blade row and the casing requires finite clearance between the rotor tips and the end-wall to avoid rubbing. Presence of this gap, relative motion of the blade tip and the end-wall, and pressure difference across the blade give rise to tip clearance flow which causes many adverse effects, including end-wall vortex cavitation. The vortex is formed by interaction of the clearance flow with the through flow on the suction side of the blade. This report formulates a correlation of the appropriate variables which predict the inception of end-wall vortex cavitation using the following approach: (1) identification of necessary parameters and relationships; (2) experimental measurements of the parameters in the High Reynolds Number Pump facility, a 42-inch diameter pump specifically designed for this purpose; (3) formulation of the correlation model from relationships among the measured variables; and (4) verification of the model with existing databases. The resulting model provides guidance to turbomachinery designers. The model of end-wall vortex cavitation successfully correlates the subject data existing databases. An optimum tip clearance was theoretically identified. The correlation model contains the boundary layer, lift coefficient, tip clearance, vortex core size, and tip geometry as input variables. Submodels have been developed for the core radius and tip lift coefficient as a function of tip clearance. Laser velocimeter measurements shown that additional circulation is shed into the tip vortex form the suction side trailing edge. GRA

N90-11983# Massachusetts Inst. of Tech., Cambridge. Computational Fluid Dynamics Lab.
COMPUTATIONAL METHODS FOR COMPLEX FLOWFIELDS Final Technical Report, 1 Jun. 1987 - 31 May 1989
Earll M. Murman and Judson R. Baron 5 Jul. 1989 290 p
(Grant AF-AFOSR-0218-87; AF Proj. 2307)
(AD-A211485; AFOSR-89-1072TR) Avail: NTIS HC A13/MF A02 CSCL 20/4

Development of solution algorithms for complex flowfields has been the objective of this research. Embedded subdomains were used to resolve relevant physical processes in a global flow around aerodynamic bodies. Adaptive approaches were studied and developed for the two- and three-dimensional Euler equations and two-dimensional Navier Stokes equations using finite volume and finite element methods. A new approach is reported for combining expert system approaches with adaptive procedural algorithms into a totally integrated methodology. Recent results on formulation of outflow boundary conditions for the Navier-Stokes equations and compact high-order schemes for the Euler equations are also presented. Additional tasks included: studying the performance of CFD algorithms on several parallel processors; a short study on turbulent spot measurements; and the prediction of dispersive errors in numerical solution of the Euler equations. GRA

N90-11984# Aerospace Corp., El Segundo, CA. Engineering Group.
THREE-DIMENSIONAL, TWO-PHASE, TRANSONIC, CANTED NOZZLE FLOWS Final Report, 1986 - 1988
I-Shih Chang 2 Dec. 1988 55 p
(Contract F04701-88-C-0089)
(AD-A211528; TR-0089(4530-04)-1; SD-TR-89-38) Avail: NTIS HC A04/MF A01 CSCL 20/4

A time-dependent numerical scheme, in conjunction with a three-dimensional, body-fitted coordinate transformation technique, is used for the solution of subsonic-transonic-supersonic flows: both gas-only, one-phase and fully coupled, gas-particle, two-phase flows inside three-dimensional canted nozzles of arbitrary configurations. The emphasis of the study is placed upon the transonic flow solution, which has been a bottleneck in many three-dimensional nozzle flow studies. Precise interpretation of flow variables in a canted nozzle is obtained through the simultaneous solution of multiple flow regions for motor aft closure and nozzle with two different coordinate centerlines. Numerical calculations are carried out for the seven-segment Titan IV solid rocket motor aft closure and nozzle internal flow field. The results of the three-dimensional flow analysis are in good agreement with available test data, and constitute the first rigorous numerical solution for canted nozzle flows since the inception of the Titan solid rocket motor program more than 25 years ago. GRA

N90-11985# Naval Surface Warfare Center, Silver Spring, MD.
VISCOUS SPLIT ALGORITHMS FOR THE TIME DEPENDENT INCOMPRESSIBLE NAVIER-STOKES EQUATIONS Final Report, 1986 - 1988
William G. Szymczak 6 Jun. 1989 15 p
(AD-A211592; NSWC-TR-89-136) Avail: NTIS HC A02/MF A01 CSCL 20/4

For problems involving the processes of convection and diffusion, a viscous split algorithm is one in which each process is solved separately. The emphasis is on the application of this procedure to obtain numerical solutions to the incompressible Navier-Stokes equations. A second order Godunov method is used to solve the convection step of the algorithm. The diffusion step (Stokes equation) is solved by the Galerkin Finite Difference Method which projects the solution onto a discreetly divergence free space using local mesh basis functions. Numerical results for both steady and unsteady flows are presented. GRA

N90-11986# Carnegie-Mellon Univ., Pittsburgh, PA. Dept. of Mathematics.
EFFICIENT FINITE ELEMENT SOLUTION OF NAVIER-STOKES EQUATIONS AND RELATED TOPICS Final Technical Report, 1 Jun. 1984 - 31 May 1989
R. A. Nicolaides 1989 6 p
(Grant AF-AFOSR-0137-84; AF Proj. 2304)
(AD-A211647; AFOSR-89-1180TR) Avail: NTIS HC A02/MF A01 CSCL 20/4

Research efforts were directed towards a number of different topics connected with numerical methods for incompressible fluid flows. The subject groupings were as follows: (1) Finite element techniques, Stability of discretizations, Stream function methods and pressure recovery, Nonconforming schemes; (2) Vortex techniques, Higher order vortex algorithms, Analysis and computation; (3) Solution algorithms, Deflated conjugate gradients, Iterative methods for arbitrary meshes, Domain decomposition methods; (4) Fluid mechanics and phase transitions, Cahn-Hilliard equation analysis and algorithms, Stationary and evolutionary cases; (5) Complementary volume methods, Vorticity-velocity methods, Primitive variable methods; and (6) Control theory. GRA

N90-11987# Mission Research Corp., Albuquerque, NM.
SOME NEW ALGORITHMS FOR BOUNDARY VALUE PROBLEMS IN SMOOTH PARTICLE HYDRODYNAMICS Technical Report, 6 Jun. 1988 - 6 Jun. 1989
Phil M. Campbell 6 Jun. 1989 47 p
(Contract DNA001-88-C-0079)
(AD-A211728; MRC/ABQ-R-1100; DNA-TR-88-286) Avail: NTIS HC A03/MF A01 CSCL 20/4

A rederivation of the basic equations of smoothed particle hydrodynamics is given that removes some of the intuitive elements in earlier work. New algorithms are obtained for hydrodynamics with heat flow that include boundary terms. These algorithms permit application of the method to systems driven by external pressures or heat sources. Hydrodynamic work terms are different in the new algorithms and these terms may eliminate some difficulties encountered with expressions found in the literature. The method developed for thermal diffusion yields the fluxes directly and may be extended to a flux limited diffusion formulation of radiation transport. GRA

N90-11988# Pennsylvania State Univ., University Park. Dept. of Mechanical Engineering.
EXPERIMENTAL RESEARCH ON SWEPT SHOCK WAVE/BOUNDARY LAYER INTERACTIONS Final Report, 1 Apr. 1986 - 31 Mar. 1989
Gary S. Settles 28 Jun. 1989 43 p
(Grant AF-AFOSR-0082-86; AF Proj. 2307)
(AD-A211744; PSU-ME-R-88/89-0068; AFOSR-89-1055TR)
Avail: NTIS HC A03/MF A01 CSCL 20/4

An experimental research effort on the subject of swept shock wave interactions with turbulent boundary layers is reported. The research relied largely on nonintrusive, laser based optical flow diagnostics. Experiments were carried out to define the Mach number influence, flowfield structure, and quantitative skin friction behavior of fin generated swept interactions over the supersonic range from March 2.5 to 4.0, including weak, moderate, and strong interactions. The results have given new insight into the fin interaction flowfield structure, which involves a jet impingement process caused by shockwave bifurcation. High skin friction levels were measured in the vicinity of this jet impingement and were used for the validation of computational predictions carried out by others. GRA

N90-11989# Technische Univ., Delft (Netherlands). Faculty of Technical Mathematics and Informatics.
ON THE COMPUTATION OF NORMAL MODES OF A ROTATING, VISCOUS, INCOMPRESSIBLE FLUID WITH A CAPILLARY FREE BOUNDARY
R. M. S. M. Schulkes 1989 27 p
(Rept-89-01; ISSN-0922-5641; ETN-89-95111) Copyright Avail: NTIS HC A03/MF A01

A method for the computation of normal modes of a rotating, viscous, incompressible fluid with a capillary free boundary is studied. The variational formulation of the linearized problem leads, using a finite element discretization, to a quadratic eigenvalue problem. This problem is solved efficiently using an inverse iteration procedure. The effect on the eigenfrequencies of viscosity, boundary conditions, contact angle and angular velocity of the container is investigated for a variety of container shapes. ESA

N90-11990# European Space Agency, Paris (France).
CALCULATION ON FILM PREPARATION AND FILM MOTION OF A SWIRL ATOMIZER
Tom Schork and Zoltan Farago (Deutsche Forschungs- und Versuchsanstalt fuer Luft- und Raumfahrt, Hardthausen, Germany, F.R.) May 1989 86 p Transl. into ENGLISH for Berechnungen zur Filmaufbereitung und Filmbewegung einer Druckdrallduese (Hardthausen, Fed. Republic of Germany, DFVLR) 80 p Original language document was announced as N88-16962
(ESA-TT-1096; DFVLR-FB-87-25; ETN-89-95156) Avail: NTIS HC A05/MF A01; original German version available from DFVLR, VB-PL-DO, Postfach 90 60 58, 5000 Cologne, Fed. Republic of Germany, 31 DM

The calculation methods for integral hydraulic parameters of a swirl atomizer are presented. The time average mass flow, the film thickness and the film angle are taken into account. The total angular momentum is described by Bernoulli equation. Stability criteria to describe the vortex flow are presented. The film contour after leaving the nozzle is calculated by the force balance between the surface and inertia forces. The mass flows and film thicknesses are interpreted as time averages of periodic fluctuations. A possible extension for calculating spill atomizers (with open and semi open spill flows) and a possible procedure for taking into account viscosity effects, are described. ESA

N90-11991# Deutsche Forschungs- und Versuchsanstalt fuer Luft- und Raumfahrt, Goettingen (Germany, F.R.). Abteilung Messphysik.
ABSOLUTE DETERMINATION OF THE WALL SHEAR STRESS BY MEANS OF AN INTERFEROMETER Ph.D. Thesis - Goettingen Univ.
Jaime MarquezOlivares Mar. 1989 84 p In GERMAN; ENGLISH summary
(DFVLR-FB-89-13; ISSN-0171-1342; ETN-89-95309) Avail: NTIS HC A05/MF A01; DFVLR, VB-PL-DO, Postfach 90 60 58, 5000 Cologne, Federal Republic of Germany, 26 deutsche marks

The feasibility of determining the oil film thickness in a model designed to determine wall shear stress interferometrically is investigated. Determination of the oil film thickness can be achieved from inside the model. The measurements were undertaken on a flat plate in the low turbulence wind tunnel of the DFVLR (Deutsche Forshungs und Versuchsanstalt fur Luft und Raumfahrt) in Gottingen (RFA). Absolute data of the wall shear stresses obtained agrees within two percent with data deduced from a Blasius profile. In the case of a turbulent boundary layer the values increased by a factor of 1.6. The determination of the viscosity of the oil by means of the same optical set-up yields values which agree with data issued by the manufacturers. ESA

N90-11992# Deutsche Forschungs- und Versuchsanstalt fuer Luft- und Raumfahrt, Goettingen (Germany, F.R.). Abteilung Grenzschichten und Unterschalt Stroemungen.
NUMERICAL COMPUTATION OF THE VISCOUS FLOW FIELD AROUND A PROLATE SPHEROID Ph.D. Thesis -Technische Univ. Claustha
Florian Menter Mar. 1989 106 p In GERMAN; ENGLISH summary
(DFVLR-FB-89-22; ISSN-0171-1342; ETN-89-95317) Avail: NTIS HC A06/MF A01; DFVLR, VB-PL-DO, Postfach 90 60 58, 5000 Cologne, Federal Republic of Germany, 31.50 deutsche marks

Three dimensional boundary layer equations are solved using the Keller and the Zick-Zack Box methods. To observe the influence of the boundary conditions on the solution in regions with strong viscous-inviscid interaction, different boundary conditions are used (potential flow and experimental pressure distribution, as well as half-inverse boundary conditions). The Parabolized Navier-Stokes-(PNS) equations are solved using a space-marching finite-difference method. The numerical results are compared with each other and with the experimental results. The solutions of the PNS-equations are in close agreement with the experimental results. ESA

N90-11993 Gesellschaft fuer Mathematik und Datenverarbeitung, Saint Augustin (Germany, F.R.). Inst. fuer Methodische Grundlagen.
A MULTIGRID ALGORITHM FOR THE INCOMPRESSIBLE NAVIER-STOKES EQUATION
Anton Schueller Mar. 1989 15 p
(GMD-374; ISSN-0723-0508; ETN-89-95349) Copyright Avail: Fachinformationszentrum Karlsruhe, 7514 Eggenstein-Leopoldshafen 2, Federal Republic of Germany

A reformulation of the incompressible Navier-Stokes problem is derived. The continuity equation is replaced by a Poisson-like equation for the pressure. The corresponding discrete nonlinear system of equations has advantageous features for the numerical solution. For this system a multigrid algorithm is proposed. The smoothing scheme is a collective point relaxation. This algorithm is efficient for low and moderate values of Reynolds number. It can be easily vectorized and parallelized. The generalization to time dependent flows is possible. ESA

35 INSTRUMENTATION AND PHOTOGRAPHY

Includes remote sensors; measuring instruments and gages; detectors; cameras and photographic supplies; and holography.

For aerial photography see *43 Earth Resources and Remote Sensing.* For related information see also *06 Aircraft Instrumentation,* and *19 Spacecraft Instrumentation.*

N90-11994# Texas A&M Univ., College Station.
FIELD EVALUATION OF THE MULTI-DEPTH DEFLECTOMETERS Interim Research Report, Sep. 1986 - Sep. 1988
T. Scullion, J. Uzan, J. I. Yazdani, and P. Chan Sep. 1988 58 p Sponsored by Federal Highway Administration, Austin, TX and Texas State Dept. of Highways and Public Transportation, Austin
(PB89-207708; TTI-2-18-87-1123-2; RR-1123-2; FHWA/TX-88/1123-2) Avail: NTIS HC A04/MF A01 CSCL 14B

The Multi-Depth Deflectometer (MDD) is an LVDT deflection measuring device which is retrofitted into pavement layers. A maximum of six MDD modules may be installed in a single 1.5-inch diameter hole. The modules are clamped against the sides of the hole at the required depths and the center core is attached to an anchor located approximately 7 feet below the pavement surface. The MDD can measure either the relative elastic deflection or the total permanent deformation of each layer in the pavement system. By placing multiple modules in a single hole, the vertical strains induced in pavement layers can be measured. The report describes the installation of Multi-Depth Deflectometers at the Texas A and M Research Annex. The pavement response under both Falling Weight Deflectometer and truck loading is described, together with an analysis procedure to backcalculate layer moduli from depth deflection readings. The MDD results obtained are extremely promising. The device is relatively inexpensive and durable. It shows a great potential in assisting in several areas of pavement research, including backcalculation analysis, tire pressure and rutting studies. Author

N90-11995# Department of the Navy, Washington, DC.
APPARATUS AND METHOD FOR MONITORING PRESSURE LEAKS FROM A SEALED SYSTEM Patent Application
Jeanne A. Welch, inventor (to Navy) 5 Jun. 1989 14 p
(AD-D014168; US-Patent-Appl-SN-361074) Avail: NTIS HC A03/MF A01 CSCL 13/11

The present invention described herein relates to the field of measuring pressure changes in sealed systems. More specifically, the invention relates to measuring pressure changes in sealed lamps. The invention especially relates to measuring pressure changes due to leaks in sealed lamps used in an infrared jammer. Lamps used in infrared jamming and other applications contain evacuated or pressurized gases in a sealed chamber. Such lamps are surrounded by sealed envelopes. When leaks occur into the evacuated chamber, catastrophic lamp failure or implosion may occur resulting in injury to personnel and extensive property damage. GRA

N90-11996# Department of the Navy, Washington, DC.
MAGNETOSTRICTIVE TORQUE SENSOR Patent Application
Howard T. Savage, inventor (to Navy), Arthur E. Clark, inventor (to Navy), Marilyn Wun-Fogie, inventor (to Navy), Lawrence T. Kabacoff, inventor (to Navy), Antonio Herando, inventor (to Navy), and Bruce Beihoff, inventor (to Navy) 21 Jun. 1989 14 p
(AD-D014169; US-Patent-Appl-SN-374112) Avail: NTIS HC A03/MF A01 CSCL 14/2

Magnetostrictive wire having a low surface-to-volume ratio established by a constant non-planar cross-section, is helically deformed into contact with a shaft under a stress maintaining the wire in fixed relation to the shaft surface. Magnetic anisotropy is imparted to the wire by twist thereof about its cross-sectional axis while the wire is being helically deformed into contact with the shaft surface to form a torque sensor through which accurate torque detection is achieved. GRA

N90-11997# Department of the Navy, Washington, DC.
INFRARED DETECTOR ARRAY Patent Application
Tak-Kin Chu, inventor (to Navy) 27 Jun. 1989 13 p
(AD-D014170; US-Patent-Appl-SN-371884) Avail: NTIS HC A03/MF A01 CSCL 17/5

An infrared detector array is constructed by depositing a plurality of non-contiguous strips of infrared radiation responsive, semiconductor material on a base substrate. A contiguous metal semiconductor contact is then overlaid on the plurality of strips thereby forming an individual detector element wherever the metal contact crosses one of the plurality of strips. GRA

N90-11998# Los Alamos National Lab., NM.
EXPLODING METALLIC FOIL FUSE MODELING AT LOS ALAMOS
Irvin R. Lindemuth, Robert E. Reinovsky, and James H. Goforth 1989 6 p Presented at the 5th International Conference on Megagauss Magnetic Field Generation and Related Topics, Novosibirsk, USSR, 3-7 Jul. 1989
(Contract W-7405-eng-36)
(DE89-016970; LA-UR-89-2921; CONF-890710-17) Avail: NTIS HC A02/MF A01

A first-principles computational model of exploding metallic foil behavior was developed at Los Alamos. The model couples zero-dimensional magnetohydrodynamics with ohmic heating and electrical circuit equations and uses the Los Alamos SESAME atomic data base computer library to determine the foil material's temperature- and density-dependent pressure, specific energy, and electrical conductivity. The model encompasses many previously successful empirical models and offers plausible physical explanations of phenomena not treated by the empirical models. In addition to addressing the electrical circuit performance of an exploding foil, the model provides information on the temporal evolution of the foil material's density, temperature, pressure, electrical conductivity, and expansion and translational velocities. The physical insight gained by computational studies of two opening switch concepts being developed for application in an FCG-driven 1-MJ-class imploding plasma z-pinch experiment are reported. The first concept considered is a conventional electrically exploded fuse, which was demonstrated to operate at 16 MA driven by the 15-MJ-class FCG to be used in the 1 MJ implosion experiment. The second concept considered is a Type 2 explosively formed fuse (EFF), which was demonstrated to operate at the 8 MA level by a 1-MJ-class FCG. DOE

N90-11999*# Sverdrup Technology, Inc., Cleveland, OH.
DROPLET SIZING INSTRUMENTATION USED FOR ICING RESEARCH: OPERATION, CALIBRATION, AND ACCURACY Final Report
Edward A. Hovenac Aug. 1989 53 p Sponsored by FAA, Atlantic City International Airport, NJ
(Contract NAS3-25266)
(NASA-CR-182293; E-4538; NAS 1.26:182293; DOT/FAA/CD-89/13) Avail: NTIS HC A04/MF A01 CSCL 14B

The accuracy of the Forward Scattering Spectrometer Probe (FSSP) is determined using laboratory tests, wind tunnel comparisons, and computer simulations. Operation in an icing environment is discussed and a new calibration device for the FSSP (the rotating pinhole) is demonstrated to be a valuable tool. Operation of the Optical Array Probe is also presented along with a calibration device (the rotating reticle) which is suitable for performing detailed analysis of that instrument. Author

N90-12000# Los Alamos National Lab., NM.
LAGRANGIAN ANALYSIS OF MIV (MAGNETIC IMPULSE-VELOCITY) GAUGE EXPERIMENTS ON PBX 9502 USING THE MASS-DISPLACEMENT MOMENT FUNCTION
Charles A. Forest, Jerry Wackerle, Jerry J. Dick, Stephen A. Sheffield, and Donald R. Pettit 1989 24 p Presented at the 9th International Symposium on Detonation, Portland, OR, 28 Aug. - 1 Sep. 1989
(Contract W-7405-eng-36)
(DE89-016612; LA-UR-89-2898; CONF-890811-28) Avail: NTIS HC A03/MF A01

Magnetic Impulse-Velocity (MIV) gauges were used to measure the impulse and particle-velocity fields at discrete Lagrangian positions in two samples of the triaminotrinitrobenzene (TATB) explosive PBX 9502. Each sample was shock driven by a 6.4 mm layer of reacting superfine TATB ((rho)(sub 0) = 1.80 g/cm(sup 3)), which was itself shocked by a gas driven projectile. The gauge histories of particle velocity and impulse, and the derived displacement history were simultaneously fit to the partial derivatives of the mass-displacement moment function employing a single set of parameters. (The function also gives volume, energy, pressure and their time derivatives.) With an assumed mixture equation of state, the reaction extent and reaction rate were calculated. The two experiments were compared and rate correlations were examined. DOE

N90-12001# Fermi National Accelerator Lab., Batavia, IL.
SCINTILLATING FIBER RIBBON - TUNGSTEN CALORIMETER
A. Bross, M. Crisler, B. Kross, and J. Wrbanek (Illinois Univ. at Urbana-Champaign, Savoy.) 14 Jul. 1989 5 p
(Contract DE-AC02-76CH-03000)
(DE89-016705; FNAL-TM-1588) Avail: NTIS HC A01/MF A01

An ultra-high density scintillating fiber and tungsten calorimeter used as an active beam-dump for electrons are described. Data showing the calorimeter response to electrons with momenta between 50 and 350 GeV/c are presented. DOE

N90-12002# Lawrence Livermore National Lab., CA.
SHOCK PRESSURE DETERMINATION IN DETONATOR WIRES
A. M. Frank and G. R. Gathers 21 Jul. 1989 5 p Presented at the American Physical Society Topical Conference on Shock Compression of Condensed Matter, Albuquerque, NM, 14-17 Aug. 1989
(Contract W-7405-eng-48)
(DE89-017756; UCRL-100687; CONF-890812-46) Avail: NTIS HC A01/MF A01

High resolution microstreak photographs were used to record shock waves from water immersed, exploding detonator wires. Shock velocities were read directly from the photographs, and pressures were computed from known Hugoniot data. Wires were gold or aluminum, 35 microns in diameter by 1 mm long. The field of the streak camera covered a spatial width of about 1 mm and a time interval of 200 to 500 ns with resolutions of about 5 microns and 1 ns, respectively. Initial hand reduction of data, and the quadratic form of the Hugoniot, resulted in substantial data spread. Computer image analysis reduced the spread, although questions of interpretation and accuracy remain. Observation included waves generated by melting of the wire and by rebound of the melt wave. Shockwave pressures of over 15 kbar were generated, predominantly by the rebound wave from the burst, which overtakes the initial burst wave. DOE

N90-12003# Lawrence Livermore National Lab., CA.
A MICROCHANNEL PLATE INTENSIFIED, SUBNANOSECOND, X-RAY IMAGING CAMERA
M. R. Carter, B. J. McKinley, and K. G. Tirsell Jul. 1989 18 p Presented at the 9th International Conference on Vacuum Ultraviolet Radiation Physics, Honolulu, HI, 14-18 Aug. 1989
(Contract W-7405-eng-48)
(DE89-017781; UCRL-100784; CONF-890809-1) Avail: NTIS HC A03/MF A01

A microchannel plate intensified, subnanosecond X-ray detector was developed for X-ray imaging experiments. It consists of an X-ray photocathode, a microchannel plate, electrostatic focusing optics and a subnanosecond phosphor. The detector is used for 1-D imaging and spectroscopic measurements. Signals are recorded using either a 1-D Reticon camera or a streak camera. The microchannel plates employ an X-ray photocathode (CuI or

CsI) deposited on the front surface of the microchannel plate to enhance their soft X-ray efficiency. Electrostatic focusing of the electrons exiting the microchannel plate also enhances the gain of the detector by an order of magnitude. The electrons are accelerated to 20 kV before striking a fast phosphor (Indium doped Cadmium Sulfide). The detector output is coupled to a Reticon camera or a streak camera with a fiber optic array. More than 20 microchannel plate intensified detectors were built and calibrated. Efficiencies in excess of 1000 (Watts/sq cm) output per (Watt/sq cm) input) were demonstrated. The time response of the detector is less than 500 ps. The efficiency of the CuI and CsI X-ray photocathodes were measured from 450 eV to 1300 eV at the Stanford Synchrotron Radiation Laboratory. Data are presented on the efficiency, time response, spectral response and the spatial resolution of the detectors. DOE

N90-12004# Lawrence Livermore National Lab., CA. Lab. for Experimental Astrophysics.
HIGH RESOLUTION X-RAY SPECTROSCOPY USING GERMANIUM MICROCALORIMETERS
E. Silver, S. Labov, F. Goulding, N. Madden, D. Landis, J. Beeman, T. Pfafman, L. Melkonian, I. Millett, and Y. Wai (California Univ., Berkeley.) 26 Jul. 1989 11 p Presented at the 33rd SPIE Annual International Technical Symposium on Optical and Optoelectronic Applied Science and Engineering, San Diego, CA, 6-11 Aug. 1989
(Contract W-7405-eng-48)
(DE89-017784; UCRL-101721; CONF-890836-14) Avail: NTIS HC A03/MF A01

Cryogenically cooled microcalorimeters were used for high resolution X-ray spectroscopy. Using neutron transmutation doped (NTD) germanium thermistors as the X-ray absorber, an energy resolution of 70 eV was achieved at a temperature of 0.3 K. There is strong evidence for incomplete conversion of X-ray energy into thermal energy when the photon is absorbed in the bulk of the NTD germanium. It is believed that the nonthermal energy component manifests as ionization, none of which is converted to thermal energy within the measurement time of the system. As in an ionization detector, the division between ionization and thermal energy is statistically uncertain and leads to a lower limit to the energy resolution measured using either the thermal or ionization signal. Complete conversion to thermal energy with no loss to ionization appears to occur when the X-ray is absorbed by the metallic contacts. This is discussed in the context of the most recent 0.3 K experiments. DOE

N90-12005# Wentworth Inst., Boston, MA.
DESIGN OF SCIENTIFIC PAYLOADS AND COMPONENTS Final Technical Report, Dec. 1982 - Jun. 1988
Richard B. Gates 15 May 1989 55 p
(Contract F19628-83-C-0014; AF Proj. 2698)
(AD-A211819; AFGL-TR-88-0326) Avail: NTIS HC A04/MF A01 CSCL 17/5

The primary task was to provide design, engineering, and fabrication support for AFGL toward the development of payloads for infrared measurements and other physical science experiments in space. Specific services provided included mechanical design and analysis of mechanical pieces and electro-mechanical devices, development of cost effective fabrication techniques, testing, and field support of the hardware. Also provided were the design, fabrication, assembly, testing, and integration of electronic devices including PCB's and their circuitry. Efforts consisted of design and fabrication of one-of-a-kind payloads and flight instruments, ground equipment, field launch services, and refurbishment of recovered payloads and instruments. GRA

N90-12006 Physics and Electronics Lab. TNO, The Hague (Netherlands).
FAST AND OBJECTIVE MRTD MEASUREMENT
A. N. DeJong and S. J. M. Bakker Jun. 1988 23 p Sponsored by the Netherlands Ministry of Defense
(FEL-1988-24; TD88-3269; ETN-89-95073) Copyright Avail: TNO Physics and Electronics Laboratory, P.O. Box 96864, 2509 JG The Hague, Netherlands

The method to measure the Minimum Resolvable Temperature Difference (MRTD) of a thermal imager is described. It is based upon simple targets, a CCD camera, an IBM PC with frame-grabber unit, and fast computation algorithms. The classical method and the proposed one are compared. A plot of the MRTD measurement of a prototype thermal imager with a tilted line target is given. In the described method the following features are outlined: the MRTD is obtained in an objective way, it can be measured in the field; the method is fast and cheap (+ or - 15 minutes) compared to the classical method, because the targets are simple, no expensive collimator system is necessary, the temperature stability can be relatively low, and there is no need for expensive observers. It is recommended to look for possibilities to reach an international agreement about an MRTD measurement. ESA

N90-12007# Deutsche Forschungs- und Versuchsanstalt fuer Luft- und Raumfahrt, Brunswick (Germany, F.R.). Abteilung Flugversuchstechnik.
DEVICES AND PROCEDURES FOR THE CALIBRATION OF SENSORS AND MEASUREMENT: SYSTEMS OF THE FLIGHT TEST SUPPORT SYSTEM ATTAS
Rudolf Oliva and Dieter Otto Dec. 1988 94 p In GERMAN; ENGLISH summary
(DFVLR-Mitt-89-06; ISSN-0176-7739; ETN-89-95297; AD-B134983L) Avail: NTIS HC A05/MF A01; DFVLR, VB-PL-DO, Postfach 90 60 58, 5000 Cologne, Fed. Republic of Germany, 50 DM

A detailed description of devices used in the calibration of sensors of the flight test support system ATTAS (Advanced Technologies Testing Aircraft System) is presented. The devices were developed and manufactured by the Flight Test Engineering Division of the Institute for Flight Mechanics. The installation of the devices and calibration procedures are described. Proposals for improvement of calibration devices and procedures are discussed. ESA

N90-12008# Deutsche Forschungs- und Versuchsanstalt fuer Luft- und Raumfahrt, Oberpfaffenhofen (West Germany). Inst. for Optoelectronics.
INFRARED TEMPERATURE MEASUREMENT WITH AUTOMATIC CONSIDERATION OF EMISSIVITY
Volker Tank (Deutsche Forschungs- und Versuchsanstalt fuer Luft- und Raumfahrt, Oberpfaffenhofen, West Germany) Jul. 1989 217 p Transl. into ENGLISH of Infrarottemperaturmessung mit Selbsttaetiger Beruecksichtigung des Emissionsgrads (Oberpfaffenhofen, Fed. Republic of Germany, DFVLR), Mar. 1988 176 p Original language document was announced as N89-10271
(ESA-TT-1131; DFVLR-FB-88-22; ETN-89-95518) Avail: NTIS HC A10/MF A01; original German version available from DFVLR, VB-PL-DO, Postfach 90 60 58, 5000 Cologne, Fed. Republic of Germany

The theoretical and practical development of a system, for contactless infrared temperature measurement, is discussed. The components, the data reduction and the calibration procedures are investigated. A method, which measures spectral radiances of an object in ten narrow infrared bands is used. It is based on a balancing calculation of this data. The temperatures of the object and its environment as well as the object's emissivity are computed. The method is also suitable for strongly reflecting objects below the temperature of glow. Examples of measurements are included. ESA

36 LASERS AND MASERS

Includes parametric amplifiers.
For related information see also *76 Solid-State Physics.*

N90-12009*# Oklahoma State Univ., Stillwater. Dept. of Physics.
GROWTH AND CHARACTERIZATION OF MATERIALS FOR TUNABLE LASERS IN THE NEAR INFRARED SPECTRAL REGION Semiannual Progress Report, 1 Feb. - 31 Jul. 1989
Richard C. Powell and Joel J. Martin 23 Aug. 1989 35 p
(Grant NAG1-694)
(NASA-CR-185832; NAS 1.26:185832) Avail: NTIS HC A03/MF A01 CSCL 20E

Laser spectroscopy, crystal growth, and radiation damage research was performed. The laser spectroscopy effort focused on understanding the effects of excited state absorption processes involving pump photons. This was performed on a variety of rare earth ions in different hosts. The crystal growth and radiation damage effort focused on LiFY4 (YLF) doped with rare earth ions. The results of this work is described. Author

N90-12010# National Oceanic and Atmospheric Administration, Boulder, CO. Wave Propagation Lab.
PROPAGATION OF AN ELLIPTICAL LASER BEAM THROUGH THE TURBULENT ATMOSPHERE (VERTICAL BEAMS)
Richard J. Lataitis and James H. Churnside May 1989 19 p
(Contract ASL-87-8013)
(PB89-208680; NOAA-TM-ERL-WPL-165) Avail: NTIS HC A03/MF A01 CSCL 20E

The effect of a turbulence gradient on the mean irradiance profile of an elliptical beam is calculated. It is concluded that in a turbulent atmosphere the peak irradiance can be shifted to a point further from the ground. Also, the vertical symmetry of the beam can be perturbed because of greater horizontal beam spreading at lower heights where turbulence is stronger. However, the effect is significant only for highly elliptical beams, and only when the horizontal beam divergence is determined by turbulence. GRA

N90-12011*# Maryland Univ., College Park. Inst. for Physical Science and Technology.
PROGRESS OF RESEARCH ON WATER VAPOR LIDAR Progress Report, period ending 31 Jul. 1989
Thomas D. Wilkerson and U. N. Singh Oct. 1989 65 p
(Contract NCC1-25)
(NASA-CR-185970; NAS 1.26:185970; BN-1104) Avail: NTIS HC A04/MF A01 CSCL 20E

Research is summarized on applications of stimulated Raman scattering (SRS) of laser light into near infrared wavelengths suitable for atmospheric monitoring. Issues addressed are conversion efficiency, spectral purity, optimization of operating conditions, and amplification techniques. A Raman cell was developed and built for the laboratory program, and is now available to NASA-Langley, either as a design or as a completed cell for laboratory or flight applications. The Raman cell has been approved for flight in NASA's DC-8 aircraft. The self-seeding SRS technique developed here is suggested as an essential improvement for tunable near-IR DIAL applications at wavelengths of order 1 micrometer or greater. Author

N90-12012# Los Alamos National Lab., NM.
ZEEMAN INTERFEROMETRY
R. G. Johnston 1989 8 p Presented at the 33rd SPIE Annual International Technical Symposium on Optical and Optoelectronic Applied Science and Engineering, San Diego, CA, 6-11 Aug. 1989
(Contract W-7405-eng-36)
(DE89-015296; LA-UR-89-2500; CONF-890836-11) Avail: NTIS HC A02/MF A01

The use of a two-frequency, Zeeman effect laser permits simple, stable, rapid, and highly accurate interferometry. There are a number of interesting applications. Three of them are discussed here. DOE

N90-12013# Dortmund Univ. (Germany, F.R.). Abteilung Physik.
CONSTRUCTION OF A PICOSECOND LASER SYSTEM FOR THE INVESTIGATION OF SEMICONDUCTORS USING NONLINEAR OPTICAL METHODS Ph.D. Thesis [AUFBAU EINER PIKOSEKUNDEN-LASERANLAGE ZUR UNTERSUCCHUNG VON HALBLEITERN MIT HILFE NICHTLINEARER OPTISCHER METHODEN]
Reinhard Wille 1988 146 p In GERMAN Sponsored by Deutsche Forschungsgemeinschaft, Bonn, Fed. Republic of Germany
(ETN-89-94664) Avail: NTIS HC A07/MF A01

A picosecond laser system is developed, which opens a variety of investigation possibilities in the field of dynamic processes in solid state physics. The most important component is an actively mode-coupled Nd-YAG laser, giving 100 ps pulses. A synchronously coupled dye laser gives 50 ps pulses, providing a 60 micro-eV spectral resolution. It is demonstrated that in the range of these pulse lengths, interesting time-resolved phenomena can be expected. For the investigation of multiple quantum well (MQW) structures, requiring a laser source with very small photon energy, the pulse of a CO2-laser is shortened by reflection on an optically generated e-h plasma in a Ge-plate. This pulse is used to study the dynamic stark effect, and the energy difference between both subbands in an undoped MQW structure. ESA

N90-12014# Swedish Inst. for Materials Testing, Boras.
COMPARISON OF I2-STABILIZED HE-NE LASERS
Leslie Pendrill, Ove Poulsen, and Harald Simonsen 1989 29 p
Prepared in cooperation with Aarhus Univ., Denmark
(PB89-219844; SP-RAPP-1989:23) Avail: NTIS HC A03/MF A01 CSCL 20E

Two iodine-stabilized HeNe lasers (wavelength 0.633 micrometer) were compared in frequency at Arthus University, Institute of Physics, Denmark in December 1988. The designs of the two lasers were such that the lasers should satisfy the requirements specified by the International Conference for Weights and Measures in connection with the present definition of the unit of length, one meter. Full details are given of the comparison procedure, including some construction details of the lasers of importance in determining system performance. A discussion of a least-squares analysis of the measurements is also included. GRA

N90-12015# Lawrence Livermore National Lab., CA.
LASER IONIZATION MASS SPECTROSCOPY
Luis J. Bernardez, III and W. J. Siekhaus (Allied-Signal Aerospace Co., Kansas City, MO.) Oct. 1989 10 p Presented at the 3rd Annual IMOG Conference for UCRL 100290, Kansas City, MO, 18 Oct. 1989
(Contract W-7405-eng-48)
(DE89-008039; UCRL-100290; CONF-891068-1) Avail: NTIS HC A02/MF A01

Laser Ionization Mass Spectroscopy (LIMS) is a simple technique with several advantages and disadvantages over standard mass spectroscopy techniques. The LIMS technique uses a laser to vaporize a small portion of a sample. The vapor from the sample consists of a mixture of charged and neutral atoms or fragments. Using electrostatic grids, the ions (positive or negative) are given a known amount of kinetic energy and sent down a time-of-flight tube. The time it takes the ions to travel down the flight tube is recorded. Knowing the ions' energy, the length of the flight tube, and the time it takes the ions to travel that distance, the masses of the ions can be calculated. The instrument used is a LIMA 3 made by Cambridge Mass Spectrometry. It has a Quanta Ray DCR-11 Nd:YAG laser, which was frequency-quadrupled to 266 nm. The laser spot size is typically between 2 and 5 microns in diameter and the pulse width is between 5 and 10 nanoseconds. The energy of the laser is continually variable between 0.1 and 3.0 millijoules. The detector is a 17-stage venetian-blind multiplier made by Thorn EMI. The analysis is carried out under vacuum, usually between 10(exp -8) and 10(exp -9) Torr. The LIMA 3 has several useful features such as: a He-Ne pilot laser used to target the Nd:YAG laser; a microscope (which is used to view the sample through the laser optics); and a precision sample stage for accurate sample alignment. DOE

N90-12016# Los Alamos National Lab., NM.
A PROPOSED LINAC CAVITY RF DRIVE SYSTEM FOR THE LOS ALAMOS EXTREME ULTRAVIOLET FREE-ELECTRON LASER
W. Joel D. Johnson 1989 10 p Presented at the 11th International Free Electron Laser Conference, Naples, FL, 28 Aug. - 1 Sep. 1989
(Contract W-7405-eng-36)
(DE89-016614; LA-UR-89-2894; CONF-8908134-1) Avail: NTIS HC A02/MF A01

Since 1979, scientists and engineers at the Los Alamos National Laboratory have designed, constructed, and operated a radio-frequency (RF) linac free-electron laser (FEL) at wavelengths from 9 to 45 (mu)m. Coupled with success of other research centers investigating wavelengths from the visible to far-infrared, Los Alamos is now proposing a vacuum-ultraviolet and soft X-ray referred to henceforth as extreme ultraviolet, (XUV) FEL oscillator/Self-Amplified Spontaneous Emission amplifier with beam energies ranging from 100 MeV to 1 GeV. This paper will focus on the first milestone of the proposed Los Alamos XUV project, i.e., a 250-MeV linac with approximately 50 mA of average current, producing photons with wavelengths below 1000 (angstrom). DOE

N90-12017# Allied-Signal Corp., Morristown, NJ.
NEW LASER MATERIALS Final Report, 1 Jan. - 30 Sep. 1988
Bruce H. T. Chai, Marge Long, Robert C. Morris, and Dave Narasimhan Jun. 1989 45 p Prepared in cooperation with Lawrence Livermore National Lab., CA
(Contract W-7405-eng-48)
(DE89-017524; UCRL-15867-Vol-4) Avail: NTIS HC A03/MF A01

In the 1987 final report we reported the progress in both the search for ICF reactor laser and the pump laser for the 10 MJ research laser. In this contract period, the effort was mainly concentrated in search of new materials suitable for the 10 MJ research laser's pump laser, since it now has a greater degree of urgency. The data is to find a high efficiency chromium laser free running near 800 nm to match the absorption band of Nd. The long lifetime Nd laser acts as an energy storage media and is finally lased near 1.06(mu)m. The laser is then frequently tripled and guided to the fusion target. In order to achieve the necessary overall efficiency, the chromium pump laser has to be very efficient (better than 5 percent). The present search effort has been directed towards the identification of suitable Cr laser materials. In this report we shall list most of the experiments that we have conducted during the contract period, including the unsuccessful ones. We shall discuss in more detail those materials that showed promising signs, since we have done more work and more thought has been given to them. On this basis we will divide the discussion in two separate sections: (A) new chromium doped crystalline compounds, and (B) exploratory work and speculations on new compounds. DOE

N90-12018# Los Alamos National Lab., NM.
COMPARISON OF LASER AND NEUTRAL PARTICLE BEAM DISCRIMINATION
Gregory H. Canavan Sep. 1989 16 p
(Contract W-7405-eng-36)
(DE89-017786; LA-11572-MS) Avail: NTIS HC A03/MF A01

The relative ability of lasers and neutral particle beams (NPBs) to discriminate reentry vehicle (RV) and anti-satellite (ASAT) decoys is pivotal in assessing their relative worth as strategic defenses. Their ability is evaluated and their relative contributions are assessed. It is concluded that NPBs can typically discriminate about 100 times as many objects as can lasers, and do so with significantly greater certainty. DOE

N90-12019# Sandia National Labs., Albuquerque, NM.
PULSED-LASER-EXCITED RAMAN SPECTRA OF SHOCK COMPRESSED TRIAMINOTRINITROBENZENE
Wayne M. Trott and Anita M. Renlund 1989 20 p Presented at the 9th International Symposium on Detonation, Portland, OR, 28 Aug. - 1 Sep. 1989
(Contract DE-AC04-76DP-00789)
(DE90-000668; SAND-88-2483C; CONF-890811-31) Avail: NTIS HC A03/MF A01

Pulsed-laser-excited Raman scattering methods were used to examine sustained shock compression of 1,3,5-triamino 2,4,6-trinitrobenzene (TATB) at an optical window interface. Records of vibrational frequency shifts and line shape changes were obtained under variable and well-controlled shock loading using a 63 mm-diameter compressed gas gun to provide a planar impact geometry. To facilitate interpretation of the shock data. Raman spectra of TATB samples at elevated temperatures and ambient pressure were also acquired. Raman modes identified with the nitro and amino groups in TATB exhibit complex behavior arising from interactions associated with the extensive intra- and intermolecular hydrogen bonding network in this material. The distinct (and frequently competing) effects of pressure and temperature on these modes are discussed in relation to the known insensitivity of TATB to shock initiation. DOE

N90-12020# Georgia Inst. of Tech., Atlanta. Electromagnetics Lab.
MEGALIDAR Interim Report, 1 Aug. 1987 - 31 Jan. 1988
A. K. Garrison, G. W. Grams, E. M. Patterson, and D. W. Roberts 8 Feb. 1989 90 p
(Contract F33615-86-C-1051)
(AD-A212074; AFWAL-TR-88-1128) Avail: NTIS HC A05/MF A01 CSCL 17/9

An investigation is presented of the applicability of the 100-inch collimator facility to a LIDAR measurements program for AFWAL/AARI-3 at Wright-Patterson AFB. Particular measurements of atmospheric parameters and phenomena are suggested. The performance of the 100-inch LIDAR for observing Rayleigh and Raman backscattering from various altitudes were simulated assuming different laser powers and signal averaging times and the results are presented and discussed. A review of the kinds of LIDAR measurements that are required for broad coverage of atmospheric phenomena as well as a review of the technology required to instrument these measurements are given. The current status of the collimator is summarized and changes in the collimator optics to accommodate a 10.6-micrometer LIDAR are suggested. Preliminary designs for transmitter and receiver modules to facilitate the use of the collimator as a multi-LIDAR facility are discussed. GRA

N90-12021# Illinois Univ., Chicago. Lab. for Atomic, Molecular, and Radiation Physics.
LASER PRODUCTION OF SOFT X RAYS BY MULTIQUANTUM PROCESSES AND THE EXCITATION OF ATOMIC INNER-SHELL STATES Progress Report
Charles K. Rhodes, Ting Shan Luk, Armon McPherson, and Keith Boyer 6 Jul. 1989 58 p Sponsored by AFOSR; NSF; and Strategic Defense Initiative Organization
(Contract N00014-87-K-0558)
(AD-A211372) Avail: NTIS HC A04/MF A01 CSCL 20/5

Atomic and molecular materials exhibit complex behavior when exposed to strong externally applied fields. This research goal is to understand the nonlinear processes governing the coupling of intense radiation to atomic and molecular matter. The general amplitude under study is N gamma + X yields X superscript q+ + qe(-) + gamma prime, a class of processes which involves ionization with the collateral production of energetic electrons and radiation. Recently developed ultraviolet light sources are enabling the attainment of focal intensities such that the strong field regime can now be systematically studied. It was anticipated that such conditions would produce unusual excited states of matter and that expectation has been confirmed by recent experimental findings revealing the direct multiphoton production of inner-orbital

(2 sigma/g) excited states of N2+ and N2(2+). Indeed, it can be shown that the strong-field coupling represents a unique mode of interaction which combines (1) the application of strong electromagnetic forces with (2) a very small collateral transfer of energy. This regime is impossible to achieve with charged particle collisions or with low intensity radiation of any frequency. Interactions of this type are particularly effective in exciting electronic motions along specific molecular axes enabling the generation of new forms of highly excited matter regardless of molecular structure or composition. GRA

N90-12022# LTV Missiles and Electronics Group, Dallas, TX. Missiles Div.
A NONLINEAR-OPTICAL METHOD FOR COMBINING HIGH POWER LASER BEAMS Report, 1 Apr. 1988 - 30 Apr. 1989
Jay S. Chivian, C. A. Glosson, W. D. Cotten, C. D. Cantrell, III, and S. F. DiMarco 28 Apr. 1989 55 p
(Contract N00014-87-C-0114)
(AD-A211730; Rept-3-45400/9R-57) Avail: NTIS HC A04/MF A01 CSCL 20/6

The overall program goal was to investigate concepts for laser-controlled optics based on near-resonance non-linear dispersion in gases, and to demonstrate a laser-induced grating capable of high power laser beam combining. The theoretical work extended the previous year's effort in giving a more detailed view of those aspects which might prevent observation of a grating, and led to optimization of experimental parameters. Modifications and improvements were made to the experimental apparatus. No grating was observed over a wide range of experimental conditions, although the apparatus was capable of such demonstration had a grating existed. The most likely cause of trouble appears to be the complexity of the SF6 medium chosen for demonstration. As an apparatus check, a medium (e.g., vanadium dioxide) can be used in which it is known that a grating can be demonstrated. Measurements were extended on the effect of noble gas admixtures into SF6 on the absorption of 16.26 micrometers radiation; helium suppresses absorption, argon and xenon enhance absorption. It would be worthwhile to continue these studies in light of information to be gained regarding the effect of collisions on absorption spectra in molecular species. GRA

N90-12023# Fraunhofer Inst. fuer Physikalische Messtechnik, Freiburg (Germany, F.R.).
DEVELOPMENT OF MICROSTRUCTURED DH DIODE LASERS AND DETECTORS FOR THE NEAR AND MEDIUM IR SPECTRAL DOMAIN USING MOLECULAR BEAM EPITAXY [ENTWICKLUNG MIKROSTRUKTURIERTER DH-DIODENLASER UND DETEKTOREN FUER DEN NAHEN UND MITTLEREN INFRAROTEN SPEKTRALBERETCH UNTER EINSATZ VON MOLEKULARSTRAHLEPITAXIE]
A. Lambrecht, H. Boettner, and M. Tacke 31 Aug. 1988 149 p In GERMAN; ENGLISH summary
(Contract BMFT-13-N-5281-A5)
(IPM-15/1988; ETN-89-94620) Avail: Fachinformationszentrum Karlruhe 2, 7514 Eggenstein-Leopoldshafen 2, Fed. Republic of Germany

High Vacuum Molecular Beam Epitaxy (HV-MBE) is applied for the first time to develop infrared DH lasers and detectors. The operation temperature of DH lasers is further increased. Mainly lasers with PbEuSe in the active zone are produced. The short wavelength limit is further reduced to 2.9 micron in continuous wave operation. Lasers with very low threshold current are produced using mesa etching. First tests with the ternary material PbSrSe are conducted. In pulsed operation the worldwide highest operation temperature (17 C) for an IR (infrared) diode laser was obtained. The first HV-MBE laser is tested and found to be functional. ESA

N90-12024# European Space Agency, Paris (France).
LASER SOUNDING FROM SPACE: REPORT OF THE ESA TECHNOLOGY WORKING GROUP ON SPACE LASER SOUNDING AND RANGING
H. Lutz, ed., B. Battrick, ed., and E. Armandillo, ed. (European Space Agency. European Space Research and Technology Center, ESTEC, Noordwijk, Netherlands) Jan. 1989 64 p Original contains color illustrations
(ESA-SP-1108; ISSN-0379-6566; ETN-89-95011) Copyright Avail: NTIS HC A04/MF A01

The purpose and principles of spaceborne lidar are described, giving particular attention to candidates for space deployment, including simple backscatter lidar for measuring of cloud top height, cloud extend and optical properties, differential absorption lidar providing high vertical resolution measurements of humidity, temperature and pressure, a wind profiling lidar with the unique capability of improved weather forecasting and global dynamics, and a ranging and altimeter lidar for very accurate measurement of surface features, including ground, sea and ice cap height for solid earth studies. ESA

37 MECHANICAL ENGINEERING

Includes auxiliary systems (nonpower); machine elements and processes; and mechanical equipment.

N90-12025# Draper (Charles Stark) Lab., Inc., Cambridge, MA.
COMPUTER-AIDED DESIGN OF FLEXIBLE ASSEMBLY SYSTEMS Final Report, 15 Aug. 1986 - 31 Jan. 1988
Daniel E. Whitney, Thomas L. DeFazio, Richard E. Gustavson, Stephen C. Graves, Kurt Cooprider, Carol A. Holmes, Charles J. Klein, Mancheung Lui, and Suguna Pappu (Massachusetts Inst. of Tech., Cambridge.) 1988 107 p
(Grant NSF DMC-84-17949)
(PB89-216253; CSDL-R-2033; NSF/ENG-88038) Avail: NTIS HC A06/MF A01 CSCL 13H

The goal of the project is to better understand product and system design issues associated with flexible assembly. As a result of prior research and extensive work with industry on these topics, researchers identified the following knowledge gaps for study: (1) development of a systematic methodology for coordinated design of products and processes, especially assembly; (2) determination, enumeration, and evaluation of alternate assembly sequences; (3) economic analysis methods for assembly systems and processes, including the effects of inspection and rework; and (4) assembly system design methods, especially those which can create designs for systems that must handle model mix. Author

N90-12026# Battelle Columbus Labs., OH. Gas Appliance Technology Center.
AN ASSESSMENT OF TECHNOLOGY FOR SELF-POWERED GAS APPLIANCES: A GATC (GAS APPLIANCE TECHNOLOGY CENTER) Task Report, Jul. 1988 - Jan. 1989
Albert E. Weller and George H. Stickford 31 Jan. 1989 165 p
(Contract GRI-5086-241-1219)
(PB89-219265; GRI-89/0093) Avail: NTIS HC A08/MF A01 CSCL 13I

The study assessed the potential technical and economic feasibility of self-powered appliances, and identified candidate appliances and matching energy technologies for self-powered appliances. This assessment included residential and small commercial appliances that have a potential for near-term application. Author

N90-12027# Du Pont de Nemours (E. I.) and Co., Aiken, SC. Savannah River Lab.
RESISTANCE WELDING LARGE PARTS
W. R. Kanne 1989 9 p Presented at the IMOG Joining Subgroup Meeting, Amarillo, TX, 25-27 Oct. 1989
(Contract DE-AC09-76SR-00001)
(DE89-010462; DP-MS-89-20; CONF-891088-1) Avail: NTIS HC A02/MF A01

An ongoing program at Savannah River to develop resistance welding techniques for fabrication of vessels will be described in this report. Resistance upset welding has advantages over the fusion welding techniques presently used to fabricate bodies of vessels. Advantages include the high reliability, quality, and yield experienced with our present resistance welding processes (less than 0.5 percent rejects for pinch and reclamation welds). The process is fast (about one second) and easily controlled (only three primary variables: current, force, and time). The metallurgical properties of these solid state welds are closer to those of the base metal since there is no resolidified zone and the heat affected zone is small. DOE

N90-12028# Dartmouth Coll., Hanover, NH. School of Engineering.
THERMOMECHANICAL CONTACT PHENOMENA AND WEAR OF SLIDING COMPONENTS Final Report, 1 Jan. 1987 - 31 Dec. 1988
Francis E. Kennedy, Jr., Beda M. M. Espinoza, Susanne M. Pepper, and Lin Tang 31 Jul. 1989 68 p
(Contract N00014-87-K-0125)
(AD-A211290) Avail: NTIS HC A04/MF A01 CSCL 20/11

The objectives were to better understand the tribological behavior of ceramic coated rings sliding against carbon graphite and thermocracking that occurs with some of the ceramic coatings. Sliding wear tests were conducted on Inconel 625 substrates coated with four different hard materials: chromium oxide, chromium carbide, titanium nitride, and tungsten carbide. Tests were also run to determine the corrosion behavior of the ceramic coated rings in seawater. Surface profilometry, mass loss measurements, and microscopy were used to characterize wear, cracking and corrosion phenomena. Residual stresses and preferred orientations of one of the coatings (TiN) were determined by x ray diffractometry methods and hardness and modulus of elasticity of the TiN coatings were measured by nanoindentation hardness testing. Coupled with the experimental work was a theoretical analysis of temperatures and stresses in the contact region of the ceramic coating during sliding. The influence of various material and geometric parameters on coating cracking or spalling was studied in the analytical work. GRA

N90-12029# Sheffield Univ. (England). Dept. of Control Engineering.
AN OPTIMUM TRAJECTORY PLANNER FOR ROBOT MANIPULATORS IN JOINT-SPACE AND UNDER PHYSICAL CONSTRAINTS
A. M. S. Zalzala and A. S. Morris Nov. 1988 51 p
(RR-349; ETN-89-95136) Avail: NTIS HC A04/MF A01

A trajectory algorithm is developed, where the minimum-time history of the movement of the robot end-effector is defined. Planning is made in the joint-mode by combining a new approach to polynomial splines along with an exhaustive search technique to identify the best minimum-time trajectory. The uniqueness of this algorithm emerges from the unique combination of cubic and quadratic polynomials, and the ability to perform the search on local parts of each joint trajectory. A scaling process is applied to these local segments to ensure maximum performance. All physical and dynamical limitations inherent in the manipulator design, in addition to any geometric constraints imposed on the path are taken into consideration. Simulation programs and results are reported for a Puma 600 robot manipulator. ESA

N90-12030# Sheffield Univ. (England). Dept. of Control Engineering.
ON THE COMPLEXITY ANALYSIS OF THE CORIOLIS AND CENTRIPETAL EFFECTS OF A 6 DOF ROBOT MANIPULATOR
A. Y. Zomaya and A. S. Morris Oct. 1988 12 p
(RR-344; ETN-89-95131) Avail: NTIS HC A03/MF A01

The equations used in calculating the different forces and torques which control the movement of a robot manipulator are perfected. They involve a considerable amount of differential and nonlinear terms with high computational complexity. Centripetal and Coriolis effects based on the Lagrangian formulation, have been simplified and a lower order form produced which has reduced computational complexity. Simulation results for a robot arm are used to check for the validity of the derivation. ESA

N90-12031# Sheffield Univ. (England). Dept. of Control Engineering.
THE DYNAMIC PERFORMANCE OF ROBOT MANIPULATORS UNDER DIFFERENT OPERATING CONDITIONS
A. Y. Zomaya and A. S. Morris Oct. 1988 23 p
(RR-345; ETN-89-95132) Avail: NTIS HC A03/MF A01

A simplified symbolic Lagrangian representation of the different terms is presented, with emphasis on the Coriolis and centripetal effects. The accuracy and computational efficiency of this formulation is demonstrated by simulation of a Stanford and Puma 560 manipulator. Quantitative measurements and error analysis are included on the significance of Coriolis and centripetal terms under different load and speed conditions. How this representation can be used in studying the different interconnected relationships between the manipulator joints, speeds, loads, and actuation forces of a robot arm are discussed. ESA

N90-12032# Technische Univ., Delft (Netherlands). Faculty of Technical Mathematics and Informatics.
THREE-DIMENSIONAL VISCOELASTIC BODIES IN STEADY STATE FRICTIONAL ROLLING CONTACT WITH GENERALIZATION TO KNOTHE ROLLING
J. J. Kalker 1989 20 p
(Rept-89-23; ISSN-0922-5641; ETN-89-95582) Copyright Avail: NTIS HC A03/MF A01

The problem of three dimensional viscoelastic bodies in steady state frictional rolling contact is solved by largely reducing it to methods of solving contact problems in the theory of elasticity. The rolling bodies are approximated by half-spaces for the purpose of calculating the viscoelastic field only. The surface displacement due to certain simple loadings that move, unchanging, over the viscoelastic half-space with rolling velocity is calculated. The surface displacement is found as the convolution of the elastic solution with the relaxation function. This relaxation function is a decreasing exponential which renders the convolution a Laplace integral, which can be evaluated numerically. Rolling contact is controlled by several parameters of which the mutual approach of the rolling bodies, and the creepages are mentioned. The viscoelastic theory first derived, is applied to find the response of the rolling bodies to harmonic variations of the controlling parameters (Knothe rolling). ESA

N90-12033*# Illinois Univ., Chicago. Dept. of Mechanical Engineering.
GENERATION AND TOOTH CONTACT ANALYSIS OF SPIRAL BEVEL GEARS WITH PREDESIGNED PARABOLIC FUNCTIONS OF TRANSMISSION ERRORS Final Report
Faydor L. Litvin and Hong-Tao Lee Washington NASA Nov. 1989 215 p
(Grant NAG3-783; DA Proj. 1L1-62209-A-47-A)
(NASA-CR-4259; E-4977; AVSCOM-TR-89-C-014; NAS 1.26:4259) Avail: NTIS HC A10/MF A02 CSCL 13I

A new approach for determination of machine-tool settings for spiral bevel gears is proposed. The proposed settings provide a predesigned parabolic function of transmission errors and the desired location and orientation of the bearing contact. The predesigned parabolic function of transmission errors is able to absorb piece-wise linear functions of transmission errors that are caused by the gear misalignment and reduce gear noise. The gears are face-milled by head cutters with conical surfaces or surfaces of revolution. A computer program for simulation of meshing, bearing contact and determination of transmission errors for misaligned gear has been developed. Author

38 QUALITY ASSURANCE AND RELIABILITY

Includes product sampling procedures and techniques; and quality control.

N90-12034*# National Aeronautics and Space Administration. Lewis Research Center, Cleveland, OH.
MODEL 0A WIND TURBINE GENERATOR FMEA Final Report
William E. Klein (National Aeronautics and Space Administration. Plum Brook Reactor Facility, Sandusky, OH.) and Vincent R. Lalli Oct. 1989 8 p Proposed for presentation at the 1990 Annual Reliability and Maintainability Symposium, Los Angeles, CA, 23-25 Jan. 1990; cosponsored by ASME, ASQC, IIE, IEEE, SOLE, IES, AIAA, SSS, and SRE
(Contract DE-AB29-79ET-20370)
(NASA-TM-102378; E-5117; NAS 1.15:102378; DOE/NASA/20370-23) Avail: NTIS HC A02/MF A01 CSCL 10A

The results of Failure Modes and Effects Analysis (FMEA) conducted for the Wind Turbine Generators are presented. The FMEA was performed for the functional modes of each system, subsystem, or component. The single-point failures were eliminated for most of the systems. The blade system was the only exception. The qualitative probability of a blade separating was estimated at level D-remote. Many changes were made to the hardware as a result of this analysis. The most significant change was the addition of the safety system. Operational experience and need to improve machine availability have resulted in subsequent changes to the various systems which are also reflected in this FMEA. Author

N90-12035# Aeritalia S.p.A., Turin (Italy). Gruppo Velivoli da Combattimento.
IN SERVICE LIFE MONITORING SYSTEM USING G-METER READINGS AND MASS CONFIGURATION CONTROL
T. Giacobbe 1987 16 p Presented at the Associazione Italiana per la Fatica in Aeronautica, Milan, Italy, 16-17 Mar. 1987
(ETN-89-95218) Avail: NTIS HC A03/MF A01

The Interim Monitoring System (IMS) is described. This system is based on the g meter readings and allows it to know the fatigue life consumed, before the utilization of the maintenance recorder system. The fatigue life consumption is considerably lower than the theoretical one, if the contractual maneuver spectrum is applied. (The ratio between contractual flight hours and actual flight hours is about 0.25). The results are comparable to those employing Tornado. The usefulness of the system, related to the true life consumption and not to the flight hours, is stressed. ESA

N90-12036# National Inst. of Standards and Technology, Gaithersburg, MD. Office of nondestructive evaluation.
NDE (NON-DESTRUCTIVE EVALUATION) PUBLICATIONS, 1985
Leonard Mordfin, ed. Aug. 1989 43 p
(PB89-229025; NISTIR-89/4131) Avail: NTIS HC A03/MF A01 CSCL 14D

Bibliographic citations, with selected abstracts, for 131 publications that appeared in the open literature, primarily during calendar year 1985, are given. A detailed subject index is included as well as information on how copies of many of the publications may be obtained. Author

39 STRUCTURAL MECHANICS

Includes structural element design and weight analysis; fatigue; and thermal stress.

For applications see *05 Aircraft Design, Testing and Performance* and *18 Spacecraft Design, Testing and Performance.*

N90-12037 Worcester Polytechnic Inst., MA.
ERROR ESTIMATION AND SELF-ADAPTIVE MESH REFINEMENT FOR BOUNDARY ELEMENT METHOD Ph.D. Thesis
Kwo-Yih Jong 1989 168 p
Avail: Univ. Microfilms Order No. DA8912384

An a posteriori error estimate and self-adaptive h-refinement technique are developed for boundary element solutions. Two-dimensional and axisymmetric problems for potential and elasticity are investigated. Due to the boundary element discretization process, errors associated with the potential (displacement) and flux (traction) are found based on a given mesh. The local (element) L sub 2 error norm is formulated for the potential (displacement) or flux (traction) which exists in each element. The error norm is evaluated for the unknown quantity in each element. The global boundary L sub 2 error norm is found by summing the local boundary L sub 2 error norms. The evaluation of the local error norms is based on a projection process of adjacent boundary element solutions. A self-adaptive technique that requires minimal user interaction to activate the refinement process is proposed. Coupling the error estimates with the h-refinement strategy, a new mesh is obtained within a user prescribed tolerance. Only one refinement pass is needed, thus providing the least engineering and computational expenses. The reliability and accuracy of this technique are demonstrated by potential and elasticity examples. The proposed algorithm can be easily implemented as part of the postprocessor in an existing boundary element software system. Dissert. Abstr.

N90-12038# National Inst. of Standards and Technology, Gaithersburg, MD. Applied and Computational Mathematics Div.
MECHANISM FOR SHEAR BAND FORMATION IN THE HIGH STRAIN RATE TORSION TEST
Timothy J. Burns Jun. 1989 46 p
(PB89-215370; NISTIR-89/4121) Avail: NTIS HC A03/MF A01 CSCL 20K

An asymptotics argument is given, which shows that rigid unloading from the ends of the thin-walled tubular specimen, enchanced by conductive heat transfer, is a plausible mechanism for adiabatic shear band formation during the high strain rate torsion test. The argument assumes that thickness variations, as well as elastic and dynamic effects in the tube, can be ignored, but that heat conduction and heat-sink thermal boundary conditions must be included. The proposed mechanism is supported by a numerical analysis of a mathematical model of the torsion test, which is based on recent torsional Kolsky bar experimental work of Marchand and Duffy (1988), on a physical model of thermoelastic-plastic flow due to Wallace (1985), and on a phenomenological Arrhenius model of the plastic flow surface. The numerical technique used is the semi-discretization method of lines. GRA

N90-12039# National Aerospace Lab., Tokyo (Japan). First Airframe Div.
AXIAL COMPRESSION BUCKLING TEST ON THE H-2 LAUNCH VEHICLE SATELLITE FAIRING STRUCTURAL ELEMENT PROTOTYPE (ALUMINUM SURFACE PLATE/ALUMINUM HONEYCOMB SANDWICHED CURVED SURFACE PLATE)
Syunji Endoh, Yoshio Noguchi, Kunihiko Ohtake, Kouichi Ono, and Sachio Fukushima (National Space Development Agency, Tokyo, Japan) Jan. 1987 23 p In JAPANESE
(NAL-TM-563; ISSN-0452-2982; JTN-88-80058) Avail: NTIS HC A03/MF A01

The H-2 Launch Vehicle, which the National Space Development Agency of Japan (NASDA) is developing as the main launch vehicle for the 1990's, will have the capacity of launching a 2-ton class satellite into a geostationary orbit. The satellite fairing is being developed using Japanese technology. The NASDA has already finished the conceptual design of the launch vehicle and has decided to use a sandwich construction of aluminum surface plates and an aluminum honeycomb core as the construction format of the fairing structure. The satellite fairing is a large shell structure. Its buckling strength is an important structural design condition. Buckling of a sandwich structure can be divided into two types, namely, general instability and wrinkling. Intracell buckling also occurs with the honeycomb sandwich construction which uses honeycomb as the core, and poses a stability problem specific to the honeycomb board. These buckling phenomena are possible in plastic regions depending on the load resistance ability of the surface plate. The results of axial compression and buckling tests of a partial structural element model of the fairing, namely, the aluminum honeycomb sandwiched curved surface plates, are discussed. NASDA

N90-12040# George Washington Univ., Washington, DC. Graduate School of Engineering and Applied Science.

ACTIVE CONTROL OF THE FORCED AND TRANSIENT RESPONSE OF A FINITE BEAM M.S. Thesis

John Theodore Post 20 Oct. 1989 91 p
Avail: NTIS HC A05/MF A01

When studying structural vibrations resulting from a concentrated source, many structures may be modelled as a finite beam excited by a point source. The theoretical limit on cancelling the resulting beam vibrations by utilizing another point source as an active controller is explored. Three different types of excitation are considered, harmonic, random, and transient. In each case, a cost function is defined and minimized for numerous parameter variations. For the case of harmonic excitation, the cost function is obtained by integrating the mean squared displacement over a region of the beam in which control is desired. A controller is then found to minimize this cost function in the control interval. The control interval and controller location are continuously varied for several frequencies of excitation. The results show that control over the entire beam length is possible only when the excitation frequency is near a resonant frequency of the beam, but control over a subregion may be obtained even between resonant frequencies at the cost of increasing the vibration outside of the control region. For random excitation, the cost function is realized by integrating the expected value of the displacement squared over the interval of the beam in which control is desired. This is shown to yield the identical cost function as obtained by integrating the cost function for harmonic excitation over all excitation frequencies. As a result, it is always possible to reduce the cost function for random excitation whether controlling the entire beam or just a subregion, without ever increasing the vibration outside the region in which control is desired. The last type of excitation considered is a single, transient pulse. A cost function representative of the beam vibration is obtained by integrating the transient displacement squared over a region of the beam and over all time. The form of the controller is chosen a priori as either one or two delayed pulses. Delays constrain the controller to be causal. The best possible control is then examined while varying the region of control and the controller location. It is found that control is always possible using either one or two control pulses. The two pulse controller gives better performance than a single pulse controller, but finding the optimal delay time for the additional controllers increases as the square of the number of control pulses. Author

N90-12041*# National Aeronautics and Space Administration. Lewis Research Center, Cleveland, OH.

EFFECTS OF MISTUNING AND MATRIX STRUCTURE ON THE TOPOLOGY OF FREQUENCY RESPONSE CURVES

Dare Afolabi Oct. 1989 48 p
(NASA Order C-99066-G)
(NASA-TM-102290; ICOMP-89-17; E-4960; NAS 1.15:102290)
Avail: NTIS HC A03/MF A01 CSCL 20K

The stability of a frequency response curve under mild perturbations of the system's matrix is investigated. Using recent developments in the theory of singularities of differentiable maps, it is shown that the stability of a response curve depends on the structure of the system's matrix. In particular, the frequency response curves of a cylic system are shown to be unstable. Consequently, slight parameter variations engendered by mistuning will induce a significant difference in the topology of the forced response curves, if the mistuning transformation crosses the bifurcation set. Author

N90-12042*# National Aeronautics and Space Administration. Hugh L. Dryden Flight Research Facility, Edwards, CA.

EFFECT OF CONTROL SURFACE MASS UNBALANCE ON THE STABILITY OF A CLOSED-LOOP ACTIVE CONTROL SYSTEM

E. Nissim (Technion - Israel Inst. of Tech., Haifa.) Oct. 1989 26 p
(NASA-TP-2952; H-1534; NAS 1.60:2952) Avail: NTIS HC A03/MF A01 CSCL 20K

The effects on stability of inertial forces arising from closed-loop activation of mass-unbalanced control surfaces are studied analytically using inertial energy approach, similar to the aerodynamic energy approach used for flutter suppression. The limitations of a single control surface like a leading-edge (LE) control or a trailing-edge (TE) control are demonstrated and compared to the superior combined LE-TE mass unbalanced system. It is shown that a spanwise section for sensor location can be determined which ensures minimum sensitivity to the mode shapes of the aircraft. It is shown that an LE control exhibits compatibility between inertial stabilization and aerodynamic stabilization, and that a TE control lacks such compatibility. The results of the present work should prove valuable, both for the purpose of flutter suppression using mass unbalanced control surfaces, or for the stabilization of structural modes of large space structures by means of inertial forces. Author

N90-12043# Technische Hogeschool, Delft (Netherlands). Faculty of Aerospace Engineering.

BUCKLING OF AXIALLY COMPRESSED IMPERFECT ORTHOTROPIC SHELLS WITH ELASTIC EDGE SUPPORTS

J. Arbocz, P. G. Vermeulen (Netherlands Agency for Aerospace Programs, Delft.), and J. vanGeer Mar. 1988 45 p Presented at the 26th IUTAM Congress, Lyngby, DE, Aug. 1984
(PB89-217038; LR-540) Avail: NTIS HC A03/MF A01 CSCL 20K

A rigorous solution is presented for the case of axially compressed stiffened cylindrical shells with general imperfections, where the edge supports are provided by symmetrical or unsymmetrical elastic rings. The circumferential dependence is eliminated by a truncated Fourier series. The resulting nonlinear 2-point boundary value problem is solved numerically via the Shooting Method. The changing deformation patterns resulting from the different degrees of interaction between the given initial imperfections and the specified end rings are displayed. Recommendations are made as to the minimum stiffnesses required for optimal load carrying configurations. GRA

N90-12044# Westinghouse Hanford Co., Richland, WA.

WIND/SEISMIC COMPARISONS FOR UPGRADING EXISTING STRUCTURES

Richard A. Giller Oct. 1989 11 p Presented at the 2nd DOE Natural Phenomena Hazards Mitigation Conference, Knoxville, TN, 3-5 Oct. 1989
(Contract DE-AC06-87RL-10930)
(DE89-016055; WHC-SA-0601; CONF-8910192-2) Avail: NTIS HC A03/MF A01

This paper depicts the analysis procedures and methods used to evaluate three existing building structures for extreme wind loads. The three structures involved in this evaluation are located at the U.S. Department of Energy's Hanford Site near Richland, Washington. This site is characterized by open flat grassland with few surrounding obstructions and has extreme winds in lieu of tornados as a design basis accident condition. This group of buildings represents a variety of construction types, including a concrete stack, a concrete load-bearing wall structure, and a rigid steel-frame building. The three structures included in this group have recently been evaluated for response to the design basis earthquake that included non-linear time history effects. The resulting loads and stresses from the wind analyses were compared to the loads and stresses resulting from seismic analyses. This approach eliminated the need to prepare additional capacity calculations that were already contained in the seismic evaluations. DOE

N90-12045# Los Alamos National Lab., NM.
A NUMERICAL LABORATORY FOR GRANULAR SOLIDS
B. C. Trent and L. G. Margolin (Lawrence Livermore National Lab., CA.) 1989 12 p Presented at the 1st US Conference on Discrete Element Methods, Golden, CO, 19-20 Oct. 1989
(Contract W-7405-eng-36)
(DE89-016367; LA-UR-89-2768; CONF-8910198-2) Avail: NTIS HC A03/MF A01

The behavior of cemented granular material is complex and difficult to characterize. Physical tests on laboratory-size specimens are time consuming and often inconclusive, due to the variable nature of the bulk material. As an alternate approach, we have used the distinct element method to construct numerical samples of cemented granular material. The model allows us to verify which are the important microphysical processes determining material behavior. We can do parameter studies, continuously varying the material properties of the bonding material and the topology of the bonds themselves, to see how the macroscopic properties depend upon the microscopic structure. We illustrate our program with two types of calculations. The first series consists of measuring the macroscopic p-wave and the s-wave speeds of the numerical sample, and using them to infer elastic properties of the bulk material. We also investigate how the number and size of the bonds influence bulk response. In the second series, we look at crack growth in granular materials. The Griffith theory of crack growth assumes an ideally flat crack. In granular materials and in our simulation, the crack is formed when many consecutive bonds in the material are broken. DOE

N90-12046# Oak Ridge National Lab., TN.
AN APPLICATION OF THE J-INTEGRAL TO AN INCREMENTAL ANALYSIS OF BLUNTING CRACK BEHAVIOR
J. G. Merkle 1989 27 p Presented at the European Symposium on Elastic-Plastic Fracture Mechanics, Freiburg, Federal Rep. of Germany, 9-12 Oct. 1989
(Contract DE-AC05-84OR-21400)
(DE89-016844; CONF-8910199-1) Avail: NTIS HC A03/MF A01

This paper describes an analytical approach to estimating the elastic-plastic stresses and strains near the tip of a blunting crack with a finite root radius. Rice's original derivation of the path independent J-integral considered the possibility of a finite crack tip root radius. For this problem Creager's elastic analysis gives the relation between the stress intensity factor K(sub I) and the near tip stresses. It can be shown that the relation K(sub I)(exp 2) = E'J holds when the root radius is finite. Recognizing that elastic-plastic behavior is incrementally linear then allows a derivation to be performed for a bielastic specimen having a crack tip region of reduced modulus, and the result differentiated to estimate elastic-plastic behavior. The result is the incremental form of Neuber's equation. This result does not require the assumption of any particular stress-strain relation. However by assuming a pure power law stress-strain relation and using Ilyushin's principle, the ordinary deformation theory form of Neuber's equation, K(sub sigma) K(sub epsilon) = K(sub t)(exp 2), is obtained. Applications of the incremental form of Neuber's equation have already been made to fatigue and fracture analysis. This paper helps to provide a theoretical basis for these methods previously considered semiempirical. DOE

N90-12047*# National Aeronautics and Space Administration. John F. Kennedy Space Center, Cocoa Beach, FL.
COMPUTATION OF GENERALIZED MODAL LOADS IN AN ACOUSTIC FIELD DEFINE BY A DISTRIBUTION OF CORRELATED PRESSURES
Valentin Sepcenko Aug. 1989 76 p
(Contract NAS10-11451)
(NASA-CR-186041; NAS 1.26:186041; KSC-DM-3265) Avail: NTIS HC A05/MF A01 CSCL 20K

This report is an aid to designers of structures with large area-to-mass ratios that are subject to high acoustic pressures during rocket launches. A means is provided for determining generalized modal loads using AJ-coefficients. AJ-coefficients are a measure of a vibroacoustic coupling between the structure and the acoustic field. Author

N90-12048# Army Armament Research and Development Command, Watervliet, NY.
AUTOFRETTAGE-STRESS DISTRIBUTION UNDER LOAD AND RETAINED STRESSES AFTER DEPRESSURIZATION Final Report
Boaz Avitzur Jul. 1989 46 p
(AD-A212090; ARCCB-TR-89019) Avail: NTIS HC A03/MF A01 CSCL 20/11

Autofrettage is a process in which a thick-walled tube is pressurized internally beyond its elastic limit. Reaching the elastic limit initiates plastic flow at the tube's bore (inner surface, r equals a). Gradual increases of the pressure at the bore are accompanied by a progressive thickening of the plastically deformed inner sleeve. This plastically deformed sleeve is in the range a less than or equal to r less than or equal to rho, with the elastic-plastic interface at r equals rho where a less than or equal to rho less than or equal to b. This process is commonly used in manufacturing some thick-walled pressure vessels which generated an interest in correlating the imposed pressure (usually an internal one) with the elastic plastic interface at r equals rho, and with the distribution of the retained state of stress throughout the wall thickness upon the removal of that pressure. In this report, four different methods of calculating such stresses are presented and compared. The methods are based on the following assumed yield criteria and deformation conditions: (1) Tresca's yield criterion; (2) Tresca's yield criterion times 2/square root of 3; (3) Mises' yield criterion in plane-stress; and (4) Mises' yield criterion in plane-strain. GRA

N90-12049# Army Lab. Command, Watertown, MA. Material Technology Lab.
A C(SUPERSCRIPT)-ANISOPARAMETRIC THREE-NODE SHALLOW SHELL ELEMENT FOR GENERAL SHELL ANALYSIS Final Report
Alexander Tessler Aug. 1989 25 p
(AD-A212094; MTL-TR-89-72) Avail: NTIS HC A03/MF A01 CSCL 12/1

A highly desirable three-node shallowly curved shell element is proposed for general shell analysis. Constrained-type C (sup 0) anisoparametric interpolations are derived for the membrane and transverse displacement fields by the use of explicit edge constraints. Pertinent issues on shell theory and infinite element approximation are addressed. Several numerical studies are carried out which demonstrate the effectiveness of this new triangular element in the regime of thin and moderately thick shells. GRA

N90-12050# Johns Hopkins Univ., Baltimore, MD. Dept. of Materials Science and Engineering.
MATERIALS CHARACTERIZATION USING HOLOGRAPHIC MAPPING OF TRANSIENT LAMB WAVES Technical Report, Jan. 1988 - Apr. 1989
Michael J. Ehrlich and James W. Wagner May 1989 82 p
(Contract N00014-82-K-0741)
(AD-A211414) Avail: NTIS HC A05/MF A01 CSCL 20/11

The testing of engineering materials is traditionally done using contact ultrasonic techniques or potentially destructive mechanical tests. For many materials, elastic properties are a function of both position and direction, owing to material anisotropy and inhomogeneities arising from process variation and defects. In order to determine these elastic properties as a function of position or direction using conventional techniques, it is necessary to scan the testing apparatus over the surface of the material. In contrast, holographic methods offer a means of full field determination of the elastic properties. Toward this end, the spatial propagation of antisymmetric Lamb waves in nearly homogeneous isotropic plates was investigated. Using high speed pulsed holographic techniques coupled with excitation of ultrasonic waves, surface displacements arising from Lamb wave propagation in thin plates result in interference patterns super sign imposed on the holographic reconstruction of the speciment image. The determination of Lamb wave group velocities utilizing a technique which uses only features of the spatial waveform has been demonstrated to yield results in good agreement with elastic plate theory. In addition, preliminary results show that the same holographic techniques may prove a useful tool in the characterization and evaluation of laminated composite plates. GRA

N90-12051# California Inst. of Tech., Pasadena. Graduate Aeronautical Labs.

AN EXPERIMENTAL AND ANALYTICAL PROGRAM TO DEVELOP CRACK TIP FRACTURE CRITERIA Final Report, 1 Sep. 1984 - 31 Oct. 1988

C. R. Schultheisz and W. G. Knauss 19 Jul. 1989 174 p
(Grant AF-AFOSR-0254-84; AF Proj. 2302)
(AD-A211565; AFOSR-89-1181TR) Avail: NTIS HC A08/MF A01 CSCL 20/11

The large plastic deformations at the tip of a crack in a ductile heat treatment of 4340 steel are studied numerically and experimentally. The numerical simulation of the experiment uses a small strain, incremental plasticity law, with a power law hardening behavior. Both the inplane and outplane deformations are measured on the same specimens at the same time. The experimental technique of moire interferometry is used to measure the inplane displacements. This technique is described in detail, including an analysis of the effort of outplane rotations on the use of the technique. A three beam interferometer and a four beam interferometer are compared. The outplane displacements are measured with a Twyman-Green interferometer. The analysis of this data is still underway and will be forward when completed. The numerical model is described in detail. The material properties are determined from a uniaxial test on specimens taken from the same bar as the fracture specimens and with identical heat treatment. A numerical model of the fracture specimen having 7581 degrees of freedom is used to provide data for comparison between 400 N (linear behavior) up to 75000 N (catastrophic failure of the steel specimen) in fourteen steps. GRA

N90-12052# ESDU International Ltd., London (England).

NATURAL FREQUENCIES OF SINGLY-CURVED LAMINATED PLATES WITH SIMPLY-SUPPORTED EDGES

Jun. 1989 32 p
(ESDU-89011; ISBN-0-85679-682-4; ISSN-0141-3961; ISSN-0958-0360) Avail: ESDU

This Data Item 89011, an addition to the Acoustic Fatigue and Composites Subseries, gives a FORTRAN program listing for the calculation of the lower natural frequencies of rectangular thin plates (thickness/shorter dimension ratio less than 0.05), either flat or with shallow curvative (shorter dimension/radius ratio very much less than unity). The input is structured to treat fibre-reinforced laminated plates particularly conveniently, but will also deal with isotropic materials. The effects of a uniformly distributed in-plane biaxial loading can be included but, if compressive, should not exceed 30 percent of the buckling load. In-plane shear is neglected, as are shear deformation and rotary inertia, and the method relies on small deflection, linear plate theory. The program is restricted to plates in which the shear coupling terms in the stiffness matrix are zero. The program was used to illustrate graphically for a typical laminated plate the effects of varying curvature and of varying the in-plane loading. The input format is explained in detail, and a worked example illustrates it and the format of the output. The program is available on magnetic media as ESDUpac 8811. ESDU

N90-12053# Royal Aerospace Establishment, Farnborough (England).

DEFORMATION OF ELECTRON BEAM WELDED Ti-6Al-4V ALLOY SHEET UNDER SUPERPLASTIC CONDITIONS

P. G. Partridge and D. V. Dunford 29 Jul. 1988 8 p Presented at the 6th World Conference on Titanium, Cannes, France, 6-9 Jun. 1988
(RAE-TM-MAT/STR-1109; BR108269; ETN-89-94201) Copyright Avail: Defence Research Information Centre, Kentigem House, 65 Brown Street, Glasgow, G2 8EX, Scotland

The effect of fusion welds on superplastic deformation of titanium alloy was studied. Electron beam welds in Ti-6Al-4V sheet deformed under superplastic conditions (at 800 or 925 C at a strain rate of 0.0002/sec) were less superplastic and deformed less than the adjacent sheet. This caused severe local thinning of the sheet when the weld direction deviated from the principal strain direction. However, deformation removed weld undercuts and caused acicular weld microstructures to become more like the equiaxed sheet microstructure. The implications for the superplastic forming of components from welded sheet, bar, and extrusions are discussed. ESA

N90-12054# Royal Aerospace Establishment, Farnborough (England).

EFFECT OF SUPERPLASTIC DEFORMATION ON THE SURFACE ROUGHNESS OF SHEET

P. G. Partridge and D. V. Dunford 29 Jul. 1988 8 p Presented at the International Conference on Superplasticity and Superplastic Forming, Blaine, WA, 1-4 Aug. 1988
(RAE-TM-MAT/STR-1112; BR108126; ETN-89-94202) Copyright Avail: Defence Research Information Centre, Kentigem House, 65 Brown Street, Glasgow, G2 8EX, Scotland

The arithmetic mean of the departure of the profile from the mean line (Ra value) was determined for titanium and aluminum alloy sheets before and after superplastic deformation. The significance of Ra values for forming and bonding of sheet is discussed. The surface roughness of thin sheet increases with increase in superplastic strain and with increase in grain size. The increase is greater in Al-alloys than in Ti-alloys. The increase in roughness could have implications for surface reactions, diffusion bonding, and for fatigue properties, especially for very thin sections. ESA

N90-12055# National Aerospace Lab., Amsterdam (Netherlands). Structures and Materials Div.

WISPER: A STANDARDIZED FATIGUE LOAD SEQUENCE FOR HAWT-BLADES

A. A. tenHave 25 May 1988 9 p Presented at the 1988 ECWEC Conference, Herning, Denmark, 6-10 Jun. 1988
(NLR-MP-88029-U; ETN-89-95055) Avail: NTIS HC A02/MF A01

A variable-amplitude test loading sequence for use in the fatigue evaluation of horizontal axis wind turbine (HAWT) blades is described. The WISPER sequence is derived from flap load measurements on nine different European wind turbines, covering different materials, a wide range of rotor-diameters and various geographical locations. The principles behind the data processing procedures of WISPER are explained. The subsequent development steps that led from basic input data to a final loading standard are shown. Information is supplied to enable potential users of the new standard to judge its validity and applicability to their purposes. Quantitative data not given here will be the subject of a third publication, giving a complete description of WISPER and its precise derivation steps. ESA

N90-12056# National Aerospace Lab., Amsterdam (Netherlands). Structures and Materials Div.

APPLICATION OF MATRIX CORRECTION METHODS ON A PLATE AND A TRUSS STRUCTURE

A. deBoer, H. H. Ottens, B. W. Kooi, and J. J. Wijker (Fokker B.V., Amsterdam, Netherlands) 17 Jun. 1988 19 p Presented at the StruCoMe 88 Conference, Paris, France, 2-4 Nov. 1988
(NLR-MP-88042-U; ETN-89-95056) Avail: NTIS HC A03/MF A01

Matrix correction methods proposed by Chen, Baruch, Berman, and Ceasar are evaluated using a simple plate and a truss structure. The plate experimental data is obtained from an impact test. The truss structure data is simulated. The structures are modeled using a finite element approach. To facilitate the comparison between measured and calculated results, the Guyan static condensation method is applied in calculating the natural frequencies and mode shapes. It is concluded that the physical relevance of the updated matrices is lost and that matrix correction methods are only suitable for special applications in combination with other methods. ESA

N90-12057*# National Aeronautics and Space Administration. Langley Research Center, Hampton, VA.
AIRFRAME STRUCTURAL DYNAMIC CONSIDERATIONS IN ROTOR DESIGN OPTIMIZATION
Raymond G. Kvaternik and T. Sreekanta Murthy (Planning Research Corp., Hampton, VA.) Aug. 1989 27 p
(NASA-TM-101646; NAS 1.15:101646) Avail: NTIS HC A03/MF A01 CSCL 20K

An an overview and discussion of those aspects of airframe structural dynamics that have a strong influence on rotor design optimization is provided. Primary emphasis is on vibration requirements. The vibration problem is described, the key vibratory forces are identified, the role of airframe response in rotor design is summarized, and the types of constraints which need to be imposed on rotor design due to airframe dynamics are discussed. Some considerations of ground and air resonance as they might affect rotor design are included. Author

N90-12058*# Textron Bell Helicopter, Fort Worth, TX.
INVESTIGATION OF DIFFICULT COMPONENT EFFECTS ON FINITE ELEMENT MODEL VIBRATION PREDICTION FOR THE BELL AH-1G HELICOPTER. VOLUME 1: GROUND VIBRATION TEST RESULTS
R. V. Dompka Oct. 1989 212 p
(Contract NAS1-17496)
(NASA-CR-181916-Vol-1; NAS 1.26:181916-Vol-1) Avail: NTIS HC A10/MF A02 CSCL 20K

Under the NASA-sponsored Design Analysis Methods for VIBrationS (DAMVIBS) program, a series of ground vibration tests and NASTRAN finite element model (FEM) correlations were conducted on the Bell AH-1G helicopter gunship to investigate the effects of difficult components on the vibration response of the airframe. Previous correlations of the AH-1G showed good agreement between NASTRAN and tests through 15 to 20 Hz, but poor agreement in the higher frequency range of 20 to 30 Hz. Thus, this effort emphasized the higher frequency airframe vibration response correlations and identified areas that need further R and T work. To conduct the investigations, selected difficult components (main rotor pylon, secondary structure, nonstructural doors/panels, landing gear, engine, fuel, etc.) were systematically removed to quantify their effects on overall vibratory response of the airframe. The entire effort was planned and documented, and the results reviewed by NASA and industry experts in order to ensure scientific control of the testing, analysis, and correlation exercise. In particular, secondary structure and damping had significant effects on the frequency response of the airframe above 15 Hz. Also, the nonlinear effects of thrust stiffening and elastomer mounts were significant on the low frequency pylon modes below main rotor 1p (5.4 Hz). The results of the ground vibration testing are presented. Author

42 GEOSCIENCES (GENERAL)

N90-12059*# National Aeronautics and Space Administration. Marshall Space Flight Center, Huntsville, AL.
NASA/MSFC FY88 GLOBAL SCALE ATMOSPHERIC PROCESSES RESEARCH PROGRAM REVIEW
Greg S. Wilson, ed., Fred W. Leslie, ed., and J. E. Arnold, ed. Feb. 1989 92 p Review held in Huntsville, AL
(NASA-TM-100357; ES41; NAS 1.15:100357) Avail: NTIS HC A05/MF A01 CSCL 04B

Interest in environmental issues and the magnitude of the environmental changes continues. One way to gain more understanding of the atmosphere is to make measurements on a global scale from space. The Earth Observation System is a series of new sensors to measure globally atmospheric parameters. Analysis of satellite data by developing algorithms to interpret the radiance information improves the understanding and also defines requirements for these sensors. One measure of knowledge of the atmosphere lies in the ability to predict its behavior. Use of numerical and experimental models provides a better understanding of these processes. These efforts are described in the context of satellite data analysis and fundamental studies of atmospheric dynamics which examine selected processes important to the global circulation. For individual titles, see N90-12060 through N90-12083.

N90-12060*# Pennsylvania State Univ., University Park. Dept. of Meteorology.
STRATIFORM CLOUDS AND THEIR INTERACTION WITH ATMOSPHERIC MOTIONS Abstract Only c46
John H. E. Clark and N. Shirer Hampton *In* NASA, Marshall Space Flight Center, NASA/MSFC FY88 Global Scale Atmospheric Processes Research Program Review Feb. 1989 p 1-5 (For primary document see N90-12059 03-42)
Avail: NTIS HC A05/MF A01 CSCL 04A

During the 1987 to 1988 academic year, three projects were finished and plans were made to redirect and focus work in a proposal now being reviewed. The completed work involves study of waves on an equatorial beta-plane in shear flow, investigation of the influence of orography on the index cycle, and analysis of a model of cloud street development in a thermally-forced, sheared environment. The proposed work involves study of boundary layer circulations supporting stratocumulus decks and investigation of how the radiative effects of these clouds modulate larger-scale flows such as those associated with the index oscillation. Author

N90-12061*# Purdue Univ., West Lafayette, IN. Dept. of Earth and Atmospheric Sciences.
SYNOPTIC/PLANETARY-SCALE INTERACTIONS AND BLOCKING OVER THE NORTH ATLANTIC OCEAN Abstract Only c47
Phillip J. Smith *In* NASA, Marshall Space Flight Center, NASA/MSFC FY88 Global Scale Atmospheric Processes Research Program Review Feb. 1989 p 7-8 (For primary document see N90-12059 03-42)
Avail: NTIS HC A05/MF A01 CSCL 04B

The focus was on the development of a blocking anticyclone that formed over the North Atlantic in January 1979 and a marine cyclone that deepened explosively prior to the onset of the block. The extended height tendency equation was used as the primary diagnostic tool. Focusing on the domain encompassing the migrating ridge that eventually formed the block, it was found that vorticity advection played the dominant role in the development of the ridge and the formation of the block. Also of interest was an attempt to evaluate the relative importance of synoptic-scale, planetary-scale, and synoptic/planetary-scale interactions as the block developed. To accomplish this, all data fields were partitioned into synoptic and planetary-scale components using a Barnes-type filter. Finally, the cyclone was diagnosed by examining the low level static stability fields associated with the cyclone's development. Author

N90-12062*# National Aeronautics and Space Administration. Marshall Space Flight Center, Huntsville, AL.
GLOBAL ATMOSPHERIC MOISTURE VARIABILITY Abstract Only c47
Franklin R. Robertson, Bonnie F. James, Kay Chi, and Huo-Jin Huang (North Carolina Univ., Asheville.) *In its* NASA/MSFC FY88 Global Scale Atmospheric Processes Research Program Review, Feb. 1989 p 9-11 (For primary document see N90-12059 03-42)
Avail: NTIS HC A05/MF A01 CSCL 04B

Research efforts during FY-88 have focused on completion of several projects relating to analysis of FGGE data during SOP-1 and on expanded studies of global atmospheric moisture. In particular, a revised paper on the relationship between diabatic heating and baroclinicity in the South Pacific Convergence Zone (SPCZ) was submitted. A summary of completed studies on diagnostic convective parameterization was presented at the Satellite Meteorology and Oceanography Convergence last February. These investigations of diabatic heating in the SPCZ have demonstrated the requirement for a more quantitative description of atmospheric moisture. As a result, efforts were directed toward use of passive remote microwave measurements from the Nimbus-7 SMMR and the DOD's Special Sensor Microwave Imager (SSMI/I) as critical sources of moisture data. Activities this year are summarized. Author

N90-12063*# Yale Univ., New Haven, CT. Dept. of Geology and Geophysics.
APPLICATION OF DYNAMICAL SYSTEMS THEORY TO GLOBAL WEATHER PHENOMENA REVEALED BY SATELLITE IMAGERY Abstract Only c47
Barry Saltzman, Wesley Ebisuzaki, Kirk A. Maasch, Robert Oglesby, Lionel Pandolfo, and Chung-Muh Tang (Universities Space Research Association, Columbia, MD.) *In* NASA, Marshall Space Flight Center, NASA/MSFC FY88 Global Scale Atmospheric Processes Research Program Review Feb. 1989 p 13-15 (For primary document see N90-12059 03-42)
Avail: NTIS HC A05/MF A01 CSCL 04B

Theoretical studies of low frequency and seasonal weather variability; dynamical properties of observational and general circulation model (GCM)-generated records; effects of the hydrologic cycle and latent heat release on extratropical weather; and Earth-system science studies are summarized. B.G.

N90-12064*# Illinois State Water Survey, Champaign. Climate and Meteorology Section.
VARIATIONAL OBJECTIVE ANALYSIS FOR CYCLONE STUDIES c47
Gary L. Achtemeier *In* NASA, Marshall Space Flight Center, NASA/MSFC FY88 Global Scale Atmospheric Processes Research Program Review Feb. 1989 p 17-21 (For primary document see N90-12059 03-42)
Avail: NTIS HC A05/MF A01 CSCL 04B

Significant accomplishments during 1987 to 1988 are summarized with regard to each of the major project components. Model 1 requires satisfaction of two nonlinear horizontal momentum equations, the integrated continuity equation, and the hydrostatic equation. Model 2 requires satisfaction of model 1 plus the thermodynamic equation for a dry atmosphere. Model 3 requires satisfaction of model 2 plus the radiative transfer equation. Model 4 requires satisfaction of model 3 plus a moisture conservation equation and a parameterization for moist processes. B.G.

N90-12065*# National Aeronautics and Space Administration. Marshall Space Flight Center, Huntsville, AL.
DYNAMICS AND ENERGETICS OF THE SOUTH PACIFIC CONVERGENCE ZONE DURING FGGE SOP-1 AND SOUTH PACIFIC CONVERGENCE ZONE AND GLOBAL-SCALE Annual Report, 1 Jul. 1987 - 30 Jun. 1988 Abstract Only c47
Dayton G. Vincent, Franklin R. Robertson, Huo-Jin Huang, Deirdre M. Kann, James W. Hurrell, and Catherine B. Pedigo (Purdue Univ., West Lafayette, IN.) *In* NASA, Marshall Space Flight Center, NASA/MSFC FY88 Global Scale Atmospheric Processes Research Program Review Feb. 1989 p 23-26 (For primary document see N90-12059 03-42)
(Contracts NAS8-35187; NAS8-37127)
Avail: NTIS HC A05/MF A01 CSCL 04B

Significant accomplishments (papers published, conference presentations, and education degrees) are presented. The focus of the current research is outlined. Plans for the coming year are discussed briefly. B.G.

N90-12066*# FWG Associates, Inc., Tullahoma, TN.
LOW LEVEL REMOTE SENSING: OROGRAPHIC WINDS Abstract Only c47
Walter Frost *In* NASA, Marshall Space Flight Center, NASA/MSFC FY88 Global Scale Atmospheric Processes Research Program Review Feb. 1989 p 27-28 (For primary document see N90-12059 03-42)
Avail: NTIS HC A05/MF A01 CSCL 04B

The orographic flow data set was obtained from a flight program to measure the influence of orographic features on turbulence momentum, heat, and moisture fluxes. The NASA B-57 aircraft instrumented with probes for measuring the three fluctuating wind speed components, temperature, and humidity was the primary measuring vehicle. Ancillary measurements were made with several ground-based sensors. These include the NOAA radar wind profilers, the Boulder wind network, the PROFS mesoscale surface network, the Boulder Atmospheric Observatory 300 m tower, special rawinsonde observations, and the NOAA/WPL Doppler lidar. The major objective of the flight program was to provide planetary boundary layer parameter information for new and current general circulation computer models. A numerical code, WINDER, based on a discrete element technique was run to numerically model the water tunnel simulated flow. Comparison of the analytical model with the experimental results is very good. Physical fluid dynamic principles embedded in the computational model and visual and hot wire anemometer measurements from the simulation are being rationalized to develop a physical understanding of the vortex flow. The results will be interpreted as they pertain to full scale atmospheric flows. Author

N90-12067*# National Aeronautics and Space Administration. Marshall Space Flight Center, Huntsville, AL.
LOW LEVEL REMOTE SENSING: THE DOPPLER RADAR WIND PROFILER Abstract Only c47
Gregory S. Forbes, William Syrett (Pennsylvania State Univ., University Park.), and Catherine Carlson *In its* NASA/MSFC FY88 Global Scale Atmospheric Processes Research Program Review Feb. 1989 p 29-30 (For primary document see N90-12059 03-42)
Avail: NTIS HC A05/MF A01 CSCL 04B

Mesoscale phenomena such as thunderstorm and sea breeze frontal circulations are being investigated using a 50 MHz Doppler wind profiler at the Kennedy Space Center. The profiler installation will begin October 1, 1988 and will be completed by February 17, 1989. The focus of current research and plans for next year include: examination of vertical velocities associated with local thunderstorm activity and sea breeze frontal circulations and compare the vertical velocities to conceptual mesoscale models; implementation of space-time conversion analysis techniques to blend profiler data with National Meteorological Center's model output and other wind data such as jimsphere, windsonde and rawinsonde for mesoscale analysis; development of suggestions for use of wind profiler data in mesoscale analysis and forecasting at Kennedy Space Center; and problems detection in the quality of the profiler data during this research project. Researchers will work closely with MSFC to identify and solve the data quality problems. Author

N90-12068*# Alabama Univ., Huntsville. Dept. of Mathematics and Statistics.
STUDIES OF BAROCLINIC INSTABILITY IN THE PRESENCE OF SURFACE TOPOGRAPHY AND STRATOSPHERIC OZONE Abstract Only c46
Nathaniel D. Reynolds *In* NASA, Marshall Space Flight Center, NASA/MSFC FY88 Global Scale Atmospheric Processes Research

Program Review Feb. 1989 p 31-32 (For primary document see N90-12059 03-42)
Avail: NTIS HC A05/MF A01 CSCL 04A

Major goals are to gain a better understanding of the planetary-scale tropospheric/stratospheric circulation and to better utilize global-scale routine measurements from satellites. The focus on the latter goal is determining the relationship between total column ozone measurements and the tropopause altitude. Author

N90-12069*# Alabama Univ., Huntsville. Atmospheric Science and Remote Sensing Lab.

GLOBAL DISTRIBUTION OF MOISTURE, EVAPORATION-PRECIPITATION, AND DIABATIC HEATING RATES Abstract Only c47

John R. Christy *In* NASA, Marshall Space Flight Center, NASA/MSFC FY88 Global Scale Atmospheric Processes Research Program Review Feb. 1989 p 33-34 (For primary document see N90-12059 03-42)
Avail: NTIS HC A05/MF A01 CSCL 04B

Global archives were established for ECMWF 12-hour, multilevel analysis beginning 1 January 1985; day and night IR temperatures, and solar incoming and solar absorbed. Routines were written to access these data conveniently from NASA/MSFC MASSTOR facility for diagnostic analysis. Calculations of diabatic heating rates were performed from the ECMWF data using 4-day intervals. Calculations of precipitable water (W) from 1 May 1985 were carried out using the ECMWF data. Because a major operational change on 1 May 1985 had a significant impact on the moisture field, values prior to that date are incompatible with subsequent analyses. Author

N90-12070*# Texas A&M Univ., College Station. Dept. of Meteorology.

TROPICAL PACIFIC MOISTURE VARIABILITY Abstract Only c47

James P. McGuirk *In* NASA, Marshall Space Flight Center, NASA/MSFC FY88 Global Scale Atmospheric Processes Research Program Review Feb. 1989 p 35-37 (For primary document see N90-12059 03-42)
Avail: NTIS HC A05/MF A01 CSCL 04B

Research objectives are to: (1) describe the synoptic scale variability of moisture over the tropical Pacific Ocean; (2) describe the systems leading to this variability; and (3) develop and implement satellite analysis procedures to facilitate (1) and (2) over the data sparse Pacific. Author

N90-12071*# Arizona Univ., Tucson.

DISTURBANCES IN THE ARIZONA MONSOON c47

Robert Gall, Benjamin Herman, and John Reagan *In* NASA, Marshall Space Flight Center, NASA/MSFC FY88 Global Scale Atmospheric Processes Research Program Review Feb. 1989 p 39-45 (For primary document see N90-12059 03-42)
Avail: NTIS HC A05/MF A01 CSCL 04B

Numerical modeling simulations of tropical squall lines were begun to determine the role of large scale terrain features over Arizona and Mexico in their initiation and propagation. Installation was completed for a short-base, high resolution lightning location and detection network in and around Tucson. Data from a Doppler wind profiler is being analyzed to determine the role of large scale heating over the inter-mountain plateau region in governing local diurnal wind variations and possible relationships to the monsoon flow. The portable solar photometer for determining high temporal resolution values of the local precipitable water vapor was completed and calibrated. The assembly is nearly completed for a multi-channel microwave passive radiometer to determine local temperature and water vapor profiles. Author

N90-12072*# Florida State Univ., Tallahassee. Geophysical Fluid Dynamics Inst.

DYNAMICS OF BAROCLINIC WAVE SYSTEMS Abstract Only c47

Albert Barcilon and Hengyi Weng *In* NASA, Marshall Space Flight Center, NASA/MSFC FY88 Global Scale Atmospheric Processes Research Program Review Feb. 1989 p 47-48 (For primary document see N90-12059 03-42)
Avail: NTIS HC A05/MF A01 CSCL 04B

The research carried out in the past year dealt with nonlinear baroclinic wave dynamics. The model consisted of an Eady baroclinic basic state and uneven Elkman dissipation at the top and bottom boundaries with/without slopes. The method of solution used a truncated spectral expansion with three zonal waves and one or two meridional modes. Numerical experiments were performed on synoptic scale waves or planetary scale waves with/without wave-wave interaction. Author

N90-12073*# Miami Univ., FL. School of Marine and Atmospheric Science.

THE EFFECT OF LATENT HEAT RELEASE ON SYNOPTIC-TO-PLANETARY WAVE INTERACTIONS AND ITS IMPLICATION FOR SATELLITE OBSERVATIONS: THEORETICAL MODELING Abstract Only c47

Lee E. Branscome and Rainer Bleck *In* NASA, Marshall Space Flight Center, NASA/MSFC FY88 Global Scale Atmospheric Processes Research Program Review Feb. 1989 p 49-51 (For primary document see N90-12059 03-42)
Avail: NTIS HC A05/MF A01 CSCL 04B

Simple models are being developed to simulate interaction of planetary and synoptic-scale waves incorporating the effects of large-scale topography; eddy heat and momentum fluxes (or nonlinear dynamics); radiative heating/cooling; and latent heat release (precipitation) in synoptic-scale waves. The importance of latent heat release is determined in oceanic storm tracks for temporal variability and time-mean behavior of planetary waves. The model results were compared with available observations of planetary and synoptic-scale wave variability and time-mean circulation. The usefulness of monitoring precipitation in oceanic storm tracks by satellite observing systems was ascertained. The modeling effort includes two different low-order quasi-geostrophic models-time-dependent version and climatological mean version. The modeling also includes a low-order primitive equation model. A time-dependent, multi-level version will be used to validate the two-level Q-G models and examine effects of spherical geometry. Author

N90-12074*# Virginia Univ., Charlottesville. Dept. of Environmental Sciences.

THE EFFECT OF LATENT HEAT RELEASE ON SYNOPTIC-TO-PLANETARY SCALE WAVE INTERACTIONS: OBSERVATIONAL STUDY Abstract Only c47

Stephen Colucci and Steven Greco *In* NASA, Marshall Space Flight Center, NASA/MSFC FY88 Global Scale Atmospheric Processes Research Program Review Feb. 1989 p 53-54 (For primary document see N90-12059 03-42)
Avail: NTIS HC A05/MF A01 CSCL 04B

A blocking pattern which formed over eastern North America following the landfall of Hurricane Juan during November 1985 was investigated. It is hypothesize that latent heat released in the Hurricane's rainfall was either directly or indirectly responsible for the large observed 500 mb height rises over eastern Canada during the formation of this block. This idea is evaluated with a diagnostic model for the height tendency field which includes latent heat release as a forcing function. The total column heating is calculated using satellite-derived precipitation estimates. These estimates are qualitatively congruent with observations, but overestimate light rainfall and underestimate heavy rainfall. The calculations reveal that the direct contribution of the heating to the 500 mb height tendency field is small relative to the quasigeostrophic forcing. However, maxima in heating coincide with regions where anticyclonic potential vorticity is generated. Once such region is just upstream of the location of large 500 mb height rises in the incipient block. An indirect role is proposed for the heating in this case. Specifically, anticyclonic potential vorticity is generated near the heating maxima; this vorticity is then advected downstream, forcing the 500 mb heights to rise and the block to develop. Author

N90-12075*# Iowa State Univ. of Science and Technology, Ames. Dept. of Earth Sciences.
USE OF SATELLITE DATA AND MODELING TO ASSESS THE INFLUENCE OF STRATOSPHERIC PROCESSES ON THE TROPOSPHERE Abstract Only **c46**
Terrence R. Nathan and Douglas N. Yarger *In* NASA, Marshall Space Flight Center, NASA/MSFC FY88 Global Scale Atmospheric Processes Research Program Review Feb. 1989 p 55-58 (For primary document see N90-12059 03-42)
Avail: NTIS HC A05/MF A01 CSCL 04A

The research is comprised of the following tasks: use of simple analytical and numerical models of a coupled troposphere-stratosphere system to examine the effects of radiation and ozone on planetary wave dynamics and the tropospheric circulation; use of satellite data obtained from the Nimbus 7 Limb Infrared Monitor of the Stratosphere (LIMS) instrument and Solar Backscattered Ultraviolet (SBUV) experiment, in conjunction with National Meteorological Center (NMC) data, to determine the planetary wave vertical structures, dominant wave spectra, ozone spectra, and time variations in diabatic heating rate; and synthesis of the modeling and observational results to provide a better understanding of the effects that stratospheric processes have on tropospheric dynamics. Author

N90-12076*# Colorado Univ., Boulder. Dept. of Astrophysical, Planetary and Atmospheric Sciences.
LABORATORY AND THEORETICAL MODELS OF PLANETARY-SCALE INSTABILITIES AND WAVES Abstract Only **c46**
John E. Hart and Juri Toomre *In* NASA, Marshall Space Flight Center, NASA/MSFC FY88 Global Scale Atmospheric Processes Research Program Review Feb. 1989 p 59-63 (For primary document see N90-12059 03-42)
Avail: NTIS HC A05/MF A01 CSCL 04A

The continuous low-g environment of the orbiting space shuttle provided a setting for conducting geophysical fluid model experiments with a completely consistent representation of sphericity and the resultant radial gravity found on astrogeophysical objects. This is possible because in zero gravity an experiment can be constructed that has its own radial buoyancy forces. The dielectric forces in a liquid, which are linearly dependent on fluid temperature, give rise to an effectively radial buoyancy force when a radial electrostatic field is applied. The Geophysical Fluid Flow Cell (GFFC) experiment is an implementation of this idea in which fluid is contained between two rotating hemispheres that are differentially heated and stressed with a large ac voltage. The GFFC flew on Spacelab 3 in May 1985. Data in the form of global Schlieren images of convective patterns were obtained for a large variety of configurations. These included situations of rapid rotation (large Taylor numbers), low rotation, large and small thermal forcing, and situations with applied meridional temperature gradients. The analysis and interpretation of the GFFC-85 data are being conducted. Improvements were developed to the GFFC instrument that will allow for real-time (TV) display of convection data and for near-real-time interactive experiments. These experiments, on the transition to global turbulence, the breakdown of rapidly rotating convective planforms and other phenomena, are scheduled to be carried out on the International Microgravity Laboratory (IML-1) aboard the shuttle in June 1990. Author

N90-12077*# National Aeronautics and Space Administration. Marshall Space Flight Center, Huntsville, AL.
LABORATORY AND THEORETICAL STUDIES OF BAROCLINIC PROCESSES Abstract Only **c47**
Timothy Miller, Fred W. Leslie, Dan Fitzjarrald, Nathaniel D. Reynolds, Shih-Hung Chou, Karen Payne, and Joseph Fehribach (Alabama Univ., Huntsville.) *In* NASA, Marshall Space Flight Center, NASA/MSFC FY88 Global Scale Atmospheric Processes Research Review Program Feb. 1989 p 65-68 (For primary document see N90-12059 03-42)
Avail: NTIS HC A05/MF A01 CSCL 04B

An understanding is being developed for processes which may be important in the atmosphere, and the definition and analysis of baroclinic experiments utilizing the geophysical fluid flow cells (GFFC) apparatus in microgravity space flights. Included are studies using numerical codes, theoretical models, and terrestrial laboratory experiments. The numerical modeling is performed in three stages: calculation of steady axisymmetric flow, calculation of fastest-growing linear eigenmodes, and nonlinear effects (first, wave-mean flow interactions, then wave-wave interactions). The code can accommodate cylindrical, spherical, or channel geometry. It uses finite differences in the vertical and meridional directions, and is spectral in the azimuthal. The theoretical work was mostly in the area of effects of topography upon the baroclinic instability problem. The laboratory experiments are performed in a cylindrical annulus which has a temperture gradient imposed upon the lower surface and an approximately isothermal outer wall, with the upper and inner surfaces being nominally thermally insulating. Author

N90-12078*# Hawaii Univ., Honolulu. Hawaii Inst. of Geophysics.
AEROSOL IN THE PACIFIC TROPOSPHERE Abstract Only **c46**
Antony D. Clarke *In* NASA, Marshall Space Flight Center, NASA/MSFC FY88 Global Scale Atmospheric Processes Research Program Review Feb. 1989 p 69-71 (For primary document see N90-12059 03-42)
Avail: NTIS HC A05/MF A01 CSCL 04A

The use of near real-time optical techniques is emphasized for the measurement of mid-tropospheric aerosol over the Central Pacific. The primary focus is on measurement of the aerosol size distribution over the range of particle diameters from 0.15 to 5.0 microns that are essential for modeling CO2 backscatter values in support of the laser atmospheric wind sounder (LAWS) program. The measurement system employs a LAS-X (Laser Aerosol Spectrometer-PMS, Boulder, CO) with a custom 256 channel pulse height analyzer and software for detailed measurement and analysis of aerosol size distributions. A thermal preheater system (Thermo Optic Aerosol Descriminator (TOAD) conditions the aerosol in a manner that allows the discrimination of the size distribution of individual aerosol components such as sulfuric acid, sulfates and refractory species. This allows assessment of the relative contribution of each component to the BCO2 signal. This is necessary since the different components have different sources, exhibit independent variability and provide different BCO2 signals for a given mass and particle size. Field activities involve experiments designed to examine both temporal and spatial variability of these aerosol components from ground based and aircraft platforms. Author

N90-12079*# Universities Space Research Association, Huntsville, AL. Earth Science and Applications Div.
AEROSOL BACKSCATTER STUDIES SUPPORTING LAWS Abstract Only **c47**
Jeffry Rothermel *In* NASA, Marshall Space Flight Center, NASA/MSFC FY88 Global Scale Atmospheric Processes Research Program Review Feb. 1989 p 73-74 (For primary document see N90-12059 03-42)
Avail: NTIS HC A05/MF A01 CSCL 04B

Optimized Royal Signals and Radar Establishment (RSRE), Laser True Airspeed System (LATAS) algorithm for low backscatter conditions was developed. The algorithm converts backscatter intensity measurements from focused continuous-wave (CW) airborne Doppler lidar into backscatter coefficients. The performance of optimized algorithm under marginal backscatter signal conditions was evaluated. The 10.6 micron CO2 aerosol backscatter climatologies were statistically analyzed. Climatologies reveal clean background aerosol mode near 10(exp -10)/kg/sq m/sr (mixing ratio units) through middle and upper troposhere, convective mode associated with planetary boundary layer convective activity, and stratospheric mode associated with volcanically-generated aerosols. Properties of clean background mode are critical to design and simulation studies of Laser Atmospheric Wind Sounder (LAWS), a MSFC facility Instrument on the Earth Observing System (Eos). Previous intercomparisons suggested correlation between aerosol backscatter at CO2 wavelength and water vapor. Field measurements of backscatter profiles with MSFC ground-based Doppler lidar system (GBDLS) were initiated in late FY-88 to coincide with independent program of local rawinsonde releases and overflights by Multi-spectral Atmospheric Mapping Sensor (MAMS), a multi-channel infrared radiometer capable of measuring horizontal and vertical moisture distributions. Design and performance simulation studies for LAWS would benefit from the existence of a relationship between backscatter and water vapor. Author

N90-12080*# Alabama Univ., Huntsville.
GLOBAL BACKSCATTER ASSESSMENT Abstract Only c46
David A. Bowdle *In* NASA, Marshall Space Flight Center, NASA/MSFC FY88 Global Scale Atmospheric Processes Research Program Review Feb. 1989 p 75-78 (For primary document see N90-12059 03-42)
Avail: NTIS HC A05/MF A01 CSCL 04A

The focus of this effort is the development of a global-scale model of aerosol backscatter for laser atmospheric wind sounder (LAWS) design and performance studies. Background parameters are derived from aerosol data sets with global-scale spatial and/or temporal coverage, using objective statistical decomposition and/or a priori stratification based on supplementary data. Backscatter coefficients at the LAWS design wavelength are derived from background aerosol physical, chemical, and optical data, or from direct backscatter measurements at other wavelengths, using background conversion factors. Direct measurements of aerosol backscatter at 10.6 microns from the Royal Signals and Radar Establishment (RSRE) and the Wave Propagation Laboratory (WPL) were selected. The RSRE backscatter data processing code were optimized under low backscatter conditions, performed detailed analyses of collocated intercomparisons between the two lidars, and assisted in the analysis of the long-term backscatter climatologies from the two lidars. Timely presentation of global backscattering experiment (GLOBE) research results to the global geophysical community is required. Author

N90-12081*# Simpson Weather Associates, Inc., Charlottesville, VA.
LAWS SIMULATION: SAMPLING STRATEGIES AND WIND COMPUTATION ALGORITHMS c47
G. D. A. Emmitt, S. A. Wood, and S. H. Houston *In* NASA, Marshall Space Flight Center, NASA/MSFC FY88 Global Scale Atmospheric Processes Research Program Review Feb. 1989 p 79-86 (For primary document see N90-12059 03-42)
Avail: NTIS HC A05/MF A01 CSCL 04B

In general, work has continued on developing and evaluating algorithms designed to manage the Laser Atmospheric Wind Sounder (LAWS) lidar pulses and to compute the horizontal wind vectors from the line-of-sight (LOS) measurements. These efforts fall into three categories: Improvements to the shot management and multi-pair algorithms (SMA/MPA); observing system simulation experiments; and ground-based simulations of LAWS. Author

N90-12082*# Georgia Inst. of Tech., Atlanta.
MEASUREMENTS OF AEROSOL PROPERTIES NEEDED TO INFER BACKSCATTER CHARACTERISTICS IN SUPPORT OF THE NASA DOPPLER LIDAR PROGRAM Abstract Only c46
E. M. Patterson, M. S. Black, and C. O. Pollard *In* NASA, Marshall Space Flight Center, NASA/MSFC FY88 Global Scale Atmospheric Processes Research Program Review Feb. 1989 p 87-90 (For primary document see N90-12059 03-42)
Avail: NTIS HC A05/MF A01 CSCL 04A

During the first year two areas of work were emphasized, analysis of aerosol data to provide improved estimates of backscatter over the Pacific ocean and development of a global model for backscatter at different wavelengths and preparation and planning for the aircraft flights of the GLOVE program. Significant progress was made in each of these areas. The analytical work is a continuation of the GAMETAG analysis, and was directed toward the development of a backscatter model for the Pacific Oceanic free troposphere. This has included a further evaluation of relationships between the optical effects at different wavelengths, a comparison of modeled optical effects at differing temporal resolutions, and an investigation of the effects of sampling on the modeled results. An initial investigation of the predictability of 9 to 10 micrometers Beta values from other data sets as well as some preliminary comparisons of the modeling results with experimental data. The comparison of the optical effects was extended to make the comparisons for different sets of time bases between 1 and 20 minutes. Author

N90-12083*# Pennsylvania State Univ., University Park.
INFRARED BACKSCATTERING Abstract Only c46
Craig F. Bohren, Timothy J. Nevitt, and Shermila Brito Singham *In* NASA, Marshall Space Flight Center, NASA/MSFC FY88 Global Scale Atmospheric Processes Research Program Review Feb. 1989 p 91-94 (For primary document see N90-12059 03-42)
Avail: NTIS HC A05/MF A01 CSCL 04A

All particles in the atmosphere are not spherical. Moreover, the scattering properties of randomly oriented nonspherical particles are not equivalent to those of spherical particles no matter how the term equivalent is defined. This is especially true for scattering in the backward direction and at the infrared wavelengths at which some atmospheric particles have strong absorption bands. Thus calculations based on Mie theory of infrared backscattering by dry or insoluble atmospheric particles are suspect. To support this assertion, it was noted that peaks in laboratory-measured infrared backscattering spectra show appreciable shifts compared with those calculated using Mie theory. One example is ammonium sulfate. Some success was had in modeling backscattering spectra of ammonium sulfate particles using a simple statistical theory called the continuous distribution of ellipsoids (CDE) theory. In this theory, the scattering properties of an ensemble are calculated. Recently a modified version of this theory was applied to measured spectra of scattering by kaolin particles. The particles were platelike, so the probability distribution of ellipsoidal shapes was chosen to reflect this. As with ammonium sulfate, the wavelength of measured peak backscattering is shifted longward of that predicted by Mie theory. Author

N90-12084*# National Academy of Sciences - National Research Council, Washington, DC. Committee on Earth Sciences.
STRATEGY FOR EARTH EXPLORERS IN GLOBAL EARTH SCIENCES
1988 64 p
(Contract NASw-3482)
(NASA-CR-185933; NAS 1.26:185933; PB89-198907) Avail: NTIS HC A04/MF A01 CSCL 08G

The goal of the current NASA Earth System Science initiative is to obtain a comprehensive scientific understanding of the Earth as an integrated, dynamic system. The centerpiece of the Earth System Science initiative will be a set of instruments carried on polar orbiting platforms under the Earth Observing System program. An Earth Explorer program can open new vistas in the earth sciences, encourage innovation, and solve critical scientific problems. Specific missions must be rigorously shaped by the demands and opportunities of high quality science and must complement the Earth Observing System and the Mission to Planet Earth. The committee believes that the proposed Earth Explorer program provides a substantial opportunity for progress in the earth sciences, both through independent missions and through missions designed to complement the large scale platforms and international research programs that represent important national commitments. The strategy presented is intended to help ensure the success of the Earth Explorer program as a vital stimulant to the study of the planet. Author

43 EARTH RESOURCES AND REMOTE SENSING

Includes remote sensing of earth resources by aircraft and spacecraft; photogrammetry; and aerial photography.

For instrumentation see *35 Instrumentation and Photography.*

N90-12085# Alaska Univ., Fairbanks. Geophysical Inst.
REMOTE SENSING DATA ACQUISITION, ANALYSIS AND ARCHIVAL Final Report
William J. Stringer Nov. 1988 61 p Sponsored by Minerals Management Service, Anchorage, AK; Alaska Outer Continental Shelf Office and National Ocean Service, Anchorage, AK
(PB89-142566) Avail: NTIS HC A04/MF A01 CSCL 05B

The current status is described of the remotely sensed data archive at the University of Alaska in support of the outer continental shelf environmental research and assessment needs. The archive primarily consists of data from NOAA and LANDSAT satellites, but it also includes passive microwave imagery, aerial photography, and side looking airborne radar data. In addition, research on certain aspects of sea ice distribution and movement in the northern Bering, Chukchi and Beaufort Seas is summarized, such as snow melt flooding along the North Slope of Alaska, factor causing immobilization or rapid movement of sea ice through the Bering Strait, and distribution of floe size in the Beaufort Sea. As a major effort, the size and recurrence of 22 polynyi in the northern Bering and Chukchi Seas is documented, and these features are related to available data on winds and air temperature. Author

N90-12086# National Oceanographic Instrumentation Center, Washington, DC. Satellite Applications Lab.
SATELLITE-DERIVED RAINFALL ESTIMATES AND PROPAGATION CHARACTERISTICS ASSOCIATED WITH THE MESOSCALE CONVECTIVE SYSTEMS (MCSs)
Juying Xie and Roderick A. Scofield May 1989 56 p
(PB89-213417; NOAA-TM-NESDIS-25) Avail: NTIS HC A04/MF A01 CSCL 04B

One of the challenges of a satellite meteorologist is estimating flash flood-producing rainfall from Mesoscale Convective Systems (MCSs). Presented here are satellite-derived rainfall estimates using the Scofield/Oliver Technique for flash flood producing MCSs. The verification and accuracy of the estimates are presented as well as a recommendation for improving the rainfall algorithm. Another challenge for the operational meteorologist is predicting how much more rainfall will occur and where will it move. This type of prediction involves determining where MCSs will propagate. Most of the flash floods in the study were produced by backward propagating MCSs. Synoptic patterns are presented for forward and backward propagating MCSs. These patterns form the basis for objective and interactive methods for short range flash flood forecasting for MCSs. Author

N90-12087 Deutsche Geodaetische Kommission, Munich (Germany, F.R.).
TIME AND FREQUENCY IN GEODESY MEASURING METHODS Ph.D. Thesis - Technischen Univ., Munich [ZEIT UND FREQUENZ IM MESSVERFAHREN DER GEODAESIE]
Wolfgang Schlueter Frankfurt am Main, Fed. Republic of Germany Inst. fuer Angewande Geodaesie 1988 203 p In GERMAN
(Ser-C-337; Mitt-177; ISSN-0071-9196; ETN-89-94649) Copyright Avail: Institut fuer Angewandte Geodesie, Richard-Strauss-Allee 11, D-6000, Frankfurt am Main 70, Fed. Republic of Germany

The techniques of time control and frequency generation are discussed with a view to geodetic applications. Starting from the astronomical time units and scales used in astrogeodetic positioning, the transition to atomic is depicted. The generation of local time scales with clocks, their operation and properties, as well as time comparison methods are described. The accuracies of time control and frequency generation which can be obtained during geodetic measurements are discussed, taking as example the time system of the station Wettzell. ESA

N90-12088# Deutsche Forschungs- und Versuchsanstalt fuer Luft- und Raumfahrt, Oberpfaffenhofen (West Germany). Abteilung Fernerkundungsanwendungen.
INVESTIGATION OF THE USEFULNESS OF LANDSAT 5 THEMATIC MAPPER DATA FOR MAPPING FOREST DISEASE Ph.D. Thesis - Technische Univ. Berlin
Bernhard Foerster Jan. 1989 200 p In GERMAN; ENGLISH summary
(DFVLR-FB-89-06; ISSN-0171-1342; ETN-89-95303) Avail: NTIS HC A09/MF A01; DFVLR, VB-PL-DO, Postfach 90 60 58, 5000 Cologne, Federal Republic of Germany, 68 deutsche marks

The usefulness of LANDSAT 5 thematic mapper data for mapping forest disease in spruce stands (Picea abies) in the northern part of te Harz mountains, Germany, is investigated. In order to take the different illuminations in this mountainous area into account, six illumination classes calculated from a digital terrain model were used. The result of a detailed signature analysis showed, that the pixelwise difference of the channels TM4-TM5 is best suited for an estimation of the quota of highly damaged spruce trees. The digital classification based on this difference is compared with the result of an aerial photo interpretation of the disease. ESA

N90-12089# Deutsche Forschungs- und Versuchsanstalt fuer Luft- und Raumfahrt, Oberpfaffenhofen (West Germany). Abteilung fuer Optische Fernerkundung.
SIGNATURE ANALYSIS AND CLASSIFICATION OF PINE OF DIFFERENT VITALITY CLASSES USING AIRBORNE THEMATIC MAPPER DATA Ph.D. Thesis - Ludwig-Maximilians Univ.
Karin Herrmann Feb. 1989 188 p In GERMAN; ENGLISH summary Original contains color illustrations
(DFVLR-FB-89-07; ISSN-0171-1342; ETN-89-95304) Avail: NTIS HC A09/MF A01; DFVLR, VB-PL-DO, Postfach 90 60 58, 5000 Cologne, Federal Republic of Germany, 78 deutsche marks

The use of the airborne thematic mapper Daedalus 1268 in assessing, mapping and monitoring forest decline areas since 1986 is described. Symptoms on Scotch pine (Pinus sylvestris L.) like chlorosis and needle loss are investigated. Spectral signatures of individual pine crowns are collected and analyzed. Procedures to optimize the classification of various damaged pine areas are developed and different verification methods are examined. ESA

N90-12090*# National Aeronautics and Space Administration. Goddard Inst. for Space Studies, New York, NY.
GLOBAL DATA BASES ON DISTRIBUTION, CHARACTERISTICS AND METHANE EMISSION OF NATURAL WETLANDS: DOCUMENTATION OF ARCHIVED DATA TAPE
Elaine Matthews Nov. 1989 22 p
(NASA-TM-4153; Rept-90-005; NAS 1.15:4153) Avail: NTIS HC A03/MF A01 CSCL 13B

Global digital data bases on the distribution and environmental characteristics of natural wetlands, compiled by Matthews and Fung (1987), were archived for public use. These data bases were developed to evaluate the role of wetlands in the annual emission of methane from terrestrial sources. Five global 1 deg latitude by 1 deg longitude arrays are included on the archived tape. The arrays are: (1) wetland data source, (2) wetland type, (3) fractional inundation, (4) vegetation type, and (5) soil type. The first three data bases on wetland locations were published by Matthews and Fung (1987). The last two arrays contain ancillary information about these wetland locations: vegetation type is from the data of Matthews (1983) and soil type from the data of Zobler (1986). Users should consult original publications for complete discussion of the data bases. This short paper is designed only to document the tape, and briefly explain the data sets and their initial application to estimating the annual emission of methane from natural wetlands. Included is information about array characteristics such as dimensions, read formats, record lengths, blocksizes and value ranges, and descriptions and translation tables for the individual data bases. Author

N90-12091* National Aeronautics and Space Administration, Washington, DC.
EARTH RESOURCES: A CONTINUING BIBLIOGRAPHY WITH INDEXES (ISSUE 63)
Oct. 1989 128 p
(NASA-SP-7041(63); NAS 1.21:7041(63)) Avail: NTIS HC A07; NTIS standing order as PB89-903800, $15.50 domestic, $31.00 foreign CSCL 08B

This bibliography lists 449 reports, articles, and other documents introduced into the NASA scientific and technical information system between July 1 and September 31, 1989. Emphasis is placed on the use of remote sensing and geophysical instrumentation in spacecraft and aircraft to survey and inventory natural resources and urban areas. Subject matter is grouped according to agriculture and forestry, environmental changes and cultural resources, geodesy and cartography, geology and mineral resources, oceanography and marine resources, hydrology and water management, data processing and distribution systems, and instrumentation and sensors. Author

44 ENERGY PRODUCTION AND CONVERSION

Includes specific energy conversion systems, e.g., fuel cells; global sources of energy; geophysical conversion; and windpower.

For related information see also *07 Aircraft Propulsion and Power, 20 Spacecraft Propulsion and Power,* and *28 Propellants and Fuels.*

N90-12092# Helsinki Univ. of Technology, Espoo (Finland). Lab. of Thermal Engineering.
ANALYSIS OF THE EFFICIENCY OF A DIELECTRIC SOLAR ENERGY COLLECTOR
Markku J. Lampinen, Kari Kirjavainen, and Thomas Pylkkaenen 1989 53 p Prepared in cooperation with Tampere Univ. of Technology, Finland
(PB89-212716; Rept-33; ISBN-951-754-830-3) Avail: NTIS HC A04/MF A01 CSCL 10A

The research investigated the possibilities of various dielectric materials for the conversion of thermal energy into electrical energy. The main application considered was the operation of such a condenser as a collector of solar energy. The research concentrated on two particular materials and on estimating the efficiency obtainable from them. One of these was a ferro-electrical material, a solid phase solution consisting of BaTiO3 and BaZrO3, the dipole moment of which changes very vigorously with rising temperature. The other material investigated was electrothermomechanical film, which is a porous plastics film containing methanol liquid and gas. Author

N90-12093# Colorado State Univ., Fort Collins.
ANALYSIS OF LOSS MECHANISMS IN POLYCRYSTALLINE THIN-FILM SOLAR CELLS Annual Subcontract Report, 1 Apr. 1988 - 31 Mar. 1989
J. R. Sites Jul. 1989 30 p
(Contracts DE-AC02-83CH-10093; XL-8-18080-1)
(DE89-009454; SERI/STR-211-3545) Avail: NTIS HC A03/MF A01

The goal for thin-film polycrystalline solar cell analysis is to increase the useful information extracted from relatively straightforward electrical measurements. The strategy is to: (1) systemize measurements and reporting; (2) evaluate possible analytical techniques to increase precision and avoid pitfalls; (3) organize results in terms of quantitative values for individual sources and current and voltage loss; and (4) insist on a viable physical explanation of each loss mechanism. This report describes the past year's activities, which have focused on analytical techniques related to the primary cause of low fill factor (diode quality and series resistance) and those related to interpreting capacitance measurements. DOE

N90-12094# Sandia National Labs., Albuquerque, NM.
PHOTOVOLTAIC SYSTEM RESEARCH STATUS
H. N. Post, G. J. Jones, and M. G. Thomas 1989 6 p Presented at the World Congress of the International Solar Energy Society, Kobe, Japan, 4-8 Sep. 1989
(Contract DE-AC04-76DP-00789)
(DE89-016764; SAND-89-2009C; CONF-890923-1) Avail: NTIS HC A02/MF A01

After a decade of photovoltaic system research, most system related issues have been successfully resolved. Current system research activities are now oriented toward maintaining and updating the comprehensive database on system performance established by previous research efforts, integrating new components into system designs, and transferring the accumulated information to industry and users of the technology. This paper presents a brief overview of the status of system research in the United States, emphasizing three key activities - field evaluation, balance-of-system hardware development, and technology transfer. DOE

N90-12095# Pacific Northwest Lab., Richland, WA.
USER'S GUIDE FOR A PERSONAL COMPUTER MODEL OF TURBULENCE AT A WIND TURBINE ROTOR
J. R. Connell, D. C. Powell, and G. L. Gower Aug. 1989 170 p
(Contract DE-AC06-76RL-01830)
(DE89-017753; PNL-6959) Avail: NTIS HC A08/MF A01

This document is primarily: (1) a user's guide for the personal computer (PC) version of the code for the PNL computational model of the rotationally sampled wind speed (RODASIM11), and (2) a brief guide to the growing literature on the subject of rotationally sampled turbulence, from which the model is derived. The model generates values of turbulence experienced by single points fixed in the rotating frame of reference of an arbitrary wind turbine blade. The character of the turbulence depends on the specification of mean wind speed, the variance of turbulence, the crosswind and along-wind integral scales of turbulence, mean wind shear, and the hub height, radius, and angular speed of rotation of any point at which wind fluctuation is to be calculated. DOE

N90-12096# Aquanautics Corp., Alameda, CA.
LONG ENDURANCE UNDERWATER POWER SYSTEM Quarterly Report, Apr. - Jun. 1989
4 Aug. 1989 62 p
(Contract N00014-87-C-0335)
(AD-A211386) Avail: NTIS HC A04/MF A01 CSCL 10/2

As part of DARPA's Artificial Gill program, Aquanautics is developing an underwater power source that uses an ambient pressure solid polymer electrolyte (SPE) hydrogen/oxygen fuel cell with an artificial gill that extracts dissolved oxygen from seawater and an Alwatt aluminum corrosion cell that generates the hydrogen. The innovation in this concept is a direct carrier feed fuel cell (CFFC) process which allows the fuel cell to operate at ambient pressure without a costly deep water pressure vessel. Activities during this quarter include: direct feed of oxygen carrier into fuel cell; new batches of electrodes were ordered. These are with a different ion-exchange membrane called Nafion (manufactured by Dupont) as against Raipore (mfd. by RAI Research). There was some concern that hydrogen at high pressures would leak out through the membrane which led to calculation of the hydrogen leakage; it appears that at 6000 m, the loss will be around 20 percent. Eight rectangular membrane cartridges were ordered. The factors varied were type of membrane (solid vs. microporous) and fiber to fiber distance. Theoretical study for sizing of the gill and pumping power required was carried out. Integration of the gill and fuel cell was carried out where oxygen extracted from synthetic ocean water was used in the fuel cell. There was no unforeseen problem. Hydrogen generation using an Alwatt battery was obtained and tested. GRA

N90-12097# Washington Univ., Seattle. Tri-Cities Univ. Center.
GRADED BANDGAP SOLAR CELLS Final Report, 1 Sep. 1984 - 30 Sep. 1988
Larry C. Olsen Jun. 1989 41 p
(Grant AF-AFOSR-0355-85; AF Proj. 2301)
(AD-A211537; AFOSR-89-1186TR) Avail: NTIS HC A03/MF A01 CSCL 10/3

This program has emphasized investigations of graded bandgap solar cells. The key objective was to determine the feasibility of obtaining high efficiencies with a graded emitter heterojunction structure. The Al(x)Ga(1-x)As ternary system was selected for actual device fabrication and characterization. Interpretation of photoresponse data for graded devices indicated that the minority carrier diffusion length was essentially zero for x equal to or greater than .25. This property of the AlGaAs films made it impossible to obtain the expected photocurrent from the graded devices. However, studies were carried out which clearly indicated that the structures with graded emitters were characterized by an enhanced photoresponse relative to homojunction devices. GRA

N90-12098# Texas A&M Univ., College Station. Center for Electro-Chemical Systems and Hydrogen Research.
A LIGHTWEIGHT SOLID POLYMER ELECTROLYTE FUEL CELL WITH STACK POWER DENSITY OF 3 kW/LB (7 kW/kg)
A. John Appleby 1989 10 p
(Contract N00014-88-K-0389)
(AD-A211542; AD-E951378) Avail: NTIS HC A02/MF A01 CSCL 10/3

The objectives of the solid polymer electrolyte fuel cell project are: (1) Investigations of physico-chemical properties of various solid polymer electrolyte electrode kinetics at Pt/solid polymer electrolyte interfaces; (2) Optimization of low and high Pt-loading gas diffusion electrode conditions, structures, membrane bonding to obtain most effective electrocatalyst membrane interface and hence attain maximum fuel cell performance; and (3) Mathematical modeling of electrochemical, mass transfer and heat generation characteristics associated with cell operation to optimize fuel cell thermal and water management. GRA

N90-12099# Deutsche Forschungs- und Versuchsanstalt fuer Luft- und Raumfahrt, Stuttgart (Germany, F.R.). Hauptabteilung Angewandte Datentechnik.
TYPE-SPECIFIC DYNAMIC MEASUREMENTS ON WIND TURBINES AT THE TEST SITE SCHNITTLINGEN (GERMANY, F.R.) Final Report, 30 Jun. 1988
Helmut Boehnisch, Alfred Kussmann, Klaus Reiniger (Deutsche Forschungs- und Versuchsanstalt fuer Luft- und Raumfahrt, Oberpfaffenhofen, West Germany), and Reimer Thiesen 23 Dec. 1988 102 p In GERMAN; ENGLISH summary Report will also be announced as translation (ESA-TT-1174)
(Contract BMFT-03-E-8156-A)
(DFVLR-Mitt-88-31; ISSN-0176-7739; ETN-89-95295) Avail: NTIS HC A06/MF A01; DFVLR, VB-PL-DO, Postfach 90 60 58, 5000 Cologne, Fed. Republic of Germany, 38.50 DM

Results of research on recording high dynamical data from rotating systems are presented. Two telemetry PCM (pulse code modulation) systems are used. The data of high-speed short-term measurement campaigns and of the long-time measurements are preprocessed on the test site process computers for averaging and first verification. Final evaluation of the data is done off-line on the DFVLR (Deutsche Forschungs und Versuchsanstalt fuer Luft und Raumfahrt) main frame computers. Of special interest are weather conditions, particularly their influence on the behavior of the control system and on the performance of wind turbines. Typical analyzed data of the tested turbines and interesting weather conditions are presented. A list of experiences and recommendations on wind test work are given. ESA

N90-12100# Keuring van Electrotechnische Materialen N.V., Arnhem (Netherlands).
[ACTIVITIES REPORT ON KEMA R AND D] Annual Report, 1987
W. Nagel, ed. and A. J. vanLoon, ed. 1988 51 p
(ST-Rept-Vol-6-No-12; ISBN-9-03-530072-6; ISSN-0167-8590; ETN-89-95469) Avail: NTIS HC A04/MF A01

The KEMA Research and Development (R and D) activities performed in 1987 are presented. Seven research programs are included: the generation of electricity with fossil fuels, nuclear energy, environmental research, transmission, distribution and consumption, new generating systems (mainly wind energy) and their economy, and measurements and diagnostics. The costs of R and D, the organization of KEMA and of the KEMA R and D division are presented. ESA

45 ENVIRONMENT POLLUTION

Includes atmospheric, noise, thermal, and water pollution.

N90-12101*# National Academy of Sciences - National Research Council, Washington, DC.
OZONE DEPLETION, GREENHOUSE GASES, AND CLIMATE CHANGE
Harold A. Mooney, D. James Baker, Jr., Francis P. Bretherton, Kevin C. Burke, William C. Clark, Margaret B. Davis, Robert E. Dickinson, John Imbrie, Thomas F. Malone, and Michael B. McElroy (Harvard Univ., Cambridge, MA.) et al 1989 135 p Sponsored in part by NASA, NSF, NOAA, Dept. of Agriculture, DOD, DOE, Dept. of the Interior, DOT, and EPA
(Grant NA87-AA-D-CP041)
(NASA-CR-185323; NAS 1.26:185323; LC-88-31544; ISBN-0-309-03945-2) Avail: NTIS HC A07/MF A01 CSCL 13B

This symposium was organized to study the unusual convergence of a number of observations, both short and long term that defy an integrated explanation. Of particular importance are surface temperature observations and observations of upper atmospheric temperatures, which have declined significantly in parts of the stratosphere. There has also been a dramatic decline in ozone concentration over Antarctica that was not predicted. Significant changes in precipitation that seem to be latitude dependent have occurred. There has been a threefold increase in methane in the last 100 years; this is a problem because a source does not appear to exist for methane of the right isotopic composition to explain the increase. These and other meteorological global climate changes are examined in detail. E.R.

N90-12102*# National Aeronautics and Space Administration, Washington, DC.
FINAL ENVIRONMENTAL IMPACT STATEMENT FOR THE GALILEO MISSION (TIER 2)
May 1989 299 p
(NASA-TM-101825; NAS 1.15:101825) Avail: NTIS HC A13/MF A02 CSCL 13B

This Final Environmental Impact Statement (FEIS) addresses the proposed action of completing the preparation and operation of the Galileo spacecraft, including its planned launch on the Space Transportation System (STS) Shuttle in October 1989, and the alternative of canceling further work on the mission. The Tier 1 (program level) EIS (NASA 1988a) considered the Titan IV launch vehicle as an alternative booster stage for launch in May 1991 or later. The May 1991 Venus launch opportunity is considered a planetary back-up for the Magellan (Venus Radar Mapper) mission, the Galileo mission, and the Ulysses mission. Plans were underway to enable the use of a Titan IV launch vehicle for the planetary back-up. However, in November 1988, the U.S. Air Force, which procures the Titan IV for NASA, notified NASA that it could not provide a Titan IV vehicle for the May 1991 launch opportunity due to high priority Department of Defense requirements. Consequently, NASA terminated all mission planning for the Titan IV planetary back-up. A minimum of 3 years is required to implement mission-specific modifications to the basic Titan IV launch configuration; therefore, insufficient time is available to use a Titan

IV vehicle in May 1991. Thus, the Titan IV launch vehicle is no longer a feasible alternative to the STS/Inertial Upper Stage (IUS) for the May 1991 launch opportunity. Author

N90-12103# Environmental Protection Agency, Research Triangle Park, NC. Atmospheric Research and Exposure Assessment Lab.

EVALUATION AND SENSITIVITY ANALYSES RESULTS OF THE MESOPUFF 2 MODEL WITH CAPTEX (CROSS-APPALACHIAN TRACER EXPERIMENT) MEASUREMENTS Final Report, Jun. 1986 - Dec. 1988

James M. Goodwitch Jun. 1989 110 p
(PB89-198253; EPA/600/3-89/056) Avail: NTIS HC A06/MF A01 CSCL 13B

The MESOPUFF 2 regional Lagrangian puff model was evaluated and tested against measurements from the Cross-Appalachian Tracer Experiment (CAPTEX) data base in an effort to assess its ability to simulate the transport and dispersion of a nonreactive, nondepositing tracer plume out to distances of over 1000 km. The model applied a mixed layer averaged wind field to simulate boundary layer transport and Gaussian dispersion parameters to govern puff growth. The model overpredicted peak and mean concentrations; modeled mean values were within a factor of two of observed values in four experiments. Graphical maps confirmed that the scatter among concentration pairs was primarily due to notable spatial displacements between observed and modeled tracer plumes. Analysis of plume centroid positions was employed to give quantitative information about the difference in downwind distances and separation between the observed and modeled plume patterns versus time. Diagnostic test run results, where optional single level wind fields and optional dispersion methods were exercised, are also compared to default model run results and to observed values. Sensitivity test runs focused on variations in the dry deposition and chemical transformation parameters for SOx. Author

N90-12104# Environmental Protection Agency, Research Triangle Park, NC. Office of Air Quality Planning and Standards.

REVIEW OF THE NATIONAL AMBIENT AIR QUALITY STANDARDS FOR LEAD: EXPOSURE ANALYSIS METHODOLOGY AND VALIDATION Final Staff Report

Jeff Cohen, Allan Marcus, Donna Sledge, Dave McLamb, Gail Brion, and John Haines Jun. 1989 172 p Prepared in cooperation with New York Univ. Medical Center; PEI Associates, Inc., Durham, NC; and Alliance Technologies Corp., Chapel Hill, NC
(PB89-207914; EPA/450/2-89-011) Avail: NTIS HC A08/MF A01 CSCL 13B

Relevant information is summarized on multi-media lead exposure and the modeling methodologies that EPA staff believes should be considered for the review of the national ambient air quality standards for lead are presented. Results of validating one of these methodologies are also presented. The significant downward trends in gasoline lead emissions and lead concentrations in the diet are accounted for in these methodologies. Young children, pregnant women (as exposure surrogates for the fetus), and middle-aged men are identified as particularly susceptible to lead. Three different exposure methodologies, developed from a wide variety of data are described: the uptake/biokinetic and aggregate air lead models, both applicable to young children, and the disaggregate air lead model, which is applicable to both young children and adults. The uptake/biokinetic model allows explicit projections of future lead concentrations in different media and in turn can estimate the impacts of these changes on different age groups of children. It is this flexibility that makes the uptake/biokinetic model adaptable for a wide range of predictive exposure assessments and why it was the focus of the validation exercises. Results of these exercises indicate good concordance between predicted and observed blood lead levels in children living near different lead point sources. GRA

N90-12105# Radian Corp., Austin, TX.

POTENTIAL TECHNOLOGIES FOR COLLECTION AND DESTRUCTION OF CFCS (CHLOROFLUOROCARBONS), HALONS, AND RELATED COMPOUNDS Final Report, Mar. 1988 - May 1989

Kirk E. Hummel and Thomas P. Nelson Jul. 1989 98 p
(Contract EPA-68-02-4286)
(PB89-219968; EPA/600/2-89/037) Avail: NTIS HC A05/MF A01 CSCL 13B

Recommendations of a multidisciplinary panel of experts are given on new or novel technologies (or modifications of existing technologies) which show the most promise for the collection and destruction of chlorofluorocarbons and related compounds. Panel members met in a roundtable format to discuss their experiences and relate them to the compounds of interest. The panel identified technologies holding the most promise and suggested general areas of research and development needed to develop collection and destruction technologies. GRA

N90-12106# Jet Propulsion Lab., California Inst. of Tech., Pasadena.

GLOBAL ENVIRONMENTAL EFFECTS OF IMPACT-GENERATED AEROSOLS: RESULTS FROM A GENERAL CIRCULATION MODEL

Curt Covey, Steven J. Ghan, John J. Walton, and Paul R. Weissman Feb. 1989 23 p Presented at the Snowbird Conference on Global Catastrophies in Earth History, Snowbird, UT, 20-23 Oct. 1989 Submitted for publication Prepared in cooperation with Lawrence Livermore National Lab., CA
(Contract W-7405-eng-48)
(DE89-008033; UCRL-98894; CONF-891065-1) Avail: NTIS HC A03/MF A01

Interception of sunlight by the high altitude worldwide dust cloud generated by impact of a large asteroid or comet would lead to substantial land surface cooling, according to the three-dimensional atmospheric general circulation model (GCM). This result is qualitatively similar to conclusions drawn from an earlier study that employed a one-dimensional atmospheric model, but in the GCM simulation the heat capacity of the oceans, not included in the one-dimensional model, substantially mitigates land surface cooling. On the other hand, the low heat capacity of the GCM's land surface allows temperatures to drop more rapidly in the initial stages of cooling than in the one-dimensional model study. GCM-simulated climatic changes in the scenario of asteroid/comet winter are more severe than in nuclear winter because the assumed aerosol amount is large enough to intercept all sunlight falling on earth. Impacts of smaller objects could also lead to dramatic, though of course less severe, climatic changes, according to the GCM. An asteroid or comet impact would not lead to anything approaching complete global freezing, but quite reasonable to assume that impacts would dramatically alter the climate in at least a patchy sense. DOE

N90-12107# Oak Ridge National Lab., TN.

POLICIES TO ENCOURAGE PRIVATE SECTOR RESPONSES TO POTENTIAL CLIMATE CHANGE

Robin A. Cantor, Donald W. Jones, Paul N. Leiby, and Steve Rayner 1989 12 p Presented at the 11th Annual North American Conference of the International Association for Energy Economists, Los Angeles, CA, 16-18 Oct. 1989
(Contract DE-AC05-84OR-21400)
(DE89-017244; CONF-8910162-3) Avail: NTIS HC A03/MF A01

The Oak Ridge National Laboratory (ORNL) recently completed work on a report commissioned by the U.S. Congress from the Department of Energy entitled, A Compendium of Options for Government Policy to Encourage Private Sector Responses to Potential Climate Change, (US DOE 1989). Four classes of incentives (regulatory, fiscal, informational, and RD and D) were surveyed in the context of greenhouse-related activities in five economic sectors. For each activity general policies and specific options were considered. The paper presented here does not summarize the DOE study but identifies some of the lessons ORNL staff learned during the study about policies to deal with potential global warming. DOE

N90-12108# Lawrence Livermore National Lab., CA. Atmospheric and Geophysical Sciences Div.

A STATISTICAL INTERCOMPARISON OF TEMPERATURE AND PRECIPITATION PREDICTED BY FOUR GENERAL CIRCULATION MODELS WITH HISTORICAL DATA

Stanley L. Grotch Aug. 1989 29 p Presented at the Workshop on Greenhouse-Gas Induced Climate Change: A Critical Appraisal of Simultations and Observations, Amherst, MA, 8-12 May 1989
(Contract W-7405-eng-48)
(DE89-017785; UCRL-101726; CONF-8905106-1) Avail: NTIS HC A03/MF A01

A detailed intercomparison was made of the results produced by 4 different General Circulation Models (GCMs) that were used to estimate the climatic consequences of a doubling of CO2 concentration. Two variables, surface air temperature and precipitation, annually and seasonally averaged, are compared for both the current climate and for the predicted equilibrium changes after a doubling of the atmospheric CO2 concentration. The major question considered here is: How well the predictions from different GCMs agree with each other and with historical climatology over different aeral extents, from the global scale down to the range of only several gridpoints. Although the models often agree well when estimating averages over large areas, substantial disagreements become apparent as the spatial scale is reduced. At scales below continental, the correlations observed between different model predictions are often very poor. The implications for investigation of climatic impacts on a regional scale are profound. For these two important variables, at least, the poor agreement between model simulations of the current climate on the regional scale calls into question the ability of these models to quantitatively estimate future climatic change on anything approaching the scale of a few (less than 10) gridpoints, which is essential if these results are to be used in meaningful resource assessment studies. DOE

N90-12109*# National Center for Atmospheric Research, Boulder, CO.

GLOBAL TROPOSPHERIC CHEMISTRY: CHEMICAL FLUEXES IN THE GLOBAL ATMOSPHERE

Donald H. Lenschow, ed. and Bruce B. Hicks, ed. May 1989 112 p Report on the Workshop on Measurements of Surface Exchange and Flux Divergence of Chemical Species in the Global Atmosphere, New York, NY, Oct. 1987; sponsored by NASA, NSF and NOAA Sponsored by NASA, Washington, DC and NOAA, Rockville, MD
(Grant NSF ATM-87-09659)
(NASA-CR-186090; NAS 1.26:186090; PB89-218739) Avail: NTIS HC A06/MF A01 CSCL 13B

In October 1987, NSF, NASA, and NOAA jointly sponsored a workshop at Columbia University to assess the experimental tools and analysis procedures in use and under development to measure and understand gas and particle fluxes across this critical air-surface boundary. Results are presented for that workshop. It is published to summarize the present understanding of the various measurement techniques that are available, identify promising new technological developments for improved measurements, and stimulate thinking about this important measurement challenge. GRA

N90-12110# National Academy of Sciences - National Research Council, Washington, DC. Commission on Physical Sciences, Mathematics and Resources.

OZONE DEPLETION, GREENHOUSE GASES, AND CLIMATE CHANGE

1989 137 p
(PB89-216097; LC-88-31544; ISBN-0-309-03945-2) Avail: NTIS HC A07/MF A01 CSCL 13B

Ozone depletion in the stratosphere and increases in greenhouse gases in the troposphere are both subjects of growing concern-even alarm-among scientists, policymakers, and the public. At the same time, recent data show that these atmospheric developments are interconnected and in turn profoundly affect climatic conditions. To arrive at a better understanding of this complex relationship, major institutions in the field of atmospheric study convened a symposium of noted researchers. Here, researchers present the results of their most recent research, with the most up-to-date data and theories available on ozone depletion, greenhouse gases and climatic change. Author

N90-12111# Bundesministerium fuer Forschung und Technologie, Bonn (Germany, F.R.).

OZONE RESEARCH PROGRAM (GERMAN CONTRIBUTION TO CLIMATE AND ATMOSPHERE RESEARCH) [OZONFORSCHUNGSPROGRAMM. DEUTSCHER BEITRAG ZUR KLIMAT UND ATMOSPHAERENFORSCHUNG]

20 Dec. 1988 43 p In GERMAN
(Rept-46-88; ETN-89-94621) Avail: NTIS HC A03/MF A01

The plans for coordinated research activities in the Federal Republic of Germany aiming at the explanation of chemical and dynamic processes in the stratosphere are outlined. The main goals are the determination of the type and importance of the ozone concentration change, the explanation of the origins of this change, and reliable predictions of future evolutions. This requires common and coordinated efforts in field measurements, laboratory studies, and the further development of multidimensional, coupled chemical and dynamic models as well as the diagnosis of available meteorological data. ESA

N90-12112# Deutsche Forschungs- und Versuchsanstalt fuer Luft- und Raumfahrt, Freiburg (Germany, F.R.). Abteilung Luftbildmessung und Fernerkundung der Universitaet Freiburg.

INVESTIGATION ON ANALYZING COMPUTER-AIDED FOREST DISEASE CLASSIFICATIONS Thesis - Freiburg Univ.

Steffan Kuntz 17 Jul. 1989 162 p In GERMAN; ENGLISH summary Original contains color illustrations
(DFVLR-FB-89-16; ISSN-0171-1342; ETN-89-95312) Avail: NTIS HC A08/MF A01; DFVLR, VB-PL-DO, Postfach 90 60 58, 5000 Cologne, Federal Republic of Germany, 64 deutsche marks

Computer-aided forest disease classifications based on multispectral airborne scanner data are presented. Problems encountered in trying to check the results are described. Airborne scanner data from different altitudes were investigated. Computer-aided classifications methodologies for statistically checking the results were developed and tested over damaged forest areas. The quality of the classification could be improved when digital terrain information is involved. ESA

46 GEOPHYSICS

Includes aeronomy; upper and lower atmosphere studies; ionospheric and magnetospheric physics; and geomagnetism.

For space radiation see *93 Space Radiation.*

N90-12113# National Center for Atmospheric Research, Boulder, CO. Atmospheric Technology Div.

MEETING REVIEW: THE SECOND NCAR (NATIONAL CENTER FOR ATMOSPHERIC RESEARCH) RESEARCH AIRCRAFT FLEET WORKSHOP

Warren B. Johnson and William A. Cooper May 1989 94 p Workshop held in Boulder, CO, 15-16 Apr. 1987; sponsored by NSF
(Grant NSF ATM-87-09659)
(PB89-200901; NCAR/TN-332-PROC) Avail: NTIS HC A05/MF A01 CSCL 04A

A workshop was held at NCAR 15 to 16 April 1987 to assess the scientific needs for atmospheric research aircraft in the next 15 years, and to recommend how the composition of the NCAR aircraft fleet should evolve to meet those needs. The workshop was attended by approximately 75 atmospheric and oceanic scientists and research managers representing all of the scientific areas served by the NCAR Research Aviation Facility. The NCAR group that planned the workshop recognized that the products of the meeting would be most credible and valuable if they reflected the viewpoints of a representative cross section of scientists from a broad spectrum of disciplines and interests, and accordingly prepared the invitation list to provide the needed balance and breadth. The workshop followed up on a previous meeting (the First NCAR Research Aviation Facility Fleet Workshop) that was held in February 1982 with similar purposes. Author

N90-12114# Physical Sciences, Inc., Andover, MA.

LABCEDE FLUORESCENCE INVESTIGATIONS Final Report, 30 Nov. 1984 - 29 Feb. 1988

B. D. Green, B. L. Upschulte, W. J. Marinelli, L. G. Piper, K. L. Holtzclaw, J. C. Person, M. E. Fraser, W. J. Kessler, H. C. Murphy, and A. T. Lintz Aug. 1988 555 p
(Contract F19628-84-C-0057; AF Proj. 2310)
(AD-A210678; PSI-TR-756; AFGL-TR-88-0186) Avail: NTIS HC A24/MF A03 CSCL 04/1

A wide variety of projects to measure and interpret the fluorescence arising from electron excitation of atmospheric gases are covered. Excitation of nitrogen B-state is Franck Condon at low pressure but as pressure increases to tens of mtorr, collisional transfer from the A-state into the lowest B-state vibrational levels is observed. The middle levels of the B-state show little variation with pressure even though they strongly coupled to W-state levels. The N2a(1 pi g) state was observed via LBH emission at 0.2 micrometers. Substantial vibrational redistribution rather than electronic quenching was observed. Again nested electronic states in particular the a'-state are involved in the relaxation. Level-specific investigations of the N2a, v=0 relaxation by a variety of gases including N2 and oxygen is also reported. Electron impact excitation cross sections for N2(+) A, v=2-7 were measured at sufficiently low pressures that quenching effects can be removed. Data from two infrared spectrometers are used to determine the contributions of various N2 transitions to the IR spectrum observed in LABCEDE. Emission from N2/O2 irradiated mixtures were also studied. Ozone fluorescence is observed. Data from early field mission seemed to indicate that the auroral fluorescence spectrum was different under sunlit conditions. The LABCEDE Facility was used to provide an understanding of electron/N2 molecular scattering processes. GRA

N90-12115*# National Aeronautics and Space Administration. Goddard Space Flight Center, Greenbelt, MD.

PROCESSING OF DMSP MAGNETIC DATA AND ITS USE IN GEOMAGNETIC FIELD MODELING

J. R. Ridgway, T. J. Sabaka, D. Chinn (Science Applications Research, Lanham, MD.), and R. A. Langel Nov. 1989 63 p
(Contract NAS5-20440)
(NASA-TM-100750; Rept-90B00020; NAS 1.15:100750) Avail: NTIS HC A04/MF A01 CSCL 08G

The DMSP F-7 satellite is an operational Air Force meteorological satellite which carried a magnetometer for geophysical measurements. The magnetometer was located within the body of the spacecraft in the presence of large spacecraft fields. In addition to stray magnetic fields, the data have inherent position and time inaccuracies. Algorithms were developed to identify and remove time varying magnetic field noise from the data. Techniques developed for Magsat were then modified and used to attempt determination of the spacecraft fields, of any rotation between the magnetometer axes and the spacecraft axes, and of any scale changes within the magnetometer itself. The corrected data were then used to attempt to model the geomagnetic field. This was done in combination with data from Magsat, from the standard magnetic observatories, from aeromagnetic and other survey data, and from DE-2 spacecraft field data. Future DMSP missions can be upgraded in terms of geomagnetic measurements by upgrading the time and position information furnished with the data, placing the magnetometer at the end of the boom, upgrading the attitude determination at the magnetometer, and increasing the accuracy of the magnetometer. Author

N90-12116# Finnish Meteorological Inst., Helsinki.

CALCULATED SOLAR RADIATION INCIDENT UPON SLOPES OF DIFFERENT ORIENTATED SURFACES IN FINLAND

Bengt Tammelin and Reijo Hyvonen 1989 41 p In FINNISH; ENGLISH summary
(FMI-MP-8; ISBN-951-697-270-5) Avail: NTIS HC A03/MF A01

Solar radiation on inclined surfaces was calculated using as basic data measured hourly values of global and diffuse radiation. Hourly values for incoming direct radiation on a vertical surface having the same azimuth as the sun were put into a average solar map (grids 2.5 x 2.5 degrees). This was first done to be able to calculate easily the incoming radiation for a large number of buildings in different surroundings. These monthly mean values for each grid were used to calculate the incoming radiation on inclined surfaces. Diffuse radiation was handled isotropically. The mean monthly figures are presented for south-, middle and north-Finland assuming an elevation of 5 degrees for the horizon. Author

N90-12117*# International Council of Scientific Unions, Urbana, IL. Scientific Committee on Solar-Terrestrial Physics.

MIDDLE ATMOSPHERE PROGRAM. HANDBOOK FOR MAP, VOLUME 28

C. H. Liu, ed. and Belva Edwards, ed. Aug. 1989 685 p
Proceedings of 4th Workshop on Technical and Scientific Aspects of MST Radar, Kyoto, Japan, 28 Nov. - 2 Dec. 1988 Sponsored by NASA, Washington and UNESCO
(NASA-CR-184972; NAS 1.26:184972; MAP-Handbook-28) Avail: NTIS HC A99/MF A04; also available from SCOSTEP Secretariat, Illinois Univ., 1406 West Green Street, Urbana, IL 61801 CSCL 04A

Extended abstracts from the fourth workshop on the technical and scientific aspects of MST (mesosphere stratosphere troposphere) radar are presented. Individual sessions addressed the following topics: meteorological applications of MST and ST radars, networks, and campaigns; dynamics of the equatorial middle atmosphere; interpretation of radar returns from clear air; techniques for studying gravity waves and turbulence; intercomparison and calibration of wind and wave measurements at various frequencies; progress in existing and planned MST and ST radars; hardware design for MST and ST radars and boundary layer/lower troposphere profilers; signal processing; and data management. M.G.

N90-12118# Kiruna Geophysical Inst. (Sweden).

DISTRIBUTION OF AURORAL PRECIPITATION AT MIDNIGHT DURING A MAGNETIC STORM

J. Sandahl, L. Eliasson, A. Pellinen-Wannberg, G. Rostoker, L. P. Block, R. E. Erlandson, E. Friis-Christensen, B. Jacobsen, H. Luehr, and J. S. Murphree (Calgary Univ., Alberta) Apr. 1989 47 p
Submitted for publication
(PB89-213136; IRF-Preprint-113) Avail: NTIS HC A03/MF A01 CSCL 04A

On the night of November 4, 1986 a very complex precipitation pattern was observed by the Swedish satellite Viking in the magnetic midnight sector over Scandinavia and Svalbard. The pass took place during a magnetic storm, but during substorm recovery phase. Going from north to south the satellite first encountered a plasma region of bps-type and then a region of cps-type. Then, however, a new region of bps-type was traversed. The quite intense most equatorward aurora corresponded to a plasma region which was not of ordinary cps-type but contained sharp quasimonoenergetic peaks. The high latitude midnight sector was totally dominated by eastward convection. The Harang discontinuity had passed northern Scandinavia the first time as early as between 18 and 20 MLT, more than three hours before the Viking pass. It is suggested that the particle precipitation pattern and the general shape of the aurora as observed by the Viking imager can be explained in a natural way by the convection pattern. The northernmost bps- and cps-type regions originated in the morning side convection cell while the more equatorward population of bps-type had drifted in from the evening side. Author

N90-12119# Los Alamos National Lab., NM.
COHERENCY PROPERTIES OF STRONG LANGMUIR TURBULENCE
Harvey A. Rose, D. F. DuBois, and David Russell 1989 4 p
Presented at the International Workshop on Nonlinear and Turbulent Processes in Physics, Kiev, USSR, Oct. 1989
(Contract W-7405-eng-36)
(DE89-009290; LA-UR-89-895; CONF-891073-1) Avail: NTIS HC A01/MF A01

Strongly correlated Langmuir wave collapse has been observed in two dimensional simulations of Zakharov's model in a regime characterized by strong ion sound wave damping and an external drive frequency, omega(sub 0), close to but less than the plasma frequency, (omega(sub p) - omega(sub 0))/omega(sub 0) is greater than epsilon with epsilon being approximately equal to 0.005. Caviton-caviton interactions induce temporal correlations between different collapse sites on a time scale the order of a collapse cycle, and on a longer time scale site locations migrate possibly leading to strong spatial correlations. Certain features of ionospheric incoherent scatter radar (ISR) spectra are consistent with such correlations. DOE

N90-12120# Massachusetts Inst. of Tech., Cambridge. Dept. of Earth, Atmospheric, and Planetary Sciences.
INVESTIGATIONS OF EURASIAN SEISMIC SOURCES AND UPPER MANTLE STRUCTURE Final Technical Report, 9 Jun. 1987 - 8 Nov. 1988
Thomas H. Jordan, Justin S. Revenaugh, and Lind S. Gee 25 May 1989 309 p
(Contract F19628-87-K-0040; NSF EAR-87-08548; ARPA Order 5299)
(AD-A211806; GL-TR-89-0143) Avail: NTIS HC A14/MF A02 CSCL 08/11

A new set of waveform-analysis procedures to recover phase and amplitude information from seismograms was evaluated. These procedures appear to be capable of making fundamentally new observations about the structure of the earth's interior. They were used to measure travel times and quality factors of body waves, including those embedded in complex wavetrains, as well as dispersion and attenuation of surface waves, including higher modes. These techniques were applied to three component seismograms to investigate the structure of the Eurasian upper mantle, made observations of shear wave splitting on long period records of multiply reflected S waves bottoming in the upper mantle beneath the Russian and Siberian platforms. Dispersion of Love and Rayleigh waves over these paths shows discrepancies of comparable or larger magnitude with respect to smooth isotropic structures, consistent with a model of the uppermost mantle having significant apparent vertical anisotropy. Although the splitting and dispersion data can be fit by smooth anisotropic models, we investigated the apparent anisotropy associated with fine-scale (rough) structure beneath stable Eurasia. The data was fitted with a rough isotropic model having an rms shear velocity fluctuation that varies from 14 percent in the uppermost mantle to zero at 400-km depth. The fluctuations are larger than the variation expected for even a diverse assemblage of upper mantle ultrabasic rocks, which was taken as evidence for some sort of intrinsic (local) anisotropy. GRA

N90-12121# Atmospheric Radiation Consultants, Acton, MA.
RETRIEVAL OF ATOMIC OXYGEN AND TEMPERATURE IN THE THERMOSPHERE. PART 2: FEASIBILITY OF AN EXPERIMENT BASED ON LIMB EMISSION IN THE OI LINES Final Report, Feb. 1987 - Apr. 1989
A. S. Zachor and B. K. Yap (Yap Analytics, Inc., Lexington, MA.) 30 May 1989 42 p
(Contract F19628-87-C-0053)
(AD-A211807; GL-TR-89-0145-Pt-2) Avail: NTIS HC A03/MF A01 CSCL 04/1

A viable technique for remote sensing of the atomic oxygen density and translational temperature profiles above 80 km altitude, where oxygen atoms are involved in important chemical, collisional and radiative cooling processes, would have enormous value. The two profiles can, in principle, be recovered simultaneously from limb scan data obtained near wave length 147 and/or 63 microns corresponding to the intermultiplet transitions in the ground electronic state of atomic oxygen. An approach in which the limb radiance data represents just one of the lines observed at high spectral resolution was considered in part 1; recovery of the temperature relies mainly on Doppler broadening. Here, in Part 2, feasibility is evaluated of the experiment concept when the data is a pair of limb radiance profiles corresponding to the two unresolved OI lines; temperature retrieval relies mostly on the difference in upper state populations. GRA

N90-12122# Hawaii Univ., Honolulu. Inst. of Geophysics.
HYDROPHONE INVESTIGATIONS OF EARTHQUAKES AND EXPLOSION GENERATED HIGH-FREQUENCY SEISMIC PHASES Final Technical Report, 1 Nov. 1985 - 31 May 1989
Daniel A. Walker 30 Jun. 1989 81 p
(Grant AF-AFOSR-0339-89; AF Proj. 2309)
(AD-A212055; AFOSR-89-1206TR) Avail: NTIS HC A05/MF A01 CSCL 17/10

Brief descriptions of published papers, in-house reports, or abstracts sponsored by this grant are presented. A sampling of highlights from these investigations includes: (1) There is a strong correlation between ocean surface wind velocities and ocean bottom noise in the frequency range of 0.5 to 30 Hz; (2) Sites favorable for the detection of weak short-period signals may be found on the deep ocean bottom in regions with low wind; (3) The yield of large explosions might be disguised by siting the explosion at a location that selectively defocuses energy towards continents where most seismic stations are located; (4) The Wake Island array provides very stable measures of yield; (5) A moderate underground nuclear explosion appropriately placed in a subduction zone (e.g., the Kuril-Kamchatka portion of the circum-Pacific arc) could escape detection by the existing conventional network of continental and island seismic stations; (6) A new trench extending over 5000 km from the Marianas trench to the Tonga trench may be forming in the southwest Pacific; and (7) A significant number of earthquakes, unreported by the conventional world wide network of seismic stations, are located within the interior of the Northwestern Pacific Basin. GRA

N90-12123# Johns Hopkins Univ., Laurel, MD. Applied Physics Lab.
INVESTIGATION OF ATMOSPHERIC EMISSIONS IN ULTRAVIOLET, VACUUM ULTRAVIOLET, AND EXTREME ULTRAVIOLET WAVELENGTH Final Report
Ching-I. Meng Jul. 1989 108 p
(Grant AF-AFOSR-0057-86; AF Proj. 2310)
(AD-A212169; AFOSR-89-1227TR) Avail: NTIS HC A06/MF A01 CSCL 04/1

The research had three objectives: (1) To understand the morphology of atmospheric optical UV emissions over the polar region associated with the solar and magnetospheric particle precipitations; (2) To understand the morphology of the middle and low latitude airglow; and (3) To investigate the UV background of the atmospheric emissions for possible application for remote sensing. The focus of data analysis started on UV and FUV spectra taken from the polar orbiting S3-4 satellite. To this date, the S3-4 has provided the only satellite measurement with the composite data set of the FUV (sometimes called Vacuum Ultraviolet) and UV wavelength regions. The S3-4 data set is suitable for the analyses of diffuse auroral emissions, and the study revealed the characteristic wavelength which can be used for remote sensing and 2-D image in the auroral precipitating electron energetics. The comparison of the observation to a transport model calculation, led to the contribution of defining some atmospheric constants currently in debate. The close examination of anomalous emission spectra led to the discovery of the UV spectra caused by energetic O(+) precipitation. Finally, the Doppler shift of proton auroral La was observed for the first time. GRA

N90-12124# Air Force Geophysics Lab., Hanscom AFB, MA.
COMPARISON OF THE LOWTRAN 7 CODE AND S3-4 SATELLITE MEASUREMENTS OF UV RADIANCE
R. E. Huffman, L. A. Hall, and F. J. LeBlanc (Northwest Research Associates, Inc., Bellevue, WA.) 8 Aug. 1989 8 p Submitted for publication
(AF Proj. 4643)
(AD-A211356; AFGL-TR-89-0195) Avail: NTIS HC A02/MF A01 CSCL 04/1

Atmospheric radiance measurements and model calculations in the 200 to 290 nm wavelength region are found to be in good agreement. The calculations are made using the recently released LOWTRAN 7 transmission and radiance code. The measurements were made in 1978 from the S3-4 satellite. The model is in excellent agreement in regard to radiance level and to spectral variability in this region for the daytime, mid-latitude measurements. Under twilight conditions, the lack of airglow and fluorescence emission sources in the code lead to differences. Additions to the model to provide better agreement are under consideration, but as the present time, the code can be used for a wide range of atmospheric problems. GRA

N90-12125# Air Force Geophysics Lab., Hanscom AFB, MA.
ESTIMATED UV CLUTTER LEVELS AT 10-100 METER SENSOR PIXEL RESOLUTION EXTRAPOLATED FROM RECENT POLAR BEAR MEASUREMENTS
M. Wohlers, R. Huguenin, M. Weinberg (Aerodyne Research, Inc., Billerica, MA.), R. E. Huffman, R. W. Eastes, and F. P. Delgreco 7 Aug. 1989 11 p Submitted for publication
(AD-A211357; AFGL-TR-89-0191) Avail: NTIS HC A02/MF A01 CSCL 17/5

There is continuing need for information about the earth background clutter at ultraviolet wavelengths. The methodology and the results obtained at 1304 are described. A wavelength from an analysis of th AFGL Polar Bear Experiment. The basic measurement equipment provided data of a spatial resolution of 20 km over a large portion of the earth. The instrumentation also provided sampled outputs as the footprint scanned along the measurement track. The combination of the fine scanning and large area coverage provided opportunity for a spatial power spectral analysis that in turn provided a means for extrapolation to finer-spatial scale; a companion paper discusses the physical basis for this extrapolation. GRA

N90-12126# Air Force Geophysics Lab., Hanscom AFB, MA.
SPATIAL CHARACTERISTICS OF AIRGLOW AND SOLAR SCATTER RADIANCE FROM THE EARTH'S ATMOSPHERE
R. Huguenin, R. Wohlers, M. Weinberg (Aerodyne Research, Inc., Billerica, MA.), R. E. Huffman, R. W. Eastes, and F. P. Delgreco 9 Aug. 1989 13 p Submitted for publication
(Contracts F19628-87-C-0206; F19628-89-C-0091)
(AD-A211358; AFGL-TR-89-0200) Avail: NTIS HC A02/MF A01 CSCL 04/1

Data measured by the Polar BEAR/AIRS UV Experiment were processed to extract spatial radiance characteristics. Photometer mode 1304A dayside data measured on Julian Day 219, 1897, near mid-day were analysed. The spatial structure of thermospheric dayside radiance at 1304A appeared to be controlled principally by turbulence over spatial scales of 10 million to 100 meters, with modifications imposed by Rayleigh scattering effects and magnetospherically forced phenomena. Spatial structure can be adequately modeled fractally, using dimensions based on Kolmogorov formalism modified by the Rayleigh scattering phase function. Mean radiance can be modeled using existing models of radiant intensity, resonance scattering, and absorption combined with thermospheric composition and general circulation models, such as MSIS-83, scaled to the mean and RHS intensities measured by Polar BEAR. The results can be incorporated in a background radiance simulation model that will provide a means for testing and refining phenomenological models of the structured earth background. This will be important not only for improving physical and chemical models of atmospheric features and processes, but it will allow parametric predictions of spatial structure and clutter to be developed for sensor applications. GRA

N90-12127# Air Force Geophysics Lab., Hanscom AFB, MA.
UV IONOSPHERIC REMOTE SENSING WITH THE POLAR BEAR SATELLITE
F. P. Delgreco, R. W. Eastes, and R. E. Huffman 8 Aug. 1989 6 p Submitted for publication
(AF Proj. 4643)
(AD-A211359; AFGL-TR-89-0199) Avail: NTIS HC A02/MF A01 CSCL 17/5

Some recent work interpreting and analyzing data obtained by the AIRS sensor on the Polar BEAR satellite is briefly described. The Polar BEAR satellite was launched in November 1986 into a nearly circular 1000 km orbit with an orbital inclination of 89.5 degrees and a nodal regression of 0.05 degrees per day. In the course of a year the satellite experiences all local times twice a year. One of the instruments on Polar BEAR is the Auroral Ionospheric Remote Sensor (AIRS). AIRS was described previously and some of the early data from that instrument also was presented. Briefly, in its primary operating mode AIRS was designed to return four simultaneous images of the atmospheric radiation at Northern latitudes, in the far and near ultraviolet (UV) and the visible at 6300 A. Two of the data streams originate from photomultipliers at the exit plane of a one eighth meter far UV spectrometer. The other two data streams originate at photomultipliers behind narrow band UV and visible filters. A single telescope illuminates both the spectrometer entrance slit and the filtered detectors. In the normal imaging mode of operation, on a three second cycle the line of sight of all four channels is deflected from horizon to horizon perpendicular to the orbital path by a plane mirror at the entrance to the telescope. GRA

N90-12128# Saint Louis Univ., MO. Geophysics Lab.
SEISMIC WAVE ATTENUATION AND YIELD DETERMINATION AT REGIONAL DISTANCES Final Report, 1 May 1987 - 30 Apr. 1989
B. J. Mitchell, O. W. Nuttli, J. K. Xie, H. Al-Shukri, and A. Correig 25 May 1989 131 p
(Contract F19628-87-K-0036)
(AD-A211548; AFGL-TR-89-0142) Avail: NTIS HC A07/MF A01 CSCL 08/11

Work was completed on yield determination at the Soviet test site on Novaya Zemlya. Magnitudes and yields, determined for 30 explosions using Lg amplitudes recorded in northwestern Europe, ranged between 2.5 and 4900 kt, the largest since April 1976 being about 145 kt. Studies were completed on seismic wave attenuation of surface waves at intermediate periods and of Lg waves at 1 Hz in several regions of the world. Limits were determined for the degree of frequency dependence of Q sub beta which can occur in the crust in stable and tectonically active regions. A stochastic convolution model was proposed for Lg coda at distances greater than 200 km which considers the effects of dispersion scattering and mode conversions at those distances. A back projection tomographic method was developed to regionalize large scale lateral variations of coda Q for Lg waves which traverse long continental paths. A seismically active region in the New Madrid seismic zone was found to be characterized by lower than normal Q values. In the western United States it was found that Q values in the upper mantle vary laterally, becoming smaller from east to west. Crust of the Basin and Range province has a low-Q upper crust overlying a lower crust with higher Q values. GRA

N90-12129# RDP, Inc., Waltham, MA.
TEC (TOTAL ELECTRON CONTENT) MODELS Report, 3 Feb. 1988 - 2 Feb. 1989
Andrew J. Mazzella, Jr., Kevin P. Larson, and Peter Dickson 15 Mar. 1989 26 p
(Contract F19628-88-C-0039)
(AD-A211553; AFGL-TR-89-0092; SR-2) Avail: NTIS HC A03/MF A01 CSCL 04/1

Models of the ionosphere were developed and utilized to evaluate Total Electron Content for various specified transmission paths from the ground into space. GRA

N90-12130# Westinghouse Electric Corp., Middletown, RI. Oceanic Div.
EFFECTS ON ELECTROMAGNETIC WAVE PROPAGATION AND ROCKET VAPOR TRAILS OF INTENSE TURBULENCE GENERATED BY BREAKING INTERNAL GRAVITY WAVES Final Report, Aug. 1986 - Sep. 1987
John R. Grant 14 Aug. 1989 15 p
(Contract N00014-86-C-0662)
(AD-A211755; WOD/CO/HYDRO-87/09) Avail: NTIS HC A03/MF A01 CSCL 04/1

The effects on laser propagation of turbulence produced by breaking internal gravity waves in the mesosphere is investigated. At the time of this writing the major parameter, (C sub n) sq., needed for this investigation was computed for a representative case. The case is a narrow band wave generated at the ground and propagating upward; breaking eventually occurs over altitudes from less than 40 to greater than 93 kilometers, the upper limit of the calculation. The calculation itself, if not strictly from first principles, involves only a relatively small amount of approximation to the Navier-Stokes equations, both for the wave motion and the turbulence. The evolution of (C sub n) sq. is followed from its inception in the breaking part of the wave phase, its growth in magnitude and coalescence across the phases, to its subsequent decay as the turbulence dies away. Peak values of about 10 to the -17th power/m to the 2/3 power are observed in (C sub n) sq. With these results, effects such as variance in intensity and phase, beam spread and beam wander may be computed. GRA

N90-12060*# Pennsylvania State Univ., University Park. Dept. of Meteorology.
STRATIFORM CLOUDS AND THEIR INTERACTION WITH ATMOSPHERIC MOTIONS Abstract Only
John H. E. Clark and N. Shirer Hampton *In* NASA, Marshall Space Flight Center, NASA/MSFC FY88 Global Scale Atmospheric Processes Research Program Review Feb. 1989 p 1-5 (For primary document see N90-12059 03-42)
Avail: NTIS HC A05/MF A01 CSCL 04A

N90-12068*# Alabama Univ., Huntsville. Dept. of Mathematics and Statistics.
STUDIES OF BAROCLINIC INSTABILITY IN THE PRESENCE OF SURFACE TOPOGRAPHY AND STRATOSPHERIC OZONE Abstract Only
Nathaniel D. Reynolds *In* NASA, Marshall Space Flight Center, NASA/MSFC FY88 Global Scale Atmospheric Processes Research Program Review Feb. 1989 p 31-32 (For primary document see N90-12059 03-42)
Avail: NTIS HC A05/MF A01 CSCL 04A

N90-12075*# Iowa State Univ. of Science and Technology, Ames. Dept. of Earth Sciences.
USE OF SATELLITE DATA AND MODELING TO ASSESS THE INFLUENCE OF STRATOSPHERIC PROCESSES ON THE TROPOSPHERE Abstract Only
Terrence R. Nathan and Douglas N. Yarger *In* NASA, Marshall Space Flight Center, NASA/MSFC FY88 Global Scale Atmospheric Processes Research Program Review Feb. 1989 p 55-58 (For primary document see N90-12059 03-42)
Avail: NTIS HC A05/MF A01 CSCL 04A

N90-12076*# Colorado Univ., Boulder. Dept. of Astrophysical, Planetary and Atmospheric Sciences.
LABORATORY AND THEORETICAL MODELS OF PLANETARY-SCALE INSTABILITIES AND WAVES Abstract Only
John E. Hart and Juri Toomre *In* NASA, Marshall Space Flight Center, NASA/MSFC FY88 Global Scale Atmospheric Processes Research Program Review Feb. 1989 p 59-63 (For primary document see N90-12059 03-42)
Avail: NTIS HC A05/MF A01 CSCL 04A

N90-12078*# Hawaii Univ., Honolulu. Hawaii Inst. of Geophysics.
AEROSOL IN THE PACIFIC TROPOSPHERE Abstract Only
Antony D. Clarke *In* NASA, Marshall Space Flight Center, NASA/MSFC FY88 Global Scale Atmospheric Processes Research Program Review Feb. 1989 p 69-71 (For primary document see N90-12059 03-42)
Avail: NTIS HC A05/MF A01 CSCL 04A

N90-12080*# Alabama Univ., Huntsville.
GLOBAL BACKSCATTER ASSESSMENT Abstract Only
David A. Bowdle *In* NASA, Marshall Space Flight Center, NASA/MSFC FY88 Global Scale Atmospheric Processes Research Program Review Feb. 1989 p 75-78 (For primary document see N90-12059 03-42)
Avail: NTIS HC A05/MF A01 CSCL 04A

N90-12082*# Georgia Inst. of Tech., Atlanta.
MEASUREMENTS OF AEROSOL PROPERTIES NEEDED TO INFER BACKSCATTER CHARACTERISTICS IN SUPPORT OF THE NASA DOPPLER LIDAR PROGRAM Abstract Only
E. M. Patterson, M. S. Black, and C. O. Pollard *In* NASA, Marshall Space Flight Center, NASA/MSFC FY88 Global Scale Atmospheric Processes Research Program Review Feb. 1989 p 87-90 (For primary document see N90-12059 03-42)
Avail: NTIS HC A05/MF A01 CSCL 04A

N90-12083*# Pennsylvania State Univ., University Park.
INFRARED BACKSCATTERING Abstract Only
Craig F. Bohren, Timothy J. Nevitt, and Shermila Brito Singham *In* NASA, Marshall Space Flight Center, NASA/MSFC FY88 Global Scale Atmospheric Processes Research Program Review Feb. 1989 p 91-94 (For primary document see N90-12059 03-42)
Avail: NTIS HC A05/MF A01 CSCL 04A

47 METEOROLOGY AND CLIMATOLOGY

Includes weather forecasting and modification.

N90-12131# Air Force Systems Command, Wright-Patterson AFB, OH. Foreign Technology Div.
CONTEMPORARY CHINA'S METEOROLOGICAL ENTERPRISES (SELECTED PORTIONS)
9 Jun. 1989 30 p Transl. into ENGLISH from Dangdai Zhongguo de Qiziany Shiye, Chuban She (Beijin, People's Republic of China), 1984 p 24-44; 186-188; 208-211; 420-421
(AD-A210697; FTD-ID(RS)T-0390-89) Avail: NTIS HC A03/MF A01 CSCL 04/2

Two chapters are presented from a translation of a Chinese meteorological journal. Chapter 2: The network of meteorological stations and posts; Chapter 8: Meteorological service. GRA

N90-12132# National Center for Atmospheric Research, Boulder, CO.
INVESTIGATIONS OF POLAR AIR STREAM CYCLOGENESIS BASED ON NUMERICAL SIMULATIONS WITH A MESOSCALE MODEL Ph.D. Thesis - Washington Univ.
Warren Blier 1989 280 p
(Grants NSF ATM-87-09659; NSF ATM-81-03697; NSF ATM-83-18842)
(PB89-214563; NCAR/CT-120) Avail: NTIS HC A13/MF A02 CSCL 04B

Extratropical cyclogenesis has long been considered through the paradigm provided by the Norwegian cyclone model, in which cyclone evolution occurs through a wave development along a polar front separating tropical and polar air masses. However, smaller scale cyclones are observed to form on the cold air side of the polar front, especially over oceanic regions during the winter half of the year. It is to the evolution of these cyclones that the phrase polar air stream is applied. Author

N90-12133*# Mesoscale Environmental Simulations and Operations, Inc., Hampton, VA.

DEVELOPMENT OF HIGH RESOLUTION SIMULATIONS OF THE ATMOSPHERIC ENVIRONMENT USING THE MASS MODEL Final Report

Michael L. Kaplan, John W. Zack, and V. Mohan Karyampudi 30 Nov. 1989 80 p
(Contract NAS5-30145)
(NASA-CR-186040; NAS 1.26:186040) Avail: NTIS HC A05/MF A01 CSCL 04B

Numerical simulations were performed with a very high resolution (7.25 km) version of the MASS model (Version 4.0) in an effort to diagnose the vertical wind shear and static stability structure during the Shuttle Challenger disaster which occurred on 28 January 1986. These meso-beta scale simulations reveal that the strongest vertical wind shears were concentrated in the 200 to 150 mb layer at 1630 GMT, i.e., at about the time of the disaster. These simulated vertical shears were the result of two primary dynamical processes. The juxtaposition of both of these processes produced a shallow (30 mb deep) region of strong vertical wind shear, and hence, low Richardson number values during the launch time period. Comparisons with the Cape Canaveral (XMR) rawinsonde indicates that the high resolution MASS 4.0 simulation more closely emulated nature than did previous simulations of the same event with the GMASS model. Author

N90-12134# National Severe Storms Forecast Center, Kansas City, MO.

SEVERE LOCAL STORM WARNING VERIFICATION: 1988 Final Technical Report

Leo A. Grenier, John T. Halmstad, and Preston W. Leftwich, Jr. Jun. 1989 28 p
(PB89-226310; NOAA-TM-NWS-NSSFC-23) Avail: NTIS HC A03/MF A01 CSCL 04B

Tornado and severe thunderstorm warnings are issued by local offices of the National Weather Service. Routine verification of these warnings is accomplished at the National Severe Storms Forecast Center. Verification results are highlighted for the year 1988. Stations in the Central and southern regions again issued most of the warnings and experienced most of the severe local storm events. On a national scale, verification scores improved slightly. Continued improvement in the False Alarm Ratio and the Critical Success Index are evident. After a slight decrease in the Probability of Detection in 1987 it also resumed an upward trend. GRA

N90-12135# National Inst. of Standards and Technology, Gaithersburg, MD. Center for Electronics and Electrical Engineering.

LIGHTNING AND SURGE PROTECTION OF PHOTOVOLTAIC INSTALLATIONS: TWO CASE HISTORIES, VULCANO AND KYTHNOS

Francois D. Martzloff Jun. 1989 78 p Sponsored by Sandia National Labs., Albuquerque, NM
(PB89-229058; NISTIR-89/4113) Avail: NTIS HC A05/MF A01 CSCL 04B

Two installations of photovoltaic systems were damaged during lightning storms. The two sites were visited and the damaged equipment that was still available on the site was examined for analysis of the suspected occurrence. The evidence, however, is insufficient to conclude that all the observed damage was caused by the direct effect of a lightning flash. A possible scenario may be that lightning-induced overvoltages caused insulation breakdown at the edges of the photovaltaic modules, with subsequent damage done by the dc current of the array. Other surge protection considerations are also addressed, and suggestions presented for further investigations. GRA

N90-12136# Naval Ocean Systems Center, San Diego, CA.

AIRBORNE PROFILES TAKEN NEAR SAN NICOLAS ISLAND, CALIFORNIA, DURING OPERATION FIRE (FIRST ISCCP (INTERNATIONAL SATELLITE CLOUD CLIMATOLOGY PROJECT) REGIONAL EXPERIMENT) (1987): AEROSOL SIZE DISTRIBUTIONS, AIR AND SURFACE TEMPERATURES, CLOUD TOP TEMPERATURES, AND RELATIVE HUMIDITIES Final Report, Jun. - Sep. 1987

Douglas R. Jensen Feb. 1989 141 p
(AD-A211664; NOSC/TD-1533) Avail: NTIS HC A07/MF A01 CSCL 04/2

During June and July, 1987, Project FIRE was conducted in the Southern California offshore area. First ISCCP Regional Experimental (FIRE) is a cloud research program to validate/update the International Satellite Cloud Climatology Project (ISCCP) database and cloud/radiation parameterizations used in the general circulation models. Coordinated surface, aircraft, and satellite observations of marine stratocumulus cloud within and just above the marine boundary layer were made by a myriad of participants. Data are presented from airborne profiles taken near San Nichols Island, CA, during Operation FIRE (1987). Aerosol size distributions, air and surface temperatures, cloud top temperatures, and relative humidities are tabulated. The NOSC airborne platform was employed to investigate the low-level horizontal variability of the marine-boundary-layer structure. GRA

N90-12137 Physics and Electronics Lab. TNO, The Hague (Netherlands).

CALIBRATION OF A VISIOCEILOMETER, A HAND HELD LIDAR SYSTEM

G. J. Kunz Sep. 1988 54 p
(Contract A83/K/058)
(FEL-1988-73; TD88-4405; ETN-89-95081) Copyright Avail: TNO Physics and Electronics Lab., P.O. Box 96864, 2509 JG The Hague, Netherlands

The calibration of a modified laser range finder, in the lidar mode, is described. The visioceilometer is applied for visibility and cloud height measurements. An inconvenience of the visioceilometer is the mains powered cassette recorder combined with the battery powered lidar and processing unit. The laser transmitter is suited for lidar applications (the laser energy varies about 20 percent). The receiver seems to have different calibration parameters than it was assumed. The signal bandwidth and sample frequency are suited for lidar aplications. Overloading the detection system has little influence on the lidar signal. The logarithmic transfer function for small signals can be compensated with a second order curve. A point of uncertainty is the reference level of the output signal. ESA

N90-12138 Physics and Electronics Lab. TNO, The Hague (Netherlands).

A CLOSER LOOK AT THE VISIOCEILOMETER

G. J. Kunz Mar. 1989 83 p Original contains color illustrations
(Contract A83/K/058)
(FEL-1989-80; TD89-1857; ETN-89-95084) Copyright Avail: TNO Physics and Electronics Lab., P.O. Box 96864, 2509 JG The Hague, Netherlands

The properties of the visioceilometer, a small prototype commercial lidar systems, are reported. The receiver and its related problems are discussed. The measured maximum range is compared with the calculated one. Measured data is presented and compared with the results of an experimental Mini Lidar. The calibration of the visioceilometer lidar is very critical at high visibilities. A straight-line fit to the calibration data is not adequate under these conditions. A fifth-order fit is used. Strong horizontal irregularities were not observed. The shot-to-shot changes in the slope of the range-compensated curves suggests that there are irregularities with dimensions on the order of the range capacity of the lidars, or greater. ESA

N90-12139# World Meteorological Organization, Geneva (Switzerland).
WORLD WEATHER WATCH: IMPLEMENTATION Status Report No. 14
1989 96 p
(WMO-714; ISBN-92-63-10714-9; ETN-89-95173) Copyright
Avail: NTIS MF A01; World Meteorological Organization, Case Postale no. 5, CH-1211 Geneva 20, Switzerland

The World Weather Watch (WWW) plan and the 1988-1997 implementation program are reported. The purpose of the plan is to give to the members a conceptual framework for the further longterm development of their national meteorological services and WWW components. The plan assumes that the primary function of the WWW remains unaltered, but requirements for specific services increase. In the scope of the report the global systems involving observation, data processing and telecommunication are studied. The monitoring of the operation of the WWW and the WWW operational information system are considered. ESA

N90-12140 Royal Netherlands Meteorological Inst., De Bilt. Physical Meteorology Dept.
CRAU 1987: THE KNMI CONTRIBUTION
W. Kohsiek, J. G. vanderVliet, and W. A. A. Monna 1988 56 p
(KNMI-TR-110; ISSN-0169-1708; ETN-89-95596) Copyright
Avail: Royal Netherlands Meteorological Inst., P.O. Box 201, 3730 de Bilt, Wilhelminalaan 10, Netherlands

The results obtained from the Crau experiment are reported. The purpose of the experiment is to study the exchange of heat and moisture between the Earth's surface and the atmosphere over homogeneous and nonhomogeneous terrain in relation to satellite observations of surface temperature, and to investigate the behavior of the atmospheric surface layer if dry, warm air is advected over a wet, cool surface. Several measuring stations are installed in the region of Crau (France). The measuring instruments, the data collection and processing are presented. Synoptical observations and micrometeorological measurements are effectuated. ESA

N90-12141 Royal Netherlands Meteorological Inst., De Bilt. Physical Meteorology Dept.
DESCRIPTION OF A SOFTWARE LIBRARY FOR THE CALCULATION OF SURFACE FLUXES
A. C. M. Beljaars, A. A. M. Holtslag, and R. M. vanWestrhenen 1988 38 p
(KNMI-TR-112; ISSN-0169-1708; ETN-89-95597) Copyright
Avail: Royal Netherlands Meteorological Inst., P.O. Box 201, 3730 de Bilt, Wilhelminalaan 10, Netherlands

A set of Fortran-77 routines, and the demo programs are described. The basic routines are FLXN1, FLXN2, FLXN3 and FLXSE1. They are based on parameterizaton schemes. They can be applied to observations above land as well as over sea. The purpose is the measurement of the surface fluxes of heat, water vapor and momentum, to determine the state of the atmospheric boundary layer. An example of the diurnal variation of the sensible and latent heat flux, calculated with the full parameterization in comparison with observations, is given. ESA

N90-12142*# Wisconsin Univ., Madison. Space Science and Engineering Center.
LIGHTNING DATA STUDY IN CONJUNCTION WITH GEOSTATIONARY SATELLITE DATA Final Report, 23 Jun. 1984 - 22 Dec. 1987
Brian Auvine and David W. Martin Dec. 1987 88 p
(Contract NAS8-35981)
(NASA-CR-179286; NAS 1.26:179286) Avail: NTIS HC A05/MF A01 CSCL 04B

During the summer of 1985, cloud-to-ground stroke lightning were collected. Thirty minute samples of lightning were compared with GOES IR fractional cold cloud coverage computed for three temperature thresholds (213, 243, and 273 K) twice daily (morning and evening). It was found that satellite measurements of cold cloud have a relationship to the flashrate and, in a more limited way, to the polarity and numbers of return strokes. Results varied little by location. Lightning, especially positive strokes, was found to be correlated with fractional cloud coverage, especially for clouds at or below 213 K. Other data and correlations are discussed. Author

N90-12061*# Purdue Univ., West Lafayette, IN. Dept. of Earth and Atmospheric Sciences.
SYNOPTIC/PLANETARY-SCALE INTERACTIONS AND BLOCKING OVER THE NORTH ATLANTIC OCEAN Abstract Only
Phillip J. Smith *In* NASA, Marshall Space Flight Center, NASA/MSFC FY88 Global Scale Atmospheric Processes Research Program Review Feb. 1989 p 7-8 (For primary document see N90-12059 03-42)
Avail: NTIS HC A05/MF A01 CSCL 04B

N90-12062*# National Aeronautics and Space Administration. Marshall Space Flight Center, Huntsville, AL.
GLOBAL ATMOSPHERIC MOISTURE VARIABILITY Abstract Only
Franklin R. Robertson, Bonnie F. James, Kay Chi, and Huo-Jin Huang (North Carolina Univ., Asheville.) *In its* NASA/MSFC FY88 Global Scale Atmospheric Processes Research Program Review, Feb. 1989 p 9-11 (For primary document see N90-12059 03-42)
Avail: NTIS HC A05/MF A01 CSCL 04B

N90-12063*# Yale Univ., New Haven, CT. Dept. of Geology and Geophysics.
APPLICATION OF DYNAMICAL SYSTEMS THEORY TO GLOBAL WEATHER PHENOMENA REVEALED BY SATELLITE IMAGERY Abstract Only
Barry Saltzman, Wesley Ebisuzaki, Kirk A. Maasch, Robert Oglesby, Lionel Pandolfo, and Chung-Muh Tang (Universities Space Research Association, Columbia, MD.) *In* NASA, Marshall Space Flight Center, NASA/MSFC FY88 Global Scale Atmospheric Processes Research Program Review Feb. 1989 p 13-15 (For primary document see N90-12059 03-42)
Avail: NTIS HC A05/MF A01 CSCL 04B

N90-12064*# Illinois State Water Survey, Champaign. Climate and Meteorology Section.
VARIATIONAL OBJECTIVE ANALYSIS FOR CYCLONE STUDIES
Gary L. Achtemeier *In* NASA, Marshall Space Flight Center, NASA/MSFC FY88 Global Scale Atmospheric Processes Research Program Review Feb. 1989 p 17-21 (For primary document see N90-12059 03-42)
Avail: NTIS HC A05/MF A01 CSCL 04B

N90-12065*# National Aeronautics and Space Administration. Marshall Space Flight Center, Huntsville, AL.
DYNAMICS AND ENERGETICS OF THE SOUTH PACIFIC CONVERGENCE ZONE DURING FGGE SOP-1 AND SOUTH PACIFIC CONVERGENCE ZONE AND GLOBAL-SCALE Annual Report, 1 Jul. 1987 - 30 Jun. 1988 Abstract Only
Dayton G. Vincent, Franklin R. Robertson, Huo-Jin Huang, Deirdre M. Kann, James W. Hurrell, and Catherine B. Pedigo (Purdue Univ., West Lafayette, IN.) *In* NASA, Marshall Space Flight Center, NASA/MSFC FY88 Global Scale Atmospheric Processes Research Program Review Feb. 1989 p 23-26 (For primary document see N90-12059 03-42)
(Contracts NAS8-35187; NAS8-37127)
Avail: NTIS HC A05/MF A01 CSCL 04B

N90-12066*# FWG Associates, Inc., Tullahoma, TN.
LOW LEVEL REMOTE SENSING: OROGRAPHIC WINDS Abstract Only
Walter Frost *In* NASA, Marshall Space Flight Center, NASA/MSFC FY88 Global Scale Atmospheric Processes Research Program Review Feb. 1989 p 27-28 (For primary document see N90-12059 03-42)
Avail: NTIS HC A05/MF A01 CSCL 04B

N90-12067*# National Aeronautics and Space Administration. Marshall Space Flight Center, Huntsville, AL.
LOW LEVEL REMOTE SENSING: THE DOPPLER RADAR WIND PROFILER Abstract Only
Gregory S. Forbes, William Syrett (Pennsylvania State Univ., University Park.), and Catherine Carlson *In its* NASA/MSFC FY88 Global Scale Atmospheric Processes Research Program Review Feb. 1989 p 29-30 (For primary document see N90-12059 03-42)
Avail: NTIS HC A05/MF A01 CSCL 04B

N90-12069*# Alabama Univ., Huntsville. Atmospheric Science and Remote Sensing Lab.
GLOBAL DISTRIBUTION OF MOISTURE, EVAPORATION-PRECIPITATION, AND DIABATIC HEATING RATES Abstract Only
John R. Christy *In* NASA, Marshall Space Flight Center, NASA/MSFC FY88 Global Scale Atmospheric Processes Research Program Review Feb. 1989 p 33-34 (For primary document see N90-12059 03-42)
Avail: NTIS HC A05/MF A01 CSCL 04B

N90-12070*# Texas A&M Univ., College Station. Dept. of Meteorology.
TROPICAL PACIFIC MOISTURE VARIABILITY Abstract Only
James P. McGuirk *In* NASA, Marshall Space Flight Center, NASA/MSFC FY88 Global Scale Atmospheric Processes Research Program Review Feb. 1989 p 35-37 (For primary document see N90-12059 03-42)
Avail: NTIS HC A05/MF A01 CSCL 04B

N90-12071*# Arizona Univ., Tucson.
DISTURBANCES IN THE ARIZONA MONSOON
Robert Gall, Benjamin Herman, and John Reagan *In* NASA, Marshall Space Flight Center, NASA/MSFC FY88 Global Scale Atmospheric Processes Research Program Review Feb. 1989 p 39-45 (For primary document see N90-12059 03-42)
Avail: NTIS HC A05/MF A01 CSCL 04B

N90-12072*# Florida State Univ., Tallahassee. Geophysical Fluid Dynamics Inst.
DYNAMICS OF BAROCLINIC WAVE SYSTEMS Abstract Only
Albert Barcilon and Hengyi Weng *In* NASA, Marshall Space Flight Center, NASA/MSFC FY88 Global Scale Atmospheric Processes Research Program Review Feb. 1989 p 47-48 (For primary document see N90-12059 03-42)
Avail: NTIS HC A05/MF A01 CSCL 04B

N90-12073*# Miami Univ., FL. School of Marine and Atmospheric Science.
THE EFFECT OF LATENT HEAT RELEASE ON SYNOPTIC-TO-PLANETARY WAVE INTERACTIONS AND ITS IMPLICATION FOR SATELLITE OBSERVATIONS: THEORETICAL MODELING Abstract Only
Lee E. Branscome and Rainer Bleck *In* NASA, Marshall Space Flight Center, NASA/MSFC FY88 Global Scale Atmospheric Processes Research Program Review Feb. 1989 p 49-51 (For primary document see N90-12059 03-42)
Avail: NTIS HC A05/MF A01 CSCL 04B

N90-12074*# Virginia Univ., Charlottesville. Dept. of Environmental Sciences.
THE EFFECT OF LATENT HEAT RELEASE ON SYNOPTIC-TO-PLANETARY SCALE WAVE INTERACTIONS: OBSERVATIONAL STUDY Abstract Only
Stephen Colucci and Steven Greco *In* NASA, Marshall Space Flight Center, NASA/MSFC FY88 Global Scale Atmospheric Processes Research Program Review Feb. 1989 p 53-54 (For primary document see N90-12059 03-42)
Avail: NTIS HC A05/MF A01 CSCL 04B

N90-12077*# National Aeronautics and Space Administration. Marshall Space Flight Center, Huntsville, AL.
LABORATORY AND THEORETICAL STUDIES OF BAROCLINIC PROCESSES Abstract Only
Timothy Miller, Fred W. Leslie, Dan Fitzjarrald, Nathaniel D. Reynolds, Shih-Hung Chou, Karen Payne, and Joseph Fehribach (Alabama Univ., Huntsville.) *In* NASA, Marshall Space Flight Center, NASA/MSFC FY88 Global Scale Atmospheric Processes Research Review Program Feb. 1989 p 65-68 (For primary document see N90-12059 03-42)
Avail: NTIS HC A05/MF A01 CSCL 04B

N90-12079*# Universities Space Research Association, Huntsville, AL. Earth Science and Applications Div.
AEROSOL BACKSCATTER STUDIES SUPPORTING LAWS Abstract Only
Jeffry Rothermel *In* NASA, Marshall Space Flight Center, NASA/MSFC FY88 Global Scale Atmospheric Processes Research Program Review Feb. 1989 p 73-74 (For primary document see N90-12059 03-42)
Avail: NTIS HC A05/MF A01 CSCL 04B

N90-12081*# Simpson Weather Associates, Inc., Charlottesville, VA.
LAWS SIMULATION: SAMPLING STRATEGIES AND WIND COMPUTATION ALGORITHMS
G. D. A. Emmitt, S. A. Wood, and S. H. Houston *In* NASA, Marshall Space Flight Center, NASA/MSFC FY88 Global Scale Atmospheric Processes Research Program Review Feb. 1989 p 79-86 (For primary document see N90-12059 03-42)
Avail: NTIS HC A05/MF A01 CSCL 04B

48 OCEANOGRAPHY

Includes biological, dynamic, and physical oceanography; and marine resources.

For related information see also *43 Earth Resources and Remote Sensing.*

N90-12143# National Oceanic and Atmospheric Administration, Seattle, WA. Marine Environmental Lab.
OBSERVATIONS OF LONG ROSSBY WAVES IN THE NORTHERN TROPICAL PACIFIC
William S. Kessler (Washington Univ., Seattle.) Mar. 1989 178 p
(PB89-196331; NOAA-TM-ERL-PMEL-86; CONTRIB-1113) Avail: NTIS HC A09/MF A01 CSCL 08C

The report documents the occurrence of waves from historical data and to show that much of the observed low-frequency pycnocline variability in the northern tropical Pacific may be represented by a simple model expressing the physical processes of Ekman pumping, the radiation of long (non-dispersive) Rossby waves due to such pumping in mid-basin, and the radiation of long Rossby waves from observed eastern boundary thermocline depth fluctuations. GRA

N90-12144# Woods Hole Oceanographic Inst., MA.
SIMILARITY RELATIONS OF WIND WAVES IN FINITE DEPTH M.S. Thesis
Padmaraj Vengayil Nov. 1988 96 p
(Grant NA86-AA-D-SG090)
(PB89-198113; WHOI-88-49) Avail: NTIS HC A05/MF A01 CSCL 08C

Three formulations for the rear face of a growing windsea spectrum in finite depth are tested using spectral measurements from Lake St. Clair. Assuming spectral similarity in wave number space relations between the energy, equillibrium parameters and peak wave number are derived. Using a regression analysis, relations are obtained from the data and compared to the theoretical relations. Results indicate that the formulation based on a high-frequency f(sup 4) tail is better than the f(sup 5) high-frequency tail. Based on the effective fetch formulation, wave propagation directions are calculated. Relations between the spectral parameters, growth-stage variables and fetch are also determined from the data. The relations indicate a weak dependence of the spectral parameters on depth. Various source terms in the energy balance equation for wave growth in finite depth water are estimated for two cases of wave evolution. The relative importance of wind input, bottom dissipation, white-capping dissipation and nonlinear transfer in the evolution of the spectra is analyzed. GRA

N90-12145# Woods Hole Oceanographic Inst., MA.
OBSERVATIONS AND MODELLING OF DEEP EQUATORIAL CURRENTS IN THE CENTRAL PACIFIC PH.D. Thesis
Rui Vasques deMelo Ponte Jan. 1988 186 p
(Grant NSF OCE-86-00052)
(PB89-198139; WHOI-88-9) Copyright Avail: NTIS HC A09/MF A01 CSCL 08C

Analysis of vertical profiles of absolute horizontal velocity collected in January 1981, February 1982 and April 1982 in the central equatorial Pacific as part of the Pacific Equatorial Ocean Dynamics (PEQUOD) program, revealed two significant narrow band spectral peaks in the zonal velocity records, centered at vertical wavelengths of 560 and 350 stretched meters (sm). Both signals were present in all three cruises, but the 350 sm peak showed a more steady character in amplitude and a higher signal-to-noise ratio. In addition, its vertical scales corresponded to the scales of the conspicuous alternating flows generically called the equatorial deep jets. Meridional velocity and vertical displacement spectra did not show any such energetic features. Time lagged coherence results suggested upward phase propagation at time scales of about 4 years. East-west phase lines computed from zonally lagged coherences, tilted downward towards the west, implying westward phase propagation. GRA

N90-12146# Woods Hole Oceanographic Inst., MA.
DYNAMICS OF THE EQUATORIAL UNDERCURRENT AND ITS TERMINATION PH.D. Thesis
Sophie Wacongne Jan. 1988 267 p
(Grants NSF OCE-82-14771; NSF OCE-82-08744; NSF OCE-85-14885)
(PB89-198147; WHOI-88-10) Copyright Avail: NTIS HC A12/MF A02 CSCL 08C

The dissertation studies the zonal weakening, eastern termination and seasonal variations of the Atlantic equatorial undercurrent (EUC). A detailed analysis of the Atlantic EUC simulated by Philander and Pacanowski's (1986) general circulation model provides a novel description of the dynamical regimes governing various regions of a nonlinear stratified undercurrent. Only in a narrow deep western region does a purely inertial regime exist. Elsewhere frictional processes cannot be ignored. In qualitative agreement with observations, the bulk of the mid-basin model EUC terminates in the overlying westward surface flow while only a small fraction (deeper layers) terminates at the eastern coast. The model EUC core is found above the thermocline in the west, below in the east, because vertical friction erodes the upper eastward momentum more efficiently than lateral friction erodes the lower one. A new analysis of current measurements in the Gulf of Guinea suggests that, although the measurements are inadequate the definitive conclusions, Lukas' claim of a spring surge of the Pacific EUC to the eastern coast and a seasonal branching of the EUC into a coastal southeastward undercurrent may hold for the Atlantic Ocean. GRA

N90-12147# National Oceanic and Atmospheric Administration, Seattle, WA. Pacific Marine Environmental Lab.
EQUATORIAL OCEANIC RESPONSE TO FORCING ON TIME SCALES FROM DAYS TO MONTHS
Benjamin S. Giese (Washington Univ., Seattle.) Apr. 1989 107 p
(PB89-206775; NOAA-TM-ERL-PMEL-87; CONTRIB-1115) Avail: NTIS HC A06/MF A01 CSCL 08C

Episodes of westerly wind in the western Pacific may be an important source of sea surface temperature variability in the eastern Pacific on monthly, seasonal and interannual time scales. In the report the authors use a combination of data, linear theory and an ocean general circulation model to examine remote response to western Pacific wind forcing. GRA

N90-12148# Naval Underwater Systems Center, Newport, RI. Weapon Systems Technology and Assessment Dept.
DOPPLER STATISTICS OF OCEAN VELOCITY VARIABILITY
L. Goodman and A. Jilling 1 Nov. 1988 46 p
(AD-A211687; NUSC-TR-6734) Avail: NTIS HC A03/MF A01 CSCL 20/1

This report examines the returned acoustic signal fluctuations from the backscattering of particles embedded in a model ocean velocity microstructure field. Particular attention is given to the separate role of scatterer relative location. It is shown that the fourth-order statistic of the returned signal or, equivalently, the variance of the pulse-to-pulse returned complex signal correlation function contains information on the spatial structure of the fluid velocity correlation function. A key parameter in this relationship is the ratio of the spatial scale of the fluid velocity field to the along-range scale size of the scattering volume. A sensitivity analysis is performed on the theoretical results comparing the limits of performance of a coherent Doppler estimate of microstructure velocity with those of an estimate involving the use of the higher order statistical relationship, termed stochastic Doppler. GRA

N90-12149# Coast Guard, Washington, DC. Office of Research and Development.
STATISTICAL MODELS FOR THE OPTIMAL ESTIMATION OF OCEANIC FIELDS Interim Report
L. C. Sun, Arthur A. Allen, and Clare B. Billing, Jr. Jun. 1989 127 p
(AD-A211786; USCG-D-10-89; RDC-10/87) Avail: NTIS HC A07/MF A01 CSCL 08/3

An investigation is being conducted into the drift and leeway of survivors and survivor crafts as part of the improvement of probability of detection in search and rescue. Part of this effort uses freely drifting buoys that transmit their positions to a shore/ship-based receiver to provide an estimate of the surface current field. The data sets are in the form of drift tracks from each drifter. To analyze the irregular spaced drifter tracks, objective analysis techniques were applied to produce optimal estimations of surface current fields on a regularly spaced grid. Transformation of a data set onto a regularly spaced grid allows use of many other standard computer analysis programs. A computer program using this technique was previously successfully applied to large oceanographic data sets of many drifter tracks. The objective analysis program was converted for use on Hewlett Packard microcomputers and applied to a much more limited data set from 6 drifters, the results being that objective analysis can effectively work with small data sets. The effect of very limited data sets on the outcome of the estimated fields was checked by removing drifters, one at a time, from the data set of 6 drifters. The fields generated by the reduced number of drifters were then compared to the results with the best estimate field determined by all 6 drifters. GRA

51 LIFE SCIENCES (GENERAL)

N90-12150# National Inst. of Standards and Technology, Gaithersburg, MD. Center for Fire Research.
SYNERGISTIC EFFECTS OF NITROGEN DIOXIDE AND CARBON DIOXIDE FOLLOWING ACUTE INHALATION EXPOSURES IN RATS
Barbara C. Levin, Maya Paabo, Lane Highbarger, and Nancy Eller May 1989 45 p Presented at Society of Toxicology Annual Meeting, Atlanta, GA, Feb. 1989 Sponsored in part by the Society of the Plastics Industry, Inc., New York, NY

(PB89-214779; NISTIR-89/4105) Avail: NTIS HC A03/MF A01 CSCL 06P

All fires occurring in air produce carbon dioxide (C02). Fire involving nitrogen-containing products will also generate nitrogen dioxide (N02), a pulmonary irritant. In Fischer 344 male rats, the LC50 (30 minute exposure plus 14 day post-exposure observation period) for N02 was 200 ppm (with 95 percent confidence limits of 43 to 51 percent); whereas, the LC50 for N02 in the presence of 5 percent C02 was 90 ppm (with 90 percent confidence limits ranging from 70-120 ppm). Exposure to N02 increased the methemoglobin (MetHb) levels in the arterial blood. At the end of the 30 minute exposures, the MetHb levels were 2-3 times higher in the animals exposed to the combination of N02 (200 ppm) and C02 (5 percent) than in those exposed to N02 only. Deaths from N02 were all post-exposure and occurred earlier in the presence of N02 plus 5 percent C02 than in the absence of the C02. The time of death was concentration-dependent when both gases were present. At death, evidence of hemorrage and extensive edema was observed in the lungs. The mean lung wet weight/body weight ratio from rats exposed to 200 ppm N02 with and without 5 percent C02 was 3-4 times that of non-exposed rats. More edema was noted with N02 and C02 than with N02 alone. GRA

N90-12151*# National Aeronautics and Space Administration. Ames Research Center, Moffett Field, CA.

THE RODENT RESEARCH ANIMAL HOLDING FACILITY AS A BARRIER TO ENVIRONMENTAL CONTAMINATION

P. D. Savage, Jr., G. C. Jahns, B. P. Dalton, R. P. Hogan, and A. E. Wray (General Electric Co., Moffett Field, CA.) Sep. 1989 11 p Presented at the 19th Intersociety Conference on Environmental Systems, San Diego, CA, 24-26 Jul. 1989

(NASA-TM-102237; A-89183; NAS 1.15:102237) Avail: NTIS HC A03/MF A01 CSCL 06C

The rodent Research Animal Holding Facility (RAHF), developed by NASA Ames Research Center (ARC) to separately house rodents in a Spacelab, was verified as a barrier to environmental contaminants during a 12-day biocompatibility test. Environmental contaminants considered were solid particulates, microorganisms, ammonia, and typical animal odors. The 12-day test conducted in August 1988 was designed to verify that the rodent RAHF system would adequately support and maintain animal specimens during normal system operations. Additional objectives of this test were to demonstrate that: (1) the system would capture typical particulate debris produced by the animal; (2) microorganisms would be contained; and (3) the passage of animal odors was adequately controlled. In addition, the amount of carbon dioxide exhausted by the RAHF system was to be quantified. Of primary importance during the test was the demonstration that the RAHF would contain particles greater than 150 micrometers. This was verified after analyzing collection plates placed under exhaust air ducts and rodent cages during cage maintenance operations, e.g., waste tray and feeder changeouts. Microbiological testing identified no additional organisms in the test environment that could be traced to the RAHF. Odor containment was demonstrated to be less than barely detectable. Ammonia could not be detected in the exhaust air from the RAHF system. Carbon dioxide levels were verified to be less than 0.35 percent. Author

N90-12152* Lockheed Engineering and Sciences Co., Washington, DC.

USSR SPACE LIFE SCIENCES DIGEST, ISSUE 24

Lydia Razran Hooke, ed., Ronald Teeter, ed., P. Lynn Donaldson, ed., Victoria Garshnek, ed., and Joseph Rowe, ed. (Library of Congress, Washington, DC.) Washington NASA Nov. 1989 112 p

(Contract NASw-4292)

(NASA-CR-3922(28)-Issue-24; NAS 1.26:3922(28)-Issue-24)

Avail: Issuing Activity CSCL 06C

This is the twenty-fourth issue of NASA's USSR Space Life Sciences Digest. It contains abstracts of 39 journal papers or book chapters published in Russian. In addition, reviews of two recent Soviet books are translated. The abstracts in this issue have been identified as relevant to 25 areas of space biology and medicine: adaptation, aviation medicine, biological rhythms, cardiovascular and respiratory systems, cytology, developmental biology, endocrinology, equipment and instrumentation, genetics, habitability and environment effects, hemetology, human performance, immunology, life support systems, man-machine systems, mathematical modeling, metabolism, microbiology, morphology, musculoskeletal system, neurophysiology, operational medicine, psychology, radiobiology, and space medicine. Author

N90-12153* Lockheed Engineering and Sciences Co., Washington, DC.

USSR SPACE LIFE SCIENCES DIGEST, ISSUE 22

Lydia Razran Hooke, ed., Ronald Teeter, ed., P. Lynn Donaldson, ed., Victoria Garshnek, ed., and Joseph Rowe, ed. (Library of Congress, Washington, DC.) Washington NASA Aug. 1989 137 p

(Contract NASw-4292)

(NASA-CR-3922(26)-Issue-22; NAS 1.26:3922(26)-Issue-22)

Avail: Issuing Activity CSCL 06C

This is the twenty-second issue of NASA's USSR Space Life Sciences Digest. It contains abstracts of 56 journal papers or book chapters published in Russian and of a Soviet monograph reviewing the literature on chronobiology. The complete contents of two issues of the Soviet Journal Space Biology and Aerospace Medicine are covered. Selected abstracts are illustrated with figures and tables from the original. A special feature presents a translation of an interview with two Mir cosmonauts. The abstracts in this issue have been identified as relevant to 29 areas of space biology and medicine. These areas are: adaptation, biological rhythms, biospherics, body fluids, botany, cardiovascular and respiratory systems, developmental biology, endocrinology, enzymology, equipment and instrumentation, genetics, gravitational biology, habitability and environmental effects, hematology, human performance, immunology, life support systems, mathematical modeling, metabolism, microbiology, musculoskeletal system, neurophysiology, nutrition, operational medicine, perception, psychology, radiobiology, reproductive system, and space biology and medicine. Author

N90-12154* Lockheed Engineering and Sciences Co., Washington, DC.

USSR SPACE LIFE SCIENCES DIGEST, ISSUE 23

Lydia Razran Hooke, ed., P. Lynn Donaldson, ed., Ronald Teeter, ed., Victoria Garshnek, ed., and Joseph Rowe, ed. (Library of Congress, Washington, DC.) Washington NASA Aug. 1989 123 p

(Contract NASw-4292)

(NASA-CR-3922(27)-Issue-23; NAS 1.26:3922(27)-Issue-23)

Avail: Issuing Activity CSCL 06C

This is the twenty-third issue of NASA's USSR Space Life Sciences Digest. It contains abstracts of 47 journal papers or book chapters published in Russian and of five Soviet monographs and one book review. Selected abstracts are illustrated with figures and tables from the original. A special feature provides a translation of a discussion on biomedical support of manned flights to Mars. The abstracts in this issue have been identified as relevant to 32 areas of space biology and medicine. These areas are: adaptation, aviation medicine, biological rhythms, biospherics, body fluids, botany, cardiovascular and respiratory systems, cytology, developmental biology, endocrinology, enzymology, equipment and instrumentation, gastrointestinal system, genetics, group dynamics, habitability and environmental effects, hematology, human performance, immunology, life support systems, man-machine systems, mathematical modeling, metabolism, microbiology, musculoskeletal system, neurophysiology, nutrition, operational medicine, perception, psychology, radiobiology, and reproductive system. Author

N90-12155# Cincinnati Univ., OH. Dept. of Microbiological and Molecular Genetics.

GENETIC ENGINEERING OF ENHANCED MICROBIAL NITRIFICATION Environmental Research Brief, Aug. 1983 - 1988 Sep.

Michael Carsiotis and Sunil Khanna Jun. 1989 10 p
(Grant EPA-CR-810888)
(PB89-208334; EPA/600/M-89/011) Avail: NTIS HC A02/MF A01 CSCL 06C

Experiments were conducted to introduce genetic information in the form of antibiotic or mercuric ion resistance genes into Nitrobacter hamburgenesis strain X14. The resistance genes were either stable components of broad host range plasmids or transposable genes on plasmids presumably unable to replicate in strain X14. Four methods for plasmid transformation as well as conjugation with various donor strains of Escherichia coli failed. The leuB gene containing DNA was restriction-mapped and the 1.3 kilobase pair gene was subcloned into a vector suitable for use in DNA sequencing. To date, a tentative sequence comprising about 1300 bases was obtained. Although the primary goal of developing a procedure for introducing genetic material into a nitrifying organism is not yet achieved, the results achieved have produced useful information on the genomic organization of Nitrobacter as well as a plasmid-borne library of genes from that organism. Future experiments can be made with this library in order to provide additional basic information on Nitrobacter's genome. GRA

N90-12156# North Carolina State Univ., Raleigh.
MEMBRANE FUSION: THE ROLE OF POLYPHOSPHATIDYLINOSITOL Final Report, Mar. 1986 - Mar. 1989
Wendy F. Boss and Jeffrey J. Wheeler 24 Jul. 1989 5 p
(Contract DAAL03-86-G-0035)
(AD-A211289; ARO-23767.7-LS-F) Avail: NTIS HC A02/MF A01 CSCL 06/1

It was found that the presence of the phospholipid, lysophosphatidylinositol monophosphate (LPIP) correlates positively with the fusion potential of fusogenic carrot cells. There was no correlation with the presence of phosphatidylinositol monophosphate (PIP) and phosphatidylinositol bisphosphate (PIP2) and fusion. Nor was there evidence for the need for PIP or PIP2 turnover in order for the cells to be fusion permissive. LPIP was synthesized primarily from the phosphorylation of lysophosphatidylinositol. Lysolipids were found to decrease the phosphorylation of PI and PIP suggesting a mechanism for regulating the biosynthesis of the polyphosphoinositides which are key components of the signal transduction pathway in many animal cells. GRA

N90-12157# Duke Univ., Durham, NC.
BORON ANALOGUES OF AMINO ACIDS AND DERIVATIVES Final Report, 1 Sep. 1987 - 30 Nov. 1988
Bernard F. Spielvogel, Barbara Ramsay Shaw, and Robert G. Ghirardelli 19 Jul. 1989 5 p
(Contract DAAL03-87-C-0029)
(AD-A211311; ARO-25263.1-CH) Avail: NTIS HC A01/MF A01 CSCL 06/15

The principal goal of this research was the synthesis and characterization of boron analogues of important biologically active molecules such as the amino acids. During this period of research syntheses were developed for amides of a variety of simple boron analogues of common amino acids such as saline. Peptides containing boron were completed. Synthetic approaches were developed for boron analogues of phosphonates. Collaborative studies on the biological activity of many of these compounds were carried out by Professor Iris H. Hall at the University of North Carolina. Significant antitumor and hypolipidemic activity were found in animal model studies. GRA

N90-12158# California Univ., Irvine.
SYNAPTIC PLASTICITY AND MEMORY FORMATION Final Technical Report, Apr. 1986 - Mar. 1989
Gary Lynch 30 May 1989 11 p
(Grant AF-AFOSR-0099-86; AF Proj. 2312)
(AD-A211368; AFOSR-89-1141TR) Avail: NTIS HC A02/MF A01 CSCL 05/8

The purpose of the proposed research was to test and elaborate on an hypothesis regarding cellular mechanisms responsible for storing recognition memory in mammalian telencephalon. The encoding process proposed involves: (1) an unusual pattern of physiological activity in the relevant neural pathways, (2) influx of calcium into dendritic spines postsynaptic to the active axons, (3) activation of the calcium-sensitive protease, calpain, (4) partial degradation of spectrin, a cytoskeleton protein that regulates membrane surface chemistry and possibly spine shape, and (5) anatomical reorganization of postsynaptic structure resulting in a stable increase of postsynaptic potentials. Central to the hypothesis is the phenomenon of long-term potentiation (LTP) of synaptic transmission; much of the research conducted in the past three years has been aimed at characterizing the physiological and biochemical steps responsible for this remarkably persistent synaptic change and examining its role in memory storage. We have also hypothesized that excessive activation of the calpain system can lead to the neuronal degeneration that is associated with experimental age-related neuropathologies. GRA

N90-12159# Utah Univ., Salt Lake City.
INVESTIGATION OF RESONANT ac-dc MAGNETIC FIELD EFFECTS Final Report, May 1986 - Jul. 1989
Carl H. Durney, Jiri Janata, Catherine Rappaport, Mark Kaminski, and Cindy Bruckner-Lea 10 Jul. 1989 45 p
(Contract N00014-86-K-0230; RR04108)
(AD-A211612; UTEC-89-036) Avail: NTIS HC A03/MF A01 CSCL 06/7

Recently reported observations by others indicate that a combination of a weak dc magnetic field and extra low frequency ac magnetic fields can produce resonant effects in biological systems. The study of resonant magnetic field effects consist of three parts: calculations aimed at identifying the basic mechanism underlying the resonance, measurements of the effects of combined dc and ac magnetic fields on the dc current through plain (containing no channels) planar phospholipid membranes, and measurements of the effects of combined dc and ac magnetic fields on the binding of metallochromic dyes and calmodulin to calcium. The calculations provided insight and a physical mechanism that explains both frequency and amplitude windows in an elementary model consisting of one charged particle in a viscous medium. The combined dc-ac magnetic fields did affect the dc current through planar phospholipid membranes, but not in every membrane, and not consistently at the same values of magnetic field strength and frequency. No effect of the magnetic fields were seen on the binding of metallochromic dyes and calmodulin to calcium. None of the measurements showed any resonant response like the cyclotron like resonance reported in the literature in diatoms and lymphocytes. GRA

52 AEROSPACE MEDICINE

Includes physiological factors; biological effects of radiation; and effects of weightlessness on man and animals.

N90-12160# New York Univ., New York. Dept. of Psychology.
VISUAL MOTION PERCEPTION Interim Report, 1 Feb. 1988 - 31 Jan. 1989
George Sperling 31 Jan. 1989 7 p
(Grant AF-AFOSR-0140-88; AF Proj. 2313)
(AD-A210994; AFOSR-89-1021TR) Avail: NTIS HC A02/MF A01 CSCL 06/4

Two separate motion-computation systems and the derivation of the functional properties of each were explored. A dynamic stimulus was demonstrated that caused the first- and second-order motion perception systems to perceive motion in opposite directions, depending on viewing distance. Motion/texture interactions-stimuli were discovered that are accessible only to second order motion analysis and then only after their texture has first been extracted. It was also demonstrated that perceiving 3D structure from 2D visual inputs depends primarily on the first-order motion perception system. A new spatial interaction was also found in which a textured area surrounded by a similar high-contrast texture appears to be of lower contrast when surrounded by neutral gray. This remarkable phenomenon contradicts all current theories of lightness perception. GRA

N90-12161# Naval Health Research Center, San Diego, CA. Applied Physiology Dept.
DEMONSTRATION OF REPLICABLE DIMENSIONS OF HEALTH BEHAVIORS Interim Report
Ross R. Vickers, Jr., Terry L. Conway, and Linda K. Hervig 6 Oct. 1988 24 p
(AD-A211920; NHRC-88-41) Avail: NTIS HC A03/MF A01 CSCL 06/5

Appropriate health behaviors are necessary to ensure health and well-being, thereby keeping military personnel ready to perform their jobs which may demand exceptional efforts at key times. An understanding of factors influencing health behaviors would be more readily achieved if general dimensions could be identified to delineate sets of health behaviors that consistently co-occur. Prior research has suffered from the use of only brief lists of health behaviors, failure to systematically select health behaviors to represent hypothesized health behavior dimensions, and failure to replicate findings across samples. The present study was designed to extend prior efforts by determining the number of dimensions of health behavior that could be reliably identified in two samples of Navy personnel. A set of 40 health behavior items was chosen to represent four major dimensions of health behavior that prior work suggested were present in groups representing a wide range of social and demographic backgrounds. GRA

N90-12162# Illinois Inst. of Tech., Chicago.
COMPUTER GENERATION OF A TUTORIAL DIALOGUE Quarterly Progress Report, 1 Jun. - 31 Aug. 1989
Martha Evens, Joel Michael, and Allen Rovick 31 Aug. 1989 7 p
(Contract N00014-89-J-1952)
(AD-A211976) Avail: NTIS HC A02/MF A01 CSCL 12/5

The main focus was on the taping of human-to-human tutoring sessions and the analysis of the transcripts of those sessions with regard to both language and content. The language analysis involves study of vocabulary, syntax, semantics, and discourse for use in the understanding of ill-formed input and the generation of responses. The analysis of content focuses on tutoring rules, modeling rules, and the underlying knowledge used by the tutor. The development of the lexical functional grammar rules and lexicon for the cardiovascular sublanguage, the development of a cardiovascular knowledge base for the tutoring system, a Prolog prototype for the tutor being built, and the initial plans for a tutoring system in Lisp to support the research in text generation are all being examined in detail. The context of the work is an attempt to build an intelligent version of a remarkably effective conventional tutoring program, CIRCSIM, designed and implemented in Basic. CIRCSIM is intended to tutor first year medical students in the complex negative feedback processes used by the human body to maintain blood pressure. GRA

N90-12163# Army Research Inst. of Environmental Medicine, Natick, MA.
THE EFFECT OF CAFFEINE ON ENDURANCE TIME TO EXHAUSTION AT HIGH ALTITUDE
Charles S. Fulco, Paul B. Rock, Laurie A. Trad, Madeline S. Rose, Vincent A. Forte, Jr., Patricia M. Young, and Allen Cymerman 27 Apr. 1989 43 p
(AD-A212069) Avail: NTIS HC A03/MF A01 CSCL 06/15

Endurance time to exhaustion (ETX) is increased at high altitude (HA) but only after 2 weeks of continued exposure. The increase is thought to be related to a delayed depletion of muscle glycogen, secondary to HA-induced increases in the mobilization and utilization of free fatty acids (FFA). It was determined if caffeine (CAF), which stimulates FFA mobilization, could prolong ETX earlier in the HA exposure. Eight untrained men (17 to 24 yr) performed 2 ETX cycling bouts at 79 to 85 percent of their altitude-specific maximal oxygen consumption in each of 3 phases: at sea level (SL), after 1 h simulated exposure (acute), and after 2 weeks (chronic) at 4300 m. Subjects received either a CAF (4 mg/kg) or a placebo drink in a double-bind cross-over design 1 h prior to each ETX bout in each phase. Subjective ratings of perceived exertion (PE) and cardiac output (CO) were obtained during exercise. Daily caloric intake and composition were held constant. CAF did not alter ETX at SL but was increased by 54 percent (22.0 to 35.0 min, p=.04) and 24 percent (30.8 to 38.5 min, p=0.11) during acute and chronic HA exposure, respectively. The improvements in ETX were determined not to be associated with substrate mobilization and utilization, or to a reduction in PE. GRA

N90-12164# Army Research Inst. of Environmental Medicine, Natick, MA.
HEATSTROKE PATHOPHYSIOLOGY: THE ENERGY DEPLETION MODEL Report, May - Jun. 1989
Roger W. Hubbard 12 Jun. 1989 42 p
(AD-A212156; USARIEM-M59-89) Avail: NTIS HC A03/MF A01 CSCL 06/10

This symposium focuses on exertional heatstroke, with emphasis on predisposing factors, clinical observations, diagnosis, treatment and recovery. The serious challenge to cardiovascular stability presented by exercise hyperthermia and some aspects of regulatory failure were reviewed in the introduction. The intent of this review, to describe how heat stress is translated into heat strain at the cellular level, is not to downplay the seriousness of the systemic condition. If we are successful, this may stimulate further interest on the impact of heat on the cell as a model for other factors which alter membrane integrity and permeability, lead to new experimental paradigms, and improve the diagnosis and treatment of other disorders such as toxic, hypovolemic or ischemic shock. This review may also stimulate interesting research regarding more subtle threats to homeostasis such as chronic exercise, hypohydration and thirst, ion imbalance, and sleep deprivation. We have discussed the relationship of this concept to carbohydrate metabolism, thirst, and the cellular aspects of heat illness treatment. This article will attempt to integrate and extend some of those ideas. GRA

N90-12165# Army Research Inst. of Environmental Medicine, Natick, MA.
HUMAN BODY REGIONAL CONVECTIVE HEAT TRANSFER DETERMINATION USING SUBLIMATING NAPHTHALENE DISKS
Stephen KW. Chang and Richard R. Gonzalez Jul. 1989 22 p
(DA Proj. 3E1-62787-A8-78)
(AD-A212170; ARIEM-M66-89) Avail: NTIS HC A03/MF A01 CSCL 06/4

The regional convective heat transfer coefficients(hc) on the human body were determined using sublimating naphthalene disks. Circular naphthalene disks were affixed to various body segments of a stationary, life size manikin, under constant temperature and wind speed in an environmental chamber. The amount of naphthalene weight loss through sublimation was translated into hc using the Chilton-Colburn j-factor analogy between heat and mass transfer. The regional convective heat transfer coefficients can be determined by using strictly the heat-mass transfer analogy, excluding any supplementary technique of cylindrical body segment approximations or other shape extrapolations. The logarithmic mean density factor for naphthalene sublimating in air (PAM,n) was also determined. PAM,n for the naphthalene-air sublimation environment is only one third of the water vapor-air diffusion environment (PAM). PAM,n is an essential factor for extracting the correct hc value from the naphthalene mass transfer data. GRA

N90-12166# California Univ., Irvine. Center for the Neurobiology of Learning and Memory.
ADAPTIVE INFORMATION PROCESSING IN AUDITORY CORTEX Annual Report, 1 Jun. 1988 - 31 May 1989
Norman M. Weinberger 31 May 1989 51 p
(Contract N00014-87-K-0433)
(AD-A211294) Avail: NTIS HC A04/MF A01 CSCL 06/4

The principles of biological intelligence are of central importance to the understanding of brain function and to the development of devices based on the extraordinary computing and information processing abilities of brains. Adaptive cognitive and behavioral performance must be based on principles of brain function that have been selected in evolution so that organisms can successfully cope with environmental demands. Although these principles are not yet known, they may be advantageously approached by analyzing how they modify information processing within the brain. Central to adaptive information processing as expressed in the mammalian brain, are the cerebral neocortex and associative learning. In both fields, new perspectives are emerging. In particular, information processing in sensory neocortex involves the operation of active learning processes which transform receptive fields. These and related findings provide a basis for understanding the functional role of sensory cortical physiological plasticity and for a bridge between physiological plasticity and adaptive information processing in the cerebral cortex. GRA

N90-12167# Army Aeromedical Research Lab., Fort Rucker, AL.

VISUAL ACUITY AND STEREOPSIS WITH NIGHT VISION GOGGLES Final Report

Roger W. Wiley Jun. 1989 30 p
(AD-A211552; USAARL-89-9) Avail: NTIS HC A03/MF A01 CSCL 17/5

Measurements of visual performance (stereopsis and visual resolution) were acquired to compare results achieved using unaided monocular and binocular viewing, monocular and binocular viewing with the AN/PVS-5A night vision goggles, and models A and B of the AN/PVS-7 biocular night vision goggles. All of the goggles were equipped with 2nd generation tubes. Using a modified Howard-Dolman apparatus to assess stereopsis, all of the goggle-assisted thresholds were very much larger than stereoscopic thresholds achieved with unaided binocular vision. Statistical analysis of the results indicated that stereopsis through night vision goggles, regardless of the model or viewing condition, is essentially eliminated and equivalent to the threshold obtained with unaided monocular viewing. In comparison, spatial resolution capability with all of the goggle systems is superior to performance with unaided vision. In agreement with previously published data, visual acuity with the goggles is approximately 20/50, but only for high contrast targets and simulated full moon ambient light levels. As light levels decrease to quarter moon conditions or target contrasts are reduced to more realistic values, visual spatial resolution with the goggles is much poorer. For infantry use, any differences in visual performance between monocular, biocular, and binocular designs probably are not operationally meaningful. GRA

N90-12168# Central Inst. for the Deaf, Saint Louis, MO.

BINAURAL MASKING: AN ANALYSIS OF MODELS Final Technical Report, 15 Jul. 1986 - 14 Mar. 1989

Robert H. Gilkey 1 Aug. 1989 15 p
(Grant AF-AFOSR-0298-86; AF Proj. 2313)
(AD-A211578; AFOSR-89-1164TR) Avail: NTIS HC A03/MF A01 CSCL 05/8

The overall goal of this program of research is to specify the processes used by the auditory system to detect signals presented in noisy backgrounds. A wide variety of experimental approaches were used to examine these processes. The data suggest that subjects often detect the signal as a change in the spectral/temporal pattern of stimulus information. These results conflict with the classical models of simple auditory masking that suggest that subjects restrict their analysis to a narrow frequency band and a brief temporal window. Quantitative models of the process that compares information across spectral/temporal regions were developed, which combine excitatory and inhibitory components. While it has traditionally been assumed that quite different mechanisms govern monaural and binaural masking phenomena, very similar models were successfully applied to the two sets of data. Other significant results include a more complete description on internal noise processes, evidence that the external masker is not cancelled by the binaural processor, empirical and theoretical evaluations of the efficiency of psychophysical procedures, and hardware and software developments to aid psychoacoustic research. Overall, the work examined issues and models of contemporary interest and thus has implications for auditory theory in general and for the study of auditory pattern analysis and auditory masking in specific. GRA

N90-12169# Retina Foundation, Boston, MA. Eye Research Inst.

EYE MOVEMENTS AND SPATIAL PATTERN VISION Final Report, 1 Mar. 1986 - 30 Apr. 1989

Lawrence E. Arend 15 Jul. 1989 12 p
(Grant AF-AFOSR-0128-86; AF Proj. 2313)
(AD-A211650; AFOSR-89-1151TR) Avail: NTIS HC A03/MF A01 CSCL 06/4

Models of lightness and color perception must take account of human color constancy, a tendency for apparent surface color to be relatively independent of the color and intensity of the illuminating light source. Observers matched the lightness and brightnesses of regions in simple and complex achromatic spatial patterns. The data showed that the observers' knowledge of the surface reflectances (revealed by lightness matches) was unaffected by changing brightness of the same surfaces (revealed by brightness matches). In the analogous chromatic experiments, observers matched the hue and saturation of patches or the patches' apparent surface colors. The observers' knowledge of the surface colors was not as reliable as in the achromatic case. Patches' hues and saturations matched when their chromaticities were approximately the same. Shifts of hue attributable to simultaneous color contrast were in the correct direction but too small to produce hue constancy. GRA

N90-12170# State Univ. of New York, Buffalo. Dept. of Psychology.

CELLULAR AND MOLECULAR MECHANISMS OF HIGH PRESSURE INOTROPY IN CARDIAC MUSCLE Annual Report, 1 Aug. 1988 - 31 Jul. 1989

Perry M. Hogan and Stephen R. Besch 1 Aug. 1989 20 p
(Contract N00014-88-K-0550; RR04108)
(AD-A211695) Avail: NTIS HC A03/MF A01 CSCL 06/10

Cardiac muscle subjected to increased hydrostatic pressure from 2 to 150 atmospheres respond with an increase in developed tension, a phenomenon we refer to as high pressure inotropy (HPI). Experiments were performed on papillary muscles isolated from adolescent rabbit hearts to test the possibility that HPI is due to a preferential action of pressure to partially inhibit the activity of the sodium-potassium pump of the cell membrane leading to calcium accumulation through reduced sodium-calcium exchange. Ouabain, a cardiac glycoside known to inhibit pump activity, prevented the development of HPI when applied before pressure was increased. Both ouabain and pressure altered the time course of mechanical restitution and the development of the resting state contraction in a similar manner that could be mimicked by a computer model when the calcium extrusion ordinarily occurring during each cardiac cycle was substantially retarded. Finally, we reported on progress made to develop a microfluorimeter for measuring cytosolic calcium in single cardiac myocytes under hyperbaric conditions. GRA

N90-12171# Air Force Occupational and Environmental Health Lab., Brooks AFB, TX.

BASE LEVEL MANAGEMENT OF RADIO FREQUENCY RADIATION PROTECTION PROGRAM Final Report

Steven E. Rademacher and Noel D. Montgomery Apr. 1989 98 p
(AD-A211787; AFOEHL-89-023RC0111DRA) Avail: NTIS HC A05/MF A01 CSCL 06/7

AFOEHL developed this report to assist the base level aerospace medical team manage their radio frequency radiation protection program. This report supersedes USAFOEHL Report 80-42, A Practical R-F Guide for BEES. GRA

N90-12172# Deutsche Forschungs- und Versuchsanstalt fuer Luft- und Raumfahrt, Cologne (Germany, F.R.). Inst. fuer Flugmedizin.
STUDIES ON PREDICTING THE RESYNCHRONIZATION OF THE CIRCADIAN SYSTEM AFTER TRANSMEDIAN FLIGHTS Ph.D. Thesis - Technische Hochschule, Aachen
Michael Ripkens Feb. 1989 122 p In GERMAN; ENGLISH summary Report will also be announced as translation (ESA-TT-1177)
(DFVLR-FB-89-10; ISSN-0171-1342; ETN-89-95307) Avail: NTIS HC A06/MF A01; DFVLR, VB-PL-DO, Postafach 90 60 58, 5000 Cologne, Federal Republic of Germany, 40 deutsche marks

Resynchronization in the circadian rhythms of different body functions after timeshifts of 6 and 9 hours is studied. Three flight experiments involving eight subjects each were carried out to determine whether the speed of adaptation could be predicted from the individual rhythm parameters of preflight control days. Significant correlations were found only in a few single cases for some functions. Since, in addition, the consistency grade was too small, the hypothesis of a reliable predictiveness of the individual adaptation speed had to be refused. This statement should not be generalized, as the number of subjects was too small and the applied procedure did not permit more general conclusions. ESA

N90-12173* National Aeronautics and Space Administration, Washington, DC.
AEROSPACE MEDICINE AND BIOLOGY: A CONTINUING BIBLIOGRAPHY WITH INDEXES (SUPPLEMENT 329)
Nov. 1989 66 p
(NASA-SP-7011(329); NAS 1.21:7011(329)) Avail: NTIS HC A04; NTIS standing order as PB89-912300, $10.50 domestic, $21.00 foreign CSCL 06E

This bibliography lists 184 reports, articles and other documents introduced into the NASA Scientific and Technical Information System during October 1989. Subject coverage includes: aerospace medicine and psychology, life support systems and controlled environments, safety equipment, exobiology and extraterrestrial life, and flight crew behavior and performance. Author

53 BEHAVIORAL SCIENCES

Includes psychological factors; individual and group behavior; crew training and evaluation; and psychiatric research.

N90-12174*# Essex Corp., Orlando, FL.
MICROCOMPUTER-BASED TESTS FOR REPEATED-MEASURES: METRIC PROPERTIES AND PREDICTIVE VALIDITIES
Robert S. Kennedy, Dennis R. Baltzley, William P. Dunlap, Robert L. Wilkes, and Lois-Ann Kuntz 1 May 1989 34 p
(Contracts NAS9-17326; NSF ISI-85-21282; DAMD17-85-C-5095)
(NASA-CR-185517; NAS 1.26:185517; EOTR-89-02) Avail: NTIS HC A03/MF A01 CSCL 05I

A menu of psychomotor and mental acuity tests were refined. Field applications of such a battery are, for example, a study of the effects of toxic agents or exotic environments on performance readiness, or the determination of fitness for duty. The key requirement of these tasks is that they be suitable for repeated-measures applications, and so questions of stability and reliability are a continuing, central focus of this work. After the initial (practice) session, seven replications of 14 microcomputer-based performance tests (32 measures) were completed by 37 subjects. Each test in the battery had previously been shown to stabilize in less than five 90-second administrations and to possess retest reliabilities greater than $r = 0.707$ for three minutes of testing. However, all the tests had never been administered together as a battery and they had never been self-administered. In order to provide predictive validity for intelligence measurement, the Wechsler Adult Intelligence Scale-Revised and the Wonderlic Personnel Test were obtained on the same subjects. Author

N90-12175*# Essex Corp., Orlando, FL.
A MENU OF SELF-ADMINISTERED MICROCOMPUTER-BASED NEUROTOXICOLOGY TESTS
Robert S. Kennedy, Robert L. Wilkes, Lois-Ann Kuntz, and Dennis R. Baltzley Nov. 1988 25 p
(Contract NAS9-17326)
(NASA-CR-185518; NAS 1.26:185518; EOTR-88-10) Avail: NTIS HC A03/MF A01 CSCL 05I

This study examined the feasibility of repeated self-administration of a newly developed battery of mental acuity tests. Researchers developed this battery to be used to screen the fitness for duty of persons in at-risk occupations (astronauts, race car drivers), or those who may be exposed to environmental stress, toxic agents, or disease. The menu under study contained cognitive and motor tests implemented on a portable microcomputer including: a five-test core battery, lasting six minutes, which had demonstrable reliabilities and stability from several previous repeated-measures studies, and also 13 new tests, lasting 42 minutes, which had appeared in other batteries but had not yet been evaluated for repeated-measures implementation in this medium. Sixteen subjects self-administered the battery over 10 repeated sessions. The hardware performed well throughout the study and the tests appeared to be easily self-administered. Stabilities and reliabilities of the test from the core battery were comparable to those obtained previously under more controlled experimental conditions. Analyses of metric properties of the remaining 13 tests produced eight additional tests with satisfactory properties. Although the average retest reliability was high, cross-correlations between tests were low, indicating factorial richness. The menu can be used to form batteries of flexible total testing time which are likely to tap different mental processes and functions. Author

N90-12176# North Carolina State Univ., Raleigh. Dept. of Electrical and Computer Engineering.
THREE DIMENSIONAL OBJECT RECOGNITION EMPLOYING COMBINED VISUAL AND TACTILE SENSING Final Project Report, 1 Jul. 1985 - 31 Aug. 1988
Ren C. Luo, Horng-Hai Loh, and Patrick Robinson Dec. 1988 56 p
(Grant NSF DMC-85-05166)
(PB89-219489; NSF/ENG-88037) Avail: NTIS HC A04/MF A01 CSCL 05I

The objective of the project was the development of a combined use of 2-D visual and 2-D tactile information for 3-D object recognition purposes. A conventional video camera is used to obtain the top view of an object. Two tactile sensing arrays mounted on a robot gripper are also used to measure information about the lateral surfaces of an object. Three dimensional reference models are established as a hierarchical decision tree. Measuring the available features derived from the sensor information of an object, a decision tree is traversed to identify and label the sensed object. Developments include: (1) a system capable of performing the tasks in an integrated fashion; (2) the construction of an effective and efficient way of discriminating objects; and (3) new algorithms for dealing with tactile information developed and implemented in the form of an automatic decision tree generation generator. Author

N90-12177# Washington Univ., Seattle. Dept. of Psychology.
METACOGNITION AND RETRIEVAL FROM LONG-TERM MEMORY AT MOUNT EVEREST Final Report, 13 May 1988 - 23 Jun. 1989
Thomas O. Nelson 27 Jun. 1989 19 p
(Grant AF-AFOSR-0226-88; AF Proj. 2313)
(AD-A211629; AFOSR-89-1113TR) Avail: NTIS HC A03/MF A01 CSCL 05/8

Behavioral data were collected from climbers at various altitudes on Mount Everest. In contrast to earlier findings that altitude impairs the acquisition of information into memory, no

changes were found in the accuracy or latency of retrieving information from memory, even at extreme altitudes above 21,000 ft (6,400 m). This lack of effect on retrieval occurred for both the recall and recognition of answers to general information questions (e.g., what is the capital of Finland). Self confidence about the accuracy of recent retrieval was also not affected by altitude. However, the feeling of knowing (i.e., self confidence about upcoming retrieval) declined at extreme altitudes and remained lower even after return to Kathmandu. This pattern of results is close to opposite of the pattern obtained when the independent variable is alcohol intoxication and the same test battery is employed. These and related results are described in an attempt to give a relatively comprehensive picture of the climbers' performance, and suggestions are offered for future research.
GRA

54 MAN/SYSTEM TECHNOLOGY AND LIFE SUPPORT

Includes human engineering; biotechnology; and space suits and protective clothing.

For related information see also *16 Space Transportation*.

N90-12178*# Good Samaritan Hospital and Medical Center, Portland, OR. Dept. of Neuro-otology.
AGE-RELATED CHANGES IN HUMAN POSTURE CONTROL: MOTOR COORDINATION TESTS
R. J. Peterka and F. O. Black 1989 13 p
(Grant NAG9-117)
(NASA-CR-185855; NAS 1.26:185855) Avail: NTIS HC A03/MF A01 CSCL 05H

Postural responses to support surface displacements were measured in 214 normal human subjects ranging in age from 7 to 81 years. Motor tests measured leg muscle Electromyography (EMG) latencies, body sway, and the amplitude and timing of changes in center of pressure displacements in response to sudden forward and backward horizontal translations of the support surface upon which the subjects stood. There were small increases in both EMG latencies and the time to reach the peak amplitude of center of pressure responses with increasing age. The amplitude of center of pressure responses showed little change with age if the amplitude measures were normalized by a factor related to subject height. In general, postural responses to sudden translations showed minimal changes with age, and all age related trends which were identified were small relative to the variability within the population.
Author

N90-12179# Pennsylvania State Univ., University Park. Dept. of Engineering Science and Mechanics.
WRIST ORIENTATION EFFECT ON GRIP STRENGTH AND ENDURANCE Final Report
Jean Landa Pytel and Thomas J. Mackin 28 Nov. 1988 25 p
(Grant PHS-OH-02178)
(PB89-200935) Avail: NTIS HC A03/MF A01 CSCL 05H

The study provides basic data about some factors that may affect the ability of an individual to apply a gripping force. The study determines the effect of wrist orientation on grip strength and grip endurance. Twenty men and 20 women were used as subjects. They were asked to apply a maximum static force to a grip dynamometer and maintain a maximum contraction until their gripping force falls to 70 percent of the peak. The duration of the grip force application was used as a measure of fatigue time or endurance. Peak forces and linear impulses (to determine how the gripping force changed) of the gripping forces at various wrist orientations were measured and related to the maximum values generated by each subject. Wrist orientations varied by 15-degree increments in wrist angle in four directions: plantar flexion, dorsiflexion, ulnar deviation and radial deviation. Relative changes in peak force, fatigue time and linear impulse were evaluated for all the subjects at all wrist positions and also compared between sex groups. This type of basic data is of use to those people who are concerned with musculoskeletal disorders. They will be able to suggest changes in the manner in which a tool is held in order to decrease the susceptibility of an individual to musculoskeletal disorders.
GRA

N90-12180# California Univ., Irvine. Dept. of Cognitive Sciences.
DISCRIMINATING RIGID FROM NONRIGID MOTION Studies in the Cognitive Sciences
Myron L. Braunstein, Donald D. Hoffman, and Frank E. Pollick 31 Jul. 1989 38 p
(Contracts N00014-88-K-0354; N00014-87-G-0135; NSF BNS-88-19565; NSF IRI-87-00924; RR04209)
(AD-A211794; UCI-51) Avail: NTIS HC A03/MF A01 CSCL 05/8

Theoretical investigations of structure from motion have demonstrated that an ideal observer can discriminate rigid from nonrigid motion from two views of as few as four points. Three experiments are reported that demonstrate similar abilities in human observers: In one experiment 4 of 6 subjects made this discrimination from two views of four points; the remaining subjects required five points. Accuracy in discriminating rigid from nonrigid motion depended on the amount of nonrigidity in the nonrigid structure. The measure on nonrigidity was based on the variance of the interpoint distances over views. The ability to detect a rigid group dropped sharply as noise points (points not part of the rigid group) were added to the display. It is concluded that human observers do extremely well in discriminating between nonrigid and fully rigid motion, but do quite poorly at segregating points in a display on the basis of rigidity.
GRA

N90-12181# Naval Personnel Research and Development Center, San Diego, CA.
THE EFFECT OF INCENTIVES ON THE RELIABILITY AND VALIDITY OF COGNITIVE SPEED TESTS Technical Report, FY 1987 - FY 1988
Dennis P. Saccuzzo, Gerald E. Larson, and James Brown (San Diego State Univ., CA.) Jul. 1989 50 p
(AD-A211346; NPRDC-TR-89-14) Avail: NTIS HC A03/MF A01 CSCL 05/8

In the present study, financial incentives were used to motivate test takers, so that the effect of motivation on elementary cognitive tests could be determined. One hundred and nine male and female volunteer college students were tested on a battery of microcomputerized cognitive tests. One hundred of these subjects returned for a second session in which they were randomly assigned to an incentive or no incentive condition and then retested. The effort expended on the tests were measured via heart rate, skin conductance, and a self-report questionnaire pertaining to the perceived level of difficulty of the tests and amount of effort expended on them. Criterion measures, including the Advanced Otis-Lennon Test of Mental Abilities, Standard and Advanced Raven Progressive Matrices, and scores on the Scholastic Aptitude Test were also taken. The findings revealed that incentives led to better performance only on the most complex task in the study. In no case, however, did incentives affect the overall IQ-performance correlation for the tests used in the battery. These results support the view that correlations between cognitive speed and intelligence reflect common mental capacities, rather than some affective variable such as motivation.
GRA

55 SPACE BIOLOGY

Includes exobiology; planetary biology; and extraterrestrial life.

No abstracts in this category.

59 MATHEMATICAL AND COMPUTER SCIENCES (GENERAL)

N90-12182*# Institute for Computer Applications in Science and Engineering, Hampton, VA.
THE NONCONVEX MULTI-DIMENSIONAL RIEMANN PROBLEM FOR HAMILTON-JACOBI EQUATIONS Final Report
Stanley Osher (California Univ., Los Angeles.) Aug. 1989 11 p Submitted for publication Sponsored in part by DARPA
(Contracts NAS1-18107; NAG1-270; NSF DMS-88-11863; N00014-86-K-0691)
(NASA-CR-181887; ICASE-89-53; NAS 1.26:181887) Avail: NTIS HC A03/MF A01 CSCL 12A

Simple inequalities for the Riemann problem for a Hamilton-Jacobi equation in N space dimension when neither the initial data nor the Hamiltonian need be convex (or concave) are presented. The initial data is globally continuous, affine in each orthant, with a possible jump in normal derivative across each coordinate plane, x sub i = 0. The inequalities become equalities wherever a maxmin equals a minmax and thus an exact closed form solution to this problem is then obtained. Author

N90-12183*# Institute for Computer Applications in Science and Engineering, Hampton, VA.
REQUIREMENTS FOR MULTIDISCIPLINARY DESIGN OF AEROSPACE VEHICLES ON HIGH PERFORMANCE COMPUTERS Final Report
Robert G. Voigt Sep. 1989 12 p Presented at the NATO Advanced Research Workshop on Supercomputing
(Contract NAS1-18605)
(NASA-CR-181915; NAS 1.26:181915; ICASE-89-70) Avail: NTIS HC A03/MF A01 CSCL 12A

The design of aerospace vehicles is becoming increasingly complex as the various contributing disciplines and physical components become more tightly coupled. This coupling leads to computational problems that will be tractable only if significant advances in high performance computing systems are made. Some of the modeling, algorithmic and software requirements generated by the design problem are discussed. Author

60 COMPUTER OPERATIONS AND HARDWARE

Includes hardware for computer graphics, firmware, and data processing.

For components see *33 Electronics and Electrical Engineering.*

N90-12184# Xerox Palo Alto Research Center, CA. Systems Science Lab.
COLOR PRINTING FOR COMPUTER GRAPHICS. OR: HOW TO GET IT OFF YOUR SCREEN AND ONTO PAPER, IN COLOR
Maureen C. Stone Dec. 1988 42 p Submitted for publication
(PB89-208110; PARC-EDL-88-5) Avail: NTIS HC A03/MF A01 CSCL 09B

Members of the computer graphics community are expert at producing high quality images on monitors. Rarely, however, are they satisfied with the results of reproducing these images on paper. Part of the dissatisfaction is inevitable as some aspects of images rendered on monitors can never be reproduced on paper. However, part of the problem is simply ignorance, and knowledge of the strengths and weaknesses of printing systems can be used to produce better results. Here, it is explained why transferring a monitor image to a printed page is difficult, and some techniques that can be used to improve the results are given. Author

N90-12185# National Aerospace Lab., Tokyo (Japan). Computer Center.
BASIC PROGRAM FOR RASTER SCAN DISPLAY UNIT
Toshio Isobe, Syunji Suematsu, and Keiko Oguchi Dec. 1986 51 p In JAPANESE
(NAL-TM-560; ISSN-0452-2982; JTN-88-80056) Avail: NTIS HC A04/MF A01

In recent scientific and technical computer systems, graphics display is a necessary output device. On raster scan display using a computer, one can assign data to each picture element displayed. This enables the production of real images such as photographs or television images. In the computer center of National Aerospace Laboratory (NAL), raster scan displays have been installed and connected to large-scale computers. Described here are the hardware configuration of installed raster scan displays and basic display programs prepared for the displays. Also covered is the operation method of the entire system and the use of subroutines. Every prepared program is written in the FORTRAN subroutine format. The unique display function and raster scan common display function are clearly separated for standardization of the subroutines. A program written using the X-Y plotter subroutine can also be displayed on raster scan display without modification. Image drawing is enabled in the data input format based on the integrity of the data structure of the arithmetic operation results. NASDA

N90-12186 Department of the Navy, Washington, DC.
OPTICAL ARITHMETIC LOGIC USING THE MODIFIED SIGNED-DIGIT REDUNDANT NUMBER REPRESENTATION Patent
Mark E. Lasher, inventor (to Navy), Richard P. Bocker, inventor (to Navy), Barry L. Drake, inventor (to Navy), and Thomas B. Henderson, inventor (to Navy) 13 Jun. 1989 21 p Filed 29 Dec. 1986
(AD-D014176; US-Patent-4,838,646; US-Patent-Appl-SN-947142; US-Patent-Class-350-169) Avail: U.S. Patent and Trademark Office CSCL 12/9

Optical architectures are presented for performing fully parallel, carry-free computation with a trinary, modified signal-digit number representation to allow addition, subtraction and multiplication. Two different optical schemes involving position and polarization encoding enable the fabrication of modular trinary logic systems that accommodate trinary numbers of different magnitudes. The optical systems made up of redundant three-dimensional modules provide a designer with latitude to simultaneously carry out addition, subtraction or multiplication optically and with reduced complexity. GRA

N90-12187# Massachusetts Inst. of Tech., Cambridge. Artificial Intelligence Lab.
THE J-MACHINE: A FINE GRAIN CONCURRENT COMPUTER
William J. Dally, Andrew A. Chien, Stuart Fiske, Waldemar Horwat, John Keen, Michael Larivee, Rich Lethin, Peter Nuth, Scott Wills, and Paul Carrick (INTEL Corp., Santa Clara, CA.) et al May 1989 17 p Submitted for publication Sponsored by NSF; General Electric Corp.; and IBM Corp.
(Contracts N00014-88-K-0738; N00014-87-K-0825; N00014-85-K-0124)
(AD-A211909; VLSI-MEMO-89-532) Avail: NTIS HC A03/MF A01 CSCL 12/7

The J-Machine is a fine-grain concurrent computer that provides low-overhead primitive mechanisms for communication, synchronization, and translation. Communication mechanisms are provided that permit a node to send a message to any other node in the machine in less than 2 microsecs. On message arrival, a task is created and dispatched in less than 1 microsecs. A translation mechanism supports a global virtual address space. These mechanisms efficiently support most proposed models of concurrent computation. The hardware is an ensemble of up to 65,536 nodes each containing a 36-bit processor, 4K 36-bit words of memory, and a router. The nodes are connected by a high-speed 3-D mesh network. This design was chosen to make the most efficient use of available chip and board area. GRA

N90-12188# Massachusetts Inst. of Tech., Cambridge. Lab. for Computer Science.
SEQUENTIAL SEARCHING IN MULTIDIMENSIONAL MONOTONE ARRAYS

Alok Aggarwal (International Business Machines Corp., Yorktown Heights, NY.) and James K. Park Jun. 1989 37 p Submitted for publication
(Contracts N00014-87-K-0825; N00014-86-K-0593)
(AD-A211938; VLSI-MEMO-89-540) Avail: NTIS HC A03/MF A01 CSCL 12/6

Shared-memory multiprocessors commonly use shared variables for synchronization. Our simulations of real parallel applications show that large-scale cache-coherent multiprocessors suffer significant amounts of invalidation traffic due to synchronization. Large multiprocessors that do not cache synchronization variables are often more severely impacted. If this synchronization traffic is not reduced or managed adequately, synchronization references can cause severe congestion in the network. We propose a class of adaptive backoff methods that do not use any extra hardware and can significantly reduce the memory traffic to synchronization variables. These methods use synchronization state to reduce polling of synchronization variables. Our simulations show that when the number of processors participating in a barrier synchronization is small compared to the time of arrival of the processors, reductions of 20 percent to over 95 percent in synchronization traffic can be achieved at no extra cost. In other situations adaptive backoff techniques result in a tradeoff between reduced network accesses and increased processor idle time. GRA

N90-12189# Royal Signals and Radar Establishment, Malvern (England).

ON THE DESIGN AND IMPLEMENTATION OF A SECURE COMPUTER SYSTEM

P. F. Terry and S. R. Wiseman Jun. 1988 59 p
(Contract A94C/2711)
(RSRE-Memo-4188; BR108095; ETN-89-94081) Copyright
Avail: Defence Research Information Centre, Kentigern House, 65 Brown Street, Glasgow, G2 8EX, Scotland

The SMITE capability based computer architecture implementing a security policy model is proposed for use in government and military environments where high assurance of complex confidentiality and integrity based security policies is required. The SMITE security policy modeling approach is a state transition based model which can express notions of security such as government confidentiality, integrity issues, and commercial policies with equal facility and in a coherent manner. The approach is suitable for use in high assurance systems where proof of consistency with security axioms is required and can be refined to implementation in a straight forward manner for the SMITE architecture. ESA

N90-12190# Royal Signals and Radar Establishment, Malvern (England).

A SECURITY MODEL AND ITS IMPLEMENTATION

S. R. Wiseman and C. L. Harrold Sep. 1988 39 p
(RSRE-Memo-4222; BR108825; ETN-89-94085) Copyright
Avail: Defence Research Information Centre, Kentigern House, 65 Brown Street, Glasgow, G2 8EX, Scotland

A computer security model which allows the notions of confidentiality and integrity to be expressed in one coherent framework is proposed. Confidentiality is taken to be solely concerned with the observation of classified information, while separation of duty is employed as the technique for assuring the integrity of the security labels which are the basis of confidentiality. Discretionary access control is modeled by access control lists whose integrity is also provided by separation of duty controls. The specification of a simple system is given as an example of the techniques, and methods for implementation are discussed. ESA

61 COMPUTER PROGRAMMING AND SOFTWARE

Includes computer programs, routines, alogorithms, and specific applications, e.g., CAD/CAM.

N90-12191# National Aerospace Lab., Tokyo (Japan). Computer Center.

SOFTWARE PACKAGE FOR 3-DIMENSIONAL GRAPHIC DISPLAY UNIT

Kazuyo Suematsu and Toshio Isobe Dec. 1986 41 p In JAPANESE
(NAL-TM-559; ISSN-0452-2982; JTN-88-80055) Avail: NTIS HC A03/MF A01

Graphics processing is a powerful means to efficiently process numeric data that is output in large quantities. Under the present conditions, however, a unique graphics output library is supported for each graphics processor. When a different device is used with a previously prepared drawing program, graphics output library learning of the device and program modification become required. A long period of time and burden is required of the user for graphics processing. GCP (Graphic Control Package) is a graphics processing software package that enables the user to develop drawing programs without being concerned with the device for reduction of the users burden. Researchers started development work to enable the use of this software package on all the graphics processors connected to the National Aerospace Laboratory (NAL) computer system. They have completed software package development of the three-dimensional graphics display device named SAPIENS manufactured by Muto Industries Ltd. and installed at the calculation center. The functions of the software package are discussed. NASDA

N90-12192*# Institute for Computer Applications in Science and Engineering, Hampton, VA.

PARAMETER IDENTIFICATION FOR AN ABSTRACT CAUCHY PROBLEM BY QUASILINEARIZATION Final Report

Dennis W. Brewer, John A. Burns, and Eugene M. Cliff (Virginia Polytechnic Inst. and State Univ., Blacksburg.) Oct. 1989 36 p Submitted for publication
(Contracts NAS1-18107; F49620-87-C-0116; F49620-87-C-0088; AF-AFOSR-0079-89; AF-AFOSR-0472-89; AF-AFOSR-0001-89)
(NASA-CR-181933; NAS 1.26:181933; ICASE-89-75) Avail: NTIS HC A03/MF A01 CSCL 09B

A parameter identification problem is considered in the context of a linear abstract Cauchy problem with a parameter-dependent evolution operator. Conditions are investigated under which the gradient of the state with respect to a parameter possesses smoothness properties which lead to local convergence of an estimation algorithm based on quasi-linearization. Numerical results are presented concerning estimation of unknown parameters in delay-differential equations. Author

N90-12193*# Institute for Computer Applications in Science and Engineering, Hampton, VA.

THE USE OF LANCZOS'S METHOD TO SOLVE THE LARGE GENERALIZED SYMMETRIC DEFINITE EIGENVALUE PROBLEM Final Report

Mark T. Jones and Merrell L. Patrick (Duke Univ., Durham, NC.) Sep. 1989 60 p
(Contract NAS1-18605; NAG1-466; AF-AFOSR-0117-88)
(NASA-CR-181914; NAS 1.26:181914; ICASE-89-69) Avail: NTIS HC A04/MF A01 CSCL 09B

The generalized eigenvalue problem, Kx = Lambda Mx, is of significant practical importance, especially in structural enginering where it arises as the vibration and buckling problem. A new algorithm, LANZ, based on Lanczos's method is developed. LANZ uses a technique called dynamic shifting to improve the efficiency and reliability of the Lanczos algorithm. A new algorithm for solving the tridiagonal matrices that arise when using Lanczos's method is described. A modification of Parlett and Scott's selective orthogonalization algorithm is proposed. Results from an implementation of LANZ on a Convex C-220 show it to be superior to a subspace iteration code. Author

N90-12194# Argonne National Lab., IL. Mathematics and Computer Science Div.

TOOLS TO AID IN THE DEVELOPMENT HIGH-PERFORMANCE ALGORITHMS

Jack Dongarra, Danny Sorensen, and Orlie Brewer 1989 12 p Presented at the Parallel and Distributed Algorithms Conference, Bonas, France, 3-6 Oct. 1989
(Contract W-31-109-eng-38)
(DE89-012395; CONF-8910108-1) Avail: NTIS HC A03/MF A01

This paper discusses two tools that aid in the development of parallel algorithms for high-performance computers. We describe the SCHEDULE package which provides an environment for developing and analyzing new parallel algorithms in FORTRAN that require sophisticated synchronization at a large-grain level. This package provides portability of a user's code and also has a graphics postprocessor for performance analysis and debugging. We also discuss a graphics tool useful for studying memory access patterns of algorithms. DOE

N90-12195# Allied-Signal Aerospace Co., Kansas City, MO.

REASONING ABOUT CHANGE AND EXCEPTIONS IN AUTOMATED PROCESS PLANNING

S. L. Brooks and K. E. Hummel Aug. 1989 7 p Presented at the AAAI Spring Symposium for AI in Manufacturing, Stanford, CA, 28 Mar. 1989
(Contract DE-AC04-76DP-00613)
(DE89-017706; KCP-613-4099; CONF-8903164-1) Avail: NTIS HC A02/MF A01

Automated process planning is generally defined as the automatic planning of the manufacturing procedures for producing a part from a computer aided design (CAD) based product definition. The knowledge in this domain is largely heuristic and has been a good application of expert systems for developing an automated planner. We are currently developing an automated process planning system, XCUT, using the HERB rule-based expert system shell which employs hierarchical abstraction and object-oriented programming. Two areas where we have found the AI techniques implemented in HERB lacking for our domain are reasoning about change and exceptions. To reason about change is the frame problem, where after applying an action the planner must determine what facts are still true. Reasoning about exceptions is determining when general heuristics can be used or not. In AI terms reasoning about exceptions is default reasoning or in terms of ATMS is hypothetical reasoning. The focus of this paper will explore both the need and the ways we plan to augment the XCUT system for reasoning about change and exceptions. DOE

N90-12196# Lawrence Livermore National Lab., CA.

LOW-COST THREE-DIMENSIONAL STEREOSCOPIC DISPLAY TECHNIQUE FOR COMPUTER-AIDED DESIGN

Peter A. Luft and Gary Bradley Sep. 1989 11 p Presented at the Computer Graphics World Computervision International User Conference, Boston, MA, 10-13 Sep. 1989
(Contract W-7405-eng-48)
(DE89-017732; UCRL-100718-Rev-1; CONF-8909111-1-Rev-1) Avail: NTIS HC A03/MF A01

This paper describes a procedure for obtaining low-cost stereoscopic imagery on any computer-aided design system that has color capability and that models its data in 3-D form. This technique works independently of installed hardware or software. Stereoscopic imagery is valuable in the design process because it simplifies and clarifies complex computer-modeled parts and assemblies. Thus, the design and manufacturing processes benefit from better communication and fewer errors. DOE

N90-12197# Massachusetts Inst. of Tech., Cambridge. Artificial Intelligence Lab.

EXPERIENCE WITH CST: PROGRAMMING AND IMPLEMENTATION

Waldemar Horwat, Andrew A. Chien, and William J. Dally May 1989 12 p Submitted for publication Sponsored in part by NSF, Washington, DC; General Electric Corp., Fairfield, CT and ONR, Washington, DC
(Contracts N00014-88-K-0738; N00014-87-K-0825; N00014-85-K-0124)
(AD-A211882; VLSI-MEMO-89-530) Avail: NTIS HC A03/MF A01 CSCL 12/5

CST is an object-oriented concurrent programming language based on Small talk-80 that supports concurrency using locks, asynchronous messages, and distributed objects. CST is described: the language and its implementation. Example programs and initial programming experience with CST is described. An implementation of CST (Concurrent Small Talk) generates native code for the J-machine, a fine-grained concurrent computer. Some novel compiler optimizations developed in conjunction with that implementation are also described. GRA

N90-12198# Massachusetts Inst. of Tech., Cambridge. Microsystems Research Center.

AN APPROXIMATE MAX-FLOW MIN-CUT THEOREM FOR UNIFORM MULTICOMMODITY FLOW PROBLEMS WITH APPLICATIONS TO APPROXIMATION ALGORITHMS

Tom Leighton and Satish Rao May 1989 12 p Submitted for publication Sponsored by NSF; IBM; and AT and T Bell Labs.
(Contracts N00014-80-C-0622; N00014-87-K-0825; N00014-86-K-0593; DAAL03-86-K-0171; AF-AFOSR-0076-86)
(AD-A211908; VLSI-MEMO-89-542) Avail: NTIS HC A03/MF A01 CSCL 12/4

In this paper, we consider a multicommodity flow problem where for each pair of vertices, (u,v), we are required to send f half-units of commodity (u,v) from u to v and f half-units of commodity (u,v) for v to u without violating capacity constraints. Our main result is an algorithm for performing the task provided that the capacity of each cut exceeds the demand across the cut by a theta(log n) factor. The condition on cuts is required in the worst case, and is trivially within a theta(log n) factor of optimal for any flow problem. The result is of interest because it can be used to construct the first poly-log times optimal approximation algorithms for a wide variety of problems, including minimum quotient separators, 1/3-2/3 separators, bifurcators, crossing number and VLSI layout area. The result can also be used to efficiently route packets in arbitrary distributed networks. For example, we can prove that any n-node bounded degree graph, G, with minimum edge expansion alpha can be configured off-line to simulate any n-node bounded degree graph H in O(log n/alpha) steps using constant size queues. GRA

N90-12199# Massachusetts Inst. of Tech., Cambridge. Microsystems Research Center.

PARALLEL GRAPH CONTRACTION

Cynthia A. Phillips May 1989 12 p
(Contracts N00014-87-K-0825; N00014-86-K-0593)
(AD-A211916; VLSI-MEMO-89-535) Avail: NTIS HC A03/MF A01 CSCL 12/4

The parallel tree contraction technique of Miller and Reif has proved to be a valuable tool in many parallel graph algorithms. This paper provides a similar contraction technique that applies not only to trees, but also to general graphs. It also provides a second, potentially faster contraction techniques for bounded-degree graphs (and general graphs when an embedding is known). The technique of parallel contraction is used in a more general setting. It is shown that a remarkably simple contraction algorithm that uses (n + e)/lg n processors reduces a connected n-node e-edge graph to a single node in O(lg squared n) steps and a second simple algorithm which uses the first as a subroutine. GRA

N90-12200*# University of Southern California, Marina del Rey. Information Sciences Inst.

THE CONDITIONAL-EVENT APPROACH TO DISTRIBUTED SIMULATION

K. M. Chandy and R. Sherman Jun. 1989 26 p
(Contracts NCC2-539; N00014-87-K-0022)
(NASA-CR-185890; NAS 1.26:185890; AD-A212009; ISI/RR-88-226) Avail: NTIS HC A03/MF A01 CSCL 09/2

A new conservative approach to distributed simulation that appears to be efficient is proposed. Performance measures of the simulator executing queueing network models are discussed. This work departs from earlier work on distributed simulation in two aspects. The topological structure of simulators described in the literature mirrors the structure of the physical system. By contrast, this method, messages are used for a variety of purposes, and the process interconnection structure of the simulator need not reflect the structure of the physical system. The second difference between the method proposed here and that used in the literature is the use of conditional events, and extension of the concept that forms the basis for sequential simulation. Experimental results on the Intel iPSC/1 running Cosmic C are reported. GRA

N90-12201# National Inst. of Standards and Technology, Gaithersburg, MD. Advanced Systems Div.

PROCESSING RATE SENSITIVITIES OF A HETEROGENEOUS MULTIPROCESSOR

Gordon E. Lyon Aug. 1989 12 p Sponsored by DARPA, Arlington, VA and DOE, Washington, DC
(PB89-229017; NISTIR-89/4128) Avail: NTIS HC A03/MF A01 CSCL 09B

A recent trend in multiprocessor evaluation has been to seek fundamental but easily parameterized performance characterizations. Freed of specialized detail, simplified models can convey good insight while applying easily and widely. A simple performance estimator and alternate scheduling schemes can, from very modest effort, highlight some first-order improvement tradeoffs in multiprocessors. An application example of a quicksort is used to demonstrate the approach. Author

N90-12202# California Univ., Irvine. Dept. of Mechanical Engineering.

DESIGN MECHANISM FOR INTERACTIVE GRAPHICS MECHANISM DESIGN Report, 1 May 1986 - 31 Aug. 1988

J. Michael McCarthy and R. M. C. Bodduluri 9 Mar. 1989 90 p
(Grant NSF DMC-85-16114)
(PB89-219513; NSF/ENG-89007) Avail: NTIS HC A05/MF A01 CSCL 09B

Computer techniques were developed for the design of modern mechanical systems. The focus, initially, was on mechanisms to control the rotation of a body. The result was the interactive design software Sphinx, which designed a linkage to guide a body through four specified orientations. This was generalized to provide a design for any number of specified orientations. The next step was to generalize the design methodology to multi-degree of freedom spherical chains such as occur in the wrist mechanism of robots. Multi-degree of freedom closed chains were addressed. These chains could be designed but their movement from place to place could not be planned. Finally, software for the design of the dynamic performance of these mechanisms is being pursued using the principles of time-optimal control. Initial results of the work have solved the problem of time-optimal movement of a multi-degree of freedom closed chain. GRA

N90-12203# University of Southern California, Marina del Rey. Information Sciences Inst.

A SINGLE-PHASE CLOCKED NOR/NOR CMOS PROGRAMMABLE SEQUENTIAL ARRAY STRUCTURE

Shih-Lien Lu Apr. 1989 13 p
(Contracts MDA903-86-C-0178; F29601-87-C-0069)
(AD-A211297; ISI/RR-89-230) Avail: NTIS HC A02/MF A01 CSCL 09/1

A static CMOS Programmable Sequential Array (PSA) structure is presented, which uses a precharge CMOS NOR/NOR logic structure to implement combinational logic. It is fast, it consumes no static power, and it imposes no limits on the number of input terms. Only one input clock is required while additional clocks are generated by the PSA structure. Static latches are added to the output. Results will remain unchanged with the absence of a high clock signal. This single-phase clocking technique, with statistically latched outputs, permits this proposed PSA to be used for many different system overall timing strategies. The proposed methodology has been implemented with MOSIS scalable design rules and has been adapted into the Berkeley VLSI CAD tool system--MPLA's tiling format. An automatically generated example is given. GRA

N90-12204# University of Southern California, Marina del Rey. Information Sciences Inst.

ISI'S (INFORMATION SCIENCES INSTITUTE) SDI ARCHITECTURE SIMULATOR: AN EXPERIMENT IN ADDING NEW SOFTWARE TO THE SYSTEM

Scott Carter and David Mizell Jul. 1989 14 p
(Contract N00014-87-K-0022)
(AD-A211314; ISI/RR-89-223) Avail: NTIS HC A02/MF A01 CSCL 12/5

The design of ISI's SDI architecture simulator was intended to minimize the software development necessary to add new simulation models to the system or to refine the detail of existing ones. The key software design approach used to accomplish this goal was the modeling of each simulated defense system component by a software object called a technology module. Each technology module provided a carefully defined abstract interface between the component model and the rest of the simulation system, particularly the simulation models of battle managers. The first test of the validity of this software design approach is documented. A new technology module modeling a kinetic kill vehicle (KKV) was added to the simulator. Although this technology module had an impact on several parts of the simulation system in the form of new data structures and functions that had to be created, the integration of the new module was accomplished without the necessity of replacing any existing code. GRA

N90-12205# Carnegie-Mellon Univ., Pittsburgh, PA. Software Engineering Inst.

SCHEDULING SPORADIC AND APERIODIC EVENTS IN A HARD REAL-TIME SYSTEM Final Report

Brinkley Sprunt, Lui Sha, and John Lehoczky Apr. 1989 47 p
(Contract F19628-85-C-0003)
(AD-A211344; CMU/SEI-89-TR-11; ESD-TR-89-19) Avail: NTIS HC A03/MF A01 CSCL 12/5

A real-time system consists of both aperiodic and periodic tasks. Periodic tasks have regular arrival times and hard deadlines. Aperiodic tasks have irregular arrival times and either soft or hard deadlines. In this paper, we present a new algorithm, the Sporadic Server algorithm, that greatly improves response times for soft-deadline aperiodic tasks and can guarantee hard deadlines for both periodic and aperiodic tasks. The operation of the Sporadic Server algorithm, its performance, and schedulability analysis are discussed and compared with previous, published aperiodic service algorithms. Real-time systems are used to control physical processes that range in complexity from automobile ignition systems to controllers for flight systems and nuclear power plants. In these systems, the correctness of system functions depends upon not only the results of computation but also the times at which results are produced. GRA

N90-12206# Carnegie-Mellon Univ., Pittsburgh, PA. Software Engineering Inst.

ADOPTION OF SOFTWARE ENGINEERING INNOVATIONS IN ORGANIZATIONS Final Report

Judy Bayer and Nancy Melone Apr. 1989 150 p Sponsored by DOD, Washington, DC
(AD-A211573; CMU/SEI-89-TR-17; ESD-TR-89-25) Avail: NTIS HC A07/MF A01 CSCL 12/5

Designing effective strategies to facilitate the adoption of new software engineering technologies is a complex endeavor. The experiences are considered of organizations in the defense industry that have considered and in many cases adopted any one of five software engineering technologies: structured programming, program design languages, software cost models, complexity metrics, and Ada. In all, 296 respondents participated. These respondents represented approx. 120 business units within approximately 75 defense contractor organizations. Data were collected using a structured survey instrument administered over the telephone. The motivations behind technology acquisition and adoption decisions, the use of various technology transfer mechanisms during the stages of the adoption process, and the relationship between technology transfer mechanisms and the timing, pass through, and smoothness of adoption process stages are all examined. Adoption is assumed to be a multistage process that may proceed in a linear or nonlinear fashion. Also explored is the relationship between managerial level of the advocate (i.e., top management, middle management, technical management, and broad-based support) and the speed and smoothness of technology acquisition and adoption. GRA

N90-12207# SRI International Corp., Menlo Park, CA. Computer Science Lab.
STRUCTURE BASED FORMAL METHODS FOR SOFTWARE ENGINEERING Final Report
Mark Moriconi 27 Jul. 1989 52 p
(Contract N00014-83-C-0300)
(AD-A211660) Avail: NTIS HC A04/MF A01 CSCL 12/4

It is widely recognized that the cost of software is far out stripping that of hardware, and that software repair, improvement, and enhancement typically consume the major portion of the cost. There are several reasons for the high cost of modification. Research on rapid prototyping is expected to help in this regard. Another reason is that a system implementation may not meet its requirements. Approaches to this problem include testing, formal verification, and runtime assertion checking. However, the dominant source of cost is system modification, which is necessitated by changes in requirements and in the support environment. If the design or the implementation of a large system is changed, the incremental cost of an individual change can be unacceptably high because a seemingly minor change to one part of a system can have unforeseen and subtle consequences in another part. Some changes always will have far reaching effects.The root cause is the implementation goal of good performance which usually dominates and conflicts with the goals of maintaining clarity and structure. Formal techniques were devised that can substantially reduce the cost of modifying large systems, especially those systems that have been optimized for performance. The techniques were implemented and apply to a class of sequential systems containing such objects as modules, procedures, and variables. The ways in which objects can be related is limited at present, reducing design and implementation flexibility. GRA

N90-12208# Messerschmitt-Boelkow-Blohm G.m.b.H., Ottobrunn (Germany, F.R.). Unternehmensbereich Drehfluegler.
GENERAL DATA PROCESSING SUPPORT FROM PROJECT PLANNING TO WORKSHOP CONTROL [DURCHGAENGIGE DV-UNTERSTUETZUNG VON DER PROJEKTIERUNG BIS ZU WERKSTATTSTEUERUNG]
Dierk Minke Dec. 1987 33 p In GERMAN
(MBB-UD-526/88-PUB; ETN-89-94619) Avail: NTIS HC A03/MF A01

The data processing support in aeronautics and space programs from the first idea to the construction is illustrated by a practical example from the field of aircraft development. The iterative process of development, optimization and permission of highly loaded aircraft components is depicted. The organization of the construction of the prototype, resulting from the development phase, and the implementation of data processing systems are described. The use of data processing systems is most meaningful in the domains of planning, administration, and feedback information of orders. A concept for the integration of standard software packages is presented. ESA

N90-12209# Technische Univ., Delft (Netherlands). Faculty of Technical Mathematics and Informatics.
A LANGUAGE FOR ASSEMBLY INSTRUCTIONS
Afke vanRijn 1988 31 p
(Rept-88-90; ISSN-0922-5641; ETN-89-95432) Copyright Avail: NTIS HC A03/MF A01

A language for off-line programming of a flexible assembly cell is introduced. The flexible assembly cell is called DIAC (Delft intelligent assembly cell) and the language DJ (DIAC jargon). The language constructions and the aims of DJ are described. DJ is a language intended for use in a restricted, technical domain, by a designer programming the cell for a specific product. The language is placed in a general context by comparison with existing literature on robot programming. ESA

N90-12210# Technische Univ., Delft (Netherlands). Faculty of Technical Mathematics and Informatics.
A POLYNOMIAL METHOD OF APPROXIMATE WEIGHTED CENTERS FOR LINEAR PROGRAMMING
C. Roos and D. denHertog 1989 26 p
(Rept-89-13; ISSN-0922-5641; ETN-89-95446) Copyright Avail: NTIS HC A03/MF A01

A generalization of the central path following method is proposed, both for the problem in standard form and for its dual problem. Weighted trajectories are defined by means of the weighted logarithmic barrier function. Through each strictly feasible point such a weighted trajectory is constructed. The algorithm can start in any strictly feasible point, and follows the weighted trajectory through this point. Hence, compared with the central path following method, the weighted trajectory following method is shown to advantage in not requiring to start sufficiently close to the central path as to require irksome transformations. Polynomiality is proved under a condition. The proof is surprisingly simple and elegant. ESA

N90-12211*# National Aeronautics and Space Administration. Ames Research Center, Moffett Field, CA.
A SIMPLIFIED SELF-ADAPTIVE GRID METHOD, SAGE
C. Davies and E. Venkatapathy (Eloret Corp., Sunnyvale, CA.) Oct. 1989 51 p
(NASA-TM-102198; A-89156; NAS 1.15:102198) Avail: NTIS HC A04/MF A01 CSCL 09B

The formulation of the Self-Adaptive Grid Evolution (SAGE) code, based on the work of Nakahashi and Deiwert, is described in the first section of this document. The second section is presented in the form of a user guide which explains the input and execution of the code, and provides many examples. Application of the SAGE code, by Ames Research Center and by others, in the solution of various flow problems has been an indication of the code's general utility and success. Although the basic formulation follows the method of Nakahashi and Deiwert, many modifications have been made to facilitate the use of the self-adaptive grid method for single, zonal, and multiple grids. Modifications to the methodology and the simplified input options make this current version a flexible and user-friendly code. Author

62 COMPUTER SYSTEMS

Includes computer networks and special application computer systems.

N90-12212*# California Univ., Irvine. Dept. of Electrical and Computer Engineering.
EFFICIENT DIAGNOSIS OF MULTIPROCESSOR SYSTEMS UNDER PROBABILISTIC MODELS
Douglas M. Blough, Gregory F. Sullivan, and Gerald M. Masson (Johns Hopkins Univ., Baltimore, MD.) 1989 27 p
(Grant NsG-1442)
(NASA-CR-185965; NAS 1.26:185965) Avail: NTIS HC A03/MF A01 CSCL 09B

The problem of fault diagnosis in multiprocessor systems is considered under a probabilistic fault model. The focus is on minimizing the number of tests that must be conducted in order to correctly diagnose the state of every processor in the system with high probability. A diagnosis algorithm that can correctly diagnose the state of every processor with probability approaching one in a class of systems performing slightly greater than a linear number of tests is presented. A nearly matching lower bound on the number of tests required to achieve correct diagnosis in arbitrary systems is also proven. Lower and upper bounds on the number of tests required for regular systems are also presented. A class of regular systems which includes hypercubes is shown to be correctly diagnosable with high probability. In all cases, the number of tests required under this probabilistic model is shown to be significantly less than under a bounded-size fault set model. Because the number of tests that must be conducted is a measure of the diagnosis overhead, these results represent a dramatic improvement in the performance of system-level diagnosis techniques. Author

N90-12213*# Illinois Univ., Urbana-Champaign. Coordinated Science Lab.

PARALLEL IMPLEMENTATION AND EVALUATION OF MOTION ESTIMATION SYSTEM ALGORITHMS ON A DISTRIBUTED MEMORY MULTIPROCESSOR USING KNOWLEDGE BASED MAPPINGS

Alok Nidhi Choudhary (Syracuse Univ., NY.), Mun K. Leung, Thomas S. Huang, and Janak H. Patel Oct. 1989 28 p Presented at the Computer Architectures Vision and Pattern Recognition Conference

(Grants NAG1-613; NSF IRI-87-05400)

(NASA-CR-185984; NAS 1.26:185984; UILU-ENG-89-2235; CSG-112) Avail: NTIS HC A03/MF A01 CSCL 09B

Several techniques to perform static and dynamic load balancing techniques for vision systems are presented. These techniques are novel in the sense that they capture the computational requirements of a task by examining the data when it is produced. Furthermore, they can be applied to many vision systems because many algorithms in different systems are either the same, or have similar computational characteristics. These techniques are evaluated by applying them on a parallel implementation of the algorithms in a motion estimation system on a hypercube multiprocessor system. The motion estimation system consists of the following steps: (1) extraction of features; (2) stereo match of images in one time instant; (3) time match of images from different time instants; (4) stereo match to compute final unambiguous points; and (5) computation of motion parameters. It is shown that the performance gains when these data decomposition and load balancing techniques are used are significant and the overhead of using these techniques is minimal. Author

N90-12214*# Illinois Univ., Urbana-Champaign. Coordinated Science Lab.

NOVEL TECHNIQUES FOR DATA DECOMPOSITION AND LOAD BALANCING FOR PARALLEL PROCESSING OF VISION SYSTEMS: IMPLEMENTATION AND EVALUATION USING A MOTION ESTIMATION SYSTEM

Alok Nidhi Choudhary, Mun K. Leung, Thomas S. Huang, and Janak H. Patel Oct. 1989 45 p

(Grants NAG1-613; NSF IRI-87-05400)

(NASA-CR-185991; NAS 1.26:185991; UILU-ENG-89-2234; CSG-111) Avail: NTIS HC A03/MF A01 CSCL 09B

Computer vision systems employ a sequence of vision algorithms in which the output of an algorithm is the input of the next algorithm in the sequence. Algorithms that constitute such systems exhibit vastly different computational characteristics, and therefore, require different data decomposition techniques and efficient load balancing techniques for parallel implementation. However, since the input data for a task is produced as the output data of the previous task, this information can be exploited to perform knowledge based data decomposition and load balancing. Presented here are algorithms for a motion estimation system. The motion estimation is based on the point correspondence between the involved images which are a sequence of stereo image pairs. Researchers propose algorithms to obtain point correspondences by matching feature points among stereo image pairs at any two consecutive time instants. Furthermore, the proposed algorithms employ non-iterative procedures, which results in saving considerable amounts of computation time. The system consists of the following steps: (1) extraction of features; (2) stereo match of images in one time instant; (3) time match of images from consecutive time instants; (4) stereo match to compute final unambiguous points; and (5) computation of motion parameters. Author

N90-12215*# Illinois Univ., Urbana-Champaign. Coordinated Science Lab.

PARALLEL ARCHITECTURES AND PARALLEL ALGORITHMS FOR INTEGRATED VISION SYSTEMS Ph.D. Thesis

Alok Nidhi Choudhary Sep. 1989 187 p

(Grant NAG1-613)

(NASA-CR-185990; NAS 1.26:185990; UILU-ENG-89-2231; CSG-108) Avail: NTIS HC A09/MF A01 CSCL 09B

Computer vision is regarded as one of the most complex and computationally intensive problems. An integrated vision system (IVS) is a system that uses vision algorithms from all levels of processing to perform for a high level application (e.g., object recognition). An IVS normally involves algorithms from low level, intermediate level, and high level vision. Designing parallel architectures for vision systems is of tremendous interest to researchers. Several issues are addressed in parallel architectures and parallel algorithms for integrated vision systems. Author

N90-12216# California Inst. of Tech., Pasadena. Dept. of Electrical Engineering.

OPTICAL COMPUTING BASED ON THE HOPFIELD MODEL FOR NEURAL NETWORKS Final Report

Demetri Psaltis, Ken-Yuh Hsu, and Hsin-Yu Li 1989 64 p

(Contract N00014-85-K-2035)

(AD-A211824) Avail: NTIS HC A04/MF A01 CSCL 06/4

Associative memories are one of the most interesting applications of neural networks. In general, an associative memory stores a set of information, called memories. The information is stored in a format such that when an external stimulus is presented into the system, the system evolves to a stable state that is closest to the input data. This process can be viewed as a content-addressable memory since the stored memory is retrieved by the contents of the input and not by the specific address. In other words, the memory can recognize distorted inputs as long as the input provides sufficient information. Later the characteristics of the associative memory are shown by presenting distorted versions of the stored images, e.g., rotated, scaled, shifted ones, etc. to the system and see how it converges. GRA

N90-12217# Royal Signals and Radar Establishment, Malvern (England).

PARALLEL PROCESSING ON TRANSPUTER ARRAYS FOR THE RECOGNITION OF OBJECTS IN INFRARED IMAGES

S. A. Baker Sep. 1988 16 p

(RSRE-Memo-4197; BR108826; ETN-89-94083) Avail: Defence Research Information Centre, Kentigern House, 65 Brown Street, Glasgow, G2 8EX, Scotland

Image processing algorithms were mapped on to transputer arrays, and object classification based on the autocorrelation function was applied to infrared images. Using the OCCAM programming language, parallel processing techniques were developed to make use of the concurrency available for communication and calculation. The results for this problem are assessed and conclusions drawn on the use of transputers and OCCAM for parallel processing. During low level image processing all the transputers in the network are doing the same operations at the same time and so there are no problems of efficiency, or need for load balancing. Feature extraction and calculation are much more data-dependent and so it is more difficult to design a problem-solving strategy which uses all the transputers as efficiently as possible. Communications handling is the more complicated task from the programmer's point of view, while the coding of the numerical algorithms is relatively easy (particularly with the checking mechanisms available in the OCCAM compiler). Any solution using parallel processing techniques needs to take into account how much programming time is required, not only for designing and coding but also for testing and debugging. ESA

N90-12218# Sheffield Univ. (England). Dept. of Control Engineering.
DISTRIBUTED VLSI ARCHITECTURE FOR FAST JACOBIAN AND INVERSE JACOBIAN FORMULATIONS
A. Y. Zomaya and A. S. Morris Oct. 1988 36 p
(RR-346; ETN-89-95133) Avail: NTIS HC A03/MF A01

Parallel processing techniques are used to reduce the computational time for the kinematical description of robot manipulators. The development system used to implement the algorithms consists of an Inmos Transputer (a Very Large Scale Integration (VLSI) single chip computer) running the OCCAM concurrent programing language. This system is used to construct and evaluate the performance and cost effectiveness of several methods proposed for solving the Jacobian and inverse Jacobian problems with special attention to the case of a robot operating in the neighborhood of singular points. Detailed analysis is performed and successful results obtained for a six degrees of freedom robot arm (Puma 560). Execution time comparisons between Von Neumann (uniprocessing) and parallel processing architectures are included to show the superiority of the latter approach. ESA

63 CYBERNETICS

Includes feedback and control theory, artificial intelligence, robotics and expert systems.

For related information see also *54 Man/System Technology and Life Support.*

N90-12219# Oak Ridge National Lab., TN.
NAVIGATION OF ROBOTIC SYSTEMS Foreign Trip Report, 10-29 Aug. 1989
David B. Reister 13 Sep. 1989 5 p
(Contract DE-AC05-84OR-21400)
(DE89-017507; ORNL/FTR-3366) Avail: NTIS HC A01/MF A01

K. Asai, the general manager of the computing center at the Japan Atomic Energy Research Institute (JAERI), invited the traveler to perform research at JAERI and to learn about the Human Acts Simulation Program (HASP). The traveler performed research on a methodology for the self-location of a robot navigating in an unstructured environment and had several discussions about HASP. DOE

N90-12220# Illinois Univ., Urbana-Champaign. Coordinated Science Lab.
ADAPTIVE FEEDBACK LINEARIZATION: STABILITY AND ROBUSTNESS M.S. Thesis
Ioannis Kanellakopoulos Jan. 1989 83 p
(Grant NSF ECS-87-15811)
(PB89-219497; UILU-ENG-89-2207; DC-111; NSF/ENG-89010) Avail: NTIS HC A05/MF A01 CSCL 09B

A new direct adaptive regulation scheme is proposed for nonlinear systems satisfying an extended matching condition. For this class of systems, the usual overparameterization in parameter estimates is avoided. Conditions are given, under which some of the obtained local results become global. It is also shown how these results can be applied to the more general problem of adaptive tracking, under the assumption of exponentially minimum phase systems. Finally, the robustness of the regulation scheme with respect to unmodeled dynamics is examined and quantified, and comparison between adaptive and nonadaptive control is carried out. GRA

N90-12221# Massachusetts Inst. of Tech., Cambridge. Artificial Intelligence Lab.
TAXONOMIC SYNTAX FOR FIRST ORDER INFERENCE
David McAllester and Bob Given Jun. 1989 37 p
(Contract N00014-86-K-0180)
(AD-A211618; AI-M-1134) Avail: NTIS HC A03/MF A01 CSCL 05/7

Most knowledge representation languages are based on classes and taxonomic relationships between classes. Taxonomic hierarchies without defaults or exceptions are semantically equivalent to a collection of formulas in first order predicate calculus. Although designers of knowledge representation languages often express an intuitive feeling that there must be some advantage to representing facts as taxonomic relationships rather than first order formulas, there are few, if any, technical results supporting this intuition. We attempt to remedy this situation by presenting a taxonomic syntax for first order predicate calculus and a series of theorems that support the claim that taxonomic syntax is superior to classical syntax. GRA

N90-12222# Stanford Univ., CA. Inst. for Research on Learning.
COMPUTER-BASED TUTORS FOR EXPLAINING AND MANAGING THE PROCESS OF DIAGNOSTIC REASONING Final Report, Mar. 1985 - Dec. 1988
William J. Clancey Dec. 1988 11 p
(Contract N00014-85-K-0305)
(AD-A211738) Avail: NTIS HC A03/MF A01 CSCL 12/9

AI (Artificial Intelligence)-based instructional programs, often called intelligent tutoring systems (ITS), use qualitative modeling techniques to represent: (1) processes in the subject domain (e.g., a steam propulsion plant, an electronic circuit); (2) problem solving processes (e.g., diagnostic strategy, programming methods); and (3) communication processes (e.g., the Socratic method, case method discourse, and rhetorical principles in explanation) (qualitative student models). Typically, instructional programs may represent only one or two kinds of these processes. When a simulation model of problem solving processes is incorporated in the program, a basis is provided for evaluating and assisting the student in a very general way. Such programs, which can solve the same problems given to a student, are called knowledge based tutors (knowledge based tutoring). Early in the research, the importance of representing problem solving processes in a well structured procedural language was identified. In a sequence of programs, basic AI techniques were identified for achieving the separation of domain facts from a diagnostic procedure (NEOMYCIN), and the advantages of this separation for explanation and student modeling (IMAGE, ODYSSEUS). The generalization of the work has had a significant impact on expert systems and tutoring research. GRA

N90-12223# Sheffield Univ. (England). Dept. of Control Engineering.
ROBOT INVERSE DYNAMICS COMPUTATION VIA VLSI DISTRIBUTED ARCHITECTURES
A. Y. Zomaya and A. S. Morris Feb. 1989 30 p
(RR-350; ETN-89-95137) Avail: NTIS HC A03/MF A01

Algorithms that compute highly coupled dynamic equations in real time dynamic control of robot manipulators (due to advances in (VLSI) very large scale integration technology) are presented. A semi-customized symbolic form of the Lagrange-Euler formulation is divided into subtasks and distributed on a parallel processing system. This network is used to introduce parallelism by using different task allocation strategies which flow naturally from the Lagrange-Euler formulation. The cost effectiveness and speed of the scheme is demonstrated by applying it to a case study (Stanford arm). Comparisons are made between uniprocessing (Von Neumann) and parallel implementations of the algorithm. Several measures such as utilization, efficiency, and speedup are used to evaluate the performance of the employed networks and task allocations. ESA

N90-12224# Sheffield Univ. (England). Dept. of Control Engineering.

CAN PERCEPTRONS FIND LYAPUNOV FUNCTIONS: AN ALGORITHMIC APPROACH TO SYSTEMS STABILITY

S. P. Banks and R. F. Harrison 6 Jun. 1989 12 p
(RR-365; ETN-89-95232) Avail: NTIS HC A03/MF A01

The problem of finding a Lyapunov function using a simple neural network is discussed. The Rosenblatt single layer perceptron is used for this purpose. It is shown that the problem can be cast in a form suitable for solution. The importance of such a complete machine implementation of an algorithm which determines Lyapunov functions in the field of systems theory is discussed. ESA

N90-12225# Sheffield Univ. (England). Dept. of Control Engineering.

FAST FORWARD DYNAMICS ALGORITHM FOR ROBOT ARMS USING MULTIPROCESSING

A. Y. Zomaya and A. S. Morris Jun. 1989 26 p
(RR-367; ETN-89-95234) Avail: NTIS HC A03/MF A01

Parallel and distributed processing techniques are used to compute the direct dynamics problem involved in real time computer modeling and simulation of robot manipulators. A parallel implementation of a simplified Lagrange-Euler formulation is used to solve the dynamics. The resulting system of linear equations is solved using Gaussian elimination with simple row interchange. Both algorithms are distributed over a Multiple-Instruction Multiple-Data (MIMD) stream computer architecture. The system is constructed from VLSI (very large scale integration) building blocks called the Transputer. Quantification of the speed and utilization measures are given to demonstrate the cost effectiveness of the parallel approach. The problem is solved for a six degrees of freedom robot arm. ESA

N90-12226# Royal Signals and Radar Establishment, Malvern (England). Speech Research Unit.

A HYBRID OPTIMISATION STRATEGY FOR ADAPTIVE FEED-FORWARD LAYERED NETWORKS

Andrew Webb and David Lowe 9 Sep. 1988 25 p
(RSRE-Memo-4193; BR108038; ETN-89-94082) Copyright
Avail: Defense Research Information Centre, Kentigem House, 65 Brown Street, Glasgow, G2 8EX, Scotland

An optimization strategy for solving for the weight values of a general adaptive feedforward layered network with linear output units is considered. The weight values of the final layer of the network are determined using linear techniques based on a singular value decomposition of the outputs of the hidden units. The set of weight values governing the transformation of the data prior to this final layer is found using a nonlinear optimization strategy. Nonlinear optimization strategies combined with the linear method are compared with an approach which solves for all the weights of the network using nonlinear techniques on a range of problems. The results show that a hybrid approach generally leads to a minimization of the error at the output of a network in fewer iteration compared with a fully nonlinear optimization strategy. For certain problems (e.g. high-dimensional, confusable, inherently noisy data) the results suggest that it is more efficient to train a network (according to least squares minimization) by using a hybrid technique which solves for the network parameters layer by layer. ESA

N90-12227*# National Aeronautics and Space Administration. Ames Research Center, Moffett Field, CA.

GROUND-STATE CODING IN PARTIALLY CONNECTED NEURAL NETWORKS

Yoram Baram (Technion - Israel Inst. of Tech., Haifa.) Oct. 1989 21 p
(NASA-TM-102239; A-89256; NAS 1.15:102239) Avail: NTIS HC A03/MF A01 CSCL 09B

Patterns over (-1,0,1) define, by their outer products, partially connected neural networks, consisting of internally strongly connected, externally weakly connected subnetworks. The connectivity patterns may have highly organized structures, such as lattices and fractal trees or nests. Subpatterns over (-1,1) define the subcodes stored in the subnetwork, that agree in their common bits. It is first shown that the code words are locally stable stares of the network, provided that each of the subcodes consists of mutually orthogonal words or of, at most, two words. Then it is shown that if each of the subcodes consists of two orthogonal words, the code words are the unique ground states (absolute minima) of the Hamiltonian associated with the network. The regions of attraction associated with the code words are shown to grow with the number of subnetworks sharing each of the neurons. Depending on the particular network architecture, the code sizes of partially connected networks can be vastly greater than those of fully connected ones and their error correction capabilities can be significantly greater than those of the disconnected subnetworks. The codes associated with lattice-structured and hierarchical networks are discussed in some detail. Author

64 NUMERICAL ANALYSIS

Includes iteration, difference equations, and numerical approximation.

N90-12228*# Illinois Univ., Chicago.

THE REALIZATION OF INPUT-OUTPUT MAPS USING BIALGEBRAS

Robert Grossman and Richard G. Larson [1989] 14 p
(Grants NAG2-513; NSF DMS-87-01085)
(NASA-CR-185362; NAS 1.26:185362) Avail: NTIS HC A03/MF A01 CSCL 12A

The theory of bialgebras is used to prove a state space realization theorem for input/output maps of dynamical systems. This approach allows for the consideration of the classical results of Fliess and more recent results on realizations involving families of trees. Two examples of applications of the theorum are given. Author

N90-12229# Wisconsin Univ., Madison. Center for Mathematical Sciences.

HOMOCLINIC ORBITS FOR A CLASS OF HAMILTONIAN SYSTEMS Summary Report

Paul H. Rabinowitz Jun. 1989 9 p
(Contracts DAAL03-87-K-0043; N00014-88-K-0134; NSF MCS-81-10556)
(AD-A210562; CMS-TSR-89-36) Avail: NTIS HC A02/MF A01 CSCL 12/2

This document establishes the existence of a homoclinic solution of a Hamiltonian system assuming that the potential V is T periodic in t, grows more rapidly than quadratically as the value of 9 approaches limit of infinity and satisfies some other technical conditions. The homoclinic solution is obtained as the limit of subharmonic solutions of (asterisk). The subharmonic solutions are found using a minimax argument. GRA

N90-12230*# Institute for Computer Applications in Science and Engineering, Hampton, VA.

CONVERGENCE RESULTS FOR PSEUDOSPECTRAL APPROXIMATIONS OF HYPERBOLIC SYSTEMS BY A PENALTY TYPE BOUNDARY TREATMENT Final Report

Daniele Funaro and David Gottlieb (Brown Univ., Providence, RI.) Sep. 1989 21 p
(Contract NAS1-18605)
(NASA-CR-181929; NAS 1.26:181929; ICASE-89-59) Avail: NTIS HC A03/MF A01 CSCL 12A

A new method of imposing boundary conditions in the pseudospectral approximation of hyperbolic systems of equations is proposed. It is suggested to collocate the equations, not only at the inner grid points, but also at the boundary points and use the boundary conditions as penalty terms. In the pseudo-spectral Legrendre method with the new boundary treatment, a stability analysis for the case of a constant coefficient hyperbolic system is presented and error estimates are derived. Author

N90-12231*# National Aeronautics and Space Administration. Lewis Research Center, Cleveland, OH.
A LEAST-SQUARES FINITE ELEMENT METHOD FOR INCOMPRESSIBLE NAVIER-STOKES PROBLEMS
Bo-nan Jiang Oct. 1989 22 p
(NASA Order C-99066-G)
(NASA-TM-102385; E-5124; ICOMP-89-28; NAS 1.15:102385)
Avail: NTIS HC A03/MF A01 CSCL 12A

A least-squares finite element method, based on the velocity-pressure-vorticity formulation, is developed for solving steady incompressible Navier-Stokes problems. This method leads to a minimization problem rather than to a saddle-point problem by the classic mixed method, and can thus accommodate equal-order interpolations. This method has no parameter to tune. The associated algebraic system is symmetric, and positive definite. Numerical results for the cavity flow at Reynolds number up to 10,000 and the backward-facing step flow at Reynolds number up to 900 are presented. Author

N90-12232*# Institute for Computer Applications in Science and Engineering, Hampton, VA.
NUMERICAL EXPERIENCE WITH A CLASS OF ALGORITHMS FOR NONLINEAR OPTIMIZATION USING INEXACT FUNCTION AND GRADIENT INFORMATION Final Report
Richard G. Carter Jun. 1989 37 p Submitted for publication
(Contract NAS1-18605)
(NASA-CR-181927; NAS 1.26:181927; ICASE-89-46) Avail: NTIS HC A03/MF A01 CSCL 12A

For optimization problems associated with engineering design, parameter estimation, image reconstruction, and other optimization/simulation applications, low accuracy function and gradient values are frequently much less expensive to obtain than high accuracy values. Here, researchers investigate the computational performance of trust region methods for nonlinear optimization when high accuracy evaluations are unavailable or prohibitively expensive, and confirm earlier theoretical predictions when the algorithm is convergent even with relative gradient errors of 0.5 or more. The proper choice of the amount of accuracy to use in function and gradient evaluations can result in orders-of-magnitude savings in computational cost. Author

N90-12233# Lawrence Livermore National Lab., CA.
MICROSCOPIC APPROACH TO THE GENERATOR COORDINATE METHOD
Q. Haider, D. Gogny (Commissariat a l'Energie Atomique, Bruyeres-le-Chatel, France), and M. S. Weiss 22 Aug. 1989 38 p Sponsored by NRL
(Contract W-7405-eng-48)
(DE89-016701; UCID-21807) Avail: NTIS HC A03/MF A01

Different theoretical problems are solved which are associated with the calculation of the kernel occurring in the Hill-Wheeler integral equations within the framework of generator coordinate method. In particular, the Wick's theorem is extended to nonorthogonal Bogoliubov states. Expressions for the overlap between Bogoliubov states and for the generalized density matrix are also derived. These expressions are valid even when using an incomplete basis, as in the case of actual calculations. Finally, the Hill-Wheeler formalism is developed for a finite range interaction and the Skyrme force, and evaluated for the latter. DOE

N90-12234# Mound Lab., Miamisburg, OH.
OPERATIONAL MEASURES OF CENTRAL TENDENCY
Gary L. Silver 28 Aug. 1989 27 p
(Contract DE-AC04-88DP-43495)
(DE89-016959; MLM-3598) Avail: NTIS HC A03/MF A01

New operational formulas can be used in place of the average for estimating the center point of data. The new formulas are often more accurate than the average on known functions and their predictive properties resemble the median. One of them is used in a new method of bivariate interpolation on four points in rectangular array. New operational formulas for estimating slopes at the endpoints of three-point curves are presented. DOE

N90-12235# Stanford Univ., CA. Inst. for Mathematical Studies in the Social Sciences.
A DYNAMIC PROOF OF THE FROBENIUS-PERRON THEOREM FOR METZLER MATRICES
Kenneth J. Arrow Apr. 1989 11 p
(Contract N00014-86-K-0216)
(AD-A211839; TR-542) Avail: NTIS HC A03/MF A01 CSCL 12/1

Matrices with non-negative off-diagonal elements have many applications in mathematical economics and other fields of investigation. Economists have called them Metzler matrices. An important property, especially for the study of stability of dynamic systems, is that the largest real part of the characteristic roots is itself a characteristic root and has a semi-positive characteristic vector. There is a less well-known property of linear dynamic systems governed by Metzler matrices: if the forcing term is a non-negative vector and if the system starts in the positive orthant, it will remain there forever. The result does not appear to be derivable from the standard Frobenius-Perron theorem. Its proof is not very hard, however. The question is then raised, whether the Frobenius-Perron result is derivable simply from this theorem. This note shows that the answer is affirmative. The result may very possibly be useful for expository purposes. GRA

N90-12236# Massachusetts Inst. of Tech., Cambridge. Dept. of Mathematics.
DYNAMIC EMBEDDING OF TREES IN HYPERCUBES WITH CONSTANT DILATION AND LOAD
Tom Leighton, Mark Newman, and Eric Schwabe May 1989 12 p Submitted for publication Sponsored in part by NSF, Washington, DC
(Contracts N00014-80-C-0622; N00014-87-K-0825; DAAL03-86-K-0171; AF-AFOSR-0078-86)
(AD-A211884; VLSI-MEMO-89-543) Avail: NTIS HC A03/MF A01 CSCL 12/4

Parallel computations often yield computation structures which are trees; the shape of such a tree evolves over time as the computation progresses. However, parallel computers are usually designed as networks of processors with fixed connections; it is therefore important to embed the dynamic structure of a computation efficiently in a fixed network. The problem of dynamically embedding an evolving binary tree with at most N nodes in an N-node hypercube is considered. A simple randomized algorithm is presented which uses only local control and guarantees constant dilation, while maintaining constant load with high probability; this is the first load-balancing algorithm which achieves constant dilation. We also prove that random solutions to this problem are highly desirable, by demonstrating that any deterministic embedding algorithm which maintains constant load must have omega (square root of log N) dilation. GRA

N90-12237# Massachusetts Inst. of Tech., Cambridge. Microsystems Research Center.
FOUR VECTOR-MATRIX PRIMITIVES
Ajit Agrawal, Guy E. Blelloch, Robert L. Krawitz (Thinking Machines Corp., Cambridge, MA.), and Cynthia A. Phillips May 1989 13 p Submitted for publication Sponsored in part by International Business Machines Corp., Armonk, NY
(Contract N00014-87-K-0825)
(AD-A211889; VLSI-MEMO-89-536) Avail: NTIS HC A03/MF A01 CSCL 12/5

A set of powerful primitive matrix operations is discussed which allow easy specification of parallel matrix routines. The hypercube implementation demonstrates that the additional expressive power need not reduce performance and can, in fact, improve performance by providing automatic load balancing in the case where there are more matrix elements than processors. Some routines based on these primitives and other simple parallel operations give some timings for the primitives and routines for the implementation on the Connection Machine. One expects to generalize these implementations of the primitives so they work on processor grids whose row and column sizes are not powers of two, and to allow a vector extracted from a row off a matrix to be distributed to or deposited in either a row or column of another matrix. The primitives should be available to higher level languages so that they can be easily used. GRA

N90-12238# Massachusetts Inst. of Tech., Cambridge. Microsystems Research Center.

FAST COMPUTATION USING FAULTY HYPERCUBES

Johan Hastad (Royal Inst. of Tech., Stockholm, Sweden), Tom Leighton, and Mark Newman May 1989 15 p Submitted for publication Sponsored by NSF and IBM Corp.
(Contracts N00014-80-C-0622; N00014-87-K-0825; DAAL03-86-X-0171; AF-AFOSR-0078-86)
(AD-A211910; VLSI-MEMO-89-546) Avail: NTIS HC A03/MF A01 CSCL 12/4

The computational power of a hypercube containing a potentially large number of randomly located faulty components is considered. Researchers describe a randomized algorithm which embeds an N-node hypercube in an N-node hypercube with faulty processors. Provided that the processors of the N-node hypercube are faulty with probability p less than 1, and that the faults are independently distributed, we show that with high probability, the faulty hypercube can emulate the fault-free hypercube with only constant slowdown. In other words, an N-node hypercube with faults can simulate T steps of an N-node fault-free hypercube in O(T) steps. The embedding is easy to construct in polylogarithmic time using only local control. Also described are O (log N)-step routing algorithms which ensure the delivery of messages with high probability even when a constant fraction of the nodes and edges have failed. The routing results represent the first adaptive routing algorithms for which an effective theoretical analysis has been achieved. GRA

N90-12239# Massachusetts Inst. of Tech., Cambridge. Microsystems Research Center.

SEQUENTIAL DESIGN OF EXPERIMENTS WITH PHYSICALLY BASED MODELS 23 M.S. Thesis

Michele E. Storm May 1989 82 p
(Contract MDA972-88-K-0008)
(AD-A211918; VLSI-MEMO-89-529) Avail: NTIS HC A05/MF A01 CSCL 12/1

The application of physically based models to sequential optimization was explored and the benefits measured by comparison to optimizations performed using control variable polynomial models. The optimization algorithm developed is based on the sequential use of local (weighted) linear regression models. A new operating point or design is recommended at the optimum of the model within the region where the model is considered valid. This region, within which extrapolations based on the model are believed to be sufficiently accurate, is defined by constraints based on the estimated predictive error of the model and the distance from the data. A new model is created after each data point is collected. As a test case, the sequential optimizer was applied to the design of a paper helicopter for maximum time of flight. The physically based model of the paper helicopter was developed through the use of dimensional analysis, a technique which groups variables according to their dimensions. It was found that the physically based model improved the design of the helicopter more rapidly than the polynomial models. For example, in one comparison of the physical model and the linear model, the physical model reached the optimum design after four sequential designs, while the linear model hadn't reached the optimum after ten designs. GRA

N90-12240# Massachusetts Inst. of Tech., Cambridge. Lab. for Information and Decision Systems.

ON THE COMMUNICATION COMPLEXITY OF SOLVING A POLYNOMIAL EQUATION

Zhi-Quan Luo and John N. Tsitsiklis Jul. 1989 21 p
(Contracts N00014-84-K-0519; DAAL03-86-K-0171)
(AD-A211945; LIDS-P-1876) Avail: NTIS HC A03/MF A01 CSCL 12/7

In a computer network where a set of processors wish to perform some computational task, communication can sometimes become a bottleneck, especially when communication resources are scarce. This is particularly so, in the area of parallel and VLSI computation where communication issues have been studied extensively. In such contexts, it is desirable to design algorithms that require as little information exchange as possible. Problems of minimizing the amount of exchanged information also arise in the context of decentralized signal processing, where each local processor collects some partial data to be processed collectively. The communication complexity (i.e., the minimum possible amount of information exchange) of some particular computational tasks are thoroughly examined. Generally speaking, communication complexity depends both on the topology of a computer network and on the nature of the computational task under consideration. The topological issues are ignored by assuming that there are only two processors, say P1 and P2. GRA

N90-12241# Admiralty Research Lab., Teddington (England).

CALCULATION OF TRANSIENT RESPONSE FROM TIME-HARMONIC SPECTRUM

J. H. James Jun. 1989 24 p
(AD-A211972; ARE-TR-89308; DRIC-BR-110719) Avail: NTIS HC A03/MF A01 CSCL 12/1

The theory behind a FORTRAN program which facilitates computations of transient response is described. Discrete values of a time-harmonic spectrum are used, via quadratic interpolation and weighting by the transform of a selected time function, to provide samples for transient response calculations done by numerical evaluation of a Fourier integral using the fast Fourier transform (FFT) algorithm. Examples of motion, radiation and scattering transient responses of simple dynamical systems demonstrate that the program is a valuable research tool. This report is an update of previous work GRA

N90-12242# Stanford Univ., CA. Dept. of Operations Research.

SMALL SAMPLE THEORY FOR STEADY STATE CONFIDENCE INTERVALS

Chia-Hon Chien Jun. 1989 99 p
(Contract DAAL03-88-K-0063)
(AD-A212097; TR-37; ARO-25839.12-MA) Avail: NTIS HC A05/MF A01 CSCL 12/3

The goal of this dissertation is to develop a nonparametric method for obtaining a confidence interval for the mean of a stationary sequence. As indicated in the literature, nonparametric confidence intervals in practice often have undesirable small-sample asymmetry and coverage characteristics. These phenomena are partially due to the fact that the third and fourth cumulants of the point estimator for the stationary mean, unlike those of the standard normal random variable, are not zero. We will apply Edgeworth and Cornish-Fisher expansions to obtain asymptotic expansions for the errors associated with confidence intervals. The analysis isolates various elements that contribute to errors and makes it possible for us to estimate each element and hopefully correct the errors to a smaller order. We will use Glynn's method to develop first and second order pivots for the confidence intervals. Furthermore, these procedures also improve the asymptotic order of confidence interval accuracy. GRA

N90-12243# Helsinki Univ. of Technology, Espoo (Finland). Inst. of Mathematics.

SOME NOTES ON PERTURBATIONS OF DIFFERENTIAL-ALGEBRAIC EQUATIONS

Benedict Leimkuhler May 1989 25 p
(PB89-218564; MAT-A266; ISBN-951-754-896-6) Avail: NTIS HC A03/MF A01 CSCL 12A

A differential-algebraic equation (DAE) for which the constraints and differential equations are separated may be thought of as an ordinary differential equation in a manifold. Numerical software for such a DAE is most easily applicable if the index (the number of differentiations of the constraints necessary to yield an ODE) is one or zero. Recently, it has been suggested to solve some high index DAEs by differentiating the constraints. This procedure results in a DAE of reduced index. The effect of perturbations on these differentiated-constraint formulations is considered. A generalization of a state-space form is developed to help compare the behavior of solutions of these reformulations with solutions of the original DAE. Author

N90-12244# Stanford Univ., CA. Systems Optimization Lab.
A MATRIX FACTORIZATION AND ITS APPLICATION TO LARGE-SCALE LINEAR PROGRAMMING
Pierre F. DeMazancourt Jul. 1989 89 p
(Contracts N00014-89-J-1659; DE-FG03-87ER-25030; DE-FG03-87ER-25028; NSF ECS-87-15153; NSF DDM-88-14253; NSF DMS-88-00589)
(AD-A211293; SOL-89-10) Avail: NTIS HC A05/MF A01
CSCL 12/4

As an alternative to the Lower-Upper (LU) matrix factorization, a factorization is considered that uses the lower triangular part of the original matrix as one factor and computes the other factors as a product of rank-one update matrices. After reviewing and improving the time complexity, the requirements, the stability and the efficiency of this method, a stable factorization algorithms is derived which was implemented in FORTRAN77 within the framework of the simplex algorithm for linear programming. A comparison of the numerical results with those obtained through the code MINOS 5.3 indicate that the method may be more efficient than an ordinary LU decomposition for some matrices whose order ranges between 28 and 1481, especially when these matrices are almost triangular. GRA

N90-12245# Purdue Univ., West Lafayette, IN. Dept. of Statistics.
ON FINDING THE LARGEST NORMAL MEAN AND ESTIMATING THE SELECTED MEAN
Shanti S. Gupta and Klaus J. Miescke (Illinois Univ., Chicago.) Aug. 1989 24 p
(Contract N00014-88-K-0170; AF-AFOSR-0347-83)
(AD-A211628; TR-89-23C) Avail: NTIS HC A03/MF A01
CSCL 12/3

For k greater than or = 2 independent normal populations with unknown means and a common known variance the problem of selecting the population with the largest mean and simultaneously estimating the mean of the selected population is considered in the decision theoretic approach following Cohen and Sackrowitz (1988). Under several loss functions with two additive components due to selection and due to estimation, Bayes decision rules are derived and studied. Both the case of equal sample sizes and the case of unequal sample sizes are treated. The natural rule, which selects in terms of the largest sample mean and then estimates based on the sample mean of the selected population, is critically examined in all situations considered. GRA

N90-12246# Wayne State Univ., Detroit, MI. Dept. of Mathematics.
EMPIRICAL BAYES ESTIMATION OF BINOMIAL PARAMETER WITH SYMMETRIC PRIORS
TaChen Liang Jun. 1989 13 p Prepared in cooperation with Purdue Univ., West Lafayette, IN
(Contract N00014-88-K-0170; NSF DMS-87-02620)
(AD-A211646; TR-89-13) Avail: NTIS HC A03/MF A01
CSCL 12/3

The problem of estimating the binomial parameter via the nonparametric empirical Bayes approach is examined. This estimation problem has some surprising phenomenon that estimators which are asymptotically optimal in the usual empirical Bayes sense do not exist (Robbins (1956, 1964)). However, as pointed out by Liang (1984) and Gupta and Liang (1986), it is possible to construct asymptotically optimal empirical Bayes estimators if the unknown priors a monotone empirical Bayes estimator is constructed by using the isotonic regression method. This estimator is asymptotically optimal in the usual empirical Bayes sense. The corresponding rate of convergence is investigated and shown to be at least of order 1/n where n is the number of past observations at hand. GRA

N90-12247# Sheffield Univ. (England). Dept. of Control Engineering.
GLOBAL LINEAR REPRESENTATIONS OF NONLINEAR SYSTEMS AND THE ADJOINT MAP
S. P. Banks Dec. 1988 23 p
(RR-347; ETN-89-95134) Avail: NTIS HC A03/MF A01

Two methods of global linearization of nonlinear systems on a manifold are described. The first consists of an expansion of the vector field in terms of a basis of the space of square integrable vector fields. The second method uses the adjoint representation of the Lie algebra of vector fields to obtain an infinite dimensional matrix representation of the system. A connection between the two approaches is developed. The first method is an essentially local procedure, but the adjoint representation provides a globally valid matrix representation of the vector field. ESA

N90-12248# Sheffield Univ. (England). Dept. of Control Engineering.
RATIONAL EXPANSION FOR NONLINEAR INPUT-OUTPUT MAPS
B. Chanane and S. P. Banks Dec. 1988 22 p
(RR-348; ETN-89-95135) Avail: NTIS HC A03/MF A01

A method of rational expansion for nonlinear input-output maps based on the rational expansion of functions of several complex variables is introduced. If truncated, this series reduces to a ratio of truncated Volterra series and as such it is expected to produce a better approximation in a smaller number of terms. To derive this representation, results from the theory of functions of several complex variables are needed. Rational expansion for single-input single-output systems is presented. The result is extended to the multidimensional case. A feedback version is presented in which the output is written in terms of input and output. ESA

N90-12249# Sheffield Univ. (England). Dept. of Control Engineering.
MAPPING NONLINEAR INTEGRO-DIFFERENTIAL EQUATIONS INTO THE FREQUENCY DOMAIN
S. A. Billings and J. C. PeytonJones 12 Jul. 1989 22 p
(RR-366; ETN-89-95233) Avail: NTIS HC A03/MF A01

An analytical relationship between nonlinear integro-differential equations and the generalized frequency response functions is derived. This provides insight into the relationships between the time and frequency domain representations of nonlinear systems and exposes the sensitivity of the frequency domain characteristics to parameters in the differential equation model. The frequency domain effects of changing physical characteristics such as the mass, damping and stiffness in Duffings equation can be readily investigated to provide engineering insight into system characteristics. ESA

N90-12250# Technische Univ., Delft (Netherlands). Faculty of Technical Mathematics and Informatics.
ON THE DIFFERENTIABLE MANIFOLD OF FIXED ORDER STABLE LINEAR SYSTEMS
B. Hanzon 1989 18 p
(Rept-88-89; ISSN-0922-5641; ETN-89-95431) Copyright Avail: NTIS HC A03/MF A01

Investigations are carried out into problem areas of system theory. Results of Helmke, Ober and Hanzon are generalized by the demonstration that the space of asymptotically stable linear systems of fixed order and the corresponding space of all linear systems are real analytically diffeomorphic differentiable manifolds. One-to-one correspondences between smooth parametrizations on the two manifolds, and of Riemannian metrics between the two manifolds is implied. A one-to-one correspondence between smooth canonical forms on the two corresponding principal fiber bundles is demonstrated. ESA

N90-12251# Technische Univ., Delft (Netherlands). Faculty of Technical Mathematics and Informatics.
SMOOTH LINEARIZATION OF HYPERBOLIC FIXED POINTS WITHOUT RESONANCE CONDITIONS

Sebastian vanStrien 1989 27 p
(Rept-89-03; ISSN-0922-5641; ETN-89-95437) Copyright Avail: NTIS HC A03/MF A01

Theorems an smooth linearization of hyperbolic fixed points are studied. The theorem of Hartman-Grobman, on the conjugacy of diffeomorphisms with a hyperbolic fixed point to linear diffeomorphisms, is discussed. A theorem is given relating to differentiable conjugacy, which is Hoelder, and does not require resonance conditions. The theorem is proved, for a special case, by the demonstration that the blown-up vector field and the blown-up linear part are conjugate, in a case by case analysis. ESA

N90-12252# Technische Univ., Delft (Netherlands). Faculty of Technical Mathematics and Informatics.
SOME OBSERVATIONS ON THE CONVERGENCE BEHAVIOR OF GMRES
Yunqing Huang (Xian Jiaotong Univ., China) and Henk A. vanderVorst 1989 41 p
(Rept-89-09; ISSN-0922-5641; ETN-89-95443) Copyright Avail: NTIS HC A03/MF A01

The Generalized Minimal Residual (GMRES) method, proposed by Saad and Schultz, is an iterative method for the approximate solution of linear systems of equations Ax=b with A possibly nonsymmetric. It has appeared to be a competitive method for certain classes of problems, especially for many systems which arise after discretization of partial differential equations. Numerical experiments in which the convergence behavior is observed and where the effects of changing the spectral properties of A are traced, are reported. Major observations are summarized. ESA

N90-12253# Technische Univ., Delft (Netherlands). Faculty of Technical Mathematics and Informatics.
A SIMPLE PROOF OF A DIFFERENTIAL EQUATION FOR GENERALIZATIONS OF LAGUERRE POLYNOMIALS
J. Koekoek and Roelof Koekoek 1989 12 p
(Rept-89-15; ISSN-0922-5641; ETN-89-95448) Copyright Avail: NTIS HC A03/MF A01

A simple proof is given for a second order differential equation satisfied by polynomials which are orthogonal with respect to an inner product. The proof is outlined and provides an easier method for the generalization of Laguerre polynomials. ESA

N90-12254# Grenoble-1 Univ. (France). Lab. des Techniques de lInformatique, des Mathematiques, de la Microelectronique et de la Microscop
A STUDY OF THE ASYMPTOTIC BEHAVIOR OF LINEAR DIFFERENCE EQUATIONS WITH POLYNOMIAL COEFFICIENTS [SOLUTIONS ASYMPTOTIQUES D'EQUATIONS AUX DIFFERENCES A COEFFICIENTS POLYNOMIAUX]
M. A. Barkatou Oct. 1988 25 p In FRENCH; ENGLISH summary Sponsored by the CNRS
(IMAG-RR-743-M; ETN-89-95493) Avail: NTIS HC A03/MF A01

Methods of solving linear difference equations with polynomial coefficients are described. The solutions have integral representations and may be expanded asymptotically using the saddle point method. Two methods of solving such equations are presented: the direct method and the Ramis method. The procedure and logic behind each step of the procedure is explained. ESA

N90-12255# Grenoble-1 Univ. (France). Lab. des Techniques de l'Informatique, des Mathematiques, de la Microelectronique et de la Microscop
ASYMPTOTIC BIAS OF AUTOREGRESSIVE ESTIMATORS
Pham Dinh Tuan Oct. 1988 31 p
(IMAG-RR-745-M; ETN-89-95495) Avail: NTIS HC A03/MF A01

Explicit formulas for the asymptotic bias of various estimators for the parameters of a scalar autoregressive process of general order are derived. The least squares (ordinary or forward-backward), the Burg's, Kay's and maximum likelihood estimators are shown to have the same asymptotic bias. The Yule-Walker estimator however posseses an additional bias which could be unacceptably high in some cases. ESA

N90-12256# Grenoble-1 Univ. (France). Lab. des Techniques de l'Informatique, des Mathematiques, de la Microelectronique et de la Microscop
INF-CONVOLUTION SPLINES
Pierre-Jean Laurent Oct. 1988 19 p
(IMAG-RR-749-M; ETN-89-95496) Avail: NTIS HC A03/MF A01

Inf-convolution splines introduced for the representation of functions presenting singularities (discontinuities, peaks) are described. The energy functions to be minimized are the inf-convolution of a semi-Hilbertian function and the indicator function of a linear subspace containing the singularities. The principle is extended to interpolating or smoothing splines based on the inf-convolution of a finite number of arbitrary semi-Hilbertian functions. Characterization theorems are given using the notion of semi-kernel. Several algorithms are proposed. ESA

N90-12257# Grenoble-1 Univ. (France). Lab. des Techniques de l'Informatique, des Mathematiques, de la Microelectronique et de la Microscop
SPLINES AND EQUATIONS OF NONLINEAR PARAMETERS
D. Girard and P. J. Laurent Nov. 1988 31 p Presented at the Congress on Mathematical Methods for CAGD, Oslo, Norway, 16-22 Jun. 1988 Submitted for publication
(IMAG-RR-750-M; ETN-89-95497) Avail: NTIS HC A03/MF A01

Given the approximate values z sub i and points t sub 1 to t sub n of a function f having some particular features (determined by alpha), the researchers smooth the data and simultaneously estimate alpha. Alpha can be the location of peaks or discontinuities, the value of a period, etc. The idea of using the smoothing spline corresponding to a well chosen quadratic smoothness criterion L sub alpha is explained. By using the inf-convolution of several quadratic functionals such a criterion can be built. Characterizations and computational methods for the resulting splines are presented. The choice of both the smoothing parameter and alpha by the generalized cross-validation method is discussed. Several algorithms are given and their efficiency shown on several types of numerical examples. ESA

N90-12258# Ecole Nationale Superieure des Telecommunications, Paris (France). Dept. Images.
OPTIMAL MATCHING OF 3-D CONVEX POLYHEDRA
Isabelle Bloch-Boulanger, Henri Maitre, and Michel Minoux (Paris VI Univ., France) Feb. 1989 27 p Submitted for publication
(Grant CIFRE-252/88)
(Telecom-Paris-89C003; ETN-89-95504) Avail: NTIS HC A03/MF A01

A method to find the best matching of two convex three-dimensional polyhedra, by minimizing a proximity measure over all possible relative positions of the two polyhedra, is proposed. The measure depends on the translation and the rotation performed on one of the polyhedra. This measure is chosen in such a way that it has good regularity properties. A calculation of this proximity measure is proposed. It is based on a barycentric representation of the surface points of the polyhedra and on projected gradient and conjugate gradient techniques. An optimization technique to minimize the proximity measure between convex polyhedra is developed. This method does not assume any correspondence knowledge between the vertices of the two polyhedra. It provides good results on random convex polyhedra. ESA

N90-12259# Sheffield Univ. (England). Dept. of Control Engineering.
ORTHOGONAL LEAST SQUARES METHODS AND THEIR APPLICATION TO NONLINEAR SYSTEM IDENTIFICATION
S. Chen, S. A. Billings, and W. Luo Aug. 1988 32 p
(Grant SERC-GR/D/30587)
(RR-343; ETN-89-95130) Avail: NTIS HC A03/MF A01

identification algorithms which combine structure determination and parameter estimation are developed based on well-known orthogonal least squares methods. These algorithms can provide information about the structure, or which terms to include in the model, and final parameter estimates for a class of multivariable discrete-time nonlinear stochastic systems which are linear in the parameters. It is shown that these estimators efficiently combine structure determination with parameter estimation to provide powerful procedures for identifying parsimonious models of structure-unknown systems. The applications to both simulated and real data are demonstrated. ESA

N90-12260# Technische Univ., Delft (Netherlands). Faculty of Technical Mathematics and Informatics.
THE CONVERGENCE BEHAVIOR OF SOME ITERATIVE SOLUTION METHODS
Henk A. vanderVorst 1989 16 p
(Rept-89-19; ISSN-0922-5641; ETN-89-95578) Copyright Avail: NTIS HC A03/MF A01

Among the most competitive methods for solving large sparse linear systems of equations, the conjugate gradients, generalized minimum residual, and conjugate gradients squared, methods are investigated. An overview of these methods is given with particular focus on their convergence behavior. Understanding the convergence behavior, in view of (spectral) properties of the given matrix, may be of help in applying these methods successfully and in selecting or modifying suitable preconditioning matrices. ESA

N90-12261# Technische Univ., Delft (Netherlands). Faculty of Technical Mathematics and Informatics.
ANALYSIS OF A SYSTEM OF TWO WEAKLY NONLINEAR COUPLED HARMONIC OSCILLATORS ARISING FROM THE FIELD OF WIND-INDUCED VIBRATIONS
C. G. A. vanderBeek 1989 43 p
(Rept-89-22; ISSN-0922-5641; ETN-89-95581) Copyright Avail: NTIS HC A03/MF A01

A model problem originating from the phenomenon of galloping overhead transmission lines is presented. A non-Hamiltonian system of two weakly nonlinear coupled harmonic oscillators is considered. For the lower order frequency ratios the influence of the coupling terms on the occurrence and (local) stability of periodic motions is studied, as well as the global behavior of the solutions. Since this system may be considered as a model for the wind induced vibrations of an oscillator with two degrees of freedom, an interpretation of the result is included. ESA

N90-12262# Technische Univ., Delft (Netherlands). Faculty of Technical Mathematics and Informatics.
AUGMENTATIONS OF GRAMMATICAL CATEGORIES IN DISTRIBUTIONAL-ALGEBRAIC MODELS OF NATURAL LANGUAGES
Maria Polkowska-Semeniuk and Lech T. Polkowski 1989 25 p
(Rept-89-24; ISSN-0922-5641; ETN-89-95583) Copyright Avail: NTIS HC A03/MF A01

In a continuing study distributional-algebraic models of natural languages are investigated. Facts about distributional models of languages are given which shed light on more advanced topics of the theory and prepare the ground for discussion on anaphora in the frames of the theory. Rank in generalized grammatical categories is addressed and augmentations of a generalized grammatical category are given. ESA

N90-12263# Technische Univ., Delft (Netherlands). Faculty of Technical Mathematics and Informatics.
GENERALIZATIONS OF LAGUERRE POLYNOMIALS
Roelof Koekoek 1989 20 p
(Rept-89-25; ISSN-0922-5641; ETN-89-95584) Copyright Avail: NTIS HC A03/MF A01

A study of polynomials which are generalizations of the classical generalized Laguerre polynomials is presented. Properties of the polynomials are given and coefficients defined in such a way that the polynomials are orthogonal with respect to an inner product. A proof of a second order differential equation for the polynomials is given. Representations as a hypergeometric series and a Christoffel-Darboux type formula are given. ESA

N90-12264# Technische Univ., Delft (Netherlands). Faculty of Technical Mathematics and Informatics.
A MULTIGRID METHOD COMBINED WITH DEFECT CORRECTION FOR FREE CONVECTION PROBLEMS AT HIGH RAYLEIGH NUMBERS
S. Zeng and P. Wesseling 1989 42 p
(Rept-89-27; ISSN-0922-5641; ETN-89-95586) Copyright Avail: NTIS HC A03/MF A01

The application of a multigrid method to the computation of free convection flow at high Rayleigh number is described. The differential equations are discretized by a hybrid scheme, which is a combination of central and upwind differences. Convergence problems are encountered at high Rayleigh numbers. One remedy is to introduce a direct solver on the coarsest grid, and to limit the coarsness of the grid. Another remedy, less costly, is to introduce artificial diffusion. The resulting loss of discretization accuracy is compensated by defect correction. The discretization error, the convergence behavior and the computing time are studied by means of numerical experiments. ESA

N90-12265# Technische Univ., Delft (Netherlands). Faculty of Technical Mathematics and Informatics.
SOME TECHNIQUES FOR ANAPHORA RESOLUTION IN ALGEBRAIC LINGUISTICS
Maria Polkowska-Semeniuk and Lech T. Polkowski 1989 21 p
(Rept-89-28; ISSN-0922-5641; ETN-89-95587) Copyright Avail: NTIS HC A03/MF A01

In a continuing study, basic foundations of the distributional-algebraic approach to natural languages previously laid out, are applied, to describe in formal terms, the phenomenon of anaphora. Cases where an anaphoric reference is ambiguous are addressed. The opposite point of view to that adopted in artificial intelligence, where extra information is provided by which proper anaphoric references can be selected, is adopted, so that all possible anaphoric references are built. The notions of multi-anaphora resolution and a way of defining them is described. An example, using a simple text, is detailed as an illustration of the approach. ESA

N90-12266*# Institute for Computer Applications in Science and Engineering, Hampton, VA.
A MULTIDOMAIN SPECTRAL COLLOCATION METHOD FOR THE STOKES PROBLEM Final Report
G. Sacchi Landriani and H. Vandeven (Paris VI Univ., France) May 1989 33 p Submitted for publication
(Contract NAS1-18107)
(NASA-CR-181876; ICASE-89-42; NAS 1.26:181876) Avail: NTIS HC A03/MF A01 CSCL 12A

A multidomain spectral collocation scheme is proposed for the approximation of the two-dimensional Stokes problem. It is shown that the discrete velocity vector field is exactly divergence-free and we prove error estimates both for the velocity and the pressure. Author

65 STATISTICS AND PROBABILITY

Includes data sampling and smoothing; Monte Carlo method; and stochastic processes.

N90-12267# Stanford Univ., CA. Dept. of Operations Research.
A UNIFIED FRAMEWORK FOR SIMULATING MARKOVIAN MODELS OF HIGHLY DEPENDABLE SYSTEMS
Ambuj Goyal, Perwez Shahabuddin, Philip Heidelberger, Victor F. Nicola (IBM Watson Research Center, Yorktown Heights, NY.), and Peter W. Glynn Jul. 1989 42 p
(Contract DAAL03-88-K-0063)

(AD-A212164; TR-39; ARO-25839.15-MA) Avail: NTIS HC A03/MF A01 CSCL 12/4

A unified framework for simulating Markovian models of highly dependable systems is presented. Since the failure event is a rare event, the estimation of system dependability measures using standard simulation requires very long simulation runs. It is shown that a variance reduction technique called Importance Sampling can be used to speed up the simulation by many orders of magnitude over standard simulation. This technique can be combined very effectively with regenerative simulation to estimate measures such as steady state availability and mean time to failure. Moreover, it can be combined with conditional Monte Carlo methods to quickly estimate transient measures such as reliability, expected interval availability and the distribution of interval availability. The effectiveness of these methods is shown by using them to simulate large dependability models. Also discussed is how these methods can be implemented in a software package to compute both transient and steady state measures simultaneously from the same sample run. GRA

N90-12268# Stanford Univ., CA. Dept. of Statistics.
COMPUTER PROBLEMS IN GOODNESS-OF-FIT
Michael A. Stephens 10 Aug. 1989 21 p
(Contract N00014-89-J-1627)
(AD-A211411; TR-420) Avail: NTIS HC A02/MF A01 CSCL 12/3

Several problems are discussed involving the use of the computer in statistics. These have arisen in connection with the author's work in goodness-of-fit, but occur in many other applications. The subjects treated are: estimating percentage points by Monte Carlo simulation and by Pearson curve fitting; estimation of asymptotic percentage points and approximations to the covariance matrix of order statistics and its inverse. GRA

N90-12269# Purdue Univ., West Lafayette, IN. Dept. of Statistics.
ON A CLASSIFICATION PROBLEM: RANKING AND SELECTION APPROACH
Shanti S. Gupta and Lii-Yuh Leu (National Central Univ., Chung-Li, Taiwan) Aug. 1989 21 p
(Contract N00014-88-K-0170; NSF DMS-87-02620)
(AD-A211627; TR-89-27C) Avail: NTIS HC A03/MF A01 CSCL 05/9

A classification problem based on ranking and selection approach is examined. It is assumed that the populations follow multivariate normal distribution. The corresponding selection problem is to choose the population with the smallest Mahalanobis distance. The subset selection approach is considered. Sometimes the indifference zone approach is also proposed. It should be pointed out that, for the subset selection approach, it is not assumed that the individual to be classified belongs to one of the several given categories. GRA

N90-12270# Purdue Univ., West Lafayette, IN. Dept. of Statistics.
ON THE ASYMPTOTIC OPTIMALITY OF CERTAIN EMPIRICAL BAYES SIMULTANEOUS TESTING PROCEDURES
Shanti S. Gupta and TaChen Liang (Wayne State Univ., Detroit, MI.) Jul. 1989 23 p
(Contract N00014-88-K-0170; NSF DMS-86-06964)
(AD-A211649; TR-89-22C) Avail: NTIS HC A03/MF A01 CSCL 12/3

The problem of simultaneous testing for n-component decisions is examined. Under the specific statistical model, the n components share certain similarity. Thus, empirical Bayes approach is employed. A general formulation is given of this empirical Bayes decision problem with a specialization to the problem of selecting good Poisson populations. Three empirical Bayes methods are used to incorporate information from different sources for making a decision for each of the n components. They are: nonparametric empirical Bayes, parametric empirical Bayes and hierarchical empirical Bayes. For each of them, a corresponding empirical Bayes decision rule is proposed. The asymptotic optimality properties and the convergence rates of the three empirical Bayes rules are investigated. It is shown that each of the three empirical Bayes rules, the rate of convergence is at least of order 0(exp(-cn + ln n)) for some positive constant c, where the value of c varies depending on the empirical Bayes rule used. GRA

N90-12271# Sheffield Univ. (England). Dept. of Control Engineering.
FAST SAMPLING AND STABILITY OF NONLINEAR SAMPLED DATA SYSTEMS. PART 2: SAMPLING RATE ESTIMATIONS
Y. Zheng, D. H. Owens (Strathclyde Univ., Glasgow, Scotland), and S. A. Billings Aug. 1988 42 p
(RR-341; ETN-89-95128) Avail: NTIS HC A03/MF A01

A time-domain approach is used to study the effect of fast sampling on the stability of a class of nonlinear sampled data systems which have the property that their underlying continuous systems are stable on a certain domain. A relationship between sampling rate and an estimated domain of attraction of the system is obtained by extending the analysis already developed. The relationship indicates that a faster sampling rate can increase the estimated domain of attraction of the sampled data system. A better understanding of the effect of sampling on the behavior of a sampled data system is obtained. Methods of designing a sampled data system in the best interests of economic instrumentation and system performance are presented. ESA

N90-12272# Sheffield Univ. (England). Dept. of Control Engineering.
MODELING AND ANALYSIS OF NONLINEAR TIME SERIES
S. Chen and S. A. Billings Mar. 1989 27 p
(Grant SERC-GR/D/30587)
(RR-355; ETN-89-95140) Avail: NTIS HC A03/MF A01

Modeling of nonlinear time series is reviewed and results are obtained by employing ideas from nonlinear control systems identification. Both global and local conditions for stationarity and invertibility are established for the general nonlinear time series model and it is shown how these results provide a framework for time series estimators. Methods of computing multistep ahead predictions are studied and the usefulness of polynomial models is discussed. ESA

N90-12273# Technische Univ., Delft (Netherlands). Faculty of Technical Mathematics and Informatics.
SOME 1(SUB P) INVARIANT PROBABILITY MEASURES
Jolanta Misiewicz and Roger Cooke 1989 12 p
(Rept-88-91; ISSN-0922-5641; ETN-89-95433) Copyright Avail: NTIS HC A03/MF A01

Some 1(sub p) invariant measures are investigated with reference to the exchangeability of such measures. A representation of infinite dimensional processes, which are 1(sub p) invariant up to a scale vector, as mixtures of independent, not identically distributed processes, is given. This generalizes a theorem of Berman, who generalized a classical result for spherically invariant measures. The processes are not exchangeable and not stationary. A proof technique is given, which is simpler than that of Berman, and uses only the fact that completely monotonic functions are Laplace transforms. ESA

N90-12274# Technische Univ., Delft (Netherlands). Faculty of Technical Mathematics and Informatics.
FUZZY LOGIC AND THE GENERALIZED MODUS PONENS
Hans Hellendoorn 1989 31 p
(Rept-88-92; ISSN-0922-5641; ETN-89-95434) Copyright Avail: NTIS HC A03/MF A01

The generalized modus ponens in fuzzy logic is investigated. Fuzzy logic and possibility theory in general is addressed. Hedges, strict implication and the generalized modus ponens are discussed. Driankov's criteria are discussed as a good approach to fuzzy logic. Criteria is proposed concerning the generalized modus ponens and the behavior of the fuzzy inference rule, and assumptions required for the proposition explained. ESA

N90-12275# Technische Univ., Delft (Netherlands). Faculty of Technical Mathematics and Informatics.
ESTIMATING FUNCTIONALS RELATED TO A DENSITY BY A CLASS OF STATISTICS BASED ON SPACINGS
Bert vanEs 1989 16 p
(Grant SMC-611-303-013)
(Rept-89-11; ISSN-0922-5641; ETN-89-95445) Copyright Avail: NTIS HC A03/MF A01

The estimation of functionals of a probability density of the elements of a sample X(sub 1) to X(sub n), is considered. A class of statistics based on spacings of increasing order is discussed and it is shown that these statistics are consistent estimators of the functionals considered. Special attention is paid to entropy estimation. In particular an asymptotic normality for this case is derived. ESA

N90-12276# Sheffield Univ. (England). Dept. of Control Engineering.
FAST SAMPLING AND STABILITY OF NONLINEAR SAMPLED-DATA SYSTEMS. PART 1: EXISTENCE THEOREMS
D. H. Owens (Strathclyde Univ., Glasgow, Scotland), Y. Zheng, and S. A. Billings Aug. 1988 18 p
(RR-340-Pt-1; ETN-89-95127) Avail: NTIS HC A03/MF A01

How the choice of sampling interval is related to the stability of a class of nonlinear sampled-data systems, and in particular how fast sampling may stabilize a sampled-data system when the underlying continuous system is known to be stable is investigated. Two fast sampling theorems are derived for a class of nonlinear sampled-data systems and it is shown that, provided the underlying continuous system is stable, there exists a maximum sampling interval such that when the system is sampled below this interval it will remain stable. A special class of nonlinear sampled-data systems are studied and an analytical relationship between sampling rates and the domains of attraction of the system is derived. ESA

N90-12277# Sheffield Univ. (England). Dept. of Control Engineering.
SLOW SAMPLING AND STABILITY OF NONLINEAR SAMPLED-DATA SYSTEMS
Y. Zheng, D. H. Owens (Strathclyde Univ., Glasgow, Scotland), and S. A. Billings Aug. 1988 22 p
(RR-342; ETN-89-95129) Avail: NTIS HC A03/MF A01

A technique for stabilizing a class of sampled data system using slow sampling is described. A relationship between the minimum sampling period and an estimated domain of attraction for the system is established. The technique allows for random sampling rates provided that all sampling periods are within an allowable range which ensures the system stability. Examples are given that show how the stability criteria can be easily applied even though results may be conservative in some cases. ESA

66 SYSTEMS ANALYSIS

Includes mathematical modeling; network analysis; and operations research.

No abstracts in this category.

67 THEORETICAL MATHEMATICS

Includes topology and number theory.

N90-12278# Technische Univ., Delft (Netherlands). Faculty of Technical Mathematics and Informatics.
A LONG TIME TAIL FOR RANDOM WALK IN RANDOM SCENERY
F. denHollander, J. Naudts, and P. Scheunders (Antwerp Univ., Belgium) 1989 36 p Sponsored by the Inst. pour l'Encouragement de la Recherche Scientifique dans l'Industrie et l'Agriculture
(Rept-89-08; ISSN-0922-5641; ETN-89-95442) Copyright Avail: NTIS HC A03/MF A01

A model of a random walk on a lattice with a random black and white coloring assigned to its sites is investigated. Walk and coloring are independent. The asymptotic behavior of the interarrival times between the successive visits of the walk to black sites is investigated, in particular in the occurrence of a long time tail in the decay of the average interarrival times to a limiting value. Numerical calculations are presented. The transition matrix between black sites is shown to be itself the solution of difference equations. This method of studying random walk problems by numerical solution of difference equations is thus applied twice, in calculating the matrix and then its iteration. ESA

N90-12279# Technische Univ., Delft (Netherlands). Faculty of Technical Mathematics and Informatics.
LIKELIHOOD CROSS-VALIDATION BANDWIDTH SELECTION FOR NONPARAMETRIC KERNEL DENSITY ESTIMATORS
Bert vanEs 1989 32 p
(Grant SMC-611-303-013)
(Rept-89-10; ISSN-0922-5641; ETN-89-95444) Copyright Avail: NTIS HC A03/MF A01

One of the major problems in kernel density estimation, the choice of bandwith, is addressed. The first order properties of the likelihood cross-validation bandwidth selection method, introduced by Habbema, Hermans and Van den Broek (1974) and Duin (1976) are reviewed. This method was modified by Marron (1985) to obtain an asymptotic optimality property for Lipschitz densities. For densities with jumps the modified method is shown to lose this optimality property. The asymptotic normality of the distance of the likehood cross-validation bandwidth to the minimizer of a suitable integrated squared error is established. Comparisons with related results for least cross-validation are included. ESA

70 PHYSICS (GENERAL)

For precision time and time interval (PTTI) see *35 Instrumentation and Photography;* for geophysics, astrophysics or solar physics see *46 Geophysics, 90 Astrophysics,* or *92 Solar Physics.*

N90-12280# Department of the Army, Washington, DC.
PERIODIC PERMANENT MAGNET STRUCTURES Patent Application
Herbert A. Leupold, inventor (to Army) 3 Jul. 1989 14 p
(AD-D014173; US-Patent-Appl-SN-375218) Avail: NTIS HC A03/MF A01 CSCL 20/7

Periodic permanent magnet structures comprise a plurality of paired axially aligned sections of hollow spherical flux sources each of which produces a uniform high-field in its central cavity. Each pair of sections is mounted on opposite sides of a respective plate of permeable material. The magnetic field orientations in the central cavities are axially directed and alternate or reverse in direction from section to section. An axial bore hole drilled through the sections and plates provides a continuous channel or path through which a beam of charged particles will travel. GRA

N90-12281# Department of the Navy, Washington, DC.
THIN FILM MAGNETIC MEMORY ELEMENTS Patent Application
Gary Z. Prinz, inventor (to Navy) 1 Jun. 1989 21 p
(AD-D014178; US-Patent-Appl-SN-360173) Avail: NTIS HC A03/MF A01 CSCL 12/6

This invention is directed to a high density magnetic film memory storage device, and more particularly to such a memory storage device wherein the individual storage elements are patterned on a substrate using the intrinsic and structural anisotropies of the particular magnetic film, such that fringing fields about each storage element are eliminated. The first commercial random access nonvolatile magnetic memories were magnetic core systems in which circular magnetic ferrite cores were used as memory element, were arranged in large three-dimensional arrays, and were coupled to selected wire wraps for reading and writing. GRA

N90-12282*# National Aeronautics and Space Administration. Lewis Research Center, Cleveland, OH.
PARAMETRIC STUDY OF POWER ABSORPTION FROM ELECTROMAGNETIC WAVES BY SMALL FERRITE SPHERES
Gerald W. Englert Nov. 1989 22 p
(NASA-TP-2949; E-4601; NAS 1.60:2949) Avail: NTIS HC A03/MF A01 CSCL 20C

Algebraic expressions in terms of elementary mathematical functions are derived for power absorption and dissipation by eddy currents and magnetic hysteresis in ferrite spheres. Skin depth is determined by using a variable inner radius in descriptive integral equations. Numerical results are presented for sphere diameters less than one wavelength. A generalized power absorption parameter for both eddy currents and hysteresis is expressed in terms of the independent parameters involving wave frequency, sphere radius, resistivity, and complex permeability. In general, the hysteresis phenomenon has a greater sensitivity to these independent parameters than do eddy currents over the ranges of independent parameters studied herein. Working curves are presented for obtaining power losses from input to the independent parameters. Author

N90-12283# Nationaal Inst. voor Kernfysica en Hoge Energiefysica, Amsterdam (Netherlands).
OPERATOR PRODUCT COEFFICIENTS IN NON-DIAGONAL CONFORMAL FIELD THEORIES
Juergen Fuchs Nov. 1988 11 p
(PB89-216873; NIKHEF-H-87-19) Avail: NTIS HC A03/MF A01 CSCL 20C

The problems involved in the determination of operator product coefficients in nondiagonal conformal field theories (RCFTs) are explained. The methods of Dotsenko and Fateev are used to derive formulae which allow computing these coefficients. A careful treatment of the issue of uniqueness of the results proves to be necessary. It is deemed appropriate to analyze the four-point functions of RCFTs in sufficient detail so as to be able to determine unambiguously the operator product coefficients of these theories. The outcome of such an analysis is examined (details will appear elsewhere). It turns out that the methods of Dotsenko and Fateev are sufficient to attack the nondiagonal case, provided the subtle issue of uniqueness of the four-point functions is taken care of. The formulae are somewhat unwieldy, but can be easily evaluated on a computer. The results apply directly to the case of c less than 1 RCFTs and to A1 Wess-Zumino-Witten theories where the differential equations for the four-point functions are known explicitly, but analogous considerations will be valid for any RCFT. GRA

N90-12284# California Univ., Berkeley. Lawrence Berkeley Lab. Accelerator and Fusion Research Div.
THE EFFECT OF FLUX CREEP ON THE MAGNETIZATION FIELD IN THE SSC DIOPOLE MAGNETS
W. S. Gilber, R. F. Althaus, P. J. Barale, R. W. Benjegerdes, M. A. Green, M. I. Green, and R. M. Scanlan Jun. 1989 9 p
Presented at the International Cryogenic Materials Conference, Los Angeles, CA, 24-28 Jul. 1989
(Contract DE-AC03-76SF-00098)
(DE90-000124; LBL-26598; CONF-890701-6) Avail: NTIS HC A02/MF A01

The sextuple fields of model SSC dipole magnets were observed to change with time when the magnets are held at constant current under conditions similar to injection into the SSC accelerator. The changes in the sextupole component have close to a linear log time dependence, and is felt to be caused by flux creep decay of the magnetization currents in the superconductor filaments. Measurements of this decay were made under various conditions. The conditions include various central field inductions and changes of field prior to when the decay was measured. The measured field decay in the dipole's sextupole is proportional to the magnitude and sign of the sextupole due to magnetization which was measured at the start of the decay. This suggests that the decay is a bulk superconductivity flux creep. Proximity coupling appears to play only a minor role in the flux creep according to recent LBL measurements with a stable power supply. DOE

N90-12285# Technische Univ., Vienna (Austria). Inst. of Applied and Technical Physics.
ANISOTROPY AND MICROSTRUCTURE OF HIGH-COERCIVITY RARE EARTH PERMANENT MAGNETS Final Technical Report
Josef Fidler, Roland Grossinger, Hans Kirchmayr, and Peter Skalicky Jun. 1989 27 p
(Contract DAJA45-86-C-0010)
(AD-A211905; R/D-5295-MS-01) Avail: NTIS HC A03/MF A01 CSCL 20/3

In Nd2Fe14B-based permanent magnets the coercivity is in practice only 20 to 40 percent of the theoretical limits. The aim of this study is to investigate Nd-Fe-B based compounds with respect to their magnetic anisotropy behavior and to characterize the microstructure of sintered Nd-Fe-B based permanent magnets. The anisotropy field HA was determined by using the Singular Point Detection (SPD) technique, and the microstructural investigations were carried out on a JEOL 200 CS analytical transmission electron microscope equipped with a high take-off energy dispersive (EDS) x ray analyzer. GRA

N90-12286# Boston Univ., MA. Dept. of Physics.
KINETICS OF DIFFUSION-CONTROLLED REACTIONS Final Report, 1 Jan. 1986 - 30 Jun. 1989
Sidney Redner 22 Aug. 1989 14 p
(Contract DAAL03-86-K-0025)
(AD-A212161; ARO-23084.11-CH) Avail: NTIS HC A03/MF A01 CSCL 20/5

There were three primary goals of this project. First, we elucidated fundamental aspects of the kinetics of diffusion-controlled reactions. While the rate equations provide a useful starting point for treating reaction kinetics, this approach neglects the effects of fluctuations, and these can play a dominant role in governing the kinetics in the diffusion controlled limit. Thus, it is crucial to determine exactly when and in what manner fluctuations manifest themselves. A second broad goal of this project was to map out the kinetics of General Classes of aggregating and fragmenting systems. Intriguing non-universal behavior was found for aggregation processes in which there is more than one type of monomeric species. Novel steady-state properties were found in an aggregating system with localized input and output. A scaling theory was also developed to understand the kinetics of fragmentation processes. Our very general approach allowed us to classify essentially all previous results into simple universality classes. Finally the dynamics of random multiplicative processes were studied, and the role of correlations in determining statistical properties was elucidated. GRA

N90-12287# Washington State Univ., Pullman. Dept. of Chemistry.
LUMINESCENCE IN APPLIED MAGNETIC FIELDS Final Report, 16 May 1987 - 15 May 1989
G. A. Crosby 15 Aug. 1989 5 p
(Contract N00014-87-K-0444)
(AD-A211551; TR-9-ONR) Avail: NTIS HC A01/MF A01 CSCL 07/5

Metal complexes and solids were synthesized and subjected to photoexcitation measurements under the influence of externally applied magnetic fields. The photoluminescence of complexes of rhodium (I) and iridium (I) displayed both field induced emission bands and a many fold shortening of the excited state lifetime. Both the decay rates and the induced emission band intensities showed a quadratic dependence on the applied field. A several fold shortening of the phosphorescence from the octaphosphitoplatinum (II) anion under an applied field (50 T) was also observed. Spectroscopic studies of several bis (N-heterocyclic) complexes of copper (I) were also concluded and complete group theoretic assignments of the charge transfer excited states were made. The technique of Thermal Modulation was perfected and applied to the study of the exited states of transition metal complexes with near degenerate emitting states. GRA

N90-12288# European Space Agency, Paris (France).
EQUILIBRIUM SOLUTIONS OF A SPHERICAL PENDULUM WITH ROTATING POINT OF SUSPENSION AND FRICTION
Ernst A. Bockemueller (Deutsche Forschungs- und Versuchsanstalt fuer Luft- und Raumfahrt, Brunswick, Germany, F.R.) Jun. 1989 40 p Transl. into ENGLISH of Gleichgewichtsloesungen des Sphaerischen Pendels mit Rotierendem Aufhaengepunkt und Widerstand (Brunswick, Fed. Republic of Germany, DFVLR) 45 p Original language document previously announced as N89-19966
(ESA-TT-1139; DFVLR-Mitt-88-24; ETN-89-95519) Avail: NTIS HC A03/MF A01; original German version available from DFVLR, VB-PL-DO, Postfach 90 60 58, 5000 Cologne, Fed. Republic of Germany

The analysis of a rotating pendulum with rotating point of suspension and friction is performed. For this nonlinear system with time dependent constraints, the equilibrium solutions in the rotating coordinate system are studied. The analysis leads to the conclusions that the number and the stability of these solutions depend on the system parameters. The investigations show that the velocity coupling between the degrees of freedom is decisive for the stablity of the solutions. ESA

71 ACOUSTICS

Includes sound generation, transmission and attenuation. For noise pollution see *45 Environmental Pollution.*

N90-12289* National Aeronautics and Space Administration. Pasadena Office, CA.
ACOUSTIC CONTROLLED ROTATION AND ORIENTATION Patent
Martin B. Barmatz, inventor (to NASA) and James L. Allen, inventor (to NASA) (Jet Propulsion Lab., California Inst. of Tech., Pasadena.) 31 Jan. 1989 10 p Filed 29 Oct. 1986
(NASA-Case-NPO-16995-1-CU; US-Patent-4,800,756; US-Patent-Class-73-505; US-Patent-Class-73-571; US-Patent-Appl-SN-924297) Avail: U.S. Patent and Trademark Office CSCL 20A

Acoustic energy is applied to a pair of locations spaced about a chamber, to control rotation of an object levitated in the chamber. Two acoustic transducers applying energy of a single acoustic mode, one at each location, can (one or both) serve to levitate the object in three dimensions as well as control its rotation. Slow rotation is achieved by initially establishing a large phase difference and/or pressure ratio of the acoustic waves, which is sufficient to turn the object by more than 45 deg, which is immediately followed by reducing the phase difference and/or pressure ratio to maintain slow rotation. A small phase difference and/or pressure ratio enables control of the angular orientation of the object without rotating it. The sphericity of an object can be measured by its response to the acoustic energy.
Official Gazette of the U.S. Patent and Trademark Office

N90-12290*# Rensselaer Polytechnic Inst., Troy, NY. Dept. of Mathematical Sciences.
ACOUSTICAL EFFECTS OF A LARGE RIDGE ON LOW-FREQUENCY SOUND PROPAGATION IN STATIONARY AND MOVING ATMOSPHERES
J. S. Robertson, M. J. Jacobson, W. L. Siegmann, and D. P. Santandrea 20 Nov. 1989 29 p
(Grant NAG1-929)
(NASA-CR-186001; NAS 1.26:186001; RPI-181) Avail: NTIS HC A03/MF A01 CSCL 20A

The effects of a ridge on a low-frequency acoustic propagation in quiescent and windy atmospheres are investigated using a parabolic approximation. A logarithmic wind-speed profile, commonly employed to model atmospheric wind currents, is modified and used to model two-dimensional atmospheric flow over a triangularly-shaped hill. The parabolic equation is solved using an implicit finite-difference algorithm. Several examples are examined to determine the combined effects of source-ridge distance, ridge dimensions, wind-speed profile, and CW source frequency on the received acoustic field. Author

N90-12291# Technische Hogeschool, Delft (Netherlands). Faculty of Aerospace Engineering.
NOISE DATA OF FOUR SMALL PROPELLER-DRIVEN AIRPLANES
G. J. J. Ruijgrok and D. M. vanPaassen Aug. 1988 39 p
(PB89-216980; LR-544) Avail: NTIS HC A03/MF A01 CSCL 20A

Maximum observed noise levels in terms of dBA are presented for four typical small propeller-driven airplaines. The data are derived from the results of inflight noise recordings taken by the Faculty of Aerospace Engineering of Delft University of Technology. Maximum levels versus distance as a function of powersetting are given wherever possible. GRA

N90-12292*# National Aeronautics and Space Administration. Langley Research Center, Hampton, VA.
PREDICTION OF THE THERMAL ENVIRONMENT AND THERMAL RESPONSE OF SIMPLE PANELS EXPOSED TO RADIANT HEAT
Travis L. Turner and Robert L. Ash (Old Dominion Univ., Norfolk, VA.) Oct. 1989 58 p
(NASA-TM-101660; NAS 1.15:101660) Avail: NTIS HC A04/MF A01 CSCL 20A

A method of predicting the radiant heat flux distribution produced by a bank of tubular quartz heaters was applied to a radiant system consisting of a single unreflected lamp irradiating a flat metallic incident surface. In this manner, the method was experimentally verified for various radiant system parameter settings and used as a source of input for a finite element thermal analysis. Two finite element thermal analyses were applied to a thermal system consisting of a thin metallic panel exposed to radiant surface heating. A two-dimensional steady-state finite element thermal analysis algorithm, based on Galerkin's Method of Weighted Residuals (GFE), was formulated specifically for this problem and was used in comparison to the thermal analyzers of the Engineering Analysis Language (EAL). Both analyses allow conduction, convection, and radiation boundary conditions. Differences in the respective finite element formulation are discussed in terms of their accuracy and resulting comparison discrepancies. The thermal analyses are shown to perform well for the comparisons presented here with some important precautions about the various boundary condition models. A description of the experiment, corresponding analytical modeling, and resulting comparisons are presented. Author

N90-12293# Naval Ocean Systems Center, San Diego, CA.
NUMERICAL SOLUTION OF ACOUSTIC-STRUCTURE INTERACTION PROBLEMS Final Report
H. A. Schenck and G. W. Benthien Apr. 1989 35 p
(AD-A211505; NOSC/TR-1263) Avail: NTIS HC A03/MF A01 CSCL 20/1

A technique is described for solving steady state coupled structure-acoustics problems that has been implemented by the transducer modeling group at the NOSC. This technique is applicable to both structural radiation problems and structural scattering problems. The structural portion of the problem is modeled using a standard finite element program. The particular program used at NOSC is MARTSAM, but virtually any general finite element code could be used. The acoustical portion of the problem is modeled using the Combined Helmholtz Integral Equation Formulation (CHIEF). This technique was implemented at NOSC in a computer program that is also called CHIEF. A technique is described for solving steady coupled structure-acoustics problems. GRA

72 ATOMIC AND MOLECULAR PHYSICS

Includes atomic structure, electron properties, and molecular spectra.

N90-12294# Lawrence Livermore National Lab., CA.
ATOMIC AND MOLECULAR SURFACE AND VOLUME PROCESSES IN THE ANALYSIS OF NEGATIVE HYDROGEN DISCHARGES
J. R. Hiskes and A. M. Karo 3 Jul. 1989 9 p Presented at the NATO Advanced Study Institute on Non-equilibrium Processes in Partially Ionized Gases, Acquafredda di Maratea, Italy, 4-17 Jun. 1989
(Contract W-7405-eng-48; AF-AFOSR-ISSA-89-0039)
(DE89-015705; UCRL-101309; CONF-890697-1) Avail: NTIS HC A02/MF A01

The principal source of negative ion generation in hydrogen discharges is now recognized to be low-energy electron attachment to H2(nu prime prime) molecules excited to the middle portion of the vibrational spectrum. Electron excitation processes are generally taken to be the principal source of H2(nu prime prime) generation, with high-energy excitations through the singlet spectrum being the principal excitation process populating the active portion of the vibrational spectrum. A description of the collisional re-excitation from level (nu)(prime)(prime), to level (nu)(prime)(prime), requires 15 x 15 matrix of cross sections linking all initial and final levels. These cross sections were evaluated and incorporated into the modelling code. An additional source of vibrational excitation may be derived from recombination of H2(+) and H3(+) ions on the surfaces of the discharge. In this case the molecular ions will impinge with kinetic energies given by the plasma potential, 1 to 10 eV. The evaluation of H2(nu prime prime) resulting from the surface recombination process is reported. The use of low work function materials for the discharge surfaces makes possible two additional sources of negative ions: the direct dormation of negative ions by hydrogen atoms rebounding from the surface, and the dissociation of H2(-) ions formed in the surface selvage. DOE

N90-12295# Oak Ridge National Lab., TN.
BEAM DYNAMICS OF A LIQUID METAL ION SOURCE
J. H. Whealton, P. S. Meszaros, K. E. Rothe, R. J. Raridon, and P. M. Ryan 1989 14 p Presented at the International Conference on Ion Sources, Berkeley, CA, 9-15 Jul. 1989
(Contract DE-AC05-84OR-21400)
(DE89-015856; CONF-890703-13) Avail: NTIS HC A03/MF A01

RMS emittance growth of liquid metal ion sources is studied. Processes included are nonlinear expansion through extractor and accelerator fringe fields, nonlinear beam space charge, plasma effects near needle, and waves (either ion-acoustic or space charge limited as considered by V. I. Dudnikov). This investigation consists of 2-D analysis of appropriate Vlasov-Poisson equations in both steady-state and time-dependent formulations. Various geometries will be considered such as some used by G. Alton of ORNL. DOE

N90-12296# Los Alamos National Lab., NM.
DAVYDOV SOLUTIONS AT 300 KELVIN: THE FINAL SEARCH
P. S. Lomdahl and W. C. Kerr (Wake Forest Univ., Winston-Salem, NC.) 1989 10 p Presented at the NATO Workshop on Localization of Energy in Proteins, (Denmark), 1-5 Aug. 1989
(Contract W-7405-eng-36)
(DE89-015248; LA-UR-89-2453; CONF-8908122-2) Avail: NTIS HC A02/MF A01

The original proposal by Professor A. S. Davydov of a soliton mechanism for localization and transport of energy along linear chain molecules provided the impetus for several research efforts which explored the properties of these nonlinear entities in differing degrees of realism. The general conclusion from all of this work is that the nonlinear equations of motion which have been used to describe these systems have soliton-like solutions when they are solved in the deterministic limit. This limit corresponds to the absolute zero of temperature, because it ignores the influence of random thermal perturbations on the system. However, the questions of existence and importance of the Davydov soliton remain controversial when non-zero temperature effects are taken into account, because numerical simulations and theoretical calculations done by independent research groups have reached diametrically opposed conclusions. Our 1985 paper was the first to simulate thermal perturbations at biologically relevant temperature (300 K). Since publishing that paper, we have done simulations for collisions of phonon wave packets with Davydov solitons and have also taken into account the presence of multiple quanta of the high frequency oscillator field in the Davydov equations of motion. We present these results here. However, for the major question about the temperature effects on the Davydov soliton, our conclusions remain unchanged. DOE

N90-12297# Los Alamos National Lab., NM.
QUANTUM-MECHANICAL DERIVATION OF THE DAVYDOV EQUATIONS FOR MULTI-QUANTA STATES
W. C. Kerr (Wake Forest Univ., Winston-Salem, NC.) and P. S. Lomdahl 1989 9 p Presented at the NATO Workshop on Localization of Energy in Proteins, Denmark, 1-5 Aug. 1989
(Contract W-7405-eng-36)
(DE89-015250; LA-UR-89-2446; CONF-8908122-1) Avail: NTIS HC A02/MF A01

The purpose here is to present a derivation of the Davydov equations which employs only quantum-mechanical techniques. The derivation here is more general than the previous treatment of this problem because an Ansatz is used which has present several quanta of the high frequency oscillator system rather than just one quantum. Since some steps of the calculation are the same as those in the paper which treats the single quantum case, reference will be made to that paper for some of the those details. DOE

N90-12298*# Stanford Univ., CA. Center for Space Science and Astrophysics.
THE BEHAVIOR OF BEAMS OF RELATIVISTIC NON-THERMAL ELECTRONS UNDER THE INFLUENCE OF COLLISIONS AND SYNCHROTRON LOSSES
James M. McTiernan (California Univ., Berkeley.) and Vahe Petrosian Nov. 1989 59 p
(Grants NsG-7092; NGR-05-020-668; NSF ATM-83-20439)
(NASA-CR-185983; NAS 1.26:185983) Avail: NTIS HC A04/MF A01 CSCL 20H

For many astrophysical situations, such as in solar flares or cosmic gamma-ray bursts, continuum gamma rays with energies up to hundreds of MeV were observed, and can be interpreted to be due to bremsstrahlung radiation by relativistic electrons. The region of acceleration for these particles is not necessarily the same as the region in which the radiation is produced, and the effects of the transport of the electrons must be included in the general problem. Hence it is necessary to solve the kinetic equation for relativistic electrons, including all the interactions and loss mechanisms relevant at such energies. The resulting kinetic equation for non-thermal electrons, including the effects of Coulomb collisions and losses due to synchrotron emission, was solved analytically in some simple limiting cases, and numerically for the general cases including constant and varying background plasma density and magnetic field. New approximate analytic solutions are presented for collision dominated cases, for small pitch angles and all energies, synchrotron dominated cases, both steady-state and time dependent, for all pitch angles and energies, and for cases when both synchrotron and collisional energy losses are important, but for relativistic electrons. These analytic solutions are compared to the full numerical results in the proper limits. These results will be useful for calculation of spectra and angular distribution of the radiation (x rays, gamma-rays, and microwaves) emitted via synchrotron or bremsstrahlung processes by the electrons. These properties and their relevance to observations will be observed in subsequent papers. Author

N90-12299# Los Alamos National Lab., NM. Theoretical Div.
NEW DEVELOPMENTS IN THE AB INITIO TREATMENT OF LOW ENERGY ELECTRON COLLISIONS WITH MOLECULES
B. I. Schneider, T. N. Rescigno, C. William McCurdy, and Byron H. Lengsfield, III (Lawrence Livermore National Lab., CA.) 1989 16 p Presented at the International Conference on the Physics of Electronic and Atomic Collisions, New Haven, CT, 23-25 Jul. 1989 Submitted for publication
(Contract W-7405-eng-36)
(DE89-015294; LA-UR-89-2506; CONF-8907135-1) Avail: NTIS HC A03/MF A01

Although there has been substantial progress in the ab initio treatment of low energy electron scattering from small diatomic and polyatomic molecules in the last few years a number of problems still remain. Most current research has focused on the calculation of fixed nuclei scattering amplitudes in the static-exchange (SE) approximation. A few calculations have gone beyond this approximation to include electron correlation and/or vibrational and rotational effects, the latter often within the framework of model or parameterized potentials. In this article we review a number of developments which have occurred since the last electron molecule satellite meeting at Daresbury Laboratory in July 1987. Our primary objective shall be to point out the strengths and weaknesses of current computational capabilities and to describe a new approach to electron polyatomic collisions using the complex Kohn method. DOE

N90-12300# Argonne National Lab., IL. Physics Div.
MONTE CARLO STUDIES OF NUCLEI AND QUANTUM LIQUID DROPS
V. R. Pandharipande (Illinois Univ., Urbana-Champaign.) and S. C. Pieper 1989 12 p Presented at the Symposium on the Occasion of the 40th Anniversary of the Nuclear Shell Model, Argonne, IL, 25-27 May 1989
(Contract W-31-109-eng-38)
(DE89-016914; CONF-890583-3) Avail: NTIS HC A03/MF A01

The progress in application of variational and Green's function Monte Carlo methods to nuclei is reviewed. The nature of single particle orbitals in correlated quantum liquid drops is discussed, and it is suggested that the difference between quasiparticle and mean field orbitals may be of importance in nuclear structure physics. DOE

N90-12301# Oak Ridge National Lab., TN.
SYNCHROTRON-RADIATION EXPERIMENTS WITH RECOIL IONS
Jon C. Levin (Tennessee Univ., Knoxville.) 1989 8 p Presented at the 16th International Conference on the Physics of Electronic and Atomic Collisions, New York, NY, 26 Jul. - 1 Aug. 1989
(Contract DE-AC05-84OR-21400)
(DE89-017579; CONF-890708-7) Avail: NTIS HC A02/MF A01

Studies of atoms, ions and molecules with synchrotron radiation have generally focused on measurements of properties of the electrons ejected during, or after, the photoionization process. Much can also be learned, however, about the atomic or molecular relaxation process by studies of the residual ions or molecular fragments following inner-shell photoionization. Measurements are reported of mean kinetic energies of highly charged argon, krypton, and xenon recoil ions produced by vacancy cascades following inner-shell photoionization using white and monochromatic synchrotron x radiation. Energies are much lower than for the same charge-state ions produced by charged-particle impact. The results may be applicable to design of future angle-resolved ion-atom collision experiments. Photoion charge distributions are presented and compared with other measurements and calculations. Related experiments with synchrotron-radiation produced recoil ion, including photoionization of stored ions and measurement of shakeoff in near-threshold excitation, are briefly discussed. DOE

N90-12302# Oak Ridge National Lab., TN.
FLUCTUATIONS IN TRANSVERSE ENERGY AND MULTIPLICITY, ENERGY DENSITIES, AND NEUTRAL PION SPECTRA IN NUCLEUS-NUCLEUS COLLISIONS AT 200 GeV/NUCLEON
F. Plasil, R. Albrecht, T. C. Awes, C. Baktash, P. Beckmann, F. Berger, R. Bock, G. Claesson, G. Clewing, and L. Dragon (Muenster Univ., Germany, F.R.) 1989 18 p Presented at the International Nuclear Physics Conference, Sao Paulo, Brazil, 20-26 Aug. 1989
(Contract DE-AC05-84OR-21400)
(DE89-017583; CONF-890826-3) Avail: NTIS HC A03/MF A01

The main goal of the CERN heavy-ion experiments is the search for an indication that the predicted state of deconfined quarks and gluons, the quark-gluon plasma (QGP), has been produced. The quantity most crucial to the probability of QGP formation is the thermalized energy density attained during the heavy-ion reaction. The amount of energy radiated transverse to the beam direction is the experimental quantity which is believed to be a measure of the amount of energy deposition in the reaction, and hence to reflect the energy density attained. In this presentation we consider the systematics of transverse energy production at CERN SPS energies, and we use the results to make estimates, under various assumptions, of attained energy densities. Measurements of direct photons and lepton pairs are considered to be among the most promising methods for studies of the QGP. In contrast to hadrons, direct photons are not expected to undergo any interactions after their creation. The measurement of direct photons was undertaken. This is a difficult task due to the presence of a high background of photons from the decay of neutral pions. The pion (sup 0) spectra themselves, however, provide us with the opportunity to study the excited reaction zone during the hadronization phase. We present here measurements of neutral pions produced in O-16 + Au collisions at 200 GeV/nucleon. DOE

N90-12303# Aerospace Corp., El Segundo, CA. Aerophysics Lab.
SPIN-ORBIT RELAXATION RATES OF Bi(6p(3)) 2D(3/2) FOLLOWING PHOTOLYSIS OF Bi(CH3)3 AT LAMBDA = 193 nm
J. S. Holloway, J. B. Koffend, and R. F. Heidner, III 7 Jul. 1989 32 p
(Contract F04701-88-C-0089)
(AD-A211792; TR-0089(4604)-1; SD-TR-89-49) Avail: NTIS HC A03/MF A01 CSCL 07/4

Rate coefficients for the collisional relaxation of the first excited spin-orbit state of Bismuth (6p3, 2D3/2) have been measured at 295 K for argon, carbon dioxide, sulfur hexaflouride, hydrogen, deuterium, hydrogen flouride. The excited Bi atoms were prepared by excimer laser photolysis of trimethyl bismuth (TMB) at 193 nm and monitored directly in emission. The rate coefficient for quenching by the precursor TMB and a lower limit for removal by CH3 photofragments have also been established. Where applicable, our results are compared with the earlier work of Bevan and Husain and of Trainor. The suitability of long-range interaction models is discussed for those cases where isotopic substitution leads to markedly different quenching rates. GRA

N90-12304# Gordon Research Conferences, Inc., Kingston, RI.
GORDON CONFERENCE ON ATOMIC PHYSICS Final Report
Thomas J. McIlrath and David Wineland Apr. 1989 9 p Conference held in Wolfeboro, NH, 6-10 Jul. 1987
(Grant AF-AFOSR-0214-87; AF Proj. 2301)
(AD-A211946; AFOSR-89-1112TR) Avail: NTIS HC A02/MF A01 CSCL 20/5

Topics covered included Atoms in High Magnetic Fields, Atoms in High Optical Fields, Multi-electron Excitation of Atoms, Relativistic Spectra of Atoms, Atoms in Traps, Quantum Jumps, Squeezed States, Muon Induced Fusion, Microwave Ionization of Atoms and Chaos in Atomic Ionization. A poster session was held in addition to the morning and evening sessions. GRA

N90-12305# Jet Propulsion Lab., California Inst. of Tech., Pasadena.
ION FORMATION BY ELECTRON IMPACT Final Report, 31 May 1985 - 30 Nov. 1988
Santosh K. Srivastava 30 Nov. 1988 53 p
(Grants AF-AFOSR-ISSA-87-0036; AF-AFOSR-ISSA-88-0014; AF-AFOSR-ISSA-85-0070; AF-AFOSR-ISSA-86-0036; AF Proj. 2301)
(AD-A211367; AFOSR-89-1102TR) Avail: NTIS HC A04/MF A01 CSCL 20/5

Dissociative attachment and polar dissociation cross sections were measured for the following molecules: HC1, NO, N2O, C6H6, SiH4, Si2H6, and LiH. Direct ionization and dissociative ionization cross sections were determined for the following molecules: H2, D2, N2, O2, He, Ne, Ar, Kr, Xe, H2O, Co, CO2, CH4, SiH4, Sih4, Si2H6, N2*, and NH3. An experimental apparatus for a pulsed extraction technique was fabricated and successfully tested. GRA

N90-12306# Bowling Green State Univ., OH. Center for Photochemical Sciences.
LIFETIME OF SINGLET OXYGEN IN AQUEOUS HYDROGEN PEROXIDE (BHP) Final Report, 18 Sep. 1987 - 22 Feb. 1989
M. A. J. Rodgers and M. A. Shand May 1989 24 p
(Contract F29601-87-K-0076)
(AD-A211545; AFWL-TR-89-07) Avail: NTIS HC A03/MF A01 CSCL 20/5

Singlet delta oxygen lifetime in deuterated basic hydrogen peroxide was measured. The contributing bimolecular rate constants were measured as a function of temperature. The measured lifetime of 20 microseconds compared favorably to the lifetime of 24 microseconds arrived at by using contributing bimolecular rates. GRA

N90-12307# Stanford Univ., CA.
STATE-RESOLVED REACTION DYNAMICS Final Report, 1 Nov. 1985 - 31 Oct. 1988
Richard N. Zare 12 Jul. 1989 25 p
(Contract F49620-86-C-0016)
(AD-A211613; AFOSR-89-1060TR) Avail: NTIS HC A03/MF A01 CSCL 20/5

A single time-of-flight (TOF) photoelectron spectrometer is to be used in conjunction with the Multiphoton Ionization Photoelectron (MPI) of jet-cooled molecules. This apparatus will measure energy and single resolved photoelectron spectra. Such information was of direct use in measuring the internal state distribution of Resonance Enhanced Multiphoton Ionization Photoelectron (REMPI) formed ions used in ion-molecule reaction studies. The laser induced fluorescence (LIF) technique was developed to probe ion species. The ions produced directly from REMPI can have their rotational propensity roles in photoionization processes. The ions produced from a reaction between the state selected ions generated by REMPI and other molecules can be observed for studying state to state ion molecule reaction dynamics. The reactions of ammonia cations with neutral molecule, were conducted using a tandem quadropole mass spectrometer. A new tapole ion trap was proposed to increase vastly the control over and understanding of biomolecular ion-molecular reactions. To make the quadropole/octapole/quadropole ion trap operational it was necessary to solve the technically challenging problem of interfacing three dissimilar radio frequency (RF) devices. GRA

N90-12308# Swedish Inst. of Space Physics, Kiruna.
ON THE ROLE OF COULOMB FORCES IN ATOMIC RADIATIVE EMISSION
Sten Yngstrom Oct. 1988 19 p
(IRF-Preprint-106; ETN-89-95158) Avail: NTIS HC A03/MF A01

It is shown how the generalized Coulomb interaction (electric and magnetic fields of force) competes with the radiative interaction. It causes overall inhibition of the radiative capability of atoms and ions in a gaseous sample of matter. Basic quantum mechanical aspects of the electromagnetic interaction are discussed in a heuristic introduction. A treatment in the formalism of relativistic quantum electrodynamics, is effectuated. ESA

N90-12309 Max-Planck-Inst. fuer Physik und Astrophysik, Garching (Germany, F.R.). Werner-Heisenberg-Inst. fuer Physik.
EXPERIMENTAL TEST OF PCAC HYPOTHESIS IN THE REACTIONS MU NEUTRINO-PROTON GIVING MUON(-)-PROTON-PION(+) AND MU ANTINEUTRINO-PROTON GIVING MUON(+)-PROTON-PION(-) IN THE DELTA (1232) REGION
G. T. Jones, R. W. L. Jones, B. W. Kennedy, S. W. ONeale, D. R. O. Morrison, M. M. Mobayen, S. Wainstein (Imperial Coll. of Science and Technology, London, England), M. Aderholz, D. Hantke, and E. Hoffmann et al Apr. 1989 31 p
(MPE-PAE/Exp.El.199; ETN-89-95337) Copyright Avail: Fachinformationszentrum Karlsruhe, 7514 Eggenstein-Leopoldshafen 2, Federal Republic of Germany

Data on the mu neutrino-proton and mu anti-neutrino proton giving respectively muon(-)-proton-pion(+) and muon(+)-proton-pion(-) in the delta (1232) is presented. A test of the PCAC hypothesis is performed. The analysis is based on 1081 events in the neutrino and on 180 events in the antineutrino reaction, obtained in the big European bubble chamber experiment. The experimental cross sections for the neutrino and the antineutrino reaction are determined. The four-momentum transfer squared and the invariant hadionic mass distributions, the density matrix elements of the delta resonance, and moments of the pion angular distributions, are discussed. At low four-momentum transfer squared, the data confirm the PCAC hypothesis and the discrepancy, observed between the experimental and theoretical cross sections for the mu neutrino-proton reaction, is understood as being due to inadequate pion off-mass-shell corrections. ESA

73 NUCLEAR AND HIGH-ENERGY PHYSICS

Includes elementary and nuclear particles; and reactor theory.

For space radiation see *93 Space Radiation.*

N90-12310# Tokyo Univ., Tanashi (Japan). Inst. for Nuclear Study.
FABRICATION OF MODULATED VANES FOR A SPLIT-COAXIAL RFQ
T. Fujino (National Lab. for High Energy Physics, Ibaraki, Japan), S. Arai, T. Fukushima, N. Sakamoto, and E. Tojyo Sep. 1988 23 p In JAPANESE; ENGLISH summary
(DE88-757235; INS-T-485) Avail: NTIS (US Sales Only) HC A03/MF A01

Modulated vanes installed in a split-coaxial RFQ were fabricated at the INS machine shop. Each modulated vane, 205 cm long, is assembled by connecting 11 short vane pieces. The pieces were machined with an NC lathe operated like a milling machine. A ball end mill is mounted in the rotor and a vane piece is fixed by a special vise attached at the tool post; the vise moves vertically, and the tool post dose two-dimensionally in the horizontal plane. In the report, the development of the vise attachment, the calculation of the vane-tip geometry, the NC program, the machining process are described. DOE

N90-12311# Purdue Univ., West Lafayette, IN. Dept. of Physics.
AN EXPERIMENTAL HIGH ENERGY PHYSICS PROGRAM Progress Report, Jan. 1988 - May 1989
J. A. Gaidos, F. J. Loeffler, R. L. McIlwain, D. H. Miller, T. R. Palfrey, and E. I. Shibata 1 May 1989 27 p
(Contract DE-AC02-76ER-01428)
(DE89-014695; DOE/ER-01428/T1) Avail: NTIS HC A03/MF A01

The CLEO detector accumulated, (approximately 480,000 B-mesons) the world's largest sample of B decays, before being shutdown in May 1988 for the installation of CLEO II. This data sample came from 335 pb(-1) accumulated at the upsilon (4S). The Cornell Electron Storage Ring set new luminosity records, reaching 3.5 pb(-1) in a single day. These data are being intensively analyzed and 21 papers were given at the Baltimore APS meeting. Among the highlights are: confirmation of B(sup 0)(bar B)(sup 0) mixing; discovery of the charm-strange baryon xi (sub c)(sup 0); limits on b yields u decay; and non-observation of B yields p(bar p)pi(pi), which was reported by the ARGUS collaboration. The construction of CLEO II is proceeding on schedule. The new 1.5 T superconducting magnet has passed all tests and all of the detector elements have been installed. This includes a 7800 CsI crystals electromagnetic shower calorimeter. The data from the Gamma Ray Astrophysics experiment show a significant signal for high energy gamma ray emission from Cygnus X-3 and also confirm the previously reported anomalous period from Her X-1. Meanwhile, the old 6 mirror telescope has been refitted with 26 high resolution mirrors and improved fast electronics. GRANDE, the next generation detector based on the water Cherenkov technique, has been formally proposed to HEPAP. The detector will search for neutrino emission in the Southern Hemisphere and gamma radiation in the Northern Hemisphere. DOE

N90-12312# Lawrence Livermore National Lab., CA.
DART: A SIMULATION CODE FOR CHARGED PARTICLE BEAMS, REVISION 1
R. C. White, W. L. Barr, and R. W. Moir 31 Jul. 1989 44 p
Revised
(Contract W-7405-eng-48)
(DE89-016697; UCID-21330-Rev-1) Avail: NTIS HC A03/MF A01

A recently modified version of the 2-D code, DART, is presented which can simulate the behavior of a beam of charged particles whose trajectories are determined by electric and magnetic fields. This code was originally used to design laboratory-scale and full-scale beam direct converters. Since then, its utility was expanded to allow more general applications. The simulation includes space charge, secondary electrons, and the ionization of neutral gas. A beam can contain up to nine superimposed beamlets of different energy and species. The calculation of energy conversion efficiency and the method of specifying the electrode geometry are described. Basic procedures for using the code are given, and sample input and output fields are shown. DOE

N90-12313# Pacific Northwest Lab., Richland, WA.
NUCLEAR CLOSED-CYCLE GASEOUS HEAT ENGINE CONCEPT
B. A. Ross and M. K. Drost May 1989 6 p Presented at the 24th Intersociety Energy Conversion Engineering Conference, Washington, DC, 6-11 Aug. 1989
(Contract DE-AC06-76RL-01830)
(DE89-016824; PNL-SA-17011; CONF-890815-25) Avail: NTIS HC A02/MF A01

A nuclear closed-cycle gaseous heat engine concept is presented in which mechanical or electrical power is produced from the fission of uranium hexafluoride (UF6). The engine consists of a reaction chamber and piston, a regenerator, a cooler, and an expansion/compression cylinder and piston. The concept is envisioned to be useful for applications where heat sources (fossil fuel) are not easily obtained, such as for remote terrestrial or space power generation. Potential advantages include simplicity, easily transportable fuel, and reliability. The major unresolved issues include corrosion, nuclear/thermodynamic interactions, and the relatively low operating speed of the engine. DOE

N90-12314 National Physical Lab., Teddington (England). Div. of Radiation Science and Acoustics.
USE OF THE NPL LINAC FOR X RAY DOSIMETRY
J. E. Burns and J. W. G. Dale Jul. 1989 53 p
(NPL-RSA(EXT)-6; ISSN-0955-9655; ETN-89-95538) Copyright
Avail: National Physical Lab., Teddington, Middlesex, TW11 OLW, United Kingdom

The procedures adopted to control the National Physical Laboratory (NPL), UK, linear accelerator (linac) in order to achieve accurate dosimetry of x radiation are described. Attention is paid to the procedures for aligning the x ray beam with the optical axis, and to the means by which the energy of the x ray beam is kept constant. Aspects of the building and machine that are relevant to the metrology of ionizing radiation are described. Guidelines for setting up a linear accelerator for x ray dosimetry are provided. ESA

74 OPTICS

Includes light phenomena; and optical devices.
For lasers see *36 Lasers and Masers.*

N90-12315# National Oceanic and Atmospheric Administration, Boulder, CO. Wave Propagation Lab.
TURBULENCE EFFECTS ON REFLECTED OPTICAL PATTERNS (ATMOSPHERE AND STRUCTURE)
Richard J. Lataitis and James H. Churnside May 1989 16 p
(Contract ASL-87-8013)
(PB89-208094; NOAA-TM-ERL-WPL-166) Avail: NTIS HC A03/MF A01 CSCL 20F

The vacuum irradiance pattern produced by an optical beam illuminating a distant receiving plane is distorted by atmospheric turbulence. The distortion manifests itself as a wander and breathing of the beam spot. Reflected optical patterns exhibit the same type of distortion but to a degree that depends on the type of reflector. The reflected irradiance pattern is described in terms of several length scales of interest. Numerically derived optical patterns for a spherical wave reflected from a plane retroflector are also presented. Various reflector diameters and turbulence strengths are considered. GRA

N90-12316# Breault Research Organization, Tucson, AZ.
KINEMATIC DESIGN NC OPTICAL GENERATOR Final Report
William P. Kuhn 31 Aug. 1989 65 p
Avail: NTIS HC A04/MF A01

The purpose of this research was to design a low cost, versatile, 3-axis numerical control aspheric generator using all rotary motions. In addition, the generator was to have the capability of grinding glass, metals and ceramics and the ability to generate off axis or non-rotationally symmetric aspherics. The research carried out during this study was a review of various methods of implementing 3 axis motion using all rotary bearings. Traditional orthogonal axis methods of achieving this motion were found lacking in accuracy and very costly. The study then turned to a generator based on kinematic design with a minimum number of constraints to the rotary motions. The results of this research showed that the kinematic design met or exceeded all the proposed goals for this study. The design has a minimum number of components and depends for its accuracy only on the lengths of the two actuators controlling the grinding wheel position. The rotary motion joints are all spherical ball joints except for one that is a flexure pivot. The proposed generator uses commercially available components and has few custom parts to keep the cost down. Special software allows the easy fabrication of non-rotationally symmetric optics and a large grinding wheel radius minimizes mid spatial frequency surface errors and roughness. Author

N90-12317# Sandia National Labs., Albuquerque, NM.
OPERATING EXPERIENCE WITH THE SANDIA TERMINAL SWITCHING NETWORK AND FIBER OPTIC LOOP
L. F. Tolendino, S. D. Nelson, S. A. Gossage, and D. L. Bickel 1989 8 p Presented at the MILCOM, Boston, MA, 15-18 Oct. 1989
(Contract DE-AC04-76DP-00789)
(DE89-007422; SAND-88-3472C; CONF-891059-1) Avail: NTIS HC A02/MF A01

At Sandia National Laboratories, Albuquerque, secure data communications is provided by a system whose major elements include a fiber loop, technical control centers, and a terminal switching network. The optical fiber loop supplies the advantages of high bandwidth, negligible cross talk, and immunity to interference. The technical control centers, as elements on the fiber optic loop, focus regional communications and simplify distribution. The terminal switching network utilizes the optical fiber loop and the technical control centers' distribution and control capabilities to layer management and security onto the Sandia network. Other functions, such as Ethernet interconnections, also utilize the fiber loop and technical control centers. By designing data communications around this set of trusted elements, Sandia has implemented a robust, secure system without sacrificing performance or responsiveness. The experience revolves around maintaining a system that reliably serves thousands of users, responds quickly to problems and user relocations, and evolves to support new technologies while meeting stringent security requirements. DOE

N90-12318# Oak Ridge National Lab., TN.
A SURVEY OF CAMERA ERROR SOURCES IN MACHINE VISION SYSTEMS
W. B. Jatko 1989 5 p Presented at the Sensor's Expo 1989, Cleveland, OH, 12-14 Sep. 1989
(Contract DE-AC05-84OR-21400)
(DE89-014072; CONF-890996-5) Avail: NTIS HC A01/MF A01

In machine vision applications, such as an automated inspection line, television cameras are commonly used to record scene intensity in a computer memory or frame buffer. Scene data from the image sensor can then be analyzed with a wide variety of feature-detection techniques. Many algorithms found in textbooks on image processing make the implicit simplifying assumption of an ideal input image with clearly defined edges and uniform illumination. The ideal image model is helpful to aid the student in understanding the principles of operation, but when these algorithms are blindly applied to real-world images the results can be unsatisfactory. This paper examines some common measurement errors found in camera sensors and their underlying causes, and possible methods of error compensation. The role of the camera in a typical image-processing system is discussed, with emphasis on the origination of signal distortions. The effects of such things as lighting, optics, and sensor characteristics are considered. DOE

N90-12319# Sandia National Labs., Albuquerque, NM.
DISTANCE AND CLEARANCE PERCEPTION USING FORWARD-LOOKING, VEHICULAR TELEVISION SYSTEMS
Dwight P. Miller 1989 12 p Presented at the 32nd Human Factors Society Annual Meeting, Anaheim, CA, 14-28 Oct. 1989 Sponsored by Army Missile Command
(Contract DE-AC04-76DP-00789)
(DE89-014740; SAND-88-1958C; CONF-8910129-1) Avail: NTIS HC A03/MF A01

During off-road navigation, drivers often must make size, distance, and clearance judgments of terrain features and obstacles in order to choose safe navigational routes. These same judgments must be made in the teleoperation of land vehicles using forward-looking television systems. This study evaluated how well subjects perceived size, distance, and clearance using monochrome and color television systems. Thirty-eight subjects (Ss) estimated the size, distance, and separation of two obstacles using video imagery produced by a forward-looking, vehicle-mounted camera. Results indicate that Ss typically overestimated distances, and when in error judging clearance, tended to overestimate the gap between the objects. These biases were expected due to the well documented minification effect of television using standard lenses. More surprising was the somewhat larger bias evidenced by Ss using color versus those using monochrome imagery. This paper will describe the research methodology, the results obtained, potential reasons for the results, discuss the plans for continuing research in this area, and assess the implications these findings may have on teleoperated vehicle design. DOE

N90-12320# Brookhaven National Lab., Upton, NY.
THE NATIONAL SYNCHROTRON LIGHT SOURCE AND ITS APPLICATIONS
G. P. Williams 1989 13 p Presented at the International Conference on Synchrotron Radiation Application, Hefei, China, 9-12 May 1989
(Contract DE-AC02-76CH-00016)
(DE89-017605; BNL-43105; CONF-8905210-1) Avail: NTIS HC A03/MF A01

We describe the National Synchrotron Light Source facility including its beamlines and operational characteristics. Research results on selected beamlines on the VUV ring which highlight new experimental capabilities are described since they are more relevant to the program at HESYRL. Examples chosen are spin-polarized photoemission, infra-red surface science, high resolution core level spectroscopy, x ray lithography, photoelectron/Auger coincidence spectroscopy and high electron momentum resolution surface studies. DOE

N90-12321# Connecticut Univ., Storrs. Dept. of Physics.
ENERGY TRANSFER AND NON-LINEAR OPTICAL PROPERTIES AT NEAR ULTRAVIOLET WAVELENGTHS: RARE EARTH 4f(YIELDS)5d TRANSITIONS IN CRYSTALS AND GLASSES Progress Report, 1 Jun. 1984 - 31 Nov. 1989
Douglas S. Hamilton Sep. 1989 69 p
(Contract DE-FG02-84ER-45056)
(DE90-000065; DOE/ER-45056/8) Avail: NTIS HC A04/MF A01

The project has considered several aspects of the optical properties of lanthanide (rare-earth) doped crystals and glasses at near ultraviolet wavelengths. These include two-photon absorption, excited state absorption, excited-state photoionization and color center formation, two-step photoconductivity, optical gain, energy transfer, nonradiative relaxation and optical grating formation. These research projects are considered in more detail in the following section. The publications, conference presentation and thesis are listed which were completed under the auspices of this grant. A summary of the personnel supported by this grant and their accomplishments is then presented. DOE

N90-12322# California Univ., Berkeley. Lawrence Berkeley Lab. Engineering Div.
OPTICAL DATA TRANSMISSION SYSTEMS IN RADIATION ENVIRONMENT
Branko Leskovar May 1989 9 p Presented at the International Conference on Operability of Nuclear Systems in Normal and Adverse Environments, Lyon, France, 18-22 Sep. 1989
(Contract DE-AC03-76SF-00098)
(DE90-000174; LBL-26473; CONF-890911-8) Avail: NTIS HC A02/MF A01

The rapidly expanding field of optical data transmission includes a wide variety of particle accelerator, detector and nuclear power facility applications in which transmission systems are required to withstand exposure to the radiation background. Fiber optic links provide several major advantages over conventional electronic data transmission systems. These include immunity to electromagnetic interference and low transmission losses for very high data rates. The state of the art of optical transmitters, low loss fiber waveguides and receivers in radiation environment is reviewed and summarized. Emphasis is placed on the effects of irradiation on the performance of light emitting and laser diodes, optical fiber waveguides, photodiodes and associated electronics components and subassemblies. DOE

N90-12323# Naval Ocean Systems Center, Kailua, HI.
SMALL-RADIUS BENDING LOSS IN SINGLE-MODE FIBERS
Neil Kamikawa and Ching-Ten Chang (San Diego State Univ., CA.) Jul. 1989 7 p
(AD-A211822) Avail: NTIS HC A02/MF A01 CSCL 20/6

Single mode fibers with smaller mode-field radii and, therefore, tighter confinement of the mode field should exhibit lower bending losses. However, bending tests conducted on six different types of single mode fibers showed that a smaller mode field radius does not necessarily insure lower losses for bend radii between 1.25 and 8 mm. For a given bend radius, the measured losses depend on both the refractive index profile and mode-field radius. Refractive index profiles and mode-field radii are required to evaluate small radius bending losses in single mode fibers. Tests show that a refractive-index depression in the core center may reduce bending loss sensitivity. GRA

N90-12324# Minnesota Univ., Saint Paul. Dept. of Psychology.
A CONFERENCE ON THREE-DIMENSIONAL REPRESENTATION HELD IN UNIVERSITY OF MINNESOTA ON 24-26 MAY 1989 Final Report, 1 Jan. - 31 Dec. 1989
Irving Biederman Jun. 1989 52 p Conference held in Minneapolis, MN, 24-26 May 1989
(Grant AF-AFOSR-0232-89; AF Proj. 2313)
(AD-A211630; AFOSR-89-1090TR) Avail: NTIS HC A04/MF A01 CSCL 06/4

This is the final report for a conference grant entitled: A conference on Three-Dimensional Representation. The two and one-half day conference was held at the University of Minn. on May 24 to 26, 1989 to evaluate the current status of problem associated with three-dimensional representations from current computational, psychological, development, and neurophysiological perspectives. Nineteen presentations were made spanning these approaches. One hundred sixty-six individuals attended the conference. Of 44 evaluations received, 75 percent rated the conference as excellent, 20 percent as good, and 5 percent as fair. None rated it poor. The report consists of the original and revised program, conference abstracts evaluation summary and the rooster of attendees. GRA

N90-12325# Florida Univ., Gainesville. Dept. of Chemical Engineering.
LINEAR (PASSIVE) AND NON-LINEAR GUIDED AND STUDIES IN GLASS Final Report, 1 May 1988 - 30 Apr. 1989
R. V. Ramaswamy Jul. 1989 10 p
(Grant AF-AFOSR-0199-88; AF Proj. 2303)
(AD-A211693; AFOSR-89-1142TR) Avail: NTIS HC A02/MF A01 CSCL 20/6

The primary object of the project is to investigate theoretically as well as experimentally the ion-exchange process and solgel technology for fabrication of passive integrated optical circuits in glass for signal processing applications. This report deals with the progress made in both the ion-exchange and the gel-silica waveguide technology. The study involved several sub-projects: (1) Passive, low-loss waveguides and tapers by Ag+ -Na+ exchange; (2) Surface and buried channel waveguides by K+ -Na exchange; (3) Fabrication and characterization of 3 dB cross-couplers; and (4) Laser-assisted fabrication of waveguides in gel-silica. GRA

N90-12326# European Space Agency, Paris (France).
MEASUREMENT OF PRESSURE FLUCTUATIONS IN A RESONANT CHAMBER WITH LASER-INDUCED IODINE FLUORESCENCE
Bernhard Stahl and Ulf Michel (Deutsche Forschungs- und Versuchsanstalt fuer Luft- und Raumfahrt, Berlin, Germany, F.R.) Feb. 1989 84 p Transl. into ENGLISH of Messung von Druckschwankungen in einer Resonanzkammer mit Laserinduzierter Jod-Fluoreszenz (Berlin, Fed. Republic of Germany, DFVLR), 75 p Original language document was announced as N88-27551
(ESA-TT-1123; DFVLR-FB-87-53; ETN-89-95157) Avail: NTIS HC A05/MF A01; original German version available from DFVLR, VB-PL-DO, Postfach 90 60 58, 5000 Cologne, Fed. Republic of Germany, 23 DM

The feasibility of measuring pressure fluctuations with laser induced iodine fluorescence is investigated. An evacuable resonant chamber containing a gas mixture of iodine and nitrogen is applied. The intensity of fluorescent light is measured as a function of the thermodynamic state of the gas mixture, the laser light power and the laser frequency. The experimental results show that the noncontact measurement of pressure fluctuations is possible only under restricted boundary conditions. ESA

75 PLASMA PHYSICS

Includes magnetohydrodynamics and plasma fusion.
For ionospheric plasmas see *46 Geophysics*. For space plasmas see *90 Astrophysics*.

N90-12327# Massachusetts Inst. of Tech., Cambridge. Dept. of Nuclear Engineering.
CONFINEMENT OF MULTIPLY CHARGED IONS IN AN ECRH MIRROR PLASMA Ph.D. Thesis
Clinton Craig Petty Jun. 1989 170 p
(Contract DE-AC02-78ET-51013)
(DE89-016052; DOE/ET-51013/271; PFC/RR-89-9) Avail: NTIS HC A08/MF A01

This thesis is an experimental study of multiply charged ions in the Constance B mirror experiment. By measuring the ion densities, end loss fluxes and ion temperatures, the parallel confinement times for the first five charge states of oxygen and neon plasmas are determined. The parallel ion confinement times increase with charge state and peak on axis, both indications of an ion-confining potential dip created by the hot electrons. The radial profile of ion end loss is usually hollow due to large ion radial transport (tau sub parallel(i) is approximately tau sub perpendicular(i)), with the peak fluxes occurring at the edge of the electron cyclotron resonance zone. Several attempts are made to increase the end loss of selected ion species. Using minority ICRH, the end loss flux of resonant ions increases by 20 percent in cases when radial transport induced by ICRH is not too severe. A large antenna voltage can also extinguish the plasma. By adding helium to an oxygen plasma, the end loss of O(6+) increases by 80 due to decreased ion radial transport. An ion model is developed to predict the ion densities, end loss fluxes and confinement times in the plasma center using the ion particle balance equations, the quasineutrality condition and theoretical confinement time formulas. The model generally agrees with the experimental data for oxygen and neon plasmas to within experimental error. Under certain conditions spatial diffusion appears to determine the parallel ion confinement time of the highest charge states. For oxygen plasmas during ICRH, the measured parallel confinement time of the resonant ions is much shorter than their theoretical value, probably due to rf diffusion of the ions into the loss cone. DOE

N90-12328# Wisconsin Univ., Madison.
STELLARATOR TRANSPORT THEORY
W. N. G. Hitchon 1989 20 p
(Contract DE-FG02-85ER-53201)
(DE89-016371; DOE/ER-53201/2) Avail: NTIS HC A03/MF A01

A program of research in Stellarator Transport Theory is described, with emphasis on kinetic modeling of divertor plasmas. A very efficient numerical solution of the kinetic equation was developed. It was implemented first for the ions, self-consistently with the electrostatic potential, Phi, assuming quasineutrality and a Boltzmann distribution of electron density. The presheath problem was solved, confirming analytic work in the collisionless limit and extending the earlier work to collisional cases. The effect of a transverse electric field on divertor flows in IMS is to redistribute the diverted flux. It was shown (experimentally) that vector E x vector B drifts are responsible. Thus the presheath model was used to examine the effect of magnetic mirrors along a diverted field line, both on the diverted fluxes and on the electrostatic potential. The calculated variation delta phi is approximately O(T sub e) can be expected to set up significant flows. Numerical calculations of the stellarator ambipolar electric field and bootstrap current were done. Further analytical and computational work on ripple transport is under way, in conjunction with IPP-Garching and as part of the U.S.-USSR collaboration. Our earlier analytic calculations of stellarator ripple transport have also been modified to apply to tokamaks. DOE

N90-12329# Ceskoslovenska Akademie Ved, Prague. Inst. of Plasma Physics.

CALCULATIONS OF SOFT X RAY EMISSION OF REB-HEATED PLASMA

J. Raus and V. Babicky Jan. 1989 43 p
(IPPCZ-287) Avail: NTIS HC A03/MF A01

Time dependent spectrum of hydrogen plasma with 1 percent oxygen impurity in spectral range 5 eV to 5 KeV is calculated by using the corona model in the approximation of constant electron temperature (of the order of tens of eV) for interpretation of radiation measurements made on REBEX experiment by means of vacuum x ray diodes and submicrometer nitrocellulose filters. Author

N90-12330# Ceskoslovenska Akademie Ved, Prague. Inst. of Plasma Physics.

NON-STATIONARY COMPUTER MODEL OF THE ASYMPTOTIC REGION OF AN ELECTRIC ARC GAS HEATER

J. Jenista and Z. Sedlacek Feb. 1989 25 p
(IPPCZ-288) Avail: NTIS HC A03/MF A01

A method is presented for the numerical solution of the non-stationary energy balance equation in the asymptotic region of an electric arc gas heater with axial gas supply which makes it possible to distinguish between stable and unstable solutions and to examine in detail the transient phenomena occurring during the formation of the stationary state. Author

N90-12331# Ceskoslovenska Akademie Ved, Prague. Inst. of Plasma Physics.

ELECTRON CYCLOTRON EMISSION AND ABSORPTION EXPERIMENT ON THE CASTOR TOKAMAK

S. I. Fedorenko (Academy of Sciences, USSR, Moscow), J. Stockel, M. Valovic, and F. Zacek Nov. 1988 16 p
(IPPCZ-285) Avail: NTIS HC A03/MF A01

Electron cyclotron radiation and absorption measurements on the CASTOR tokamak are reported. Emission spectra are obtained with fast-scanning Fourier spectrometer and InSb detectors, working in the spectral range 30 to 300 GHz and receiving two orthogonal polarization components simultaneously. When the plasma loop voltage is high, runaway electrons give rise to intense broad-band emission. Runaway particles can be removed by increasing the plasma density. The electron temperature profile was deduced from thermal emission and absorption around second cyclotron harmonics. From non-thermal emission second and third harmonics, the energy and number of non-thermal particles could be calculated. During the lower-hybrid-current-drive (LHCD) experiments, presence of 60 KeV electrons with density of 1.10(16)/cu.m. was deduced from emission spectra. Author

N90-12332# Ceskoslovenska Akademie Ved, Prague. Inst. of Plasma Physics.

CONTROL OF PLASMA POSITION IN THE CASTOR TOKAMAK

M. Valovic Nov. 1988 18 p
(IPPCZ-284) Avail: NTIS HC A03/MF A01

A servo system for control of plasma position in the CASTOR tokamak is described. The plasma is maintained in prescribed position with accuracy of 3 mm. Author

N90-12333# Montana State Univ., Bozeman. Dept. of Electrical Engineering.

COMPUTER CONTROLLED MHD POWER CONSOLIDATION AND PULSE-GENERATION SYSTEM Technical Progress Report, Oct. 1987 - Mar. 1988

R. Johnson 1989 53 p
(Contract DE-AC22-87PC-79680)
(DE89-015600; DOE/PC-79680/T1) Avail: NTIS HC A04/MF A01

The major goal of this project is to establish the feasibility of a power conversion technology which will permit the direct synthesis of computer programmable pulse power. Feasibility will be established in this project by demonstration of direct synthesis of commercial frequency power by means of computer control. The power input to the conversion system is assumed to be a magnetohydrodynamic (MHD) Faraday connected generator which may be viewed as a multi-terminal d.c. source. This consolidation/inversion process is referred to subsequently as Pulse-Amplitude-Synthesis-and-Control (PASC). A secondary goal is to deliver a controller subsystem consisting of a computer, software, and computer interface board which can serve as one of the building blocks for a possible Phase 2 prototype system. This report covers the initial six months portion of the project and includes discussions on the following areas: (1) selection of a control computer with software tool kit for development of the PASC controller contract requirement; (2) problem formulation considerations for simulation of the PASC technique on digital computers; (3) initial simulation results for the PASC transformer, including simulation results obtained using SPICE and the INTEG program; (4) a survey of available gate-turn-off (GTO's), power semiconductors, power field effect transistors (PFET's), and fiber optics signal cabling and transducers. DOE

N90-12334# Los Alamos National Lab., NM.

HIGHLIGHTS OF PAPERS PRESENTED AT THE WORKSHOP ON COLD FUSION PHENOMENA

Sep. 1989 26 p Workshop held in Santa Fe, NM, 23-25 May 1989
(Contract W-7405-eng-36)
(DE89-016956; LA-11686-C; CONF-8905126-Summ) Avail: NTIS HC A03/MF A01

Highlights are presented of formal oral papers presented at the Workshop on Cold Fusion Phenomena. General topics covered are: physics of fusion reactions; neutron and gamma-ray spectroscopy; colorimetry; and applicable condensed-matter physics, electrochemistry, and analytical chemistry. DOE

N90-12335# California Univ., Los Angeles. Dept. of Electrical Engineering.

WAVE PARTICLE INTERACTIONS Final Report, 6 Nov. 1987 - 31 Oct. 1988

Chan Joshi, R. Williams, C. Clayton, and T. Katsouleas Apr. 1989 107 p Prepared in cooperation with Lawrence Livermore National Lab., CA
(Contract W-7405-eng-48)
(DE89-017527; UCRL-21225) Avail: NTIS HC A06/MF A01

A three dimensional simulation technique, which incorporates the random selection of electron initial coordinates and momenta, has been used to model the motion of energetic electrons which are injected colinearly into a relativistic plasma wave. The model predicts the resulting energy spectrum, angular distribution, number density and spatial positions of electrons which exchange energy with the plasma wave. These predictions are applicable to the laser-plasma beatwave experiments at UCLA which use CO2 laser wavelength 9.6 and 10.3 microns. Some of the predictions are applicable to beatwave experiments at Rutherford Laboratories which use Nd:glass laser wavelength of 1.06 and 1.05 microns and for experiments that may use 10.3 and 10.6 micron wavelengths. These experiments differ according to the phase velocity of the plasma wave produced by the beating of the two laser beams in a resonant density plasma. The predictions of this model have been useful for optimizing the electron detection apparatus of the UCLA experiments. DOE

N90-12336# Lawrence Livermore National Lab., CA.

AN ELECTROMAGNETIC FINITE ELEMENT PARTICLE CODE ON AN UNSTRUCTURED GRID

John J. Ambrosiano and Rainald Lohner (George Washington Univ., Washington, DC.) Jun. 1989 6 p Presented at the 13th Conference on the Numerical Simulation of Plasmas, Santa Fe, NM, 17-20 Sep. 1989
(Contract W-7405-eng-48)
(DE89-017532; UCRL-101322; CONF-890931-8) Avail: NTIS HC A02/MF A01

The need to perform plasma simulations in bounded regions of possibly complicated shape has generated a great deal of interest in nontraditional formulations of particle codes.

Well-established methods based on rectangular Cartesian grids are too inflexible to fit complex geometries well. Some of the unconventional approaches taken thus far include curvilinear coordinates, finite volume formulations and finite element methods. One of the most promising new strategies, in terms of geometrical flexibility, is to use unstructured grids. A structured grid connects each node to a fixed number of neighboring nodes. This makes it easy to specify the relationship between a node and its neighbors, but also makes it difficult to map such a grid into complicated geometries without patching several grids together into a composite. In contrast, one may form an unstructured grid by placing nodes anywhere in the domain as required by the shape of the boundary or the demands of the calculation. There are two obvious difficulties that occur when one abandons structured grids: solving the field equations, and locating the particles. In this paper we describe work in progress at Lawrence Livermore National Laboratory to develop a two-dimensional electromagnetic particle code on an unstructured grid. We discuss methods for obtaining the fields and for tracing the particles. DOE

N90-12337# Lawrence Livermore National Lab., CA.
TEMPORAL AND SPATIAL FILTERING REMEDIES FOR DISPERSION IN ELECTROMAGNETIC PARTICLE CODES
Peter W. Rambo, John J. Ambrosiano, Alex Friedman, and Dale E. Nielsen, Jr. Jul. 1989 5 p Presented at the 13th Conference on the Numerical Simulation of Plasmas, Santa Fe, NM, 17-20 Sep. 1989
(Contract W-7405-eng-48)
(DE89-017534; UCRL-101395; CONF-890931-7) Avail: NTIS HC A01/MF A01

There has been considerable interest over the last decade in the physics of intense electromagnetic signals in plasmas, much of it in the context of laser fusion and pulsar astrophysics. Simulations of these phenomena test the limits of particle simulation and in particular the standard leapfrog algorithm for advancing the electromagnetic fields. As shock fronts and sheaths develop within the plasma in response to intense electromagnetic waves, numerical dispersion intrinsic to the leapfrog algorithm can cause unphysical ripples to appear in the field solution which can interact with particles. Fourier analysis of the leapfrog scheme in 1D yields the dispersion relation for a Courant number (nu) (triple bond) c(Delta)t/(Delta)x = 0.5. As we can see, the phase velocity of the modes falls off the light line at high k(Delta)x. Thus modes that are poorly resolved will tend to disperse and trail the main pulse as ripples. There are several approaches to finding a remedy for these ripples. High-order finite difference methods can be considerably less dispersive. Also, improving resolution can move the physics to lower k(Delta)x where the dispersion is less. Often these options are not available, either because of difficulty in implementation or because computer resources are insufficient. This leaves filtering as the main option, with two routes to schemes that remove high k(Delta)x modes -- temporal and spatial filtering. In this paper we present techniques to remove dispersion from particle simulations using both methods. DOE

N90-12338# Cornell Univ., Ithaca, NY. Lab. of Plasma Studies.
GENERATION AND FOCUSING OF PULSED INTENSE ION BEAMS Final Report, 1 Jul. 1987 - 30 Sep. 1988
D. A. Hammer, B. R. Kusse, and R. N. Sudan 3 Aug. 1989 6 p
(Contract DE-FC08-87DP-10618)
(DE89-017558; DOE/DP-10618/T2) Avail: NTIS HC A02/MF A01

This paper discusses the following experiments: ion diode experiments at 0.5 x 10(exp 12) W on the LION accelerator; spectroscopic studies of ion diodes; ion beam-plasma channel transport research; and plasma opening switch experiments. Theoretical studies of plasma opening switches are also presented. DOE

N90-12339# Lawrence Livermore National Lab., CA.
PROPERTIES OF STRONGLY COUPLED MULTI-IONIC PLASMAS
Hugh E. DeWitt, W. L. Slattery, and Guy S. Stringfellow (California Univ., Santa Cruz.) Aug. 1989 13 p Presented at the 24th Yamada Conference on Strongly Coupled Plasma Physics, Tokyo, Japan, 29 Aug. - 2 Sep. 1989
(Contract W-7405-eng-48)
(DE89-017782; UCRL-101753; CONF-8908133-2) Avail: NTIS HC A03/MF A01

A reexamination of the one component plasma fluid equation of state using new Monte Carlo results gives the EOS as -9/10 Gamma + b Gamma sup s with s (approx.) 1/3 rather than the 1/4 value obtained previously. The EOS for the bcc crystalline phase indicates that first order anharmonic corrections are present. A recalculation of the freezing transition leaves the bcc transition unchanged at about Gamma = 178, but the transition to fcc is lower, about 192. For ionic mixtures the HNC equations were solved and give a nearly perfect agreement with the linear mixing rule. DOE

N90-12340# Lawrence Livermore National Lab., CA.
MICROWAVE TOKAMAK EXPERIMENT (MTX) OHMIC HEATING SYSTEM
M. C. Jackson 13 Sep. 1989 4 p Presented at the 13th International Symposium on Fusion Engineering, Knoxville, TN, 2-6 Oct. 1989 Submitted for publication
(Contract W-7405-eng-48)
(DE89-017892; UCRL-101103; CONF-891007-1) Avail: NTIS HC A01/MF A01

The ohmic heating system for the Microwave Tokamak Experiment (MTX) at Lawrence Livermore National Laboratory (LLNL) provides both the voltage for the initial breakdown phase and the energy to drive the plasma current to a value of 400 kA or greater. Providing this voltage and flux swing requires a one-turn loop voltage of about 25 volts (11 kV across the coil) and a magnetic flux swing of 2 volt- seconds. This voltage and flux swing are accomplished by charging the ohmic heating coils to 20 kA, at which point the current is commutated off into a resistor generating the 11 kV across the coil. When the current passes through zero, another power supply drives the current in the opposite polarity to 20 kA, thus completing the full 2 volt-second flux swing. This paper describes the design features and performance of the ohmic heating circuit, with emphasis on the commutation circuit. In addition, the paper describes the use of the ohmic heating system for discharge cleaning and the changeover procedure. DOE

N90-12341# College of William and Mary, Williamsburg, VA.
THEORETICAL PLASMA PHYSICS Progress Report, 31 Oct. 1988 - 31 Oct. 1989
Allen H. Boozer and George Vahala Aug. 1989 9 p
(Contract DE-FG05-84ER-53176)
(DE90-000009; DOE/ER-53176/5) Avail: NTIS HC A02/MF A01

During the past year we have studied stellarator equilibria with quasi-helical symmetry and the relation between the trajectories of the exact and the drift Hamiltonian. The relation between these trajectories is particularly important to issue of (alpha) particle confinement in a reactor. Work has also been done on the bootstrap current in the absence of symmetry, the effects of tearing modes on the current profile in a tokamak, and models of plasma turbulence. In addition, considerable time was spent during the year by Allen Boozer chairing the task force on Alternate Transport as part of the DOE transport initiative. DOE

N90-12342# Texas Univ., Austin. Dept. of Physics.
EXPERIMENTAL RESEARCH IN HIGH ENERGY PHYSICS Progress Report, 1 Jul. 1989 - 31 Dec. 1989
Jack L. Ritchie Aug. 1989 10 p
(Contract DE-FG05-89ER-40515)
(DE90-000061; DOE/ER-40515/1) Avail: NTIS HC A02/MF A01

Experiment 791 is located in the B5 neutral beam at the Alternating Gradient Synchrotron at the Brookhaven National Laboratory. The spectrometer combines precise tracking with good particle identification capability. The excellent mass resolution (sigma = 1.4 MeV) of the spectrometer can be seen from reconstructed K(sub L) yields pi(+)pi(-) events. High rate capability is achieved by fully-custom high speed front-end electronics, a massively parallel readout architecture, and a multi-level trigger system. The progress on E791 can be broken into two categories: the completion of the analysis of data taken in 1988 and publication of those results and the completion of a major data taking run in the early part of 1989. These will be discussed separately. DOE

N90-12343# Oregon Univ., Eugene. Chemical Physics Inst.
ELECTRON ATTACHMENT AND MOLECULAR FRAGMENTATION IN LASER-EXCITED PLASMAS Final Report, 5 May 1988 - 4 May 1989
J. L. Hardwick and J. T. Moseley 10 Aug. 1989 13 p
(Contract DAAL03-88-K-0070)
(AD-A212098; ARO-25624.3-PH) Avail: NTIS HC A03/MF A01 CSCL 07/5

Production of O(-) from thermal electrons was identified during the laser excitation of NO. O(-) is produced during excitation near 226 nm, corresponding to absorption in the (0,0) band of the A-X band system of NO. Electrons with energy limited to less than 0.5 eV completely suppress the endothermic production of O(-) from NO(X2II). Dissociative attachment occurs from the A2(+) electronic state of NO and produces both O(-) and N in their ground electronic states. This is the first reported case of dissociative attachment of electrons to an optically prepared excited electronic state. GRA

N90-12344# Naval Research Lab., Washington, DC.
ADVANCED CONCEPTS THEORY Final Annual Report, Jan. - Dec. 1988
3 Aug. 1989 157 p
(Contract MIPR-88-577)
(AD-A211665; NRL-MR-6517) Avail: NTIS HC A08/MF A01 CSCL 20/9

This report details the work of the Plasma Radiation Branch with respect to several critical problems concerning the design of z pinch implosions and the optimization of their radiative output. Separate sections describe progress in the analysis of z pinch experiments, the development of atomic, electron, plasma and MHD dynamical models to describe z pinch implosions, and the analysis of plasma opening switches. GRA

76 SOLID-STATE PHYSICS

Includes superconductivity.

For related information, see also *33 Electronics and Electrical Engineering* and *36 Lasers and Masers.*

N90-12345*# National Aeronautics and Space Administration. Marshall Space Flight Center, Huntsville, AL.
CHARACTERIZATIONS OF ELECTRICAL PROPERTIES OF HIGHT(SUB c) SUPERCONDUCTING MATERIALS Center Director's Discretionary Fund Final Report
R. C. Sisk and P. N. Peters Sep. 1989 15 p
(NASA-TM-100380; NAS 1.15:100380) Avail: NTIS HC A03/MF A01 CSCL 20L

The automated data acquisition system developed in the Space Science Laboratory at Marshall Space Flight Center for measuring electrical properties of high temperature superconductors is described. The acquisition system, consisting of a computer and computer-controlled hardware, allows large numbers of voltage, current, temperature, and magnetic measurements to be performed on bulk and thin film samples. Typical results are shown characterizing transition temperature (T sub c), critical current density (J sub c), and magnetic properties of bulk high T(sub c) materials as a function of temperature. Author

N90-12346# Department of the Navy, Washington, DC.
PROCESS FOR SINGLE CRYSTAL GROWTH OF HIGH T(SUB c) SUPERCONDUCTORS Patent Application
William Lechter, inventor (to Navy), Louis Toth, inventor (to Navy), and Das Badri, inventor (to Navy) 25 May 1989 11 p
(AD-D014167; US-Patent-Appl-SN-356496) Avail: NTIS HC A03/MF A01 CSCL 20/3

Large oriented crystals greater than one millimeter in length of high T(sub c) superconducting compounds are grown by mixing starting materials in the correct proportions to make the superconducting compound, forming a mixture. The CO2 is removed from the mixture and the ternary oxide of the compound is formed from the mixture. Next, the mixture is formed into a self-supporting green body and sintered at a sintering temperature at which the top of the self supporting green body is molten and the bottom surface is solid. The self-supporting green body is held at the sintering temperature for a time, forming a sintered body. Next, the sintered body is cooled so that crystals form. After this step, the crystals can be further processed to increase their superconducting properties. Finally, the crystals are removed and processed for use. GRA

N90-12347# Department of the Navy, Washington, DC.
NIOBIUM AND NIOBIUM NITRIDE CONTACTS ON SEMICONDUCTING MATERIAL Patent Application
Edward Cukauskas, inventor (to Navy), William Carter, inventor (to Navy), Jeffrey Pond, inventor (to Navy), and Harvey Newman, inventor (to Navy) 30 Jun. 1989 19 p
(AD-D014177; US-Patent-Appl-SN-374101) Avail: NTIS HC A03/MF A01 CSCL 20/12

This invention related generally to a metallization layer of niobium or niobium nitride on a semiconductor in an integrated circuit structure which can function from the superconducting temperature regime to above room temperature. Niobium or niobium nitride is deposited onto a heated gallium arsenide substrate. This metallization will maintain chemical stability after high temperature post processing. These materials provide a low resistivity metallization suitable for Schottky contacts used over a wide operating temperature range and are superconducting at low temperatures. GRA

N90-12348*# National Aeronautics and Space Administration. Lewis Research Center, Cleveland, OH.
FORTRAN PROGRAM FOR X RAY PHOTOELECTRON SPECTROSCOPY DATA REFORMATTING
Phillip B. Abel Nov. 1989 10 p
(NASA-TP-2957; E-4867; NAS 1.60:2957) Avail: NTIS HC A02/MF A01 CSCL 20L

A FORTRAN program has been written for use on an IBM PC/XT or AT or compatible microcomputer (personal computer, PC) that converts a column of ASCII-format numbers into a binary-format file suitable for interactive analysis on a Digital Equipment Corporation (DEC) computer running the VGS-5000 Enhanced Data Processing (EDP) software package. The incompatible floating-point number representations of the two computers were compared, and a subroutine was created to correctly store floating-point numbers on the IBM PC, which can be directly read by the DEC computer. Any file transfer protocol having provision for binary data can be used to transmit the resulting file from the PC to the DEC machine. The data file header required by the EDP programs for an x ray photoelectron spectrum is also written to the file. The user is prompted for the relevant experimental parameters, which are then properly coded into the format used internally by all of the VGS-5000 series EDP packages. Author

N90-12349# Sandia National Labs., Albuquerque, NM.
ENERGY RELAXATION OF LIGHT HOLES IN InAs(.15)Sb(.85)/InSb MULTIPLE QUANTUM WELLS
C. P. Tigges, J. E. Schirber, H. P. Hjalmarson, I. J. Fritz, and L. R. Dawson 1989 9 p Presented at the 6th International Conference on Hot Carriers in Semiconductors, Scottsdale, AZ, 23-28 Jul. 1989
(Contract DE-AC04-76DP-00789)
(DE89-016035; SAND-89-1875C; CONF-8907133-1) Avail: NTIS HC A02/MF A01

The energy relaxation rate of light in-plane in InAs(.15)Sb(.85)/InSb quantum wells was measured using a Shubnikov-de Haas technique. In this Type 2 system, the holes reside in the InSb layers; strain reverses the heavy-light hole ordering and thus light holes are the charge carriers. The samples consist of 20 to 100 InAs(.15)Sb(.85)/InSb periods 100/200 A thick. The InAsSb barriers are doped with Be. The total carrier concentration is obtained from Hall data. Shubnikov-de Haas oscillation amplitudes are measured and used to determine the light hole temperature for a given applied power. The steady state power per carrier is equated to the energy relaxation rate to determine the carrier temperature T(sub H). Data are compared with theory and experiment for light holes in InGaAs/GaAs quantum wells. DOE

N90-12350# Technische Hogeschool, Delft (Netherlands). Afd. der Elektrotechniek.
ELECTROLITIC DEPOSITED OHMIC CONTACTS ON III-V COMPOUND SEMICONDUCTORS: A REVIEW
S. Blasko, M. J. Geerts, and J. C. vandenHeuvel 1988 21 p
(PB89-217400) Avail: NTIS HC A03/MF A01 CSCL 20L

The electroplating technology for ohmic contacts on group III-V compound semiconductors is reviewed. The reviewed technology is divided into four parts: the semiconductor surface preparation before electroplating; the choice of the metals or the metal alloys, their composition and thickness; the modes of the metal electroplating on the semiconductors and the heat treatment after the metal deposition. The values of specific contact resistance obtained by electroplating are in several cases comparable to those made by vacuum deposition. GRA

N90-12351# Helsinki Univ. of Technology, Espoo (Finland). Low Temperature Lab.
INTERNAL MAGNUS EFFECTS IN SUPERFLUID 3He-A
R. H. Salmelin, M. M. Salomaa, and V. P. Mineev (Academy of Sciences, USSR, Moscow) 1989 14 p Sponsored by Koerber-Stiftung, Hamburg, Fed. Republic of Germany; Academy of Finland; Finnish Cultural Foundation; and Magnus Ehrnrooth Foundation
(PB89-212617; TKK-F-A646; ISBN-951-754-869-9) Avail: NTIS HC A03/MF A01 CSCL 20L

The orbital angular momentum of the coherently aligned Cooper pairs in superfluid (3)He-A is transmitted to an object immersed in the condensate. The authors evaluate the quasiparticle-scattering asymmetry experienced by a negative ion; this leads to a measurable, purely quantum-mechanical Magnus force deflecting the ion's trajectory. Close to T(sub c), possible hydrodynamic Magnus effects are smaller by the factor delta sub A/(k sub B)(T sub c). Author

N90-12352# Oak Ridge National Lab., TN.
CHARACTERIZATION OF THE STRUCTURE AND CHEMISTRY OF DEFECTS IN MATERIALS: PROCEEDINGS, VOLUME 138
Bennett C. Larson, ed., Manfred Ruehle, ed., and David N. Seidman, ed. (Northwestern Univ., Evanston, IL.) 1988 589 p Symposium held in Boston, MA, 28 Nov. - 3 Dec. 1988
(Contract DE-AC05-84OR-21400)
(DE89-014796; CONF-8811195-Vol-138) Avail: NTIS HC A25/MF A04

Research programs, presented at the materials research symposium, on defects in materials are presented. Major areas include: point defects, defect aggregates, and ordering; defects in non-metals and semiconductors; atomic resolution imaging of defects; and gain boundaries, interfaces, and layered materials. Individual projects are processed separately for the data bases. DOE

N90-12353# Sandia National Labs., Albuquerque, NM.
FIELD-ASSISTED BONDING OF SINGLE CRYSTAL QUARTZ
Randall D. Watkins, Clinton D. Tuthill, Richard M. Curlee, Dale R. Koehler, and Charles F. Joerg 1989 27 p Presented at the 11th Quartz Devices Conference, Kansas City, MO, 28-31 Aug. 1989
(Contract DE-AC04-76DP-00789)
(DE89-015407; SAND-89-0814C; CONF-8908132-1) Avail: NTIS HC A03/MF A01

A technique to produce strong, hermetic bonds between plates of single crystal quartz using a modified field-assisted bonding process is presented. Field-assisted bonding is a technique traditionally used to join glass to metals at temperatures well below normal glass softening temperatures. To promote reactivity between quartz within an electrical field at temperatures well below quartz transformation temperatures, thin films of silicon metal and glass were vapor deposited onto adjacent quartz plates. Thermal stresses caused by expansion mismatch between the quartz and the films were of concern. These stresses were reduced by determining the minimum film thicknesses capable of yielding sufficient reactivity for bonding. Processing studies were conducted to optimize bond integrity, and bonds were characterized by hermeticity, thermal shock, and mechanical shock. Packages produced under the most ideal conditions were able to survive greater than 1000 psi shock loads. DOE

N90-12354# Lawrence Livermore National Lab., CA.
SUPERCONDUCTIVITY AND MAGNETIC SCATTERING IN THE Nd(SUB 2-x)Ce(SUB x)CuO(SUB 4-DELTA)
J. L. Peng, R. N. Shelton, and H. B. Radousky (California Univ., Livermore.) Jul. 1989 3 p Presented at the International Conference on Materials and Mechanisms of Superconductivity, Stanford, CA, 23-28 Jul. 1989 Submitted for publication
(Contract W-7405-eng-48)
(DE89-016524; UCRL-100695; CONF-890718-26) Avail: NTIS HC A01/MF A01

Samples of Nd(sub 2-x)Ce(sub x)CuO(sub 4-delta) were prepared by annealing both in air and under vacuum. Electrical resistivity measurements showed that these materials in their normal state demonstrate a Kondo anomaly resulting from a combination of magnetic and phonon scatterings. DOE

N90-12355# Argonne National Lab., IL.
COMPUTER SIMULATIONS OF TWO-DIMENSIONAL QUASIPERIODIC CRYSTAL AND RANDOM TILING MODELS
Katherine J. Strandburg Aug. 1989 18 p Presented at the 4th Adriatico Research Conference (AARC '89) on Quasicrystals, Trieste, Italy, 4-7 Jul. 1989
(Contract W-31-109-eng-38)
(DE89-016909; CONF-8907138-1) Avail: NTIS HC A03/MF A01

The recent discovery of quasicrystalline materials exhibiting resolution-limited diffraction peaks focusses attention on those quasicrystalline models which predict long-range translational order. Two such models have been suggested: the quasiperiodic crystal model (for which the Penrose tiling is the prototype) and the random tiling model (analogous to allowing arbitrary spacefilling arrangements of the Penrose rhombuses). Physically, the two models are distinguished by primary dependence on energy and entropy, respectively, in stabilizing the quasicrystal phase. Here we describe computer simulation results for simple two-dimensional realizations of each model. DOE

N90-12356# Argonne National Lab., IL.
STRUCTURE-PROPERTY RELATIONSHIPS AS AN AID IN THE RATIONAL DESIGN OF (BETA)-(ET)(SUB 2)X ORGANIC SUPERCONDUCTORS
Jack M. Williams, Hau H. Wang, Aravinda M. Kini, Mark A. Beno, Urs Geiser, Arthur J. Schultz, K. Douglas Carlson, John R. Ferraro, and Myung-Hwan Whangbo 1989 6 p Presented at the NATO Advanced Study Institute on Lower-Dimensional Systems and Molecular Electronics, Spetses, Greece, 12-23 Jun. 1989 Submitted for publication
(Contracts W-31-109-eng-38; DE-FG05-86ER-45259)
(DE89-016912; CONF-8906205-1) Avail: NTIS HC A02/MF A01

The organic electron-donor molecule ET, 1, was the current central focus of research in organic superconductors because it forms numerous solid phases with anions, X(-), of which the beta-(ET) sub 2 X materials, X = IBr2(-), AuI2(-), and I3(-), are ambient pressure superconductors with T sub c's = 2.8 K, 4.9 K, and 1.5 K (and 8 K at p greater than 0.5 kbar), respectively. The synthesis of these materials was summarized in detail in the literature and is discussed. DOE

N90-12357# Oak Ridge National Lab., TN.
ION BEAM DEPOSITION OF EPITAXIAL GERMANIUM AND GALLIUM ARSENIDE LAYERS Foreign Trip Report, 2-18 Jun. 1989
T. E. Haynes Jul. 1989 23 p
(Contract DE-AC05-84OR-21400)
(DE89-017439; ORNL/FTR-3308) Avail: NTIS HC A03/MF A01

The traveler presented an invited paper entitled, Ion Beam Deposition of Epitaxial Germanium and Gallium Arsenide Layers, at the Twelfth Symposium on Ion Sources and Ion-Assisted Technology (ISIAT '89) in Tokyo. During informal conversations at this meeting, the traveler was informed about a new Japanese initiative, sponsored by the Ministry of International Trade and Industry and an industrial consortium, to establish an Ion Engineering Research Center, whose purpose will be to provide sophisticated equipment and technology base for exploring and developing new applications of ion beam processing. The traveler also visited five Japanese laboratories involved in research on ion-solid interactions. Developments in ionized cluster beam (ICB) deposition were emphasized at ISIAT '89 and during visits to Kyoto University, where the ICB technique was pioneered, and to Mitsubishi Electric's Itami Works, where commercial ICB systems are now being produced. Discussions at Osaka University concentrated on the application of focused ion beams for maskless patterning of submicron devices and on recent studies of one-dimensional quantum effects in semiconductor wires. At Hitachi Research Laboratory, basic research on thin-film growth was described, as well as progress toward the development of a variable frequency RF quadrupole accelerator for ion implantation. DOE

N90-12358# Lawrence Livermore National Lab., CA.
ELECTRON-POSITRON MOMENTUM DISTRIBUTION MEASUREMENTS OF HIGH-T(SUB c) SUPERCONDUCTORS AND RELATED SYSTEMS
A. L. Wachs, P. E. A. Turchi, R. H. Howell, Y. C. Jean, M. J. Fluss, R. N. West, J. H. Kaiser, S. Rayner, H. Hahghighi, and K. L. Merkle (Argonne National Lab., IL.) et al Jun. 1989 4 p Presented at the International Conference on Materials and Mechanisms of Superconductivity - High-Temperature Superconductors, Stanford, CA, 23-28 Jul. 1989 Prepared in cooperation with Paris-Sud Univ., Orsay (France)
(Contract W-7405-eng-48)
(DE89-017538; UCRL-100596; CONF-890718-27) Avail: NTIS HC A01/MF A01

We discuss our measurements of the 2D-angular correlation of positron annihilation radiation (ACAR) in La(sub 2)CuO(sub 4), YBa(sub 2)Cu(sub 3)O(sub 7) (YBCO), and NiO. The measurements for NiO are the first such 2D-ACAR measurements; the YBCO results are of a higher statistical quality than previously reported in the literature. The data are compared with complementary theoretical calculations and with each other. We discuss the implication of our analysis for ACAR studies of similar and related systems. DOE

N90-12359# Argonne National Lab., IL.
RF PERFORMANCE OF POLYCRYSTALLINE HIGH-T(SUB c) SUPERCONDUCTORS
C. L. Bohn, J. R. Delayen, and C. T. Roche 1989 12 p Presented at the 4th Workshop on RF Superconductivity, Ibaraki-Ken, Japan, 14-18 Aug. 1989 Sponsored in part by Army
(Contract W-31-109-eng-38)
(DE89-017671; CONF-8908145-1) Avail: NTIS HC A03/MF A01

The RF properties were measured of bulk and thick film high T(sub c) superconductors as functions of temperature, frequency, and RF field amplitude. The RF surface resistance typically depended strongly on field amplitude, but the samples remained superconducting up to the highest fields applied (approx. 640 gauss). For example, at 220 MHz, the surface resistance of a bulk polycrystalline YBa2Cu3O(7-x) sample ranged from (approx. less than or = 2 micro-ohms) at approx. less than or = 0.05 gauss and 4.2 K to 6.3 micro-ohms at 640 gauss and 77 K. The stability of the RF properties of this sample after storage both in air and in vacuum was also investigated. DOE

N90-12360# Argonne National Lab., IL. Materials Science Div.
ANOMALOUS ION-CHANNELING BEHAVIOR ACROSS THE SUPERCONDUCTING TRANSITION IN HIGH-T(SUB c) MATERIALS
L. E. Rehn, R. P. Sharma, P. M. Baldo, and J. Z. Liu Jul. 1989 21 p Presented at the 13th International Conference on Atomic Collisions in Solids, Aarhus, Denmark, 7-11 Aug. 1989
(Contract W-31-109-eng-38)
(DE89-017677; CONF-890821-3) Avail: NTIS HC A03/MF A01

Axial channeling scans with minimum RBS yields of less than or = 2 percent were obtained for 1.5 MeV He-4 ions incident along the c-axis in YBa2Cu3O(7-delta) and ErBa2Cu3O(7-delta) single crystals. Large variations in the FWHM of the (001) channeling dip were observed for temperatures between 30 and 300 K. An abrupt, (approx.) 8 percent increase was measured as the temperature was lowered through the superconducting transition T(sub c); the rela tive increase across T(sub c) in the width of the axial dip was even larger for angles of incidence less than the critical angle. A simple analytical procedure for polyatomic materials yields isotropic, average thermal vibrational amplitudes that agree well with considerably less precise neutron powder diffraction results on sintered samples. The individual contribution to the angular channeling dip from the row of Er and Ba atoms parallel to the c-axis can be isolated in the RBS scans of the Er compound. This separation reveals normal (Debye-type) behavior for atoms in the Er-Ba row, demonstrating that the anomalous changes are due solely to atomic displacements in the Cu-O row. Finally, x ray studies using specimens with different O stoichiometries reveal that the anomalous change in the FWHM shifts in temperature in direct proportion to the change in T(sub c). DOE

N90-12361# Argonne National Lab., IL. Materials and Components Technology Div.
HIGH-TEMPERATURE SUPERCONDUCTING CURRENT LEADS FOR CRYOGENIC APPARATUS
John R. Hull 1989 7 p Presented at the 24th Intersociety Energy Conversion Engineering Conference, Arlington, VA, 6-11 Aug. 1989
(Contract W-31-109-eng-38)
(DE89-017680; CONF-890815-28) Avail: NTIS HC A02/MF A01

The use of high temperature superconductors (HTSC) for cryostat current leads is analyzed for operation between liquid helium and liquid nitrogen temperatures in the conduction cooled and vapor cooled cases. Present fabrication methods are sufficient to produce such leads for most known applications. Thermophysical data suggest that performance of leads of HTSC operated in the normal state is nearly as good as that of pure metal leads. If leads of HTSC are optimized for the normal state and then operated in the superconducting state, helium boiloff can be reduced by about a factor of two. For leads longer than the normal-state optimum, the helium boiloff can be reduced further, but the system must be guarded against thermal runaway. For temperature perturbations, the lead may enter a metastable state where a large fraction of the length remains normal. DOE

N90-12362# California Univ., Davis. Dept. of Physics.
PREPARATION AND CHARACTERIZATION OF SINGLE PHASE Ba(1-x)KxBiO3
T. J. Folkerts, R. N. Shelton, and H. B. Radousky (Lawrence Livermore National Lab., CA.) Jul. 1989 3 p Presented at the International Conference on Materials and Mechanisms of Superconductivity - High-Temperature Superconductors, Stanford,

CA, 23-28 Jul. 1989
(Contract W-7405-eng-48)
(DE89-017735; UCRL-100094; CONF-890718-28) Avail: NTIS HC A01/MF A01

High quality single phase samples of Ba sub 1-chi K sub chi BiO3 (BKBO) were made across the range of compositions from 0 less than chi less than 0.5. Powder X-ray diffraction data indicates pure single phase materials for all potassium concentrations. Samples with chi less than 0.35 are nonsuperconducting while those with chi greater than 0.35 show sharp superconducting transitions from both resistivity and magnetization measurements. Care during sample preparation is vital for obtaining quality samples of this material. DOE

N90-12363# Lawrence Livermore National Lab., CA.
SUBNANOSECOND LINEAR GaAs PHOTOCONDUCTIVE SWITCHING, REVISION 1
R. L. Druce, M. D. Pocha, K. L. Griffin, and W. W. Hofer 1989 7 p Presented at the 7th Institute of Electrical and Electronics Engineers Pulsed Power Conference, Monterey, CA, 12-14 Jun. 1989 Revised
(Contract W-7405-eng-48)
(DE89-017739; UCRL-100357-Rev-1; CONF-890665-48-Rev-1) Avail: NTIS HC A02/MF A01

Research was conducted in photoconductive switching for the purpose of generating subnanosecond pulses in the 25 to 50kV range. The very fast recombination rates of Gallium Arsenide (GaAs) was exploited to explore the potential of GaAs as a closing and opening switch when operating in the linear mode (the linear mode is defined such that one carrier pair is generated for each photon absorbed). The closing time of a linear GaAs switch is theoretically limited by the characteristics of the laser pulse used to activate the switch (the carrier generation time in GaAs is (approx. 10(-14) sec) while the opening time is theoretically limited by the recombination time of the carriers. The recombination time is several ns for commercially available semi-insulating GaAs. Doping or neutron irradiation can reduce the recombination time to less than 100 ps. Switch closing times of less than 200 ps with a 100 ps duration laser pulse and opening times of less than 400 ps with neutron irradiated GaAs at fields of tens of kV/cm was observed. The illumination source was a Nd:YAG laser operating at 1.06 microns. DOE

N90-12364# Lawrence Livermore National Lab., CA.
THE CHARACTERIZATION OF Nb3Sn SUPERCONDUCTORS FOR USE IN MAGNETS OF 19 T AND GREATER
L. T. Summers, M. J. Strum, and J. R. Miller Aug. 1989 8 p Presented at the International Cryogenic Materials Conference, Los Angeles, CA, 24-28 Jul. 1989
(Contract W-7405-eng-48)
(DE89-017758; UCRL-100270; CONF-890701-5) Avail: NTIS HC A02/MF A01

Increased resolution of NMR spectrometry will require the use of very high field Nb3Sn superconducting magnets. The results are reported of the investigation into mechanical and temperature effects on internal-Sn superconductors similar to those proposed for use in a 900 MHz, 21 T NMR magnet system. Thermal precompression was found to be about 0.225 percent, and the irreversible strain was about 0.8 percent. Fatigue degradation was not observed at cyclic intrinsic strains below 0.575 percent. Additions of reinforcing steel in cable conductors was found to reduce the critical current by as much as 50 percent compared to similar, unreinforced cables. Reduction of the testing temperature to 2.3 K did not increase the critical current in steel reinforced cables to a level significantly above that of unreinforced samples. DOE

N90-12365# Oak Ridge National Lab., TN.
EFFECTS OF GRAIN BOUNDARY CHEMISTRY ON CRITICAL CURRENT DENSITY IN OXIDE SUPERCONDUCTORS
D. M. Kroeger 11 Sep. 1989 17 p Presented at the NATO Advanced Study Inst. on Physics and Materials Science of High Temperature Superconductors, Bad Windsheim, Fed. Republic of Germany, 13-26 Aug. 1989
(Contract DE-AC05-84OR-21400)
(DE89-017780; ORNL/FTR-3367) Avail: NTIS HC A03/MF A01

A NATO Advanced Study Institute on Physics and Materials Science of High Temperature Superconductors was attended and this paper was presented. Work of particular interest to the ORNL program on superconductivity described preparation and properties of a randomly oriented polycrystalline silver/B-Sr-Ca-Cu-O composite conductor which does not exhibit weak-link behavior at 4.2 K. These results provide a basis for optimism concerning bulk applications of oxide superconductors. DOE

N90-12366# Brookhaven National Lab., Upton, NY.
SINGLE CRYSTAL DIFFRACTION
J. Axe, J. Brown, J. Cable, S. Mason, and B. Schoenborn 1989 6 p Presented at the DOE Workshop for Advanced Neutron Source, Oak Ridge, TN, 9 Jun. 1989
(Contract DE-AC02-76CH-00016)
(DE90-000024; BNL-43114; CONF-8906213-1; BIO-4531) Avail: NTIS HC A02/MF A01

Crystallographic techniques are used in many scientific fields, and, at first instance, all applications appear to use the same theory and instrumentation. However a closer look at the requirements posed by the different fields reveals that the strategies for both analysis and data collection employ quite different approaches, based on widely different demands. In the following sections we highlight the differences between the major usages of neutron crystallography. From a perusal of the different requirements, it is clear that several different instruments are required, some with overlapping characteristics. We do not specifically address the number of instruments required in each category, but some comments on the total usage are given in each section. DOE

N90-12367# Colorado State Univ., Fort Collins. Dept. of Electrical Engineering.
BEAM ASSISTED FABRICATION OF 3-5/SI MONOLITHIC DEVICES Final Report, Sep. 1986 - Mar. 1989
Gary Y. Robinson, George J. Collins, and Raj Solanki (Oregon Graduate Center for Study and Research, Beaverton.) 1 May 1989 6 p
(Contract F49620-86-K-0021)
(AD-A212046; AFOSR-89-1159TR) Avail: NTIS HC A02/MF A01 CSCL 20/12

The results of a two-year project to explore new methods for deposition of 3-5 semiconducting film on silicon substrates are summarized. Gas-source molecular beam epitaxy was used for the first time to achieve heteroepitaxy of InP on Si. The InP films contain low concentrations of impurities (less than 400 ppb), luminescence under optical excitation, and exhibit high structural quality. Laser-assisted epitaxy was used for selective area growth of GaP and InP on Si using a new phosphorous precursor, and in situ removal of oxide on Si was achieved photochemically. Plasma-assisted chemical vapor deposition of AlN films has been carried out at low substrate temperatures using an electron beam to excite a remote plasma. GRA

N90-12368# Helsinki Univ. of Technology, Espoo (Finland). Low Temperature Lab.
FLARE-IN TEXTURE IN ROTATING SUPERFLUID (3)He-B
M. M. Salomaa 1989 18 p
(PB89-218994; TKK-F-A641; ISBN-951-754-823-0) Avail: NTIS HC A03/MF A01 CSCL 20L

A new first-order phase transition is proposed to manifest itself in rotating (3)He-B for the vortex-free state, owing to counterflow. The flare-out texture becomes unstable towards a new flare-in texture, which is suggested to explain the transition to a previously unidentified state characterized by a signal corresponding to beta = 90 deg, i.e., with the vector (n circumflex) perpendicular to (H vector)(Norm Omega vector)(z circumflex). This transition may be observable also in other experiments, such as ultrasonic measurements, on the vortex-free state of rotating (3)He-B. GRA

N90-12369# Helsinki Univ. of Technology, Espoo (Finland). Low Temperature Lab.
RESONANT QUASIPARTICLE-ION SCATTERING IN ANISOTROPIC SUPERFLUID (3)He
R. H. Salmelin and M. M. Salomaa 1989 68 p
(PB89-221618; TKK-F-A647; ISBN-951-754-877-X) Avail: NTIS HC A04/MF A01 CSCL 20L

Low-energy excitations in quantum fluids are most directly encountered by ions. In the superfluid phases of (3)He the relevant elementary excitations are Bogoliubov quasiparticles which undergo repeated scattering off an ion in the presence of a divergent density of states. A quantum-mechanical calculation is given of the resonant (3)He quasiparticle-scattering-limited mobility for negative ions in the anisotropic bulk (3)He-A (A phase) and (3)He-P (polar phase) which is exact when the quasiparticles scatter elastically. A new numerical scheme is developed to solve the singular equations for quasiparticle-ion scattering in the A and P phases. The (3)He quasiparticle-ion cross sections are discussed, which allow one to account for the mobility data with essentially no free parameters. The calculated mobility thus facilitates an introduction of ion spectroscopy to extract useful information on fundamental properties of the superfluid state, such as the temperature dependence of the energy gap in (3)He-A. GRA

N90-12370# Helsinki Univ. of Technology, Espoo (Finland). Low Temperature Lab.
COLLECTIVE-MODE SPECTROSCOPY OF TEXTURES IN SUPERFLUID (3)He-B
M. M. Salomaa and G. E. Volovik (Academy of Sciences, USSR, Moscow) 13 Mar. 1989 40 p
(PB89-221634; TKK-F-A642; ISBN-951-754-846-X) Avail: NTIS HC A03/MF A01 CSCL 20L

A phenomenological theory for the propagation of the real squashing modes in superfluid (3)He-B is presented. This allows one to calculate the splitting of the rsq mode spectrum caused by the combined effects of magnetic field, dispersion, and texture in the experimentally important range of magnetic fields from 0 to 1000 Gauss. This serves to provide a tool for the rsq mode spectroscopy of the textures in (3)He-B. In particular, a new gyrosonic effect is suggested: the intensity of the rsq modes generated in textures depends on the sense of rotation, even when the axis of rotation coincides with the direction of the ultrasound propagation. GRA

N90-12371# Army Lab. Command, Watertown, MA.
EFFECT OF ANNEALING CONDITIONS ON THE STRUCTURAL AND SUPERCONDUCTING PROPERTIES OF Y-Ba-Cu-O FILMS
Jae Ryu, Yizhou Huang, Carmine Vittoria, Daniel F. Ryder, Jr. (Tufts Univ., Medford, MA.), James V. Marzik, Richard Benfer, and William A. Spurgeon May 1989 17 p Submitted for publication
(DA Proj. 1L1-61102-AH-42)
(AD-A211308; MTL-TR-89-41) Avail: NTIS HC A02/MF A01 CSCL 20/3

The effect of various annealing treatments on ion beam sputter deposited Y1Ba2Cu(y)O(7-x)(y=3 and 5) amorphous thin films was studied using scanning electron microscopy (SEM), x ray diffraction and dc resistivity measurements. SEM analysis showed that the morphology of the films were clearly divided into three categories: an equiaxial grain structure, a well oriented grid like microstructure and a textured platelet structure. The equiaxial grain structure (random orientation according to x ray diffraction measurements) was obtained when the film was annealed at slow heating and cooling rates in an oxygen atmosphere. The grid like microstructure (b/c-axes oriented normal to the plane) was obtained in Cu-rich composition (y=5) by rapid thermal annealing. A textured platelet microstructure (c-axis oriented normal to the plane) was obtained using slow heating rates and by carefully controlling the gas environment at the temperature region near the orthorhombic tetragonal transition. Thus, the ability was demonstrated to control the morphology and orientation of the film by varying the annealing process. GRA

N90-12372# Cornell Univ., Ithaca, NY. School of Electrical Engineering.
ULTRA HIGH SPEED COMPOUND SEMICONDUCTORS AND REAL TIME SIGNAL PROCESSING Annual Report, 1 May 1988 - 30 Apr. 1989
J. Peter Krusius 1 May 1989 47 p
(Contract F49620-87-C-0044)
(AD-A211394) Avail: NTIS HC A03/MF A01 CSCL 20/12

This report is the annual report on research conducted under the auspices of the Joint Services Electronics Program at Cornell University. The research is grouped under two themes: (1) ultra high speed compound semiconductors, and (2) real time signal processing. Results on organometallic vapor phase epitaxy (OMVPE) materials growth, femtosecond laser probing of hot carriers, and ensemble Monte Carlo simulations are reported on under the first theme. Accomplishments on VLSI algorithms, fault tolerant architectures, and architectures with multiple functional units for signal processing are given under the second theme. GRA

N90-12373# Stanford Univ., CA. Electronics Lab.
SURFACE, INTERFACE, AND BULK PROPERTIES OF HIGH T(SUB c) SUPERCONDUCTORS Final Report, 30 Sep. 1987 - 29 Apr. 1989
William E. Spicer, Z. X. Shen, Per Lindberg, Daniel Dessau, and Barrett Wells 30 Jun. 1989 12 p
(Grant AF-AFOSR-0389-87; AF Proj. 2306)
(AD-A211490; AFOSR-89-1104TR) Avail: NTIS HC A02/MF A01 CSCL 20/12

Extensive studies were performed on Bi2Sr2CaCu2O8 material ever since its discovery in early 1988. Single crystals, polycrystalline pellets and thin film samples of the Bi2Sr2CaCu2O8 material were examined using various photoemission related techniques. Especially the single crystalline Bi2Sr2CaCu2O8 material was found to have an extraordinary inertness in ultrahigh vacuum conditions, allowing a detailed examination of the surface electronic structure. Consequently, most of the investigations were focused on the single crystalline materials. Low-Energy Electron Diffraction (LEED) was used to confirm the single crystallinity of the in situ cleaved crystals of Bi2Sr2CaCu2O8. Sharp diffraction spots indicative of long range periodicity were observed. The observed LEED pattern showed that the Bi2Sr2CaCu2O8 material preferentially cleaves parallel to the a-b plane. In addition, a superstructure was seen extending along one of the symmetry axes in the a-b plane. The superstructure was found to have a periodicity about 5 times as long as the cell dimensions of the a and b axes, in agreement with the bulk structure. GRA

N90-12374# Minnesota Univ., Saint Paul. School of Physics and Astronomy.
HIGH TEMPERATURE SUPERCONDUCTING COMPOUNDS Technical Report, 1 Sep. 1987 - 28 Feb. 1989
Allen M. Goldman and Martha L. Mecartney 31 Mar. 1989 14 p
(Grant AF-AFOSR-0372-87; AF Proj. 2306)
(AD-A211511; AFOSR-89-1107TR) Avail: NTIS HC A02/MF A01 CSCL 20/3

High T(sub c) superconductors were investigated in both bulk and thin film form. Investigations were carried out on the magnetic properties of both polycrystalline and single crystal forms of YBa2Cu3O7 focussing on time-dependent effects. Single crystals of this material were studied using scanning tunneling microscopy. Techniques for fabricating thin films were developed. These include sputtering using spherical targets and co-evaporation using pure ozone as an oxidant. The latter permits the in situ formation of films without any post-deposition annealing step. Superconducting fluctuations and the Kosterlize-Thouless transition were studied in the T1-Ba-Ca-Cu-O films. GRA

N90-12375# Virginia Univ., Charlottesville. Dept. of Electrical Engineering.
SIS (SUPERCONDUCTOR-INSULATOR-SUPERCONDUCTOR) MIXER RESEARCH Final Technical Report, Nov. 1987 - Nov. 1988
Marc J. Feldman Jul. 1989 18 p
(Grant AF-AFOSR-0056-86; AF Proj. 2305)
(AD-A211607; UVA/525659/EE90/101; AFOSR-89-1165TR)
Avail: NTIS HC A03/MF A01 CSCL 09/1

Theoretical and experimental research has been conducted to elucidate the basic physics behind the properties of Superconductor Insulator Superconductor (SIS) tunnel junction receiving devices. The saturation behavior of the SIS mixer and the SIS direct detector was calculated. The direct detector was found to saturate at far higher powers than previously believed, allowing the possibility of practical application. SIS mixer saturation was measured using both monochromatic and thermal signals, and these experiments dramatically verified the theoretical expression. Quantum noise in the quantum theory of mixing was identified as the residual remaining when the usual noise sources are minimized. The quantum noise limit was shown to be reached in only two special cases. Computer calculations determined that the behavior of SIS receivers divides into two frequencies regimes, the cross over frequency depending upon junction quality. The properties of these two regimes were delineated. A study of the role of the image termination of SIS mixers found that the nonlinear quantum reactance results in an effective time delay at the input port. Many aspects of the operation of SIS mixers at submillimeter wavelengths were clarified. Niobium nitride edge junctions with excellent current voltage characteristics were fabricated using a novel barrier formation process. GRA

N90-12376# Evans (Charles) and Associates, Redwood City, CA.
DEVELOPMENT AND EVALUATION OF AN INSTRUMENT FOR RAPID ELECTROREFLECTANCE OF SEMICONDUCTOR MATERIALS Final Technical Report, 1 Feb. 1988 - 30 Apr. 1989
Michael H. Herman 30 Jun. 1989 73 p
(Contract N00014-88-C-0221; ARPA Order 5325)
(AD-A211690; CEVANS/057/FR-8901) Avail: NTIS HC A04/MF A01 CSCL 20/12

The applications of electron beam electroreflectance (EBER) to Hg(1-x)Cd(x)Te (MCT) and other semiconductor systems are desired. Temperature dependences of the E1 optical gap of MCT are in agreement with the results of other researchers. For an epitaxial sample, alpha E (1)/alpha T of -(6.7 to 8.2) x .0001 eV/K has been obtained. This value is consistent with that determined by Berlouis. We find a larger thermal coefficient for epitaxial MCT on CdTe than for bulk MCT. We have also measured the E(1) Delta (1) band gap to be nearly 0.63 eV above the E1 transition energy. MCT is more sensitive to electron beam current intensity than other materials due to its relatively poor thermal conductivity. The lineshape observed at .001 A/sq.cm appears to be from thermoreflectance (TR), based upon calculations and detailed experimental studies. Therefore, EBER determinations of the temperature dependence of the E1 and E1+Delta (1) band gap energies demonstrate a large variance. We have collaborated with other researchers on EBER evaluation of MCT growth and dry-etch processes. We have extended EBER studies to other technologically important crystal systems related to MCT. We have found correlations between the EBER measurements of CdTe samples and surface preparation methods. GRA

N90-12377# Army Lab. Command, Watertown, MA. Material Technology Lab.
SYNTHESIS AND MICROSTRUCTURE OF HIGHLY ORIENTED PbTIO3 THIN FILMS PREPARED BY A SOL-GEL METHOD Final Report
Daniel F. Ryder, Jr., Chiahong Chen, and William A. Spurgeon Jun. 1989 16 p Prepared in cooperation with Tufts Univ., Medford, MA
(AD-A211735; MTL-TR-89-55) Avail: NTIS HC A03/MF A01 CSCL 20/2

While orientation of microstructure to enhance electrical characteristics is, in general, not a major issue in the development of ceramic dielectrics, there are specific exceptions where system performance is improved by film orientation. The electrical poling of ferroelectric ceramics to produce piezoelectric transducer and pyroelectric detector components is a case in point. Relative to thin film devices, there is, then, the need to develop economical processes for the fabrication of highly oriented ferroelectrics. In this work, the sol-gel method was investigated as a potential technique for the deposition of oriented and epitaxial PbTiO3 thin films. Thin films of PbTiO3 were deposited on fused silica, resistor grade alumina, and single crystal (100) MgO by a sol-gel processing method. While the films deposited on silica and alumina substrates were randomly oriented and polycrystalline, highly (100) oriented PbTi03 films were grown on the MgO single crystals. The peroviskite-type structure was observed with films deposited on the single crystal MgO and annealed at temperatures as low as 470 C, while a pyrochlore-type structure was observed with films of fused silica and alumina processed in a similar manner. All films heat treated at temperatures in excess of 570 C showed significant formation of a second PbTi3O7 phase. The films were characterized by electron microscopy and glancing incidence angle x ray diffraction. GRA

77 THERMODYNAMICS AND STATISTICAL PHYSICS

Includes quantum mechanics; theoretical physics; and Bose and Fermi statistics.

For related information see also *25 Inorganic and Physical Chemistry* and *34 Fluid Mechanics and Heat Transfer.*

N90-12378# Institute for Advanced Study, Princeton, NJ.
BORDERED SURFACES, OFF-SHELL AMPLITUDES, SEWING, AND STRING FIELD THEORY
Steven Carlip Apr. 1989 43 p Presented at the 25th Karpacz Winter School of Theoretical Physics, Karpacz, Poland, 20 Feb. - 5 Mar. 1989
(Contract DE-AC02-76ER-02220)
(DE90-000006; CONF-8902132-1; IASSNS-HEP-89/29) Avail: NTIS HC A03/MF A01

These lectures will deal with the current status of the sewing problem. The rationale for this approach is that any nonperturbative string theory must reproduce the Polyakov path integral as a perturbation series. If our experience in ordinary field theory is a guide, and admittedly it may not be, the terms in such a perturbation series, like Feynman diagrams, are likely to be built up from simple vertices and propagators, which can themselves be represented as (off-shell) Polyakov amplitudes. Hence an understanding of how to put together simple components into more complicated world sheet amplitudes is likely to give us much-needed information about the structure of nonperturbative string theory. To understand sewing, we must first understand the building blocks, off-shell Polyakov amplitudes. This is the subject of my first lecture. Next, we will explore the sewing of conformal field theories at a fixed conformal structure, that is, the reconstruction of correlation functions for a fixed surface (Sigma) from those on a pair of surfaces (Sigma)(sub 1) and (Sigma)(sub 2) obtained by cutting (Sigma) along a closed curve. We will then look at the problem of sewing amplitudes, integrals of correlation functions over moduli space. This will necessitate an understanding of how to build the moduli space of a complicated surface from simpler moduli spaces. Finally, we will briefly examine vertices and string field theories. DOE

N90-12379# Universal Energy Systems, Inc., Dayton, OH.
STUDIES ON THE STARTUP TRANSIENTS AND PERFORMANCE OF A GAS LOADED SODIUM HEAT PIPE Ph.D. Thesis - Dayton Univ. Interim Technical Report, 29 Jun. 1987 - 30 Nov. 1988

Rengasamy Ponnappan Jun. 1989 247 p
(Contract F33615-87-C-2738; AF Proj. 3145)
(AD-A211880; UES-799-TR-87-001; WRDC-TR-89-2046) Avail: NTIS HC A11/MF A02 CSCL 20/13

High temperature liquid metal heat pipes have exhibited difficulties starting up from frozen state due to inherent low near-room temperature vapor pressures associated with working fluids. Inert gas loading is a possible solution to the frozen state startup problem. A few research papers give results of this technique. The applicability of the method to heat pipes with arterial grooves and long adiabatic lengths is unknown. The present study deals with the design, fabrication and startup testing of a gas loaded sodium heat pipe of the double walled type with grooved artery channel and long adiabatic section. GRA

N90-12380# Aerospace Corp., El Segundo, CA. Electronics Research Lab.
THERMAL MODEL FOR DOUBLE-DRIFT IMPATT DIODES ON DIAMOND HEAT SINKS
Geza Csanky 31 Aug. 1989 46 p
(Contract F04701-88-C-0089)
(AD-A211746; TR-0089(4925-02)-3; SD-TR-89-57) Avail: NTIS HC A03/MF A01 CSCL 20/13

A thermal model of double-drift IMPATT diodes on diamond heat sinks was developed. The thermal model approximates the temperature dependent thermal conductivities of Si and diamond (Type II) by means of simple empirical formulas. The application of the thermal model to three IMPATT diode lits indicates that under life test, junction temperatures are greater than 700 C, while the metal/Si interface temperatures exceed 500 C. An explanation of the failure mechanism is presented. Designs that result in a lower junction temperature are proposed. GRA

N90-12381# ESDU International Ltd., London (England).
AN INTRODUCTION TO EFFECTIVENESS: NTU RELATIONSHIPS
Aug. 1989 27 p
(ESDU-89016; ISBN-0-85679-688-3; ISSN-0141-402X) Avail: ESDU

ESDU 89016 introduces the method, used in the thermal design or in estimating the thermal performance of heat exchangers, using the analysis of the heat transfer in a counter-current exchanger to derive the fundamental relationships. The quantities involved (heat transfer effectiveness, thermal capacity ratio and number of heat transfer units (N sub TU)) are defined. An alternative approach, the F-factor method, is introduced and the relationship between it and the effectiveness - N sub TU method is explained; by considering the steps involved in the assessment of the performance of a given exchanger for given inlet conditions, the methods are compared. Although the methods assume constant specific heat capacity and a constant local value of heat transfer coefficient between the streams, example calculations show that no major errors are introduced when those properties are varying slowly; the use of average values for them is adequate. The relationships cannot be used, however, when sudden property changes occur (such as with the onset of boiling or condensation). The data provided in ESDU 86018, 87020 and 88021 are introduced with an explanation of the asymptotic values (maximum effectiveness irrespective of size) and crossover values (when both streams have the same temperature) included for each type of exchanger considered, and there is an index showing which types are treated in each document. Author

N90-12382 National Physical Lab., Teddington (England). Div. of Materials Applications.
A CRITICAL ASSESSMENT OF THERMODYNAMIC AND PHASE DIAGRAM DATA FOR THE Ga-In SYSTEM
B. C. Rugg (Sheffield Univ., England) and T. G. Chart Mar. 1989 24 p
(NPL-DMA(A)-174; ISSN-0143-7313; ETN-89-95539) Copyright Avail: National Physical Lab., Teddington, Middlesex, TW11 0LW, United Kingdom

Thermodynamic and phase diagram data for the liquid and solid phases of the gallium-indium system are critically assessed. An optimized set of thermodynamic parameters consistent with the experimental data is presented which employs the Redlich-Kister/Margules formalism. The calculated phase equilibria and optimized thermodynamic values are compared with those determined experimentally. There is uncertainty in the literature concerning portions of the phase diagram, namely the liquidus in the vicinity of the eutectic composition and the solid solubility of gallium in indium. The calculated phase diagram and optimized thermodynamic parameters prove to be in agreement with more recent data. ESA

80 SOCIAL SCIENCES (GENERAL)

Includes educational matters.

N90-12383# Massachusetts Inst. of Tech., Cambridge.
DESIGNING AND DESIGNING KNOWLEDGE IN ENGINEERING AND ARCHITECTURE Final Report
L. L. Bucciarelli, Stephen M. Ervin, Aaron Fleisher, Gabriela Goldschmidt, Mark D. Gross, Donald A. Schon, and Glenn Wiggins 14 Apr. 1989 255 p
(Grant NSF DMC-86-11357)
(PB89-219521; NSF/ENG-89006) Avail: NTIS HC A12/MF A02 CSCL 13B

The volume contains a collection of reports. Included are: Summary Report CM2: a Constraint Based Design Environment; CM2: A Constraint Manager for Design Exploration on the Macintosh; Computer-aided diagramming and the Generator-Test Cycle; Grammatical Architecture; Kings of Seeing and their Functions in Designing; Architectural Sketching: Seeing As and Seeing That; and Engineering Design as Negotiation: A Design Exercise. Author

81 ADMINISTRATION AND MANAGEMENT

Includes management planning and research.

N90-12384# National Academy of Sciences - National Research Council, Washington, DC. Commission on Engineering and Technical Systems.
TWENTY-FIVE YEARS OF SERVICE, 1962-1987: PROCEEDINGS OF THE AIR FORCE STUDIES BOARD SYMPOSIUM ON AIR FORCE RESEARCH AND DEVELOPMENT, NOVEMBER 16, 1987
1988 183 p Symposium held in Washington, DC, 16 Nov. 1987
(Contract F49620-87-C-0122)
(PB89-198915) Avail: NTIS HC A09/MF A01 CSCL 05A

The Air Force Studies Board celebrated 25 consecutive years of service to the National Research Council and the United States Air Force on November 16, 1987, with a symposium reviewing the last 25 years of Air Force research and development, and projecting lessons learned into the future. During the intervening 25 years the AFSB has maintained a close relationship with successive AFSC commanders and has published 86 studies on such diverse topics as jet and rocket propulsion, optics, satellite time transfer, battle management, and avionics troubleshooting. Author

N90-12385*# National Aeronautics and Space Administration, Washington, DC.
WORKING WITH PEOPLE TO IMPROVE PRODUCTIVITY AND QUALITY: A BIBLIOGRAPHY WITH INDEXES, 1984-1988
Oct. 1989 72 p
(NASA-SP-7078; NAS 1.21:7078) Avail: NTIS HC A04 CSCL 05A

This bibliography contains 253 anotated references to reports and journal articles entered into the NASA scientific and technical information database 1984 to 1988. Author

N90-12386# Oak Ridge Gaseous Diffusion Plant, TN.
THE APPLICATION OF QUALITY ASSURANCE TO ENGINEERING MANAGEMENT
George J. Kidd, Jr. Apr. 1989 11 p Presented at the 2nd International Conference on Engineering Management, Toronto, Ontario, 16-18 Oct. 1989
(Contract DE-AC05-84OT-21400)
(DE89-009955; K/QT-282; CONF-891075-1) Avail: NTIS HC A03/MF A01

The need for quality in the products that our industries produce has long been recognized and accepted. In recent years it has also been recognized that the concern for quality must also be applied to the raw materials going into the products and to the processes used to produce them. Only very recently has it been recognized that the same concern for quality must be applied during the engineering processes that precede the manufacturing phase of the product cycle. For this idea to be understood and accepted by the engineering community, it will be necessary to apply these same concepts of quality to the engineering-management function. This paper describes a systems-analysis-based approach of quality assurance that provides a simple, straightforward process for determining which outputs from the various management tasks are significant. It also relates what can and should be tracked and evaluated and who is responsible. The process has four aspects: system description, planning, execution, and evaluation. DOE

N90-12387# Defense Logistics Agency, Alexandria, VA. Operations Research and Economic Analysis Office.
FORECASTING CONTRACTING WORKLOAD Final Report
Kurt F. Schwarz and Thomas L. Brooks, IV Apr. 1989 25 p
(AD-A211935) Avail: NTIS HC A03/MF A01 CSCL 05/1

This study explored the possibility of forecasting Defense Logistics Agency (DLA) contracting workload from indicators of service activity. The premise of this analysis is that DLA's contracting workload is somehow related to Service activity; an increase in Service activity will lead to a corresponding increase in DLA workload. We examined the use of regression analysis and mathematical modeling for forecasting DLA workload. We found that we could not forecast DLA's contracting workload directly from service activity (given the variables we examined). We were able to forecast DLA's supply operations workload (expressed by item demand) from Service activity in some cases. Then, we could forecast some of DLA's stocked item contracting workload indirectly by using the forecasts of item demand, but we were unable to forecast any of DLA's nonstocked contracting workload. Based upon the inability to accurately forecast DLA's contracting workload from service activity, we recommend continued use of DLA's current workload forecasting techniques. GRA

82 DOCUMENTATION AND INFORMATION SCIENCE

Includes information management; information storage and retrieval technology; technical writing; graphic arts; and micrography.

For computer documentation see *61 Computer Programming and Software.*

N90-12388* National Aeronautics and Space Administration. Lewis Research Center, Cleveland, OH.
CRISS-CROSS DIRECTORY OF NASA N NUMBERS AND DOD AD NUMBERS. VOLUME 2, PART 1: AD TO N, 1979-1986. N TO AD, 1962-1986
George Mandel, ed. Feb. 1988 449 p Prepared in cooperation with Special Libraries Association, Chicago, IL
(NASA-TM-101814; NAS 1.15:101814) Avail: MS 60-1, NASA Lewis Research Center, 21000 Brookpark Road, Cleveland, OH 44135 HC $55.00. Make checks available to Aerospace Div., SLA CSCL 05B

This directory presents a tabular listing of DOD AD report numbers and corresponding NASA N numbers for the periods 1979-1986 (AD to N) and 1962-1986 (N to AD). In addition, tables are provided that map the various NASA Research Report series to N numbers. Those series include Conference Papers (CP), Contractor Reports (CR), Educational Publications (EP), Reference Publications (RP), Special Publications (SP), Technical Papers (TP), Technical Translations (TT), and Technical Memorandums (TM). Part 1 of the directory includes the AD to N listing, Research Report tables, and a portion of the N to AD listing. Author

N90-12389* National Aeronautics and Space Administration. Lewis Research Center, Cleveland, OH.
CRISS-CROSS DIRECTORY OF NASA N NUMBERS AND DOD AD NUMBERS. VOLUME 2, PART 2: AD TO N, 1979-1986. N TO AD, 1962-1986
George Mandel Feb. 1988 451 p Prepared in cooperation with Special Libraries Association, Chicago, IL
(NASA-TM-101815; NAS 1.15:101815) Avail: MS 60-1, NASA Lewis Research Center, 21000 Brookpark Road, Cleveland, OH 44135 HC $55.00. Make checks available to Aerospace Div., SLA CSCL 05B

This directory presents a tabular listing of DOD AD report numbers and corresponding NASA N numbers for the periods 1979-1986 (AD to N) and 1962-1986 (N to AD). In addition, tables mapping the various NASA Research Report series to N numbers are provided. Part 2 of the directory continues the N to AD listing. Author

N90-12390# National Library of Medicine, Bethesda, MD. Collection Access Section.
NATIONAL LIBRARY OF MEDICINE DOCLINE (TRADENAME) MANUAL
Mar. 1989 134 p Sponsored by Dept. of Health and Human Services, Washington, DC
(PB89-188676) Avail: NTIS HC A07/MF A01 CSCL 05B

DOCLINE(R) is the National Library of Medicine's automated interlibrary loan request routing system. The system was developed to improve document delivery service by routing loan requests quickly and efficiently throughout the Regional Medical Library network. Simplicity and ease of use are design features of DOCLINE. Loan requests can be created, edited, routed, received, and filled without special training. Users can also check the status of a request for which they are either the borrowing or the lending library. A series of menus and system prompts guides the user through the steps necessary to accomplish these functions. The manual presents a tutorial, a reference section, and sample transactions. GRA

N90-12391# Department of Energy, Oak Ridge, TN. Office of Scientific and Technical Information.
PROGRAM DISTRIBUTION FOR UNCLASSIFIED SCIENTIFIC AND TECHNICAL REPORTS: INSTRUCTIONS AND CATEGORY SCOPE NOTES, REVISION 75
W. F. Simpson, Jr., ed. and D. Amburn, ed. Aug. 1989 108 p
(DE89-005395; DOE/OSTI-4500-Rev-75) Avail: NTIS HC A06/MF A01

The DOE Office of Scientific and Technical Information (OSTI) in conjunction with DOE Program Offices establishes distribution categories for research, development, and technological reports emanating from DOE programs. The revised category numbers and scope notes contained in this publication were coordinated between OSTI and DOE Program Offices with input from DOE Field Offices. Decisions regarding whether reports will be distributed are made by Program Offices in conjunction with DOE Field Offices and OSTI. This revision of DOE/OSTI-4500 contains the revised distribution category numbers and scope notes along with the printed copy requirement, which shows the number of copies required to make program distribution. DOE

N90-12392# Vrije Univ., Amsterdam (Netherlands). Dept. of Mathematics and Computer Science.
ROLE OF CONCEPTUAL MODELS IN THE DESIGN AND USE

OF INFORMATION SYSTEMS
Roel Wieringa Feb. 1989 39 p
(PB89-217376) Avail: NTIS HC A03/MF A01 CSCL 05B

Three different roles of conceptual models (CM's) in the design and use of information systems (IS's) are investigated. The representative role of a CM is that it is an abstract representation of the universe of discourse (UoD) of the IS; as such it prescribes the structure and behavior of a database (DB) containing a representation of the UoD. A second, normative role of a CM is that it contains prescriptions for the behavior of entities in the UoD. If these prescriptions are implemented in a DB, the DB is used to eliminate possible behaviors of UoD entities. A third role of CM's emerges when a computer is viewed as a symbol-manipulating machine capable of performing speech acts like commanding and promising. A symbol-manipulating machine is capable of uttering sentences (usually in written form), which take on a certain meaning assigned to them by social convention (just as it is a convention that a traffic light tells us to stop when it is red). These conventions are stored in a CM known to the people at whom the speech act is directed. A CM playing this role is called institutional. These three roles are analyzed, using some results from analytic philosophy, and placed in the context of IS design and use. GRA

N90-12393# Helsinki Univ. (Finland). Dept. of Computer Science.
PROBLEM OF INCOMPLETE INFORMATION IN RELATIONAL DATABASES
Gosta Grahne Mar. 1989 170 p
(PB89-217533; A-1989-1; ISBN-951-45-4941-4) Avail: NTIS HC A08/MF A01 CSCL 05B

The basic semantic assumption is that an incomplete database is a set of complete databases (relations). It is shown that there are two natural lattice structures on the set of all sets of relations. There are several candidate tools for storing and manipulating databases with incomplete information. The generalizations of relations is examined. These generalizations, called tables allow variables representing unknown values as entries, as well as entries constraining the variables. Four increasingly (syntactically) stricter classes of tables are defined and their abilities to serve as a basis for implementing incomplete databases are studied along with the operations on them. It turns out that the new class of Horn tables is the most significant from a practical point of view. In this class of tables, positive existential queries are efficiently evaluated and in some cases least fixpoint (recursive) queries. In Horn tables, the information contained in one join dependency is efficiently incorporated and a set of equality generating dependencies, as well as hold the result of a subclass of the update operations. Author

N90-12394# Helsinki Univ. (Finland). Dept. of Computer Science.
INTEROPERABILITY OF HETEROGENEOUS INFORMATION SYSTEMS: THE COST 11(ter) PROJECT Final Report
Henry Tirri, ed. Mar. 1989 120 p
(PB89-217541; A-1989-2; ISBN-951-45-4948-1) Avail: NTIS HC A06/MF A01 CSCL 05B

Project IHIS was formed 1987 as a sequel to the COST 11(ter) project DAISY (Distribution Aspects of Information Systems) to carry out cooperative European research in the area of distributed information systems, including the emerging topic of distributed knowledge based systems. Realizing the many facets of the problems in interoperability, the project was organized as a collection of subprojects, each with a special interest area. The four subtopics to be studied are knowledge based integration, multidatabase languages, generalized transaction model, and performance issues. GRA

N90-12395# National Inst. of Standards and Technology, Gaithersburg, MD. Information Systems Engineering Div.
DETAILED DESCRIPTION OF THE KNOWLEDGE-BASED SYSTEM FOR PHYSICAL DATABASE DESIGN, VOLUME 2 Interim Report, Jul. 1985 - Dec. 1988
Christopher E. Dabrowski Aug. 1989 177 p
(PB89-229033; NISTIR-89/4139/2) Avail: NTIS HC A09/MF A01 CSCL 05B

A knowledge based system for physical database design was developed at the National Computer Systems Laboratory. The system was previously described in NIST Special Publication 500-151. The knowledge base for the system is described in detail. The description includes a complete explanation of each component of the knowledge base together with the actual rules used by the system. Author

N90-12396# National Bureau of Standards, Gaithersburg, MD. Tribology Group.
DEVELOPMENT AND USE OF A TRIBOLOGY RESEARCH-IN-PROGRESS DATABASE
S. Jahanmir and M. B. Peterson Jul. 1989 316 p
(PB89-228274; NISTIR-89/4112) Avail: NTIS HC A14/MF A02 CSCL 05B

Preliminary efforts leading to the development of a research-in-progress database on tribology are described. The database contains brief abstracts of current tribology research being conducted by industry, universities, research institutes and government laboratories based on a survey of active researchers. It also contains information on the types of activities, general areas of interest, program objectives, and tribology applications. The primary program objectives cited in connection with the tribology activities include long life, low maintenance, failure-free machinery, fundamental understanding, and materials development for improved performance. K.C.D.

N90-12397# Oak Ridge National Lab., TN.
BUILDING A USER-FRIENDLY DATA DICTIONARY SYSTEM IN ORACLE
J. P. Loftis and W. E. Friggle 1989 9 p Presented at the International ORACLE User Group Week, Dallas, TX, 1-6 Oct. 1989
(Contract DE-AC05-84OR-21400)
(DE89-014878; CONF-8910154-1) Avail: NTIS HC A02/MF A01

For some time now developers of software systems have recognized the need to capture information about the system and to build a framework for retrieving this information so that it can be easily accessible to end users. Current trends, such as the Information Research Dictionary System (IRDS) standard, IBM's Repository, and a growing interest in Computer Aided Software Engineering (CASE) tools in the U.S. and the Integrated Project Support Environment. dictionary tools that capture information critical to the development and maintenance of a system throughout its life cycle. This paper describes the development of a menu-driven system dictionary in ORACLE for a design prototype system currently under development at Oak Ridge National Laboratory (ORNL). It addresses integration of ORACLE's data dictionary tables with the system dictionary, and possible avenues of future research regarding the design and implementation of an IRDS. DOE

N90-12398# Department of Energy, Washington, DC. Office of Energy Research.
FEDIX: AN ON-LINE INFORMATION SERVICE FOR UNIVERSITIES AND OTHER RESEARCH ORGANIZATIONS: USER'S GUIDE, VERSION 2.0, RELEASE 1
Oct. 1989 45 p
(DE89-016695; DOE/ER-0423) Avail: NTIS HC A03/MF A01

FEDIX is a system of on-line databases providing information on Federal Government programs of interest to colleges and universities. The system currently contains information on the Department of Energy's energy-related equipment program, DOE research and development programs, faculty/student education programs, and DOE's minority assistance programs. DOE's sub-system is referred to as DOEINFO. Databases containing information on Office of Naval Research and National Aeronautics and Space Administration programs will be developed in the fall of 1989 and will be available on-line in FY 1990. It is anticipated that other government agencies will soon be providing information on their programs. DOE

N90-12399# Lawrence Livermore National Lab., CA.
CALS (COMPUTER-AIDED ACQUISITION AND LOGISTIC SUPPORT) TEST NETWORK INFORMATION EXCHANGE: USER'S MANUAL
12 Jun. 1989 18 p Prepared for Air Force Logistics Command
(Contract W-7405-eng-48)
(DE89-016700; UCID-21679; CTN-89-007) Avail: NTIS HC A03/MF A01

The DOD Computer-aided Acquisition and Logistic Support (CALS) Test Network is conducting tests of the military standard for the Automated Interchange of Technical Information (MIL-STD-1840A) and its companion suite of military specifications. The CTN is a DOD- sponsored confederation of voluntary participants from industry and government, managed jointly by a technical staff at Air Force Logistics Command (AFLC) and Lawrence Livermore National Laboratory (LLNL). The objective of CTN tests is to demonstrate and evaluate the interchange and functional use of digital data information between industry and government using the CALS standards. The CTN Information Exchange (CTN Info-X) is a combination of information services for participants and sponsors of the work of the CALS Test Network. This manual tells how to access and use the CALS Info-X. DOE

N90-12400# Defense Applied Information Technology Center, Alexandria, VA. Hypermedia Lab.
DOD GATEWAY INFORMATION SYSTEM (DGIS) COMMON COMMAND LANGUAGE: A RETROSPECTIVE ON THE INTRODUCTION OF PROLOG AS THE DEVELOPMENT TOOL
Duc T. Tran, Allen D. Kuhn, and Randy L. Bixby May 1989 20 p
(AD-A211941; DAITC/TR-89/6; DTIC-TR-89/16) Avail: NTIS HC A03/MF A01 CSCL 12/5

The introduction of PROLOG into the Common Command Language (CCL) development is reviewed. The advantages of using PROLOG as an artificial intelligence tool for developing fifth-generation programs are shown, in comparison with doing traditional third-generation programming. A brief is given on actual PROLOG programming, then the reasons for going to PROLOG are explained. The approach to CCL using knowledge bases and blackboard architecture is described. The goals of CCL as an interface on the DOD Gateway Information System (DGIS) are to provide a standard program for accessing databases, provide maintainability with syntax and semantic changes as they occur, and provide adaptability to future requirements and enhancements. GRA

N90-12401# Ohio State Univ., Columbus. Dept. of Computer and Information Science.
DISTRIBUTED KNOWLEDGE-BASED SYSTEMS Final Report, 1 Nov. 1986 - 31 Oct. 1988
B. Chandrasekaran 15 Mar. 1989 329 p
(Grant AF-AFOSR-0090-87; AF Proj. 2304)
(AD-A211984; AFOSR-89-0428TR) Avail: NTIS HC A15/MF A02 CSCL 12/9

An introduction to and survey of recent research in the generic task approach to task-specific, knowledge-based systems is presented. Knowledge based systems using task specific architectures are steadily winning recognition as significant improvements over earlier attempts at building expert systems. There are generic problem solving strategies out of which complex knowledge based reasoning systems can be built. These generic strategies make use of knowledge organized in forms that are appropriate to the task and its characteristic control regime, and in that way help encode the expert's knowledge of a domain in a deeper way than is obtained using a typical rule based system. The research has developed the basic methodology of the generic task approach, has explored how deeper models and causal reasoning may be of use in problem solving systems, has helped in the production of a generic task toolset to encourage research on integration and useful in practical applications, and has examined ways in which the efficiency and robustness of systems can be improved-by learning, making use of parallelism, and by considering new environments for implementing generic tasks. GRA

N90-12402# National Inst. of Standards and Technology, Gaithersburg, MD. Center for Electronics and Electrical Engineering.
CENTER FOR ELECTRONICS AND ELECTRICAL ENGINEERING TECHNICAL PUBLICATION ANNOUNCEMENTS COVERING CENTER PROGRAMS, JANUARY-MARCH 1989 WITH 1989 CEEE EVENTS CALENDAR
E. J. Walters, comp. Jul. 1989 20 p
(PB89-228308; NISTIR-89/4118) Avail: NTIS HC A03/MF A01 CSCL 05B

The report is the twentieth issue of a quarterly publication providing information on the technical work of the National Institute of Standards and Technology (formerly the National Bureau of Standards) Center for Electronics and Electrical Engineering. The issue covers the first quarter of calendar year 1989. Abstracts are provided by technical area for papers published during the quarter. Author

N90-12403# Carnegie-Mellon Univ., Pittsburgh, PA. Software Engineering Inst.
A REAL-TIME LOCKING PROTOCOL Final Report
Lui Sha, Ragunathan Rajkumar, Sang Son, and Chun-Hyon Chang (Kon-Kuk Univ., Seoul, Republic of Korea) Apr. 1989 26 p
(Contract F19628-85-C-0003)
(AD-A211514; CMU/SEI-89-TR-18; ESD-TR-89-26) Avail: NTIS HC A03/MF A01 CSCL 12/5

When a database system is used in a real-time application, the consistency control prototype must satisfy not only the consistency of shared data but also the timing constraints of the application. A priority-driven two-phase lock protocol called the read- or write-priority ceiling protocol was examined. It is shown that this protocol is free of deadlock, and in addition a high-priority transaction can be blocked by lower priority transactions for at most the duration of a single embedded transaction. The system performance was examined experimentally. GRA

N90-12404# Deutsche Forschungs- und Versuchsanstalt fuer Luft- und Raumfahrt, Oberpfaffenhofen (West Germany). Abteilung Regelung.
ANDECS-PERLUDE 2.0: A DATABASED, INTERACTIVE SYSTEM OF CONTROL SOFTWARE USER'S GUIDE
Hans-Dieter Joos Mar. 1988 119 p In GERMAN; ENGLISH summary
(DFVLR-Mitt-89-07; ISSN-0176-7739; ETN-89-95298) Avail: NTIS HC A06/MF A01; DFVLR, VB-PL-DO, Postfach 90 60 58, 5000 Cologne, Fed. Republic of Germany, 42.50 DM

A software package for control applications, ANDECS-PRELUDE (ANalysis and Design of Control Systems-PRELiminary Utilities DEpository), is described. The ANDECS-PRELUDE package supplies the user by a database system and an interactive environment for control analysis and design procedures. It is an open software system in the sense that user defined applications can be easily added to it. It includes a data and method base system for technical and scientific applications. The system theory and control methods in ANDECS-PRELUDE are those of the control engineering software library RAPS (regulator analysis and synthesis programs). The procedures in ANDECS-PRELUDE use predefined composed control oriented data structures. This avoids user problems with data interfaces between different procedures. ESA

N90-12405# Royal Aerospace Establishment, Farnborough (England).
INTRODUCTION TO THE MIL-STD-1553B SERIAL MULTIPLEX DATA BUS
D. R. Bracknell 7 Sep. 1988 32 p

(RAE-TM-M-9; BR108268; ETN-89-94335) Copyright Avail: Defence Research Information Centre, Kentigem House, 65 Brown Street, Glasgow, G2 8EX, Scotland

The Mil-Std-1553B serial, digital, multiplex data bus standard used in military real time system applications is introduced. The standard is now finding applications in the commercial and industrial sector because of its inherent flexibility and durability in harsh environments. The history and main features of the standard are presented, together with an indication of why it was developed and how it is applied in systems design. It is compared with three commercial counterparts (ARINC 429, BITBUS and ETHERNET) and possible developments are discussed. ESA

N90-12466*# Colorado Univ., Boulder. Dept. of Atmospheric, Planetary, and Astrophysical Sciences.

ACCESS TO MAX '91 INFORMATION VIA COMPUTER NETWORKS

Alan L. Kiplinger (National Oceanic and Atmospheric Administration, Boulder, CO.) *In* NASA, Goddard Space Flight Center, Max '91 Workshop 2: Developments in Observations and Theory for Solar Cycle 22 1989 p 60-64 (For primary document see N90-12459 03-92)

Avail: NTIS HC A17/MF A03 CSCL 05B

83 ECONOMICS AND COST ANALYSIS

Includes cost effectiveness studies.

N90-12406# Systems Control Technology, Inc., Arlington, VA.

ROTORCRAFT LOW ALTITUDE CNS BENEFIT/COST ANALYSIS: ROTORCRAFT OPERATIONS DATA Final Report

Brian E. Mee, Deborah Peisen, and Margaret B. Renton Sep. 1989 160 p

(Contract DTFA01-87-C-00014)

(DOT/FAA/DS-89/9; SCT-89RR-47) Avail: NTIS HC A08/MF A01

Communications, navigation, and surveillance (CNS) services are readily available at the altitudes flown by most fixed wing aircraft. They are not, however, always available at the lower altitudes at which most rotary wing aircraft operate. The objective is to determine if there is an economic basis for improvement of these low altitude CNS services within the National Airspace System (NAS) in order to better support rotorcraft operations. The Rotorcraft Master Plan advocates the establishment of additional CNS facilities as well as the analysis and development of systems to satisfy the increasing demand for widespread IFR rotorcraft operations within the NAS. The findings will aid the FAA decisionmaking in that regard. In view of prior implementation decisions on Loran-C, the emphasis is on communications and surveillance. Background data is provided on the rotorcraft industry as it exists today, as well as forecasts to the year 2007 for the purpose of providing operational data for analysis of long term CNS benefits and costs. Rotorcraft missions are described; those most likely to benefit from increased availability of CNS services are selected; the probability is identified of various combinations within selected rotorcraft operating areas; and an inventory is presented of rotorcraft activity by mission and location. Author

84 LAW, POLITICAL SCIENCE AND SPACE POLICY

Includes NASA appropriation hearings; aviation law; space law and policy; international law; international cooperation; and patent policy.

N90-12407# National Science Foundation, Washington, DC. Div. of Science Resources Studies.

FEDERAL FUNDS FOR RESEARCH AND DEVELOPMENT: FISCAL YEARS 1986, 1987, AND 1988. VOLUME 36: DETAILED STATISTICAL TABLES

1988 264 p

(PB89-223523; NSF-87-314-Vol-36) Avail: NTIS HC A12/MF A02 CSCL 05C

The 163 tables present data on Federal research and development (R and D) funding for the 1986 through 1988 period. The data, provided by Federal agencies through an annual survey, cover research and development by individual agency, character of work (basic research, applied research, and development), and performing sector. Research funding by field of science/engineering is available for all performing sectors and for research performed at universities and colleges. Data are provided on R and D plant obligations by agency and also for R and D and R and D plants at individual Federally Funded Research and Development Centers. In addition, data are available on foreign performers and the distribution of R and D obligations by State. Historical data for major categories is provided for the 1967 through 1988 period. Author

N90-12408# National Science Foundation, Washington, DC. Div. of Science Resources Studies.

FEDERAL FUNDS FOR RESEARCH AND DEVELOPMENT. FISCAL YEARS 1987, 1988, AND 1989. VOLUME 37: DETAILED STATISTICAL TABLES

1989 113 p

(PB89-223531; NSF-89-304-Vol-37) Avail: NTIS HC A06/MF A01 CSCL 05C

The tables present data on Federal research and development (R and D) funding for the 1987 through 1989 period. The data, provided by Federal agencies through an annual survey, cover research and development by individual agency, character of work (basic research, applied research, and development), and performing sector. Research funding by field of science/engineering is available for all performing sectors and for research performed at universities and colleges. Data are provided on R and D plant obligations by agency and also for R and D and R and D plants at individual Federally Funded Research and Development Centers. In addition, data are available on foreign performers and the distribution of R and D obligations by State. Historical data for major categories is provided for the 1968 through 1989 period. Data for 1988 and 1989 are estimated since they do not represent final actions. Author

N90-12409# Strategic Defense Initiative Organization, Washington, DC.

FY 1990/FY 1991 BIENNIAL BUDGET DESCRIPTIVE SUMMARIES FOR THE STRATEGIC DEFENSE INITIATIVE ORGANIZATION

Jan. 1989 193 p LIMITED REPRODUCIBILITY: Availability: Document partially illegible

(AD-A211985) Avail: NTIS HC A09/MF A01 CSCL 05/1

This document has been prepared to provide information on the Strategic Defense Initiative Organization (SDIO) Research, Development, Test and Evaluation (RDT and E) program to the congressional committees during the FY 1990/FY 1991 budget hearings. The descriptive summaries provide narrative and fiscal information on the SDIO program elements and the projects contained therein. GRA

85 URBAN TECHNOLOGY AND TRANSPORTATION

Includes applications of space technology to urban problems; technology transfer; technology assessment; and surface and mass transportation.

For related information see also *03 Air Transportation and Safety, 16 Space Transportation,* and *44 Energy Production and Conversion.*

N90-12410# North Carolina Univ., Chapel Hill. Dept. of Environmental Sciences and Engineering.

METHANOL FUELED VEHICLES AND PHOTOCHEMICAL MODELS: AN EVALUATION OF THE STATE OF KNOWLEDGE

Terry Keating May 1989 480 p
(Grant EPA-U913-890-01-0)
(PB89-214225; EPA/600/9-89/064) Avail: NTIS HC A21/MF A03 CSCL 13F

The study is part of the National Network for Environmental Management Studies conducted under the auspices of the Office of Cooperative Environmental Management-U.S. Environmental Protection Agency. The study is an evaluation of the ability of state-of-the-art photochemical mechanisms to assess the impacts of methanol fueled vehicles on ambient levels of ozone, formaldehyde and peroxyacetylnitrate. The evaluation involves comparing the predictions of the California Institute of Technology Mechanism, Carbon Bond Mechanism 4, and the Carter-Atkinson-Lurmann Mechanism to observations from a series of smog chamber experiments previously conducted at the University of North Carolina. The evaluation demonstrates that the performance of the mechanisms decreases with increasing reactivity of the background mixture of ambient hydrocarbons. Author

N90-12411# Eaton Corp., Southfield, MI.
DSEP (DUAL SHAFT ELECTRIC PROPULSION) OPERATION AND MAINTENANCE MANUAL FOR THE NVH AND TB-2 VEHICLES: ADVANCED DUAL SHAFT ELECTRIC PROPULSION SYSTEM TECHNOLOGY DEVELOPMENT PROGRAM
D. Canini, I. Kalns, W. Kelledes, A. North, W. ONeil, and R. Saul Aug. 1989 145 p
(Contract DE-AC07-84NV-10366)
(DE89-017549; DOE/NV-10366/9; Eaton-TR-89041) Avail: NTIS HC A07/MF A01

This document serves as an operation and maintenance manual for the Advanced Dual Shaft Electric Propulsion (DSEP) vehicles. The DSEP vehicles are converted Chrysler minivans. The NVH vehicle is based on a 1987 Dodge Ram van, and the TB-2 vehicle is based on a 1988 Dodge caravan. The DSEP vehicles are battery-powered. DOE

88 SPACE SCIENCES (GENERAL)

No abstracts in this category.

89 ASTRONOMY

Includes radio, gamma-ray, and infrared astronomy, and astrometry.

N90-12412 Colorado Univ., Boulder.
ON THE ANALYSIS OF LINE PROFILE VARIATIONS: A STATISTICAL APPROACH Ph.D. Thesis
Stephan Robert McCandliss 1988 267 p
Avail: Univ. Microfilms Order No. DA8912208

This study is concerned with the empirical characterization of the line profile variations (LPV), which occur in many Of and Wolf-Rayet stars. The goal of the analysis is to gain insight into the physical mechanisms producing the variations. The analytic approach uses a statistical method to quantify the significance of the LPV and to identify those regions in the line profile which are undergoing statistically significant variations. Line positions and flux variations are then measured and subject to temporal and correlative analysis. Previous studies of LPV have for the most part been restricted to observations of a single line. Important information concerning the range and amplitude of the physical mechanisms involved can be obtained by simultaneously observing spectral features formed over a range of depths in the extended mass losing atmospheres of massive, luminous stars. Time series of a Wolf-Rayet and two Of stars with nearly complete spectral coverage from 3940A to 6610A and with spectral resolution of R = 10000 are analyzed here. Dissert. Abstr.

90 ASTROPHYSICS

Includes cosmology; celestial mechanics; space plasmas; and interstellar and interplanetary gases and dust.
For related information see also *75 Plasma Physics.*

N90-12413# Universidade Federal do Rio de Janeiro (Brazil). Inst. de Fisica.
SCALAR FIELDS VERSUS BLACK HOLES
A. J. Accioly and M. S. Oliveira (Universidade Estadual de Paulista, Sao Paulo, Brazil) 1988 9 p
(DE89-611967; IFT-P-30/88) Avail: NTIS (US Sales Only) HC A02/MF A01

It is shown that if a body is endowed with a scalar charge, the event horizon associated with the modified Schwarzchild solution is reduced to a point, this avoiding the black holes formation. The discussion is restricted to ordinary scalar fields and conformally invariant scalar fields, respectively. DOE

N90-12414# Sao Paulo Univ. (Brazil). Inst. de Fisica.
TWO DIMENSIONAL CONFORMAL SUPERGRAVITY AND CRITICAL BEHAVIOR
E. Abdalla, M. C. B. Abdalla, and A. Zadra (Universidade Estadual de Paulista, Sao Paulo, Brazil) 1988 12 p
(DE89-611968; IFT-P-40/88) Avail: NTIS (US Sales Only) HC A03/MF A01

A recent construction of Z-D gravity is generalized to the supersymmetric case. Anomalous dimensions are found. A super Kac-Moody SL (Z,R) algebra is obtained as a starting point using the anomaly equation for the graviton/gravitino system. DOE

N90-12415# Chalmers Univ. of Technology, Goeteborg (Sweden). Dept. of Radio and Space Science.
GALAX: A TWO-DIMENSIONAL N-BODY CODE FOR DISK GALAXY DYNAMICS
Magnus Thomasson 1989 73 p
(PB89-217780; RR-162) Avail: NTIS HC A04/MF A01 CSCL 03B

One way to do experiments with galactic dynamics is to use simulations on a large computer. A 2-D N-body program is described in polar coordinates, intended for studies of isolated and tidally perturbed disk galaxies. The particles are divided in two groups with different velocity dispersions. It is possible to let the cold particles, then representing gas clouds, collide inelastically. Several different kinds of velocity curves and corresponding surface densities and potentials can be used. The program was tested in many ways to verify that it works correctly. A number of programs for presentation of the results of the simulations are also described. Author

N90-12416# National Oceanic and Atmospheric Administration, Boulder, CO. Space Environment Lab.
MHD (MAGNETOHYDRODYNAMIC) MODELING OF SOLAR AND INTERPLANETARY PROCESSES Final Report, 1 Oct. 1986 - 30 Sep. 1988
Murray Dryer Apr. 1989 27 p
(AFGL Order GLH7-6017; AFGL Order GLH8-6004)
(PB89-215461; SEL-1216) Avail: NTIS HC A03/MF A01 CSCL 03B

Magnetohydrodynamic (MHD) numerical modeling and simulations were used as tools to understand the physics of energy and momentum transport from the solar surface through the corona to interplanetary space. Possible physical mechanisms were identified and synthesis calculations were performed using self-consistent MHD theory via numerical and analytical methods. Solar and interplanetary (remote-sensing and in situ) observations play important roles in the synthesis strategy. The models, unique in the field of solar/interplanetary physics, include both 2 1/2-D and 3-D time-dependent codes that could lead to future operational status in geomagnetic storm forecasting procedures. A Bibliography of related papers is included. GRA

N90-12417# Los Alamos National Lab., NM. Applied Theoretical Physics Div.

EFFECTS OF MAIN-SEQUENCE MASS LOSS ON THE TURNOFF AGES OF POPULATION 1 CLUSTERS

Joyce A. Guzik 1989 9 p Presented at the 5th Astrophysics Meeting on Astrophysical Ages and Dating Methods, Paris, France, 26-29 Jun. 1989
(Contract W-7405-eng-36)
(DE89-016755; LA-UR-89-2961; CONF-8906206-1) Avail: NTIS HC A02/MF A01

Willson, Bowen, and Struck-Marcell have proposed that stars of spectral types A through early-G lose a significant portion of their mass during the early main-sequence phase. The proposed mass loss is driven by pulsation, and facilitated by rapid rotation. One implication of this hypothesis is that the main-sequence turnoff is an invalid indicator of cluster age, as present turnoff stars may have had higher projenitor masses; hence clusters appear older than they actually are. This paper presents examples of cluster HR diagrams synthesized with mass-losing stars of solar metallicity, initial masses 1-2 M, and exponentially-decreasing mass-loss rates with e-folding times 1 to 2 Gyr. The increases in apparent turnoff age of Pop. I clusters, and the potential of the hypothesis to account for blue stragglers as normal stars that have not lost mass (or lost mass more slowly) are discussed. DOE

N90-12418# Lawrence Livermore National Lab., CA.

PARTICLE PHYSICS AND COSMOLOGY USING STELLAR EVOLUTION THEORY Final Report

Joseph I. Silk 1989 3 p
(Contract W-7405-eng-48)
(DE89-017529; UCRL-21240) Avail: NTIS HC A01/MF A01

Georg Raffelt has completed several projects in the field of astro-particle physics. They were largely aimed at getting a better understanding of specific questions of particle physics and cosmology by using stellar evolution theory and the pertinent astronomical data as a laboratory. DOE

N90-12419# Lawrence Livermore National Lab., CA.

DETAILED PHOTONUCLEAR CROSS-SECTION CALCULATIONS AND ASTROPHYSICAL APPLICATIONS

D. G. Gardner, M. A. Gardner, and R. W. Hoff 15 Jun. 1989 27 p Presented at the WEIN '89: International Symposium on Weak and Electromagnetic Interactions in Nuclei, Montreal, Quebec, 15-19 May 1989
(Contract W-7405-eng-48)
(DE89-017531; UCRL-100547; CONF-8905187-3) Avail: NTIS HC A03/MF A01

We have investigated the role of an isomeric state and its coupling to the ground state (g.s.) via photons and neutron inelastic scattering in a stellar environment by making detailed photonuclear and neutron cross-section calculations for (176)Lu and (210)Bi. In the case of (176)Lu, the g.s. would function as an excellent galactic slow- (s-) process chronometer were it not for the 3.7-h isomer at 123 KeV. Our calculations predicted much larger photon cross sections for production of the isomer, as well as a lower threshold, than had been assumed based on earlier measurements. These two factors combine to indicate that an enormous correction, a factor of 10(7), must be applied to shorten the current estimate of the half-life against photoexcitation of (176)Lu as a function of temperature. This severely limits the use of (176)Lu as a stellar chronometer and indicates a significantly lower temperature at which the two states reach thermal equilibrium. For (210)Bi, our preliminary calculations of the production and destruction of the 3 times 10(6) y isomeric state by neutrons and photons suggest that the (210)Bi isomer may not be destroyed by photons as rapidly as assumed in certain stellar environments. This leads to an alternate production path of (207)Pb and significantly affects presently interpreted lead isotopic abundances. DOE

N90-12420# Oak Ridge National Lab., TN. Metals and Ceramics Div.

AN ATOM PROBE STUDY OF PHASE DECOMPOSITION IN THREE IRON METEORITES

M. K. Miller and K. F. Russell 1989 18 p Presented at the Symposium on Physical Metallurgy of Controlled Expansion Invar-Type Alloys, Las Vegas, NV, 28 Feb. 1989
(Contract DE-AC05-84OR-21400)
(DE89-017581; CONF-8902117-2) Avail: NTIS HC A03/MF A01

An atom probe field-ion microscopy characterization of the Cape York, Twin City and Santa Catharina iron-nickel meteorites has been performed. This investigation has revealed that the taenite, corresponding to an interface region between the cloudy zone and the clear taenite 2 (CT2) region in the Cape York meteorite and the matrix of the Twin City and Santa Catharina meteorites, has phase separated to form an ultra-fine scale duplex microstructure. The composition of these two phases was determined to be 50 at. percent Ni and approximately 15 at. percent Ni. These compositions correspond to the equiatomic FeNi L1(sub 0)-ordered phase and a disordered face centered cubic phase. DOE

N90-12421# Royal Inst. of Tech., Stockholm (Sweden). Dept. of Plasma Physics.

THE PHYSICS OF DOUBLE LAYERS AND THEIR ROLE IN ASTROPHYSICS

Michael A. Raadu Apr. 1989 132 p Submitted for publication Sponsored by the Swedish Natural Science Research Council
(TRITA-EPP-89-03; ISSN-0348-7539; ETN-89-95923) Avail: NTIS HC A07/MF A01

The electrostatic Double Layers (DL's) and their astrophysical applications are reviewed. The existence criteria for DL's are discussed. It is shown that the current driven instabilities can lead to DL formation, and account for the flunctuations associated with strong DL's. A class of weak DL's is described using the modified Korteweg-Devries equation, and the conditions for the emergence of a DL from arbitrary initial conditions are specified. Simulation studies of strong DL formation are effectuated. They reveal important dynamical features. Weak DL's are found in simulations of ion acoustic instabilities. A strong coupling between a DL and the global current system is observed. The results of theoretical, simulation and observational investigations of magnetospheric DL's are presented. ESA

N90-12422# Royal Aerospace Establishment, Farnborough (England).

TIME-WEIGHTED ACCUMULATIONS ap(TAU) AND Kp(TAU)

Gordon L. Wrenn 25 Jul. 1988 9 p Repr. from Journal of Geophysical Research, v. 92, no. A9 (United States), 1 Sep. 1987 p 10,125-10,129
(RAE-TR-88050; RAE-Space-672; BR108279; ETN-89-94337)
Copyright Avail: Defence Research Information Centre, Kentigern House, 65 Brown Street, Glasgow, G2 8EX, Scotland

The planetary geomagnetic indices Kp and ap used in space geophysics are discussed. They provide an estimate of maximum magnetic perturbation within a 3 hr period. Many geophysical properties are clearly related to the indices, through energy transfer form a common disturbance source, but direct correlation is often lacking because of poor matching between the frequency of sampling and the physical response functions. The index ap (tau) is a simple accumulation of the linear ap calculated with an attenuation factor tau included to take account of natural temporal relaxation. The case for ap (tau) and the related Kp (tau) is made using applications to the variability of the plasma environment in the ionosphere and inner magnetosphere. These examples of improved correlation suggest that time-weighted integration might profitably be applied to other indices. ESA

91 LUNAR AND PLANETARY EXPLORATION

Includes planetology; and manned and unmanned flights. For spacecraft design or space stations see *18 Spacecraft Design, Testing and Performance.*

N90-12423*# Lunar and Planetary Inst., Houston, TX.
ABSTRACTS FOR THE VENUS GEOSCIENCE TUTORIAL AND VENUS GEOLOGIC MAPPING WORKSHOP Abstracts Only
1989 62 p Workshop held in Flagstaff, AZ, 12-15 Jun. 1989
(Contract NASw-4066)
(NASA-CR-185432; NAS 1.26:185432; LPI-Contrib-708) Avail: NTIS HC A04/MF A01 CSCL 03B

Abstracts and tutorial are presented from the workshop. Representative titles are: Geology of Southern Guinevere Planitia, Venus, Based on Analyses of Goldstone Radar Data; Tessera Terrain: Characteristics and Models of Origin; Venus Volcanism; Rate Estimates from Laboratory Studies of Sulfur Gas-Solid Reactions; and A Morphologic Study of Venus Ridge Belts. For individual titles, see N90-12424 through N90-12453.

N90-12424*# Washington Univ., Saint Louis, MO. Dept. of Earth and Planetary Sciences.
GEOLOGY OF SOUTHERN GUINEVERE PLANITIA, VENUS, BASED ON ANALYSES OF GOLDSTONE RADAR DATA Abstract Only
R. E. Arvidson, J. J. Plaut, R. F. Jurgens, R. S. Saunders, and M. A. Slade (Jet Propulsion Lab., California Inst. of Tech., Pasadena.) *In* Lunar and Planetary Inst., Abstracts for the Venus Geoscience Tutorial and Venus Geologic Mapping Workshop 1989 p 1 (For primary document see N90-12423 03-91)
Avail: NTIS HC A04/MF A01 CSCL 03B

The ensemble of 41 backscatter images of Venus acquired by the S Band (12.6 cm) Goldstone radar system covers approx. 35 million km and includes the equatorial portion of Guinevere Planitia, Navka Planitia, Heng-O Chasma, and Tinatin Planitia, and parts of Devana Chasma and Phoebe Regio. The images and associated altimetry data combine relatively high spatial resolution (1 to 10 km) with small incidence angles (less than 10 deg) for regions not covered by either Venera Orbiter or Arecibo radar data. Systematic analyses of the Goldstone data show that: (1) Volcanic plains dominate, including groups of small volcanic constructs, radar bright flows on a NW-SE arm of Phoebe Regio and on Ushas Mons and circular volcano-tectonic depressions; (2) Some of the regions imaged by Goldstone have high radar cross sections, including the flows on Ushas Mons and the NW-SE arm of Phoebe Regio, and several other unnamed hills, ridged terrains, and plains areas; (3) A 1000 km diameter multiringed structure is observed and appears to have a morphology not observed in Venera data (The northern section corresponds to Heng-O Chasma); (4) A 150 km wide, 2 km deep, 1400 km long rift valley with upturned flanks is located on the western flank of Phoebe Regio and extends into Devana Chasma; (5) A number of structures can be discerned in the Goldstone data, mainly trending NW-SE and NE-SW, directions similar to those discerned in Pioneer-Venus topography throughout the equatorial region; and (6) The abundance of circular and impact features is similar to the plains global average defined from Venera and Arecibo data, implying that the terrain imaged by Goldstone has typical crater retention ages, measured in hundreds of millions of years. The rate of resurfacing is less than or equal to 4 km/Ga. Author

N90-12425*# Brown Univ., Providence, RI. Dept. of Geological Sciences.
CHARACTERISTICS, DISTRIBUTION AND GEOLOGIC/TERRAIN ASSOCIATIONS OF SMALL DOME-LIKE HILLS ON VENUS
J. C. Aubele and E. N. Slyuta (Academy of Sciences, USSR, Moscow) *In* Lunar and Planetary Inst., Abstracts for the Venus Geoscience Tutorial and Venus Geologic Mapping Workshop 1989 p 2-3 (For primary document see N90-12423 03-91)
Avail: NTIS HC A04/MF A01 CSCL 03B

Approximately 22,000 small dome-like hills were recognized on the northern 20 percent of the surface of Venus imaged by Verera 15/16. These features were described as generally circular in planimetric outline, with a range in basal diameter from the effective resolution of the Venera images (1 to 2 km) up to 20 km. The General Characteristics, Dome Distribution and Terrain Unit and Geologic Feature Associations are discussed. Author

N90-12426*# Brown Univ., Providence, RI. Dept. of Geological Sciences.
TESSERA TERRAIN: CHARACTERISTICS AND MODELS OF ORIGIN
D. L. Bindschadler and James W. Head *In* Lunar and Planetary Inst., Abstracts for the Venus Geoscience Tutorial and Venus Geologic Mapping Workshop 1989 p 4-5 (For primary document see N90-12423 03-91)
Avail: NTIS HC A04/MF A01 CSCL 03B

Tessera terrain consists of complexly deformed regions characterized by sets of ridges and valleys that intersect at angles ranging from orthogonal to oblique, and were first viewed in Venera 15/16 SAR data. Tesserae cover more area (approx. 15 percent of the area north of 30 deg N) than any of the other tectonic units mapped from the Venera data and are strongly concentrated in the region between longitudes 0 deg E and 150 deg E. Tessera terrain is concentrated between a proposed center of crustal extension and divergence in Aphrodite and a region of intense deformation, crustal convergence, and orogenesis in western Ishtar Terra. Thus, the tectonic processes responsible for tesserae are an important part of Venus tectonics. As part of an effort to understand the formation and evolution of this unusual terrain type, the basic characteristics of the tesserae were compared to the predictions made by a number of tectonic models. The basic characteristics of tessera terrain are described and the models and some of their basic predictions are briefly discussed. Author

N90-12427*# Brown Univ., Providence, RI. Dept. of Geological Sciences.
DIVERGENT PLATE BOUNDARIES AND CRUSTAL SPREADING ON VENUS: EVIDENCE FROM APHRODITE TERRA
L. S. Crumpler and James W. Head *In* Lunar and Planetary Inst., Abstracts for the Venus Geoscience Tutorial and Venus Geologic Mapping Workshop 1989 p 6-7 (For primary document see N90-12423 03-91)
Avail: NTIS HC A04/MF A01 CSCL 03B

The modes of lithospheric heat transfer and the tectonic styles may differ between Earth and Venus, depending on how the high surface temperature (700 K = 430 C), dense and opaque atmosphere (approx. 10 MPa = 100 bars), lack of water oceans, and the other known ways in which Venus differs from Earth, influence basic lithospheric processes, thermal gradient, upper mantle temperature, thermal and chemical evolution, and convection. A fundamental question is whether the lithosphere of Venus is horizontally stable, like the other terrestrial planets, or is mobile like that on Earth. The variety of characteristics, their integrated relationships, and their predictable behavior throughout Western Aphrodite Terra are similar to those features known to occur in association with the terrestrial seafloor at spreading centers and divergent plate boundaries. It is concluded that Western Aphrodite Terra represents the site of crustal spreading centers and divergent plate boundaries. The extent of similar characteristics and processes elsewhere on Venus outside of the 13,000 km long Western and Eastern Aphrodite Terra rise is unknown at the present, but their presence in other areas of the equatorial highlands, suggested from recent analysis, may be tested with forthcoming Magellan data. Author

N90-12428*# Massachusetts Inst. of Tech., Cambridge. Dept. of Earth, Atmospheric, and Planetary Sciences.
VENUS VOLCANISM: RATE ESTIMATES FROM LABORATORY STUDIES OF SULFUR GAS-SOLID REACTIONS

K. Ehlers, B. Fegley, Jr., and R. G. Prinn *In* Lunar and Planetary Inst., Abstracts for the Venus Geoscience Tutorial and Venus Geologic Mapping Workshop 1989 p 8-9 (For primary document see N90-12423 03-91)
(Grant NSF ATM-87-10102)
Avail: NTIS HC A04/MF A01 CSCL 03B

Thermochemical reactions between sulfur-bearing gases in the atmosphere of Venus and calcium-, iron-, magnesium-, and sulfur-bearing minerals on the surface of Venus are an integral part of a hypothesized cycle of thermochemical and photochemical reactions responsible for the maintenance of the global sulfuric acid cloud cover on Venus. SO2 is continually removed from the Venus atmosphere by reaction with calcium bearing minerals on the planet's surface. The rate of volcanism required to balance SO2 depletion by reactions with calcium bearing minerals on the Venus surface can therefore be deduced from a knowledge of the relevant gas-solid reaction rates combined with reasonable assumptions about the sulfur content of the erupted material (gas + magma). A laboratory program was carried out to measure the rates of reaction between SO2 and possible crustal minerals on Venus. The reaction of CaCO3(calcite) + SO2 yields CaSO4 (anhydrite) + CO was studied. Brief results are given. Author

N90-12429*# Jet Propulsion Lab., California Inst. of Tech., Pasadena.

POTENTIAL FOR OBSERVING AND DISCRIMINATING IMPACT CRATERS AND COMPARABLE VOLCANIC LANDFORMS ON MAGELLAN RADAR IMAGES Abstract Only

J. P. Ford *In* Lunar and Planetary Inst., Abstracts for the Venus Geoscience Tutorial and Venus Geologic Mapping Workshop 1989 p 10 (For primary document see N90-12423 03-91)
Avail: NTIS HC A04/MF A01 CSCL 03B

Observations of small terrestrial craters by Seasat synthetic aperture radar (SAR) at high resolution (approx. 25 m) and of comparatively large Venusian craters by Venera 15/16 images at low resolution (1000 to 2000 m) and shorter wavelength show similarities in the radar responses to crater morphology. At low incidence angles, the responses are dominated by large scale slope effects on the order of meters; consequently it is difficult to locate the precise position of crater rims on the images. Abrupt contrasts in radar response to changing slope (hence incidence angle) across a crater produce sharp tonal boundaries normal to the illumination. Crater morphology that is radially symmetrical appears on images to have bilateral symmetry parallel to the illumination vector. Craters are compressed in the distal sector and drawn out in the proximal sector. At higher incidence angles obtained with the viewing geometry of SIR-A, crater morphology appears less compressed on the images. At any radar incidence angle, the distortion of a crater outline is minimal across the medial sector, in a direction normal to the illumination. Radar bright halos surround some craters imaged by SIR-A and Venera 15 and 16. The brightness probably denotes the radar response to small scale surface roughness of the surrounding ejecta blankets. Similarities in the radar responses of small terrestrial impact craters and volcanic craters of comparable dimensions emphasize the difficulties in discriminating an impact origin from a volcanic origin in the images. Similar difficulties will probably apply in discriminating the origin of small Venusian craters, if they exist. Because of orbital considerations, the nominal incidence angel of Magellan radar at the center of the imaging swath will vary from about 45 deg at 10 deg N latitude to about 16 deg at the north pole and at 70 deg S latitude. Impact craters and comparable volcanic landforms will show bilateral symmetry parallel to the illumination vector and will appear increasingly compressed toward higher latitudes. Author

N90-12430*# Jet Propulsion Lab., California Inst. of Tech., Pasadena.

CONTRASTING LANDFORM PERCEPTION WITH VARIED RADAR ILLUMINATION GEOMETRIES AND AT SIMULATED RESOLUTIONS OF VENERA AND MAGELLAN Abstract Only

J. P. Ford and R. E. Arvidson (Washington Univ., Saint Louis, MO.) *In* Lunar and Planetary Inst., Abstracts for the Venus Geoscience Tutorial and Venus Geologic Mapping Workshop 1989 p 11 (For primary document see N90-12423 03-91)
Avail: NTIS HC A04/MF A01 CSCL 03B

The high sensitivity of imaging radars to slope at moderate to low incidence angles enhances the perception of linear topography on images. It reveals broad spatial patterns that are essential to landform mapping and interpretation. As radar responses are strongly directional, the ability to discriminate linear features on images varies with their orientation. Landforms that appear prominent on images where they are transverse to the illumination may be obscure to indistinguishable on images where they are parallel to it. Landform detection is also influenced by the spatial resolution in radar images. Seasat radar images of the Gran Desierto Dunes complex, Sonora, Mexico; the Appalachian Valley and Ridge Province; and accreted terranes in eastern interior Alaska were processed to simulate both Venera 15 and 16 images (1000 to 3000 km resolution) and image data expected from the Magellan mission (120 to 300 m resolution. The Gran Desierto Dunes are not discernable in the Venera simulation, whereas the higher resolution Magellan simulation shows dominant dune patterns produced from differential erosion of the rocks. The Magellan simulation also shows that fluvial processes have dominated erosion and exposure of the folds. Author

N90-12431*# Massachusetts Inst. of Tech., Cambridge. Center for Space Research.

VENUS SURFACE PROPERTIES DEDUCED FROM RADAR AND RADIOMETRY Abstract Only

P. G. Ford *In* Lunar and Planetary Inst., Abstracts for the Venus Geoscience Tutorial and Venus Geologic Mapping Workshop 1989 p 12 (For primary document see N90-12423 03-91)
Avail: NTIS HC A04/MF A01 CSCL 03B

The brightness of surface features on side looking radar images of Venus is determined by many factors: the angles of incidence and reflection, polarization, surface geometry and composition, and so forth. The contribution from surface properties themselves can only be deduced by combining several types of measurement. For instance, without additional information, it is impossible to distinguish the effects of changes in surface roughness from those in dielectric constant. In common with the Moon and Mars, the surface of Venus appears to scatter radar waves in two ways: small-scale surface inhomogeneities, i.e., those smaller than the incident wavelength, depolarize and scatter the energy over a wide range of angles. The Pioneer Venus radar mapper experiment made three overlapping sets of measurements of the equatorial region of Venus from 15 deg S latitude to 45 deg N; the backscatter cross section at a range of incidence angles, the shape and intensity of radar echoes from the nadir, and the microwave brightness temperature of the surface. These techniques developed during the analysis of Pioneer Venus data will be used during the Magellan mission to extract measurements of surface slopes and dielectric constants over all areas covered by the SAR and altimeter antennae, with a resolution of about 10 km. A knowledge of the mechanisms that govern surface scattering will also be useful in the analysis of higher resolution side looking radar images, particularly in distinguishing the effects of changing roughness from those caused by a long range surface tilt or changing dielectric constant. Author

N90-12432*# Brown Univ., Providence, RI. Dept. of Geological Sciences.

A MORPHOLOGIC STUDY OF VENUS RIDGE BELTS

S. L. Frank and James W. Head *In* Lunar and Planetary Inst., Abstracts for the Venus Geoscience Tutorial and Venus Geologic Mapping and Workshop 1989 p 13-14 (For primary document see N90-12423 03-91)
Avail: NTIS HC A04/MF A01 CSCL 03B

Ridge belts, first identified in the Venera 15/16 images are distinguished as linear regions of concentrated, parallel to anastomosing, ridges. They are tens to several hundreds of km wide, hundreds to over one thousand km long, and composed of individual ridges 5 to 20 km wide and up to 200 km long. The

ridges appear symmetrical in the radar images and are either directly adjacent to each other or separated by mottled plains. Cross-strike lineaments, visible as dark or bright lines, are common within the ridge belts, and some truncate individual ridges. In places the ridge belt may be offset by these lineaments, but such offset is rarely consistent across the ridge belt. Once the mode of formation of these ridge belts is understood, their distribution and orientation will help to constrain the homogeneity and orientation of the stresses over the period of ridge belt formation. The look direction for the Venera system was to the west, so ridges appear as pairs of bright and dark lineaments, with the bright line to the east of the dark. The term ridge was used in a general sense to refer to a linear rise. The use of this term is restricted to rises which have a sharp transition from bright to dark at the crest, and are 5 to 15 km wide. These ridges are either continuous or discontinuous. The continuous ridges are over 30 km long and form coherent ridge belts, while the discontinuous ridges are less than 30 km long and do not form a coherent ridge belt. The continuous ridges were divided into 3 components: (1) Anastomosing ridges, in which the individual ridges are sinuous and often meet and cross at small angles, are the most common component; (2) The parallel ridge component also consists of well defined ridges, often with plains separating the individual ridges, but the ridges are more linear and rarely intersect one another; and (3) Parallel ridged plains are composed of indistinct ridges, some of which do not have a distinctive bright-dark pattern. The nature of deformation within the ridge belts is complex and not fully understood at present. Some belts show distinct signs of compression, while others have symmetrical patterns expected in extensional environments. Thus the ridge belts may have formed by more than one style of deformation; some may be extensional, while others are compressional. All the ridge belts are being systematically mapped, especially for symmetrical relationships.
Author

N90-12433*# Arizona State Univ., Tempe. Dept. of Geology.
EVIDENCE FOR VOLCANISM IN NW ISHTAR TERRA, VENUS
L. Gaddis and Ronald Greeley *In* Lunar and Planetary Inst., Abstracts for the Venus Geoscience Tutorial and Venus Geologic Mapping Workshop 1989 p 15-16 (For primary document see N90-12423 03-91)
Avail: NTIS HC A04/MF A01 CSCL 03B

Venera 15/16 radar data for an area in NW Ishtar Terra, Venus, show an area with moderate radar return and a smooth textured surface which embays low lying areas of the surrounding mountainous terrain. Although this unit may be an extension of the lava plains of Lakshmi Planum to the southeast, detailed study suggests a separate volcanic center in NW Ishtar Terra. Lakshmi Planum, on the Ishtar Terra highland, exhibits major volcanic and tectonic features. On the Venera radar image radar brightness is influenced by slope and roughness; radar-facing slopes (east-facing) and rough surfaces (approx. 8 cm average relief) are bright, while west-facing slopes and smooth surfaces are dark. A series of semi-circular features, apparently topographic depressions, do not conform in orientation to major structural trends in this region of NW Ishtar Terra. The large depression in NW Ishtar Terra is similar to the calderas of Colette and Sacajawea Paterae, as all three structures are large irregular depressions. NW Ishtar Terra appears to be the site of a volcanic center with a complex caldera structure, possibly more than one eruptive vent, and associated lobed flows at lower elevations. The morphologic similarity between this volcanic center and those of Colette and Sacajawea suggests that centralized eruptions have been the dominant form of volcanism in Ishtar. The location of this volcanic center at the intersection of two major compressional mountain belts and the large size of the calders (with an inferred larg/deep magma source) support a crustal thickening/melting rather than a hot-spot origin for these magmas.
Author

N90-12434*# National Aeronautics and Space Administration. Goddard Space Flight Center, Greenbelt, MD.
ANALYSIS OF RADAR IMAGES OF THE ACTIVE VOLCANIC ZONE AT KRAFLA, ICELAND: THE EFFECTS OF LOOK AZIMUTH BIASING
J. B. Garvin and R. S. Williams, Jr. (Geological Survey, Reston, VA.) *In* Lunar and Planetary Inst., Abstracts for the Venus Geoscience Tutorial and Venus Geologic Mapping Workshop 1989 p 17-18 (For primary document see N90-12423 03-91)
Avail: NTIS HC A04/MF A01 CSCL 03B

The geomorphic expression of Mid-Ocean-Ridge (MOR) volcanism in a subaerial setting occurs uniquely on Earth in Iceland, and the most recent MOR eruptive activity has been concentrated in the Northeastern Volcanic Zone in an area known as Krafla. Within the Krafla region are many of the key morphologic elements of MOR-related basaltic volcanism, as well as volcanic explosion craters, subglacial lava shields, tectonic fissure swarms known as gjar, and basaltic-andesite flows with well developed ogives (pressure-ridges). The objective was to quantify the degree to which the basic volcanic and structural features can be mapped from directional SAR imagery as a function of the look azimuth. To accomplish this, the current expression of volcanic and tectonic constructs was independently mapped within the Krafla region on the E, W, and N-looking SAR images, as well as from SPOT Panchromatic imagery acquired in 1987. The initial observations of the E, W, and N images indicates that fresh a'a lava surfaces are extremely radar bright (rough at 3 cm to meter scales) independent of look direction; this suggests that these flows do not have strong flow direction related structures at meter and cm scales, which is consistent with typical Icelandic a'a lava surfaces in general. The basic impression from a preliminary analysis of the effects of look azimuth biasing on interpretation of the geology of an active MOR volcanic zone is that up to 30 percent of the diagnostic features can be missed at any given look direction, but that having two orthogonal look direction images is probably sufficient to prevent gross misinterpretation.
Author

N90-12435*# National Aeronautics and Space Administration. Goddard Space Flight Center, Greenbelt, MD.
RADAR SCATTERING MECHANISMS WITHIN THE METEOR CRATER EJECTA BLANKET: GEOLOGIC IMPLICATIONS AND RELEVANCE TO VENUS
J. B. Garvin, B. A. Campbell, S. H. Zisk, Gerald G. Schaber, and C. Evans (Maryland Univ., Greenbelt.) *In* Lunar and Planetary Inst., Abstracts for the Venus Geoscience Tutorial and Venus Geologic Mapping Workshop 1989 p 19-20 (For primary document see N90-12423 03-91)
Avail: NTIS HC A04/MF A01 CSCL 03B

Simple impact craters are known to occur on all of the terrestrial planets and the morphologic expression of their ejecta blankets is a reliable indicator of their relative ages on the Moon, Mars, Mercury, and most recently for Venus. It will be crucial for the interpretation of the geology of Venus to develop a reliable means of distinguishing smaller impact landforms from volcanic collapse and explosion craters, and further to use the observed SAR characteristics of crater ejecta blankets (CEB) as a means of relative age estimation. With these concepts in mind, a study was initiated of the quantitative SAR textural characteristics of the ejecta blanket preserved at Meteor Crater, Arizona, the well studied 1.2 km diameter simple crater that formed approx. 49,000 years ago from the impact of an octahedrite bolide. While Meteor Crater was formed as the result of an impact into wind and water lain sediments and has undergone recognizable water and wind related erosion, it nonetheless represents the only well studied simple impact crater on Earth with a reasonably preserved CEB. Whether the scattering behavior of the CEB can provide an independent perspective on its preservation state and style of erosion is explored. Finally, airborne laser altimeter profiles of the microtopography of the Meteor Crater CEB were used to further quantify the subradar pizel scale topographic slopes and RMS height variations for comparisons with the scattering mechanisms computed from SAR polarimetry. A preliminary assessment was summarized of the L-band radar scattering mechanisms within the

Meteor Crater CEB as derived from a NASA/JPL DC-8 SAR Polarimetry dataset acquired in 1988, and the dominant scattering behavior was compared with microtopographic data (laser altimeter profiles and 1:10,000 scale topographic maps). Author

N90-12436*# Arizona State Univ., Tempe. Dept. of Geology.

AEOLIAN PROCESSES ON VENUS

Ronald Greeley *In* Lunar and Planetary Inst., Abstracts for the Venus Geoscience Tutorial and Venus Geologic Mapping Workshop 1989 p 21-22 (For primary document see N90-12423 03-91)

Avail: NTIS HC A04/MF A01 CSCL 03B

This review assesses the potential aeolian regime on Venus as derived from spacecraft observations, laboratory simulations, and theoretical considerations. The two requirements for aeolian processes (a supply of small, loose particles and winds of sufficient strength to move them) appear to be met on Venus. Venera 9, 10, 13, and 14 images show particles considered to be sand and silt size on the surface. In addition, dust spurts (grains 5 to 50 microns in diameter) observed via lander images and inferred from the Pioneer-Venus nephalometer experiments suggest that the particles are loose and subject to movement. Although data on near surface winds are limited, measurements of 0.3 to 1.2 m/sec from the Venera lander and Pioneer-Venus probes appear to be well within the range required for sand and dust entrainment. Aeolian activity involves the interaction of the atmosphere, lithosphere, and loose particles. Thus, there is the potential for various physical and chemical weathering processes that can effect not only rates of erosion, but changes in the composition of all three components. The Venus Simulator is an apparatus used to simulate weathering under venusian conditions at full pressure (to 112 bars) and temperature (to 800 K). In one series of tests, the physical modifications of windblown particles and rock targets were assessed and it was shown that particles become abraded even when moved by gentle winds. However, little abrasion occurs on the target faces. Thus, compositional signatures for target rocks may be more indicative of the windblown particles than of the bedrock. From these and other considerations, aeolian modifications of the venusian surface may be expected to occur as weathering, erosion, transportation, and deposition of surficial materials. Depending upon global and local wind regimes, there may be distinctive sources and sinks of windblown materials. Radar imaging, especially as potentially supplied via the Magellan mission, may enable the identification of such areas on Venus. Author

N90-12437*# Brown Univ., Providence, RI. Dept. of Geological Sciences.

ARCHITECTURE OF OROGENIC BELTS AND CONVERGENT ZONES IN WESTERN ISHTAR TERRA, VENUS

James W. Head, R. W. VorderBruegge, and L. S. Crumpler *In* Lunar and Planetary Inst., Abstracts for the Venus Geoscience Tutorial and Venus Geologic Mapping Workshop 1989 p 24-25 (For primary document see N90-12423 03-91)

Avail: NTIS HC A04/MF A01 CSCL 03B

Linear mountain belts in Ishtar Terra were recognized from Pioneer-Venus topography, and later Arecibo images showed banded terrain interpreted to represent folds. Subsequent analyses showed that the mountains represented orogenic belts, and that each had somewhat different features and characteristics. Orogenic belts are regions of focused shortening and compressional deformation and thus provide evidence for the nature of such deformation, processes of crustal thickening (brittle, ductile), and processes of crustal loss. Such information is important in understanding the nature of convergent zones on Venus (underthrusting, imbrication, subduction), the implications for rates of crustal recycling, and the nature of environments of melting and petrogenesis. The basic elements of four convergent zones and orogenic belts in western Ishtar Terra are identified and examined, and then assess the architecture of these zones (the manner in which the elements are arrayed), and their relationships. The basic nomenclature of the convergent zones is shown. Author

N90-12438*# Jet Propulsion Lab., California Inst. of Tech., Pasadena.

DEDUCING THE AGE OF THE DENSE VENUS ATMOSPHERE Abstract Only

R. Kahn *In* Lunar and Planetary Inst., Abstracts for the Venus Geoscience Tutorial and Venus Geologic Mapping Workshop 1989 p 26 Previously announced in IAA as A82-31258 (For primary document see N90-12423 03-91)

Avail: NTIS HC A04/MF A01 CSCL 03B

It is shown how crater size-density counts may be used to help constrain the history of the Venus atmosphere, based on the predictions of simple but reasonable models for crater production, surface erosion, and the effects of atmospheric drag and breakup on incident meteors in the Venus atmosphere. In particular, if the atmosphere is young, the old (uneroded) surfaces will have crater densities upward of 0.0001/sq km and a ratio of small (4 km) craters to large (128 km) craters near 1000. If the atmosphere is old and the breakup mechanism is dominant, absolute crater densities on Venus surfaces will be diminished by several orders of magnitude relative to the young atmosphere case. If atmospheric drag is dominant, the absolute crater density will be lowered by perhaps an order of magnitude relative to the young atmosphere case, and the ratio of small to large craters will be reduced to a value near 10 to the 1.5 power. Once a large fraction of Venus surface has been imaged at kilometer resolution, as the Venus Orbiting Imaging Radar project promises to do, it could be possible to make an early determination of the age of the Venus atmosphere. Author

N90-12439*# Geological Survey, Flagstaff, AZ.

CLOTHO TESSERA, VENUS: A FRAGMENT OF FORTUNA TESSERA

Richard C. Kozak and Gerald G. Schaber *In* Lunar and Planetary Inst., Abstracts for the Venus Geoscience Tutorial and Venus Geologic Mapping Workshop 1989 p 27-28 (For primary document see N90-12423 03-91)

Avail: NTIS HC A04/MF A01 CSCL 03B

Clotho Tessera, adjacent to southeast Lakshmi Planum, may provide additional evidence for lateral crustal motions, and a model for the origin of small tessera fragments. Clotho Tessera and Lakshmi Planum are so noticeably different, and in such close proximity, it is difficult to derive a reasonable model of their formation in situ. Squeezing of material out from beneath Lakshmi has been suggested as an origin for Moira Tessera, which is also adjacent to Lakshmi and 1400 km west of Clotho. However, a logical model of juxtaposition of the two different terrains, originally from points once distant, can be made for Clotho and Lakshmi (and perhaps other small tesserae as well). It is suggested that Clotho Tessera was once part of Fortuna Tessera, but was cut off by a transcurrent fault zone (the DLZ) striking perpendicular to the Sigrun rift and carried westward where it collided with Lakshmi Planum (forming Danu Montes). A gravity anomaly along the southern border of Lakshmi, in the area of Danu Montes, was interpreted as indicating subduction there, providing additional supporting evidence for the collision hypothesis. Diffusion of the DLZ with proximity to Sigrun Fossae may be due to either higher ductility near the postulated Sigrun rift, or to burial by flows away from the rift nearer to Valkyrie Fossae. Other possible examples of migrating tesserae occur elsewhere: small pieces of Ananke Tessera can be fit back together as though they had rifted apart, and the spreading apart of Ananke and Virilis Tesserae has been suggested because of their symmetric locations about the axis of an inferred spreading zone. Other tessera fragments appear to have been isolated by rifting, with little, if any, significant lateral motion (e.g., Meni and Tellus Tesserae, and Thethus and Fortuna Tesserae). The migrating terrain model for Clotho Tessera supports Sukhanov's interpretation of tesseral fragments as rafts of lighter crustal material. Author

N90-12440*# Geological Survey, Flagstaff, AZ.

TECTONISM ON VENUS: A REVIEW Abstract Only

Richard C. Kozak and Gerald G. Schaber *In* Lunar and Planetary Inst., Abstracts for the Venus Geoscience Tutorial and Venus

Geologic Mapping Workshop 1989 p 29 (For primary document see N90-12423 03-91)
Avail: NTIS HC A04/MF A01 CSCL 03B

Venus is more similar to Earth than to any other planet. It has elevated regions associated with marginal fold and thrust belts, fracture zones that extend tens of thousands of kilometers, crustal swells and shields that are hundreds of kilometers in diameter and 1 to 2 km high, and sublinear accumulations of volcanic cones and domes that stretch for thousands of kilometers across the plains. The Venusian surface is, however, distinctly different from Earth's in that: (1) its elevated terrains cannot be distinguished from its low plains on a hypsometric curve; (2) trenches have not been found plainsward of the marginal belts; (3) fracture zones bear no resemblance to mid-oceanic ridges; and (4) some features, such as the ridge-belt zone near 210 deg E, seem to have no terrestrial analog. Various theories about tectonism on Venus and Earth of other authors are reviewed. Author

N90-12441*# Geological Survey, Menlo Park, CA.

CRATER IDENTIFICATION AND RESOLUTION OF LUNAR RADAR IMAGES Abstract Only

H. J. Moore and T. W. Thompson (Jet Propulsion Lab., California Inst. of Tech., Pasadena.) *In* Lunar and Planetary Inst., Abstracts for the Venus Geoscience Tutorial and Venus Geologic Mapping Workshop 1989 p 32 Previously announced in IAA as A89-10879 (For primary document see N90-12423 03-91)
Avail: NTIS HC A04/MF A01 CSCL 03B

The relations between the identification of dominant lunar landforms, craters, and radar images at three resolutions are investigated. Although the percentage of craters that can be identified is found to increase with diameter or relief for any given resolution, it is noted that craters have not been identified at all diameters and relief. It is shown that the relation between the percentage of identified craters and their dimensions depends on the size-frequency distributions of both diameters and relief, and that crater identification depends strongly on the resolution of the radar image. Author

N90-12442*# Southern Methodist Univ., Dallas, TX. Dept. of Geological Sciences.

VENUS: MANTLE CONVECTION, HOTSPOTS, AND TECTONICS Abstract Only

R. J. Phillips *In* Lunar and Planetary Inst., Abstracts for the Venus Geoscience Tutorial and Venus Geologic Mapping Workshop 1989 p 33-34 (For primary document see N90-12423 03-91)
Avail: NTIS HC A04/MF A01 CSCL 03B

The putative paradigm that planets of the same size and mass have the same tectonic style led to the adaptation of the mechanisms of terrestrial plate tectonics as the a priori model of the way Venus should behave. Data acquired over the last decade by Pioneer Venus, Venera, and ground-based radar have modified this view sharply and have illuminated the lack of detailed understanding of the plate tectonic mechanism. For reference, terrestrial mechanisms are briefly reviewed. Venusian lithospheric divergence, hotspot model, and horizontal deformation theories are proposed and examined. Author

N90-12443*# Washington Univ., Saint Louis, MO. Dept. of Earth and Planetary Sciences.

RADAR SCATTERING FROM DESERT TERRAINS, PISGAH/LAVIC REGION, CALIFORNIA: IMPLICATIONS FOR MAGELLAN

J. J. Plaut, R. E. Arvidson, and S. Wall (Jet Propulsion Lab., California Inst. of Tech., Pasadena.) *In* Lunar and Planetary Inst., Abstracts for the Venus Geoscience Tutorial and Venus Geologic Mapping Workshop 1989 p 35-36 (For primary document see N90-12423 03-91)
Avail: NTIS HC A04/MF A01 CSCL 03B

A major component of the 1988 Mojave Field Experiment involved the simultaneous acquisition of quad-polarization multifrequency airborne Synthetic Aperture Radar (SAR) imaging radar data and ground measurements thought to be relevant to the radar scattering behavior of a variety of desert surfaces. In preparation for the Magellan mission to Venus, the experiment was designed to explore the ability of SAR to distinguish types of geological surfaces, and the effects of varying incidence angles on the appearance of such surfaces. The airborne SAR system acquired images at approx. 10 m resolution, at 3 incidence angles (30, 40, 50 degs) and at 3 wavelengths (P:68 cm, L:24 cm, C:5.6 cm). The polarimetric capabilities of the instrument allow the simulation of any combination of transmit and receive polarizations during data reduction. Calibrated trihedral corner reflectors were deployed within each scene to permit absolute radiometric calibration of the image data. Initial analyses of this comprehensive radar data set is reported, with emphasis on implications for interpretation of Magellan data. Author

N90-12444*# Brown Univ., Providence, RI. Dept. of Geological Sciences.

LAKSHMI PLANUM: A DISTINCTIVE HIGHLAND VOLCANIC PROVINCE

Kari M. Roberts and James W. Head *In* Lunar and Planetary Inst., Abstracts for the Venus Geoscience Tutorial and Venus Geologic Mapping Workshop 1989 p 37-38 (For primary document see N90-12423 03-91)
Avail: NTIS HC A04/MF A01 CSCL 03B

Lakshmi Planum, a broad smooth plain located in western Ishtar Terra and containing two large oval depressions (Colette and Sacajawea), has been interpreted as a highland plain of volcanic origin. Lakshmi is situated 3 to 5 km above the mean planetary radius and is surrounded on all sides by bands of mountains interpreted to be of compressional tectonic origin. Four primary characteristics distinguish Lakshmi from other volcanic regions known on the planet, such as Beta Regio: (1) high altitude, (2) plateau-like nature, (3) the presence of very large, low volcanic constructs with distinctive central calderas, and (4) its compressional tectonic surroundings. Building on the previous work of Pronin, the objective is to establish the detailed nature of the volcanic deposits on Lakshmi, interpret eruption styles and conditions, sketch out an eruption history, and determine the relationship between volcanism and the tectonic environment of the region. Author

N90-12445*# Geological Survey, Flagstaff, AZ.

VOLCANISM ON VENUS: LARGE SHIELDS AND MAJOR ACCUMULATIONS OF SMALL DOMES

Gerald G. Schaber and Richard C. Kozak *In* Lunar and Planetary Inst., Abstracts for the Venus Geoscience Tutorial and Venus Geologic Mapping Workshop 1989 p 39-40 (For primary document see N90-12423 03-91)
Avail: NTIS HC A04/MF A01 CSCL 03B

The outer layers of the Venusian lithosphere appear to dissipate heat from the interior through mantle-driven thermal anomalies (hot spots, swells). As a result, Venus exhibits diverse forms of thin-skin tectonism and magmatic transfer to and extrusion from countless numbers of volcanic centers (e.g., shields, paterae, domes) and volcano-tectonic complexes (e.g., coronae, arachnoids). What is known about the distribution and morphologies of major Venusian shields is summarized, and the evidence for possible structural control of major accumulations as long as 5000 km of small volcanic domes is described. Author

N90-12446*# Geological Survey, Flagstaff, AZ.

IMPACT CRATERING AND THE SURFACE AGE OF VENUS: THE PRE-MAGELLAN CONTROVERSY

Gerald G. Schaber, E. M. Shoemaker, C. S. Shoemaker, and Richard C. Kozak *In* Lunar and Planetary Inst., Abstracts for the Venus Geoscience Tutorial and Venus Geologic Mapping Workshop 1989 p 41-42 (For primary document see N90-12423 03-91)
Avail: NTIS HC A04/MF A01 CSCL 03B

The average surface age of a planet is a major indicator of the level of its geologic activity and thus of the dynamics of its interior. Radar images obtained by Venera 15/16 from the northern quarter of the Venus (lat 30 to 90 degs) reveal about 150 features

that resemble impact craters, and they were so interpreted by Soviet investigators B. A. Ivanov, A. T. Basilevsky, and their colleagues. These features range in diameter from about 10 to 145 km. Their areal density is remarkably similar to the density of impact structures found on the American and European continental shields. The basic difference between the Soviet and American estimates of the average surface age of Venus's northern quarter is due to which crater-production rate is used for the Venusian environment. Cratering rates based on the lunar and terrestrial cratering records, as well as statistical calculations based on observed and predicted Venus-crossing asteroids and comets, have been used in both the Soviet and American calculations. The single largest uncertainty in estimating the actual cratering rates near Venus involves the shielding effect of the atmosphere.
Author

N90-12447*# Brown Univ., Providence, RI.
GEOLOGY OF THE VENUS EQUATORIAL REGION FROM PIONEER VENUS RADAR IMAGING
D. A. Senske and James W. Head *In* Lunar and Planetary Inst., Abstracts for the Venus Geoscience Tutorial and Venus Geologic Mapping Workshop 1989 p 43-44 (For primary document see N90-12423 03-91)
Avail: NTIS HC A04/MF A01 CSCL 03B

The surface characteristics and morphology of the equatorial region of Venus were first described by Masursky et al. who showed this part of the planet to be characterized by two topographic provinces, rolling plains and highlands, and more recently by Schaber who described and interpreted tectonic zones in the highlands. Using Pioneer Venus (PV) radar image data (15 deg S to 45 deg N), Senske and Head examined the distribution, characteristics, and deposits of individual volcanic features in the equatorial region, and in addition classified major equatorial physiographic and tectonic units on the basis of morphology, topographic signature, and radar properties derived from the PV data. Included in this classification are: plains (undivided), inter-highland tectonic zones, tectonically segmented linear highlands, upland rises, tectonic junctions, dark halo plains, and upland plateaus. In addition to the physiographic units, features interpreted as coronae and volcanic mountains have also been mapped. The latter four of the physiographic units along with features interpreted to be coronae.
Author

N90-12448*# Stanford Univ., CA. Dept. of Geophysics.
VENUS AND THE ARCHEAN EARTH: THERMAL CONSIDERATIONS Abstract Only
N. H. Sleep *In* Lunar and Planetary Inst., Abstracts for the Venus Geoscience Tutorial and Venus Geologic Mapping Workshop 1989 p 46 (For primary document see N90-12423 03-91)
Avail: NTIS HC A04/MF A01 CSCL 03B

The Archean Era of the Earth is not a direct analog of the present tectonics of Venus. In this regard, it is useful to review the state of the Archean Earth. Most significantly, the temperature of the adiabatic interior of the Earth was 200 to 300 C hotter than the current temperature. Preservation biases limit what can be learned from the Archean record. Archean oceanic crust, most of the planetary surface at any one time, has been nearly all subducted. More speculatively, the core of the Earth has probably cooled more slowly than the mantle. Thus the temperature contrast above the core-mantle boundary and the vigor of mantle plumes has increased with time on the Earth. The most obvious difference between Venus and the present Earth is the high surface temperature and hence a low effective viscosity of the lithosphere. In addition, the temperature contrast between the adiabatic interior and the surface, which drives convection, is less on Venus than on the Earth. It appears that the hot lithosphere enhanced tectonics on the early Venus significantly enough that its interior cooled faster than the Earth's. The best evidence for a cool interior of Venus comes from long wavelength gravity anomalies. The low interior temperatures retard seafloor spreading on Venus. The high surface temperatures on Venus enhance crustal deformation. That is, the lower crust may become ductile enough to permit significant flow between the upper crust and the mantle. There is thus some analogy to modern and ancient areas of high heat flow on the Earth. Archean crustal blocks typically remained stable for long intervals and thus overall are not good analogies to the deformation style on Venus.
Author

N90-12449*# Brown Univ., Providence, RI. Dept. of Geological Sciences.
CORONAE ON VENUS OBSERVATIONS AND MODELS OF ORIGIN
E. R. Stofan *In* Lunar and Planetary Inst., Abstracts for the Venus Geoscience Tutorial and Venus Geologic Mapping Workshop 1989 p 47-48 (For primary document see N90-12423 03-91)
Avail: NTIS HC A04/MF A01 CSCL 03B

The Venera 15/16 spacecraft revealed a number of features of unknown origin including coronae, elongate to circular structures with a complex interior surrounded by an annulus of concentric ridges. Eighteen coronae were identified in Venera 15/16 data of Venus; an additional thirteen possible coronae are found in Pioneer Venus and Arecibo data. Coronae, with maximum widths of 160 to over 650 km, are found primarily in two clusters in the Northern Hemisphere located to the east and west of Ishtar Terra. Another possible cluster is located in Themis Regio in the Southern Hemisphere. The majority of coronae are at least partially raised less than 1.5 km above the surrounding region, and over half are partially surrounded by a peripheral trough. A sequence of events for coronae has been determined through mapping. Prior to corona formation, regional compression or extension creates bands of lineaments along which coronae tend to later form. During the early stages of corona formation, relatively raised topography is produced by uplift and volcanic construction. The evolution of coronae and their general characteristics have been compared to two models of corona origin: hotspots and sinking mantle diapirs. In the hotspot or rising mantle diapir model, heating and melting at depth create uplift at the surface. Uplift is accompanied by central extension, facilitating volcanism. Gravitational relaxation of the uplifted region follows producing the compressional features within the annulus and the peripheral trough. Both models can predict the major characteristics and evolutionary sequence of coronae. The sinking diapir model does predict an early-time low and central compression as well as broadening and shallowing of the peripheral trough with time, all of which are not observed at current data resolution. In addition, the sinking mantle diapir mode predicts more simultaneous formation of the high topography, annulus and trough unlike the hotspot or rising mantle diapir mode. High resolution Magellan data will be used to distinguish between the two models of corona origin.
Author

N90-12450*# Cornell Univ., Ithaca, NY. Dept. of Geological Sciences.
CRUSTAL DEFORMATION: EARTH VS VENUS Abstract Only
D. L. Turcotte *In* Lunar and Planetary Inst., Abstracts for the Venus Geoscience Tutorial and Venus Geologic Mapping Workshop 1989 p 49 (For primary document see N90-12423 03-91)
Avail: NTIS HC A04/MF A01 CSCL 03B

It is timely to consider the possible tectonic regimes on Venus both in terms of what is known about Venus and in terms of deformation mechanisms operative on the earth. Plate tectonic phenomena dominate tectonics on the earth. Horizontal displacements are associated with the creation of new crust at ridges and destruction of crust at trenches. The presence of plate tectonics on Venus is debated, but there is certainly no evidence for the trenches associated with subduction on the earth. An essential question is what kind of tectonics can be expected if there is no plate tectonics on Venus. Mars and the Moon are reference examples. Volcanic constructs appear to play a dominant role on Mars but their role on Venus is not clear. On single plate planets and satellites, tectonic structures are often associated with thermal stresses. Cooling of a planet leads to thermal contraction and surface compressive features. Delamination has been propsed for Venus by several authors. Delamination is associated with the subduction of the mantle lithosphere and possibly the lower crust but not the upper crust. The surface manifestations of delamination are unclear. There is some evidence that delamination is occurring beneath the Transverse Ranges in California. Delamination will certainly lead to lithospheric thinning and is likely to lead to uplift and crustal thinning. Author

N90-12451*# Brown Univ., Providence, RI. Dept. of Geological Sciences.

EASTERN ISHTAR TERRA: TECTONIC EVOLUTION DERIVED FROM RECOGNIZED FEATURES

R. W. VorderBruegge and James W. Head *In* Lunar and Planetary Inst., Abstracts for the Venus Geoscience Tutorial and Venus Geologic Mapping Workshop 1989 p 50-51 (For primary document see N90-12423 03-91)
Avail: NTIS HC A04/MF A01 CSCL 03B

Previous analyses have recognized several styles and orientations of compressional deformation, crustal convergence, and crustal thickening in Eastern Ishtar Terra. An east to west sense of crustal convergence through small scale folding, thrusting, and buckling is reflected in the high topography and ridge-and-valley morphology of Maxwell Montes and the adjacent portion of Fortuna Tessera. This east to west convergence was accompanied by up to 1000 km of lateral motion and large scale strike-slip faulting within two converging shear zones which has resulted in the present morphology of Maxwell Montes. A more northeast to southwest sense of convergence through large scale buckling and imbrication is reflected in large, northwest-trending scarps along the entire northern boundary of Ishtar Terra, with up to 2 km of relief present at many of the scarps. It was previously suggested that both styles of compression have occurred at the expense of pre-existing tessera regions which have then been overprinted by the latest convergence event. The difference in style is attributed mostly to differences in the properties of the crust converging with the tessera blocks. If one, presumably thick, tessera block converges with another tessera region, then the widespread, distributed style of deformation occurs, as observed in western Fortuna Tessera. However, if relatively thin crust (such as suggested for the North Polar Plains converges with thicker tessera regions, then localized deformation occurs, as reflected in the scarps along Northern Ishtar Terra. The purpose is to identify the types of features observed in Eastern Ishtar Terra. Their potential temporal and spatial relationships, is described, possible origins for them is suggested, and how the interpretation of some of these features has led to the multiple-style tectonic evolution model described is shown.
Author

N90-12452*# Arizona State Univ., Tempe. Dept. of Geology.

STRESS DISTRIBUTION AND TOPOGRAPHY OF TELLUS REGIO, VENUS

David R. Williams and Ronald Greeley *In* Lunar and Planetary Inst., Abstracts for the Venus Geoscience Tutorial and Venus Geologic Mapping Workshop 1989 p 52-53 (For primary document see N90-12423 03-91)
Avail: NTIS HC A04/MF A01 CSCL 03B

The Tellus Regio area of Venus represents a subset of a narrow latitude band where Pioneer Venus Orbiter (PVO) altimetry data, line-of-sight (LOS) gravity data, and Venera 15/16 radar images have all been obtained with good resolution. Tellus Regio also has a wide variety of surface morphologic features, elevations ranging up to 2.5 km, and a relatively low LOS gravity anomaly. This area was therefore chosen in order to examine the theoretical stress distributions resulting from various models of compensation of the observed topography. These surface stress distributions are then compared with the surface morphology revealed in the Venera 15/16 radar images. Conclusions drawn from these comparisons will enable constraints to be put on various tectonic parameters relevant to Tellus Regio. The stress distribution is calculated as a function of the topography, the equipotential anomaly, and the assumed model parameters. The topography data is obtained from the PVO altimetry. The equipotential anomaly is estimated from the PVO LOS gravity data. The PVO LOS gravity represents the spacecraft accelerations due to mass anomalies within the planet. These accelerations are measured at various altitudes and angles to the local vertical and therefore do not lend themselves to a straightforward conversion. A minimum variance estimator of the LOS gravity data is calculated, taking into account the various spacecraft altitudes and LOS angles and using the measured PVO topography as an a priori constraint. This results in an estimated equivalent surface mass distribution, from which the equipotential anomaly is determined. Author

N90-12453*# National Aeronautics and Space Administration. Lyndon B. Johnson Space Center, Houston, TX.

THREE AGES OF VENUS

Charles A. Wood and Cassandra R. Coombs *In* Lunar and Planetary Inst., Abstracts for the Venus Geoscience Tutorial and Venus Geologic Mapping Workshop 1989 p 54-55 (For primary document see N90-12423 03-91)
Avail: NTIS HC A04/MF A01 CSCL 03B

A central question for any planet is the age of its surface. Based on comparative planetological arguments, Venus should be as young and active as the Earth (Wood and Francis). The detection of probable impact craters in the Venera radar images provides a tool for estimating the age of the surface of Venus. Assuming somewhat different crater production rates, Bazilevskiy et al. derived an age of 1 + or - 0.5 billion years, and Schaber et al. and Wood and Francis estimated an age of 200 to 400 million years. The known impact craters are not randomly distributed, however, thus some area must be older and others younger than this average age. Ages were derived for major geologic units on Venus using the Soviet catalog of impact craters (Bazilevskiy et al.), and the most accessible geologic unit map (Bazilevskiy). The crater counts are presented for (diameters greater than 20 km), areas, and crater densities for the 7 terrain units and coronae. The procedure for examining the distribution of craters is superior to the purely statistical approaches of Bazilevskiy et al. and Plaut and Arvidson because the bins are larger (average size 16 x 10(6) sq km) and geologically significant. Crater densities define three distinct groups: relatively heavily cratered (Lakshmi, mountain belts), moderately cratered (smooth and rolling plains, ridge belts, and tesserae), and essentially uncratered (coronae and domed uplands). Following Schaber et al., Grieve's terrestrial cratering rate of 5.4 + or - 2.7 craters greater than 20 km/10(9) yrs/10(6) sq km was used to calculate ages for the geologic units on Venus. To improve statistics, the data was aggregated into the three crater density groups, deriving the ages. For convenience, the three similar age groups are given informal time stratigraphic unit names, from youngest to oldest: Ulfrunian, Sednaian, Lakshmian. Author

N90-12454*# National Aeronautics and Space Administration, Washington, DC.

REPORTS OF PLANETARY GEOLOGY AND GEOPHYSICS PROGRAM, 1988

Henry E. Holt, ed. Oct. 1989 529 p
(NASA-TM-4130; NAS 1.15:4130) Avail: NTIS HC A23/MF A03 CSCL 03B

This is a compilation of abstracts of reports from Principal Investigators of NASA's Planetary Geology and Geophysics Program, Office of Space Science and Applications. The purpose is to document in summary form research work conducted in this program during 1988. Each report reflects significant accomplishments within the area of the author's funded grant or contract. Author

N90-12455# Lawrence Livermore National Lab., CA.

HIGH PRESSURE STUDIES OF PLANETARY MATTER

Marvin Ross Jun. 1989 4 p Presented at the AIRAPT and EHPRG International High Pressure Science and Technology Conference, Paderborn, Fed. Republic of Germany, 17-21 Jul. 1989
(Contract W-7405-eng-48)
(DE89-017738; UCRL-101436; CONF-890798-11) Avail: NTIS HC A01/MF A01

Those materials which are of greatest interest to the physics of the deep planetary interiors are Fe, H2, He and the Ices. These are sufficiently diverse and intensively studied to offer an overview of present day high pressure research. DOE

92 SOLAR PHYSICS

Includes solar activity, solar flares, solar radiation and sunspots.

For related information see *93 Space Radiation.*

N90-12456*# National Aeronautics and Space Administration. Marshall Space Flight Center, Huntsville, AL.
ON THE STATISTICS OF EL NINO OCCURRENCES AND THE RELATIONSHIP OF EL NINO TO VOLCANIC AND SOLAR/GEOMAGNETIC ACTIVITY
Robert M. Wilson Washington Sep. 1989 62 p
(NASA-TP-2948; NAS 1.60:2948) Avail: NTIS HC A04/MF A01 CSCL 03B

El Nino is conventionally defined as an anomalous and persistent warming of the waters off the coasts of Ecuador and Peru in the eastern equatorial Pacific, having onset usually in Southern Hemispheric summer/fall. Some of the statistical aspects of El Nino occurrences are examined, especially as they relate to the normal distribution and to possible associations with volcanic, solar, and geomagnetic activity. With regard to the very strong El Nino of 1982 to 1983, it is noted that, although it may very well be related to the 1982 eruptions of El Chichon, the event occurred essentially on time (with respect to the past behavior of elapsed times between successive El Nino events; a moderate-to-stronger El Nino was expected during the interval 1978 to 1982, assuming that El Nino occurrences are normally distributed, having a mean elapsed time between successive onsets of 4 years and a standard deviation of 2 years and a last known occurrence in 1976). Also, although not widely recognized, the whole of 1982 was a record year for geomagnetic activity (based on the aa geomagnetic index, with the aa index registering an all time high in February 1982), perhaps, important for determining a possible trigger for this and other El Nino events. A major feature is an extensive bibliography (325 entries) on El Nino and volcanic-solar-geomagnetic effects on climate. Also, included is a tabular listing of the 94 major volcanic eruptions of 1835 to 1986. Author

N90-12457# Los Alamos National Lab., NM.
THE BAKSAN GALLIUM SOLAR NEUTRINO EXPERIMENT
V. N. Gavrin, A. I. Abazov, D. N. Abdurashitov, O. L. Anosov, O. V. Bychuk, S. N. Danshin, L. A. Eroshkina, E. L. Faizov, V. I. Gayevsky, and S. V. Girin et al 1989 13 p Presented at the International Conference: Inside the Sun, Versailles, France, 22-26 May 1989
(Contract W-7405-eng-36)
(DE89-016036; LA-UR-89-2779; CONF-890520-2) Avail: NTIS HC A03/MF A01

A radiochemical Ga(71)-Ge(71) experiment to determine the integral flux of neutrinos from the sun was constructed at the Baksan Neutrino Observatory in the USSR. Measurements have begun with 30 tonnes of gallium. The experiment is being expanded with the addition of another 30 tonnes. The motivation, experimental procedures, and present status of this experiment are presented. DOE

N90-12458*# Stanford Univ., CA. Dept. of Applied Physics.
THE HARD X RAYS AND GAMMA-RAYS FROM SOLAR FLARES
James M. McTiernan and Vahe Petrosian Nov. 1989 35 p
(Grants NsG-7092; NSF ATM-83-20439)
(NASA-CR-185982; NAS 1.26:185982) Avail: NTIS HC A03/MF A01 CSCL 03B

Radiation of energies from 10 KeV to greater than 10 MeV has been observed during solar flares, and is interpreted to be due to bremsstrahlung by relativistic electrons. A complete treatment of this problem requires solution of the kinetic equation for relativistic electrons and inclusion of synchrotron energy losses. Using the electron distributions obtained from numerical solutions of this equation the bremsstrahlung spectra in the impulsive x ray and gamma-ray regimes are calculated, and the variation of these spectral indices and directivities with energy and observation angle are described. The dependences of these characteristics of the radiation of changes in the solar atmospheric model, including the convergence of the magnetic field, the injected electron spectral index, and most importantly, in the anisotropy of the injected electrons and of the convergence of the magnetic field are also described. The model results are compared with stereoscopic observations of individual flares and the constraints that this data sets on the models are discussed. Author

N90-12459*# National Aeronautics and Space Administration. Goddard Space Flight Center, Greenbelt, MD.
MAX '91 WORKSHOP 2: DEVELOPMENTS IN OBSERVATIONS AND THEORY FOR SOLAR CYCLE 22
Robert M. Winglee, ed. (Colorado Univ., Boulder.) and Brian R. Dennis, ed. 1989 377 p Workshop held in Laurel, MD, 8-9 Jun. 1989
(NASA-TM-101893; NAS 1.15:101893) Avail: NTIS HC A17/MF A03 CSCL 03B

Papers and observatory reports presented at the second workshop of the Max '91 program are compiled along with discussion group summaries and invited reviews. The four discussion groups addressed the following subjects: high-energy flare physics; coordinated magnetograph observations; flare theory and modeling; and Max '91 communications and coordination. A special session also took place on observations of Active Region 5395 and the associated flares of March 1989. Other topics covered during the workshop include the scientific objectives of solar gamma ray observations, the solar capabilities of each of the four instruments on the Gamma Ray Observatory, and access to Max '91 information. For individual titles, see N90-12460 through N90-12491.

N90-12460*# New Hampshire Univ., Durham.
HIGH ENERGY FLARE PHYSICS GROUP SUMMARY
J. M. Ryan and J. D. Kurfess (Naval Research Lab., Washington, DC.) *In* NASA, Goddard Space Flight Center, Max '91 Workshop 2: Developments in Observations and Theory for Solar Cycle 22 1989 p 1-16 (For primary document see N90-12459 03-92)
Avail: NTIS HC A17/MF A03 CSCL 03B

The contributions of the High Energy Flare Physics Special Session in the American Astronomical Society Solar Physics Division Meeting are reviewed. Oral and poster papers were presented on observatories and instruments available for the upcoming solar maximum. Among these are the space-based Gamma Ray Observatory, the Solar Flare and Cosmic Burst Gamma Ray Experiment on the Ulysses spacecraft, the Soft X Ray Telescope on the spacecraft Solar-A, and the balloon-based Gamma Ray Imaging Device. Ground based observatories with new capabilities include the BIMA mm-wave interferometer (Univ. of California, Berkeley; Univ. of Illinois; Univ. of Maryland), Owens Valley Radio Observatory and the Very Large Array. The highlights of the various instrument performances are reported and potential data correlations and collaborations are suggested. Author

N90-12461*# National Aeronautics and Space Administration. Goddard Space Flight Center, Greenbelt, MD.
MAGNETOGRAPH GROUP SUMMARY
Harrison P. Jones *In its* Max '91 Workshop 2: Developments in Observations and Theory for Solar Cycle 22 1989 p 17-26 (For primary document see N90-12459 03-92)
Avail: NTIS HC A17/MF A03 CSCL 03B

The Magnetograph Group focussed on the techniques and many practical problems of interleaving ground-based measurements of magnetic fields from diverse sites and instruments to address the original scientific objectives. The predominant view of the discussion group was that present instrumentation and analysis resources do not warrant immediate, specific plans for further worldwide campaigns of cooperative magnetograph observing. The several reasons for this view, together with many caveats, qualifications, and suggestions for future work are presented. Author

N90-12462*# National Aeronautics and Space Administration. Goddard Space Flight Center, Greenbelt, MD.

THEORY AND MODELING GROUP

Gordon D. Holman *In its* Max '91 Workshop 2: Developments in Observations and Theory for Solar Cycle 22 1989 p 27-30 (For primary document see N90-12459 03-92)
Avail: NTIS HC A17/MF A03 CSCL 03B

The primary purpose of the Theory and Modeling Group meeting was to identify scientists engaged or interested in theoretical work pertinent to the Max '91 program, and to encourage theorists to pursue modeling which is directly relevant to data which can be expected to result from the program. A list of participants and their institutions is presented. Two solar flare paradigms were discussed during the meeting -- the importance of magnetic reconnection in flares and the applicability of numerical simulation results to solar flare studies. Author

N90-12463*# California Univ., San Diego.

SCIENTIFIC OBJECTIVES OF SOLAR GAMMA-RAY OBSERVATIONS

R. E. Lingenfelter *In* NASA, Goddard Space Flight Center, Max '91 Workshop 2: Developments in Observations and Theory for Solar Cycle 22 1989 p 33-34 (For primary document see N90-12459 03-92)
Avail: NTIS HC A17/MF A03 CSCL 03B

Solar flare neutrons and gamma rays are produced by nuclear interactions of flare accelerated ions in the solar atmosphere. A rich variety of such gamma ray and neutron observations have been made by the Solar Maximum Mission (SSM), other satellite, balloon and ground based detectors, and they have provided a wealth of unique information on the nature of particle acceleration in flares and on the flare process itself. What we have learned from these observations is briefly reviewed, and what we can hope to learn from more sensitive new observations to be made with the Gamma Ray Observatory (GRO), the Max '91 balloon program, and the Nuclear Astrophysics Explorer is outlined. Author

N90-12464*# National Aeronautics and Space Administration. Goddard Space Flight Center, Greenbelt, MD.

THE GAMMA-RAY OBSERVATORY: AN OVERVIEW

Donald A. Kniffen *In its* Max '91 Workshop 2: Developments in Observations and Theory for Solar Cycle 22 1989 p 35-45 (For primary document see N90-12459 03-92)
Avail: NTIS HC A17/MF A03 CSCL 03B

The Gamma-Ray Observatory (GRO) is a 16,000 kg spacecraft containing four instruments which span almost six decades of energy from about 50 keV to about 30 GeV. It will provide the first opportunity to make simultaneous observations over such a broad band of gamma-ray energies. GRO is assembled and undergoing testing prior to its scheduled June 4, 1990 launch aboard the Space Shuttle. The orbit will be circular with an altitude of 450 km and with an inclination of 28 degrees. Data will be recorded at 32 kilobits per second and dumped once per orbit via the Tracking and Data Relay Satellite System (TDRSS). The spacecraft is three-axis stabilized and timing will be maintained to .1 ms. The observing schedule will begin with an all sky survey, consisting of 30 two week pointings, covering the first 15 months of science operations. Following observations will emphasize source studies and deep searches. Originally selected as a Principal Class spacecraft with a two year mission, extension of the mission to six to ten years makes a vigorous Guest Investigator Program both possible and desirable. Such a program will be fully in place by the third year of the mission, with limited opportunities earlier. Each of the four instruments has a capability for observing both gamma-ray bursts and solar flare gamma-rays, and there is some solar neutron capability. Correlated observations with those at other wavelengths is also receiving considerable attention in the mission planning. Author

N90-12465*# Stanford Univ., CA.

WHEN AND WHERE TO LOOK TO OBSERVE MAJOR SOLAR FLARES

T. Bai *In* NASA, Goddard Space Flight Center, Max '91 Workshop 2: Developments in Observations and Theory for Solar Cycle 22 1989 p 46-59 (For primary document see N90-12459 03-92)
Avail: NTIS HC A17/MF A03 CSCL 03B

When and where to look is an important issue to observers planning to observe major solar flares. Prediction of major flares is also important because they influence the Earth's environment. Techniques for utilizing recently discovered solar hot spots and a solar activity periodicity of about 154 days in determining when and where to look to catch major flares are discussed. Author

N90-12466*# Colorado Univ., Boulder. Dept. of Atmospheric, Planetary, and Astrophysical Sciences.

ACCESS TO MAX '91 INFORMATION VIA COMPUTER NETWORKS c82

Alan L. Kiplinger (National Oceanic and Atmospheric Administration, Boulder, CO.) *In* NASA, Goddard Space Flight Center, Max '91 Workshop 2: Developments in Observations and Theory for Solar Cycle 22 1989 p 60-64 (For primary document see N90-12459 03-92)
Avail: NTIS HC A17/MF A03 CSCL 05B

Various types of flare information, activity, active region reports, x ray plots and daily Campaign Action notices are now available on SPAN, and INTERNET. Although this system was developed for use by Max '91 participants during campaigns, it is updated daily and maintained at times outside of campaigns. Thus it is available for general use outside of campaigns. The Space Environment Laboratory maintains VAX and Apollo systems, both of which are on INTERNET. The VAX is also on the SPAN network as node SELVAX or 9555. Details of access to files on the VAX are given. Author

N90-12467*# Naval Research Lab., Washington, DC. Center for Space Research.

CAPABILITIES OF GRO/OSSE FOR OBSERVING SOLAR FLARES

J. D. Kurfess, W. N. Johnson, G. H. Share, E. O. Hulburt, S. M. Matz, and R. J. Murphy (Universities Space Research Association, Columbia, MD.) *In* NASA, Goddard Space Flight Center, Max '91 Workshop 2: Developments in Observations and Theory for Solar Cycle 22 1989 p 65-74 (For primary document see N90-12459 03-92)
Avail: NTIS HC A17/MF A03 CSCL 03B

The launch of the Gamma Ray Observatory (GRO) near solar maximum makes solar flare studies early in the mission particularly advantageous. The Oriented Scintillation Spectrometer Experiment (OSSE) on GRO, covering the energy range 0.05 to 150 MeV, has some significant advantages over the previous generation of satellite-borne gamma-ray detectors for solar observations. The OSSE detectors will have about 10 times the effective area of the Gamma-Ray Spectrometer (GRS) on Solar Maximum Mission (SMM) for both photons and high-energy neutrons. The OSSE also has the added capability of distinguishing between high-energy neutrons and photons directly. The OSSE spectral accumulation time (approx. 4s) is four times faster than that of the SMM/GRS; much better time resolution is available in selected energy ranges. These characteristics will allow the investigation of particle acceleration in flares based on the evolution of the continuum and nuclear line components of flare spectra, nuclear emission in small flares, the anisotropy of continuum emission in small flares, and the relative intensities of different nuclear lines. The OSSE observational program will be devoted primarily to non-solar sources. Therefore, solar observations require planning and special configurations. The instrumental and operational characteristics of OSSE are discussed in the context of undertaking solar observations. The opportunities for guest investigators to participate in solar flare studies with OSSE is also presented. Author

N90-12468*# Institute for the Study of Earth, Oceans and Space, Durham, NH.

THE SOLAR GAMMA RAY AND NEUTRON CAPABILITIES OF COMPTEL ON THE GAMMA RAY OBSERVATORY

James M. Ryan and John A. Lockwood *In* NASA, Goddard Space Flight Center, Max '91 Workshop 2: Developments in Observations and Theory for Solar Cycle 22 1989 p 75-95 Sponsored by Max Planck Institut fuer Extraterrestrische Physik, Garching, Fed. Republic of Germany; Space Research Organization of the Netherlands, Leiden, Netherlands; and Space Science Dept. of ESA/ESTEC, Noordwijk, Netherlands (For primary document see N90-12459 03-92)
(Contract NAS5-26645)
Avail: NTIS HC A17/MF A03 CSCL 03B

The imaging Compton telescope COMPTEL on the Gamma Ray Observatory (GRO) has unusual spectroscopic capabilities for measuring solar gamma-ray and neutron emission. The launch of the GRO is scheduled for June 1990 near the peak of the sunspot cycle. With a 30 to 40 percent probability for the Sun being in the COMPTEL field-of-view during the sunlit part of an orbit, a large number of flares will be observed above the 800 keV gamma-ray threshold of the telescope. The telescope energy range extends to 30 MeV with high time resolution burst spectra available from 0.1 to 10 MeV. Strong Compton tail suppression of instrumental gamma-ray interactions will facilitate improved spectral analysis of solar flare emissions. In addition, the high signal to noise ratio for neutron detection and measurement will provide new neutron spectroscopic capabilities. Specifically, a flare similar to that of 3 June 1982 will provide spectroscopic data on greater than 1500 individual neutrons, enough to construct an unambiguous spectrum in the energy range of 20 to 200 MeV. Details of the instrument and its response to solar gamma-rays and neutrons will be presented. Author

N90-12469*# National Aeronautics and Space Administration. Goddard Space Flight Center, Greenbelt, MD.

THE BATSE EXPERIMENT ON THE GAMMA RAY OBSERVATORY: SOLAR FLARE HARD X RAY AND GAMMA-RAY CAPABILITIES

G. J. Fishman, C. A. Meegan, R. B. Wilson, T. A. Parnell, W. S. Paciesas, G. N. Pendleton, H. S. Hudson, J. L. Matteson, L. E. Peterson (California Univ., San Diego.), and T. L. Cline et al *In its* Max '91 Workshop 2: Developments in Observations and Theory for Solar Cycle 22 1989 p 96-106 (For primary document see N90-12459 03-92)
Avail: NTIS HC A17/MF A03 CSCL 03B

The Burst and Transient Source Experiment (BATSE) for the Gamma Ray Observatory (GRO) consists of eight detector modules that provide full-sky coverage for gamma-ray bursts and other transient phenomena such as solar flares. Each detector module has a thin, large-area scintillation detector (2025 sq cm) for high time-resolution studies, and a thicker spectroscopy detector (125 sq cm) to extend the energy range and provide better spectral resolution. The total energy range of the system is 15 keV to 100 MeV. These 16 detectors and the associated onboard data system should provide unprecedented capabilities for observing rapid spectral changes and gamma-ray lines from solar flares. The presence of a solar flare can be detected in real-time by BATSE; a trigger signal is sent to two other experiments on the GRO. The launch of the GRO is scheduled for June 1990, so that BATSE can be an important component of the Max '91 campaign. Author

N90-12470*# Max-Planck-Inst. fuer Extraterrestrische Physik, Garching (Germany, F.R.).

THE SOLAR FLARE AND COSMIC GAMMA-RAY BURST EXPERIMENT ABOARD THE ULYSSES SPACECRAFT

Michel Boer, Michael Sommer, and Kevin Hurley (California Univ., Berkeley.) *In* NASA, Goddard Space Flight Center, Max '91 Workshop 2: Developments in Observations and Theory for Solar Cycle 22 1989 p 107-109 (For primary document see N90-12459 03-92)
Avail: NTIS HC A17/MF A03 CSCL 03B

The HUS-Ulysses team has prepared an instrument for the Ulysses spacecraft consisting of 2 Csi detectors and 2 Si surface barrier detectors for measuring x rays in the range 5 to 200 keV with up to 8 ms time resolution. The prime objectives of the experiment are the study of solar flares and cosmic gamma-ray bursts. The Ulysses mission will leave the ecliptic during the forthcoming solar maximum. The total time above ecliptic latitudes + or - 70 degrees is expected to be 230 days. The solar data can be used in conjunction with other experiments to measure the directivity of the emission and for correlative studies. Author

N90-12471*# Tufts Univ., Medford, MA. Dept. of Physics and Astronomy.

VLA-MAX '91 TESTS OF HIGH ENERGY FLARE PHYSICS

Kenneth R. Lang and Robert F. Willson *In* NASA, Goddard Space Flight Center, Max '91 Workshop 2: Developments in Observations and Theory for Solar Cycle 22 1989 p 110-118 (For primary document see N90-12459 03-92)
Avail: NTIS HC A17/MF A03 CSCL 03B

The potential for the Very Large Array (VLA) contributions during the coming maximum in solar activity is illustrated by unpublished observations of solar flares on 28 May, 8 June, 24 June, and 30 September 1988. Some of this data appears in the two papers by Willson et al., referenced in this article. The VLA can be used to spatially resolve flaring active regions and their magnetic fields. These results can be compared with simultaneous x ray and gamma ray observations from space. Examples are provided in which spatially separated radio sources are resolved for the pre-burst, impulsive and decay phases of solar flares. The emergence of precursor coronal loops probably triggers the release of stored magnetic energy in adjacent coronal loops. Noise storm enhancements can originate in large-scale coronal loops on opposite sides of the visible solar disk. An interactive feedback mechanism may exist between activity in high-lying 90 cm coronal loops and lower-lying 20 cm ones. Author

N90-12472*# Maryland Univ., College Park.

FIRST INTERFEROMETRIC OBSERVATIONS WITH ARC-SEC. RESOLUTION OF SOLAR RADIO BURSTS AT MILLIMETER WAVELENGTHS

Mukul R. Kundu, S. M. White, N. Gopalswamy, and J. H. Bieging (California Univ., Berkeley.) *In* NASA, Goddard Space Flight Center, Max '91 Workshop 2: Developments in Observations and Theory for Solar Cycle 22 1989 p 119-130 (For primary document see N90-12459 03-92)
Avail: NTIS HC A17/MF A03 CSCL 03B

The Berkeley-Maryland-Illinois Array (BIMA) is briefly described in the context of solar observations. Specific areas of research that could be performed using BIMA during the Solar Maximum Mission (SMM) in 1991 are outlined. Some preliminary results of flare observations during March 1989 are presented. Author

N90-12473*# National Aeronautics and Space Administration. Goddard Space Flight Center, Greenbelt, MD.

OBSERVATIONAL GOALS FOR MAX '91 TO IDENTIFY THE CAUSATIVE AGENT FOR IMPULSIVE BURSTS

D. A. Batchelor *In its* Max '91 Workshop 2: Developments in Observations and Theory for Solar Cycle 22 1989 p 131-142 (For primary document see N90-12459 03-92)
Avail: NTIS HC A17/MF A03 CSCL 03B

Recent studies of impulsive hard x ray and microwave bursts suggest that a propagating causative agent with a characteristic velocity of the order of 1000 km/s is responsible for these bursts. The results of these studies are summarized and observable distinguishing characteristics of the various possible agents are highlighted, with emphasis on key observational goals for the Max '91 campaigns. The most likely causative agents suggested by the evidence are shocks, thermal conduction fronts, and propagating modes of magnetic reconnection in flare plasmas. With new instrumentation planned for Max '91, high spatial resolution observations of hard x ray sources have the potential to identify the agent by revealing detailed features of source spatial evolution. Observations with the Very Large Array and other radio imaging instruments are of great importance, as well as detailed modeling of coronal loop structures to place limits on their density and temperature profiles. With the combined hard x ray and microwave imaging observations, aided by loop model results, the simplest causative agent to rule out would be the propagating modes of magnetic reconnection. To fit the observational evidence, reconnection modes would need to travel at approximately the same velocity (the Alfven velocity) in different coronal structures that vary in length by a factor of 10(exp 3). Over such a vast range in loop lengths, it is difficult to believe that the Alfven velocity is constant. Thermal conduction fronts would be suggested by sources that expand along the direction of B and exhibit relatively little particle precipitation. Particle acceleration due to shocks could produce more diverse radially expanding source geometries with precipitation at loop footprints. Author

N90-12474*# National Aeronautics and Space Administration. Goddard Space Flight Center, Greenbelt, MD.

SOLAR FLARE GAMMA-RAY AND HARD X RAY IMAGING WITH THE GRID-ON-A-BALLOON

Larry E. Orwig, C. J. Crannell, Brian R. Dennis, R. Starr, G. J. Hurford, H. S. Hudson, F. vanBeek, M. E. Greene, W. N. Johnson, and J. P. Norris (Naval Research Lab., Washington, DC.) et al *In its* Max '91 Workshop 2: Developments in Observations and Theory for Solar Cycle 22 1989 p 143-157 (For primary document see N90-12459 03-92)

Avail: NTIS HC A17/MF A03 CSCL 03B

A primary scientific objective for solar flare research during the rapidly approaching maximum in solar activity is the imaging of gamma-ray and hard x ray sources of solar flare emissions. These goals will be pursued by the Gamma Ray Imaging Device (GRID) instrument, one of three instruments recently selected for NASA's Max '91 Solar Balloon Program. The GRID instrument is based on the technique of Fourier transform imaging and utilizes scanning modulation grid collimator optics to provide full-Sun imaging with 1.9-arcsecond resolution over the energy range from 20 to 700 keV at time resolutions from 0.1 to 2 s. The GRID telescope will employ 32 subcollimators, each composed of a matched pair of high-Z collimator grids separated by 5.2 meters and a phoswich scintillation spectrometer detector having no spatial resolution. The subcollimators and integrally-mounted fine aspect system are contained within a telescope canister which will be pointed to 0.1 degree accuracy and cyclically scanned to produce source modulation. The 32 subcollimators provide a uniform distribution of grid slit orientations and a logarithmic distribution of slit spacings corresponding to angular dimensions of 1.9 arcseconds to several arcminutes. The instrument is several orders of magnitude more sensitive than the HXIS instrument on the Solar Maximum Mission (SMM) and nearly 10 times more sensitive than any similar instrument scheduled to fly during the next solar maximum. The payload, designed for long-duration high-altitude balloon capability, is scheduled for its first science flight (8 to 14 days duration) from the Antarctic in January of 1992. Author

N90-12475*# Lockheed Missiles and Space Co., Palo Alto, CA. Research Lab.

THE SOFT X RAY TELESCOPE FOR SOLAR-A

W. A. Brown, L. W. Acton, M. E. Bruner, J. R. Lemen, and K. T. Strong *In* NASA, Goddard Space Flight Center, Max '91 Workshop 2: Developments in Observations and Theory for Solar Cycle 22 1989 p 158-172 (For primary document see N90-12459 03-92)

(Contract NAS8-37334)

Avail: NTIS HC A17/MF A03 CSCL 03B

The Solar-A satellite being prepared by the Institute for Sapce and Astronautical Sciences (ISAS) in Japan is dedicated to high energy observations of solar flares. The Soft X Ray Telescope (SXT) is being prepared to provide filtered images in the 2 to 60 A interval. The flight model is now undergoing tests in the 1000 foot tunnel at MSFC. Launch will be in September 1991. Earlier resolution and efficiency tests on the grazing incidence mirror have established its performance in soft x rays. The one-piece, two mirror grazing incidence telescope is supported in a strain free mount separated from the focal plane assembly by a carbon-epoxy metering tube whose windings and filler are chosen to minimize thermal and hygroscopic effects. The CCD detector images both the x ray and the concentric visible light aspect telescope. Optical filters provide images at 4308 and 4700 A. The SXT will be capable of producing over 8000 of the smallest partial frame images per day, or fewer but larger images, up to 1024 x 1024 pixel images. Image sequence with two or more of the five x ray analysis filters, with automatic exposure compensation to optimize the charge collection by the CCD detector, will be used to provide plasma diagnostics. Calculations using a differential emission measure code were used to optimize filter selection over the range of emission measure variations and to avoid redundancy, but the filters were chosen primarily to give ratios that are monotonic in plasma temperature. Author

N90-12476*# National Aeronautics and Space Administration. Goddard Space Flight Center, Greenbelt, MD.

PRE-PULSES: SIGNATURE OF A TRIGGER PROCESS IN SHORT (LESS THAN 60 SECS) SOLAR HARD X RAY FLARES

U. Deasi and Larry E. Orwig *In its* Max '91 Workshop 2: Developments in Observations and Theory for Solar Cycle 22 1989 p 173-182 (For primary document see N90-12459 03-92)

Avail: NTIS HC A17/MF A03 CSCL 03B

The continuing study of short hard x ray events (less than 60 sec duration) from the Solar Maximum Mission (SMM) Hard X ray Burst Spectrometer (HXRBS) instrument has revealed a unique feature. A well-separated distinctly identifiable, narrow (2 to 6 sec wide) pulse occurs prior to the start of the longer-flare lasting emission activity. Light curves are presented for eight events showing this feature. The pre-pulses show symmetrical rise and fall times. Spectral evolution of the pre-pulses are presented and their evolution compared to that of the main event spectra. It is argued that this feature be the elementary flare burst (de Jager, 1978). These pre-pulses could be a signature of the magnetic reconnection phenomenon discussed by Sturrock et al., (1984). Author

N90-12477*# Osservatorio Astrofisico di Arcetri, Florence (Italy).

FLARE MODEL SENSITIVITY OF THE BALMER SPECTRUM

A. Falchi, R. Falciani, L. A. Smaldone (Naples Univ., Italy), and G. P. Tozzi *In* NASA, Goddard Space Flight Center, Max '91 Workshop 2: Developments in Observations and Theory for Solar Cycle 22 1989 p 183-197 (For primary document see N90-12459 03-92)

Avail: NTIS HC A17/MF A03 CSCL 03B

Careful studies of various chromospheric spectral signatures are very important in order to explore their possible sensitivity to the modifications of the thermodynamic quantities produced by the flare occurrence. Pioneer work of Canfield and co-workers have shown how the H alpha behavior is able to indicate different changes in the atmospheric parameters structure associated to the flare event. It was decided to study the behavior of the highest Balmer lines and of the Balmer continuum in different solar flare model atmospheres. These spectral features, originating in the deep photosphere in a quiet area, may have a sensitivity different from H alpha to the modification of a flare atmosphere. The details of the method used to compute the Stark profile of the higher Balmer line (n is greater than or equal to 6) and their merging were extensively given elsewhere (Donati-Falchi et al., 1985; Falchi et al., 1989). The models used were developed by Ricchiazzi in his thesis (1982) evaluating the chromospheric response to both the nonthermal electron flux, for energy greater than 20 kev, (F sub 20) and to the thermal conduction, (F sub c). The effect of the coronal pressure values (P sub O) at the apex of the flare loop is also included. Author

N90-12478*# National Aeronautics and Space Administration. Goddard Space Flight Center, Greenbelt, MD.

JOULE HEATING AND RUNAWAY ELECTRON ACCELERATION IN A SOLAR FLARE

Gordon D. Holman, Mukul R. Kundu, and Sharad R. Kane (California Univ., Berkeley.) *In its* Max '91 Workshop 2: Developments in Observations and Theory for Solar Cycle 22 1989 p 198-203 (For primary document see N90-12459 03-92)
Avail: NTIS HC A17/MF A03 CSCL 03B

The hard and soft x ray and microwave emissions from a solar flare (May 14, 1980) were analyzed and interpreted in terms of Joule heating and runaway electron acceleration in one or more current sheets. It is found that all three emissions can be generated with sub-Dreicer electric fields. The soft x ray emitting plasma can only be heated by a single current sheet if the resistivity in the sheet is well above the classical, collisional resistivity of 10(exp 7) K, 10(exp 11)/cu cm plasma. If the hard x ray emission is from thermal electrons, anomalous resistivity or densities exceeding 3 x 10(exp 12)/cu cm are required. If the hard x ray emission is from nonthermal electrons, the emissions can be produced with classical resistivity in the current sheets if the heating rate is approximately 4 times greater than that deduced from the soft x ray data (with a density of 10(exp 10)/cu cm in the soft x ray emitting region), if there are at least 10(exp 4) current sheets, and if the plasma properties in the sheets are characteristic of the superhot plasma observed in some flares by Lin et al., and with Hinotori. Most of the released energy goes directly into bulk heating, rather than accelerated particles. Author

N90-12479*# Colorado Univ., Boulder. Dept. of Astrophysical, Planetary, and Atmospheric Sciences.

HEATING AND ACCELERATION OF CORONAL AND CHROMOSPHERIC IONS DURING SOLAR FLARES

M. E. McKean, Robert M. Winglee, and G. A. Dulk *In* NASA, Goddard Space Flight Center, Max '91 Workshop 2: Developments in Observations and Theory for Solar Cycle 22 1989 p 204-218 (For primary document see N90-12459 03-92)
(Grants NAGw-91; NsG-7287; NSF ATM-87-19371)
Avail: NTIS HC A17/MF A03 CSCL 03B

One-dimensional, electrostatic, particle-in-cell simulations are used to explore two mechanisms proposed to explain turbulent broadening of soft x ray emission lines of heavy ions observed during solar flares and the presence of blue-shifted components. Results from the simulations are in qualitative agreement with the observations. Author

N90-12480*# Colorado Univ., Boulder. Dept. of Astrophysical, Planetary, and Atmospheric Sciences.

CHROMOSPHERIC-CORONAL COUPLING DURING SOLAR FLARES: CURRENT SYSTEMS AND PARTICLE ACCELERATION

Robert M. Winglee, M. E. McKean, and G. A. Dulk *In* NASA, Goddard Space Flight Center, Max '91 Workshop 2: Developments in Observations and Theory for Solar Cycle 22 1989 p 219-228 (For primary document see N90-12459 03-92)
(Grants NAGw-91; NAGw-1587; NsG-7287; NSF ATM-87-19371)
Avail: NTIS HC A17/MF A03 CSCL 03B

Two-dimensional (three velocity) electrostatic particle simulations are used to investigate the particle heating and acceleration associated with the impulsive phase of a solar flare. A crossfield current in the high corona (which is presumably driven by reconnection processes) is used to initiate the flare. Due to the differential motion of the electrons and ions, currents, and associated quasi-static electric fields are generated with the primary current and balancing return current being on adjacent field lines. These currents extend from the corona down into the chromosphere. Electrons can be accelerated to energies exceeding 100 keV on short time scales via the quasi-static fields and wave-particle interactions. The spectra of these electrons has a broken power-law distribution which hardens in time. The spatially separate primary and return currents are closed by the cross-field acceleration of the ambient ions into the primary current regions. These ions are then accelerated upwards into the corona by the same quasi-static electric field accelerating the electrons downwards. This acceleration can account for the broadened stationary and weak blue shifted component seen in soft x ray line emissions and enhancements in heavy ion abundances seen in the solar wind in associations with solar flares. Author

N90-12481*# Stanford Univ., CA. Center for Space Science and Astrophysics.

DEVELOPMENT OF A NUMERICAL SOLUTION TO THE TIME DEPENDENT KINETIC EQUATION

Russell J. Hamilton, Edward T. Lu, and Vahe Petrosian *In* NASA, Goddard Space Flight Center, Max '91 Workshop 2: Developments in Observations and Theory for Solar Cycle 22 1989 p 233-232 (For primary document see N90-12459 03-92)
(Grants NsG-7092; NSF ATM-87-05084)
Avail: NTIS HC A17/MF A03 CSCL 03B

A numerical solution was developed for the time dependent Fokker-Planck equation for arbitrary distributions of electrons injected into a magnetized plasma. The code which includes energy loss and pitch angle scattering due to Coulomb collisions and changes in pitch angle due to inhomogeneous magnetic fields was calibrated and tested. The numerical method is versatile so that other scattering or radiation terms can be easily included. Using this code many processes associated with the impulsive phase of solar flares will be investigated. Author

N90-12482*# National Oceanic and Atmospheric Administration, Boulder, CO. Space Environment Lab.

SOME OF THE TERRESTRIAL EFFECTS OF AR 5395

D. Speich *In* NASA, Goddard Space Flight Center, Max '91 Workshop 2: Developments in Observations and Theory for Solar Cycle 22 1989 p 233-241 (For primary document see N90-12459 03-92)
Avail: NTIS HC A17/MF A03 CSCL 03B

Active Region 5395 was extraordinary for both its flare production for a complete disk transit and for one of the largest geomagnetic storms on record. Some of the more dramatic terrestrial effects resulting from the flare activity are briefly discussed. B.G.

N90-12483*# Herzberg Inst. of Astrophysics, Pentiction (British Columbia).

THE 10.7-cm MICROWAVE OBSERVATIONS OF AR 5395 AND RELATED TERRESTRIAL EFFECTS

V. Gaizauskas, T. J. Hughes, and K. F. Tapping *In* NASA, Goddard Space Flight Center, Max '91 Workshop 2: Developments in Observations and Theory for Solar Cycle 22 1989 p 242-245 (For primary document see N90-12459 03-92)
Avail: NTIS HC A17/MF A03 CSCL 03B

The 10.7 cm flux patrols in Canada recorded 4 Great Bursts (peaks greater than 500 sfu) during the disk passage of AR 5395 in March 1989. The Great Bursts of 16 and 17 March were simple events of great amplitude and with half-life durations of only several minutes. Earlier Great Bursts, originating on 6 March towards the NE limb and on 10 March closer to the central meridian, belong to an entirely different category of event. Each started with a very strong impulsive event lasting just minutes. After an initial recovery, however, the emission climbed back to level as greater or greater than the initial impulsive burst. The events of 6 and 10 March stayed above the Great Burst threshold for at least 100 minutes. The second component of long duration in these cases is associated with Type 4 continuum emission and thus very likely with CMEs. Major geomagnetic disturbances did not occur as a result of the massive complex event of 6 March or the two simple but strong events of 16 and 17 March. But some 55 hours after the peak in the long-enduring burst of 10 March, a storm began which qualifies as the fourth strongest geomagnetic storm in Canada since 1932. The vertical component of the earth's field measured during the storm by a fluxgate magnetometer at a station in Manitoba is presented. Within a minute of the sudden commencement of this storm, a series of breakdowns began in the transmission system of Hydro-Quebec which resulted in a total loss of power, on a bitterly cold winter's day, for at least 10 hours. The loss of power provoked an enormous outcry from the public resulting in the power utilities being more receptive to the need to monitor solar as well as geomagnetic activity. Author

N90-12484*# Johns Hopkins Univ., Laurel, MD. Applied Physics Lab.

INTERPLANETARY ENERGETIC PARTICLE OBSERVATIONS OF THE MARCH 1989 EVENTS

E. T. Sarris (Thrace Univ., Xanthe, Greece) and S. M. Krimigis *In* NASA, Goddard Space Flight Center, Max '91 Workshop 2: Developments in Observations and Theory for Solar Cycle 22 1989 p 246-247 (For primary document see N90-12459 03-92)
Avail: NTIS HC A17/MF A03 CSCL 03B

The IMP-8 spacecraft placed in an elongated orbit of approximately R(sub E) x R(sub E) orbit around the Earth was the only monitor of the energetic particle environment of the near interplanetary space during the period of the solar particle events associated with the Active Region 5395 in March 1989. Measurements of energetic ion and electron intensities were obtained in a series of channels within the energy range: 0.3 to 440 MeV for photons, 0.6 to 52 MeV/nuc for alpha particles, 0.7 to 3.3 MeV/nuc for nuclei with Z greater than or equal to 3, 3 to 9 MeV/nuc with Z greater than or equal to 20, and 0.2 to 2.5 MeV for electrons. The responses of selected energy channels during the period 5 to 23 March 1989 are displayed. It is clearly noted that the most prominent energetic ion intensity enhancements in that time interval were associated with the interplanetary shock wave of March 13 (07:42 UT) as well as that of March 8 (17:56 UT), which have distinct particle acceleration signatures. These shock waves play a major role in determining the near Earth energetic ion intensities during the above period by accelerating and modulating the ambient solar energetic particle population, which was already present in high intensities in the interplanetary medium due to the superposition of a series of solar flare particle events originating in AR 5395. The differential ion intensities at the lowest energy channel of the CPME experiment, which were associated with the March 13 shock wave, reached the highest level in the life of the IMP-8 spacecraft at this energy. At high energies, the shock associated intensity peak was smaller by less than a factor of 3 than the maxima of solar flare particle intensities from some other major flares, in particular from those with sites well connected to the Earth's magnetic flux tubes. Author

N90-12485*# National Aeronautics and Space Administration. Goddard Space Flight Center, Greenbelt, MD.

THE SMM UV OBSERVATIONS OF ACTIVE REGION 5395

Stephen A. Drake (ST Systems Corp., Lanham, MD.) and Joseph B. Gurman *In its* Max '91 Workshop 2: Developments in Observations and Theory for Solar Cycle 22 1989 p 248-258 (For primary document see N90-12459 03-92)
Avail: NTIS HC A17/MF A03 CSCL 03B

The Ultraviolet Spectrometer and Polarimeter (UVSP) on the Solar Maximum Mission (SMM) spacecraft was used extensively to study the spatial morphology and time variability of solar active regions in the far UV (at approx. wavelength of 1370 A) since July 1985. The normal spatial resolution of UVSP observations in this 2nd-order mode is 10 sec., and the highest temporal resolution is 64 milliseconds. To make a full-field, 4 min. by 4 min. image this wavelength using 5 sec. raster steps takes about 3 minutes. UVSP can also make observations of the Sun at approx. wavelength of 2790 with 3 sec. spatial resolution when operated in its 1st-order mode; a full-field image at this wavelength (a so-called SNEW image) takes about 8 minutes. UVSP made thousands of observations (mostly in 2nd-order) of AR 5395 during its transit across the visible solar hemisphere (from 7 to 19 March, inclusive). During this period, UVSP's duty cycle for observing AR 5395 was roughly 40 percent, with the remaining 60 percent of the time being fairly evenly divided between aeronomy studies of the Earth's atmosphere and dead time due to Earth occultation of the Sun. UVSP observed many of the flares tagged to AR 5395, including 26 GOES M-level flares and 3 X-level flares, one of which produced so much UV emission that the safety software of UVSP turned off the detector to avoid damage due to saturation. Images and light curves of some of the more spectacular of the AR 5395 events are presented. Author

N90-12486*# National Aeronautics and Space Administration. Goddard Space Flight Center, Greenbelt, MD.

HARD X RAY HIGHLIGHTS OF AR 5395

R. A. Schwartz (ST Systems Corp., Lanham, MD.) and Brian R. Dennis *In its* Max '91 Workshop 2: Developments in Observations and Theory for Solar Cycle 22 1989 p 267-275 (For primary document see N90-12459 03-92)
Avail: NTIS HC A17/MF A03 CSCL 03B

Active Region 5395 produced an exceptional series of hard x ray bursts notable for their frequency, intensity, and impulsivity. Over the two weeks from March 6 to 19, 447 hard x ray flares were observed by the Hard X Ray Burst Spectrometer on Solar Maximum Mission (HXRBS/SMM), a rate of approx. 35 per day which exceeded the previous high by more than 50 percent. During one 5 day stretch, more than 250 flares were detected, also a new high. The three largest GOES X-flares were observed by HXRBS and had hard x ray rates over 100,000 s(exp -1) compared with only ten flares above 100,000(exp -1) during the previous nine years of the mission. An ongoing effort for the HXRBS group has been the correlated analysis of hard x ray data with flare data at other wavelengths with the most recent emphasis on those measurements with spatial information. During a series of bursts from AR 5395 at 1644 to 1648 UT on 12 March 1989, simultaneous observations were made by HXRBS and UVSP (Ultra Violet Spectrometer Polarimeter) on SMM, the two-element Owens Valley Radio Observatory (OVRO) interferometric array, and R. Canfield's H-alpha Echelle spectrograph at the National Solar Observatory at Sacramento Peak. The data show strong correlations in the hard x ray, microwave, and UV lightcurves. This event will be the subject of a combined analysis. Author

N90-12487*# Lockheed Missiles and Space Co., Palo Alto, CA. Research Lab.

INVESTIGATION OF ACTIVE REGIONS AT HIGH RESOLUTION BY BALLOON FLIGHTS OF THE SOLAR OPTICAL UNIVERSAL POLARIMETER (SOUP)

T. Tarbell, Z. Frank, C. Gilbreth, R. Shine, A. Title, K. Topka, and J. Wolfson *In* NASA, Goddard Space Flight Center, Max '91 Workshop 2: Developments in Observations and Theory for Solar Cycle 22 1989 p 310-319 (For primary document see N90-12459 03-92)
(Contracts NAS8-32805; NAS5-26813)
Avail: NTIS HC A17/MF A03 CSCL 03B

SOUP is a versatile, visible-light solar observatory, built for space or balloon flight. It is designed to study magnetic and velocity fields in the solar atmosphere with high spatial resolution and temporal uniformity, which cannot be achieved from the surface of the earth. The SOUP investigation is carried out by the Lockheed Palo Alto Research Laboratory, under contract to NASA's Marshall Space Flight Center. Co-investigators include staff members at a dozen observatories and universities in the U.S. and Europe. The primary objectives of the SOUP experiment are: to measure vector magnetic and velocity fields in the solar atmosphere with much better spatial resolution than can be achieved from the ground; to study the physical processes that store magnetic energy in active regions and the conditions that trigger its release; and to understand how magnetic flux emerges, evolves, combines, and disappears on spatial scales of 400 to 100,000 km. SOUP is designed to study intensity, magnetic, and velocity fields in the photosphere and low chromosphere with 0.5 arcsec resolution, free of atmospheric disturbances. The instrument includes: a 30 cm Cassegrain telescope; an active mirror for image stabilization; broadband film and TV cameras; a birefringent filter, tunable over 5100 to 6600 A with 0.05 A bandpass; a 35 mm film camera and a digital CCD camera behind the filter; and a high-speed digital image processor. Author

N90-12488*# New Mexico Univ., Albuquerque. Dept. of Physics and Astronomy.

THE ONSET OF THE SOLAR ACTIVE CYCLE 22

H. S. Ahluwalia *In* NASA, Goddard Space Flight Center, Max '91 Workshop 2: Developments in Observations and Theory for Solar Cycle 22 1989 p 320-323 (For primary document see

N90-12459 03-92)
(Grant NAGw-1468)
Avail: NTIS HC A17/MF A03 CSCL 03B

There is a great deal of interest in being able to predict the main characteristics of a solar activity cycle (SAC). One would like to know, for instance, how large the amplitude (R sub m) of a cycle is likely to be, i.e., the annual mean of the sunspot numbers at the maximum of SAC. Also, how long a cycle is likely to last, i.e., its period. It would also be interesting to be able to predict the details, like how steep the ascending phase of a cycle is likely to be. Questions like these are of practical importance to NASA in planning the launch schedule for the low altitude, expensive spacecrafts like the Hubble Space Telescope, the Space Station, etc. Also, one has to choose a proper orbit, so that once launched the threat of an atmospheric drag on the spacecraft is properly taken into account. Cosmic ray data seem to indicate that solar activity cycle 22 will surpass SAC 21 in activity. The value of R sub m for SAC 22 may approach that of SAC 19. It would be interesting to see whether this prediction is borne out. Researchers are greatly encouraged to proceed with the development of a comprehensive prediction model which includes information provided by cosmic ray data. Author

N90-12489*# Hawaii Univ., Honolulu. Inst. for Astronomy.
AN IMAGING VECTOR MAGNETOGRAPH FOR THE NEXT SOLAR MAXIMUM Progress Report
D. L. Mickey, B. J. LaBonte, and R. C. Canfield *In* NASA, Goddard Space Flight Center, Max '91 Workshop 2: Developments in Observations and Theory for Solar Cycle 22 1989 p 324-327 (For primary document see N90-12459 03-92)
Avail: NTIS HC A17/MF A03 CSCL 03B

Researchers describe the conceptual design of a new imaging vector magnetograph currently being constructed at the University of Hawaii. The instrument combines a modest solar telescope with a rotating quarter-wave plate, an acousto-optical tunable prefilter as a blocker for a servo-controlled Fabry-Perot etalon, CCD cameras, and on-line digital image processing. Its high spatial resolution (1/2 arcsec pixel size) over a large field of view (5 by 5 arcmin) will be sufficient to significantly measure, for the first time, the magnetic energy dissipated in major solar flares. Its millisecond tunability and wide spectral range (5000 to 7000 A) enable nearly simultaneous vector magnetic field measurements in the gas-pressure-dominated photosphere and magnetically-dominated chromosphere, as well as effective co-alignment with Solar-A's X ray images. Researchers expect to have the instrument in operation at Mees Solar Observatory (Haleakala) in early 1991. They have chosen to use tunable filters as wavelength-selection elements in order to emphasize the spatial relationships between magnetic field elements, and to permit construction of a compact, efficient instrument. This means that spectral information must be obtained from sequences of images, which can cause line profile distortions due to effects of atmospheric seeing. Author

N90-12490*# California Inst. of Tech., Pasadena. Solar Astronomy.
THE OWENS VALLEY SOLAR ARRAY
G. J. Hurford and D. E. Gary *In* NASA, Goddard Space Flight Center, Max '91 Workshop 2: Developments in Observations and Theory for Solar Cycle 22 1989 p 328-337 (For primary document see N90-12459 03-92)
(Grants NAGw-1706; NSF ATM-86-10330; NSF AST-87-02682)
Avail: NTIS HC A17/MF A03 CSCL 03B

Solar microwave emission contains essential information for the study of the coronal magnetic structure of active regions and of thermal and nonthermal flare electrons. To exploit this potential requires BOTH imaging and spectroscopy with sufficient resolution to resolve spatial and spectral features. The VLA provides excellent solar imaging (when in the C and D configurations) but inadequate spectral coverage. The existing Owens Valley system has excellent spectral coverage but imaging that is adequate only for very simple sources. The Owens Valley system is currently undergoing an expansion, which when completed in October 1990 will provide a SOLAR-DEDICATED 5 antenna array (10 baselines). By using frequency-synthesis, this will provide a significant imaging capability in addition to its current spectral coverage. Author

N90-12491*# National Aeronautics and Space Administration. Goddard Space Flight Center, Greenbelt, MD.
A HIGH-SPEED DIGITAL CAMERA SYSTEM FOR THE OBSERVATION OF RAPID H-ALPHA FLUCTUATIONS IN SOLAR FLARES
Alan L. Kiplinger (Colorado Univ., Boulder.), Brian R. Dennis, and Larry E. Orwig *In its* Max '91 Workshop 2: Developments in Observations and Theory for Solar Cycle 22 1989 p 346-348 (For primary document see N90-12459 03-92)
Avail: NTIS HC A17/MF A03 CSCL 03B

Researchers developed a prototype digital camera system for obtaining H-alpha images of solar flares with 0.1 s time resolution. They intend to operate this system in conjunction with SMM's Hard X Ray Burst Spectrometer, with x ray instruments which will be available on the Gamma Ray Observatory and eventually with the Gamma Ray Imaging Device (GRID), and with the High Resolution Gamma-Ray and Hard X Ray Spectrometer (HIREGS) which are being developed for the Max '91 program. The digital camera has recently proven to be successful as a one camera system operating in the blue wing of H-alpha during the first Max '91 campaign. Construction and procurement of a second and possibly a third camera for simultaneous observations at other wavelengths are underway as are analyses of the campaign data. Author

93 SPACE RADIATION

Includes cosmic radiation; and inner and outer earth's radiation belts.

For biological effects of radiation see *52 Aerospace Medicine*. For theory see *73 Nuclear and High-Energy Physics*.

N90-12492*# Chicago Univ., IL. Dept. of Astronomy and Astrophysics.
COSMIC STRINGS AND ULTRA-HIGH ENERGY COSMIC RAYS
Pijushpani Bhattacharjee Sep. 1989 16 p Prepared in cooperation with Fermi National Accelerator Lab., Batavia, IL
(Grant NAGw-1340)
(NASA-CR-185924; NAS 1.26:185924; Fermilab-Pub-89/196-A)
Avail: NTIS HC A03/MF A01 CSCL 03B

The flux is calculated of ultrahigh energy protons due to the process of cusp evaporation from cosmic string loops. For the standard value of the dimensionless cosmic string parameter epsilon is identical to G(sub mu) approx. = 10(exp -6), the flux is several orders of magnitude below the observed cosmic ray flux of ultrahigh energy protons. However, the flux at any energy initially increases as the value of epsilon is decreased. This at first suggests that there may be a lower limit on the value of epsilon, which would imply a lower limit on the temperature of a cosmic string forming phase transition in the early universe. However, the calculation shows that this is not the case -- the particle flux at any energy reaches its highest value at epsilon approx. = 10(exp -15) and it then decreases for further decrease of the value of epsilon. This is due to the fact that for too small values of epsilon (less than 10(exp -15)), the energy loss of the loops through the cusp evaporation process itself (rather than gravitational energy loss of the loops) becomes the dominant factor that controls the behavior of the number density of the loops at the relevant times of emission of the particles. The highest flux at any energy remains at least four orders of magnitude below the observed flux. There is thus no lower limit on epsilon. Author

N90-12493# Air Force Geophysics Lab., Hanscom AFB, MA.
VACUUM ULTRAVIOLET BACKGROUNDS FROM SPACE - TEN YEARS AFTER
R. E. Huffman, J. C. Larrabee, and F. J. LeBlanc (Northwest Research Associates, Inc., Bellevue, WA.) Aug. 1989 11 p

Presented at the 33rd SPIE Symposium, San Diego, CA, 6-11 Aug. 1989
(AF Proj. 4643)
(AD-A211353; AFGL-TR-89-0197) Avail: NTIS HC A02/MF A01 CSCL 17/5

The past ten years has seen progress in the understanding of the ultraviolet background of the earth's atmosphere. These airglow, auroral, and scattering emission sources set limits on the usefulness of UV for space observations. They also, however, enable several types of passive remote sensing; such as, electron density profiles, neutral density and composition, and auroral location and strength. The paper describes our measurements and data analysis in these areas. UV imaging of the aurora has been achieved by four experiments, and these are briefly reviewed. UV imaging has opened up a new way to study solar-terrestrial relationships. GRA

99 GENERAL

N90-12494# Messerschmitt-Boelkow-Blohm G.m.b.H., Munich (Germany, F.R.).
ON THE OCCASION OF THE 100TH BIRTHDAY OF ERNST HEINKEL [ZUM 100. GEBURTSTAG VON ERNST HEINKEL]
H. Dieter Koehler and Hans J. Ebert, ed. 1988 49 p In GERMAN
(MBB/LW/3015/S/PUB/321; ETN-89-94614) Avail: NTIS HC A03/MF A01

On the occasion of the one hundredth birthday of Ernst Heinkel, it's contributions to the German aerospace development and industry, and international aviation are outlined, including the aircrafts He70, He111, He112, He176, He177, He118, He274, He116, He119, He115, He59, He114, He60, He59, He100V8, He280, He280V1. ESA

SUBJECT INDEX

SCIENTIFIC AND TECHNICAL AEROSPACE REPORTS VOLUME 28 NUMBER 3

Typical Subject Index Listing

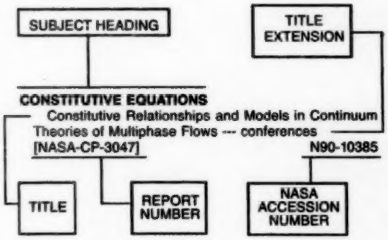

The subject heading is a key to the subject content of the document. Titles, report numbers, and accession numbers of pertinent documents are provided under each subject heading. When the title is insufficiently descriptive of the document content, a title extension has been added, separated from the title by three hyphens. The report number helps to indicate the type of document cited (e.g., NASA report, NASA translation, NASA contractor report). The NASA accession number is the number by which the document abstracts are arranged in this journal and by which the document is sold or requested. The titles, with title extensions if present, are arranged under each subject heading in ascending accession number order. The subject headings have been selected from the latest revision of the *NASA Thesaurus* (NASA SP-7064).

A

A-300 AIRCRAFT
Comparison of the results of tests on A300 aircraft in the RAE 5 metre and ONERA F1 wind tunnels
[RAE-TM-AERO-2130] N90-11768

ABILITIES
Effects of the advanced map interpretation and terrain analysis course on contour-level navigation performance
[AD-A212163] N90-11723

ABSORPTION SPECTRA
A nonlinear-optical method for combining high power laser beams
[AD-A211730] N90-12022

ABSORPTIVITY
A SAW Slanted Array Correlator (SAC) with separate amplitude compensation channel
[AD-D014174] N90-11914

ACCELEROMETERS
In service life monitoring system using g-meter readings and mass configuration control
[ETN-89-95218] N90-12035

ACCESS CONTROL
A security model and its implementation
[RSRE-MEMO-4222] N90-12190

ACCIDENT PREVENTION
UK airmisses involving commercial air transport
[CAA-2/88] N90-11718

ACCUMULATIONS
Time-weighted accumulations ap(tau) and Kp(tau)
[RAE-TR-88050] N90-12422

ACOUSTIC ATTENUATION
A SAW Slanted Array Correlator (SAC) with separate amplitude compensation channel
[AD-D014174] N90-11914

ACOUSTIC EXCITATION
Materials characterization using holographic mapping of transient lamb waves
[AD-A211414] N90-12050

ACOUSTIC INSTABILITY
The physics of double layers and their role in astrophysics
[TRITA-EPP-89-03] N90-12421

ACOUSTIC LEVITATION
Acoustic controlled rotation and orientation
[NASA-CASE-NPO-16995-1-CU] N90-12289

ACOUSTIC PROPAGATION
Transport composite fuselage technology: Impact dynamics and acoustic transmission
[NASA-CR-4035] N90-11821

ACOUSTIC SCATTERING
Numerical solution of acoustic-structure interaction problems
[AD-A211505] N90-12293

ACOUSTIC SIMULATION
Acoustic-thermal environment for USB flap structure. Report 1: Ground simulation test results
[NAL-TM-567] N90-11697

ACOUSTICS
Analysis of two-pass Modified Hough Transform (MHT) technique for the detection of wake like signals
[AD-A211982] N90-11924
NDE (Non-Destructive Evaluation) publications, 1985
[PB89-229025] N90-12036
Computation of generalized modal loads in an acoustic field define by a distribution of correlated pressures
[NASA-CR-186041] N90-12047
Acoustical effects of a large ridge on low-frequency sound propagation in stationary and moving atmospheres
[NASA-CR-186001] N90-12290

ACOUSTO-OPTICS
An imaging vector magnetograph for the next solar maximum N90-12489

ACTIVATION
Mechanism of electrochemical activation of carbon electrodes: Role of graphite lattice defects
[AD-A211644] N90-11845
Synaptic plasticity and memory formation
[AD-A211368] N90-12158

ACTIVE CONTROL
Active control of unsteady and separated flow structures
[AD-A212109] N90-11707
Independent Orbiter Assessment (IOA): Analysis of the active thermal control subsystem
[NASA-CR-185553] N90-11782
Active control of the forced and transient response of a finite beam N90-12040
Effect of control surface mass unbalance on the stability of a closed-loop active control system
[NASA-TP-2952] N90-12042

ACTUATORS
Solid-State Sensor and Actuator
[AD-A211427] N90-11961

ADAPTATION
USSR Space Life Sciences Digest, Issue 22
[NASA-CR-3922(26)-ISSUE-22] N90-12153
USSR Space Life Sciences Digest, Issue 23
[NASA-CR-3922(27)-ISSUE-23] N90-12154
Studies on predicting the resynchronization of the circadian system after transmedian flights
[DFVLR-FB-89-10] N90-12172
A simplified self-adaptive grid method, SAGE
[NASA-TM-102198] N90-12211

ADAPTIVE CONTROL
Adaptive control law design for model uncertainty compensation
[AD-A211712] N90-11758
Adaptive information processing in auditory cortex
[AD-A211294] N90-12166
Adaptive feedback linearization: Stability and robustness
[PB89-219497] N90-12220
A hybrid optimisation strategy for adaptive feed-forward layered networks
[RSRE-MEMO-4193] N90-12226

ADHESION
Fundamental tribological properties of ion-beam-deposited boron nitride films
[NASA-TM-102088] N90-11881

ADHESIVE BONDING
Design of glued joints, elastoplastic adhesives
[DRIC-T-8168] N90-11894

ADIABATIC CONDITIONS
Global distribution of moisture, evaporation-precipitation, and diabatic heating rates
N90-12069

ADJOINTS
Global linear representations of nonlinear systems and the adjoint map
[RR-347] N90-12247

ADSORPTION
Photolysis of spacecraft contaminants
[AD-A211715] N90-11801

ADVECTION
Synoptic/planetary-scale interactions and blocking over the North Atlantic Ocean N90-12061

AEOLIAN TONES
Aeolian processes on Venus N90-12436

AERIAL PHOTOGRAPHY
Ice runways near the South Pole
[AD-A211606] N90-11908

AEROACOUSTICS
Review and analysis of the DNW/Model 360 rotor acoustic data base
[NASA-TM-102253] N90-11692

AERODYNAMIC CHARACTERISTICS
The determination of the aerodynamic characteristics of an ogive-cylinder body in subsonic, curved, incompressible flow, and an assessment of the effect of flow curvature
[REPT-87-13] N90-11712

AERODYNAMIC FORCES
Normal-force-curve and pitching-moment-curve slopes of forebody-cylinder combinations at zero angle of attack for Mach numbers up to 5
[ESDU-89008] N90-11709

AERODYNAMIC STABILITY
Unsteady aerodynamics with applications to flight mechanics
[AD-A211944] N90-11706
Active control of unsteady and separated flow structures
[AD-A212109] N90-11707
Stability and control derivatives of the De Havilland DHC-2 BEAVER aircraft
[PB89-217525] N90-11754
Effect of control surface mass unbalance on the stability of a closed-loop active control system
[NASA-TP-2952] N90-12042

AERODYNAMIC STALLING
Stall/spin/flight simulation
[DOT/FAA/CT-88/28] N90-11765

AERODYNAMICS
Aeronautical engineering: A continuing bibliography with indexes (supplement 243)
[NASA-SP-7037(243)] N90-11693
Aeronautical engineering: A continuing bibliography with indexes (supplement 244)
[NASA-SP-7037(244)] N90-11694
Computer simulation of aircraft aerodynamics
[NASA-TM-102221] N90-11699
Effect of control surface mass unbalance on the stability of a closed-loop active control system
[NASA-TP-2952] N90-12042

AERONAUTICAL ENGINEERING
Aeronautical engineering: A continuing bibliography with indexes (supplement 243)
[NASA-SP-7037(243)] N90-11693
Aeronautical engineering: A continuing bibliography with indexes (supplement 244)
[NASA-SP-7037(244)] N90-11694
AFRAPT (Air Force Research in Aero Propulsion Technology) Trainee Program
[AD-A211540] N90-11744

AEROSOLS
Aerosol in the Pacific troposphere N90-12078
Aerosol backscatter studies supporting LAWS
N90-12079
Global backscatter assessment N90-12080

Measurements of aerosol properties needed to infer backscatter characteristics in support of the NASA Doppler Lidar program N90-12082

Airborne profiles taken near San Nicolas Island, California, during Operation FIRE (First ISCCP (International Satellite Cloud Climatology Project) regional experiment) (1987): Aerosol size distributions, air and surface temperatures, cloud top temperatures, and relative humidities
[AD-A211664] N90-12136

AEROSPACE ENGINEERING

Evolution of flight commands in Aeritalia design
[ETN-89-95211] N90-11759

Choice and characterization of new materials for aerospace applications
[ETN-89-95219] N90-11819

The evolution of light alloys in the aerospace industry
[ETN-89-95216] N90-11872

Requirements for multidisciplinary design of aerospace vehicles on high performance computers
[NASA-CR-181915] N90-12183

On the occasion of the 100th birthday of Ernst Heinkel
[MBB/LW/3015/S/PUB/321] N90-12494

AEROSPACE INDUSTRY

On the occasion of the 100th birthday of Ernst Heinkel
[MBB/LW/3015/S/PUB/321] N90-12494

AEROSPACE MEDICINE

USSR Space Life Sciences Digest, Issue 24
[NASA-CR-3922(28)-ISSUE-24] N90-12152

USSR Space Life Sciences Digest, Issue 22
[NASA-CR-3922(26)-ISSUE-22] N90-12153

USSR Space Life Sciences Digest, Issue 23
[NASA-CR-3922(27)-ISSUE-23] N90-12154

Aerospace medicine and biology: A continuing bibliography with indexes (supplement 329)
[NASA-SP-7011(329)] N90-12173

AEROSPACE SYSTEMS

AFRAPT (Air Force Research in Aero Propulsion Technology) Trainee Program
[AD-A211540] N90-11744

AEROSPACE VEHICLES

Requirements for multidisciplinary design of aerospace vehicles on high performance computers
[NASA-CR-181915] N90-12183

AFTERBURNING

Measurement effects on the calculation of in-flight thrust for an F404 turbofan engine
[NASA-TM-4140] N90-11741

AGE FACTOR

Age-related changes in human posture control: Motor coordination tests
[NASA-CR-185855] N90-12178

AGING (MATERIALS)

Aging of CFRP due to longterm storage in heated air
[ESA-TT-1124] N90-11893

A model for long-term creep and the effects of physical ageing in poly (butylene terephthalate)
[NPL-DMA(A)-182] N90-11895

AH-1G HELICOPTER

Investigation of difficult component effects on finite element model vibration prediction for the Bell AH-1G helicopter. Volume 1: Ground vibration test results
[NASA-CR-181916-VOL-1] N90-12058

AIR

Air breakdown photography in the picosecond domain
[DE89-016775] N90-11830

An empirical formula for gas switch breakdown delay
[DE89-017233] N90-11947

AIR FLOW

Air velocity mapping of environmental test chambers
[AD-A212082] N90-11764

AIR LAND INTERACTIONS

Global tropospheric chemistry: Chemical fluxes in the global atmosphere
[NASA-CR-186090] N90-12109

AIR LOCKS

Independent Orbiter Assessment (IOA): Analysis of the life support and airlock support subsystems
[NASA-CR-185539] N90-11786

AIR POLLUTION

Improved pattern recognition techniques for real time operation
[AD-A211395] N90-11840

Evaluation and sensitivity analyses results of the MESOPUFF 2 model with CAPTEX (Cross-Appalachian Tracer Experiment) measurements
[PB89-198253] N90-12103

Methanol fueled vehicles and photochemical models: An evaluation of the state of knowledge
[PB89-214225] N90-12410

AIR QUALITY

Final environmental impact statement for the Galileo Mission (Tier 2)
[NASA-TM-101825] N90-12102

Review of the national ambient air quality standards for lead: Exposure analysis methodology and validation
[PB89-207914] N90-12104

AIR TRAFFIC CONTROL

A simulation study of landing time allocation procedures for use in computer-assisted air traffic management systems
[AD-A212159] N90-11722

On the generation of a variable structure airport surface traffic control system
[AD-A211306] N90-11724

The 1987 survey of track keeping and altitudes on Heathrow and Gatwick standard instrument departure routes (DAY)
[CAA-PAPER-88010] N90-11729

AIR WATER INTERACTIONS

Investigations of polar air stream cyclogenesis based on numerical simulations with a mesoscale model
[PB89-214563] N90-12132

Equatorial oceanic response to forcing on time scales from days to months
[PB89-206775] N90-12147

On the statistics of El Nino occurrences and the relationship of El Nino to volcanic and solar/geomagnetic activity
[NASA-TP-2948] N90-12456

AIRCRAFT ACCIDENT INVESTIGATION

Post crash flight analysis: Visualizing flight recorder data
[AD-A212063] N90-11715

AIRCRAFT APPROACH SPACING

UK airmisses involving commercial air transport, May-August 1988
[ISSN-0951-6301] N90-11717

AIRCRAFT CONFIGURATIONS

Robust control design for flight control
[AD-A211957] N90-11756

AIRCRAFT CONSTRUCTION MATERIALS

Choice and characterization of new materials for aerospace applications
[ETN-89-95219] N90-11819

A new test procedure for a wing made with carbon fiber composites
[ETN-89-95220] N90-11820

The evolution of light alloys in the aerospace industry
[ETN-89-95216] N90-11872

Aluminium alloy development for aero engines
[PNR90548] N90-11874

AIRCRAFT CONTROL

Robust control design for flight control
[AD-A211957] N90-11756

Evolution of flight commands in Aeritalia design
[ETN-89-95211] N90-11759

AIRCRAFT DESIGN

Wind tunnel test of CAD USB-STOL semi-borne prototype
[NAL-TM-566] N90-11696

Computer simulation of aircraft aerodynamics
[NASA-TM-102221] N90-11699

Development of direct-inverse 3-D methods for applied transonic aerodynamic wing design and analysis
[NASA-CR-186036] N90-11733

A design procedure for the handling qualities optimization of the X-29A aircraft
[NASA-TM-4142] N90-11753

Evolution of flight commands in Aeritalia design
[ETN-89-95211] N90-11759

Stall/spin/flight simulation
[DOT/FAA/CT-88/28] N90-11765

The aerodynamic experimental center of Aeritalia: Combat aircraft group
[ETN-89-95213] N90-11766

Choice and characterization of new materials for aerospace applications
[ETN-89-95219] N90-11819

The evolution of light alloys in the aerospace industry
[ETN-89-95216] N90-11872

General data processing support from project planning to workshop control
[MBB-UD-526/88-PUB] N90-12208

On the occasion of the 100th birthday of Ernst Heinkel
[MBB/LW/3015/S/PUB/321] N90-12494

AIRCRAFT ENGINES

Future military powerplants — fighter aircraft engines
[PNR90554] N90-11749

Aluminium alloy development for aero engines
[PNR90548] N90-11874

AIRCRAFT EQUIPMENT

Numerical simulation of aeroplane response to a lightning injection
[ETN-89-95271] N90-11716

AIRCRAFT HAZARDS

Meeting review: The Second NCAR (National Center for Atmospheric Research) Research Aircraft Fleet Workshop
[PB89-200901] N90-12113

AIRCRAFT INSTRUMENTS

Devices and procedures for the calibration of sensors and measurement: Systems of the flight test support system ATTAS
[DFVLR-MITT-89-06] N90-12007

AIRCRAFT LANDING

A simulation study of landing time allocation procedures for use in computer-assisted air traffic management systems
[AD-A212159] N90-11722

Ice runways near the South Pole
[AD-A211606] N90-11908

AIRCRAFT MAINTENANCE

The RB199: An in-service success
[PNR90544] N90-11746

AIRCRAFT MODELS

Stability and control derivatives of the De Havilland DHC-2 BEAVER aircraft
[PB89-217525] N90-11754

Sequential design of experiments with physically based models 23
[AD-A211918] N90-12239

AIRCRAFT NOISE

Propfan Test Assessment (PTA): Flight test report
[NASA-CR-182278] N90-11738

AIRCRAFT SAFETY

Aircraft cabin fire suppression by means of an interior water spray system
[CAA-PAPER-88014] N90-11719

The 1987 survey of track keeping and altitudes on Heathrow and Gatwick standard instrument departure routes (DAY)
[CAA-PAPER-88010] N90-11729

AIRCRAFT STABILITY

Stability and control derivatives of the De Havilland DHC-2 BEAVER aircraft
[PB89-217525] N90-11754

AIRCRAFT STRUCTURES

Transport composite fuselage technology: Impact dynamics and acoustic transmission
[NASA-CR-4035] N90-11821

AIRCRAFT SURVIVABILITY

In service life monitoring system using g-meter readings and mass configuration control
[ETN-89-95218] N90-12035

AIRFOILS

The structure of separated flow regions occurring near the leading edge of airfoils - including transition
[NASA-CR-185853] N90-11695

AIRFRAMES

Airframe structural dynamic considerations in rotor design optimization
[NASA-TM-101646] N90-12057

Investigation of difficult component effects on finite element model vibration prediction for the Bell AH-1G helicopter. Volume 1: Ground vibration test results
[NASA-CR-181916-VOL-1] N90-12058

AIRGLOW

Investigation of atmospheric emissions in ultraviolet, vacuum ultraviolet, and extreme ultraviolet wavelength
[AD-A212169] N90-12123

Comparison of the LOWTRAN 7 code and S3-4 satellite measurements of UV radiance
[AD-A211356] N90-12124

Spatial characteristics of airglow and solar scatter radiance from the earth's atmosphere
[AD-A211358] N90-12126

AIRPORTS

A simulation study of landing time allocation procedures for use in computer-assisted air traffic management systems
[AD-A212159] N90-11722

ALANINE

Boron analogues of amino acids and derivatives
[AD-A211311] N90-12157

ALASKA

HIPAS 1987-88: ULF research and campaign support
[AD-A211720] N90-11933

ALGEBRA

The realization of input-output maps using bialgebras
[NASA-CR-185362] N90-12228

Some notes on perturbations of differential-algebraic equations
[PB89-218564] N90-12243

Augmentations of grammatical categories in distributional-algebraic models of natural languages
[REPT-89-24] N90-12262

Some techniques for anaphora resolution in algebraic linguistics
[REPT-89-28] N90-12265

Two dimensional conformal supergravity and critical behavior
[DE89-611968] N90-12414

ALGORITHMS

The upwind control volume scheme for unstructured triangular grids
[NASA-TM-101664] N90-11703
On the generation of a variable structure airport surface traffic control system
[AD-A211306] N90-11724
Vision-based navigation for autonomous ground vehicles
[AD-A211584] N90-11725
Resistive block methods for electrostatic field solutions with internal elements
[DE89-017535] N90-11920
Nearly optimal algorithms and bounds for multilayer channel routing
[AD-A211913] N90-11955
Redundancies and don't cares in sequential logic synthesis
[AD-A211931] N90-11956
A design methodology for self-tuning control of systems with inherent conflicts
[PB89-219505] N90-11960
Viscous split algorithms for the time dependent incompressible Navier-Stokes equations
[AD-A211592] N90-11985
Efficient finite element solution of Navier-Stokes equations and related topics
[AD-A211647] N90-11986
Some new algorithms for boundary value problems in smooth particle hydrodynamics
[AD-A211728] N90-11987
A multigrid algorithm for the incompressible Navier-Stokes equation
[GMD-374] N90-11993
Error estimation and self-adaptive mesh refinement for boundary element method N90-12037
Aerosol backscatter studies supporting LAWS N90-12079
LAWS simulation: Sampling strategies and wind computation algorithms N90-12081
Processing of DMSP magnetic data and its use in geomagnetic field modeling
[NASA-TM-100750] N90-12115
The use of Lanczos's method to solve the large generalized symmetric definite eigenvalue problem
[NASA-CR-181914] N90-12193
Tools to aid in the development high-performance algorithms
[DE89-012395] N90-12194
An approximate max-flow min-cut theorem for uniform multicommodity flow problems with applications to approximation algorithms
[AD-A211908] N90-12198
Parallel graph contraction
[AD-A211916] N90-12199
Scheduling sporadic and aperiodic events in a hard real-time system
[AD-A211344] N90-12205
Parallel architectures and parallel algorithms for integrated vision systems
[NASA-CR-185990] N90-12215
Can perceptrons find Lyapunov functions: An algorithmic approach to systems stability
[RR-365] N90-12224
Fast forward dynamics algorithm for robot arms using multiprocessing
[RR-367] N90-12225
Numerical experience with a class of algorithms for nonlinear optimization using inexact function and gradient information
[NASA-CR-181927] N90-12232
Dynamic embedding of trees in hypercubes with constant dilation and load
[AD-A211884] N90-12236
Fast computation using faulty hypercubes
[AD-A211910] N90-12238
Sequential design of experiments with physically based models 23
[AD-A211918] N90-12239
On the communication complexity of solving a polynomial equation
[AD-A211945] N90-12240
A matrix factorization and its application to large-scale linear programming
[AD-A211293] N90-12244
Orthogonal least squares methods and their application to nonlinear system identification
[RR-343] N90-12259
Temporal and spatial filtering remedies for dispersion in electromagnetic particle codes
[DE89-017534] N90-12337

Problem of incomplete information in relational databases
[PB89-217533] N90-12393

ALIGNMENT

Periodic permanent magnet structures
[AD-D014173] N90-12280
Use of the NPL linac for x ray dosimetry --- linear accelerator (linac)
[NPL-RSA(EXT)-6] N90-12314

ALKALI METALS

Neutron scattering studies of premartensitic phenomena
[DE90-000025] N90-11863

ALLOCATIONS

A simulation study of landing time allocation procedures for use in computer-assisted air traffic management systems
[AD-A212159] N90-11722

ALLOYS

Formation and modification of surface alloys by excimer laser melting and resolidification
[DE89-016968] N90-11856
Electronic structure of transition metal alloys and intermetallics: Charge transfer and its implications for Moessbauer effect measurements
[DE89-017603] N90-11860
Kinetic processes in advanced alloys
[AD-A212049] N90-11867
Current research in advanced materials
[DE89-017466] N90-11884

ALPHA PARTICLES

Theoretical plasma physics
[DE90-000009] N90-12341

ALTITUDE SIMULATION

Contrasting landform perception with varied radar illumination geometries and at simulated resolutions of Venera and Magellan N90-12430

ALUMINIDES

Weldability of ductile nickel aluminides
[DE89-017452] N90-11859
Low temperature formation of titanium aluminide films using physical vapor deposition
[AD-A211877] N90-11866

ALUMINUM

Investigations into the infiltration kinetics, wettability, and interfacial bond strength of Al/SiC composites
[AD-A211924] N90-11815
Deformation behavior of SiC/2014 Al metal-matrix composite
[AD-A212095] N90-11816

ALUMINUM ALLOYS

Effects of a heat cycle on material strength
[NAL-TM-562] N90-11737
Elevated temperature aluminum-titanium alloy by powder metallurgy process
[AD-D014165] N90-11852
A study of the hot workability of Al-8.5 wt pct Mg alloys for armor plate applications
[AD-A211680] N90-11868
Effect of fretting on fatigue strength of aluminium alloys
[ESDU-89004] N90-11870
Aluminium alloy development for aero engines
[PNR90548] N90-11874
Axial compression buckling test on the H-2 launch vehicle satellite fairing structural element prototype (aluminum surface plate/aluminum honeycomb sandwiched curved surface plate)
[NAL-TM-563] N90-12039

ALUMINUM OXIDES

Processing and characterization of alumina platelet-reinforced mullite composites
[DE90-000057] N90-11814
Significance of oxide skins on powder for the quality of PM Al material — PM (press molded)
[DFVLR-FB-89-11] N90-11873
Flexure strength of advanced ceramics: A round robin exercise
[AD-A212101] N90-11889

AMINO ACIDS

Boron analogues of amino acids and derivatives
[AD-A211311] N90-12157

AMPLIFICATION

Base level management of radio frequency radiation protection program
[AD-A211787] N90-12171

AMPLITUDES

Bordered surfaces, off-shell amplitudes, sewing, and string field theory
[DE90-000006] N90-12378

ANALYSIS OF VARIANCE

Application of dimensional analysis to statistical process modeling
[AD-A211881] N90-11905

ANGLE OF ATTACK

Normal-force-curve and pitching-moment-curve slopes of forebody-cylinder combinations at zero angle of attack for Mach numbers up to 5
[ESDU-89008] N90-11709
Flutter clearance of the F-18 high-angle-of-attack research vehicle with experimental wingtip instrumentation pods
[NASA-TM-4148] N90-11732

ANISOTROPY

International seminar on the inelastic behavior of solids: Models and utilization
[DE89-017420] N90-11858
Anisotropy and microstructure of high-coercivity rare earth permanent magnets
[AD-A211905] N90-12285

ANNEALING

On-orbit annealing of gallium arsenide solar cell arrays
[AD-A212087] N90-11900
Effect of annealing conditions on the structural and superconducting properties of Y-Ba-Cu-O films
[AD-A211308] N90-12371

ANODES

Plasma-anode electron gun research
[AD-A211547] N90-11773

ANOXIA

Synergistic effects of nitrogen dioxide and carbon dioxide following acute inhalation exposures in rats
[PB89-214779] N90-12150

ANTARCTIC REGIONS

Improving snow roads and airstrips in Antarctica
[AD-A211588] N90-11907
Ice runways near the South Pole
[AD-A211606] N90-11908

ANTENNA ARRAYS

Proceedings of the 1988 Antenna Applications Symposium, volume 1
[AD-A211396] N90-11928
Theory and simulation of the operation of a Doppler direction finder in a multipath environment
[FEL-1988-56] N90-11939
The Owens Valley solar array N90-12490

ANTENNA COMPONENTS

Dielectric covered microstrip patch antennas
[AD-A211577] N90-11963

ANTENNA DESIGN

Recent advances to NEC (Numerical Electromagnetics Code): Applications and validation
[DE89-009231] N90-11917
Dielectric covered microstrip patch antennas
[AD-A211577] N90-11963

ANTICYCLONES

Synoptic/planetary-scale interactions and blocking over the North Atlantic Ocean N90-12061

ANTINEUTRINOS

Experimental test of PCAC hypothesis in the reactions mu neutrino-proton giving muon(-)-proton-pion(+) and mu antineutrino-proton giving muon(+)-proton-pion(-) in the delta (1232) region — partial conserved axial current
[MPE-PAE/EXP.EL.199] N90-12309

ANTIREFLECTION COATINGS

Vanadium dioxide protective devices
[AD-A212018] N90-11887

APPLICATIONS PROGRAMS (COMPUTERS)

NRL/VOA modifications to IONCAP as of 12 July 1988
[AD-A211546] N90-11929
Description of a software library for the calculation of surface fluxes
[KNMI-TR-112] N90-12141
A language for assembly instructions
[REPT-88-90] N90-12209

APPROACH

Simulations for computer centerline approach
[DOT/FAA/CT-TN89/41] N90-11726

APPROPRIATIONS

Federal funds for research and development: Fiscal years 1986, 1987, and 1988. Volume 36: Detailed statistical tables
[PB89-223523] N90-12407
Federal funds for research and development. Fiscal years 1987, 1988, and 1989. Volume 37: Detailed statistical tables
[PB89-223531] N90-12408

APPROXIMATION

An approximate max-flow min-cut theorem for uniform multicommodity flow problems with applications to approximation algorithms
[AD-A211908] N90-12198
Convergence results for pseudospectral approximations of hyperbolic systems by a penalty type boundary treatment
[NASA-CR-181929] N90-12230
Rational expansion for nonlinear input-output maps
[RR-348] N90-12248

Non-stationary computer model of the asymptotic region of an electric arc gas heater
[IPPCZ-288] N90-12330

ARCHITECTURE
Designing and designing knowledge in engineering and architecture
[PB89-219521] N90-12383

ARCHITECTURE (COMPUTERS)
Spacelab system analysis Marshall Avionics System Testbed (MAST)
[NASA-CR-183804] N90-11802
A distributed pipelined architecture of the recursive Lagrangian equations of motion for robot manipulators with VLSI implementation — VLSI (very large scale integration)
[RR-353] N90-11966
Optical arithmetic logic using the modified signed-digit redundant number representation
[AD-D014176] N90-12186
On the design and implementation of a secure computer system
[RSRE-MEMO-4186] N90-12189
Software package for 3-dimensional graphic display unit
[NAL-TM-559] N90-12191
ISI's (Information Sciences Institute) SDI architecture simulator: An experiment in adding new software to the system
[AD-A211314] N90-12204
Parallel architectures and parallel algorithms for integrated vision systems
[NASA-CR-185990] N90-12215
Distributed VLSI architecture for fast Jacobian and inverse Jacobian formulations
[RR-346] N90-12218
Robot inverse dynamics computation via VLSI distributed architectures
[RR-350] N90-12223
Ground-state coding in partially connected neural networks
[NASA-TM-102239] N90-12227
Distributed knowledge-based systems
[AD-A211984] N90-12401

AREA NAVIGATION
Simulations for computer centerline approach
[DOT/FAA/CT-TN89/41] N90-11726

ARGON
Spin-orbit relaxation rates of Bi(6p(3)) 2D(3/2) following photolysis of Bi(CH3)3 at lambda = 193 nm
[AD-A211792] N90-12303

ARIZONA
Disturbances in the Arizona Monsoon N90-12071

ARMED FORCES (UNITED STATES)
Twenty-five years of service, 1962-1987: Proceedings of the Air Force Studies Board Symposium on Air Force Research and Development, November 16, 1987
[PB89-198915] N90-12384

ARMOR
A study of the hot workability of Al-8.5 wt pct Mg alloys for armor plate applications
[AD-A211680] N90-11868

ARRAYS
On-orbit annealing of gallium arsenide solar cell arrays
[AD-A212087] N90-11900
A SAW Slanted Array Correlator (SAC) with separate amplitude compensation channel
[AD-D014174] N90-11914
Infrared detector array
[AD-D014170] N90-11997
Sequential searching in multidimensional monotone arrays
[AD-A211938] N90-12188

ARSENIDES
Energy relaxation of light holes in InAs(.15)Sb(.85)/InSb multiple quantum wells
[DE89-016035] N90-12349

ARTIFICIAL INTELLIGENCE
Three dimensional object recognition employing combined visual and tactile sensing
[PB89-219489] N90-12176
Navigation of robotic systems
[DE89-017507] N90-12219
Taxonomic syntax for first order inference
[AD-A211618] N90-12221
DOD Gateway Information System (DGIS) common command language: A retrospective on the introduction of prolog as the development tool
[AD-A211941] N90-12400

ARTIFICIAL SATELLITES
On-orbit annealing of gallium arsenide solar cell arrays
[AD-A212087] N90-11900

ASSEMBLING
Computer-aided design of flexible assembly systems
[PB89-216253] N90-12025

ASSESSMENTS
A critical assessment of thermodynamic and phase diagram data for the Ga-In system
[NPL-DMA(A)-174] N90-12382

ASSOCIATIVE PROCESSING (COMPUTERS)
Optical computing based on the Hopfield model for neural networks
[AD-A211824] N90-12216

ASTRONOMICAL MODELS
Theory and modeling group N90-12462

ASTROPHYSICS
Detailed photonuclear cross-section calculations and astrophysical applications
[DE89-017531] N90-12419

ASYMPTOTES
Asymptotic bias of autoregressive estimators
[IMAG-RR-745-M] N90-12255

ASYMPTOTIC METHODS
Hopf bifurcation in the driven cavity
[NASA-TM-102334] N90-11969
A study of the asymptotic behavior of linear difference equations with polynomial coefficients
[IMAG-RR-743-M] N90-12254

ASYMPTOTIC PROPERTIES
Likelihood cross-validation bandwidth selection for nonparametric kernel density estimators
[REPT-89-10] N90-12279

ASYMPTOTIC SERIES
Small sample theory for steady state confidence intervals
[AD-A212097] N90-12242

ATLANTIC OCEAN
Synoptic/planetary-scale interactions and blocking over the North Atlantic Ocean N90-12061
Dynamics of the equatorial undercurrent and its termination
[PB89-198147] N90-12146

ATMOSPHERIC BOUNDARY LAYER
Airborne profiles taken near San Nicolas Island, California, during Operation FIRE (First ISCCP (International Satellite Cloud Climatology Project) regional experiment) (1987): Aerosol size distributions, air and surface temperatures, cloud top temperatures, and relative humidities
[AD-A211664] N90-12136
Description of a software library for the calculation of surface fluxes
[KNMI-TR-112] N90-12141

ATMOSPHERIC CHEMISTRY
Global tropospheric chemistry: Chemical fluexes in the global atmosphere
[NASA-CR-186090] N90-12109
LABCEDE fluorescence investigations
[AD-A210678] N90-12114

ATMOSPHERIC CIRCULATION
Stratiform clouds and their interaction with atmospheric motions N90-12060
Studies of baroclinic instability in the presence of surface topography and stratospheric ozone N90-12068
Use of satellite data and modeling to asses the influence of stratospheric processes on the troposphere
N90-12075
Laboratory and theoretical models of planetary-scale instabilities and waves N90-12076
Development of high resolution simulations of the atmospheric environment using the MASS model
[NASA-CR-186040] N90-12133

ATMOSPHERIC COMPOSITION
Progress of research on water vapor lidar
[NASA-CR-185970] N90-12011
Studies of baroclinic instability in the presence of surface topography and stratospheric ozone N90-12068
Aerosol in the Pacific troposphere N90-12078
Ozone depletion, greenhouse gases, and climate change
[NASA-CR-185323] N90-12101
A statistical intercomparison of temperature and precipitation predicted by four general circulation models with historical data
[DE89-017785] N90-12108

ATMOSPHERIC EFFECTS
Deducing the age of the dense Venus atmosphere
N90-12438

ATMOSPHERIC ENTRY
Project AENEAS: A feasibility study for crew emergency return vehicle
[PB89-217020] N90-11799

ATMOSPHERIC GENERAL CIRCULATION MODELS
NASA/MSFC FY88 Global Scale Atmospheric Processes Research Program Review
[NASA-TM-100357] N90-12059
Stratiform clouds and their interaction with atmospheric motions N90-12060
Application of dynamical systems theory to global weather phenomena revealed by satellite imagery
N90-12063
Variational objective analysis for cyclone studies
N90-12064
Dynamics and energetics of the South Pacific Convergence Zone during FGGE SOP-1 and South Pacific Convergence Zone and global-scale N90-12065
Low level remote sensing: Orographic winds
N90-12066
Global backscatter assessment N90-12080
Measurements of aerosol properties needed to infer backscatter characteristics in support of the NASA Doppler Lidar program N90-12082
Global environmental effects of impact-generated aerosols: Results from a general circulation model
[DE89-008033] N90-12106
A statistical intercomparison of temperature and precipitation predicted by four general circulation models with historical data
[DE89-017785] N90-12108

ATMOSPHERIC HEAT BUDGET
Crau 1987: The KNMI contribution — KNMI (Royal Netherlands Meteorological Institute)
[KNMI-TR-110] N90-12140

ATMOSPHERIC HEATING
Global distribution of moisture, evaporation-precipitation, and diabatic heating rates
N90-12069

ATMOSPHERIC MODELS
Comparison of the LOWTRAN 7 code and S3-4 satellite measurements of UV radiance
[AD-A211356] N90-12124
Spatial characteristics of airglow and solar scatter radiance from the earth's atmosphere
[AD-A211358] N90-12126
TEC (Total Electron Content) models
[AD-A211553] N90-12129
Investigations of polar air stream cyclogenesis based on numerical simulations with a mesoscale model
[PB89-214563] N90-12132
Development of high resolution simulations of the atmospheric environment using the MASS model
[NASA-CR-186040] N90-12133
Airborne profiles taken near San Nicolas Island, California, during Operation FIRE (First ISCCP (International Satellite Cloud Climatology Project) regional experiment) (1987): Aerosol size distributions, air and surface temperatures, cloud top temperatures, and relative humidities
[AD-A211664] N90-12136
Deducing the age of the dense Venus atmosphere
N90-12438

ATMOSPHERIC MOISTURE
Global atmospheric moisture variability N90-12062
Variational objective analysis for cyclone studies
N90-12064
Low level remote sensing: Orographic winds
N90-12066
Global distribution of moisture, evaporation-precipitation, and diabatic heating rates
N90-12069
Tropical Pacific moisture variability N90-12070

ATMOSPHERIC PHYSICS
Middle Atmosphere Program. Handbook for MAP, volume 28
[NASA-CR-184972] N90-12117
Comparison of the LOWTRAN 7 code and S3-4 satellite measurements of UV radiance
[AD-A211356] N90-12124

ATMOSPHERIC SCATTERING
Propagation of an elliptical laser beam through the turbulent atmosphere (vertical beams)
[PB89-208680] N90-12010

ATMOSPHERIC SOUNDING
Laser sounding from space: Report of the ESA Technology Working Group on Space Laser Sounding and Ranging
[ESA-SP-1108] N90-12024
LAWS simulation: Sampling strategies and wind computation algorithms N90-12081
Middle Atmosphere Program. Handbook for MAP, volume 28
[NASA-CR-184972] N90-12117

ATMOSPHERIC TEMPERATURE
Ozone depletion, greenhouse gases, and climate change
[NASA-CR-185323] N90-12101
A statistical intercomparison of temperature and precipitation predicted by four general circulation models with historical data
[DE89-017785] N90-12108
Retrieval of atomic oxygen and temperature in the thermosphere. Part 2: Feasibility of an experiment based on limb emission in the OI lines
[AD-A211807] N90-12121

ATMOSPHERIC TURBULENCE
Some implications of the isotropic momentarily frozen assumptions for the SPAN-MAT program
[NASA-CR-181937] N90-11704
Propagation of an elliptical laser beam through the turbulent atmosphere (vertical beams)
[PB89-208680] N90-12010
Turbulence effects on reflected optical patterns (atmosphere and structure)
[PB89-208094] N90-12315

ATOMIC ENERGY LEVELS
Laser production of soft x rays by multiquantum processes and the excitation of atomic inner-shell states
[AD-A211372] N90-12021
Spin-orbit relaxation rates of Bi(6p(3)) 2D(3/2) following photolysis of Bi(CH3)3 at lambda = 193 nm
[AD-A211792] N90-12303

ATOMIC PHYSICS
Atomic and molecular surface and volume processes in the analysis of negative hydrogen discharges
[DE89-015705] N90-12294
Gordon Conference on Atomic Physics
[AD-A211946] N90-12304

ATOMIC STRUCTURE
Electronic structure of transition metal alloys and intermetallics: Charge transfer and its implications for Moessbauer effect measurements
[DE89-017603] N90-11860

ATOMIZERS
Calculation on film preparation and film motion of a swirl atomizer
[ESA-TT-1096] N90-11990

ATTITUDE CONTROL
Low-speed wind-tunnel study of reaction control-jet effectiveness for hover and transition of a STOVL fighter concept
[NASA-TM-4147] N90-11751

AUDITORY PERCEPTION
Binaural masking: An analysis of models
[AD-A211578] N90-12168

AUDITORY SIGNALS
Binaural masking: An analysis of models
[AD-A211578] N90-12168

AUGER SPECTROSCOPY
Quantitative interpretation of auger lineshapes and electron/photon stimulated desorption
[AD-A211550] N90-11842

AURORAS
LABCEDE fluorescence investigations
[AD-A210678] N90-12114
Distribution of auroral precipitation at midnight during a magnetic storm
[PB89-213136] N90-12118
UV ionospheric remote sensing with the polar BEAR satellite
[AD-A211359] N90-12127
Vacuum ultraviolet backgrounds from space - ten years after
[AD-A211353] N90-12493

AUSTENITIC STAINLESS STEELS
The effects of temperature on fatigue crack propagation in 310 austenitic stainless steel
[DE90-000136] N90-11865

AUTOMATIC CONTROL
Kinematic design NC optical generator N90-12316

AUTOMATIC PILOTS
Pilotless airplanes
[AD-A211719] N90-11734
Independent Orbiter Assessment (IOA): FMEA/CIL assessment
[NASA-CR-185550] N90-11783

AUTONOMOUS NAVIGATION
Vision-based navigation for autonomous ground vehicles
[AD-A211584] N90-11725

AUTONOMY
Vision-based navigation for autonomous ground vehicles
[AD-A211584] N90-11725

AUTOREGRESSIVE PROCESSES
Adaptive noise cancellation for a class of nonlinear 2R filter
[RR-351] N90-11965
Asymptotic bias of autoregressive estimators
[IMAG-RR-745-M] N90-12255

AVALANCHE DIODES
Thermal model for double-drift IMPATT diodes on diamond heat sinks
[AD-A211746] N90-12380

AVIONICS
Spacelab system analysis Marshall Avionics System Testbed (MAST)
[NASA-CR-183804] N90-11802

AXIAL FLOW PUMPS
An investigation of end-wall vortex cavitation in a high Reynolds number axial-flow pump
[AD-A211426] N90-11982

AXISYMMETRIC FLOW
Three component laser Doppler measurements in an axisymmetric jet
[NASA-CR-181908] N90-11702

B

BACKGROUND NOISE
Binaural masking: An analysis of models
[AD-A211578] N90-12168

BACKGROUND RADIATION
Spatial characteristics of airglow and solar scatter radiance from the earth's atmosphere
[AD-A211358] N90-12126

BACKSCATTERING
Aerosol backscatter studies supporting LAWS
N90-12079
Global backscatter assessment N90-12080
Measurements of aerosol properties needed to infer backscatter characteristics in support of the NASA Doppler Lidar program N90-12082
Infrared backscattering N90-12083
Doppler statistics of ocean velocity variability
[AD-A211687] N90-12148

BACTERIA
Genetic engineering of enhanced microbial nitrification
[PB89-208334] N90-12155

BALANCE
Effect of control surface mass unbalance on the stability of a closed-loop active control system
[NASA-TP-2952] N90-12042

BALLISTIC MISSILE DECOYS
Comparison of laser and neutral particle beam discrimination
[DE89-017786] N90-12018

BALLOON-BORNE INSTRUMENTS
Design of scientific payloads and components
[AD-A211819] N90-12005
Solar flare gamma-ray and hard x ray imaging with the GRID-on-a-balloon N90-12474

BALMER SERIES
Flare model sensitivity of the Balmer spectrum
N90-12477

BANDWIDTH
Likelihood cross-validation bandwidth selection for nonparametric kernel density estimators
[REPT-89-10] N90-12279

BARIUM
Atomic and molecular surface and volume processes in the analysis of negative hydrogen discharges
[DE89-015705] N90-12294

BAROCLINIC INSTABILITY
Dynamics and energetics of the South Pacific Convergence Zone during FGGE SOP-1 and South Pacific Convergence Zone and global-scale N90-12065
Studies of baroclinic instability in the presence of surface topography and stratospheric ozone N90-12068
Laboratory and theoretical studies of baroclinic processes N90-12077

BAROCLINIC WAVES
Dynamics of baroclinic wave systems N90-12072

BAROCLINITY
Global atmospheric moisture variability N90-12062

BAROTROPIC FLOW
Laboratory and theoretical studies of baroclinic processes N90-12077

BARRIERS
The rodent research animal holding facility as a barrier to environmental contamination
[NASA-TM-102237] N90-12151

BARS
Deformation of Ti-6Al-4V bar and extrusion under superplastic forming conditions
[RAE-TM-MAT/STR-1110] N90-11875

BAYES THEOREM
On finding the largest normal mean and estimating the selected mean
[AD-A211628] N90-12245
Empirical Bayes estimation of binomial parameter with symmetric priors
[AD-A211646] N90-12246
On the asymptotic optimality of certain empirical Bayes simultaneous testing procedures
[AD-A211649] N90-12270

BEAM SWITCHING
Cryogenic Schottky-mixer receiver front-end for 40-50 GHz
[PB89-221667] N90-11959

BEAMS (RADIATION)
Microwave instability near transition energy
[DE90-000107] N90-11922
Propagation of an elliptical laser beam through the turbulent atmosphere (vertical beams)
[PB89-208680] N90-12010
Turbulence effects on reflected optical patterns (atmosphere and structure)
[PB89-208094] N90-12315

BEAMS (SUPPORTS)
Active control of the forced and transient response of a finite beam N90-12040
Computation of generalized modal loads in an acoustic field define by a distribution of correlated pressures
[NASA-CR-186041] N90-12047

BEDROCK
Volcanism on Venus: Large shields and major accumulations of small domes N90-12445

BEND TESTS
Small-radius bending loss in single-mode fibers
[AD-A211822] N90-12323

BENDING
Small-radius bending loss in single-mode fibers
[AD-A211822] N90-12323

BENZENE
Calculation of the refractive index change in dissociating shocked benzene
[DE89-017737] N90-11833

BERYLLIUM
A rate-dependent constitutive model for Be
[DE89-017755] N90-11861

BETA PARTICLES
An experimental high energy physics program
[DE89-014695] N90-12311

BIAS
Asymptotic bias of autoregressive estimators
[IMAG-RR-745-M] N90-12255

BIBLIOGRAPHIES
Aeronautical engineering: A continuing bibliography with indexes (supplement 243)
[NASA-SP-7037(243)] N90-11693
Aeronautical engineering: A continuing bibliography with indexes (supplement 244)
[NASA-SP-7037(244)] N90-11694
NDE (Non-Destructive Evaluation) publications, 1985
[PB89-229025] N90-12036
Earth resources: A continuing bibliography with indexes (issue 63)
[NASA-SP-7041(63)] N90-12091
Aerospace medicine and biology: A continuing bibliography with indexes (supplement 329)
[NASA-SP-7011(329)] N90-12173
Working with people to improve productivity and quality: A bibliography with indexes, 1984-1988
[NASA-SP-7078] N90-12385
Center for Electronics and Electrical Engineering technical publication announcements covering Center programs, January-March 1989 with 1989 CEEE events calendar
[PB89-228308] N90-12402

BINARY DATA
FORTRAN program for x ray photoelectron spectroscopy data reformatting
[NASA-TP-2957] N90-12348

BINAURAL HEARING
Binaural masking: An analysis of models
[AD-A211578] N90-12168

BINOMIALS
Empirical Bayes estimation of binomial parameter with symmetric priors
[AD-A211646] N90-12246

BIOASTRONAUTICS
Aerospace medicine and biology: A continuing bibliography with indexes (supplement 329)
[NASA-SP-7011(329)] N90-12173

BIOCHEMISTRY
Synaptic plasticity and memory formation
[AD-A211368] N90-12158
Cellular and molecular mechanisms of high pressure inotropy in cardiac muscle
[AD-A211695] N90-12170

BIODEGRADATION
Synaptic plasticity and memory formation
[AD-A211368] N90-12158

BIOFEEDBACK
Computer generation of a tutorial dialogue
[AD-A211976] N90-12162

BIOGEOCHEMISTRY
Global tropospheric chemistry: Chemical fluexes in the global atmosphere
[NASA-CR-186090] N90-12109

BIOGRAPHY
Space flight (selected articles)
[AD-A212068] N90-11769

BIOLOGICAL EFFECTS
Aerospace medicine and biology: A continuing bibliography with indexes (supplement 329)
[NASA-SP-7011(329)] N90-12173

BIOSYNTHESIS
Membrane fusion: The role of polyphosphatidylinositol
[AD-A211269] N90-12156
BISMUTH
Spin-orbit relaxation rates of Bi(6p(3)) 2D(3/2) following photolysis of Bi(CH3)3 at lambda = 193 nm
[AD-A211792] N90-12303
BIVARIATE ANALYSIS
Operational measures of central tendency
[DE89-016959] N90-12234
BLACK HOLES (ASTRONOMY)
Scalar fields versus black holes
[DE89-611967] N90-12413
BLADE TIPS
Acoustical effects of a large ridge on low-frequency sound propagation in stationary and moving atmospheres
[NASA-CR-186001] N90-12290
BLADE-VORTEX INTERACTION
Review and analysis of the DNW/Model 360 rotor acoustic data base
[NASA-TM-102253] N90-11692
BLASIUS FLOW
Absolute determination of the wall shear stress by means of an interferometer
[DFVLR-FB-89-13] N90-11991
BODIES OF REVOLUTION
Incompressible flow about ellipsoids of revolution
[REPT-88-02] N90-11713
BODY FLUIDS
USSR Space Life Sciences Digest, Issue 22
[NASA-CR-3922(26)-ISSUE-22] N90-12153
BODY TEMPERATURE
Human body regional convective heat transfer determination using sublimating naphthalene disks
[AD-A212170] N90-12165
BOILERS
Independent Orbiter Assessment (IOA): Assessment of the hydraulics/water spray boiler subsystem
[NASA-CR-185537] N90-11792
BONDING
Apparatus and method for monitoring pressure leaks from a sealed system
[AD-D014168] N90-11995
Field-assisted bonding of single crystal quartz
[DE89-015407] N90-12353
BORIDES
Collective-mode spectroscopy of textures in superfluid (3)He-B
[PB89-221634] N90-12370
BORN APPROXIMATION
Clutter models for subsurface electromagnetic applications
[PB89-229678] N90-11925
BORON
Boron analogues of amino acids and derivatives
[AD-A211311] N90-12157
BORON NITRIDES
Static tensile and tensile creep testing of four boron nitride coated ceramic fibers at elevated temperatures
[NASA-CR-184999] N90-11807
Fundamental tribological properties of ion-beam-deposited boron nitride films
[NASA-TM-102088] N90-11881
BOUNDARY ELEMENT METHOD
Error estimation and self-adaptive mesh refinement for boundary element method N90-12037
BOUNDARY LAYER CONTROL
Active control of unsteady and separated flow structures
[AD-A212109] N90-11707
BOUNDARY LAYER EQUATIONS
Numerical computation of the viscous flow field around a prolate spheroid
[DFVLR-FB-89-22] N90-11992
BOUNDARY LAYER FLOW
An experimental study of surface roughness effects on turbulent boundary layer flow and heat transfer
[AD-A212099] N90-11980
Numerical computation of the viscous flow field around a prolate spheroid
[DFVLR-FB-89-22] N90-11992
Evaluation and sensitivity analyses results of the MESOPUFF 2 model with CAPTEX (Cross-Appalachian Tracer Experiment) measurements
[PB89-198253] N90-12103
BOUNDARY LAYER SEPARATION
Active control of unsteady and separated flow structures
[AD-A212109] N90-11707
Control of turbulent mixing layers
[AD-A211413] N90-11708
Simulation of glancing shock wave and boundary layer interaction
[NASA-TM-102233] N90-11970
BOUNDARY LAYER TRANSITION
The structure of separated flow regions occurring near the leading edge of airfoils - including transition
[NASA-CR-185853] N90-11695
Normal-force-curve and pitching-moment-curve slopes of forebody-cylinder combinations at zero angle of attack for Mach numbers up to 5
[ESDU-89008] N90-11709
BOUNDARY VALUE PROBLEMS
Nearly optimal algorithms and bounds for multilayer channel routing
[AD-A211913] N90-11955
Some new algorithms for boundary value problems in smooth particle hydrodynamics
[AD-A211728] N90-11987
On the computation of normal modes of a rotating, viscous, incompressible fluid with a capillary free boundary
[REPT-89-01] N90-11989
Buckling of axially compressed imperfect orthotropic shells with elastic edge supports
[PB89-217038] N90-12043
Convergence results for pseudospectral approximations of hyperbolic systems by a penalty type boundary treatment
[NASA-CR-181929] N90-12230
BOXES (CONTAINERS)
The rodent research animal holding facility as a barrier to environmental contamination
[NASA-TM-102237] N90-12151
BREMSSTRAHLUNG
The behavior of beams of relativistic non-thermal electrons under the influence of collisions and synchrotron losses
[NASA-CR-185983] N90-12298
BROADBAND
Performance of four rake modems over the non-disturbed wideband HF channel
[AD-A211569] N90-11930
Television systems with enhanced image quality for new broadband channels
[ETN-89-94622] N90-11936
BROWNIAN MOVEMENTS
Stochastic propagation of an array of parallel cracks: Exploratory work on matrix fatigue damage in composite laminates
[DE89-017837] N90-11813
BUBBLE CHAMBERS
Experimental test of PCAC hypothesis in the reactions mu neutrino-proton giving muon(-)-proton-pion(+) and mu antineutrino-proton giving muon(+)-proton-pion(-) in the delta (1232) region — partial conserved axial current
[MPE-PAE/EXP.EL.199] N90-12309
BUCKLING
Axial compression buckling test on the H-2 launch vehicle satellite fairing structural element prototype (aluminum surface plate/aluminum honeycomb sandwiched curved surface plate)
[NAL-TM-563] N90-12039
Buckling of axially compressed imperfect orthotropic shells with elastic edge supports
[PB89-217038] N90-12043
The use of Lanczos's method to solve the large generalized symmetric definite eigenvalue problem
[NASA-CR-181914] N90-12193
BUILDINGS
Wind/seismic comparisons for upgrading existing structures
[DE89-016055] N90-12044
BUOYS
Statistical models for the optimal estimation of oceanic fields
[AD-A211786] N90-12149
BURNING RATE
Flammability, smoke, and dry arc tracking tests of aircraft electrical wire insulations
[DOT/FAA/CT-89/21] N90-11714
Ignition characteristics of the nickel-based alloy UNS N07718 in pressurized oxygen
[NASA-CR-185932] N90-11850
BUTENES
A model for long-term creep and the effects of physical ageing in poly (butylene terephthalate)
[NPL-DMA(A)-182] N90-11895

C

C-130 AIRCRAFT
Improving snow roads and airstrips in Antarctica
[AD-A211588] N90-11907
CAFFEINE
The effect of caffeine on endurance time to exhaustion at high altitude
[AD-A212069] N90-12163
CALCIUM
Investigation of resonant ac-dc magnetic field effects
[AD-A211612] N90-12159
CALCULUS
Taxonomic syntax for first order inference
[AD-A211618] N90-12221
CALCULUS OF VARIATIONS
Monte Carlo studies of nuclei and quantum liquid drops
[DE89-016914] N90-12300
CALIBRATING
Design and calibration of an electrodynamic driver for the Space Thermoacoustic Refrigerator (STAR)
[AD-A212022] N90-11906
Calibration and de-embedding of microwave measurements using any combination of one- or two-port standards
[PB89-212674] N90-11916
Contribution of the precision determination of noise powers in the MHz and lower GHz frequency range
[PTB-E-33] N90-11935
Droplet sizing instrumentation used for icing research: Operation, calibration, and accuracy
[NASA-CR-182293] N90-11999
Scintillating fiber ribbon - tungsten calorimeter
[DE89-016705] N90-12001
Devices and procedures for the calibration of sensors and measurement: Systems of the flight test support system ATTAS
[DFVLR-MITT-89-06] N90-12007
CALIFORNIA
Airborne profiles taken near San Nicolas Island, California, during Operation FIRE (First ISCCP (International Satellite Cloud Climatology Project) regional experiment) (1987): Aerosol size distributions, air and surface temperatures, cloud top temperatures, and relative humidities
[AD-A211664] N90-12136
CALORIMETERS
Scintillating fiber ribbon - tungsten calorimeter
[DE89-016705] N90-12001
High resolution X-ray spectroscopy using germanium microcalorimeters
[DE89-017784] N90-12004
CAMERAS
A survey of camera error sources in machine vision systems
[DE89-014072] N90-12318
An imaging vector magnetograph for the next solar maximum N90-12489
A high-speed digital camera system for the observation of rapid H-alpha fluctuations in solar flares N90-12491
CAPACITANCE
Analysis of loss mechanisms in polycrystalline thin-film solar cells
[DE89-009454] N90-12093
CARBIDES
Creep strength of niobium alloys, Nb-1%Zr and PWC-11
[NASA-TM-102390] N90-11854
CARBOHYDRATE METABOLISM
Heatstroke pathophysiology: The energy depletion model
[AD-A212156] N90-12164
CARBON
Plasma-deposited amorphous hydrogenated carbon films and their tribological properties
[NASA-TM-102379] N90-11880
CARBON DIOXIDE
Policies to encourage private sector responses to potential climate change
[DE89-017244] N90-12107
A statistical intercomparison of temperature and precipitation predicted by four general circulation models with historical data
[DE89-017785] N90-12108
Synergistic effects of nitrogen dioxide and carbon dioxide following acute inhalation exposures in rats
[PB89-214779] N90-12150
Spin-orbit relaxation rates of Bi(6p(3)) 2D(3/2) following photolysis of Bi(CH3)3 at lambda = 193 nm
[AD-A211792] N90-12303
CARBON DIOXIDE LASERS
Construction of a picosecond laser system for the investigation of semiconductors using nonlinear optical methods
[ETN-89-94664] N90-12013
CARBON FIBER REINFORCED PLASTICS
A new test procedure for a wing made with carbon fiber composites
[ETN-89-95220] N90-11820
Aging of CFRP due to longterm storage in heated air
[ESA-TT-1124] N90-11893

CARBON FIBERS
Carbon fiber reinforced glass matrix composites for structural space based applications
[AD-A211682] N90-11818

CARBON MONOXIDE
Catalyst for carbon monoxide oxidation
[NASA-CASE-LAR-14155-1-SB] N90-11823
Catalogic hydrogenation of carbon monoxide
[DE89-017813] N90-11834

CARBURIZING
Advances and directions of ion nitriding/carburizing
[NASA-TM-102398] N90-11902

CARDIOVASCULAR SYSTEM
USSR Space Life Sciences Digest, Issue 22
[NASA-CR-3922(26)-ISSUE-22] N90-12153
USSR Space Life Sciences Digest, Issue 23
[NASA-CR-3922(27)-ISSUE-23] N90-12154
Heatstroke pathophysiology: The energy depletion model
[AD-A212156] N90-12164

CAST ALLOYS
A study of the hot workability of Al-8.5 wt pct Mg alloys for armor plate applications
[AD-A211680] N90-11868

CATALOGS (PUBLICATIONS)
Criss-cross directory of NASA N numbers and DOD AD numbers. Volume 2, part 1: AD to N, 1979-1986. N to AD, 1962-1986
[NASA-TM-101814] N90-12388
Criss-cross directory of NASA N numbers and DOD AD numbers. Volume 2, part 2: AD to N, 1979-1986. N to AD, 1962-1986
[NASA-TM-101815] N90-12389

CATALYSIS
Natural gas to liquids
[DE89-000982] N90-11828

CATALYSTS
Catalyst for carbon monoxide oxidation
[NASA-CASE-LAR-14155-1-SB] N90-11823
In-situ spectroscopic studies of transition metal macrocycles as catalysts for the electrochemical reduction of oxygen
[PB89-219273] N90-11826
Conversion of methane to liquid hydrocarbons
[DE89-017547] N90-11831
Catalogic hydrogenation of carbon monoxide
[DE89-017813] N90-11834

CATIONS
X ray diffraction patterns of metal aurocyanides
[DE89-015188] N90-11851

CAUCHY PROBLEM
The nonconvex multi-dimensional Riemann problem for Hamilton-Jacobi equations
[NASA-CR-181887] N90-12182
Parameter identification for an abstract Cauchy problem by quasilinearization
[NASA-CR-181933] N90-12192

CAVITATION FLOW
An investigation of end-wall vortex cavitation in a high Reynolds number axial-flow pump
[AD-A211426] N90-11982

CAVITIES
Periodic permanent magnet structures
[AD-D014173] N90-12280

CAVITY RESONATORS
Measurement of pressure fluctuations in a resonant chamber with laser-induced iodine fluorescence
[ESA-TT-1123] N90-12326

CEILINGS (METEOROLOGY)
Calibration of a visioceilometer, a hand held lidar system
[FEL-1988-73] N90-12137
A closer look at the visioceilometer
[FEL-1989-80] N90-12138

CELLS (BIOLOGY)
Heatstroke pathophysiology: The energy depletion model
[AD-A212156] N90-12164

CEMENTS
A numerical laboratory for granular solids
[DE89-016367] N90-12045

CENTRIPETAL FORCE
On the complexity analysis of the coriolis and centripetal effects of a 6 DOF robot manipulator --- Degrees of Freedom (DOF)
[RR-344] N90-12030

CERAMIC COATINGS
Vanadium dioxide protective devices
[AD-A212018] N90-11887
Thermomechanical contact phenomena and wear of sliding components
[AD-A211290] N90-12028

CERAMIC FIBERS
Static tensile and tensile creep testing of four boron nitride coated ceramic fibers at elevated temperatures
[NASA-CR-184999] N90-11807

CERAMIC MATRIX COMPOSITES
Inorganic composite materials in Japan: Status and trends
[PB89-230015] N90-11810

CERAMICS
Carbon fiber reinforced glass matrix composites for structural space based applications
[AD-A211682] N90-11818
Sliding seal materials for low heat rejection engines
[NASA-CR-182262] N90-11862
Photolithography: A new tool for ceramic science
[DE90-000135] N90-11885
Densification of particulate ceramic composites: The role of heterogeneities
[DE90-000177] N90-11886
Structure/reactivity relationships of polysilazane preceramics
[AD-A212028] N90-11888
Flexure strength of advanced ceramics: A round robin exercise
[AD-A212101] N90-11889
New mechanism for toughening ceramic materials
[AD-A211651] N90-11892
Effect of annealing conditions on the structural and superconducting properties of Y-Ba-Cu-O films
[AD-A211308] N90-12371
Synthesis and microstructure of highly oriented PbTiO3 thin films prepared by a sol-gel method
[AD-A211735] N90-12377

CEREBRAL CORTEX
Adaptive information processing in auditory cortex
[AD-A211294] N90-12166

CHANNEL FLOW
Near-planar TS waves and longitudinal vortices in channel flow: Nonlinear interaction and focusing
[NASA-CR-181928] N90-11696

CHANNEL NOISE
Multi-stage noise-reducing system
[AD-D014179] N90-11942

CHANNELS (DATA TRANSMISSION)
A new approach to HF (High Frequency) channel modeling and simulation. Part 1: Deterministic model
[PB89-203962] N90-11913
Introduction to the Mil-Std-1553B serial multiplex data bus
[RAE-TM-M-9] N90-12405

CHARACTERIZATION
Choice and characterization of new materials for aerospace applications
[ETN-89-95219] N90-11819

CHARGE CARRIERS
Graded bandgap solar cells
[AD-A211537] N90-12097
Energy relaxation of light holes in InAs(.15)Sb(.85)/InSb multiple quantum wells
[DE89-016035] N90-12349

CHARGE COUPLED DEVICES
Fast and objective MRTD measurement
[FEL-1988-24] N90-12006
An imaging vector magnetograph for the next solar maximum N90-12489

CHARGE DISTRIBUTION
Synchrotron-radiation experiments with recoil ions
[DE89-017579] N90-12301

CHARGE TRANSFER
Electronic structure of transition metal alloys and intermetallics: Charge transfer and its implications for Moessbauer effect measurements
[DE89-017603] N90-11860

CHARGED PARTICLES
Molecular dynamics study of the primitive model of 1-3 electrolyte studies
[AD-A211653] N90-11846
Laser production of soft x rays by multiquantum processes and the excitation of atomic inner-shell states
[AD-A211372] N90-12021
Confinement of multiply charged ions in an ECRH mirror plasma
[DE89-016052] N90-12327

CHEBYSHEV APPROXIMATION
Elimination of spurious eigenvalues in the Chebyshev tau spectral method
[PB89-209282] N90-11967

CHEMICAL ANALYSIS
Structure/reactivity relationships of polysilazane preceramics
[AD-A212028] N90-11888
An atom probe study of phase decomposition in three iron meteorites
[DE89-017581] N90-12420

CHEMICAL CLEANING
Cleaning of printed circuit assemblies with surface-mounted components
[DE89-013609] N90-11945

CHEMICAL COMPOSITION
Coating galvanized steel
[AD-A211775] N90-11869
Correlating microemulsion fuel composition, structure and combustion properties
[DE89-017779] N90-11898
KIVA reactive hydrodynamics code applied to detonations in high vacuum
[DE89-016979] N90-11974

CHEMICAL ENGINEERING
Structure/reactivity relationships of polysilazane preceramics
[AD-A212028] N90-11888
Application of dimensional analysis to statistical process modeling
[AD-A211881] N90-11905

CHEMICAL EXPLOSIONS
Sensitivity relationships in energetic materials
[DE89-016967] N90-11897
VISAR wave profile measurements in supra-compressed HE
[DE89-017736] N90-11976

CHEMICAL REACTION CONTROL
State-resolved reaction dynamics
[AD-A211613] N90-12307

CHEMICAL REACTIONS
In-situ cure monitoring of composites by fiber-optic molecular sensors
[AD-A211495] N90-11817
Shock dissociation of molecular fluids: A possibility of first-order phase change
[DE89-016647] N90-11829
Phase behavior of pure and mixed systems at high pressure
[DE89-017734] N90-11832
Synthesis and chemistry of strained and conjugated fluorocarbons
[AD-A211633] N90-11844
State-resolved reaction dynamics
[AD-A211613] N90-12307

CHEMISORPTION
Self-assembled organic monolayer films
[AD-A212006] N90-11838

CHIRAL DYNAMICS
Eigensolutions for the reflection problem involving the interface of two chiral half spaces
[PB89-221592] N90-11926

CHLOROCARBONS
Potential technologies for collection and destruction of CFCs (Chlorofluorocarbons), halons, and related compounds
[PB89-219968] N90-12105

CHROMIUM
New laser materials
[DE89-017524] N90-12017

CHROMIUM ALLOYS
Precipitation strengthened high strength, high conductivity Cu-Cr-Nb alloys produced by chill block melt spinning
[NASA-CR-185144] N90-11853
Fracture toughness data base for HT9 and modified 9Cr-1Mo irradiated in several reactors up to approximately 100 dpa
[DE90-000111] N90-11864

CHROMOSPHERE
Flare model sensitivity of the Balmer spectrum
N90-12477
Heating and acceleration of coronal and chromospheric ions during solar flares N90-12479
Chromospheric-coronal coupling during solar flares: Current systems and particle acceleration N90-12480

CHRONOLOGY
Impact cratering and the surface age of Venus: The Pre-Magellan controversy N90-12446

CIRCADIAN RHYTHMS
Studies on predicting the resynchronization of the circadian system after transmedian flights
[DFVLR-FB-89-10] N90-12172

CIRCUIT DIAGRAMS
Nearly optimal algorithms and bounds for multilayer channel routing
[AD-A211913] N90-11955

CIRCUITS
A digital model for level-clocked circuitry
[AD-A211937] N90-11957
Linear (passive) and non-linear guided and studies in glass
[AD-A211693] N90-12325

CIRCULAR TUBES
Mechanism for shear band formation in the high strain rate torsion test
[PB89-215370] N90-12038

CLAMPS
Effect of fretting on fatigue strength of aluminium alloys
[ESDU-89004] N90-11870

CLASSIFICATIONS
Investigation on analyzing computer-aided forest disease classifications
[DFVLR-FB-89-16] N90-12112
Program distribution for unclassified scientific and technical reports: Instructions and category scope notes, revision 75
[DE89-005395] N90-12391
CLEARANCES
Flutter clearance of the F-18 high-angle-of-attack research vehicle with experimental wingtip instrumentation pods
[NASA-TM-4148] N90-11732
An investigation of end-wall vortex cavitation in a high Reynolds number axial-flow pump
[AD-A211426] N90-11982
CLIMATE CHANGE
Ozone depletion, greenhouse gases, and climate change
[NASA-CR-185323] N90-12101
Global environmental effects of impact-generated aerosols: Results from a general circulation model
[DE89-008033] N90-12106
Policies to encourage private sector responses to potential climate change
[DE89-017244] N90-12107
Ozone depletion, greenhouse gases, and climate change
[PB89-216097] N90-12110
CLIMATOLOGY
Airborne profiles taken near San Nicolas Island, California, during Operation FIRE (First ISCCP (International Satellite Cloud Climatology Project) regional experiment) (1987): Aerosol size distributions, air and surface temperatures, cloud top temperatures, and relative humidities
[AD-A211664] N90-12136
CLOCKS
A digital model for level-clocked circuitry
[AD-A211937] N90-11957
CLOSED CYCLES
Nuclear closed-cycle gaseous heat engine concept
[DE89-016824] N90-12313
CLOTHING
New Fabric Development Program
[AD-A211549] N90-11891
CLOUD COVER
Lightning data study in conjunction with geostationary satellite data
[NASA-CR-179286] N90-12142
CLOUD HEIGHT INDICATORS
Calibration of a visioceilometer, a hand held lidar system
[FEL-1988-73] N90-12137
CLOUDS (METEOROLOGY)
Further guide for the retrieval of dropsize distributions in water clouds with a ground-based clear-air-sensing Doppler radar
[PB89-196000] N90-11911
Lightning data study in conjunction with geostationary satellite data
[NASA-CR-179286] N90-12142
CLUTTER
Clutter models for subsurface electromagnetic applications
[PB89-229678] N90-11925
ASR-9 weather channel test report
[AD-A211749] N90-11934
Modeling of diffraction reflection and clutter loss in UHF radio wave propagation
[FEL-1988-28] N90-11938
Estimated UV clutter levels at 10-100 meter sensor pixel resolution extrapolated from recent polar bear measurements
[AD-A211357] N90-12125
CMOS
A single-phase clocked NOR/NOR CMOS programmable sequential array structure
[AD-A211297] N90-12203
COASTS
Airborne profiles taken near San Nicolas Island, California, during Operation FIRE (First ISCCP (International Satellite Cloud Climatology Project) regional experiment) (1987): Aerosol size distributions, air and surface temperatures, cloud top temperatures, and relative humidities
[AD-A211664] N90-12136
COATINGS
Coatings for gas turbine compressors
[NLR-MP-88045-U] N90-11750
Method of modifying the dielectric properties of an organic polymer film
[AD-D014171] N90-11879
Ion-assisted deposition of high-temperature lubricious surfaces
[DE89-012397] N90-11883
COBALT ALLOYS
Determination and description of the long term creep behavior of high temperature gas turbine materials
[ETN-89-94985] N90-11871
CODING
Optical arithmetic logic using the modified signed-digit redundant number representation
[AD-D014176] N90-12186
Ground-state coding in partially connected neural networks
[NASA-TM-102239] N90-12227
COEFFICIENTS
The realization of input-output maps using bialgebras
[NASA-CR-185362] N90-12228
Generalizations of Laguerre polynomials
[REPT-89-25] N90-12263
COERCIVITY
Anisotropy and microstructure of high-coercivity rare earth permanent magnets
[AD-A211905] N90-12285
COGNITION
Adaptive information processing in auditory cortex
[AD-A211294] N90-12166
Metacognition and retrieval from long-term memory at Mount Everest
[AD-A211629] N90-12177
The effect of incentives on the reliability and validity of cognitive speed tests
[AD-A211346] N90-12181
Optical computing based on the Hopfield model for neural networks
[AD-A211824] N90-12216
COHERENT LIGHT
Propagation of an elliptical laser beam through the turbulent atmosphere (vertical beams)
[PB89-208680] N90-12010
COLD CATHODE TUBES
Plasma-anode electron gun research
[AD-A211547] N90-11773
COLD HARDENING
Precipitation strengthened high strength, high conductivity Cu-Cr-Nb alloys produced by chill block melt spinning
[NASA-CR-185144] N90-11853
COLLECTION
Potential technologies for collection and destruction of CFCs (Chlorofluorocarbons), halons, and related compounds
[PB89-219968] N90-12105
COLLISION AVOIDANCE
UK airmisses involving commercial air transport, May-August 1988
[ISSN-0951-6301] N90-11717
UK airmisses involving commercial air transport
[CAA-2/88] N90-11718
COLLISIONS
The time evaluation of the number of space probes and debris at different orbit heights with a view to a future collision risk in space
[R-8716] N90-11772
Global environmental effects of impact-generated aerosols: Results from a general circulation model
[DE89-008033] N90-12106
COLLOCATION
A multidomain spectral collocation method for the Stokes problem
[NASA-CR-181876] N90-12266
COLOR
Multicolor electrochromic displays exploratory development
[AD-A212004] N90-11721
Transport systems research vehicle color display system operations manual
[NASA-TM-101577] N90-11736
COLOR VISION
Eye movements and spatial pattern vision
[AD-A211650] N90-12169
COMBUSTION
Analytical studies of three-dimensional combustion processes
[AD-A211903] N90-11837
COMBUSTION CHAMBERS
Steam cooled rich-burn combustor liner
[NASA-CASE-LEW-13609-1] N90-11824
COMBUSTION TEMPERATURE
Program for high speed computation of physical properties of propellants and combustion gas of an LH2/LOX rocket engine
[NAL-TM-564] N90-11803
COMMAND LANGUAGES
DOD Gateway Information System (DGIS) common command language: A retrospective on the introduction of prolog as the development tool
[AD-A211941] N90-12400
COMMERCIAL AIRCRAFT
UK airmisses involving commercial air transport
[CAA-2/88] N90-11718
COMMUNICATION
Rotorcraft low altitude CNS benefit/cost analysis: Rotorcraft operations data
[DOT/FAA/DS-89/9] N90-12406
COMMUNICATION EQUIPMENT
Independent Orbiter Assessment (IOA): Assessment of the communication and tracking subsystem, volume 1
[NASA-CR-185528-VOL-1] N90-11789
Independent Orbiter Assessment (IOA): Assessment of the communication and tracking subsystem, volume 2
[NASA-CR-185528-VOL-2] N90-11790
Independent Orbiter Assessment (IOA): Assessment of the communication and tracking subsystem, volume 3
[NASA-CR-185528-VOL-3] N90-11791
COMMUNICATION NETWORKS
Satellite-matrix-switched, time-division-multiple-access network simulator
[NASA-TP-2944] N90-11915
DOD Gateway Information System (DGIS) common command language: A retrospective on the introduction of prolog as the development tool
[AD-A211941] N90-12400
COMMUNICATION SATELLITES
Petite Amateur Navy Satellite (PANSAT)
[NASA-CR-186049] N90-11800
Satellite-matrix-switched, time-division-multiple-access network simulator
[NASA-TP-2944] N90-11915
COMPACTING
Improving snow roads and airstrips in Antarctica
[AD-A211588] N90-11907
COMPETITION
Manufacturing and the manufacturing engineer in the year 2000, revision
[DE89-017707] N90-11904
COMPLEX COMPOUNDS
Luminescence in applied magnetic fields
[AD-A211551] N90-12287
COMPLEX VARIABLES
Rational expansion for nonlinear input-output maps
[RR-348] N90-12248
COMPLEXITY
On the complexity analysis of the coriolis and centripetal effects of a 6 DOF robot manipulator --- Degrees of Freedom (DOF)
[RR-344] N90-12030
COMPOSITE MATERIALS
Thermal conduction of SSC (Superconducting Super Collider) wire
[DE89-016710] N90-11811
Processing and characterization of alumina platelet-reinforced mullite composites
[DE90-000057] N90-11814
Investigations into the infiltration kinetics, wettability, and interfacial bond strength of Al/SiC composites
[AD-A211924] N90-11815
In-situ cure monitoring of composites by fiber-optic molecular sensors
[AD-A211495] N90-11817
Choice and characterization of new materials for aerospace applications
[ETN-89-95219] N90-11819
Current research in advanced materials
[DE89-017466] N90-11884
Densification of particulate ceramic composites: The role of heterogeneities
[DE90-000177] N90-11886
Flexure strength of advanced ceramics: A round robin exercise
[AD-A212101] N90-11889
COMPOSITE STRUCTURES
An integrated methodology for optimizing structural composite damping
[NASA-TM-102343] N90-11808
Transport composite fuselage technology: Impact dynamics and acoustic transmission
[NASA-CR-4035] N90-11821
Natural frequencies of singly-curved laminated plates with simply-supported edges
[ESDU-89011] N90-12052
COMPRESSIBLE FLOW
Experimental research on swept shock Wave/Boundary layer interactions
[AD-A211744] N90-11988
COMPRESSING
Axial compression buckling test on the H-2 launch vehicle satellite fairing structural element prototype (aluminum surface plate/aluminum honeycomb sandwiched curved surface plate)
[NAL-TM-563] N90-12039

COMPUTATION
Calculated solar radiation incident upon slopes of different orientated surfaces in Finland
[FMI-MP-8] N90-12116
The J-Machine: A fine grain concurrent computer
[AD-A211909] N90-12187
Scheduling sporadic and aperiodic events in a hard real-time system
[AD-A211344] N90-12205
Fast computation using faulty hypercubes
[AD-A211910] N90-12238
COMPUTATIONAL ASTROPHYSICS
The physics of double layers and their role in astrophysics
[TRITA-EPP-89-03] N90-12421
COMPUTATIONAL FLUID DYNAMICS
Computer simulation of aircraft aerodynamics
[NASA-TM-102221] N90-11699
Analytical studies of three-dimensional combustion processes
[AD-A211903] N90-11837
Hopf bifurcation in the driven cavity
[NASA-TM-102334] N90-11969
Simulation of glancing shock wave and boundary layer interaction
[NASA-TM-102233] N90-11970
Numerical analysis, scientific computing and fundamental studies of fluid mechanics
[DE89-017554] N90-11975
Near-wall, three-dimensional turbulence measurements: A challenge for laser velocimetry
[NASA-TM-102252] N90-11978
Computational methods for complex flowfields
[AD-A211485] N90-11983
A simplified self-adaptive grid method, SAGE
[NASA-TM-102198] N90-12211
COMPUTATIONAL GRIDS
The upwind control volume scheme for unstructured triangular grids
[NASA-TM-101664] N90-11703
Error estimation and self-adaptive mesh refinement for boundary element method N90-12037
A simplified self-adaptive grid method, SAGE
[NASA-TM-102198] N90-12211
A multigrid method combined with defect correction for free convection problems at high Rayleigh numbers
[REPT-89-27] N90-12264
An electromagnetic finite element particle code on an unstructured grid
[DE89-017532] N90-12336
COMPUTER AIDED DESIGN
Wind tunnel test of CAD USB-STOL semi-borne prototype
[NAL-TM-566] N90-11696
Development of direct-inverse 3-D methods for applied transonic aerodynamic wing design and analysis
[NASA-CR-186036] N90-11733
Advanced technology in military gas turbine design and manufacture
[PNR90545] N90-11747
Coupling rule-based and object-oriented programming for the classification of machined features
[DE89-017705] N90-11903
Recent advances to NEC (Numerical Electromagnetics Code): Applications and validation
[DE89-009231] N90-11917
Computer-aided design of flexible assembly systems
[PB89-216253] N90-12025
Requirements for multidisciplinary design of aerospace vehicles on high performance computers
[NASA-CR-181915] N90-12183
Reasoning about change and exceptions in automated process planning
[DE89-017706] N90-12195
Low-cost three-dimensional stereoscopic display technique for computer-aided design
[DE89-017732] N90-12196
Design mechanism for interactive graphics mechanism design
[PB89-219513] N90-12202
Structure based formal methods for software engineering
[AD-A211660] N90-12207
General data processing support from project planning to workshop control
[MBB-UD-526/88-PUB] N90-12208
Designing and designing knowledge in engineering and architecture
[PB89-219521] N90-12383
ANDECS-PERLUDE 2.0: A databased, interactive system of control software user's guide
[DFVLR-MITT-89-07] N90-12404
COMPUTER AIDED MANUFACTURING
Advanced technology in military gas turbine design and manufacture
[PNR90545] N90-11747
General data processing support from project planning to workshop control
[MBB-UD-526/88-PUB] N90-12208
Fabrication of modulated vanes for a split-coaxial RFQ
[DE88-757235] N90-12310
COMPUTER ASSISTED INSTRUCTION
Effects of the advanced map interpretation and terrain analysis course on contour-level navigation performance
[AD-A212163] N90-11723
Computer generation of a tutorial dialogue
[AD-A211976] N90-12162
Computer-based tutors for explaining and managing the process of diagnostic reasoning
[AD-A211738] N90-12222
COMPUTER GRAPHICS
Vision-based navigation for autonomous ground vehicles
[AD-A211584] N90-11725
Color printing for computer graphics. Or: How to get it off your screen and onto paper, in color
[PB89-206110] N90-12184
Basic program for raster scan display unit
[NAL-TM-560] N90-12185
Software package for 3-dimensional graphic display unit
[NAL-TM-559] N90-12191
Low-cost three-dimensional stereoscopic display technique for computer-aided design
[DE89-017732] N90-12196
Design mechanism for interactive graphics mechanism design
[PB89-219513] N90-12202
Designing and designing knowledge in engineering and architecture
[PB89-219521] N90-12383
COMPUTER INFORMATION SECURITY
On the design and implementation of a secure computer system
[RSRE-MEMO-4188] N90-12189
A security model and its implementation
[RSRE-MEMO-4222] N90-12190
Operating experience with the Sandia terminal switching network and fiber optic loop
[DE89-007422] N90-12317
COMPUTER NETWORKS
The conditional-event approach to distributed simulation
[NASA-CR-185890] N90-12200
On the communication complexity of solving a polynomial equation
[AD-A211945] N90-12240
Operating experience with the Sandia terminal switching network and fiber optic loop
[DE89-007422] N90-12317
Interoperability of heterogeneous information systems: The COST 11(ter) Project
[PB89-217541] N90-12394
Access to Max '91 information via computer networks
N90-12466
COMPUTER PROGRAMMING
Coupling rule-based and object-oriented programming for the classification of machined features
[DE89-017705] N90-11903
Software package for 3-dimensional graphic display unit
[NAL-TM-559] N90-12191
Experience with CST: Programming and implementation
[AD-A211882] N90-12197
A single-phase clocked NOR/NOR CMOS programmable sequential array structure
[AD-A211297] N90-12203
ISI's (Information Sciences Institute) SDI architecture simulator: An experiment in adding new software to the system
[AD-A211314] N90-12204
Adoption of software engineering innovations in organizations
[AD-A211573] N90-12206
Structure based formal methods for software engineering
[AD-A211660] N90-12207
A language for assembly instructions
[REPT-88-90] N90-12209
Computer-based tutors for explaining and managing the process of diagnostic reasoning
[AD-A211738] N90-12222
COMPUTER PROGRAMS
Some implications of the isotropic momentarily frozen assumptions for the SPAN-MAT program
[NASA-CR-181937] N90-11704
Development of direct-inverse 3-D methods for applied transonic aerodynamic wing design and analysis
[NASA-CR-186036] N90-11733
Program for high speed computation of physical properties of propellants and combustion gas of an LH2/LOX rocket engine
[NAL-TM-564] N90-11803
Recent advances to NEC (Numerical Electromagnetics Code): Applications and validation
[DE89-009231] N90-11917
KIVA reactive hydrodynamics code applied to detonations in high vacuum
[DE89-016979] N90-11974
Generation and tooth contact analysis of spiral bevel gears with predesigned parabolic functions of transmission errors
[NASA-CR-4259] N90-12033
Natural frequencies of singly-curved laminated plates with simply-supported edges
[ESDU-89011] N90-12052
WISPER: A standardized fatigue load sequence for HAWT-blades
[NLR-MP-88029-U] N90-12055
Aerosol backscatter studies supporting LAWS
N90-12079
Development of high resolution simulations of the atmospheric environment using the MASS model
[NASA-CR-186040] N90-12133
Structure based formal methods for software engineering
[AD-A211660] N90-12207
A simplified self-adaptive grid method, SAGE
[NASA-TM-102198] N90-12211
Navigation of robotic systems
[DE89-017507] N90-12219
Four vector-matrix primitives
[AD-A211889] N90-12237
Numerical solution of acoustic-structure interaction problems
[AD-A211505] N90-12293
Non-stationary computer model of the asymptotic region of an electric arc gas heater
[IPPCZ-288] N90-12330
FORTRAN program for x ray photoelectron spectroscopy data reformatting
[NASA-TP-2957] N90-12348
GALAX: A two-dimensional N-body code for disk galaxy dynamics
[PB89-217780] N90-12415
COMPUTER STORAGE DEVICES
Sequential searching in multidimensional monotone arrays
[AD-A211938] N90-12188
Optical computing based on the Hopfield model for neural networks
[AD-A211824] N90-12216
Thin film magnetic memory elements
[AD-D014178] N90-12281
COMPUTER SYSTEMS DESIGN
Basic program for raster scan display unit
[NAL-TM-560] N90-12185
On the design and implementation of a secure computer system
[RSRE-MEMO-4188] N90-12189
Adoption of software engineering innovations in organizations
[AD-A211573] N90-12206
Detailed description of the knowledge-based system for physical database design, volume 2
[PB89-229033] N90-12395
COMPUTER SYSTEMS PERFORMANCE
Software package for 3-dimensional graphic display unit
[NAL-TM-559] N90-12191
Processing rate sensitivities of a heterogeneous multiprocessor
[PB89-229017] N90-12201
A unified framework for simulating Markovian models of highly dependable systems
[AD-A212164] N90-12267
Detailed description of the knowledge-based system for physical database design, volume 2
[PB89-229033] N90-12395
COMPUTER SYSTEMS PROGRAMS
Software package for 3-dimensional graphic display unit
[NAL-TM-559] N90-12191
ANDECS-PERLUDE 2.0: A databased, interactive system of control software user's guide
[DFVLR-MITT-89-07] N90-12404
COMPUTER SYSTEMS SIMULATION
Human Operator Simulator (HOS) 4 user's guide
[AD-A212007] N90-11763
COMPUTER TECHNIQUES
Effects of the advanced map interpretation and terrain analysis course on contour-level navigation performance
[AD-A212163] N90-11723
Computer generation of a tutorial dialogue
[AD-A211976] N90-12162

Design mechanism for interactive graphics mechanism design
[PB89-219513] N90-12202

Novel techniques for data decomposition and load balancing for parallel processing of vision systems: Implementation and evaluation using a motion estimation system
[NASA-CR-185991] N90-12214

Some techniques for anaphora resolution in algebraic linguistics
[REPT-89-28] N90-12265

Computer problems in goodness-of-fit
[AD-A211411] N90-12268

COMPUTER VISION

Three dimensional object recognition employing combined visual and tactile sensing
[PB89-219489] N90-12176

Parallel implementation and evaluation of motion estimation system algorithms on a distributed memory multiprocessor using knowledge based mappings
[NASA-CR-185984] N90-12213

Novel techniques for data decomposition and load balancing for parallel processing of vision systems: Implementation and evaluation using a motion estimation system
[NASA-CR-185991] N90-12214

Parallel architectures and parallel algorithms for integrated vision systems
[NASA-CR-185990] N90-12215

A survey of camera error sources in machine vision systems
[DE89-014072] N90-12318

COMPUTERIZED SIMULATION

Computer simulation of aircraft aerodynamics
[NASA-TM-102221] N90-11699

Post crash flight analysis: Visualizing flight recorder data
[AD-A212063] N90-11715

Numerical simulation of aeroplane response to a lightning injection
[ETN-89-95271] N90-11716

A simulation study of landing time allocation procedures for use in computer-assisted air traffic management systems
[AD-A212159] N90-11722

Simulations for computer centerline approach
[DOT/FAA/CT-TN89/41] N90-11726

STOVL propulsion system volume dynamics approximations
[NASA-TM-102397] N90-11740

Human Operator Simulator (HOS) 4 user's guide
[AD-A212007] N90-11763

Program for high speed computation of physical properties of propellants and combustion gas of an LH2/LOX rocket engine
[NAL-TM-564] N90-11803

Analysis of opposed jet hydrogen-air counter flow diffusion flame
[NASA-CR-182366] N90-11825

Computer simulations of radiation damage in amorphous solids
[PB89-212682] N90-11827

Microwave instability near transition energy
[DE90-000107] N90-11922

Theory and simulation of the operation of a Doppler direction finder in a multipath environment
[FEL-1988-56] N90-11939

Development of high frequency spice models for ferrite core inductors and transformers
[DE89-015121] N90-11946

Simulation of glancing shock wave and boundary layer interaction
[NASA-TM-102233] N90-11970

The dynamic performance of robot manipulators under different operating conditions
[RR-345] N90-12031

Generation and tooth contact analysis of spiral bevel gears with predesigned parabolic functions of transmission errors
[NASA-CR-4259] N90-12033

Disturbances in the Arizona Monsoon N90-12071

Laboratory and theoretical models of planetary-scale instabilities and waves N90-12076

User's guide for a personal computer model of turbulence at a wind turbine rotor
[DE89-017753] N90-12095

Development of high resolution simulations of the atmospheric environment using the MASS model
[NASA-CR-186040] N90-12133

Low-cost three-dimensional stereoscopic display technique for computer-aided design
[DE89-017732] N90-12196

The conditional-event approach to distributed simulation
[NASA-CR-185890] N90-12200

ISI's (Information Sciences Institute) SDI architecture simulator: An experiment in adding new software to the system
[AD-A211314] N90-12204

Fast forward dynamics algorithm for robot arms using multiprocessing
[RR-367] N90-12225

A unified framework for simulating Markovian models of highly dependable systems
[AD-A212164] N90-12267

DART: A simulation code for charged particle beams, revision 1
[DE89-016697] N90-12312

Computer controlled MHD power consolidation and pulse-generation system
[DE89-015600] N90-12333

Wave particle interactions
[DE89-017527] N90-12335

Temporal and spatial filtering remedies for dispersion in electromagnetic particle codes
[DE89-017534] N90-12337

Computer simulations of two-dimensional quasiperiodic crystal and random tiling models
[DE89-016909] N90-12355

GALAX: A two-dimensional N-body code for disk galaxy dynamics
[PB89-217780] N90-12415

COMPUTERS

The J-Machine: A fine grain concurrent computer
[AD-A211909] N90-12187

CONCURRENT PROCESSING

The J-Machine: A fine grain concurrent computer
[AD-A211909] N90-12187

Experience with CST: Programming and implementation
[AD-A211882] N90-12197

Parallel processing on transputer arrays for the recognition of objects in infrared images
[RSRE-MEMO-4197] N90-12217

CONDENSED MATTER PHYSICS

Highlights of papers presented at the workshop on Cold Fusion Phenomena
[DE89-016956] N90-12334

CONFERENCES

Proceedings of the 1988 Antenna Applications Symposium, volume 1
[AD-A211396] N90-11928

Proceedings of the Workshop on Compound Semiconductor Devices and Integrated Circuits (13th) held in Cabourg, France on 10-12 May 1989
[AD-A211848] N90-11954

Solid-State Sensor and Actuator
[AD-A211427] N90-11961

Indexes for the proceedings of the symposia (international) on detonation, 1951 through 1985
[DE89-015178] N90-11972

Global tropospheric chemistry: Chemical fluexes in the global atmosphere
[NASA-CR-186090] N90-12109

Ozone depletion, greenhouse gases, and climate change
[PB89-216097] N90-12110

Meeting review: The Second NCAR (National Center for Atmospheric Research) Research Aircraft Fleet Workshop
[PB89-200901] N90-12113

Middle Atmosphere Program. Handbook for MAP, volume 28
[NASA-CR-184972] N90-12117

Heatstroke pathophysiology: The energy depletion model
[AD-A212156] N90-12164

Gordon Conference on Atomic Physics
[AD-A211946] N90-12304

A Conference on Three-Dimensional Representation held in University of Minnesota on 24-26 May 1989
[AD-A211630] N90-12324

Max '91 Workshop 2: Developments in Observations and Theory for Solar Cycle 22
[NASA-TM-101893] N90-12459

CONFIDENCE LIMITS

Small sample theory for steady state confidence intervals
[AD-A212097] N90-12242

CONFORMAL MAPPING

Bordered surfaces, off-shell amplitudes, sewing, and string field theory
[DE90-000006] N90-12378

CONJUGATION

Synthesis and chemistry of strained and conjugated fluorocarbons
[AD-A211633] N90-11844

CONSTITUTIVE EQUATIONS

International seminar on the inelastic behavior of solids: Models and utilization
[DE89-017420] N90-11858

A rate-dependent constitutive model for Be
[DE89-017755] N90-11861

CONSTRAINTS

Some notes on perturbations of differential-algebraic equations
[PB89-218564] N90-12243

CONTAMINANTS

Photolysis of spacecraft contaminants
[AD-A211715] N90-11801

The rodent research animal holding facility as a barrier to environmental contamination
[NASA-TM-102237] N90-12151

CONTINENTAL SHELVES

Remote sensing data acquisition, analysis and archival
[PB89-142566] N90-12085

CONTRACTION

Parallel graph contraction
[AD-A211916] N90-12199

CONTRACTS

Forecasting contracting workload
[AD-A211935] N90-12387

CONTRAILS

Effects on electromagnetic wave propagation and rocket vapor trails of intense turbulence generated by breaking internal gravity waves
[AD-A211755] N90-12130

CONTROL SURFACES

Effect of control surface mass unbalance on the stability of a closed-loop active control system
[NASA-TP-2952] N90-12042

CONTROL SYSTEMS DESIGN

Applications of flight control system methods to an advanced combat rotorcraft
[NASA-TM-101054] N90-11752

A design procedure for the handling qualities optimization of the X-29A aircraft
[NASA-TM-4142] N90-11753

Robust control design for flight control
[AD-A211957] N90-11756

Independent Orbiter Assessment (IOA): Assessment of the electrical power distribution and control subsystem, volume 1
[NASA-CR-185557-VOL-1] N90-11779

Independent Orbiter Assessment (IOA): Assessment of the electrical power distribution and control subsystem, volume 2
[NASA-CR-185557-VOL-2] N90-11780

Independent Orbiter Assessment (IOA): Assessment of the electrical power distribution and control subsystem, volume 3
[NASA-CR-185557-VOL-3] N90-11781

Computer controlled MHD power consolidation and pulse-generation system
[DE89-015600] N90-12333

CONTROL THEORY

Adaptive control law design for model uncertainty compensation
[AD-A211712] N90-11758

Efficient finite element solution of Navier-Stokes equations and related topics
[AD-A211647] N90-11986

CONTROLLABILITY

A design procedure for the handling qualities optimization of the X-29A aircraft
[NASA-TM-4142] N90-11753

CONTROLLERS

Independent Orbiter Assessment (IOA): Assessment of the reaction control system, volume 1
[NASA-CR-185543-VOL-1] N90-11793

Independent Orbiter Assessment (IOA): Assessment of the reaction control system, volume 2
[NASA-CR-185543-VOL-2] N90-11794

Independent Orbiter Assessment (IOA): Assessment of the reaction control system, volume 3
[NASA-CR-185543-VOL-3] N90-11795

Independent Orbiter Assessment (IOA): Assessment of the reaction control system, volume 4
[NASA-CR-185543-VOL-4] N90-11796

Independent Orbiter Assessment (IOA): Assessment of the reaction control system, volume 5
[NASA-CR-185543-VOL-5] N90-11797

A design methodology for self-tuning control of systems with inherent conflicts
[PB89-219505] N90-11960

Control of plasma position in the CASTOR tokamak
[IPPCZ-284] N90-12332

CONVECTION

Viscous split algorithms for the time dependent incompressible Navier-Stokes equations
[AD-A211592] N90-11985

CONVECTIVE HEAT TRANSFER

Convective heat transfer in hypobaric environments
[AD-A212060] N90-11979

Human body regional convective heat transfer determination using sublimating naphthalene disks
[AD-A212170] N90-12165

CONVERGENCE
Global atmospheric moisture variability N90-12062
Dynamics and energetics of the South Pacific Convergence Zone during FGGE SOP-1 and South Pacific Convergence Zone and global-scale N90-12065
Convergence results for pseudospectral approximations of hyperbolic systems by a penalty type boundary treatment
[NASA-CR-181929] N90-12230
Some observations on the convergence behavior of GMRES
[REPT-89-09] N90-12252
The convergence behavior of some iterative solution methods
[REPT-89-19] N90-12260
A multigrid method combined with defect correction for free convection problems at high Rayleigh numbers
[REPT-89-27] N90-12264

CONVEXITY
Optimal matching of 3-D convex polyhedra
[TELECOM-PARIS-89C003] N90-12258

CONVOLUTION INTEGRALS
Inf-convolution splines
[IMAG-RR-749-M] N90-12256

COOLING
Steam cooled rich-burn combustor liner
[NASA-CASE-LEW-13609-1] N90-11824

COPOLYMERIZATION
Suppression of side chain crystallization and transformation of monotropic mesophases into enantiotropic mesophases by copolymerization of the parent polymers' monomer pairs containing constitutional isomeric mesogenic side groups
[AD-A209066] N90-11878

COPOLYMERS
Suppression of side chain crystallization and transformation of monotropic mesophases into enantiotropic mesophases by copolymerization of the parent polymers' monomer pairs containing constitutional isomeric mesogenic side groups
[AD-A209066] N90-11878

COPPER
Temperature dependent effects during Ag deposition on Cu(110)
[DE89-016987] N90-11857

COPPER ALLOYS
Precipitation strengthened high strength, high conductivity Cu-Cr-Nb alloys produced by chill block melt spinning
[NASA-CR-185144] N90-11853

COPPER OXIDES
High-temperature superconducting current leads for cryogenic apparatus
[DE89-017680] N90-12361
Effects of grain boundary chemistry on critical current density in oxide superconductors
[DE89-017780] N90-12365
Effect of annealing conditions on the structural and superconducting properties of Y-Ba-Cu-O films
[AD-A211308] N90-12371
High temperature superconducting compounds
[AD-A211511] N90-12374

CORIOLIS EFFECT
On the complexity analysis of the coriolis and centripetal effects of a 6 DOF robot manipulator --- Degrees of Freedom (DOF)
[RR-344] N90-12030

CORONAS
Venus and the Archean Earth: Thermal considerations N90-12448

CORRECTION
Application of matrix correction methods on a plate and a truss structure
[NLR-MP-88042-U] N90-12056
A multigrid method combined with defect correction for free convection problems at high Rayleigh numbers
[REPT-89-27] N90-12264

CORRELATION
Lightning data study in conjunction with geostationary satellite data
[NASA-CR-179286] N90-12142

CORRELATORS
A SAW Slanted Array Correlator (SAC) with separate amplitude compensation channel
[AD-D014174] N90-11914

CORROSION
Thermomechanical contact phenomena and wear of sliding components
[AD-A211290] N90-12028
Long endurance underwater power system
[AD-A211386] N90-12096

CORROSION TESTS
Coatings for gas turbine compressors
[NLR-MP-88045-U] N90-11750

COSMIC RAYS
Cosmic strings and ultra-high energy cosmic rays
[NASA-CR-185924] N90-12492

COSMIC X RAYS
The BATSE experiment on the Gamma Ray Observatory: Solar flare hard x ray and gamma-ray capabilities N90-12469
Solar flare gamma-ray and hard x ray imaging with the GRID-on-a-balloon N90-12474

COSMOLOGY
Particle physics and cosmology using stellar evolution theory
[DE89-017529] N90-12418

COST ANALYSIS
Adoption of software engineering innovations in organizations
[AD-A211573] N90-12206
Rotorcraft low altitude CNS benefit/cost analysis: Rotorcraft operations data
[DOT/FAA/DS-89/9] N90-12406

COSTS
Structure based formal methods for software engineering
[AD-A211660] N90-12207

COTTON FIBERS
New Fabric Development Program
[AD-A211549] N90-11891

COUETTE FLOW
Numerical analysis, scientific computing and fundamental studies of fluid mechanics
[DE89-017554] N90-11975

COULOMB POTENTIAL
On the role of Coulomb forces in atomic radiative emission
[IRF-PREPRINT-106] N90-12308

COUNTERFLOW
Analysis of opposed jet hydrogen-air counter flow diffusion flame
[NASA-CR-182366] N90-11825

COUPLING
Chromospheric-coronal coupling during solar flares: Current systems and particle acceleration N90-12480

COUPLINGS
Docking system for spacecraft
[NASA-CASE-MSC-21327-1] N90-11798

CRACK PROPAGATION
Effects of a heat cycle on material strength
[NAL-TM-562] N90-11737
Stochastic propagation of an array of parallel cracks: Exploratory work on matrix fatigue damage in composite laminates
[DE89-017837] N90-11813
Processing and characterization of alumina platelet-reinforced mullite composites
[DE90-000057] N90-11814
The effects of temperature on fatigue crack propagation in 310 austenitic stainless steel
[DE90-000136] N90-11865
Fractographic and microstructural analysis of fatigue crack growth in a Ti-6Al-4V fan disc forging
[NLR-MP-88028-U] N90-11877
A numerical laboratory for granular solids
[DE89-016367] N90-12045
An application of the J-integral to an incremental analysis of blunting crack behavior
[DE89-016844] N90-12046

CRACK TIPS
An application of the J-integral to an incremental analysis of blunting crack behavior
[DE89-016844] N90-12046
An experimental and analytical program to develop crack tip fracture criteria
[AD-A211565] N90-12051

CRACKS
Stochastic propagation of an array of parallel cracks: Exploratory work on matrix fatigue damage in composite laminates
[DE89-017837] N90-11813
Weldability of ductile nickel aluminides
[DE89-017452] N90-11859
A numerical laboratory for granular solids
[DE89-016367] N90-12045

CRASH LANDING
Post crash flight analysis: Visualizing flight recorder data
[AD-A212063] N90-11715

CREEP PROPERTIES
Determination and description of the long term creep behavior of high temperature gas turbine materials
[ETN-89-94985] N90-11871
The effect of flux creep on the magnetization field in the SSC diopole magnets
[DE90-000124] N90-12284

CREEP STRENGTH
Creep strength of niobium alloys, Nb-1%Zr and PWC-11
[NASA-TM-102390] N90-11854

CREEP TESTS
Creep and fracture behavior of heat resistant steels in characteristic cases of variable fatigue loading
[ETN-89-94671] N90-11855
A model for long-term creep and the effects of physical ageing in poly (butylene terephthalate)
[NPL-DMA(A)-182] N90-11895

CRITICAL POINT
Vapour pressures and critical points of liquids. Halogenated hydrocarbons
[ESDU-89006] N90-11848

CROSS FLOW
Doubly-fluted tubes and enhanced tubes in confined crossflow
[PB89-217921] N90-11971

CROSS POLARIZATION
Eigensolutions for the reflection problem involving the interface of two chiral half spaces
[PB89-221592] N90-11926

CROSSLINKING
Positron annihilation studies of interpenetrating polymer networks
[AD-A212162] N90-11890

CRYOGENIC COOLING
Design and calibration of an electrodynamic driver for the Space Thermoacoustic Refrigerator (STAR)
[AD-A212022] N90-11906

CRYOGENIC EQUIPMENT
Cryogenic Schottky-mixer receiver front-end for 40-50 GHz
[PB89-221667] N90-11959
High-temperature superconducting current leads for cryogenic apparatus
[DE89-017680] N90-12361

CRYOGENIC TEMPERATURE
Cryogenic free jets
[ESA-TT-1128] N90-11767

CRYOSTATS
High-temperature superconducting current leads for cryogenic apparatus
[DE89-017680] N90-12361

CRYSTAL DEFECTS
Computer simulations of radiation damage in amorphous solids
[PB89-212682] N90-11827
Mechanism of electrochemical activation of carbon electrodes: Role of graphite lattice defects
[AD-A211644] N90-11845
Characterization of the Structure and Chemistry of Defects in Materials: Proceedings, volume 138
[DE89-014796] N90-12352

CRYSTAL GROWTH
Growth and characterization of materials for tunable lasers in the near infrared spectral region
[NASA-CR-185832] N90-12009
New laser materials
[DE89-017524] N90-12017
Process for single crystal growth of high T(sub c) superconductors
[AD-D014167] N90-12346
Characterization of the Structure and Chemistry of Defects in Materials: Proceedings, volume 138
[DE89-014796] N90-12352

CRYSTAL LATTICES
Deformation and defects in Laves-phase intermetallic compounds
[DE89-017798] N90-11862

CRYSTAL STRUCTURE
Deformation and defects in Laves-phase intermetallic compounds
[DE89-017798] N90-11862
New laser materials
[DE89-017524] N90-12017
Computer simulations of two-dimensional quasiperiodic crystal and random tiling models
[DE89-016909] N90-12355
Effect of annealing conditions on the structural and superconducting properties of Y-Ba-Cu-O films
[AD-A211308] N90-12371
Synthesis and microstructure of highly oriented PbTiO3 thin films prepared by a sol-gel method
[AD-A211735] N90-12377

CRYSTALLIZATION
Low temperature formation of titanium aluminide films using physical vapor deposition
[AD-A211877] N90-11866
Suppression of side chain crystallization and transformation of monotropic mesophases into enantiotropic mesophases by copolymerization of the parent polymers' monomer pairs containing constitutional isomeric mesogenic side groups
[AD-A209066] N90-11878

CRYSTALLOGRAPHY
Single crystal diffraction
[DE90-000024] N90-12366
CRYSTALS
Energy transfer and non-linear optical properties at near ultraviolet wavelengths: Rare earth 4f(yields)5d transitions in crystals and glasses
[DE90-000065] N90-12321
Computer simulations of two-dimensional quasiperiodic crystal and random tiling models
[DE89-016909] N90-12355
Anomalous ion-channeling behavior across the superconducting transition in high-T(sub c) materials
[DE89-017677] N90-12360
CURING
In-situ cure monitoring of composites by fiber-optic molecular sensors
[AD-A211495] N90-11817
CURRENT DENSITY
Resistive block methods for electrostatic field solutions with internal elements
[DE89-017535] N90-11920
Superconducting switch program
[AD-A211580] N90-11964
Effects of grain boundary chemistry on critical current density in oxide superconductors
[DE89-017780] N90-12365
CURRENT DISTRIBUTION
The physics of double layers and their role in astrophysics
[TRITA-EPP-89-03] N90-12421
CURVATURE
Natural frequencies of singly-curved laminated plates with simply-supported edges
[ESDU-89011] N90-12052
CURVE FITTING
Computer problems in goodness-of-fit
[AD-A211411] N90-12268
CUTTING
Autonomous space processor for orbital debris
[NASA-CR-186043] N90-11770
CYANIDES
X ray diffraction patterns of metal aurocyanides
[DE89-015188] N90-11851
CYCLOGENESIS
Investigations of polar air stream cyclogenesis based on numerical simulations with a mesoscale model
[PB89-214563] N90-12132
CYCLONES
Variational objective analysis for cyclone studies
N90-12064
CYCLOTRON RADIATION
Electron cyclotron emission and absorption experiment on the CASTOR tokamak
[IPPCZ-285] N90-12331
CYCLOTRON RESONANCE
Investigation of resonant ac-dc magnetic field effects
[AD-A211612] N90-12150
CYLINDRICAL BODIES
Normal-force-curve and pitching-moment-curve slopes of forebody-cylinder combinations at zero angle of attack for Mach numbers up to 5
[ESDU-89008] N90-11709
CYTOLOGY
Cellular and molecular mechanisms of high pressure inotropy in cardiac muscle
[AD-A211695] N90-12170

D

D REGION
HIPAS 1987-88: ULF research and campaign support
[AD-A211720] N90-11933
DAMAGE ASSESSMENT
Computer simulations of radiation damage in amorphous solids
[PB89-212682] N90-11827
Lightning and surge protection of photovoltaic installations: Two case histories, Vulcano and Kythnos
[PB89-229056] N90-12135
DAMPING
An integrated methodology for optimizing structural composite damping
[NASA-TM-102343] N90-11808
DATA ACQUISITION
Contemporary China's meteorological enterprises (selected portions)
[AD-A210697] N90-12131
Noise data of four small propeller-driven airplanes
[PB89-216980] N90-12291
Characterizations of electrical properties of highT(sub c) superconducting materials
[NASA-TM-100380] N90-12345
CALS (Computer-aided Acquisition and Logistic Support) Test Network information exchange: User's manual
[DE89-016700] N90-12399
DATA BASE MANAGEMENT SYSTEMS
Program distribution for unclassified scientific and technical reports: Instructions and category scope notes, revision 75
[DE89-005395] N90-12391
Role of conceptual models in the design and use of information systems
[PB89-217376] N90-12392
Problem of incomplete information in relational databases
[PB89-217533] N90-12393
Interoperability of heterogeneous information systems: The COST 11(ter) Project
[PB89-217541] N90-12394
A real-time locking protocol
[AD-A211514] N90-12403
DATA BASES
Review and analysis of the DNW/Model 360 rotor acoustic data base
[NASA-TM-102253] N90-11692
Remote sensing data acquisition, analysis and archival
[PB89-142566] N90-12085
Global data bases on distribution, characteristics and methane emission of natural wetlands: Documentation of archived data tape
[NASA-TM-4153] N90-12090
Airborne profiles taken near San Nicolas Island, California, during Operation FIRE (First ISCCP (International Satellite Cloud Climatology Project) regional experiment) (1987): Aerosol size distributions, air and surface temperatures, cloud top temperatures, and relative humidities
[AD-A211664] N90-12136
Statistical models for the optimal estimation of oceanic fields
[AD-A211786] N90-12149
Interoperability of heterogeneous information systems: The COST 11(ter) Project
[PB89-217541] N90-12394
Detailed description of the knowledge-based system for physical database design, volume 2
[PB89-229033] N90-12395
Development and use of a tribology research-in-progress database
[PB89-228274] N90-12396
FEDIX: An on-line information service for universities and other research organizations: User's guide, version 2.0, release 1
[DE89-016695] N90-12398
ANDECS-PERLUDE 2.0: A databased, interactive system of control software user's guide
[DFVLR-MITT-89-07] N90-12404
DATA FLOW ANALYSIS
An approximate max-flow min-cut theorem for uniform multicommodity flow problems with applications to approximation algorithms
[AD-A211908] N90-12198
DATA LINKS
Independent Orbiter Assessment (IOA): Assessment of the communication and tracking subsystem, volume 1
[NASA-CR-185528-VOL-1] N90-11789
Independent Orbiter Assessment (IOA): Assessment of the communication and tracking subsystem, volume 2
[NASA-CR-185528-VOL-2] N90-11790
Independent Orbiter Assessment (IOA): Assessment of the communication and tracking subsystem, volume 3
[NASA-CR-185528-VOL-3] N90-11791
DATA PROCESSING
Navigation experiment NAVEX: Data storage and processing
[DFVLR-MITT-89-09] N90-11727
NASA/MSFC FY88 Global Scale Atmospheric Processes Research Program Review
[NASA-TM-100357] N90-12059
Global distribution of moisture, evaporation-precipitation, and diabatic heating rates
N90-12069
Laboratory and theoretical models of planetary-scale instabilities and waves N90-12076
UV ionospheric remote sensing with the polar BEAR satellite
[AD-A211359] N90-12127
World Weather Watch: Implementation
[WMO-714] N90-12139
Crau 1987: The KNMI contribution — KNMI (Royal Netherlands Meteorological Institute)
[KNMI-TR-110] N90-12140
General data processing support from project planning to workshop control
[MBB-UD-526/88-PUB] N90-12208
Operating experience with the Sandia terminal switching network and fiber optic loop
[DE89-007422] N90-12317
Single crystal diffraction
[DE90-000024] N90-12366
Problem of incomplete information in relational databases
[PB89-217533] N90-12393
DATA PROCESSING TERMINALS
Software package for 3-dimensional graphic display unit
[NAL-TM-559] N90-12191
DATA RECORDING
A closer look at the visioceilometer
[FEL-1989-80] N90-12138
DATA SAMPLING
Fast sampling and stability of nonlinear sampled data systems. Part 2: Sampling rate estimations
[RR-341] N90-12271
Fast sampling and stability of nonlinear sampled-data systems. Part 1: Existence theorems
[RR-340-PT-1] N90-12276
Slow sampling and stability of nonlinear sampled-data systems
[RR-342] N90-12277
DATA SMOOTHING
Splines and equations of nonlinear parameters
[IMAG-RR-750-M] N90-12257
DATA STORAGE
Navigation experiment NAVEX: Data storage and processing
[DFVLR-MITT-89-09] N90-11727
DATA SYSTEMS
Fast sampling and stability of nonlinear sampled-data systems. Part 1: Existence theorems
[RR-340-PT-1] N90-12276
Slow sampling and stability of nonlinear sampled-data systems
[RR-342] N90-12277
Building a user-friendly data dictionary system in ORACLE
[DE89-014878] N90-12397
DATA TRANSMISSION
Optical data transmission systems in radiation environment
[DE90-000174] N90-12322
DECELERATION
An open-loop transient thermodynamic model of the Cougar turbojet
[AD-A211774] N90-11745
DECISION MAKING
On the generation of a variable structure airport surface traffic control system
[AD-A211306] N90-11724
On the asymptotic optimality of certain empirical Bayes simultaneous testing procedures
[AD-A211649] N90-12270
DECISION THEORY
On finding the largest normal mean and estimating the selected mean
[AD-A211628] N90-12245
DECOMPOSITION
A multidomain spectral collocation method for the Stokes problem
[NASA-CR-181876] N90-12266
An atom probe study of phase decomposition in three iron meteorites
[DE89-017581] N90-12420
DEFECTS
Deformation and defects in Laves-phase intermetallic compounds
[DE89-017798] N90-11862
DEFENSE INDUSTRY
Adoption of software engineering innovations in organizations
[AD-A211573] N90-12206
DEFENSE PROGRAM
Forecasting contracting workload
[AD-A211935] N90-12387
FY 1990/FY 1991 biennial budget descriptive summaries for the Strategic Defense Initiative Organization
[AD-A211985] N90-12409
DEFLECTION
Field evaluation of the multi-depth deflectometers
[PB89-207708] N90-11994
DEFORMATION
Deformation and defects in Laves-phase intermetallic compounds
[DE89-017798] N90-11862
Field evaluation of the multi-depth deflectometers
[PB89-207708] N90-11994
Crustal deformation: Earth vs Venus N90-12450
DEGASSING
Significance of oxide skins on powder for the quality of PM Al material — PM (press molded)
[DFVLR-FB-89-11] N90-11873

DELAY
Navigation experiment NAVEX: The equipment delay times in the Spacelab mission D1
[DFVLR-MITT-89-10] N90-11728
DELTA WINGS
Unsteady aerodynamics with applications to flight mechanics
[AD-A211944] N90-11706
DENSIFICATION
Densification of particulate ceramic composites: The role of heterogeneities
[DE90-000177] N90-11886
DEPLETION
Ozone depletion, greenhouse gases, and climate change
[PB89-216097] N90-12110
DEPOSITION
Photolysis of spacecraft contaminants
[AD-A211715] N90-11801
Temperature dependent effects during Ag deposition on Cu(110)
[DE89-016987] N90-11857
Plasma-deposited amorphous hydrogenated carbon films and their tribological properties
[NASA-TM-102379] N90-11880
Fundamental tribological properties of ion-beam-deposited boron nitride films
[NASA-TM-102088] N90-11881
Ion-assisted deposition of high-temperature lubricious surfaces
[DE89-012397] N90-11883
Ion beam deposition of epitaxial germanium and gallium arsenide layers
[DE89-017439] N90-12357
High temperature superconducting compounds
[AD-A211511] N90-12374
DERIVATION
Incompressible flow about ellipsoids of revolution
[REPT-88-02] N90-11713
DESIGN ANALYSIS
Performance and quality of a wing type parachute: Parametric analysis
[REPT-88-19] N90-11710
Development of direct-inverse 3-D methods for applied transonic aerodynamic wing design and analysis
[NASA-CR-186036] N90-11733
Design of a solar sail mission to Mars
[NASA-CR-186045] N90-11771
An integrated methodology for optimizing structural composite damping
[NASA-TM-102343] N90-11808
Current research in advanced materials
[DE89-017466] N90-11884
Kinematic design NC optical generator N90-12316
An introduction to effectiveness: NTU relationships
[ESDU-89016] N90-12381
DESORPTION
Photolysis of spacecraft contaminants
[AD-A211715] N90-11801
Quantitative interpretation of auger lineshapes and electron/photon stimulated desorption
[AD-A211550] N90-11842
DESTRUCTION
Potential technologies for collection and destruction of CFCs (Chlorofluorocarbons), halons, and related compounds
[PB89-219968] N90-12105
DETECTION
Improved pattern recognition techniques for real time operation
[AD-A211395] N90-11840
Microwave signal detection using modulation of polymeric optical waveguides
[DE89-017545] N90-11921
Statistical models for the optimal estimation of oceanic fields
[AD-A211786] N90-12149
DETECTORS
Control of plasma position in the CASTOR tokamak
[IPPCZ-284] N90-12332
DETONATION
A critical assessment of models available for the shock initiation of heterogeneous explosives
[MRL-TR-89-17] N90-11896
Sensitivity relationships in energetic materials
[DE89-016967] N90-11897
Indexes for the proceedings of the symposia (international) on detonation, 1951 through 1985
[DE89-015178] N90-11972
KIVA reactive hydrodynamics code applied to detonations in high vacuum
[DE89-016979] N90-11974
VISAR wave profile measurements in supra-compressed HE
[DE89-017736] N90-11976
Lagrangian analysis of MIV (Magnetic Impulse-Velocity) gauge experiments on PBX 9502 using the mass-displacement moment function
[DE89-016612] N90-12000
Shock pressure determination in detonator wires
[DE89-017756] N90-12002
DETONATION WAVES
Wave combustors for trans-atmospheric vehicles
[NASA-TM-102238] N90-11742
Indexes for the proceedings of the symposia (international) on detonation, 1951 through 1985
[DE89-015178] N90-11972
DEUTERIUM
Spin-orbit relaxation rates of Bi(6p(3)) 2D(3/2) following photolysis of Bi(CH3)3 at lambda = 193 nm
[AD-A211792] N90-12303
DHC 2 AIRCRAFT
Stability and control derivatives of the De Havilland DHC-2 BEAVER aircraft
[PB89-217525] N90-11754
DIAMONDS
Thermal model for double-drift IMPATT diodes on diamond heat sinks
[AD-A211746] N90-12380
DICTIONARIES
Building a user-friendly data dictionary system in ORACLE
[DE89-014878] N90-12397
DIELECTRIC PROPERTIES
Method of modifying the dielectric properties of an organic polymer film
[AD-D014171] N90-11879
Time-domain analytic and numeric analysis of vertical dipoles in front of dielectric planar interface
[PB89-221642] N90-11927
DIELECTRICS
Spectral-domain analysis of finite frequency selective surfaces
[AD-A211669] N90-11932
Dielectric covered microstrip patch antennas
[AD-A211577] N90-11963
Analysis of the efficiency of a dielectric solar energy collector
[PB89-212716] N90-12092
DIESEL ENGINES
Sliding seal materials for low heat rejection engines
[NASA-CR-182262] N90-11882
DIFFERENCE EQUATIONS
Some observations on the convergence behavior of GMRES
[REPT-89-09] N90-12252
A study of the asymptotic behavior of linear difference equations with polynomial coefficients
[IMAG-RR-743-M] N90-12254
A long time tail for random walk in random scenery
[REPT-89-08] N90-12278
DIFFERENTIAL EQUATIONS
The realization of input-output maps using bialgebras
[NASA-CR-185362] N90-12228
Some notes on perturbations of differential-algebraic equations
[PB89-218564] N90-12243
Mapping nonlinear integro-differential equations into the frequency domain
[RR-366] N90-12249
A simple proof of a differential equation for generalizations of Laguerre polynomials
[REPT-89-15] N90-12253
DIFFRACTION PATTERNS
X ray diffraction patterns of metal aurocyanides
[DE89-015188] N90-11851
DIFFUSION
Kinetics of diffusion-controlled reactions
[AD-A212161] N90-12286
DIFFUSION ELECTRODES
Effect of electrical double layer on transport limited currents at microelectrodes
[AD-A211586] N90-11843
DIFFUSION FLAMES
Analysis of opposed jet hydrogen-air counter flow diffusion flame
[NASA-CR-182366] N90-11825
DIGITAL COMPUTERS
Processing rate sensitivities of a heterogeneous multiprocessor
[PB89-229017] N90-12201
DIGITAL FILTERS
Improved pattern recognition techniques for real time operation
[AD-A211395] N90-11840
DIGITAL SIMULATION
A digital model for level-clocked circuitry
[AD-A211937] N90-11957
Experimental investigation of a planar shock wave over a double wedge
[AD-A211366] N90-11981
DIGITAL SYSTEMS
Applications of flight control system methods to an advanced combat rotorcraft
[NASA-TM-101054] N90-11752
On-orbit annealing of gallium arsenide solar cell arrays
[AD-A212087] N90-11900
Video imaging systems: A survey
[DE89-016920] N90-11919
A digital model for level-clocked circuitry
[AD-A211937] N90-11957
DIGITAL TECHNIQUES
Engine controls for the 1990's
[PNR90546] N90-11748
DIMENSIONAL ANALYSIS
Application of dimensional analysis to statistical process modeling
[AD-A211881] N90-11905
DIODES
Calculations of soft x ray emission of REB-heated plasma
[IPPCZ-287] N90-12329
DIPOLE MOMENTS
Time-domain analytic and numeric analysis of vertical dipoles in front of dielectric planar interface
[PB89-221642] N90-11927
DIRECTIONAL ANTENNAS
Theory and simulation of the operation of a Doppler direction finder in a multipath environment
[FEL-1988-56] N90-11939
DIRECTORIES
Criss-cross directory of NASA N numbers and DOD AD numbers. Volume 2, part 1: AD to N, 1979-1986. N to AD, 1962-1986
[NASA-TM-101814] N90-12388
Criss-cross directory of NASA N numbers and DOD AD numbers. Volume 2, part 2: AD to N, 1979-1986. N to AD, 1962-1986
[NASA-TM-101815] N90-12389
DISEASES
Investigation on analyzing computer-aided forest disease classifications
[DFVLR-FB-89-16] N90-12112
DISK GALAXIES
GALAX: A two-dimensional N-body code for disk galaxy dynamics
[PB89-217780] N90-12415
DISPERSING
Performance of four rake modems over the non-disturbed wideband HF channel
[AD-A211589] N90-11930
DISPLAY DEVICES
Multicolor electrochromic displays exploratory development
[AD-A212004] N90-11721
Transport systems research vehicle color display system operations manual
[NASA-TM-101577] N90-11736
Independent Orbiter Assessment (IOA): Analysis of the displays and controls subsystem
[NASA-CR-185563] N90-11774
Analysis of two-pass Modified Hough Transform (MHT) technique for the detection of wake like signals
[AD-A211982] N90-11924
Color printing for computer graphics. Or: How to get it off your screen and onto paper, in color
[PB89-208110] N90-12184
Basic program for raster scan display unit
[NAL-TM-560] N90-12185
Software package for 3-dimensional graphic display unit
[NAL-TM-559] N90-12191
DISSIPATION
Dynamics of baroclinic wave systems N90-12072
DISSOCIATION
Shock dissociation of molecular fluids: A possibility of first-order phase change
[DE89-016647] N90-11829
Atomic and molecular surface and volume processes in the analysis of negative hydrogen discharges
[DE89-015705] N90-12294
Ion formation by electron impact
[AD-A211367] N90-12305
DISTORTION
Microwave instability near transition energy
[DE90-000107] N90-11922
DISTRIBUTED PROCESSING
Spacelab system analysis Marshall Avionics System Testbed (MAST)
[NASA-CR-183804] N90-11802
Parallel implementation and evaluation of motion estimation system algorithms on a distributed memory multiprocessor using knowledge based mappings
[NASA-CR-185984] N90-12213
Distributed VLSI architecture for fast Jacobian and inverse Jacobian formulations
[RR-346] N90-12218

Fast forward dynamics algorithm for robot arms using multiprocessing
[RR-367] N90-12225
DISTRIBUTION (PROPERTY)
Distribution of auroral precipitation at midnight during a magnetic storm
[PB89-213136] N90-12118
Electron-positron momentum distribution measurements of high-T(sub c) superconductors and related systems
[DE89-017536] N90-12358
DISTRIBUTION FUNCTIONS
Molecular dynamics study of the primitive model of 1-3 electrolyte studies
[AD-A211653] N90-11846
Some 1(sub p) invariant probability measures
[REPT-88-91] N90-12273
DIVERGENCE
A multidomain spectral collocation method for the Stokes problem
[NASA-CR-181876] N90-12266
DOCUMENTATION
Criss-cross directory of NASA N numbers and DOD AD numbers. Volume 2, part 1: AD to N, 1979-1986. N to AD, 1962-1986
[NASA-TM-101814] N90-12388
Criss-cross directory of NASA N numbers and DOD AD numbers. Volume 2, part 2: AD to N, 1979-1986. N to AD, 1962-1986
[NASA-TM-101815] N90-12389
DOMAINS
A multidomain spectral collocation method for the Stokes problem
[NASA-CR-181876] N90-12266
DOMES (GEOLOGY)
Characteristics, distribution and geologic/terrain associations of small dome-like hills on Venus
N90-12425
Volcanism on Venus: Large shields and major accumulations of small domes N90-12445
DOPPLER EFFECT
Theory and simulation of the operation of a Doppler direction finder in a multipath environment
[FEL-1988-56] N90-11939
Doppler statistics of ocean velocity variability
[AD-A211687] N90-12148
DOPPLER RADAR
Further guide for the retrieval of dropsize distributions in water clouds with a ground-based clear-air-sensing Doppler radar
[PB89-196000] N90-11911
Low level remote sensing: The Doppler Radar wind profiler N90-12067
Measurements of aerosol properties needed to infer backscatter characteristics in support of the NASA Doppler Lidar program N90-12082
DOSIMETERS
Use of the NPL linac for x ray dosimetry — linear accelerator (linac)
[NPL-RSA(EXT)-6] N90-12314
DOWNWASH
Analysis of heliport environmental data: Indianapolis downtown heliport, Wall Street heliport. Volume 2: Wall Street heliport data plots
[DOT/FAA/CT-TN87/54-VOL-2] N90-11761
DRAG REDUCTION
An experimental investigation of helicopter rotor hub fairing drag characteristics
[NASA-TM-102182] N90-11701
DRAWING
Designing and designing knowledge in engineering and architecture
[PB89-219521] N90-12383
DROP SIZE
Further guide for the retrieval of dropsize distributions in water clouds with a ground-based clear-air-sensing Doppler radar
[PB89-196000] N90-11911
DROPS (LIQUIDS)
Conceptual design of liquid droplet radiator shuttle-attached experiment
[NASA-CR-185164] N90-11805
Conceptual design of liquid droplet radiator shuttle-attached experiment technical requirements document
[NASA-CR-185165] N90-11806
Further guide for the retrieval of dropsize distributions in water clouds with a ground-based clear-air-sensing Doppler radar
[PB89-196000] N90-11911
Droplet sizing instrumentation used for icing research: Operation, calibration, and accuracy
[NASA-CR-182293] N90-11999
Monte Carlo studies of nuclei and quantum liquid drops
[DE89-016914] N90-12300
DUCTED ROCKET ENGINES
Analytical studies of three-dimensional combustion processes
[AD-A211903] N90-11837
DUCTILITY
Weldability of ductile nickel aluminides
[DE89-017452] N90-11859
A study of the hot workability of Al-8.5 wt pct Mg alloys for armor plate applications
[AD-A211680] N90-11868
DYE LASERS
Construction of a picosecond laser system for the investigation of semiconductors using nonlinear optical methods
[ETN-89-94664] N90-12013
DYNAMIC CHARACTERISTICS
Molecular dynamics study of the primitive model of 1-3 electrolyte studies
[AD-A211653] N90-11846
DYNAMIC CONTROL
Adaptive control law design for model uncertainty compensation
[AD-A211712] N90-11758
Robot inverse dynamics computation via VLSI distributed architectures
[RR-350] N90-12223
DYNAMIC MODELS
Adaptive control law design for model uncertainty compensation
[AD-A211712] N90-11758
DYNAMIC STRUCTURAL ANALYSIS
Effects of mistuning and matrix structure on the topology of frequency response curves
[NASA-TM-102290] N90-12041
Airframe structural dynamic considerations in rotor design optimization
[NASA-TM-101646] N90-12057
DYNAMICAL SYSTEMS
Application of dynamical systems theory to global weather phenomena revealed by satellite imagery
N90-12063
The realization of input-output maps using bialgebras
[NASA-CR-185362] N90-12228

E

EARTH ATMOSPHERE
Spatial characteristics of airglow and solar scatter radiance from the earth's atmosphere
[AD-A211358] N90-12126
Crau 1987: The KNMI contribution — KNMI (Royal Netherlands Meteorological Institute)
[KNMI-TR-110] N90-12140
Vacuum ultraviolet backgrounds from space - ten years after
[AD-A211353] N90-12493
EARTH CORE
Investigations of Eurasian seismic sources and upper mantle structure
[AD-A211806] N90-12120
EARTH CRUST
Global environmental effects of impact-generated aerosols: Results from a general circulation model
[DE89-008033] N90-12106
EARTH IONOSPHERE
UV ionospheric remote sensing with the polar BEAR satellite
[AD-A211359] N90-12127
TEC (Total Electron Content) models
[AD-A211553] N90-12129
EARTH LIMB
Retrieval of atomic oxygen and temperature in the thermosphere. Part 2: Feasibility of an experiment based on limb emission in the OI lines
[AD-A211807] N90-12121
EARTH MANTLE
Investigations of Eurasian seismic sources and upper mantle structure
[AD-A211806] N90-12120
EARTH OBSERVATIONS (FROM SPACE)
Laser sounding from space: Report of the ESA Technology Working Group on Space Laser Sounding and Ranging
[ESA-SP-1108] N90-12024
Strategy for earth explorers in global earth sciences
[NASA-CR-185933] N90-12084
EARTH OBSERVING SYSTEM (EOS)
Strategy for earth explorers in global earth sciences
[NASA-CR-185933] N90-12084
EARTH ORBITS
The time evaluation of the number of space probes and debris at different orbit heights with a view to a future collision risk in space
[R-8718] N90-11772
EARTH RESOURCES
Earth resources: A continuing bibliography with indexes (issue 63)
[NASA-SP-7041(63)] N90-12091
EARTH SURFACE
Crustal deformation: Earth vs Venus N90-12450
EARTHQUAKE RESISTANT STRUCTURES
Wind/seismic comparisons for upgrading existing structures
[DE89-016055] N90-12044
EARTHQUAKES
Hydrophone investigations of earthquakes and explosion generated high-frequency seismic phases
[AD-A212055] N90-12122
ECONOMIC IMPACT
Manufacturing and the manufacturing engineer in the year 2000, revision
[DE89-017707] N90-11904
EDDY CURRENTS
Parametric study of power absorption from electromagnetic waves by small ferrite spheres
[NASA-TP-2949] N90-12282
EDGES
Interlaminar stress concentration in fiber composites
[ETN-89-94670] N90-11809
EFFERENT NERVOUS SYSTEMS
Age-related changes in human posture control: Motor coordination tests
[NASA-CR-185855] N90-12178
EFFICIENCY
A method to model fuze-performance. Part 3: Diffraction of electromagnetic radiation by an edge
[FEL-1989-22-PT-3] N90-11940
EIGENVALUES
Elimination of spurious eigenvalues in the Chebyshev tau spectral method
[PB89-209282] N90-11967
On the computation of normal modes of a rotating, viscous, incompressible fluid with a capillary free boundary
[REPT-89-01] N90-11989
The use of Lanczos's method to solve the large generalized symmetric definite eigenvalue problem
[NASA-CR-181914] N90-12193
EJECTORS
Investigation of advanced mixer-ejector exhaust system
[AD-A211943] N90-11705
EL NINO
On the statistics of El Nino occurrences and the relationship of El Nino to volcanic and solar/geomagnetic activity
[NASA-TP-2948] N90-12456
ELASTIC ANISOTROPY
Materials characterization using holographic mapping of transient lamb waves
[AD-A211414] N90-12050
ELASTIC DEFORMATION
Deformation behavior of SiC/2014 Al metal-matrix composite
[AD-A212095] N90-11816
An application of the J-integral to an incremental analysis of blunting crack behavior
[DE89-016844] N90-12046
ELASTIC PLATES
Materials characterization using holographic mapping of transient lamb waves
[AD-A211414] N90-12050
ELASTIC PROPERTIES
International seminar on the inelastic behavior of solids: Models and utilization
[DE89-017420] N90-11858
New mechanism for toughening ceramic materials
[AD-A211651] N90-11892
Buckling of axially compressed imperfect orthotropic shells with elastic edge supports
[PB89-217038] N90-12043
Autofrettage-stress distribution under load and retained stresses after depressurization
[AD-A212090] N90-12048
Numerical solution of acoustic-structure interaction problems
[AD-A211505] N90-12293
ELASTOPLASTICITY
Design of glued joints, elastoplastic adhesives
[DRIC-T-8168] N90-11894
ELECTRIC ARCS
Non-stationary computer model of the asymptotic region of an electric arc gas heater
[IPPCZ-288] N90-12330
ELECTRIC BATTERIES
Assessment of thin film batteries based on polymer electrolytes. Part 1: Energy density
[AD-A212111] N90-11958

ELECTRIC CONNECTORS
Nearly optimal algorithms and bounds for multilayer channel routing
[AD-A211913] N90-11955
High-temperature superconducting current leads for cryogenic apparatus
[DE89-017680] N90-12361
ELECTRIC CONTACTS
Niobium and niobium nitride contacts on semiconducting material
[AD-D014177] N90-12347
Electrolitic deposited ohmic contacts on III-V compound semiconductors: A review
[PB89-217400] N90-12350
ELECTRIC CURRENT
HIPAS 1987-88: ULF research and campaign support
[AD-A211720] N90-11933
The characterization of Nb3Sn superconductors for use in magnets of 19 T and greater
[DE89-017758] N90-12364
ELECTRIC DIPOLES
Time-domain analytic and numeric analysis of vertical dipoles in front of dielectric planar interface
[PB89-221642] N90-11927
ELECTRIC DISCHARGES
Simulation of the EMP (Electromagnetic Pulse) from ESD (Electrostatic Discharge)
[DE89-014484] N90-11918
An empirical formula for gas switch breakdown delay
[DE89-017233] N90-11947
ELECTRIC FIELDS
Clutter models for subsurface electromagnetic applications
[PB89-229678] N90-11925
Stellarator transport theory
[DE89-016371] N90-12328
Field-assisted bonding of single crystal quartz
[DE89-015407] N90-12353
ELECTRIC GENERATORS
Independent Orbiter Assessment (IOA): Assessment of the Electrical Power Distribution and Control/Electrical Power Generation (EPD and C/EPG) FMEA/CIL
[NASA-CR-185542] N90-11785
An assessment of technology for self-powered gas appliances: A GATC (Gas Appliance Technology Center)
[PB89-219265] N90-12026
ELECTRIC MOTOR VEHICLES
Safety considerations for sodium-sulfur batteries for electric vehicles
[DE89-017682] N90-11949
DSEP (Dual Shaft Electric Propulsion) operation and maintenance manual for the NVH and TB-2 vehicles: Advanced Dual Shaft Electric Propulsion System technology development program
[DE89-017549] N90-12411
ELECTRIC POTENTIAL
Effect of electrical double layer on transport limited currents at microelectrodes
[AD-A211586] N90-11843
ELECTRIC POWER SUPPLIES
Independent Orbiter Assessment (IOA): Assessment of the reaction control system, volume 3
[NASA-CR-185543-VOL-3] N90-11795
ELECTRIC POWER TRANSMISSION
Independent Orbiter Assessment (IOA): Assessment of the reaction control system, volume 1
[NASA-CR-185543-VOL-1] N90-11793
Independent Orbiter Assessment (IOA): Assessment of the reaction control system, volume 2
[NASA-CR-185543-VOL-2] N90-11794
Independent Orbiter Assessment (IOA): Assessment of the reaction control system, volume 4
[NASA-CR-185543-VOL-4] N90-11796
Independent Orbiter Assessment (IOA): Assessment of the reaction control system, volume 5
[NASA-CR-185543-VOL-5] N90-11797
ELECTRIC SPARKS
Air breakdown photography in the picosecond domain
[DE89-016775] N90-11830
ELECTRIC WELDING
Resistance welding large parts
[DE89-010462] N90-12027
ELECTRIC WIRE
Flammability, smoke, and dry arc tracking tests of aircraft electrical wire insulations
[DOT/FAA/CT-89/21] N90-11714
ELECTRICAL ENGINEERING
Center for Electronics and Electrical Engineering technical publication announcements covering Center programs, January-March 1989 with 1989 CEEE events calendar
[PB89-228308] N90-12402
ELECTRICAL INSULATION
Flammability, smoke, and dry arc tracking tests of aircraft electrical wire insulations
[DOT/FAA/CT-89/21] N90-11714
ELECTRICAL PROPERTIES
Characterizations of electrical properties of highT(sub c) superconducting materials
[NASA-TM-100380] N90-12345
ELECTRICAL RESISTANCE
Resistance welding large parts
[DE89-010462] N90-12027
ELECTRICAL RESISTIVITY
Resistive block methods for electrostatic field solutions with internal elements
[DE89-017535] N90-11920
RF performance of polycrystalline high-T(sub c) superconductors
[DE89-017671] N90-12359
ELECTRO-OPTICS
Sensitivity of optoelectronic receivers
[AD-A211823] N90-11923
Proceedings of the Workshop on Compound Semiconductor Devices and Integrated Circuits (13th) held in Cabourg, France on 10-12 May 1989
[AD-A211848] N90-11954
ELECTROACOUSTIC TRANSDUCERS
Design and calibration of an electrodynamic driver for the Space Thermoacoustic Refrigerator (STAR)
[AD-A212022] N90-11906
ELECTROACOUSTICS
Design and calibration of an electrodynamic driver for the Space Thermoacoustic Refrigerator (STAR)
[AD-A212022] N90-11906
ELECTROCHEMICAL OXIDATION
Mechanism of electrochemical activation of carbon electrodes: Role of graphite lattice defects
[AD-A211644] N90-11845
ELECTROCHEMISTRY
In-situ spectroscopic studies of transition metal macrocycles as catalysts for the electrochemical reduction of oxygen
[PB89-219273] N90-11826
Effect of electrical double layer on transport limited currents at microelectrodes
[AD-A211586] N90-11843
Highlights of papers presented at the workshop on Cold Fusion Phenomena
[DE89-016956] N90-12334
Effects of grain boundary chemistry on critical current density in oxide superconductors
[DE89-017780] N90-12365
ELECTRODEPOSITION
Fe-Ni-Cr alloys for coatings and electroforms
[PB89-195846] N90-11849
ELECTRODES
Multicolor electrochromic displays exploratory development
[AD-A212004] N90-11721
Mechanism of electrochemical activation of carbon electrodes: Role of graphite lattice defects
[AD-A211644] N90-11845
ELECTROLYTES
Effect of electrical double layer on transport limited currents at microelectrodes
[AD-A211586] N90-11843
Molecular dynamics study of the primitive model of 1-3 electrolyte studies
[AD-A211653] N90-11846
Assessment of thin film batteries based on polymer electrolytes. Part 1: Energy density
[AD-A212111] N90-11958
ELECTROLYTIC CELLS
Multicolor electrochromic displays exploratory development
[AD-A212004] N90-11721
A lightweight solid polymer electrolyte fuel cell with stack power density of 3 kW/lb (7 kW/kg)
[AD-A211542] N90-12098
ELECTROMAGNETIC COMPATIBILITY
Handbook of radio wave propagation loss (100-20,000 MHz), part 2
[PB89-195473] N90-11912
ELECTROMAGNETIC FIELDS
Resistive block methods for electrostatic field solutions with internal elements
[DE89-017535] N90-11920
An electromagnetic finite element particle code on an unstructured grid
[DE89-017532] N90-12336
Temporal and spatial filtering remedies for dispersion in electromagnetic particle codes
[DE89-017534] N90-12337
ELECTROMAGNETIC INTERACTIONS
Laser production of soft x rays by multiquantum processes and the excitation of atomic inner-shell states
[AD-A211372] N90-12021
On the role of Coulomb forces in atomic radiative emission
[IRF-PREPRINT-106] N90-12308
ELECTROMAGNETIC NOISE
Sensitivity of optoelectronic receivers
[AD-A211823] N90-11923
SIS (Superconductor-Insulator-Superconductor) mixer research
[AD-A211607] N90-12375
ELECTROMAGNETIC NOISE MEASUREMENT
Contribution of the precision determination of noise powers in the MHz and lower GHz frequency range
[PTB-E-33] N90-11935
ELECTROMAGNETIC PULSES
Simulation of the EMP (Electromagnetic Pulse) from ESD (Electrostatic Discharge)
[DE89-014484] N90-11918
ELECTROMAGNETIC RADIATION
A new approach to HF (High Frequency) channel modeling and simulation. Part 1: Deterministic model
[PB89-203962] N90-11913
A method to model fuze-performance. Part 3: Diffraction of electromagnetic radiation by an edge
[FEL-1989-22-PT-3] N90-11940
Parametric study of power absorption from electromagnetic waves by small ferrite spheres
[NASA-TP-2949] N90-12282
ELECTROMAGNETIC WAVE TRANSMISSION
Effects on electromagnetic wave propagation and rocket vapor trails of intense turbulence generated by breaking internal gravity waves
[AD-A211755] N90-12130
ELECTROMAGNETISM
Recent advances to NEC (Numerical Electromagnetics Code): Applications and validation
[DE89-009231] N90-11917
ELECTROMAGNETS
An electromagnetic finite element particle code on an unstructured grid
[DE89-017532] N90-12336
Temporal and spatial filtering remedies for dispersion in electromagnetic particle codes
[DE89-017534] N90-12337
ELECTROMECHANICAL DEVICES
Design of scientific payloads and components
[AD-A211819] N90-12005
ELECTROMYOGRAPHY
Age-related changes in human posture control: Motor coordination tests
[NASA-CR-185855] N90-12178
ELECTRON ACCELERATION
Joule heating and runaway electron acceleration in a solar flare N90-12476
ELECTRON ATTACHMENT
Electron attachment and molecular fragmentation in laser-excited plasmas
[AD-A212098] N90-12343
ELECTRON BEAM WELDING
Deformation of electron beam welded Ti-6Al-4V alloy sheet under superplastic conditions
[RAE-TM-MAT/STR-1109] N90-12053
ELECTRON BEAMS
A beam induced upset during the flight of the ECHO-7 rocket
[NASA-CR-186089] N90-11755
Development and evaluation of an instrument for rapid electroreflectance of semiconductor materials
[AD-A211690] N90-12376
ELECTRON CAPTURE
Electron attachment and molecular fragmentation in laser-excited plasmas
[AD-A212098] N90-12343
ELECTRON DENSITY (CONCENTRATION)
TEC (Total Electron Content) models
[AD-A211553] N90-12129
Stellarator transport theory
[DE89-016371] N90-12328
ELECTRON DENSITY PROFILES
Vacuum ultraviolet backgrounds from space - ten years after
[AD-A211353] N90-12493
ELECTRON DISTRIBUTION
LABCEDE fluorescence investigations
[AD-A210678] N90-12114
Development of a numerical solution to the time dependent kinetic equation N90-12481
ELECTRON EMISSION
Plasma-anode electron gun research
[AD-A211547] N90-11773
ELECTRON ENERGY
Calculations of soft x ray emission of REB-heated plasma
[IPPCZ-287] N90-12329
ELECTRON GUNS
Plasma-anode electron gun research
[AD-A211547] N90-11773
Switched power workshop: Introduction and summary
[DE90-000036] N90-11952

ELECTRON IMPACT
Ion formation by electron impact
[AD-A211367] N90-12305
ELECTRON ORBITALS
Spin-orbit relaxation rates of Bi(6p(3)) 2D(3/2) following photolysis of Bi(CH3)3 at lambda = 193 nm
[AD-A211792] N90-12303
ELECTRON SCATTERING
Laser production of soft x rays by multiquantum processes and the excitation of atomic inner-shell states
[AD-A211372] N90-12021
LABCEDE fluorescence investigations
[AD-A210678] N90-12114
New developments in the ab initio treatment of low energy electron collisions with molecules
[DE89-015294] N90-12299
ELECTRON SPECTROSCOPY
Quantitative interpretation of auger lineshapes and electron/photon stimulated desorption
[AD-A211550] N90-11842
FORTRAN program for x ray photoelectron spectroscopy data reformatting
[NASA-TP-2957] N90-12348
ELECTRON STATES
Quantitative interpretation of auger lineshapes and electron/photon stimulated desorption
[AD-A211550] N90-11842
Spin-orbit relaxation rates of Bi(6p(3)) 2D(3/2) following photolysis of Bi(CH3)3 at lambda = 193 nm
[AD-A211792] N90-12303
ELECTRON TRANSFER
Iron (III) initiated autoxidation of 1,2,3,4-tetrahydrocarbazole: An example of electron transfer
[AD-A211857] N90-11836
Mechanism of electrochemical activation of carbon electrodes: Role of graphite lattice defects
[AD-A211644] N90-11845
ELECTRON TRANSITIONS
LABCEDE fluorescence investigations
[AD-A210678] N90-12114
ELECTRON TUNNELING
SIS (Superconductor-Insulator-Superconductor) mixer research
[AD-A211607] N90-12375
ELECTRONIC CONTROL
Engine controls for the 1990's
[PNR90546] N90-11748
ELECTRONIC EQUIPMENT
Numerical simulation of aeroplane response to a lightning injection
[ETN-89-95271] N90-11716
Advanced light source master oscillator
[DE90-000123] N90-11953
Design of scientific payloads and components
[AD-A211819] N90-12005
ELECTRONIC SPECTRA
Quantitative interpretation of auger lineshapes and electron/photon stimulated desorption
[AD-A211550] N90-11842
Ion formation by electron impact
[AD-A211367] N90-12305
ELECTRONS
Quantitative interpretation of auger lineshapes and electron/photon stimulated desorption
[AD-A211550] N90-11842
Electron-positron momentum distribution measurements of high-T(sub c) superconductors and related systems
[DE89-017538] N90-12358
ELECTROPLATING
Electrolitic deposited ohmic contacts on III-V compound semiconductors: A review
[PB89-217400] N90-12350
ELECTROSTATIC CHARGE
Simulation of the EMP (Electromagnetic Pulse) from ESD (Electrostatic Discharge)
[DE89-014484] N90-11918
The physics of double layers and their role in astrophysics
[TRITA-EPP-89-03] N90-12421
ELECTROSTATICS
Molecular dynamics study of the primitive model of 1-3 electrolyte studies
[AD-A211653] N90-11846
Resistive block methods for electrostatic field solutions with internal elements
[DE89-017535] N90-11920
ELLIPSOIDS
Incompressible flow about ellipsoids of revolution
[REPT-88-02] N90-11713
EMBEDDED COMPUTER SYSTEMS
Dynamic embedding of trees in hypercubes with constant dilation and load
[AD-A211884] N90-12236
EMBEDDING
Calibration and de-embedding of microwave measurements using any combination of one- or two-port standards
[PB89-212674] N90-11916
EMERGENCIES
Project AENEAS: A feasibility study for crew emergency return vehicle
[PB89-217020] N90-11799
EMERGENCY LIFE SUSTAINING SYSTEMS
Project AENEAS: A feasibility study for crew emergency return vehicle
[PB89-217020] N90-11799
EMISSION
Global data bases on distribution, characteristics and methane emission of natural wetlands: Documentation of archived data tape
[NASA-TM-4153] N90-12090
On the role of Coulomb forces in atomic radiative emission
[IRF-PREPRINT-106] N90-12308
EMISSION SPECTRA
Retrieval of atomic oxygen and temperature in the thermosphere. Part 2: Feasibility of an experiment based on limb emission in the OI lines
[AD-A211807] N90-12121
Investigation of atmospheric emissions in ultraviolet, vacuum ultraviolet, and extreme ultraviolet wavelength
[AD-A212169] N90-12123
Electron cyclotron emission and absorption experiment on the CASTOR tokamak
[IPPCZ-285] N90-12331
EMISSIVITY
Infrared temperature measurement with automatic consideration of emissivity
[ESA-TT-1131] N90-12008
EMULSIONS
Correlating microemulsion fuel composition, structure and combustion properties
[DE89-017779] N90-11898
ENDOCRINOLOGY
USSR Space Life Sciences Digest, Issue 23
[NASA-CR-3922(27)-ISSUE-23] N90-12154
ENERGETIC PARTICLES
Interplanetary energetic particle observations of the March 1989 events N90-12484
Cosmic strings and ultra-high energy cosmic rays
[NASA-CR-185924] N90-12492
ENERGY CONSUMPTION
Activities report on KEMA R and D
[ST-REPT-VOL-6-NO-12] N90-12100
ENERGY CONVERSION
An assessment of technology for self-powered gas appliances: A GATC (Gas Appliance Technology Center)
[PB89-219265] N90-12026
ENERGY CONVERSION EFFICIENCY
Analysis of the efficiency of a dielectric solar energy collector
[PB89-212716] N90-12092
ENERGY DISTRIBUTION
Fluctuations in transverse energy and multiplicity, energy densities, and neutral pion spectra in nucleus-nucleus collisions at 200 GeV/nucleon
[DE89-017583] N90-12302
ENERGY GAPS (SOLID STATE)
Graded bandgap solar cells
[AD-A211537] N90-12097
ENERGY SPECTRA
Wave particle interactions
[DE89-017527] N90-12335
ENERGY TECHNOLOGY
Activities report on KEMA R and D
[ST-REPT-VOL-6-NO-12] N90-12100
FEDIX: An on-line information service for universities and other research organizations: User's guide, version 2.0, release 1
[DE89-016695] N90-12398
ENERGY TRANSFER
Laser production of soft x rays by multiquantum processes and the excitation of atomic inner-shell states
[AD-A211372] N90-12021
Quantum-mechanical derivation of the Davydov equations for multi-quanta states
[DE89-015250] N90-12297
Energy transfer and non-linear optical properties at near ultraviolet wavelengths: Rare earth 4f(yields)5d transitions in crystals and glasses
[DE90-000065] N90-12321
ENGINE CONTROL
An open-loop transient thermodynamic model of the Cougar turbojet
[AD-A211774] N90-11745
Engine controls for the 1990's
[PNR90546] N90-11748
ENGINE DESIGN
Wave combustors for trans-atmospheric vehicles
[NASA-TM-102238] N90-11742
Advanced technology in military gas turbine design and manufacture
[PNR90545] N90-11747
Engine controls for the 1990's
[PNR90546] N90-11748
Future military powerplants --- fighter aircraft engines
[PNR90554] N90-11749
Nuclear closed-cycle gaseous heat engine concept
[DE89-016824] N90-12313
ENGINE PARTS
Effects of a heat cycle on material strength
[NAL-TM-562] N90-11737
Advanced technology in military gas turbine design and manufacture
[PNR90545] N90-11747
Aluminium alloy development for aero engines
[PNR90548] N90-11874
ENGINEERING MANAGEMENT
The application of quality assurance to engineering management
[DE89-009955] N90-12386
ENGINES
Nuclear closed-cycle gaseous heat engine concept
[DE89-016824] N90-12313
ENTROPY
Estimating functionals related to a density by a class of statistics based on spacings
[REPT-89-11] N90-12275
ENVIRONMENT EFFECTS
Coatings for gas turbine compressors
[NLR-MP-88045-U] N90-11750
Final environmental impact statement for the Galileo Mission (Tier 2)
[NASA-TM-101825] N90-12102
Global environmental effects of impact-generated aerosols: Results from a general circulation model
[DE89-008033] N90-12106
ENVIRONMENTAL MONITORING
Investigation on analyzing computer-aided forest disease classifications
[DFVLR-FB-89-16] N90-12112
ENVIRONMENTAL SURVEYS
Investigation on analyzing computer-aided forest disease classifications
[DFVLR-FB-89-16] N90-12112
ENVIRONMENTAL TESTS
Air velocity mapping of environmental test chambers
[AD-A212082] N90-11764
ENZYMOLOGY
USSR Space Life Sciences Digest, Issue 22
[NASA-CR-3922(26)-ISSUE-22] N90-12153
EPITAXY
Proceedings of the Workshop on Compound Semiconductor Devices and Integrated Circuits (13th) held in Cabourg, France on 10-12 May 1989
[AD-A211848] N90-11954
Development and evaluation of an instrument for rapid electroreflectance of semiconductor materials
[AD-A211690] N90-12376
EQUATIONS OF MOTION
Stall/spin/flight simulation
[DOT/FAA/CT-88/28] N90-11765
DART: A simulation code for charged particle beams, revision 1
[DE89-016697] N90-12312
Non-stationary computer model of the asymptotic region of an electric arc gas heater
[IPPCZ-288] N90-12330
EQUATIONS OF STATE
Phase behavior of pure and mixed systems at high pressure
[DE89-017734] N90-11832
VISAR wave profile measurements in supra-compressed HE
[DE89-017736] N90-11976
Characteristics of flyer impact for one-dimensional shock-wave study applications
[DE89-017887] N90-11977
Properties of strongly coupled multi-ionic plasmas
[DE89-017782] N90-12339
EQUATORIAL REGIONS
Observations and modelling of deep equatorial currents in the central Pacific
[PB89-198139] N90-12145
Dynamics of the equatorial undercurrent and its termination
[PB89-198147] N90-12146
Geology of the Venus equatorial region from Pioneer Venus radar imaging N90-12447
EQUILIBRIUM EQUATIONS
Equilibrium solutions of a spherical pendulum with rotating point of suspension and friction
[ESA-TT-1139] N90-12288

ERROR ANALYSIS
Discrete filtering techniques applied to sequential GPS range measurements
[NASA-CR-177472] N90-11730
Convergence results for pseudospectral approximations of hyperbolic systems by a penalty type boundary treatment
[NASA-CR-181929] N90-12230
ERRORS
Error estimation and self-adaptive mesh refinement for boundary element method N90-12037
A survey of camera error sources in machine vision systems
[DE89-014072] N90-12318
ESTIMATES
Error estimation and self-adaptive mesh refinement for boundary element method N90-12037
Likelihood cross-validation bandwidth selection for nonparametric kernel density estimators
[REPT-89-10] N90-12279
ESTIMATING
Statistical models for the optimal estimation of oceanic fields
[AD-A211786] N90-12149
On finding the largest normal mean and estimating the selected mean
[AD-A211628] N90-12245
Empirical Bayes estimation of binomial parameter with symmetric priors
[AD-A211646] N90-12246
Splines and equations of nonlinear parameters
[IMAG-RR-750-M] N90-12257
Fast sampling and stability of nonlinear sampled data systems. Part 2: Sampling rate estimations
[RR-341] N90-12271
Estimating functionals related to a density by a class of statistics based on spacings
[REPT-89-11] N90-12275
ETALONS
An imaging vector magnetograph for the next solar maximum N90-12489
EULER EQUATIONS OF MOTION
The upwind control volume scheme for unstructured triangular grids
[NASA-TM-101664] N90-11703
EULER-LAGRANGE EQUATION
A distributed pipelined architecture of the recursive Lagrangian equations of motion for robot manipulators with VLSI implementation — VLSI (very large scale integration)
[RR-353] N90-11966
EUROPEAN SPACE PROGRAMS
Laser sounding from space: Report of the ESA Technology Working Group on Space Laser Sounding and Ranging
[ESA-SP-1108] N90-12024
EVALUATION
Numerical simulation of aeroplane response to a lightning injection
[ETN-89-95271] N90-11716
EVAPORATION
Global distribution of moisture, evaporation-precipitation, and diabatic heating rates
N90-12069
EVOLUTION (DEVELOPMENT)
Evolution of flight commands in Aeritalia design
[ETN-89-95211] N90-11759
EXCIMER LASERS
Formation and modification of surface alloys by excimer laser melting and resolidification
[DE89-016968] N90-11856
EXHAUST FLOW SIMULATION
Steady and unsteady potential flow around thin annular wings and engines with simulation of jet engine flow
[DFVLR-FB-89-18] N90-11711
EXHAUST NOZZLES
Investigation of advanced mixer-ejector exhaust system
[AD-A211943] N90-11705
EXHAUSTION
The effect of caffeine on endurance time to exhaustion at high altitude
[AD-A212069] N90-12163
EXOBIOLOGY
USSR Space Life Sciences Digest, Issue 24
[NASA-CR-3922(28)-ISSUE-24] N90-12152
Aerospace medicine and biology: A continuing bibliography with indexes (supplement 329)
[NASA-SP-7011(329)] N90-12173
EXPERIMENT DESIGN
Conceptual design of liquid droplet radiator shuttle-attached experiment
[NASA-CR-185164] N90-11805
Conceptual design of liquid droplet radiator shuttle-attached experiment technical requirements document
[NASA-CR-185165] N90-11806
EXPERT SYSTEMS
Coupling rule-based and object-oriented programming for the classification of machined features
[DE89-017705] N90-11903
Reasoning about change and exceptions in automated process planning
[DE89-017706] N90-12195
Computer-based tutors for explaining and managing the process of diagnostic reasoning
[AD-A211738] N90-12222
Distributed knowledge-based systems
[AD-A211984] N90-12401
EXPLODING WIRES
Shock pressure determination in detonator wires
[DE89-017756] N90-12002
EXPLOSIONS
Indexes for the proceedings of the symposia (international) on detonation, 1951 through 1985
[DE89-015178] N90-11972
Exploding metallic foil fuse modeling at Los Alamos
[DE89-016970] N90-11998
EXPLOSIVES
A critical assessment of models available for the shock initiation of heterogeneous explosives
[MRL-TR-89-17] N90-11896
Sensitivity relationships in energetic materials
[DE89-016967] N90-11897
Indexes for the proceedings of the symposia (international) on detonation, 1951 through 1985
[DE89-015178] N90-11972
Lagrangian analysis of MIV (Magnetic Impulse-Velocity) gauge experiments on PBX 9502 using the mass-displacement moment function
[DE89-016612] N90-12000
EXTRAPOLATION
Sequential design of experiments with physically based models 23
[AD-A211918] N90-12239
EXTREME ULTRAVIOLET RADIATION
Investigation of atmospheric emissions in ultraviolet, vacuum ultraviolet, and extreme ultraviolet wavelength
[AD-A212169] N90-12123
EXTREMELY LOW RADIO FREQUENCIES
HIPAS 1987-88: ULF research and campaign support
[AD-A211720] N90-11933
EXTRUDING
Deformation of Ti-6Al-4V bar and extrusion under superplastic forming conditions
[RAE-TM-MAT/STR-1110] N90-11875
Deformation of extruded titanium alloys under superplastic conditions
[RAE-TM-MAT/STR-1111] N90-11876
EYE MOVEMENTS
Eye movements and spatial pattern vision
[AD-A211650] N90-12169

F

F-18 AIRCRAFT
Flutter clearance of the F-18 high-angle-of-attack research vehicle with experimental wingtip instrumentation pods
[NASA-TM-4148] N90-11732
F-86 AIRCRAFT
Scientific justification and development plan for a mid-sized jet research aircraft
[PB89-208995] N90-11731
FABRICATION
Manufacturing and the manufacturing engineer in the year 2000, revision
[DE89-017707] N90-11904
High gain flux compression generator fabrication issues
[DE89-017888] N90-11951
Design of scientific payloads and components
[AD-A211819] N90-12005
Fabrication of modulated vanes for a split-coaxial RFQ
[DE88-757235] N90-12310
Beam assisted fabrication of 3-5/Si monolithic devices
[AD-A212046] N90-12367
FABRICS
New Fabric Development Program
[AD-A211549] N90-11891
FABRY-PEROT INTERFEROMETERS
An imaging vector magnetograph for the next solar maximum N90-12489
FACTORIZATION
A matrix factorization and its application to large-scale linear programming
[AD-A211293] N90-12244
FAILURE ANALYSIS
Model 0A wind turbine generator FMEA
[NASA-TM-102378] N90-12034
FAILURE MODES
Independent Orbiter Assessment (IOA): Analysis of the displays and controls subsystem
[NASA-CR-185563] N90-11774
Independent Orbiter Assessment (IOA): Assessment of the orbiter main propulsion system FMEA/CIL, volume 1
[NASA-CR-185559-VOL-1] N90-11775
Independent Orbiter Assessment (IOA): Assessment of the main propulsion subsystem FMEA/CIL, volume 2
[NASA-CR-185559-VOL-2] N90-11776
Independent Orbiter Assessment (IOA): Assessment of the main propulsion subsystem FMEA/CIL, volume 3
[NASA-CR-18559-VOL-3] N90-11777
Independent Orbiter Assessment (IOA): Assessment of the main propulsion subsystem FMEA/CIL, volume 4
[NASA-CR-185559-VOL-4] N90-11778
Independent Orbiter Assessment (IOA): Assessment of the electrical power distribution and control subsystem, volume 1
[NASA-CR-185557-VOL-1] N90-11779
Independent Orbiter Assessment (IOA): Assessment of the electrical power distribution and control subsystem, volume 2
[NASA-CR-185557-VOL-2] N90-11780
Independent Orbiter Assessment (IOA): Assessment of the electrical power distribution and control subsystem, volume 3
[NASA-CR-185557-VOL-3] N90-11781
Independent Orbiter Assessment (IOA): Analysis of the active thermal control subsystem
[NASA-CR-185553] N90-11782
Independent Orbiter Assessment (IOA): FMEA/CIL assessment
[NASA-CR-185550] N90-11783
Independent Orbiter Assessment (IOA): Assessment of the guidance, navigation, and control subsystem FMEA/CIL
[NASA-CR-185552] N90-11784
Independent Orbiter Assessment (IOA): Assessment of the Electrical Power Distribution and Control/Electrical Power Generation (EPD and C/EPG) FMEA/CIL
[NASA-CR-185542] N90-11785
Independent Orbiter Assessment (IOA): Analysis of the life support and airlock support subsystems
[NASA-CR-185539] N90-11786
Independent Orbiter Assessment (IOA): Assessment of the orbital maneuvering system FMEA/CIL, volume 1
[NASA-CR-185544-VOL-1] N90-11787
Independent Orbiter Assessment (IOA): Assessment of the orbital maneuvering subsystem, volume 2
[NASA-CR-185544-VOL-2] N90-11788
Independent Orbiter Assessment (IOA): Assessment of the communication and tracking subsystem, volume 1
[NASA-CR-185528-VOL-1] N90-11789
Independent Orbiter Assessment (IOA): Assessment of the communication and tracking subsystem, volume 2
[NASA-CR-185528-VOL-2] N90-11790
Independent Orbiter Assessment (IOA): Assessment of the communication and tracking subsystem, volume 3
[NASA-CR-185528-VOL-3] N90-11791
Independent Orbiter Assessment (IOA): Assessment of the hydraulics/water spray boiler subsystem
[NASA-CR-185537] N90-11792
Independent Orbiter Assessment (IOA): Assessment of the reaction control system, volume 1
[NASA-CR-185543-VOL-1] N90-11793
Independent Orbiter Assessment (IOA): Assessment of the reaction control system, volume 3
[NASA-CR-185543-VOL-3] N90-11795
Independent Orbiter Assessment (IOA): Assessment of the reaction control system, volume 4
[NASA-CR-185543-VOL-4] N90-11796
Independent Orbiter Assessment (IOA): Assessment of the reaction control system, volume 5
[NASA-CR-185543-VOL-5] N90-11797
Model 0A wind turbine generator FMEA
[NASA-TM-102378] N90-12034
FAIRINGS
An experimental investigation of helicopter rotor hub fairing drag characteristics
[NASA-TM-102182] N90-11701
Axial compression buckling test on the H-2 launch vehicle satellite fairing structural element prototype (aluminum surface plate/aluminum honeycomb sandwiched curved surface plate)
[NAL-TM-563] N90-12039
FALSE ALARMS
Severe local storm warning verification: 1988
[PB89-226310] N90-12134
FAN BLADES
Fractographic and microstructural analysis of fatigue crack growth in a Ti-6Al-4V fan disc forging
[NLR-MP-88028-U] N90-11877

FAR ULTRAVIOLET RADIATION
Photolysis of spacecraft contaminants
[AD-A211715] N90-11801
Investigation of atmospheric emissions in ultraviolet, vacuum ultraviolet, and extreme ultraviolet wavelength
[AD-A212169] N90-12123
The SMM UV observations of Active Region 5395
N90-12465
Vacuum ultraviolet backgrounds from space - ten years after
[AD-A211353] N90-12493
FARADAY EFFECT
Effect of electrical double layer on transport limited currents at microelectrodes
[AD-A211586] N90-11843
FAST FOURIER TRANSFORMATIONS
Calculation of transient response from time-harmonic spectrum
[AD-A211972] N90-12241
FATIGUE (BIOLOGY)
Heatstroke pathophysiology: The energy depletion model
[AD-A212156] N90-12164
FATIGUE (MATERIALS)
Effects of a heat cycle on material strength
[NAL-TM-562] N90-11737
Stochastic propagation of an array of parallel cracks: Exploratory work on matrix fatigue damage in composite laminates
[DE89-017837] N90-11813
FATIGUE LIFE
Creep and fracture behavior of heat resistant steels in characteristic cases of variable fatigue loading
[ETN-89-94671] N90-11855
In service life monitoring system using g-meter readings and mass configuration control
[ETN-89-95218] N90-12035
FATIGUE TESTS
Creep and fracture behavior of heat resistant steels in characteristic cases of variable fatigue loading
[ETN-89-94671] N90-11855
Effect of fretting on fatigue strength of aluminium alloys
[ESDU-89004] N90-11870
Determination and description of the long term creep behavior of high temperature gas turbine materials
[ETN-89-94965] N90-11871
WISPER: A standardized fatigue load sequence for HAWT-blades
[NLR-MP-88029-U] N90-12055
FAULT TOLERANCE
An open-loop transient thermodynamic model of the Cougar turbojet
[AD-A211774] N90-11745
Redundancies and don't cares in sequential logic synthesis
[AD-A211931] N90-11956
FEASIBILITY ANALYSIS
Feasibility of graphics voice telephones for the post 2000 era
[FEL-1988-26] N90-11937
Computer controlled MHD power consolidation and pulse-generation system
[DE89-015600] N90-12333
FEDERAL BUDGETS
Forecasting contracting workload
[AD-A211935] N90-12387
FY 1990/FY 1991 biennial budget descriptive summaries for the Strategic Defense Initiative Organization
[AD-A211985] N90-12409
FEEDBACK CONTROL
Control of turbulent mixing layers
[AD-A211413] N90-11708
Adaptive control law design for model uncertainty compensation
[AD-A211712] N90-11758
Effect of control surface mass unbalance on the stability of a closed-loop active control system
[NASA-TP-2952] N90-12042
Adaptive feedback linearization: Stability and robustness
[PB89-219497] N90-12220
Operating experience with the Sandia terminal switching network and fiber optic loop
[DE89-007422] N90-12317
FEEDFORWARD CONTROL
A hybrid optimisation strategy for adaptive feed-forward layered networks
[RSRE-MEMO-4193] N90-12226
FERRITES
Development of high frequency spice models for ferrite core inductors and transformers
[DE89-015121] N90-11946
Parametric study of power absorption from electromagnetic waves by small ferrite spheres
[NASA-TP-2949] N90-12282
FERROELECTRICITY
Analysis of the efficiency of a dielectric solar energy collector
[PB89-212716] N90-12092
FIBER COMPOSITES
An integrated methodology for optimizing structural composite damping
[NASA-TM-102343] N90-11808
Interlaminar stress concentration in fiber composites
[ETN-89-94670] N90-11809
Carbon fiber reinforced glass matrix composites for structural space based applications
[AD-A211682] N90-11818
FIBER OPTICS
In-situ cure monitoring of composites by fiber-optic molecular sensors
[AD-A211495] N90-11817
High power, solid state RF pulse generators
[AD-D014172] N90-11941
Operating experience with the Sandia terminal switching network and fiber optic loop
[DE89-007422] N90-12317
Optical data transmission systems in radiation environment
[DE90-000174] N90-12322
Small-radius bending loss in single-mode fibers
[AD-A211822] N90-12323
FIELD THEORY (PHYSICS)
Operator product coefficients in non-diagonal conformal field theories
[PB89-216873] N90-12283
Bordered surfaces, off-shell amplitudes, sewing, and string field theory
[DE90-000006] N90-12378
FIGHTER AIRCRAFT
Problems related to the acquisition, processing and utilization of the modal parameters measured in flight tests in order to obtain the full envelope for flutter
[ETN-89-95210] N90-11735
Future military powerplants — fighter aircraft engines
[PNR90554] N90-11749
Low-speed wind-tunnel study of reaction control-jet effectiveness for hover and transition of a STOVL fighter concept
[NASA-TM-4147] N90-11751
The aerodynamic experimental center of Aeritalia: Combat aircraft group
[ETN-89-95213] N90-11766
FILM THICKNESS
Calculation on film preparation and film motion of a swirl atomizer
[ESA-TT-1096] N90-11990
Absolute determination of the wall shear stress by means of an interferometer
[DFVLR-FB-89-13] N90-11991
FINITE DIFFERENCE THEORY
Effect of electrical double layer on transport limited currents at microelectrodes
[AD-A211586] N90-11843
Viscous split algorithms for the time dependent incompressible Navier-Stokes equations
[AD-A211592] N90-11985
FINITE ELEMENT METHOD
Computational methods for complex flowfields
[AD-A211485] N90-11983
Efficient finite element solution of Navier-Stokes equations and related topics
[AD-A211647] N90-11986
A C(Superscript)-Anisoparametric three-node shallow shell element for general shell analysis
[AD-A212094] N90-12049
Investigation of difficult component effects on finite element model vibration prediction for the Bell AH-1G helicopter. Volume 1: Ground vibration test results
[NASA-CR-181916-VOL-1] N90-12058
A least-squares finite element method for incompressible Navier-Stokes problems
[NASA-TM-102385] N90-12231
Numerical solution of acoustic-structure interaction problems
[AD-A211505] N90-12293
An electromagnetic finite element particle code on an unstructured grid
[DE89-017532] N90-12336
FINLAND
Calculated solar radiation incident upon slopes of different orientated surfaces in Finland
[FMI-MP-8] N90-12116
FINS
Simulation of glancing shock wave and boundary layer interaction
[NASA-TM-102233] N90-11970
FIRE EXTINGUISHERS
Aircraft cabin fire suppression by means of an interior water spray system
[CAA-PAPER-88014] N90-11719
FIRE PREVENTION
Aircraft cabin fire suppression by means of an interior water spray system
[CAA-PAPER-88014] N90-11719
FIREPROOFING
Aircraft cabin fire suppression by means of an interior water spray system
[CAA-PAPER-88014] N90-11719
FISCHER-TROPSCH PROCESS
Natural gas to liquids
[DE89-000982] N90-11828
FIXED POINTS (MATHEMATICS)
On the differentiable manifold of fixed order stable linear systems
[REPT-88-89] N90-12250
FLAME PROPAGATION
Premixed turbulent flame propagation
[AD-A211489] N90-11841
FLAMMABILITY
Flammability, smoke, and dry arc tracking tests of aircraft electrical wire insulations
[DOT/FAA/CT-89/21] N90-11714
FLEXIBILITY
Flexure strength of advanced ceramics: A round robin exercise
[AD-A212101] N90-11889
FLEXIBLE BODIES
Computer-aided design of flexible assembly systems
[PB89-216253] N90-12025
FLEXING
Flexure strength of advanced ceramics: A round robin exercise
[AD-A212101] N90-11889
FLIGHT CHARACTERISTICS
Unsteady aerodynamics with applications to flight mechanics
[AD-A211944] N90-11706
Comparison of flying qualities derived from in-flight and ground-based simulators for a jet-transport airplane for the approach and landing pilot tasks
[NASA-TP-2962] N90-11757
FLIGHT CONTROL
Applications of flight control system methods to an advanced combat rotorcraft
[NASA-TM-101054] N90-11752
Robust control design for flight control
[AD-A211957] N90-11756
Comparison of flying qualities derived from in-flight and ground-based simulators for a jet-transport airplane for the approach and landing pilot tasks
[NASA-TP-2962] N90-11757
Adaptive control law design for model uncertainty compensation
[AD-A211712] N90-11758
FLIGHT ENVELOPES
Stability and control derivatives of the De Havilland DHC-2 BEAVER aircraft
[PB89-217525] N90-11754
FLIGHT INSTRUMENTS
Independent Orbiter Assessment (IOA): Analysis of the displays and controls subsystem
[NASA-CR-185563] N90-11774
Design of scientific payloads and components
[AD-A211819] N90-12005
FLIGHT MANAGEMENT SYSTEMS
Navigation experiment NAVEX: The equipment delay times in the Spacelab mission D1
[DFVLR-MITT-89-10] N90-11728
FLIGHT MECHANICS
Unsteady aerodynamics with applications to flight mechanics
[AD-A211944] N90-11706
FLIGHT OPERATIONS
Independent Orbiter Assessment (IOA): Analysis of the displays and controls subsystem
[NASA-CR-185563] N90-11774
FLIGHT OPTIMIZATION
Sequential design of experiments with physically based models 23
[AD-A211918] N90-12239
FLIGHT PATHS
The 1987 survey of track keeping and altitudes on Heathrow and Gatwick standard instrument departure routes (DAY)
[CAA-PAPER-88010] N90-11729
FLIGHT RECORDERS
Post crash flight analysis: Visualizing flight recorder data
[AD-A212063] N90-11715
FLIGHT SAFETY
UK airmisses involving commercial air transport
[CAA-2/88] N90-11718

FLIGHT SIMULATION
Stability and control derivatives of the De Havilland DHC-2 BEAVER aircraft
[PB89-217525] N90-11754
Comparison of flying qualities derived from in-flight and ground-based simulators for a jet-transport airplane for the approach and landing pilot tasks
[NASA-TP-2962] N90-11757
Stall/spin/flight simulation
[DOT/FAA/CT-88/28] N90-11765
FLIGHT TEST INSTRUMENTS
Devices and procedures for the calibration of sensors and measurement: Systems of the flight test support system ATTAS
[DFVLR-MITT-89-06] N90-12007
FLIGHT TESTS
Problems related to the acquisition, processing and utilization of the modal parameters measured in flight tests in order to obtain the full envelope for flutter
[ETN-89-95210] N90-11735
Propfan Test Assessment (PTA): Flight test report
[NASA-CR-182278] N90-11738
Propfan Test Assessment (PTA)
[NASA-CR-185138] N90-11739
Devices and procedures for the calibration of sensors and measurement: Systems of the flight test support system ATTAS
[DFVLR-MITT-89-06] N90-12007
FLOODS
Satellite-derived rainfall estimates and propagation characteristics associated with the Mesoscale Convective Systems (MCSs)
[PB89-213417] N90-12086
FLOW CHARACTERISTICS
The determination of the aerodynamic characteristics of an ogive-cylinder body in subsonic, curved, incompressible flow, and an assessment of the effect of flow curvature
[REPT-87-13] N90-11712
Numerical computation of the viscous flow field around a prolate spheroid
[DFVLR-FB-89-22] N90-11992
FLOW DISTRIBUTION
The structure of separated flow regions occurring near the leading edge of airfoils - including transition
[NASA-CR-185853] N90-11695
Investigation of advanced mixer-ejector exhaust system
[AD-A211943] N90-11705
Computation of ramjet internal flowfields
[AD-A212001] N90-11743
Analytical studies of three-dimensional combustion processes
[AD-A211903] N90-11837
Experimental investigation of a planar shock wave over a double wedge
[AD-A211366] N90-11981
Computational methods for complex flowfields
[AD-A211485] N90-11983
Three-dimensional, two-phase, transonic, canted nozzle flows
[AD-A211528] N90-11984
Experimental research on swept shock Wave/Boundary layer interactions
[AD-A211744] N90-11988
FLOW EQUATIONS
A multigrid method combined with defect correction for free convection problems at high Rayleigh numbers
[REPT-89-27] N90-12264
FLOW GEOMETRY
Analytical studies of three-dimensional combustion processes
[AD-A211903] N90-11837
FLOW STABILITY
Elimination of spurious eigenvalues in the Chebyshev tau spectral method
[PB89-209282] N90-11967
A study of the temporal stability of multiple cell vortices
[NASA-CR-4261] N90-11968
FLOW VELOCITY
Some implications of the isotropic momentarily frozen assumptions for the SPAN-MAT program
[NASA-CR-181937] N90-11704
Air velocity mapping of environmental test chambers
[AD-A212082] N90-11764
FLOW VISUALIZATION
Application of the wide-field shadowgraph technique to rotor wake visualization
[NASA-TM-102222] N90-11700
Advanced technology in military gas turbine design and manufacture
[PNR90545] N90-11747
Experimental research on swept shock Wave/Boundary layer interactions
[AD-A211744] N90-11988
FLUID BOUNDARIES
On the computation of normal modes of a rotating, viscous, incompressible fluid with a capillary free boundary
[REPT-89-01] N90-11989
FLUID DYNAMICS
Some new algorithms for boundary value problems in smooth particle hydrodynamics
[AD-A211728] N90-11987
Dynamics of baroclinic wave systems N90-12072
A least-squares finite element method for incompressible Navier-Stokes problems
[NASA-TM-102385] N90-12231
FLUID FLOW
Analytical studies of three-dimensional combustion processes
[AD-A211903] N90-11837
FLUID JETS
Three component laser Doppler measurements in an axisymmetric jet
[NASA-CR-181908] N90-11702
FLUID MANAGEMENT
Independent Orbiter Assessment (IOA): Assessment of the orbiter main propulsion system FMEA/CIL, volume 1
[NASA-CR-185559-VOL-1] N90-11775
Independent Orbiter Assessment (IOA): Assessment of the main propulsion subsystem FMEA/CIL, volume 2
[NASA-CR-185559-VOL-2] N90-11776
Independent Orbiter Assessment (IOA): Assessment of the main propulsion subsystem FMEA/CIL, volume 3
[NASA-CR-18559-VOL-3] N90-11777
Independent Orbiter Assessment (IOA): Assessment of the main propulsion subsystem FMEA/CIL, volume 4
[NASA-CR-185559-VOL-4] N90-11778
FLUID MECHANICS
Numerical analysis, scientific computing and fundamental studies of fluid mechanics
[DE89-017554] N90-11975
FLUORESCENCE
In-situ cure monitoring of composites by fiber-optic molecular sensors
[AD-A211495] N90-11817
LABCEDE fluorescence investigations
[AD-A210678] N90-12114
Comparison of the LOWTRAN 7 code and S3-4 satellite measurements of UV radiance
[AD-A211356] N90-12124
FLUOROCARBONS
Synthesis and chemistry of strained and conjugated fluorocarbons
[AD-A211633] N90-11844
Potential technologies for collection and destruction of CFCs (Chlorofluorocarbons), halons, and related compounds
[PB89-219968] N90-12105
FLUOROHYDROCARBONS
Synthesis and chemistry of strained and conjugated fluorocarbons
[AD-A211633] N90-11844
FLUTTER
Flutter clearance of the F-18 high-angle-of-attack research vehicle with experimental wingtip instrumentation pods
[NASA-TM-4148] N90-11732
Effect of control surface mass unbalance on the stability of a closed-loop active control system
[NASA-TP-2952] N90-12042
FLUTTER ANALYSIS
Problems related to the acquisition, processing and utilization of the modal parameters measured in flight tests in order to obtain the full envelope for flutter
[ETN-89-95210] N90-11735
FLUX DENSITY
Assessment of thin film batteries based on polymer electrolytes. Part 1: Energy density
[AD-A212111] N90-11958
Fluctuations in transverse energy and multiplicity, energy densities, and neutral pion spectra in nucleus-nucleus collisions at 200 GeV/nucleon
[DE89-017583] N90-12302
FLY BY WIRE CONTROL
Engine controls for the 1990's
[PNR90546] N90-11748
FOCUSING
Near-planar TS waves and longitudinal vortices in channel flow: Nonlinear interaction and focusing
[NASA-CR-181928] N90-11698
Generation and focusing of pulsed intense ion beams
[DE89-017558] N90-12338
FOKKER-PLANCK EQUATION
Development of a numerical solution to the time dependent kinetic equation N90-12481
FOLDS (GEOLOGY)
Architecture of orogenic belts and convergent zones in Western Ishtar Terra, Venus N90-12437
Tectonism on Venus: A review N90-12440
FORCED VIBRATION
Active control of the forced and transient response of a finite beam N90-12040
FOREBODIES
Normal-force-curve and pitching-moment-curve slopes of forebody-cylinder combinations at zero angle of attack for Mach numbers up to 5
[ESDU-89008] N90-11709
FORECASTING
Manufacturing and the manufacturing engineer in the year 2000, revision
[DE89-017707] N90-11904
Forecasting contracting workload
[AD-A211935] N90-12387
FOREST MANAGEMENT
Investigation on analyzing computer-aided forest disease classifications
[DFVLR-FB-89-16] N90-12112
FORMAT
FORTRAN program for x ray photoelectron spectroscopy data reformatting
[NASA-TP-2957] N90-12348
FORMULATIONS
Effective permeability of mixtures
[PB89-218952] N90-11839
FORTRAN
Manual for Program PSTRESS: Peel stress computation
[NASA-CR-178408] N90-11822
Calculation of transient response from time-harmonic spectrum
[AD-A211972] N90-12241
FORTRAN program for x ray photoelectron spectroscopy data reformatting
[NASA-TP-2957] N90-12348
FORWARD SCATTERING
Droplet sizing instrumentation used for icing research: Operation, calibration, and accuracy
[NASA-CR-182293] N90-11999
FOSSIL FUELS
Activities report on KEMA R and D
[ST-REPT-VOL-6-NO-12] N90-12100
FRACTOGRAPHY
Fractographic and microstructural analysis of fatigue crack growth in a Ti-6Al-4V fan disc forging
[NLR-MP-88028-U] N90-11877
Flexure strength of advanced ceramics: A round robin exercise
[AD-A212101] N90-11889
FRACTURE MECHANICS
Deformation behavior of SiC/2014 Al metal-matrix composite
[AD-A212095] N90-11816
Fundamental tribological properties of ion-beam-deposited boron nitride films
[NASA-TM-102088] N90-11881
An application of the J-integral to an incremental analysis of blunting crack behavior
[DE89-016844] N90-12046
An experimental and analytical program to develop crack tip fracture criteria
[AD-A211565] N90-12051
FRACTURE STRENGTH
Fracture toughness data base for HT9 and modified 9Cr-1Mo irradiated in several reactors up to approximately 100 dpa
[DE90-000111] N90-11864
FRAGMENTATION
Kinetics of diffusion-controlled reactions
[AD-A212161] N90-12286
Electron attachment and molecular fragmentation in laser-excited plasmas
[AD-A212098] N90-12343
FRANCE
Crau 1987: The KNMI contribution --- KNMI (Royal Netherlands Meteorological Institute)
[KNMI-TR-110] N90-12140
FREE CONVECTION
A multigrid method combined with defect correction for free convection problems at high Rayleigh numbers
[REPT-89-27] N90-12264
FREE ELECTRON LASERS
A proposed linac cavity RF drive system for the Los Alamos extreme ultraviolet free-electron laser
[DE89-016614] N90-12016
FREE JETS
Cryogenic free jets
[ESA-TT-1128] N90-11767
FREEZING
Studies on the startup transients and performance of a gas loaded sodium heat pipe
[AD-A211880] N90-12379
FREQUENCY MEASUREMENT
Time and frequency in geodesy measuring methods
[SER-C-337] N90-12087

FREQUENCY MODULATION
Fabrication of modulated vanes for a split-coaxial RFQ
[DE88-757235] N90-12310

FREQUENCY MULTIPLIERS
Design, construction and test of a frequency doubler for 183 GHz
[PB89-212591] N90-11944

FREQUENCY RESPONSE
Effects of mistuning and matrix structure on the topology of frequency response curves
[NASA-TM-102290] N90-12041

FRETTING
Effect of fretting on fatigue strength of aluminium alloys
[ESDU-89004] N90-11870

FRICTION
Three-dimensional viscoelastic bodies in steady state frictional rolling contact with generalization to Knothe rolling
[REPT-89-23] N90-12032

FUEL CELLS
Fuel cells for vehicle propulsion applications: A thermodynamic systems analysis
[DE89-017689] N90-11950
A lightweight solid polymer electrolyte fuel cell with stack power density of 3 kW/lb (7 kW/kg)
[AD-A211542] N90-12098

FUEL COMBUSTION
Analysis of opposed jet hydrogen-air counter flow diffusion flame
[NASA-CR-182366] N90-11825
Correlating microemulsion fuel composition, structure and combustion properties
[DE89-017779] N90-11898

FUEL CONTROL
Independent Orbiter Assessment (IOA): Assessment of the orbiter main propulsion system FMEA/CIL, volume 1
[NASA-CR-185559-VOL-1] N90-11775
Independent Orbiter Assessment (IOA): Assessment of the main propulsion subsystem FMEA/CIL, volume 2
[NASA-CR-185559-VOL-2] N90-11776
Independent Orbiter Assessment (IOA): Assessment of the main propulsion subsystem FMEA/CIL, volume 3
[NASA-CR-18559-VOL-3] N90-11777
Independent Orbiter Assessment (IOA): Assessment of the main propulsion subsystem FMEA/CIL, volume 4
[NASA-CR-185559-VOL-4] N90-11778

FUEL SYSTEMS
Independent Orbiter Assessment (IOA): Assessment of the orbiter main propulsion system FMEA/CIL, volume 1
[NASA-CR-185559-VOL-1] N90-11775
Independent Orbiter Assessment (IOA): Assessment of the main propulsion subsystem FMEA/CIL, volume 2
[NASA-CR-185559-VOL-2] N90-11776
Independent Orbiter Assessment (IOA): Assessment of the main propulsion subsystem FMEA/CIL, volume 3
[NASA-CR-18559-VOL-3] N90-11777
Independent Orbiter Assessment (IOA): Assessment of the main propulsion subsystem FMEA/CIL, volume 4
[NASA-CR-185559-VOL-4] N90-11778

FUELS
Methanol fueled vehicles and photochemical models: An evaluation of the state of knowledge
[PB89-214225] N90-12410

FUNCTIONAL ANALYSIS
Visual motion perception
[AD-A210994] N90-12160

FUNCTIONALS
Estimating functionals related to a density by a class of statistics based on spacings
[REPT-89-11] N90-12275

FUNCTIONS (MATHEMATICS)
Smooth linearization of hyperbolic fixed points without resonance conditions
[REPT-89-03] N90-12251

FURNACES
Modelling and control of a diffusion/LPCVD furnace
[REPT-88-97] N90-11910

FUSELAGES
Transport composite fuselage technology: Impact dynamics and acoustic transmission
[NASA-CR-4035] N90-11821

FUZZY SETS
Fuzzy logic and the generalized modus ponens
[REPT-88-92] N90-12274

G

GALERKIN METHOD
Viscous split algorithms for the time dependent incompressible Navier-Stokes equations
[AD-A211592] N90-11985

GALILEO PROJECT
Final environmental impact statement for the Galileo Mission (Tier 2)
[NASA-TM-101825] N90-12102

GALLIUM ALLOYS
A critical assessment of thermodynamic and phase diagram data for the Ga-In system
[NPL-DMA(A)-174] N90-12382

GALLIUM ARSENIDES
On-orbit annealing of gallium arsenide solar cell arrays
[AD-A212087] N90-11900
Ion beam deposition of epitaxial germanium and gallium arsenide layers
[DE89-017439] N90-12357
Subnanosecond linear GaAs photoconductive switching, revision 1
[DE89-017739] N90-12363
Development and evaluation of an instrument for rapid electroreflectance of semiconductor materials
[AD-A211690] N90-12376

GALLIUM ISOTOPES
The Baksan gallium solar neutrino experiment
[DE89-016036] N90-12457

GAMMA RAY ASTRONOMY
Scientific objectives of solar gamma-ray observations
N90-12463
The Gamma-Ray Observatory: An overview
N90-12464

GAMMA RAY BURSTS
The BATSE experiment on the Gamma Ray Observatory: Solar flare hard x ray and gamma-ray capabilities
N90-12469
The solar flare and cosmic gamma-ray burst experiment aboard the Ulysses spacecraft N90-12470

GAMMA RAY OBSERVATORY
The Gamma-Ray Observatory: An overview
N90-12464
Capabilities of GRO/OSSE for observing solar flares
N90-12467
The solar gamma ray and neutron capabilities of COMPTEL on the Gamma Ray Observatory N90-12468
The BATSE experiment on the Gamma Ray Observatory: Solar flare hard x ray and gamma-ray capabilities
N90-12469

GAMMA RAY SPECTROMETERS
Capabilities of GRO/OSSE for observing solar flares
N90-12467
A high-speed digital camera system for the observation of rapid H-alpha fluctuations in solar flares N90-12491

GAMMA RAY TELESCOPES
The solar gamma ray and neutron capabilities of COMPTEL on the Gamma Ray Observatory N90-12468
Solar flare gamma-ray and hard x ray imaging with the GRID-on-a-balloon N90-12474

GAMMA RAYS
An experimental high energy physics program
[DE89-014695] N90-12311
The hard x rays and gamma-rays from solar flares
[NASA-CR-185982] N90-12458
The BATSE experiment on the Gamma Ray Observatory: Solar flare hard x ray and gamma-ray capabilities
N90-12469
The solar flare and cosmic gamma-ray burst experiment aboard the Ulysses spacecraft N90-12470

GAS DISSOCIATION
An empirical formula for gas switch breakdown delay
[DE89-017233] N90-11947

GAS MIXTURES
An empirical formula for gas switch breakdown delay
[DE89-017233] N90-11947
A nonlinear-optical method for combining high power laser beams
[AD-A211730] N90-12022

GAS PRESSURE
Apparatus and method for monitoring pressure leaks from a sealed system
[AD-D014168] N90-11995

GAS TURBINE ENGINES
Advanced technology in military gas turbine design and manufacture
[PNR90545] N90-11747

GAS TURBINES
Determination and description of the long term creep behavior of high temperature gas turbine materials
[ETN-89-94985] N90-11871

GAS-SOLID INTERACTIONS
Venus volcanism: Rate estimates from laboratory studies of sulfur gas-solid reactions N90-12428

GASES
Non-stationary computer model of the asymptotic region of an electric arc gas heater
[IPPCZ-288] N90-12330

GATES (CIRCUITS)
A single-phase clocked NOR/NOR CMOS programmable sequential array structure
[AD-A211297] N90-12203

GAUGE INVARIANCE
Two dimensional conformal supergravity and critical behavior
[DE89-611968] N90-12414

GEAR TEETH
Generation and tooth contact analysis of spiral bevel gears with predesigned parabolic functions of transmission errors
[NASA-CR-4259] N90-12033

GEARS
Generation and tooth contact analysis of spiral bevel gears with predesigned parabolic functions of transmission errors
[NASA-CR-4259] N90-12033

GENE EXPRESSION
Genetic engineering of enhanced microbial nitrification
[PB89-208334] N90-12155

GENES
Genetic engineering of enhanced microbial nitrification
[PB89-208334] N90-12155

GENETIC ENGINEERING
Genetic engineering of enhanced microbial nitrification
[PB89-208334] N90-12155

GENETICS
USSR Space Life Sciences Digest, Issue 22
[NASA-CR-3922(26)-ISSUE-22] N90-12153
Genetic engineering of enhanced microbial nitrification
[PB89-208334] N90-12155

GEOCHRONOLOGY
Three ages of Venus N90-12453

GEODESY
Time and frequency in geodesy measuring methods
[SER-C-337] N90-12087

GEODETIC ACCURACY
Time and frequency in geodesy measuring methods
[SER-C-337] N90-12087

GEOMAGNETISM
HIPAS 1987-88: ULF research and campaign support
[AD-A211720] N90-11933
Processing of DMSP magnetic data and its use in geomagnetic field modeling
[NASA-TM-100750] N90-12115
Time-weighted accumulations ap(tau) and Kp(tau)
[RAE-TR-88050] N90-12422
On the statistics of El Nino occurrences and the relationship of El Nino to volcanic and solar/geomagnetic activity
[NASA-TP-2948] N90-12456

GEOPHYSICAL FLUID FLOW CELLS
Laboratory and theoretical models of planetary-scale instabilities and waves N90-12076
Laboratory and theoretical studies of baroclinic processes N90-12077

GEOPHYSICS
Global atmospheric moisture variability N90-12062
Dynamics of baroclinic wave systems N90-12072
Processing of DMSP magnetic data and its use in geomagnetic field modeling
[NASA-TM-100750] N90-12115
Reports of planetary geology and geophysics program, 1988
[NASA-TM-4130] N90-12454

GEOTEMPERATURE
Ozone depletion, greenhouse gases, and climate change
[NASA-CR-185323] N90-12101

GERMANIUM
High resolution X-ray spectroscopy using germanium microcalorimeters
[DE89-017784] N90-12004
Ion beam deposition of epitaxial germanium and gallium arsenide layers
[DE89-017439] N90-12357

GLASS
Carbon fiber reinforced glass matrix composites for structural space based applications
[AD-A211682] N90-11818
Current research in advanced materials
[DE89-017466] N90-11884
Linear (passive) and non-linear guided and studies in glass
[AD-A211693] N90-12325

GLIDE PATHS
ILS mathematical modeling study of the effects of proposed hangar construction at the Orlando International Airport, Runway 17R, Orlando, Florida
[DOT/FAA/CT-TN89/52] N90-11762

GLOBAL ATMOSPHERIC RESEARCH PROGRAM
Dynamics and energetics of the South Pacific Convergence Zone during FGGE SOP-1 and South Pacific Convergence Zone and global-scale N90-12065

GLOBAL POSITIONING SYSTEM
Sentinel satellite positional precision derived from the NAVSTAR global positioning system
[AD-A211876] N90-11720

Discrete filtering techniques applied to sequential GPS range measurements
[NASA-CR-177472] N90-11730

GLOBAL TRACKING NETWORK
World Weather Watch: Implementation
[WMO-714] N90-12139

GLOW DISCHARGES
Advances and directions of ion nitriding/carburizing
[NASA-TM-102398] N90-11902

GLUCOSIDES
Cellular and molecular mechanisms of high pressure inotropy in cardiac muscle
[AD-A211695] N90-12170

GLUES
Design of glued joints, elastoplastic adhesives
[DRIC-T-8168] N90-11894

GLYCOLYSIS
Heatstroke pathophysiology: The energy depletion model
[AD-A212156] N90-12164

GOGGLES
Visual acuity and stereopsis with night vision goggles
[AD-A211552] N90-12167

GOLD
X ray diffraction patterns of metal aurocyanides
[DE89-015188] N90-11851

GOODNESS OF FIT
Computer problems in goodness-of-fit
[AD-A211411] N90-12268

GRAIN BOUNDARIES
Elevated temperature aluminum-titanium alloy by powder metallurgy process
[AD-D014165] N90-11852
Kinetic processes in advanced alloys
[AD-A212049] N90-11867
Characterization of the Structure and Chemistry of Defects in Materials: Proceedings, volume 138
[DE89-014796] N90-12352
Effects of grain boundary chemistry on critical current density in oxide superconductors
[DE89-017780] N90-12365

GRAIN SIZE
Kinetic processes in advanced alloys
[AD-A212049] N90-11867

GRAMMARS
Computer generation of a tutorial dialogue
[AD-A211976] N90-12162
Augmentations of grammatical categories in distributional-algebraic models of natural languages
[REPT-89-24] N90-12262

GRANULAR MATERIALS
A numerical laboratory for granular solids
[DE89-016367] N90-12045

GRAPHIC ARTS
Post crash flight analysis: Visualizing flight recorder data
[AD-A212063] N90-11715

GRAPHITE
Calculation of the refractive index change in dissociating shocked benzene
[DE89-017737] N90-11833

GRAPHS (CHARTS)
Parallel graph contraction
[AD-A211916] N90-12199

GRATINGS (SPECTRA)
A nonlinear-optical method for combining high power laser beams
[AD-A211730] N90-12022

GRAVITATIONAL EFFECTS
USSR Space Life Sciences Digest, Issue 22
[NASA-CR-3922(26)-ISSUE-22] N90-12153

GRAVITY WAVES
Effects on electromagnetic wave propagation and rocket vapor trails of intense turbulence generated by breaking internal gravity waves
[AD-A211755] N90-12130

GREEN'S FUNCTIONS
Spectral-domain analysis of finite frequency selective surfaces
[AD-A211669] N90-11932

GREENHOUSE EFFECT
Ozone depletion, greenhouse gases, and climate change
[NASA-CR-185323] N90-12101
Policies to encourage private sector responses to potential climate change
[DE89-017244] N90-12107
Ozone depletion, greenhouse gases, and climate change
[PB89-216097] N90-12110

GRINDING MACHINES
Kinematic design NC optical generator N90-12316

GROUND STATIONS
Discrete filtering techniques applied to sequential GPS range measurements
[NASA-CR-177472] N90-11730

GROUND SUPPORT EQUIPMENT
Design of scientific payloads and components
[AD-A211819] N90-12005

GROUND TESTS
Acoustic-thermal environment for USB flap structure. Report 1: Ground simulation test results
[NAL-TM-567] N90-11697

H

HABITS
Demonstration of replicable dimensions of health behaviors
[AD-A211920] N90-12161

HALL EFFECT
Superconductivity and magnetic scattering in the Nd(sub 2-x)Ce(sub x)CuO(sub 4-delta)
[DE89-016524] N90-12354

HALOGEN COMPOUNDS
Vapour pressures and critical points of liquids. Halogenated hydrocarbons
[ESDU-89006] N90-11848

HAMILTON-JACOBI EQUATION
The nonconvex multi-dimensional Riemann problem for Hamilton-Jacobi equations
[NASA-CR-181887] N90-12182

HAMILTONIAN FUNCTIONS
Ground-state coding in partially connected neural networks
[NASA-TM-102239] N90-12227
Homoclinic orbits for a class of Hamiltonian systems
[AD-A210562] N90-12229

HANGARS
ILS mathematical modeling study of the effects of proposed hangar construction at the Orlando International Airport, Runway 17R, Orlando, Florida
[DOT/FAA/CT-TN89/52] N90-11762

HARDNESS
Improving snow roads and airstrips in Antarctica
[AD-A211588] N90-11907

HARDNESS TESTS
Thermomechanical contact phenomena and wear of sliding components
[AD-A211290] N90-12028

HARMONIC ANALYSIS
Processing of DMSP magnetic data and its use in geomagnetic field modeling
[NASA-TM-100750] N90-12115

HARMONIC CONTROL
Active control of the forced and transient response of a finite beam N90-12040

HARMONIC OSCILLATORS
Analysis of a system of two weakly nonlinear coupled harmonic oscillators arising from the field of wind-induced vibrations
[REPT-89-22] N90-12261

HARMONICS
Homoclinic orbits for a class of Hamiltonian systems
[AD-A210562] N90-12229
Calculation of transient response from time-harmonic spectrum
[AD-A211972] N90-12241

HAZARDS
Base level management of radio frequency radiation protection program
[AD-A211787] N90-12171

HEALTH PHYSICS
Final environmental impact statement for the Galileo Mission (Tier 2)
[NASA-TM-101825] N90-12102

HEARING
Adaptive information processing in auditory cortex
[AD-A211294] N90-12166

HEART
Cellular and molecular mechanisms of high pressure inotropy in cardiac muscle
[AD-A211695] N90-12170

HEART RATE
The effect of caffeine on endurance time to exhaustion at high altitude
[AD-A212069] N90-12163

HEAT EXCHANGERS
Application of process integration to utilities, combined heat and power, and heat pumps
[ESDU-89001] N90-11909
An introduction to effectiveness: NTU relationships
[ESDU-89016] N90-12381

HEAT FLUX
Low level remote sensing: Orographic winds
N90-12066
Description of a software library for the calculation of surface fluxes
[KNMI-TR-112] N90-12141

HEAT PIPES
Studies on the startup transients and performance of a gas loaded sodium heat pipe
[AD-A211880] N90-12379

HEAT RADIATORS
Independent Orbiter Assessment (IOA): Analysis of the active thermal control subsystem
[NASA-CR-185553] N90-11782

HEAT RESISTANT ALLOYS
Creep and fracture behavior of heat resistant steels in characteristic cases of variable fatigue loading
[ETN-89-94671] N90-11855
Determination and description of the long term creep behavior of high temperature gas turbine materials
[ETN-89-94985] N90-11871

HEAT SINKS
Thermal model for double-drift IMPATT diodes on diamond heat sinks
[AD-A211746] N90-12380

HEAT STROKE
Heatstroke pathophysiology: The energy depletion model
[AD-A212156] N90-12164

HEAT TRANSFER
Application of process integration to utilities, combined heat and power, and heat pumps
[ESDU-89001] N90-11909
Convective heat transfer in hypobaric environments
[AD-A212060] N90-11979
Prediction of the thermal environment and thermal response of simple panels exposed to radiant heat
[NASA-TM-101660] N90-12292
An introduction to effectiveness: NTU relationships
[ESDU-89016] N90-12381

HEAT TRANSFER COEFFICIENTS
Modelling and control of a diffusion/LPCVD furnace
[REPT-88-97] N90-11910

HEAT TREATMENT
An experimental and analytical program to develop crack tip fracture criteria
[AD-A211565] N90-12051

HEATERS
Prediction of the thermal environment and thermal response of simple panels exposed to radiant heat
[NASA-TM-101660] N90-12292

HEATING
Microwave Tokamak Experiment (MTX) ohmic heating system
[DE89-017892] N90-12340

HEATING EQUIPMENT
Non-stationary computer model of the asymptotic region of an electric arc gas heater
[IPPCZ-288] N90-12330

HEAVY IONS
Fluctuations in transverse energy and multiplicity, energy densities, and neutral pion spectra in nucleus-nucleus collisions at 200 GeV/nucleon
[DE89-017583] N90-12302
Heating and acceleration of coronal and chromospheric ions during solar flares N90-12479

HEINKEL AIRCRAFT
On the occasion of the 100th birthday of Ernst Heinkel
[MBB/LW/3015/S/PUB/321] N90-12494

HELICOPTER DESIGN
Controller design for active vibration suppression of a helicopter
[DFVLR-FB-89-20] N90-11760

HELICOPTER ENGINES
Coatings for gas turbine compressors
[NLR-MP-88045-U] N90-11750

HELICOPTER WAKES
Application of the wide-field shadowgraph technique to rotor wake visualization
[NASA-TM-102222] N90-11700
Analysis of heliport environmental data: Indianapolis downtown heliport, Wall Street heliport. Volume 2: Wall Street heliport data plots
[DOT/FAA/CT-TN87/54-VOL-2] N90-11761

HELICOPTERS
An experimental investigation of helicopter rotor hub fairing drag characteristics
[NASA-TM-102182] N90-11701
Sequential design of experiments with physically based models 23
[AD-A211918] N90-12239
Rotorcraft low altitude CNS benefit/cost analysis: Rotorcraft operations data
[DOT/FAA/DS-89/9] N90-12406

HELIPORTS
Analysis of heliport environmental data: Indianapolis downtown heliport, Wall Street heliport. Volume 2: Wall Street heliport data plots
[DOT/FAA/CT-TN87/54-VOL-2] N90-11761

HELIUM
Independent Orbiter Assessment (IOA): Assessment of the reaction control system, volume 1
[NASA-CR-185543-VOL-1] N90-11793
Independent Orbiter Assessment (IOA): Assessment of the reaction control system, volume 2
[NASA-CR-185543-VOL-2] N90-11794
Independent Orbiter Assessment (IOA): Assessment of the reaction control system, volume 3
[NASA-CR-185543-VOL-3] N90-11795
Independent Orbiter Assessment (IOA): Assessment of the reaction control system, volume 4
[NASA-CR-185543-VOL-4] N90-11796
Independent Orbiter Assessment (IOA): Assessment of the reaction control system, volume 5
[NASA-CR-185543-VOL-5] N90-11797
High pressure studies of planetary matter
[DE89-017738] N90-12455

HELIUM ISOTOPES
Flare-in texture in rotating superfluid (3)He-B
[PB89-218994] N90-12368
Resonant quasiparticle-ion scattering in anisotropic superfluid (3)He
[PB89-221618] N90-12369
Collective-mode spectroscopy of textures in superfluid (3)He-B
[PB89-221634] N90-12370

HELIUM-NEON LASERS
Zeeman interferometry
[DE89-015296] N90-12012
Comparison of I2-stabilized HE-NE lasers
[PB89-219644] N90-12014

HETEROGENEITY
Densification of particulate ceramic composites: The role of heterogeneities
[DE90-000177] N90-11886

HETEROJUNCTIONS
Graded bandgap solar cells
[AD-A211537] N90-12097
Development and evaluation of an instrument for rapid electroreflectance of semiconductor materials
[AD-A211690] N90-12376

HEURISTIC METHODS
Premixed turbulent flame propagation
[AD-A211489] N90-11841
Reasoning about change and exceptions in automated process planning
[DE89-017706] N90-12195
On the role of Coulomb forces in atomic radiative emission
[IRF-PREPRINT-106] N90-12308

HIGH ALTITUDE BREATHING
The effect of caffeine on endurance time to exhaustion at high altitude
[AD-A212069] N90-12163

HIGH ALTITUDE ENVIRONMENTS
Metacognition and retrieval from long-term memory at Mount Everest
[AD-A211629] N90-12177

HIGH ENERGY INTERACTIONS
Plasma-anode electron gun research
[AD-A211547] N90-11773
An experimental high energy physics program
[DE89-014695] N90-12311
Experimental research in high energy physics
[DE90-000061] N90-12342

HIGH FREQUENCIES
A new approach to HF (High Frequency) channel modeling and simulation. Part 1: Deterministic model
[PB89-203962] N90-11913
Development of high frequency spice models for ferrite core inductors and transformers
[DE89-015121] N90-11946

HIGH POWER LASERS
A nonlinear-optical method for combining high power laser beams
[AD-A211730] N90-12022
Ultra high speed compound semiconductors and real time signal processing
[AD-A211394] N90-12372

HIGH PRESSURE
Cellular and molecular mechanisms of high pressure inotropy in cardiac muscle
[AD-A211695] N90-12170
High pressure studies of planetary matter
[DE89-017738] N90-12455

HIGH RESOLUTION
High temperature and high resolution UV photoelectron spectroscopy using supersonic molecular beams
[DE90-000176] N90-11835
Television systems with enhanced image quality for new broadband channels
[ETN-89-94622] N90-11936
High resolution X-ray spectroscopy using germanium microcalorimeters
[DE89-017784] N90-12004

HIGH REYNOLDS NUMBER
An investigation of end-wall vortex cavitation in a high Reynolds number axial-flow pump
[AD-A211426] N90-11982

HIGH STRENGTH ALLOYS
Precipitation strengthened high strength, high conductivity Cu-Cr-Nb alloys produced by chill block melt spinning
[NASA-CR-185144] N90-11853

HIGH TEMPERATURE
High temperature and high resolution UV photoelectron spectroscopy using supersonic molecular beams
[DE90-000176] N90-11835
Elevated temperature aluminum-titanium alloy by powder metallurgy process
[AD-D014165] N90-11852

HIGH TEMPERATURE AIR
Aging of CFRP due to longterm storage in heated air
[ESA-TT-1124] N90-11893

HIGH TEMPERATURE FLUIDS
Studies on the startup transients and performance of a gas loaded sodium heat pipe
[AD-A211880] N90-12379

HIGH TEMPERATURE GASES
Reactive ion etching of sputtered silicon carbide and tungsten thin films for device applications
[AD-A211711] N90-11847

HIGH TEMPERATURE SUPERCONDUCTORS
Superconducting switch program
[AD-A211580] N90-11964
Characterizations of electrical properties of highT(sub c) superconducting materials
[NASA-TM-100380] N90-12345
RF performance of polycrystalline high-T(sub c) superconductors
[DE89-017671] N90-12359
Anomalous ion-channeling behavior across the superconducting transition in high-T(sub c) materials
[DE89-017677] N90-12360
High-temperature superconducting current leads for cryogenic apparatus
[DE89-017680] N90-12361
Preparation and characterization of single phase Ba(1-x)KxBiO3
[DE89-017735] N90-12362
Effects of grain boundary chemistry on critical current density in oxide superconductors
[DE89-017780] N90-12365
Surface, interface, and bulk properties of high T(sub c) superconductors
[AD-A211490] N90-12373
High temperature superconducting compounds
[AD-A211511] N90-12374

HIGH TEMPERATURE TESTS
Static tensile and tensile creep testing of four boron nitride coated ceramic fibers at elevated temperatures
[NASA-CR-184999] N90-11807

HIGH VACUUM
KIVA reactive hydrodynamics code applied to detonations in high vacuum
[DE89-016979] N90-11974

HILBERT TRANSFORMATION
Inf-convolution splines
[IMAG-RR-749-M] N90-12256

HISTORIES
The fuel cell in space: Yesterday, today and tomorrow
[NASA-TM-102366] N90-11804

HOLES (ELECTRON DEFICIENCIES)
Quantitative interpretation of auger lineshapes and electron/photon stimulated desorption
[AD-A211550] N90-11842
Energy relaxation of light holes in InAs(.15)Sb(.85)/InSb multiple quantum wells
[DE89-016035] N90-12349

HOLOGRAPHIC INTERFEROMETRY
Materials characterization using holographic mapping of transient lamb waves
[AD-A211414] N90-12050

HOLOGRAPHY
Materials characterization using holographic mapping of transient lamb waves
[AD-A211414] N90-12050

HONEYCOMB CORES
Axial compression buckling test on the H-2 launch vehicle satellite fairing structural element prototype (aluminum surface plate/aluminum honeycomb sandwiched curved surface plate)
[NAL-TM-563] N90-12039

HOT PRESSING
Processing and characterization of alumina platelet-reinforced mullite composites
[DE90-000057] N90-11814
Photolithography: A new tool for ceramic science
[DE90-000135] N90-11885

HOT WORKING
A study of the hot workability of Al-8.5 wt pct Mg alloys for armor plate applications
[AD-A211680] N90-11868

HOVERING
Low-speed wind-tunnel study of reaction control-jet effectiveness for hover and transition of a STOVL fighter concept
[NASA-TM-4147] N90-11751

HUBS
An experimental investigation of helicopter rotor hub fairing drag characteristics
[NASA-TM-102182] N90-11701

HUMAN BEHAVIOR
Demonstration of replicable dimensions of health behaviors
[AD-A211920] N90-12161

HUMAN FACTORS ENGINEERING
Human Operator Simulator (HOS) 4 user's guide
[AD-A212007] N90-11763
Project AENEAS: A feasibility study for crew emergency return vehicle
[PB89-217020] N90-11799
New Fabric Development Program
[AD-A211549] N90-11891
Wrist orientation effect on grip strength and endurance
[PB89-200935] N90-12179

HUMAN PERFORMANCE
USSR Space Life Sciences Digest, Issue 24
[NASA-CR-3922(28)-ISSUE-24] N90-12152
USSR Space Life Sciences Digest, Issue 23
[NASA-CR-3922(27)-ISSUE-23] N90-12154
Adaptive information processing in auditory cortex
[AD-A211294] N90-12166

HURRICANES
The effect of latent heat release on synoptic-to-planetary scale wave interactions: Observational study
N90-12074

HYDRAULIC CONTROL
Independent Orbiter Assessment (IOA): Assessment of the hydraulics/water spray boiler subsystem
[NASA-CR-185537] N90-11792

HYDRAULIC EQUIPMENT
Independent Orbiter Assessment (IOA): Assessment of the hydraulics/water spray boiler subsystem
[NASA-CR-185537] N90-11792

HYDROCARBON COMBUSTION
Computation of ramjet internal flowfields
[AD-A212001] N90-11743

HYDROCARBON FUEL PRODUCTION
Correlating microemulsion fuel composition, structure and combustion properties
[DE89-017779] N90-11898

HYDROCARBONS
Conversion of methane to liquid hydrocarbons
[DE89-017547] N90-11831
Vapour pressures and critical points of liquids. Halogenated hydrocarbons
[ESDU-89006] N90-11848

HYDRODYNAMICS
A critical assessment of models available for the shock initiation of heterogeneous explosives
[MRL-TR-89-17] N90-11896
KIVA reactive hydrodynamics code applied to detonations in high vacuum
[DE89-016979] N90-11974
Some new algorithms for boundary value problems in smooth particle hydrodynamics
[AD-A211728] N90-11987

HYDROGEN
High pressure studies of planetary matter
[DE89-017738] N90-12455
A high-speed digital camera system for the observation of rapid H-alpha fluctuations in solar flares N90-12491

HYDROGEN ATOMS
Spin-orbit relaxation rates of Bi(6p(3)) 2D(3/2) following photolysis of Bi(CH3)3 at lambda = 193 nm
[AD-A211792] N90-12303

HYDROGEN IONS
Atomic and molecular surface and volume processes in the analysis of negative hydrogen discharges
[DE89-015705] N90-12294

HYDROGEN OXYGEN FUEL CELLS
Long endurance underwater power system
[AD-A211386] N90-12096

HYDROGEN PEROXIDE
Lifetime of singlet oxygen in aqueous hydrogen peroxide (BHP)
[AD-A211545] N90-12306

HYDROGENATION
Catalogic hydrogenation of carbon monoxide
[DE89-017813] N90-11834

HYDROPHONES
Hydrophone investigations of earthquakes and explosion generated high-frequency seismic phases
[AD-A212055] N90-12122
HYDROSTATIC PRESSURE
Cellular and molecular mechanisms of high pressure inotropy in cardiac muscle
[AD-A211695] N90-12170
HYPERBOLIC COORDINATES
Smooth linearization of hyperbolic fixed points without resonance conditions
[REPT-89-03] N90-12251
HYPERBOLIC FUNCTIONS
Convergence results for pseudospectral approximations of hyperbolic systems by a penalty type boundary treatment
[NASA-CR-181929] N90-12230
HYPERCUBE MULTIPROCESSORS
Efficient diagnosis of multiprocessor systems under probabilistic models
[NASA-CR-185965] N90-12212
Parallel implementation and evaluation of motion estimation system algorithms on a distributed memory multiprocessor using knowledge based mappings
[NASA-CR-185984] N90-12213
Novel techniques for data decomposition and load balancing for parallel processing of vision systems: Implementation and evaluation using a motion estimation system
[NASA-CR-185991] N90-12214
Dynamic embedding of trees in hypercubes with constant dilation and load
[AD-A211884] N90-12236
Four vector-matrix primitives
[AD-A211889] N90-12237
Fast computation using faulty hypercubes
[AD-A211910] N90-12238
HYPERONS
An experimental high energy physics program
[DE89-014695] N90-12311
HYPERSONIC COMBUSTION
Wave combustors for trans-atmospheric vehicles
[NASA-TM-102238] N90-11742
HYPERSONIC VEHICLES
Adaptive control law design for model uncertainty compensation
[AD-A211712] N90-11758
HYPERTHERMIA
Heatstroke pathophysiology: The energy depletion model
[AD-A212156] N90-12164
HYPOBARIC ATMOSPHERES
Convective heat transfer in hypobaric environments
[AD-A212060] N90-11979
HYSTERESIS
Development of high frequency spice models for ferrite core inductors and transformers
[DE89-015121] N90-11946
Parametric study of power absorption from electromagnetic waves by small ferrite spheres
[NASA-TP-2949] N90-12282

I

ICE
Ice runways near the South Pole
[AD-A211606] N90-11908
High pressure studies of planetary matter
[DE89-017738] N90-12455
ICE MAPPING
Remote sensing data acquisition, analysis and archival
[PB89-142566] N90-12085
ICELAND
Analysis of radar images of the active volcanic zone at Krafla, Iceland: The effects of look azimuth biasing
N90-12434
IDENTIFYING
Experimental research in high energy physics
[DE90-000061] N90-12342
IGNITION TEMPERATURE
Ignition characteristics of the nickel-based alloy UNS N07718 in pressurized oxygen
[NASA-CR-185932] N90-11850
IMAGE ANALYSIS
Characteristics, distribution and geologic/terrain associations of small dome-like hills on Venus
N90-12425
Potential for observing and discriminating impact craters and comparable volcanic landforms on Magellan radar images N90-12429
Contrasting landform perception with varied radar illumination geometries and at simulated resolutions of Venera and Magellan N90-12430
Venus surface properties deduced from radar and radiometry N90-12431
A morphologic study of Venus Ridge belts
N90-12432
Evidence for volcanism in NW Ishtar Terra, Venus
N90-12433
Analysis of radar images of the active volcanic zone at Krafla, Iceland: The effects of look azimuth biasing
N90-12434
Radar scattering mechanisms within the meteor crater ejecta blanket: Geologic implications and relevance to Venus N90-12435
Aeolian processes on Venus N90-12436
Architecture of orogenic belts and convergent zones in Western Ishtar Terra, Venus N90-12437
Tectonism on Venus: A review N90-12440
Crater identification and resolution of lunar radar images N90-12441
Radar scattering from desert terrains, Pisgah/Lavic Region, California: Implications for Magellan
N90-12443
Lakshmi Planum: A distinctive highland volcanic province N90-12444
Impact cratering and the surface age of Venus: The Pre-Magellan controversy N90-12446
Geology of the Venus equatorial region from Pioneer Venus radar imaging N90-12447
Venus and the Archean Earth: Thermal considerations
N90-12448
Eastern Ishtar Terra: Tectonic evolution derived from recognized features N90-12451
Stress distribution and topography of Tellus Regio, Venus N90-12452
IMAGE INTENSIFIERS
A microchannel plate intensified, subnanosecond, X-ray imaging camera
[DE89-017781] N90-12003
IMAGE PROCESSING
Video imaging systems: A survey
[DE89-016920] N90-11919
Analysis of two-pass Modified Hough Transform (MHT) technique for the detection of wake like signals
[AD-A211982] N90-11924
Fast and objective MRTD measurement
[FEL-1988-24] N90-12006
Discriminating rigid from nonrigid motion
[AD-A211794] N90-12180
Basic program for raster scan display unit
[NAL-TM-560] N90-12185
Parallel implementation and evaluation of motion estimation system algorithms on a distributed memory multiprocessor using knowledge based mappings
[NASA-CR-185984] N90-12213
Novel techniques for data decomposition and load balancing for parallel processing of vision systems: Implementation and evaluation using a motion estimation system
[NASA-CR-185991] N90-12214
Parallel architectures and parallel algorithms for integrated vision systems
[NASA-CR-185990] N90-12215
Parallel processing on transputer arrays for the recognition of objects in infrared images
[RSRE-MEMO-4197] N90-12217
A survey of camera error sources in machine vision systems
[DE89-014072] N90-12318
Investigation of active regions at high resolution by balloon flights of the Solar Optical Universal Polarimeter (SOUP) N90-12487
An imaging vector magnetograph for the next solar maximum N90-12489
IMAGE RESOLUTION
Television systems with enhanced image quality for new broadband channels
[ETN-89-94622] N90-11936
Fast and objective MRTD measurement
[FEL-1988-24] N90-12006
IMAGES
Vision-based navigation for autonomous ground vehicles
[AD-A211584] N90-11725
A high-speed digital camera system for the observation of rapid H-alpha fluctuations in solar flares N90-12491
IMAGING TECHNIQUES
Video imaging systems: A survey
[DE89-016920] N90-11919
The Owens Valley solar array N90-12490
IMPACT RESISTANCE
Transport composite fuselage technology: Impact dynamics and acoustic transmission
[NASA-CR-4035] N90-11821
IMPLOSIONS
Apparatus and method for monitoring pressure leaks from a sealed system
[AD-D014168] N90-11995
Advanced concepts theory
[AD-A211665] N90-12344
IN-FLIGHT MONITORING
Measurement effects on the calculation of in-flight thrust for an F404 turbofan engine
[NASA-TM-4140] N90-11741
INCENTIVES
The effect of incentives on the reliability and validity of cognitive speed tests
[AD-A211346] N90-12181
INCOMPRESSIBLE FLOW
Steady and unsteady potential flow around thin annular wings and engines with simulation of jet engine flow
[DFVLR-FB-89-18] N90-11711
Incompressible flow about ellipsoids of revolution
[REPT-88-02] N90-11713
Efficient finite element solution of Navier-Stokes equations and related topics
[AD-A211647] N90-11986
A least-squares finite element method for incompressible Navier-Stokes problems
[NASA-TM-102385] N90-12231
INCOMPRESSIBLE FLUIDS
On the computation of normal modes of a rotating, viscous, incompressible fluid with a capillary free boundary
[REPT-89-01] N90-11989
A multigrid algorithm for the incompressible Navier-Stokes equation
[GMD-374] N90-11993
INDEXES (DOCUMENTATION)
Aeronautical engineering: A continuing bibliography with indexes (supplement 243)
[NASA-SP-7037(243)] N90-11693
Aeronautical engineering: A continuing bibliography with indexes (supplement 244)
[NASA-SP-7037(244)] N90-11694
Indexes for the proceedings of the symposia (international) on detonation, 1951 through 1985
[DE89-015178] N90-11972
Earth resources: A continuing bibliography with indexes (issue 63)
[NASA-SP-7041(63)] N90-12091
Aerospace medicine and biology: A continuing bibliography with indexes (supplement 329)
[NASA-SP-7011(329)] N90-12173
Criss-cross directory of NASA N numbers and DOD AD numbers. Volume 2, part 1: AD to N, 1979-1986. N to AD, 1962-1986
[NASA-TM-101814] N90-12388
Criss-cross directory of NASA N numbers and DOD AD numbers. Volume 2, part 2: AD to N, 1979-1986. N to AD, 1962-1986
[NASA-TM-101815] N90-12389
INDIUM ALLOYS
A critical assessment of thermodynamic and phase diagram data for the Ga-In system
[NPL-DMA(A)-174] N90-12382
INDIUM ANTIMONIDES
Energy relaxation of light holes in InAs(.15)Sb(.85)/InSb multiple quantum wells
[DE89-016035] N90-12349
INDIUM PHOSPHIDES
Beam assisted fabrication of 3-5/Si monolithic devices
[AD-A212046] N90-12367
INDUCTION MOTORS
Adjustable speed drive study, part 1
[DE89-017654] N90-11948
INDUCTORS
Development of high frequency spice models for ferrite core inductors and transformers
[DE89-015121] N90-11946
INELASTIC SCATTERING
Detailed photonuclear cross-section calculations and astrophysical applications
[DE89-017531] N90-12419
INERTIA
Effect of control surface mass unbalance on the stability of a closed-loop active control system
[NASA-TP-2952] N90-12042
INFERENCE
Doppler statistics of ocean velocity variability
[AD-A211687] N90-12148
INFILTRATION
Investigations into the infiltration kinetics, wettability, and interfacial bond strength of Al/SiC composites
[AD-A211924] N90-11815
INFORMATION DISSEMINATION
National Library of Medicine DOCLINE (tradename) manual
[PB89-188676] N90-12390
INFORMATION PROCESSING (BIOLOGY)
Adaptive information processing in auditory cortex
[AD-A211294] N90-12166
Metacognition and retrieval from long-term memory at Mount Everest
[AD-A211629] N90-12177

INFORMATION RETRIEVAL
Program distribution for unclassified scientific and technical reports: Instructions and category scope notes, revision 75
[DE89-005395] N90-12391
Problem of incomplete information in relational databases
[PB89-217533] N90-12393
Interoperability of heterogeneous information systems: The COST 11(ter) Project
[PB89-217541] N90-12394
INFORMATION SYSTEMS
Operating experience with the Sandia terminal switching network and fiber optic loop
[DE89-007422] N90-12317
Program distribution for unclassified scientific and technical reports: Instructions and category scope notes, revision 75
[DE89-005395] N90-12391
Role of conceptual models in the design and use of information systems
[PB89-217376] N90-12392
Interoperability of heterogeneous information systems: The COST 11(ter) Project
[PB89-217541] N90-12394
Building a user-friendly data dictionary system in ORACLE
[DE89-014878] N90-12397
FEDIX: An on-line information service for universities and other research organizations: User's guide, version 2.0, release 1
[DE89-016695] N90-12398
DOD Gateway Information System (DGIS) common command language: A retrospective on the introduction of prolog as the development tool
[AD-A211941] N90-12400
Access to Max '91 information via computer networks
N90-12466
INFORMATION TRANSFER
FEDIX: An on-line information service for universities and other research organizations: User's guide, version 2.0, release 1
[DE89-016695] N90-12398
DOD Gateway Information System (DGIS) common command language: A retrospective on the introduction of prolog as the development tool
[AD-A211941] N90-12400
INFRARED DETECTORS
Improved pattern recognition techniques for real time operation
[AD-A211395] N90-11840
Vanadium dioxide protective devices
[AD-A212018] N90-11887
Infrared detector array
[AD-D014170] N90-11997
Infrared temperature measurement with automatic consideration of emissivity
[ESA-TT-1131] N90-12008
Development of microstructured DH diode lasers and detectors for the near and medium IR spectral domain using molecular beam epitaxy
[IPM-15/1988] N90-12023
INFRARED IMAGERY
Parallel processing on transputer arrays for the recognition of objects in infrared images
[RSRE-MEMO-4197] N90-12217
INFRARED LASERS
Development of microstructured DH diode lasers and detectors for the near and medium IR spectral domain using molecular beam epitaxy
[IPM-15/1988] N90-12023
INFRARED RADIATION
Infrared temperature measurement with automatic consideration of emissivity
[ESA-TT-1131] N90-12008
Infrared backscattering N90-12083
INFRARED SPECTROMETERS
Improved pattern recognition techniques for real time operation
[AD-A211395] N90-11840
INFRARED SPECTROSCOPY
Improved pattern recognition techniques for real time operation
[AD-A211395] N90-11840
INPUT/OUTPUT ROUTINES
Rational expansion for nonlinear input-output maps
[RR-348] N90-12248
INSPECTION
Stochastic propagation of an array of parallel cracks: Exploratory work on matrix fatigue damage in composite laminates
[DE89-017837] N90-11813
INSTRUMENT LANDING SYSTEMS
ILS mathematical modeling study of the effects of proposed hangar construction at the Orlando International Airport, Runway 17R, Orlando, Florida
[DOT/FAA/CT-TN89/52] N90-11762
INTEGRAL EQUATIONS
Microscopic approach to the generator coordinate method
[DE89-016701] N90-12233
Mapping nonlinear integro-differential equations into the frequency domain
[RR-366] N90-12249
INTEGRATED CIRCUITS
Proceedings of the Workshop on Compound Semiconductor Devices and Integrated Circuits (13th) held in Cabourg, France on 10-12 May 1989
[AD-A211848] N90-11954
Nearly optimal algorithms and bounds for multilayer channel routing
[AD-A211913] N90-11955
Linear (passive) and non-linear guided and studies in glass
[AD-A211693] N90-12325
Niobium and niobium nitride contacts on semiconducting material
[AD-D014177] N90-12347
Beam assisted fabrication of 3-5/Si monolithic devices
[AD-A212046] N90-12367
INTEGRATED LIBRARY SYSTEMS
National Library of Medicine DOCLINE (tradename) manual
[PB89-188676] N90-12390
INTERACTIVE CONTROL
Manual for Program PSTRESS: Peel stress computation
[NASA-CR-178408] N90-11822
Design mechanism for interactive graphics mechanism design
[PB89-219513] N90-12202
ANDECS-PERLUDE 2.0: A databased, interactive system of control software user's guide
[DFVLR-MITT-89-07] N90-12404
INTERFACES
Human Operator Simulator (HOS) 4 user's guide
[AD-A212007] N90-11763
Short period multilayers: Interface dominated structures
[DE89-017536] N90-11812
Power up modification for video switcher microprocessor interface for sensor system processing system
[AD-A211543] N90-11962
INTERFERENCE DRAG
An experimental investigation of helicopter rotor hub fairing drag characteristics
[NASA-TM-102182] N90-11701
INTERFEROMETERS
Absolute determination of the wall shear stress by means of an interferometer
[DFVLR-FB-89-13] N90-11991
INTERMETALLICS
Electronic structure of transition metal alloys and intermetallics: Charge transfer and its implications for Moessbauer effect measurements
[DE89-017603] N90-11860
Deformation and defects in Laves-phase intermetallic compounds
[DE89-017798] N90-11862
INTERMOLECULAR FORCES
Phase behavior of pure and mixed systems at high pressure
[DE89-017734] N90-11832
INTERNAL WAVES
Effects on electromagnetic wave propagation and rocket vapor trails of intense turbulence generated by breaking internal gravity waves
[AD-A211755] N90-12130
INTERPLANETARY SPACE
MHD (magnetohydrodynamic) modeling of solar and interplanetary processes
[PB89-215461] N90-12416
Interplanetary energetic particle observations of the March 1989 events N90-12484
INTERPOLATION
Operational measures of central tendency
[DE89-016959] N90-12234
Calculation of transient response from time-harmonic spectrum
[AD-A211972] N90-12241
Inf-convolution splines
[IMAG-RR-749-M] N90-12256
INTERPROCESSOR COMMUNICATION
On the communication complexity of solving a polynomial equation
[AD-A211945] N90-12240
DOD Gateway Information System (DGIS) common command language: A retrospective on the introduction of prolog as the development tool
[AD-A211941] N90-12400
INTERVALS
Small sample theory for steady state confidence intervals
[AD-A212097] N90-12242
INVARIANCE
Some 1(sub p) invariant probability measures
[REPT-88-91] N90-12273
INVISCID FLOW
Calculation on film preparation and film motion of a swirl atomizer
[ESA-TT-1096] N90-11990
IODINE
Measurement of pressure fluctuations in a resonant chamber with laser-induced iodine fluorescence
[ESA-TT-1123] N90-12326
ION BEAMS
Reactive ion etching of sputtered silicon carbide and tungsten thin films for device applications
[AD-A211711] N90-11847
Fundamental tribological properties of ion-beam-deposited boron nitride films
[NASA-TM-102088] N90-11881
Ion-assisted deposition of high-temperature lubricious surfaces
[DE89-012397] N90-11883
Photolithography: A new tool for ceramic science
[DE90-000135] N90-11885
Advances and directions of ion nitriding/carburizing
[NASA-TM-102398] N90-11902
Beam dynamics of a liquid metal ion source
[DE89-015856] N90-12295
Generation and focusing of pulsed intense ion beams
[DE89-017558] N90-12338
Anomalous ion-channeling behavior across the superconducting transition in high-T(sub c) materials
[DE89-017677] N90-12360
ION EXCHANGING
Long endurance underwater power system
[AD-A211386] N90-12096
Linear (passive) and non-linear guided and studies in glass
[AD-A211693] N90-12325
ION EXTRACTION
Ion formation by electron impact
[AD-A211367] N90-12305
ION IMPACT
Plasma-anode electron gun research
[AD-A211547] N90-11773
Ion formation by electron impact
[AD-A211367] N90-12305
ION IMPLANTATION
Characterization of the Structure and Chemistry of Defects in Materials: Proceedings, volume 138
[DE89-014796] N90-12352
Ion beam deposition of epitaxial germanium and gallium arsenide layers
[DE89-017439] N90-12357
ION PLATING
Ion-assisted deposition of high-temperature lubricious surfaces
[DE89-012397] N90-11883
ION PRODUCTION RATES
Atomic and molecular surface and volume processes in the analysis of negative hydrogen discharges
[DE89-015705] N90-12294
ION RECOMBINATION
Atomic and molecular surface and volume processes in the analysis of negative hydrogen discharges
[DE89-015705] N90-12294
ION SCATTERING
Resonant quasiparticle-ion scattering in anisotropic superfluid (3)He
[PB89-221618] N90-12369
ION SOURCES
Beam dynamics of a liquid metal ion source
[DE89-015856] N90-12295
Generation and focusing of pulsed intense ion beams
[DE89-017558] N90-12338
Ion beam deposition of epitaxial germanium and gallium arsenide layers
[DE89-017439] N90-12357
ION TRAPS (INSTRUMENTATION)
State-resolved reaction dynamics
[AD-A211613] N90-12307
IONIZATION
Laser ionization mass spectroscopy
[DE89-008039] N90-12015
IONIZATION CROSS SECTIONS
Ion formation by electron impact
[AD-A211367] N90-12305

IONIZED GASES

Properties of strongly coupled multi-ionic plasmas
[DE89-017782] N90-12339

IONOSPHERIC CURRENTS

HIPAS 1987-88: ULF research and campaign support
[AD-A211720] N90-11933

IONOSPHERIC HEATING

HIPAS 1987-88: ULF research and campaign support
[AD-A211720] N90-11933

Coherency properties of strong Langmuir turbulence
[DE89-009290] N90-12119

IONOSPHERIC NOISE

NRL/VOA modifications to IONCAP as of 12 July 1988
[AD-A211546] N90-11929

IONOSPHERIC PROPAGATION

NRL/VOA modifications to IONCAP as of 12 July 1988
[AD-A211546] N90-11929

IRIDIUM

Luminescence in applied magnetic fields
[AD-A211551] N90-12287

IRON

Iron (III) initiated autoxidation of 1,2,3,4-tetrahydrocarbazole: An example of electron transfer
[AD-A211857] N90-11836

High pressure studies of planetary matter
[DE89-017738] N90-12455

IRON METEORITES

An atom probe study of phase decomposition in three iron meteorites
[DE89-017581] N90-12420

IRRADIATION

Fracture toughness data base for HT9 and modified 9Cr-1Mo irradiated in several reactors up to approximately 100 dpa
[DE90-000111] N90-11864

ISOTROPY

Some implications of the isotropic momentarily frozen assumptions for the SPAN-MAT program
[NASA-CR-181937] N90-11704

ITERATIVE SOLUTION

On the computation of normal modes of a rotating, viscous, incompressible fluid with a capillary free boundary
[REPT-89-01] N90-11989

Some observations on the convergence behavior of GMRES
[REPT-89-09] N90-12252

The convergence behavior of some iterative solution methods
[REPT-89-19] N90-12260

A long time tail for random walk in random scenery
[REPT-89-08] N90-12278

J

J INTEGRAL

An application of the J-integral to an incremental analysis of blunting crack behavior
[DE89-016844] N90-12046

JACOBI MATRIX METHOD

Distributed VLSI architecture for fast Jacobian and inverse Jacobian formulations
[RR-346] N90-12218

JET AIRCRAFT

Comparison of flying qualities derived from in-flight and ground-based simulators for a jet-transport airplane for the approach and landing pilot tasks
[NASA-TP-2962] N90-11757

JET ENGINE FUELS

The prediction of middle distillate fuel properties using liquid chromatography-proton nuclear magnetic resonance spectroscopy data
[AD-A211879] N90-11899

JET ENGINES

Effects of a heat cycle on material strength
[NAL-TM-562] N90-11737

The RB199: An in-service success
[PNR90544] N90-11746

Coatings for gas turbine compressors
[NLR-MP-88045-U] N90-11750

Aluminium alloy development for aero engines
[PNR90548] N90-11874

JET FLOW

Steady and unsteady potential flow around thin annular wings and engines with simulation of jet engine flow
[DFVLR-FB-89-18] N90-11711

Low-speed wind-tunnel study of reaction control-jet effectiveness for hover and transition of a STOVL fighter concept
[NASA-TM-4147] N90-11751

Cryogenic free jets
[ESA-TT-1128] N90-11767

JET STREAMS (METEOROLOGY)

Investigations of polar air stream cyclogenesis based on numerical simulations with a mesoscale model
[PB89-214563] N90-12132

JOINTS (JUNCTIONS)

Investigations into the infiltration kinetics, wettability, and interfacial bond strength of Al/SiC composites
[AD-A211924] N90-11815

JUDGMENTS

Metacognition and retrieval from long-term memory at Mount Everest
[AD-A211629] N90-12177

K

KALMAN FILTERS

Discrete filtering techniques applied to sequential GPS range measurements
[NASA-CR-177472] N90-11730

KERNEL FUNCTIONS

Likelihood cross-validation bandwidth selection for nonparametric kernel density estimators
[REPT-89-10] N90-12279

KINEMATICS

Kinematic design NC optical generator N90-12316

KINETIC ENERGY

Davydov solutions at 300 Kelvin: The final search
[DE89-015248] N90-12296

Synchrotron-radiation experiments with recoil ions
[DE89-017579] N90-12301

KINETIC EQUATIONS

Kinetics of diffusion-controlled reactions
[AD-A212161] N90-12286

The behavior of beams of relativistic non-thermal electrons under the influence of collisions and synchrotron losses
[NASA-CR-185983] N90-12298

Stellarator transport theory
[DE89-016371] N90-12328

Development of a numerical solution to the time dependent kinetic equation N90-12481

KINETIC FRICTION

Equilibrium solutions of a spherical pendulum with rotating point of suspension and friction
[ESA-TT-1139] N90-12288

KINETICS

Photolysis of spacecraft contaminants
[AD-A211715] N90-11801

Investigations into the infiltration kinetics, wettability, and interfacial bond strength of Al/SiC composites
[AD-A211924] N90-11815

KNOWLEDGE

Designing and designing knowledge in engineering and architecture
[PB89-219521] N90-12383

KNOWLEDGE BASES (ARTIFICIAL INTELLIGENCE)

Parallel implementation and evaluation of motion estimation system algorithms on a distributed memory multiprocessor using knowledge based mappings
[NASA-CR-185984] N90-12213

Computer-based tutors for explaining and managing the process of diagnostic reasoning
[AD-A211738] N90-12222

Interoperability of heterogeneous information systems: The COST 11(ter) Project
[PB89-217541] N90-12394

Detailed description of the knowledge-based system for physical database design, volume 2
[PB89-229033] N90-12395

Distributed knowledge-based systems
[AD-A211984] N90-12401

KRYPTON FLUORIDE LASERS

Air breakdown photography in the picosecond domain
[DE89-016775] N90-11830

L

LAGUERRE FUNCTIONS

A simple proof of a differential equation for generalizations of Laguerre polynomials
[REPT-89-15] N90-12253

Generalizations of Laguerre polynomials
[REPT-89-25] N90-12263

LAMB WAVES

Materials characterization using holographic mapping of transient lamb waves
[AD-A211414] N90-12050

LAMINAR FLOW

Elimination of spurious eigenvalues in the Chebyshev tau spectral method
[PB89-209282] N90-11967

Numerical analysis, scientific computing and fundamental studies of fluid mechanics
[DE89-017554] N90-11975

LAMINAR MIXING

Premixed turbulent flame propagation
[AD-A211489] N90-11841

LAMINATES

Interlaminar stress concentration in fiber composites
[ETN-89-94670] N90-11809

Short period multilayers: Interface dominated structures
[DE89-017536] N90-11812

Stochastic propagation of an array of parallel cracks: Exploratory work on matrix fatigue damage in composite laminates
[DE89-017837] N90-11813

Aging of CFRP due to longterm storage in heated air
[ESA-TT-1124] N90-11893

LANDFORMS

Acoustical effects of a large ridge on low-frequency sound propagation in stationary and moving atmospheres
[NASA-CR-186001] N90-12290

Contrasting landform perception with varied radar illumination geometries and at simulated resolutions of Venera and Magellan N90-12430

A morphologic study of Venus Ridge belts
N90-12432

LANDING SITES

Improving snow roads and airstrips in Antarctica
[AD-A211588] N90-11907

Ice runways near the South Pole
[AD-A211606] N90-11908

LANGUAGES

Augmentations of grammatical categories in distributional-algebraic models of natural languages
[REPT-89-24] N90-12262

LAPLACE TRANSFORMATION

Some 1(sub p) invariant probability measures
[REPT-88-91] N90-12273

LASER ANEMOMETERS

Near-wall, three-dimensional turbulence measurements: A challenge for laser velocimetry
[NASA-TM-102252] N90-11978

LASER APPLICATIONS

LAWS simulation: Sampling strategies and wind computation algorithms N90-12081

LASER BEAMS

Comparison of laser and neutral particle beam discrimination
[DE89-017786] N90-12018

A nonlinear-optical method for combining high power laser beams
[AD-A211730] N90-12022

LASER CAVITIES

A proposed linac cavity RF drive system for the Los Alamos extreme ultraviolet free-electron laser
[DE89-016614] N90-12016

LASER DOPPLER VELOCIMETERS

Three component laser Doppler measurements in an axisymmetric jet
[NASA-CR-181908] N90-11702

LASER INDUCED FLUORESCENCE

State-resolved reaction dynamics
[AD-A211613] N90-12307

Measurement of pressure fluctuations in a resonant chamber with laser-induced iodine fluorescence
[ESA-TT-1123] N90-12326

LASER INTERFEROMETRY

Zeeman interferometry
[DE89-015296] N90-12012

LASER MATERIALS

New laser materials
[DE89-017524] N90-12017

Development of microstructured DH diode lasers and detectors for the near and medium IR spectral domain using molecular beam epitaxy
[IPM-15/1988] N90-12023

LASER OUTPUTS

Propagation of an elliptical laser beam through the turbulent atmosphere (vertical beams)
[PB89-208680] N90-12010

Comparison of I2-stabilized HE-NE lasers
[PB89-219844] N90-12014

LASER PLASMA INTERACTIONS

Electron attachment and molecular fragmentation in laser-excited plasmas
[AD-A212098] N90-12343

LASER PLASMAS

Switched power workshop: Introduction and summary
[DE90-000036] N90-11952

Temporal and spatial filtering remedies for dispersion in electromagnetic particle codes
[DE89-017534] N90-12337

LASER RANGE FINDERS

Calibration of a visioceilometer, a hand held lidar system
[FEL-1988-73] N90-12137

A closer look at the visiocellometer
[FEL-1989-80] N90-12138

LASER SPECTROSCOPY
Growth and characterization of materials for tunable lasers in the near infrared spectral region
[NASA-CR-185832] N90-12009
Laser ionization mass spectroscopy
[DE89-008039] N90-12015

LATENT HEAT
The effect of latent heat release on synoptic-to-planetary wave interactions and its implication for satellite observations: Theoretical modeling N90-12073
The effect of latent heat release on synoptic-to-planetary scale wave interactions: Observational study N90-12074

LATTICES (MATHEMATICS)
A long time tail for random walk in random scenery
[REPT-89-08] N90-12278

LEAD (METAL)
Review of the national ambient air quality standards for lead: Exposure analysis methodology and validation
[PB89-207914] N90-12104

LEAD TITANATES
Synthesis and microstructure of highly oriented PbTiO3 thin films prepared by a sol-gel method
[AD-A211735] N90-12377

LEAD ZIRCONATE TITANATES
New mechanism for toughening ceramic materials
[AD-A211651] N90-11892

LEADING EDGES
The structure of separated flow regions occurring near the leading edge of airfoils - including transition
[NASA-CR-185853] N90-11695

LEAKAGE
Apparatus and method for monitoring pressure leaks from a sealed system
[AD-D014168] N90-11995
Long endurance underwater power system
[AD-A211386] N90-12096

LEARNING
Synaptic plasticity and memory formation
[AD-A211368] N90-12158
Adaptive information processing in auditory cortex
[AD-A211294] N90-12166

LEAST SQUARES METHOD
A least-squares finite element method for incompressible Navier-Stokes problems
[NASA-TM-102385] N90-12231
Asymptotic bias of autoregressive estimators
[IMAG-RR-745-M] N90-12255
Orthogonal least squares methods and their application to nonlinear system identification
[RR-343] N90-12259

LENGTH
Comparison of I2-stabilized HE-NE lasers
[PB89-219844] N90-12014

LIAPUNOV FUNCTIONS
Can perceptrons find Lyapunov functions: An algorithmic approach to systems stability
[RR-365] N90-12224

LIE GROUPS
Global linear representations of nonlinear systems and the adjoint map
[RR-347] N90-12247

LIFE SCIENCES
USSR Space Life Sciences Digest, Issue 24
[NASA-CR-3922(28)-ISSUE-24] N90-12152

LIFE SUPPORT SYSTEMS
Independent Orbiter Assessment (IOA): Analysis of the life support and airlock support subsystems
[NASA-CR-185539] N90-11786
USSR Space Life Sciences Digest, Issue 24
[NASA-CR-3922(28)-ISSUE-24] N90-12152
USSR Space Life Sciences Digest, Issue 23
[NASA-CR-3922(27)-ISSUE-23] N90-12154

LIGHT (VISIBLE RADIATION)
Turbulence effects on reflected optical patterns (atmosphere and structure)
[PB89-208094] N90-12315

LIGHT ALLOYS
The evolution of light alloys in the aerospace industry
[ETN-89-95216] N90-11872

LIGHT CURVE
Pre-pulses: Signature of a trigger process in short (less than 60 secs) solar hard x ray flares N90-12476

LIGHT SCATTERING
Droplet sizing instrumentation used for icing research: Operation, calibration, and accuracy
[NASA-CR-182293] N90-11999

LIGHT SOURCES
Advanced light source master oscillator
[DE90-000123] N90-11953
The national synchrotron light source and its applications
[DE89-017605] N90-12320

LIGHT TRANSMISSION
Turbulence effects on reflected optical patterns (atmosphere and structure)
[PB89-208094] N90-12315

LIGHTNING
Numerical simulation of aeroplane response to a lightning injection
[ETN-89-95271] N90-11716
Lightning and surge protection of photovoltaic installations: Two case histories, Vulcano and Kythnos
[PB89-229058] N90-12135
Lightning data study in conjunction with geostationary satellite data
[NASA-CR-179286] N90-12142

LINE OF SIGHT
LAWS simulation: Sampling strategies and wind computation algorithms N90-12081

LINE SPECTRA
Quantitative interpretation of auger lineshapes and electron/photon stimulated desorption
[AD-A211550] N90-11842

LINEAR ACCELERATORS
A proposed linac cavity RF drive system for the Los Alamos extreme ultraviolet free-electron laser
[DE89-016614] N90-12016
Use of the NPL linac for x ray dosimetry --- linear accelerator (linac)
[NPL-RSA(EXT)-6] N90-12314

LINEAR EQUATIONS
A study of the asymptotic behavior of linear difference equations with polynomial coefficients
[IMAG-RR-743-M] N90-12254
The convergence behavior of some iterative solution methods
[REPT-89-19] N90-12260

LINEAR PREDICTION
The convergence behavior of some iterative solution methods
[REPT-89-19] N90-12260

LINEAR PROGRAMMING
A polynomial method of approximate weighted centers for linear programming
[REPT-89-13] N90-12210
A matrix factorization and its application to large-scale linear programming
[AD-A211293] N90-12244

LINEAR QUADRATIC GAUSSIAN CONTROL
Modelling and control of a diffusion/LPCVD furnace
[REPT-88-97] N90-11910

LINEAR SYSTEMS
Adaptive feedback linearization: Stability and robustness
[PB89-219497] N90-12220
A dynamic proof of the Frobenius-Perron theorem for Metzler matrices
[AD-A211839] N90-12235
On the differentiable manifold of fixed order stable linear systems
[REPT-88-89] N90-12250
Some observations on the convergence behavior of GMRES
[REPT-89-09] N90-12252
The convergence behavior of some iterative solution methods
[REPT-89-19] N90-12260

LINEAR TRANSFORMATIONS
Global linear representations of nonlinear systems and the adjoint map
[RR-347] N90-12247

LINEARITY
Convective heat transfer in hypobaric environments
[AD-A212060] N90-11979

LINEARIZATION
Parameter identification for an abstract Cauchy problem by quasilinearization
[NASA-CR-181933] N90-12192
Smooth linearization of hyperbolic fixed points without resonance conditions
[REPT-89-03] N90-12251

LINGUISTICS
Augmentations of grammatical categories in distributional-algebraic models of natural languages
[REPT-89-24] N90-12262
Some techniques for anaphora resolution in algebraic linguistics
[REPT-89-28] N90-12265

LININGS
Steam cooled rich-burn combustor liner
[NASA-CASE-LEW-13609-1] N90-11824

LIPIDS
Membrane fusion: The role of polyphosphatidylinositol
[AD-A211289] N90-12156

LIQUID CHROMATOGRAPHY
The prediction of middle distillate fuel properties using liquid chromatography-proton nuclear magnetic resonance spectroscopy data
[AD-A211879] N90-11899

LIQUID HYDROGEN
Program for high speed computation of physical properties of propellants and combustion gas of an LH2/LOX rocket engine
[NAL-TM-564] N90-11803

LIQUID METALS
Beam dynamics of a liquid metal ion source
[DE89-015856] N90-12295

LIQUID OXYGEN
Program for high speed computation of physical properties of propellants and combustion gas of an LH2/LOX rocket engine
[NAL-TM-564] N90-11803

LIQUID SODIUM
Studies on the startup transients and performance of a gas loaded sodium heat pipe
[AD-A211880] N90-12379

LIQUID SURFACES
Self-assembled organic monolayer films
[AD-A212006] N90-11838

LIQUID-SOLID INTERFACES
Self-assembled organic monolayer films
[AD-A212006] N90-11838

LIQUIDS
Natural gas to liquids
[DE89-000982] N90-11828
Conversion of methane to liquid hydrocarbons
[DE89-017547] N90-11831
Shock-induced reaction in several liquids
[DE89-016594] N90-11973

LITHIUM
Assessment of thin film batteries based on polymer electrolytes. Part 1: Energy density
[AD-A212111] N90-11958

LOAD DISTRIBUTION (FORCES)
A new test procedure for a wing made with carbon fiber composites
[ETN-89-95220] N90-11820

LOAD TESTS
A new test procedure for a wing made with carbon fiber composites
[ETN-89-95220] N90-11820
WISPER: A standardized fatigue load sequence for HAWT-blades
[NLR-MP-88029-U] N90-12055

LOADS (FORCES)
The dynamic performance of robot manipulators under different operating conditions
[RR-345] N90-12031

LOCAL AREA NETWORKS
Spacelab system analysis Marshall Avionics System Testbed (MAST)
[NASA-CR-183804] N90-11802

LOCKING
A real-time locking protocol
[AD-A211514] N90-12403

LOGIC CIRCUITS
Redundancies and don't cares in sequential logic synthesis
[AD-A211931] N90-11956
Optical arithmetic logic using the modified signed-digit redundant number representation
[AD-D014176] N90-12186
A single-phase clocked NOR/NOR CMOS programmable sequential array structure
[AD-A211297] N90-12203

LOOK ANGLES (ELECTRONICS)
Analysis of radar images of the active volcanic zone at Krafla, Iceland: The effects of look azimuth biasing N90-12434

LOSSES
Analysis of loss mechanisms in polycrystalline thin-film solar cells
[DE89-009454] N90-12093
Effects of main-sequence mass loss on the turnoff ages of population 1 clusters
[DE89-016755] N90-12417

LOVE WAVES
Investigations of Eurasian seismic sources and upper mantle structure
[AD-A211806] N90-12120

LOW ALTITUDE
Rotorcraft low altitude CNS benefit/cost analysis: Rotorcraft operations data
[DOT/FAA/DS-89/9] N90-12406

LOW FREQUENCIES
Acoustical effects of a large ridge on low-frequency sound propagation in stationary and moving atmospheres
[NASA-CR-186001] N90-12290

LOW SPEED WIND TUNNELS
Comparison of the results of tests on A300 aircraft in the RAE 5 metre and ONERA F1 wind tunnels
[RAE-TM-AERO-2130] N90-11768

LOW TEMPERATURE
Thermal model for double-drift IMPATT diodes on diamond heat sinks
[AD-A211746] N90-12380

LOW TEMPERATURE PHYSICS
Highlights of papers presented at the workshop on Cold Fusion Phenomena
[DE89-016956] N90-12334

LUBRICANTS
Plasma-deposited amorphous hydrogenated carbon films and their tribological properties
[NASA-TM-102379] N90-11880

LUMINAIRES
Apparatus and method for monitoring pressure leaks from a sealed system
[AD-D014168] N90-11995

LUMINOUS INTENSITY
Luminescence in applied magnetic fields
[AD-A211551] N90-12287

LUNAR CRATERS
Crater identification and resolution of lunar radar images N90-12441

LUNAR TOPOGRAPHY
Crater identification and resolution of lunar radar images N90-12441

M

MACH NUMBER
Normal-force-curve and pitching-moment-curve slopes of forebody-cylinder combinations at zero angle of attack for Mach numbers up to 5
[ESDU-89008] N90-11709

MACHINING
Fabrication of modulated vanes for a split-coaxial RFQ
[DE88-757235] N90-12310

MAGNESIUM ALLOYS
A study of the hot workability of Al-8.5 wt pct Mg alloys for armor plate applications
[AD-A211680] N90-11868

MAGNETIC COMPRESSION
High gain flux compression generator fabrication issues
[DE89-017888] N90-11951

MAGNETIC CORES
Thin film magnetic memory elements
[AD-D014178] N90-12281

MAGNETIC DIPOLES
The effect of flux creep on the magnetization field in the SSC diopole magnets
[DE90-000124] N90-12284

MAGNETIC DISTURBANCES
The 10.7-cm microwave observations of AR 5395 and related terrestrial effects N90-12483

MAGNETIC EFFECTS
Investigation of resonant ac-dc magnetic field effects
[AD-A211612] N90-12159
The 10.7-cm microwave observations of AR 5395 and related terrestrial effects N90-12483

MAGNETIC FIELDS
Development of high frequency spice models for ferrite core inductors and transformers
[DE89-015121] N90-11946
Periodic permanent magnet structures
[AD-D014173] N90-12280
Luminescence in applied magnetic fields
[AD-A211551] N90-12287
Stellarator transport theory
[DE89-016371] N90-12328
Superconductivity and magnetic scattering in the Nd(sub 2-x)Ce(sub x)CuO(sub 4-delta)
[DE89-016524] N90-12354

MAGNETIC FILMS
Thin film magnetic memory elements
[AD-D014178] N90-12281

MAGNETIC FLUX
High gain flux compression generator fabrication issues
[DE89-017888] N90-11951
Investigation of resonant ac-dc magnetic field effects
[AD-A211612] N90-12159
Investigation of active regions at high resolution by balloon flights of the Solar Optical Universal Polarimeter (SOUP) N90-12487

MAGNETIC MATERIALS
Effective permeability of mixtures
[PB89-218952] N90-11839

MAGNETIC PUMPING
Gordon Conference on Atomic Physics
[AD-A211946] N90-12304

MAGNETIC SIGNALS
HIPAS 1987-88: ULF research and campaign support
[AD-A211720] N90-11933

MAGNETIC SIGNATURES
Magnetograph group summary N90-12461
An imaging vector magnetograph for the next solar maximum N90-12489

MAGNETIC STORAGE
Thin film magnetic memory elements
[AD-D014178] N90-12281

MAGNETIC STORMS
Distribution of auroral precipitation at midnight during a magnetic storm
[PB89-213136] N90-12118
Some of the terrestrial effects of AR 5395
N90-12482

MAGNETIZATION
The effect of flux creep on the magnetization field in the SSC diopole magnets
[DE90-000124] N90-12284
Preparation and characterization of single phase Ba(1-x)KxBiO3
[DE89-017735] N90-12362

MAGNETOHYDRODYNAMIC GENERATORS
Computer controlled MHD power consolidation and pulse-generation system
[DE89-015600] N90-12333

MAGNETOHYDRODYNAMIC WAVES
HIPAS 1987-88: ULF research and campaign support
[AD-A211720] N90-11933

MAGNETOHYDRODYNAMICS
Exploding metallic foil fuse modeling at Los Alamos
[DE89-016970] N90-11998
Non-stationary computer model of the asymptotic region of an electric arc gas heater
[IPPCZ-288] N90-12330
Advanced concepts theory
[AD-A211665] N90-12344
MHD (magnetohydrodynamic) modeling of solar and interplanetary processes
[PB89-215461] N90-12416

MAGNETOMETERS
HIPAS 1987-88: ULF research and campaign support
[AD-A211720] N90-11933

MAGNETOSTRICTION
Magnetostrictive torque sensor
[AD-D014169] N90-11996

MAGNUS EFFECT
Internal Magnus effects in superfluid 3He-A
[PB89-212617] N90-12351

MAIN SEQUENCE STARS
Effects of main-sequence mass loss on the turnoff ages of population 1 clusters
[DE89-016755] N90-12417

MAINTAINABILITY
The RB199: An in-service success
[PNR90544] N90-11746

MAINTENANCE
Improving snow roads and airstrips in Antarctica
[AD-A211588] N90-11907
DSEP (Dual Shaft Electric Propulsion) operation and maintenance manual for the NVH and TB-2 vehicles: Advanced Dual Shaft Electric Propulsion System technology development program
[DE89-017549] N90-12411

MAN MACHINE SYSTEMS
USSR Space Life Sciences Digest, Issue 24
[NASA-CR-3922(28)-ISSUE-24] N90-12152

MAN-COMPUTER INTERFACE
ISI's (Information Sciences Institute) SDI architecture simulator: An experiment in adding new software to the system
[AD-A211314] N90-12204

MANIFOLDS (MATHEMATICS)
Some notes on perturbations of differential-algebraic equations
[PB89-218564] N90-12243
Global linear representations of nonlinear systems and the adjoint map
[RR-347] N90-12247

MANIPULATORS
A distributed pipelined architecture of the recursive Lagrangian equations of motion for robot manipulators with VLSI implementation — VLSI (very large scale integration)
[RR-353] N90-11966
An optimum trajectory planner for robot manipulators in joint-space and under physical constraints
[RR-349] N90-12029
On the complexity analysis of the coriolis and centripetal effects of a 6 DOF robot manipulator — Degrees of Freedom (DOF)
[RR-344] N90-12030
The dynamic performance of robot manipulators under different operating conditions
[RR-345] N90-12031
Navigation of robotic systems
[DE89-017507] N90-12219
Fast forward dynamics algorithm for robot arms using multiprocessing
[RR-367] N90-12225

MANUALS
Transport systems research vehicle color display system operations manual
[NASA-TM-101577] N90-11736
DSEP (Dual Shaft Electric Propulsion) operation and maintenance manual for the NVH and TB-2 vehicles: Advanced Dual Shaft Electric Propulsion System technology development program
[DE89-017549] N90-12411

MANUFACTURING
Coupling rule-based and object-oriented programming for the classification of machined features
[DE89-017705] N90-11903
Manufacturing and the manufacturing engineer in the year 2000, revision
[DE89-017707] N90-11904
Application of dimensional analysis to statistical process modeling
[AD-A211881] N90-11905
Reasoning about change and exceptions in automated process planning
[DE89-017706] N90-12195

MANY BODY PROBLEM
GALAX: A two-dimensional N-body code for disk galaxy dynamics
[PB89-217780] N90-12415

MAPPING
Air velocity mapping of environmental test chambers
[AD-A212082] N90-11764
Mapping nonlinear integro-differential equations into the frequency domain
[RR-366] N90-12249

MAPS
Effects of the advanced map interpretation and terrain analysis course on contour-level navigation performance
[AD-A212163] N90-11723

MARINE METEOROLOGY
Hydrophone investigations of earthquakes and explosion generated high-frequency seismic phases
[AD-A212055] N90-12122
Airborne profiles taken near San Nicolas Island, California, during Operation FIRE (First ISCCP (International Satellite Cloud Climatology Project) regional experiment) (1987): Aerosol size distributions, air and surface temperatures, cloud top temperatures, and relative humidities
[AD-A211664] N90-12136

MARKOV PROCESSES
A unified framework for simulating Markovian models of highly dependable systems
[AD-A212164] N90-12267

MARS (PLANET)
Design of a solar sail mission to Mars
[NASA-CR-186045] N90-11771

MASS
Effects of main-sequence mass loss on the turnoff ages of population 1 clusters
[DE89-016755] N90-12417

MASS DISTRIBUTION
Effect of control surface mass unbalance on the stability of a closed-loop active control system
[NASA-TP-2952] N90-12042

MASS SPECTROMETERS
Experimental research in high energy physics
[DE90-000061] N90-12342

MASS SPECTROSCOPY
Laser ionization mass spectroscopy
[DE89-008039] N90-12015

MASS TRANSFER
A lightweight solid polymer electrolyte fuel cell with stack power density of 3 kW/lb (7 kW/kg)
[AD-A211542] N90-12098
Human body regional convective heat transfer determination using sublimating naphthalene disks
[AD-A212170] N90-12165

MASSIVELY PARALLEL PROCESSORS
The upwind control volume scheme for unstructured triangular grids
[NASA-TM-101664] N90-11703

MATCHED FILTERS
Analysis of two-pass Modified Hough Transform (MHT) technique for the detection of wake like signals
[AD-A211982] N90-11924

MATCHING
Optimal matching of 3-D convex polyhedra
[TELECOM-PARIS-89C003] N90-12258

MATERIALS RECOVERY
Correlating microemulsion fuel composition, structure and combustion properties
[DE89-017779] N90-11898

MATHEMATICAL LOGIC
A digital model for level-clocked circuitry
[AD-A211937] N90-11957
Optical arithmetic logic using the modified signed-digit redundant number representation
[AD-D014176] N90-12186
Some techniques for anaphora resolution in algebraic linguistics
[REPT-89-28] N90-12265
Fuzzy logic and the generalized modus ponens
[REPT-88-92] N90-12274

MATHEMATICAL MODELS
The upwind control volume scheme for unstructured triangular grids
[NASA-TM-101664] N90-11703
Robust control design for flight control
[AD-A211957] N90-11756
ILS mathematical modeling study of the effects of proposed hangar construction at the Orlando International Airport, Runway 17R, Orlando, Florida
[DOT/FAA/CT-TN89/52] N90-11762
An integrated methodology for optimizing structural composite damping
[NASA-TM-102343] N90-11808
Analysis of opposed jet hydrogen-air counter flow diffusion flame
[NASA-CR-182366] N90-11825
International seminar on the inelastic behavior of solids: Models and utilization
[DE89-017420] N90-11858
A rate-dependent constitutive model for Be
[DE89-017755] N90-11861
A critical assessment of models available for the shock initiation of heterogeneous explosives
[MRL-TR-89-17] N90-11896
Application of dimensional analysis to statistical process modeling
[AD-A211881] N90-11905
Modelling and control of a diffusion/LPCVD furnace
[REPT-88-97] N90-11910
Recent advances to NEC (Numerical Electromagnetics Code): Applications and validation
[DE89-009231] N90-11917
Clutter models for subsurface electromagnetic applications
[PB89-229678] N90-11925
Modeling of diffraction reflection and clutter loss in UHF radio wave propagation
[FEL-1988-28] N90-11938
A digital model for level-clocked circuitry
[AD-A211937] N90-11957
KIVA reactive hydrodynamics code applied to detonations in high vacuum
[DE89-016979] N90-11974
Exploding metallic foil fuse modeling at Los Alamos
[DE89-016970] N90-11998
An experimental and analytical program to develop crack tip fracture criteria
[AD-A211565] N90-12051
Disturbances in the Arizona Monsoon N90-12071
The effect of latent heat release on synoptic-to-planetary wave interactions and its implication for satellite observations: Theoretical modeling N90-12073
The effect of latent heat release on synoptic-to-planetary scale wave interactions: Observational study
N90-12074
Use of satellite data and modeling to asses the influence of stratospheric processes on the troposphere
N90-12075
Laboratory and theoretical models of planetary-scale instabilities and waves N90-12076
Laboratory and theoretical studies of baroclinic processes N90-12077
A lightweight solid polymer electrolyte fuel cell with stack power density of 3 kW/lb (7 kW/kg)
[AD-A211542] N90-12098
Evaluation and sensitivity analyses results of the MESOPUFF 2 model with CAPTEX (Cross-Appalachian Tracer Experiment) measurements
[PB89-198253] N90-12103
Review of the national ambient air quality standards for lead: Exposure analysis methodology and validation
[PB89-207914] N90-12104
Processing of DMSP magnetic data and its use in geomagnetic field modeling
[NASA-TM-100750] N90-12115
Investigations of Eurasian seismic sources and upper mantle structure
[AD-A211806] N90-12120
Seismic wave attenuation and yield determination at regional distances
[AD-A211548] N90-12128
The conditional-event approach to distributed simulation
[NASA-CR-185890] N90-12200
Efficient diagnosis of multiprocessor systems under probabilistic models
[NASA-CR-185965] N90-12212
Sequential design of experiments with physically based models 23
[AD-A211918] N90-12239
Mapping nonlinear integro-differential equations into the frequency domain
[RR-366] N90-12249
Augmentations of grammatical categories in distributional-algebraic models of natural languages
[REPT-89-24] N90-12262
On the asymptotic optimality of certain empirical Bayes simultaneous testing procedures
[AD-A211649] N90-12270
Modeling and analysis of nonlinear time series
[RR-355] N90-12272
Numerical solution of acoustic-structure interaction problems
[AD-A211505] N90-12293
Non-stationary computer model of the asymptotic region of an electric arc gas heater
[IPPCZ-288] N90-12330
Role of conceptual models in the design and use of information systems
[PB89-217376] N90-12392
Problem of incomplete information in relational databases
[PB89-217533] N90-12393
Flare model sensitivity of the Balmer spectrum
N90-12477

MATRICES (MATHEMATICS)
Microscopic approach to the generator coordinate method
[DE89-016701] N90-12233
A dynamic proof of the Frobenius-Perron theorem for Metzler matrices
[AD-A211839] N90-12235
Four vector-matrix primitives
[AD-A211889] N90-12237
A matrix factorization and its application to large-scale linear programming
[AD-A211293] N90-12244
A long time tail for random walk in random scenery
[REPT-89-08] N90-12278

MATRIX MATERIALS
Carbon fiber reinforced glass matrix composites for structural space based applications
[AD-A211682] N90-11818

MATRIX METHODS
Application of matrix correction methods on a plate and a truss structure
[NLR-MP-88042-U] N90-12056

MAXWELL EQUATION
Non-stationary computer model of the asymptotic region of an electric arc gas heater
[IPPCZ-288] N90-12330

MEAN
On finding the largest normal mean and estimating the selected mean
[AD-A211628] N90-12245

MEASURING INSTRUMENTS
Field evaluation of the multi-depth deflectometers
[PB89-207708] N90-11994
Lagrangian analysis of MIV (Magnetic Impulse-Velocity) gauge experiments on PBX 9502 using the mass-displacement moment function
[DE89-016612] N90-12000
Devices and procedures for the calibration of sensors and measurement: Systems of the flight test support system ATTAS
[DFVLR-MITT-89-06] N90-12007

MECHANICAL DRIVES
Adjustable speed drive study, part 1
[DE89-017654] N90-11948

MECHANICAL PROPERTIES
Coating galvanized steel
[AD-A211775] N90-11869
Effect of fretting on fatigue strength of aluminium alloys
[ESDU-89004] N90-11870

MECHANICAL SHOCK
A critical assessment of models available for the shock initiation of heterogeneous explosives
[MRL-TR-89-17] N90-11896

MEDICAL SCIENCE
National Library of Medicine DOCLINE (tradename) manual
[PB89-188676] N90-12390

MELT SPINNING
Precipitation strengthened high strength, high conductivity Cu-Cr-Nb alloys produced by chill block melt spinning
[NASA-CR-185144] N90-11853

MELTING
Formation and modification of surface alloys by excimer laser melting and resolidification
[DE89-016968] N90-11856

MEMBRANES
Membrane fusion: The role of polyphosphatidylinositol
[AD-A211289] N90-12156

MEMORY
Synaptic plasticity and memory formation
[AD-A211368] N90-12158
Metacognition and retrieval from long-term memory at Mount Everest
[AD-A211629] N90-12177

MEMORY (COMPUTERS)
Ground-state coding in partially connected neural networks
[NASA-TM-102239] N90-12227
Thin film magnetic memory elements
[AD-D014178] N90-12281

MENTAL PERFORMANCE
A menu of self-administered microcomputer-based neurotoxicology tests
[NASA-CR-185518] N90-12175
The effect of incentives on the reliability and validity of cognitive speed tests
[AD-A211346] N90-12181
Computer-based tutors for explaining and managing the process of diagnostic reasoning
[AD-A211738] N90-12222

MESONS
An experimental high energy physics program
[DE89-014695] N90-12311

MESOSCALE PHENOMENA
Low level remote sensing: The Doppler Radar wind profiler N90-12067
Satellite-derived rainfall estimates and propagation characteristics associated with the Mesoscale Convective Systems (MCSs)
[PB89-213417] N90-12086

MESSAGE PROCESSING
The J-Machine: A fine grain concurrent computer
[AD-A211909] N90-12187

METAL COATINGS
Fe-Ni-Cr alloys for coatings and electroforms
[PB89-195846] N90-11849
Electrolitic deposited ohmic contacts on III-V compound semiconductors: A review
[PB89-217400] N90-12350

METAL CRYSTALS
A rate-dependent constitutive model for Be
[DE89-017755] N90-11861

METAL FATIGUE
The effects of temperature on fatigue crack propagation in 310 austenitic stainless steel
[DE90-000136] N90-11865
Effect of fretting on fatigue strength of aluminium alloys
[ESDU-89004] N90-11870

METAL FILMS
Reactive ion etching of sputtered silicon carbide and tungsten thin films for device applications
[AD-A211711] N90-11847
Low temperature formation of titanium aluminide films using physical vapor deposition
[AD-A211877] N90-11866

METAL FOILS
Exploding metallic foil fuse modeling at Los Alamos
[DE89-016970] N90-11998

METAL IONS
X ray diffraction patterns of metal aurocyanides
[DE89-015188] N90-11851
Beam dynamics of a liquid metal ion source
[DE89-015856] N90-12295

METAL MATRIX COMPOSITES
Inorganic composite materials in Japan: Status and trends
[PB89-230015] N90-11810
Deformation behavior of SiC/2014 Al metal-matrix composite
[AD-A212095] N90-11816
Low temperature formation of titanium aluminide films using physical vapor deposition
[AD-A211877] N90-11866

METAL PLATES
Axial compression buckling test on the H-2 launch vehicle satellite fairing structural element prototype (aluminum surface plate/aluminum honeycomb sandwiched curved surface plate)
[NAL-TM-563] N90-12039

METAL POWDER
Fe-Ni-Cr alloys for coatings and electroforms
[PB89-195846] N90-11849

METAL SHEETS
Deformation of extruded titanium alloys under superplastic conditions
[RAE-TM-MAT/STR-1111] N90-11876

Effect of superplastic deformation on the surface roughness of sheet
[RAE-TM-MAT/STR-1112] N90-12054

METAL SURFACES
Quantitative interpretation of auger lineshapes and electron/photon stimulated desorption
[AD-A211550] N90-11842

METALLIZING
Reactive ion etching of sputtered silicon carbide and tungsten thin films for device applications
[AD-A211711] N90-11847
Niobium and niobium nitride contacts on semiconducting material
[AD-D014177] N90-12347

METEORITE CRATERS
Radar scattering mechanisms within the meteor crater ejecta blanket: Geologic implications and relevance to Venus N90-12435
Deducing the age of the dense Venus atmosphere N90-12438

METEORITIC MICROSTRUCTURES
An atom probe study of phase decomposition in three iron meteorites
[DE89-017581] N90-12420

METEOROLOGICAL PARAMETERS
ASR-9 weather channel test report
[AD-A211749] N90-11934
MEGALIDAR
[AD-A212074] N90-12020

METEOROLOGICAL RADAR
ASR-9 weather channel test report
[AD-A211749] N90-11934
Middle Atmosphere Program. Handbook for MAP, volume 28
[NASA-CR-184972] N90-12117

METEOROLOGICAL RESEARCH AIRCRAFT
Scientific justification and development plan for a mid-sized jet research aircraft
[PB89-208995] N90-11731
Meeting review: The Second NCAR (National Center for Atmospheric Research) Research Aircraft Fleet Workshop
[PB89-200901] N90-12113

METEOROLOGICAL SERVICES
ASR-9 weather channel test report
[AD-A211749] N90-11934
Contemporary China's meteorological enterprises (selected portions)
[AD-A210697] N90-12131
World Weather Watch: Implementation
[WMO-714] N90-12139

METEOROLOGY
Scientific justification and development plan for a mid-sized jet research aircraft
[PB89-208995] N90-11731

METHANE
Conversion of methane to liquid hydrocarbons
[DE89-017547] N90-11831
Global data bases on distribution, characteristics and methane emission of natural wetlands: Documentation of archived data tape
[NASA-TM-4153] N90-12090

METHOD OF MOMENTS
Spectral-domain analysis of finite frequency selective surfaces
[AD-A211669] N90-11932

METHYL ALCOHOL
Methanol fueled vehicles and photochemical models: An evaluation of the state of knowledge
[PB89-214225] N90-12410

METHYL COMPOUNDS
Suppression of side chain crystallization and transformation of monotropic mesophases into enantiotropic mesophases by copolymerization of the parent polymers' monomer pairs containing constitutional isomeric mesogenic side groups
[AD-A209066] N90-11878

METROLOGY
Use of the NPL linac for x ray dosimetry --- linear accelerator (linac)
[NPL-RSA(EXT)-6] N90-12314
Center for Electronics and Electrical Engineering technical publication announcements covering Center programs, January-March 1989 with 1989 CEEE events calendar
[PB89-228308] N90-12402

MEXICO
Disturbances in the Arizona Monsoon N90-12071

MICROCHANNEL PLATES
A microchannel plate intensified, subnanosecond, X-ray imaging camera
[DE89-017781] N90-12003

MICROCOMPUTERS
Microcomputer-based tests for repeated-measures: Metric properties and predictive validities
[NASA-CR-185517] N90-12174
A menu of self-administered microcomputer-based neurotoxicology tests
[NASA-CR-185518] N90-12175
Basic program for raster scan display unit
[NAL-TM-560] N90-12185

MICROELECTRONICS
High resolution X-ray spectroscopy using germanium microcalorimeters
[DE89-017784] N90-12004
Beam assisted fabrication of 3-5/Si monolithic devices
[AD-A212046] N90-12367

MICROPROCESSORS
Power up modification for video switcher microprocessor interface for sensor system processing system
[AD-A211543] N90-11962

MICROSTRIP ANTENNAS
Dielectric covered microstrip patch antennas
[AD-A211577] N90-11963

MICROSTRIP TRANSMISSION LINES
Calibration and de-embedding of microwave measurements using any combination of one- or two-port standards
[PB89-212674] N90-11916

MICROSTRUCTURE
Processing and characterization of alumina platelet-reinforced mullite composites
[DE90-000057] N90-11814
Mechanism of electrochemical activation of carbon electrodes: Role of graphite lattice defects
[AD-A211644] N90-11845
Low temperature formation of titanium aluminide films using physical vapor deposition
[AD-A211877] N90-11866
Fractographic and microstructural analysis of fatigue crack growth in a Ti-6Al-4V fan disc forging
[NLR-MP-88028-U] N90-11877
Photolithography: A new tool for ceramic science
[DE90-000135] N90-11885
Correlating microemulsion fuel composition, structure and combustion properties
[DE89-017779] N90-11898
Development of microstructured DH diode lasers and detectors for the near and medium IR spectral domain using molecular beam epitaxy
[IPM-15/1988] N90-12023
Anisotropy and microstructure of high-coercivity rare earth permanent magnets
[AD-A211905] N90-12285
Characterization of the Structure and Chemistry of Defects in Materials: Proceedings, volume 138
[DE89-014796] N90-12352
Effect of annealing conditions on the structural and superconducting properties of Y-Ba-Cu-O films
[AD-A211308] N90-12371
Synthesis and microstructure of highly oriented PbTiO3 thin films prepared by a sol-gel method
[AD-A211735] N90-12377

MICROWAVE EMISSION
The Owens Valley solar array N90-12490

MICROWAVE EQUIPMENT
Microwave signal detection using modulation of polymeric optical waveguides
[DE89-017545] N90-11921

MICROWAVE FREQUENCIES
Design, construction and test of a frequency doubler for 183 GHz
[PB89-212591] N90-11944

MICROWAVE LANDING SYSTEMS
Simulations for computer centerline approach
[DOT/FAA/CT-TN89/41] N90-11726
Independent Orbiter Assessment (IOA): FMEA/CIL assessment
[NASA-CR-185550] N90-11783

MICROWAVE RADIOMETERS
Venus surface properties deduced from radar and radiometry N90-12431

MICROWAVE SCATTERING
Propagation of an elliptical laser beam through the turbulent atmosphere (vertical beams)
[PB89-208680] N90-12010

MICROWAVE SOUNDING
Middle Atmosphere Program. Handbook for MAP, volume 28
[NASA-CR-184972] N90-12117

MICROWAVE SWITCHING
Channelized coplanar waveguide pin-diode switches
[NASA-TM-102289] N90-11943

MICROWAVE TRANSMISSION
Channelized coplanar waveguide pin-diode switches
[NASA-TM-102289] N90-11943

MICROWAVES
Calibration and de-embedding of microwave measurements using any combination of one- or two-port standards
[PB89-212674] N90-11916
Microwave signal detection using modulation of polymeric optical waveguides
[DE89-017545] N90-11921
Microwave instability near transition energy
[DE90-000107] N90-11922
Microwave Tokamak Experiment (MTX) ohmic heating system
[DE89-017892] N90-12340

MIDAIR COLLISIONS
UK airmisses involving commercial air transport, May-August 1988
[ISSN-0951-6301] N90-11717
UK airmisses involving commercial air transport
[CAA-2/88] N90-11718

MIDDLE ATMOSPHERE
Middle Atmosphere Program. Handbook for MAP, volume 28
[NASA-CR-184972] N90-12117

MIE SCATTERING
Infrared backscattering N90-12083

MILITARY HELICOPTERS
Applications of flight control system methods to an advanced combat rotorcraft
[NASA-TM-101054] N90-11752

MILITARY TECHNOLOGY
Post crash flight analysis: Visualizing flight recorder data
[AD-A212063] N90-11715
Feasibility of graphics voice telephones for the post 2000 era
[FEL-1988-26] N90-11937
Twenty-five years of service, 1962-1987: Proceedings of the Air Force Studies Board Symposium on Air Force Research and Development, November 16, 1987
[PB89-198915] N90-12384
FY 1990/FY 1991 biennial budget descriptive summaries for the Strategic Defense Initiative Organization
[AD-A211985] N90-12409

MILLIMETER WAVES
Calibration and de-embedding of microwave measurements using any combination of one- or two-port standards
[PB89-212674] N90-11916
First interferometric observations with arc-sec. resolution of solar radio bursts at millimeter wavelengths N90-12472

MILLING
Photolithography: A new tool for ceramic science
[DE90-000135] N90-11885

MIRRORS
Kinematic design NC optical generator N90-12316

MISSION PLANNING
Wave combustors for trans-atmospheric vehicles
[NASA-TM-102238] N90-11742
Strategy for earth explorers in global earth sciences
[NASA-CR-185933] N90-12084

MIXED CRYSTALS
Process for single crystal growth of high T(sub c) superconductors
[AD-D014167] N90-12346

MIXERS
Investigation of advanced mixer-ejector exhaust system
[AD-A211943] N90-11705

MIXING CIRCUITS
Cryogenic Schottky-mixer receiver front-end for 40-50 GHz
[PB89-221667] N90-11959
SIS (Superconductor-Insulator-Superconductor) mixer research
[AD-A211607] N90-12375

MIXING LAYERS (FLUIDS)
Control of turbulent mixing layers
[AD-A211413] N90-11708
Cryogenic free jets
[ESA-TT-1128] N90-11767

MIXTURES
Effective permeability of mixtures
[PB89-218952] N90-11839

MODAL RESPONSE
Computation of generalized modal loads in an acoustic field define by a distribution of correlated pressures
[NASA-CR-186041] N90-12047

MODELS
An open-loop transient thermodynamic model of the Cougar turbojet
[AD-A211774] N90-11745
Proceedings of the Workshop on Compound Semiconductor Devices and Integrated Circuits (13th) held in Cabourg, France on 10-12 May 1989
[AD-A211848] N90-11954
Thermal model for double-drift IMPATT diodes on diamond heat sinks
[AD-A211746] N90-12380

MODEMS
Performance of four rake modems over the non-disturbed wideband HF channel
[AD-A211589] N90-11930

MOIRE INTERFEROMETRY
An experimental and analytical program to develop crack tip fracture criteria
[AD-A211565] N90-12051

MOISTURE
Crau 1987: The KNMI contribution --- KNMI (Royal Netherlands Meteorological Institute)
[KNMI-TR-110] N90-12140
Description of a software library for the calculation of surface fluxes
[KNMI-TR-112] N90-12141

MOISTURE METERS
Crau 1987: The KNMI contribution — KNMI (Royal Netherlands Meteorological Institute)
[KNMI-TR-110] N90-12140

MOJAVE DESERT (CA)
Radar scattering from desert terrains, Pisgah/Lavic Region, California: Implications for Magellan
N90-12443

MOLECULAR BEAM EPITAXY
Development of microstructured DH diode lasers and detectors for the near and medium IR spectral domain using molecular beam epitaxy
[IPM-15/1988] N90-12023
Beam assisted fabrication of 3-5/Si monolithic devices
[AD-A212046] N90-12367

MOLECULAR BEAMS
High temperature and high resolution UV photoelectron spectroscopy using supersonic molecular beams
[DE90-000176] N90-11835

MOLECULAR BIOLOGY
Cellular and molecular mechanisms of high pressure inotropy in cardiac muscle
[AD-A211695] N90-12170

MOLECULAR COLLISIONS
New developments in the ab initio treatment of low energy electron collisions with molecules
[DE89-015294] N90-12299
Spin-orbit relaxation rates of Bi(6p(3)) 2D(3/2) following photolysis of Bi(CH3)3 at lambda = 193 nm
[AD-A211792] N90-12303

MOLECULAR EXCITATION
Spin-orbit relaxation rates of Bi(6p(3)) 2D(3/2) following photolysis of Bi(CH3)3 at lambda = 193 nm
[AD-A211792] N90-12303
Electron attachment and molecular fragmentation in laser-excited plasmas
[AD-A212098] N90-12343

MOLECULAR STRUCTURE
Molecular dynamics study of the primitive model of 1-3 electrolyte studies
[AD-A211653] N90-11846
Suppression of side chain crystallization and transformation of monotropic mesophases into enantiotropic mesophases by copolymerization of the parent polymers' monomer pairs containing constitutional isomeric mesogenic side groups
[AD-A209066] N90-11878
Structure/reactivity relationships of polysilazane preceramics
[AD-A212028] N90-11888
The prediction of middle distillate fuel properties using liquid chromatography-proton nuclear magnetic resonance spectroscopy data
[AD-A211879] N90-11899
Laser production of soft x rays by multiquantum processes and the excitation of atomic inner-shell states
[AD-A211372] N90-12021

MOLECULES
State-resolved reaction dynamics
[AD-A211613] N90-12307

MOLYBDENUM ALLOYS
Fracture toughness data base for HT9 and modified 9Cr-1Mo irradiated in several reactors up to approximately 100 dpa
[DE90-000111] N90-11864

MOMENTUM
Low level remote sensing: Orographic winds
N90-12066
Description of a software library for the calculation of surface fluxes
[KNMI-TR-112] N90-12141
Electron-positron momentum distribution measurements of high-T(sub c) superconductors and related systems
[DE89-017538] N90-12358

MONITORS
Progress of research on water vapor lidar
[NASA-CR-185970] N90-12011

MONOMERS
Suppression of side chain crystallization and transformation of monotropic mesophases into enantiotropic mesophases by copolymerization of the parent polymers' monomer pairs containing constitutional isomeric mesogenic side groups
[AD-A209066] N90-11878

MONOTONE FUNCTIONS
Sequential searching in multidimensional monotone arrays
[AD-A211938] N90-12188

MONSOONS
Disturbances in the Arizona Monsoon N90-12071

MONTE CARLO METHOD
Microwave instability near transition energy
[DE90-000107] N90-11922
A unified framework for simulating Markovian models of highly dependable systems
[AD-A212164] N90-12267
Monte Carlo studies of nuclei and quantum liquid drops
[DE89-016914] N90-12300

MORPHOLOGY
Temperature dependent effects during Ag deposition on Cu(110)
[DE89-016987] N90-11857
On the differentiable manifold of fixed order stable linear systems
[REPT-88-89] N90-12250
A morphologic study of Venus Ridge belts
N90-12432

MOSSBAUER EFFECT
Electronic structure of transition metal alloys and intermetallics: Charge transfer and its implications for Moessbauer effect measurements
[DE89-017603] N90-11860

MOTION PERCEPTION
Visual motion perception
[AD-A210994] N90-12160
Discriminating rigid from nonrigid motion
[AD-A211794] N90-12180

MOTION SIMULATION
Molecular dynamics study of the primitive model of 1-3 electrolyte studies
[AD-A211653] N90-11846

MOTION STABILITY
Analysis of a system of two weakly nonlinear coupled harmonic oscillators arising from the field of wind-induced vibrations
[REPT-89-22] N90-12261

MOTIVATION
The effect of incentives on the reliability and validity of cognitive speed tests
[AD-A211346] N90-12181

MOTOR VEHICLES
Distance and clearance perception using forward-looking, vehicular television systems
[DE89-014740] N90-12319
Methanol fueled vehicles and photochemical models: An evaluation of the state of knowledge
[PB89-214225] N90-12410

MOUNTAINS
Ice runways near the South Pole
[AD-A211606] N90-11908

MULLITES
Processing and characterization of alumina platelet-reinforced mullite composites
[DE90-000057] N90-11814

MULTIPATH TRANSMISSION
Theory and simulation of the operation of a Doppler direction finder in a multipath environment
[FEL-1988-56] N90-11939

MULTIPLEXING
Introduction to the Mil-Std-1553B serial multiplex data bus
[RAE-TM-M-9] N90-12405

MULTIPROCESSING (COMPUTERS)
Sequential searching in multidimensional monotone arrays
[AD-A211938] N90-12188
Processing rate sensitivities of a heterogeneous multiprocessor
[PB89-229017] N90-12201
Efficient diagnosis of multiprocessor systems under probabilistic models
[NASA-CR-185965] N90-12212
Parallel architectures and parallel algorithms for integrated vision systems
[NASA-CR-185990] N90-12215
Fast forward dynamics algorithm for robot arms using multiprocessing
[RR-367] N90-12225

MULTISPECTRAL BAND SCANNERS
Investigation on analyzing computer-aided forest disease classifications
[DFVLR-FB-89-16] N90-12112

MULTIVARIATE STATISTICAL ANALYSIS
On a classification problem: Ranking and selection approach
[AD-A211627] N90-12269

MUSCLES
Cellular and molecular mechanisms of high pressure inotropy in cardiac muscle
[AD-A211695] N90-12170

MUSCULAR FATIGUE
The effect of caffeine on endurance time to exhaustion at high altitude
[AD-A212069] N90-12163

MUSCULAR STRENGTH
Wrist orientation effect on grip strength and endurance
[PB89-200935] N90-12179

MYOCARDIUM
Cellular and molecular mechanisms of high pressure inotropy in cardiac muscle
[AD-A211695] N90-12170

N

NAPHTHALENE
Human body regional convective heat transfer determination using sublimating naphthalene disks
[AD-A212170] N90-12165

NARROWBAND
A new approach to HF (High Frequency) channel modeling and simulation. Part 1: Deterministic model
[PB89-203962] N90-11913

NASTRAN
Investigation of difficult component effects on finite element model vibration prediction for the Bell AH-1G helicopter. Volume 1: Ground vibration test results
[NASA-CR-181916-VOL-1] N90-12058

NATIONAL AIRSPACE SYSTEM
UK airmisses involving commercial air transport, May-August 1988
[ISSN-0951-6301] N90-11717
Rotorcraft low altitude CNS benefit/cost analysis: Rotorcraft operations data
[DOT/FAA/DS-89/9] N90-12406

NATIONAL SEVERE STORMS PROJECT
Severe local storm warning verification: 1988
[PB89-226310] N90-12134

NATURAL GAS
Natural gas to liquids
[DE89-000982] N90-11828

NAVIER-STOKES EQUATION
Hopf bifurcation in the driven cavity
[NASA-TM-102334] N90-11969
Viscous split algorithms for the time dependent incompressible Navier-Stokes equations
[AD-A211592] N90-11985
Efficient finite element solution of Navier-Stokes equations and related topics
[AD-A211647] N90-11986
Numerical computation of the viscous flow field around a prolate spheroid
[DFVLR-FB-89-22] N90-11992
A multigrid algorithm for the incompressible Navier-Stokes equation
[GMD-374] N90-11993
A least-squares finite element method for incompressible Navier-Stokes problems
[NASA-TM-102385] N90-12231
Non-stationary computer model of the asymptotic region of an electric arc gas heater
[IPPCZ-288] N90-12330

NAVIGATION
Navigation of robotic systems
[DE89-017507] N90-12219

NAVIGATION INSTRUMENTS
Navigation experiment NAVEX: Data storage and processing
[DFVLR-MITT-89-09] N90-11727
Navigation experiment NAVEX: The equipment delay times in the Spacelab mission D1
[DFVLR-MITT-89-10] N90-11728

NAVSTAR SATELLITES
Sentinel satellite positional precision derived from the NAVSTAR global positioning system
[AD-A211876] N90-11720

NEAR INFRARED RADIATION
Growth and characterization of materials for tunable lasers in the near infrared spectral region
[NASA-CR-185832] N90-12009

NEGATIVE IONS
Atomic and molecular surface and volume processes in the analysis of negative hydrogen discharges
[DE89-015705] N90-12294

NEODYMIUM LASERS
Construction of a picosecond laser system for the investigation of semiconductors using nonlinear optical methods
[ETN-89-94664] N90-12013
Laser ionization mass spectroscopy
[DE89-008039] N90-12015
New laser materials
[DE89-017524] N90-12017

NETWORK ANALYSIS
Calibration and de-embedding of microwave measurements using any combination of one- or two-port standards
[PB89-212674] N90-11916

NETWORK CONTROL
A hybrid optimisation strategy for adaptive feed-forward layered networks
[RSRE-MEMO-4193] N90-12226

NEURAL NETS
Optical computing based on the Hopfield model for neural networks
[AD-A211824] N90-12216
Can perceptrons find Lyapunov functions: An algorithmic approach to systems stability
[RR-365] N90-12224
Ground-state coding in partially connected neural networks
[NASA-TM-102239] N90-12227

NEUROMUSCULAR TRANSMISSION
Synaptic plasticity and memory formation
[AD-A211368] N90-12158

NEUROPHYSIOLOGY
Synaptic plasticity and memory formation
[AD-A211368] N90-12158

NEUTRAL PARTICLES
Comparison of laser and neutral particle beam discrimination
[DE89-017786] N90-12018

NEUTRINOS
Experimental test of PCAC hypothesis in the reactions mu neutrino-proton giving muon(-)-proton-pion(+) and mu antineutrino-proton giving muon(+)-proton-pion(-) in the delta (1232) region — partial conserved axial current
[MPE-PAE/EXP.EL.199] N90-12309
The Baksan gallium solar neutrino experiment
[DE89-016036] N90-12457

NEUTRON DIFFRACTION
Neutron scattering studies of premartensitic phenomena
[DE90-000025] N90-11863
Single crystal diffraction
[DE90-000024] N90-12366

NEUTRON SCATTERING
Neutron scattering studies of premartensitic phenomena
[DE90-000025] N90-11863

NICKEL ALLOYS
Ignition characteristics of the nickel-based alloy UNS N07718 in pressurized oxygen
[NASA-CR-185932] N90-11850
Weldability of ductile nickel aluminides
[DE89-017452] N90-11859
Determination and description of the long term creep behavior of high temperature gas turbine materials
[ETN-89-94985] N90-11871

NIGHT SKY
Distribution of auroral precipitation at midnight during a magnetic storm
[PB89-213136] N90-12118

NIGHT VISION
Visual acuity and stereopsis with night vision goggles
[AD-A211552] N90-12167

NIOBIUM
Niobium and niobium nitride contacts on semiconducting material
[AD-D014177] N90-12347

NIOBIUM ALLOYS
Precipitation strengthened high strength, high conductivity Cu-Cr-Nb alloys produced by chill block melt spinning
[NASA-CR-185144] N90-11853
Creep strength of niobium alloys, Nb-1%Zr and PWC-11
[NASA-TM-102390] N90-11854

NIOBIUM COMPOUNDS
The characterization of Nb3Sn superconductors for use in magnets of 19 T and greater
[DE89-017758] N90-12364

NITRIDES
Niobium and niobium nitride contacts on semiconducting material
[AD-D014177] N90-12347

NITRIDING
Advances and directions of ion nitriding/carburizing
[NASA-TM-102398] N90-11902

NITROGEN DIOXIDE
Synergistic effects of nitrogen dioxide and carbon dioxide following acute inhalation exposures in rats
[PB89-214779] N90-12150

NITROGEN OXIDES
Electron attachment and molecular fragmentation in laser-excited plasmas
[AD-A212098] N90-12343

NOISE INTENSITY
Noise data of four small propeller-driven airplanes
[PB89-216980] N90-12291

NOISE PROPAGATION
NRL/VOA modifications to IONCAP as of 12 July 1988
[AD-A211546] N90-11929
Acoustical effects of a large ridge on low-frequency sound propagation in stationary and moving atmospheres
[NASA-CR-186001] N90-12290

NOISE REDUCTION
Review and analysis of the DNW/Model 360 rotor acoustic data base
[NASA-TM-102253] N90-11692
Multi-stage noise-reducing system
[AD-D014179] N90-11942
Adaptive noise cancellation for a class of nonlinear 2R filter
[RR-351] N90-11965
Noise data of four small propeller-driven airplanes
[PB89-216980] N90-12291

NONDESTRUCTIVE TESTS
NDE (Non-Destructive Evaluation) publications, 1985
[PB89-229025] N90-12036

NONLINEAR EQUATIONS
Global linear representations of nonlinear systems and the adjoint map
[RR-347] N90-12247
Rational expansion for nonlinear input-output maps
[RR-348] N90-12248
Mapping nonlinear integro-differential equations into the frequency domain
[RR-366] N90-12249
Splines and equations of nonlinear parameters
[IMAG-RR-750-M] N90-12257

NONLINEAR FILTERS
Adaptive noise cancellation for a class of nonlinear 2R filter
[RR-351] N90-11965

NONLINEAR OPTICS
Construction of a picosecond laser system for the investigation of semiconductors using nonlinear optical methods
[ETN-89-94664] N90-12013

NONLINEAR SYSTEMS
Mapping nonlinear integro-differential equations into the frequency domain
[RR-366] N90-12249
Orthogonal least squares methods and their application to nonlinear system identification
[RR-343] N90-12259
Analysis of a system of two weakly nonlinear coupled harmonic oscillators arising from the field of wind-induced vibrations
[REPT-89-22] N90-12261
Fast sampling and stability of nonlinear sampled data systems. Part 2: Sampling rate estimations
[RR-341] N90-12271
Modeling and analysis of nonlinear time series
[RR-355] N90-12272
Fast sampling and stability of nonlinear sampled-data systems. Part 1: Existence theorems
[RR-340-PT-1] N90-12276
Slow sampling and stability of nonlinear sampled-data systems
[RR-342] N90-12277

NONLINEARITY
Near-planar TS waves and longitudinal vortices in channel flow: Nonlinear interaction and focusing
[NASA-CR-181928] N90-11698
Numerical experience with a class of algorithms for nonlinear optimization using inexact function and gradient information
[NASA-CR-181927] N90-12232
Linear (passive) and non-linear guided and studies in glass
[AD-A211693] N90-12325

NONPARAMETRIC STATISTICS
Small sample theory for steady state confidence intervals
[AD-A212097] N90-12242
Empirical Bayes estimation of binomial parameter with symmetric priors
[AD-A211646] N90-12246

NONTHERMAL RADIATION
The behavior of beams of relativistic non-thermal electrons under the influence of collisions and synchrotron losses
[NASA-CR-185983] N90-12298

NORMAL DENSITY FUNCTIONS
On a classification problem: Ranking and selection approach
[AD-A211627] N90-12269

NORTH AMERICA
The effect of latent heat release on synoptic-to-planetary scale wave interactions: Observational study
N90-12074

NORTHERN HEMISPHERE
UV ionospheric remote sensing with the polar BEAR satellite
[AD-A211359] N90-12127
Coronae on Venus observations and models of origin
N90-12449

NOTCH TESTS
Interlaminar stress concentration in fiber composites
[ETN-89-94670] N90-11809

NOZZLE DESIGN
Three-dimensional, two-phase, transonic, canted nozzle flows
[AD-A211528] N90-11984

NOZZLE FLOW
Investigation of advanced mixer-ejector exhaust system
[AD-A211943] N90-11705
Three-dimensional, two-phase, transonic, canted nozzle flows
[AD-A211528] N90-11984

NUCLEAR ELECTRIC POWER GENERATION
Activities report on KEMA R and D
[ST-REPT-VOL-6-NO-12] N90-12100

NUCLEAR EXPLOSIONS
Hydrophone investigations of earthquakes and explosion generated high-frequency seismic phases
[AD-A212055] N90-12122
Seismic wave attenuation and yield determination at regional distances
[AD-A211548] N90-12128

NUCLEAR FUSION
Gordon Conference on Atomic Physics
[AD-A211946] N90-12304
Highlights of papers presented at the workshop on Cold Fusion Phenomena
[DE89-016956] N90-12334

NUCLEAR HEAT
Nuclear closed-cycle gaseous heat engine concept
[DE89-016824] N90-12313

NUCLEAR PHYSICS
Gordon Conference on Atomic Physics
[AD-A211946] N90-12304

NUCLEAR REACTORS
Wind/seismic comparisons for upgrading existing structures
[DE89-016055] N90-12044

NUCLEAR STRUCTURE
Monte Carlo studies of nuclei and quantum liquid drops
[DE89-016914] N90-12300

NUCLEI (NUCLEAR PHYSICS)
Fluctuations in transverse energy and multiplicity, energy densities, and neutral pion spectra in nucleus-nucleus collisions at 200 GeV/nucleon
[DE89-017583] N90-12302
Detailed photonuclear cross-section calculations and astrophysical applications
[DE89-017531] N90-12419

NUCLEON-NUCLEON INTERACTIONS
Fluctuations in transverse energy and multiplicity, energy densities, and neutral pion spectra in nucleus-nucleus collisions at 200 GeV/nucleon
[DE89-017583] N90-12302
Experimental test of PCAC hypothesis in the reactions mu neutrino-proton giving muon(-)-proton-pion(+) and mu antineutrino-proton giving muon(+)-proton-pion(-) in the delta (1232) region — partial conserved axial current
[MPE-PAE/EXP.EL.199] N90-12309

NUMERICAL ANALYSIS
Computation of ramjet internal flowfields
[AD-A212001] N90-11743
Numerical analysis, scientific computing and fundamental studies of fluid mechanics
[DE89-017554] N90-11975

NUMERICAL CONTROL
Scheduling sporadic and aperiodic events in a hard real-time system
[AD-A211344] N90-12205
Computer controlled MHD power consolidation and pulse-generation system
[DE89-015600] N90-12333

NUMERICAL DIFFERENTIATION
On the differentiable manifold of fixed order stable linear systems
[REPT-88-89] N90-12250
NUMERICAL INTEGRATION
Spectral-domain analysis of finite frequency selective surfaces
[AD-A211669] N90-11932
NUMERICAL WEATHER FORECASTING
NASA/MSFC FY88 Global Scale Atmospheric Processes Research Program Review
[NASA-TM-100357] N90-12059

O

OBJECT PROGRAMS
ISI's (Information Sciences Institute) SDI architecture simulator: An experiment in adding new software to the system
[AD-A211314] N90-12204
OBSERVATION
When and where to look to observe major solar flares
N90-12465
OBSERVATION AIRCRAFT
Pilotless airplanes
[AD-A211719] N90-11734
OCEAN BOTTOM
Hydrophone investigations of earthquakes and explosion generated high-frequency seismic phases
[AD-A212055] N90-12122
OCEAN CURRENTS
Observations and modelling of deep equatorial currents in the central Pacific
[PB89-198139] N90-12145
Dynamics of the equatorial undercurrent and its termination
[PB89-198147] N90-12146
OCEAN DYNAMICS
Observations of long Rossby waves in the northern tropical Pacific
[PB89-196331] N90-12143
Observations and modelling of deep equatorial currents in the central Pacific
[PB89-198139] N90-12145
Dynamics of the equatorial undercurrent and its termination
[PB89-198147] N90-12146
OCEAN SURFACE
Hydrophone investigations of earthquakes and explosion generated high-frequency seismic phases
[AD-A212055] N90-12122
Equatorial oceanic response to forcing on time scales from days to months
[PB89-206775] N90-12147
OCEAN TEMPERATURE
Equatorial oceanic response to forcing on time scales from days to months
[PB89-206775] N90-12147
OCEANOGRAPHIC PARAMETERS
Statistical models for the optimal estimation of oceanic fields
[AD-A211786] N90-12149
OCEANS
Doppler statistics of ocean velocity variability
[AD-A211687] N90-12148
OGIVES
The determination of the aerodynamic characteristics of an ogive-cylinder body in subsonic, curved, incompressible flow, and an assessment of the effect of flow curvature
[REPT-87-13] N90-11712
OHMIC DISSIPATION
Microwave Tokamak Experiment (MTX) ohmic heating system
[DE89-017892] N90-12340
Joule heating and runaway electron acceleration in a solar flare N90-12478
OLFACTORY PERCEPTION
Synaptic plasticity and memory formation
[AD-A211368] N90-12158
ON-LINE SYSTEMS
National Library of Medicine DOCLINE (tradename) manual
[PB89-188676] N90-12390
FEDIX: An on-line information service for universities and other research organizations: User's guide, version 2.0, release 1
[DE89-016695] N90-12398
OPERATOR PERFORMANCE
Human Operator Simulator (HOS) 4 user's guide
[AD-A212007] N90-11763
OPERATORS (MATHEMATICS)
Parameter identification for an abstract Cauchy problem by quasilinearization
[NASA-CR-181933] N90-12192
Operator product coefficients in non-diagonal conformal field theories
[PB89-216873] N90-12283
OPTICAL COMMUNICATION
MEGALIDAR
[AD-A212074] N90-12020
OPTICAL DATA PROCESSING
Fast and objective MRTD measurement
[FEL-1988-24] N90-12006
Optical computing based on the Hopfield model for neural networks
[AD-A211824] N90-12216
Optical data transmission systems in radiation environment
[DE90-000174] N90-12322
OPTICAL EQUIPMENT
Applications of flight control system methods to an advanced combat rotorcraft
[NASA-TM-101054] N90-11752
Kinematic design NC optical generator N90-12316
OPTICAL FILTERS
A method to model fuze-performance. Part 3: Diffraction of electromagnetic radiation by an edge
[FEL-1989-22-PT-3] N90-11940
OPTICAL PATHS
Turbulence effects on reflected optical patterns (atmosphere and structure)
[PB89-208094] N90-12315
Linear (passive) and non-linear guided and studies in glass
[AD-A211693] N90-12325
OPTICAL PROPERTIES
Energy transfer and non-linear optical properties at near ultraviolet wavelengths: Rare earth 4f(yields)5d transitions in crystals and glasses
[DE90-000065] N90-12321
Characterization of the Structure and Chemistry of Defects in Materials: Proceedings, volume 138
[DE89-014796] N90-12352
OPTICAL RADAR
Progress of research on water vapor lidar
[NASA-CR-185970] N90-12011
MEGALIDAR
[AD-A212074] N90-12020
Laser sounding from space: Report of the ESA Technology Working Group on Space Laser Sounding and Ranging
[ESA-SP-1108] N90-12024
Measurements of aerosol properties needed to infer backscatter characteristics in support of the NASA Doppler Lidar program N90-12082
Calibration of a visioceilometer, a hand held lidar system
[FEL-1988-73] N90-12137
OPTICAL SWITCHING
Vanadium dioxide protective devices
[AD-A212018] N90-11887
OPTICAL WAVEGUIDES
Microwave signal detection using modulation of polymeric optical waveguides
[DE89-017545] N90-11921
OPTIMAL CONTROL
A hybrid optimisation strategy for adaptive feed-forward layered networks
[RSRE-MEMO-4193] N90-12226
OPTIMIZATION
A design procedure for the handling qualities optimization of the X-29A aircraft
[NASA-TM-4142] N90-11753
Controller design for active vibration suppression of a helicopter
[DFVLR-FB-89-20] N90-11760
An integrated methodology for optimizing structural composite damping
[NASA-TM-102343] N90-11808
Nearly optimal algorithms and bounds for multilayer channel routing
[AD-A211913] N90-11955
Airframe structural dynamic considerations in rotor design optimization
[NASA-TM-101646] N90-12057
Statistical models for the optimal estimation of oceanic fields
[AD-A211786] N90-12149
A hybrid optimisation strategy for adaptive feed-forward layered networks
[RSRE-MEMO-4193] N90-12226
Numerical experience with a class of algorithms for nonlinear optimization using inexact function and gradient information
[NASA-CR-181927] N90-12232
Optimal matching of 3-D convex polyhedra
[TELECOM-PARIS-89C003] N90-12258
On the asymptotic optimality of certain empirical Bayes simultaneous testing procedures
[AD-A211649] N90-12270
ORBIT CALCULATION
Sentinel satellite positional precision derived from the NAVSTAR global positioning system
[AD-A211876] N90-11720
ORBIT MANEUVERING ENGINE (SPACE SHUTTLE)
Independent Orbiter Assessment (IOA): Assessment of the orbital maneuvering system FMEA/CIL, volume 1
[NASA-CR-185544-VOL-1] N90-11787
Independent Orbiter Assessment (IOA): Assessment of the orbital maneuvering subsystem, volume 2
[NASA-CR-185544-VOL-2] N90-11788
ORBITS
Homoclinic orbits for a class of Hamiltonian systems
[AD-A210562] N90-12229
ORGANIC CHEMISTRY
Self-assembled organic monolayer films
[AD-A212006] N90-11838
ORGANIC COMPOUNDS
Structure-property relationships as an aid in the rational design of (beta)-(ET)(sub 2)X organic superconductors
[DE89-016912] N90-12356
ORGANOMETALLIC COMPOUNDS
Ultra high speed compound semiconductors and real time signal processing
[AD-A211394] N90-12372
OROGRAPHY
Stratiform clouds and their interaction with atmospheric motions N90-12060
Low level remote sensing: Orographic winds
N90-12066
ORR-SOMMERFELD EQUATIONS
Elimination of spurious eigenvalues in the Chebyshev tau spectral method
[PB89-209282] N90-11967
ORTHOGONAL FUNCTIONS
Orthogonal least squares methods and their application to nonlinear system identification
[RR-343] N90-12259
ORTHOGONALITY
Generalizations of Laguerre polynomials
[REPT-89-25] N90-12263
ORTHOTROPIC SHELLS
Buckling of axially compressed imperfect orthotropic shells with elastic edge supports
[PB89-217038] N90-12043
OSCILLATIONS
Analysis of a system of two weakly nonlinear coupled harmonic oscillators arising from the field of wind-induced vibrations
[REPT-89-22] N90-12261
OSCILLATORS
Advanced light source master oscillator
[DE90-000123] N90-11953
OVERVOLTAGE
Lightning and surge protection of photovoltaic installations: Two case histories, Vulcano and Kythnos
[PB89-229058] N90-12135
OXIDATION
Catalyst for carbon monoxide oxidation
[NASA-CASE-LAR-14155-1-SB] N90-11823
Conversion of methane to liquid hydrocarbons
[DE89-017547] N90-11831
OXIDATION-REDUCTION REACTIONS
Iron (III) initiated autoxidation of 1,2,3,4-tetrahydrocarbazole: An example of electron transfer
[AD-A211857] N90-11836
Effect of electrical double layer on transport limited currents at microelectrodes
[AD-A211586] N90-11843
OXIDE FILMS
Significance of oxide skins on powder for the quality of PM Al material — PM (press molded)
[DFVLR-FB-89-11] N90-11873
OXIDES
Mechanism of electrochemical activation of carbon electrodes: Role of graphite lattice defects
[AD-A211644] N90-11845
OXYGEN
In-situ spectroscopic studies of transition metal macrocycles as catalysts for the electrochemical reduction of oxygen
[PB89-219273] N90-11826
Ignition characteristics of the nickel-based alloy UNS N07718 in pressurized oxygen
[NASA-CR-185932] N90-11850
Lifetime of singlet oxygen in aqueous hydrogen peroxide (BHP)
[AD-A211545] N90-12306
OXYGEN ATOMS
Retrieval of atomic oxygen and temperature in the thermosphere. Part 2: Feasibility of an experiment based on limb emission in the OI lines
[AD-A211807] N90-12121

OXYGEN CONSUMPTION

The effect of caffeine on endurance time to exhaustion at high altitude
[AD-A212069] N90-12163

OXYGEN SPECTRA

Retrieval of atomic oxygen and temperature in the thermosphere. Part 2: Feasibility of an experiment based on limb emission in the OI lines
[AD-A211807] N90-12121

OZONE

Studies of baroclinic instability in the presence of surface topography and stratospheric ozone N90-12068

Use of satellite data and modeling to asses the influence of stratospheric processes on the troposphere
N90-12075

Ozone depletion, greenhouse gases, and climate change
[PB89-216097] N90-12110

OZONE DEPLETION

Ozone depletion, greenhouse gases, and climate change
[NASA-CR-185323] N90-12101

Ozone Research Program (German contribution to climate and atmosphere research)
[REPT-46-88] N90-12111

OZONOSPHERE

Ozone Research Program (German contribution to climate and atmosphere research)
[REPT-46-88] N90-12111

P

P-I-N JUNCTIONS

Channelized coplanar waveguide pin-diode switches
[NASA-TM-102289] N90-11943

PACIFIC OCEAN

Dynamics and energetics of the South Pacific Convergence Zone during FGGE SOP-1 and South Pacific Convergence Zone and global-scale N90-12065

Tropical Pacific moisture variability N90-12070

Hydrophone investigations of earthquakes and explosion generated high-frequency seismic phases
[AD-A212055] N90-12122

Observations of long Rossby waves in the northern tropical Pacific
[PB89-196331] N90-12143

Observations and modelling of deep equatorial currents in the central Pacific
[PB89-198139] N90-12145

Equatorial oceanic response to forcing on time scales from days to months
[PB89-206775] N90-12147

PACKETS (COMMUNICATION)

An approximate max-flow min-cut theorem for uniform multicommodity flow problems with applications to approximation algorithms
[AD-A211908] N90-12198

PANELS

Prediction of the thermal environment and thermal response of simple panels exposed to radiant heat
[NASA-TM-101660] N90-12292

PAPER (MATERIAL)

Color printing for computer graphics. Or: How to get it off your screen and onto paper, in color
[PB89-208110] N90-12184

PARACHUTE DESCENT

Performance and quality of a wing type parachute: Parametric analysis
[REPT-88-19] N90-11710

PARALLEL PROCESSING (COMPUTERS)

Tools to aid in the development high-performance algorithms
[DE89-012395] N90-12194

Parallel graph contraction
[AD-A211916] N90-12199

Parallel implementation and evaluation of motion estimation system algorithms on a distributed memory multiprocessor using knowledge based mappings
[NASA-CR-185984] N90-12213

Novel techniques for data decomposition and load balancing for parallel processing of vision systems: Implementation and evaluation using a motion estimation system
[NASA-CR-185991] N90-12214

Parallel architectures and parallel algorithms for integrated vision systems
[NASA-CR-185990] N90-12215

Parallel processing on transputer arrays for the recognition of objects in infrared images
[RSRE-MEMO-4197] N90-12217

Distributed VLSI architecture for fast Jacobian and inverse Jacobian formulations
[RR-346] N90-12218

Robot inverse dynamics computation via VLSI distributed architectures
[RR-350] N90-12223

Fast forward dynamics algorithm for robot arms using multiprocessing
[RR-367] N90-12225

Dynamic embedding of trees in hypercubes with constant dilation and load
[AD-A211884] N90-12236

PARAMETER IDENTIFICATION

Parameter identification for an abstract Cauchy problem by quasilinearization
[NASA-CR-181933] N90-12192

PARAMETERIZATION

Performance and quality of a wing type parachute: Parametric analysis
[REPT-88-19] N90-11710

Structure based formal methods for software engineering
[AD-A211660] N90-12207

Adaptive feedback linearization: Stability and robustness
[PB89-219497] N90-12220

Numerical experience with a class of algorithms for nonlinear optimization using inexact function and gradient information
[NASA-CR-181927] N90-12232

PARTICLE ACCELERATION

Heating and acceleration of coronal and chromospheric ions during solar flares N90-12479

Chromospheric-coronal coupling during solar flares: Current systems and particle acceleration N90-12480

PARTICLE BEAMS

Comparison of laser and neutral particle beam discrimination
[DE89-017786] N90-12018

DART: A simulation code for charged particle beams, revision 1
[DE89-016697] N90-12312

PARTICLE COLLISIONS

Atomic and molecular surface and volume processes in the analysis of negative hydrogen discharges
[DE89-015705] N90-12294

The behavior of beams of relativistic non-thermal electrons under the influence of collisions and synchrotron losses
[NASA-CR-185983] N90-12298

New developments in the ab initio treatment of low energy electron collisions with molecules
[DE89-015294] N90-12299

Fluctuations in transverse energy and multiplicity, energy densities, and neutral pion spectra in nucleus-nucleus collisions at 200 GeV/nucleon
[DE89-017583] N90-12302

GALAX: A two-dimensional N-body code for disk galaxy dynamics
[PB89-217780] N90-12415

PARTICLE DIFFUSION

Some new algorithms for boundary value problems in smooth particle hydrodynamics
[AD-A211728] N90-11987

PARTICLE INTERACTIONS

Molecular dynamics study of the primitive model of 1-3 electrolyte studies
[AD-A211653] N90-11846

Laser production of soft x rays by multiquantum processes and the excitation of atomic inner-shell states
[AD-A211372] N90-12021

Wave particle interactions
[DE89-017527] N90-12335

PARTICLE PRECIPITATION

Distribution of auroral precipitation at midnight during a magnetic storm
[PB89-213136] N90-12118

PARTICLE SIZE DISTRIBUTION

Droplet sizing instrumentation used for icing research: Operation, calibration, and accuracy
[NASA-CR-182293] N90-11999

Aerosol in the Pacific troposphere N90-12078

PARTICLE THEORY

Particle physics and cosmology using stellar evolution theory
[DE89-017529] N90-12418

PARTICLE TRAJECTORIES

Experimental test of PCAC hypothesis in the reactions mu neutrino-proton giving muon(-)-proton-pion(+) and mu antineutrino-proton giving muon(+)-proton-pion(-) in the delta (1232) region --- partial conserved axial current
[MPE-PAE/EXP.EL.199] N90-12309

Confinement of multiply charged ions in an ECRH mirror plasma
[DE89-016052] N90-12327

PARTICLES

Doppler statistics of ocean velocity variability
[AD-A211687] N90-12148

Experimental research in high energy physics
[DE90-000061] N90-12342

PARTICULATE SAMPLING

Aerosol in the Pacific troposphere N90-12078

Measurements of aerosol properties needed to infer backscatter characteristics in support of the NASA Doppler Lidar program N90-12082

PARTICULATES

Densification of particulate ceramic composites: The role of heterogeneities
[DE90-000177] N90-11886

PATTERN RECOGNITION

Improved pattern recognition techniques for real time operation
[AD-A211395] N90-11840

Eye movements and spatial pattern vision
[AD-A211650] N90-12169

A survey of camera error sources in machine vision systems
[DE89-014072] N90-12318

PAVEMENTS

Field evaluation of the multi-depth deflectometers
[PB89-207708] N90-11994

PAYLOADS

Design of scientific payloads and components
[AD-A211819] N90-12005

PEELING

Manual for Program PSTRESS: Peel stress computation
[NASA-CR-178408] N90-11822

PENALTY FUNCTION

Convergence results for pseudospectral approximations of hyperbolic systems by a penalty type boundary treatment
[NASA-CR-181929] N90-12230

PENDULUMS

Equilibrium solutions of a spherical pendulum with rotating point of suspension and friction
[ESA-TT-1139] N90-12288

PEPTIDES

Boron analogues of amino acids and derivatives
[AD-A211311] N90-12157

PERFORMANCE PREDICTION

Review and analysis of the DNW/Model 360 rotor acoustic data base
[NASA-TM-102253] N90-11692

Some implications of the isotropic momentarily frozen assumptions for the SPAN-MAT program
[NASA-CR-181937] N90-11704

Prediction of the thermal environment and thermal response of simple panels exposed to radiant heat
[NASA-TM-101660] N90-12292

PERFORMANCE TESTS

Performance of four rake modems over the non-disturbed wideband HF channel
[AD-A211589] N90-11930

PERMANENT MAGNETS

Periodic permanent magnet structures
[AD-D014173] N90-12280

Anisotropy and microstructure of high-coercivity rare earth permanent magnets
[AD-A211905] N90-12285

PERMEABILITY

Effective permeability of mixtures
[PB89-218952] N90-11839

PERTURBATION

Some notes on perturbations of differential-algebraic equations
[PB89-218564] N90-12243

PETRI NETS

On the generation of a variable structure airport surface traffic control system
[AD-A211306] N90-11724

PHASE TRANSFORMATIONS

Shock dissociation of molecular fluids: A possibility of first-order phase change
[DE89-016647] N90-11829

New mechanism for toughening ceramic materials
[AD-A211651] N90-11892

Properties of strongly coupled multi-ionic plasmas
[DE89-017782] N90-12339

Flare-in texture in rotating superfluid (3)He-B
[PB89-218994] N90-12368

A critical assessment of thermodynamic and phase diagram data for the Ga-In system
[NPL-DMA(A)-174] N90-12382

PHASE VELOCITY

Investigations of Eurasian seismic sources and upper mantle structure
[AD-A211806] N90-12120

PHASED ARRAYS

Proceedings of the 1988 Antenna Applications Symposium, volume 1
[AD-A211396] N90-11928

PHOSPHORIC ACID
Membrane fusion: The role of polyphosphatidylinositol [AD-A211289] N90-12156

PHOSPHORYLATION
Membrane fusion: The role of polyphosphatidylinositol [AD-A211289] N90-12156

PHOTOCHEMICAL REACTIONS
Methanol fueled vehicles and photochemical models: An evaluation of the state of knowledge [PB89-214225] N90-12410
Venus volcanism: Rate estimates from laboratory studies of sulfur gas-solid reactions N90-12428

PHOTOCONDUCTIVITY
High power, solid state RF pulse generators [AD-D014172] N90-11941
Energy transfer and non-linear optical properties at near ultraviolet wavelengths: Rare earth 4f(yields)5d transitions in crystals and glasses [DE90-000065] N90-12321
Subnanosecond linear GaAs photoconductive switching, revision 1 [DE89-017739] N90-12363

PHOTODIODES
Switched power workshop: Introduction and summary [DE90-000036] N90-11952

PHOTOELECTRIC EMISSION
State-resolved reaction dynamics [AD-A211613] N90-12307
Surface, interface, and bulk properties of high T(sub c) superconductors [AD-A211490] N90-12373

PHOTOELECTRON SPECTROSCOPY
High temperature and high resolution UV photoelectron spectroscopy using supersonic molecular beams [DE90-000176] N90-11835

PHOTOIONIZATION
Synchrotron-radiation experiments with recoil ions [DE89-017579] N90-12301
Energy transfer and non-linear optical properties at near ultraviolet wavelengths: Rare earth 4f(yields)5d transitions in crystals and glasses [DE90-000065] N90-12321
Electron attachment and molecular fragmentation in laser-excited plasmas [AD-A212098] N90-12343

PHOTOLITHOGRAPHY
Photolithography: A new tool for ceramic science [DE90-000135] N90-11885

PHOTOLUMINESCENCE
Luminescence in applied magnetic fields [AD-A211551] N90-12287

PHOTOLYSIS
Photolysis of spacecraft contaminants [AD-A211715] N90-11801
Spin-orbit relaxation rates of Bi(6p(3)) 2D(3/2) following photolysis of Bi(CH3)3 at lambda = 193 nm [AD-A211792] N90-12303

PHOTOMETRY
Spatial characteristics of airglow and solar scatter radiance from the earth's atmosphere [AD-A211358] N90-12126

PHOTONS
Quantitative interpretation of auger lineshapes and electron/photon stimulated desorption [AD-A211550] N90-11842
Laser production of soft x rays by multiquantum processes and the excitation of atomic inner-shell states [AD-A211372] N90-12021

PHOTONUCLEAR REACTIONS
Detailed photonuclear cross-section calculations and astrophysical applications [DE89-017531] N90-12419

PHOTOSENSITIVITY
Graded bandgap solar cells [AD-A211537] N90-12097

PHOTOSPHERE
MHD (magnetohydrodynamic) modeling of solar and interplanetary processes [PB89-215461] N90-12416

PHOTOVOLTAIC CELLS
Lightning and surge protection of photovoltaic installations: Two case histories, Vulcano and Kythnos [PB89-229058] N90-12135

PHOTOVOLTAIC CONVERSION
Photovoltaic system research status [DE89-016764] N90-12094

PHTHALOCYANIN
Multicolor electrochromic displays exploratory development [AD-A212004] N90-11721

PHYSICAL FITNESS
Demonstration of replicable dimensions of health behaviors [AD-A211920] N90-12161

PHYSICAL OPTICS
A method to model fuze-performance. Part 3: Diffraction of electromagnetic radiation by an edge [FEL-1989-22-PT-3] N90-11940

PHYSICAL PROPERTIES
The prediction of middle distillate fuel properties using liquid chromatography-proton nuclear magnetic resonance spectroscopy data [AD-A211879] N90-11899

PHYSIOLOGICAL EFFECTS
Synergistic effects of nitrogen dioxide and carbon dioxide following acute inhalation exposures in rats [PB89-214779] N90-12150

PHYSIOLOGICAL FACTORS
Wrist orientation effect on grip strength and endurance [PB89-200935] N90-12179

PHYSIOLOGICAL TESTS
Wrist orientation effect on grip strength and endurance [PB89-200935] N90-12179

PICOSECOND PULSES
Air breakdown photography in the picosecond domain [DE89-016775] N90-11830

PIONS
Fluctuations in transverse energy and multiplicity, energy densities, and neutral pion spectra in nucleus-nucleus collisions at 200 GeV/nucleon [DE89-017583] N90-12302

PIPELINING (COMPUTERS)
A distributed pipelined architecture of the recursive Lagrangian equations of motion for robot manipulators with VLSI implementation — VLSI (very large scale integration) [RR-353] N90-11966

PIPES (TUBES)
Doubly-fluted tubes and enhanced tubes in confined crossflow [PB89-217921] N90-11971
Autofrettage-stress distribution under load and retained stresses after depressurization [AD-A212090] N90-12048

PISTONS
Sliding seal materials for low heat rejection engines [NASA-CR-182262] N90-11882

PITCH (INCLINATION)
Unsteady aerodynamics with applications to flight mechanics [AD-A211944] N90-11706

PITCH (MATERIAL)
Carbon fiber reinforced glass matrix composites for structural space based applications [AD-A211682] N90-11818

PITCHING MOMENTS
Normal-force-curve and pitching-moment-curve slopes of forebody-cylinder combinations at zero angle of attack for Mach numbers up to 5 [ESDU-89008] N90-11709

PITTING
Coatings for gas turbine compressors [NLR-MP-88045-U] N90-11750

PIXELS
Estimated UV clutter levels at 10-100 meter sensor pixel resolution extrapolated from recent polar bear measurements [AD-A211357] N90-12125

PLANE WAVES
Experimental investigation of a planar shock wave over a double wedge [AD-A211366] N90-11981

PLANETARY CORES
High pressure studies of planetary matter [DE89-017738] N90-12455

PLANETARY CRATERS
Potential for observing and discriminating impact craters and comparable volcanic landforms on Magellan radar images N90-12429
Deducing the age of the dense Venus atmosphere N90-12438
Impact cratering and the surface age of Venus: The Pre-Magellan controversy N90-12446

PLANETARY CRUSTS
Divergent plate boundaries and crustal spreading on Venus: Evidence from Aphrodite Terra N90-12427
Tectonism on Venus: A review N90-12440
Crustal deformation: Earth vs Venus N90-12450

PLANETARY EVOLUTION
Deducing the age of the dense Venus atmosphere N90-12438
Clotho Tessera, Venus: A fragment of Fortuna Tessera N90-12439
Eastern Ishtar Terra: Tectonic evolution derived from recognized features N90-12451
Reports of planetary geology and geophysics program, 1988 [NASA-TM-4130] N90-12454

PLANETARY GEOLOGY
Abstracts for the Venus Geoscience Tutorial and Venus Geologic Mapping Workshop [NASA-CR-185432] N90-12423
Geology of Southern Guinevere Planitia, Venus, based on analyses of Goldstone radar data N90-12424
Characteristics, distribution and geologic/terrain associations of small dome-like hills on Venus N90-12425
Tessera terrain: Characteristics and models of origin N90-12426
Contrasting landform perception with varied radar illumination geometries and at simulated resolutions of Venera and Magellan N90-12430
Venus surface properties deduced from radar and radiometry N90-12431
A morphologic study of Venus Ridge belts N90-12432
Evidence for volcanism in NW Ishtar Terra, Venus N90-12433
Radar scattering mechanisms within the meteor crater ejecta blanket: Geologic implications and relevance to Venus N90-12435
Aeolian processes on Venus N90-12436
Architecture of orogenic belts and convergent zones in Western Ishtar Terra, Venus N90-12437
Clotho Tessera, Venus: A fragment of Fortuna Tessera N90-12439
Crater identification and resolution of lunar radar images N90-12441
Venus: Mantle convection, hotspots, and tectonics N90-12442
Radar scattering from desert terrains, Pisgah/Lavic Region, California: Implications for Magellan N90-12443
Lakshmi Planum: A distinctive highland volcanic province N90-12444
Volcanism on Venus: Large shields and major accumulations of small domes N90-12445
Impact cratering and the surface age of Venus: The Pre-Magellan controversy N90-12446
Geology of the Venus equatorial region from Pioneer Venus radar imaging N90-12447
Venus and the Archean Earth: Thermal considerations N90-12448
Crustal deformation: Earth vs Venus N90-12450
Eastern Ishtar Terra: Tectonic evolution derived from recognized features N90-12451
Three ages of Venus N90-12453
Reports of planetary geology and geophysics program, 1988 [NASA-TM-4130] N90-12454

PLANETARY MANTLES
Divergent plate boundaries and crustal spreading on Venus: Evidence from Aphrodite Terra N90-12427
Venus: Mantle convection, hotspots, and tectonics N90-12442
Venus and the Archean Earth: Thermal considerations N90-12448

PLANETARY MAPPING
Abstracts for the Venus Geoscience Tutorial and Venus Geologic Mapping Workshop [NASA-CR-185432] N90-12423
Characteristics, distribution and geologic/terrain associations of small dome-like hills on Venus N90-12425
Tessera terrain: Characteristics and models of origin N90-12426
Divergent plate boundaries and crustal spreading on Venus: Evidence from Aphrodite Terra N90-12427
Potential for observing and discriminating impact craters and comparable volcanic landforms on Magellan radar images N90-12429
Architecture of orogenic belts and convergent zones in Western Ishtar Terra, Venus N90-12437
Clotho Tessera, Venus: A fragment of Fortuna Tessera N90-12439
Venus: Mantle convection, hotspots, and tectonics N90-12442
Lakshmi Planum: A distinctive highland volcanic province N90-12444
Volcanism on Venus: Large shields and major accumulations of small domes N90-12445
Impact cratering and the surface age of Venus: The Pre-Magellan controversy N90-12446
Eastern Ishtar Terra: Tectonic evolution derived from recognized features N90-12451
Three ages of Venus N90-12453

PLANETARY METEOROLOGY
Synoptic/planetary-scale interactions and blocking over the North Atlantic Ocean N90-12061
Application of dynamical systems theory to global weather phenomena revealed by satellite imagery N90-12063

PLANETARY WAVES
Application of dynamical systems theory to global weather phenomena revealed by satellite imagery N90-12063
The effect of latent heat release on synoptic-to-planetary wave interactions and its implication for satellite observations: Theoretical modeling N90-12073
The effect of latent heat release on synoptic-to-planetary scale wave interactions: Observational study N90-12074
Laboratory and theoretical models of planetary-scale instabilities and waves N90-12076
Observations of long Rossby waves in the northern tropical Pacific
[PB89-196331] N90-12143
PLANNING
Coupling rule-based and object-oriented programming for the classification of machined features
[DE89-017705] N90-11903
An optimum trajectory planner for robot manipulators in joint-space and under physical constraints
[RR-349] N90-12029
Reasoning about change and exceptions in automated process planning
[DE89-017706] N90-12195
PLANT DISEASES
Investigation of the usefulness of LANDSAT 5 thematic mapper data for mapping forest disease
[DFVLR-FB-89-06] N90-12088
Signature analysis and classification of pine of different vitality classes using airborne thematic mapper data
[DFVLR-FB-89-07] N90-12089
PLANTS (BOTANY)
Global data bases on distribution, characteristics and methane emission of natural wetlands: Documentation of archived data tape
[NASA-TM-4153] N90-12090
PLASMA CLOUDS
A beam induced upset during the flight of the ECHO-7 rocket
[NASA-CR-186089] N90-11755
PLASMA CONTROL
Confinement of multiply charged ions in an ECRH mirror plasma
[DE89-016052] N90-12327
Control of plasma position in the CASTOR tokamak
[IPPCZ-284] N90-12332
PLASMA CURRENTS
Plasma-anode electron gun research
[AD-A211547] N90-11773
PLASMA DIAGNOSTICS
Confinement of multiply charged ions in an ECRH mirror plasma
[DE89-016052] N90-12327
The soft x ray telescope for Solar-A N90-12475
PLASMA DIFFUSION
Proceedings of the Workshop on Compound Semiconductor Devices and Integrated Circuits (13th) held in Cabourg, France on 10-12 May 1989
[AD-A211848] N90-11954
PLASMA DIODES
Generation and focusing of pulsed intense ion beams
[DE89-017558] N90-12338
PLASMA ELECTRODES
Plasma-anode electron gun research
[AD-A211547] N90-11773
PLASMA ETCHING
Reactive ion etching of sputtered silicon carbide and tungsten thin films for device applications
[AD-A211711] N90-11847
PLASMA INTERACTIONS
Plasma-anode electron gun research
[AD-A211547] N90-11773
PLASMA JETS
Plasma-anode electron gun research
[AD-A211547] N90-11773
PLASMA LAYERS
The physics of double layers and their role in astrophysics
[TRITA-EPP-89-03] N90-12421
PLASMA PHYSICS
Theoretical plasma physics
[DE90-000009] N90-12341
MHD (magnetohydrodynamic) modeling of solar and interplanetary processes
[PB89-215461] N90-12416
PLASMA PINCH
Advanced concepts theory
[AD-A211665] N90-12344
PLASMA RADIATION
Advanced concepts theory
[AD-A211665] N90-12344
PLASMA SPECTRA
Calculations of soft x ray emission of REB-heated plasma
[IPPCZ-287] N90-12329
PLASMA TEMPERATURE
The soft x ray telescope for Solar-A N90-12475
PLASMA WAVES
Coherency properties of strong Langmuir turbulence
[DE89-009290] N90-12119
Wave particle interactions
[DE89-017527] N90-12335
PLASMA-ELECTROMAGNETIC INTERACTION
A beam induced upset during the flight of the ECHO-7 rocket
[NASA-CR-186089] N90-11755
PLASMAS (PHYSICS)
Plasma-deposited amorphous hydrogenated carbon films and their tribological properties
[NASA-TM-102379] N90-11880
Advances and directions of ion nitriding/carburizing
[NASA-TM-102398] N90-11902
Electron cyclotron emission and absorption experiment on the CASTOR tokamak
[IPPCZ-285] N90-12331
Control of plasma position in the CASTOR tokamak
[IPPCZ-284] N90-12332
Joule heating and runaway electron acceleration in a solar flare N90-12478
Development of a numerical solution to the time dependent kinetic equation N90-12481
PLASTIC DEFORMATION
Deformation of Ti-6Al-4V bar and extrusion under superplastic forming conditions
[RAE-TM-MAT/STR-1110] N90-11875
Deformation of extruded titanium alloys under superplastic conditions
[RAE-TM-MAT/STR-1111] N90-11876
A model for long-term creep and the effects of physical ageing in poly (butylene terephthalate)
[NPL-DMA(A)-182] N90-11895
An application of the J-integral to an incremental analysis of blunting crack behavior
[DE89-016844] N90-12046
Autofrettage-stress distribution under load and retained stresses after depressurization
[AD-A212090] N90-12048
An experimental and analytical program to develop crack tip fracture criteria
[AD-A211565] N90-12051
Deformation of electron beam welded Ti-6Al-4V alloy sheet under superplastic conditions
[RAE-TM-MAT/STR-1109] N90-12053
Effect of superplastic deformation on the surface roughness of sheet
[RAE-TM-MAT/STR-1112] N90-12054
PLASTIC FLOW
Autofrettage-stress distribution under load and retained stresses after depressurization
[AD-A212090] N90-12048
PLATES (STRUCTURAL MEMBERS)
Application of matrix correction methods on a plate and a truss structure
[NLR-MP-88042-U] N90-12056
PLATES (TECTONICS)
Divergent plate boundaries and crustal spreading on Venus: Evidence from Aphrodite Terra N90-12427
PLUMES
Investigation of advanced mixer-ejector exhaust system
[AD-A211943] N90-11705
POINT DEFECTS
Characterization of the Structure and Chemistry of Defects in Materials: Proceedings, volume 138
[DE89-014796] N90-12352
POISSON EQUATION
A multigrid algorithm for the incompressible Navier-Stokes equation
[GMD-374] N90-11993
POLAR METEOROLOGY
Investigations of polar air stream cyclogenesis based on numerical simulations with a mesoscale model
[PB89-214563] N90-12132
POLARIMETERS
The SMM UV observations of Active Region 5395 N90-12485
POLICIES
Policies to encourage private sector responses to potential climate change
[DE89-017244] N90-12107
POLLUTION CONTROL
Potential technologies for collection and destruction of CFCs (Chlorofluorocarbons), halons, and related compounds
[PB89-219968] N90-12105
POLYATOMIC MOLECULES
New developments in the ab initio treatment of low energy electron collisions with molecules
[DE89-015294] N90-12299
POLYCRYSTALS
Analysis of loss mechanisms in polycrystalline thin-film solar cells
[DE89-009454] N90-12093
RF performance of polycrystalline high-T(sub c) superconductors
[DE89-017671] N90-12359
Surface, interface, and bulk properties of high T(sub c) superconductors
[AD-A211490] N90-12373
POLYESTER RESINS
New Fabric Development Program
[AD-A211549] N90-11891
POLYETHYLENES
Assessment of thin film batteries based on polymer electrolytes. Part 1: Energy density
[AD-A212111] N90-11958
POLYHEDRONS
Optimal matching of 3-D convex polyhedra
[TELECOM-PARIS-89C003] N90-12258
POLYMER MATRIX COMPOSITES
Inorganic composite materials in Japan: Status and trends
[PB89-230015] N90-11810
POLYMERIC FILMS
Method of modifying the dielectric properties of an organic polymer film
[AD-D014171] N90-11879
POLYMERIZATION
Method of modifying the dielectric properties of an organic polymer film
[AD-D014171] N90-11879
POLYNOMIALS
Sequential design of experiments with physically based models 23
[AD-A211918] N90-12239
On the communication complexity of solving a polynomial equation
[AD-A211945] N90-12240
A simple proof of a differential equation for generalizations of Laguerre polynomials
[REPT-89-15] N90-12253
Generalizations of Laguerre polynomials
[REPT-89-25] N90-12263
Modeling and analysis of nonlinear time series
[RR-355] N90-12272
POLYSTYRENE
Positron annihilation studies of interpenetrating polymer networks
[AD-A212162] N90-11890
POSITION (LOCATION)
Doppler statistics of ocean velocity variability
[AD-A211687] N90-12148
Acoustic controlled rotation and orientation
[NASA-CASE-NPO-16995-1-CU] N90-12289
POSITRON ANNIHILATION
Positron annihilation studies of interpenetrating polymer networks
[AD-A212162] N90-11890
Electron-positron momentum distribution measurements of high-T(sub c) superconductors and related systems
[DE89-017538] N90-12358
POSITRONS
Electron-positron momentum distribution measurements of high-T(sub c) superconductors and related systems
[DE89-017538] N90-12358
POSTFLIGHT ANALYSIS
Post crash flight analysis: Visualizing flight recorder data
[AD-A212063] N90-11715
POSTURE
Age-related changes in human posture control: Motor coordination tests
[NASA-CR-185855] N90-12178
POTENTIAL ENERGY
Phase behavior of pure and mixed systems at high pressure
[DE89-017734] N90-11832
POTENTIAL FLOW
Steady and unsteady potential flow around thin annular wings and engines with simulation of jet engine flow
[DFVLR-FB-89-18] N90-11711
POWDER (PARTICLES)
Significance of oxide skins on powder for the quality of PM Al material — PM (press molded)
[DFVLR-FB-89-11] N90-11873
Densification of particulate ceramic composites: The role of heterogeneities
[DE90-000177] N90-11886
POWDER METALLURGY
Elevated temperature aluminum-titanium alloy by powder metallurgy process
[AD-D014165] N90-11852
Current research in advanced materials
[DE89-017466] N90-11884

POWER AMPLIFIERS

Control of plasma position in the CASTOR tokamak [IPPCZ-284] N90-12332

POWER CONDITIONING

Photovoltaic system research status [DE89-016764] N90-12094

POWER MODULES (STS)

Independent Orbiter Assessment (IOA): Assessment of the electrical power distribution and control subsystem, volume 1 [NASA-CR-185557-VOL-1] N90-11779

Independent Orbiter Assessment (IOA): Assessment of the electrical power distribution and control subsystem, volume 2 [NASA-CR-185557-VOL-2] N90-11780

Independent Orbiter Assessment (IOA): Assessment of the electrical power distribution and control subsystem, volume 3 [NASA-CR-185557-VOL-3] N90-11781

PRECIPITATION (METEOROLOGY)

Global distribution of moisture, evaporation-precipitation, and diabatic heating rates N90-12069

A statistical intercomparison of temperature and precipitation predicted by four general circulation models with historical data [DE89-017785] N90-12108

PRECIPITATION HARDENING

Precipitation strengthened high strength, high conductivity Cu-Cr-Nb alloys produced by chill block melt spinning [NASA-CR-185144] N90-11853

PRECISION

Contribution of the precision determination of noise powers in the MHz and lower GHz frequency range [PTB-E-33] N90-11935

PREDICTION ANALYSIS TECHNIQUES

Computational methods for complex flowfields [AD-A211465] N90-11983

PREDICTIONS

Studies on predicting the resynchronization of the circadian system after transmedian flights [DFVLR-FB-89-10] N90-12172

The onset of the solar active cycle 22 N90-12488

PREMIXED FLAMES

Premixed turbulent flame propagation [AD-A211489] N90-11841

PRESSURE DISTRIBUTION

Computation of generalized modal loads in an acoustic field define by a distribution of correlated pressures [NASA-CR-186041] N90-12047

PRESSURE EFFECTS

Phase behavior of pure and mixed systems at high pressure [DE89-017734] N90-11832

Ignition characteristics of the nickel-based alloy UNS N07718 in pressurized oxygen [NASA-CR-185932] N90-11850

VISAR wave profile measurements in supra-compressed HE [DE89-017736] N90-11976

Characteristics of flyer impact for one-dimensional shock-wave study applications [DE89-017887] N90-11977

Shock pressure determination in detonator wires [DE89-017756] N90-12002

High pressure studies of planetary matter [DE89-017738] N90-12455

PRESSURE MEASUREMENT

Measurement of pressure fluctuations in a resonant chamber with laser-induced iodine fluorescence [ESA-TT-1123] N90-12326

PRESSURE OSCILLATIONS

Measurement of pressure fluctuations in a resonant chamber with laser-induced iodine fluorescence [ESA-TT-1123] N90-12326

PRESSURE VESSELS

Autofrettage-stress distribution under load and retained stresses after depressurization [AD-A212090] N90-12048

PRESSURIZING

Independent Orbiter Assessment (IOA): Assessment of the reaction control system, volume 1 [NASA-CR-185543-VOL-1] N90-11793

Independent Orbiter Assessment (IOA): Assessment of the reaction control system, volume 2 [NASA-CR-185543-VOL-2] N90-11794

Independent Orbiter Assessment (IOA): Assessment of the reaction control system, volume 3 [NASA-CR-185543-VOL-3] N90-11795

Independent Orbiter Assessment (IOA): Assessment of the reaction control system, volume 4 [NASA-CR-185543-VOL-4] N90-11796

Independent Orbiter Assessment (IOA): Assessment of the reaction control system, volume 5 [NASA-CR-185543-VOL-5] N90-11797

Apparatus and method for monitoring pressure leaks from a sealed system [AD-D014168] N90-11995

Autofrettage-stress distribution under load and retained stresses after depressurization [AD-A212090] N90-12048

PRIMERS (COATINGS)

Coating galvanized steel [AD-A211775] N90-11869

PRIMITIVE EQUATIONS

Four vector-matrix primitives [AD-A211889] N90-12237

PRINTED CIRCUITS

Cleaning of printed circuit assemblies with surface-mounted components [DE89-013609] N90-11945

PRINTING

Color printing for computer graphics. Or: How to get it off your screen and onto paper, in color [PB89-208110] N90-12184

PROBABILITY DENSITY FUNCTIONS

Estimating functionals related to a density by a class of statistics based on spacings [REPT-89-11] N90-12275

Likelihood cross-validation bandwidth selection for nonparametric kernel density estimators [REPT-89-10] N90-12279

PROBABILITY THEORY

Statistical models for the optimal estimation of oceanic fields [AD-A211786] N90-12149

Efficient diagnosis of multiprocessor systems under probabilistic models [NASA-CR-185965] N90-12212

On a classification problem: Ranking and selection approach [AD-A211627] N90-12269

Some 1(sub p) invariant probability measures [REPT-88-91] N90-12273

Fuzzy logic and the generalized modus ponens [REPT-88-92] N90-12274

PROBLEM SOLVING

Eigensolutions for the reflection problem involving the interface of two chiral half spaces [PB89-221592] N90-11926

Viscous split algorithms for the time dependent incompressible Navier-Stokes equations [AD-A211592] N90-11985

The nonconvex multi-dimensional Riemann problem for Hamilton-Jacobi equations [NASA-CR-181887] N90-12182

The use of Lanczos's method to solve the large generalized symmetric definite eigenvalue problem [NASA-CR-181914] N90-12193

Taxonomic syntax for first order inference [AD-A211618] N90-12221

Computer-based tutors for explaining and managing the process of diagnostic reasoning [AD-A211738] N90-12222

Microscopic approach to the generator coordinate method [DE89-016701] N90-12233

On the communication complexity of solving a polynomial equation [AD-A211945] N90-12240

A multigrid method combined with defect correction for free convection problems at high Rayleigh numbers [REPT-89-27] N90-12264

Distributed knowledge-based systems [AD-A211984] N90-12401

PROCEDURES

Coupling rule-based and object-oriented programming for the classification of machined features [DE89-017705] N90-11903

PROCESS CONTROL (INDUSTRY)

Current research in advanced materials [DE89-017466] N90-11884

PRODUCTIVITY

Working with people to improve productivity and quality: A bibliography with indexes, 1984-1988 [NASA-SP-7078] N90-12385

PROGRAMMING LANGUAGES

Experience with CST: Programming and implementation [AD-A211882] N90-12197

Adoption of software engineering innovations in organizations [AD-A211573] N90-12206

Structure based formal methods for software engineering [AD-A211660] N90-12207

A language for assembly instructions [REPT-88-90] N90-12209

PROJECT MANAGEMENT

Twenty-five years of service, 1962-1987: Proceedings of the Air Force Studies Board Symposium on Air Force Research and Development, November 16, 1987 [PB89-198915] N90-12384

PROLATE SPHEROIDS

Numerical computation of the viscous flow field around a prolate spheroid [DFVLR-FB-89-22] N90-11992

PROP-FAN TECHNOLOGY

Propfan Test Assessment (PTA): Flight test report [NASA-CR-182278] N90-11738

Propfan Test Assessment (PTA) [NASA-CR-185138] N90-11739

PROPAGATION VELOCITY

Shock pressure determination in detonator wires [DE89-017756] N90-12002

PROPELLANT STORAGE

Independent Orbiter Assessment (IOA): Assessment of the orbital maneuvering system FMEA/CIL, volume 1 [NASA-CR-185544-VOL-1] N90-11787

Independent Orbiter Assessment (IOA): Assessment of the reaction control system, volume 1 [NASA-CR-185543-VOL-1] N90-11793

Independent Orbiter Assessment (IOA): Assessment of the reaction control system, volume 2 [NASA-CR-185543-VOL-2] N90-11794

Independent Orbiter Assessment (IOA): Assessment of the reaction control system, volume 3 [NASA-CR-185543-VOL-3] N90-11795

Independent Orbiter Assessment (IOA): Assessment of the reaction control system, volume 4 [NASA-CR-185543-VOL-4] N90-11796

Independent Orbiter Assessment (IOA): Assessment of the reaction control system, volume 5 [NASA-CR-185543-VOL-5] N90-11797

PROPELLANT TRANSFER

Independent Orbiter Assessment (IOA): Assessment of the orbiter main propulsion system FMEA/CIL, volume 1 [NASA-CR-185559-VOL-1] N90-11775

Independent Orbiter Assessment (IOA): Assessment of the main propulsion subsystem FMEA/CIL, volume 2 [NASA-CR-185559-VOL-2] N90-11776

Independent Orbiter Assessment (IOA): Assessment of the main propulsion subsystem FMEA/CIL, volume 3 [NASA-CR-18559-VOL-3] N90-11777

Independent Orbiter Assessment (IOA): Assessment of the main propulsion subsystem FMEA/CIL, volume 4 [NASA-CR-185559-VOL-4] N90-11778

PROPELLER NOISE

Noise data of four small propeller-driven airplanes [PB89-216980] N90-12291

PROPULSION

Fuel cells for vehicle propulsion applications: A thermodynamic systems analysis [DE89-017689] N90-11950

PROPULSION SYSTEM CONFIGURATIONS

STOVL propulsion system volume dynamics approximations [NASA-TM-102397] N90-11740

Independent Orbiter Assessment (IOA): Assessment of the orbiter main propulsion system FMEA/CIL, volume 1 [NASA-CR-185559-VOL-1] N90-11775

Independent Orbiter Assessment (IOA): Assessment of the main propulsion subsystem FMEA/CIL, volume 2 [NASA-CR-185559-VOL-2] N90-11776

Independent Orbiter Assessment (IOA): Assessment of the main propulsion subsystem FMEA/CIL, volume 3 [NASA-CR-18559-VOL-3] N90-11777

Independent Orbiter Assessment (IOA): Assessment of the main propulsion subsystem FMEA/CIL, volume 4 [NASA-CR-185559-VOL-4] N90-11778

PROPULSIVE EFFICIENCY

Fuel cells for vehicle propulsion applications: A thermodynamic systems analysis [DE89-017689] N90-11950

PROTECTIVE COATINGS

Vanadium dioxide protective devices [AD-A212018] N90-11887

PROTOCOL (COMPUTERS)

A real-time locking protocol [AD-A211514] N90-12403

PROTON FLUX DENSITY

Cosmic strings and ultra-high energy cosmic rays [NASA-CR-185924] N90-12492

PROTON MAGNETIC RESONANCE

The prediction of middle distillate fuel properties using liquid chromatography-proton nuclear magnetic resonance spectroscopy data [AD-A211879] N90-11899

PROXIMITY

Optimal matching of 3-D convex polyhedra [TELECOM-PARIS-89C003] N90-12258

PSYCHOLOGICAL TESTS
Microcomputer-based tests for repeated-measures: Metric properties and predictive validities
[NASA-CR-185517] N90-12174
A menu of self-administered microcomputer-based neurotoxicology tests
[NASA-CR-185518] N90-12175
The effect of incentives on the reliability and validity of cognitive speed tests
[AD-A211346] N90-12181

PSYCHOMOTOR PERFORMANCE
Microcomputer-based tests for repeated-measures: Metric properties and predictive validities
[NASA-CR-185517] N90-12174
A menu of self-administered microcomputer-based neurotoxicology tests
[NASA-CR-185518] N90-12175

PUBLIC HEALTH
Demonstration of replicable dimensions of health behaviors
[AD-A211920] N90-12161

PULSE CODE MODULATION
Type-specific dynamic measurements on wind turbines at the test site Schnittlingen (Germany, F.R.)
[DFVLR-MITT-88-31] N90-12099

PULSE DURATION
Pre-pulses: Signature of a trigger process in short (less than 60 secs) solar hard x ray flares N90-12476

PULSE GENERATORS
Simulation of the EMP (Electromagnetic Pulse) from ESD (Electrostatic Discharge)
[DE89-014484] N90-11918
High power, solid state RF pulse generators
[AD-D014172] N90-11941
High gain flux compression generator fabrication issues
[DE89-017888] N90-11951
Computer controlled MHD power consolidation and pulse-generation system
[DE89-015600] N90-12333
Subnanosecond linear GaAs photoconductive switching, revision 1
[DE89-017739] N90-12363

PULSED RADIATION
Generation and focusing of pulsed intense ion beams
[DE89-017558] N90-12338

PULSES
High power, solid state RF pulse generators
[AD-D014172] N90-11941

PYROLYSIS
Structure/reactivity relationships of polysilazane preceramics
[AD-A212028] N90-11888

Q

QUADRATIC EQUATIONS
Calculation of transient response from time-harmonic spectrum
[AD-A211972] N90-12241

QUALITY CONTROL
Working with people to improve productivity and quality: A bibliography with indexes, 1984-1988
[NASA-SP-7078] N90-12385
The application of quality assurance to engineering management
[DE89-009955] N90-12386

QUANTUM ELECTRODYNAMICS
On the role of Coulomb forces in atomic radiative emission
[IRF-PREPRINT-106] N90-12308

QUANTUM ELECTRONICS
SIS (Superconductor-Insulator-Superconductor) mixer research
[AD-A211607] N90-12375

QUANTUM MECHANICS
Quantum-mechanical derivation of the Davydov equations for multi-quanta states
[DE89-015250] N90-12297
Resonant quasiparticle-ion scattering in anisotropic superfluid (3)He
[PB89-221618] N90-12369

QUANTUM THEORY
Monte Carlo studies of nuclei and quantum liquid drops
[DE89-016914] N90-12300
Gordon Conference on Atomic Physics
[AD-A211946] N90-12304

QUANTUM WELLS
Energy relaxation of light holes in InAs(.15)Sb(.85)/InSb multiple quantum wells
[DE89-016035] N90-12349

QUARTZ
Field-assisted bonding of single crystal quartz
[DE89-015407] N90-12353

QUARTZ CRYSTALS
Field-assisted bonding of single crystal quartz
[DE89-015407] N90-12353

QUEUEING THEORY
A simulation study of landing time allocation procedures for use in computer-assisted air traffic management systems
[AD-A212159] N90-11722
The conditional-event approach to distributed simulation
[NASA-CR-185890] N90-12200

R

RADAR ASTRONOMY
Geology of Southern Guinevere Planitia, Venus, based on analyses of Goldstone radar data N90-12424

RADAR ECHOES
Pacific marine radar sea scatter experimental results
[AD-A211593] N90-11931

RADAR GEOLOGY
Abstracts for the Venus Geoscience Tutorial and Venus Geologic Mapping Workshop
[NASA-CR-185432] N90-12423
Geology of Southern Guinevere Planitia, Venus, based on analyses of Goldstone radar data N90-12424
Tessera terrain: Characteristics and models of origin N90-12426

RADAR IMAGERY
Potential for observing and discriminating impact craters and comparable volcanic landforms on Magellan radar images N90-12429
Contrasting landform perception with varied radar illumination geometries and at simulated resolutions of Venera and Magellan N90-12430
Venus surface properties deduced from radar and radiometry N90-12431
A morphologic study of Venus Ridge belts N90-12432
Evidence for volcanism in NW Ishtar Terra, Venus N90-12433
Analysis of radar images of the active volcanic zone at Krafla, Iceland: The effects of look azimuth biasing N90-12434
Crater identification and resolution of lunar radar images N90-12441
Radar scattering from desert terrains, Pisgah/Lavic Region, California: Implications for Magellan N90-12443
Geology of the Venus equatorial region from Pioneer Venus radar imaging N90-12447
Stress distribution and topography of Tellus Regio, Venus N90-12452

RADAR MEASUREMENT
Middle Atmosphere Program. Handbook for MAP, volume 28
[NASA-CR-184972] N90-12117

RADAR RANGE
Base level management of radio frequency radiation protection program
[AD-A211787] N90-12171

RADAR SCATTERING
Pacific marine radar sea scatter experimental results
[AD-A211593] N90-11931
Spectral-domain analysis of finite frequency selective surfaces
[AD-A211669] N90-11932
Radar scattering mechanisms within the meteor crater ejecta blanket: Geologic implications and relevance to Venus N90-12435
Radar scattering from desert terrains, Pisgah/Lavic Region, California: Implications for Magellan N90-12443

RADIANCE
Retrieval of atomic oxygen and temperature in the thermosphere. Part 2: Feasibility of an experiment based on limb emission in the OI lines
[AD-A211807] N90-12121
Comparison of the LOWTRAN 7 code and S3-4 satellite measurements of UV radiance
[AD-A211356] N90-12124
Spatial characteristics of airglow and solar scatter radiance from the earth's atmosphere
[AD-A211358] N90-12126

RADIANT HEATING
Prediction of the thermal environment and thermal response of simple panels exposed to radiant heat
[NASA-TM-101660] N90-12292

RADIATION ABSORPTION
Parametric study of power absorption from electromagnetic waves by small ferrite spheres
[NASA-TP-2949] N90-12282

RADIATION DAMAGE
Photolysis of spacecraft contaminants
[AD-A211715] N90-11801
Growth and characterization of materials for tunable lasers in the near infrared spectral region
[NASA-CR-185832] N90-12009

RADIATION DETECTORS
A microchannel plate intensified, subnanosecond, X-ray imaging camera
[DE89-017781] N90-12003
Electron cyclotron emission and absorption experiment on the CASTOR tokamak
[IPPCZ-285] N90-12331

RADIATION DISTRIBUTION
On the role of Coulomb forces in atomic radiative emission
[IRF-PREPRINT-106] N90-12308

RADIATION EFFECTS
Computer simulations of radiation damage in amorphous solids
[PB89-212682] N90-11827
Fracture toughness data base for HT9 and modified 9Cr-1Mo irradiated in several reactors up to approximately 100 dpa
[DE90-000111] N90-11864
Use of satellite data and modeling to asses the influence of stratospheric processes on the troposphere N90-12075
Investigation of resonant ac-dc magnetic field effects
[AD-A211612] N90-12159
Optical data transmission systems in radiation environment
[DE90-000174] N90-12322

RADIATION MEASUREMENT
Calculations of soft x ray emission of REB-heated plasma
[IPPCZ-287] N90-12329
Electron cyclotron emission and absorption experiment on the CASTOR tokamak
[IPPCZ-285] N90-12331

RADIATION MEASURING INSTRUMENTS
Center for Electronics and Electrical Engineering technical publication announcements covering Center programs, January-March 1989 with 1989 CEEE events calendar
[PB89-228308] N90-12402

RADIATION PROTECTION
Base level management of radio frequency radiation protection program
[AD-A211787] N90-12171

RADIATION PYROMETERS
Infrared temperature measurement with automatic consideration of emissivity
[ESA-TT-1131] N90-12008

RADIATION SOURCES
An experimental high energy physics program
[DE89-014695] N90-12311

RADIATIVE LIFETIME
Lifetime of singlet oxygen in aqueous hydrogen peroxide (BHP)
[AD-A211545] N90-12306

RADIATIVE TRANSFER
Stratiform clouds and their interaction with atmospheric motions N90-12060
The effect of latent heat release on synoptic-to-planetary wave interactions and its implication for satellite observations: Theoretical modeling N90-12073

RADII
Small-radius bending loss in single-mode fibers
[AD-A211822] N90-12323

RADIO COMMUNICATION
Independent Orbiter Assessment (IOA): Assessment of the communication and tracking subsystem, volume 1
[NASA-CR-185528-VOL-1] N90-11789
Independent Orbiter Assessment (IOA): Assessment of the communication and tracking subsystem, volume 2
[NASA-CR-185528-VOL-2] N90-11790
Independent Orbiter Assessment (IOA): Assessment of the communication and tracking subsystem, volume 3
[NASA-CR-185528-VOL-3] N90-11791
A new approach to HF (High Frequency) channel modeling and simulation. Part 1: Deterministic model
[PB89-203962] N90-11913

RADIO DIRECTION FINDERS
Theory and simulation of the operation of a Doppler direction finder in a multipath environment
[FEL-1988-56] N90-11939

RADIO FILTERS
Adaptive noise cancellation for a class of nonlinear 2R filter
[RR-351] N90-11965

RADIO FREQUENCIES
High power, solid state RF pulse generators
[AD-D014172] N90-11941
Base level management of radio frequency radiation protection program
[AD-A211787] N90-12171

RF performance of polycrystalline high-T(sub c) superconductors
[DE89-017671] N90-12359

RADIO INTERFEROMETERS
First interferometric observations with arc-sec. resolution of solar radio bursts at millimeter wavelengths
N90-12472

RADIO TELESCOPES
Cryogenic Schottky-mixer receiver front-end for 40-50 GHz
[PB89-221667] N90-11959

RADIO TRANSMISSION
TEC (Total Electron Content) models
[AD-A211553] N90-12129

RADIO WAVES
Handbook of radio wave propagation loss (100-20,000 MHz), part 2
[PB89-195473] N90-11912
Modeling of diffraction reflection and clutter loss in UHF radio wave propagation
[FEL-1988-28] N90-11938
Base level management of radio frequency radiation protection program
[AD-A211787] N90-12171

RADIOBIOLOGY
USSR Space Life Sciences Digest, Issue 23
[NASA-CR-3922(27)-ISSUE-23] N90-12154

RADIOCHEMISTRY
The Baksan gallium solar neutrino experiment
[DE89-016036] N90-12457

RADIOGRAPHY
NDE (Non-Destructive Evaluation) publications, 1985
[PB89-229025] N90-12036

RAIN
Global atmospheric moisture variability N90-12062
Satellite-derived rainfall estimates and propagation characteristics associated with the Mesoscale Convective Systems (MCSs)
[PB89-213417] N90-12086

RAMAN SPECTRA
Progress of research on water vapor lidar
[NASA-CR-185970] N90-12011
Pulsed-laser-excited Raman spectra of shock compressed triaminotrinitrobenzene
[DE90-000668] N90-12019
MEGALIDAR
[AD-A212074] N90-12020

RAMJET ENGINES
Computation of ramjet internal flowfields
[AD-A212001] N90-11743
Analytical studies of three-dimensional combustion processes
[AD-A211903] N90-11837

RANDOM SAMPLING
Slow sampling and stability of nonlinear sampled-data systems
[RR-342] N90-12277

RANDOM VARIABLES
Fast computation using faulty hypercubes
[AD-A211910] N90-12238

RANDOM WALK
A long time tail for random walk in random scenery
[REPT-89-08] N90-12278

RANGE (EXTREMES)
A closer look at the visioceilometer
[FEL-1989-80] N90-12138

RANGEFINDING
Discrete filtering techniques applied to sequential GPS range measurements
[NASA-CR-177472] N90-11730

RANKING
On a classification problem: Ranking and selection approach
[AD-A211627] N90-12269

RAPID QUENCHING (METALLURGY)
Kinetic processes in advanced alloys
[AD-A212049] N90-11867

RARE EARTH ALLOYS
Anisotropy and microstructure of high-coercivity rare earth permanent magnets
[AD-A211905] N90-12285

RARE GASES
A nonlinear-optical method for combining high power laser beams
[AD-A211730] N90-12022

RASTER SCANNING
Basic program for raster scan display unit
[NAL-TM-560] N90-12185

RATES (PER TIME)
Spin-orbit relaxation rates of Bi(6p(3)) 2D(3/2) following photolysis of Bi(CH3)3 at lambda = 193 nm
[AD-A211792] N90-12303

RAYLEIGH NUMBER
A multigrid method combined with defect correction for free convection problems at high Rayleigh numbers
[REPT-89-27] N90-12264

RAYLEIGH SCATTERING
MEGALIDAR
[AD-A212074] N90-12020
Spatial characteristics of airglow and solar scatter radiance from the earth's atmosphere
[AD-A211358] N90-12126

RAYLEIGH WAVES
Investigations of Eurasian seismic sources and upper mantle structure
[AD-A211806] N90-12120

RAYON
New Fabric Development Program
[AD-A211549] N90-11891

REACTION KINETICS
Natural gas to liquids
[DE89-000982] N90-11828
Conversion of methane to liquid hydrocarbons
[DE89-017547] N90-11831
Synthesis and chemistry of strained and conjugated fluorocarbons
[AD-A211633] N90-11844
Mechanism of electrochemical activation of carbon electrodes: Role of graphite lattice defects
[AD-A211644] N90-11845
Kinetic processes in advanced alloys
[AD-A212049] N90-11867
Shock-induced reaction in several liquids
[DE89-016594] N90-11973
VISAR wave profile measurements in supra-compressed HE
[DE89-017736] N90-11976
Kinetics of diffusion-controlled reactions
[AD-A212161] N90-12286
Spin-orbit relaxation rates of Bi(6p(3)) 2D(3/2) following photolysis of Bi(CH3)3 at lambda = 193 nm
[AD-A211792] N90-12303

REACTIVITY
KIVA reactive hydrodynamics code applied to detonations in high vacuum
[DE89-016979] N90-11974

REAL TIME OPERATION
Improved pattern recognition techniques for real time operation
[AD-A211395] N90-11840
Scheduling sporadic and aperiodic events in a hard real-time system
[AD-A211344] N90-12205
Ultra high speed compound semiconductors and real time signal processing
[AD-A211394] N90-12372
A real-time locking protocol
[AD-A211514] N90-12403

RECEIVERS
Sensitivity of optoelectronic receivers
[AD-A211823] N90-11923

RECOGNITION
Synaptic plasticity and memory formation
[AD-A211368] N90-12158
A Conference on Three-Dimensional Representation held in University of Minnesota on 24-26 May 1989
[AD-A211630] N90-12324

RECOIL IONS
Synchrotron-radiation experiments with recoil ions
[DE89-017579] N90-12301

RECONNAISSANCE AIRCRAFT
Pilotless airplanes
[AD-A211719] N90-11734

RECTANGULAR PLATES
Natural frequencies of singly-curved laminated plates with simply-supported edges
[ESDU-89011] N90-12052

REDUCED GRAVITY
Nonintrusive inertial vibration isolation technology for microgravity space experiments
[NASA-TM-102386] N90-11901

REDUCTION (CHEMISTRY)
In-situ spectroscopic studies of transition metal macrocycles as catalysts for the electrochemical reduction of oxygen
[PB89-219273] N90-11826

REDUNDANCY
Redundancies and don't cares in sequential logic synthesis
[AD-A211931] N90-11956
Optical arithmetic logic using the modified signed-digit redundant number representation
[AD-D014176] N90-12186

REENTRY VEHICLES
Comparison of laser and neutral particle beam discrimination
[DE89-017786] N90-12018

REFLECTANCE
Spectral-domain analysis of finite frequency selective surfaces
[AD-A211669] N90-11932
Development and evaluation of an instrument for rapid electroreflectance of semiconductor materials
[AD-A211690] N90-12376

REFLECTION
Eigensolutions for the reflection problem involving the interface of two chiral half spaces
[PB89-221592] N90-11926

REFRACTIVITY
Calculation of the refractive index change in dissociating shocked benzene
[DE89-017737] N90-11833
Small-radius bending loss in single-mode fibers
[AD-A211822] N90-12323

REFRIGERATORS
Design and calibration of an electrodynamic driver for the Space Thermoacoustic Refrigerator (STAR)
[AD-A212022] N90-11906

REGENERATIVE FUEL CELLS
The fuel cell in space: Yesterday, today and tomorrow
[NASA-TM-102366] N90-11804

REGRESSION ANALYSIS
Forecasting contracting workload
[AD-A211935] N90-12387

RELATIVISTIC ELECTRON BEAMS
The behavior of beams of relativistic non-thermal electrons under the influence of collisions and synchrotron losses
[NASA-CR-185983] N90-12298

RELIABILITY
The RB199: An in-service success
[PNR90544] N90-11746
The effect of incentives on the reliability and validity of cognitive speed tests
[AD-A211346] N90-12181
A unified framework for simulating Markovian models of highly dependable systems
[AD-A212164] N90-12267

REMOTE CONTROL
Pilotless airplanes
[AD-A211719] N90-11734

REMOTE SENSING
NASA/MSFC FY88 Global Scale Atmospheric Processes Research Program Review
[NASA-TM-100357] N90-12059
Low level remote sensing: The Doppler Radar wind profiler N90-12067
Remote sensing data acquisition, analysis and archival
[PB89-142566] N90-12085
Earth resources: A continuing bibliography with indexes (issue 63)
[NASA-SP-7041(63)] N90-12091
UV ionospheric remote sensing with the polar BEAR satellite
[AD-A211359] N90-12127

REMOTE SENSORS
Improved pattern recognition techniques for real time operation
[AD-A211395] N90-11840
Earth resources: A continuing bibliography with indexes (issue 63)
[NASA-SP-7041(63)] N90-12091
Investigation of atmospheric emissions in ultraviolet, vacuum ultraviolet, and extreme ultraviolet wavelength
[AD-A212169] N90-12123

REMOVAL
Autonomous space processor for orbital debris
[NASA-CR-186043] N90-11770

REPLACING
Scientific justification and development plan for a mid-sized jet research aircraft
[PB89-208995] N90-11731

REQUIREMENTS
Conceptual design of liquid droplet radiator shuttle-attached experiment technical requirements document
[NASA-CR-185165] N90-11806
Meeting review: The Second NCAR (National Center for Atmospheric Research) Research Aircraft Fleet Workshop
[PB89-200901] N90-12113

RESCUE OPERATIONS
Statistical models for the optimal estimation of oceanic fields
[AD-A211786] N90-12149

RESEARCH
Development and use of a tribology research-in-progress database
[PB89-228274] N90-12396

RESEARCH AND DEVELOPMENT
Inorganic composite materials in Japan: Status and trends
[PB89-230015] N90-11810
An optimum trajectory planner for robot manipulators in joint-space and under physical constraints
[RR-349] N90-12029

Twenty-five years of service, 1962-1987: Proceedings of the Air Force Studies Board Symposium on Air Force Research and Development, November 16, 1987
[PB89-198915] N90-12384

Federal funds for research and development: Fiscal years 1986, 1987, and 1988. Volume 36: Detailed statistical tables
[PB89-223523] N90-12407

Federal funds for research and development. Fiscal years 1987, 1988, and 1989. Volume 37: Detailed statistical tables
[PB89-223531] N90-12408

RESEARCH FACILITIES

AFRAPT (Air Force Research in Aero Propulsion Technology) Trainee Program
[AD-A211540] N90-11744

RESEARCH MANAGEMENT

Ozone Research Program (German contribution to climate and atmosphere research)
[REPT-46-88] N90-12111

RESIDENTIAL ENERGY

An assessment of technology for self-powered gas appliances: A GATC (Gas Appliance Technology Center)
[PB89-219265] N90-12026

RESIDUAL STRESS

Thermomechanical contact phenomena and wear of sliding components
[AD-A211290] N90-12028

Autofrettage-stress distribution under load and retained stresses after depressurization
[AD-A212090] N90-12048

RESIN BONDING

A lightweight solid polymer electrolyte fuel cell with stack power density of 3 kW/lb (7 kW/kg)
[AD-A211542] N90-12098

RESISTANCE HEATING

Joule heating and runaway electron acceleration in a solar flare N90-12478

RESONANCE

Resonant quasiparticle-ion scattering in anisotropic superfluid (3)He
[PB89-221618] N90-12369

RESONANCE SCATTERING

Spatial characteristics of airglow and solar scatter radiance from the earth's atmosphere
[AD-A211358] N90-12126

RESONANT FREQUENCIES

Natural frequencies of singly-curved laminated plates with simply-supported edges
[ESDU-89011] N90-12052

RESPIRATION

Synergistic effects of nitrogen dioxide and carbon dioxide following acute inhalation exposures in rats
[PB89-214779] N90-12150

RHODIUM

Luminescence in applied magnetic fields
[AD-A211551] N90-12287

RHYTHM (BIOLOGY)

USSR Space Life Sciences Digest, Issue 22
[NASA-CR-3922(26)-ISSUE-22] N90-12153

RIBBON PARACHUTES

Performance and quality of a wing type parachute: Parametric analysis
[REPT-88-19] N90-11710

RIBBONS

Scintillating fiber ribbon - tungsten calorimeter
[DE89-016705] N90-12001

RIDGES

Coronae on Venus observations and models of origin
N90-12449

RIEMANN MANIFOLD

On the differentiable manifold of fixed order stable linear systems
[REPT-88-89] N90-12250

RING WINGS

Steady and unsteady potential flow around thin annular wings and engines with simulation of jet engine flow
[DFVLR-FB-89-18] N90-11711

ROADS

Improving snow roads and airstrips in Antarctica
[AD-A211588] N90-11907

ROBOTICS

Autonomous space processor for orbital debris
[NASA-CR-186043] N90-11770

A distributed pipelined architecture of the recursive Lagrangian equations of motion for robot manipulators with VLSI implementation --- VLSI (very large scale integration)
[RR-353] N90-11966

An optimum trajectory planner for robot manipulators in joint-space and under physical constraints
[RR-349] N90-12029

On the complexity analysis of the coriolis and centripetal effects of a 6 DOF robot manipulator --- Degrees of Freedom (DOF)
[RR-344] N90-12030

The dynamic performance of robot manipulators under different operating conditions
[RR-345] N90-12031

Three dimensional object recognition employing combined visual and tactile sensing
[PB89-219489] N90-12176

Design mechanism for interactive graphics mechanism design
[PB89-219513] N90-12202

A language for assembly instructions
[REPT-88-90] N90-12209

Distributed VLSI architecture for fast Jacobian and inverse Jacobian formulations
[RR-346] N90-12218

Navigation of robotic systems
[DE89-017507] N90-12219

Robot inverse dynamics computation via VLSI distributed architectures
[RR-350] N90-12223

Fast forward dynamics algorithm for robot arms using multiprocessing
[RR-367] N90-12225

ROBOTS

Autonomous space processor for orbital debris
[NASA-CR-186043] N90-11770

Navigation of robotic systems
[DE89-017507] N90-12219

A survey of camera error sources in machine vision systems
[DE89-014072] N90-12318

ROBUSTNESS (MATHEMATICS)

Robust control design for flight control
[AD-A211957] N90-11756

Adaptive feedback linearization: Stability and robustness
[PB89-219497] N90-12220

ROCKET ENGINES

Independent Orbiter Assessment (IOA): Assessment of the reaction control system, volume 1
[NASA-CR-185543-VOL-1] N90-11793

Independent Orbiter Assessment (IOA): Assessment of the reaction control system, volume 2
[NASA-CR-185543-VOL-2] N90-11794

Independent Orbiter Assessment (IOA): Assessment of the reaction control system, volume 3
[NASA-CR-185543-VOL-3] N90-11795

Independent Orbiter Assessment (IOA): Assessment of the reaction control system, volume 4
[NASA-CR-185543-VOL-4] N90-11796

Independent Orbiter Assessment (IOA): Assessment of the reaction control system, volume 5
[NASA-CR-185543-VOL-5] N90-11797

ROCKET NOZZLES

Three-dimensional, two-phase, transonic, canted nozzle flows
[AD-A211528] N90-11984

ROCKET-BORNE INSTRUMENTS

Design of scientific payloads and components
[AD-A211819] N90-12005

RODENTS

The rodent research animal holding facility as a barrier to environmental contamination
[NASA-TM-102237] N90-12151

RODS

Fe-Ni-Cr alloys for coatings and electroforms
[PB89-195846] N90-11849

ROLL FORMING

A study of the hot workability of Al-8.5 wt pct Mg alloys for armor plate applications
[AD-A211680] N90-11868

ROLLING CONTACT LOADS

Three-dimensional viscoelastic bodies in steady state frictional rolling contact with generalization to Knothe rolling
[REPT-89-23] N90-12032

ROTARY STABILITY

Equilibrium solutions of a spherical pendulum with rotating point of suspension and friction
[ESA-TT-1139] N90-12288

ROTATING FLUIDS

On the computation of normal modes of a rotating, viscous, incompressible fluid with a capillary free boundary
[REPT-89-01] N90-11989

Flare-in texture in rotating superfluid (3)He-B
[PB89-218994] N90-12368

ROTATING SPHERES

Equilibrium solutions of a spherical pendulum with rotating point of suspension and friction
[ESA-TT-1139] N90-12288

ROTATION

Acoustic controlled rotation and orientation
[NASA-CASE-NPO-16995-1-CU] N90-12289

ROTOR BLADES (TURBOMACHINERY)

Review and analysis of the DNW/Model 360 rotor acoustic data base
[NASA-TM-102253] N90-11692

An investigation of end-wall vortex cavitation in a high Reynolds number axial-flow pump
[AD-A211426] N90-11982

WISPER: A standardized fatigue load sequence for HAWT-blades
[NLR-MP-88029-U] N90-12055

Airframe structural dynamic considerations in rotor design optimization
[NASA-TM-101646] N90-12057

ROTORS

An experimental investigation of helicopter rotor hub fairing drag characteristics
[NASA-TM-102182] N90-11701

User's guide for a personal computer model of turbulence at a wind turbine rotor
[DE89-017753] N90-12095

RUNWAYS

Improving snow roads and airstrips in Antarctica
[AD-A211588] N90-11907

Ice runways near the South Pole
[AD-A211606] N90-11908

S

SADDLE POINTS

A study of the asymptotic behavior of linear difference equations with polynomial coefficients
[IMAG-RR-743-M] N90-12254

SAFETY DEVICES

Aircraft cabin fire suppression by means of an interior water spray system
[CAA-PAPER-88014] N90-11719

SAFETY FACTORS

Safety considerations for sodium-sulfur batteries for electric vehicles
[DE89-017682] N90-11949

SAFETY MANAGEMENT

UK airmisses involving commercial air transport
[CAA-2/88] N90-11718

SAMPLING

Estimated UV clutter levels at 10-100 meter sensor pixel resolution extrapolated from recent polar bear measurements
[AD-A211357] N90-12125

Surface, interface, and bulk properties of high T(sub c) superconductors
[AD-A211490] N90-12373

SATELLITE ANTENNAS

Proceedings of the 1988 Antenna Applications Symposium, volume 1
[AD-A211396] N90-11928

SATELLITE DESIGN

Petite Amateur Navy Satellite (PANSAT)
[NASA-CR-186049] N90-11800

SATELLITE IMAGERY

NASA/MSFC FY88 Global Scale Atmospheric Processes Research Program Review
[NASA-TM-100357] N90-12059

Application of dynamical systems theory to global weather phenomena revealed by satellite imagery
N90-12063

The effect of latent heat release on synoptic-to-planetary wave interactions and its implication for satellite observations: Theoretical modeling N90-12073

Use of satellite data and modeling to asses the influence of stratospheric processes on the troposphere
N90-12075

Characteristics, distribution and geologic/terrain associations of small dome-like hills on Venus
N90-12425

SATELLITE OBSERVATION

Comparison of the LOWTRAN 7 code and S3-4 satellite measurements of UV radiance
[AD-A211356] N90-12124

UV ionospheric remote sensing with the polar BEAR satellite
[AD-A211359] N90-12127

Coronae on Venus observations and models of origin
N90-12449

Interplanetary energetic particle observations of the March 1989 events N90-12484

SCALARS

Scalar fields versus black holes
[DE89-611967] N90-12413

SCATTERING

Calculation of transient response from time-harmonic spectrum
[AD-A211972] N90-12241

Internal Magnus effects in superfluid 3He-A
[PB89-212617] N90-12351

Superconductivity and magnetic scattering in the Nd(sub 2-x)Ce(sub x)CuO(sub 4-delta)
[DE89-016524] N90-12354

SCATTERING CROSS SECTIONS
Pacific marine radar sea scatter experimental results
[AD-A211593] N90-11931

SCHEDULING
Processing rate sensitivities of a heterogeneous multiprocessor
[PB89-229017] N90-12201
Scheduling sporadic and aperiodic events in a hard real-time system
[AD-A211344] N90-12205

SCHOTTKY DIODES
Design, construction and test of a frequency doubler for 183 GHz
[PB89-212591] N90-11944

SCHWARZSCHILD METRIC
Scalar fields versus black holes
[DE89-611967] N90-12413

SCIENTISTS
Space flight (selected articles)
[AD-A212068] N90-11769

SCINTILLATION
Scintillating fiber ribbon - tungsten calorimeter
[DE89-016705] N90-12001

SEA ICE
Remote sensing data acquisition, analysis and archival
[PB89-142566] N90-12085

SEA STATES
Pacific marine radar sea scatter experimental results
[AD-A211593] N90-11931

SEA WATER
Long endurance underwater power system
[AD-A211386] N90-12096

SEALING
Apparatus and method for monitoring pressure leaks from a sealed system
[AD-D014168] N90-11995

SEALS (STOPPERS)
Sliding seal materials for low heat rejection engines
[NASA-CR-182262] N90-11682

SEARCH RADAR
ASR-9 weather channel test report
[AD-A211749] N90-11934

SECONDARY EMISSION
Plasma-anode electron gun research
[AD-A211547] N90-11773

SEEBECK EFFECT
Superconductivity and magnetic scattering in the Nd(sub 2-x)Ce(sub x)CuO(sub 4-delta)
[DE89-016524] N90-12354

SEISMIC WAVES
Wind/seismic comparisons for upgrading existing structures
[DE89-016055] N90-12044
Hydrophone investigations of earthquakes and explosion generated high-frequency seismic phases
[AD-A212055] N90-12122
Seismic wave attenuation and yield determination at regional distances
[AD-A211548] N90-12126

SEISMOLOGY
Hydrophone investigations of earthquakes and explosion generated high-frequency seismic phases
[AD-A212055] N90-12122

SELECTION
Likelihood cross-validation bandwidth selection for nonparametric kernel density estimators
[REPT-89-10] N90-12279

SELECTIVE SURFACES
Spectral-domain analysis of finite frequency selective surfaces
[AD-A211669] N90-11932

SELF ORGANIZING SYSTEMS
Can perceptrons find Lyapunov functions: An algorithmic approach to systems stability
[RR-365] N90-12224

SEMANTICS
Computer generation of a tutorial dialogue
[AD-A211976] N90-12162
Taxonomic syntax for first order inference
[AD-A211618] N90-12221
Some techniques for anaphora resolution in algebraic linguistics
[REPT-89-28] N90-12265
DOD Gateway Information System (DGIS) common command language: A retrospective on the introduction of prolog as the development tool
[AD-A211941] N90-12400

SEMICONDUCTING FILMS
Beam assisted fabrication of 3-5/Si monolithic devices
[AD-A212046] N90-12367

SEMICONDUCTOR DIODES
Channelized coplanar waveguide pin-diode switches
[NASA-TM-102289] N90-11943
Analysis of loss mechanisms in polycrystalline thin-film solar cells
[DE89-009454] N90-12093

SEMICONDUCTOR LASERS
Development of microstructured DH diode lasers and detectors for the near and medium IR spectral domain using molecular beam epitaxy
[IPM-15/1988] N90-12023

SEMICONDUCTOR PLASMAS
Reactive ion etching of sputtered silicon carbide and tungsten thin films for device applications
[AD-A211711] N90-11847

SEMICONDUCTORS (MATERIALS)
Reactive ion etching of sputtered silicon carbide and tungsten thin films for device applications
[AD-A211711] N90-11847
Application of dimensional analysis to statistical process modeling
[AD-A211881] N90-11905
Infrared detector array
[AD-D014170] N90-11997
Construction of a picosecond laser system for the investigation of semiconductors using nonlinear optical methods
[ETN-89-94664] N90-12013
Niobium and niobium nitride contacts on semiconducting material
[AD-D014177] N90-12347
Electrolitic deposited ohmic contacts on III-V compound semiconductors: A review
[PB89-217400] N90-12350
Ultra high speed compound semiconductors and real time signal processing
[AD-A211394] N90-12372
Development and evaluation of an instrument for rapid electroreflectance of semiconductor materials
[AD-A211690] N90-12376

SENSITIVITY
Sensitivity relationships in energetic materials
[DE89-016967] N90-11897

SENSORIMOTOR PERFORMANCE
Age-related changes in human posture control: Motor coordination tests
[NASA-CR-185855] N90-12178

SENSORS
Devices and procedures for the calibration of sensors and measurement: Systems of the flight test support system ATTAS
[DFVLR-MITT-89-06] N90-12007

SENTINEL SYSTEM
Sentinel satellite positional precision derived from the NAVSTAR global positioning system
[AD-A211876] N90-11720

SEPARATED FLOW
The structure of separated flow regions occurring near the leading edge of airfoils - including transition
[NASA-CR-185853] N90-11695
Numerical analysis, scientific computing and fundamental studies of fluid mechanics
[DE89-017554] N90-11975

SERIES EXPANSION
Rational expansion for nonlinear input-output maps
[RR-348] N90-12248

SERVICE LIFE
The RB199: An in-service success
[PNR90544] N90-11746
In service life monitoring system using g-meter readings and mass configuration control
[ETN-89-95218] N90-12035
Long endurance underwater power system
[AD-A211386] N90-12096

SERVOCONTROL
Control of plasma position in the CASTOR tokamak
[IPPCZ-284] N90-12332

SHADOWGRAPH PHOTOGRAPHY
Application of the wide-field shadowgraph technique to rotor wake visualization
[NASA-TM-102222] N90-11700

SHAFTS (MACHINE ELEMENTS)
Magnetostrictive torque sensor
[AD-D014169] N90-11996

SHALLOW SHELLS
A C(Superscript)-Anisoparametric three-node shallow shell element for general shell analysis
[AD-A212094] N90-12049

SHEAR LAYERS
Control of turbulent mixing layers
[AD-A211413] N90-11708

SHEAR STRESS
Manual for Program PSTRESS: Peel stress computation
[NASA-CR-178408] N90-11822
Absolute determination of the wall shear stress by means of an interferometer
[DFVLR-FB-89-13] N90-11991

SHELL THEORY
A C(Superscript)-Anisoparametric three-node shallow shell element for general shell analysis
[AD-A212094] N90-12049

SHIPS
Statistical models for the optimal estimation of oceanic fields
[AD-A211786] N90-12149

SHOCK HEATING
Shock dissociation of molecular fluids: A possibility of first-order phase change
[DE89-016647] N90-11829

SHOCK LAYERS
Experimental research on swept shock Wave/Boundary layer interactions
[AD-A211744] N90-11988

SHOCK LOADS
Calculation of the refractive index change in dissociating shocked benzene
[DE89-017737] N90-11833
VISAR wave profile measurements in supra-compressed HE
[DE89-017736] N90-11976

SHOCK WAVE INTERACTION
Experimental research on swept shock Wave/Boundary layer interactions
[AD-A211744] N90-11988

SHOCK WAVE PROPAGATION
Shock-induced reaction in several liquids
[DE89-016594] N90-11973

SHOCK WAVES
Wave combustors for trans-atmospheric vehicles
[NASA-TM-102238] N90-11742
Calculation of the refractive index change in dissociating shocked benzene
[DE89-017737] N90-11833
A rate-dependent constitutive model for Be
[DE89-017755] N90-11861
Simulation of glancing shock wave and boundary layer interaction
[NASA-TM-102233] N90-11970
Characteristics of flyer impact for one-dimensional shock-wave study applications
[DE89-017887] N90-11977
Experimental investigation of a planar shock wave over a double wedge
[AD-A211366] N90-11981
Lagrangian analysis of MIV (Magnetic Impulse-Velocity) gauge experiments on PBX 9502 using the mass-displacement moment function
[DE89-016612] N90-12000
Shock pressure determination in detonator wires
[DE89-017756] N90-12002
Pulsed-laser-excited Raman spectra of shock compressed triaminotrinitrobenzene
[DE90-000668] N90-12019
Interplanetary energetic particle observations of the March 1989 events N90-12484

SHORT TAKEOFF AIRCRAFT
Wind tunnel test of CAD USB-STOL semi-borne prototype
[NAL-TM-566] N90-11696
Acoustic-thermal environment for USB flap structure. Report 1: Ground simulation test results
[NAL-TM-567] N90-11697
STOVL propulsion system volume dynamics approximations
[NASA-TM-102397] N90-11740
Low-speed wind-tunnel study of reaction control-jet effectiveness for hover and transition of a STOVL fighter concept
[NASA-TM-4147] N90-11751

SHOT NOISE
LAWS simulation: Sampling strategies and wind computation algorithms N90-12081

SIGNAL DETECTION
In-situ cure monitoring of composites by fiber-optic molecular sensors
[AD-A211495] N90-11817
Microwave signal detection using modulation of polymeric optical waveguides
[DE89-017545] N90-11921
Analysis of two-pass Modified Hough Transform (MHT) technique for the detection of wake like signals
[AD-A211982] N90-11924
Hydrophone investigations of earthquakes and explosion generated high-frequency seismic phases
[AD-A212055] N90-12122
Binaural masking: An analysis of models
[AD-A211578] N90-12168

SIGNAL DETECTORS
Analysis of two-pass Modified Hough Transform (MHT) technique for the detection of wake like signals
[AD-A211982] N90-11924

SIGNAL MEASUREMENT
Doppler statistics of ocean velocity variability
[AD-A211687] N90-12146
SIGNAL PROCESSING
Simulations for computer centerline approach
[DOT/FAA/CT-TN89/41] N90-11726
Improved pattern recognition techniques for real time operation
[AD-A211395] N90-11840
Adaptive noise cancellation for a class of nonlinear 2R filter
[RR-351] N90-11965
Aerosol backscatter studies supporting LAWS
N90-12079
On the communication complexity of solving a polynomial equation
[AD-A211945] N90-12240
Linear (passive) and non-linear guided and studies in glass
[AD-A211693] N90-12325
Ultra high speed compound semiconductors and real time signal processing
[AD-A211394] N90-12372
SIGNAL REFLECTION
ILS mathematical modeling study of the effects of proposed hangar construction at the Orlando International Airport, Runway 17R, Orlando, Florida
[DOT/FAA/CT-TN89/52] N90-11762
SIGNAL TO NOISE RATIOS
Analysis of two-pass Modified Hough Transform (MHT) technique for the detection of wake like signals
[AD-A211982] N90-11924
SILICON CARBIDES
Investigations into the infiltration kinetics, wettability, and interfacial bond strength of Al/SiC composites
[AD-A211924] N90-11815
Reactive ion etching of sputtered silicon carbide and tungsten thin films for device applications
[AD-A211711] N90-11847
SILICON FILMS
Self-assembled organic monolayer films
[AD-A212006] N90-11838
SILICON NITRIDES
Flexure strength of advanced ceramics: A round robin exercise
[AD-A212101] N90-11889
SILICON POLYMERS
Structure/reactivity relationships of polysilazane preceramics
[AD-A212028] N90-11888
SILVER
Temperature dependent effects during Ag deposition on Cu(110)
[DE89-016987] N90-11857
SIMULATION
Computation of ramjet internal flowfields
[AD-A212001] N90-11743
SIMULATORS
Human Operator Simulator (HOS) 4 user's guide
[AD-A212007] N90-11763
Satellite-matrix-switched, time-division-multiple-access network simulator
[NASA-TP-2944] N90-11915
SINGLE CRYSTALS
Process for single crystal growth of high T(sub c) superconductors
[AD-D014167] N90-12346
Field-assisted bonding of single crystal quartz
[DE89-015407] N90-12353
Surface, interface, and bulk properties of high T(sub c) superconductors
[AD-A211490] N90-12373
High temperature superconducting compounds
[AD-A211511] N90-12374
SINGLE EVENT UPSETS
A beam induced upset during the flight of the ECHO-7 rocket
[NASA-CR-186089] N90-11755
SINTERING
Processing and characterization of alumina platelet-reinforced mullite composites
[DE90-000057] N90-11814
Flexure strength of advanced ceramics: A round robin exercise
[AD-A212101] N90-11889
SIS (SUPERCONDUCTORS)
SIS (Superconductor-Insulator-Superconductor) mixer research
[AD-A211607] N90-12375
SITE SELECTION
Ice runways near the South Pole
[AD-A211606] N90-11908
SIZE DETERMINATION
Droplet sizing instrumentation used for icing research: Operation, calibration, and accuracy
[NASA-CR-182293] N90-11999
SIZE DISTRIBUTION
Further guide for the retrieval of dropsize distributions in water clouds with a ground-based clear-air-sensing Doppler radar
[PB89-196000] N90-11911
SLIDING FRICTION
Thermomechanical contact phenomena and wear of sliding components
[AD-A211290] N90-12028
SLOPES
Calculated solar radiation incident upon slopes of different orientated surfaces in Finland
[FMI-MP-8] N90-12116
Operational measures of central tendency
[DE89-016959] N90-12234
SMOKE
Flammability, smoke, and dry arc tracking tests of aircraft electrical wire insulations
[DOT/FAA/CT-89/21] N90-11714
SMOOTHING
Inf-convolution splines
[IMAG-RR-749-M] N90-12256
SODIUM SULFUR BATTERIES
Safety considerations for sodium-sulfur batteries for electric vehicles
[DE89-017682] N90-11949
SOFTWARE ENGINEERING
Transport systems research vehicle color display system operations manual
[NASA-TM-101577] N90-11736
Requirements for multidisciplinary design of aerospace vehicles on high performance computers
[NASA-CR-181915] N90-12183
Adoption of software engineering innovations in organizations
[AD-A211573] N90-12206
SOFTWARE TOOLS
Tools to aid in the development high-performance algorithms
[DE89-012395] N90-12194
SOILS
Global data bases on distribution, characteristics and methane emission of natural wetlands: Documentation of archived data tape
[NASA-TM-4153] N90-12090
SOL-GEL PROCESSES
Linear (passive) and non-linear guided and studies in glass
[AD-A211693] N90-12325
Synthesis and microstructure of highly oriented PbTiO3 thin films prepared by a sol-gel method
[AD-A211735] N90-12377
SOLAR ACTIVITY
MHD (magnetohydrodynamic) modeling of solar and interplanetary processes
[PB89-215461] N90-12416
Access to Max '91 information via computer networks
N90-12466
SOLAR ACTIVITY EFFECTS
Some of the terrestrial effects of AR 5395
N90-12482
Interplanetary energetic particle observations of the March 1989 events N90-12484
SOLAR ATMOSPHERE
The hard x rays and gamma-rays from solar flares
[NASA-CR-185982] N90-12458
Investigation of active regions at high resolution by balloon flights of the Solar Optical Universal Polarimeter (SOUP) N90-12487
SOLAR CELLS
On-orbit annealing of gallium arsenide solar cell arrays
[AD-A212087] N90-11900
Analysis of loss mechanisms in polycrystalline thin-film solar cells
[DE89-009454] N90-12093
Graded bandgap solar cells
[AD-A211537] N90-12097
SOLAR COLLECTORS
Analysis of the efficiency of a dielectric solar energy collector
[PB89-212716] N90-12092
SOLAR CORONA
MHD (magnetohydrodynamic) modeling of solar and interplanetary processes
[PB89-215461] N90-12416
Heating and acceleration of coronal and chromospheric ions during solar flares N90-12479
Chromospheric-coronal coupling during solar flares: Current systems and particle acceleration N90-12480
The Owens Valley solar array N90-12490
SOLAR COSMIC RAYS
The onset of the solar active cycle 22 N90-12488
SOLAR CYCLES
Max '91 Workshop 2: Developments in Observations and Theory for Solar Cycle 22
[NASA-TM-101893] N90-12459
When and where to look to observe major solar flares
N90-12465
SOLAR ENERGY
Analysis of the efficiency of a dielectric solar energy collector
[PB89-212716] N90-12092
Photovoltaic system research status
[DE89-016764] N90-12094
SOLAR FLARES
The hard x rays and gamma-rays from solar flares
[NASA-CR-185982] N90-12458
Max '91 Workshop 2: Developments in Observations and Theory for Solar Cycle 22
[NASA-TM-101893] N90-12459
High energy flare physics group summary N90-12460
Magnetograph group summary N90-12461
Theory and modeling group N90-12462
Scientific objectives of solar gamma-ray observations
N90-12463
The Gamma-Ray Observatory: An overview
N90-12464
When and where to look to observe major solar flares
N90-12465
Access to Max '91 information via computer networks
N90-12466
Capabilities of GRO/OSSE for observing solar flares
N90-12467
The solar gamma ray and neutron capabilities of COMPTEL on the Gamma Ray Observatory N90-12468
The BATSE experiment on the Gamma Ray Observatory: Solar flare hard x ray and gamma-ray capabilities
N90-12469
The solar flare and cosmic gamma-ray burst experiment aboard the Ulysses spacecraft N90-12470
VLA-Max '91 tests of high energy flare physics
N90-12471
First interferometric observations with arc-sec. resolution of solar radio bursts at millimeter wavelengths
N90-12472
Observational goals for Max '91 to identify the causative agent for impulsive bursts N90-12473
Solar flare gamma-ray and hard x ray imaging with the GRID-on-a-balloon N90-12474
The soft x ray telescope for Solar-A N90-12475
Pre-pulses: Signature of a trigger process in short (less than 60 secs) solar hard x ray flares N90-12476
Flare model sensitivity of the Balmer spectrum
N90-12477
Joule heating and runaway electron acceleration in a solar flare N90-12478
Heating and acceleration of coronal and chromospheric ions during solar flares N90-12479
Chromospheric-coronal coupling during solar flares: Current systems and particle acceleration N90-12480
Some of the terrestrial effects of AR 5395
N90-12482
The 10.7-cm microwave observations of AR 5395 and related terrestrial effects N90-12483
The SMM UV observations of Active Region 5395
N90-12485
Hard x ray highlights of AR 5395 N90-12486
An imaging vector magnetograph for the next solar maximum N90-12489
The Owens Valley solar array N90-12490
A high-speed digital camera system for the observation of rapid H-alpha fluctuations in solar flares N90-12491
SOLAR INSTRUMENTS
High energy flare physics group summary N90-12460
SOLAR MAGNETIC FIELD
Magnetograph group summary N90-12461
Investigation of active regions at high resolution by balloon flights of the Solar Optical Universal Polarimeter (SOUP) N90-12487
An imaging vector magnetograph for the next solar maximum N90-12489
The Owens Valley solar array N90-12490
SOLAR MAXIMUM MISSION
Capabilities of GRO/OSSE for observing solar flares
N90-12467
The BATSE experiment on the Gamma Ray Observatory: Solar flare hard x ray and gamma-ray capabilities
N90-12469
The solar flare and cosmic gamma-ray burst experiment aboard the Ulysses spacecraft N90-12470
VLA-Max '91 tests of high energy flare physics
N90-12471
Observational goals for Max '91 to identify the causative agent for impulsive bursts N90-12473
Solar flare gamma-ray and hard x ray imaging with the GRID-on-a-balloon N90-12474
The SMM UV observations of Active Region 5395
N90-12485
Hard x ray highlights of AR 5395 N90-12486
A high-speed digital camera system for the observation of rapid H-alpha fluctuations in solar flares N90-12491

SOLAR NEUTRONS
Scientific objectives of solar gamma-ray observations N90-12463
The solar gamma ray and neutron capabilities of COMPTEL on the Gamma Ray Observatory N90-12468
SOLAR OBSERVATORIES
High energy flare physics group summary N90-12460
Investigation of active regions at high resolution by balloon flights of the Solar Optical Universal Polarimeter (SOUP) N90-12487
SOLAR PHYSICS
MHD (magnetohydrodynamic) modeling of solar and interplanetary processes
[PB89-215461] N90-12416
The hard x rays and gamma-rays from solar flares
[NASA-CR-185982] N90-12458
Max '91 Workshop 2: Developments in Observations and Theory for Solar Cycle 22
[NASA-TM-101893] N90-12459
High energy flare physics group summary N90-12460
Magnetograph group summary N90-12461
Theory and modeling group N90-12462
Scientific objectives of solar gamma-ray observations N90-12463
The Gamma-Ray Observatory: An overview N90-12464
VLA-Max '91 tests of high energy flare physics N90-12471
Observational goals for Max '91 to identify the causative agent for impulsive bursts N90-12473
SOLAR RADIATION
Photolysis of spacecraft contaminants
[AD-A211715] N90-11801
Calculated solar radiation incident upon slopes of different orientated surfaces in Finland
[FMI-MP-8] N90-12116
The SMM UV observations of Active Region 5395 N90-12485
The Owens Valley solar array N90-12490
SOLAR RADIO BURSTS
The solar gamma ray and neutron capabilities of COMPTEL on the Gamma Ray Observatory N90-12468
First interferometric observations with arc-sec. resolution of solar radio bursts at millimeter wavelengths N90-12472
Observational goals for Max '91 to identify the causative agent for impulsive bursts N90-12473
SOLAR SAILS
Design of a solar sail mission to Mars
[NASA-CR-186045] N90-11771
SOLAR SPECTRA
The hard x rays and gamma-rays from solar flares
[NASA-CR-185982] N90-12458
A high-speed digital camera system for the observation of rapid H-alpha fluctuations in solar flares N90-12491
SOLAR TERRESTRIAL INTERACTIONS
On the statistics of El Nino occurrences and the relationship of El Nino to volcanic and solar/geomagnetic activity
[NASA-TP-2948] N90-12456
Some of the terrestrial effects of AR 5395 N90-12482
The 10.7-cm microwave observations of AR 5395 and related terrestrial effects N90-12483
SOLAR WIND
MHD (magnetohydrodynamic) modeling of solar and interplanetary processes
[PB89-215461] N90-12416
SOLAR X-RAYS
The hard x rays and gamma-rays from solar flares
[NASA-CR-185982] N90-12458
Pre-pulses: Signature of a trigger process in short (less than 60 secs) solar hard x ray flares N90-12476
Joule heating and runaway electron acceleration in a solar flare N90-12478
Chromospheric-coronal coupling during solar flares: Current systems and particle acceleration N90-12480
Hard x ray highlights of AR 5395 N90-12486
A high-speed digital camera system for the observation of rapid H-alpha fluctuations in solar flares N90-12491
SOLID ELECTROLYTES
Long endurance underwater power system
[AD-A211386] N90-12096
A lightweight solid polymer electrolyte fuel cell with stack power density of 3 kW/lb (7 kW/kg)
[AD-A211542] N90-12098
SOLID LUBRICANTS
Ion-assisted deposition of high-temperature lubricious surfaces
[DE89-012397] N90-11883
SOLID PHASES
Structure-property relationships as an aid in the rational design of (beta)-(ET)(sub 2)X organic superconductors
[DE89-016912] N90-12356
SOLID PROPELLANT ROCKET ENGINES
Three-dimensional, two-phase, transonic, canted nozzle flows
[AD-A211528] N90-11984
SOLID STATE DEVICES
Solid-State Sensor and Actuator
[AD-A211427] N90-11961
SIS (Superconductor-Insulator-Superconductor) mixer research
[AD-A211607] N90-12375
SOLID SURFACES
Quantitative interpretation of auger lineshapes and electron/photon stimulated desorption
[AD-A211550] N90-11842
SOLIDIFICATION
Formation and modification of surface alloys by excimer laser melting and resolidification
[DE89-016968] N90-11856
Kinetic processes in advanced alloys
[AD-A212049] N90-11867
SOLIDS
Computer simulations of radiation damage in amorphous solids
[PB89-212682] N90-11827
International seminar on the inelastic behavior of solids: Models and utilization
[DE89-017420] N90-11858
A numerical laboratory for granular solids
[DE89-016367] N90-12045
SOLITARY WAVES
Davydov solutions at 300 Kelvin: The final search
[DE89-015248] N90-12296
SOLVENTS
Cleaning of printed circuit assemblies with surface-mounted components
[DE89-013609] N90-11945
SONAR
Doppler statistics of ocean velocity variability
[AD-A211687] N90-12148
SOUNDING ROCKETS
A beam induced upset during the flight of the ECHO-7 rocket
[NASA-CR-186089] N90-11755
SPACE CHARGE
A beam induced upset during the flight of the ECHO-7 rocket
[NASA-CR-186089] N90-11755
Plasma-anode electron gun research
[AD-A211547] N90-11773
DART: A simulation code for charged particle beams, revision 1
[DE89-016697] N90-12312
SPACE DEBRIS
Autonomous space processor for orbital debris
[NASA-CR-186043] N90-11770
The time evaluation of the number of space probes and debris at different orbit heights with a view to a future collision risk in space
[R-8718] N90-11772
SPACE DETECTION AND TRACKING SYSTEM
Independent Orbiter Assessment (IOA): Assessment of the communication and tracking subsystem, volume 1
[NASA-CR-185528-VOL-1] N90-11789
Independent Orbiter Assessment (IOA): Assessment of the communication and tracking subsystem, volume 2
[NASA-CR-185528-VOL-2] N90-11790
Independent Orbiter Assessment (IOA): Assessment of the communication and tracking subsystem, volume 3
[NASA-CR-185528-VOL-3] N90-11791
SPACE FLIGHT
Space flight (selected articles)
[AD-A212068] N90-11769
SPACE FLIGHT TRACKING AND DATA NETWORK
Navigation experiment NAVEX: Data storage and processing
[DFVLR-MITT-89-09] N90-11727
Navigation experiment NAVEX: The equipment delay times in the Spacelab mission D1
[DFVLR-MITT-89-10] N90-11728
SPACE NAVIGATION
Independent Orbiter Assessment (IOA): Assessment of the guidance, navigation, and control subsystem FMEA/CIL
[NASA-CR-185552] N90-11784
SPACE PERCEPTION
Visual motion perception
[AD-A210994] N90-12160
Visual acuity and stereopsis with night vision goggles
[AD-A211552] N90-12167
Discriminating rigid from nonrigid motion
[AD-A211794] N90-12180
Distance and clearance perception using forward-looking, vehicular television systems
[DE89-014740] N90-12319
A Conference on Three-Dimensional Representation held in University of Minnesota on 24-26 May 1989
[AD-A211630] N90-12324
SPACE POWER REACTORS
Creep strength of niobium alloys, Nb-1%Zr and PWC-11
[NASA-TM-102390] N90-11854
SPACE PROBES
The time evaluation of the number of space probes and debris at different orbit heights with a view to a future collision risk in space
[R-8718] N90-11772
SPACE PROCESSING
On-orbit annealing of gallium arsenide solar cell arrays
[AD-A212087] N90-11900
SPACE SHUTTLE MAIN ENGINE
Independent Orbiter Assessment (IOA): Assessment of the orbiter main propulsion system FMEA/CIL, volume 1
[NASA-CR-185559-VOL-1] N90-11775
Independent Orbiter Assessment (IOA): Assessment of the main propulsion subsystem FMEA/CIL, volume 2
[NASA-CR-185559-VOL-2] N90-11776
Independent Orbiter Assessment (IOA): Assessment of the main propulsion subsystem FMEA/CIL, volume 3
[NASA-CR-18559-VOL-3] N90-11777
Independent Orbiter Assessment (IOA): Assessment of the main propulsion subsystem FMEA/CIL, volume 4
[NASA-CR-185559-VOL-4] N90-11778
SPACE SHUTTLE ORBITERS
Independent Orbiter Assessment (IOA): Analysis of the displays and controls subsystem
[NASA-CR-185563] N90-11774
Independent Orbiter Assessment (IOA): Assessment of the orbiter main propulsion system FMEA/CIL, volume 1
[NASA-CR-185559-VOL-1] N90-11775
Independent Orbiter Assessment (IOA): Assessment of the main propulsion subsystem FMEA/CIL, volume 2
[NASA-CR-185559-VOL-2] N90-11776
Independent Orbiter Assessment (IOA): Assessment of the main propulsion subsystem FMEA/CIL, volume 3
[NASA-CR-18559-VOL-3] N90-11777
Independent Orbiter Assessment (IOA): Assessment of the main propulsion subsystem FMEA/CIL, volume 4
[NASA-CR-185559-VOL-4] N90-11778
Independent Orbiter Assessment (IOA): Assessment of the electrical power distribution and control subsystem, volume 1
[NASA-CR-185557-VOL-1] N90-11779
Independent Orbiter Assessment (IOA): Assessment of the electrical power distribution and control subsystem, volume 2
[NASA-CR-185557-VOL-2] N90-11780
Independent Orbiter Assessment (IOA): Assessment of the electrical power distribution and control subsystem, volume 3
[NASA-CR-185557-VOL-3] N90-11781
Independent Orbiter Assessment (IOA): Analysis of the active thermal control subsystem
[NASA-CR-185553] N90-11782
Independent Orbiter Assessment (IOA): FMEA/CIL assessment
[NASA-CR-185550] N90-11783
Independent Orbiter Assessment (IOA): Assessment of the guidance, navigation, and control subsystem FMEA/CIL
[NASA-CR-185552] N90-11784
Independent Orbiter Assessment (IOA): Assessment of the Electrical Power Distribution and Control/Electrical Power Generation (EPD and C/EPG) FMEA/CIL
[NASA-CR-185542] N90-11785
Independent Orbiter Assessment (IOA): Analysis of the life support and airlock support subsystems
[NASA-CR-185539] N90-11786
Independent Orbiter Assessment (IOA): Assessment of the orbital maneuvering system FMEA/CIL, volume 1
[NASA-CR-185544-VOL-1] N90-11787
Independent Orbiter Assessment (IOA): Assessment of the orbital maneuvering subsystem, volume 2
[NASA-CR-185544-VOL-2] N90-11788
Independent Orbiter Assessment (IOA): Assessment of the communication and tracking subsystem, volume 1
[NASA-CR-185528-VOL-1] N90-11789
Independent Orbiter Assessment (IOA): Assessment of the communication and tracking subsystem, volume 2
[NASA-CR-185528-VOL-2] N90-11790
Independent Orbiter Assessment (IOA): Assessment of the communication and tracking subsystem, volume 3
[NASA-CR-185528-VOL-3] N90-11791
Independent Orbiter Assessment (IOA): Assessment of the hydraulics/water spray boiler subsystem
[NASA-CR-185537] N90-11792
Independent Orbiter Assessment (IOA): Assessment of the reaction control system, volume 1
[NASA-CR-185543-VOL-1] N90-11793

Independent Orbiter Assessment (IOA): Assessment of the reaction control system, volume 2
[NASA-CR-185543-VOL-2] N90-11794

Independent Orbiter Assessment (IOA): Assessment of the reaction control system, volume 3
[NASA-CR-185543-VOL-3] N90-11795

Independent Orbiter Assessment (IOA): Assessment of the reaction control system, volume 4
[NASA-CR-185543-VOL-4] N90-11796

Independent Orbiter Assessment (IOA): Assessment of the reaction control system, volume 5
[NASA-CR-185543-VOL-5] N90-11797

SPACE SHUTTLE PAYLOADS

Conceptual design of liquid droplet radiator shuttle-attached experiment
[NASA-CR-185164] N90-11805

SPACE SHUTTLES

Nonintrusive inertial vibration isolation technology for microgravity space experiments
[NASA-TM-102386] N90-11901

Final environmental impact statement for the Galileo Mission (Tier 2)
[NASA-TM-101825] N90-12102

SPACE STATIONS

Docking system for spacecraft
[NASA-CASE-MSC-21327-1] N90-11798

SPACE TRANSPORTATION SYSTEM FLIGHTS

Independent Orbiter Assessment (IOA): Analysis of the active thermal control subsystem
[NASA-CR-185553] N90-11782

SPACE-TIME FUNCTIONS

Scalar fields versus black holes
[DE89-611967] N90-12413

SPACEBORNE EXPERIMENTS

Petite Amateur Navy Satellite (PANSAT)
[NASA-CR-186049] N90-11800

Nonintrusive inertial vibration isolation technology for microgravity space experiments
[NASA-TM-102386] N90-11901

The BATSE experiment on the Gamma Ray Observatory: Solar flare hard x ray and gamma-ray capabilities
N90-12469

SPACEBORNE LASERS

Laser sounding from space: Report of the ESA Technology Working Group on Space Laser Sounding and Ranging
[ESA-SP-1108] N90-12024

SPACECRAFT COMMUNICATION

Design of a solar sail mission to Mars
[NASA-CR-186045] N90-11771

Independent Orbiter Assessment (IOA): Assessment of the communication and tracking subsystem, volume 1
[NASA-CR-185528-VOL-1] N90-11789

Independent Orbiter Assessment (IOA): Assessment of the communication and tracking subsystem, volume 2
[NASA-CR-185528-VOL-2] N90-11790

Independent Orbiter Assessment (IOA): Assessment of the communication and tracking subsystem, volume 3
[NASA-CR-185528-VOL-3] N90-11791

SPACECRAFT COMPONENTS

Independent Orbiter Assessment (IOA): Analysis of the life support and airlock support subsystems
[NASA-CR-185539] N90-11786

Docking system for spacecraft
[NASA-CASE-MSC-21327-1] N90-11798

SPACECRAFT CONSTRUCTION MATERIALS

Axial compression buckling test on the H-2 launch vehicle satellite fairing structural element prototype (aluminum surface plate/aluminum honeycomb sandwiched curved surface plate)
[NAL-TM-563] N90-12039

SPACECRAFT CONTAMINATION

Photolysis of spacecraft contaminants
[AD-A211715] N90-11801

The rodent research animal holding facility as a barrier to environmental contamination
[NASA-TM-102237] N90-12151

SPACECRAFT CONTROL

Independent Orbiter Assessment (IOA): Analysis of the displays and controls subsystem
[NASA-CR-185563] N90-11774

SPACECRAFT DESIGN

Project AENEAS: A feasibility study for crew emergency return vehicle
[PB89-217020] N90-11799

Requirements for multidisciplinary design of aerospace vehicles on high performance computers
[NASA-CR-181915] N90-12183

SPACECRAFT DOCKING

Docking system for spacecraft
[NASA-CASE-MSC-21327-1] N90-11798

SPACECRAFT GUIDANCE

Independent Orbiter Assessment (IOA): Assessment of the guidance, navigation, and control subsystem FMEA/CIL
[NASA-CR-185552] N90-11784

SPACECRAFT INSTRUMENTS

Independent Orbiter Assessment (IOA): Analysis of the displays and controls subsystem
[NASA-CR-185563] N90-11774

The Gamma-Ray Observatory: An overview
N90-12464

SPACECRAFT LAUNCHING

Computation of generalized modal loads in an acoustic field define by a distribution of correlated pressures
[NASA-CR-186041] N90-12047

Final environmental impact statement for the Galileo Mission (Tier 2)
[NASA-TM-101825] N90-12102

SPACECRAFT MANEUVERS

Independent Orbiter Assessment (IOA): Assessment of the reaction control system, volume 1
[NASA-CR-185543-VOL-1] N90-11793

Independent Orbiter Assessment (IOA): Assessment of the reaction control system, volume 2
[NASA-CR-185543-VOL-2] N90-11794

Independent Orbiter Assessment (IOA): Assessment of the reaction control system, volume 3
[NASA-CR-185543-VOL-3] N90-11795

Independent Orbiter Assessment (IOA): Assessment of the reaction control system, volume 4
[NASA-CR-185543-VOL-4] N90-11796

Independent Orbiter Assessment (IOA): Assessment of the reaction control system, volume 5
[NASA-CR-185543-VOL-5] N90-11797

SPACECRAFT POWER SUPPLIES

Independent Orbiter Assessment (IOA): Assessment of the electrical power distribution and control subsystem, volume 1
[NASA-CR-185557-VOL-1] N90-11779

Independent Orbiter Assessment (IOA): Assessment of the electrical power distribution and control subsystem, volume 2
[NASA-CR-185557-VOL-2] N90-11780

Independent Orbiter Assessment (IOA): Assessment of the electrical power distribution and control subsystem, volume 3
[NASA-CR-185557-VOL-3] N90-11781

Independent Orbiter Assessment (IOA): Assessment of the Electrical Power Distribution and Control/Electrical Power Generation (EPD and C/EPG) FMEA/CIL
[NASA-CR-185542] N90-11785

Independent Orbiter Assessment (IOA): Assessment of the reaction control system, volume 1
[NASA-CR-185543-VOL-1] N90-11793

Independent Orbiter Assessment (IOA): Assessment of the reaction control system, volume 2
[NASA-CR-185543-VOL-2] N90-11794

Independent Orbiter Assessment (IOA): Assessment of the reaction control system, volume 3
[NASA-CR-185543-VOL-3] N90-11795

Independent Orbiter Assessment (IOA): Assessment of the reaction control system, volume 4
[NASA-CR-185543-VOL-4] N90-11796

Independent Orbiter Assessment (IOA): Assessment of the reaction control system, volume 5
[NASA-CR-185543-VOL-5] N90-11797

The fuel cell in space: Yesterday, today and tomorrow
[NASA-TM-102366] N90-11804

SPACECRAFT PROPULSION

Independent Orbiter Assessment (IOA): Assessment of the orbiter main propulsion system FMEA/CIL, volume 1
[NASA-CR-185559-VOL-1] N90-11775

Independent Orbiter Assessment (IOA): Assessment of the main propulsion subsystem FMEA/CIL, volume 2
[NASA-CR-185559-VOL-2] N90-11776

Independent Orbiter Assessment (IOA): Assessment of the main propulsion subsystem FMEA/CIL, volume 3
[NASA-CR-18559-VOL-3] N90-11777

Independent Orbiter Assessment (IOA): Assessment of the main propulsion subsystem FMEA/CIL, volume 4
[NASA-CR-185559-VOL-4] N90-11778

Independent Orbiter Assessment (IOA): Assessment of the reaction control system, volume 1
[NASA-CR-185543-VOL-1] N90-11793

Independent Orbiter Assessment (IOA): Assessment of the reaction control system, volume 2
[NASA-CR-185543-VOL-2] N90-11794

Independent Orbiter Assessment (IOA): Assessment of the reaction control system, volume 3
[NASA-CR-185543-VOL-3] N90-11795

Independent Orbiter Assessment (IOA): Assessment of the reaction control system, volume 4
[NASA-CR-185543-VOL-4] N90-11796

Independent Orbiter Assessment (IOA): Assessment of the reaction control system, volume 5
[NASA-CR-185543-VOL-5] N90-11797

SPACECRAFT RADIATORS

Conceptual design of liquid droplet radiator shuttle-attached experiment
[NASA-CR-185164] N90-11805

Conceptual design of liquid droplet radiator shuttle-attached experiment technical requirements document
[NASA-CR-185165] N90-11806

SPACECRAFT RELIABILITY

Independent Orbiter Assessment (IOA): Analysis of the displays and controls subsystem
[NASA-CR-185563] N90-11774

Independent Orbiter Assessment (IOA): Assessment of the orbiter main propulsion system FMEA/CIL, volume 1
[NASA-CR-185559-VOL-1] N90-11775

Independent Orbiter Assessment (IOA): Assessment of the main propulsion subsystem FMEA/CIL, volume 2
[NASA-CR-185559-VOL-2] N90-11776

Independent Orbiter Assessment (IOA): Assessment of the main propulsion subsystem FMEA/CIL, volume 3
[NASA-CR-18559-VOL-3] N90-11777

Independent Orbiter Assessment (IOA): Assessment of the main propulsion subsystem FMEA/CIL, volume 4
[NASA-CR-185559-VOL-4] N90-11778

Independent Orbiter Assessment (IOA): Assessment of the electrical power distribution and control subsystem, volume 1
[NASA-CR-185557-VOL-1] N90-11779

Independent Orbiter Assessment (IOA): Assessment of the electrical power distribution and control subsystem, volume 2
[NASA-CR-185557-VOL-2] N90-11780

Independent Orbiter Assessment (IOA): Assessment of the electrical power distribution and control subsystem, volume 3
[NASA-CR-185557-VOL-3] N90-11781

Independent Orbiter Assessment (IOA): Analysis of the active thermal control subsystem
[NASA-CR-185553] N90-11782

Independent Orbiter Assessment (IOA): FMEA/CIL assessment
[NASA-CR-185550] N90-11783

Independent Orbiter Assessment (IOA): Assessment of the guidance, navigation, and control subsystem FMEA/CIL
[NASA-CR-185552] N90-11784

Independent Orbiter Assessment (IOA): Assessment of the Electrical Power Distribution and Control/Electrical Power Generation (EPD and C/EPG) FMEA/CIL
[NASA-CR-185542] N90-11785

Independent Orbiter Assessment (IOA): Analysis of the life support and airlock support subsystems
[NASA-CR-185539] N90-11786

Independent Orbiter Assessment (IOA): Assessment of the orbital maneuvering system FMEA/CIL, volume 1
[NASA-CR-185544-VOL-1] N90-11787

Independent Orbiter Assessment (IOA): Assessment of the orbital maneuvering subsystem, volume 2
[NASA-CR-185544-VOL-2] N90-11788

Independent Orbiter Assessment (IOA): Assessment of the communication and tracking subsystem, volume 1
[NASA-CR-185528-VOL-1] N90-11789

Independent Orbiter Assessment (IOA): Assessment of the communication and tracking subsystem, volume 2
[NASA-CR-185528-VOL-2] N90-11790

Independent Orbiter Assessment (IOA): Assessment of the communication and tracking subsystem, volume 3
[NASA-CR-185528-VOL-3] N90-11791

Independent Orbiter Assessment (IOA): Assessment of the hydraulics/water spray boiler subsystem
[NASA-CR-185537] N90-11792

Independent Orbiter Assessment (IOA): Assessment of the reaction control system, volume 1
[NASA-CR-185543-VOL-1] N90-11793

Independent Orbiter Assessment (IOA): Assessment of the reaction control system, volume 2
[NASA-CR-185543-VOL-2] N90-11794

Independent Orbiter Assessment (IOA): Assessment of the reaction control system, volume 3
[NASA-CR-185543-VOL-3] N90-11795

Independent Orbiter Assessment (IOA): Assessment of the reaction control system, volume 4
[NASA-CR-185543-VOL-4] N90-11796

Independent Orbiter Assessment (IOA): Assessment of the reaction control system, volume 5
[NASA-CR-185543-VOL-5] N90-11797

SPACECRAFT TRACKING

Independent Orbiter Assessment (IOA): Assessment of the communication and tracking subsystem, volume 1
[NASA-CR-185528-VOL-1] N90-11789

Independent Orbiter Assessment (IOA): Assessment of the communication and tracking subsystem, volume 2
[NASA-CR-185528-VOL-2] N90-11790

Independent Orbiter Assessment (IOA): Assessment of the communication and tracking subsystem, volume 3
[NASA-CR-185528-VOL-3] N90-11791

SPACECREWS

Project AENEAS: A feasibility study for crew emergency return vehicle
[PB89-217020] N90-11799

SPACELAB
Navigation experiment NAVEX: The equipment delay times in the Spacelab mission D1
[DFVLR-MITT-89-10] N90-11728
Spacelab system analysis Marshall Avionics System Testbed (MAST)
[NASA-CR-183804] N90-11802

SPALLATION
Deformation behavior of SiC/2014 Al metal-matrix composite
[AD-A212095] N90-11816

SPARK GAPS
An empirical formula for gas switch breakdown delay
[DE89-017233] N90-11947

SPATIAL DISTRIBUTION
Doppler statistics of ocean velocity variability
[AD-A211687] N90-12148
Visual motion perception
[AD-A210994] N90-12160
Eye movements and spatial pattern vision
[AD-A211650] N90-12169

SPATIAL FILTERING
Temporal and spatial filtering remedies for dispersion in electromagnetic particle codes
[DE89-017534] N90-12337

SPATIAL RESOLUTION
Estimated UV clutter levels at 10-100 meter sensor pixel resolution extrapolated from recent polar bear measurements
[AD-A211357] N90-12125

SPECIFICATIONS
Advanced light source master oscillator
[DE90-000123] N90-11953
CALS (Computer-aided Acquisition and Logistic Support) Test Network information exchange: User's manual
[DE89-016700] N90-12399

SPECTRA
Spectral-domain analysis of finite frequency selective surfaces
[AD-A211669] N90-11932
Fluctuations in transverse energy and multiplicity, energy densities, and neutral pion spectra in nucleus-nucleus collisions at 200 GeV/nucleon
[DE89-017583] N90-12302

SPECTRAL BANDS
Growth and characterization of materials for tunable lasers in the near infrared spectral region
[NASA-CR-185832] N90-12009

SPECTRAL ENERGY DISTRIBUTION
Pacific marine radar sea scatter experimental results
[AD-A211593] N90-11931

SPECTRAL METHODS
Convergence results for pseudospectral approximations of hyperbolic systems by a penalty type boundary treatment
[NASA-CR-181929] N90-12230

SPECTRAL SENSITIVITY
In-situ cure monitoring of composites by fiber-optic molecular sensors
[AD-A211495] N90-11817

SPECTRAL SIGNATURES
Flare model sensitivity of the Balmer spectrum
N90-12477

SPECTROMETERS
Droplet sizing instrumentation used for icing research: Operation, calibration, and accuracy
[NASA-CR-182293] N90-11999
Electron cyclotron emission and absorption experiment on the CASTOR tokamak
[IPPCZ-285] N90-12331

SPECTROSCOPY
Positron annihilation studies of interpenetrating polymer networks
[AD-A212162] N90-11890
The national synchrotron light source and its applications
[DE89-017605] N90-12320

SPECTRUM ANALYSIS
Calculation of transient response from time-harmonic spectrum
[AD-A211972] N90-12241

SPECULAR REFLECTION
Analysis of two-pass Modified Hough Transform (MHT) technique for the detection of wake like signals
[AD-A211982] N90-11924

SPEED CONTROL
Adjustable speed drive study, part 1
[DE89-017654] N90-11948

SPHERES
Parametric study of power absorption from electromagnetic waves by small ferrite spheres
[NASA-TP-2949] N90-12282

SPHERICAL HARMONICS
Processing of DMSP magnetic data and its use in geomagnetic field modeling
[NASA-TM-100750] N90-12115

SPIN DYNAMICS
Spin-orbit relaxation rates of Bi(6p(3)) 2D(3/2) following photolysis of Bi(CH3)3 at lambda = 193 nm
[AD-A211792] N90-12303

SPIN STABILIZATION
Stall/spin/flight simulation
[DOT/FAA/CT-88/28] N90-11765

SPIN-ORBIT INTERACTIONS
Spin-orbit relaxation rates of Bi(6p(3)) 2D(3/2) following photolysis of Bi(CH3)3 at lambda = 193 nm
[AD-A211792] N90-12303

SPLINE FUNCTIONS
Inf-convolution splines
[IMAG-RR-749-M] N90-12256
Splines and equations of nonlinear parameters
[IMAG-RR-750-M] N90-12257

SPREAD SPECTRUM TRANSMISSION
Performance of four rake modems over the non-disturbed wideband HF channel
[AD-A211589] N90-11930

SQUALLS
Disturbances in the Arizona Monsoon N90-12071

STABILITY
On the differentiable manifold of fixed order stable linear systems
[REPT-88-89] N90-12250
Fast sampling and stability of nonlinear sampled-data systems. Part 1: Existence theorems
[RR-340-PT-1] N90-12276
Slow sampling and stability of nonlinear sampled-data systems
[RR-342] N90-12277

STABILITY DERIVATIVES
Stability and control derivatives of the De Havilland DHC-2 BEAVER aircraft
[PB89-217525] N90-11754

STABILITY TESTS
Performance and quality of a wing type parachute: Parametric analysis
[REPT-88-19] N90-11710

STANDARDS
Calibration and de-embedding of microwave measurements using any combination of one- or two-port standards
[PB89-212674] N90-11916
Comparison of I2-stabilized HE-NE lasers
[PB89-218844] N90-12014
WISPER: A standardized fatigue load sequence for HAWT-blades
[NLR-MP-88029-U] N90-12055
Review of the national ambient air quality standards for lead: Exposure analysis methodology and validation
[PB89-207914] N90-12104
CALS (Computer-aided Acquisition and Logistic Support) Test Network information exchange: User's manual
[DE89-016700] N90-12399
Introduction to the Mil-Std-1553B serial multiplex data bus
[RAE-TM-M-9] N90-12405

STAR CLUSTERS
Effects of main-sequence mass loss on the turnoff ages of population 1 clusters
[DE89-016755] N90-12417

STARTING
Studies on the startup transients and performance of a gas loaded sodium heat pipe
[AD-A211880] N90-12379

STATIC TESTS
Static tensile and tensile creep testing of four boron nitride coated ceramic fibers at elevated temperatures
[NASA-CR-184999] N90-11807

STATICS
ASR-9 weather channel test report
[AD-A211749] N90-11934

STATISTICAL ANALYSIS
Infrared backscattering N90-12083
A statistical intercomparison of temperature and precipitation predicted by four general circulation models with historical data
[DE89-017785] N90-12108
Statistical models for the optimal estimation of oceanic fields
[AD-A211786] N90-12149
Visual acuity and stereopsis with night vision goggles
[AD-A211552] N90-12167
Federal funds for research and development: Fiscal years 1986, 1987, and 1988. Volume 36: Detailed statistical tables
[PB89-223523] N90-12407
Federal funds for research and development. Fiscal years 1987, 1988, and 1989. Volume 37: Detailed statistical tables
[PB89-223531] N90-12408
On the analysis of line profile variations: A statistical approach N90-12412

STATISTICAL TESTS
Computer problems in goodness-of-fit
[AD-A211411] N90-12268
On the asymptotic optimality of certain empirical Bayes simultaneous testing procedures
[AD-A211649] N90-12270

STATORS
High gain flux compression generator fabrication issues
[DE89-017888] N90-11951

STEADY FLOW
Steady and unsteady potential flow around thin annular wings and engines with simulation of jet engine flow
[DFVLR-FB-89-18] N90-11711

STEADY STATE
Dynamics of baroclinic wave systems N90-12072
Small sample theory for steady state confidence intervals
[AD-A212097] N90-12242

STEADY STATE CREEP
Three-dimensional viscoelastic bodies in steady state frictional rolling contact with generalization to Knothe rolling
[REPT-89-23] N90-12032

STEAM
Steam cooled rich-burn combustor liner
[NASA-CASE-LEW-13609-1] N90-11824

STEELS
Fe-Ni-Cr alloys for coatings and electroforms
[PB89-195846] N90-11849
Creep and fracture behavior of heat resistant steels in characteristic cases of variable fatigue loading
[ETN-89-94671] N90-11855
Coating galvanized steel
[AD-A211775] N90-11869
An experimental and analytical program to develop crack tip fracture criteria
[AD-A211565] N90-12051

STELLAR EVOLUTION
Particle physics and cosmology using stellar evolution theory
[DE89-017529] N90-12418

STELLAR SPECTRA
On the analysis of line profile variations: A statistical approach N90-12412

STELLARATORS
Stellarator transport theory
[DE89-016371] N90-12328
Theoretical plasma physics
[DE90-000009] N90-12341

STEREOSCOPY
Low-cost three-dimensional stereoscopic display technique for computer-aided design
[DE89-017732] N90-12196
Parallel implementation and evaluation of motion estimation system algorithms on a distributed memory multiprocessor using knowledge based mappings
[NASA-CR-185984] N90-12213
Novel techniques for data decomposition and load balancing for parallel processing of vision systems: Implementation and evaluation using a motion estimation system
[NASA-CR-185991] N90-12214

STOCHASTIC PROCESSES
Seismic wave attenuation and yield determination at regional distances
[AD-A211548] N90-12128
Doppler statistics of ocean velocity variability
[AD-A211687] N90-12148

STOKES THEOREM (VECTOR CALCULUS)
A multidomain spectral collocation method for the Stokes problem
[NASA-CR-181876] N90-12266

STORAGE RINGS (PARTICLE ACCELERATORS)
Advanced light source master oscillator
[DE90-000123] N90-11953
The national synchrotron light source and its applications
[DE89-017605] N90-12320

STORM SUPPRESSION
ASR-9 weather channel test report
[AD-A211749] N90-11934

STRAIN RATE
Deformation behavior of SiC/2014 Al metal-matrix composite
[AD-A212095] N90-11816
Deformation and defects in Laves-phase intermetallic compounds
[DE89-017798] N90-11862
Mechanism for shear band formation in the high strain rate torsion test
[PB89-215370] N90-12038

STRATIGRAPHY
Three ages of Venus N90-12453

STRATOCUMULUS CLOUDS

Stratiform clouds and their interaction with atmospheric motions N90-12060

STRATOSPHERE

Studies of baroclinic instability in the presence of surface topography and stratospheric ozone N90-12068

Use of satellite data and modeling to asses the influence of stratospheric processes on the troposphere N90-12075

STREAK CAMERAS

A microchannel plate intensified, subnanosecond, X-ray imaging camera [DE89-017781] N90-12003

STREAK PHOTOGRAPHY

Air breakdown photography in the picosecond domain [DE89-016775] N90-11830

STRESS (PHYSIOLOGY)

Heatstroke pathophysiology: The energy depletion model [AD-A212156] N90-12164

Microcomputer-based tests for repeated-measures: Metric properties and predictive validities [NASA-CR-185517] N90-12174

A menu of self-administered microcomputer-based neurotoxicology tests [NASA-CR-185518] N90-12175

STRESS ANALYSIS

Mechanism for shear band formation in the high strain rate torsion test [PB89-215370] N90-12038

STRESS CONCENTRATION

Interlaminar stress concentration in fiber composites [ETN-89-94670] N90-11809

Autofrettage-stress distribution under load and retained stresses after depressurization [AD-A212090] N90-12048

STRESS DISTRIBUTION

Autofrettage-stress distribution under load and retained stresses after depressurization [AD-A212090] N90-12048

Stress distribution and topography of Tellus Regio, Venus N90-12452

STRESS RELIEVING

Steam cooled rich-burn combustor liner [NASA-CASE-LEW-13609-1] N90-11824

STRING THEORY

Operator product coefficients in non-diagonal conformal field theories [PB89-216873] N90-12283

Bordered surfaces, off-shell amplitudes, sewing, and string field theory [DE90-000006] N90-12378

Cosmic strings and ultra-high energy cosmic rays [NASA-CR-185924] N90-12492

STRIP TRANSMISSION LINES

Dielectric covered microstrip patch antennas [AD-A211577] N90-11963

STRONGLY COUPLED PLASMAS

Properties of strongly coupled multi-ionic plasmas [DE89-017782] N90-12339

STRUCTURAL ANALYSIS

Fractographic and microstructural analysis of fatigue crack growth in a Ti-6Al-4V fan disc forging [NLR-MP-88028-U] N90-11877

Flexure strength of advanced ceramics: A round robin exercise [AD-A212101] N90-11889

Wind/seismic comparisons for upgrading existing structures [DE89-016055] N90-12044

Numerical solution of acoustic-structure interaction problems [AD-A211505] N90-12293

STRUCTURAL DESIGN

The fuel cell in space: Yesterday, today and tomorrow [NASA-TM-102366] N90-11804

Application of process integration to utilities, combined heat and power, and heat pumps [ESDU-89001] N90-11909

STRUCTURAL ENGINEERING

The use of Lanczos's method to solve the large generalized symmetric definite eigenvalue problem [NASA-CR-181914] N90-12193

Designing and designing knowledge in engineering and architecture [PB89-219521] N90-12383

STRUCTURAL PROPERTIES (GEOLOGY)

Coronae on Venus observations and models of origin N90-12449

STRUCTURAL STABILITY

Wind/seismic comparisons for upgrading existing structures [DE89-016055] N90-12044

STRUCTURAL VIBRATION

Problems related to the acquisition, processing and utilization of the modal parameters measured in flight tests in order to obtain the full envelope for flutter [ETN-89-95210] N90-11735

Investigation of difficult component effects on finite element model vibration prediction for the Bell AH-1G helicopter. Volume 1: Ground vibration test results [NASA-CR-181916-VOL-1] N90-12058

STUDENTS

AFRAPT (Air Force Research in Aero Propulsion Technology) Trainee Program [AD-A211540] N90-11744

Computer generation of a tutorial dialogue [AD-A211976] N90-12162

SUBLIMATION

Human body regional convective heat transfer determination using sublimating naphthalene disks [AD-A212170] N90-12165

SUBSONIC FLOW

Computation of ramjet internal flowfields [AD-A212001] N90-11743

SUBSONIC WIND TUNNELS

The aerodynamic experimental center of Aeritalia: Combat aircraft group [ETN-89-95213] N90-11766

SUBSTRATES

Method of modifying the dielectric properties of an organic polymer film [AD-D014171] N90-11879

A SAW Slanted Array Correlator (SAC) with separate amplitude compensation channel [AD-D014174] N90-11914

Infrared detector array [AD-D014170] N90-11997

SULFURIC ACID

Venus volcanism: Rate estimates from laboratory studies of sulfur gas-solid reactions N90-12428

SUN

Investigation of active regions at high resolution by balloon flights of the Solar Optical Universal Polarimeter (SOUP) N90-12487

SUNSPOT CYCLE

The onset of the solar active cycle 22 N90-12488

SUNSPOTS

The onset of the solar active cycle 22 N90-12488

SUPERCONDUCTING FILMS

Effect of annealing conditions on the structural and superconducting properties of Y-Ba-Cu-O films [AD-A211308] N90-12371

SUPERCONDUCTING MAGNETS

The characterization of Nb3Sn superconductors for use in magnets of 19 T and greater [DE89-017758] N90-12364

SUPERCONDUCTING SUPER COLLIDER

Thermal conduction of SSC (Superconducting Super Collider) wire [DE89-016710] N90-11811

SUPERCONDUCTIVITY

Thermal conduction of SSC (Superconducting Super Collider) wire [DE89-016710] N90-11811

Characterization of the Structure and Chemistry of Defects in Materials: Proceedings, volume 138 [DE89-014796] N90-12352

Superconductivity and magnetic scattering in the Nd(sub 2-x)Ce(sub x)CuO(sub 4-delta) [DE89-016524] N90-12354

Structure-property relationships as an aid in the rational design of (beta)-(ET)(sub 2)X organic superconductors [DE89-016912] N90-12356

Anomalous ion-channeling behavior across the superconducting transition in high-T(sub c) materials [DE89-017677] N90-12360

High temperature superconducting compounds [AD-A211511] N90-12374

SUPERCONDUCTORS

Quantitative interpretation of auger lineshapes and electron/photon stimulated desorption [AD-A211550] N90-11842

Process for single crystal growth of high T(sub c) superconductors [AD-D014167] N90-12346

Structure-property relationships as an aid in the rational design of (beta)-(ET)(sub 2)X organic superconductors [DE89-016912] N90-12356

Electron-positron momentum distribution measurements of high-T(sub c) superconductors and related systems [DE89-017538] N90-12358

The characterization of Nb3Sn superconductors for use in magnets of 19 T and greater [DE89-017758] N90-12364

SUPERFLUIDITY

Internal Magnus effects in superfluid 3He-A [PB89-212617] N90-12351

Flare-in texture in rotating superfluid (3)He-B [PB89-218994] N90-12368

Resonant quasiparticle-ion scattering in anisotropic superfluid (3)He [PB89-221618] N90-12369

Collective-mode spectroscopy of textures in superfluid (3)He-B [PB89-221634] N90-12370

SUPERGRAVITY

Two dimensional conformal supergravity and critical behavior [DE89-611968] N90-12414

SUPERHIGH FREQUENCIES

Geology of Southern Guinevere Planitia, Venus, based on analyses of Goldstone radar data N90-12424

SUPERLATTICES

Short period multilayers: Interface dominated structures [DE89-017536] N90-11812

SUPERPLASTICITY

Deformation of Ti-6Al-4V bar and extrusion under superplastic forming conditions [RAE-TM-MAT/STR-1110] N90-11875

Deformation of extruded titanium alloys under superplastic conditions [RAE-TM-MAT/STR-1111] N90-11876

Deformation of electron beam welded Ti-6Al-4V alloy sheet under superplastic conditions [RAE-TM-MAT/STR-1109] N90-12053

Effect of superplastic deformation on the surface roughness of sheet [RAE-TM-MAT/STR-1112] N90-12054

SUPERSONIC COMBUSTION

Computation of ramjet internal flowfields [AD-A212001] N90-11743

SUPERSONIC COMBUSTION RAMJET ENGINES

Computation of ramjet internal flowfields [AD-A212001] N90-11743

SUPERSYMMETRY

Two dimensional conformal supergravity and critical behavior [DE89-611968] N90-12414

SURFACE ACOUSTIC WAVE DEVICES

A SAW Slanted Array Correlator (SAC) with separate amplitude compensation channel [AD-D014174] N90-11914

SURFACE FINISHING

Formation and modification of surface alloys by excimer laser melting and resolidification [DE89-016968] N90-11856

Coating galvanized steel [AD-A211775] N90-11869

SURFACE NAVIGATION

Effects of the advanced map interpretation and terrain analysis course on contour-level navigation performance [AD-A212163] N90-11723

Distance and clearance perception using forward-looking, vehicular television systems [DE89-014740] N90-12319

SURFACE PROPERTIES

Formation and modification of surface alloys by excimer laser melting and resolidification [DE89-016968] N90-11856

Spectral-domain analysis of finite frequency selective surfaces [AD-A211669] N90-11932

RF performance of polycrystalline high-T(sub c) superconductors [DE89-017671] N90-12359

Surface, interface, and bulk properties of high T(sub c) superconductors [AD-A211490] N90-12373

Venus surface properties deduced from radar and radiometry N90-12431

SURFACE REACTIONS

Self-assembled organic monolayer films [AD-A212006] N90-11838

Synaptic plasticity and memory formation [AD-A211368] N90-12158

SURFACE ROUGHNESS

An experimental study of surface roughness effects on turbulent boundary layer flow and heat transfer [AD-A212099] N90-11980

Effect of superplastic deformation on the surface roughness of sheet [RAE-TM-MAT/STR-1112] N90-12054

SURFACE ROUGHNESS EFFECTS

An experimental study of surface roughness effects on turbulent boundary layer flow and heat transfer [AD-A212099] N90-11980

SURFACE TEMPERATURE

Crau 1987: The KNMI contribution --- KNMI (Royal Netherlands Meteorological Institute) [KNMI-TR-110] N90-12140

Description of a software library for the calculation of surface fluxes
[KNMI-TR-112] N90-12141

SURFACE VEHICLES
Vision-based navigation for autonomous ground vehicles
[AD-A211584] N90-11725

SURFACE WAVES
Investigations of Eurasian seismic sources and upper mantle structure
[AD-A211806] N90-12120
Seismic wave attenuation and yield determination at regional distances
[AD-A211548] N90-12128
Similarity relations of wind waves in finite depth
[PB89-198113] N90-12144

SURGES
Lightning and surge protection of photovoltaic installations: Two case histories, Vulcano and Kythnos
[PB89-229058] N90-12135
Studies on the startup transients and performance of a gas loaded sodium heat pipe
[AD-A211880] N90-12379

SURVEILLANCE
Rotorcraft low altitude CNS benefit/cost analysis: Rotorcraft operations data
[DOT/FAA/DS-89/9] N90-12406

SURVEILLANCE RADAR
ASR-9 weather channel test report
[AD-A211749] N90-11934

SURVEYS
Ice runways near the South Pole
[AD-A211606] N90-11908

SUSPENDING (HANGING)
Equilibrium solutions of a spherical pendulum with rotating point of suspension and friction
[ESA-TT-1139] N90-12288

SWIRLING
Calculation on film preparation and film motion of a swirl atomizer
[ESA-TT-1096] N90-11990

SWITCHES
An empirical formula for gas switch breakdown delay
[DE89-017233] N90-11947
Superconducting switch program
[AD-A211580] N90-11964

SWITCHING
Switched power workshop: Introduction and summary
[DE90-000036] N90-11952

SWITCHING CIRCUITS
Power up modification for video switcher microprocessor interface for sensor system processing system
[AD-A211543] N90-11962
Subnanosecond linear GaAs photoconductive switching, revision 1
[DE89-017739] N90-12363

SYNAPSES
Synaptic plasticity and memory formation
[AD-A211368] N90-12158

SYNCHRONISM
Studies on predicting the resynchronization of the circadian system after transmedian flights
[DFVLR-FB-89-10] N90-12172
Sequential searching in multidimensional monotone arrays
[AD-A211938] N90-12188

SYNCHROTRON RADIATION
The behavior of beams of relativistic non-thermal electrons under the influence of collisions and synchrotron losses
[NASA-CR-185983] N90-12298
Synchrotron-radiation experiments with recoil ions
[DE89-017579] N90-12301
The national synchrotron light source and its applications
[DE89-017605] N90-12320

SYNOPTIC METEOROLOGY
Synoptic/planetary-scale interactions and blocking over the North Atlantic Ocean N90-12061
Tropical Pacific moisture variability N90-12070
The effect of latent heat release on synoptic-to-planetary wave interactions and its implication for satellite observations: Theoretical modeling N90-12073

SYNTAX
Computer generation of a tutorial dialogue
[AD-A211976] N90-12162
Taxonomic syntax for first order inference
[AD-A211618] N90-12221
DOD Gateway Information System (DGIS) common command language: A retrospective on the introduction of prolog as the development tool
[AD-A211941] N90-12400

SYNTHESIS (CHEMISTRY)
Synthesis and chemistry of strained and conjugated fluorocarbons
[AD-A211633] N90-11844
Suppression of side chain crystallization and transformation of monotropic mesophases into enantiotropic mesophases by copolymerization of the parent polymers' monomer pairs containing constitutional isomeric mesogenic side groups
[AD-A209066] N90-11878
Boron analogues of amino acids and derivatives
[AD-A211311] N90-12157
Structure-property relationships as an aid in the rational design of (beta)-(ET)(sub 2)X organic superconductors
[DE89-016912] N90-12356
Synthesis and microstructure of highly oriented PbTiO3 thin films prepared by a sol-gel method
[AD-A211735] N90-12377

SYSTEM EFFECTIVENESS
Transport systems research vehicle color display system operations manual
[NASA-TM-101577] N90-11736

SYSTEM FAILURES
Independent Orbiter Assessment (IOA): Analysis of the life support and airlock support subsystems
[NASA-CR-185539] N90-11786

SYSTEM GENERATED ELECTROMAGNETIC PULSES
A beam induced upset during the flight of the ECHO-7 rocket
[NASA-CR-186089] N90-11755

SYSTEM IDENTIFICATION
Adaptive noise cancellation for a class of nonlinear 2R filter
[RR-351] N90-11965
Orthogonal least squares methods and their application to nonlinear system identification
[RR-343] N90-12259
Fuzzy logic and the generalized modus ponens
[REPT-88-92] N90-12274

SYSTEMS ANALYSIS
Spacelab system analysis Marshall Avionics System Testbed (MAST)
[NASA-CR-183804] N90-11802
On the complexity analysis of the coriolis and centripetal effects of a 6 DOF robot manipulator --- Degrees of Freedom (DOF)
[RR-344] N90-12030

SYSTEMS ENGINEERING
A design methodology for self-tuning control of systems with inherent conflicts
[PB89-219505] N90-11960
Requirements for multidisciplinary design of aerospace vehicles on high performance computers
[NASA-CR-181915] N90-12183
DOD Gateway Information System (DGIS) common command language: A retrospective on the introduction of prolog as the development tool
[AD-A211941] N90-12400

SYSTEMS INTEGRATION
Parallel architectures and parallel algorithms for integrated vision systems
[NASA-CR-185990] N90-12215

SYSTEMS STABILITY
Can perceptrons find Lyapunov functions: An algorithmic approach to systems stability
[RR-365] N90-12224

T

TABLES (DATA)
Federal funds for research and development: Fiscal years 1986, 1987, and 1988. Volume 36: Detailed statistical tables
[PB89-223523] N90-12407
Federal funds for research and development. Fiscal years 1987, 1988, and 1989. Volume 37: Detailed statistical tables
[PB89-223531] N90-12408

TAKEOFF
The 1987 survey of track keeping and altitudes on Heathrow and Gatwick standard instrument departure routes (DAY)
[CAA-PAPER-88010] N90-11729

TANKS (CONTAINERS)
On the computation of normal modes of a rotating, viscous, incompressible fluid with a capillary free boundary
[REPT-89-01] N90-11989

TARGET DRONE AIRCRAFT
Pilotless airplanes
[AD-A211719] N90-11734

TARGETS
Visual acuity and stereopsis with night vision goggles
[AD-A211552] N90-12167

TATB
Pulsed-laser-excited Raman spectra of shock compressed triaminotrinitrobenzene
[DE90-000668] N90-12019

TAXONOMY
Taxonomic syntax for first order inference
[AD-A211618] N90-12221

TECHNOLOGICAL FORECASTING
Future military powerplants --- fighter aircraft engines
[PNR90554] N90-11749

TECHNOLOGY ASSESSMENT
An assessment of technology for self-powered gas appliances: A GATC (Gas Appliance Technology Center)
[PB89-219265] N90-12026

TECHNOLOGY TRANSFER
Adoption of software engineering innovations in organizations
[AD-A211573] N90-12206
Development and use of a tribology research-in-progress database
[PB89-228274] N90-12396

TECTONICS
Tessera terrain: Characteristics and models of origin N90-12426
Tectonism on Venus: A review N90-12440
Venus: Mantle convection, hotspots, and tectonics N90-12442
Lakshmi Planum: A distinctive highland volcanic province N90-12444
Crustal deformation: Earth vs Venus N90-12450
Eastern Ishtar Terra: Tectonic evolution derived from recognized features N90-12451

TELECOMMUNICATION
World Weather Watch: Implementation
[WMO-714] N90-12139
The J-Machine: A fine grain concurrent computer
[AD-A211909] N90-12187

TELEMETRY
Type-specific dynamic measurements on wind turbines at the test site Schnittlingen (Germany, F.R.)
[DFVLR-MITT-88-31] N90-12099

TELEOPERATORS
Distance and clearance perception using forward-looking, vehicular television systems
[DE89-014740] N90-12319

TELEPHONY
Feasibility of graphics voice telephones for the post 2000 era
[FEL-1988-26] N90-11937

TELESCOPES
An imaging vector magnetograph for the next solar maximum N90-12489

TELEVISION CAMERAS
Distance and clearance perception using forward-looking, vehicular television systems
[DE89-014740] N90-12319

TELEVISION SYSTEMS
Television systems with enhanced image quality for new broadband channels
[ETN-89-94622] N90-11936
Distance and clearance perception using forward-looking, vehicular television systems
[DE89-014740] N90-12319

TEMPERATURE CONTROL
Design of a solar sail mission to Mars
[NASA-CR-186045] N90-11771
Independent Orbiter Assessment (IOA): Analysis of the active thermal control subsystem
[NASA-CR-185553] N90-11782
Modelling and control of a diffusion/LPCVD furnace
[REPT-88-97] N90-11910

TEMPERATURE DEPENDENCE
Temperature dependent effects during Ag deposition on Cu(110)
[DE89-016987] N90-11857

TEMPERATURE DISTRIBUTION
Cryogenic free jets
[ESA-TT-1128] N90-11767

TEMPERATURE EFFECTS
Effects of a heat cycle on material strength
[NAL-TM-562] N90-11737
Carbon fiber reinforced glass matrix composites for structural space based applications
[AD-A211682] N90-11818
Phase behavior of pure and mixed systems at high pressure
[DE89-017734] N90-11832
Elevated temperature aluminum-titanium alloy by powder metallurgy process
[AD-D014165] N90-11852
The effects of temperature on fatigue crack propagation in 310 austenitic stainless steel
[DE90-000136] N90-11865
New mechanism for toughening ceramic materials
[AD-A211651] N90-11892
Sensitivity relationships in energetic materials
[DE89-016967] N90-11897
Davydov solutions at 300 Kelvin: The final search
[DE89-015248] N90-12296

Lifetime of singlet oxygen in aqueous hydrogen peroxide (BHP)
[AD-A211545] N90-12306
The characterization of Nb3Sn superconductors for use in magnets of 19 T and greater
[DE89-017758] N90-12364
Effect of annealing conditions on the structural and superconducting properties of Y-Ba-Cu-O films
[AD-A211308] N90-12371

TEMPERATURE GRADIENTS
Fast and objective MRTD measurement
[FEL-1988-24] N90-12006

TEMPERATURE MEASUREMENT
Infrared temperature measurement with automatic consideration of emissivity
[ESA-TT-1131] N90-12008
Center for Electronics and Electrical Engineering technical publication announcements covering Center programs, January-March 1989 with 1989 CEEE events calendar
[PB89-228308] N90-12402

TEMPERATURE PROFILES
Disturbances in the Arizona Monsoon N90-12071

TEMPORAL DISTRIBUTION
A study of the temporal stability of multiple cell vortices
[NASA-CR-4261] N90-11968
Time-weighted accumulations ap(tau) and Kp(tau)
[RAE-TR-88050] N90-12422

TENSILE CREEP
Static tensile and tensile creep testing of four boron nitride coated ceramic fibers at elevated temperatures
[NASA-CR-184999] N90-11807

TENSILE STRENGTH
Effects of a heat cycle on material strength
[NAL-TM-562] N90-11737

TENSILE TESTS
Static tensile and tensile creep testing of four boron nitride coated ceramic fibers at elevated temperatures
[NASA-CR-184999] N90-11807

TEREPHTHALATE
A model for long-term creep and the effects of physical ageing in poly (butylene terephthalate)
[NPL-DMA(A)-182] N90-11895

TERNARY SYSTEMS
Process for single crystal growth of high T(sub c) superconductors
[AD-D014167] N90-12346

TERRADYNAMICS
Clotho Tessera, Venus: A fragment of Fortuna Tessera N90-12439

TERRAIN
Tessera terrain: Characteristics and models of origin
N90-12426
Radar scattering from desert terrains, Pisgah/Lavic Region, California: Implications for Magellan
N90-12443

TERRAIN ANALYSIS
Effects of the advanced map interpretation and terrain analysis course on contour-level navigation performance
[AD-A212163] N90-11723

TEST FACILITIES
Spacelab system analysis Marshall Avionics System Testbed (MAST)
[NASA-CR-183804] N90-11802

TEXTURES
Collective-mode spectroscopy of textures in superfluid (3)He-B
[PB89-221634] N90-12370

THEMATIC MAPPERS (LANDSAT)
Investigation of the usefulness of LANDSAT 5 thematic mapper data for mapping forest disease
[DFVLR-FB-89-06] N90-12088
Signature analysis and classification of pine of different vitality classes using airborne thematic mapper data
[DFVLR-FB-89-07] N90-12089

THEMATIC MAPPING
Investigation of the usefulness of LANDSAT 5 thematic mapper data for mapping forest disease
[DFVLR-FB-89-06] N90-12088
Signature analysis and classification of pine of different vitality classes using airborne thematic mapper data
[DFVLR-FB-89-07] N90-12089

THEOREM PROVING
A dynamic proof of the Frobenius-Perron theorem for Metzler matrices
[AD-A211839] N90-12235
Smooth linearization of hyperbolic fixed points without resonance conditions
[REPT-89-03] N90-12251
Generalizations of Laguerre polynomials
[REPT-89-25] N90-12263

THEOREMS
An approximate max-flow min-cut theorem for uniform multicommodity flow problems with applications to approximation algorithms
[AD-A211908] N90-12198
Taxonomic syntax for first order inference
[AD-A211618] N90-12221
The realization of input-output maps using bialgebras
[NASA-CR-185362] N90-12228

THEORETICAL PHYSICS
Theoretical plasma physics
[DE90-000009] N90-12341

THERMAL ANALYSIS
Prediction of the thermal environment and thermal response of simple panels exposed to radiant heat
[NASA-TM-101660] N90-12292

THERMAL CONDUCTIVITY
Program for high speed computation of physical properties of propellants and combustion gas of an LH2/LOX rocket engine
[NAL-TM-564] N90-11803
Thermal conduction of SSC (Superconducting Super Collider) wire
[DE89-016710] N90-11811
RF performance of polycrystalline high-T(sub c) superconductors
[DE89-017671] N90-12359
Development and evaluation of an instrument for rapid electroreflectance of semiconductor materials
[AD-A211690] N90-12376

THERMAL DECOMPOSITION
Flammability, smoke, and dry arc tracking tests of aircraft electrical wire insulations
[DOT/FAA/CT-89/21] N90-11714

THERMAL DEGRADATION
Aging of CFRP due to longterm storage in heated air
[ESA-TT-1124] N90-11893

THERMAL DIFFUSION
Some new algorithms for boundary value problems in smooth particle hydrodynamics
[AD-A211728] N90-11987

THERMAL EMISSION
Electron cyclotron emission and absorption experiment on the CASTOR tokamak
[IPPCZ-285] N90-12331

THERMAL ENERGY
High resolution X-ray spectroscopy using germanium microcalorimeters
[DE89-017784] N90-12004
Analysis of the efficiency of a dielectric solar energy collector
[PB89-212716] N90-12092

THERMAL ENVIRONMENTS
Acoustic-thermal environment for USB flap structure. Report 1: Ground simulation test results
[NAL-TM-567] N90-11697

THERMAL FATIGUE
Acoustic-thermal environment for USB flap structure. Report 1: Ground simulation test results
[NAL-TM-567] N90-11697

THERMAL MAPPING
Fast and objective MRTD measurement
[FEL-1988-24] N90-12006

THERMAL RESISTANCE
Creep strength of niobium alloys, Nb-1%Zr and PWC-11
[NASA-TM-102390] N90-11854

THERMAL SIMULATION
Acoustic-thermal environment for USB flap structure. Report 1: Ground simulation test results
[NAL-TM-567] N90-11697

THERMAL STABILITY
Sensitivity relationships in energetic materials
[DE89-016967] N90-11897

THERMAL STRESSES
Effects of a heat cycle on material strength
[NAL-TM-562] N90-11737

THERMOCHEMISTRY
Molecular dynamics study of the primitive model of 1-3 electrolyte studies
[AD-A211653] N90-11846
Positron annihilation studies of interpenetrating polymer networks
[AD-A212162] N90-11890

THERMODYNAMIC PROPERTIES
Analysis of opposed jet hydrogen-air counter flow diffusion flame
[NASA-CR-182366] N90-11825
Application of process integration to utilities, combined heat and power, and heat pumps
[ESDU-89001] N90-11909
Thermal model for double-drift IMPATT diodes on diamond heat sinks
[AD-A211746] N90-12380
A critical assessment of thermodynamic and phase diagram data for the Ga-In system
[NPL-DMA(A)-174] N90-12382
Flare model sensitivity of the Balmer spectrum
N90-12477

THERMODYNAMICS
An open-loop transient thermodynamic model of the Cougar turbojet
[AD-A211774] N90-11745
Fuel cells for vehicle propulsion applications: A thermodynamic systems analysis
[DE89-017689] N90-11950
Thermomechanical contact phenomena and wear of sliding components
[AD-A211290] N90-12028
Studies on the startup transients and performance of a gas loaded sodium heat pipe
[AD-A211880] N90-12379
An introduction to effectiveness: NTU relationships
[ESDU-89016] N90-12381

THERMOELECTRIC COOLING
Design and calibration of an electrodynamic driver for the Space Thermoacoustic Refrigerator (STAR)
[AD-A212022] N90-11906

THERMOGRAPHY
NDE (Non-Destructive Evaluation) publications, 1985
[PB89-229025] N90-12036

THERMOGRAVIMETRY
Structure/reactivity relationships of polysilazane preceramics
[AD-A212028] N90-11888

THERMOHYDRAULICS
Doubly-fluted tubes and enhanced tubes in confined crossflow
[PB89-217921] N90-11971

THERMONUCLEAR REACTIONS
Highlights of papers presented at the workshop on Cold Fusion Phenomena
[DE89-016956] N90-12334

THERMOPHYSICAL PROPERTIES
Mechanism for shear band formation in the high strain rate torsion test
[PB89-215370] N90-12038

THERMOSPHERE
Retrieval of atomic oxygen and temperature in the thermosphere. Part 2: Feasibility of an experiment based on limb emission in the OI lines
[AD-A211807] N90-12121
Spatial characteristics of airglow and solar scatter radiance from the earth's atmosphere
[AD-A211358] N90-12126

THIN FILMS
Reactive ion etching of sputtered silicon carbide and tungsten thin films for device applications
[AD-A211711] N90-11847
Temperature dependent effects during Ag deposition on Cu(110)
[DE89-016987] N90-11857
Method of modifying the dielectric properties of an organic polymer film
[AD-D014171] N90-11879
Plasma-deposited amorphous hydrogenated carbon films and their tribological properties
[NASA-TM-102379] N90-11880
Vanadium dioxide protective devices
[AD-A212018] N90-11887
Microwave signal detection using modulation of polymeric optical waveguides
[DE89-017545] N90-11921
Assessment of thin film batteries based on polymer electrolytes. Part 1: Energy density
[AD-A212111] N90-11958
Analysis of loss mechanisms in polycrystalline thin-film solar cells
[DE89-009454] N90-12093
Thin film magnetic memory elements
[AD-D014178] N90-12281
Characterizations of electrical properties of highT(sub c) superconducting materials
[NASA-TM-100380] N90-12345
Field-assisted bonding of single crystal quartz
[DE89-015407] N90-12353
Ion beam deposition of epitaxial germanium and gallium arsenide layers
[DE89-017439] N90-12357
Synthesis and microstructure of highly oriented PbTiO3 thin films prepared by a sol-gel method
[AD-A211735] N90-12377

THIN PLATES
Natural frequencies of singly-curved laminated plates with simply-supported edges
[ESDU-89011] N90-12052

THIN WALLS
Mechanism for shear band formation in the high strain rate torsion test
[PB89-215370] N90-12038

THREAT EVALUATION

UK airmisses involving commercial air transport, May-August 1988
[ISSN-0951-6301] N90-11717

THREE DIMENSIONAL BODIES

Three-dimensional viscoelastic bodies in steady state frictional rolling contact with generalization to Knothe rolling
[REPT-89-23] N90-12032

THREE DIMENSIONAL FLOW

Three component laser Doppler measurements in an axisymmetric jet
[NASA-CR-181908] N90-11702

Simulation of glancing shock wave and boundary layer interaction
[NASA-TM-102233] N90-11970

Near-wall, three-dimensional turbulence measurements: A challenge for laser velocimetry
[NASA-TM-102252] N90-11978

Three-dimensional, two-phase, transonic, canted nozzle flows
[AD-A211528] N90-11984

THREE DIMENSIONAL MODELS

Analytical studies of three-dimensional combustion processes
[AD-A211903] N90-11837

THREE DIMENSIONAL MOTION

A Conference on Three-Dimensional Representation held in University of Minnesota on 24-26 May 1989
[AD-A211630] N90-12324

THRUST MEASUREMENT

Measurement effects on the calculation of in-flight thrust for an F404 turbofan engine
[NASA-TM-4140] N90-11741

TILT ROTOR AIRCRAFT

Application of the wide-field shadowgraph technique to rotor wake visualization
[NASA-TM-102222] N90-11700

TILTING ROTORS

Application of the wide-field shadowgraph technique to rotor wake visualization
[NASA-TM-102222] N90-11700

TIMBER INVENTORY

Investigation of the usefulness of LANDSAT 5 thematic mapper data for mapping forest disease
[DFVLR-FB-89-06] N90-12088

TIMBER VIGOR

Signature analysis and classification of pine of different vitality classes using airborne thematic mapper data
[DFVLR-FB-89-07] N90-12089

TIME DEPENDENCE

Development of a numerical solution to the time dependent kinetic equation N90-12481

TIME DIVISION MULTIPLE ACCESS

Satellite-matrix-switched, time-division-multiple-access network simulator
[NASA-TP-2944] N90-11915

TIME FUNCTIONS

Time-weighted accumulations ap(tau) and Kp(tau)
[RAE-TR-88050] N90-12422

TIME MEASUREMENT

Time and frequency in geodesy measuring methods
[SER-C-337] N90-12087

TIME OPTIMAL CONTROL

Sequential design of experiments with physically based models 23
[AD-A211918] N90-12239

TIME SERIES ANALYSIS

Fast sampling and stability of nonlinear sampled data systems. Part 2: Sampling rate estimations
[RR-341] N90-12271

Modeling and analysis of nonlinear time series
[RR-355] N90-12272

On the analysis of line profile variations: A statistical approach N90-12412

TIME TEMPERATURE PARAMETER

Aging of CFRP due to longterm storage in heated air
[ESA-TT-1124] N90-11893

TIN COMPOUNDS

The characterization of Nb3Sn superconductors for use in magnets of 19 T and greater
[DE89-017756] N90-12364

TISSUES (BIOLOGY)

Membrane fusion: The role of polyphosphatidylinositol
[AD-A211269] N90-12156

Investigation of resonant ac-dc magnetic field effects
[AD-A211612] N90-12159

TITANIUM ALLOYS

Elevated temperature aluminum-titanium alloy by powder metallurgy process
[AD-D014165] N90-11852

Deformation of Ti-6Al-4V bar and extrusion under superplastic forming conditions
[RAE-TM-MAT/STR-1110] N90-11875

Deformation of extruded titanium alloys under superplastic conditions
[RAE-TM-MAT/STR-1111] N90-11876

Deformation of electron beam welded Ti-6Al-4V alloy sheet under superplastic conditions
[RAE-TM-MAT/STR-1109] N90-12053

TOKAMAK DEVICES

Electron cyclotron emission and absorption experiment on the CASTOR tokamak
[IPPCZ-285] N90-12331

Control of plasma position in the CASTOR tokamak
[IPPCZ-284] N90-12332

Microwave Tokamak Experiment (MTX) ohmic heating system
[DE89-017692] N90-12340

TOLLMIEN-SCHLICHTING WAVES

Near-planar TS waves and longitudinal vortices in channel flow: Nonlinear interaction and focusing
[NASA-CR-181928] N90-11698

TOPOGRAPHY

Geology of Southern Guinevere Planitia, Venus, based on analyses of Goldstone radar data N90-12424

Contrasting landform perception with varied radar illumination geometries and at simulated resolutions of Venera and Magellan N90-12430

Stress distribution and topography of Tellus Regio, Venus N90-12452

TORQUE

Magnetostrictive torque sensor
[AD-D014169] N90-11996

TORSION

Deformation behavior of SiC/2014 Al metal-matrix composite
[AD-A212095] N90-11816

TORSIONAL STRESS

Mechanism for shear band formation in the high strain rate torsion test
[PB89-215370] N90-12038

TOUCH

Three dimensional object recognition employing combined visual and tactile sensing
[PB89-219489] N90-12176

TOUGHNESS

Deformation behavior of SiC/2014 Al metal-matrix composite
[AD-A212095] N90-11816

TOXIC HAZARDS

Aircraft cabin fire suppression by means of an interior water spray system
[CAA-PAPER-88014] N90-11719

TOXICOLOGY

Microcomputer-based tests for repeated-measures: Metric properties and predictive validities
[NASA-CR-185517] N90-12174

A menu of self-administered microcomputer-based neurotoxicology tests
[NASA-CR-185518] N90-12175

TRACE CONTAMINANTS

Evaluation and sensitivity analyses results of the MESOPUFF 2 model with CAPTEX (Cross-Appalachian Tracer Experiment) measurements
[PB89-198253] N90-12103

TRACKING (POSITION)

The 1987 survey of track keeping and altitudes on Heathrow and Gatwick standard instrument departure routes (DAY)
[CAA-PAPER-88010] N90-11729

TRACKING STATIONS

Navigation experiment NAVEX: Data storage and processing
[DFVLR-MITT-89-09] N90-11727

TRAJECTORIES

A polynomial method of approximate weighted centers for linear programming
[REPT-89-13] N90-12210

TRAJECTORY ANALYSIS

Design of a solar sail mission to Mars
[NASA-CR-186045] N90-11771

A polynomial method of approximate weighted centers for linear programming
[REPT-89-13] N90-12210

TRAJECTORY OPTIMIZATION

An optimum trajectory planner for robot manipulators in joint-space and under physical constraints
[RR-349] N90-12029

TRANSATMOSPHERIC VEHICLES

Wave combustors for trans-atmospheric vehicles
[NASA-TM-102238] N90-11742

TRANSFER FUNCTIONS

A new approach to HF (High Frequency) channel modeling and simulation. Part 1: Deterministic model
[PB89-203962] N90-11913

TRANSFORMERS

Development of high frequency spice models for ferrite core inductors and transformers
[DE89-015121] N90-11946

TRANSIENT RESPONSE

Active control of the forced and transient response of a finite beam N90-12040

Calculation of transient response from time-harmonic spectrum
[AD-A211972] N90-12241

TRANSITION METALS

In-situ spectroscopic studies of transition metal macrocycles as catalysts for the electrochemical reduction of oxygen
[PB89-219273] N90-11826

Electronic structure of transition metal alloys and intermetallics: Charge transfer and its implications for Moessbauer effect measurements
[DE89-017603] N90-11860

TRANSITION TEMPERATURE

New mechanism for toughening ceramic materials
[AD-A211651] N90-11892

Anomalous ion-channeling behavior across the superconducting transition in high-T(sub c) materials
[DE89-017677] N90-12360

Preparation and characterization of single phase Ba(1-x)KxBiO3
[DE89-017735] N90-12362

TRANSMISSION LINES

High power, solid state RF pulse generators
[AD-D014172] N90-11941

An empirical formula for gas switch breakdown delay
[DE89-017233] N90-11947

TRANSMISSION LOSS

Handbook of radio wave propagation loss (100-20,000 MHz), part 2
[PB89-195473] N90-11912

Modeling of diffraction reflection and clutter loss in UHF radio wave propagation
[FEL-1988-28] N90-11938

TRANSONIC FLOW

Development of direct-inverse 3-D methods for applied transonic aerodynamic wing design and analysis
[NASA-CR-186036] N90-11733

Three-dimensional, two-phase, transonic, canted nozzle flows
[AD-A211528] N90-11984

TRANSONIC NOZZLES

Three-dimensional, two-phase, transonic, canted nozzle flows
[AD-A211528] N90-11984

TRANSPORT AIRCRAFT

Comparison of flying qualities derived from in-flight and ground-based simulators for a jet-transport airplane for the approach and landing pilot tasks
[NASA-TP-2962] N90-11757

The aerodynamic experimental center of Aeritalia: Combat aircraft group
[ETN-89-95213] N90-11766

Transport composite fuselage technology: Impact dynamics and acoustic transmission
[NASA-CR-4035] N90-11821

TRANSPORT PROPERTIES

Analysis of opposed jet hydrogen-air counter flow diffusion flame
[NASA-CR-182366] N90-11825

Effect of electrical double layer on transport limited currents at microelectrodes
[AD-A211586] N90-11843

TRANSPORT THEORY

Evaluation and sensitivity analyses results of the MESOPUFF 2 model with CAPTEX (Cross-Appalachian Tracer Experiment) measurements
[PB89-198253] N90-12103

Stellarator transport theory
[DE89-016371] N90-12328

TREES (MATHEMATICS)

Three dimensional object recognition employing combined visual and tactile sensing
[PB89-219489] N90-12176

Parallel graph contraction
[AD-A211916] N90-12199

Dynamic embedding of trees in hypercubes with constant dilation and load
[AD-A211884] N90-12236

TRENDS

The evolution of light alloys in the aerospace industry
[ETN-89-95216] N90-11872

TRIBOLOGY

Plasma-deposited amorphous hydrogenated carbon films and their tribological properties
[NASA-TM-102379] N90-11880

Fundamental tribological properties of ion-beam-deposited boron nitride films
[NASA-TM-102088] N90-11881

Development and use of a tribology research-in-progress database
[PB89-228274] N90-12396

TROPOSPHERE
Use of satellite data and modeling to asses the influence of stratospheric processes on the troposphere N90-12075
Aerosol in the Pacific troposphere N90-12078
Global tropospheric chemistry: Chemical fluxes in the global atmosphere
[NASA-CR-186090] N90-12109
TRUCKS
DSEP (Dual Shaft Electric Propulsion) operation and maintenance manual for the NVH and TB-2 vehicles: Advanced Dual Shaft Electric Propulsion System technology development program
[DE89-017549] N90-12411
TRUSSES
Application of matrix correction methods on a plate and a truss structure
[NLR-MP-88042-U] N90-12056
TUNABLE LASERS
Growth and characterization of materials for tunable lasers in the near infrared spectral region
[NASA-CR-185832] N90-12009
Progress of research on water vapor lidar
[NASA-CR-185970] N90-12011
TUNGSTEN
Reactive ion etching of sputtered silicon carbide and tungsten thin films for device applications
[AD-A211711] N90-11847
Scintillating fiber ribbon - tungsten calorimeter
[DE89-016705] N90-12001
TUNING
Effects of mistuning and matrix structure on the topology of frequency response curves
[NASA-TM-102290] N90-12041
TURBINE BLADES
Model 0A wind turbine generator FMEA
[NASA-TM-102378] N90-12034
Effects of mistuning and matrix structure on the topology of frequency response curves
[NASA-TM-102290] N90-12041
User's guide for a personal computer model of turbulence at a wind turbine rotor
[DE89-017753] N90-12095
TURBOCOMPRESSORS
Coatings for gas turbine compressors
[NLR-MP-88045-U] N90-11750
TURBOFAN ENGINES
STOVL propulsion system volume dynamics approximations
[NASA-TM-102397] N90-11740
Measurement effects on the calculation of in-flight thrust for an F404 turbofan engine
[NASA-TM-4140] N90-11741
TURBOJET ENGINES
An open-loop transient thermodynamic model of the Cougar turbojet
[AD-A211774] N90-11745
TURBOPROP ENGINES
Propfan Test Assessment (PTA)
[NASA-CR-185138] N90-11739
TURBULENCE
Premixed turbulent flame propagation
[AD-A211489] N90-11841
Computational methods for complex flowfields
[AD-A211485] N90-11983
Low level remote sensing: Orographic winds N90-12066
User's guide for a personal computer model of turbulence at a wind turbine rotor
[DE89-017753] N90-12095
Coherency properties of strong Langmuir turbulence
[DE89-009290] N90-12119
TURBULENCE EFFECTS
Effects on electromagnetic wave propagation and rocket vapor trails of intense turbulence generated by breaking internal gravity waves
[AD-A211755] N90-12130
TURBULENT BOUNDARY LAYER
Near-wall, three-dimensional turbulence measurements: A challenge for laser velocimetry
[NASA-TM-102252] N90-11978
An experimental study of surface roughness effects on turbulent boundary layer flow and heat transfer
[AD-A212099] N90-11980
Experimental research on swept shock Wave/Boundary layer interactions
[AD-A211744] N90-11988
TURBULENT FLOW
Some implications of the isotropic momentarily frozen assumptions for the SPAN-MAT program
[NASA-CR-181937] N90-11704
Control of turbulent mixing layers
[AD-A211413] N90-11708
Doubly-fluted tubes and enhanced tubes in confined crossflow
[PB89-217921] N90-11971
Near-wall, three-dimensional turbulence measurements: A challenge for laser velocimetry
[NASA-TM-102252] N90-11978
An experimental study of surface roughness effects on turbulent boundary layer flow and heat transfer
[AD-A212099] N90-11980
TURBULENT HEAT TRANSFER
An experimental study of surface roughness effects on turbulent boundary layer flow and heat transfer
[AD-A212099] N90-11980
TURBULENT MIXING
Control of turbulent mixing layers
[AD-A211413] N90-11708
TWISTING
Magnetostrictive torque sensor
[AD-D014169] N90-11996
TWO DIMENSIONAL FLOW
The upwind control volume scheme for unstructured triangular grids
[NASA-TM-101664] N90-11703
Control of turbulent mixing layers
[AD-A211413] N90-11708
TWO DIMENSIONAL MODELS
Coherency properties of strong Langmuir turbulence
[DE89-009290] N90-12119
Beam dynamics of a liquid metal ion source
[DE89-015856] N90-12295
DART: A simulation code for charged particle beams, revision 1
[DE89-016697] N90-12312
Computer simulations of two-dimensional quasiperiodic crystal and random tiling models
[DE89-016909] N90-12355
Two dimensional conformal supergravity and critical behavior
[DE89-611968] N90-12414
TWO PHASE FLOW
Three-dimensional, two-phase, transonic, canted nozzle flows
[AD-A211528] N90-11984

U

U.S.S.R.
USSR Space Life Sciences Digest, Issue 22
[NASA-CR-3922(26)-ISSUE-22] N90-12153
USSR Space Life Sciences Digest, Issue 23
[NASA-CR-3922(27)-ISSUE-23] N90-12154
U.S.S.R. SPACE PROGRAM
USSR Space Life Sciences Digest, Issue 24
[NASA-CR-3922(28)-ISSUE-24] N90-12152
ULTRAHIGH FREQUENCIES
Modeling of diffraction reflection and clutter loss in UHF radio wave propagation
[FEL-1988-28] N90-11938
ULTRASONIC SPECTROSCOPY
Collective-mode spectroscopy of textures in superfluid (3)He-B
[PB89-221634] N90-12370
ULTRASONICS
NDE (Non-Destructive Evaluation) publications, 1985
[PB89-229025] N90-12036
ULTRAVIOLET DETECTORS
Comparison of the LOWTRAN 7 code and S3-4 satellite measurements of UV radiance
[AD-A211356] N90-12124
ULTRAVIOLET LASERS
A proposed linac cavity RF drive system for the Los Alamos extreme ultraviolet free-electron laser
[DE89-016614] N90-12016
ULTRAVIOLET RADIATION
Estimated UV clutter levels at 10-100 meter sensor pixel resolution extrapolated from recent polar bear measurements
[AD-A211357] N90-12125
UV ionospheric remote sensing with the polar BEAR satellite
[AD-A211359] N90-12127
Energy transfer and non-linear optical properties at near ultraviolet wavelengths: Rare earth 4f(yields)5d transitions in crystals and glasses
[DE90-000065] N90-12321
ULTRAVIOLET SPECTRA
Investigation of atmospheric emissions in ultraviolet, vacuum ultraviolet, and extreme ultraviolet wavelength
[AD-A212169] N90-12123
Comparison of the LOWTRAN 7 code and S3-4 satellite measurements of UV radiance
[AD-A211356] N90-12124
ULTRAVIOLET SPECTROMETERS
The SMM UV observations of Active Region 5395 N90-12485
ULTRAVIOLET SPECTROSCOPY
High temperature and high resolution UV photoelectron spectroscopy using supersonic molecular beams
[DE90-000176] N90-11835
ULTRAVIOLET TELESCOPES
UV ionospheric remote sensing with the polar BEAR satellite
[AD-A211359] N90-12127
ULYSSES MISSION
The solar flare and cosmic gamma-ray burst experiment aboard the Ulysses spacecraft N90-12470
UNDERGROUND ACOUSTICS
Clutter models for subsurface electromagnetic applications
[PB89-229678] N90-11925
UNDERWATER ACOUSTICS
Doppler statistics of ocean velocity variability
[AD-A211687] N90-12148
UNDERWATER ENGINEERING
Long endurance underwater power system
[AD-A211386] N90-12096
UNIQUENESS
Operator product coefficients in non-diagonal conformal field theories
[PB89-216873] N90-12283
UNSTEADY FLOW
Unsteady aerodynamics with applications to flight mechanics
[AD-A211944] N90-11706
Active control of unsteady and separated flow structures
[AD-A212109] N90-11707
Steady and unsteady potential flow around thin annular wings and engines with simulation of jet engine flow
[DFVLR-FB-89-18] N90-11711
UPPER SURFACE BLOWN FLAPS
Acoustic-thermal environment for USB flap structure. Report 1: Ground simulation test results
[NAL-TM-567] N90-11697
USER MANUALS (COMPUTER PROGRAMS)
Human Operator Simulator (HOS) 4 user's guide
[AD-A212007] N90-11763
Manual for Program PSTRESS: Peel stress computation
[NASA-CR-178408] N90-11822
User's guide for a personal computer model of turbulence at a wind turbine rotor
[DE89-017753] N90-12095
FEDIX: An on-line information service for universities and other research organizations: User's guide, version 2.0, release 1
[DE89-016695] N90-12398
CALS (Computer-aided Acquisition and Logistic Support) Test Network information exchange: User's manual
[DE89-016700] N90-12399
ANDECS-PERLUDE 2.0: A databased, interactive system of control software user's guide
[DFVLR-MITT-89-07] N90-12404
USER REQUIREMENTS
Feasibility of graphics voice telephones for the post 2000 era
[FEL-1988-26] N90-11937
Power up modification for video switcher microprocessor interface for sensor system processing system
[AD-A211543] N90-11962

V

VACUUM
Vacuum ultraviolet backgrounds from space - ten years after
[AD-A211353] N90-12493
VACUUM APPARATUS
Calculations of soft x ray emission of REB-heated plasma
[IPPCZ-287] N90-12329
VANADIUM COMPOUNDS
A nonlinear-optical method for combining high power laser beams
[AD-A211730] N90-12022
VANADIUM OXIDES
Vanadium dioxide protective devices
[AD-A212018] N90-11887
VANES
Fabrication of modulated vanes for a split-coaxial RFQ
[DE88-757235] N90-12310
VAPOR DEPOSITION
Method of modifying the dielectric properties of an organic polymer film
[AD-D014171] N90-11879
Application of dimensional analysis to statistical process modeling
[AD-A211881] N90-11905
Beam assisted fabrication of 3-5/Si monolithic devices
[AD-A212046] N90-12367

VAPOR PHASE EPITAXY
Ultra high speed compound semiconductors and real time signal processing
[AD-A211394] N90-12372
VAPOR PRESSURE
Vapour pressures and critical points of liquids. Halogenated hydrocarbons
[ESDU-89006] N90-11848
VARACTOR DIODES
Design, construction and test of a frequency doubler for 183 GHz
[PB89-212591] N90-11944
VARIANCE (STATISTICS)
Doppler statistics of ocean velocity variability
[AD-A211687] N90-12148
VARIATIONS
On the analysis of line profile variations: A statistical approach N90-12412
VECTOR ANALYSIS
Four vector-matrix primitives
[AD-A211889] N90-12237
VECTOR SPACES
Smooth linearization of hyperbolic fixed points without resonance conditions
[REPT-89-03] N90-12251
VELOCITY DISTRIBUTION
Air velocity mapping of environmental test chambers
[AD-A212062] N90-11764
VELOCITY MEASUREMENT
Three component laser Doppler measurements in an axisymmetric jet
[NASA-CR-181908] N90-11702
Observations and modelling of deep equatorial currents in the central Pacific
[PB89-198139] N90-12145
VENUS (PLANET)
Coronae on Venus observations and models of origin N90-12449
VENUS ATMOSPHERE
Deducing the age of the dense Venus atmosphere N90-12438
Venus and the Archean Earth: Thermal considerations N90-12448
VENUS CLOUDS
Venus volcanism: Rate estimates from laboratory studies of sulfur gas-solid reactions N90-12428
VENUS SURFACE
Abstracts for the Venus Geoscience Tutorial and Venus Geologic Mapping Workshop
[NASA-CR-185432] N90-12423
Geology of Southern Guinevere Planitia, Venus, based on analyses of Goldstone radar data N90-12424
Characteristics, distribution and geologic/terrain associations of small dome-like hills on Venus N90-12425
Tessera terrain: Characteristics and models of origin N90-12426
Divergent plate boundaries and crustal spreading on Venus: Evidence from Aphrodite Terra N90-12427
Venus volcanism: Rate estimates from laboratory studies of sulfur gas-solid reactions N90-12428
Potential for observing and discriminating impact craters and comparable volcanic landforms on Magellan radar images N90-12429
Venus surface properties deduced from radar and radiometry N90-12431
A morphologic study of Venus Ridge belts N90-12432
Evidence for volcanism in NW Ishtar Terra, Venus N90-12433
Radar scattering mechanisms within the meteor crater ejecta blanket: Geologic implications and relevance to Venus N90-12435
Aeolian processes on Venus N90-12436
Architecture of orogenic belts and convergent zones in Western Ishtar Terra, Venus N90-12437
Clotho Tessera, Venus: A fragment of Fortuna Tessera N90-12439
Tectonism on Venus: A review N90-12440
Venus: Mantle convection, hotspots, and tectonics N90-12442
Lakshmi Planum: A distinctive highland volcanic province N90-12444
Volcanism on Venus: Large shields and major accumulations of small domes N90-12445
Impact cratering and the surface age of Venus: The Pre-Magellan controversy N90-12446
Geology of the Venus equatorial region from Pioneer Venus radar imaging N90-12447
Crustal deformation: Earth vs Venus N90-12450
Eastern Ishtar Terra: Tectonic evolution derived from recognized features N90-12451
Stress distribution and topography of Tellus Regio, Venus N90-12452
Three ages of Venus N90-12453
VERTICAL LANDING
STOVL propulsion system volume dynamics approximations
[NASA-TM-102397] N90-11740
VERY HIGH FREQUENCIES
Petite Amateur Navy Satellite (PANSAT)
[NASA-CR-186049] N90-11800
VERY LARGE ARRAY (VLA)
VLA-Max '91 tests of high energy flare physics N90-12471
VERY LARGE SCALE INTEGRATION
A distributed pipelined architecture of the recursive Lagrangian equations of motion for robot manipulators with VLSI implementation — VLSI (very large scale integration)
[RR-353] N90-11966
An approximate max-flow min-cut theorem for uniform multicommodity flow problems with applications to approximation algorithms
[AD-A211908] N90-12198
Distributed VLSI architecture for fast Jacobian and inverse Jacobian formulations
[RR-346] N90-12218
Robot inverse dynamics computation via VLSI distributed architectures
[RR-350] N90-12223
VIBRATION
Effects of mistuning and matrix structure on the topology of frequency response curves
[NASA-TM-102290] N90-12041
The use of Lanczos's method to solve the large generalized symmetric definite eigenvalue problem
[NASA-CR-181914] N90-12193
Analysis of a system of two weakly nonlinear coupled harmonic oscillators arising from the field of wind-induced vibrations
[REPT-89-22] N90-12261
VIBRATION DAMPING
Controller design for active vibration suppression of a helicopter
[DFVLR-FB-89-20] N90-11760
Active control of the forced and transient response of a finite beam N90-12040
VIBRATION ISOLATORS
Controller design for active vibration suppression of a helicopter
[DFVLR-FB-89-20] N90-11760
Nonintrusive inertial vibration isolation technology for microgravity space experiments
[NASA-TM-102386] N90-11901
VIBRATION MODE
Problems related to the acquisition, processing and utilization of the modal parameters measured in flight tests in order to obtain the full envelope for flutter
[ETN-89-95210] N90-11735
VIBRATION TESTS
Investigation of difficult component effects on finite element model vibration prediction for the Bell AH-1G helicopter. Volume 1: Ground vibration test results
[NASA-CR-181916-VOL-1] N90-12058
VIDEO DATA
Video imaging systems: A survey
[DE89-016920] N90-11919
VIDEO EQUIPMENT
Three dimensional object recognition employing combined visual and tactile sensing
[PB89-219489] N90-12176
VIEW EFFECTS
Analysis of radar images of the active volcanic zone at Krafla, Iceland: The effects of look azimuth biasing N90-12434
VISCOELASTICITY
Three-dimensional viscoelastic bodies in steady state frictional rolling contact with generalization to Knothe rolling
[REPT-89-23] N90-12032
VISCOUS FLOW
Hopf bifurcation in the driven cavity
[NASA-TM-102334] N90-11969
A least-squares finite element method for incompressible Navier-Stokes problems
[NASA-TM-102385] N90-12231
VISUAL ACUITY
Visual acuity and stereopsis with night vision goggles
[AD-A211552] N90-12167
Discriminating rigid from nonrigid motion
[AD-A211794] N90-12180
VISUAL DISCRIMINATION
Three dimensional object recognition employing combined visual and tactile sensing
[PB89-219489] N90-12176
Discriminating rigid from nonrigid motion
[AD-A211794] N90-12180
VISUAL PERCEPTION
Visual motion perception
[AD-A210994] N90-12160
Visual acuity and stereopsis with night vision goggles
[AD-A211552] N90-12167
Eye movements and spatial pattern vision
[AD-A211650] N90-12169
A Conference on Three-Dimensional Representation held in University of Minnesota on 24-26 May 1989
[AD-A211630] N90-12324
VISUAL STIMULI
Visual motion perception
[AD-A210994] N90-12160
VOICE DATA PROCESSING
Feasibility of graphics voice telephones for the post 2000 era
[FEL-1988-26] N90-11937
VOLCANOES
Venus volcanism: Rate estimates from laboratory studies of sulfur gas-solid reactions N90-12428
Potential for observing and discriminating impact craters and comparable volcanic landforms on Magellan radar images N90-12429
Evidence for volcanism in NW Ishtar Terra, Venus N90-12433
Analysis of radar images of the active volcanic zone at Krafla, Iceland: The effects of look azimuth biasing N90-12434
Lakshmi Planum: A distinctive highland volcanic province N90-12444
Volcanism on Venus: Large shields and major accumulations of small domes N90-12445
Coronae on Venus observations and models of origin N90-12449
On the statistics of El Nino occurrences and the relationship of El Nino to volcanic and solar/geomagnetic activity
[NASA-TP-2948] N90-12456
VOLTERRA EQUATIONS
Rational expansion for nonlinear input-output maps
[RR-348] N90-12248
VORTICES
Near-planar TS waves and longitudinal vortices in channel flow: Nonlinear interaction and focusing
[NASA-CR-181928] N90-11698
A study of the temporal stability of multiple cell vortices
[NASA-CR-4261] N90-11968
Hopf bifurcation in the driven cavity
[NASA-TM-102334] N90-11969
Numerical analysis, scientific computing and fundamental studies of fluid mechanics
[DE89-017554] N90-11975
An investigation of end-wall vortex cavitation in a high Reynolds number axial-flow pump
[AD-A211426] N90-11982
Flare-in texture in rotating superfluid (3)He-B
[PB89-218994] N90-12368

W

WALL PRESSURE
Autofrettage-stress distribution under load and retained stresses after depressurization
[AD-A212090] N90-12048
WARNING SYSTEMS
Improved pattern recognition techniques for real time operation
[AD-A211395] N90-11840
Severe local storm warning verification: 1988
[PB89-226310] N90-12134
WASHING
Coating galvanized steel
[AD-A211775] N90-11869
WASTE ENERGY UTILIZATION
Conceptual design of liquid droplet radiator shuttle-attached experiment
[NASA-CR-185164] N90-11805
Conceptual design of liquid droplet radiator shuttle-attached experiment technical requirements document
[NASA-CR-185165] N90-11806
WATER CIRCULATION
Dynamics of the equatorial undercurrent and its termination
[PB89-198147] N90-12146
WATER VAPOR
Progress of research on water vapor lidar
[NASA-CR-185970] N90-12011
WATER WAVES
Similarity relations of wind waves in finite depth
[PB89-198113] N90-12144
WAVE ATTENUATION
Seismic wave attenuation and yield determination at regional distances
[AD-A211548] N90-12128

WAVE DIFFRACTION
Modeling of diffraction reflection and clutter loss in UHF radio wave propagation
[FEL-1988-28] N90-11938
A method to model fuze-performance. Part 3: Diffraction of electromagnetic radiation by an edge
[FEL-1989-22-PT-3] N90-11940

WAVE DISPERSION
Temporal and spatial filtering remedies for dispersion in electromagnetic particle codes
[DE89-017534] N90-12337

WAVE EQUATIONS
Time-domain analytic and numeric analysis of vertical dipoles in front of dielectric planar interface
[PB89-221642] N90-11927

WAVE FUNCTIONS
Davydov solutions at 300 Kelvin: The final search
[DE89-015248] N90-12296
Quantum-mechanical derivation of the Davydov equations for multi-quanta states
[DE89-015250] N90-12297

WAVE INTERACTION
Near-planar TS waves and longitudinal vortices in channel flow: Nonlinear interaction and focusing
[NASA-CR-181928] N90-11698
Dynamics of baroclinic wave systems N90-12072
The effect of latent heat release on synoptic-to-planetary wave interactions and its implication for satellite observations: Theoretical modeling N90-12073
The effect of latent heat release on synoptic-to-planetary scale wave interactions: Observational study
N90-12074
Laboratory and theoretical studies of baroclinic processes N90-12077
Wave particle interactions
[DE89-017527] N90-12335

WAVE PROPAGATION
Handbook of radio wave propagation loss (100-20,000 MHz), part 2
[PB89-195473] N90-11912
Simulation of the EMP (Electromagnetic Pulse) from ESD (Electrostatic Discharge)
[DE89-014484] N90-11918
Eigensolutions for the reflection problem involving the interface of two chiral half spaces
[PB89-221592] N90-11926
Modeling of diffraction reflection and clutter loss in UHF radio wave propagation
[FEL-1988-28] N90-11938
Effects on electromagnetic wave propagation and rocket vapor trails of intense turbulence generated by breaking internal gravity waves
[AD-A211755] N90-12130
Observations of long Rossby waves in the northern tropical Pacific
[PB89-196331] N90-12143
Similarity relations of wind waves in finite depth
[PB89-198113] N90-12144
Wave particle interactions
[DE89-017527] N90-12335

WAVE REFLECTION
Modeling of diffraction reflection and clutter loss in UHF radio wave propagation
[FEL-1988-28] N90-11938

WAVEFORMS
Multi-stage noise-reducing system
[AD-D014179] N90-11942
Similarity relations of wind waves in finite depth
[PB89-198113] N90-12144

WAVEGUIDES
Channelized coplanar waveguide pin-diode switches
[NASA-TM-102289] N90-11943
Design, construction and test of a frequency doubler for 183 GHz
[PB89-212591] N90-11944
Optical data transmission systems in radiation environment
[DE90-000174] N90-12322
Linear (passive) and non-linear guided and studies in glass
[AD-A211693] N90-12325

WEAPON SYSTEMS
Human Operator Simulator (HOS) 4 user's guide
[AD-A212007] N90-11763

WEAR
Sliding seal materials for low heat rejection engines
[NASA-CR-182262] N90-11882
New Fabric Development Program
[AD-A211549] N90-11891

WEAR RESISTANCE
Thermomechanical contact phenomena and wear of sliding components
[AD-A211290] N90-12028

WEAR TESTS
Thermomechanical contact phenomena and wear of sliding components
[AD-A211290] N90-12028

WEATHER
World Weather Watch: Implementation
[WMO-714] N90-12139

WEATHER DATA RECORDERS
Type-specific dynamic measurements on wind turbines at the test site Schnittlingen (Germany, F.R.)
[DFVLR-MITT-88-31] N90-12099

WEATHER FORECASTING
Low level remote sensing: The Doppler Radar wind profiler N90-12067
LAWS simulation: Sampling strategies and wind computation algorithms N90-12081
Satellite-derived rainfall estimates and propagation characteristics associated with the Mesoscale Convective Systems (MCSs)
[PB89-213417] N90-12086
Contemporary China's meteorological enterprises (selected portions)
[AD-A210697] N90-12131
Development of high resolution simulations of the atmospheric environment using the MASS model
[NASA-CR-186040] N90-12133
Severe local storm warning verification: 1988
[PB89-226310] N90-12134

WEATHER STATIONS
Contemporary China's meteorological enterprises (selected portions)
[AD-A210697] N90-12131

WEATHERING
Coating galvanized steel
[AD-A211775] N90-11869

WEDGES
Experimental investigation of a planar shock wave over a double wedge
[AD-A211366] N90-11981

WEIBULL DENSITY FUNCTIONS
Pacific marine radar sea scatter experimental results
[AD-A211593] N90-11931

WEIGHTING FUNCTIONS
A polynomial method of approximate weighted centers for linear programming
[REPT-89-13] N90-12210
Time-weighted accumulations ap(tau) and Kp(tau)
[RAE-TR-88050] N90-12422

WELDABILITY
Weldability of ductile nickel aluminides
[DE89-017452] N90-11859

WELDED JOINTS
Resistance welding large parts
[DE89-010462] N90-12027

WELDING
Fracture toughness data base for HT9 and modified 9Cr-1Mo irradiated in several reactors up to approximately 100 dpa
[DE90-000111] N90-11864

WETLANDS
Global data bases on distribution, characteristics and methane emission of natural wetlands: Documentation of archived data tape
[NASA-TM-4153] N90-12090

WETTABILITY
Investigations into the infiltration kinetics, wettability, and interfacial bond strength of Al/SiC composites
[AD-A211924] N90-11815

WETTING
Self-assembled organic monolayer films
[AD-A212006] N90-11838

WHISKER COMPOSITES
Deformation behavior of SiC/2014 Al metal-matrix composite
[AD-A212095] N90-11816

WHITE NOISE
Discrete filtering techniques applied to sequential GPS range measurements
[NASA-CR-177472] N90-11730

WIND (METEOROLOGY)
Low level remote sensing: Orographic winds
N90-12066
Aeolian processes on Venus N90-12436

WIND DIRECTION
Pacific marine radar sea scatter experimental results
[AD-A211593] N90-11931

WIND EFFECTS
Wind/seismic comparisons for upgrading existing structures
[DE89-016055] N90-12044
Similarity relations of wind waves in finite depth
[PB89-198113] N90-12144
Equatorial oceanic response to forcing on time scales from days to months
[PB89-206775] N90-12147
Analysis of a system of two weakly nonlinear coupled harmonic oscillators arising from the field of wind-induced vibrations
[REPT-89-22] N90-12261

WIND PROFILES
Low level remote sensing: The Doppler Radar wind profiler N90-12067
Disturbances in the Arizona Monsoon N90-12071
Evaluation and sensitivity analyses results of the MESOPUFF 2 model with CAPTEX (Cross-Appalachian Tracer Experiment) measurements
[PB89-198253] N90-12103

WIND TUNNEL MODELS
Wind tunnel test of CAD USB-STOL semi-borne prototype
[NAL-TM-566] N90-11696

WIND TUNNEL TESTS
Wind tunnel test of CAD USB-STOL semi-borne prototype
[NAL-TM-566] N90-11696
The determination of the aerodynamic characteristics of an ogive-cylinder body in subsonic, curved, incompressible flow, and an assessment of the effect of flow curvature
[REPT-87-13] N90-11712
Low-speed wind-tunnel study of reaction control-jet effectiveness for hover and transition of a STOVL fighter concept
[NASA-TM-4147] N90-11751
The aerodynamic experimental center of Aeritalia: Combat aircraft group
[ETN-89-95213] N90-11766
Comparison of the results of tests on A300 aircraft in the RAE 5 metre and ONERA F1 wind tunnels
[RAE-TM-AERO-2130] N90-11768

WIND TURBINES
Model 0A wind turbine generator FMEA
[NASA-TM-102378] N90-12034
WISPER: A standardized fatigue load sequence for HAWT-blades
[NLR-MP-88029-U] N90-12055
User's guide for a personal computer model of turbulence at a wind turbine rotor
[DE89-017753] N90-12095
Type-specific dynamic measurements on wind turbines at the test site Schnittlingen (Germany, F.R.)
[DFVLR-MITT-88-31] N90-12099
Acoustical effects of a large ridge on low-frequency sound propagation in stationary and moving atmospheres
[NASA-CR-186001] N90-12290

WIND VELOCITY
Analysis of heliport environmental data: Indianapolis downtown heliport, Wall Street heliport. Volume 2: Wall Street heliport data plots
[DOT/FAA/CT-TN87/54-VOL-2] N90-11761
Pacific marine radar sea scatter experimental results
[AD-A211593] N90-11931

WINDPOWER UTILIZATION
Activities report on KEMA R and D
[ST-REPT-VOL-6-NO-12] N90-12100

WING PROFILES
Wind tunnel test of CAD USB-STOL semi-borne prototype
[NAL-TM-566] N90-11696

WING TIPS
Flutter clearance of the F-18 high-angle-of-attack research vehicle with experimental wingtip instrumentation pods
[NASA-TM-4148] N90-11732

WINGS
Development of direct-inverse 3-D methods for applied transonic aerodynamic wing design and analysis
[NASA-CR-186036] N90-11733
A new test procedure for a wing made with carbon fiber composites
[ETN-89-95220] N90-11820

WIRE
Thermal conduction of SSC (Superconducting Super Collider) wire
[DE89-016710] N90-11811
Magnetostrictive torque sensor
[AD-D014169] N90-11996

WOLF-RAYET STARS
On the analysis of line profile variations: A statistical approach N90-12412

WOOL
New Fabric Development Program
[AD-A211549] N90-11891

WORKLOADS (PSYCHOPHYSIOLOGY)
Forecasting contracting workload
[AD-A211935] N90-12387

WRIST
Wrist orientation effect on grip strength and endurance
[PB89-200935] N90-12179

X

X RAY DIFFRACTION
Short period multilayers: Interface dominated structures
[DE89-017536] N90-11812
X RAY IMAGERY
A microchannel plate intensified, subnanosecond, X-ray imaging camera
[DE89-017781] N90-12003
Pre-pulses: Signature of a trigger process in short (less than 60 secs) solar hard x ray flares N90-12476
X RAY IRRADIATION
Use of the NPL linac for x ray dosimetry — linear accelerator (linac)
[NPL-RSA(EXT)-6] N90-12314
X RAY SPECTROSCOPY
A microchannel plate intensified, subnanosecond, X-ray imaging camera
[DE89-017781] N90-12003
High resolution X-ray spectroscopy using germanium microcalorimeters
[DE89-017784] N90-12004
FORTRAN program for x ray photoelectron spectroscopy data reformatting
[NASA-TP-2957] N90-12348
X RAY TELESCOPES
Solar flare gamma-ray and hard x ray imaging with the GRID-on-a-balloon N90-12474
The soft x ray telescope for Solar-A N90-12475
X RAYS
Laser production of soft x rays by multiquantum processes and the excitation of atomic inner-shell states
[AD-A211372] N90-12021
Calculations of soft x ray emission of REB-heated plasma
[IPPCZ-287] N90-12329
Heating and acceleration of coronal and chromospheric ions during solar flares N90-12479
Some of the terrestrial effects of AR 5395
N90-12482
X-29 AIRCRAFT
A design procedure for the handling qualities optimization of the X-29A aircraft
[NASA-TM-4142] N90-11753

Y

YAG LASERS
Construction of a picosecond laser system for the investigation of semiconductors using nonlinear optical methods
[ETN-89-94664] N90-12013
Laser ionization mass spectroscopy
[DE89-006039] N90-12015

Z

ZEEMAN EFFECT
Zeeman interferometry
[DE89-015296] N90-12012
ZINC COATINGS
Coating galvanized steel
[AD-A211775] N90-11869
ZIRCONIUM OXIDES
New mechanism for toughening ceramic materials
[AD-A211651] N90-11892

PERSONAL AUTHOR INDEX

SCIENTIFIC AND TECHNICAL AEROSPACE REPORTS VOLUME 28 NUMBER 3

Typical Personal Author Index Listing

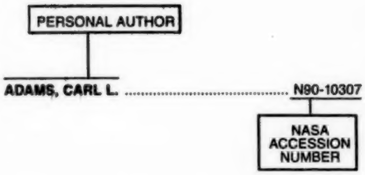

Listings in this index are arranged alphabetically by personal author. The NASA accession number denotes the number by which the citation is identified.

A

ABAZOV, A. I. N90-12457
ABDALLA, E. N90-12414
ABDALLA, M. C. B. N90-12414
ABDURASHITOV, D. N. N90-12457
ABE, D. K. N90-11951
ABEL, PHILLIP B. N90-12348
ABRAHAMSON, S. D. N90-11978
ACCIOLY, A. J. N90-12413
ACHTEMEIER, GARY L. N90-12064
ACTON, L. W. N90-12475
ADAMS, DONALD F. N90-11807
ADELMAN, HENRY G. N90-11742
ADERHOLZ, M. N90-12309
AFOLABI, DARE N90-12041
AGGARWAL, ALOK N90-12188
AGRAWAL, AJIT N90-12237
AHLUWALIA, H. S. N90-12488
AL-SHUKRI, H. N90-12128
ALBRECHT, R. N90-12302
ALCON, ROBERT R. N90-11973
ALLEN, ARTHUR A. N90-12149
ALLEN, JAMES L. N90-12289
ALLISON, J. E., JR. N90-11849
ALTEROVITZ, SAMUEL A. N90-11880
ALTHAUS, R. F. N90-12284
AMBROSIANO, JOHN J. N90-11920
N90-12336
N90-12337
AMBURN, D. N90-12391
ANDERSON, W. KYLE N90-11703
ANDRO, MONTY N90-11915
ANOSOV, O. L. N90-12457
APPLEBY, A. JOHN N90-12098
ARAI, S. N90-12310
ARBET, JIM N90-11786
ARBOCZ, J. N90-12043
AREND, LAWRENCE E. N90-12169
ARMANDILLO, E. N90-12024
ARNOLD, GRAHAM S. N90-11801
ARNOLD, J. E. N90-12059
ARROW, KENNETH J. N90-12235
ARSTENTO, G. N90-11872
ARVIDSON, R. E. N90-12424
N90-12430
N90-12443
ARZIGIAN, J. S. N90-11945
ASH, ROBERT L. N90-12292
ASHLEY, HOLT N90-11706
AUBELE, J. C. N90-12425
AUDET, NORMAN N90-11891
AUVINE, BRIAN N90-12142
AVAGNINA, GIAN MARIO N90-11759
AVITZUR, BOAZ N90-12048
AWES, T. C. N90-12302
AXE, J. N90-12366

B

BABICKY, V. N90-12329
BADRI, DAS N90-12346
BAI, T. N90-12465
BAKER, D. JAMES, JR. N90-12101
BAKER, S. A. N90-12217
BAKKER, S. J. M. N90-12006
BAKTASH, C. N90-12302
BALAVOINE, GILBERT A. N90-11888
BALDO, P. M. N90-12360
BALENA, F. J. N90-11821
BALTZLEY, DENNIS R. N90-12174
N90-12175
BANKS, S. P. N90-12224
N90-12247
N90-12248
BAPTISTE, K. N90-11953
BARALE, P. J. N90-12284
BARAM, YORAM N90-12227
BARBANTINI, E. N90-11766
BARCILON, ALBERT N90-12072
BARICKMAN, K. N90-11786
BARKATOU, M. A. N90-12254
BARKEY, DEREK A. N90-11822
BARMATZ, MARTIN B. N90-12289
BARON, JUDSON R. N90-11983
BARR, W. L. N90-12312
BARSOUM, M. N90-11810
BARTEL, H. W. N90-11738
N90-11739
BARTSCH, HERBERT N90-11871
BATCHELOR, D. A. N90-12473
BATTRICK, B. N90-12024
BAYER, JUDY N90-12206
BEARROW, M. N90-11785
BEATY, KEVIN N90-11882
BEAVER, BRUCE N90-11836
BECKMANN, P. N90-12302
BEEMAN, J. N90-12004
BEIHOFF, BRUCE N90-11996
BELJAARS, A. C. M. N90-12141
BELLO, PHILLIP A. N90-11930
BEN-DOR, G. N90-11981
BENFER, RICHARD N90-12371
BENJEGERDES, R. W. N90-12284
BENNETT, WILLIAM H. N90-11756
BENO, MARK A. N90-12356
BENTHIEN, G. W. N90-12293
BERGER, BONNIE N90-11955
BERGER, F. N90-12302
BERNARDEZ, LUIS J., III N90-12015
BESCH, STEPHEN R. N90-12170
BHATTACHARJEE, PIJUSHPANI N90-12492
BICKEL, D. L. N90-12317
BIEDERMAN, IRVING N90-12324
BIEGING, J. H. N90-12472
BILLIARD, PHILLIP A. N90-11850
BILLING, CLARE B., JR. N90-12149
BILLINGS, S. A. N90-11965
N90-12249
N90-12259
N90-12271
N90-12272
N90-12276
N90-12277
BILLMANN, BARRY R. N90-11726
BINDER, MICHAEL N90-11879
BINDSCHADLER, D. L. N90-12426
BIXBY, RANDY L. N90-12400
BLACK, F. O. N90-12178
BLACK, M. S. N90-12082
BLASKO, S. N90-12350
BLECK, RAINER N90-12073
BLELLOCH, GUY E. N90-12237
BLIER, WARREN N90-12132
BLOCH-BOULANGER, ISABELLE N90-12258
BLOCK, L. P. N90-12118
BLOUGH, DOUGLAS M. N90-12212
BOCK, R. N90-12302
BOCKEMUELLER, ERNST A. N90-12288
BOCKER, RICHARD P. N90-12186
BODDULURI, R. M. C. N90-12202
BOEHNISCH, HELMUT N90-12099
BOER, MICHEL N90-12470
BOETTNER, H. N90-12023
BOHN, C. L. N90-12359
BOHREN, CRAIG F. N90-12083
BOIE, W. N90-11936
BOISVERT, R. F. N90-11967
BOOZER, ALLEN H. N90-12341
BOSCHETTI, F. N90-11872
BOSS, WENDY F. N90-12156
BOSWORTH, JOHN T. N90-11753
BOVERIE, BILL N90-11918
BOVINO, LAWRENCE J. N90-11941
BOWDLE, DAVID A. N90-12080
BOWLES, JEFFREY V. N90-11742
BOWLING, ROBERT J. N90-11845
BOXWELL, D. A. N90-11692
BOYER, KEITH N90-12021
BRACKNELL, D. R. N90-12405
BRADLEY, GARY N90-12196
BRADY, MARTIN N90-11955
BRANSCOME, LEE E. N90-12073
BRANSFORD, JAMES W. N90-11850
BRAUNSTEIN, MYRON L. N90-12180
BRETHERTON, FRANCIS P. N90-12101
BREWER, DENNIS W. N90-12192
BREWER, ORLIE N90-12194
BRION, GAIL N90-12104
BROCKMAN, JEFF P. N90-11770
BROOKS, S. L. N90-12195
BROOKS, THOMAS L., IV N90-12387
BROSS, A. N90-12001
BROWN, DAVID R. N90-11823
BROWN, DONNA N90-11955
BROWN, GERALD V. N90-11901
BROWN, GLENN B. N90-11980
BROWN, J. N90-12366
BROWN, JAMES N90-12181
BROWN, KENNETH G. N90-11823
BROWN, P. C. N90-11738
N90-11739
BROWN, ROBERT L. N90-11907
BROWN, W. A. N90-12475
BRUCKNER-LEA, CINDY N90-12159
BRUNER, M. E. N90-12475
BUCCIANTINI, G. N90-11766
BUCCIARELLI, L. L. N90-12383
BUDD, A. J. N90-11722
BUDINGER, JAMES M. N90-11915
BUNING, H. N90-11799
BURKE, G. J. N90-11917
BURKE, KEVIN C. N90-12101
BURKE, WILLIAM J. N90-11755
BURNS, J. E. N90-12314
BURNS, JOHN A. N90-12192
BURNS, TIMOTHY J. N90-12038
BUSCH, D. E. N90-11883
BYCHUK, O. V. N90-12457
BYNUM, M. C. N90-11792

C

CABLE, J. N90-12366
CAHILL, PATRICIA L. N90-11714
CAMBIER, JEAN-LUC N90-11742
CAMPBELL, B. A. N90-12435
CAMPBELL, DAVID N90-11770
CAMPBELL, PHIL M. N90-11987
CANAVAN, GREGORY H. N90-12018
CANFIELD, R. C. N90-12489
CANINI, D. N90-12411
CANTOR, ROBIN A. N90-12107
CANTRELL, C. D., III N90-12022
CARLIP, STEVEN N90-12378
CARLSON, CATHERINE N90-12067
CARLSON, K. DOUGLAS N90-12356
CARLSON, LELAND A. N90-11733
CARRICK, PAUL N90-12187
CARSIOTIS, MICHAEL N90-12155
CARTER, BRUCE N90-11770
CARTER, M. R. N90-12003
CARTER, RICHARD G. N90-12232
CARTER, SCOTT N90-12204

CARTER, WILLIAM N90-12347
CHAI, BRUCE H. T. N90-12017
CHAMIS, C. C. N90-11808
CHAN, J. W. N90-11865
CHAN, P. N90-11994
CHANANE, B. N90-12248
CHANDRASEKARAN, B. N90-12401
CHANDY, K. M. N90-12200
CHANG, CHING-TEN N90-12323
CHANG, CHUN-HYON N90-12403
CHANG, I-SHIH N90-11984
CHANG, STEPHEN KW. N90-11764
N90-11979
N90-12165
CHART, T. G. N90-12382
CHASE, J. B. N90-11951
CHAU, H. H. N90-11977
CHAVANON, PATRICK N90-11710
CHEN, CHIAHONG N90-12377
CHEN, S. N90-12259
N90-12272
CHENG, C. C. N90-11883
CHI, KAY N90-12062
CHIEN, ANDREW A. N90-12187
N90-12197
CHIEN, CHIA-HON N90-12242
CHINN, D. N90-12115
CHIVIAN, JAY S. N90-12022
CHOU, SHIH-HUNG N90-12077
CHOU, SHUN-CHIN N90-11816
CHOUDHARY, ALOK NIDHI N90-12213
N90-12214
N90-12215
CHRISTENSEN, RICHARD N. N90-11971
CHRISTIAN, MARK JAY N90-11715
CHRISTOPHER, P. A. T. N90-11713
CHRISTY, JOHN R. N90-12069
CHU, TAK-KIN N90-11997
CHURNSIDE, JAMES H. N90-12010
N90-12315
CIPRI, F. N90-11819
CLAESSON, G. N90-12302
CLANCEY, WILLIAM J. N90-12222
CLARK, ARTHUR E. N90-11996
CLARK, JOHN H. E. N90-12060
CLARK, WILLIAM C. N90-12101
CLARKE, ANTONY D. N90-12078
CLAYTON, C. N90-12335
CLEWING, G. N90-12302
CLIFF, EUGENE M. N90-12192
CLINE, T. L. N90-12469
COGUILL, SCOTT L. N90-11807
COHEN, JEFF N90-12104
COLEMAN, HUGH W. N90-11980
COLLINS, GEORGE J. N90-12367
COLUCCI, STEPHEN N90-12074
COMPERE, A. L. N90-11898
COMPTON, J. M. N90-11783
CONNELL, J. R. N90-12095
CONNERS, TIMOTHY R. N90-11741
CONWAY, TERRY L. N90-12161
COOKE, ROGER N90-12273
COOMBS, CASSANDRA R. N90-12453
COOPER, WILLIAM A. N90-11731
N90-12113
COOPRIDER, KURT N90-12025
CORREIG, A. N90-12128
COTTEN, W. D. N90-12022
COVEY, CURT N90-12106
COX, TIMOTHY H. N90-11753
CRAIG, D. F. N90-11884
CRANE, SHARON L. N90-11972
CRANNELL, C. J. N90-12474
CRISLER, M. N90-12001
CROMBIE, MICHAEL A. N90-11720
CROSBY, G. A. N90-12287
CROWSON, ANDREW N90-11890
CRUDELE, SCOTT D. N90-11814
CRUMPLER, L. S. N90-12427
N90-12437
CSANKY, GEZA N90-12380
CUKAUSKAS, EDWARD N90-12347
CURLEE, RICHARD M. N90-12353
CURTIS, A. R. D. N90-11965
CUTLER, RAYMOND A. N90-11892
CUTTING, J. L. N90-11951
CYMERMAN, ALLEN N90-12163

D

DABROWSKI, CHRISTOPHER E. N90-12395
DAEHLER, MARK N90-11929
DALE, J. W. G. N90-12314
DALLY, WILLIAM J. N90-12187
N90-12197
DALTON, B. P. N90-12151
DANDEKAR, DATTATRAYA P. N90-11816
DANG, WENBIN N90-11817
DANIEL, STEVEN N90-11802
DANSHIN, S. N. N90-12457
DAVENPORT, J. W. N90-11860
DAVID, S. A. N90-11859
DAVIDSON, W. R. N90-11792
DAVIES, C. N90-12211
DAVIS, H. T. N90-11846
DAVIS, LARRY S. N90-11725
DAVIS, MARGARET B. N90-12101
DAVIS, PATRICIA P. N90-11823
DAWHITFIELD, Q. N90-11719
DAWSON, L. R. N90-12349
DEAL, WILLIAM E. N90-11972
DEAN, G. D. N90-11895
DEASI, U. N90-12476
DEBOER, A. N90-12056
DEFAZIO, THOMAS L. N90-12025
DEJONG, A. N. N90-12006
DEJONGHE, LUTGARD C. N90-11886
DEKONING, W. L. N90-11910
DELAYEN, J. R. N90-12359
DELGRECO, F. P. N90-12125
N90-12126
N90-12127
DEMAEL, JACQUES J. N90-11724
DEMAZANCOURT, PIERRE F. N90-12244
DENHERTOG, D. N90-12210
DENHOLLANDER, F. N90-12278
DENIERVANDERGON, A. W. N90-11857
DENNIS, BRIAN R. N90-12459
N90-12474
N90-12486
N90-12491
DESSAU, DANIEL N90-12373
DEVADAS, SRINIVAS N90-11956
DEWAARD, H. N90-11910
DEWITT, HUGH E. N90-12339
DICK, JERRY J. N90-12000
DICKINSON, ROBERT E. N90-12101
DICKSON, PETER N90-12129
DILLARD, ROY N90-11891
DIMARCO, S. F. N90-12022
DIMEO, MARK N90-11761
DIMOTAKIS, PAUL E. N90-11708
DOMPKA, R. V. N90-12058
DONALDSON, P. LYNN N90-12152
N90-12153
N90-12154
DONELSON, LESLIE N90-11770
DONGARRA, JACK N90-12194
DRAGON, L. N90-12302
DRAKE, BARRY L. N90-12186
DRAKE, STEPHEN A. N90-12485
DRAPELA, L. J. N90-11784
DRISKO, R. W. N90-11869
DRIVER, DAVID N90-11874
DROEGE, MICHAEL W. N90-11831
DROST, M. K. N90-12313
DRUCE, R. L. N90-12363
DRUMMOND, COLIN K. N90-11740
DRYER, MURRAY N90-12416
DUBOIS, D. F. N90-12119
DUFFY, R. N90-11786
DULK, G. A. N90-12479
N90-12480
DUNFORD, D. V. N90-11875
N90-11876
N90-12053
N90-12054
DUNLAP, WILLIAM P. N90-12174
DURNEY, CARL H. N90-12159
DUVAL, J. D. N90-11792

E

EARNSHAW, P. B. N90-11768
EASLEY, WESLEY C. N90-11736
EASTES, R. W. N90-12125
N90-12126
N90-12127
EASTRIDGE, RICHARD N90-11771
EATON, JOHN K. N90-11707
EBERT, HANS J. N90-12494
EBISUZAKI, WESLEY N90-12063
EDWARDS, BELVA N90-12117
EDWARDS, GLEN R. N90-11815
N90-11859
EGAWA, KOUICHI N90-11697
EHLERS, K. N90-12428
EHRLICH, MICHAEL J. N90-12050
EICHLER, P. N90-11772
ELDERING, C. A. N90-11921
ELHITMY, M. N90-11965
ELIASSON, L. N90-12118
ELLER, NANCY N90-12150
ELLIS, DAVID L. N90-11853
EMMITT, G. D. A. N90-12061
ENDOH, SYUNJI N90-11697
N90-12039
ENGLERT, GERALD W. N90-12262
ERCK, R. A. N90-11883
ERDEMIR, A. N90-11883
ERLANDSON, R. E. N90-12118
ERLICHMAN, SCOTT N90-11761
EROSHKINA, L. A. N90-12457
ERSKINE, DAVID J. N90-11833
N90-11976
ERVIN, STEPHEN M. N90-12383
ESPINOZA, BEDA M. M. N90-12028
EVANS, C. N90-12435
EVENS, MARTHA N90-12162

F

FAIZOV, E. L. N90-12457
FALCHI, A. N90-12477
FALCIANI, R. N90-12477
FARAGO, ZOLTAN N90-11990
FARRELL, KEVIN J. N90-11982
FEDORENKO, S. I. N90-12331
FEGLEY, B., JR. N90-12428
FEHRIBACH, JOSEPH N90-12077
FELDBERG, STEPHEN W. N90-11843
FELDMAN, MARC J. N90-12375
FENSKE, G. R. N90-11883
FERNANDO, G. W. N90-11860
FERRARIS, PIER LUIGI N90-11759
FERRARO, JOHN R. N90-12356
FIDLER, JOSEF N90-12285
FILLIPUCCI, M. L. N90-11951
FISHER, V. A. N90-11748
FISHMAN, G. J. N90-12469
FISHMAN, S. N90-11810
FISKE, STUART N90-12187
FITZJARRALD, DAN N90-12077
FLANDERS, K. N90-11746
FLEISHER, AARON N90-12383
FLETCHER, JAY W. N90-11752
FLUSS, M. J. N90-12358
FOERSTER, BERNHARD N90-12088
FOLKERTS, T. J. N90-12362
FORBES, GREGORY S. N90-12067
FORD, J. P. N90-12429
N90-12430
FORD, P. G. N90-12431
FOREST, CHARLES A. N90-12000
FORTE, VINCENT A., JR. N90-12163
FRANCAVILLA, T. L. N90-11964
FRANK, A. M. N90-12002
FRANK, S. L. N90-12432
FRANK, Z. N90-12487
FRANKEL, JULIUS N90-11816
FRASER, M. E. N90-12114
FRAZIER, WILLIAM E. N90-11852
N90-11912
FREUDINGER, LAWRENCE C. N90-11732
FRIEDMAN, ALEX N90-12337
FRIGGLE, W. E. N90-12397
FRIIS-CHRISTENSEN, E. N90-12118
FRITH, P. C. N90-11745
FRITZ, I. J. N90-12349
FROST, WALTER N90-12066
FUCHS, JUERGEN N90-12283
FUJIEDA, KAKUTOSHI N90-11696
FUJINO, T. N90-12310
FUJITA, TOSHIMI N90-11696
FUKUSHIMA, SACHIO N90-12039
FUKUSHIMA, T. N90-12310
FULCO, CHARLES S. N90-12163
FUNARO, DANIELE N90-12230
FUNSTON, KERRY N90-11771

G

GADDIS, L. N90-12433
GAIDOS, J. A. N90-12311
GAIZAUSKAS, V. N90-12483
GALATOLO, R. N90-11877
GALL, ROBERT N90-12071
GALLAGHER, DONALD N90-11761
GANGULY, JIBMITRA N90-11816
GARDNER, D. G. N90-12419
GARDNER, M. A. N90-12419
GARIMELLA, SRINIVAS N90-11971
GARRISON, A. K. N90-12020
GARSHNEK, VICTORIA N90-12152
N90-12153

N90-12154
GARVIN, J. B. N90-12434
N90-12435
GARY, D. E. N90-12490
GATES, RICHARD B. N90-12005
GATHERS, G. R. N90-11977
N90-12002
GAUS, NORBERT N90-11760
GAVRIN, V. N. N90-12457
GAYEVSKY, V. I. N90-12457
GEE, LIND S. N90-12120
GEERTS, M. J. N90-12350
GEISER, URS N90-12356
GHAN, STEVEN J. N90-12106
GHIRARDELLI, ROBERT G. N90-12157
GIACOBBE, T. N90-12035
GIELDA, THOMAS P. N90-11743
GIESE, BENJAMIN S. N90-12147
GILBER, W. S. N90-12284
GILBRETH, C. N90-12487
GILES, MICHAEL N90-11703
GILKEY, ROBERT H. N90-12168
GILLER, RICHARD A. N90-12044
GILLESPIE, LAROUX K. N90-11904
GIRARD, D. N90-12257
GIRIN, S. V. N90-12457
GIVEN, BOB N90-12221
GLAESER, ANDREAS M. N90-11885
GLASSMAN, IRVIN N90-11744
GLOSSON, C. A. N90-12022
GLOVER, KEITH N90-11756
GLYNN, PETER W. N90-12267
GOFORTH, JAMES H. N90-11998
GOGNY, D. N90-12233
GOLDMAN, ALLEN M. N90-12374
GOLDSCHMIDT, GABRIELA N90-12383
GONZALEZ, RICHARD R. N90-11764
N90-11979
N90-12165
GOODMAN, L. N90-12148
GOODRICH, JOHN W. N90-11969
GOODWITCH, JAMES M. N90-12103
GOPALSWAMY, N. N90-12472
GORDON, H. N90-11887
GOSSAGE, S. A. N90-12317
GOSSARD, EARL E. N90-11911
GOTTLIEB, DAVID N90-12230
GOTTSCHALL, R. N90-11810
GOULDING, F. N90-12004
GOWER, G. L. N90-12095
GOYAL, AMBUJ N90-12267
GRAHNE, GOSTA N90-12393
GRAMS, G. W. N90-12020
GRANT, JOHN R. N90-12130
GRANTHAM, WILLIAM D. N90-11757
GRAVES, STEPHEN C. N90-12025
GRECO, STEVEN N90-12074
GREELEY, RONALD N90-12433
N90-12436
N90-12452
GREEN, B. D. N90-12114
GREEN, JOHN L. N90-11816
GREEN, L. N90-11976
GREEN, M. A. N90-12284
GREEN, M. I. N90-12284
GREENE, M. E. N90-12474
GREINER, N. ROY N90-11974
GRENIER, LEO A. N90-12134
GRIFFIN, K. L. N90-12363
GRIFFITH, W. L. N90-11898
GRODSINSKY, CARLOS M. N90-11901
GROSS, MARK D. N90-12383
GROSS, ROBERT W. N90-11702
GROSSINGER, ROLAND N90-12285
GROSSMAN, ROBERT N90-12228
GROTCH, STANLEY L. N90-12108
GUADAGNO, M. N90-11735
GUBSER, D. U. N90-11964
GUETTNER, E. N90-11936
GUIFFRE, G. N90-11735
GUPTA, SHANTI S. N90-12245
N90-12269
N90-12270
GURMAN, JOSEPH B. N90-12485
GUSTAFSON, KARL N90-11969
GUSTAVSON, RICHARD E. N90-12025
GUZIK, JOYCE A. N90-12417

H

HAAS, WILBUR M. N90-11907
HAHGIGHI, H. N90-12358
HAIDER, Q. N90-12233
HAINES, JOHN N90-12104
HAIR, L. M. N90-11831
HALASI, KADOSA N90-11969
HALL, DAVID F. N90-11801
HALL, L. A. N90-12124
HALL, P. N90-11698
HALMSTAD, JOHN T. N90-12134
HAMILTON, DOUGLAS S. N90-12321
HAMILTON, M. L. N90-11864
HAMILTON, RUSSELL J. N90-12481
HAMMER, D. A. N90-12338
HAMMESFAHR, JENS N90-11727
N90-11728
HAMPTON, N. SHIRER N90-12060
HANKEY, WILBUR L. N90-11743
HANTKE, D. N90-12309
HANZON, B. N90-12250
HARDING, KERSTIN K. N90-11851
HARDWICK, J. L. N90-12343
HARRIS, DAVID ANTHONY N90-11906
HARRISON, R. F. N90-12224
HARROLD, C. L. N90-12190
HART, JOHN E. N90-12076
HARTMAN, DAN W. N90-11793
N90-11794
N90-11795
N90-11796
N90-11797
HASTAD, JOHAN N90-12238
HAUFLER, W. A. N90-11787
N90-11788
HAWKE, R. S. N90-11951
HAYNES, T. E. N90-12357
HEAD, JAMES W. N90-12426
N90-12427
N90-12432
N90-12437
N90-12444
N90-12447
N90-12451
HEIDELBERGER, PHILIP N90-12267
HEIDNER, R. F., III N90-12303
HELLENDOORN, HANS N90-12274
HENDERSON, THOMAS B. N90-12186
HENSHAW, W. F. N90-11866
HERANDO, ANTONIO N90-11996
HERMAN, BENJAMIN N90-12071
HERMAN, MICHAEL H. N90-12376
HERRMANN, KARIN N90-12089
HERVIG, LINDA K. N90-12161
HEUBAUM, FRANK H. N90-11868
HICKS, BRUCE B. N90-12109
HIGHBARGER, LANE N90-12150
HILL, DAVID A. N90-11925
HIRVONEN, JUHA-PEKKA N90-11856
HISKES, J. R. N90-12294
HITCHON, W. N. G. N90-12328
HJALMARSON, H. P. N90-12349
HO, Y. H. N90-11825
HOFER, W. W. N90-12363
HOFF, R. W. N90-12419
HOFFBAUER, M. A. N90-11857
HOFFMAN, DONALD D. N90-12180
HOFFMANN, E. N90-12309
HOFFMEYER, J. A. N90-11913
HOGAN, PERRY M. N90-12170
HOGAN, R. P. N90-12151
HOLDEN, K. A. N90-11776
N90-11777
HOLLOWAY, J. S. N90-12303
HOLMAN, GORDON D. N90-12462
N90-12478
HOLMES, CAROL A. N90-12025
HOLT, HENRY E. N90-12454
HOLTSLAG, A. A. M. N90-12141
HOLTZCLAW, K. L. N90-12114
HOOKE, LYDIA RAZRAN N90-12152
N90-12153
N90-12154
HORWAT, WALDEMAR N90-12187
N90-12197
HOSNI, M. H. N90-11980
HOUSTON, S. H. N90-12081
HOVENAC, EDWARD A. N90-11999
HOWELL, R. H. N90-12358
HSU, KEN-YUH N90-12216
HUANG, F. H. N90-11864
HUANG, HUO-JIN N90-12062
N90-12065
HUANG, THOMAS S. N90-12213
N90-12214
HUANG, YIZHOU N90-12371
HUANG, YUNQING N90-12252
HUBBARD, ROGER W. N90-12164
HUDSON, H. S. N90-12469
N90-12474
HUERKAMP, G. N90-11936
HUFFMAN, R. E. N90-12124
N90-12125
N90-12126
N90-12127
N90-12493
HUGHES, T. J. N90-12483
HUGUENIN, R. N90-12125
N90-12126
HULBURT, E. O. N90-12467
HULL, JOHN R. N90-12361
HUMMEL, K. E. N90-11903
N90-12195
HUMMEL, KIRK E. N90-12105
HUNG, CHING-MAO N90-11970
HUNG, STEPHEN THINK N90-11960
HURFORD, G. J. N90-12474
N90-12490
HURLEY, JAMES A. N90-11850
HURLEY, KEVIN N90-12470
HURRELL, JAMES W. N90-12065
HYVONEN, REIJO N90-12116

I

IKEDA, TAMEHARU N90-11737
IMBRIE, JOHN N90-12101
INGELS, FRANK N90-11802
INOUYE, MAMORU N90-11699
ISAAC, K. M. N90-11825
ISHII, ALEXANDER TOICHI N90-11957
ISOBE, TOSHIO N90-12185
N90-12191
IVANCIC, WILLIAM D. N90-11915
IWASAKI, AKIHITO N90-11696

J

JACKSON, A. C. N90-11821
JACKSON, M. C. N90-12340
JACOBSEN, B. N90-12118
JACOBSON, M. J. N90-12290
JAHANMIR, S. N90-12396
JAHNS, G. C. N90-12151
JAMES, BONNIE F. N90-12062
JAMES, J. H. N90-12241
JANATA, JIRI N90-12159
JANIK, DIETER N90-11935
JANKOWSKI, A. F. N90-11812
JANSSEN, G. J. M. N90-11939
JATKO, W. B. N90-12318
JEAN, Y. C. N90-12358
JECKO, B. N90-11716
JENISTA, J. N90-12330
JENSEN, DOUGLAS R. N90-12136
JERVIS, THOMAS R. N90-11856
JIANG, BO-NAN N90-12231
JILLING, A. N90-12148
JOERG, CHARLES F. N90-12353
JOHN, LAWRENCE E. N90-11770
JOHNSON, D. A. N90-11978
JOHNSON, LARRY E. N90-11736
JOHNSON, R. N90-12333
JOHNSON, W. JOEL D. N90-12016
JOHNSON, W. N. N90-12467
N90-12474
JOHNSON, WARREN B. N90-11731
N90-12113
JOHNSTON, R. G. N90-12012
JONES, DAVID A. N90-11896
JONES, DONALD W. N90-12107
JONES, G. J. N90-12094
JONES, G. T. N90-12309
JONES, HARRISON P. N90-12461
JONES, MARK T. N90-12193
JONES, PHILLIP L. N90-11890
JONES, R. W. L. N90-12309
JONG, KWO-YIH N90-12037
JOOS, HANS-DIETER N90-12404
JORDAN, THOMAS H. N90-12120
JOSHI, CHAN N90-12335
JURGENS, R. F. N90-12424

K

KABACOFF, LAWRENCE T. N90-11996
KAHN, JON B. N90-11798
KAHN, R. N90-12438
KAISER, J. H. N90-12358
KALKER, J. J. N90-12032
KALNS, I. N90-12411
KAMIKAWA, NEIL N90-12323
KAMINSKI, MARK N90-12159
KANE, SHARAD R. N90-12478
KANELLAKOPOULOS, IOANNIS N90-12220
KANMURI, AKIO N90-11803
KANN, DEIRDRE M. N90-12065

KANNE, W. R. N90-12027
KAPLAN, MICHAEL L. N90-12133
KARITA, TAKESHI N90-11803
KARO, A. M. N90-12294
KARYAMPUDI, V. MOHAN N90-12133
KASBEKAR, ANNAND D. N90-11890
KATSOULEAS, T. N90-12335
KATZER, EDGAR N90-11711
KAYS, R. N90-11936
KEATING, TERRY N90-12410
KEEN, JOHN N90-12187
KEFAUVER, H. LEE N90-11919
KEITH, E. I. N90-11866
KELLEDES, W. N90-12411
KENNEDY, B. W. N90-12309
KENNEDY, FRANCIS E., JR. N90-12028
KENNEDY, ROBERT S. N90-12174
N90-12175
KENNISH, RICHARD A. N90-11888
KERR, W. C. N90-12296
N90-12297
KESSLER, W. J. N90-12114
KESSLER, WILLIAM S. N90-12143
KHANNA, SUNIL N90-12155
KHORRAMI, MEHDI R. N90-11968
KIDD, GEORGE J., JR. N90-12386
KIM, ANDERSON H. N90-11941
KINDELBERGER, DAVID N90-11836
KINDLER, KNUD N90-11767
KINI, ARAVINDA M. N90-12356
KIPLINGER, ALAN L. N90-12466
N90-12491
KIRCHMAYR, HANS N90-12285
KIRJAVAINEN, KARI N90-12092
KLEIN, CHARLES J. N90-12025
KLEIN, WILLIAM E. N90-12034
KNAUSS, W. G. N90-12051
KNIFFEN, DONALD A. N90-12464
KNOESEN, ANDRE N90-11921
KOCZAK, M. J. N90-11810
KOCZAK, MICHAEL J. N90-11852
KOEHLER, DALE R. N90-12353
KOEHLER, H. DIETER N90-12494
KOEKOEK, J. N90-12253
KOEKOEK, ROELOF N90-12253
N90-12263
KOFFEND, J. B. N90-12303
KOGA, DENNIS J. N90-11707
KOHSIEK, W. N90-12140
KOLKMAN, H. J. N90-11750
KOMAR, C. A. N90-11828
KOOCHESFAHANI, MANOOCHER M. N90-11706
KOOI, B. W. N90-12056
KOOY, AD N90-11855
KOWEL, STEPHEN T. N90-11921
KOZAK, RICHARD C. N90-12439
N90-12440
N90-12445
N90-12446
KRAMER, J. F. N90-11897
KRAWITZ, ROBERT L. N90-12237
KRIMIGIS, S. M. N90-12484
KROEGER, D. M. N90-12365
KROSS, B. N90-12001
KRUMPELT, M. N90-11950
KRUSIUS, J. PETER N90-12372
KUCHNIR, M. N90-11811
KUHLMANN, JOHN M. N90-11702
KUHN, ALLEN D. N90-12400
KUHN, RICHARD E. N90-11751
KUHN, WILLIAM P. N90-12316
KUMAR, R. N90-11950
KUNDU, MUKUL R. N90-12472
N90-12478
KUNTZ, LOIS-ANN N90-12174
N90-12175
KUNTZ, STEFFAN N90-12112
KUNZ, G. J. N90-12137
N90-12138
KURFESS, J. D. N90-12460
N90-12467
KUSSE, B. R. N90-12338
KUSSMANN, ALFRED N90-12099
KVATERNIK, RAYMOND G. N90-12057
KWATNY, HAROLD G. N90-11756
KYRALA, GEORGE A. N90-11830

L

LAAKKONEN, J. N90-11827
LABARGE, W. L. N90-11821
LABONTE, B. J. N90-12489
LABOV, S. N90-12004
LAINE, RICHARD M. N90-11888
LALLI, VINCENT R. N90-12034
LAMBRECHT, A. N90-12023
LAMPINEN, MARKKU J. N90-12092
LANCE, M. B. N90-11701
LANDIS, D. N90-12004
LANDRIANI, G. SACCHI N90-12266
LANG, KENNETH R. N90-12471
LANGEL, R. A. N90-12115
LANKFORD, JAMES N90-11882
LARIVEE, MICHAEL N90-12187
LARRABEE, J. C. N90-12493
LARSON, BENNETT C. N90-12352
LARSON, GERALD E. N90-12181
LARSON, KEVIN P. N90-12129
LARSON, RICHARD G. N90-12228
LASHER, MARK E. N90-12186
LATAITIS, RICHARD J. N90-12010
N90-12315
LAURENT, P. J. N90-12257
LAURENT, PIERRE-JEAN N90-12256
LEBLANC, F. J. N90-12124
N90-12493
LECHTER, WILLIAM N90-12346
LEE, HONG-TAO N90-12033
LEE, PETER H. Y. N90-11830
LEE, R. H. N90-11883
LEE, S. Y. N90-11922
LEE, SUNG M. N90-11907
LEE, Y. T. N90-11835
LEFTWICH, PRESTON W., JR. N90-12134
LEHOCZKY, JOHN N90-12205
LEHTO, A. N90-11959
LEIBY, PAUL N. N90-12107
LEIGHTON, TOM N90-11955
N90-12198
N90-12236
N90-12238
LEIMKUHLER, BENEDICT N90-12243
LEMAL, DAVID M. N90-11844
LEMEN, J. R. N90-12475
LENGSFIELD, BYRON H., III N90-12299
LENSCHOW, DONALD H. N90-12109
LESKOVAR, BRANKO N90-12322
LESLIE, FRED W. N90-12059
N90-12077
LETHIN, RICH N90-12187
LEU, LII-YUH N90-12269
LEUNG, MUN K. N90-12213
N90-12214
LEUPOLD, HERBERT A. N90-12280
LEVIN, BARBARA C. N90-12150
LEVIN, JON C. N90-12301
LEVIS, ALEXANDER H. N90-11724
LEWIS, W. J. N90-11749
LEWKOWITZ, S. N90-11721
LI, HSIN-YU N90-12216
LIANG, TACHEN N90-12246
N90-12270
LIGHT, JEFFREY S. N90-11700
LINDBERG, PER N90-12373
LINDELL, ISMO V. N90-11839
N90-11926
LINDEMUTH, IRVIN R. N90-11998
LINGENFELTER, R. E. N90-12463
LINNARTZ, J. P. G. M. N90-11938
LINTZ, A. T. N90-12114
LITTLE, B. H. N90-11738
N90-11739
LITVIN, FAYDOR L. N90-12033
LIU, C. H. N90-12117
LIU, J. Z. N90-12360
LIVINGSTON, JAMES D. N90-11862
LLEWELYN-DAVIES, D. I. T. P. N90-11712
LO, C. C. N90-11953
LOCKWOOD, JOHN A. N90-12468
LOEFFLER, F. J. N90-12311
LOFTIS, J. P. N90-12397
LOH, HORNG-HAI N90-12176
LOHNER, RAINALD N90-12336
LOMDAHL, P. S. N90-12296
N90-12297
LONG, MARGE N90-12017
LONG, W. C. N90-11789
N90-11790
N90-11791
LOOIJE, C. E. W. N90-11877
LOPATIN, CRAIG N90-11816
LOVE, PHILIP H. N90-11980
LOWE, DAVID N90-12226
LU, EDWARD T. N90-12481
LU, SHIH-LIEN N90-12203
LUEHR, H. N90-12118
LUFT, PETER A. N90-12196
LUI, MANCHEUNG N90-12025
LUK, TING SHAN N90-12021
LUO, REN C. N90-12176
LUO, W. N90-12259
LUO, ZHI-QUAN N90-12240
LUTZ, H. N90-12024
LYNCH, GARY N90-12158
LYON, GORDON E. N90-12201

M

MA, HI-KEUNG TONY N90-11956
MAASCH, KIRK A. N90-12063
MACKIN, THOMAS J. N90-12179
MACKINNON, R. F. N90-11924
MADAN, RAM C. N90-11822
MADDEN, N. N90-12004
MAGUIRE, M. C. N90-11859
MAIGRET N90-11894
MAITRE, HENRI N90-12258
MALCOLM, PERRY R. N90-11755
MALLAT, J. N90-11959
MALONE, R. D. N90-11828
MALONE, THOMAS F. N90-12101
MAMMONE, ROBERT J. N90-11879
MANDEL, GEORGE N90-12388
N90-12389
MARCHITTI, M. N90-11735
MARCUS, ALLAN N90-12104
MARGOLIN, L. G. N90-12045
MARIANI, ELIO A. N90-11914
MARINE, MICKY C. N90-11770
MARINELLI, W. J. N90-12114
MARINO, A. J. N90-11787
MARK, W. D. N90-11704
MARQUEZOLIVARES, JAIME N90-11991
MARTEN, H. D. N90-11801
MARTIN N90-11894
MARTIN, ANTHONY G. N90-11816
MARTIN, DAVID W. N90-12142
MARTIN, JOEL J. N90-12009
MARTIN, T. H. N90-11947
MARTZLOFF, FRANCOIS D. N90-12135
MARZIK, JAMES V. N90-12371
MASON, S. N90-12366
MASSON, GERALD M. N90-12212
MATTESON, J. L. N90-12469
MATTHEWS, ELAINE N90-12090
MATZ, S. M. N90-12467
MAYES, PAUL N90-11928
MAZANEK, M. N90-11959
MAZZELLA, ANDREW J., JR. N90-12129
MCALLESTER, DAVID N90-12221
MCCANDLISS, STEPHAN ROBERT N90-12412
MCCANTS, C. N. N90-11785
MCCARTHY, J. MICHAEL N90-12202
MCCREERY, RICHARD L. N90-11845
MCCURDY, C. WILLIAM N90-12299
MCDERMOTT, KATHLEEN M. N90-11850
MCELROY, MICHAEL B. N90-12101
MCFADDEN, G. B. N90-11967
MCGUIRK, JAMES P. N90-12070
MCILRATH, THOMAS J. N90-12304
MCILWAIN, R. L. N90-12311
MCKEAN, M. E. N90-12479
N90-12480
MCKINLEY, B. J. N90-12003
MCLAMB, DAVE N90-12104
MCPHERSON, ARMON N90-12021
MCTIERNAN, JAMES M. N90-12298
N90-12458
MECARTNEY, MARTHA L. N90-12374
MEE, BRIAN E. N90-12406
MEEGAN, C. A. N90-12469
MEI, Z. N90-11865
MEISTER, MARK A. N90-11934
MELKONIAN, L. N90-12004
MELONE, NANCY N90-12206
MENEES, GENE P. N90-11742
MENG, CHING-I. N90-12123
MENRATH N90-11894
MENTER, FLORIAN N90-11992
MEREWETHER, KIM N90-11932
MERKLE, J. G. N90-12046
MERKLE, K. L. N90-12358
MESZAROS, P. S. N90-12295
MICHAEL, JOEL N90-12162
MICHAL, GARY M. N90-11853
MICHEL, ULF N90-12326
MICKEY, D. L. N90-12489
MIER-Y-TERAN, L. N90-11846
MIESCKE, KLAUS J. N90-12245
MILLER, D. H. N90-12311
MILLER, DWIGHT P. N90-12319
MILLER, HARRY B. N90-11942
MILLER, IRVIN M. N90-11823
MILLER, J. R. N90-12364
MILLER, M. K. N90-12420
MILLER, TIMOTHY N90-12077

MILLETT, I. N90-12004
MILLS, JONATHAN A. N90-11962
MINEEV, V. P. N90-12351
MINKE, DIERK N90-12208
MINOUX, MICHEL N90-12258
MISIEWICZ, JOLANTA N90-12273
MISRA, B. N90-11950
MITCHELL, B. J. N90-12128
MITTRA, RAJ N90-11932
MIYOSHI, KAZUHISA N90-11880
N90-11881
MIZELL, DAVID N90-12204
MOBAYEN, M. M. N90-12309
MOIR, R. W. N90-12312
MONNA, W. A. A. N90-12140
MONTGOMERY, NOEL D. N90-12171
MOONEY, HAROLD A. N90-12101
MOORE, H. J. N90-12441
MORDFIN, LEONARD N90-12036
MORICONI, MARK N90-12207
MORRIS, A. S. N90-11966
N90-12029
N90-12030
N90-12031
N90-12218
N90-12223
N90-12225
MORRIS, J. W., JR. N90-11865
MORRIS, PATRICK M. N90-11752
MORRIS, ROBERT C. N90-12017
MORRISON, D. R. O. N90-12309
MORROW, JOHN G. N90-11761
MORTAZAVI, M. A. N90-11921
MORTENSEN, A. N90-11810
MOSELEY, J. T. N90-12343
MUENCHAUSEN, R. E. N90-11857
MULDER, J. A. N90-11754
MULLER, RICHARD S. N90-11961
MUNSHI, M. Z. N90-11958
MURMAN, EARLL M. N90-11983
MURPHREE, J. S. N90-12118
MURPHY, GEORGE P. N90-11755
MURPHY, H. C. N90-12114
MURPHY, R. J. N90-12467
MURRAY, B. T. N90-11967
MURTHY, T. SREEKANTA N90-12057
MUYSHONDT, G. PATRICK N90-11946

N

NAGATI, M. G. N90-11765
NAGEL, W. N90-12100
NAGY, LAWRENCE A. N90-11915
NARASIMHAN, DAVE N90-12017
NASTASI, MICHAEL N90-11856
NATHAN, TERRENCE R. N90-12075
NAUDTS, J. N90-12278
NELSON, S. D. N90-12317
NELSON, THOMAS O. N90-12177
NELSON, THOMAS P. N90-12105
NEVITT, TIMOTHY J. N90-12083
NEWMAN, HARVEY N90-12347
NEWMAN, MARK N90-12236
N90-12238
NEWTON, A. RICHARD N90-11956
NICHOLS, F. A. N90-11883
NICHOLSON, M. M. N90-11721
NICOLA, VICTOR F. N90-12267
NICOLAIDES, R. A. N90-11986
NIELSEN, DALE E., JR. N90-11920
N90-12337
NIEMINEN, R. M. N90-11827
NIKOSKINEN, KEIJO I. N90-11927
NISSIM, E. N90-12042
NIU, B. N90-11835
NOGUCHI, YOSHIO N90-12039
NORMAN, THOMAS R. N90-11700
NORRIS, J. P. N90-12474
NORTH, A. N90-12411
NORTON, JOHN D. N90-11843
NUTH, PETER N90-12187
NUTTLI, O. W. N90-12128

O

ODONNELL, R. A. N90-11784
OGLESBY, ROBERT N90-12063
OGUCHI, KEIKO N90-12185
OHTAKE, KUNIHIKO N90-12039
OKIA, AMINAT N90-11771
OKUYAMA, MASAHIRO N90-11696
OLIVA, RUDOLF N90-12007
OLIVEIRA, M. S. N90-12413
OLSEN, LARRY C. N90-12097
OLSON, DAVID L. N90-11815
OLSON, JOHN V. N90-11933
ONEALE, S. W. N90-12309
ONEIL, W. N90-12411
ONO, KOUICHI N90-12039
ORR, H. N90-11887
ORR, J. S. N90-11887
ORWIG, LARRY E. N90-12474
N90-12476
N90-12491
OSHER, J. E. N90-11977
OSHER, STANLEY N90-12182
OTTENS, H. H. N90-12056
OTTO, DIETER N90-12007
OWENS, B. B. N90-11958
OWENS, D. H. N90-12271
N90-12276
N90-12277
OWENS, JOHN N90-11802

P

PAABO, MAYA N90-12150
PACIESAS, W. S. N90-12469
PACKARD, RICHARD T. N90-11845
PADOVANO, ERALDO N90-11820
PALFREY, T. R. N90-12311
PALMER, R. B. N90-11952
PAN, WEN-SEN N90-11847
PANDHARIPANDE, V. R. N90-12300
PANDOLFO, LIONEL N90-12063
PAPPU, SUGUNA N90-12025
PARK, JAMES K. N90-12188
PARKMAN, W. E. N90-11782
N90-11792
PARNELL, T. A. N90-12469
PARTRIDGE, P. G. N90-11875
N90-11876
N90-12053
N90-12054
PATEL, JANAK H. N90-12213
N90-12214
PATRICK, MERRELL L. N90-12193
PATTERSON, E. M. N90-12020
N90-12082
PATTNAIK, A. N90-11866
PAYNE, KAREN N90-12077
PEDIGO, CATHERINE B. N90-12065
PEI, G. N90-11821
PEISEN, DEBORAH N90-12406
PELLINEN-WANNBERG, A. N90-12118
PELTONEN, J. N90-11959
PENDLETON, G. N. N90-12469
PENDRILL, LESLIE N90-12014
PENG, J. L. N90-12354
PEPPER, SUSANNE M. N90-12028
PERCEC, V. N90-11878
PERKINS, D. K. N90-11866
PERSON, J. C. N90-12114
PETERKA, R. J. N90-12178
PETERS, P. N. N90-12345
PETERSON, L. E. N90-12469
PETERSON, M. B. N90-12396
PETROSIAN, VAHE N90-12298
N90-12458
N90-12481
PETTIT, DONALD R. N90-12000
PETTY, CLINTON CRAIG N90-12327
PEYTONJONES, J. C. N90-12249
PFAFMAN, T. N90-12004
PFEIFFER, SHLOMO L. N90-11805
N90-11806
PHILLIPS, CYNTHIA A. N90-12199
N90-12237
PHILLIPS, R. J. N90-12442
PICKENS, JOSEPH R. N90-11868
PIEPER, S. C. N90-12300
PIERONEK, JAMES V. N90-11934
PIETZ, K. C. N90-11784
PINCOSY, P. A. N90-11951
PIPER, L. G. N90-12114
PITMAN, W. A. N90-11821
PIZZARELLO, F. A. N90-11721
PLASIL, F. N90-12302
PLAUT, J. J. N90-12424
N90-12443
POCHA, M. D. N90-12363
POLAND, D. T. N90-11739
POLKOWSKA-SEMENIUK, MARIA N90-12262
N90-12265
POLKOWSKI, LECH T. N90-12262
N90-12265
POLLARD, C. O. N90-12082
POLLICK, FRANK E. N90-12180
PONCHAK, G. E. N90-11943
POND, JEFFREY N90-12347
PONNAPPAN, RENGASAMY N90-12379
PONTE, RUI VASQUES DEMELO N90-12145
PORTNOY, WILLIAM M. N90-11946
POST, H. N. N90-12094
POST, JOHN THEODORE N90-12040
POUCH, JOHN J. N90-11880
POULSEN, OVE N90-12014
POWELL, D. C. N90-12095
POWELL, RICHARD C. N90-12009
PREWO, K. N90-11810
PREWO, K. M. N90-11818
PRINN, R. G. N90-12428
PRINZ, GARY Z. N90-12281
PROKOPIUS, PAUL R. N90-11804
PRUST, CHET D. N90-11787
N90-11793
N90-11794
N90-11795
N90-11796
N90-11797
PRUST, E. E. N90-11774
PSALTIS, DEMETRI N90-12216
PUZZO, DEAN C. N90-11934
PYLKKAENEN, THOMAS N90-12092
PYTEL, JEAN LANDA N90-12179

Q

QUEMARD, C. N90-11768
QUINN, B. J. N90-11747
QUINN, GEORGE D. N90-11889

R

RAADU, MICHAEL A. N90-12421
RABINOWITZ, PAUL H. N90-12229
RADEMACHER, STEVEN E. N90-12171
RADOUSKY, H. B. N90-12354
N90-12362
RAEISAENEN, A. N90-11959
RAEISAENEN, ANTTI V. N90-11944
RAGNI, JAMES E. N90-11731
RAHAMAN, MOHAMED N. N90-11886
RAHN, JEFFREY A. N90-11888
RAJKUMAR, RAGUNATHAN N90-12403
RAMAKER, DAVID E. N90-11842
RAMASWAMY, R. V. N90-12325
RAMBO, PETER W. N90-12337
RAMBONE, JAMES D. N90-11762
RAMOHALLI, KUMAR N90-11770
RAMSAY, JOHN B. N90-11972
RAO, SATISH N90-12198
RAPPAPORT, CATHERINE N90-12159
RARIDON, R. J. N90-12295
RAUS, J. N90-12329
RAYNER, S. N90-12358
RAYNER, STEVE N90-12107
READ, B. E. N90-11895
REAGAN, JOHN N90-12071
REDDY, N. N. N90-11738
REDNER, SIDNEY N90-12286
REE, FRANCIS H. N90-11829
N90-11832
REHN, L. E. N90-12360
REINIGER, KLAUS N90-12099
REINOVSKY, ROBERT E. N90-11998
REISTER, DAVID B. N90-12219
RENLUND, ANITA M. N90-12019
RENTON, MARGARET B. N90-12406
RESCIGNO, T. N. N90-12299
REUTT-ROBEY, J. E. N90-11835
REVENAUGH, JUSTIN S. N90-12120
REX, D. N90-11772
REYNOLDS, NATHANIEL D. N90-12068
N90-12077
RHODES, CHARLES K. N90-12021
RIDGWAY, J. R. N90-12115
RILEY, DONALD R. N90-11751
RIPKENS, MICHAEL N90-12172
RITCHIE, JACK L. N90-12342
ROBERTS, D. W. N90-12020
ROBERTS, KARI M. N90-12444
ROBERTS, THOMAS W. N90-11703
ROBERTSON, FRANKLIN R. N90-12062
N90-12065
ROBERTSON, J. S. N90-12290
ROBINSON, GARY Y. N90-12367
ROBINSON, PATRICK N90-12176
ROCHE, C. T. N90-12359
ROCK, PAUL B. N90-12163
RODGERS, M. A. J. N90-12306
RODINA, DAN D. N90-11770
ROEDEL, JUERGEN N90-11885

ROOS, C. N90-12210
ROSE, HARVEY A. N90-12119
ROSE, MADELINE S. N90-12163
ROSS, B. A. N90-12313
ROSS, MARVIN N90-12455
ROSTOKER, G. N90-12118
ROTHE, K. E. N90-12295
ROTHERMEL, JEFFRY N90-12079
ROUSSAUD, A. N90-11716
ROVICK, ALLEN N90-12162
ROWE, JOSEPH N90-12152
N90-12153
N90-12154
RUEHLE, MANFRED N90-12352
RUGG, B. C. N90-12382
RUGGLES, M. B. N90-11858
RUIJGROK, G. J. J. N90-12291
RUIZENAAR, A. J. N90-11937
RUSSELL, DAVID N90-12119
RUSSELL, K. F. N90-12420
RUSSELL, KENNETH C. N90-11867
RYAN, J. M. N90-12460
RYAN, JAMES M. N90-12468
RYAN, P. M. N90-12295
RYDER, DANIEL F., JR. N90-12371
N90-12377
RYU, JAE N90-12371

S

SABAKA, T. J. N90-12115
SACCUZZO, DENNIS P. N90-12181
SAIIDI, MO J. N90-11783
N90-11786
SAKAMOTO, N. N90-12310
SALMELIN, R. H. N90-12351
N90-12369
SALOMAA, M. M. N90-12351
N90-12368
N90-12369
N90-12370
SALTZMAN, BARRY N90-12063
SANDAHL, J. N90-12118
SANO, MASAAKI N90-11697
SANTANDREA, D. P. N90-12290
SANTAVICCA, D. A. N90-11841
SANTORU, JOSEPH N90-11773
SARAVANOS, D. A. N90-11806
SARRIS, E. T. N90-12484
SAUL, R. N90-12411
SAUNDERS, R. S. N90-12424
SAVAGE, HOWARD T. N90-11996
SAVAGE, P. D., JR. N90-12151
SCANLAN, R. M. N90-12284
SCHABER, GERALD G. N90-12435
N90-12439
N90-12440
N90-12445
N90-12446
SCHENCK, H. A. N90-12293
SCHERSON, DANIEL A. N90-11826
SCHEUNDERS, P. N90-12278
SCHIRBER, J. E. N90-12349
SCHLICH, HUGO N90-11873
SCHLUETER, WOLFGANG N90-12087
SCHMECKPEPER, K. R. N90-11779
N90-11780
N90-11781
SCHNEIDER, B. I. N90-12299
SCHOENBORN, B. N90-12366
SCHON, DONALD A. N90-12383
SCHORK, TOM N90-11990
SCHROEDER, H. N90-11936
SCHRYER, DAVID R. N90-11823
SCHUELLER, ANTON N90-11993
SCHULKES, R. M. S. M. N90-11989
SCHULTHEISZ, C. R. N90-12051
SCHULTZ, ARTHUR J. N90-12356
SCHULTZ, DONALD F. N90-11824
SCHUMACHER, ROBERT W. N90-11773
SCHWABE, ERIC N90-12236
SCHWARTZ, R. A. N90-12486
SCHWARZ, KURT F. N90-12387
SCOFIELD, RODERICK A. N90-12086
SCOLARIS, M. N90-11872
SCOTT, JAMES N. N90-11743
SCULLION, T. N90-11994
SEDLACEK, Z. N90-12330
SEIDMAN, DAVID N. N90-12352
SELIG, WALTER S. N90-11851
SENSKE, D. A. N90-12447
SEPCENKO, VALENTIN N90-12047
SETTLES, GARY S. N90-11988
SHA, LUI N90-12205
N90-12403
SHAH, GAUTAM H. N90-11751
SHAHABUDDIN, PERWEZ N90-12267
SHALKHAUSER, MARY JO N90-11915
SHAND, M. A. N90-12306
SHAPIRO, S. M. N90-11863
SHARE, G. H. N90-12467
SHARMA, R. P. N90-12360
SHARPE, LISA M. N90-11963
SHAW, BARBARA RAMSAY N90-12157
SHEFFIELD, STEPHEN A. N90-11973
N90-12000
SHELTON, R. N. N90-12354
N90-12362
SHEN, Z. X. N90-12373
SHERMAN, R. N90-12200
SHIBATA, E. I. N90-12311
SHINE, R. N90-12487
SHIRLEY, D. A. N90-11835
SHOEMAKER, C. S. N90-12446
SHOEMAKER, E. M. N90-12446
SIEGMANN, W. L. N90-12290
SIEKHAUS, W. J. N90-12015
SIHVOLA, ARI H. N90-11839
N90-11926
SILK, JOSEPH I. N90-12418
SILVER, E. N90-12004
SILVER, GARY L. N90-12234
SILVERBERG, M. N90-11936
SILVONEN, KIMMO N90-11916
SIMONS, R. N. N90-11943
SIMONSEN, HARALD N90-12014
SIMPSON, W. F., JR. N90-12391
SINCLAIR, S. K. N90-11782
SINGH, U. N. N90-12011
SINGHAM, SHERMILA BRITO N90-12083
SISK, R. C. N90-12345
SITES, J. R. N90-12093
SKALICKY, PETER N90-12285
SKUDERA, WILLIAM J., JR. N90-11914
SLADE, M. A. N90-12424
SLATTERY, W. L. N90-12339
SLAUGHTER, B. C. N90-11775
N90-11778
SLEDGE, DONNA N90-12104
SLEEP, N. H. N90-12448
SLYUTA, E. N. N90-12425
SMALDONE, L. A. N90-12477
SMALL, GARY W. N90-11840
SMITH, F. T. N90-11698
SMITH, G. R. N90-11849
SMITH, GORDON S. N90-11851
SMITH, PHILLIP J. N90-12061
SOLANKI, RAJ N90-12367
SOMMER, MICHAEL N90-12470
SOMMERS, ROBERT S. N90-11900
SON, SANG N90-12403
SORENSEN, DANNY N90-12194
SORRELLS, J. E. N90-11758
SPALVINS, TALIVALDIS N90-11902
SPEICH, D. N90-12482
SPENCER, R. H. N90-11692
SPERLING, GEORGE N90-12160
SPICER, WILLIAM E. N90-12373
SPIELVOGEL, BERNARD F. N90-12157
SPRUNT, BRINKLEY N90-12205
SPURGEON, WILLIAM A. N90-12371
N90-12377
SRIVASTAVA, SANTOSH K. N90-12305
STAHL, BERNHARD N90-12326
STARR, R. N90-12474
STECK, ANDREW J. N90-11847
STEEL, J. N90-11719
STEINBERG, DANIEL J. N90-11861
STEINHAUSER, REINHOLD N90-11760
STEPHENS, MICHAEL A. N90-12268
STETLER, KURT A. N90-11830
STEWART, THOMAS B. N90-11801
STICKFORD, GEORGE H. N90-12026
STINE, J. R. N90-11897
STOCKEL, J. N90-12331
STODOLSKY, FRANK N90-11949
STOELLENWERK, F. N90-11936
STOFAN, E. R. N90-12449
STONE, MAUREEN C. N90-12184
STORM, C. B. N90-11897
STORM, MICHELE E. N90-12239
STRANDBURG, KATHERINE J. N90-12355
STRAUCH, RICHARD G. N90-11911
STRINGER, WILLIAM J. N90-12085
STRINGFELLOW, GUY S. N90-12339
STRONG, K. T. N90-12475
STROUB, R. H. N90-11701
STRUM, M. J. N90-12364
SUDAN, R. N. N90-12338
SUEMATSU, KAZUYO N90-12191
SUEMATSU, SYUNJI N90-12185
SUH, S. H. N90-11846
SULLIVAN, GREGORY F. N90-12212
SUMMERS, GILBERT L. N90-11731
SUMMERS, L. T. N90-12364
SUMMERS, LESLIE J. N90-11851
SUN, L. C. N90-12149
SUNG, CHONG SOOK PAIK N90-11817
SUNG, D. Y. N90-11701
SUNG, NAKHO N90-11817
SWAIN, L. J. N90-11783
SWANN, MADELINE N90-11899
SWANSON, RONALD A. N90-11816
SWIFT, G. N90-11738
SWITHINBANK, CHARLES N90-11908
SYRETT, WILLIAM N90-12067
SYVASALMI, J. N90-11959
SZYMCZAK, WILLIAM G. N90-11985

T

TACKE, M. N90-12023
TAGUE, J. L. N90-11811
TAKAHASHI, HITOSHI N90-11696
TAKALA, BRUCE E. N90-11972
TAKEMORI, H. T. N90-11951
TAMMELIN, BENGT N90-12116
TANG, CHUNG-MUH N90-12063
TANG, LIN N90-12028
TANK, VOLKER N90-12008
TAPPING, K. F. N90-12483
TARBELL, T. N90-12487
TARVER, C. N90-11976
TAYLOR, B. N90-11953
TAYLOR, ROBERT P. N90-11980
TAYLOR, T. N. N90-11857
TEETER, RONALD N90-12152
N90-12153
N90-12154
TENHAVE, A. A. N90-12055
TERRELL, DUDLEY J. N90-11723
TERRY, P. F. N90-12189
TESSLER, ALEXANDER N90-12049
THIESEN, REIMER N90-12099
THOMAS, M. G. N90-12094
THOMASSON, MAGNUS N90-12415
THOMPSON, T. W. N90-12441
TIGGES, C. P. N90-12349
TIRRI, HENRY N90-12394
TIRSELL, K. G. N90-12003
TISCHLER, MARK B. N90-11752
TITLE, A. N90-12487
TITRAN, ROBERT H. N90-11854
TJEE, R. T. H. N90-11754
TOJYO, E. N90-12310
TOLENDINO, L. F. N90-12317
TOLMUNEN, TIMO J. N90-11944
TOMAZOS, D. N90-11878
TOMLINS, P. E. N90-11895
TOMPKINS, RUTH N90-11891
TOOMRE, JURI N90-12076
TOPKA, K. N90-12487
TOTH, LOUIS N90-12346
TOWNEND, C. K. N90-11729
TOZZI, G. P. N90-12477
TRAD, LAURIE A. N90-12163
TRAHAN, W. H. N90-11774
N90-11784
TRAN, DUC T. N90-12400
TREDWAY, W. K. N90-11818
TRENT, B. C. N90-12045
TRETYAKOV, SERGEI A. N90-11926
TRIZNA, DENNIS B. N90-11931
TROTT, WAYNE M. N90-12019
TROXEL, SETH W. N90-11934
TSITSIKLIS, JOHN N. N90-12240
TUAN, PHAM DINH N90-12255
TUCKER, GEORGE T. N90-11752
TUOVINEN, J. N90-11959
TURCHI, P. E. A. N90-12358
TURCOTTE, D. L. N90-12450
TURNER, TRAVIS L. N90-12292
TUTHILL, CLINTON D. N90-12353
TWARDY, HARALD N90-11893

U

UPCHURCH, BILLY T. N90-11823
UPSCHULTE, B. L. N90-12114
UZAN, J. N90-11994

V

VAHALA, GEORGE N90-12341
VALLONE, VINCENZO N90-11820

VALOVIC, M. N90-12331
N90-12332
VANBEEK, F. N90-12474
VANDENHEUVEL, J. C. N90-12350
VANDERBEEK, C. G. A. N90-12261
VANDERVEEN, J. F. N90-11857
VANDERVLIET, J. G. N90-12140
VANDERVORST, HENK A. N90-12252
N90-12260
VANDEVEN, H. N90-12266
VANES, BERT N90-12275
N90-12279
VANGEER, J. N90-12043
VANGRAAS, FRANK N90-11730
VANKA, S. PRATAP N90-11837
VANLOON, A. J. N90-12100
VANNORMAN, JOHN D. N90-11823
VANPAASSEN, D. M. N90-12291
VANRIJN, AFKE N90-12209
VANSTRIEN, SEBASTIAN N90-12251
VANWESTRHENEN, R. M. N90-12141
VAZQUEZ, ISAURA N90-11850
VELOSKI, GARRET N90-11836
VENGAYIL, PADMARAJ N90-12144
VENKATAPATHY, E. N90-12211
VERMEULEN, P. G. N90-12043
VICKERS, ROSS R., JR. N90-12161
VIITANEN, ARI J. N90-11926
VINCENT, DAYTON G. N90-12065
VINYARD, SHANNON N90-11882
VIRKAR, ANIL V. N90-11892
VITTORIA, CARMINE N90-12371
VOGEL, M. H. N90-11940
VOGLER, L. E. N90-11913
VOIGT, ROBERT G. N90-12183
VOLKERT, RICHARD EUGENE N90-11906
VOLOVIK, G. E. N90-12370
VORDERBRUEGGE, R. W. N90-12437
N90-12451

W

WACHS, A. L. N90-12358
WACKERLE, JERRY N90-12000
WACONGNE, SOPHIE N90-12146
WAGNER, JAMES W. N90-12050
WAI, Y. N90-12004
WAINSTEIN, S. N90-12309
WAKAMATSU, YOSHIO N90-11803
WALDROP, JOAN N90-11771
WALKER, DANIEL A. N90-12122
WALL, S. N90-12443
WALLACE, A. N90-11948
WALLS, JOHN E. N90-11762
WALTERS, E. J. N90-12402
WALTON, JOHN J. N90-12106
WANG, HAU H. N90-12356
WANG, LAI-SHENG N90-11835
WANHILL, R. J. H. N90-11877
WARSHAY, MARVIN N90-11804
WATKINS, RANDALL D. N90-12353
WATSON, R. E. N90-11860
WAYLAND, BRADFORD B. N90-11834
WEBB, ANDREW N90-12226
WEBER, MARK E. N90-11934
WEHRLE, WILLIAM P. N90-11905
WEI, J. N90-11922
WEINBERG, M. N90-12125
N90-12126
WEINBERGER, NORMAN M. N90-12166
WEINER, MAURICE N90-11941
WEINERT, M. N90-11860
WEINGART, R. C. N90-11977
WEISS, M. S. N90-12233
WEISS, ROSANNE M. N90-11761
WEISSMAN, PAUL R. N90-12106
WELCH, JEANNE A. N90-11995
WELLER, ALBERT E. N90-12026
WELLS, BARRETT N90-12373
WELLS, L. J. N90-11729
WENDLAND, B. N90-11936
WENG, HENGYI N90-12072
WESSELING, P. N90-12264
WEST, R. N. N90-12358
WHANGBO, MYUNG-HWAN N90-12356
WHEALTON, J. H. N90-12295
WHEELER, JEFFREY J. N90-12156
WHITE, HENRY S. N90-11843
N90-11846
WHITE, R. C. N90-12312
WHITE, S. M. N90-12472
WHITFIELD, R. T. N90-11719
WHITNEY, DANIEL E. N90-12025
WIERINGA, ROEL N90-12392
WIGGINS, GLENN N90-12383
WIJKER, J. J. N90-12056
WILEY, ROGER W. N90-12167
WILKERSON, THOMAS D. N90-12011
WILKES, ROBERT L. N90-12174
N90-12175
WILLE, REINHARD N90-12013
WILLIAMS, DAVID R. N90-12452
WILLIAMS, G. P. N90-12320
WILLIAMS, JACK M. N90-12356
WILLIAMS, R. N90-12335
WILLIAMS, R. S., JR. N90-12434
WILLIFORD, R. E. N90-11813
WILLS, SCOTT N90-12187
WILLSON, ROBERT F. N90-12471
WILMUT, M. J. N90-11924
WILSON, GREG S. N90-12059
WILSON, R. B. N90-12469
WILSON, ROBERT M. N90-12456
WINELAND, DAVID N90-12304
WINGLEE, ROBERT M. N90-12459
N90-12479
N90-12480
WISEMAN, S. R. N90-12189
N90-12190
WITHERS, C. C. N90-11738
N90-11739
WITTLIN, G. N90-11821
WOERTLER, MARTIN N90-11809
WOHLERS, M. N90-12125
WOHLERS, R. N90-12126
WOLF, CHRISTOPHER J. N90-11726
WOLF, S. A. N90-11964
WOLFSON, J. N90-12487
WOOD, CHARLES A. N90-12453
WOOD, S. A. N90-12081
WRAY, A. E. N90-12151
WRBANEK, J. N90-12001
WRENN, GORDON L. N90-12422
WUN-FOGIE, MARILYN N90-11996
WUORI, ALBERT F. N90-11907

X

XIE, J. K. N90-12128
XIE, JUYING N90-12086

Y

YAP, B. K. N90-12121
YARGER, DOUGLAS N. N90-12075
YAZDANI, J. I. N90-11994
YEAGER, ERNEST N90-11826
YNGSTROM, STEN N90-12308
YOUNG, L. A. N90-11701
YOUNG, PATRICIA M. N90-12163
YOUNGDAHL, KAY A. N90-11888
YU, IRENE I. K. N90-11830

Z

ZACEK, F. N90-12331
ZACHOR, A. S. N90-12121
ZACK, JOHN W. N90-12133
ZADRA, A. N90-12414
ZALZALA, A. M. S. N90-11966
N90-12029
ZARE, RICHARD N. N90-12307
ZEISSE, C. R. N90-11923
ZENG, S. N90-12264
ZHENG, Y. N90-12271
N90-12276
N90-12277
ZIMMERMAN, CHRISTOPHER N90-11771
ZIMMERMAN, RICHARD S. N90-11807
ZIMMERMANN, ANITA N90-11728
ZINNER, R. A. N90-11692
ZISK, S. H. N90-12435
ZOMAYA, A. Y. N90-12030
N90-12031
N90-12218
N90-12223
N90-12225
ZRUBEK, M. NORMAN N90-11731

CORPORATE SOURCE INDEX

SCIENTIFIC AND TECHNICAL AEROSPACE REPORTS VOLUME 28 NUMBER 3

Typical Corporate Source Index Listing

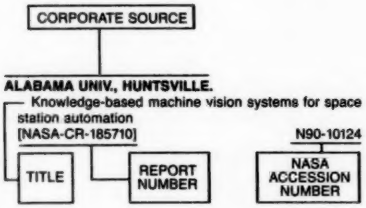
CORPORATE SOURCE
ALABAMA UNIV., HUNTSVILLE.
Knowledge-based machine vision systems for space station automation
[NASA-CR-185710]
N90-10124
TITLE
REPORT NUMBER
NASA ACCESSION NUMBER

Listings in this index are arranged alphabetically by corporate source. The title of the document provides the user with a brief description of the subject matter. The report number helps to indicate the type of document cited (e.g., NASA report, translation, NASA contractor report). The NASA accession number denotes the number by which the citation is identified. The titles are arranged under each corporate source in ascending accession number order.

A

AARHUS UNIV. (DENMARK).
Comparison of I2-stabilized HE-NE lasers
[PB89-219844] N90-12014

ADMIRALTY RESEARCH LAB., TEDDINGTON (ENGLAND).
Calculation of transient response from time-harmonic spectrum
[AD-A211972] N90-12241

AERITALIA S.P.A., TURIN (ITALY).
Problems related to the acquisition, processing and utilization of the modal parameters measured in flight tests in order to obtain the full envelope for flutter
[ETN-89-95210] N90-11735
Evolution of flight commands in Aeritalia design
[ETN-89-95211] N90-11759
The aerodynamic experimental center of Aeritalia: Combat aircraft group
[ETN-89-95213] N90-11766
Choice and characterization of new materials for aerospace applications
[ETN-89-95219] N90-11819
A new test procedure for a wing made with carbon fiber composites
[ETN-89-95220] N90-11820
The evolution of light alloys in the aerospace industry
[ETN-89-95216] N90-11872
In service life monitoring system using g-meter readings and mass configuration control
[ETN-89-95218] N90-12035

AERONAUTICAL RESEARCH LABS., MELBOURNE (AUSTRALIA).
An open-loop transient thermodynamic model of the Cougar turbojet
[AD-A211774] N90-11745

AEROSPACE CORP., EL SEGUNDO, CA.
Photolysis of spacecraft contaminants
[AD-A211715] N90-11801
Three-dimensional, two-phase, transonic, canted nozzle flows
[AD-A211528] N90-11984
Spin-orbit relaxation rates of Bi(6p(3)) 2D(3/2) following photolysis of Bi(CH3)3 at lambda = 193 nm
[AD-A211792] N90-12303
Thermal model for double-drift IMPATT diodes on diamond heat sinks
[AD-A211746] N90-12380

AIR FORCE GEOPHYSICS LAB., HANSCOM AFB, MA.
A beam induced upset during the flight of the ECHO-7 rocket
[NASA-CR-186089] N90-11755
Comparison of the LOWTRAN 7 code and S3-4 satellite measurements of UV radiance
[AD-A211356] N90-12124
Estimated UV clutter levels at 10-100 meter sensor pixel resolution extrapolated from recent polar bear measurements
[AD-A211357] N90-12125
Spatial characteristics of airglow and solar scatter radiance from the earth's atmosphere
[AD-A211358] N90-12126
UV ionospheric remote sensing with the polar BEAR satellite
[AD-A211359] N90-12127
Vacuum ultraviolet backgrounds from space - ten years after
[AD-A211353] N90-12493

AIR FORCE OCCUPATIONAL AND ENVIRONMENTAL HEALTH LAB., BROOKS AFB, TX.
Base level management of radio frequency radiation protection program
[AD-A211787] N90-12171

AIR FORCE SYSTEMS COMMAND, WRIGHT-PATTERSON AFB, OH.
Pilotless airplanes
[AD-A211719] N90-11734
Space flight (selected articles)
[AD-A212068] N90-11769
Contemporary China's meteorological enterprises (selected portions)
[AD-A210697] N90-12131

ALABAMA UNIV., HUNTSVILLE.
Studies of baroclinic instability in the presence of surface topography and stratospheric ozone N90-12068
Global distribution of moisture, evaporation-precipitation, and diabatic heating rates
N90-12069
Global backscatter assessment N90-12080

ALASKA UNIV., FAIRBANKS.
HIPAS 1987-88: ULF research and campaign support
[AD-A211720] N90-11933
Remote sensing data acquisition, analysis and archival
[PB89-142566] N90-12085

ALLIANCE TECHNOLOGIES CORP., CHAPEL HILL, NC.
Review of the national ambient air quality standards for lead: Exposure analysis methodology and validation
[PB89-207914] N90-12104

ALLIED-SIGNAL AEROSPACE CO., KANSAS CITY, MO.
Coupling rule-based and object-oriented programming for the classification of machined features
[DE89-017705] N90-11903
Manufacturing and the manufacturing engineer in the year 2000, revision
[DE89-017707] N90-11904
Reasoning about change and exceptions in automated process planning
[DE89-017706] N90-12195

ALLIED-SIGNAL CORP., MORRISTOWN, NJ.
New laser materials
[DE89-017524] N90-12017

ANACAPA SCIENCES, INC., FORT RUCKER, AL.
Effects of the advanced map interpretation and terrain analysis course on contour-level navigation performance
[AD-A212163] N90-11723

ANALYTICS, INC., WILLOW GROVE, PA.
Human Operator Simulator (HOS) 4 user's guide
[AD-A212007] N90-11763

AQUANAUTICS CORP., ALAMEDA, CA.
Long endurance underwater power system
[AD-A211386] N90-12096

ARGONNE NATIONAL LAB., IL.
Analytical studies of three-dimensional combustion processes
[AD-A211903] N90-11837
Ion-assisted deposition of high-temperature lubricious surfaces
[DE89-012397] N90-11883
Safety considerations for sodium-sulfur batteries for electric vehicles
[DE89-017682] N90-11949
Fuel cells for vehicle propulsion applications: A thermodynamic systems analysis
[DE89-017689] N90-11950
Tools to aid in the development high-performance algorithms
[DE89-012395] N90-12194
Monte Carlo studies of nuclei and quantum liquid drops
[DE89-016914] N90-12300
Computer simulations of two-dimensional quasiperiodic crystal and random tiling models
[DE89-016909] N90-12355
Structure-property relationships as an aid in the rational design of (beta)-(ET)(sub 2)X organic superconductors
[DE89-016912] N90-12356
RF performance of polycrystalline high-T(sub c) superconductors
[DE89-017671] N90-12359
Anomalous ion-channeling behavior across the superconducting transition in high-T(sub c) materials
[DE89-017677] N90-12360
High-temperature superconducting current leads for cryogenic apparatus
[DE89-017680] N90-12361

ARIZONA STATE UNIV., TEMPE.
Evidence for volcanism in NW Ishtar Terra, Venus
N90-12433
Aeolian processes on Venus N90-12436
Stress distribution and topography of Tellus Regio, Venus N90-12452

ARIZONA UNIV., TUCSON.
Autonomous space processor for orbital debris
[NASA-CR-186043] N90-11770
Disturbances in the Arizona Monsoon N90-12071

ARMY AEROMEDICAL RESEARCH LAB., FORT RUCKER, AL.
Visual acuity and stereopsis with night vision goggles
[AD-A211552] N90-12167

ARMY ARMAMENT RESEARCH AND DEVELOPMENT COMMAND, WATERVLIET, NY.
Autofrettage-stress distribution under load and retained stresses after depressurization
[AD-A212090] N90-12048

ARMY BELVOIR RESEARCH AND DEVELOPMENT CENTER, FORT BELVOIR, VA.
The prediction of middle distillate fuel properties using liquid chromatography-proton nuclear magnetic resonance spectroscopy data
[AD-A211879] N90-11899

ARMY COLD REGIONS RESEARCH AND ENGINEERING LAB., HANOVER, NH.
Ice runways near the South Pole
[AD-A211606] N90-11908

ARMY ENGINEER TOPOGRAPHIC LABS., FORT BELVOIR, VA.
Sentinel satellite positional precision derived from the NAVSTAR global positioning system
[AD-A211876] N90-11720

ARMY LAB. COMMAND, WATERTOWN, MA.
Deformation behavior of SiC/2014 Al metal-matrix composite
[AD-A212095] N90-11816
Flexure strength of advanced ceramics: A round robin exercise
[AD-A212101] N90-11889
A C(Superscript)-Anisoparametric three-node shallow shell element for general shell analysis
[AD-A212094] N90-12049
Effect of annealing conditions on the structural and superconducting properties of Y-Ba-Cu-O films
[AD-A211308] N90-12371
Synthesis and microstructure of highly oriented PbTiO3 thin films prepared by a sol-gel method
[AD-A211735] N90-12377

ARMY MISSILE COMMAND, REDSTONE ARSENAL, AL.
Power up modification for video switcher microprocessor interface for sensor system processing system
[AD-A211543] N90-11962

ARMY RESEARCH INST. OF ENVIRONMENTAL MEDICINE, NATICK, MA.
Air velocity mapping of environmental test chambers
[AD-A212082] N90-11764
Convective heat transfer in hypobaric environments
[AD-A212060] N90-11979
The effect of caffeine on endurance time to exhaustion at high altitude
[AD-A212069] N90-12163

Heatstroke pathophysiology: The energy depletion model
[AD-A212156] N90-12164
Human body regional convective heat transfer determination using sublimating naphthalene disks
[AD-A212170] N90-12165

ATMOSPHERIC RADIATION CONSULTANTS, ACTON, MA.
Retrieval of atomic oxygen and temperature in the thermosphere. Part 2: Feasibility of an experiment based on limb emission in the OI lines
[AD-A211807] N90-12121

AUBURN UNIV., AL.
Design of a solar sail mission to Mars
[NASA-CR-186045] N90-11771

B

BATTELLE COLUMBUS LABS., OH.
An assessment of technology for self-powered gas appliances: A GATC (Gas Appliance Technology Center)
[PB89-219265] N90-12026

BEN GURION UNIV. OF THE NEGEV, BEERSHEVA (ISRAEL).
Experimental investigation of a planar shock wave over a double wedge
[AD-A211366] N90-11981

BOLT, BERANEK, AND NEWMAN, INC., CAMBRIDGE, MA.
Some implications of the isotropic momentarily frozen assumptions for the SPAN-MAT program
[NASA-CR-181937] N90-11704

BOSTON UNIV., MA.
Kinetics of diffusion-controlled reactions
[AD-A212161] N90-12286

BOWLING GREEN STATE UNIV., OH.
Lifetime of singlet oxygen in aqueous hydrogen peroxide (BHP)
[AD-A211545] N90-12306

BREAULT RESEARCH ORGANIZATION, TUCSON, AZ.
Kinematic design NC optical generator N90-12316

BROOKHAVEN NATIONAL LAB., UPTON, NY.
Electronic structure of transition metal alloys and intermetallics: Charge transfer and its implications for Moessbauer effect measurements
[DE89-017603] N90-11860
Neutron scattering studies of premartensitic phenomena
[DE90-000025] N90-11863
Microwave instability near transition energy
[DE90-000107] N90-11922
Switched power workshop: Introduction and summary
[DE90-000036] N90-11952
The national synchrotron light source and its applications
[DE89-017605] N90-12320
Single crystal diffraction
[DE90-000024] N90-12366

BROWN UNIV., PROVIDENCE, RI.
Characteristics, distribution and geologic/terrain associations of small dome-like hills on Venus
N90-12425
Tessera terrain: Characteristics and models of origin
N90-12426
Divergent plate boundaries and crustal spreading on Venus: Evidence from Aphrodite Terra N90-12427
A morphologic study of Venus Ridge belts
N90-12432
Architecture of orogenic belts and convergent zones in Western Ishtar Terra, Venus N90-12437
Lakshmi Planum: A distinctive highland volcanic province N90-12444
Geology of the Venus equatorial region from Pioneer Venus radar imaging N90-12447
Coronae on Venus observations and models of origin
N90-12449
Eastern Ishtar Terra: Tectonic evolution derived from recognized features N90-12451

BUNDESMINISTERIUM FUER FORSCHUNG UND TECHNOLOGIE, BONN (GERMANY, F.R.).
Ozone Research Program (German contribution to climate and atmosphere research)
[REPT-46-88] N90-12111

BUREAU OF MINES, ALBANY, OR.
Fe-Ni-Cr alloys for coatings and electroforms
[PB89-195846] N90-11849

C

CALIFORNIA INST. OF TECH., PASADENA.
Control of turbulent mixing layers
[AD-A211413] N90-11708
Numerical analysis, scientific computing and fundamental studies of fluid mechanics
[DE89-017554] N90-11975
An experimental and analytical program to develop crack tip fracture criteria
[AD-A211565] N90-12051
Optical computing based on the Hopfield model for neural networks
[AD-A211824] N90-12216
The Owens Valley solar array N90-12490

CALIFORNIA UNIV., BERKELEY. LAWRENCE BERKELEY LAB.
High temperature and high resolution UV photoelectron spectroscopy using supersonic molecular beams
[DE90-000176] N90-11835
The effects of temperature on fatigue crack propagation in 310 austenitic stainless steel
[DE90-000136] N90-11865
Densification of particulate ceramic composites: The role of heterogeneities
[DE90-000177] N90-11886
Advanced light source master oscillator
[DE90-000123] N90-11953
The effect of flux creep on the magnetization field in the SSC diopole magnets
[DE90-000124] N90-12284
Optical data transmission systems in radiation environment
[DE90-000174] N90-12322

CALIFORNIA UNIV., DAVIS.
Microwave signal detection using modulation of polymeric optical waveguides
[DE89-017545] N90-11921
Preparation and characterization of single phase Ba(1-x)KxBiO3
[DE89-017735] N90-12362

CALIFORNIA UNIV., IRVINE.
Synaptic plasticity and memory formation
[AD-A211368] N90-12158
Adaptive information processing in auditory cortex
[AD-A211294] N90-12166
Discriminating rigid from nonrigid motion
[AD-A211794] N90-12180
Design mechanism for interactive graphics mechanism design
[PB89-219513] N90-12202
Efficient diagnosis of multiprocessor systems under probabilistic models
[NASA-CR-185965] N90-12212

CALIFORNIA UNIV., LOS ANGELES.
Wave particle interactions
[DE89-017527] N90-12335

CALIFORNIA UNIV., SAN DIEGO.
Scientific objectives of solar gamma-ray observations
N90-12463

CARNEGIE-MELLON UNIV., PITTSBURGH, PA.
Efficient finite element solution of Navier-Stokes equations and related topics
[AD-A211647] N90-11986
Scheduling sporadic and aperiodic events in a hard real-time system
[AD-A211344] N90-12205
Adoption of software engineering innovations in organizations
[AD-A211573] N90-12206
A real-time locking protocol
[AD-A211514] N90-12403

CASE WESTERN RESERVE UNIV., CLEVELAND, OH.
In-situ spectroscopic studies of transition metal macrocycles as catalysts for the electrochemical reduction of oxygen
[PB89-219273] N90-11826
Precipitation strengthened high strength, high conductivity Cu-Cr-Nb alloys produced by chill block melt spinning
[NASA-CR-185144] N90-11853
Suppression of side chain crystallization and transformation of monotropic mesophases into enantiotropic mesophases by copolymerization of the parent polymers' monomer pairs containing constitutional isomeric mesogenic side groups
[AD-A209066] N90-11878

CENTRAL INST. FOR THE DEAF, SAINT LOUIS, MO.
Binaural masking: An analysis of models
[AD-A211578] N90-12168

CENTRE AEROPORTE DE TOULOUSE (FRANCE).
Performance and quality of a wing type parachute: Parametric analysis
[REPT-88-19] N90-11710

CERAMATEC, INC., SALT LAKE CITY, UT.
New mechanism for toughening ceramic materials
[AD-A211651] N90-11892

CESKOSLOVENSKA AKADEMIE VED, PRAGUE.
Calculations of soft x ray emission of REB-heated plasma
[IPPCZ-287] N90-12329
Non-stationary computer model of the asymptotic region of an electric arc gas heater
[IPPCZ-288] N90-12330
Electron cyclotron emission and absorption experiment on the CASTOR tokamak
[IPPCZ-285] N90-12331
Control of plasma position in the CASTOR tokamak
[IPPCZ-284] N90-12332

CHALMERS UNIV. OF TECHNOLOGY, GOETEBORG (SWEDEN).
GALAX: A two-dimensional N-body code for disk galaxy dynamics
[PB89-217780] N90-12415

CHICAGO UNIV., IL.
Cosmic strings and ultra-high energy cosmic rays
[NASA-CR-185924] N90-12492

CINCINNATI UNIV., OH.
Reactive ion etching of sputtered silicon carbide and tungsten thin films for device applications
[AD-A211711] N90-11847
Genetic engineering of enhanced microbial nitrification
[PB89-208334] N90-12155

CIVIL AVIATION AUTHORITY, LONDON (ENGLAND).
UK airmisses involving commercial air transport, May-August 1988
[ISSN-0951-6301] N90-11717
UK airmisses involving commercial air transport
[CAA-2/88] N90-11718
Aircraft cabin fire suppression by means of an interior water spray system
[CAA-PAPER-88014] N90-11719
The 1987 survey of track keeping and altitudes on Heathrow and Gatwick standard instrument departure routes (DAY)
[CAA-PAPER-88010] N90-11729

COAST GUARD, WASHINGTON, DC.
Statistical models for the optimal estimation of oceanic fields
[AD-A211786] N90-12149

COLLEGE OF WILLIAM AND MARY, WILLIAMSBURG, VA.
Theoretical plasma physics
[DE90-000009] N90-12341

COLORADO SCHOOL OF MINES, GOLDEN.
Investigations into the infiltration kinetics, wettability, and interfacial bond strength of Al/SiC composites
[AD-A211924] N90-11815
Weldability of ductile nickel aluminides
[DE89-017452] N90-11859

COLORADO STATE UNIV., FORT COLLINS.
Analysis of loss mechanisms in polycrystalline thin-film solar cells
[DE89-009454] N90-12093
Beam assisted fabrication of 3-5/Si monolithic devices
[AD-A212046] N90-12367

COLORADO UNIV., BOULDER.
Laboratory and theoretical models of planetary-scale instabilities and waves N90-12076
On the analysis of line profile variations: A statistical approach N90-12412
Access to Max '91 information via computer networks
N90-12466
Heating and acceleration of coronal and chromospheric ions during solar flares N90-12479
Chromospheric-coronal coupling during solar flares: Current systems and particle acceleration N90-12480

CONNECTICUT UNIV., STORRS.
Energy transfer and non-linear optical properties at near ultraviolet wavelengths: Rare earth 4f(yields)5d transitions in crystals and glasses
[DE90-000065] N90-12321

CORNELL UNIV., ITHACA, NY.
Generation and focusing of pulsed intense ion beams
[DE89-017558] N90-12338
Ultra high speed compound semiconductors and real time signal processing
[AD-A211394] N90-12372
Crustal deformation: Earth vs Venus N90-12450

CRANFIELD INST. OF TECH., BEDFORD (ENGLAND).
The determination of the aerodynamic characteristics of an ogive-cylinder body in subsonic, curved, incompressible flow, and an assessment of the effect of flow curvature
[REPT-87-13] N90-11712
Incompressible flow about ellipsoids of revolution
[REPT-88-02] N90-11713

D

DARTMOUTH COLL., HANOVER, NH.
Synthesis and chemistry of strained and conjugated fluorocarbons
[AD-A211633] N90-11844

Thermomechanical contact phenomena and wear of sliding components
[AD-A211290] N90-12028

DAYTON UNIV., OH.
Computation of ramjet internal flowfields
[AD-A212001] N90-11743

DEFENCE RESEARCH ESTABLISHMENT PACIFIC, VICTORIA (BRITISH COLUMBIA).
Analysis of two-pass Modified Hough Transform (MHT) technique for the detection of wake like signals
[AD-A211982] N90-11924

DEFENCE RESEARCH INFORMATION CENTRE, ORPINGTON (ENGLAND).
Design of glued joints, elastoplastic adhesives
[DRIC-T-8168] N90-11894

DEFENSE APPLIED INFORMATION TECHNOLOGY CENTER, ALEXANDRIA, VA.
DOD Gateway Information System (DGIS) common command language: A retrospective on the introduction of prolog as the development tool
[AD-A211941] N90-12400

DEFENSE LOGISTICS AGENCY, ALEXANDRIA, VA.
Forecasting contracting workload
[AD-A211935] N90-12387

DEPARTMENT OF ENERGY, OAK RIDGE, TN.
Program distribution for unclassified scientific and technical reports: Instructions and category scope notes, revision 75
[DE89-005395] N90-12391

DEPARTMENT OF ENERGY, WASHINGTON, DC.
Sliding seal materials for low heat rejection engines
[NASA-CR-182262] N90-11882
FEDIX: An on-line information service for universities and other research organizations: User's guide, version 2.0, release 1
[DE89-016695] N90-12398

DEPARTMENT OF THE ARMY, WASHINGTON, DC.
Method of modifying the dielectric properties of an organic polymer film
[AD-D014171] N90-11879
A SAW Slanted Array Correlator (SAC) with separate amplitude compensation channel
[AD-D014174] N90-11914
High power, solid state RF pulse generators
[AD-D014172] N90-11941
Periodic permanent magnet structures
[AD-D014173] N90-12280

DEPARTMENT OF THE NAVY, WASHINGTON, DC.
Elevated temperature aluminum-titanium alloy by powder metallurgy process
[AD-D014165] N90-11852
Multi-stage noise-reducing system
[AD-D014179] N90-11942
Apparatus and method for monitoring pressure leaks from a sealed system
[AD-D014168] N90-11995
Magnetostrictive torque sensor
[AD-D014169] N90-11996
Infrared detector array
[AD-D014170] N90-11997
Optical arithmetic logic using the modified signed-digit redundant number representation
[AD-D014176] N90-12186
Thin film magnetic memory elements
[AD-D014178] N90-12281
Process for single crystal growth of high T(sub c) superconductors
[AD-D014167] N90-12346
Niobium and niobium nitride contacts on semiconducting material
[AD-D014177] N90-12347

DEUTSCHE FORSCHUNGS- UND VERSUCHSANSTALT FUER LUFT- UND RAUMFAHRT, BRUNSWICK (GERMANY, F.R.).
Devices and procedures for the calibration of sensors and measurement: Systems of the flight test support system ATTAS
[DFVLR-MITT-89-06] N90-12007

DEUTSCHE FORSCHUNGS- UND VERSUCHSANSTALT FUER LUFT- UND RAUMFAHRT, COLOGNE (GERMANY, F.R.).
Cryogenic free jets
[ESA-TT-1128] N90-11767
Significance of oxide skins on powder for the quality of PM Al material
[DFVLR-FB-89-11] N90-11873
Studies on predicting the resynchronization of the circadian system after transmedian flights
[DFVLR-FB-89-10] N90-12172

DEUTSCHE FORSCHUNGS- UND VERSUCHSANSTALT FUER LUFT- UND RAUMFAHRT, FREIBURG (GERMANY, F.R.).
Investigation on analyzing computer-aided forest disease classifications
[DFVLR-FB-89-16] N90-12112

DEUTSCHE FORSCHUNGS- UND VERSUCHSANSTALT FUER LUFT- UND RAUMFAHRT, GOETTINGEN (GERMANY, F.R.).
Steady and unsteady potential flow around thin annular wings and engines with simulation of jet engine flow
[DFVLR-FB-89-18] N90-11711
Absolute determination of the wall shear stress by means of an interferometer
[DFVLR-FB-89-13] N90-11991
Numerical computation of the viscous flow field around a prolate spheroid
[DFVLR-FB-89-22] N90-11992

DEUTSCHE FORSCHUNGS- UND VERSUCHSANSTALT FUER LUFT- UND RAUMFAHRT, OBERPFAFFENHOFEN (WEST GERMANY).
Navigation experiment NAVEX: Data storage and processing
[DFVLR-MITT-89-09] N90-11727
Navigation experiment NAVEX: The equipment delay times in the Spacelab mission D1
[DFVLR-MITT-89-10] N90-11728
Controller design for active vibration suppression of a helicopter
[DFVLR-FB-89-20] N90-11760
Infrared temperature measurement with automatic consideration of emissivity
[ESA-TT-1131] N90-12008
Investigation of the usefulness of LANDSAT 5 thematic mapper data for mapping forest disease
[DFVLR-FB-89-06] N90-12088
Signature analysis and classification of pine of different vitality classes using airborne thematic mapper data
[DFVLR-FB-89-07] N90-12089
ANDECS-PERLUDE 2.0: A databased, interactive system of control software user's guide
[DFVLR-MITT-89-07] N90-12404

DEUTSCHE FORSCHUNGS- UND VERSUCHSANSTALT FUER LUFT- UND RAUMFAHRT, STUTTGART (GERMANY, F.R.).
Type-specific dynamic measurements on wind turbines at the test site Schnittlingen (Germany, F.R.)
[DFVLR-MITT-88-31] N90-12099

DEUTSCHE FORSCHUNGSANSTALT FUER LUFT- UND RAUMFAHRT, BRUNSWICK (GERMANY, F.R.).
Aging of CFRP due to longterm storage in heated air
[ESA-TT-1124] N90-11893

DEUTSCHE GEODAETISCHE KOMMISSION, MUNICH (GERMANY, F.R.).
Time and frequency in geodesy measuring methods
[SER-C-337] N90-12087

DORTMUND UNIV. (GERMANY, F.R.).
Television systems with enhanced image quality for new broadband channels
[ETN-89-94622] N90-11936
Construction of a picosecond laser system for the investigation of semiconductors using nonlinear optical methods
[ETN-89-94664] N90-12013

DOUGLAS AIRCRAFT CO., INC., LONG BEACH, CA.
Manual for Program PSTRESS: Peel stress computation
[NASA-CR-178408] N90-11822

DRAPER (CHARLES STARK) LAB., INC., CAMBRIDGE, MA.
Computer-aided design of flexible assembly systems
[PB89-216253] N90-12025

DREXEL UNIV., PHILADELPHIA, PA.
Inorganic composite materials in Japan: Status and trends
[PB89-230015] N90-11810

DU PONT DE NEMOURS (E. I.) AND CO., AIKEN, SC.
Resistance welding large parts
[DE89-010462] N90-12027

DUKE UNIV., DURHAM, NC.
Positron annihilation studies of interpenetrating polymer networks
[AD-A212162] N90-11890
Boron analogues of amino acids and derivatives
[AD-A211311] N90-12157

DUQUESNE UNIV., PITTSBURGH, PA.
Iron (III) initiated autoxidation of 1,2,3,4-tetrahydrocarbazole: An example of electron transfer
[AD-A211857] N90-11836

DYNETICS, INC., HUNTSVILLE, AL.
Adaptive control law design for model uncertainty compensation
[AD-A211712] N90-11758

E

EATON CORP., SOUTHFIELD, MI.
DSEP (Dual Shaft Electric Propulsion) operation and maintenance manual for the NVH and TB-2 vehicles: Advanced Dual Shaft Electric Propulsion System technology development program
[DE89-017549] N90-12411

ECOLE NATIONALE SUPERIEURE DES TELECOMMUNICATIONS, PARIS (FRANCE).
Optimal matching of 3-D convex polyhedra
[TELECOM-PARIS-89C003] N90-12258

ENVIRONMENTAL PROTECTION AGENCY, RESEARCH TRIANGLE PARK, NC.
Evaluation and sensitivity analyses results of the MESOPUFF 2 model with CAPTEX (Cross-Appalachian Tracer Experiment) measurements
[PB89-198253] N90-12103
Review of the national ambient air quality standards for lead: Exposure analysis methodology and validation
[PB89-207914] N90-12104

ESDU INTERNATIONAL LTD., LONDON (ENGLAND).
Normal-force-curve and pitching-moment-curve slopes of forebody-cylinder combinations at zero angle of attack for Mach numbers up to 5
[ESDU-89008] N90-11709
Vapour pressures and critical points of liquids. Halogenated hydrocarbons
[ESDU-89006] N90-11848
Effect of fretting on fatigue strength of aluminium alloys
[ESDU-89004] N90-11870
Application of process integration to utilities, combined heat and power, and heat pumps
[ESDU-89001] N90-11909
Natural frequencies of singly-curved laminated plates with simply-supported edges
[ESDU-89011] N90-12052
An introduction to effectiveness: NTU relationships
[ESDU-89016] N90-12381

ESSEX CORP., ORLANDO, FL.
Microcomputer-based tests for repeated-measures: Metric properties and predictive validities
[NASA-CR-185517] N90-12174
A menu of self-administered microcomputer-based neurotoxicology tests
[NASA-CR-185518] N90-12175

EUROPEAN SPACE AGENCY, PARIS (FRANCE).
Calculation on film preparation and film motion of a swirl atomizer
[ESA-TT-1096] N90-11990
Laser sounding from space: Report of the ESA Technology Working Group on Space Laser Sounding and Ranging
[ESA-SP-1108] N90-12024
Equilibrium solutions of a spherical pendulum with rotating point of suspension and friction
[ESA-TT-1139] N90-12288
Measurement of pressure fluctuations in a resonant chamber with laser-induced iodine fluorescence
[ESA-TT-1123] N90-12326

EVANS (CHARLES) AND ASSOCIATES, REDWOOD CITY, CA.
Development and evaluation of an instrument for rapid electroreflectance of semiconductor materials
[AD-A211690] N90-12376

F

FEDERAL AVIATION ADMINISTRATION, ATLANTIC CITY, NJ.
Flammability, smoke, and dry arc tracking tests of aircraft electrical wire insulations
[DOT/FAA/CT-89/21] N90-11714
Simulations for computer centerline approach
[DOT/FAA/CT-TN89/41] N90-11726
Analysis of heliport environmental data: Indianapolis downtown heliport, Wall Street heliport. Volume 2: Wall Street heliport data plots
[DOT/FAA/CT-TN87/54-VOL-2] N90-11761
ILS mathematical modeling study of the effects of proposed hangar construction at the Orlando International Airport, Runway 17R, Orlando, Florida
[DOT/FAA/CT-TN89/52] N90-11762

FERMI NATIONAL ACCELERATOR LAB., BATAVIA, IL.
Thermal conduction of SSC (Superconducting Super Collider) wire
[DE89-016710] N90-11811
Scintillating fiber ribbon - tungsten calorimeter
[DE89-016705] N90-12001
Cosmic strings and ultra-high energy cosmic rays
[NASA-CR-185924] N90-12492

FINNISH METEOROLOGICAL INST., HELSINKI.
Calculated solar radiation incident upon slopes of different orientated surfaces in Finland
[FMI-MP-8] N90-12116
FLORIDA STATE UNIV., TALLAHASSEE.
Dynamics of baroclinic wave systems N90-12072
FLORIDA UNIV., GAINESVILLE.
Linear (passive) and non-linear guided and studies in glass
[AD-A211693] N90-12325
FRAUNHOFER INST. FUER PHYSIKALISCHE MESSTECHNIK, FREIBURG (GERMANY, F.R.).
Development of microstructured DH diode lasers and detectors for the near and medium IR spectral domain using molecular beam epitaxy
[IPM-15/1988] N90-12023
FWG ASSOCIATES, INC., TULLAHOMA, TN.
Low level remote sensing: Orographic winds N90-12066

G

GENERAL ELECTRIC CO., SCHENECTADY, NY.
Deformation and defects in Laves-phase intermetallic compounds
[DE89-017798] N90-11862
GEOLOGICAL SURVEY, FLAGSTAFF, AZ.
Clotho Tessera, Venus: A fragment of Fortuna Tessera N90-12439
Tectonism on Venus: A review N90-12440
Volcanism on Venus: Large shields and major accumulations of small domes N90-12445
Impact cratering and the surface age of Venus: The Pre-Magellan controversy N90-12446
GEOLOGICAL SURVEY, MENLO PARK, CA.
Crater identification and resolution of lunar radar images N90-12441
GEORGE WASHINGTON UNIV., WASHINGTON, DC.
Quantitative interpretation of auger lineshapes and electron/photon stimulated desorption
[AD-A211550] N90-11842
Active control of the forced and transient response of a finite beam N90-12040
GEORGIA INST. OF TECH., ATLANTA.
MEGALIDAR
[AD-A212074] N90-12020
Measurements of aerosol properties needed to infer backscatter characteristics in support of the NASA Doppler Lidar program N90-12082
GESELLSCHAFT FUER MATHEMATIK UND DATENVERARBEITUNG, SAINT AUGUSTIN (GERMANY, F.R.).
A multigrid algorithm for the incompressible Navier-Stokes equation
[GMD-374] N90-11993
GOOD SAMARITAN HOSPITAL AND MEDICAL CENTER, PORTLAND, OR.
Age-related changes in human posture control: Motor coordination tests
[NASA-CR-185855] N90-12178
GORDON RESEARCH CONFERENCES, INC., KINGSTON, RI.
Gordon Conference on Atomic Physics
[AD-A211946] N90-12304
GRENOBLE-1 UNIV. (FRANCE).
A study of the asymptotic behavior of linear difference equations with polynomial coefficients
[IMAG-RR-743-M] N90-12254
Asymptotic bias of autoregressive estimators
[IMAG-RR-745-M] N90-12255
Inf-convolution splines
[IMAG-RR-749-M] N90-12256
Splines and equations of nonlinear parameters
[IMAG-RR-750-M] N90-12257
GRUMMAN AEROSPACE CORP., BETHPAGE, NY.
Conceptual design of liquid droplet radiator shuttle-attached experiment
[NASA-CR-185164] N90-11805
Conceptual design of liquid droplet radiator shuttle-attached experiment technical requirements document
[NASA-CR-185165] N90-11806

H

HARVARD UNIV., CAMBRIDGE, MA.
Self-assembled organic monolayer films
[AD-A212006] N90-11838
HAWAII UNIV., HONOLULU.
Aerosol in the Pacific troposphere N90-12078
Hydrophone investigations of earthquakes and explosion generated high-frequency seismic phases
[AD-A212055] N90-12122
An imaging vector magnetograph for the next solar maximum N90-12489
HELSINKI UNIV. (FINLAND).
Calibration and de-embedding of microwave measurements using any combination of one- or two-port standards
[PB89-212674] N90-11916
Design, construction and test of a frequency doubler for 183 GHz
[PB89-212591] N90-11944
Problem of incomplete information in relational databases
[PB89-217533] N90-12393
Interoperability of heterogeneous information systems: The COST 11(ter) Project
[PB89-217541] N90-12394
HELSINKI UNIV. OF TECHNOLOGY, ESPOO (FINLAND).
Computer simulations of radiation damage in amorphous solids
[PB89-212682] N90-11827
Effective permeability of mixtures
[PB89-218952] N90-11839
Eigensolutions for the reflection problem involving the interface of two chiral half spaces
[PB89-221592] N90-11926
Time-domain analytic and numeric analysis of vertical dipoles in front of dielectric planar interface
[PB89-221642] N90-11927
Cryogenic Schottky-mixer receiver front-end for 40-50 GHz
[PB89-221667] N90-11959
Analysis of the efficiency of a dielectric solar energy collector
[PB89-212716] N90-12092
Some notes on perturbations of differential-algebraic equations
[PB89-218564] N90-12243
Internal Magnus effects in superfluid 3He-A
[PB89-212617] N90-12351
Flare-in texture in rotating superfluid (3)He-B
[PB89-218994] N90-12368
Resonant quasiparticle-ion scattering in anisotropic superfluid (3)He
[PB89-221618] N90-12369
Collective-mode spectroscopy of textures in superfluid (3)He-B
[PB89-221634] N90-12370
HERZBERG INST. OF ASTROPHYSICS, PENTICTION (BRITISH COLUMBIA).
The 10.7-cm microwave observations of AR 5395 and related terrestrial effects N90-12483
HUGHES RESEARCH LABS., MALIBU, CA.
Plasma-anode electron gun research
[AD-A211547] N90-11773

I

ILLINOIS INST. OF TECH., CHICAGO.
Computer generation of a tutorial dialogue
[AD-A211976] N90-12162
ILLINOIS STATE WATER SURVEY, CHAMPAIGN.
Variational objective analysis for cyclone studies N90-12064
ILLINOIS UNIV., CHICAGO.
Laser production of soft x rays by multiquantum processes and the excitation of atomic inner-shell states
[AD-A211372] N90-12021
Generation and tooth contact analysis of spiral bevel gears with predesigned parabolic functions of transmission errors
[NASA-CR-4259] N90-12033
The realization of input-output maps using bialgebras
[NASA-CR-185362] N90-12228
ILLINOIS UNIV., URBANA.
Spectral-domain analysis of finite frequency selective surfaces
[AD-A211669] N90-11932
ILLINOIS UNIV., URBANA-CHAMPAIGN.
Processing and characterization of alumina platelet-reinforced mullite composites
[DE90-000057] N90-11814
A design methodology for self-tuning control of systems with inherent conflicts
[PB89-219505] N90-11960
Parallel implementation and evaluation of motion estimation system algorithms on a distributed memory multiprocessor using knowledge based mappings
[NASA-CR-185984] N90-12213
Novel techniques for data decomposition and load balancing for parallel processing of vision systems: Implementation and evaluation using a motion estimation system
[NASA-CR-185991] N90-12214
Parallel architectures and parallel algorithms for integrated vision systems
[NASA-CR-185990] N90-12215
Adaptive feedback linearization: Stability and robustness
[PB89-219497] N90-12220
INSTITUTE FOR ADVANCED STUDY, PRINCETON, NJ.
Bordered surfaces, off-shell amplitudes, sewing, and string field theory
[DE90-000006] N90-12378
INSTITUTE FOR COMPUTER APPLICATIONS IN SCIENCE AND ENGINEERING, HAMPTON, VA.
Near-planar TS waves and longitudinal vortices in channel flow: Nonlinear interaction and focusing
[NASA-CR-181928] N90-11698
The nonconvex multi-dimensional Riemann problem for Hamilton-Jacobi equations
[NASA-CR-181887] N90-12182
Requirements for multidisciplinary design of aerospace vehicles on high performance computers
[NASA-CR-181915] N90-12183
Parameter identification for an abstract Cauchy problem by quasilinearization
[NASA-CR-181933] N90-12192
The use of Lanczos's method to solve the large generalized symmetric definite eigenvalue problem
[NASA-CR-181914] N90-12193
Convergence results for pseudospectral approximations of hyperbolic systems by a penalty type boundary treatment
[NASA-CR-181929] N90-12230
Numerical experience with a class of algorithms for nonlinear optimization using inexact function and gradient information
[NASA-CR-181927] N90-12232
A multidomain spectral collocation method for the Stokes problem
[NASA-CR-181876] N90-12266
INSTITUTE FOR TELECOMMUNICATION SCIENCES, BOULDER, CO.
A new approach to HF (High Frequency) channel modeling and simulation. Part 1: Deterministic model
[PB89-203962] N90-11913
INSTITUTE FOR THE STUDY OF EARTH, OCEANS AND SPACE, DURHAM, NH.
The solar gamma ray and neutron capabilities of COMPTEL on the Gamma Ray Observatory N90-12468
INSTITUTE OF ELECTRICAL AND ELECTRONICS ENGINEERS, NEW YORK, NY.
Solid-State Sensor and Actuator
[AD-A211427] N90-11961
INTERNATIONAL COUNCIL OF SCIENTIFIC UNIONS, URBANA, IL.
Middle Atmosphere Program. Handbook for MAP, volume 28
[NASA-CR-184972] N90-12117
IOWA STATE UNIV. OF SCIENCE AND TECHNOLOGY, AMES.
Use of satellite data and modeling to asses the influence of stratospheric processes on the troposphere N90-12075
IOWA UNIV., IOWA CITY.
Improved pattern recognition techniques for real time operation
[AD-A211395] N90-11840

J

JET PROPULSION LAB., CALIFORNIA INST. OF TECH., PASADENA.
Global environmental effects of impact-generated aerosols: Results from a general circulation model
[DE89-008033] N90-12106
Acoustic controlled rotation and orientation
[NASA-CASE-NPO-16995-1-CU] N90-12289
Ion formation by electron impact
[AD-A211367] N90-12305
Potential for observing and discriminating impact craters and comparable volcanic landforms on Magellan radar images N90-12429
Contrasting landform perception with varied radar illumination geometries and at simulated resolutions of Venera and Magellan N90-12430
Deducing the age of the dense Venus atmosphere N90-12438
JOHNS HOPKINS UNIV., BALTIMORE, MD.
Materials characterization using holographic mapping of transient lamb waves
[AD-A211414] N90-12050
JOHNS HOPKINS UNIV., LAUREL, MD.
Investigation of atmospheric emissions in ultraviolet, vacuum ultraviolet, and extreme ultraviolet wavelength
[AD-A212169] N90-12123
Interplanetary energetic particle observations of the March 1989 events N90-12484

K

KARLSRUHE UNIV. (GERMANY, F.R.).
Interlaminar stress concentration in fiber composites
[ETN-89-94670] N90-11809

KEURING VAN ELECTROTECHNISCHE MATERIALEN N.V., ARNHEM (NETHERLANDS).
Activities report on KEMA R and D
[ST-REPT-VOL-6-NO-12] N90-12100

KIRUNA GEOPHYSICAL INST. (SWEDEN).
Distribution of auroral precipitation at midnight during a magnetic storm
[PB89-213136] N90-12118

L

LAWRENCE LIVERMORE NATIONAL LAB., CA.
Short period multilayers: Interface dominated structures
[DE89-017536] N90-11812
Shock dissociation of molecular fluids: A possibility of first-order phase change
[DE89-016647] N90-11829
Conversion of methane to liquid hydrocarbons
[DE89-017547] N90-11831
Phase behavior of pure and mixed systems at high pressure
[DE89-017734] N90-11832
Calculation of the refractive index change in dissociating shocked benzene
[DE89-017737] N90-11833
X ray diffraction patterns of metal aurocyanides
[DE89-015188] N90-11851
A rate-dependent constitutive model for Be
[DE89-017755] N90-11861
Recent advances to NEC (Numerical Electromagnetics Code): Applications and validation
[DE89-009231] N90-11917
Resistive block methods for electrostatic field solutions with internal elements
[DE89-017535] N90-11920
High gain flux compression generator fabrication issues
[DE89-017888] N90-11951
VISAR wave profile measurements in supra-compressed HE
[DE89-017736] N90-11976
Characteristics of flyer impact for one-dimensional shock-wave study applications
[DE89-017887] N90-11977
Shock pressure determination in detonator wires
[DE89-017756] N90-12002
A microchannel plate intensified, subnanosecond, X-ray imaging camera
[DE89-017781] N90-12003
High resolution X-ray spectroscopy using germanium microcalorimeters
[DE89-017784] N90-12004
Laser ionization mass spectroscopy
[DE89-008039] N90-12015
New laser materials
[DE89-017524] N90-12017
Global environmental effects of impact-generated aerosols: Results from a general circulation model
[DE89-008033] N90-12106
A statistical intercomparison of temperature and precipitation predicted by four general circulation models with historical data
[DE89-017785] N90-12108
Low-cost three-dimensional stereoscopic display technique for computer-aided design
[DE89-017732] N90-12196
Microscopic approach to the generator coordinate method
[DE89-016701] N90-12233
Atomic and molecular surface and volume processes in the analysis of negative hydrogen discharges
[DE89-015705] N90-12294
DART: A simulation code for charged particle beams, revision 1
[DE89-016697] N90-12312
Wave particle interactions
[DE89-017527] N90-12335
An electromagnetic finite element particle code on an unstructured grid
[DE89-017532] N90-12336
Temporal and spatial filtering remedies for dispersion in electromagnetic particle codes
[DE89-017534] N90-12337
Properties of strongly coupled multi-ionic plasmas
[DE89-017782] N90-12339
Microwave Tokamak Experiment (MTX) ohmic heating system
[DE89-017892] N90-12340
Superconductivity and magnetic scattering in the Nd(sub 2-x)Ce(sub x)CuO(sub 4-delta)
[DE89-016524] N90-12354
Electron-positron momentum distribution measurements of high-T(sub c) superconductors and related systems
[DE89-017538] N90-12358
Subnanosecond linear GaAs photoconductive switching, revision 1
[DE89-017739] N90-12363
The characterization of Nb3Sn superconductors for use in magnets of 19 T and greater
[DE89-017758] N90-12364
CALS (Computer-aided Acquisition and Logistic Support) Test Network information exchange: User's manual
[DE89-016700] N90-12399
Particle physics and cosmology using stellar evolution theory
[DE89-017529] N90-12418
Detailed photonuclear cross-section calculations and astrophysical applications
[DE89-017531] N90-12419
High pressure studies of planetary matter
[DE89-017738] N90-12455

LIMOGES UNIV. (FRANCE).
Numerical simulation of aeroplane response to a lightning injection
[ETN-89-95271] N90-11716

LOCKHEED AERONAUTICAL SYSTEMS CO., MARIETTA, GA.
Propfan Test Assessment (PTA): Flight test report
[NASA-CR-182278] N90-11738
Propfan Test Assessment (PTA)
[NASA-CR-185138] N90-11739

LOCKHEED-CALIFORNIA CO., BURBANK.
Transport composite fuselage technology: Impact dynamics and acoustic transmission
[NASA-CR-4035] N90-11821

LOCKHEED ENGINEERING AND SCIENCES CO., WASHINGTON, DC.
USSR Space Life Sciences Digest, Issue 24
[NASA-CR-3922(28)-ISSUE-24] N90-12152
USSR Space Life Sciences Digest, Issue 22
[NASA-CR-3922(26)-ISSUE-22] N90-12153
USSR Space Life Sciences Digest, Issue 23
[NASA-CR-3922(27)-ISSUE-23] N90-12154

LOCKHEED MISSILES AND SPACE CO., PALO ALTO, CA.
The soft x ray telescope for Solar-A N90-12475
Investigation of active regions at high resolution by balloon flights of the Solar Optical Universal Polarimeter (SOUP) N90-12487

LOS ALAMOS NATIONAL LAB., NM.
Air breakdown photography in the picosecond domain
[DE89-016775] N90-11830
Formation and modification of surface alloys by excimer laser melting and resolidification
[DE89-016968] N90-11856
Temperature dependent effects during Ag deposition on Cu(110)
[DE89-016987] N90-11857
Sensitivity relationships in energetic materials
[DE89-016967] N90-11897
Indexes for the proceedings of the symposia (international) on detonation, 1951 through 1985
[DE89-015178] N90-11972
Shock-induced reaction in several liquids
[DE89-016594] N90-11973
KIVA reactive hydrodynamics code applied to detonations in high vacuum
[DE89-016979] N90-11974
Exploding metallic foil fuse modeling at Los Alamos
[DE89-016970] N90-11998
Lagrangian analysis of MIV (Magnetic Impulse-Velocity) gauge experiments on PBX 9502 using the mass-displacement moment function
[DE89-016612] N90-12000
Zeeman interferometry
[DE89-015296] N90-12012
A proposed linac cavity RF drive system for the Los Alamos extreme ultraviolet free-electron laser
[DE89-016614] N90-12016
Comparison of laser and neutral particle beam discrimination
[DE89-017786] N90-12018
A numerical laboratory for granular solids
[DE89-016367] N90-12045
Coherency properties of strong Langmuir turbulence
[DE89-009290] N90-12119
Davydov solutions at 300 Kelvin: The final search
[DE89-015248] N90-12296
Quantum-mechanical derivation of the Davydov equations for multi-quanta states
[DE89-015250] N90-12297
New developments in the ab initio treatment of low energy electron collisions with molecules
[DE89-015294] N90-12299
Highlights of papers presented at the workshop on Cold Fusion Phenomena
[DE89-016956] N90-12334
Effects of main-sequence mass loss on the turnoff ages of population 1 clusters
[DE89-016755] N90-12417
The Baksan gallium solar neutrino experiment
[DE89-016036] N90-12457

LTV MISSILES AND ELECTRONICS GROUP, DALLAS, TX.
A nonlinear-optical method for combining high power laser beams
[AD-A211730] N90-12022

LUNAR AND PLANETARY INST., HOUSTON, TX.
Abstracts for the Venus Geoscience Tutorial and Venus Geologic Mapping Workshop
[NASA-CR-185432] N90-12423

M

MARTIN MARIETTA LABS., BALTIMORE, MD.
A study of the hot workability of Al-8.5 wt pct Mg alloys for armor plate applications
[AD-A211680] N90-11868

MARYLAND UNIV., COLLEGE PARK.
Vision-based navigation for autonomous ground vehicles
[AD-A211584] N90-11725
Progress of research on water vapor lidar
[NASA-CR-185970] N90-12011
First interferometric observations with arc-sec. resolution of solar radio bursts at millimeter wavelengths
N90-12472

MASSACHUSETTS INST. OF TECH., CAMBRIDGE.
On the generation of a variable structure airport surface traffic control system
[AD-A211306] N90-11724
Kinetic processes in advanced alloys
[AD-A212049] N90-11867
Application of dimensional analysis to statistical process modeling
[AD-A211881] N90-11905
Nearly optimal algorithms and bounds for multilayer channel routing
[AD-A211913] N90-11955
Redundancies and don't cares in sequential logic synthesis
[AD-A211931] N90-11956
A digital model for level-clocked circuitry
[AD-A211937] N90-11957
Computational methods for complex flowfields
[AD-A211485] N90-11983
Investigations of Eurasian seismic sources and upper mantle structure
[AD-A211806] N90-12120
Similarity relations of wind waves in finite depth
[PB89-198113] N90-12144
Observations and modelling of deep equatorial currents in the central Pacific
[PB89-198139] N90-12145
Dynamics of the equatorial undercurrent and its termination
[PB89-198147] N90-12146
The J-Machine: A fine grain concurrent computer
[AD-A211909] N90-12187
Sequential searching in multidimensional monotone arrays
[AD-A211938] N90-12188
Experience with CST: Programming and implementation
[AD-A211882] N90-12197
An approximate max-flow min-cut theorem for uniform multicommodity flow problems with applications to approximation algorithms
[AD-A211908] N90-12198
Parallel graph contraction
[AD-A211916] N90-12199
Taxonomic syntax for first order inference
[AD-A211618] N90-12221
Dynamic embedding of trees in hypercubes with constant dilation and load
[AD-A211884] N90-12236
Four vector-matrix primitives
[AD-A211889] N90-12237
Fast computation using faulty hypercubes
[AD-A211910] N90-12238
Sequential design of experiments with physically based models 23
[AD-A211918] N90-12239
On the communication complexity of solving a polynomial equation
[AD-A211945] N90-12240
Confinement of multiply charged ions in an ECRH mirror plasma
[DE89-016052] N90-12327

Designing and designing knowledge in engineering and architecture
[PB89-219521] N90-12383
Venus volcanism: Rate estimates from laboratory studies of sulfur gas-solid reactions N90-12428
Venus surface properties deduced from radar and radiometry N90-12431

MASSACHUSETTS INST. OF TECH., LEXINGTON.
ASR-9 weather channel test report
[AD-A211749] N90-11934

MATERIALS RESEARCH LABS., ASCOT VALE (AUSTRALIA).
A critical assessment of models available for the shock initiation of heterogeneous explosives
[MRL-TR-89-17] N90-11896

MAX-PLANCK-INST. FUER EXTRATERRESTRISCHE PHYSIK, GARCHING (GERMANY, F.R.).
The solar flare and cosmic gamma-ray burst experiment aboard the Ulysses spacecraft N90-12470

MAX-PLANCK-INST. FUER PHYSIK UND ASTROPHYSIK, GARCHING (GERMANY, F.R.).
Experimental test of PCAC hypothesis in the reactions mu neutrino-proton giving muon(-)-proton-pion(+) and mu antineutrino-proton giving muon(+)-proton-pion(-) in the delta (1232) region
[MPE-PAE/EXP.EL.199] N90-12309

MCDONNELL-DOUGLAS ASTRONAUTICS CO., HOUSTON, TX.
Independent Orbiter Assessment (IOA): Analysis of the displays and controls subsystem
[NASA-CR-185563] N90-11774
Independent Orbiter Assessment (IOA): Assessment of the orbiter main propulsion system FMEA/CIL, volume 1
[NASA-CR-185559-VOL-1] N90-11775
Independent Orbiter Assessment (IOA): Assessment of the main propulsion subsystem FMEA/CIL, volume 2
[NASA-CR-185559-VOL-2] N90-11776
Independent Orbiter Assessment (IOA): Assessment of the main propulsion subsystem FMEA/CIL, volume 3
[NASA-CR-18559-VOL-3] N90-11777
Independent Orbiter Assessment (IOA): Assessment of the main propulsion subsystem FMEA/CIL, volume 4
[NASA-CR-185559-VOL-4] N90-11778
Independent Orbiter Assessment (IOA): Assessment of the electrical power distribution and control subsystem, volume 1
[NASA-CR-185557-VOL-1] N90-11779
Independent Orbiter Assessment (IOA): Assessment of the electrical power distribution and control subsystem, volume 2
[NASA-CR-185557-VOL-2] N90-11780
Independent Orbiter Assessment (IOA): Assessment of the electrical power distribution and control subsystem, volume 3
[NASA-CR-185557-VOL-3] N90-11781
Independent Orbiter Assessment (IOA): Analysis of the active thermal control subsystem
[NASA-CR-185553] N90-11782
Independent Orbiter Assessment (IOA): FMEA/CIL assessment
[NASA-CR-185550] N90-11783
Independent Orbiter Assessment (IOA): Assessment of the guidance, navigation, and control subsystem FMEA/CIL
[NASA-CR-185552] N90-11784
Independent Orbiter Assessment (IOA): Assessment of the Electrical Power Distribution and Control/Electrical Power Generation (EPD and C/EPG) FMEA/CIL
[NASA-CR-185542] N90-11785
Independent Orbiter Assessment (IOA): Analysis of the life support and airlock support subsystems
[NASA-CR-185539] N90-11786
Independent Orbiter Assessment (IOA): Assessment of the orbital maneuvering system FMEA/CIL, volume 1
[NASA-CR-185544-VOL-1] N90-11787
Independent Orbiter Assessment (IOA): Assessment of the orbital maneuvering subsystem, volume 2
[NASA-CR-185544-VOL-2] N90-11788
Independent Orbiter Assessment (IOA): Assessment of the communication and tracking subsystem, volume 1
[NASA-CR-185528-VOL-1] N90-11789
Independent Orbiter Assessment (IOA): Assessment of the communication and tracking subsystem, volume 2
[NASA-CR-185528-VOL-2] N90-11790
Independent Orbiter Assessment (IOA): Assessment of the communication and tracking subsystem, volume 3
[NASA-CR-185528-VOL-3] N90-11791
Independent Orbiter Assessment (IOA): Assessment of the hydraulics/water spray boiler subsystem
[NASA-CR-185537] N90-11792
Independent Orbiter Assessment (IOA): Assessment of the reaction control system, volume 1
[NASA-CR-185543-VOL-1] N90-11793
Independent Orbiter Assessment (IOA): Assessment of the reaction control system, volume 2
[NASA-CR-185543-VOL-2] N90-11794
Independent Orbiter Assessment (IOA): Assessment of the reaction control system, volume 3
[NASA-CR-185543-VOL-3] N90-11795
Independent Orbiter Assessment (IOA): Assessment of the reaction control system, volume 4
[NASA-CR-185543-VOL-4] N90-11796
Independent Orbiter Assessment (IOA): Assessment of the reaction control system, volume 5
[NASA-CR-185543-VOL-5] N90-11797

MESOSCALE ENVIRONMENTAL SIMULATIONS AND OPERATIONS, INC., HAMPTON, VA.
Development of high resolution simulations of the atmospheric environment using the MASS model
[NASA-CR-186040] N90-12133

MESSERSCHMITT-BOELKOW-BLOHM G.M.B.H., MUNICH (GERMANY, F.R.).
On the occasion of the 100th birthday of Ernst Heinkel
[MBB/LW/3015/S/PUB/321] N90-12494

MESSERSCHMITT-BOELKOW-BLOHM G.M.B.H., OTTOBRUNN (GERMANY, F.R.).
General data processing support from project planning to workshop control
[MBB-UD-526/88-PUB] N90-12208

MIAMI UNIV., FL.
The effect of latent heat release on synoptic-to-planetary wave interactions and its implication for satellite observations: Theoretical modeling N90-12073

MICHIGAN TECHNOLOGICAL UNIV., HOUGHTON.
Improving snow roads and airstrips in Antarctica
[AD-A211588] N90-11907

MINNESOTA UNIV., MINNEAPOLIS.
Effect of electrical double layer on transport limited currents at microelectrodes
[AD-A211586] N90-11843
Molecular dynamics study of the primitive model of 1-3 electrolyte studies
[AD-A211653] N90-11846
Assessment of thin film batteries based on polymer electrolytes. Part 1: Energy density
[AD-A212111] N90-11958

MINNESOTA UNIV., SAINT PAUL.
A Conference on Three-Dimensional Representation held in University of Minnesota on 24-26 May 1989
[AD-A211630] N90-12324
High temperature superconducting compounds
[AD-A211511] N90-12374

MISSION RESEARCH CORP., ALBUQUERQUE, NM.
Some new algorithms for boundary value problems in smooth particle hydrodynamics
[AD-A211728] N90-11987

MISSISSIPPI STATE UNIV., MISSISSIPPI STATE.
Spacelab system analysis Marshall Avionics System Testbed (MAST)
[NASA-CR-183804] N90-11802
An experimental study of surface roughness effects on turbulent boundary layer flow and heat transfer
[AD-A212099] N90-11980

MISSOURI UNIV., ROLLA.
Analysis of opposed jet hydrogen-air counter flow diffusion flame
[NASA-CR-182366] N90-11825

MITRE CORP., BEDFORD, MA.
Performance of four rake modems over the non-disturbed wideband HF channel
[AD-A211589] N90-11930

MONTANA STATE UNIV., BOZEMAN.
Computer controlled MHD power consolidation and pulse-generation system
[DE89-015600] N90-12333

MORGANTOWN TECHNOLOGY CENTER, WV.
Natural gas to liquids
[DE89-000982] N90-11828

MOUND LAB., MIAMISBURG, OH.
Operational measures of central tendency
[DE89-016959] N90-12234

N

NATIONAAL INST. VOOR KERNFYSICA EN HOGE ENERGIEFYSICA, AMSTERDAM (NETHERLANDS).
Operator product coefficients in non-diagonal conformal field theories
[PB89-216873] N90-12283

NATIONAL ACADEMY OF SCIENCES - NATIONAL RESEARCH COUNCIL, WASHINGTON, DC.
Strategy for earth explorers in global earth sciences
[NASA-CR-185933] N90-12084
Ozone depletion, greenhouse gases, and climate change
[NASA-CR-185323] N90-12101
Ozone depletion, greenhouse gases, and climate change
[PB89-216097] N90-12110
Twenty-five years of service, 1962-1987: Proceedings of the Air Force Studies Board Symposium on Air Force Research and Development, November 16, 1987
[PB89-198915] N90-12384

NATIONAL AERONAUTICS AND SPACE ADMINISTRATION, WASHINGTON, DC.
Aeronautical engineering: A continuing bibliography with indexes (supplement 243)
[NASA-SP-7037(243)] N90-11693
Aeronautical engineering: A continuing bibliography with indexes (supplement 244)
[NASA-SP-7037(244)] N90-11694
Earth resources: A continuing bibliography with indexes (issue 63)
[NASA-SP-7041(63)] N90-12091
Final environmental impact statement for the Galileo Mission (Tier 2)
[NASA-TM-101825] N90-12102
Aerospace medicine and biology: A continuing bibliography with indexes (supplement 329)
[NASA-SP-7011(329)] N90-12173
Working with people to improve productivity and quality: A bibliography with indexes, 1984-1988
[NASA-SP-7078] N90-12385
Reports of planetary geology and geophysics program, 1988
[NASA-TM-4130] N90-12454

NATIONAL AERONAUTICS AND SPACE ADMINISTRATION. AMES RESEARCH CENTER, MOFFETT FIELD, CA.
Review and analysis of the DNW/Model 360 rotor acoustic data base
[NASA-TM-102253] N90-11692
Computer simulation of aircraft aerodynamics
[NASA-TM-102221] N90-11699
Application of the wide-field shadowgraph technique to rotor wake visualization
[NASA-TM-102222] N90-11700
An experimental investigation of helicopter rotor hub fairing drag characteristics
[NASA-TM-102182] N90-11701
Wave combustors for trans-atmospheric vehicles
[NASA-TM-102238] N90-11742
Applications of flight control system methods to an advanced combat rotorcraft
[NASA-TM-101054] N90-11752
Simulation of glancing shock wave and boundary layer interaction
[NASA-TM-102233] N90-11970
Near-wall, three-dimensional turbulence measurements: A challenge for laser velocimetry
[NASA-TM-102252] N90-11978
The rodent research animal holding facility as a barrier to environmental contamination
[NASA-TM-102237] N90-12151
A simplified self-adaptive grid method, SAGE
[NASA-TM-102198] N90-12211
Ground-state coding in partially connected neural networks
[NASA-TM-102239] N90-12227

NATIONAL AERONAUTICS AND SPACE ADMINISTRATION. GODDARD INST. FOR SPACE STUDIES, NEW YORK, NY.
Global data bases on distribution, characteristics and methane emission of natural wetlands: Documentation of archived data tape
[NASA-TM-4153] N90-12090

NATIONAL AERONAUTICS AND SPACE ADMINISTRATION. GODDARD SPACE FLIGHT CENTER, GREENBELT, MD.
Processing of DMSP magnetic data and its use in geomagnetic field modeling
[NASA-TM-100750] N90-12115
Analysis of radar images of the active volcanic zone at Krafla, Iceland: The effects of look azimuth biasing N90-12434
Radar scattering mechanisms within the meteor crater ejecta blanket: Geologic implications and relevance to Venus N90-12435
Max '91 Workshop 2: Developments in Observations and Theory for Solar Cycle 22
[NASA-TM-101893] N90-12459
Magnetograph group summary N90-12461
Theory and modeling group N90-12462
The Gamma-Ray Observatory: An overview N90-12464
The BATSE experiment on the Gamma Ray Observatory: Solar flare hard x ray and gamma-ray capabilities N90-12469
Observational goals for Max '91 to identify the causative agent for impulsive bursts N90-12473
Solar flare gamma-ray and hard x ray imaging with the GRID-on-a-balloon N90-12474
Pre-pulses: Signature of a trigger process in short (less than 60 secs) solar hard x ray flares N90-12476

Joule heating and runaway electron acceleration in a solar flare N90-12478
The SMM UV observations of Active Region 5395 N90-12485
Hard x ray highlights of AR 5395 N90-12486
A high-speed digital camera system for the observation of rapid H-alpha fluctuations in solar flares N90-12491

NATIONAL AERONAUTICS AND SPACE ADMINISTRATION. HUGH L. DRYDEN FLIGHT RESEARCH FACILITY, EDWARDS, CA.
Flutter clearance of the F-18 high-angle-of-attack research vehicle with experimental wingtip instrumentation pods [NASA-TM-4148] N90-11732
Measurement effects on the calculation of in-flight thrust for an F404 turbofan engine [NASA-TM-4140] N90-11741.
A design procedure for the handling qualities optimization of the X-29A aircraft [NASA-TM-4142] N90-11753
Effect of control surface mass unbalance on the stability of a closed-loop active control system [NASA-TP-2952] N90-12042

NATIONAL AERONAUTICS AND SPACE ADMINISTRATION. JOHN F. KENNEDY SPACE CENTER, COCOA BEACH, FL.
Computation of generalized modal loads in an acoustic field define by a distribution of correlated pressures [NASA-CR-186041] N90-12047

NATIONAL AERONAUTICS AND SPACE ADMINISTRATION. LYNDON B. JOHNSON SPACE CENTER, HOUSTON, TX.
Docking system for spacecraft [NASA-CASE-MSC-21327-1] N90-11798
Three ages of Venus N90-12453

NATIONAL AERONAUTICS AND SPACE ADMINISTRATION. LANGLEY RESEARCH CENTER, HAMPTON, VA.
The upwind control volume scheme for unstructured triangular grids [NASA-TM-101664] N90-11703
Transport systems research vehicle color display system operations manual [NASA-TM-101577] N90-11736
Low-speed wind-tunnel study of reaction control-jet effectiveness for hover and transition of a STOVL fighter concept [NASA-TM-4147] N90-11751
Comparison of flying qualities derived from in-flight and ground-based simulators for a jet-transport airplane for the approach and landing pilot tasks [NASA-TP-2962] N90-11757
Catalyst for carbon monoxide oxidation [NASA-CASE-LAR-14155-1-SB] N90-11823
Airframe structural dynamic considerations in rotor design optimization [NASA-TM-101646] N90-12057
Prediction of the thermal environment and thermal response of simple panels exposed to radiant heat [NASA-TM-101660] N90-12292

NATIONAL AERONAUTICS AND SPACE ADMINISTRATION. LEWIS RESEARCH CENTER, CLEVELAND, OH.
STOVL propulsion system volume dynamics approximations [NASA-TM-102397] N90-11740
The fuel cell in space: Yesterday, today and tomorrow [NASA-TM-102366] N90-11804
An integrated methodology for optimizing structural composite damping [NASA-TM-102343] N90-11808
Steam cooled rich-burn combustor liner [NASA-CASE-LEW-13609-1] N90-11824
Creep strength of niobium alloys, Nb-1%Zr and PWC-11 [NASA-TM-102390] N90-11854
Plasma-deposited amorphous hydrogenated carbon films and their tribological properties [NASA-TM-102379] N90-11880
Fundamental tribological properties of ion-beam-deposited boron nitride films [NASA-TM-102088] N90-11881
Nonintrusive inertial vibration isolation technology for microgravity space experiments [NASA-TM-102386] N90-11901
Advances and directions of ion nitriding/carburizing [NASA-TM-102398] N90-11902
Satellite-matrix-switched, time-division-multiple-access network simulator [NASA-TP-2944] N90-11915
Channelized coplanar waveguide pin-diode switches [NASA-TM-102289] N90-11943
Hopf bifurcation in the driven cavity [NASA-TM-102334] N90-11969
Model 0A wind turbine generator FMEA [NASA-TM-102378] N90-12034
Effects of mistuning and matrix structure on the topology of frequency response curves [NASA-TM-102290] N90-12041
A least-squares finite element method for incompressible Navier-Stokes problems [NASA-TM-102385] N90-12231
Parametric study of power absorption from electromagnetic waves by small ferrite spheres [NASA-TP-2949] N90-12282
FORTRAN program for x ray photoelectron spectroscopy data reformatting [NASA-TP-2957] N90-12348
Criss-cross directory of NASA N numbers and DOD AD numbers. Volume 2, part 1: AD to N, 1979-1986. N to AD, 1962-1986 [NASA-TM-101814] N90-12388
Criss-cross directory of NASA N numbers and DOD AD numbers. Volume 2, part 2: AD to N, 1979-1986. N to AD, 1962-1986 [NASA-TM-101815] N90-12389

NATIONAL AERONAUTICS AND SPACE ADMINISTRATION. MARSHALL SPACE FLIGHT CENTER, HUNTSVILLE, AL.
NASA/MSFC FY88 Global Scale Atmospheric Processes Research Program Review [NASA-TM-100357] N90-12059
Global atmospheric moisture variability N90-12062
Dynamics and energetics of the South Pacific Convergence Zone during FGGE SOP-1 and South Pacific Convergence Zone and global-scale N90-12065
Low level remote sensing: The Doppler Radar wind profiler N90-12067
Laboratory and theoretical studies of baroclinic processes N90-12077
Characterizations of electrical properties of highT(sub c) superconducting materials [NASA-TM-100380] N90-12345
On the statistics of El Nino occurrences and the relationship of El Nino to volcanic and solar/geomagnetic activity [NASA-TP-2948] N90-12456

NATIONAL AERONAUTICS AND SPACE ADMINISTRATION. PASADENA OFFICE, CA.
Acoustic controlled rotation and orientation [NASA-CASE-NPO-16995-1-CU] N90-12289

NATIONAL AEROSPACE LAB., AMSTERDAM (NETHERLANDS).
Coatings for gas turbine compressors [NLR-MP-88045-U] N90-11750
Fractographic and microstructural analysis of fatigue crack growth in a Ti-6Al-4V fan disc forging [NLR-MP-88028-U] N90-11877
WISPER: A standardized fatigue load sequence for HAWT-blades [NLR-MP-88029-U] N90-12055
Application of matrix correction methods on a plate and a truss structure [NLR-MP-88042-U] N90-12056

NATIONAL AEROSPACE LAB., KAKUDA (JAPAN).
Program for high speed computation of physical properties of propellants and combustion gas of an LH2/LOX rocket engine [NAL-TM-564] N90-11803

NATIONAL AEROSPACE LAB., TOKYO (JAPAN).
Wind tunnel test of CAD USB-STOL semi-borne prototype [NAL-TM-566] N90-11696
Acoustic-thermal environment for USB flap structure. Report 1: Ground simulation test results [NAL-TM-567] N90-11697
Effects of a heat cycle on material strength [NAL-TM-562] N90-11737
Axial compression buckling test on the H-2 launch vehicle satellite fairing structural element prototype (aluminum surface plate/aluminum honeycomb sandwiched curved surface plate) [NAL-TM-563] N90-12039
Basic program for raster scan display unit [NAL-TM-560] N90-12185
Software package for 3-dimensional graphic display unit [NAL-TM-559] N90-12191

NATIONAL BUREAU OF STANDARDS, GAITHERSBURG, MD.
Development and use of a tribology research-in-progress database [PB89-228274] N90-12396

NATIONAL CENTER FOR ATMOSPHERIC RESEARCH, BOULDER, CO.
Scientific justification and development plan for a mid-sized jet research aircraft [PB89-208995] N90-11731
Global tropospheric chemistry: Chemical fluexes in the global atmosphere [NASA-CR-186090] N90-12109
Meeting review: The Second NCAR (National Center for Atmospheric Research) Research Aircraft Fleet Workshop [PB89-200901] N90-12113
Investigations of polar air stream cyclogenesis based on numerical simulations with a mesoscale model [PB89-214563] N90-12132

NATIONAL INST. OF STANDARDS AND TECHNOLOGY, BOULDER, CO.
Ignition characteristics of the nickel-based alloy UNS N07718 in pressurized oxygen [NASA-CR-185932] N90-11850
Clutter models for subsurface electromagnetic applications [PB89-229678] N90-11925

NATIONAL INST. OF STANDARDS AND TECHNOLOGY, GAITHERSBURG, MD.
Photolithography: A new tool for ceramic science [DE90-000135] N90-11885
Elimination of spurious eigenvalues in the Chebyshev tau spectral method [PB89-209282] N90-11967
NDE (Non-Destructive Evaluation) publications, 1985 [PB89-229025] N90-12036
Mechanism for shear band formation in the high strain rate torsion test [PB89-215370] N90-12038
Lightning and surge protection of photovoltaic installations: Two case histories, Vulcano and Kythnos [PB89-229058] N90-12135
Synergistic effects of nitrogen dioxide and carbon dioxide following acute inhalation exposures in rats [PB89-214779] N90-12150
Processing rate sensitivities of a heterogeneous multiprocessor [PB89-229017] N90-12201
Detailed description of the knowledge-based system for physical database design, volume 2 [PB89-229033] N90-12395
Center for Electronics and Electrical Engineering technical publication announcements covering Center programs, January-March 1989 with 1989 CEEE events calendar [PB89-228308] N90-12402

NATIONAL LIBRARY OF MEDICINE, BETHESDA, MD.
National Library of Medicine DOCLINE (tradename) manual [PB89-188676] N90-12390

NATIONAL OCEANIC AND ATMOSPHERIC ADMINISTRATION, BOULDER, CO.
Further guide for the retrieval of dropsize distributions in water clouds with a ground-based clear-air-sensing Doppler radar [PB89-196000] N90-11911
Propagation of an elliptical laser beam through the turbulent atmosphere (vertical beams) [PB89-208680] N90-12010
Turbulence effects on reflected optical patterns (atmosphere and structure) [PB89-208094] N90-12315
MHD (magnetohydrodynamic) modeling of solar and interplanetary processes [PB89-215461] N90-12416
Some of the terrestrial effects of AR 5395 N90-12482

NATIONAL OCEANIC AND ATMOSPHERIC ADMINISTRATION, SEATTLE, WA.
Observations of long Rossby waves in the northern tropical Pacific [PB89-196331] N90-12143
Equatorial oceanic response to forcing on time scales from days to months [PB89-206775] N90-12147

NATIONAL OCEANOGRAPHIC INSTRUMENTATION CENTER, WASHINGTON, DC.
Satellite-derived rainfall estimates and propagation characteristics associated with the Mesoscale Convective Systems (MCSs) [PB89-213417] N90-12086

NATIONAL PHYSICAL LAB., TEDDINGTON (ENGLAND).
A model for long-term creep and the effects of physical ageing in poly (butylene terephthalate) [NPL-DMA(A)-182] N90-11895
Use of the NPL linac for x ray dosimetry [NPL-RSA(EXT)-6] N90-12314
A critical assessment of thermodynamic and phase diagram data for the Ga-In system [NPL-DMA(A)-174] N90-12382

NATIONAL SCIENCE FOUNDATION, WASHINGTON, DC.
Federal funds for research and development: Fiscal years 1986, 1987, and 1988. Volume 36: Detailed statistical tables [PB89-223523] N90-12407

Federal funds for research and development. Fiscal years 1987, 1988, and 1989. Volume 37: Detailed statistical tables
[PB89-223531] N90-12408

NATIONAL SEVERE STORMS FORECAST CENTER, KANSAS CITY, MO.
Severe local storm warning verification: 1988
[PB89-226310] N90-12134

NATIONAL TELECOMMUNICATIONS AND INFORMATION ADMINISTRATION, ANNAPOLIS, MD.
Handbook of radio wave propagation loss (100-20,000 MHz), part 2
[PB89-195473] N90-11912

NAVAL CIVIL ENGINEERING LAB., PORT HUENEME, CA.
Coating galvanized steel
[AD-A211775] N90-11869

NAVAL HEALTH RESEARCH CENTER, SAN DIEGO, CA.
Demonstration of replicable dimensions of health behaviors
[AD-A211920] N90-12161

NAVAL OCEAN SYSTEMS CENTER, KAILUA, HI.
Small-radius bending loss in single-mode fibers
[AD-A211822] N90-12323

NAVAL OCEAN SYSTEMS CENTER, SAN DIEGO, CA.
Sensitivity of optoelectronic receivers
[AD-A211823] N90-11923
Airborne profiles taken near San Nicolas Island, California, during Operation FIRE (First ISCCP (International Satellite Cloud Climatology Project) regional experiment) (1987): Aerosol size distributions, air and surface temperatures, cloud top temperatures, and relative humidities
[AD-A211664] N90-12136
Numerical solution of acoustic-structure interaction problems
[AD-A211505] N90-12293

NAVAL PERSONNEL RESEARCH AND DEVELOPMENT CENTER, SAN DIEGO, CA.
The effect of incentives on the reliability and validity of cognitive speed tests
[AD-A211346] N90-12181

NAVAL POSTGRADUATE SCHOOL, MONTEREY, CA.
Post crash flight analysis: Visualizing flight recorder data
[AD-A212063] N90-11715
Petite Amateur Navy Satellite (PANSAT)
[NASA-CR-186049] N90-11800
On-orbit annealing of gallium arsenide solar cell arrays
[AD-A212087] N90-11900
Design and calibration of an electrodynamic driver for the Space Thermoacoustic Refrigerator (STAR)
[AD-A212022] N90-11906

NAVAL RESEARCH LAB., WASHINGTON, DC.
Low temperature formation of titanium aluminide films using physical vapor deposition
[AD-A211877] N90-11866
NRL/VOA modifications to IONCAP as of 12 July 1988
[AD-A211546] N90-11929
Pacific marine radar sea scatter experimental results
[AD-A211593] N90-11931
Superconducting switch program
[AD-A211580] N90-11964
Advanced concepts theory
[AD-A211665] N90-12344
Capabilities of GRO/OSSE for observing solar flares
N90-12467

NAVAL SURFACE WARFARE CENTER, SILVER SPRING, MD.
Viscous split algorithms for the time dependent incompressible Navier-Stokes equations
[AD-A211592] N90-11985

NAVAL UNDERWATER SYSTEMS CENTER, NEWPORT, RI.
Doppler statistics of ocean velocity variability
[AD-A211667] N90-12148

NAVY CLOTHING AND TEXTILE RESEARCH FACILITY, NATICK, MA.
New Fabric Development Program
[AD-A211549] N90-11891

NEW HAMPSHIRE UNIV., DURHAM.
High energy flare physics group summary N90-12460

NEW MEXICO UNIV., ALBUQUERQUE.
The onset of the solar active cycle 22 N90-12488

NEW YORK UNIV., NEW YORK.
Visual motion perception
[AD-A210994] N90-12160

NEW YORK UNIV. MEDICAL CENTER.
Review of the national ambient air quality standards for lead: Exposure analysis methodology and validation
[PB89-207914] N90-12104

NORTH CAROLINA STATE UNIV., RALEIGH.
Membrane fusion: The role of polyphosphatidylinositol
[AD-A211289] N90-12156
Three dimensional object recognition employing combined visual and tactile sensing
[PB89-219469] N90-12176

NORTH CAROLINA UNIV., CHAPEL HILL.
Methanol fueled vehicles and photochemical models: An evaluation of the state of knowledge
[PB89-214225] N90-12410

NOTRE DAME UNIV., IN.
The structure of separated flow regions occurring near the leading edge of airfoils - including transition
[NASA-CR-185853] N90-11695

O

OAK RIDGE GASEOUS DIFFUSION PLANT, TN.
The application of quality assurance to engineering management
[DE89-009955] N90-12386

OAK RIDGE NATIONAL LAB., TN.
International seminar on the inelastic behavior of solids: Models and utilization
[DE89-017420] N90-11858
Weldability of ductile nickel aluminides
[DE89-017452] N90-11859
Current research in advanced materials
[DE89-017466] N90-11884
Correlating microemulsion fuel composition, structure and combustion properties
[DE89-017779] N90-11898
An application of the J-integral to an incremental analysis of blunting crack behavior
[DE89-016844] N90-12046
Policies to encourage private sector responses to potential climate change
[DE89-017244] N90-12107
Navigation of robotic systems
[DE89-017507] N90-12219
Beam dynamics of a liquid metal ion source
[DE89-015856] N90-12295
Synchrotron-radiation experiments with recoil ions
[DE89-017579] N90-12301
Fluctuations in transverse energy and multiplicity, energy densities, and neutral pion spectra in nucleus-nucleus collisions at 200 GeV/nucleon
[DE89-017583] N90-12302
A survey of camera error sources in machine vision systems
[DE89-014072] N90-12318
Characterization of the Structure and Chemistry of Defects in Materials: Proceedings, volume 138
[DE89-014796] N90-12352
Ion beam deposition of epitaxial germanium and gallium arsenide layers
[DE89-017439] N90-12357
Effects of grain boundary chemistry on critical current density in oxide superconductors
[DE89-017780] N90-12365
Building a user-friendly data dictionary system in ORACLE
[DE89-014878] N90-12397
An atom probe study of phase decomposition in three iron meteorites
[DE89-017581] N90-12420

OHIO STATE UNIV., COLUMBUS.
Mechanism of electrochemical activation of carbon electrodes: Role of graphite lattice defects
[AD-A211644] N90-11845
Doubly-fluted tubes and enhanced tubes in confined crossflow
[PB89-217921] N90-11971
Distributed knowledge-based systems
[AD-A211984] N90-12401

OHIO UNIV., ATHENS.
Discrete filtering techniques applied to sequential GPS range measurements
[NASA-CR-177472] N90-11730

OKLAHOMA STATE UNIV., STILLWATER.
Growth and characterization of materials for tunable lasers in the near infrared spectral region
[NASA-CR-185832] N90-12009

OLD DOMINION UNIV., NORFOLK, VA.
A study of the temporal stability of multiple cell vortices
[NASA-CR-4261] N90-11968

OPTICAL COATING LAB., INC., DUNFERMLINE (SCOTLAND).
Vanadium dioxide protective devices
[AD-A212018] N90-11887

OREGON STATE UNIV., CORVALLIS.
Adjustable speed drive study, part 1
[DE89-017654] N90-11948

OREGON UNIV., EUGENE.
Electron attachment and molecular fragmentation in laser-excited plasmas
[AD-A212098] N90-12343

OSSERVATORIO ASTROFISICO DI ARCETRI, FLORENCE (ITALY).
Flare model sensitivity of the Balmer spectrum
N90-12477

P

PACIFIC NORTHWEST LAB., RICHLAND, WA.
Stochastic propagation of an array of parallel cracks: Exploratory work on matrix fatigue damage in composite laminates
[DE89-017837] N90-11813
User's guide for a personal computer model of turbulence at a wind turbine rotor
[DE89-017753] N90-12095
Nuclear closed-cycle gaseous heat engine concept
[DE89-016824] N90-12313

PARIS-SUD UNIV., ORSAY (FRANCE).
Electron-positron momentum distribution measurements of high-T(sub c) superconductors and related systems
[DE89-017538] N90-12358

PEI ASSOCIATES, INC., DURHAM, NC.
Review of the national ambient air quality standards for lead: Exposure analysis methodology and validation
[PB89-207914] N90-12104

PENNSYLVANIA STATE UNIV., UNIVERSITY PARK.
Premixed turbulent flame propagation
[AD-A211489] N90-11841
An investigation of end-wall vortex cavitation in a high Reynolds number axial-flow pump
[AD-A211426] N90-11982
Experimental research on swept shock Wave/Boundary layer interactions
[AD-A211744] N90-11988
Stratiform clouds and their interaction with atmospheric motions N90-12060
Infrared backscattering N90-12083
Wrist orientation effect on grip strength and endurance
[PB89-200935] N90-12179

PENNSYLVANIA UNIV., PHILADELPHIA.
Catalogic hydrogenation of carbon monoxide
[DE89-017813] N90-11834

PHYSICAL SCIENCES, INC., ANDOVER, MA.
LABCEDE fluorescence investigations
[AD-A210678] N90-12114

PHYSICS AND ELECTRONICS LAB. TNO, THE HAGUE (NETHERLANDS).
Feasibility of graphics voice telephones for the post 2000 era
[FEL-1988-26] N90-11937
Modeling of diffraction reflection and clutter loss in UHF radio wave propagation
[FEL-1988-28] N90-11938
Theory and simulation of the operation of a Doppler direction finder in a multipath environment
[FEL-1988-56] N90-11939
A method to model fuze-performance. Part 3: Diffraction of electromagnetic radiation by an edge
[FEL-1989-22-PT-3] N90-11940
Fast and objective MRTD measurement
[FEL-1988-24] N90-12006
Calibration of a visioceilometer, a hand held lidar system
[FEL-1988-73] N90-12137
A closer look at the visioceilometer
[FEL-1989-80] N90-12138

PHYSIKALISCH-TECHNISCHE BUNDESANSTALT, BRUNSWICK (GERMANY, F.R.).
Contribution of the precision determination of noise powers in the MHz and lower GHz frequency range
[PTB-E-33] N90-11935

PRINCETON UNIV., NJ.
AFRAPT (Air Force Research in Aero Propulsion Technology) Trainee Program
[AD-A211540] N90-11744

PURDUE UNIV., WEST LAFAYETTE, IN.
Synoptic/planetary-scale interactions and blocking over the North Atlantic Ocean N90-12061
On finding the largest normal mean and estimating the selected mean
[AD-A211628] N90-12245
Empirical Bayes estimation of binomial parameter with symmetric priors
[AD-A211646] N90-12246
On a classification problem: Ranking and selection approach
[AD-A211627] N90-12269
On the asymptotic optimality of certain empirical Bayes simultaneous testing procedures
[AD-A211649] N90-12270
An experimental high energy physics program
[DE89-014695] N90-12311

R

RADIAN CORP., AUSTIN, TX.
Potential technologies for collection and destruction of CFCs (Chlorofluorocarbons), halons, and related compounds
[PB89-219968] N90-12105

RDP, INC., WALTHAM, MA.
TEC (Total Electron Content) models
[AD-A211553] N90-12129

RENSSELAER POLYTECHNIC INST., TROY, NY.
Acoustical effects of a large ridge on low-frequency sound propagation in stationary and moving atmospheres
[NASA-CR-186001] N90-12290

RETINA FOUNDATION, BOSTON, MA.
Eye movements and spatial pattern vision
[AD-A211650] N90-12169

ROCKWELL INTERNATIONAL SCIENCE CENTER, THOUSAND OAKS, CA.
Multicolor electrochromic displays exploratory development
[AD-A212004] N90-11721

ROLLS-ROYCE LTD., DERBY (ENGLAND).
The RB199: An in-service success
[PNR90544] N90-11746
Advanced technology in military gas turbine design and manufacture
[PNR90545] N90-11747
Engine controls for the 1990's
[PNR90546] N90-11748
Future military powerplants
[PNR90554] N90-11749
Aluminium alloy development for aero engines
[PNR90548] N90-11874

ROME AIR DEVELOPMENT CENTER, GRIFFISS AFB, NY.
Proceedings of the 1988 Antenna Applications Symposium, volume 1
[AD-A211396] N90-11928
Dielectric covered microstrip patch antennas
[AD-A211577] N90-11963

ROYAL AEROSPACE ESTABLISHMENT, FARNBOROUGH (ENGLAND).
Comparison of the results of tests on A300 aircraft in the RAE 5 metre and ONERA F1 wind tunnels
[RAE-TM-AERO-2130] N90-11768
Deformation of Ti-6Al-4V bar and extrusion under superplastic forming conditions
[RAE-TM-MAT/STR-1110] N90-11875
Deformation of extruded titanium alloys under superplastic conditions
[RAE-TM-MAT/STR-1111] N90-11876
Deformation of electron beam welded Ti-6Al-4V alloy sheet under superplastic conditions
[RAE-TM-MAT/STR-1109] N90-12053
Effect of superplastic deformation on the surface roughness of sheet
[RAE-TM-MAT/STR-1112] N90-12054
Introduction to the Mil-Std-1553B serial multiplex data bus
[RAE-TM-M-9] N90-12405
Time-weighted accumulations ap(tau) and Kp(tau)
[RAE-TR-88050] N90-12422

ROYAL INST. OF TECH., STOCKHOLM (SWEDEN).
The physics of double layers and their role in astrophysics
[TRITA-EPP-89-03] N90-12421

ROYAL NETHERLANDS METEOROLOGICAL INST., DE BILT.
Crau 1987: The KNMI contribution
[KNMI-TR-110] N90-12140
Description of a software library for the calculation of surface fluxes
[KNMI-TR-112] N90-12141

ROYAL SIGNALS AND RADAR ESTABLISHMENT, MALVERN (ENGLAND).
A simulation study of landing time allocation procedures for use in computer-assisted air traffic management systems
[AD-A212159] N90-11722
On the design and implementation of a secure computer system
[RSRE-MEMO-4188] N90-12189
A security model and its implementation
[RSRE-MEMO-4222] N90-12190
Parallel processing on transputer arrays for the recognition of objects in infrared images
[RSRE-MEMO-4197] N90-12217
A hybrid optimisation strategy for adaptive feed-forward layered networks
[RSRE-MEMO-4193] N90-12226

S

SAINT LOUIS UNIV., MO.
Seismic wave attenuation and yield determination at regional distances
[AD-A211548] N90-12128

SANDIA NATIONAL LABS., ALBUQUERQUE, NM.
Simulation of the EMP (Electromagnetic Pulse) from ESD (Electrostatic Discharge)
[DE89-014484] N90-11918
Video imaging systems: A survey
[DE89-016920] N90-11919
Cleaning of printed circuit assemblies with surface-mounted components
[DE89-013609] N90-11945
An empirical formula for gas switch breakdown delay
[DE89-017233] N90-11947
Pulsed-laser-excited Raman spectra of shock compressed triaminotrinitrobenzene
[DE90-000668] N90-12019
Photovoltaic system research status
[DE89-016764] N90-12094
Operating experience with the Sandia terminal switching network and fiber optic loop
[DE89-007422] N90-12317
Distance and clearance perception using forward-looking, vehicular television systems
[DE89-014740] N90-12319
Energy relaxation of light holes in InAs(.15)Sb(.85)/InSb multiple quantum wells
[DE89-016035] N90-12349
Field-assisted bonding of single crystal quartz
[DE89-015407] N90-12353

SAO PAULO UNIV. (BRAZIL).
Two dimensional conformal supergravity and critical behavior
[DE89-611968] N90-12414

SHEFFIELD UNIV. (ENGLAND).
Adaptive noise cancellation for a class of nonlinear 2R filter
[RR-351] N90-11965
A distributed pipelined architecture of the recursive Lagrangian equations of motion for robot manipulators with VLSI implementation
[RR-353] N90-11966
An optimum trajectory planner for robot manipulators in joint-space and under physical constraints
[RR-349] N90-12029
On the complexity analysis of the coriolis and centripetal effects of a 6 DOF robot manipulator
[RR-344] N90-12030
The dynamic performance of robot manipulators under different operating conditions
[RR-345] N90-12031
Distributed VLSI architecture for fast Jacobian and inverse Jacobian formulations
[RR-346] N90-12218
Robot inverse dynamics computation via VLSI distributed architectures
[RR-350] N90-12223
Can perceptrons find Lyapunov functions: An algorithmic approach to systems stability
[RR-365] N90-12224
Fast forward dynamics algorithm for robot arms using multiprocessing
[RR-367] N90-12225
Global linear representations of nonlinear systems and the adjoint map
[RR-347] N90-12247
Rational expansion for nonlinear input-output maps
[RR-348] N90-12248
Mapping nonlinear integro-differential equations into the frequency domain
[RR-366] N90-12249
Orthogonal least squares methods and their application to nonlinear system identification
[RR-343] N90-12259
Fast sampling and stability of nonlinear sampled data systems. Part 2: Sampling rate estimations
[RR-341] N90-12271
Modeling and analysis of nonlinear time series
[RR-355] N90-12272
Fast sampling and stability of nonlinear sampled-data systems. Part 1: Existence theorems
[RR-340-PT-1] N90-12276
Slow sampling and stability of nonlinear sampled-data systems
[RR-342] N90-12277

SIMPSON WEATHER ASSOCIATES, INC., CHARLOTTESVILLE, VA.
LAWS simulation: Sampling strategies and wind computation algorithms N90-12081

SOUTHERN METHODIST UNIV., DALLAS, TX.
Venus: Mantle convection, hotspots, and tectonics
N90-12442

SOUTHWEST RESEARCH INST., SAN ANTONIO, TX.
Sliding seal materials for low heat rejection engines
[NASA-CR-182262] N90-11882

SPECIAL LIBRARIES ASSOCIATION, CHICAGO, IL.
Criss-cross directory of NASA N numbers and DOD AD numbers. Volume 2, part 1: AD to N, 1979-1986. N to AD, 1962-1986
[NASA-TM-101814] N90-12388
Criss-cross directory of NASA N numbers and DOD AD numbers. Volume 2, part 2: AD to N, 1979-1986. N to AD, 1962-1986
[NASA-TM-101815] N90-12389

SRI INTERNATIONAL CORP., MENLO PARK, CA.
Structure based formal methods for software engineering
[AD-A211660] N90-12207

STANFORD UNIV., CA.
Unsteady aerodynamics with applications to flight mechanics
[AD-A211944] N90-11706
Active control of unsteady and separated flow structures
[AD-A212109] N90-11707
Computer-based tutors for explaining and managing the process of diagnostic reasoning
[AD-A211738] N90-12222
A dynamic proof of the Frobenius-Perron theorem for Metzler matrices
[AD-A211839] N90-12235
Small sample theory for steady state confidence intervals
[AD-A212097] N90-12242
A matrix factorization and its application to large-scale linear programming
[AD-A211293] N90-12244
A unified framework for simulating Markovian models of highly dependable systems
[AD-A212164] N90-12267
Computer problems in goodness-of-fit
[AD-A211411] N90-12268
The behavior of beams of relativistic non-thermal electrons under the influence of collisions and synchrotron losses
[NASA-CR-185983] N90-12298
State-resolved reaction dynamics
[AD-A211613] N90-12307
Surface, interface, and bulk properties of high T(sub c) superconductors
[AD-A211490] N90-12373
Venus and the Archean Earth: Thermal considerations
N90-12448
The hard x rays and gamma-rays from solar flares
[NASA-CR-185982] N90-12458
When and where to look to observe major solar flares
N90-12465
Development of a numerical solution to the time dependent kinetic equation N90-12481

STATE UNIV. OF NEW YORK, BUFFALO.
Cellular and molecular mechanisms of high pressure inotropy in cardiac muscle
[AD-A211695] N90-12170

STRATEGIC DEFENSE INITIATIVE ORGANIZATION, WASHINGTON, DC.
FY 1990/FY 1991 biennial budget descriptive summaries for the Strategic Defense Initiative Organization
[AD-A211985] N90-12409

SVERDRUP TECHNOLOGY, INC., CLEVELAND, OH.
Droplet sizing instrumentation used for icing research: Operation, calibration, and accuracy
[NASA-CR-182293] N90-11999

SWEDISH INST. FOR MATERIALS TESTING, BORAS.
Comparison of I2-stabilized HE-NE lasers
[PB89-219844] N90-12014

SWEDISH INST. OF SPACE PHYSICS, KIRUNA.
On the role of Coulomb forces in atomic radiative emission
[IRF-PREPRINT-106] N90-12308

SYSTEMS CONTROL TECHNOLOGY, INC., ARLINGTON, VA.
Rotorcraft low altitude CNS benefit/cost analysis: Rotorcraft operations data
[DOT/FAA/DS-89/9] N90-12406

T

TAMPERE UNIV. OF TECHNOLOGY (FINLAND).
Analysis of the efficiency of a dielectric solar energy collector
[PB89-212716] N90-12092

TECHNISCHE HOCHSCHULE, DARMSTADT (GERMANY, F.R.).
Determination and description of the long term creep behavior of high temperature gas turbine materials
[ETN-89-94985] N90-11871

TECHNISCHE HOGESCHOOL, DELFT (NETHERLANDS).
Stability and control derivatives of the De Havilland DHC-2 BEAVER aircraft
[PB89-217525] N90-11754
Project AENEAS: A feasibility study for crew emergency return vehicle
[PB89-217020] N90-11799
Buckling of axially compressed imperfect orthotropic shells with elastic edge supports
[PB89-217038] N90-12043
Noise data of four small propeller-driven airplanes
[PB89-216980] N90-12291
Electrolitic deposited ohmic contacts on III-V compound semiconductors: A review
[PB89-217400] N90-12350
TECHNISCHE UNIV., BRUNSWICK (GERMANY, F.R.).
The time evaluation of the number of space probes and debris at different orbit heights with a view to a future collision risk in space
[R-8718] N90-11772
TECHNISCHE UNIV., DARMSTADT (GERMANY, F.R.).
Creep and fracture behavior of heat resistant steels in characteristic cases of variable fatigue loading
[ETN-89-94671] N90-11855
TECHNISCHE UNIV., DELFT (NETHERLANDS).
Modelling and control of a diffusion/LPCVD furnace
[REPT-88-97] N90-11910
On the computation of normal modes of a rotating, viscous, incompressible fluid with a capillary free boundary
[REPT-89-01] N90-11989
Three-dimensional viscoelastic bodies in steady state frictional rolling contact with generalization to Knothe rolling
[REPT-89-23] N90-12032
A language for assembly instructions
[REPT-88-90] N90-12209
A polynomial method of approximate weighted centers for linear programming
[REPT-89-13] N90-12210
On the differentiable manifold of fixed order stable linear systems
[REPT-88-89] N90-12250
Smooth linearization of hyperbolic fixed points without resonance conditions
[REPT-89-03] N90-12251
Some observations on the convergence behavior of GMRES
[REPT-89-09] N90-12252
A simple proof of a differential equation for generalizations of Laguerre polynomials
[REPT-89-15] N90-12253
The convergence behavior of some iterative solution methods
[REPT-89-19] N90-12260
Analysis of a system of two weakly nonlinear coupled harmonic oscillators arising from the field of wind-induced vibrations
[REPT-89-22] N90-12261
Augmentations of grammatical categories in distributional-algebraic models of natural languages
[REPT-89-24] N90-12262
Generalizations of Laguerre polynomials
[REPT-89-25] N90-12263
A multigrid method combined with defect correction for free convection problems at high Rayleigh numbers
[REPT-89-27] N90-12264
Some techniques for anaphora resolution in algebraic linguistics
[REPT-89-28] N90-12265
Some 1(sub p) invariant probability measures
[REPT-88-91] N90-12273
Fuzzy logic and the generalized modus ponens
[REPT-88-92] N90-12274
Estimating functionals related to a density by a class of statistics based on spacings
[REPT-89-11] N90-12275
A long time tail for random walk in random scenery
[REPT-89-08] N90-12278
Likelihood cross-validation bandwidth selection for nonparametric kernel density estimators
[REPT-89-10] N90-12279
TECHNISCHE UNIV., VIENNA (AUSTRIA).
Anisotropy and microstructure of high-coercivity rare earth permanent magnets
[AD-A211905] N90-12285
TECHNO-SCIENCES, INC., GREENBELT, MD.
Robust control design for flight control
[AD-A211957] N90-11756
TEXAS A&M UNIV., COLLEGE STATION.
Development of direct-inverse 3-D methods for applied transonic aerodynamic wing design and analysis
[NASA-CR-186036] N90-11733
Field evaluation of the multi-depth deflectometers
[PB89-207708] N90-11994
Tropical Pacific moisture variability N90-12070
A lightweight solid polymer electrolyte fuel cell with stack power density of 3 kW/lb (7 kW/kg)
[AD-A211542] N90-12098
TEXAS TECHNOLOGICAL UNIV., LUBBOCK.
Development of high frequency spice models for ferrite core inductors and transformers
[DE89-015121] N90-11946
TEXAS UNIV., AUSTIN.
Experimental research in high energy physics
[DE90-000061] N90-12342
TEXTRON BELL HELICOPTER, FORT WORTH, TX.
Investigation of difficult component effects on finite element model vibration prediction for the Bell AH-1G helicopter. Volume 1: Ground vibration test results
[NASA-CR-181916-VOL-1] N90-12058
THOMSON-CSF, ORSAY (FRANCE).
Proceedings of the Workshop on Compound Semiconductor Devices and Integrated Circuits (13th) held in Cabourg, France on 10-12 May 1989
[AD-A211848] N90-11954
TOKYO UNIV., TANASHI (JAPAN).
Fabrication of modulated vanes for a split-coaxial RFQ
[DE88-757235] N90-12310
TUFTS UNIV., MEDFORD, MA.
In-situ cure monitoring of composites by fiber-optic molecular sensors
[AD-A211495] N90-11817
Synthesis and microstructure of highly oriented PbTiO3 thin films prepared by a sol-gel method
[AD-A211735] N90-12377
VLA-Max '91 tests of high energy flare physics
N90-12471

U

UNITED TECHNOLOGIES RESEARCH CENTER, EAST HARTFORD, CT.
Investigation of advanced mixer-ejector exhaust system
[AD-A211943] N90-11705
Carbon fiber reinforced glass matrix composites for structural space based applications
[AD-A211682] N90-11818
UNIVERSAL ENERGY SYSTEMS, INC., DAYTON, OH.
Studies on the startup transients and performance of a gas loaded sodium heat pipe
[AD-A211880] N90-12379
UNIVERSIDADE FEDERAL DO RIO DE JANEIRO (BRAZIL).
Scalar fields versus black holes
[DE89-611967] N90-12413
UNIVERSITIES SPACE RESEARCH ASSOCIATION, HOUSTON, TX.
Autonomous space processor for orbital debris
[NASA-CR-186043] N90-11770
UNIVERSITIES SPACE RESEARCH ASSOCIATION, HUNTSVILLE, AL.
Aerosol backscatter studies supporting LAWS
N90-12079
UNIVERSITY OF SOUTHERN CALIFORNIA, MARINA DEL REY.
The conditional-event approach to distributed simulation
[NASA-CR-185890] N90-12200
A single-phase clocked NOR/NOR CMOS programmable sequential array structure
[AD-A211297] N90-12203
ISI's (Information Sciences Institute) SDI architecture simulator: An experiment in adding new software to the system
[AD-A211314] N90-12204
UTAH UNIV., SALT LAKE CITY.
Investigation of resonant ac-dc magnetic field effects
[AD-A211612] N90-12159

V

VIRGINIA UNIV., CHARLOTTESVILLE.
The effect of latent heat release on synoptic-to-planetary scale wave interactions: Observational study
N90-12074
SIS (Superconductor-Insulator-Superconductor) mixer research
[AD-A211607] N90-12375
VRIJE UNIV., AMSTERDAM (NETHERLANDS).
Role of conceptual models in the design and use of information systems
[PB89-217376] N90-12392

W

WASHINGTON STATE UNIV., PULLMAN.
Luminescence in applied magnetic fields
[AD-A211551] N90-12287
WASHINGTON UNIV., SEATTLE.
Structure/reactivity relationships of polysilazane preceramics
[AD-A212028] N90-11888
Graded bandgap solar cells
[AD-A211537] N90-12097
Metacognition and retrieval from long-term memory at Mount Everest
[AD-A211629] N90-12177
WASHINGTON UNIV., SAINT LOUIS, MO.
Geology of Southern Guinevere Planitia, Venus, based on analyses of Goldstone radar data N90-12424
Radar scattering from desert terrains, Pisgah/Lavic Region, California: Implications for Magellan
N90-12443
WAYNE STATE UNIV., DETROIT, MI.
Empirical Bayes estimation of binomial parameter with symmetric priors
[AD-A211646] N90-12246
WENTWORTH INST., BOSTON, MA.
Design of scientific payloads and components
[AD-A211819] N90-12005
WEST VIRGINIA UNIV., MORGANTOWN.
Three component laser Doppler measurements in an axisymmetric jet
[NASA-CR-181908] N90-11702
WESTINGHOUSE ELECTRIC CORP., MIDDLETOWN, RI.
Effects on electromagnetic wave propagation and rocket vapor trails of intense turbulence generated by breaking internal gravity waves
[AD-A211755] N90-12130
WESTINGHOUSE HANFORD CO., RICHLAND, WA.
Fracture toughness data base for HT9 and modified 9Cr-1Mo irradiated in several reactors up to approximately 100 dpa
[DE90-000111] N90-11864
Wind/seismic comparisons for upgrading existing structures
[DE89-016055] N90-12044
WICHITA STATE UNIV., KS.
Stall/spin/flight simulation
[DOT/FAA/CT-88/28] N90-11765
WISCONSIN UNIV., MADISON.
Lightning data study in conjunction with geostationary satellite data
[NASA-CR-179286] N90-12142
Homoclinic orbits for a class of Hamiltonian systems
[AD-A210562] N90-12229
Stellarator transport theory
[DE89-016371] N90-12328
WOODS HOLE OCEANOGRAPHIC INST., MA.
Similarity relations of wind waves in finite depth
[PB89-198113] N90-12144
Observations and modelling of deep equatorial currents in the central Pacific
[PB89-198139] N90-12145
Dynamics of the equatorial undercurrent and its termination
[PB89-198147] N90-12146
WORCESTER POLYTECHNIC INST., MA.
Error estimation and self-adaptive mesh refinement for boundary element method N90-12037
WORLD METEOROLOGICAL ORGANIZATION, GENEVA (SWITZERLAND).
World Weather Watch: Implementation
[WMO-714] N90-12139
WYOMING UNIV., LARAMIE.
Static tensile and tensile creep testing of four boron nitride coated ceramic fibers at elevated temperatures
[NASA-CR-184999] N90-11807

X

XEROX PALO ALTO RESEARCH CENTER, CA.
Color printing for computer graphics. Or: How to get it off your screen and onto paper, in color
[PB89-208110] N90-12184

Y

YALE UNIV., NEW HAVEN, CT.
Application of dynamical systems theory to global weather phenomena revealed by satellite imagery
N90-12063

CONTRACT NUMBER INDEX

Typical Contract Number Index Listing

AF-AFOSR-0039-88
N90-10330
CONTRACT NUMBER
NASA ACCESSION NUMBER

Listings in this index are arranged alphanumerically by contract number. Under each contract number the NASA accession numbers denoting documents that have been produced as a result of research done under that contract are arranged in ascending order. The NASA accession number denotes the number by which the citation is identified.

AF PROJ. 2301 .... N90-12097
N90-12304
N90-12305
AF PROJ. 2302 .... N90-12051
AF PROJ. 2303 .... N90-11844
N90-11845
N90-12325
AF PROJ. 2304 .... N90-11986
N90-12401
AF PROJ. 2305 .... N90-12375
AF PROJ. 2306 .... N90-12373
N90-12374
AF PROJ. 2307 .... N90-11706
N90-11707
N90-11980
N90-11983
N90-11988
AF PROJ. 2308 .... N90-11708
N90-11744
N90-11837
N90-11841
AF PROJ. 2309 .... N90-12122
AF PROJ. 2310 .... N90-12114
N90-12123
AF PROJ. 2312 .... N90-12158
AF PROJ. 2313 .... N90-12160
N90-12168
N90-12169
N90-12177
N90-12324
AF PROJ. 2418 .... N90-11867
AF PROJ. 2698 .... N90-12005
AF PROJ. 3005 .... N90-11758
AF PROJ. 3145 .... N90-12379
AF PROJ. 4600 .... N90-11928
AF PROJ. 4643 .... N90-12124
N90-12127
N90-12493
AF PROJ. 7601 .... N90-11755
AF-AFOSR-ISSA-85-0070 .... N90-12305
AF-AFOSR-ISSA-86-0036 .... N90-12305
AF-AFOSR-ISSA-87-0036 .... N90-12305
AF-AFOSR-ISSA-88-0014 .... N90-12305
AF-AFOSR-ISSA-89-0039 .... N90-12294
AF-AFOSR-0001-89 .... N90-12192
AF-AFOSR-0056-86 .... N90-12375
AF-AFOSR-0057-86 .... N90-12123
AF-AFOSR-0071-88 .... N90-11845
AF-AFOSR-0076-86 .... N90-12198
AF-AFOSR-0078-86 .... N90-11955
N90-12236
N90-12238
AF-AFOSR-0079-89 .... N90-12192
AF-AFOSR-0082-86 .... N90-11988
AF-AFOSR-0090-87 .... N90-12401
AF-AFOSR-0097-87 .... N90-11841
AF-AFOSR-0099-84 .... N90-11706
AF-AFOSR-0099-86 .... N90-12158
AF-AFOSR-0117-88 .... N90-12193
AF-AFOSR-0120-84 .... N90-11708
AF-AFOSR-0128-86 .... N90-12169
AF-AFOSR-0130-86 .... N90-11844
AF-AFOSR-0137-84 .... N90-11986
AF-AFOSR-0140-88 .... N90-12160
AF-AFOSR-0159-86 .... N90-11707
AF-AFOSR-0178-86 .... N90-11980
AF-AFOSR-0199-88 .... N90-12325
AF-AFOSR-0214-87 .... N90-12304
AF-AFOSR-0218-87 .... N90-11983
AF-AFOSR-0226-88 .... N90-12177
AF-AFOSR-0232-89 .... N90-12324
AF-AFOSR-0254-84 .... N90-12051
AF-AFOSR-0292-85 .... N90-11744
AF-AFOSR-0298-86 .... N90-12168
AF-AFOSR-0339-89 .... N90-12122
AF-AFOSR-0347-83 .... N90-12245
AF-AFOSR-0355-85 .... N90-12097
AF-AFOSR-0372-87 .... N90-12374
AF-AFOSR-0389-87 .... N90-12373
AF-AFOSR-0472-89 .... N90-12192
AFGL ORDER GLH7-6017 .... N90-12416
AFGL ORDER GLH8-6004 .... N90-12416
ARPA ORDER 5299 .... N90-12120
ARPA ORDER 5325 .... N90-12376
ASL-87-8013 .... N90-12010
N90-12315
A81/KL/134 .... N90-11939
A83/K/058 .... N90-12137
N90-12138
A84/KL/110 .... N90-11938
A86/KL/045 .... N90-11937
A94C/2711 .... N90-12189
BMFT-TK-0238-5 .... N90-11936
BMFT-01-OV-86-810 .... N90-11772
BMFT-03-E-8156-A N90-12099
BMFT-13-N-5281-A5 .... N90-12023
CIFRE-252/88 .... N90-12258
DA PROJ. 1L1-61102-AH-42 .... N90-12371
DA PROJ. 1L1-62209-A-47-A N90-12033
DA PROJ. 2Q2-63007-A-795 .... N90-11723
DA PROJ. 3E1-62787-A8-78 .... N90-11764
N90-11979
N90-12165
DA PROJ. 4A7-62707-A8-55 .... N90-11720
DAAA15-86-C-0034 .... N90-11840
DAAG46-85-C-0034 .... N90-11868
DAAL03-86-C-0015 .... N90-11890
DAAL03-86-G-0035 .... N90-12156
DAAL03-86-K-0025 .... N90-12286
DAAL03-86-K-0171 .... N90-12198
N90-12236
N90-12240
DAAL03-86-X-0171 .... N90-12238
DAAL03-87-C-0029 .... N90-12157
DAAL03-87-K-0043 .... N90-12229
DAAL03-88-G-0029 .... N90-11961
DAAL03-88-K-0063 .... N90-12242
N90-12267
DAAL03-88-K-0070 .... N90-12343
DACA76-84-C-0004 .... N90-11725
DAJA45-86-C-0010 .... N90-12285
DAJA45-87-C-0042 .... N90-11981
DAJA45-88-C-0037 .... N90-11887
DAJA45-89-M-0052 .... N90-11954
DAMD17-85-C-5095 .... N90-12174
DARPA ORDER 5994 .... N90-11892
DE-AA03-76SF-00767 .... N90-11975
DE-AB29-79ET-20370 .... N90-12034
DE-AC02-76CH-00016 .... N90-11860
N90-11863
N90-11922
N90-11952
N90-12320
N90-12366
DE-AC02-76CH-03000 .... N90-11811
N90-12001
DE-AC02-76ER-01198 .... N90-11814
DE-AC02-76ER-01428 .... N90-12311
DE-AC02-76ER-02220 .... N90-12378
DE-AC02-78ET-51013 .... N90-12327
DE-AC02-83CH-10093 .... N90-12093
DE-AC03-76SF-00098 .... N90-11835
N90-11865
N90-11885
N90-11886
N90-11953
N90-12284
N90-12322
DE-AC04-76DP-00613 .... N90-11903
N90-11904
N90-12195
DE-AC04-76DP-00789 .... N90-11918
N90-11919
N90-11945
N90-11946
N90-11947
N90-12019
N90-12094
N90-12317
N90-12319
N90-12349
N90-12353
DE-AC04-88DP-43495 .... N90-12234
DE-AC05-84OR-21400 .... N90-11858
N90-11859
N90-11884
N90-11898
N90-12046
N90-12107
N90-12219
N90-12295
N90-12301
N90-12302
N90-12318
N90-12352
N90-12357
N90-12365
N90-12397
N90-12420
DE-AC05-84OT-21400 .... N90-12386
DE-AC06-76RL-01830 .... N90-11813
N90-12095
N90-12313
DE-AC06-87RL-10930 .... N90-11864
N90-12044
DE-AC07-84NV-10366 .... N90-12411
DE-AC09-76SR-00001 .... N90-12027
DE-AC22-87PC-79680 .... N90-12333
DE-AI01-86CE-50162 .... N90-11882
DE-AI03-86SF-16310 .... N90-11854
DE-AI79-85BP-23169 .... N90-11948
DE-AS03-76ER-72012 .... N90-11975
DE-FC08-87DP-10618 .... N90-12338
DE-FG02-84ER-45056 .... N90-12321
DE-FG02-85ER-53201 .... N90-12328
DE-FG02-86ER-13615 .... N90-11834
DE-FG02-87ER-45296 .... N90-11862
DE-FG03-87ER-25028 .... N90-12244
DE-FG03-87ER-25030 .... N90-12244
DE-FG05-84ER-53176 .... N90-12341
DE-FG05-86ER-45259 .... N90-12356
DE-FG05-89ER-40515 .... N90-12342
DEN3-352 .... N90-11882
DNA001-88-C-0079 .... N90-11987
DRET-87/1497/DS/SR2 .... N90-11716
DTFA01-80-Y-10546 .... N90-11934
DTFA01-87-C-00014 .... N90-12406
DTFA03-86-C-00041 .... N90-11765
EPA-CR-810888 .... N90-12155
EPA-U913-890-01-0 .... N90-12410
EPA-68-02-4286 .... N90-12105
FY1455-88-N0617 .... N90-11837
F04701-85-C-0086 .... N90-11801
F04701-88-C-0089 .... N90-11984
N90-12303
N90-12380
F19628-83-C-0014 .... N90-12005
F19628-84-C-0057 .... N90-12114
F19628-85-C-0002 .... N90-11934
F19628-85-C-0003 .... N90-12205
N90-12403
F19628-86-C-0001 .... N90-11930
F19628-87-C-0053 .... N90-12121
F19628-87-C-0206 .... N90-12126
F19628-87-K-0036 .... N90-12128
F19628-87-K-0040 .... N90-12120
F19628-88-C-0039 .... N90-12129

F19628-89-C-0091 .... N90-12126
F29601-87-C-0069 .... N90-12203
F29601-87-K-0076 .... N90-12306
F33601-87-M-3026 .... N90-11867
F33615-86-C-1051 .... N90-12020
F33615-86-C-2615 .... N90-11743
F33615-87-C-2738 .... N90-12379
F33615-88-C-3606 .... N90-11756
F33615-88-C-3609 .... N90-11758
F49620-86-C-0016 .... N90-12307
F49620-86-C-0105 .... N90-11773
F49620-86-C-0134 .... N90-11708
F49620-86-K-0021 .... N90-12367
F49620-87-C-0044 .... N90-12372
F49620-87-C-0077 .... N90-11892
F49620-87-C-0088 .... N90-12192
F49620-87-C-0116 .... N90-12192
F49620-87-C-0122 .... N90-12384
GRI-5086-241-1219 .... N90-12026
GRI-5086-260-1403 .... N90-11826
GRI-5087-260-1538 .... N90-11971
MDA903-86-C-0178 .... N90-12203
MDA903-87-C-0523 .... N90-11723
MDA972-88-K-0006 .... N90-11905
N90-12239

MIPR-CRREL-89-12 .... N90-11908
MIPR-88-577 .... N90-12344
NAGW-91 .... N90-12479
N90-12480

NAGW-1340 .... N90-12492
NAGW-1468 .... N90-12488
NAGW-1587 .... N90-12480
NAGW-1706 .... N90-12490
NAG1-270 .... N90-12182
NAG1-466 .... N90-12193
NAG1-530 .... N90-11968
NAG1-613 .... N90-12213
N90-12214
N90-12215

NAG1-619 .... N90-11733
NAG1-694 .... N90-12009
NAG1-748 .... N90-11702
NAG1-861 .... N90-11825
NAG1-929 .... N90-12290
NAG2-470 .... N90-11807
NAG2-513 .... N90-12228
NAG3-763 .... N90-12033
NAG9-117 .... N90-12178
NASA ORDER C-99066-G N90-11969
N90-12041
N90-12231

NASW-3482 .... N90-12084
NASW-4066 .... N90-12423
NASW-4292 .... N90-12152
N90-12153
N90-12154

NASW-4435 .... N90-11770
N90-11771
N90-11800

NAS1-16521 .... N90-11704
NAS1-17496 .... N90-12058
NAS1-17698 .... N90-11821
NAS1-17970 .... N90-11822
NAS1-18107 .... N90-12182
N90-12192
N90-12266

NAS1-18605 .... N90-11698
N90-12183
N90-12193
N90-12230
N90-12232

NAS2-11969 .... N90-11730
NAS3-24339 .... N90-11738
N90-11739

NAS3-25266 .... N90-11999
NAS3-25357 .... N90-11805
N90-11806

NAS5-20440 .... N90-12115
NAS5-26645 .... N90-12468
NAS5-26813 .... N90-12487
NAS5-30145 .... N90-12133
NAS8-32805 .... N90-12487
NAS8-35187 .... N90-12065
NAS8-35981 .... N90-12142
NAS8-36717 .... N90-11802
NAS8-37127 .... N90-12065
NAS8-37334 .... N90-12475
NAS9-17326 .... N90-12174
N90-12175

NAS9-17650 .... N90-11774
N90-11775
N90-11776
N90-11777
N90-11778
N90-11779
N90-11780
N90-11781
N90-11782
N90-11783
N90-11784
N90-11785
N90-11786
N90-11787
N90-11788
N90-11789
N90-11790
N90-11791
N90-11792
N90-11793
N90-11794
N90-11795
N90-11796
N90-11797
NAS10-11451 .... N90-12047
NA86-AA-D-SG090 .... N90-12144
NA87-AA-D-CP041 .... N90-12101
NCC1-25 .... N90-12011
NCC2-539 .... N90-12200
NGR-05-020-668 .... N90-12298
NGT-50087 .... N90-11853
NSF AST-87-02682 .... N90-12490
NSF ATM-81-03697 .... N90-12132
NSF ATM-83-18842 .... N90-12132
NSF ATM-83-20439 .... N90-12298
N90-12458

NSF ATM-86-10330 .... N90-12490
NSF ATM-87-05084 .... N90-12481
NSF ATM-87-09659 .... N90-11731
N90-12109
N90-12113
N90-12132
NSF ATM-87-10102 .... N90-12428
NSF ATM-87-19371 .... N90-12479
N90-12480
NSF BNS-88-19565 .... N90-12180
NSF DDM-88-14253 .... N90-12244
NSF DMC-84-17949 .... N90-12025
NSF DMC-85-05166 .... N90-12176
NSF DMC-85-16114 .... N90-12202
NSF DMC-86-11357 .... N90-12383
NSF DMS-86-06964 .... N90-12270
NSF DMS-87-01085 .... N90-12228
NSF DMS-87-02620 .... N90-12246
N90-12269
NSF DMS-88-00589 .... N90-12244
NSF DMS-88-11863 .... N90-12182
NSF EAR-87-08548 .... N90-12120
NSF ECS-83-52185 .... N90-11955
NSF ECS-87-15153 .... N90-12244
NSF ECS-87-15811 .... N90-11960
N90-12220
NSF IRI-87-00924 .... N90-12180
NSF IRI-87-05400 .... N90-12213
N90-12214
NSF ISI-85-21282 .... N90-12174
NSF MCS-81-10556 .... N90-12229
NSF OCE-82-08744 .... N90-12146
NSF OCE-82-14771 .... N90-12146
NSF OCE-85-14885 .... N90-12146
NSF OCE-86-00052 .... N90-12145
NSG-1419 .... N90-11695
NSG-1442 .... N90-12212
NSG-5088 .... N90-11755
NSG-7092 .... N90-12298
N90-12458
N90-12481
NSG-7287 .... N90-12479
N90-12480
N00014-80-C-0622 .... N90-11955
N90-12198
N90-12236
N90-12238
N00014-80-K-0852 .... N90-11842
N00014-81-K-0605 .... N90-11847
N00014-82-K-0741 .... N90-12050
N00014-83-C-0300 .... N90-12207
N00014-84-C-0149 .... N90-11932
N00014-84-K-0519 .... N90-11724
N90-12240
N00014-85-C-0332 .... N90-11818
N00014-85-C-0415 .... N90-11721
N00014-85-K-0124 .... N90-12187
N90-12197
N00014-85-K-0305 .... N90-12222
N00014-85-K-2035 .... N90-12216
N00014-86-C-0662 .... N90-12130
N00014-86-K-0180 .... N90-12221
N00014-86-K-0216 .... N90-12235
N00014-86-K-0230 .... N90-12159
N00014-86-K-0593 .... N90-12188
N90-12198
N90-12199

N00014-86-K-0691 .... N90-12182
N00014-87-C-0114 .... N90-12022
N00014-87-C-0335 .... N90-12096
N00014-87-G-0135 .... N90-12180
N00014-87-K-0022 .... N90-12200
N90-12204
N00014-87-K-0125 .... N90-12028
N00014-87-K-0433 .... N90-12166
N00014-87-K-0444 .... N90-12287
N00014-87-K-0494 .... N90-11843
N90-11846
N00014-87-K-0558 .... N90-12021
N00014-87-K-0825 .... N90-11955
N90-11956
N90-11957
N90-12187
N90-12188
N90-12197
N90-12198
N90-12199
N90-12236
N90-12237
N90-12238
N00014-88-C-0221 .... N90-12376
N00014-88-C-0654 .... N90-11705
N00014-88-K-0134 .... N90-12229
N00014-88-K-0170 .... N90-12245
N90-12246
N90-12269
N90-12270
N00014-88-K-0240 .... N90-11933
N00014-88-K-0305 .... N90-11888
N00014-88-K-0354 .... N90-12180
N00014-88-K-0360 .... N90-11958
N00014-88-K-0389 .... N90-12098
N00014-88-K-0500 .... N90-11815
N00014-88-K-0550 .... N90-12170
N00014-88-K-0738 .... N90-12187
N90-12197
N00014-89-J-1627 .... N90-12268
N00014-89-J-1659 .... N90-12244
N00014-89-J-1828 .... N90-11878
N00014-89-J-1952 .... N90-12162
PHS-OH-02178 .... N90-12179
RAE-2028/131-XRAW N90-11712
RR013 .... N90-11842
RR04108 .... N90-12159
N90-12170
RR04209 .... N90-12180
SERC-GR/D/30587 .... N90-12259
N90-12272
SMC-611-303-013 .... N90-12275
N90-12279
TAMRF PROJ. RF-5373 .... N90-11733
W-31-109-ENG-38 .... N90-11883
N90-11949
N90-11950
N90-12194
N90-12300
N90-12355
N90-12356
N90-12359
N90-12360
N90-12361
W-7405-ENG-36 .... N90-11830
N90-11856
N90-11857
N90-11897
N90-11972
N90-11973
N90-11974
N90-11998
N90-12000
N90-12012
N90-12016
N90-12018
N90-12045
N90-12119
N90-12296
N90-12297
N90-12299
N90-12334
N90-12417
N90-12457
W-7405-ENG-48 .... N90-11812
N90-11829
N90-11831
N90-11832
N90-11833
N90-11851
N90-11861
N90-11917
N90-11920
N90-11921
N90-11951
N90-11976

N90-11977
N90-12002
N90-12003
N90-12004
N90-12015
N90-12017
N90-12106
N90-12108
N90-12196
N90-12233
N90-12294
N90-12312
N90-12335
N90-12336
N90-12337
N90-12339
N90-12340
N90-12354
N90-12358
N90-12362
N90-12363
N90-12364
N90-12399
N90-12418
N90-12419
N90-12455
XL-8-18080-1 .... N90-12093
106-30-01 .... N90-12151
505-60-01 .... N90-11699
505-60-11 .... N90-11978
505-60-31-07 .... N90-11968
505-61-51 .... N90-11700
N90-11701
N90-11752
505-61-71-02 .... N90-11702
505-61-71-07 .... N90-11751
505-62-21 .... N90-11969
N90-12041
N90-12231
505-62-71 .... N90-11740
505-63-11 .... N90-11808
505-63-11-05 .... N90-11822
505-63-21-04 .... N90-11704
505-63-51 .... N90-12033
505-63-51-01 .... N90-12057
N90-12058
505-66-01-02 .... N90-11757
505-66-11 .... N90-11730
505-66-41-22 .... N90-11736
505-66-71 .... N90-12042
505-67-21 .... N90-12227
505-68-1A N90-11999
505-90-21-01 .... N90-11698
N90-12182
N90-12183
N90-12192
N90-12193
N90-12230
N90-12232
N90-12266
506-40-11 .... N90-11742
N90-12211
506-43-1C N90-11902
506-43-11 .... N90-11880
N90-11881
N90-12348
506-44-2C N90-11943
506-48-4A N90-11806
506-80-31-02 .... N90-12292
533-02-01-03 .... N90-11703
533-02-51 .... N90-11741
N90-11753
533-02-71 .... N90-11732
534-06-23 .... N90-11821
535-03-01 .... N90-11739
553-13-00 .... N90-11853
586-01-11 .... N90-11854
591-14-3A N90-11804
650-60-23 .... N90-11915
677-43-24 .... N90-12435
694-03-03 .... N90-11901

REPORT/ACCESSION NUMBER INDEX

SCIENTIFIC AND TECHNICAL AEROSPACE REPORTS VOLUME 28 NUMBER 3

Typical Report Number Index Listing

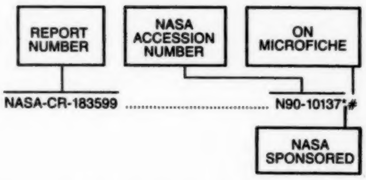

Listings in this index are arranged alphanumerically by report number. The NASA accession number denotes the number by which the citation is identified. An asterisk (*) indicates that the itemis a NASA report. A pound sign (#) indicates that the item is available on microfiche.

A-1989-1 .... N90-12393 #
A-1989-2 .... N90-12394 #
A-89006 .... N90-11752* #
A-89096 .... N90-11701* #
A-89156 .... N90-12211* #
A-89183 .... N90-12151* #
A-89213 .... N90-11692* #
A-89227 .... N90-11699* #
A-89229 .... N90-11700* #
A-89241 .... N90-11970* #
A-89251 .... N90-11742* #
A-89256 .... N90-12227* #
A-89261 .... N90-11978* #

AD-A209066 .... N90-11878 #
AD-A210562 .... N90-12229 #
AD-A210678 .... N90-12114 #
AD-A210697 .... N90-12131 #
AD-A210994 .... N90-12160 #
AD-A211289 .... N90-12156 #
AD-A211290 .... N90-12028 #
AD-A211293 .... N90-12244 #
AD-A211294 .... N90-12166 #
AD-A211297 .... N90-12203 #
AD-A211306 .... N90-11724 #
AD-A211308 .... N90-12371 #
AD-A211311 .... N90-12157 #
AD-A211314 .... N90-12204 #
AD-A211344 .... N90-12205 #
AD-A211346 .... N90-12181 #
AD-A211353 .... N90-12493 #
AD-A211356 .... N90-12124 #
AD-A211357 .... N90-12125 #
AD-A211358 .... N90-12126 #
AD-A211359 .... N90-12127 #
AD-A211366 .... N90-11981 #
AD-A211367 .... N90-12305 #
AD-A211368 .... N90-12158 #
AD-A211372 .... N90-12021 #
AD-A211386 .... N90-12096 #
AD-A211394 .... N90-12372 #
AD-A211395 .... N90-11840 #
AD-A211396 .... N90-11928 #
AD-A211411 .... N90-12268 #
AD-A211413 .... N90-11708 #
AD-A211414 .... N90-12050 #
AD-A211426 .... N90-11982 #
AD-A211427 .... N90-11961 #
AD-A211485 .... N90-11983 #
AD-A211489 .... N90-11841 #
AD-A211490 .... N90-12373 #
AD-A211495 .... N90-11817 #
AD-A211505 .... N90-12293 #
AD-A211511 .... N90-12374 #
AD-A211514 .... N90-12403 #
AD-A211528 .... N90-11984 #
AD-A211537 .... N90-12097 #
AD-A211540 .... N90-11744 #
AD-A211542 .... N90-12098 #
AD-A211543 .... N90-11962 #
AD-A211545 .... N90-12306 #
AD-A211546 .... N90-11929 #
AD-A211547 .... N90-11773 #
AD-A211548 .... N90-12128 #
AD-A211549 .... N90-11891 #
AD-A211550 .... N90-11842 #
AD-A211551 .... N90-12287 #
AD-A211552 .... N90-12167 #
AD-A211553 .... N90-12129 #
AD-A211565 .... N90-12051 #
AD-A211573 .... N90-12206 #
AD-A211577 .... N90-11963 #
AD-A211578 .... N90-12168 #
AD-A211580 .... N90-11964 #
AD-A211584 .... N90-11725 #
AD-A211586 .... N90-11843 #
AD-A211588 .... N90-11907 #
AD-A211589 .... N90-11930 #
AD-A211592 .... N90-11985 #
AD-A211593 .... N90-11931 #
AD-A211606 .... N90-11908 #
AD-A211607 .... N90-12375 #
AD-A211612 .... N90-12159 #
AD-A211613 .... N90-12307 #
AD-A211618 .... N90-12221 #
AD-A211627 .... N90-12269 #
AD-A211628 .... N90-12245 #
AD-A211629 .... N90-12177 #
AD-A211630 .... N90-12324 #
AD-A211633 .... N90-11844 #
AD-A211644 .... N90-11845 #
AD-A211646 .... N90-12246 #
AD-A211647 .... N90-11986 #
AD-A211649 .... N90-12270 #
AD-A211650 .... N90-12169 #
AD-A211651 .... N90-11892 #
AD-A211653 .... N90-11846 #
AD-A211660 .... N90-12207 #
AD-A211664 .... N90-12136 #
AD-A211665 .... N90-12344 #
AD-A211669 .... N90-11932 #
AD-A211680 .... N90-11868 #
AD-A211682 .... N90-11818 #
AD-A211687 .... N90-12148 #
AD-A211690 .... N90-12376 #
AD-A211693 .... N90-12325 #
AD-A211695 .... N90-12170 #
AD-A211711 .... N90-11847 #
AD-A211712 .... N90-11758 #
AD-A211715 .... N90-11801 #
AD-A211719 .... N90-11734 #
AD-A211720 .... N90-11933 #
AD-A211728 .... N90-11987 #
AD-A211730 .... N90-12022 #
AD-A211735 .... N90-12377 #
AD-A211738 .... N90-12222 #
AD-A211744 .... N90-11988 #
AD-A211746 .... N90-12380 #
AD-A211749 .... N90-11934 #
AD-A211755 .... N90-12130 #
AD-A211774 .... N90-11745 #
AD-A211775 .... N90-11869 #
AD-A211786 .... N90-12149 #
AD-A211787 .... N90-12171 #
AD-A211792 .... N90-12303 #
AD-A211794 .... N90-12180 #
AD-A211806 .... N90-12120 #
AD-A211807 .... N90-12121 #
AD-A211819 .... N90-12005 #
AD-A211822 .... N90-12323 #
AD-A211823 .... N90-11923 #
AD-A211824 .... N90-12216 #
AD-A211830 .... N90-11755* #
AD-A211839 .... N90-12235 #
AD-A211848 .... N90-11954 #
AD-A211857 .... N90-11836 #
AD-A211876 .... N90-11720 #
AD-A211877 .... N90-11866 #
AD-A211879 .... N90-11899 #
AD-A211880 .... N90-12379 #
AD-A211881 .... N90-11905 #
AD-A211882 .... N90-12197 #
AD-A211884 .... N90-12236 #
AD-A211889 .... N90-12237 #
AD-A211903 .... N90-11837 #
AD-A211905 .... N90-12285 #
AD-A211906 .... N90-11752* #
AD-A211908 .... N90-12198 #
AD-A211909 .... N90-12187 #
AD-A211910 .... N90-12238 #
AD-A211913 .... N90-11955 #
AD-A211916 .... N90-12199 #
AD-A211918 .... N90-12239 #
AD-A211920 .... N90-12161 #
AD-A211924 .... N90-11815 #
AD-A211931 .... N90-11956 #
AD-A211935 .... N90-12387 #
AD-A211937 .... N90-11957 #
AD-A211938 .... N90-12188 #
AD-A211941 .... N90-12400 #
AD-A211943 .... N90-11705 #
AD-A211944 .... N90-11706 #
AD-A211945 .... N90-12240 #
AD-A211946 .... N90-12304 #
AD-A211957 .... N90-11756 #
AD-A211972 .... N90-12241 #
AD-A211976 .... N90-12162 #
AD-A211982 .... N90-11924 #
AD-A211984 .... N90-12401 #
AD-A211985 .... N90-12409 #
AD-A212001 .... N90-11743 #
AD-A212004 .... N90-11721 #
AD-A212006 .... N90-11838 #
AD-A212007 .... N90-11763 #
AD-A212009 .... N90-12200* #
AD-A212018 .... N90-11887 #
AD-A212022 .... N90-11906 #
AD-A212028 .... N90-11888 #
AD-A212046 .... N90-12367 #
AD-A212049 .... N90-11867 #
AD-A212055 .... N90-12122 #
AD-A212060 .... N90-11979 #
AD-A212063 .... N90-11715 #
AD-A212068 .... N90-11769 #
AD-A212069 .... N90-12163 #
AD-A212074 .... N90-12020 #
AD-A212082 .... N90-11764 #
AD-A212087 .... N90-11900 #
AD-A212090 .... N90-12048 #
AD-A212094 .... N90-12049 #
AD-A212095 .... N90-11816 #
AD-A212097 .... N90-12242 #
AD-A212098 .... N90-12343 #
AD-A212099 .... N90-11980 #
AD-A212101 .... N90-11889 #
AD-A212109 .... N90-11707 #
AD-A212111 .... N90-11958 #
AD-A212156 .... N90-12164 #
AD-A212159 .... N90-11722 #
AD-A212161 .... N90-12286 #
AD-A212162 .... N90-11890 #
AD-A212163 .... N90-11723 #
AD-A212164 .... N90-12267 #
AD-A212169 .... N90-12123 #
AD-A212170 .... N90-12165 #

AD-B134983L .... N90-12007 #

AD-D014165 .... N90-11852 #
AD-D014167 .... N90-12346 #
AD-D014168 .... N90-11995 #
AD-D014169 .... N90-11996 #
AD-D014170 .... N90-11997 #
AD-D014171 .... N90-11879 #
AD-D014172 .... N90-11941 #
AD-D014173 .... N90-12280 #
AD-D014174 .... N90-11914 #
AD-D014176 .... N90-12186
AD-D014177 .... N90-12347 #
AD-D014178 .... N90-12281 #
AD-D014179 .... N90-11942 #

AD-E951378 .... N90-11962 #
AD-E951378 .... N90-12098 #

AFGL-ERP-1018 .... N90-11755* #

AFGL-TR-88-0186 .... N90-12114 #
AFGL-TR-88-0326 .... N90-12005 #
AFGL-TR-89-0021 .... N90-11755* #
AFGL-TR-89-0092 .... N90-12129 #
AFGL-TR-89-0142 .... N90-12128 #
AFGL-TR-89-0191 .... N90-12125 #
AFGL-TR-89-0195 .... N90-12124 #
AFGL-TR-89-0197 .... N90-12493 #
AFGL-TR-89-0199 .... N90-12127 #
AFGL-TR-89-0200 .... N90-12126 #

AFOEHL-89-023RC0111DRA .... N90-12171 #

AFOSR-89-0428TR .... N90-12401 #
AFOSR-89-1021TR .... N90-12160 #
AFOSR-89-1036TR .... N90-11708 #
AFOSR-89-1055TR .... N90-11988 #
AFOSR-89-1060TR .... N90-12307 #
AFOSR-89-1072TR .... N90-11983 #
AFOSR-89-1090TR .... N90-12324 #
AFOSR-89-1097TR .... N90-11892 #
AFOSR-89-1098TR .... N90-11844 #
AFOSR-89-1102TR .... N90-12305 #
AFOSR-89-1104TR .... N90-12373 #
AFOSR-89-1107TR .... N90-12374 #
AFOSR-89-1112TR .... N90-12304 #
AFOSR-89-1113TR .... N90-12177 #
AFOSR-89-1136TR .... N90-11706 #
AFOSR-89-1141TR .... N90-12158 #
AFOSR-89-1142TR .... N90-12325 #
AFOSR-89-1146TR .... N90-11845 #
AFOSR-89-1151TR .... N90-12169 #
AFOSR-89-1159TR .... N90-12367 #
AFOSR-89-1164TR .... N90-12168 #
AFOSR-89-1165TR .... N90-12375 #
AFOSR-89-1180TR .... N90-11986 #
AFOSR-89-1181TR .... N90-12051 #
AFOSR-89-1182TR .... N90-11744 #
AFOSR-89-1183TR .... N90-11841 #
AFOSR-89-1186TR .... N90-12097 #
AFOSR-89-1190TR .... N90-11773 #
AFOSR-89-1206TR .... N90-12122 #
AFOSR-89-1210TR .... N90-11707 #
AFOSR-89-1227TR .... N90-12123 #
AFOSR-89-1230TR .... N90-11980 #

AFWAL-TR-88-1128 .... N90-12020 #
AFWAL-TR-88-2140 .... N90-11837 #

AFWL-TR-89-07 .... N90-12306 #

AI-M-1134 .... N90-12221 #

AIAA-89-2364 .... N90-11741* #
AIAA-89-3428 .... N90-11753* #
AIAA-90-0741 .... N90-11901* #

AMSMI/TR-RD-AS-88-8 .... N90-11962 #

AR-005-707 .... N90-11896 #

ARCCB-TR-89019 .... N90-12048 #

ARE-TR-89308 .... N90-12241 #

ARI-RR-1528 .... N90-11723 #

ARIEM-M66-89 .... N90-12165 #

ARL-PROP-TM-457 .... N90-11745 #

ARL/PSU/TR-89-004 .... N90-11982 #

ARO-23084.11-CH .... N90-12286 #
ARO-23767.7-LS-F .... N90-12156 #
ARO-23992.2-MA .... N90-11890 #
ARO-25263.1-CH .... N90-12157 #
ARO-25624.3-PH .... N90-12343 #
ARO-25839.12-MA .... N90-12242 #
ARO-25839.15-MA .... N90-12267 #
ARO-26222.1-EL-CF .... N90-11961 #

ASI690-314-88 .... N90-11723 #

ATC-165 .... N90-11934 #

AVSCOM-TR-89-C-014 .... N90-12033* #

BBN-TM-938 .... N90-11704* #

BIO-4531 .... N90-12366 #

BN-1104 .... N90-12011* #

BNL-42851 .... N90-11952 #
BNL-43052 .... N90-11860 #
BNL-43105 .... N90-12320 #
BNL-43114 .... N90-12366 #
BNL-43179 .... N90-11863 #
BNL-43204 .... N90-11922 #

BRDEC-2478 .... N90-11899 #

BR108038 .... N90-12226 #
BR108095 .... N90-12189 #
BR108112 .... N90-11876 #
BR108113 .... N90-11768 #
BR108126 .... N90-12054 #
BR108268 .... N90-12405 #
BR108269 .... N90-12053 #
BR108279 .... N90-12422 #
BR108283 .... N90-11875 #
BR108365 .... N90-11894 #
BR108825 .... N90-12190 #
BR108826 .... N90-12217 #

BUMINES-RI-9213 .... N90-11849 #

CAA-PAPER-88010 .... N90-11729
CAA-PAPER-88014 .... N90-11719

CAA-2/88 .... N90-11718

CERMATEC-8961701 .... N90-11892 #

CEVANS/057/FR-8901 .... N90-12376 #

CMS-TSR-88-36 .... N90-12229 #

CMU/SEI-89-TR-11 .... N90-12205 #
CMU/SEI-89-TR-17 .... N90-12206 #
CMU/SEI-89-TR-18 .... N90-12403 #

CONF-890335-254 .... N90-11953 #
CONF-890426-29 .... N90-11885 #
CONF-890426-30 .... N90-11886 #
CONF-890492-3 .... N90-11831 #
CONF-890520-2 .... N90-12457 #
CONF-890583-3 .... N90-12300 #
CONF-890665-45 .... N90-11947 #
CONF-890665-48-REV-1 .... N90-12363 #
CONF-890697-1 .... N90-12294 #
CONF-890701-3 .... N90-11811 #
CONF-890701-5 .... N90-12364 #
CONF-890701-6 .... N90-12284 #
CONF-890701-7 .... N90-11865 #
CONF-890703-13 .... N90-12295 #
CONF-890708-7 .... N90-12301 #
CONF-890710-17 .... N90-11998 #
CONF-890710-18 .... N90-11951 #
CONF-890718-26 .... N90-12354 #
CONF-890718-27 .... N90-12358 #
CONF-890718-28 .... N90-12362 #
CONF-890738-2 .... N90-11835 #
CONF-890771-4 .... N90-11812 #
CONF-890798-11 .... N90-12455 #
CONF-890798-12 .... N90-11832 #
CONF-890803-16 .... N90-11922 #
CONF-890809-1 .... N90-12003 #
CONF-890811-28 .... N90-12000 #
CONF-890811-31 .... N90-12019 #
CONF-890812-23 .... N90-11973 #
CONF-890812-42 .... N90-11833 #
CONF-890812-43 .... N90-11976 #
CONF-890812-45 .... N90-11861 #
CONF-890812-46 .... N90-12002 #
CONF-890812-47 .... N90-11977 #
CONF-890815-25 .... N90-12313 #
CONF-890815-26 .... N90-11950 #
CONF-890815-28 .... N90-12361 #
CONF-890821-3 .... N90-12360 #
CONF-890826-3 .... N90-12302 #
CONF-890836-11 .... N90-12012 #
CONF-890836-12 .... N90-11830 #
CONF-890836-14 .... N90-12004 #
CONF-890911-8 .... N90-12322 #
CONF-890923-1 .... N90-12094 #
CONF-890931-6 .... N90-11920 #
CONF-890931-7 .... N90-12337 #
CONF-890931-8 .... N90-12336 #
CONF-890933-2 .... N90-11860 #
CONF-890996-5 .... N90-12318 #
CONF-891007-1 .... N90-12340 #
CONF-891036-1 .... N90-11883 #
CONF-891059-1 .... N90-12317 #
CONF-891065-1 .... N90-12106 #
CONF-891068-1 .... N90-12015 #
CONF-891073-1 .... N90-12119 #
CONF-891074-1 .... N90-11917 #
CONF-891075-1 .... N90-12386 #
CONF-891088-1 .... N90-12027 #
CONF-891093-1 .... N90-11857 #
CONF-8810135-7 .... N90-11952 #
CONF-8811195-VOL-138 .... N90-12352 #
CONF-8902117-2 .... N90-12420 #
CONF-8902132-1 .... N90-12378 #
CONF-8903164-1 .... N90-12195 #
CONF-8904270-1-REV .... N90-11904 #
CONF-8905106-1 .... N90-12108 #
CONF-8905126-SUMM .... N90-12334 #
CONF-8905187-3 .... N90-12419 #
CONF-8905210-1 .... N90-12320 #
CONF-8906205-1 .... N90-12356 #
CONF-8906206-1 .... N90-12417 #
CONF-8906213-1 .... N90-12366 #
CONF-8907114-2 .... N90-11863 #
CONF-8907133-1 .... N90-12349 #
CONF-8907135-1 .... N90-12299 #
CONF-8907138-1 .... N90-12355 #
CONF-8908122-1 .... N90-12297 #
CONF-8908122-2 .... N90-12296 #
CONF-8908132-1 .... N90-12353 #
CONF-8908133-2 .... N90-12339 #
CONF-8908134-1 .... N90-12016 #
CONF-8908144-1 .... N90-11949 #
CONF-8908145-1 .... N90-12359 #
CONF-8908153-1 .... N90-11903 #
CONF-8909111-1-REV-1 .... N90-12196 #
CONF-8909176-1 .... N90-11918 #
CONF-8909182-1 .... N90-11974 #
CONF-8909182-2 .... N90-11897 #
CONF-8910106-1 .... N90-11945 #
CONF-8910108-1 .... N90-12194 #
CONF-8910129-1 .... N90-12319 #
CONF-8910154-1 .... N90-12397 #
CONF-8910156-1 .... N90-11946 #
CONF-8910162-3 .... N90-12107 #
CONF-8910191-1 .... N90-11829 #
CONF-8910192-2 .... N90-12044 #
CONF-8910197-1 .... N90-11856 #
CONF-8910198-2 .... N90-12045 #
CONF-8910199-1 .... N90-12046 #

CONTRIB-1113 .... N90-12143 #
CONTRIB-1115 .... N90-12147 #

CRDEC-CR-030 .... N90-11840 #

CRREL-SP-89-22 .... N90-11907 #

CRREL-SR-89-19 .... N90-11908 #

CSDL-R-2033 .... N90-12025 #

CSG-108 .... N90-12215* #
CSG-111 .... N90-12214* #
CSG-112 .... N90-12213* #

CSM-MT-CWR-089-038 .... N90-11815 #

CT-4 .... N90-11916 #

CTN-89-007 .... N90-12399 #

DAITC/TR-89/6 .... N90-12400 #

DC-110 .... N90-11960 #
DC-111 .... N90-12220 #

DE88-757235 .... N90-12310 #
DE89-000982 .... N90-11828 #
DE89-005395 .... N90-12391 #
DE89-007422 .... N90-12317 #
DE89-008033 .... N90-12106 #
DE89-008039 .... N90-12015 #
DE89-009231 .... N90-11917 #
DE89-009290 .... N90-12119 #
DE89-009454 .... N90-12093 #
DE89-009955 .... N90-12386 #
DE89-010482 .... N90-12027 #
DE89-012395 .... N90-12194 #
DE89-012397 .... N90-11883 #
DE89-013609 .... N90-11945 #
DE89-014072 .... N90-12318 #
DE89-014484 .... N90-11918 #
DE89-014695 .... N90-12311 #
DE89-014740 .... N90-12319 #
DE89-014796 .... N90-12352 #
DE89-014878 .... N90-12397 #
DE89-015121 .... N90-11946 #
DE89-015178 .... N90-11972 #
DE89-015188 .... N90-11851 #
DE89-015248 .... N90-12296 #
DE89-015250 .... N90-12297 #
DE89-015294 .... N90-12299 #
DE89-015296 .... N90-12012 #
DE89-015407 .... N90-12353 #
DE89-015600 .... N90-12333 #

DE89-015705 N90-12294 #
DE89-015856 N90-12295 #
DE89-016035 N90-12349 #
DE89-016036 N90-12457 #
DE89-016052 N90-12327 #
DE89-016055 N90-12044 #
DE89-016367 N90-12045 #
DE89-016371 N90-12328 #
DE89-016524 N90-12354 #
DE89-016594 N90-11973 #
DE89-016612 N90-12000 #
DE89-016614 N90-12016 #
DE89-016647 N90-11829 #
DE89-016695 N90-12398 #
DE89-016697 N90-12312 #
DE89-016700 N90-12399 #
DE89-016701 N90-12233 #
DE89-016705 N90-12001 #
DE89-016710 N90-11811 #
DE89-016755 N90-12417 #
DE89-016764 N90-12094 #
DE89-016775 N90-11830 #
DE89-016824 N90-12313 #
DE89-016844 N90-12046 #
DE89-016909 N90-12355 #
DE89-016912 N90-12356 #
DE89-016914 N90-12300 #
DE89-016920 N90-11919 #
DE89-016956 N90-12334 #
DE89-016959 N90-12234 #
DE89-016967 N90-11897 #
DE89-016968 N90-11856 #
DE89-016970 N90-11998 #
DE89-016979 N90-11974 #
DE89-016987 N90-11857 #
DE89-017233 N90-11947 #
DE89-017244 N90-12107 #
DE89-017420 N90-11858 #
DE89-017439 N90-12357 #
DE89-017452 N90-11859 #
DE89-017466 N90-11884 #
DE89-017507 N90-12219 #
DE89-017524 N90-12017 #
DE89-017527 N90-12335 #
DE89-017529 N90-12418 #
DE89-017531 N90-12419 #
DE89-017532 N90-12336 #
DE89-017534 N90-12337 #
DE89-017535 N90-11920 #
DE89-017536 N90-11812 #
DE89-017538 N90-12358 #
DE89-017545 N90-11921 #
DE89-017547 N90-11831 #
DE89-017549 N90-12411 #
DE89-017554 N90-11975 #
DE89-017558 N90-12338 #
DE89-017579 N90-12301 #
DE89-017581 N90-12420 #
DE89-017583 N90-12302 #
DE89-017603 N90-11860 #
DE89-017605 N90-12320 #
DE89-017654 N90-11948 #
DE89-017671 N90-12359 #
DE89-017677 N90-12360 #
DE89-017680 N90-12361 #
DE89-017682 N90-11949 #
DE89-017689 N90-11950 #
DE89-017705 N90-11903 #
DE89-017706 N90-12195 #
DE89-017707 N90-11904 #
DE89-017732 N90-12196 #
DE89-017734 N90-11832 #
DE89-017735 N90-12362 #
DE89-017736 N90-11976 #
DE89-017737 N90-11833 #
DE89-017738 N90-12455 #
DE89-017739 N90-12363 #
DE89-017753 N90-12095 #
DE89-017755 N90-11861 #
DE89-017756 N90-12002 #
DE89-017758 N90-12364 #
DE89-017779 N90-11898 #
DE89-017780 N90-12365 #
DE89-017781 N90-12003 #
DE89-017782 N90-12339 #
DE89-017784 N90-12004 #
DE89-017785 N90-12108 #
DE89-017786 N90-12018 #
DE89-017798 N90-11862 #
DE89-017813 N90-11834 #
DE89-017837 N90-11813 #
DE89-017887 N90-11977 #
DE89-017888 N90-11951 #
DE89-017892 N90-12340 #
DE89-611967 N90-12413 #
DE89-611968 N90-12414 #

DE90-000006 N90-12378 #
DE90-000009 N90-12341 #
DE90-000024 N90-12366 #
DE90-000025 N90-11863 #
DE90-000036 N90-11952 #
DE90-000057 N90-11814 #
DE90-000061 N90-12342 #
DE90-000065 N90-12321 #
DE90-000107 N90-11922 #
DE90-000111 N90-11864 #
DE90-000123 N90-11953 #
DE90-000124 N90-12284 #
DE90-000135 N90-11885 #
DE90-000136 N90-11865 #
DE90-000174 N90-12322 #
DE90-000176 N90-11835 #
DE90-000177 N90-11886 #
DE90-000668 N90-12019 #

DFVLR-FB-87-25 N90-11990 #
DFVLR-FB-87-53 N90-12326 #
DFVLR-FB-88-05 N90-11893 #
DFVLR-FB-88-16 N90-11767 #
DFVLR-FB-88-22 N90-12008 #
DFVLR-FB-89-06 N90-12088 #
DFVLR-FB-89-07 N90-12089 #
DFVLR-FB-89-10 N90-12172 #
DFVLR-FB-89-11 N90-11873 #
DFVLR-FB-89-13 N90-11991 #
DFVLR-FB-89-16 N90-12112 #
DFVLR-FB-89-18 N90-11711 #
DFVLR-FB-89-20 N90-11760 #
DFVLR-FB-89-22 N90-11992 #

DFVLR-MITT-88-24 N90-12288 #
DFVLR-MITT-88-31 N90-12099 #
DFVLR-MITT-89-06 N90-12007 #
DFVLR-MITT-89-07 N90-12404 #
DFVLR-MITT-89-09 N90-11727 #
DFVLR-MITT-89-10 N90-11728 #

DNA-TR-88-286 N90-11987 #

DODA-AR-005-582 N90-11745 #

DOE/BP-23169/1 N90-11948 #

DOE/DP-10618/T2 N90-12338 #

DOE/ER-0423 N90-12398 #
DOE/ER-01198/T37 N90-11814 #
DOE/ER-01428/T1 N90-12311 #
DOE/ER-13615/3 N90-11834 #
DOE/ER-40515/1 N90-12342 #
DOE/ER-45056/8 N90-12321 #
DOE/ER-45296/2 N90-11862 #
DOE/ER-53176/5 N90-12341 #
DOE/ER-53201/2 N90-12328 #
DOE/ER-72012/T8 N90-11975 #

DOE/ET-51013/271 N90-12327 #

DOE/METC-89-0265 N90-11828 #

DOE/NASA/0352-3 N90-11882* #
DOE/NASA/16310-13 N90-11854* #
DOE/NASA/20370-23 N90-12034* #

DOE/NV-10366/9 N90-12411 #

DOE/OSTI-4500-REV-75 N90-12391 #

DOE/PC-79680/T1 N90-12333 #

DOT/FAA/CD-89/13 N90-11999* #

DOT/FAA/CT-TN87/54-VOL-2 N90-11761
DOT/FAA/CT-TN89/41 N90-11726 #
DOT/FAA/CT-TN89/52 N90-11762 #

DOT/FAA/CT-88/28 N90-11765 #
DOT/FAA/CT-89/21 N90-11714 #

DOT/FAA/DS-89/9 N90-12406 #

DOT/FAA/PS-89-3 N90-11934 #

DP-MS-89-20 N90-12027 #

DREP-TM-89-03 N90-11924 #

DRIC-BR-110719 N90-12241 #
DRIC-BR-110739 N90-11722 #

DRIC-T-8168 N90-11894 #

DTIC-TR-89/16 N90-12400 #

E-4538 N90-11989* #
E-4601 N90-12282* #
E-4813 N90-11915* #
E-4850 N90-11881* #
E-4867 N90-12348* #
E-4957-1 N90-11969* #
E-4959 N90-11943* #
E-4960 N90-12041* #
E-4977 N90-12033* #
E-5051 N90-11808* #
E-5084 N90-11804* #
E-5102 N90-11854* #
E-5117 N90-12034* #
E-5118 N90-11880* #
E-5124 N90-12231* #
E-5127 N90-11901* #
E-5147 N90-11740* #
E-5148 N90-11902* #

EATON-TR-89041 N90-12411 #

EOTR-88-10 N90-12175* #
EOTR-89-02 N90-12174* #

EPA/450/2-89-011 N90-12104 #
EPA/600/M-89/011 N90-12155 #
EPA/600/2-89/037 N90-12105 #
EPA/600/3-89/056 N90-12103 #
EPA/600/9-89/064 N90-12410 #

ESA-SP-1108 N90-12024 #

ESA-TT-1096 N90-11990 #
ESA-TT-1123 N90-12326 #
ESA-TT-1124 N90-11893 #
ESA-TT-1128 N90-11767 #
ESA-TT-1131 N90-12008 #
ESA-TT-1139 N90-12288 #

ESD-TR-89-19 N90-12205 #
ESD-TR-89-25 N90-12206 #
ESD-TR-89-26 N90-12403 #

ESDU-86029 N90-11709 #
ESDU-88026 N90-11709 #
ESDU-89001 N90-11909 #
ESDU-89004 N90-11870 #
ESDU-89006 N90-11848 #
ESDU-89008 N90-11709 #
ESDU-89011 N90-12052 #
ESDU-89016 N90-12381 #

ES41 N90-12059* #

ETL-0543 N90-11725 #
ETL-0544 N90-11720 #

ETN-89-94081 N90-12189 #
ETN-89-94082 N90-12226 #
ETN-89-94083 N90-12217 #
ETN-89-94085 N90-12190 #
ETN-89-94201 N90-12053 #
ETN-89-94202 N90-12054 #
ETN-89-94203 N90-11875 #
ETN-89-94328 N90-11894 #
ETN-89-94333 N90-11876 #
ETN-89-94334 N90-11768 #
ETN-89-94335 N90-12405 #
ETN-89-94337 N90-12422 #
ETN-89-94612 N90-11935 #
ETN-89-94614 N90-12494 #
ETN-89-94619 N90-12208 #
ETN-89-94620 N90-12023 #
ETN-89-94621 N90-12111 #
ETN-89-94622 N90-11936 #
ETN-89-94626 N90-11772 #
ETN-89-94649 N90-12087
ETN-89-94664 N90-12013 #
ETN-89-94670 N90-11809 #
ETN-89-94671 N90-11855 #
ETN-89-94985 N90-11871 #
ETN-89-95011 N90-12024 #
ETN-89-95024 N90-11710 #
ETN-89-95054 N90-11877 #
ETN-89-95055 N90-12055 #
ETN-89-95056 N90-12056 #
ETN-89-95057 N90-11750 #
ETN-89-95073 N90-12006
ETN-89-95074 N90-11937
ETN-89-95075 N90-11938
ETN-89-95079 N90-11939
ETN-89-95081 N90-12137
ETN-89-95083 N90-11940
ETN-89-95084 N90-12138

ETN-89-95108 .... N90-11910 #
ETN-89-95111 .... N90-11989 #
ETN-89-95127 .... N90-12276 #
ETN-89-95128 .... N90-12271 #
ETN-89-95129 .... N90-12277 #
ETN-89-95130 .... N90-12259 #
ETN-89-95131 .... N90-12030 #
ETN-89-95132 .... N90-12031 #
ETN-89-95133 .... N90-12218 #
ETN-89-95134 .... N90-12247 #
ETN-89-95135 .... N90-12248 #
ETN-89-95136 .... N90-12029 #
ETN-89-95137 .... N90-12223 #
ETN-89-95138 .... N90-11965 #
ETN-89-95139 .... N90-11966 #
ETN-89-95140 .... N90-12272 #
ETN-89-95156 .... N90-11990 #
ETN-89-95157 .... N90-12326 #
ETN-89-95158 .... N90-12308 #
ETN-89-95173 .... N90-12139 #
ETN-89-95210 .... N90-11735 #
ETN-89-95211 .... N90-11759 #
ETN-89-95213 .... N90-11766 #
ETN-89-95216 .... N90-11872 #
ETN-89-95218 .... N90-12035 #
ETN-89-95219 .... N90-11819 #
ETN-89-95220 .... N90-11820 #
ETN-89-95232 .... N90-12224 #
ETN-89-95233 .... N90-12249 #
ETN-89-95234 .... N90-12225 #
ETN-89-95249 .... N90-11717
ETN-89-95271 .... N90-11716 #
ETN-89-95295 .... N90-12099 #
ETN-89-95297 .... N90-12007 #
ETN-89-95298 .... N90-12404 #
ETN-89-95300 .... N90-11727 #
ETN-89-95301 .... N90-11728 #
ETN-89-95303 .... N90-12088 #
ETN-89-95304 .... N90-12089 #
ETN-89-95307 .... N90-12172 #
ETN-89-95308 .... N90-11873 #
ETN-89-95309 .... N90-11991 #
ETN-89-95312 .... N90-12112 #
ETN-89-95313 .... N90-11711 #
ETN-89-95315 .... N90-11760 #
ETN-89-95317 .... N90-11992 #
ETN-89-95337 .... N90-12309
ETN-89-95349 .... N90-11993
ETN-89-95390 .... N90-11893 #
ETN-89-95431 .... N90-12250 #
ETN-89-95432 .... N90-12209 #
ETN-89-95433 .... N90-12273 #
ETN-89-95434 .... N90-12274 #
ETN-89-95437 .... N90-12251 #
ETN-89-95442 .... N90-12278 #
ETN-89-95443 .... N90-12252 #
ETN-89-95444 .... N90-12279 #
ETN-89-95445 .... N90-12275 #
ETN-89-95446 .... N90-12210 #
ETN-89-95448 .... N90-12253 #
ETN-89-95469 .... N90-12100 #
ETN-89-95493 .... N90-12254 #
ETN-89-95495 .... N90-12255 #
ETN-89-95496 .... N90-12256 #
ETN-89-95497 .... N90-12257 #
ETN-89-95504 .... N90-12258 #
ETN-89-95517 .... N90-11767 #
ETN-89-95518 .... N90-12008 #
ETN-89-95519 .... N90-12288 #
ETN-89-95533 .... N90-11718
ETN-89-95534 .... N90-11729
ETN-89-95535 .... N90-11719
ETN-89-95538 .... N90-12314
ETN-89-95539 .... N90-12382
ETN-89-95540 .... N90-11895
ETN-89-95542 .... N90-11746 #
ETN-89-95543 .... N90-11747 #
ETN-89-95544 .... N90-11748 #
ETN-89-95545 .... N90-11874 #
ETN-89-95547 .... N90-11749 #
ETN-89-95575 .... N90-11712 #
ETN-89-95576 .... N90-11713 #
ETN-89-95578 .... N90-12260 #
ETN-89-95581 .... N90-12261 #
ETN-89-95582 .... N90-12032 #
ETN-89-95583 .... N90-12262 #
ETN-89-95584 .... N90-12263 #
ETN-89-95586 .... N90-12264 #
ETN-89-95587 .... N90-12265 #
ETN-89-95596 .... N90-12140
ETN-89-95597 .... N90-12141
ETN-89-95923 .... N90-12421 #

EU619 .... N90-11729

FEL-1988-24 .... N90-12006
FEL-1988-26 .... N90-11937
FEL-1988-28 .... N90-11938
FEL-1988-56 .... N90-11939
FEL-1988-73 .... N90-12137
FEL-1989-22-PT-3 .... N90-11940
FEL-1989-80 .... N90-12138

FERMILAB-PUB-89/196-A .... N90-12492* #

FHWA/TX-88/1123-2 .... N90-11994 #

FMI-MP-8 .... N90-12116 #

FNAL-TM-1588 .... N90-12001 #
FNAL-TM-1613 .... N90-11811 #

FTD-ID(RS)T-0390-89 .... N90-12131 #
FTD-ID(RS)T-0392-89 .... N90-11734 #
FTD-ID(RS)T-0594-89 .... N90-11769 #

GL-TR-89-0143 .... N90-12120 #
GL-TR-89-0145-PT-2 .... N90-12121 #

GMD-374 .... N90-11993

GRI-89/0019 .... N90-11971 #
GRI-89/0093 .... N90-12026 #
GRI-89/0123 .... N90-11826 #

H-1528 .... N90-11732* #
H-1534 .... N90-12042* #
H-1548 .... N90-11753* #
H-1556 .... N90-11741* #

IASSNS-HEP-89/29 .... N90-12378 #

ICASE-89-42 .... N90-12266* #
ICASE-89-46 .... N90-12232* #
ICASE-89-47 .... N90-11698* #
ICASE-89-53 .... N90-12182* #
ICASE-89-59 .... N90-12230* #
ICASE-89-69 .... N90-12193* #
ICASE-89-70 .... N90-12183* #
ICASE-89-75 .... N90-12192* #

ICOMP-89-17 .... N90-12041* #
ICOMP-89-21 .... N90-11969* #
ICOMP-89-26 .... N90-12231* #

IEEE-88TH0215-4 .... N90-11961 #

IFT-P-30/88 .... N90-12413 #
IFT-P-40/88 .... N90-12414 #

IMAG-RR-743-M .... N90-12254 #
IMAG-RR-745-M .... N90-12255 #
IMAG-RR-749-M .... N90-12256 #
IMAG-RR-750-M .... N90-12257 #

INS-T-485 .... N90-12310 #

IPM-15/1988 .... N90-12023 #

IPPCZ-284 .... N90-12332 #
IPPCZ-285 .... N90-12331 #
IPPCZ-287 .... N90-12329 #
IPPCZ-288 .... N90-12330 #

IRF-PREPRINT-106 .... N90-12308 #
IRF-PREPRINT-113 .... N90-12118 #

ISBN-0-309-03945-2 .... N90-12101* #
ISBN-0-309-03945-2 .... N90-12110 #
ISBN-0-85679-672-7 .... N90-11909 #
ISBN-0-85679-675-1 .... N90-11870 #
ISBN-0-85679-677-8 .... N90-11848 #
ISBN-0-85679-679-4 .... N90-11709 #
ISBN-0-85679-682-4 .... N90-12052 #
ISBN-0-85679-688-3 .... N90-12381 #
ISBN-0-947767-86-X .... N90-11713 #
ISBN-0-947767-90-8 .... N90-11712 #
ISBN-3-88314-824-5 .... N90-11935 #
ISBN-9-03-530072-6 .... N90-12100 #
ISBN-92-63-10714-9 .... N90-12139 #
ISBN-951-45-4941-4 .... N90-12393 #
ISBN-951-45-4948-1 .... N90-12394 #
ISBN-951-697-270-5 .... N90-12116 #
ISBN-951-754-313-1 .... N90-11916 #
ISBN-951-754-803-6 .... N90-11839 #
ISBN-951-754-823-0 .... N90-12368 #
ISBN-951-754-824-9 .... N90-11959 #
ISBN-951-754-826-5 .... N90-11944 #
ISBN-951-754-830-3 .... N90-12092 #
ISBN-951-754-846-X .... N90-12370 #
ISBN-951-754-869-9 .... N90-12351 #
ISBN-951-754-877-X .... N90-12369 #
ISBN-951-754-878-8 .... N90-11926 #
ISBN-951-754-896-6 .... N90-12243 #
ISBN-951-754-899-0 .... N90-11927 #

ISI/RR-88-226 .... N90-12200* #
ISI/RR-89-223 .... N90-12204 #
ISI/RR-89-230 .... N90-12203 #

ISSN-0071-9196 .... N90-12087
ISSN-0141-397X .... N90-11709 #
ISSN-0141-402X .... N90-11909 #
ISSN-0141-402X .... N90-12381 #
ISSN-0141-3961 .... N90-12052 #
ISSN-0141-4062 .... N90-11848 #
ISSN-0141-4089 .... N90-11870 #
ISSN-0143-7313 .... N90-11895
ISSN-0143-7313 .... N90-12382
ISSN-0167-8590 .... N90-12100 #
ISSN-0169-1708 .... N90-12140
ISSN-0169-1708 .... N90-12141
ISSN-0171-1342 .... N90-11711 #
ISSN-0171-1342 .... N90-11760 #
ISSN-0171-1342 .... N90-11873 #
ISSN-0171-1342 .... N90-11991 #
ISSN-0171-1342 .... N90-11992 #
ISSN-0171-1342 .... N90-12088 #
ISSN-0171-1342 .... N90-12089 #
ISSN-0171-1342 .... N90-12112 #
ISSN-0171-1342 .... N90-12172 #
ISSN-0176-7739 .... N90-11727 #
ISSN-0176-7739 .... N90-11728 #
ISSN-0176-7739 .... N90-12007 #
ISSN-0176-7739 .... N90-12099 #
ISSN-0176-7739 .... N90-12404 #
ISSN-0341-6720 .... N90-11935 #
ISSN-0348-7539 .... N90-12421 #
ISSN-0379-6566 .... N90-12024 #
ISSN-0452-2982 .... N90-11696 #
ISSN-0452-2982 .... N90-11697 #
ISSN-0452-2982 .... N90-11737 #
ISSN-0452-2982 .... N90-11803 #
ISSN-0452-2982 .... N90-12039 #
ISSN-0452-2982 .... N90-12185 #
ISSN-0452-2982 .... N90-12191 #
ISSN-0723-0508 .... N90-11993
ISSN-0922-5641 .... N90-11910 #
ISSN-0922-5641 .... N90-11989 #
ISSN-0922-5641 .... N90-12032 #
ISSN-0922-5641 .... N90-12209 #
ISSN-0922-5641 .... N90-12210 #
ISSN-0922-5641 .... N90-12250 #
ISSN-0922-5641 .... N90-12251 #
ISSN-0922-5641 .... N90-12252 #
ISSN-0922-5641 .... N90-12253 #
ISSN-0922-5641 .... N90-12260 #
ISSN-0922-5641 .... N90-12261 #
ISSN-0922-5641 .... N90-12262 #
ISSN-0922-5641 .... N90-12263 #
ISSN-0922-5641 .... N90-12264 #
ISSN-0922-5641 .... N90-12265 #
ISSN-0922-5641 .... N90-12273 #
ISSN-0922-5641 .... N90-12274 #
ISSN-0922-5641 .... N90-12275 #
ISSN-0922-5641 .... N90-12278 #
ISSN-0922-5641 .... N90-12279 #
ISSN-0951-6301 .... N90-11717
ISSN-0951-6301 .... N90-11718
ISSN-0955-9655 .... N90-12314
ISSN-0958-0360 .... N90-12052 #

JTN-88-80055 .... N90-12191 #
JTN-88-80056 .... N90-12185 #
JTN-88-80057 .... N90-11737 #
JTN-88-80058 .... N90-12039 #
JTN-88-80059 .... N90-11803 #
JTN-88-80061 .... N90-11696 #
JTN-88-80062 .... N90-11697 #

K/QT-282 .... N90-12386 #

KCP-613-4025-REV .... N90-11904 #
KCP-613-4099 .... N90-12195 #
KCP-613-4130 .... N90-11903 #

KNMI-TR-110 .... N90-12140
KNMI-TR-112 .... N90-12141

KSC-DM-3265 .... N90-12047* #

L-16609 .... N90-11757* #
L-16616 .... N90-11751* #

LA-UR-89-895 .... N90-12119 #
LA-UR-89-2446 .... N90-12297 #
LA-UR-89-2453 .... N90-12296 #
LA-UR-89-2500 .... N90-12012 #

LA-UR-89-2506 N90-12299 #
LA-UR-89-2671 N90-11830 #
LA-UR-89-2718 N90-11973 #
LA-UR-89-2768 N90-12045 #
LA-UR-89-2779 N90-12457 #
LA-UR-89-2783 N90-11974 #
LA-UR-89-2808 N90-11857 #
LA-UR-89-2894 N90-12016 #
LA-UR-89-2898 N90-12000 #
LA-UR-89-2921 N90-11998 #
LA-UR-89-2930 N90-11856 #
LA-UR-89-2936 N90-11897 #
LA-UR-89-2961 N90-12417 #

LA-11570-MS N90-11972 #
LA-11572-MS N90-12018 #
LA-11686-C N90-12334 #

LBL-25974 N90-11953 #
LBL-26473 N90-12322 #
LBL-26598 N90-12284 #
LBL-27303 N90-11885 #
LBL-27375 N90-11865 #
LBL-27583 N90-11835 #
LBL-27643 N90-11886 #

LC-87-83469 N90-11961 #
LC-88-31544 N90-12101* #
LC-88-31544 N90-12110 #
LC-88-600301 N90-11849 #

LG89ER0026 N90-11738* #
LG89ER0064 N90-11739* #

LIDS-P-1876 N90-12240 #
LIDS-P-1899 N90-11724 #

LLNL-B-034291 N90-11921 #

LPI-CONTRIB-708 N90-12423* #

LR-540 N90-12043 #
LR-544 N90-12291 #
LR-556 N90-11754 #
LR-558 N90-11799 #
LR-31038 N90-11821* #

MAE-TM-25 N90-11825* #

MAP-HANDBOOK-28 N90-12117* #

MAT-A266 N90-12243 #

MBB-UD-526/88-PUB N90-12208 #

MBB/LW/3015/S/PUB/321 N90-12494 #

MITT-177 N90-12087

MLM-3598 N90-12234 #

MML-TR-894(C) N90-11868 #

MPE-PAE/EXP.EL.199 N90-12309

MRC/ABQ-R-1100 N90-11987 #

MRL-TR-89-17 N90-11896 #

MSU-EE-FIN-20B-89 N90-11802* #

MT-CWR-089-033 N90-11859 #

MTL-TR-89-3 N90-11868 #
MTL-TR-89-41 N90-12371 #
MTL-TR-89-42 N90-11816 #
MTL-TR-89-55 N90-12377 #
MTL-TR-89-62 N90-11869 #
MTL-TR-89-72 N90-12049 #

MTR-10445 N90-11930 #

NAL-TM-559 N90-12191 #
NAL-TM-560 N90-12185 #
NAL-TM-562 N90-11737 #
NAL-TM-563 N90-12039 #
NAL-TM-564 N90-11803 #
NAL-TM-566 N90-11696 #
NAL-TM-567 N90-11697 #

NAS 1.15:4130 N90-12454* #
NAS 1.15:4140 N90-11741* #
NAS 1.15:4142 N90-11753* #
NAS 1.15:4147 N90-11751* #
NAS 1.15:4148 N90-11732* #
NAS 1.15:4153 N90-12090* #
NAS 1.15:100357 N90-12059* #
NAS 1.15:100380 N90-12345* #
NAS 1.15:100750 N90-12115* #
NAS 1.15:101054 N90-11752* #
NAS 1.15:101577 N90-11736* #
NAS 1.15:101646 N90-12057* #
NAS 1.15:101660 N90-12292* #
NAS 1.15:101664 N90-11703* #
NAS 1.15:101814 N90-12388*
NAS 1.15:101815 N90-12389*
NAS 1.15:101825 N90-12102* #
NAS 1.15:101893 N90-12459* #
NAS 1.15:102088 N90-11881* #
NAS 1.15:102182 N90-11701* #
NAS 1.15:102198 N90-12211* #
NAS 1.15:102221 N90-11699* #
NAS 1.15:102222 N90-11700* #
NAS 1.15:102233 N90-11970* #
NAS 1.15:102237 N90-12151* #
NAS 1.15:102238 N90-11742* #
NAS 1.15:102239 N90-12227* #
NAS 1.15:102252 N90-11978* #
NAS 1.15:102253 N90-11692* #
NAS 1.15:102289 N90-11943* #
NAS 1.15:102290 N90-12041* #
NAS 1.15:102334 N90-11969* #
NAS 1.15:102343 N90-11808* #
NAS 1.15:102366 N90-11804* #
NAS 1.15:102378 N90-12034* #
NAS 1.15:102379 N90-11880* #
NAS 1.15:102385 N90-12231* #
NAS 1.15:102386 N90-11901* #
NAS 1.15:102390 N90-11854* #
NAS 1.15:102397 N90-11740* #
NAS 1.15:102398 N90-11902* #
NAS 1.21:7011(329) N90-12173*
NAS 1.21:7037(243) N90-11693*
NAS 1.21:7037(244) N90-11694*
NAS 1.21:7041(63) N90-12091*
NAS 1.21:7078 N90-12385* #
NAS 1.26:3922(26)-ISSUE-22 N90-12153*
NAS 1.26:3922(27)-ISSUE-23 N90-12154*
NAS 1.26:3922(28)-ISSUE-24 N90-12152*
NAS 1.26:4035 N90-11821* #
NAS 1.26:4259 N90-12033* #
NAS 1.26:4261 N90-11968* #
NAS 1.26:18559-VOL-3 N90-11777* #
NAS 1.26:177472 N90-11730* #
NAS 1.26:178408 N90-11822* #
NAS 1.26:179286 N90-12142* #
NAS 1.26:181876 N90-12266* #
NAS 1.26:181887 N90-12182* #
NAS 1.26:181908 N90-11702* #
NAS 1.26:181914 N90-12193* #
NAS 1.26:181915 N90-12183* #
NAS 1.26:181916-VOL-1 N90-12058* #
NAS 1.26:181927 N90-12232* #
NAS 1.26:181928 N90-11698* #
NAS 1.26:181929 N90-12230* #
NAS 1.26:181933 N90-12192* #
NAS 1.26:181937 N90-11704* #
NAS 1.26:182262 N90-11882* #
NAS 1.26:182278 N90-11738* #
NAS 1.26:182293 N90-11999* #
NAS 1.26:182366 N90-11825* #
NAS 1.26:183804 N90-11802* #
NAS 1.26:184972 N90-12117* #
NAS 1.26:184999 N90-11807* #
NAS 1.26:185138 N90-11739* #
NAS 1.26:185144 N90-11853* #
NAS 1.26:185164 N90-11805* #
NAS 1.26:185165 N90-11806* #
NAS 1.26:185323 N90-12101* #
NAS 1.26:185362 N90-12228* #
NAS 1.26:185432 N90-12423* #
NAS 1.26:185517 N90-12174* #
NAS 1.26:185518 N90-12175* #
NAS 1.26:185528-VOL-1 N90-11789* #
NAS 1.26:185528-VOL-2 N90-11790* #
NAS 1.26:185528-VOL-3 N90-11791* #
NAS 1.26:185537 N90-11792* #
NAS 1.26:185539 N90-11786* #
NAS 1.26:185542 N90-11785* #
NAS 1.26:185543-VOL-1 N90-11793* #
NAS 1.26:185543-VOL-2 N90-11794* #
NAS 1.26:185543-VOL-3 N90-11795* #
NAS 1.26:185543-VOL-4 N90-11796* #
NAS 1.26:185543-VOL-5 N90-11797* #
NAS 1.26:185544-VOL-1 N90-11787* #
NAS 1.26:185544-VOL-2 N90-11788* #
NAS 1.26:185550 N90-11783* #
NAS 1.26:185552 N90-11784* #
NAS 1.26:185553 N90-11782* #
NAS 1.26:185557-VOL-1 N90-11779* #
NAS 1.26:185557-VOL-2 N90-11780* #
NAS 1.26:185557-VOL-3 N90-11781* #
NAS 1.26:185559-VOL-1 N90-11775* #
NAS 1.26:185559-VOL-2 N90-11776* #
NAS 1.26:185559-VOL-4 N90-11778* #
NAS 1.26:185563 N90-11774* #
NAS 1.26:185832 N90-12009* #
NAS 1.26:185853 N90-11695* #
NAS 1.26:185855 N90-12178* #
NAS 1.26:185890 N90-12200* #
NAS 1.26:185924 N90-12492* #
NAS 1.26:185932 N90-11850* #
NAS 1.26:185933 N90-12084* #
NAS 1.26:185965 N90-12212* #
NAS 1.26:185970 N90-12011* #
NAS 1.26:185982 N90-12458* #
NAS 1.26:185983 N90-12298* #
NAS 1.26:185984 N90-12213* #
NAS 1.26:185990 N90-12215* #
NAS 1.26:185991 N90-12214* #
NAS 1.26:186001 N90-12290* #
NAS 1.26:186036 N90-11733* #
NAS 1.26:186040 N90-12133* #
NAS 1.26:186041 N90-12047* #
NAS 1.26:186043 N90-11770* #
NAS 1.26:186045 N90-11771* #
NAS 1.26:186049 N90-11800* #
NAS 1.26:186089 N90-11755* #
NAS 1.26:186090 N90-12109* #
NAS 1.60:2944 N90-11915* #
NAS 1.60:2948 N90-12456* #
NAS 1.60:2949 N90-12282* #
NAS 1.60:2952 N90-12042* #
NAS 1.60:2957 N90-12348* #
NAS 1.60:2962 N90-11757* #
NAS 1.71:LAR-14155-1-SB N90-11823* #
NAS 1.71:MSC-21327-1 N90-11798* #

NASA-CASE-LAR-14155-1-SB N90-11823* #

NASA-CASE-LEW-13609-1 N90-11824* #

NASA-CASE-MSC-21327-1 N90-11798* #

NASA-CASE-NPO-16995-1-CU N90-12289*

NASA-CR-3922(26)-ISSUE-22 N90-12153*
NASA-CR-3922(27)-ISSUE-23 N90-12154*
NASA-CR-3922(28)-ISSUE-24 N90-12152*
NASA-CR-4035 N90-11821* #
NASA-CR-4259 N90-12033* #
NASA-CR-4261 N90-11968* #
NASA-CR-18559-VOL-3 N90-11777* #
NASA-CR-177472 N90-11730* #
NASA-CR-178408 N90-11822* #
NASA-CR-179286 N90-12142* #
NASA-CR-181876 N90-12266* #
NASA-CR-181887 N90-12182* #
NASA-CR-181908 N90-11702* #
NASA-CR-181914 N90-12193* #
NASA-CR-181915 N90-12183* #
NASA-CR-181916-VOL-1 N90-12058* #
NASA-CR-181927 N90-12232* #
NASA-CR-181928 N90-11698* #
NASA-CR-181929 N90-12230* #
NASA-CR-181933 N90-12192* #
NASA-CR-181937 N90-11704* #
NASA-CR-182262 N90-11882* #
NASA-CR-182278 N90-11738* #
NASA-CR-182293 N90-11999* #
NASA-CR-182366 N90-11825* #
NASA-CR-183804 N90-11802* #
NASA-CR-184972 N90-12117* #
NASA-CR-184999 N90-11807* #
NASA-CR-185138 N90-11739* #
NASA-CR-185144 N90-11853* #
NASA-CR-185164 N90-11805* #
NASA-CR-185165 N90-11806* #
NASA-CR-185323 N90-12101* #
NASA-CR-185362 N90-12228* #
NASA-CR-185432 N90-12423* #
NASA-CR-185517 N90-12174* #
NASA-CR-185518 N90-12175* #
NASA-CR-185528-VOL-1 N90-11789* #
NASA-CR-185528-VOL-2 N90-11790* #
NASA-CR-185528-VOL-3 N90-11791* #
NASA-CR-185537 N90-11792* #
NASA-CR-185539 N90-11786* #
NASA-CR-185542 N90-11785* #
NASA-CR-185543-VOL-1 N90-11793* #
NASA-CR-185543-VOL-2 N90-11794* #
NASA-CR-185543-VOL-3 N90-11795* #
NASA-CR-185543-VOL-4 N90-11796* #
NASA-CR-185543-VOL-5 N90-11797* #
NASA-CR-185544-VOL-1 N90-11787* #
NASA-CR-185544-VOL-2 N90-11788* #
NASA-CR-185550 N90-11783* #
NASA-CR-185552 N90-11784* #

NASA-CR-185553 .... N90-11762* #
NASA-CR-185557-VOL-1 .... N90-11779* #
NASA-CR-185557-VOL-2 .... N90-11780* #
NASA-CR-185557-VOL-3 .... N90-11781* #
NASA-CR-185559-VOL-1 .... N90-11775* #
NASA-CR-185559-VOL-2 .... N90-11776* #
NASA-CR-185559-VOL-4 .... N90-11778* #
NASA-CR-185563 .... N90-11774* #
NASA-CR-185632 .... N90-12009* #
NASA-CR-185653 .... N90-11695* #
NASA-CR-185655 .... N90-12178* #
NASA-CR-185690 .... N90-12200* #
NASA-CR-185924 .... N90-12492* #
NASA-CR-185932 .... N90-11850* #
NASA-CR-185933 .... N90-12084* #
NASA-CR-185965 .... N90-12212* #
NASA-CR-185970 .... N90-12011* #
NASA-CR-185982 .... N90-12458* #
NASA-CR-185983 .... N90-12298* #
NASA-CR-185984 .... N90-12213* #
NASA-CR-185990 .... N90-12215* #
NASA-CR-185991 .... N90-12214* #
NASA-CR-186001 .... N90-12290* #
NASA-CR-186036 .... N90-11733* #
NASA-CR-186040 .... N90-12133* #
NASA-CR-186041 .... N90-12047* #
NASA-CR-186043 .... N90-11770* #
NASA-CR-186045 .... N90-11771* #
NASA-CR-186049 .... N90-11800* #
NASA-CR-186069 .... N90-11755* #
NASA-CR-186090 .... N90-12109* #

NASA-SP-7011(329) N90-12173*
NASA-SP-7037(243) N90-11693*
NASA-SP-7037(244) N90-11694*
NASA-SP-7041(63) N90-12091*
NASA-SP-7078 .... N90-12385* #

NASA-TM-4130 .... N90-12454* #
NASA-TM-4140 .... N90-11741* #
NASA-TM-4142 .... N90-11753* #
NASA-TM-4147 .... N90-11751* #
NASA-TM-4148 .... N90-11732* #
NASA-TM-4153 .... N90-12090* #
NASA-TM-100357 .... N90-12059* #
NASA-TM-100380 .... N90-12345* #
NASA-TM-100750 .... N90-12115* #
NASA-TM-101054 .... N90-11752* #
NASA-TM-101577 .... N90-11736* #
NASA-TM-101646 .... N90-12057* #
NASA-TM-101660 .... N90-12292* #
NASA-TM-101664 .... N90-11703* #
NASA-TM-101814 .... N90-12388*
NASA-TM-101815 .... N90-12389*
NASA-TM-101825 .... N90-12102* #
NASA-TM-101893 .... N90-12459* #
NASA-TM-102088 .... N90-11881* #
NASA-TM-102182 .... N90-11701* #
NASA-TM-102198 .... N90-12211* #
NASA-TM-102221 .... N90-11699* #
NASA-TM-102222 .... N90-11700* #
NASA-TM-102233 .... N90-11970* #
NASA-TM-102237 .... N90-12151* #
NASA-TM-102238 .... N90-11742* #
NASA-TM-102239 .... N90-12227* #
NASA-TM-102252 .... N90-11978* #
NASA-TM-102253 .... N90-11692* #
NASA-TM-102269 .... N90-11943* #
NASA-TM-102290 .... N90-12041* #
NASA-TM-102334 .... N90-11969* #
NASA-TM-102343 .... N90-11808* #
NASA-TM-102366 .... N90-11804* #
NASA-TM-102378 .... N90-12034* #
NASA-TM-102379 .... N90-11880* #
NASA-TM-102385 .... N90-12231* #
NASA-TM-102386 .... N90-11901* #
NASA-TM-102390 .... N90-11854* #
NASA-TM-102397 .... N90-11740* #
NASA-TM-102398 .... N90-11902* #

NASA-TP-2944 .... N90-11915* #
NASA-TP-2948 .... N90-12456* #
NASA-TP-2949 .... N90-12282* #
NASA-TP-2952 .... N90-12042* #
NASA-TP-2957 .... N90-12348* #
NASA-TP-2962 .... N90-11757* #

NCAR/CT-120 .... N90-12132 #

NCAR/TN-332-PROC .... N90-12113 #
NCAR/TN-337-EDD .... N90-11731 #

NCEL-TN-1794 .... N90-11869 #

NCTRF-170 .... N90-11891 #

NHRC-88-41 .... N90-12161 #

NIKHEF-H-87-19 .... N90-12283 #

NISTIR-89/3909 .... N90-11925 #
NISTIR-89/3911 .... N90-11850* #
NISTIR-89/4090 .... N90-11967 #
NISTIR-89/4105 .... N90-12150 #
NISTIR-89/4112 .... N90-12396 #
NISTIR-89/4113 .... N90-12135 #
NISTIR-89/4118 .... N90-12402 #
NISTIR-89/4121 .... N90-12038 #
NISTIR-89/4128 .... N90-12201 #
NISTIR-89/4131 .... N90-12036 #
NISTIR-89/4139/2 .... N90-12395 #

NLR-MP-88028-U .... N90-11877 #
NLR-MP-88029-U .... N90-12055 #
NLR-MP-88042-U .... N90-12056 #
NLR-MP-88045-U .... N90-11750 #

NOAA-TM-ERL-PMEL-86 .... N90-12143 #
NOAA-TM-ERL-PMEL-87 .... N90-12147 #

NOAA-TM-ERL-WPL-165 .... N90-12010 #
NOAA-TM-ERL-WPL-166 .... N90-12315 #

NOAA-TM-NESDIS-25 .... N90-12086 #

NOAA-TM-NWS-NSSFC-23 .... N90-12134 #

NOSC/TD-1533 .... N90-12136 #

NOSC/TR-1263 .... N90-12293 #

NPL-DMA(A)-174 .... N90-12382
NPL-DMA(A)-182 .... N90-11895

NPL-RSA(EXT)-6 .... N90-12314

NPRDC-TR-89-14 .... N90-12181 #

NRL-MR-6393 .... N90-11866 #
NRL-MR-6506 .... N90-11931 #
NRL-MR-6508 .... N90-11964 #
NRL-MR-6514 .... N90-11929 #
NRL-MR-6517 .... N90-12344 #

NSF-87-314-VOL-36 .... N90-12407 #
NSF-89-304-VOL-37 .... N90-12408 #

NSF/ENG-88037 .... N90-12176 #
NSF/ENG-88038 .... N90-12025 #
NSF/ENG-89006 .... N90-12383 #
NSF/ENG-89007 .... N90-12202 #
NSF/ENG-89009 .... N90-11960 #
NSF/ENG-89010 .... N90-12220 #

NSWC-TR-89-136 .... N90-11985 #

NTIA-88-240-PT-1 .... N90-11913 #
NTIA-89-242-PT-2 .... N90-11912 #

NUSC-TR-6734 .... N90-12148 #

ORNL/FTR-3036 .... N90-11858 #
ORNL/FTR-3286 .... N90-11884 #
ORNL/FTR-3308 .... N90-12357 #
ORNL/FTR-3366 .... N90-12219 #
ORNL/FTR-3367 .... N90-12365 #

ORNL/SUB-85-27421/03 .... N90-11859 #

ORNL/TM-11248 .... N90-11898 #

PARC-EDL-88-5 .... N90-12184 #

PB89-142566 .... N90-12085 #
PB89-188676 .... N90-12390 #
PB89-195473 .... N90-11912 #
PB89-195846 .... N90-11849 #
PB89-196000 .... N90-11911 #
PB89-196331 .... N90-12143 #
PB89-198113 .... N90-12144 #
PB89-198139 .... N90-12145 #
PB89-198147 .... N90-12146 #
PB89-198253 .... N90-12103 #
PB89-198907 .... N90-12084* #
PB89-198915 .... N90-12384 #
PB89-200901 .... N90-12113 #
PB89-200935 .... N90-12179 #
PB89-203962 .... N90-11913 #
PB89-206775 .... N90-12147 #
PB89-207708 .... N90-11994 #
PB89-207914 .... N90-12104 #
PB89-208094 .... N90-12315 #
PB89-208110 .... N90-12184 #
PB89-208334 .... N90-12155 #
PB89-208680 .... N90-12010 #
PB89-208995 .... N90-11731 #
PB89-209282 .... N90-11967 #
PB89-212591 .... N90-11944 #
PB89-212617 .... N90-12351 #
PB89-212674 .... N90-11916 #
PB89-212682 .... N90-11827 #
PB89-212716 .... N90-12092 #
PB89-213136 .... N90-12118 #
PB89-213417 .... N90-12086 #
PB89-214225 .... N90-12410 #
PB89-214563 .... N90-12132 #
PB89-214779 .... N90-12150 #
PB89-215370 .... N90-12038 #
PB89-215461 .... N90-12416 #
PB89-216097 .... N90-12110 #
PB89-216253 .... N90-12025 #
PB89-216873 .... N90-12283 #
PB89-216980 .... N90-12291 #
PB89-217020 .... N90-11799 #
PB89-217038 .... N90-12043 #
PB89-217376 .... N90-12392 #
PB89-217400 .... N90-12350 #
PB89-217525 .... N90-11754 #
PB89-217533 .... N90-12393 #
PB89-217541 .... N90-12394 #
PB89-217780 .... N90-12415 #
PB89-217921 .... N90-11971 #
PB89-218333 .... N90-11850* #
PB89-218564 .... N90-12243 #
PB89-218739 .... N90-12109* #
PB89-218952 .... N90-11839 #
PB89-218994 .... N90-12368 #
PB89-219265 .... N90-12026 #
PB89-219273 .... N90-11826 #
PB89-219489 .... N90-12176 #
PB89-219497 .... N90-12220 #
PB89-219505 .... N90-11960 #
PB89-219513 .... N90-12202 #
PB89-219521 .... N90-12383 #
PB89-219844 .... N90-12014 #
PB89-219968 .... N90-12105 #
PB89-221592 .... N90-11926 #
PB89-221618 .... N90-12369 #
PB89-221634 .... N90-12370 #
PB89-221642 .... N90-11927 #
PB89-221667 .... N90-11959 #
PB89-223523 .... N90-12407 #
PB89-223531 .... N90-12408 #
PB89-226310 .... N90-12134 #
PB89-228274 .... N90-12396 #
PB89-228308 .... N90-12402 #
PB89-229017 .... N90-12201 #
PB89-229025 .... N90-12036 #
PB89-229033 .... N90-12395 #
PB89-229058 .... N90-12135 #
PB89-229678 .... N90-11925 #
PB89-230015 .... N90-11810 #

PFC/RR-89-9 .... N90-12327 #

PNL-SA-17011 .... N90-12313 #

PNL-6903 .... N90-11813 #
PNL-6959 .... N90-12095 #

PNR90544 .... N90-11746 #
PNR90545 .... N90-11747 #
PNR90546 .... N90-11748 #
PNR90548 .... N90-11874 #
PNR90554 .... N90-11749 #

PSI-TR-756 .... N90-12114 #

PSU-ME-R-88/89-0068 .... N90-11988 #

PTB-E-33 .... N90-11935 #

R-8718 .... N90-11772 #

R/D-5295-MS-01 .... N90-12285 #
R/D-5838-PH-01 .... N90-11981 #
R/D-6060-EE-01 .... N90-11887 #
R/D-6132-EE-02 .... N90-11954 #

RADC-TR-88-307 .... N90-11963 #
RADC-TR-89-91 .... N90-11930 #
RADC-TR-89-121-VOL-1 .... N90-11928 #

RAE-SPACE-672 .... N90-12422 #

RAE-TM-AERO-2130 .... N90-11768 #

RAE-TM-M-9 .... N90-12405 #

RAE-TM-MAT/STR-1109 N90-12053 #
RAE-TM-MAT/STR-1110 N90-11875 #
RAE-TM-MAT/STR-1111 N90-11876 #
RAE-TM-MAT/STR-1112 N90-12054 #

RAE-TR-88050 N90-12422 #

RDC-10/87 N90-12149 #

REPT-1.0-WP-VA87001-02 N90-11786* #
REPT-1.0-WP-VA87001-05 N90-11782* #
REPT-1.0-WP-VA87001-06 N90-11774* #
REPT-1.0-WP-VA88003-06 N90-11784* #
REPT-1.0-WP-VA88003-12-VOL-1 N90-11793* #
REPT-1.0-WP-VA88003-12-VOL-2 N90-11794* #
REPT-1.0-WP-VA88003-12-VOL-3 N90-11795* #
REPT-1.0-WP-VA88003-12-VOL-4 N90-11796* #
REPT-1.0-WP-VA88003-12-VOL-5 N90-11797* #
REPT-1.0-WP-VA88003-23-VOL-1 N90-11779* #
REPT-1.0-WP-VA88003-23-VOL-2 N90-11780* #
REPT-1.0-WP-VA88003-23-VOL-3 N90-11781* #
REPT-1.0-WP-VA88003-30-VOL-1 N90-11787* #
REPT-1.0-WP-VA88003-30-VOL-2 N90-11788* #
REPT-1.0-WP-VA88003-33 N90-11785* #
REPT-1.0-WP-VA88003-33-VOL-1 N90-11775* #
REPT-1.0-WP-VA88003-33-VOL-2 N90-11776* #
REPT-1.0-WP-VA88003-33-VOL-3 N90-11777* #
REPT-1.0-WP-VA88003-33-VOL-4 N90-11778* #
REPT-1.0-WP-VA88003-40 N90-11783* #
REPT-1.0-WP-VA88005-10-VOL-1 N90-11789* #
REPT-1.0-WP-VA88005-10-VOL-2 N90-11790* #
REPT-1.0-WP-VA88005-10-VOL-3 N90-11791* #
REPT-3-45400/9R-57 N90-12022 #
REPT-33 N90-12092 #
REPT-43 N90-11839 #
REPT-46 N90-11926 #
REPT-46-88 N90-12111 #
REPT-47 N90-11927 #
REPT-87-13 N90-11712 #
REPT-88-02 N90-11713 #
REPT-88-19 N90-11710 #
REPT-88-89 N90-12250 #
REPT-88-90 N90-12209 #
REPT-88-91 N90-12273 #
REPT-88-92 N90-12274 #
REPT-88-97 N90-11910 #
REPT-89-01 N90-11989 #
REPT-89-03 N90-12251 #
REPT-89-08 N90-12278 #
REPT-89-09 N90-12252 #
REPT-89-10 N90-12279 #
REPT-89-11 N90-12275 #
REPT-89-13 N90-12210 #
REPT-89-15 N90-12253 #
REPT-89-19 N90-12260 #
REPT-89-22 N90-12261 #
REPT-89-23 N90-12032 #
REPT-89-24 N90-12262 #
REPT-89-25 N90-12263 #
REPT-89-27 N90-12264 #
REPT-89-28 N90-12265 #
REPT-90-005 N90-12090* #
REPT-90B00020 N90-12115* #
REPT-186(1989) N90-11827 #
REPT-542 N90-11729

RPI-181 N90-12290* #

RR-162 N90-12415 #
RR-340-PT-1 N90-12276 #
RR-341 N90-12271 #
RR-342 N90-12277 #
RR-343 N90-12259 #
RR-344 N90-12030 #
RR-345 N90-12031 #
RR-346 N90-12218 #
RR-347 N90-12247 #
RR-348 N90-12248 #
RR-349 N90-12029 #
RR-350 N90-12223 #
RR-351 N90-11965 #
RR-353 N90-11966 #
RR-355 N90-12272 #
RR-365 N90-12224 #
RR-366 N90-12249 #
RR-367 N90-12225 #
RR-1123-2 N90-11994 #

RSRE-MEMO-4132 N90-11722 #
RSRE-MEMO-4188 N90-12189 #
RSRE-MEMO-4193 N90-12226 #
RSRE-MEMO-4197 N90-12217 #
RSRE-MEMO-4222 N90-12190 #

S-176 N90-11959 #
S-178 N90-11944 #

SAND-88-1958C N90-12319 #
SAND-88-2483C N90-12019 #
SAND-88-3472C N90-12317 #
SAND-89-0153C N90-11918 #
SAND-89-0814C N90-12353 #
SAND-89-1382C N90-11945 #
SAND-89-1626C N90-11946 #
SAND-89-1784 N90-11919 #
SAND-89-1875C N90-12349 #
SAND-89-1954C N90-11947 #
SAND-89-2009C N90-12094 #

SCT-89RR-47 N90-12406 #

SC5433.FR N90-11721 #

SD-TR-89-38 N90-11984 #
SD-TR-89-45 N90-11801 #
SD-TR-89-49 N90-12303 #
SD-TR-89-57 N90-12380 #

SEL-1216 N90-12416 #

SER-C-337 N90-12087

SERI/STR-211-3545 N90-12093 #

SNIAS-NT-18926/AG-ET N90-11894 #

SOL-89-10 N90-12244 #

SP-RAPP-1989:23 N90-12014 #

SR-2 N90-12129 #

ST-REPT-VOL-6-NO-12 N90-12100 #

SWRI-06-7963 N90-11882* #

TAMRF-5373-8903 N90-11733* #

TD88-3269 N90-12006
TD88-4381 N90-11937
TD88-4405 N90-12137
TD88-4406 N90-11938
TD89-0302 N90-11939
TD89-1167-PT-3 N90-11940
TD89-1857 N90-12138

TELECOM-PARIS-89C003 N90-12258 #

TKK-F-A641 N90-12368 #
TKK-F-A642 N90-12370 #
TKK-F-A646 N90-12351 #
TKK-F-A647 N90-12369 #

TR-4 N90-11846 #
TR-6 N90-11843 #
TR-9-ONR N90-12287 #
TR-15-ONR N90-11958 #
TR-18 N90-11888 #
TR-24 N90-11878 #
TR-37 N90-12242 #
TR-39 N90-12267 #
TR-89-WPAFB-3609-033 N90-11758 #
TR-89-13 N90-12246 #
TR-89-22C N90-12270 #
TR-89-23C N90-12245 #
TR-89-27C N90-12269 #
TR-420 N90-12268 #
TR-542 N90-12235 #
TR-0086(6403-01)-1 N90-11801 #
TR-0089(4530-04)-1 N90-11984 #
TR-0089(4604)-1 N90-12303 #
TR-0089(4925-02)-3 N90-12380 #

TRITA-EPP-89-03 N90-12421 #

TSI-89-04-06-WB N90-11756 #

TTI-2-18-87-1123-2 N90-11994 #

UCI-51 N90-12180 #

UCID-21330-REV-1 N90-12312 #
UCID-21679 N90-12399 #
UCID-21742 N90-11851 #
UCID-21807 N90-12233 #

UCRL-15867-VOL-4 N90-12017 #
UCRL-21166 N90-11921 #
UCRL-21225 N90-12335 #
UCRL-21240 N90-12418 #
UCRL-98894 N90-12106 #
UCRL-100094 N90-12362 #
UCRL-100270 N90-12364 #
UCRL-100290 N90-12015 #
UCRL-100357-REV-1 N90-12363 #
UCRL-100488 N90-11832 #
UCRL-100547 N90-12419 #
UCRL-100596 N90-12358 #
UCRL-100642 N90-11951 #
UCRL-100651 N90-11917 #
UCRL-100687 N90-12002 #
UCRL-100695 N90-12354 #
UCRL-100718-REV-1 N90-12196 #
UCRL-100784 N90-12003 #
UCRL-100804 N90-11833 #
UCRL-100835 N90-11976 #
UCRL-100869 N90-11812 #
UCRL-100901 N90-11977 #
UCRL-100943 N90-11831 #
UCRL-101103 N90-12340 #
UCRL-101309 N90-12294 #
UCRL-101322 N90-12336 #
UCRL-101395 N90-12337 #
UCRL-101396 N90-11920 #
UCRL-101433 N90-11829 #
UCRL-101436 N90-12455 #
UCRL-101616 N90-11861 #
UCRL-101721 N90-12004 #
UCRL-101726 N90-12108 #
UCRL-101753 N90-12339 #

UES-799-TR-87-001 N90-12379 #

UILU-ENG-89-2206 N90-11960 #
UILU-ENG-89-2207 N90-12220 #
UILU-ENG-89-2220 N90-11932 #
UILU-ENG-89-2231 N90-12215* #
UILU-ENG-89-2234 N90-12214* #
UILU-ENG-89-2235 N90-12213* #

US-PATENT-APPL-SN-150122 N90-11852 #
US-PATENT-APPL-SN-292121 N90-11798* #
US-PATENT-APPL-SN-298150 N90-11823* #
US-PATENT-APPL-SN-328651 N90-11942 #
US-PATENT-APPL-SN-356496 N90-12346 #
US-PATENT-APPL-SN-360173 N90-12281 #
US-PATENT-APPL-SN-361074 N90-11995 #
US-PATENT-APPL-SN-371884 N90-11997 #
US-PATENT-APPL-SN-373537 N90-11914 #
US-PATENT-APPL-SN-374101 N90-12347 #
US-PATENT-APPL-SN-374112 N90-11996 #
US-PATENT-APPL-SN-374122 N90-11941 #
US-PATENT-APPL-SN-374125 N90-11879 #
US-PATENT-APPL-SN-375218 N90-12280 #
US-PATENT-APPL-SN-452465 N90-11824* #
US-PATENT-APPL-SN-924297 N90-12289*
US-PATENT-APPL-SN-947142 N90-12186

US-PATENT-CLASS-60-730 N90-11824* #
US-PATENT-CLASS-60-732 N90-11824* #
US-PATENT-CLASS-73-505 N90-12289*
US-PATENT-CLASS-73-571 N90-12289*
US-PATENT-CLASS-165-81 N90-11824* #
US-PATENT-CLASS-165-83 N90-11824* #
US-PATENT-CLASS-165-156 N90-11824* #
US-PATENT-CLASS-350-169 N90-12186
US-PATENT-CLASS-431-352 N90-11824* #

US-PATENT-4,800,756 N90-12289*
US-PATENT-4,819,438 N90-11824* #
US-PATENT-4,834,942 N90-11852 #
US-PATENT-4,838,646 N90-12186

USAARL-89-9 N90-12167 #

USAAVSCOM-CP-89-A-002 N90-11752* #

USAAVSCOM-TM-89-A-002 N90-11692* #

USARIEM-M59-89 N90-12164 #
USARIEM-M64-89 N90-11979 #
USARIEM-M65-89 N90-11764 #

USCG-D-10-89 N90-12149 #

UTEC-89-036 N90-12159 #

UTRC/R89-917704-1 N90-11818 #
UTRC/R89-957928-3 N90-11705 #

UVA/525659/EE90/101 N90-12375 #

UW-CMRG-R-89-123 N90-11807* #

VLSI-MEMO-89-529 N90-12239 #
VLSI-MEMO-89-530 N90-12197 #
VLSI-MEMO-89-532 N90-12187 #
VLSI-MEMO-89-533 N90-11905 #
VLSI-MEMO-89-534 N90-11957 #

VLSI-MEMO-89-535 .... N90-12199 #
VLSI-MEMO-89-536 .... N90-12237 #
VLSI-MEMO-89-538 .... N90-11956 #
VLSI-MEMO-89-540 .... N90-12188 #
VLSI-MEMO-89-542 .... N90-12198 #
VLSI-MEMO-89-543 .... N90-12236 #
VLSI-MEMO-89-545 .... N90-11955 #
VLSI-MEMO-89-546 .... N90-12238 #

WHC-SA-0601 .... N90-12044 #
WHC-SA-0667 .... N90-11864 #

WHOI-88-9 .... N90-12145 #
WHOI-88-10 .... N90-12146 #
WHOI-88-49 .... N90-12144 #

WMO-714 .... N90-12139 #

WOD/CO/HYDRO-87/09 .... N90-12130 #

WRDC-TR-89-2025 .... N90-11743 #
WRDC-TR-89-2046 .... N90-12379 #
WRDC-TR-89-3061 .... N90-11758 #
WRDC-TR-89-3063 .... N90-11756 #
WRDC-TR-89-4051 .... N90-11867 #

Appendix—About STAR

Scientific and Technical Aerospace Reports (STAR) is a major component of a comprehensive National Aeronautics and Space Administration information system covering aeronautics, space, and supporting disciplines. *STAR* is issued on the 8th and 23rd of each month and announces current publications of the following types:

- NASA, NASA contractor, and NASA grantee reports
- Reports issued by other U.S. Government agencies, domestic and foreign institutions, universities, and private firms
- Translations in report form
- NASA-owned patents and patent applications
- Other U.S. Government agency and foreign patents and patent applications
- Domestic and foreign dissertations and theses

Journal, book, and conference literature, cover-to-cover journal translations, and certain foreign dissertations are announced in a companion journal, *International Aerospace Abstracts (IAA),* available on subscription from the American Institute of Aeronautics and Astronautics, Technical Information Service, 555 West 57th Street, 12th Floor, New York, NY 10019.

SUBJECT SCOPE

The subject scope of *STAR* and *IAA* includes all aspects of aeronautics and space research and development, supporting basic and applied research, and applications. Aerospace aspects of earth resources, energy development, conservation, oceanography, environmental protection, urban transportation, and other topics of high national priority are also covered.

OTHER NASA PUBLICATIONS

Other NASA publications and information services are described in the publication, *The NASA Scientific and Technical Information System ... and How to Use It,* available without charge from the NASA Scientific and Technical Information Facility, P.O. Box 8757, BWI Airport, MD 21240.

HOW TO USE *STAR* SUBJECT CATEGORIES

STAR is categorized by 10 major subject divisions broken down further into 76 specific subject categories and one general division/category. The major subject divisions are listed on page ii in the Table of Contents, together with a note for each that defines its scope and provides any cross-references. For example:

> **AERONAUTICS**
>
> Includes aeronautics (general); aerodynamics; air transportation and safety; aircraft communications and navigation; aircraft design, testing and performance; aircraft instrumentation; aircraft propulsion and power; aircraft stability and control; and research and support facilities (air).
>
> For related information see also *Astronautics.*

Each major division is further divided into as many as nine specific categories, which are identified by category numbers.

Abstracts in *STAR* are grouped by subject category, the categories appearing in sequential order. Category breaks in the abstract section are identified by the category number and title, and a scope note. Cross-references to other categories are provided as appropriate. For example:

> **02 AERODYNAMICS**
>
> Includes aerodynamics of bodies, combinations, wings, rotors, and control surfaces; and internal flow in ducts and turbomachinery.
>
> For related information see also *34 Fluid Mechanics and Heat Transfer.*

CROSS-REFERENCES

Individual *STAR* abstracts are not ordinarily cross-referenced, except for certain conference reports or book translations that have had separate abstracts written for their component papers or chapters. Citations and abstracts of the components follow immediately after those of the parent document. When the subject content of a component differs sufficiently from the general content of the parent, a cross-reference citation also is printed at the end of the category to which it normally would have been assigned if it were independent.

DOCUMENTS ON MICROFICHE

Documents on microfiche(1) are designated by a pound sign (#) following the accession number. The pound sign is used without regard to the source or quality of the microfiche.

LIMITED REPRODUCIBILITY

A Note of Limited Reproducibility appears in the citation, if one or a combination of the following factors affect the reproducibility of more than 20% of the document. These factors include: faint or broken type, color photographs, black and white photographs, foldouts, dot matrix print, charts/graphs with script notation, non-Roman alphabet, or some other factor that limits the reproducibility of that document. This notation also appears on the microfiche header, with the specific causing factor checked off on a list visible in the second frame.

AVAILABILITIES

One or more sources from which a document announced in *STAR* is available to the public is given in each citation. The most commonly indicated sources and their acronyms or abbreviations are listed below. If the publication is available from a source other than those listed, the publisher and his address will be displayed on the availability line or in combination with the corporate source line.

Avail: NTIS. Sold by the National Technical Information Service. Prices for hard copy (HC) and microfiche (MF) are indicated by a price code following the letters HC or MF in the *STAR* citation. Current values for the price codes are given in the tables on page A-7.

Initially distributed microfiche under the NTIS SRIM (Selected Research in Microfiche) is available at greatly reduced unit prices. For this service and for information concerning subscription to NASA printed reports, consult the NTIS Subscription Section, Springfield, VA 22161.

NOTE ON ORDERING DOCUMENTS: When ordering NASA publications (those followed by the * symbol), use the N accession number. NASA patent applications (only the specifications are offered) should be ordered by the US-Patent-Appl-SN number. Non-NASA publications (no asterisk) should be ordered by the AD, PB, or other *report number* shown on the last line of the citation, not by the N accession number. It is also advisable to cite the title and other bibliographic identification.

---

(1) A microfiche is a transparent sheet of film, 105 by 148 mm in size, containing as many as 60 to 98 pages of information reduced to micro images (not to exceed 26:1 reduction).

Avail: SOD (or GPO). Sold by the Superintendent of Documents, U.S. Government Printing Office, in hard copy. The current price and order number are given following the availability line. (NTIS will fill microfiche requests, as indicated above, for those documents identified by a # symbol.)

Avail: BLL (formerly NLL): British Library Lending Division, Boston Spa, Wetherby, Yorkshire, England. Photocopies available from this organization at the price shown. (If none is given, inquiry should be addressed to the BLL.)

Avail: DOE Depository Libraries. Organizations in U.S. cities and abroad that maintain collections of Department of Energy reports, usually in microfiche form, are listed in *Energy Research Abstracts.* Services available from the DOE and its depositories are described in a booklet, *DOE Technical Information Center - Its Functions and Services* (TID-4660), which may be obtained without charge from the DOE Technical Information Center.

Avail: ESDU. Pricing information on specific data, computer programs, and details on Engineering Sciences Data Unit (ESDU) topic categories can be obtained from ESDU International Ltd. Requesters in North America should use the Virginia address while all other requesters should use the London address, both of which are on page A-6.

Avail: Fachinformationszentrum, Karlsruhe. Sold by the Fachinformationszentrum Energie, Physik, Mathematik GMBH, Eggenstein Leopoldshafen, Federal Republic of Germany, at the price shown in deutschmarks (DM).

Avail: HMSO. Publications of Her Majesty's Stationery Office are sold in the U.S. by Pendragon House, Inc. (PHI), Redwood City, CA. The U.S. price (including a service and mailing charge) is given, or a conversion table may be obtained from PHI.

Avail: NASA Public Document Rooms. Documents so indicated may be examined at or purchased from the National Aeronautics and Space Administration, Public Documents Room (Room 126), 600 Independence Ave., S.W., Washington, DC 20546, or public document rooms located at NASA installations, and the NASA Pasadena Office at the Jet Propulsion Laboratory.

Avail: Univ. Microfilms. Documents so indicated are dissertations selected from *Dissertation Abstracts* and are sold by University Microfilms as xerographic copy (HC) and microfilm. All requests should cite the author and the Order Number as they appear in the citation.

Avail: US Patent and Trademark Office. Sold by Commissioner of Patents and Trademarks, U.S. Patent and Trademark Office, at the standard price of $1.50 each, postage free. (See discussion of NASA patents and patent applications below.)

Avail: (US Sales Only). These foreign documents are available to users within the United States from the National Technical Information Service (NTIS). They are available to users outside the United States through the International Nuclear Information Service (INIS) representative in their country, or by applying directly to the issuing organization.

Avail: USGS. Originals of many reports from the U.S. Geological Survey, which may contain color illustrations, or otherwise may not have the quality of illustrations preserved in the microfiche or facsimile reproduction may be examined by the public at the libraries of the USGS field offices whose addresses are listed in this Introduction. The libraries may be queried concerning the availability of specific documents and the possible utilization of local copying services, such as color reproduction.

Avail: Issuing Activity, or Corporate Author, or no indication of availability. Inquiries as to the availability of these documents should be addressed to the organization shown in the citation as the corporate author of the document.

NASA PATENTS AND PATENT APPLICATIONS

Patents and patent applications owned by NASA are announced in *STAR* under appropriate subject categories and are referenced in the *STAR* indexes. In the Report/Accession Number Index, patents are indexed by the NASA Case Number (which appears in lieu of the report number in other indexes), the U.S. Patent Number, the U.S. Patent Application Serial Number, and the U.S. Patent Class. Patent applications for which patents have not yet been issued are indexed by the NASA Case Number and the U.S. Patent Application Serial Number.

NASA *patent application specifications* are sold in paper copy and microfiche by the National Technical Information Service (NTIS). The US-Patent-Appl-SN- number should be used in ordering either paper copy or microfiche from NTIS. Printed copies of *patents* (which are not microfiched) are available for purchase from:

Commissioner of Patents and Trademarks
U.S. Patent and Trademark Office
Washington, DC 20231

When ordering patents, the U.S. Patent Number should be used, and payment must be remitted in advance, by money order or check payable to the Commissioner of Patents and Trademarks. Prepaid purchase coupons for ordering are also available from the Patent and Trademark Office. The patents and patent applications announced in *STAR* are owned by NASA and are available for royalty-free licensing. Requests for licensing terms and further information should be addressed to:

Associate General Counsel for Intellectual Property/Code GP
National Aeronautics and Space Administration
Washington, DC 20546

ELIGIBILITY AND REGISTRATION FOR NASA INFORMATION PRODUCTS AND SERVICES

A variety of services is available to organizations of the following types that have registered with NASA to receive specific services or products:

1. NASA offices and installations, contractors, subcontractors, grantees, and consultants;
2. Other U.S. Government agencies and their contractors;
3. Libraries in the United States that have arrangements with NASA to maintain collections of NASA documents for public reference;
4. Other organizations in the United States having a need for NASA documents in work related to aeronautics and space research;
5. Organizations abroad that have established reciprocal document exchange arrangements with NASA.

Only the central service points or central points of document acquisition and control within qualified organizations are eligible to register for NASA products and services. Domestic organizations that may be eligible to receive various classes of NASA publications and services should address their requests for registration or for further information to:

NASA Scientific and Technical Information Facility
ATTN: Registration Services
P.O. Box 8757
BWI Airport, MD 21240
301-621-0153

Organizations abroad should direct requests to Manager, International STI Activities, NTT, NASA Headquarters, Washington, DC 20546.

AVAILABILITY OF *STAR* ABSTRACTS ON MICROFICHE

Microfiche of the abstract sections of this issue and other issues of *STAR* are available on annual subscription from NTIS as PB90-911300, Attn: Subscriptions, 5285 Port Royal Road, Springfield, VA 22161. Annual subscription rates are $75.50 North America; $151.00 foreign. Abstract sections for previous years retroactive to 1964 are available at the current rates. Microfiche for individual *STAR* issue abstract sections are not available.

PUBLIC COLLECTIONS OF NASA DOCUMENTS

DOMESTIC: NASA and NASA-sponsored documents and a large number of aerospace publications are available to the public for reference purposes at the library maintained by the American Institute of Aeronautics and Astronautics, Technical Information Service, 555 West 57th Street, 12th Floor, New York, NY 10019

EUROPEAN: An extensive collection of NASA and NASA-sponsored publications is maintained by the British Library Lending Division, Boston Spa, Wetherby, Yorkshire, England, for public access. The British Library Lending Division also has available many of the non-NASA publications cited in *STAR*. European requesters may purchase facsimile copy or microfiche of NASA and NASA-sponsored documents, those identified by both the symbols # and * from ESA - Information Retrieval Service, European Space Agency, 8-10 rue Mario-Nikis, 75738 Paris CEDEX 15, France.

FEDERAL DEPOSITORY LIBRARY PROGRAM

In order to provide the general public with greater access to U.S. Government publications, Congress established the Federal Depository Library Program under the Government Printing Office (GPO), with 51 regional depositories responsible for permanent retention of material, inter-library loan, and reference services. At least one copy of nearly every NASA and NASA-sponsored publication, either in printed or microfiche format, is received and retained by the 51 regional depositories. A list of the regional GPO libraries, arranged alphabetically by state, appears on the inside back cover. These libraries are *not* sales outlets. A local library can contact a Regional Depository to help locate specific reports, or direct contact may be made by an individual.

ADDRESSES OF ORGANIZATIONS

American Institute of Aeronautics and Astronautics
Technical Information Service
555 West 57th Street, 12th Floor
New York, New York 10019

British Library Lending Division,
Boston Spa, Wetherby, Yorkshire,
England

Commissioner of Patents and Trademarks
U.S. Patent and Trademark Office
Washington, DC 20231

Department of Energy
Technical Information Center
P.O. Box 62
Oak Ridge, Tennessee 37830

European Space Agency-Information Retrieval Service
ESRIN
Via Galileo Galilei
00044 Frascati (Rome) Italy

Engineering Sciences Data Unit International
P.O. Box 1633
Manassas, Virginia 22110

Engineering Sciences Data Unit International, Ltd.
251-259 Regent Street
London, W1R 7AD, England

Fachinformationszentrum Energie, Physik, Mathematik
GMBH
7514 Eggenstein Leopoldshafen
Federal Republic of Germany

Her Majesty's Stationery Office
P.O. Box 569, S.E. 1
London, England

NASA Scientific and Technical Information Facility
P.O. Box 8757
BWI Airport, Maryland 21240

National Aeronautics and Space Administration
Scientific and Technical Information Division (NTT)
Washington, DC 20546

National Technical Information Service
5285 Port Royal Road
Springfield, Virginia 22161

Pendragon House, Inc.
899 Broadway Avenue
Redwood City, California 94063

Superintendent of Documents
U.S. Government Printing Office
Washington, DC 20402

University Microfilms
A Xerox Company
300 North Zeeb Road
Ann Arbor, Michigan 48106

University Microfilms, Ltd.
Tylers Green
London, England

U.S. Geological Survey Library National Center
MS 950
12201 Sunrise Valley Drive
Reston, Virginia 22092

U.S. Geological Survey Library
2255 North Gemini Drive
Flagstaff, Arizona 86001

U.S. Geological Survey
345 Middlefield Road
Menlo Park, California 94025

U.S. Geological Survey Library
Box 25046
Denver Federal Center, MS914
Denver, Colorado 80225

NTIS PRICE SCHEDULES

(Effective January 1, 1990)

Schedule A
STANDARD PRICE DOCUMENTS AND MICROFICHE

PRICE CODE	NORTH AMERICAN PRICE	FOREIGN PRICE
A01	$ 8.00	$ 16.00
A02	11.00	22.00
A03	15.00	30.00
A04-A05	17.00	34.00
A06-A09	23.00	46.00
A10-A13	31.00	62.00
A14-A17	39.00	78.00
A18-A21	45.00	90.00
A22-A25	53.00	106.00
A99	*	*
N01	60.00	120.00
N02	59.00	118.00
N03	20.00	40.00

Schedule E
EXCEPTION PRICE DOCUMENTS AND MICROFICHE

PRICE CODE	NORTH AMERICAN PRICE	FOREIGN PRICE
E01	$10.00	$ 20.00
E02	12.00	24.00
E03	14.00	28.00
E04	16.50	33.00
E05	18.50	37.00
E06	21.50	43.00
E07	24.00	48.00
E08	27.00	54.00
E09	29.50	59.00
E10	32.50	65.00
E11	35.00	70.00
E12	38.50	77.00
E13	41.00	82.00
E14	45.00	90.00
E15	48.50	97.00
E16	53.00	106.00
E17	57.50	115.00
E18	62.00	124.00
E19	69.00	138.00
E20	80.00	160.00
E99	*	*

* Contact NTIS for price quote.

IMPORTANT NOTICE

NTIS Shipping and Handling Charges
U.S., Canada, Mexico — ADD $3.00 per TOTAL ORDER
All Other Countries — ADD $4.00 per TOTAL ORDER

Exceptions — Does NOT apply to:
ORDERS REQUESTING NTIS RUSH HANDLING
ORDERS FOR SUBSCRIPTION OR STANDING ORDER PRODUCTS *ONLY*

NOTE: Each additional delivery address on an order requires a separate shipping and handling charge.

FEDERAL REGIONAL DEPOSITORY LIBRARIES

ALABAMA

AUBURN UNIV. AT MONTGOMERY LIBRARY
Documents Department
Montgomery, AL 36193
(205) 279-9110 ext.253

UNIV. OF ALABAMA LIBRARY
Reference Department/Documents
Box S
Tuscaloosa, AL 35486
(205) 348-6046

ARIZONA

DEPT. OF LIBRARY, ARCHIVES, AND PUBLIC RECORDS
Third Floor State Capitol
1700 West Washington
Phoenix, AZ 85007
(602) 255-4121

ARKANSAS

ARKANSAS STATE LIBRARY
Documents Service Section
One Capitol Mall
Little Rock, AR 72201
(501) 371-2090

CALIFORNIA

CALIFORNIA STATE LIBRARY
Govt. Publications Section
914 Capitol Mall
Sacramento, CA 95814
(916) 322-4572

COLORADO

UNIV. OF COLORADO
Norlin Library
Government Publications Division
Campus Box 184
Boulder, CO 80309
(303) 492-8834

DENVER PUBLIC LIBRARY
Govt. Pub. Department
1357 Broadway
Denver, CO 80203
(303) 571-2346

CONNECTICUT

CONNECTICUT STATE LIBRARY
231 Capitol Avenue
Hartford, CT 06106
(203) 566-4971

FLORIDA

UNIV. OF FLORIDA LIBRARIES
Documents Department
Library West
Gainesville, FL 32611
(904) 392-0367

GEORGIA

UNIV. OF GEORGIA LIBRARIES
Government Documents Dept.
Athens, GA 30602
(404) 542-8949

HAWAII

UNIV. OF HAWAII
Hamilton Library
Government Documents Collection
2550 The Mall
Honolulu, HI 96822
(808) 948-8230

IDAHO

UNIV. OF IDAHO LIBRARY
Documents Section
Moscow, ID 83843
(208) 885-6344

ILLINOIS

ILLINOIS STATE LIBRARY
Federal Documents
Centennial Building
Springfield, IL 62756
(217) 782-5012

INDIANA

INDIANA STATE LIBRARY
Serials Section
140 North Senate Avenue
Indianapolis, IN 46204
(317) 232-3686

IOWA

UNIV. OF IOWA LIBRARIES
Government Publications Dept.
Iowa City, IA 52242
(319) 335-5926

KANSAS

UNIVERSITY OF KANSAS
Spencer Research Library
Government Documents
Lawrence, KS 66045
(913) 864-4662

KENTUCKY

UNIV. OF KENTUCKY LIBRARIES
Government Publications/Maps Dept.
Lexington, KY 40506
(606) 257-8400

LOUISIANA

LOUISIANA STATE UNIVERSITY
Middleton Library
Government Documents Dept.
Baton Rouge, LA 70803
(504) 388-2570

LOUISIANA TECHNICAL UNIV.
Prescott Memorial Library
Government Documents Dept.
Ruston, LA 71272
(318) 257-4962

MAINE

UNIVERSITY OF MAINE
Raymond H. Fogler Library
Govt. Documents & Microforms Dept.
Orono, ME 04469
(207) 581-1680

MARYLAND

UNIVERSITY OF MARYLAND
McKeldin Library
Documents/Maps Room
College Park, MD 20742
(301) 454-3034

MASSACHUSETTS

BOSTON PUBLIC LIBRARY
Government Documents Dept.
666 Boylston Street
Boston, MA 02117
(617) 536-5400 ext.226

MICHIGAN

DETROIT PUBLIC LIBRARY
5201 Woodward Avenue
Detroit, MI 48202
(313) 833-1409

LIBRARY OF MICHIGAN
Government Documents
P.O. Box 30007
735 E. Michigan Avenue
Lansing, MI 48909
(517) 373-1593

MINNESOTA

UNIVERSITY OF MINNESOTA
Wilson Library
Government Publications
309 Nineteenth Avenue South
Minneapolis, MN 55455
(612) 373-7813

MISSISSIPPI

UNIV. OF MISSISSIPPI LIB.
Government Documents Dept.
106 Old Gym Bldg.
University, MS 38677
(601) 232-5857

MISSOURI

University of Missouri at Columbia Library
Government Documents
Columbia, MO 65201
(314) 882-6733

MONTANA

UNIV. OF MONTANA
Mansfield Library
Documents Division
Missoula, MT 59812
(406) 243-6700

NEBRASKA

UNIVERSITY OF NEBRASKA - LINCOLN
Love Memorial Library
Documents Department
Lincoln, NE 68588
(402) 472-2562

NEVADA

UNIV. OF NEVADA-RENO LIB.
Govt. Pub. Department
Reno, NV 89557
(702) 784-6579

NEW JERSEY

NEWARK PUBLIC LIBRARY
U.S. Documents Division
5 Washington Street
P.O. Box 630
Newark, NJ 07101
(201) 733-7812

NEW MEXICO

UNIVERSITY OF NEW MEXICO
General Library
Government Publications/Maps Dept.
Albuquerque, NM 87131
(505) 277-5441

NEW MEXICO STATE LIBRARY
325 Don Gaspar Avenue
Santa Fe, NM 87501
(505) 827-3826

NEW YORK

NEW YORK STATE LIBRARY
Documents Sect. Cultural Educ. Ctr.
Empire State Plaza
Albany, NY 12230
(518) 474-5563

NORTH CAROLINA

UNIVERSITY OF NORTH CAROLINA AT CHAPEL HILL
Davis Library 080A
BA/SS Department Documents
Chapel Hill, NC 27514
(919) 962-1151

NORTH DAKOTA

NORTH DAKOTA STATE UNIVERSITY LIBRARY
Government Documents Dept.
Fargo, ND 58105
(701) 237-8352
In cooperation with Univ. of North Dakota, Chester Fritz Library Grand Forks

OHIO

STATE LIBRARY OF OHIO
Documents Section
65 South Front Street
Columbus, OH 43266
(614) 644-7051

OKLAHOMA

OKLAHOMA DEPT. OF LIBRARIES
Government Documents
200 NE 18th Street
Oklahoma City, OK 73105
(405) 521-2502, ext. 252

OKLAHOMA STATE UNIV. LIB.
Documents Department
Stillwater, OK 74078
(405) 624-0489

OREGON

PORTLAND STATE UNIV.
Millar Library
934 SW Harrison - P.O. Box 1151
Portland, OR 97207
(503) 229-3673

PENNSYLVANIA

STATE LIBRARY OF PENN.
Government Publications Section
Box 1601
Walnut St. & Commonwealth Ave.
Harrisburg, PA 17105
(717) 787-3752

SOUTH CAROLINA

CLEMSON UNIV. COOPER LIB.
Documents Department
Clemson, SC 29634
(803) 656-5174
In cooperation with Univ. of South Carolina, Thomas Cooper Library, Columbia

TEXAS

TEXAS STATE LIBRARY
Public Services Department
P.O. Box 12927 - 1201 Brazos
Austin, TX 78711
(512) 463-5455

TEXAS TECH. UNIV. LIBRARY
Documents Department
Lubbock, TX 79409
(806) 742-2268

UTAH

UTAH STATE UNIVERSITY
Merrill Library & Learning Resources Center, UMC-30
Documents Department
Logan, UT 84322
(801) 750-2682

VIRGINIA

UNIVERSITY OF VIRGINIA
Alderman Library
Government Documents
Charlottesville, VA 22903
(804) 924-3133

WASHINGTON

WASHINGTON STATE LIBRARY
Document Section
Olympia, WA 98504
(206) 753-4027

WEST VIRGINIA

WEST VIRGINIA UNIV. LIB.
Government Documents Section
P.O. Box 6069
Morgantown, WV 26506
(304) 293-3640

WISCONSIN

ST. HIST SOC. OF WISCONSIN LIB.
Government Pub. Section
816 State Street
Madison, WI 53706
(608) 262-2781
In cooperation with Univ. of Wisconsin-Madison, Memorial Library

MILWAUKEE PUBLIC LIBRARY
Documents Division
814 West Wisconsin Avenue
Milwaukee, WI 53233
(414) 278-3065

WYOMING

WYOMING STATE LIBRARY
Supreme Court & Library Bldg.
Cheyenne, WY 82002
(307) 777-5919

National Aeronautics and
Space Administration
Code NTT
Washington, D.C.
20546

Official Business
Penalty for Private Use, $300

SPECIAL FOURTH-CLASS RATE
POSTAGE & FEES PAID
NASA
PERMIT No. G27

NASA

POSTMASTER: If Undeliverable (Section 158
Postal Manual) Do Not Return